NASA CONTRACTOR REPORT

NASA CR-1756

NASA CR-1756

THE SIMULATION OF A LARGE JET TRANSPORT AIRCRAFT

Volume I: Mathematical Model

by C. Rodney Blake

Prepared by
THE BOEING COMPANY
Wichita, Kans.
for Ames Research Center

NATIONAL AERONAUTICS AND SPACE ADMINISTRATION • WASHINGTON, D. C. • MARCH 1971

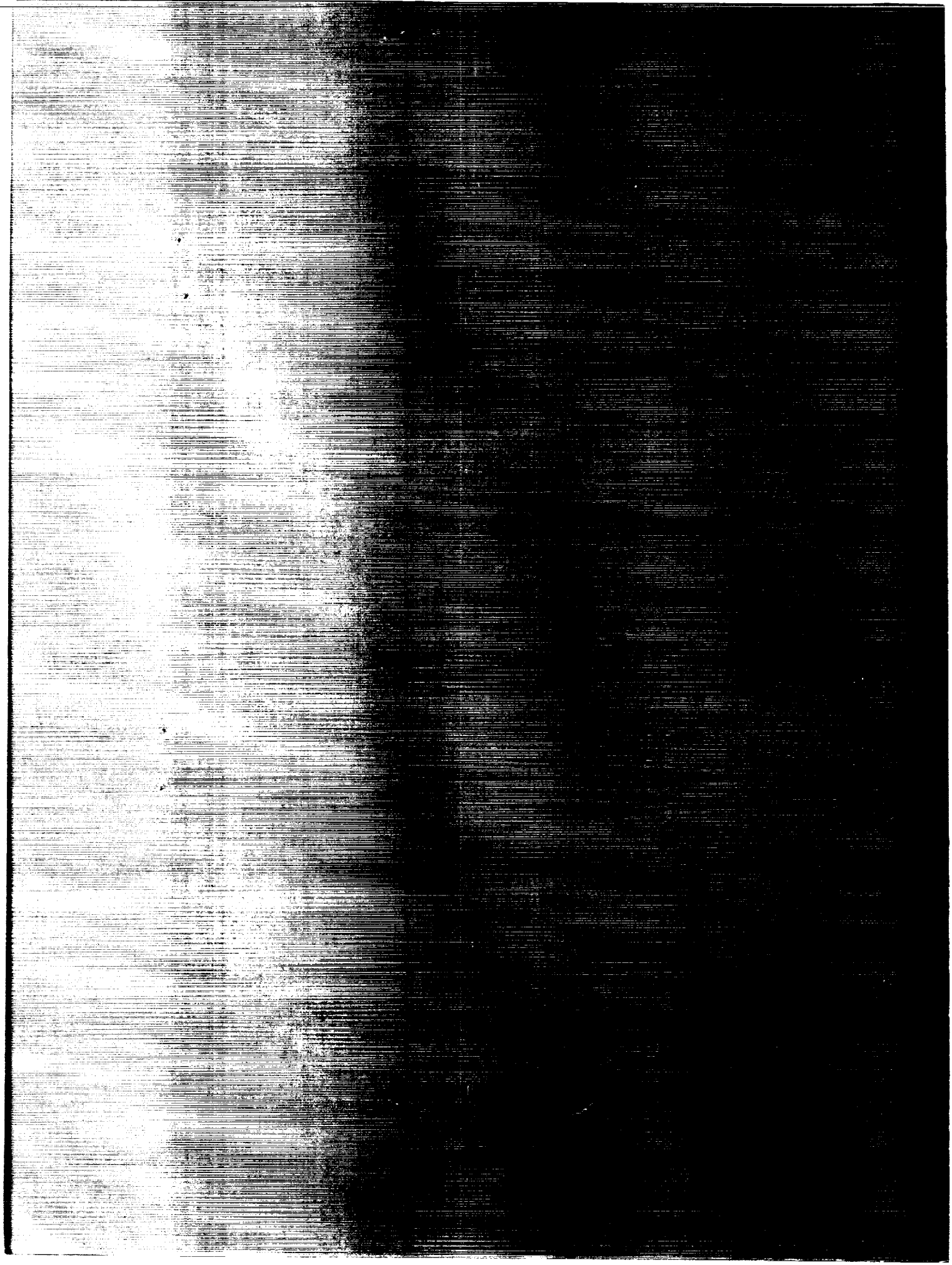

1. Report No.	2. Government Accession No.	3. Recipient's Catalog No.
NASA CR-1756		

4. Title and Subtitle	5. Report Date
"The Simulation of a Large Jet Transport Aircraft Volume I: Mathematical Model"	March 1971
	6. Performing Organization Code

7. Author(s)	8. Performing Organization Report No.
C. Rodney Hanke	10. Work Unit No.

9. Performing Organization Name and Address	11. Contract or Grant No.
The Boeing Company Wichita, Kansas	NAS 2-5524
	13. Type of Report and Period Covered
12. Sponsoring Agency Name and Address	Contractor Report
National Aeronautics and Space Administration Washington, D.C. 20546	14. Sponsoring Agency Code

15. Suppiementary Notes

16. Abstract

The mathematical models used in the manned simulation of a jumbo jet transport aircraft are described. Included are the models of the basic airframe, the longitudinal lateral and directional control systems, the high lift system, the propulsion system, and the landing gear system. In addition, the low speed buffet characteristics and atmospheric model are described.

Included is a list of necessary tests of the simulation to insure validity of the model, of the computer program, and of the quantitative values.

17. Key Words (Suggested by Author(s))	18. Distribution Statement
Simulation Mathematical Model Transport Aircraft	Unclassified-Unlimited

19. Security Classif. (of this report)	20. Security Classif. (of this page)	21. No. of Pages	22. Price*
Unclassified	Unclassified	64	$3.00

*For sale by the National Technical Information Service, Springfield, Virginia 22151

PREFACE

This report summarizes all work conducted by The Boeing Company under Task II of Contract NAS2-5524, "Design for the Simulation of Advanced Aircraft". The National Aeronautics and Space Administration Technical Monitor was Mr. John Dusterberry of the Simulation Science Division. The Boeing Company Project Leader was Mr. C. Rodney Hanke of the Wichita Division Stability, Control and Flying Qualities Organization. Technical assistance was provided by Mr. Robert A. Curnutt of the 747 Aerodynamics Staff, Everett, Washington.

TABLE OF CONTENTS

TABLE OF CONTENTS (CONTINUED)

INTRODUCTION

The Boeing Company provided NASA-Ames Research Center with mathematical models and data to simulate the flying qualities and characteristics of the Boeing 747 on the NASA Flight Simulator For Advanced Aircraft (FSAA).

The contractual report is divided into two volumes. Volume I includes a description of:

1. The work performed under the contract.
2. Generalized equations and approximations used in the simulation.
3. The form of the data furnished to NASA.
4. Nomenclature used for the report.

Volume II contains only limited rights data. These data are to be retained within the Government until The Boeing Company chooses to treat the data as non-proprietary or until September 15, 1971, whichever occurs first.

Boeing and NASA personnel established ground rules for the simulation program; these ground rules resulted in the following conditions of simulation:

1. Flaps-up and flaps-down data were incorporated into one computer program for simulation capability throughout the complete flight envelope.
2. The significant stability derivatives including control effectiveness derivatives were capable of being modified by multiplication factors (normally equal to 1.0).
3. Hydraulic system failures could be simulated by reduced control capability with the multiplication factors described in Item 2.
4. Data describing aircraft system malfunctions (asymmetric flaps, floating control surfaces, etc.) were provided, however, these data were not incorporated in the simulation.
5. Existing NASA digital computer programs were used where possible.
6. The aerodynamic data cards from the Boeing 747 digital simulation were duplicated for NASA and modified for the digital computer format at NASA-Ames. The stored data were observed visually on a scope as a part of the computer program checkout.
7. A single yaw damper system was programmed to drive both rudder segments.
8. Significant blowdown limits were included in the simulation.

9. The rudder ratio changer (limiter) was incorporated in the simulation. Rudder blowdown data were provided but were not required for the simulation.

10. The existing NASA engine simulation program was modified to simulate the 747 propulsion system. The engine simulation included forward, idle, and reverse thrust with first stage compressor RPM, engine pressure ratio, exhaust gas temperature and windmilling drag characteristics.

11. The existing NASA landing gear simulation program was modified to simulate a simplified model of the 747 landing gear. The load equalization system was accounted for by assuming that takeoff rotation occurred about a point midway between the main wing gear and body gear struts. The mathematical model of the main landing gear did not incorporate body gear steering or wing landing gear tilt.

12. Altitude and airspeed system position errors were neglected.

13. The 747 automatic flap retraction system was not incorporated in the simulation. A description of the system was provided to NASA.

14. The 747 autopilot was not included in the simulation but descriptive data on the autopilot were provided to NASA.

15. Constant fuel load was assumed for any simulation run.

NOMENCLATURE

A,B,C	Constants used in stick force program
A.Q.T.	Aft quadrant travel, in.
a	Speed of sound, ft/sec
a_o	Speed of sound, sea level standard, ft/sec
b	Wing span, ft
$\bar{c}$	Wing mean aerodynamic chord, ft
C_D	Airplane drag coefficient, $C_D = \frac{\text{Drag}}{q_D S}$
$C_{D_{Basic}}$	Basic drag coefficient for the rigid airplane at $\alpha_{F.R.L.} = 0^o$, in free air and with the landing gear retracted
C_{D_M}	Drag coefficient at Mach number
C_L	Airplane lift coefficient, $C_L = \frac{\text{Lift}}{q_D S}$
$C_{L_{Basic}}$	Basic lift coefficient for the rigid airplane at $\alpha_{F.R.L.} = 0^o$, in free air and with the landing gear retracted
C_L (c.g. -.25)	Change in pitching moment coefficient due to c.g. variation from 25% M.A.C.
C_ℓ	Airplane rolling moment coefficient, $\frac{\text{Rolling Moment}}{q_D S b}$
C_m	Airplane pitching moment, $C_m = \frac{\text{Pitching Moment}}{q_D S \bar{c}}$
$C_{m_{.25\ Basic}}$	Basic pitching moment coefficient for the rigid airplane at $\alpha_{F.R.L.} = 0^o$, in free air, with the landing gear retracted, and with the c.g. = 25% M.A.C.
C_n	Airplane yawing moment coefficient, $\frac{\text{Yawing Moment}}{q_D S b}$

C_y	Airplane side force coefficient, $\frac{\text{Side Force}}{q_D S}$
c.g.	Airplane center of gravity position as a fraction of the wing mean aerodynamic chord
C_i	Landing gear damping constant
EGT	Exhaust gas temperature
EPR	Engine pressure ratio
F_{B_i}	Tire braking force, lb
F_{G_Z}	Vertical oleo strut force, lb
F_{RX}, F_{RY}, F_{RZ}	Total body axis drag, side, and normal force exerted through the oleo struts, lb.
$F_{RX_{pi}}, F_{RY_{pi}}, F_{RZ_{pi}}$	Body axis drag, side and normal tire force for each oleo strut, lb
F_N	Net thrust, lb
F_{N_G}	Tire force normal to runway, lb
F_s, F_{si}	Tire side force, lb
F.Q.T.	Forward quadrant travel, in
FS	Stick force, lb
$FS_{\substack{\text{Mass} \\ \text{Unbalance}}}$	Stick force due to the mass unbalance of the column, lb
FSAA	Flight Simulator for Advanced Aircraft
$F\mu, F\mu_i$	Tire drag force, lb
FST	Flap screw travel
F.U.T.	Feel unit torque, in-lb
F_{WD}	Engine Windmilling Drag, lb
$F_{X_{B_O}}, F_{Y_{B_O}}, F_{Z_{B_O}}$	Tire forces in body axis for no pitch or roll rotation, lb

$F_{X_{B_\theta}}, F_{Y_{B_\theta}}, F_{Z_{B_\theta}}$	Tire forces in body axis due to pitch rotation only, lb
$F_{X_B}, F_{Y_B}, F_{Z_B}$	Tire forces in body axis due to pitch and roll rotation, lb
g	Acceleration due to gravity, ft/sec^2
G_{T_i}, H_{T_i}	Constants used to determine wheel side force
h	Pressure altitude of the airplane c.g., ft
$h_{B_{c.g._i}}$	Vertical distance from c.g. to force vector created by the tires in contact with the runway, ft
h_G	Height of the tire relative to the runway, ft
h_r	Runway altitude, ft
h_θ	Height of the tire relative to the c.g. due to the pitch angle, ft
h_ϕ	Change in height of the tire relative to the c.g. due to the bank angle, ft
ICAO	International Civil Aviation Organization
K	Drag coefficient interpolation factor
K_B	Braking constant
K_{BM}	Maximum value of braking constant
K_α	Effectiveness factor for elevator and stabilizer
K_{EGT}	Proportionality constant relating exhaust gas temperatures to N_1
K_T	Tire deflection constant
M	Mach number
MA	Mechanical advantage
M.A.C.	Wing mean aerodynamic chord, ft
M_{RX}, M_{RY}, M_{RZ}	Total body axes moments computed from the body axes forces and their distances from the c.g., ft-lb
N_1	Low pressure compressor rotor speed
n_Z	Airplane normal load factor along the Z-axis

P_f	Artificial feel unit pressure, lb/in^2
P_o	Static pressure, sea level standard day, lb/ft^2
p , q, r	Roll, pitch and yaw rates about a reference axes system, radians/sec
q_c	Impact pressure, $q_c = P_{total} - P_{static}$, lb/ft^2
q_D	Dynamic pressure, $q = 1/2\ \rho V^2$, lb/ft^2
r	Tire radius, ft
RPM	Revolutions per minute
S	Wing area, ft^2
$\mathscr{A}_{F.R.L.}$	Horizontal stabilizer angle relative to the fuselage reference line, degrees
T_{AM}	Ambient temperature, ^oR
T_o	Static temperature, sea level standard day, ^oR
T_{t_2}	Total temperature at compressor face, ^oR
T_{t_7}	Turbine discharge total temperature, ^oF
V	True airspeed, ft/sec
V_c	Calibrated airspeed, knots
V_E	Equivalent airspeed, knots
VF_i	Landing gear spring force, lb
V_G	Ground speed, knots
W	Airplane weight, lb
$X_{L_i}, Y_{L_i}, Z_{L_i}$	Distance from c.g. to the end of the fully extended landing gear strut, ft
Y_{E_I}	Effective inboard engine yawing moment arm, ft
Y_{E_O}	Effective outboard engine yawing moment arm, ft
Z_{E_I}	Effective inboard engine pitching moment arm, ft
Z_{E_O}	Effective outboard engine pitching moment arm, ft
α	Angle of attack relative to fuselage reference line, degrees
$\alpha_{W.D.P.}$	Airplane angle of attack relative to the wing design plane, degrees

β	Airplane sideslip angle, degrees
β_G	Airplane sideslip angle relative to ground velocity vector, degrees
δ_{AM}	Ambient pressure ratio, P/P_o
δ_{A_I}	Inboard aileron deflection angle, degrees
δ_{A_O}	Outboard aileron deflection angle, degrees
δ_B	Brake pedal deflection, in
δ_{column}	Control column deflection angle, degrees
δ_e	Elevator deflection angle, degrees
δ_{e_I}	Inboard elevator deflection angle, degrees
δ_{e_O}	Outboard elevator deflection angle, degrees
δ_F	Flap position
δ_P	Rudder pedal deflection, in
δ_R	Rudder deflection angle, degrees
$\delta_{R_{command}}$	Commanded rudder deflection angle, degrees
$\delta_{R_{lower}}$	Lower rudder deflection angle, degrees
$\delta_{R_{max}}$	Maximum rudder deflection angle, degrees
$\delta_{R_{upper}}$	Upper rudder deflection angle, degrees
δ_S	Nose wheel steering angle, degrees
δ_{SBH}	Speed brake handle position, degrees
δ_{SP}	Spoiler deflection angle, degrees
δ_T	Tire deflection, in
δ_W	Control wheel deflection angle, degrees
θ	Temperature ratio, T/T_o
θ_B	Airplane body axis pitch angle, radians
θ_{t_2}	Temperature ratio, T_{t_2} / T_o
ϕ_B	Airplane body axis roll angle, radians

μ_B	Coefficient of braking friction
μ_{roll}	Coefficient of rolling friction
$\frac{\partial \delta_s}{\partial \delta_p}$	Nose wheel steering gearing constant
ΔS_{T_i}	Landing gear oleo strut compression, in
$\frac{dC_D}{d\,\mathscr{a}}\,\mathscr{a}_{F.R.L.}$	Change in basic drag coefficient due to change in stabilizer angle from $\mathscr{a}_{F.R.L.} = 0^o$
$\Delta C_{D_{spoilers}}$	Change in drag coefficient due to spoiler or speedbrake deflection.
$\Delta C_{D_{\substack{landing \\ gear}}}$	Change in drag coefficient due to landing gear extension
$\Delta C_{D_{\substack{ground \\ effect}}}$	Change in drag coefficient due to ground effect
$\Delta C_{D_{sideslip}}$	Change in drag coefficient due to angle of sideslip
$\Delta C_{D_{rudders}}$	Change in drag coefficient due to rudder deflection
$(\Delta C_L)\,\alpha_{W.D.P.} = 0$	Change in basic lift coefficient due to aeroelasticity at $\alpha_{W.D.P.} = 0^o$
$\Delta\left(\frac{dC_L}{d\alpha}\right)\alpha_{W.D.P.}$	Change in basic lift coefficient due to the aeroelastic effect on the rigid airplane basic lift coefficient curve slope
$\frac{dC_L}{d\hat{\dot{\alpha}}}\left(\frac{\dot{\alpha}\bar{c}}{2V}\right)$	Change in lift coefficient due to rate of change of angle of attack
$\frac{dC_L}{d\hat{q}}\left(\frac{q\bar{c}}{2V}\right)$	Change in lift coefficient due to pitch rate
$\frac{dC_L}{dn_z}n_z$	Change in lift coefficient due to aeroelastic inertia relief caused by normal load factor
$K_\alpha\frac{dC_L}{d\,\mathscr{a}}\,\mathscr{a}_{F.R.L.}$	Change in lift coefficient due to change in stabilizer angle from $\mathscr{a}_{F.R.L.} = 0^o$
	Change in lift coefficient due to change in inboard elevator angle from $\delta_{e_I} = 0^o$
$K_\alpha\frac{dC_L}{d\delta_{e_o}}\delta_{e_o}$	Change in lift coefficient due to change in outboard elevator angle from $\delta_{e_o} = 0^o$

$\Delta C_{L_{spoilers}}$	Change in lift coefficient due to spoiler or speedbrake deflection
$\Delta C_{L_{\substack{outboard \\ ailerons}}}$	Change in lift coefficient due to outboard aileron deflection
$\Delta C_{L_{\substack{landing \\ gear}}}$	Change in lift coefficient due to landing gear extension
$\Delta C_{L_{\substack{ground \\ effect}}}$	Change in lift coefficient due to ground effect
$\frac{dC_\ell}{d\beta}\beta$	Rolling moment coefficient due to angle of sideslip
$\frac{dC_\ell}{d\hat{p}}\left(\frac{p_s b}{2V}\right)$	Rolling moment coefficient due to roll rate about the stability axis
$\frac{dC_\ell}{d\hat{r}}\left(\frac{r_s b}{2V}\right)$	Rolling moment coefficient due to yaw rate about the stability axis
$\Delta C_{\ell_{spoilers}}$	Rolling moment coefficient due to spoiler deflection
$\Delta C_{\ell_{\substack{inboard \\ ailerons}}}$	Rolling moment coefficient due to inboard aileron deflection
$\Delta C_{\ell_{\substack{outboard \\ ailerons}}}$	Rolling moment coefficient due to outboard aileron deflection
$\Delta C_{\ell_{rudders}}$	Rolling moment coefficient due to rudder deflection
$\left(\Delta C_{m_{.25}}\right)_{\alpha_{W.D.P.}=0}$	Change in pitching moment coefficient at $\alpha_{W.D.P.} = 0$ due to aeroelasticity
$\Delta\left(\frac{dCm}{d\alpha}.25\right)\alpha_{W.D.P.}$	Change in pitching moment coefficient due to the aeroelastic effect on the rigid airplane basic pitching moment coefficient curve slope
$\frac{dCm}{d\hat{\dot{\alpha}}}\left(\frac{\dot{\alpha}\bar{c}}{2V}\right)$	Change in pitching moment coefficient due to rate of change of angle of attack
$\frac{dCm}{d\hat{q}}\left(\frac{q\bar{c}}{2V}\right)$	Change in pitching moment coefficient due to pitch rate
$\frac{dCm}{dn_z}n_z$	Change in pitching moment coefficient due to aeroelastic inertia relief caused by normal load factor

$K_\alpha \frac{dCm}{d\alpha}_{.25} \alpha_{F.R.L.}$	Change in pitching moment coefficient due to change in stabilizer angle from $\alpha_{F.R.L.} = 0^o$
$K_\alpha \frac{dCm}{d\delta_{e_I}}_{.25} \delta_{e_I}$	Change in pitching moment coefficient due to change in inboard elevator angle from $\delta_{e_I} = 0^o$
$K_\alpha \frac{dCm}{d\delta_{e_O}}_{.25} \delta_{e_O}$	Change in pitching moment coefficient due to change in outboard elevator angle from $\delta_{e_O} = 0^o$
$\Delta C_{m_{.25_{spoilers}}}$	Change in pitching moment coefficient due to spoiler or speed brake deflection
$\Delta C_{m_{.25_{\substack{inboard \\ ailerons}}}}$	Change in pitching moment coefficient due to inboard aileron deflection
$\Delta C_{m_{.25_{\substack{outboard \\ ailerons}}}}$	Change in pitching moment coefficient due to outboard aileron deflection
$\Delta C_{m_{.25_{\substack{landing \\ gear}}}}$	Change in pitching moment coefficient due to landing gear extension
$\Delta C_{m_{.25_{\substack{ground \\ effect}}}}$	Change in pitching moment coefficient due to ground effect
$\Delta C_{m_{.25_{sideslip}}}$	Change in pitching moment coefficient due to angle of sideslip
$\Delta C_{m_{.25_{rudders}}}$	Change in pitching moment coefficient due to rudder deflection
$\frac{dCn}{d\beta} \beta$	Yawing moment coefficient due to angle of sideslip
$\frac{dCn}{d\hat{\dot{\beta}}} \left(\frac{\dot{\beta} b}{2V}\right)$	Yawing moment coefficient due to rate of change of sideslip angle
$\frac{dCn}{d\hat{p}} \left(\frac{p_s b}{2V}\right)$	Yawing moment coefficient due to roll rate about the stability axis
$\frac{dCn}{d\hat{r}} \left(\frac{r_s b}{2V}\right)$	Yawing moment coefficient due to yaw rate about the stability axis

$\Delta C_{n_{spoilers}}$	Yawing moment coefficient due to spoiler deflection
$\Delta C_{n_{\substack{inboard \\ ailerons}}}$	Yawing moment coefficient due to inboard aileron deflection
$\Delta C_{n_{\substack{outboard \\ ailerons}}}$	Yawing moment coefficient due to outboard aileron deflection
$\Delta C_{n_{rudders}}$	Yawing moment coefficient due to rudder deflection
$\frac{dC_Y}{d\beta}\beta$	Side force coefficient due to angle of sideslip
$\frac{dC_Y}{d\hat{p}}\left(\frac{p_s b}{2V}\right)$	Side force coefficient due to roll rate about the stability axis
$\frac{dC_Y}{d\hat{r}}\left(\frac{r_s b}{2V}\right)$	Side force coefficient due to yaw rate about the stability axis
$\Delta C_{Y_{spoilers}}$	Side force coefficient due to spoiler deflection
$\Delta C_{Y_{rudders}}$	Side force coefficient due to rudder deflection
$\frac{d(\ )}{dt} = (\cdot)$	Time derivative operation

Landing Gear Designation

$i = 1$	Nose Gear
$i = 2$	Left main landing gear
$i = 3$	Right main gear

GENERAL AIRCRAFT DESCRIPTION

The Boeing 747 is a four-fanjet intercontinental transport designed to operate from existing international airports. High lift for low speed flight is obtained with wing triple-slotted trailing flaps and Krueger type leading edge flaps. The Krueger flaps outboard of the inboard nacelle are cambered and slotted while the inboard Krueger flaps are standard unslotted. A movable stabilizer with four elevator segments provides longitudinal control for the aircraft. The lateral control is obtained with five spoiler panels, an inboard aileron between the inboard and outboard flaps, and an outboard aileron which only operates when the flaps are down. The five spoiler panels on each wing which are used for lateral control also operate symmetrically as speedbrakes in conjunction with the sixth spoiler panel. Directional control is obtained with a two-segment rudder. A general arrangement drawing of the controls and geometric dimensions of the aircraft is shown in Figure 1. A summary of the basic reference areas and geometric dimensions for the simulation is shown in Table 1.

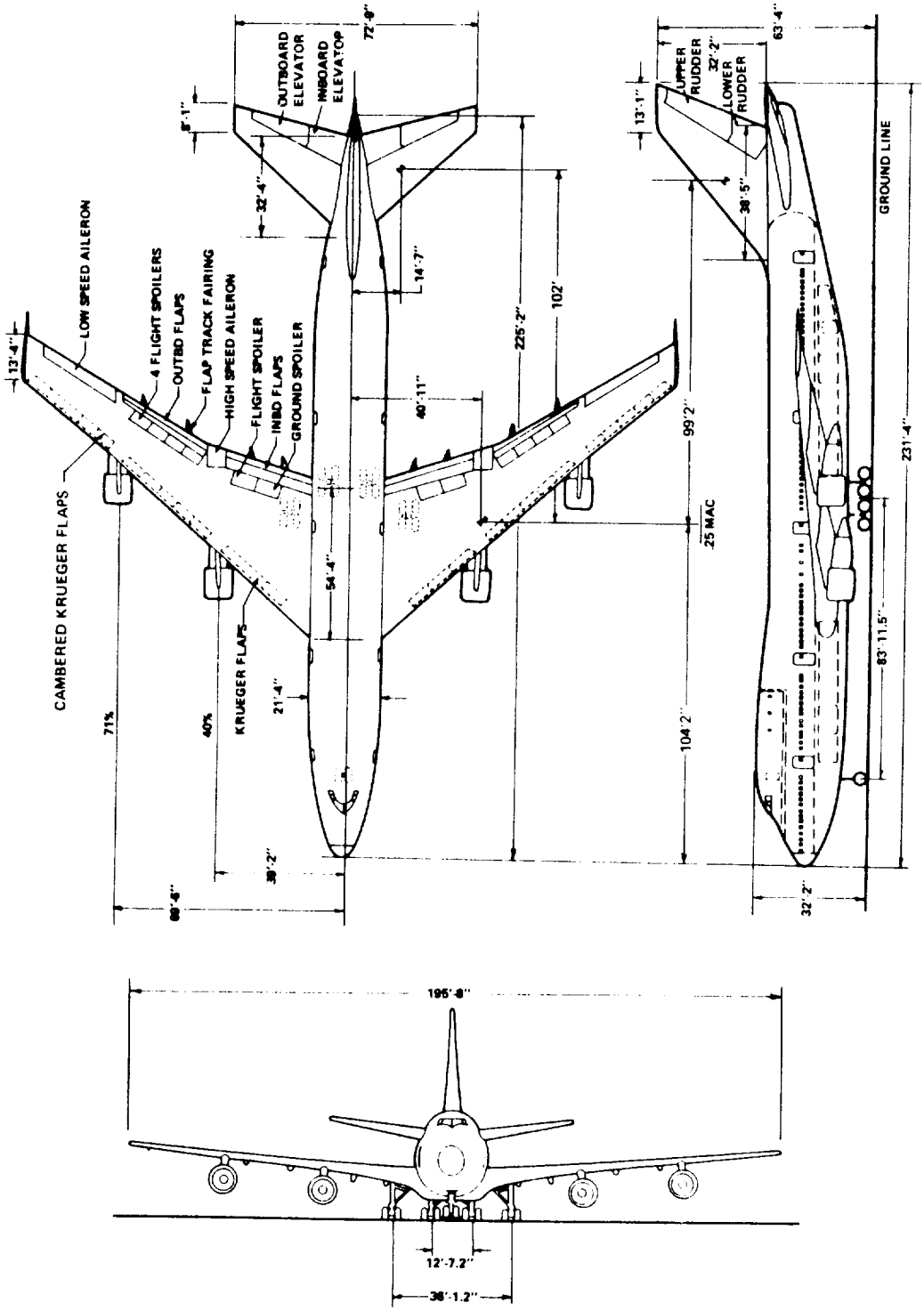

747 THREE-VIEW

FIGURE 1

ITEM	VALUE	DIMENSION
Wing Area (S)	5500	$Ft.^2$
Wing Mean Aerodynamic Chord (MAC)	27.3	Ft.
Wing Span (b)	195.7	Ft.
Wheel Base		
Wing Gear	79	Ft.
Body Gear	89	Ft.
Wheel Tread		
Wing Gear	36.2	Ft.
Body Gear	12.5	Ft.
Pilots Station to .25 MAC (ΔX)	86	Ft.
Pilots Station to Aircraft Centerline (ΔY)	1.7	Ft.
Pilots Station to Aircraft c.g. (ΔZ)	10	Ft.

SUMMARY OF AREAS AND DIMENSIONS

TABLE 1

AIRFRAME SIX DEGREE-OF-FREEDOM MODEL

This section contains the general form of equations for computing force and moment coefficients created by aerodynamic loads on the airplane. Each equation is written as a function of its significant variables. The NASA multiplication factors which can be used to modify the basic stability derivatives (ground rule 2 of the Introduction) are not included in these equations. The aerodynamic data in stability axes for these equations are included in Volume II of this report. The dimensionless force and moment coefficients (C_L, C_D, C_m, C_ℓ, C_n and C_y) were converted into dimensional forces and moments. These forces and moments were used in an existing NASA digital computer program to obtain six degree-of-freedom airframe response. Sign conventions for the control surface deflections and the aerodynamic coefficients are shown in Figure 2.

Lift Force Coefficient

The dimensionless aerodynamic lift force coefficient was computed by the following general equation for a given angle of attack:

$$
\begin{aligned}
C_L = {} & C_{L_{Basic}} + (\Delta C_L)_{\alpha_{W.D.P.}=0} + \Delta\left(\frac{dC_L}{d\alpha}\right)_{\alpha_{W.D.P.}} \\
& + \frac{dC_L}{d\left(\frac{\dot{\alpha}\bar{c}}{2V}\right)} + \frac{dC_L}{d\left(\frac{q\bar{c}}{2V}\right)} + \frac{dC_L}{dn_z} n_z + K_\alpha \frac{dC_L}{d\alpha}_{F.R.L.} \\
& + K_\alpha \frac{dC_L}{d\delta_{e_I}} \delta_{e_I} + K_\alpha \frac{dC_L}{d\delta_{e_O}} \delta_{e_O} + \Delta C_{L_{spoilers}} \\
& + \Delta C_{L_{\substack{outboard \\ ailerons}}} + \Delta C_{L_{\substack{landing \\ gear}}} + \Delta C_{L_{\substack{ground \\ effect}}} .
\end{aligned}
$$

The aerodynamic lift force data and detailed equations for obtaining the stability derivatives and control surface parameters are included in Section 2, Volume II of this report.

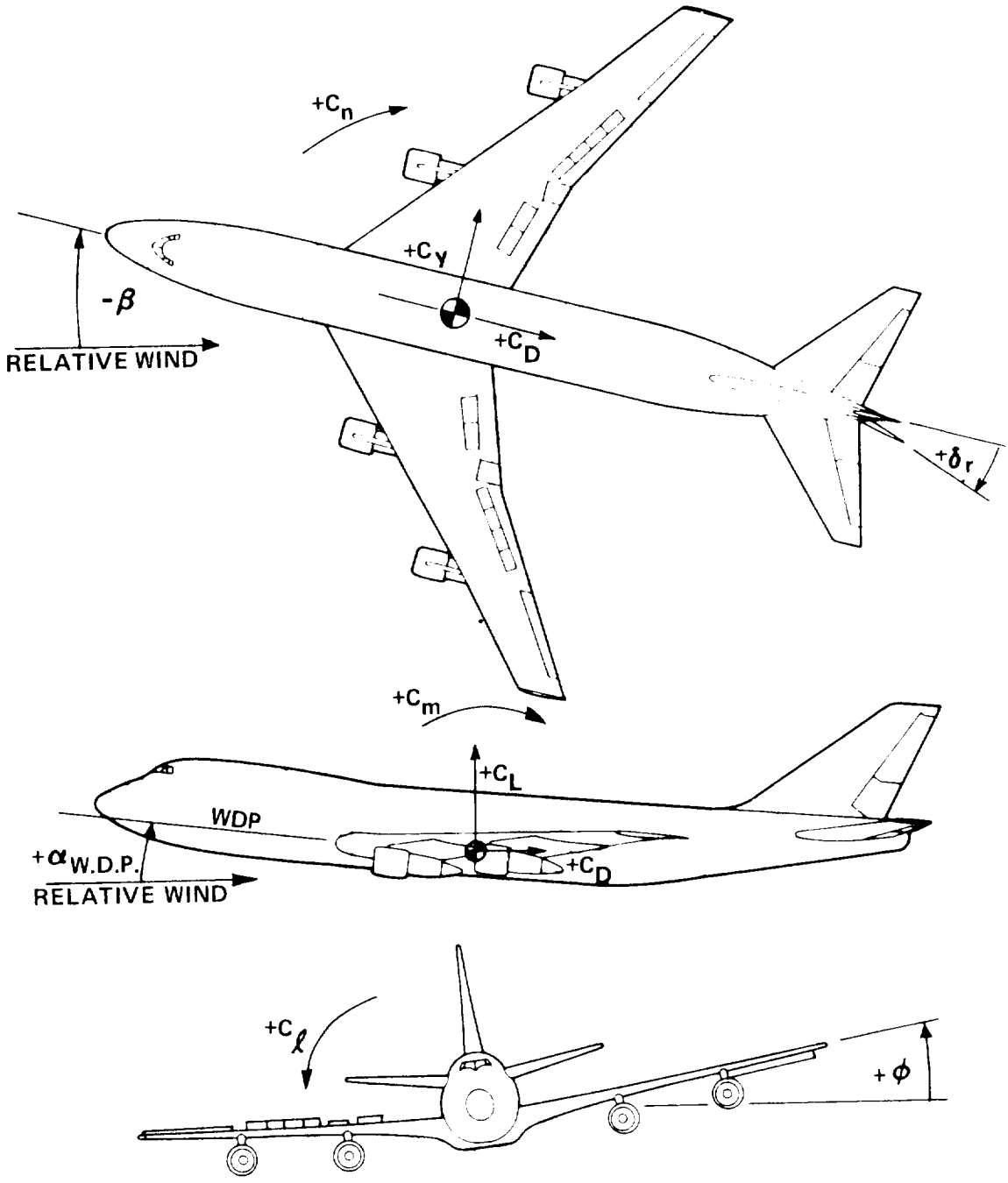

ALL CONTROL SURFACE TRAILING EDGE DOWN DEFLECTIONS ARE POSITIVE

RIGHT WING SPOILER DEFLECTION IS POSITIVE

SIGN CONVENTION
(STABILITY AXES)

FIGURE 2

Drag Force Coefficient

The dimensionless aerodynamic drag force coefficient was computed by the following general equation for a given angle of attack:

$$C_D = K\left[C_{D_{Basic}} + \frac{dC_D}{d\alpha}\alpha_{F.R.L.}\right] + \left[1-K\right]\left[C_D\right]_M + \Delta C_{D_{spoilers}} + \Delta C_{D_{\substack{landing\\gear}}} + \Delta C_{D_{\substack{ground\\effect}}} + \Delta C_{D_{sideslip}} + \Delta C_{D_{rudders}} .$$

The aerodynamic drag force data and detailed equations for obtaining the stability derivatives and control surface parameters are included in Section 3, Volume II of this report.

Pitching Moment Coefficient

The dimensionless aerodynamic pitching moment coefficient was computed by the following general equation for a given angle of attack:

$$C_m = C_{m_{.25\ Basic}} + \left(\Delta C_{m_{.25}}\right)_{\alpha\ W.D.P.=0} + \Delta\left(\frac{dCm}{d\alpha}.25\right)\alpha_{W.D.P.} + C_L\ (c.g.-.25) + \frac{dCm}{d\hat{\alpha}}\left(\frac{\dot{\alpha}\bar{c}}{2V}\right) + \frac{dCm}{d\hat{q}}\left(\frac{q\bar{c}}{2V}\right) + \frac{dCm}{dn_z}n_z + K_\alpha\frac{dCm}{d\alpha}.25\alpha_{F.R.L.} + K_\alpha\frac{dCm}{d\delta_{e_I}}.25\,\delta_{e_I} + K_\alpha\frac{dCm}{d\delta_{e_o}}.25\,\delta_{e_o} + \Delta C_{m_{.25_{spoilers}}} + \Delta C_{m_{.25_{\substack{inboard\\ailerons}}}} + \Delta C_{m_{.25_{\substack{outboard\\ailerons}}}} + \Delta C_{m_{.25_{\substack{landing\\gear}}}} + \Delta C_{m_{.25_{\substack{ground\\effect}}}} + \Delta C_{m_{.25_{sideslip}}} + \Delta C_{m_{.25_{rudders}}}$$

The aerodynamic pitching moment data and detailed equations for obtaining the stability derivatives and control surface parameters are included in Section 4, Volume II of this report.

Rolling Moment Coefficient

The dimensionless aerodynamic rolling moment coefficient was computed by the following general equation for a given angle of attack:

$$C_{\ell} = \frac{dC_{\ell}}{d\beta}\beta + \frac{dC_{\ell}}{d\hat{p}}\left(\frac{p_s b}{2V}\right) + \frac{dC_{\ell}}{d\hat{r}}\left(\frac{r_s b}{2V}\right) + \Delta C_{\ell_{spoilers}} + \Delta C_{\ell_{\substack{inboard \\ ailerons}}} + \Delta C_{\ell_{\substack{outboard \\ ailerons}}} + \Delta C_{\ell_{rudders}}.$$

The aerodynamic rolling moment data and detailed equations for obtaining the stability derivatives and control surface parameters are included in Section 5, Volume II of this report.

Yawing Moment Coefficient

The dimensionless aerodynamic yawing moment coefficient was computed by the following general equation for a given angle of attack:

$$C_n = \frac{dCn}{d\beta}\beta + \frac{dCn}{d\hat{\dot{\beta}}}\left(\frac{\dot{\beta} b}{2V}\right) + \frac{dCn}{d\hat{p}}\left(\frac{p_s b}{2V}\right) + \frac{dCn}{d\hat{r}}\left(\frac{r_s b}{2V}\right) + \Delta C_{n_{spoilers}} + \Delta C_{n_{\substack{inboard \\ ailerons}}} + \Delta C_{n_{\substack{outboard \\ ailerons}}} + \Delta C_{n_{rudders}}.$$

The aerodynamic yawing moment data and detailed equations for obtaining the stability derivatives and control surface parameters are included in Section 6, Volume II of this report.

Side Force Coefficient

The dimensionless aerodynamic side force coefficient was computed by the following general equation for a given angle of attack:

$$C_Y = \frac{dCy}{d\beta}\beta + \frac{dCy}{d\hat{p}}\left(\frac{p_s b}{2V}\right) + \frac{dCy}{d\hat{r}}\left(\frac{r_s b}{2V}\right)$$
$$+ \Delta C_{Y_{spoilers}} + \Delta C_{Y_{rudders}}.$$

The aerodynamic side force data and detailed equations for obtaining the stability derivatives and control surface parameters are included in Section 7, Volume II of this report.

LONGITUDINAL CONTROL SYSTEM

General Description

The longitudinal control system consists of two inboard and two outboard elevators and a movable horizontal stabilizer.

Under normal operation, the outboard elevator angle is equal to the inboard elevator angle at speeds below blowdown. The elevators are downrigged 2^{o} from the faired position. The control column is directly linked to the forward quadrant control mechanism. The mechanical rotation of the forward quadrant is transmitted through the control cables to the aft quadrant which controls the elevator actuators. The elevators are fully powered through irreversible hydraulic actuators connected directly to the elevators. Actual elevator deflection is limited by the hydraulic rate, the mechanical stop, or the pressure blowdown.

Control forces are synthesized in an artificial force feel unit which operates as a function of dynamic pressure and stabilizer position.

Pitch trim is available through the movable horizontal stabilizer. The stabilizer position is controlled by thumb switches on the pilot and copilot control wheels. The trim command actuates hydraulic motors which drive a jackscrew mechanism at a rate which is a function of impact pressure.

NASA Longitudinal Control Model and Approximations

A block diagram of the simulated elevator control system and the computed stick force is shown in Figure 3. The column travel in the FSAA was slightly less than the column travel in the 747. For this simulation, the column deflection of the FSAA was scaled up in the computer program such that full deflection of the FSAA column represented full deflection of the 747 column. The control column deflection in the simulator cab was converted into an equivalent forward quadrant angle on the digital computer. Aft quadrant travel was equal to the forward quadrant travel minus the amount due to cable stretch. The cable stretch was proportional to the torque generated by the artificial feel unit. The aft quadrant was converted into an elevator command which was converted into true elevator position through rate and blowdown limiters. The torque of the force feel unit was obtained as a function of aft quadrant travel and feel unit pressure. The feel unit torque was converted into cable stretch and cable load by conversion constants. The stick force produced by the cable load and the mechanical advantage was added to the stick force from the column mass balance to form the computed stick force. The computed stick force was input to the FSAA control loader to provide the pilot with the proper longitudinal force feel characteristics.

The stall warning was provided by a stick shaker model which was activated as a function of angle of attack and flap angle. The data are included in Section 2, Volume II of this report. The frequency and amplitude of the stick shaker model were varied until the evaluation pilot felt the control column "shake" was representative of the 747.

Data for the stick force simulation is presented in Section 8, Volume II of this report.

The stabilizer position was controlled by thumb switches on the pilot and copilot control wheels. A trim command drove the stabilizer trim rate as a function of impact pressure, Figure 4.

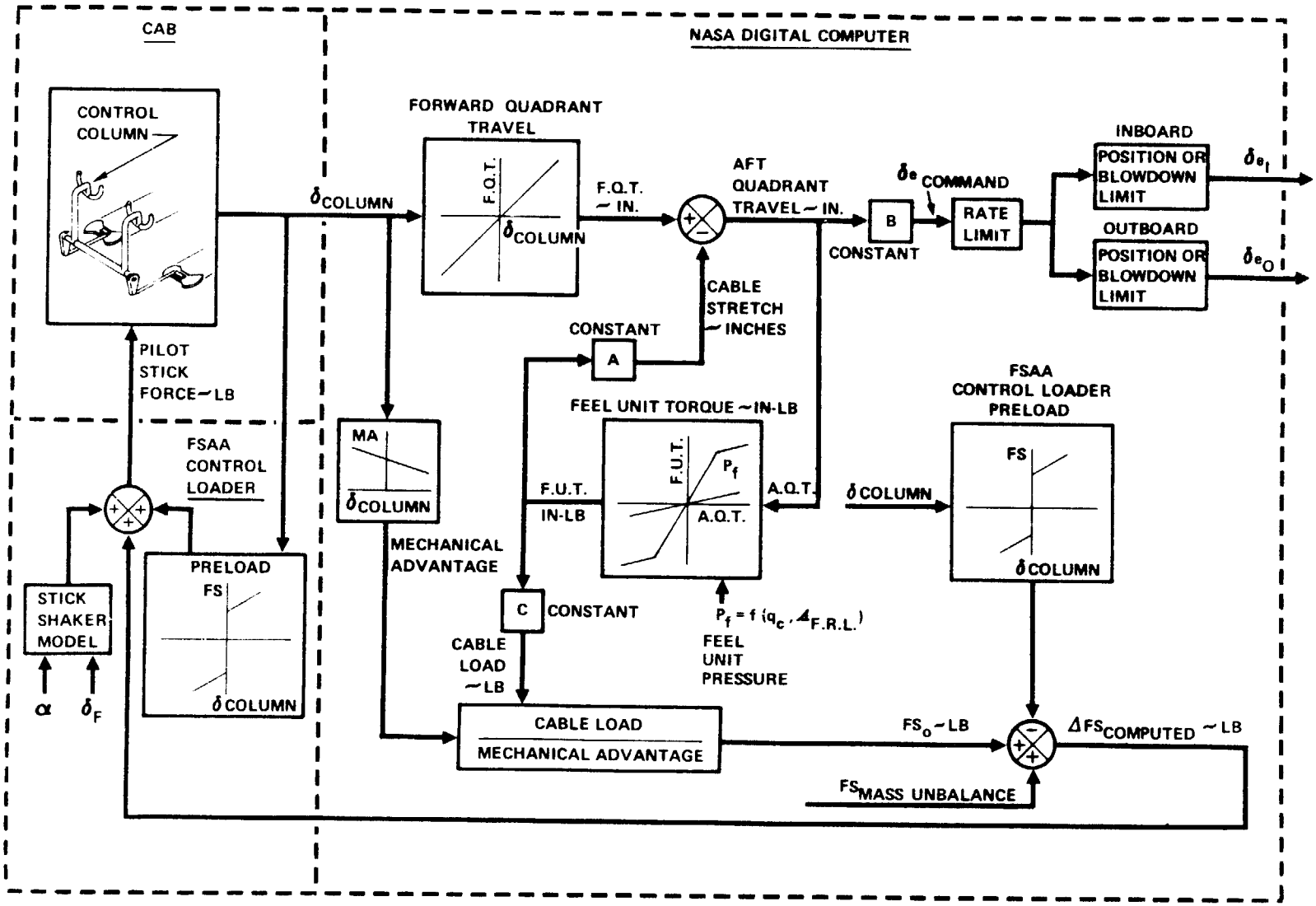

ELEVATOR AND STICK FORCE MODEL

FIGURE 3

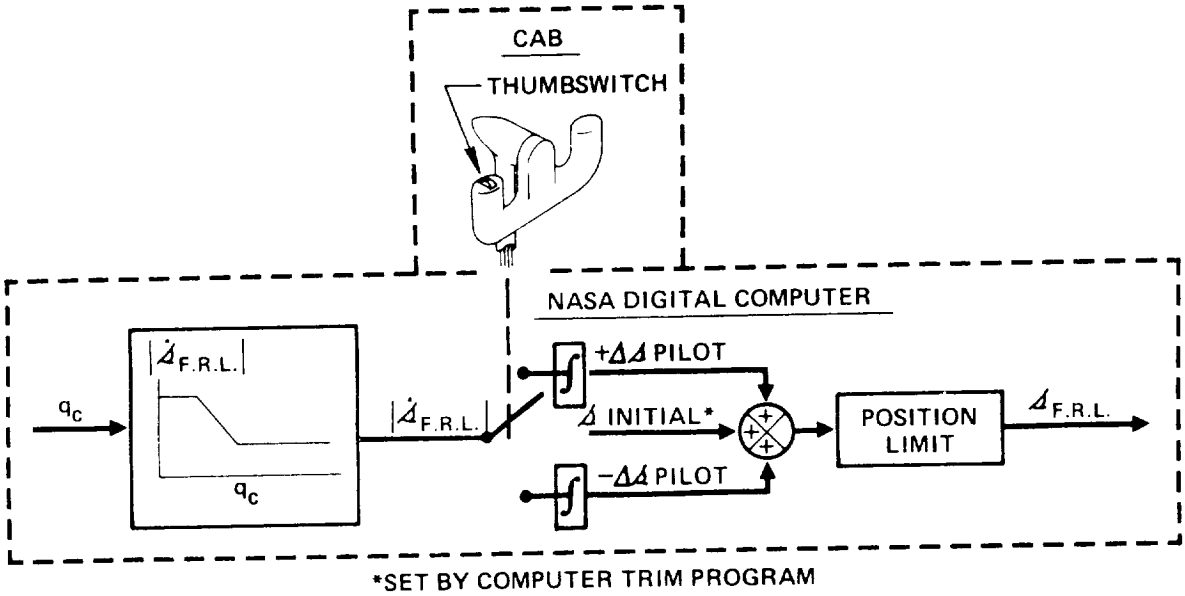

STABILIZER TRIM
FIGURE 4

LATERAL CONTROL SYSTEM

General Description

The lateral control system is a combination of inboard ailerons, outboard ailerons and spoilers. The spoilers can also be used as speedbrakes. Pilot input to the dual tandem central control actuators is provided by a cable system from each of the pilot and copilot control wheels. The actuators drive independent cable systems to the left and right wing lateral control surfaces.

The inboard ailerons operate in all flight regimes while the outboard ailerons operate only when the flaps are down. The outboard ailerons are locked out when the flaps are up.

There are six spoiler panels on each wing. Five panels are modulated by wheel and speedbrake commands and one panel on each wing is controlled by the speedbrake commands. The speedbrake handle is located on the center aisle stand. The five modulated panels on each wing are controlled from "mixer" boxes which sum the inputs from the pilot's wheel and speedbrake inputs. Wheel inputs will move the modulated spoiler panels up or down within the travel limits at any speedbrake setting.

Control wheel force is synthesized by a spring, as a function of wheel deflection.

NASA Lateral Control Model And Approximations

A block diagram of the simulated lateral control system is shown on Figure 5. The wheel deflection in the simulator cab was converted into an equivalent spoiler and aileron angle on the digital computer. Each spoiler bank deflection was computed separately. The block diagram of Figure 5 illustrates the deflection of only one spoiler panel as a function of wheel deflection for speedbrakes up and down. The commanded spoiler angle was input to the spoiler rate and deflection limiter and the output was the actual deflection for each spoiler panel.

Also shown in Figure 5 is the aileron command as a function of wheel deflection. The ailerons were rate limited. Aileron blowdown was neglected for this simulation. Aileron blowdown information is presented in Section 9 Volume II of this report. On the aircraft, the inboard ailerons are not blowdown limited during normal operations, however, the outboard ailerons can have slightly reduced authority due to blowdown near the flap placard speeds.

For the NASA simulation, wheel forces were approximated by a breakout force and a constant gradient programmed on the FSAA control loader.

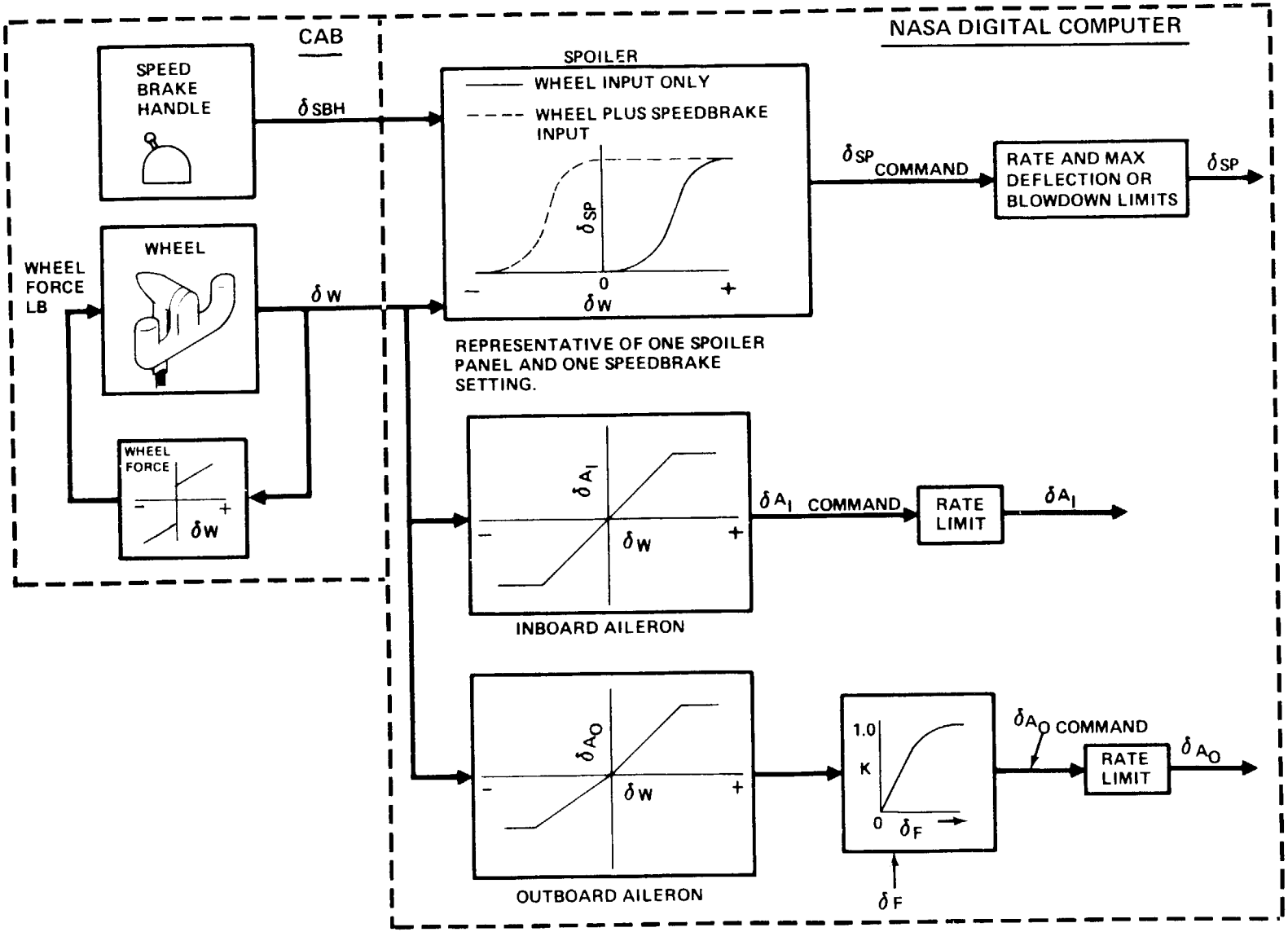

LATERAL CONTROL SYSTEM MODEL
FIGURE 5

DIRECTIONAL CONTROL SYSTEM

General Description

The directional control system consists of two rudder segments, upper and lower, each being controlled by a dual tandem actuator. Both rudder segments move together under normal operation. Rudder pedal movement is converted to rudder deflection by cables linking the forward quadrant mechanism to two ratio changers located in the empennage. The rudder ratio changer is programmed to limit maximum rudder travel to ensure safe structural limits at high airspeeds. The rudders are fully powered through irreversible dual source hydraulic actuators which are controlled by the rudder ratio changers. The actual rudder deflection is limited by the hydraulic rate limit, the pressure limit and the ratio changer.

A yaw damper is incorporated which commands rudder proportional to yaw rate and bank angle. For normal operation, the yaw damper drives both rudder segments together. Turn coordination, operative only with flaps down, is achieved by deflecting the rudder through the yaw damper. The yaw damper has its own rudder rate and deflection limits. The rudder commanded by the yaw damper does not result in any movement of the rudder pedals and does not affect the normal operation of the rudder.

Rudder pedal feel forces are provided by mechanical springs and are proportional to rudder pedal movement. Since the ratio changer reduces the rudder deflection with pedal movement as a function of airspeed, the pedal displacement and force to obtain a given rudder deflection is variable with airspeed.

NASA Directional Control Model and Approximations

A block diagram of the simulated rudder control system is shown in Figure 6. The rudder pedal deflection in the cab was converted into a fractional rudder command on the digital computer ($\delta R/\delta RMAX$). The maximum rudder deflection allowed by the rudder ratio changer was programmed as a function of calibrated airspeed. The commanded rudder deflection was obtained by multiplying the fractional rudder command by the maximum allowable rudder angle as determined by the ratio changer. The pilot's rudder command was then rate limited to obtain actual rudder deflection (less yaw damper inputs). For the NASA simulation, the maximum rudder deflection was assumed to be determined by the rudder ratio changer and not the hydraulic pressure limit (blowdown). Under most flight conditions, the actual aircraft rudder is ratio changer limited instead of hydraulic pressure limited. Rudder blowdown data is included in Section 10, Volume II of this report.

For the NASA simulation, rudder pedal forces were approximated by a breakout force and a constant gradient programmed on the FSAA control loader.

The rudder deflection due to the yaw damper system was position and rate limited, and then added to the rudder deflection due to the pilot inputs to obtain the total rudder deflection. The upper and lower rudder angles were both computed by the same mathematical functions. A block diagram with transfer functions of the yaw damper and turn coordinator systems are included in Section 10, Volume II of this report.

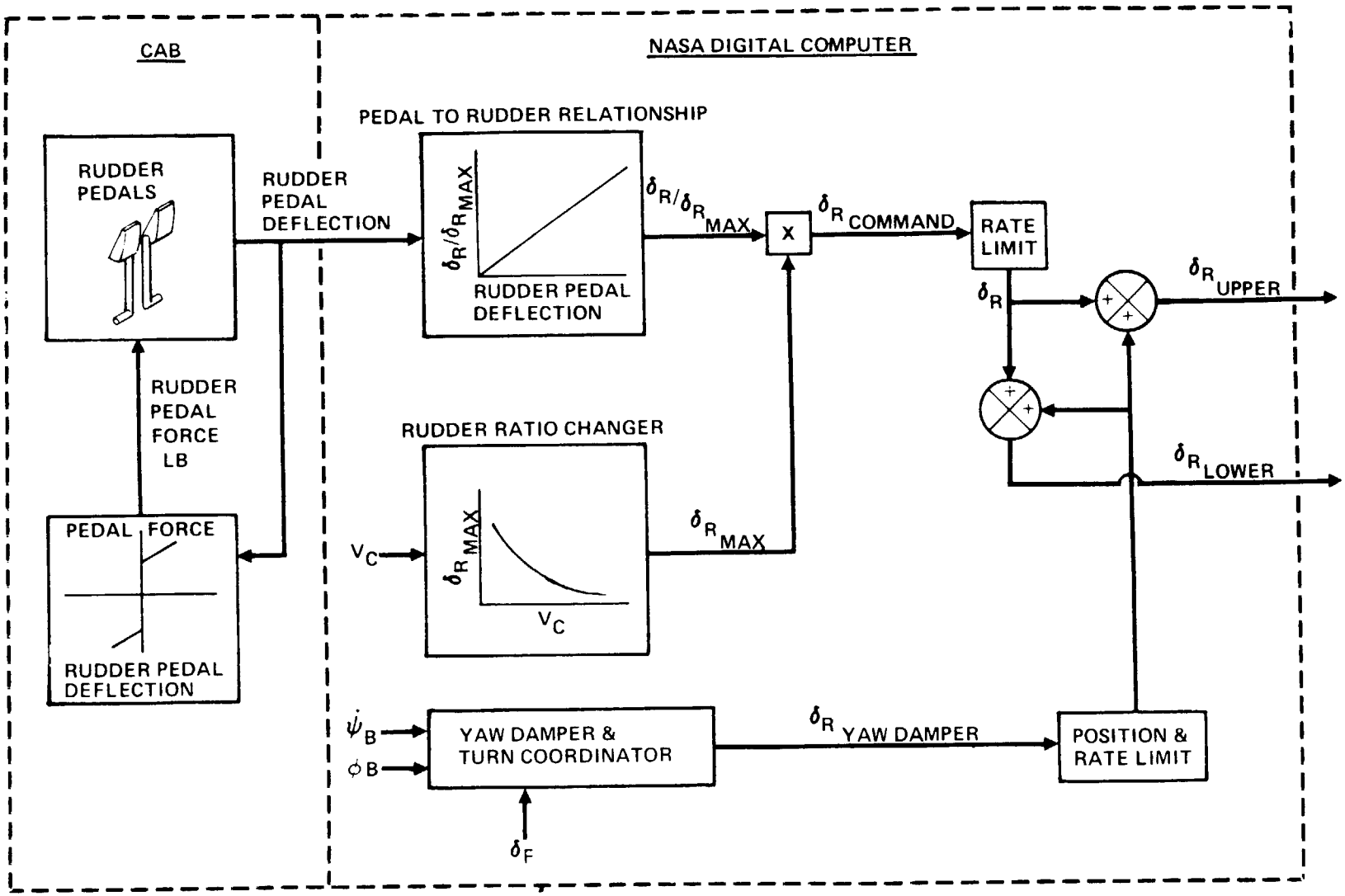

DIRECTIONAL CONTROL MODEL
FIGURE 6

HIGH LIFT SYSTEM

General Description

The 747 flap system consists of two inboard and two outboard triple slotted trailing edge flaps and Krueger type leading edge flaps, Figure 7. The Krueger flaps outboard of the inboard nacelle are cambered and slotted while the inboard Krueger flaps are standard unslotted. During extension, the outboard Krueger flaps alter in shape, flexing from a near-flat to a curved surface. The leading edge flaps are either in the full extended or retracted position as a function of the trailing edge flap position.

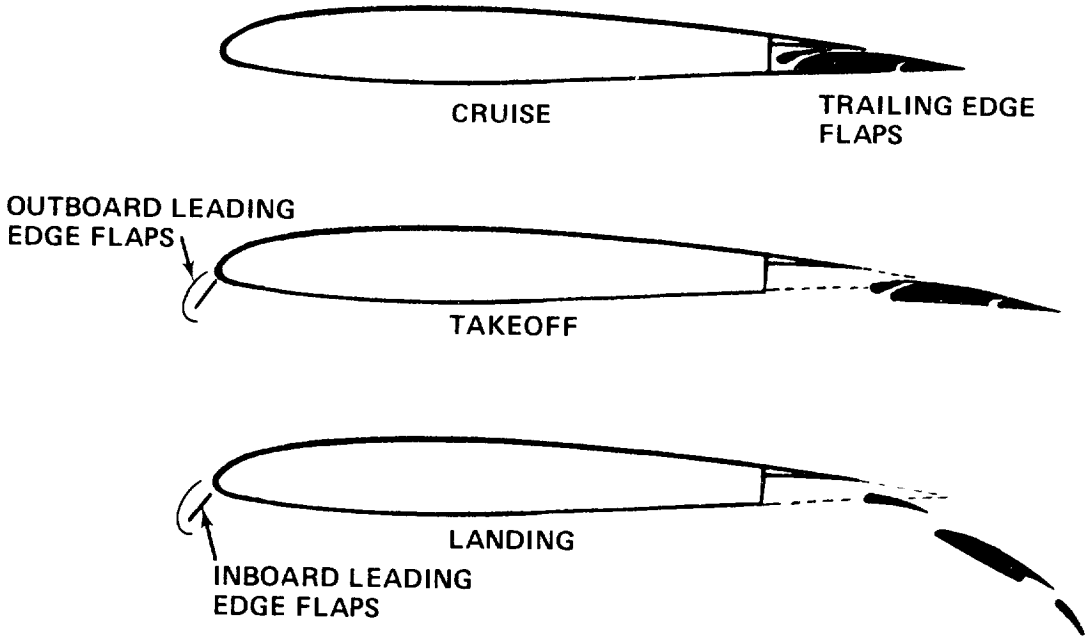

FLAP CONFIGURATION

FIGURE 7

NASA High Lift Model and Approximations

The 747 flap control lever has seven detents, 0, 1, 5, 10, 20, 25 and 30 for flap position commands. The FSAA flap control lever had five detents. Because position 1 and 5 are leading edge check positions, the five available detents were used to command flap positions 0, 10, 20, 25 and 30. FSAA flap control lever positions between 0 and 10 gave a continuous flap position between 0 and 10. For FSAA flap control lever position greater than 10, flap positions were discretely commanded for the nearest detent position.

A block diagram of the simulated flap control system is shown in Figure 8. The FSAA flap control lever commanded flap screw travel as a function of commanded flap position. The simulated flap screw was driven at a constant rate during flap extension and retraction.

All flaps down aerodynamic data presented in Volume II of this report include effects of leading edge flaps.

Aerodynamic data to simulate asymmetric flap conditions are presented in Volume II of this report. However, these data were not required for the simulation.

The flap auto-retraction system was not included in the simulation.

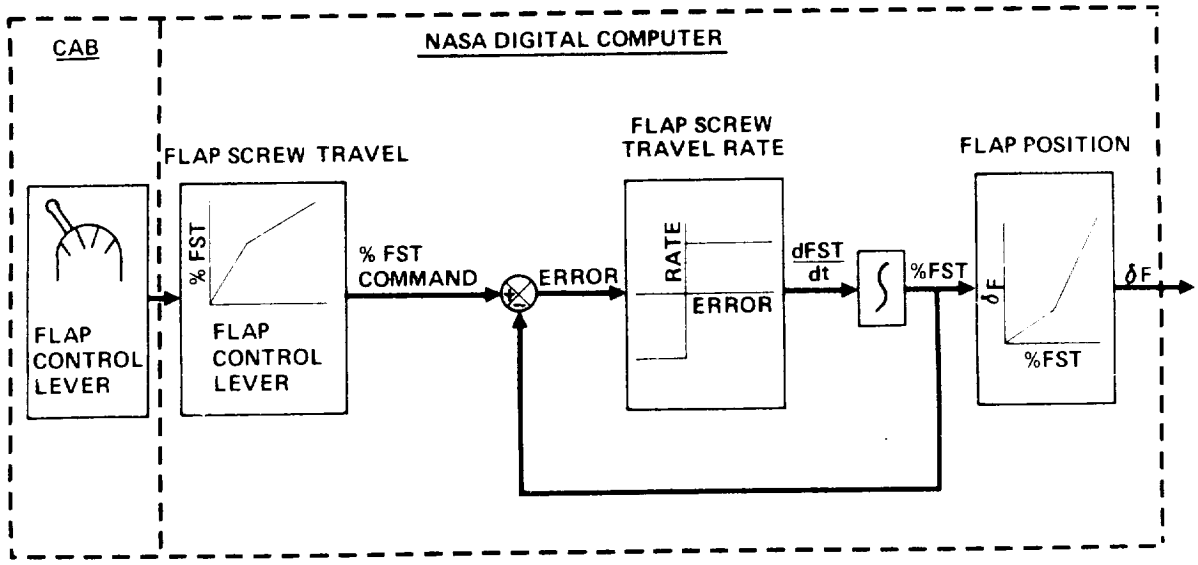

HIGH LIFT MODEL

FIGURE 8

LOW SPEED BUFFET MODEL

The NASA buffet program was tailored to match the 747 buffet characteristics. Cab buffet intensity was a function of angle of attack, flap position, and spoiler deflection. The intensity associated with angle of attack and spoiler deflection was varied until the pilot felt the buffet was representative of the 747.

Airplane buffet data is presented in Volume II of this report.

General Description

The 747 aircraft is powered by four Pratt and Whitney JT9D-3 engines having a takeoff thrust rating of 43,500 pounds on a standard sea level day. The JT9D-3 engine is an axial flow, twin spool, high compression, high bypass ratio, turbofan engine. The engines are pod mounted at approximately 40 and 71 percent of the wing semi-span.

Two thrust reversers are provided on each engine, one to reverse the bypass fan exhaust and one to reverse the turbine exhaust. A general description of the engine in normal and reverse thrust modes is shown in Figure 9.

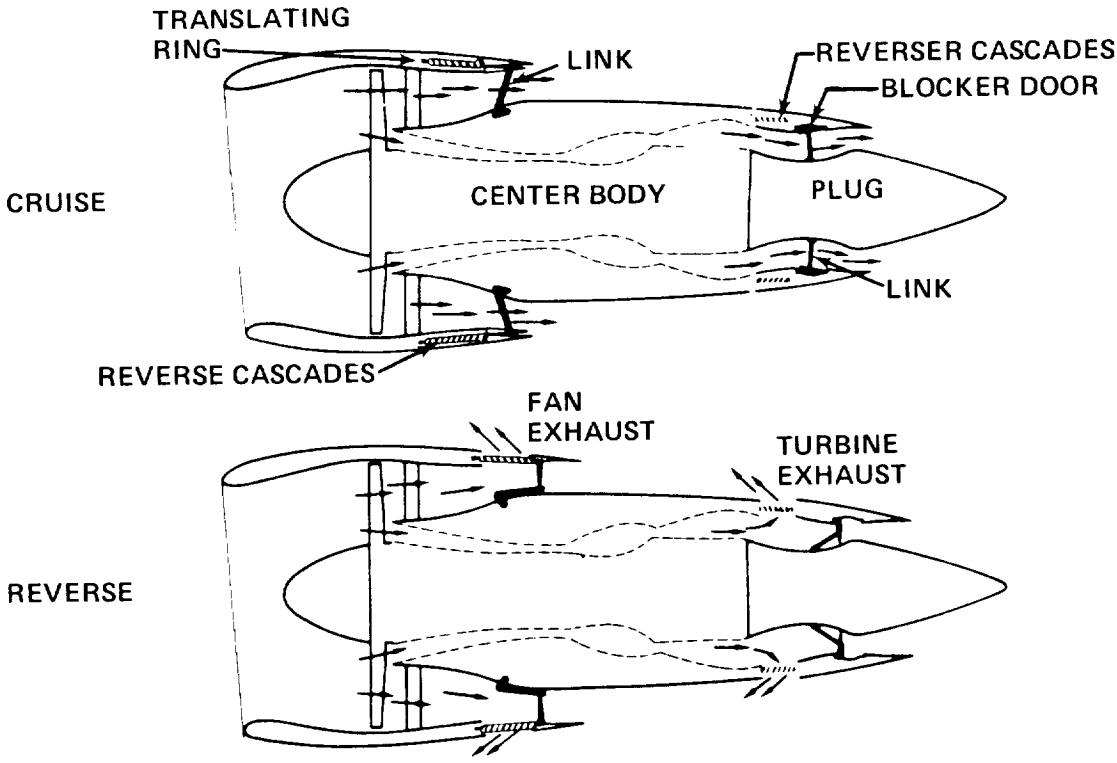

FIGURE 9

Both thrust reversers have a translating ring which is located in the outer wall of the nozzle annulus. The plug or centerbody forms the inner wall of the nozzle. During thrust reversal, the translating ring moves to the rear to block the rearward flow of the exhaust and to open the reverser cascades for flow redirection. Tailpipe blockage is accomplished by blocking doors hinged to the translating ring. Engine thrust is controlled from the engine throttle console. The reverse thrust lever is hinged to the forward thrust lever as shown in the schematic of Figure 10. On the 747 airplane, a lockout provision in the thrust lever assembly prevents simultaneous activation of the forward and reverse thrust levers. To obtain reverse thrust, the forward thrust lever must be in the idle position. The

reverse thrust lever is then moved upward to the reverse idle position. A linear time delay is required for the thrust to change from forward idle to reverse idle with no change taking place in the engine parameters (EPR, EGT, etc.).

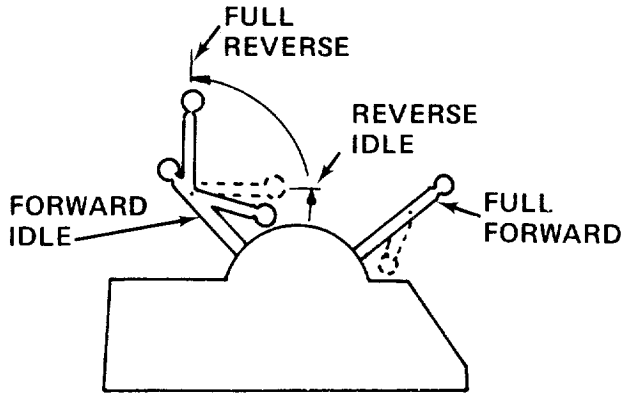

ENGINE THROTTLE CONSOLE

FIGURE 10

NASA Propulsion Model and Approximations

Engine pressure ratio was computed from the engine throttle angle as shown by the block diagram in Figure 11. The engine throttle angle was converted to engine power lever angle (fuel control angle at the engine). The hysteresis computation between the throttle angle and the power lever angle was neglected for the NASA simulation. The hysteresis in the physical mechanism of the NASA throttle mechanism was assumed to equal the hysteresis between the pilot's throttle and the fuel control on the actual airplane. The static EPR was computed as a function of ambient temperature (T_{AM}) for a known power lever angle. The static EPR was input to the NASA engine transient program. An incremental EPR (ΔEPR) was added to the output of the transient program to account for effects of altitude and Mach number. The 747 flight idle limiter was incorporated into the NASA simulation by increasing the actual EPR by a constant when the flaps were in the 25 or greater position and the landing gear was down but not on the ground.

JT9D-3 engine parameter time histories of fast and normal accelerations and decelerations for various airspeeds and altitudes were given to NASA. NASA's engine transient program was modified to approximate these characteristics. The time histories are included in Section 12, Volume II of this report.

The engine thrust simulation is shown in Figure 12. Forward net thrust was computed from EPR, Mach number and ambient pressure ratio. Reverse net thrust was assummed to be only a function of ambient pressure ratio and EPR since thrust reversers are only used from touchdown speed to 100 knots. The thrust mode (forward thrust or reverse thrust) depended upon the positioning of the throttle controls in the cab.

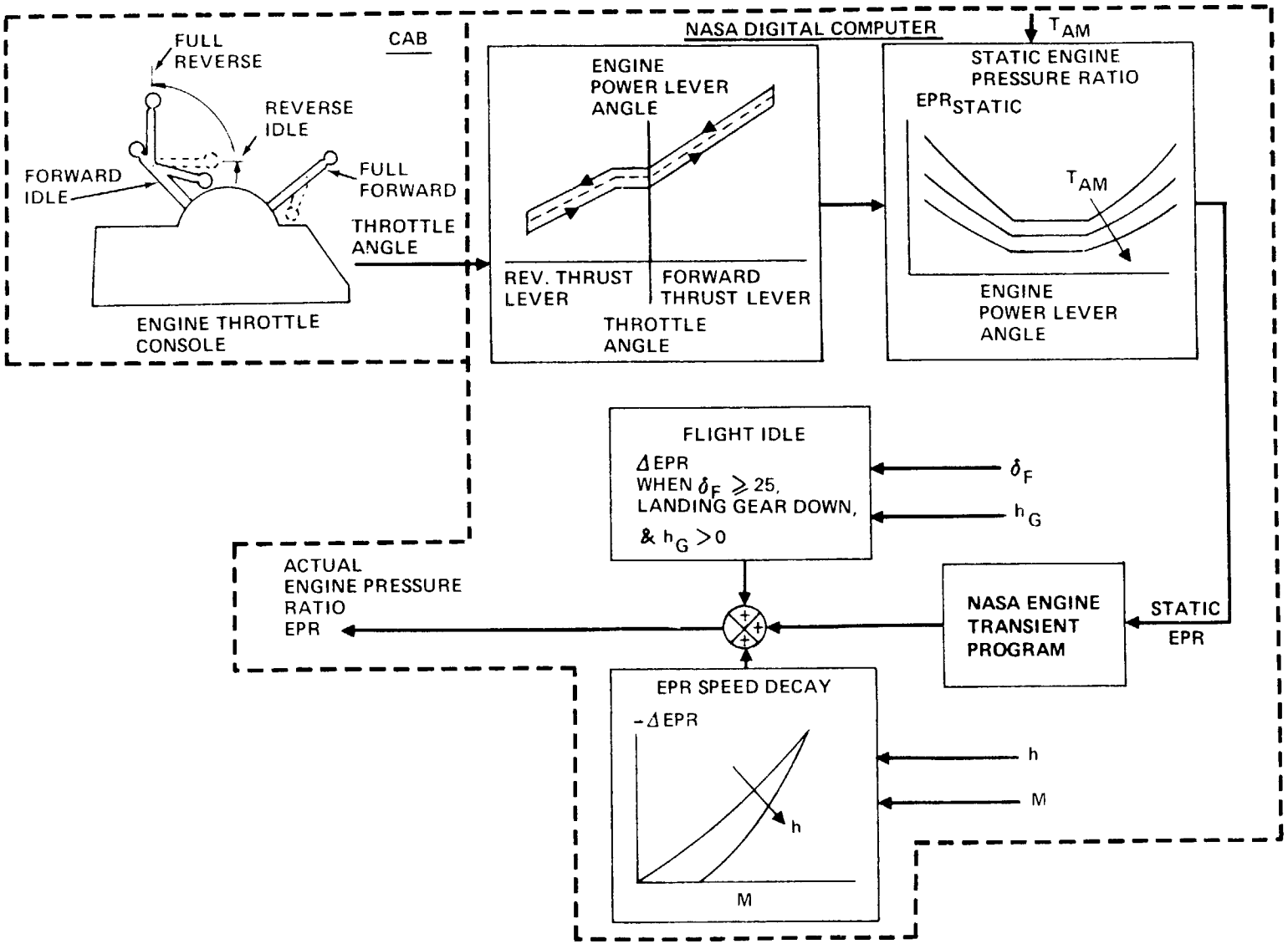

ENGINE PRESSURE RATIO SIMULATION

FIGURE 11

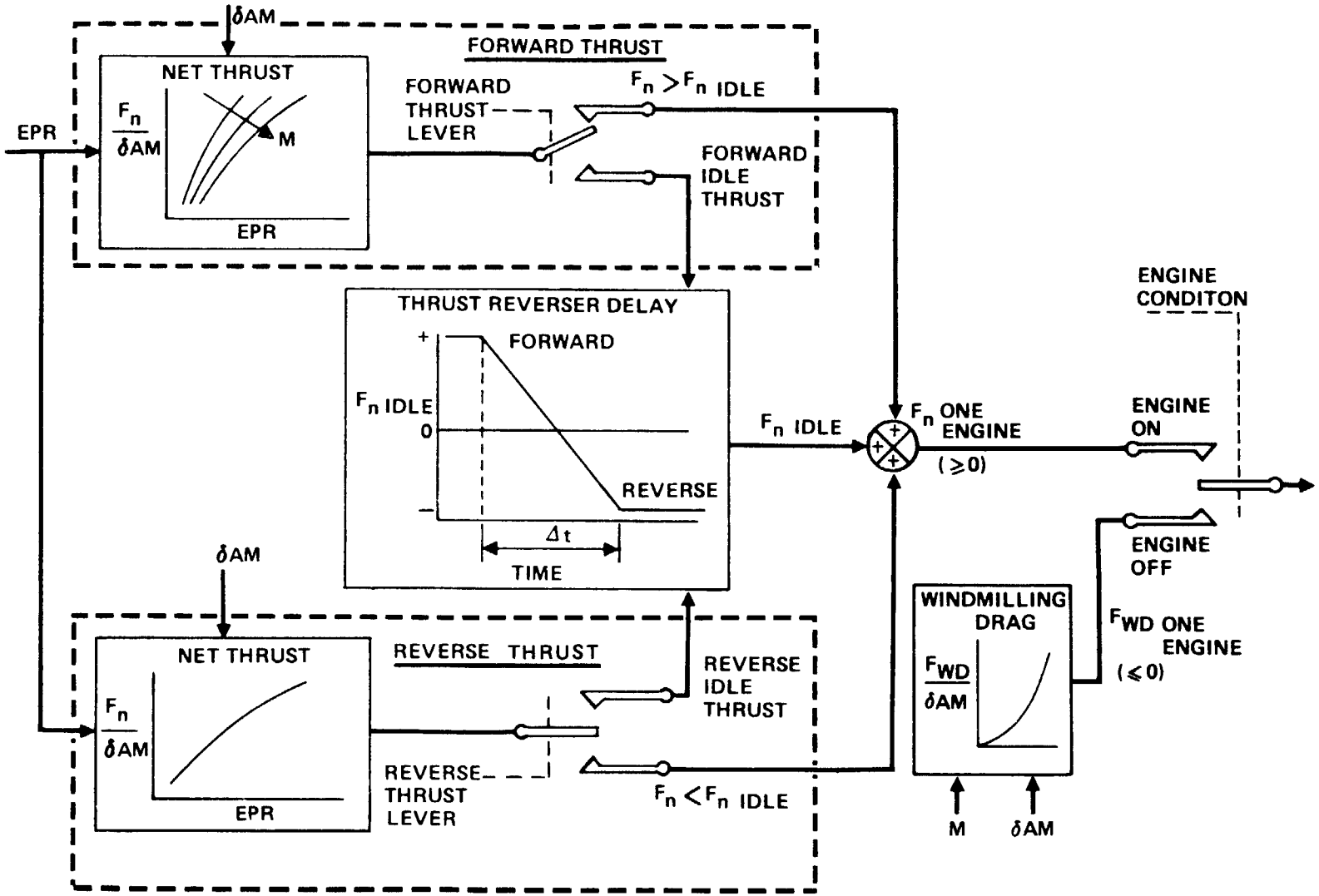

ENGINE THRUST SIMULATION

FIGURE 12

A linear transition with time was used to account for actuation of the thrust reverser mechanism when changing from forward idle thrust to reverse idle thrust.

The engine parameters displayed in the cab were EPR, exhaust gas temperature (EGT) and percent compressor RPM ($\%N_1$). A detailed method for generation of EGT and $\%N_1$ is shown in Figure 13. The temperature correction as a function of altitude was small and the compressor RPM was roughly proportional to the EGT data. Since the EGT and RPM gages were not essential to the simulation, approximations were made for the NASA simulation as shown in Figure 14.

The detailed 747 engine parameter data and the correlation of NASA thrust simulation data with actual engine data are included in Volume II of this report, Sections 12 and 14 respectively.

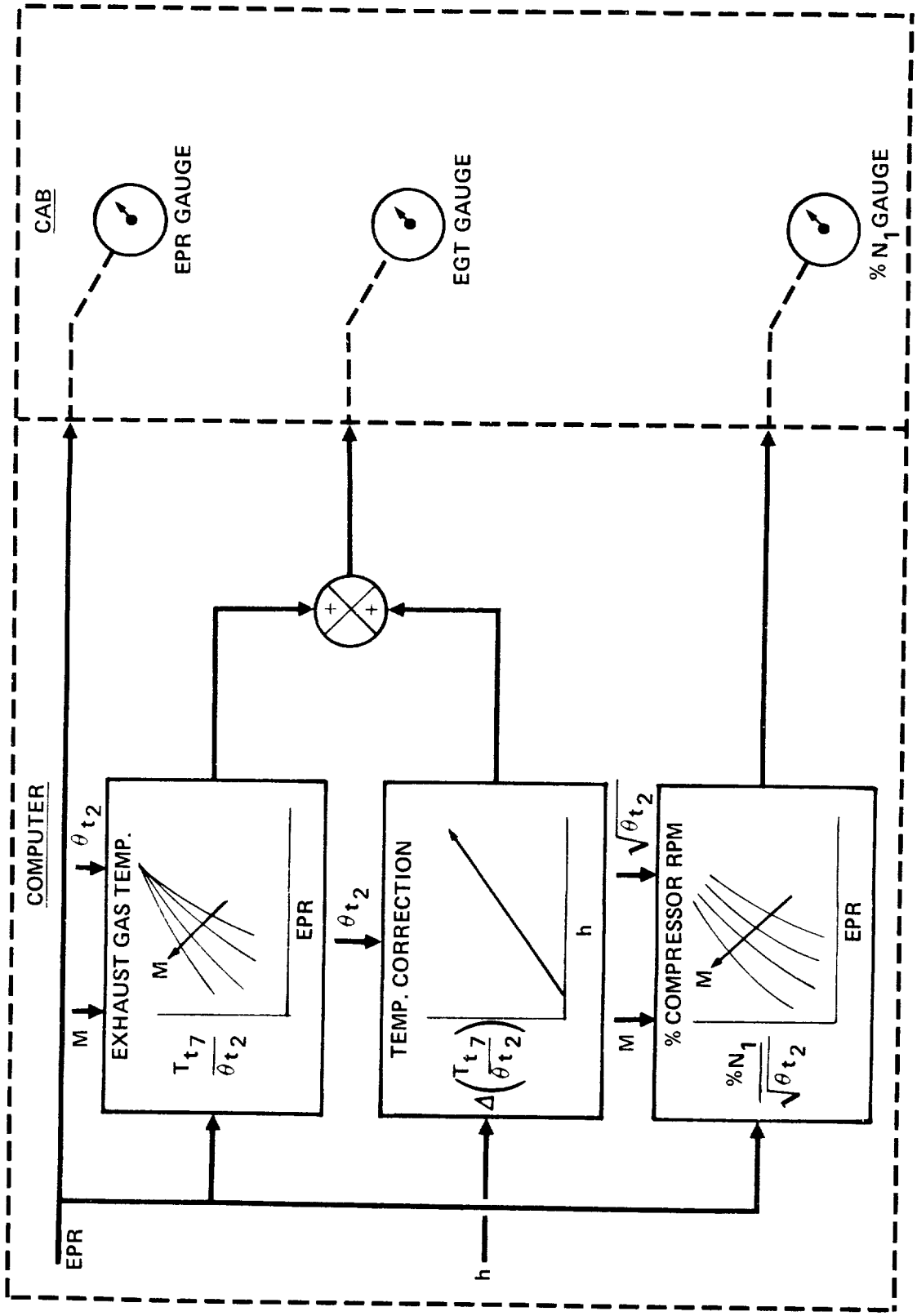

PARAMETERS FOR 747 ENGINE GAUGE DISPLAY
FIGURE 13

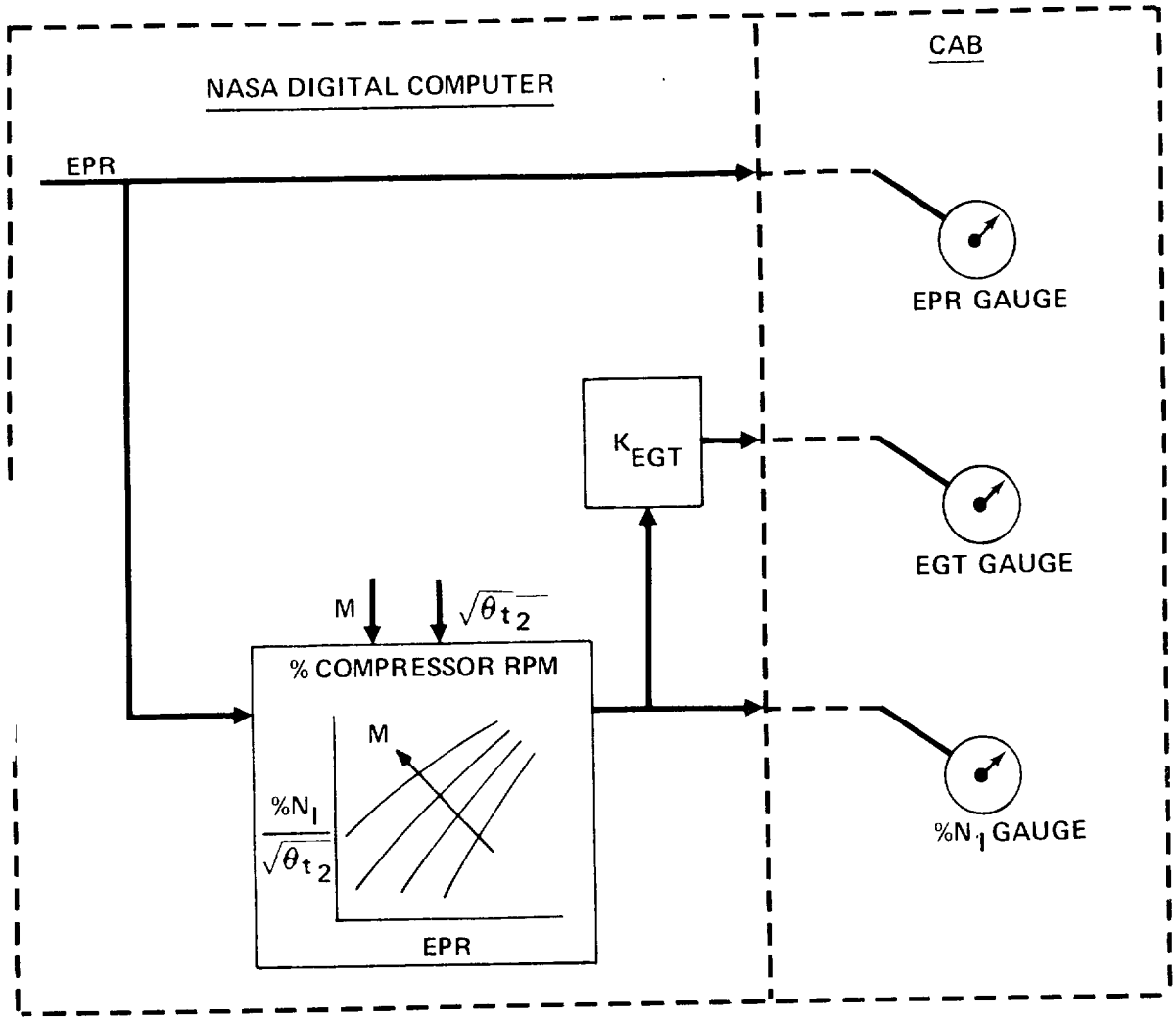

APPROXIMATIONS FOR NASA ENGINE GAUGE DISPLAY

FIGURE 14

LANDING GEAR SYSTEM

General Description

The 747 employs a four strut main landing gear system with a single strut nose gear, as illustrated in Figure 15.

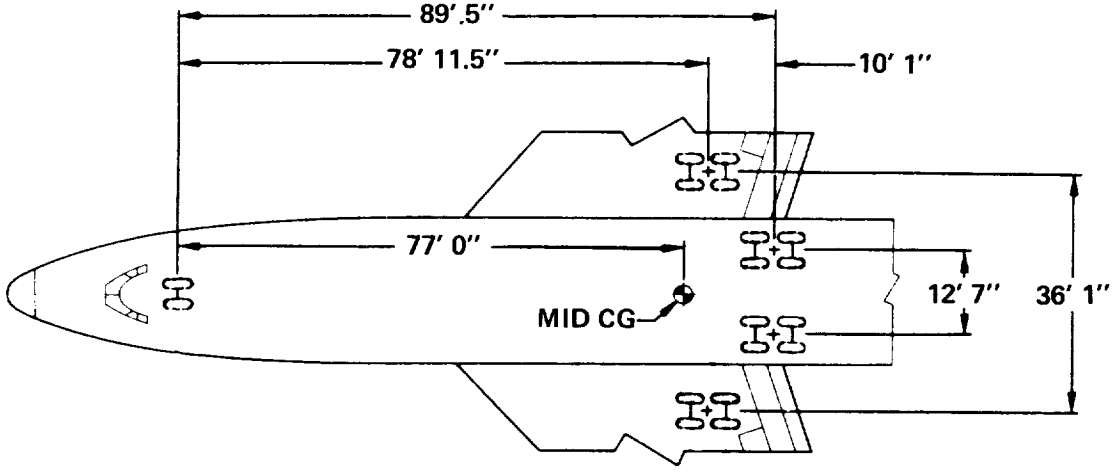

LANDING GEAR GEOMETRY

FIGURE 15

Two of the main gear struts are wing mounted and two are body mounted. Each main gear strut has a four-wheeled truck. The nose gear strut has two wheels. Because of the geometry of the wheel wells, the wing gear trucks are tilted upward 53 degrees after liftoff for retraction. The body gear trucks are tilted upward 7 degrees for retraction. Since the main landing gears are not aligned longitudinally, a load equalizer is employed to give an effective pitch rotation point midway between the wing and body gear struts.

Nose gear steering is controlled by a tiller and the rudder pedal controls. Full tiller deflection turns the nose gear 70 degrees. Full rudder-pedal travel turns the nose gear 10 degrees.

The rudder pedals command the braking system. A force of approximately 80 pounds is required to obtain maximum braking. Each wheel on the main gear struts is equipped with an anti-skid braking system.

NASA Landing Gear Model and Approximations

The following ground rules were used for the NASA simulation of the 747 landing gear system:

(1) The main body and wing gear struts were combined into an equivalent landing gear.

(2) Braking capability was provided on the equivalent main gear.

(3) Nose wheel steering as a function of rudder pedal travel was incorporated. Nose wheel

steering with a tiller was incorporated but not calibrated to the airplane.

(4) All forces generated by the landing gear contacting the runway were resolved into body axes forces and moments for computation of the airframe response.

(5) Small angle approximations were used for computing landing gear compression, compression rate, and body axes force and moment resolution.

(6) The NASA landing gear simulation was used wherever possible.

The equivalent landing gear model is shown in Figure 16.

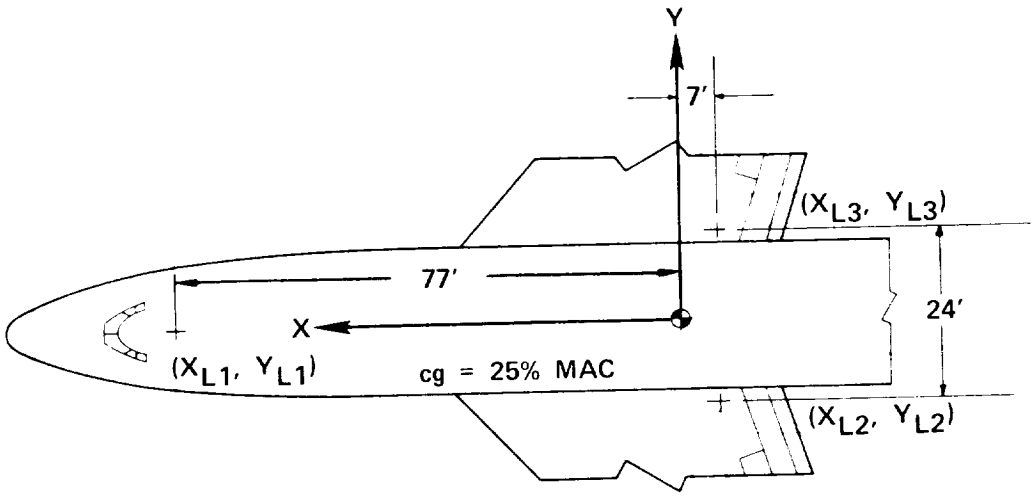

EQUIVALENT LANDING GEAR

FIGURE 16

The subscripts 1 through 3 denote the nose gear, main left gear, and main right gear respectively. The subscript "i" in the landing gear equations denotes application of the equation to simulate any one of the three landing gears.

Figures 17 through 20 show progressively in block diagram form the method used for computing landing gear forces and moments in the NASA simulation.

The distance from the c.g. to the landing gear struts was computed as a function of c.g. location as shown in Figure 17. Oleo strut compression (ΔS_{T_i}) was computed by knowing the height of the c.g. (h), the body pitch angle (θ_B), the body bank angle (ϕ_B), and the coordinates of the landing

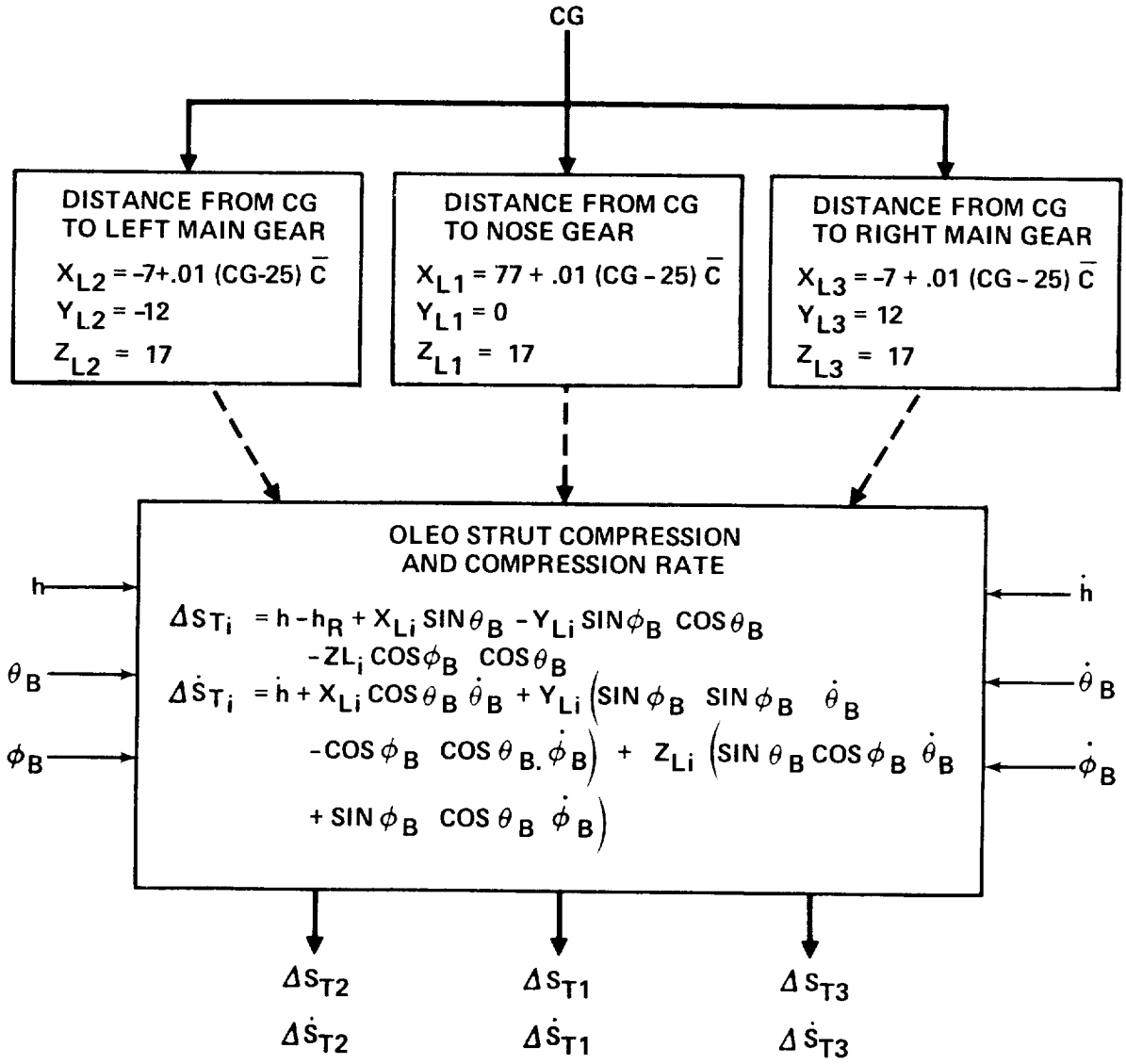

NOTE; LANDING GEAR DOES NOT CONTACT THE RUNWAY UNLESS $\Delta S_{Ti} < 0$

DETERMINATION OF OLEO STRUT COMPRESSION AND COMPRESSION RATE

FIGURE 17

gear struts. The oleo strut compression equation assumes small angle displacements. The equation for determining oleo strut compression (ΔS_{T_i}) is derived in its complete form in the Appendix. The rate of compression of the oleo strut ($\dot{\Delta S}_{T_i}$) was computed from the first derivative of the oleo strut compression equation.

The vertical oleo strut force (FG_Z) resulting from the oleo strut deflection and deflection rate were computed from the non-linear spring force and damping constant data as illustrated in the block diagram of Figure 18. Data for the spring force and damping constant parameter for the equivalent main landing gear and the nose gear are included in Section 13, Volume II, of this report.

The normal force of the tire on the runway generated by the oleo strut force F_{G_Z} is

$$F_{N_G} = \frac{F_{G_Z}}{\cos \theta_B \cos \phi_B} \quad .$$

With small angle approximations, runway normal force and oleo strut force were assumed equal. The axes system for the forces generated by the tires on the runway and the relation of these forces to aircraft body axes are shown and derived in the Appendix of this report.

Figure 19 is a block diagram illustrating the method of computing wheel side force. Tire deflection (δ_T) was computed from the runway normal force multiplied by the tire deflection constant (K_T). Wheel side force (F_s) was computed from:

$$F_{si} = \left| G_{T_i} \delta_{T_i} - H_{T_i} \delta_{T_i}^2 \right| (\delta s - \beta_G) \text{ Where}$$

β_G = airplane side slip angle relative to ground velocity vector

δ_S = nose wheel steering angle (i = 1 only).

The nose wheel steering angle was calculated from rudder pedal deflection (δ_p) when the aircraft was on the runway. The constants G_{T_i} and H_{T_i} and the nose wheel steering gearing constant $\frac{\partial \delta s}{\partial \delta p}$ are included in Section 13, Volume II of this report.

Limiting side force on the wheels was computed from the wheel normal force and a coefficient of sliding friction of 0.6.

Wheel drag force was determined from the rolling coefficient of friction and brake application as shown in the block diagram of Figure 20. Braking was available on the main gear only. The rolling coefficient of friction of 0.015 was assumed in addition to a breakout coefficient of friction varying from .014 at zero ground speed to 0 at 10 knots ground speed. The resultant coefficient of friction was combined with the wheel normal force F_N to obtain the gear drag with no braking. Braking was obtained by multiplying brake pedal deflection (δ_B) by a braking constant K_B and the aircraft mass (W/g). The braking force was limited to:

$$(F_{B_i})_{max} = \mu_B K_{BM} \frac{W}{g}$$

where the value of μ_B depended on the condition of the runway. Braking constants and gearing are included in Section 13, Volume II of this report. Brake and rolling friction are added to obtain the total retarding force on the tire.

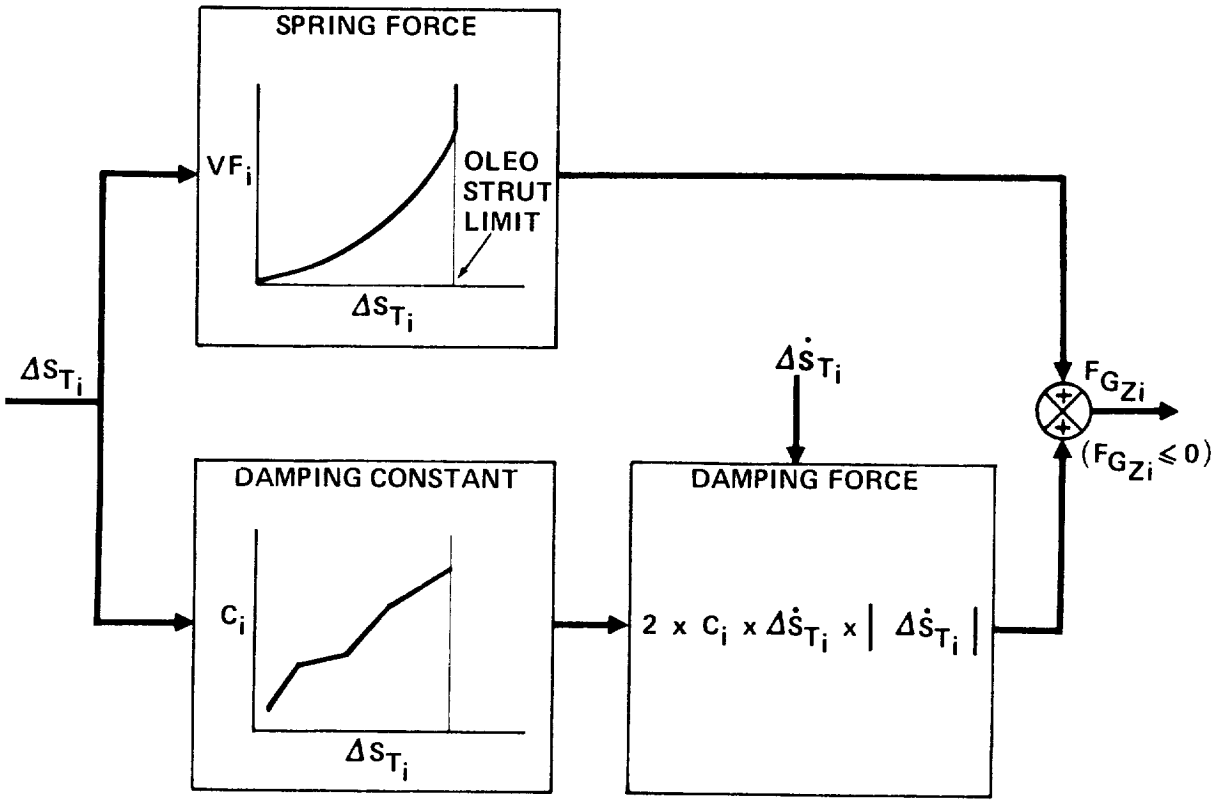

DETERMINATION OF OLEO STRUT FORCES

FIGURE 18

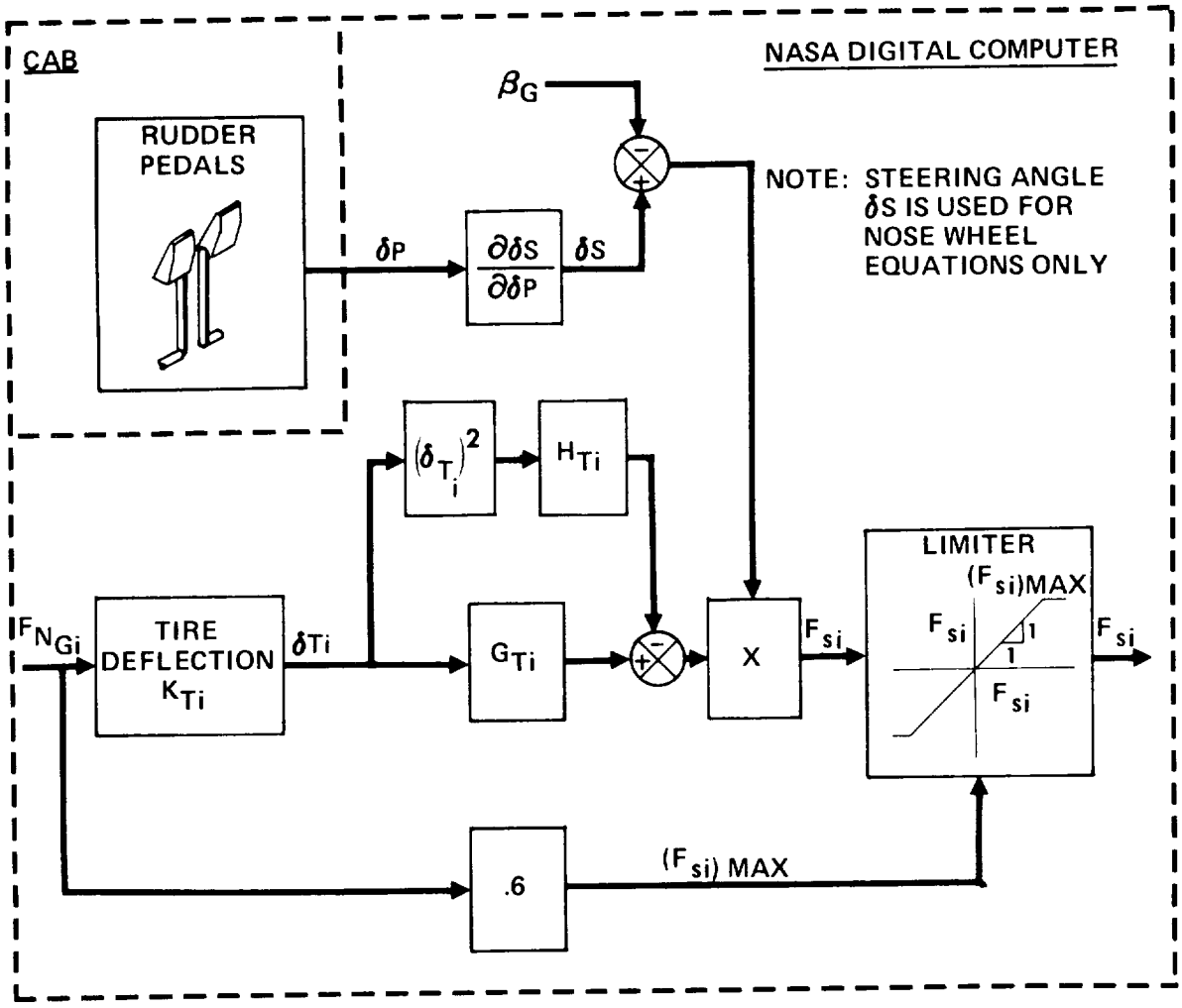

DETERMINATION OF WHEEL SIDE FORCE

FIGURE 19

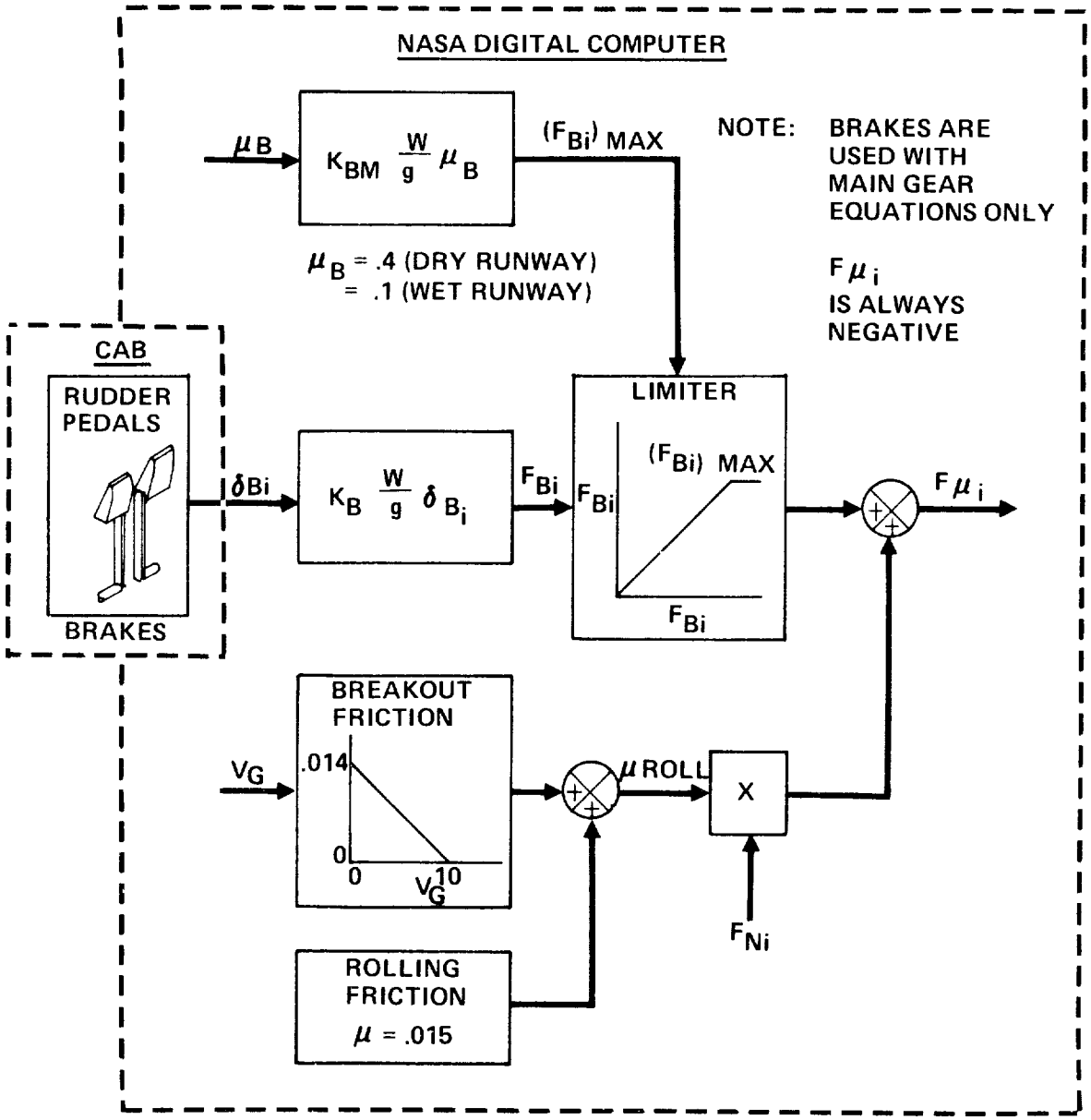

DETERMINATION OF WHEEL DRAG FORCE

FIGURE 20

Tire normal force, side force, and drag force were computed for each individual oleo strut and resolved into body axes by:

$$F_{RX_{Pi}} = F_{\mu i} - F_{G_{Zi}} \theta_B \quad \text{(FOR MAIN GEAR, i = 2,3)}$$

$$F_{RX_{Pi}} = F_{\mu i} - F_{G_{Zi}} \theta_B - F_{si} \delta_S \quad \text{(FOR NOSE GEAR, i = 1)}$$

$$F_{RY_{Pi}} = F_{si} + F_{G_{Zi}} \phi_B$$

$$F_{RZ_{Pi}} = F_{\mu i} \theta_B - F_{si} \phi_B + F_{G_{Zi}} .$$

The forces exerted on the aircraft through the oleo struts are obtained by summing the partial body axes forces.

$$F_{RX} = \sum_{i=1}^{3} F_{RX_{Pi}}$$

$$F_{RY} = \sum_{i=1}^{3} F_{RY_{Pi}}$$

$$F_{RZ} = \sum_{i=1}^{3} F_{RZ_{Pi}}$$

The vertical distance from the c.g. to the normal force, side force, and drag force vectors created by the tires in contact with the runway is

$$h_{Bc.g.i} = 17 + \Delta S_{T_i} .$$

Body axes moments were computed from the partial body axes forces and the distance from the c.g. to the runway.

$$M_{RX} = \sum_{i=1}^{3} (F_{RZ_{Pi}} Y_{Li} - F_{RY_{Pi}} h_{Bc.g.i})$$

$$M_{RY} = \sum_{i=1}^{3} (-F_{RZ_{Pi}} X_{Li} + F_{RX_{Pi}} h_{Bc.g.i})$$

$$M_{RZ} = \sum_{i=1}^{3} (F_{RY_{Pi}} X_{Li} - F_{RX_{Pi}} Y_{Li})$$

ATMOSPHERE MODEL

The ICAO standard atmosphere model was used to simulate the atmosphere's physical properties throughout the flight envelope of the 747. Table 2 shows the equation used to compute atmospheric temperature ratio (θ) and pressure ratio (δAM).

ICAO Standard Atmosphere

ALTITUDE <36,089 FT	ALTITUDE >36,089 FT
$\theta = \frac{T}{T_o} = 1\text{-}6.875 \times 10^{-6} h$	$\theta = \frac{T}{T_o} = .7518$
$\delta AM = \frac{P}{P_o} = \theta^{5.256}$	$\delta AM = \frac{P}{P_o} = .2234e^{-4.806 \times 10^{-5}(h - 36{,}089)}$

TABLE 2

The sea level standard pressure, temperature, and speed of sound are

$$P_o = 2116.2 \text{ LB/FT}^2$$

$$T_o = 518.7^o \text{ R}$$

$$a_o = 1116.4 \text{ FT/SEC}.$$

AIRSPEED EQUATIONS

The speed of sound (ft/sec) was determined from $a = 1116.4\sqrt{\theta}$. Mach number was computed from the true airspeed obtained from the airframe equations of motion,

$$M = \frac{V}{a}.$$

The compressible dynamic pressure was computed by

$$q_c = 2116.2 \quad \delta AM \left[(1 + .2M^2)^{3.5} - 1\right] \quad \text{LB/FT}^2$$

from which calibrated airspeed was computed,

$$V_c = \left\{2{,}187{,}745\left[\left(\frac{q_c}{2116.2} + 1\right)^{2/7} - 1\right]\right\}^{1/2} \quad \text{KNOTS}.$$

SIMULATION CHECKOUT

The mathematical models and data of the 747 aircraft were qualitatively and quantitatively checked to substantiate the accuracy and validity of the NASA FSAA simulation. The checkout included verification of the aerodynamic forces and moments, the solution of the equations of motion, and the simulation of flight control system characteristics. Checkout consisted of non-pilot and piloted static and dynamic flight conditions as well as an overall piloted assessment of the simulation. The quantitative results were compared to Boeing simulator and flight test data.

Quantitative non-piloted simulation checkout included the following:

1. Cockpit instruments
2. Atmosphere model
3. Engine characteristics
    a. Forward thrust
    b. Reverse thrust
    c. Transient response
4. Longitudinal trim
5. Configuration changes (trim)
    a. Flaps
    b. Landing gear
    c. Speed brakes
    d. Ground effect
6. Elevator stabilizer trades
7. Dynamics
    a. Short period
    b. Phugoid
    c. Dutch roll
8. Flight controls
    a. Force and displacement

b. Rigging

c. Blowdown

The piloted evaluation of the simulation was conducted by a Boeing and a NASA pilot. The Boeing pilot flew the motion simulator for a total of 5 hours in 3 sessions. The NASA pilot assisted in obtaining the quantitative data as well as becoming familiar with the 747 characteristics.

Piloted simulation checkout included:

A. General qualitative assessment of the following:

1. Airplane handling characteristics

a. Dutch roll mode

b. Spiral mode

c. Short period mode

d. Phugoid mode

e. Roll rate

f. Climb performance

g. Flap extension and retraction

h. Speed brakes

2. Engine response

3. Ground effect

4. Control forces

5. Takeoff (3 and 4 engine)

6. Landing

7. Stall

8. Air minimum control speed

9. Buffet

10. Stick shaker

B. Quantitative evaluation of the following:

1. Takeoff time
2. Climb performance
3. Acceleration and deceleration times in the air
4. Steady turns (elevator and stick force per g)
5. Longitudinal static stability
6. Steady sideslips
7. Roll rates
8. Air minimum control speed

The quantitative results are documented in Section 14, Volume II of this report. In addition to the test data, the pilot comments substantiated the accuracy of the simulation.

THE SIMULATION OF A JUMBO JET TRANSPORT AIRCRAFT VOLUME II: MODELING DATA

D6-30643

Prepared by

C. Rodney Hanke and Donald R. Nordwall

THE BOEING COMPANY
Wichita Division Wichita, Kansas

September 1970

for

NATIONAL AERONAUTICS AND SPACE ADMINISTRATION

Ames Research Center Moffett Field, California

PREFACE

This report summarizes all work conducted by The Boeing Company under Task II of Contract NAS2-5524, "Design for the Simulation of Advanced Aircraft". The National Aeronautics and Space Administration Technical Monitor was John Dusterberry of the Simulation Sciences Division. The Boeing Company Project Leader was Mr. C. Rodney Hanke of the Wichita Division Stability, Control and Flying Qualities Organization. Technical assistance was provided by Mr. Robert A Curnutt of the 747 Aerodynamics Staff in Everett, Washington.

TABLE OF CONTENTS

FIGURE INDEX

AD 1546 D

AD 1546 D

4.0 PITCHING MOMENT COEFFICIENT

AD 1546 D

4.0 PITCHING MOMENT COEFFICIENT (Cont'd)

5.0 ROLLING MOMENT COEFFICIENT

AD 1546 D

5.0 ROLLING MOMENT COEFFICIENT (Cont'd) PAGE

AD 1546 D

7.0 SIDE FORCE COEFFICIENT

REFERENCES:

1. Boeing Document D6-20423 "Aerodynamic Data for the 747 Flight Simulator", Revision D, March 11, 1970.

2. Boeing Document D6-30833-1 "Flight Performance Tests for Validation of the 747 Flight Simulator", June 3, 1970.

3. Boeing Document D6-13302 "JT9D-3 Turbofan Engine Operating Parameters and Performance Data for 747 Airplane Flight Simulator Design", Revision F, September 9, 1969.

4. Boeing Document D6-13703 "Boeing 747 Flight Manual", December 30, 1969.

5. Boeing Document D6-30643 "The Simulation of a Large Jet Transport Aircraft Vol. 1: Mathematical Model", 30 September 1970.

6. Boeing Document D6-13645, "747 IEFCS System Description", April 9, 1968.

1.0 INTRODUCTION

The Boeing Company provided NASA-Ames Research Center with mathematical models and data to simulate the flying qualities and characteristics of the Boeing 747 on the NASA Flight Simulator For Advanced Aircraft (FSAA).

The contractual report is divided into two volumes. Volume I includes a description of:

1. The work performed under the contract.
2. Generalized equations and approximations used in the simulation.
3. The form of the data furnished to NASA.
4. Nomenclature used for the report.

Volume II contains only limited rights data. These data are to be retained within the Government until the Boeing Company chooses to treat the data as non-proprietary or until September 15, 1971, whichever occurs first.

This document has been prepared as a summary of the 747 aerodynamic data for use in flight simulator design. This introductory section contains a description of the 747 including its flight envelope, a general description of the control systems, and a short discussion of the simulation. The following six sections of the document present the airplane aerodynamic characteristics: lift, drag, pitching moment, rolling moment, yawing moment, and side force coefficients. The next three sections describe the control characteristics for pitch, roll and yaw in the various operating modes.

Sections 11, 12 and 13 describe the characteristics of the high lift system, propulsion system and landing gear. The final section contains the results of the simulation checkout.

The appendices contain a portion of the 747 Flight Manual, buffet characteristics, autothrottle, autopilot and revised simulation data.

1.1 AIRPLANE DESCRIPTION

The Boeing 747 is a very large four-fanjet intercontinental transport designed to operate from existing international airports. To obtain the necessary low speed characteristics the wing has triple-slotted trailing flaps and Krueger type leading edge flaps. The Krueger flaps outboard of the inboard nacelle are variable cambered and slotted while the inboard Krueger flaps are standard unslotted. The main landing gear consists of a pair of wing mounted four-wheel trucks and a pair of body mounted four-wheel trucks which are slightly aft of the wing. A load equalizing system between the trucks on each side with limited travel allows the center of pitch rotation to be midway between the two pairs of trucks. Longitudinal control is obtained through four elevator segments and a movable stabilizer. The lateral control employs five spoiler panels, an inboard aileron between the inboard and outboard flaps, and an outboard aileron which operates with flaps down only on each wing. The five spoiler panels on each wing also operate symmetrically as speedbrakes in conjunction with the most inboard sixth spoiler panel. Directional control is obtained from two rudder segments. A general arrangement drawing showing these controls and pertinent dimensions is on page 1.1-2. A summary of areas and dimensions necessary for simulation is on page 1.1-3. The airplane operating limits and placards are shown on page 1.1-4.

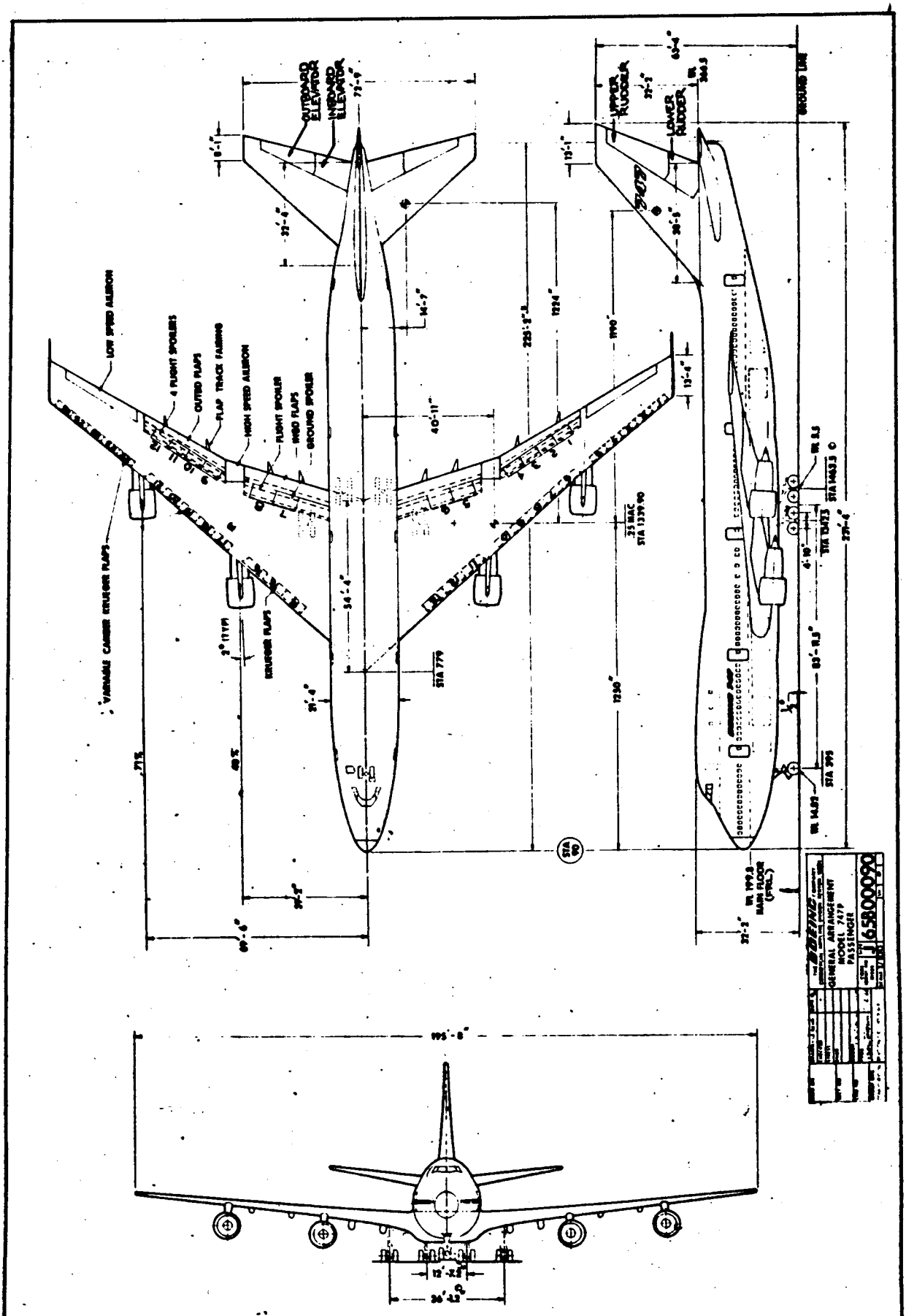
OUTBOARD ELEVATOR
INBOARD ELEVATOR
UPPER RUDDER
LOWER RUDDER
GROUND LINE
LOW SPEED AILERON
4 FLIGHT SPOILERS
OUTBD FLAPS
FLAP TRACK FAIRING
HIGH SPEED AILERON
FLIGHT SPOILER
INBD FLAPS
GROUND SPOILER
VARIABLE CAMBER KRUEGER FLAPS
KRUEGER FLAPS
STA 779
STA 995
STA 1239.90
MAIN FLOOR (APPRX.)
BOEING
GENERAL ARRANGEMENT
MODEL 747F
PASSENGER
65800090

SUMMARY OF AREAS AND DIMENSIONS

ITEM	VALUE	DIMENSION
Wing Area (S)	5500	$Ft.^2$
Wing Mean Aerodynamic Chord (MAC)	27.31	Ft.
Wing Span (b)	195.68	Ft.
Wheel Base		
Wing Gear	78.96	Ft.
Body Gear	88.96	Ft.
Wheel Tread		
Wing Gear	36.16	Ft.
Body Gear	12.5	Ft.
Effective Engine Moment Arms		
Inboard		
Y_{E_I}	39.6	Ft.
Z_{E_I}	14.6 (air)	Ft.
	9.2 (ground)	Ft.
Outboard		
Y_{E_O}	69.4	Ft.
Z_{E_O}	5.4 (air)	Ft.
	7.3 (ground)	Ft.

Note The transition between the ground and air values for the effective engine pitching arms, Z_{E_I} and Z_{E_O}, is a function of the averaged main landing gear compression ratio, η.

For $0 \leq \eta \leq 1$, $Z_{E_O} = Z_{E_{O_{AIR}}} + \eta \cdot \Delta Z_{E_O}$

$Z_{E_I} = Z_{E_{I_{AIR}}} + \eta \cdot \Delta Z_{E_I}$

where $\Delta Z_{E_O} = Z_{E_{O_{GROUND}}} - Z_{E_{O_{AIR}}} = 1.9$ FT.

$\Delta Z_{E_I} = Z_{E_{I_{GROUND}}} - Z_{E_{I_{AIR}}} = -5.4$ FT.

and $\eta = \frac{1}{36"} \sum_{n=1}^{2}$ Main Landing Gear Oleo Compression (inches).

SEE SECTION 19
FOR REVISED DATA

AD 1546 D

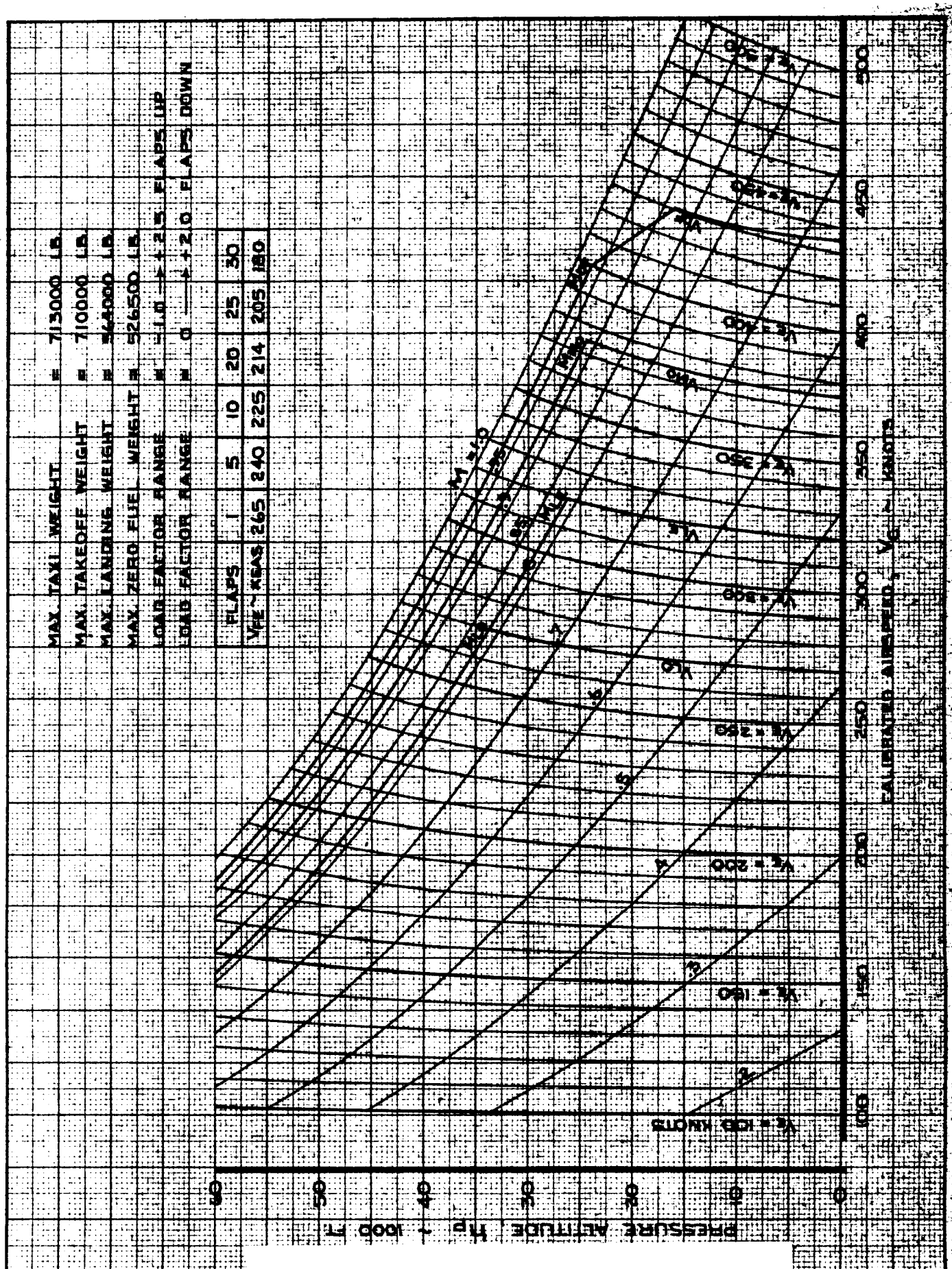

CALC	FOSTER	12-16-67			747
CHECK	HOLTZNER	12-19-67	LOW	1-12-70	LIMITS AND PLACARDS
APR			LOW	6-18-70	D6-30643 Vol. II
APR					
INK	ODEGARD	6-18-70			THE BOEING COMPANY PAGE 1.1-4

AD 461 C R4

REV. E

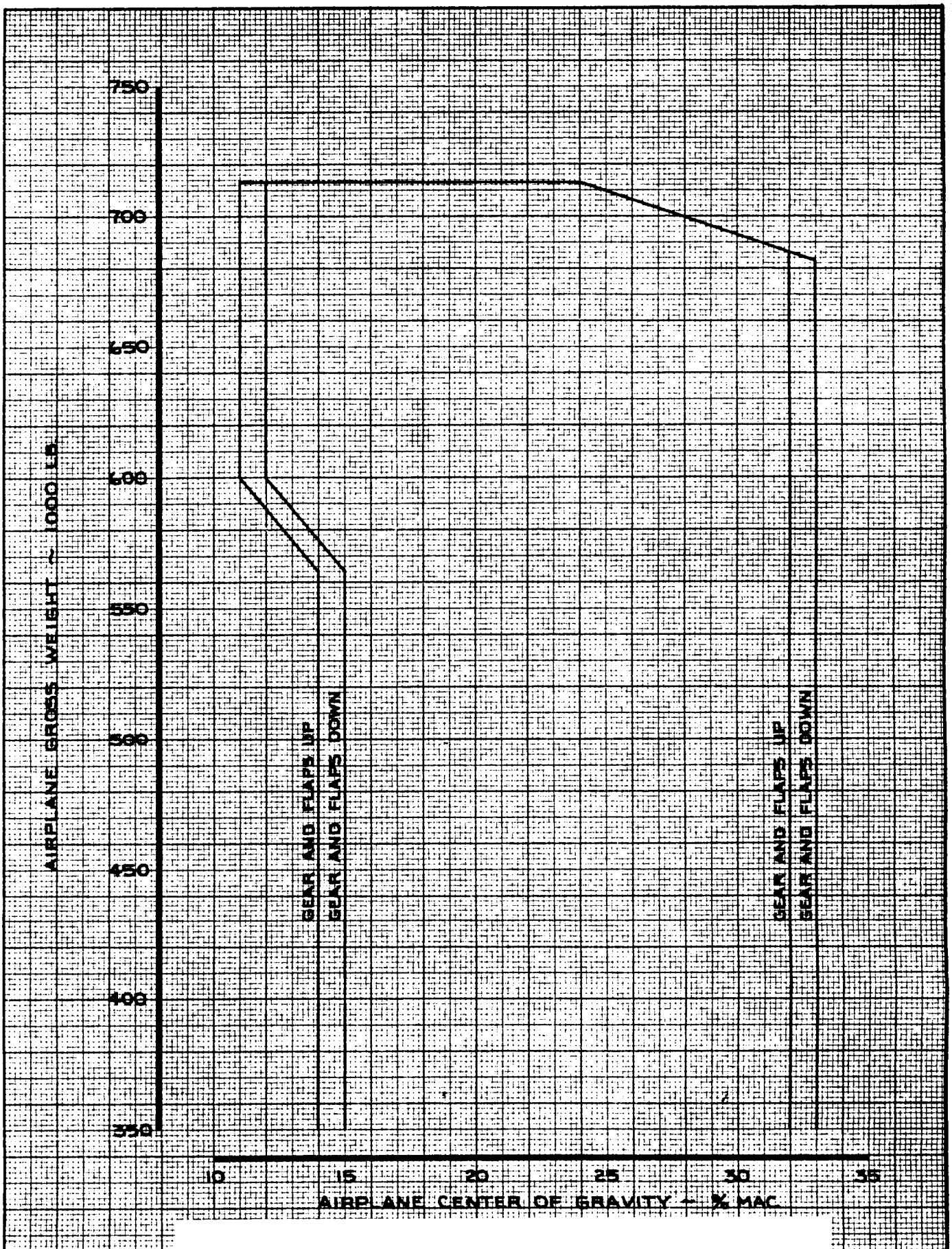

CALC	LOW	1-20-70	REVISED	DATE
CHECK				
APR				
APR				
INK	ODEGARD	1-20-70		

CENTER OF GRAVITY LIMITS

747

D6-30643 Vol. II

THE BOEING COMPANY

PAGE 1.1-5

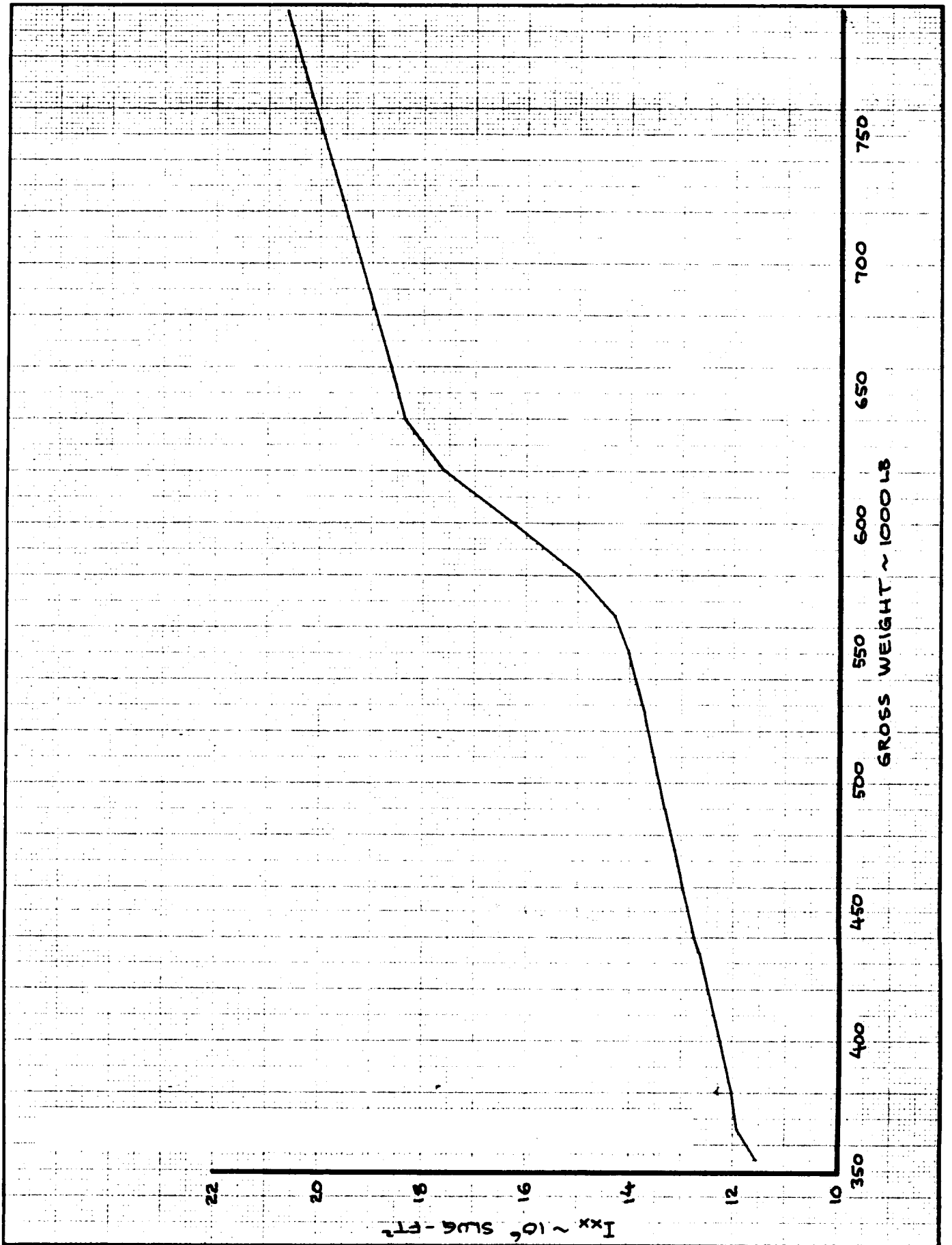

CALC			REVISED	DATE	I_{xx}, BODY AXIS MOMENT OF INERTIA
CHECK					
APR					
APR					
	DRN	JUNE 1970			THE BOEING COMPANY

747

D6-30643 VOL II

PAGE 1.1-6

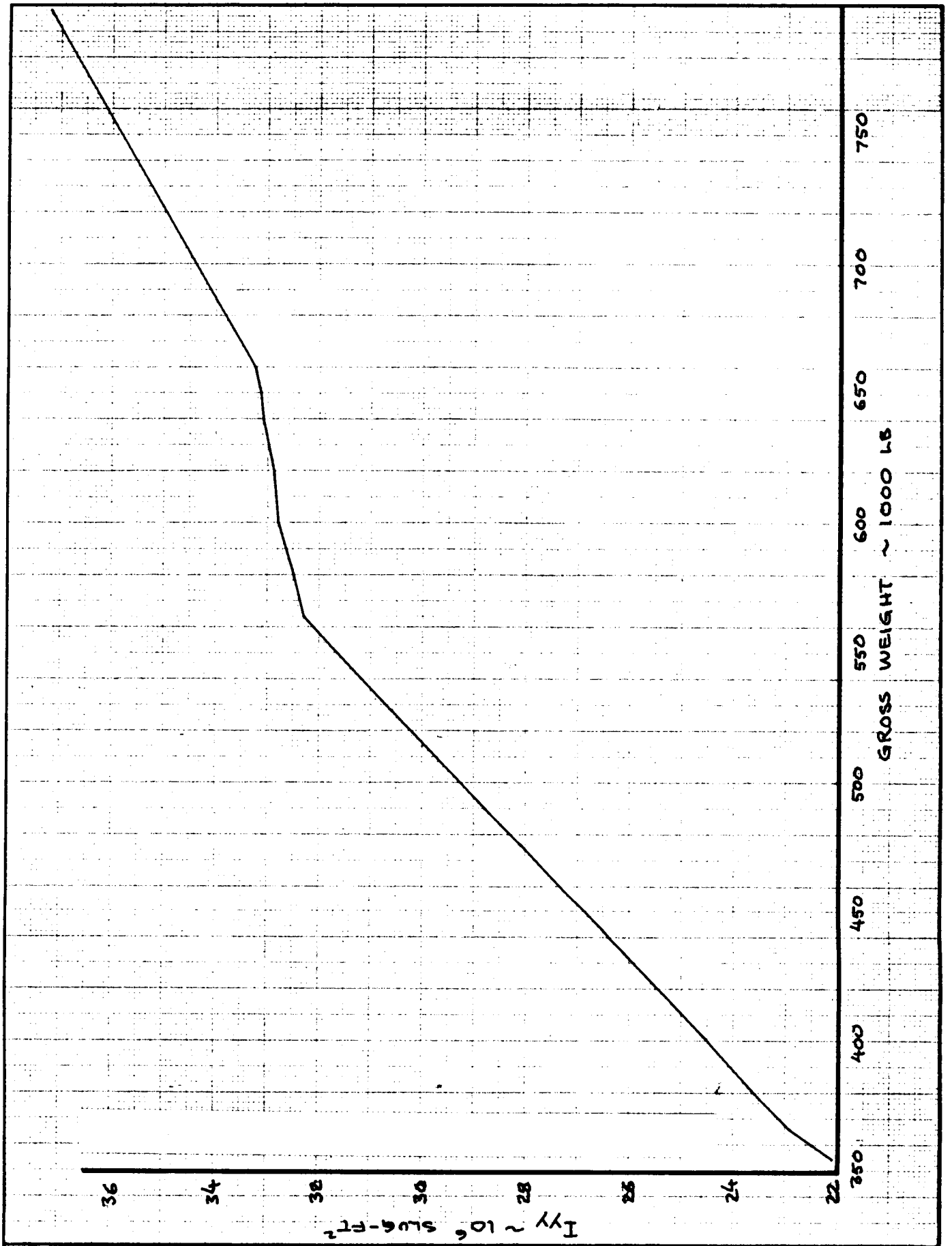

CALC			REVISED	DATE	I_{yy}, BODY AXIS MOMENT OF INERTIA
CHECK					
APR					
APR					
	DRN	JUNE 1970			THE BOEING COMPANY

747

D6-30643 VOL II

PAGE 1.1-7

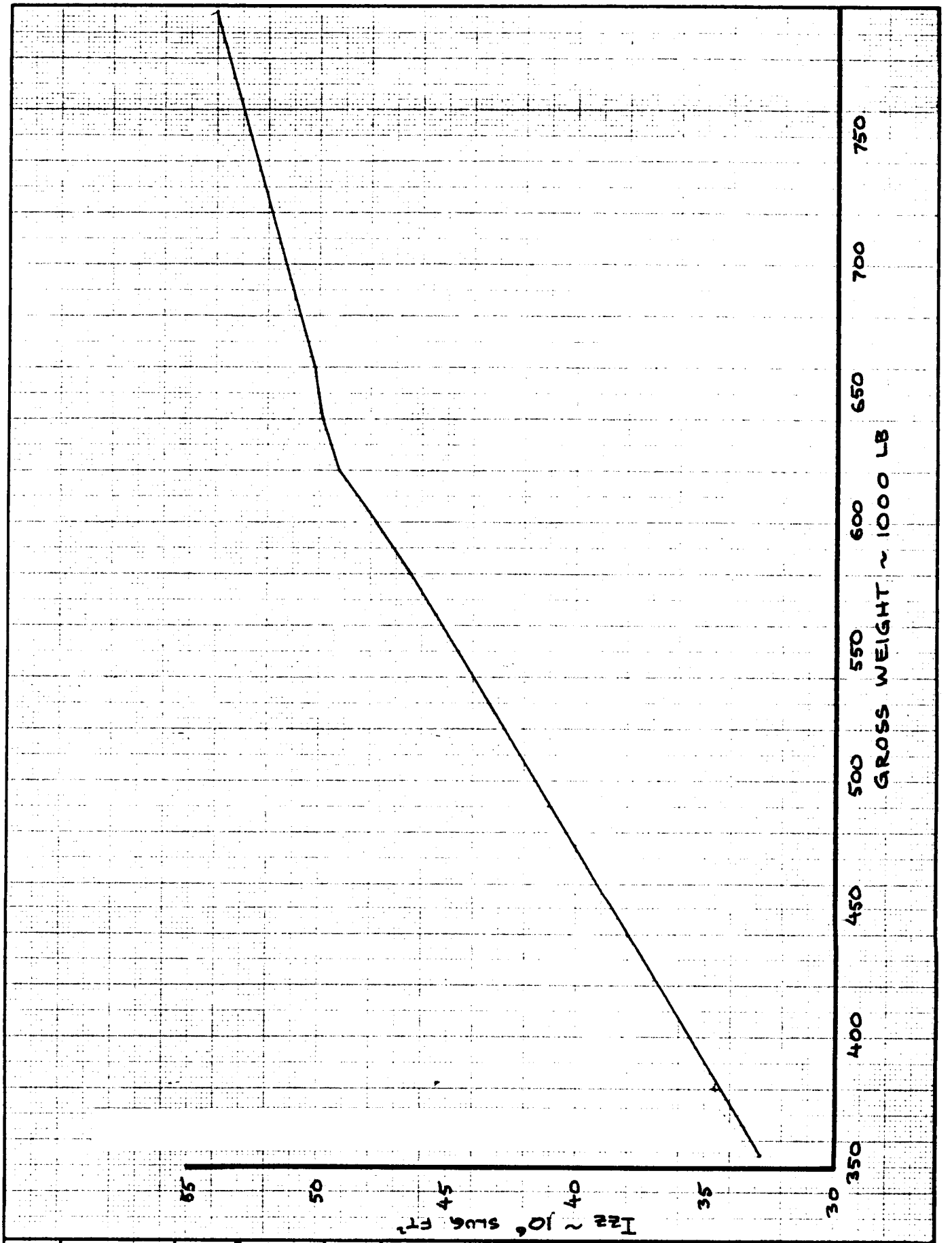

CALC			REVISED	DATE	I_{zz}, BODY AXIS MOMENT OF INERTIA
CHECK					
APR					
APR					
	DRN	JUNE 1970			THE BOEING COMPANY

747

D6-30643 VOL II

PAGE 1.1-8

AD 461 C-R4

K+E ALBANENE 1961 TRACING PAPER

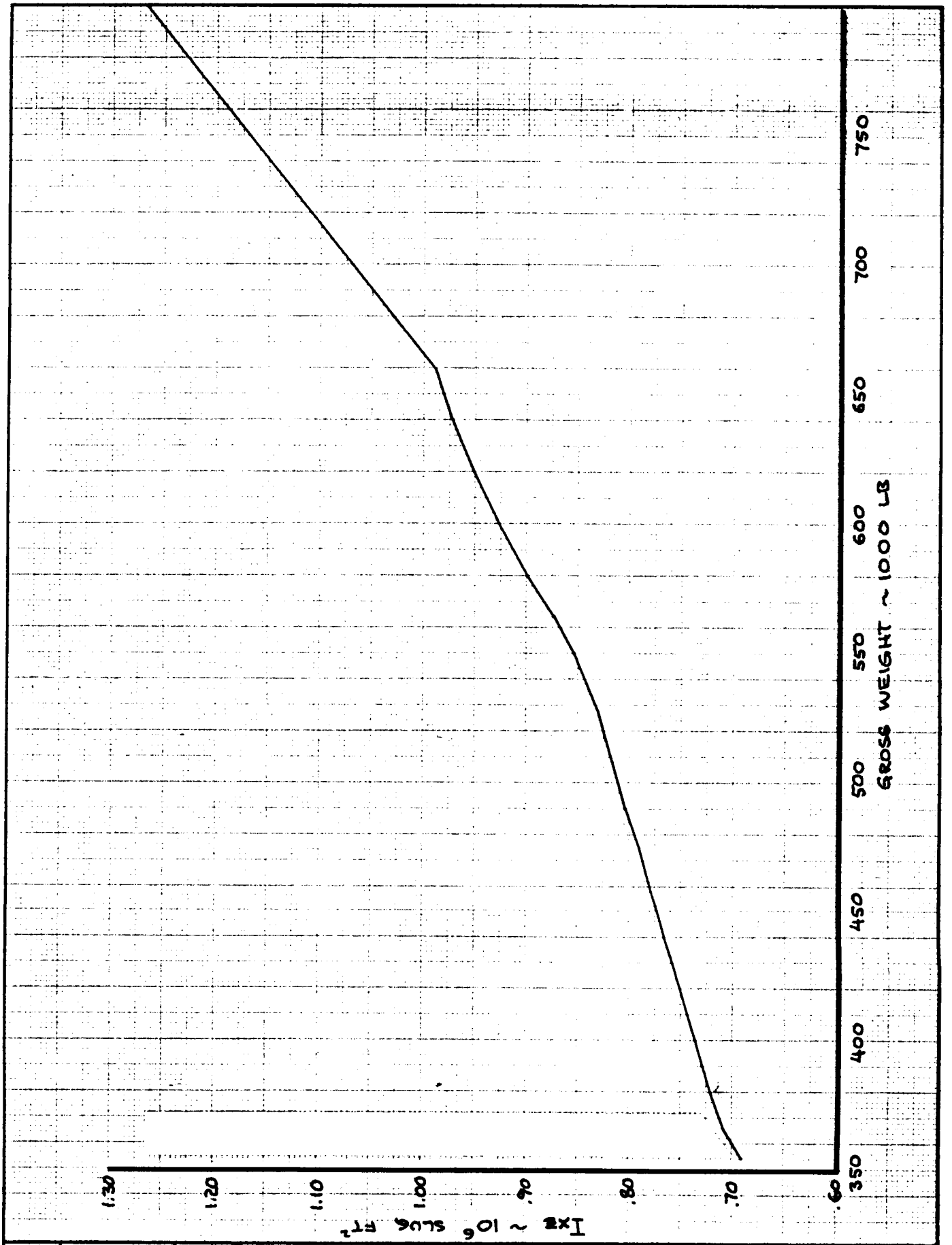

CALC			REVISED	DATE	I_{xz}, BODY AXIS PRODUCT OF INERTIA
CHECK					
APR					
APR					
	DRN	JUNE 1970			THE BOEING COMPANY

747

D6-30643 Vol III

PAGE 1.1-9

1.2 FLIGHT CONTROL SYSTEMS

All primary flight control surfaces are powered by irreversible hydraulic actuators supplied by four independent hydraulic systems. Each segment of the elevators, rudders and ailerons is driven by a single "dual-tandem" type actuator powered by various hydraulic system combinations. The flight and ground spoilers are driven by conventional single cylinder actuators individually supplied by three of the four hydraulic systems. A hydraulic schematic showing the distribution of the four hydraulic systems to the control surface actuators is shown on page 1.2-7.

All control actuators have input overtravel capability to allow unrestricted control input motion to the remaining surfaces when a given actuator is inoperative. There is no manual reversion capability on any surface in the event total hydraulic power is lost.

1.2.1 Longitudinal Controls

The longitudinal control system consists of four elevator segments and a trimmable stabilizer.

Elevators

Each of the four elevator segments is independently powered by dual-tandem actuators. Each inboard elevator actuator is powered by two hydraulic systems and each outboard elevator actuator by one hydraulic system as shown on page 1.2-7. The inboard elevators are controlled from the aft quadrant while

1.2 (Cont'd) the outboard elevators are slaved by a control cable system to the opposite inboard elevator surface. If hydraulic power to any segment is lost the segment will trail at an angle where the hinge moment is zero.

An artificial feel system is used to program the feel forces which consists of a hydraulic "q" spring modulated with stabilizer setting and a mechanical centering spring. The system is powered by hydraulic system numbers 2 and 3 normally with number 1 as a backup to number 3. Any one system will provide normal feel forces.

Stabilizer

The trimmable stabilizer is actuated by two hydraulic motors driving a single jackscrew. The power available with one or both motors is the same, but the trim rate with one motor is one-half that with both motors operating. Each motor has a rate control which varies the rate for both motors operating from 0.5 deg./sec. at low speeds to 0.2 deg./sec. at high speed. Simultaneous control of both motors is obtained either electrically by the thumb switch on each control wheel or mechanically by the control stand levers which override any electrical input signal. The autopilot system will operate either hydraulic motor.

1.2.2 Lateral Controls

The lateral control system comprises a combination of inboard and outboard ailerons and spoilers which also can be used as

1.2 (Cont'd) speedbrakes. Two dual-tandem central control actuators located in the wheel wells drive independent cable systems to the left and right wing lateral control surfaces. Pilot input to the central control actuators is provided by a cable system from each of the pilot and co-pilot control wheels.

Ailerons

Both inboard and outboard ailerons are actuated by dual-tandem actuators. The inboard ailerons operate in all flight conditions, but the outboard ailerons operate with flaps down only. A lockout mechanism which is actuated electrically by a switch on the outboard flap follow-up linkage, positions the outboard aileron actuators to neutral with flaps up. When both hydraulic systems to any aileron surface are inoperative the surface will trail at an angle where the hinge moment is zero.

Spoilers

There are six spoiler panels on each wing, five which are modulated with lateral control and speedbrake inputs and one (the most inboard panel) which is an unmodulated speedbrake only. Each panel is actuated by a single hydraulic actuator which has a check valve to prevent the panel from floating up to a zero hinge moment angle when the hydraulic system is inoperative. The five modulated panels on each wing are controlled from two "mixer boxes" which sum the inputs from the pilot's speedbrake handle and the central

1.2 (Cont'd) control actuators. Lateral control inputs will move the spoiler panels up or down within the travel limits at any speedbrake setting.

The speedbrake operation of the spoilers is divided into two functions. Moving the speedbrake handle to the "inflight" detent will raise spoiler panels 3, 4, 5 and 8, 9, 10 which are controlled through one mixer box to full deflection or blowdown angle. Before the "inflight" detent is reached, moving the speedbrake handle will raise spoiler panels 6 and 7 which are controlled directly by a two position solenoid valve, to full deflection or blowdown angle. Further handle movement to the ground detent position is possible only on the ground and will raise the remaining panels through the other mixer box.

Wheel forces are provided with a simple spring loaded follower and cam arrangement. Trim is obtained by rotating this mechanism with an electric servo motor and shifting the zero wheel force datum to the wheel angle desired. The servo motor is operated by a switch on the control stand.

1.2.3 Directional Controls

The directional control system consists of two rudder segments, each being actuated by a dual-tandem actuator. Rudder limiting is provided by a "q" programmed gear ratio changer which limits the rudder available from full pedal travel. Each rudder has a ratio changer with a comparator circuit to monitor their operation. If the two ratio changers disagree beyond the system tolerance

1.2 (Cont'd) limits, a warning light in the cockpit is activated. There are certain conditions such as one hydraulic system off operation where rudder available will be limited by actuator force capability to smaller angles than the ratio changer allows.

The rudder pedal forces are programmed by a spring loaded follower and cam arrangement similar to the lateral feel system. However, the ratio changer varies the pedal force required to obtain a given rudder angle with airspeed. This is done by installing the ratio changer between the feel system and the actuator input.

Rudder trim is obtained by rotating the feel unit with the trim knob on the control stand. The trim authority is also a function of airspeed due to the ratio changer function.

A series type yaw damper and turn coordinator system is incorporated into each rudder actuator. Rudder inputs from these systems will add to the inputs from the pedals or trim but will not feed back through the control system.

1.2.4 Flaps

The flap system consists of leading edge flaps and trailing edge flaps as shown on page 1.1-2.

The leading edge flaps comprise four sets per wing, each set being powered by a separate air motor or, as a backup, by a separate electric motor. The leading edge flaps are two-positioned (fully retracted or extended) and are programmed to operate in conjunction

1.2 (Cont'd) with the trailing edge flaps. Group A comprising leading edge flap sets (6, 7, 8), (11, 12, 13) / (14, 15, 16), (19, 20, 21) extend fully when the outboard trailing edge flaps extend to flaps 1. As the inboard trailing edge flaps extend to flaps 5, group B comprising the remaining leading edge flap sets (1, 2, 3, 4, 5), (9, 10) / (17, 18), (22, 23, 24, 25, 26) extend fully.

The two inboard trailing edge flaps are actuated by one power drive system, the two outboard by another. Each drive system consists of a hydraulic motor (see page 1.2-7) coupled through gears to a torque tube extending laterally along both wings. Each trailing edge flap is driven by two ball screw actuators powered by the turning of the appropriate torque tube. Each drive system has an electric motor for backup power. During trailing edge flap extension or retraction, an inboard trailing edge flaps asymmetry monitor automatically causes hydraulic shutoff to the inboard trailing edge flaps when the position difference between the right and left inboard trailing edge flaps exceeds a predetermined amount. An outboard trailing edge flaps asymmetry monitor operates similarly.

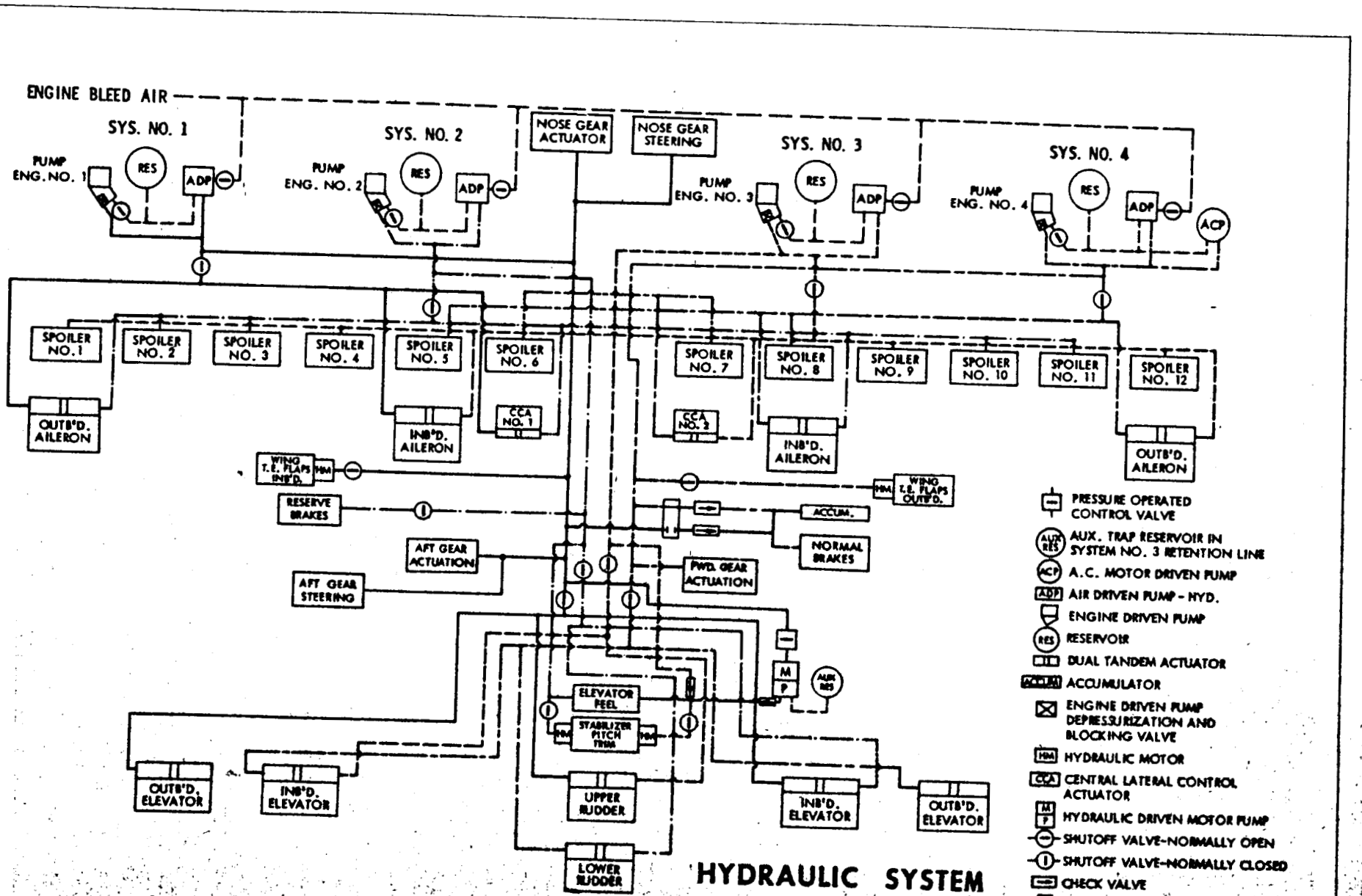
ENGINE BLEED AIR
SYS. NO. 1
SYS. NO. 2
SYS. NO. 3
SYS. NO. 4
PUMP ENG. NO. 1
PUMP ENG. NO. 2
PUMP ENG. NO. 3
PUMP ENG. NO. 4
RES
ADP
ACP
NOSE GEAR ACTUATOR
NOSE GEAR STEERING
SPOILER NO. 1
SPOILER NO. 2
SPOILER NO. 3
SPOILER NO. 4
SPOILER NO. 5
SPOILER NO. 6
SPOILER NO. 7
SPOILER NO. 8
SPOILER NO. 9
SPOILER NO. 10
SPOILER NO. 11
SPOILER NO. 12
OUTB'D. AILERON
INB'D. AILERON
CCA NO. 1
CCA NO. 2
WING T.E. FLAPS INB'D.
WING T.E. FLAPS OUT'D.
HM
RESERVE BRAKES
ACCUM.
NORMAL BRAKES
AFT GEAR ACTUATION
AFT GEAR STEERING
FWD. GEAR ACTUATION
M
P
AUX RES
ELEVATOR FEEL
STABILIZER PITCH TRIM
OUTB'D. ELEVATOR
INB'D. ELEVATOR
UPPER RUDDER
LOWER RUDDER
HYDRAULIC SYSTEM
PRESSURE OPERATED CONTROL VALVE
AUX. TRAP RESERVOIR IN SYSTEM NO. 3 RETENTION LINE
A.C. MOTOR DRIVEN PUMP
AIR DRIVEN PUMP - HYD.
ENGINE DRIVEN PUMP
RESERVOIR
DUAL TANDEM ACTUATOR
ACCUMULATOR
ENGINE DRIVEN PUMP DEPRESSURIZATION AND BLOCKING VALVE
HYDRAULIC MOTOR
CENTRAL LATERAL CONTROL ACTUATOR
HYDRAULIC DRIVEN MOTOR PUMP
SHUTOFF VALVE-NORMALLY OPEN
SHUTOFF VALVE-NORMALLY CLOSED
CHECK VALVE
BRAKE INTERCONNECT VALVE

1.3 DISCUSSION OF THE SIMULATION

An aircraft in motion is acted upon by external forces and moments resulting from thrust and gravity effects, landing gear forces, and aerodynamic loads. These force and moment components comprise the coefficients of the airplane equations of motion, which are the key to a realistic description of the aircraft's flight characteristics.

Aircraft flight simulation, then, requires continuous, real-time solution of these equations of motion, as well as an accurate representation of those systems and characteristics necessary to allow the pilot to "fly" the simulator with sufficient realism.

This document contains data which describe the forces and moments created by aerodynamic loads on the airplane. They may be functions of several variables, including altitude, airspeed, Mach number, angle of attack, rotation rates, center of gravity, ground proximity and geometry changes, such as control deflections and gear and flap extensions.

The data contained in the following sections are computed about stability axes (x_s, y_s, z_s) as shown on page 1.3-4. Stability axes differ from body axes in that the x- and z-axes are rotated about the y-axis through the angle of attack; that is, the x_s-axis lies in the plane determined by the relative wind and the body y-axis. This x_s-axis also lies in the (x-z) plane of symmetry of the

1.3 (Cont'd) airplane and is thus rotated about z_s away from the relative wind by sideslip angle, β. Forces and moments measured in this system are presented as dimensionless coefficients which are broken down into separate terms (stability derivatives) showing the effects of each important parameter.

While the use of stability axes simplifies the presentation of the aerodynamic functions, the forces and moments must be resolved to the appropriate axes systems for solution of the equations of motion. The schematic flow chart on Page 1.3-5 presents the method used to solve the dynamic equations in which the aerodynamic forces and moments are transformed into body axes. Note that the appropriate axis transformation here is to the fuselage reference line (FRL) body axes, or through the angle $\alpha_{F.R.L.}$. This allows the direct use of body axis inertias, I_{xx}, I_{yy}, I_{zz}, and I_{xz} without any inertia transformations. Note also that the wing angle of attack ($\alpha_{W.D.P.} = \alpha_{F.R.L.} + 2^{o}$) is used only in conjunction with the aerodynamic data curves - it is not used for any axis transformations.

A second item of importance is the simulation of forces and moments due to thrust. Flight testing has shown that a simple effective engine moment-arm representation accounts for thrust.

1.3 (Cont'd) At present, the thrust vector may be considered to be inclined up 2.5° from the fuselage reference line, with each engine canted inward by 2°. The corresponding thrust effects are as follows:

$$T_x = T_{\text{eng. \#1}} + T_{\text{eng. \#2}} + T_{\text{eng. \#3}} + T_{\text{eng. \#4}}$$

$$T_y = .0349\ (T_{\#1} + T_{\#2} - T_{\#3} - T_{\#4})$$

$$T_z = -.0436\ T_x$$

$$L_T = .0436\ N_T$$

$$M_T = (T_{\#1} + T_{\#4}).\ Z_{E_O} + (T_{\#2} + T_{\#3}).\ Z_{E_I}$$

$$N_T = (T_{\#1} + T_{\#4}).\ Y_{E_O} + (T_{\#2} - T_{\#3}).\ Y_{E_I}$$

The effective engine moment arm values are found on page 1.1-3. The thrust reverser effects on the lift, drag and pitching moment coefficients are presented in Section 12.5. These increments are to be added to the equations for C_L, C_D and $C_{m_{c.g.}}$ on pages 2.0-1, 3.0-1 and 4.0-1 respectively.

Sign conventions for the controls and aerodynamic coefficients are shown on page 1.3-6, while maximum control deflections are listed on page 1.3-7.

To aid in scaling, a list of maximum values is given on page 1.3-8, and a summary of nomenclature begins on page 1.3-9.

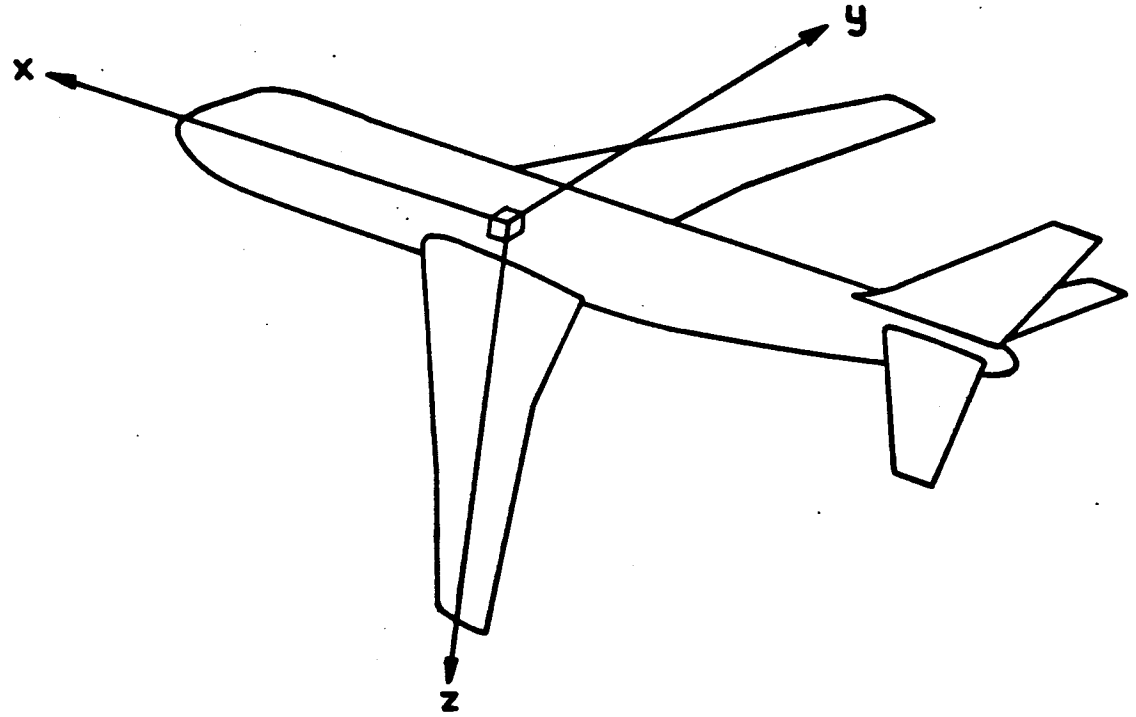

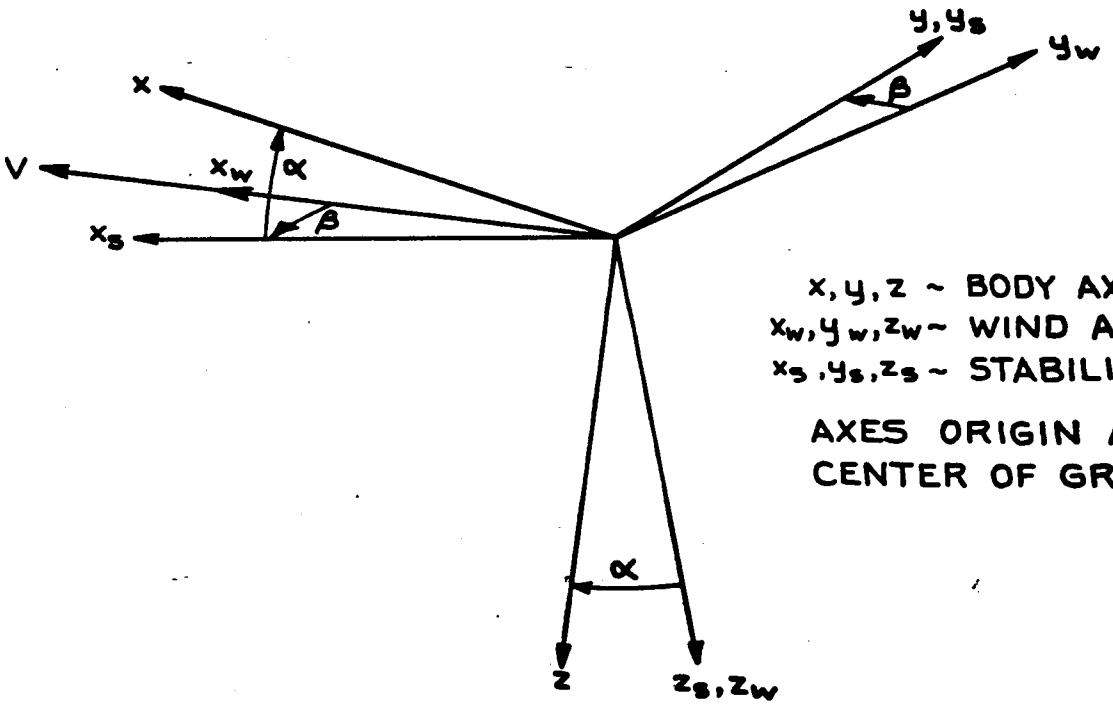

x, y, z ~ BODY AXES (FRL)
x_w, y_w, z_w ~ WIND AXES
x_s, y_s, z_s ~ STABILITY AXES

AXES ORIGIN AT THE CENTER OF GRAVITY

CALC	CURNUTT	12-20-67	REVISED	DATE	AXES SYSTEMS	747
CHECK			LOW	1-30-70		D6-30643, Vol. II
APPD						
APPD						
INK	GLENN	1-12-68			THE BOEING COMPANY RENTON, WASHINGTON	PAGE 1.3-4

TD 973 D-83

REV. D

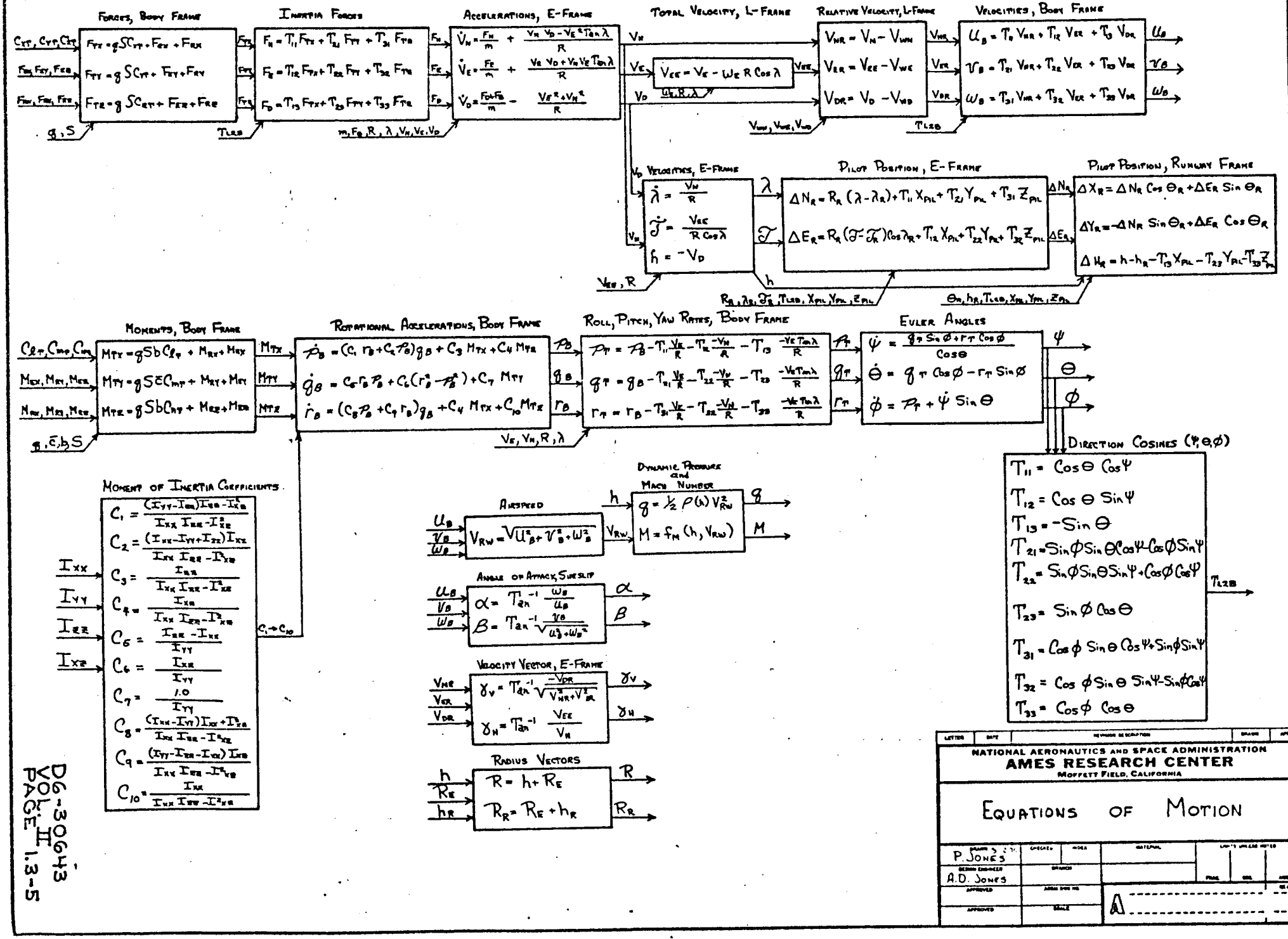

D6-30643
VOL II
PAGE 1.3-5

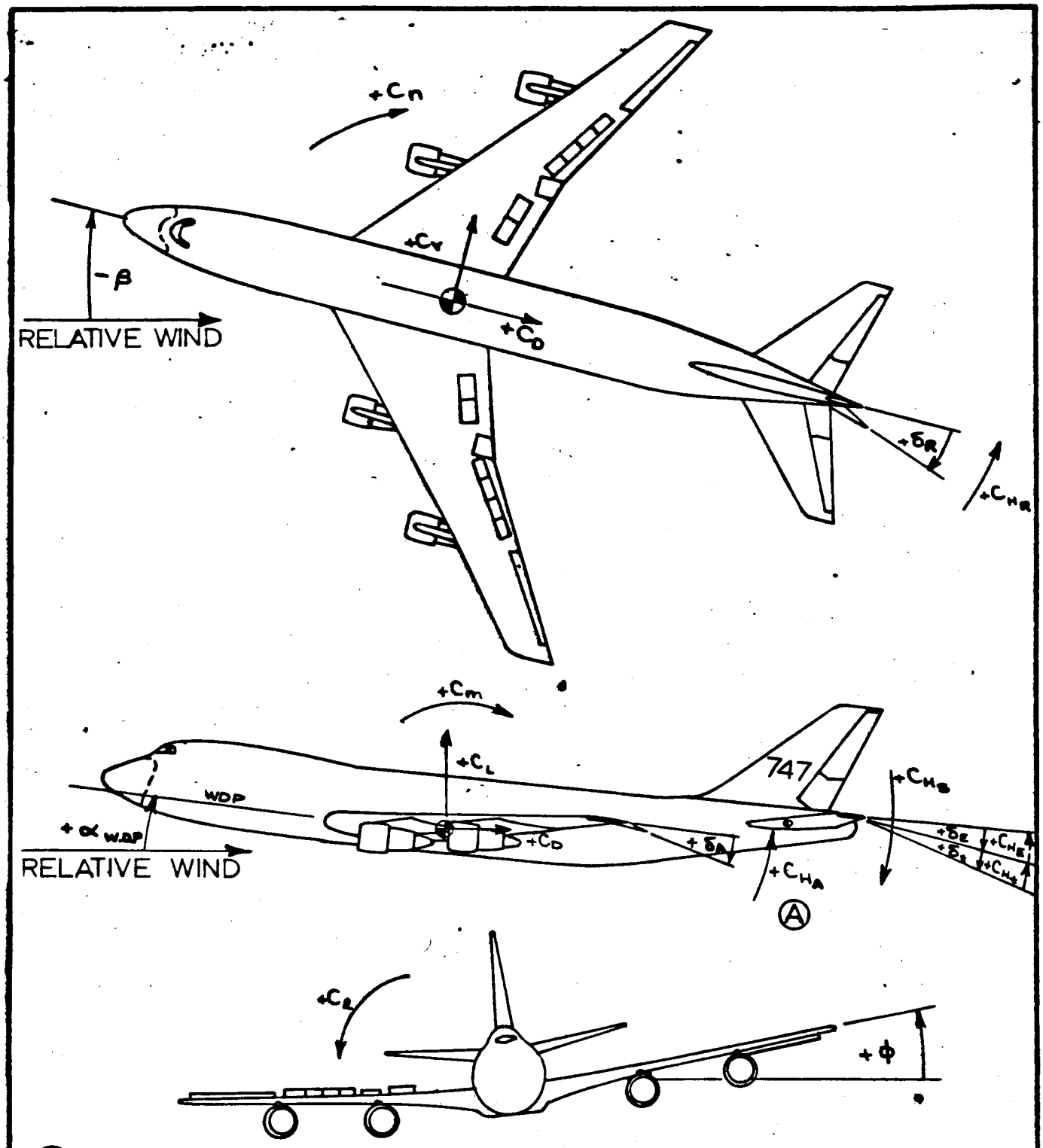

Ⓐ POSITIVE STABILIZER DEFLECTION ~ L.E. UP
FOR INDIVIDUAL AILERONS, $+\delta_A$ ~ T.E. DOWN
FOR AILERONS ON BOTH WINGS, $+\delta_A$ ~ L.H. WING T.E. DN.
R.H. WING T.E. UP

RIGHT WING SPOILER DEFLECTION IS POSITIVE.

CALC	RICHARDSON	4-3-67	REVISED	DATE
CHECK			RICHARDSON	6/6/67
APP				
APPD				
	ODEGARD	4-3-67		

SIGN CONVENTION
(STABILITY AXES)

THE BOEING COMPANY
RENTON, WASHINGTON

747
D6-30643
Vol. II
PAGE 1.3-6

TD 873 D-83

6 7000

MAXIMUM CONTROL SURFACE DEFLECTION AND RATES

Control Surface	Symbol	Maximum Displacement (deg)	Normal Operation (Full Boost) Rate (deg/sec)	One Hydraulic System Failure Rate (deg/sec)
Elevators				
Inboard	δ_{E_I}	+17	37 down	30 down
		-23	37 up	26 up
Outboard	δ_{E_O}	+17	37 down	30 down
		-23	37 up	26 up
Stabilizer	$\Delta_{F.R.L.}$			
Pilot's Thumb Switch		+ 0.5	0.5 → 0.2	0.25 → 0.1
		-10		
Control Stand Levers		+ 3	0.5 → 0.2	0.25 → 0.1
		-12		
Ailerons				
Inboard	δ_{A_I}	+20	40 down	27 down
		-20	45 up	35 up
Outboard	δ_{A_O}	+15	45 down	22 down
		-25	55 up	45 up
Spoilers	δ_{SP}			
Panels 1,2,3,4 9,10,11,12		45	75 ①	
Panels 5,8		20	75	
Panels 6,7 (Speedbrakes only)		20	25	
Rudder				
Upper	δ_{R_U}	±25	50	40
Lower	δ_{R_L}	±25	50	40

Note The deflection rates shown above are average values applicable to all flight conditions. The actual non-linear deflection rate response characteristics are presented in D6-13336, "Flight Control Systems Data For The 747 Flight Simulator".

① NASA simulation used a control wheel rate limit of 100 deg/sec in place of individual control rate limits.

AD 1345 D

MAXIMUM VALUES

Parameter	Maximum Value	Units
a_x	30	ft/sec^2
a_y	25	ft/sec^2
a_z	120	ft/sec^2
$\ddot{\theta}$	50	deg/sec^2
$\ddot{\phi}$	130	deg/sec^2
$\ddot{\psi}$	30	deg/sec^2
$\dot{\theta}$	60	deg/sec
$\dot{\phi}$	75	deg/sec
$\dot{\psi}$	30	deg/sec
$\dot{\alpha}$	40	deg/sec
$\dot{\beta}$	30	deg/sec
Altitude	45000	ft
Rate of Climb	15000	ft/min
Rate of Descent	15000	ft/min
Center of Gravity Range	0-40	%MAC

NOTE: For complete center of gravity information consult D6-13585, "Mass Properties - 747 Flight Simulator".

NOMENCLATURE

SYMBOL		DEFINITION
a_i	=	Acceleration along the "i" axis (ft/sec^2)
b	=	Wing span (ft).
C_D	=	Airplane drag coefficient. $C_D = \frac{D}{qS}$, where a positive drag force acts along the negative x_s axis.
C_L	=	Airplane lift coefficient. $C_L = \frac{LIFT}{qS}$, where a positive lift force acts along the negative z_s axis.
C_Y	=	Airplane side force coefficient. $C_Y = \frac{Y}{qS}$, where a positive side force acts along the positive y_s axis.
C_l	=	Airplane rolling moment coefficient about the reference axis, x_s . $C_l = \frac{L}{qSb}$
C_m	=	Airplane pitching moment coefficient about the reference axis, y_s . $C_m = \frac{M}{qS\bar{c}}$
C_n	=	Airplane yawing moment coefficient about the reference axis, z_s . $C_n = \frac{N}{qSb}$
C.G.	=	Airplane center of gravity position as a fraction of the wing mean aerodynamic chord.
$\bar{c}$, M.A.C.	=	Wing mean aerodynamic chord (ft).
F_p	=	Rudder pedal force, positive for a left rudder pedal force (lb).
F_s	=	Control column force, positive for a column pull force (lb).
F_w	=	Control wheel force, positive for a clockwise wheel moment (lb).

SYMBOL		DEFINITION
HM	=	Hinge moment (lb-ft).
h_p	=	Pressure altitude (ft).
I_{ij}	=	Airplane mass moment of inertia about the reference axes i, j ($slug\text{-}ft^2$).
L, M, N	=	Rolling, pitching and yawing moments about a reference axes system.
M	=	Mach number.
n_z	=	Airplane normal load factor along the z-axis. $n_z = \frac{-Z_S \cos\alpha - X_S \sin\alpha + .0436T - (Z_{\text{due to landing gear reactions}})}{mg}$
p, q, r	=	Roll, pitch and yaw rates about a reference axes system (radians/sec).
q	=	Dynamic pressure (lb/ft^2). $q = \frac{1}{2}\rho V^2 = \frac{V_E^2}{295.4}$
q_c	=	Impact pressure (lb/ft^2). $q_c = P_{TOTAL} - P_{STATIC} = 2116.2166\,\delta\left[(1 + .2M^2)^{3.5} - 1\right]$
S	=	Wing area (ft^2).
T	=	Engine thrust (lb).
V	=	True airspeed (ft/sec).
V_C	=	Calibrated airspeed (knots). $V_C = 1479.1026 \sqrt{(q_c/2116.2166 + 1)^{2/7} - 1}$
V_E	=	Equivalent airspeed (knots). $V_E = \sigma^{1/2} \cdot V / 1.689$

AD 1346 D

SYMBOL		DEFINITION
W	=	Airplane gross weight (lb).
X, Y, Z	=	Axial force, side force, and normal force along a reference system.
x, y, z	=	Body axes system described in Section 1.3.
x_s, y_s, z_s	=	Stability axes system described in Section 1.3.
x_w, y_w, z_w	=	Wind axes system described in Section 1.3.
Y_{E_I}	=	Effective inboard engine yawing arm (ft).
Y_{E_O}	=	Effective outboard engine yawing arm (ft).
Z_{E_I}	=	Effective inboard engine pitching arm (ft).
Z_{E_O}	=	Effective outboard engine pitching arm (ft).
$\alpha, \alpha_{F.R.L.}$	=	Airplane angle of attack relative to the fuselage reference line (degrees).
$\alpha_{W.D.P.}$	=	Airplane angle of attack relative to the wing design plane (degrees).
β	=	Airplane sideslip angle (degrees).
δ	=	Air pressure ratio.
δ_A	=	Aileron deflection angle (degrees).
δ_{A_I}	=	Inboard aileron deflection angle (degrees).
δ_{A_O}	=	Outboard aileron deflection angle (degrees).
δ_C	=	Control column deflection angle, positive for rearward column movement (degrees).
δ_E	=	Elevator deflection angle (degrees).
δ_{E_I}	=	Inboard elevator deflection angle (degrees).
δ_{E_O}	=	Outboard elevator deflection angle (degrees).
δ_F	=	Flap setting

AD 1846 D

SYMBOL		DEFINITION
δ_P	=	Rudder pedal deflection angle, positive for positive rudder deflection (degrees).
δ_R	=	Rudder deflection angle (degrees).
δ_{R_L}	=	Lower rudder deflection angle (degrees).
δ_{R_U}	=	Upper rudder deflection angle (degrees).
δ_{SP}	=	Spoiler deflection angle (degrees).
δ_W	=	Control wheel deflection angle, positive for a clockwise wheel movement (degrees).
$\Delta_{F.R.L.}$	=	Horizontal stabilizer angle relative to the fuselage reference line (degrees).
θ	=	Airplane Euler pitch angle.
ϕ	=	Airplane Euler roll angle.
ψ	=	Airplane Euler yaw angle.
ρ	=	Air mass density (slugs/ft^3).
σ	=	Air density ratio

SUBSCRIPT

F.R.L.	=	Fuselage reference line (any body water line).
W.D.P.	=	Wing design plane.

As used with V_E and M placards:—

FE	=	Operational flaps extended placard.
LO	=	Landing gear operating placard.
LE	=	Landing gear extended placard. (Note: The landing gear cannot be extended above the LO limit, but flight to LE limits is possible).

RD 1546 D

SUBSCRIPT

MO	=	Maximum operating limit.
DF	=	Design dive flight placard.

The time derivative operation normally denoted by $\frac{d}{dt}$ is replaced in this document by the dot derivative notation, $\frac{d(\ )}{dt} = (\dot{})$ AND $\frac{d^2(\ )}{dt^2} = (\ddot{})$.

AD 1546 D

2.0 LIFT FORCE COEFFICIENT

The dimensionless aerodynamic lift force coefficient is given in terms of its significant components by the equation below.

At a given $\alpha_{W.D.P.}$,

$$
\begin{aligned}
C_L = {} & C_{L_{BASIC}} + (\Delta C_L)_{\alpha_{W.D.P.}=0^\circ} + \Delta\left(\frac{dC_L}{d\alpha}\right)\cdot\alpha_{W.D.P.} \\
& + \frac{dC_L}{d\hat{\alpha}}\cdot\left(\frac{\dot{\alpha}\bar{c}}{2V}\right) + \frac{dC_L}{d\hat{q}}\cdot\left(\frac{q\bar{c}}{2V}\right) + \frac{dC_L}{dn_z}\cdot n_z \\
& + K_\alpha\cdot\frac{dC_L}{d\delta}\cdot\delta_{F.R.L.} + K_\alpha\cdot\frac{dC_L}{d\delta_{E_I}}\cdot\delta_{E_I} + K_\alpha\cdot\frac{dC_L}{d\delta_{E_O}}\cdot\delta_{E_O} \\
& + \Delta C_{L_{SPOILERS}} + \Delta C_{L_{OUTBOARD\ AILERONS}} + \Delta C_{L_{LANDING\ GEAR}} \\
& + \Delta C_{L_{GROUND\ EFFECT}} + \left[\Delta C_{L_{FLAP\ FAILURE}}\right]^*
\end{aligned}
$$

where,

$C_{L_{BASIC}}$ = Basic lift coefficient for the rigid airplane at $\delta_{F.R.L.}=0^\circ$, in free air and with the landing gear retracted. For low speed, $C_{L_{BASIC}}$ is plotted on page 2.0-7. For flaps up, $C_{L_{BASIC}}$ is plotted on page 2.0-8.

$(\Delta C_L)_{\alpha_{W.D.P.}=0^\circ}$ = Change in basic lift coefficient at $\alpha_{W.D.P.}=0^\circ$ due to aeroelasticity. For low speed, $(\Delta C_L)_{\alpha_{W.D.P.}=0^\circ}$

$[\ ]^*$ NOT IN NASA SIMULATION

AD 1566 D

2.0 (Cont'd)

is plotted on page 2.0-9. For flaps up, $(\Delta C_L)_{\alpha_{W.B.P.}=0^\circ}$ is plotted on page 2.0-10.

$\Delta\left(\frac{dC_L}{d\alpha}\right)_{\alpha_{W.B.P.}}$ = Change in basic lift coefficient due to the aeroelastic effect on the rigid airplane basic lift coefficient curve slope. For low speed, $\Delta\left(\frac{dC_L}{d\alpha}\right)$ is plotted on page 2.0-11. For flaps up, $\Delta\left(\frac{dC_L}{d\alpha}\right)$ is plotted on page 2.0-12.

$\frac{dC_L}{d\hat{\dot{\alpha}}}\cdot\left(\frac{\dot{\alpha}\bar{c}}{2V}\right)$ = Change in basic lift coefficient due to rate of change of angle of attack. $\frac{dC_L}{d\hat{\dot{\alpha}}}$ is plotted on page 2.0-13.

$\frac{dC_L}{d\hat{q}}\cdot\left(\frac{q\bar{c}}{2V}\right)$ = Change in basic lift coefficient due to pitch rate.

$$\frac{dC_L}{d\hat{q}} = K_{\hat{q}}\cdot\frac{dC_{L_{2D}}}{d\hat{q}}$$

where $\frac{dC_{L_{2D}}}{d\hat{q}}$ and the center of gravity factor, $K_{\hat{q}}$ are plotted on page 2.0-14.

$\frac{dC_L}{dn_z}\cdot n_z$ = Change in basic lift coefficient due to aeroelastic inertia relief caused by normal load factor, n_z. For low speed, $\frac{dC_L}{dn_z}$ is plotted on page 2.0-15. For flaps up, $\frac{dC_L}{dn_z}$ is plotted on page 2.0-16.

$K_\alpha\cdot\frac{dC_L}{d\delta}\cdot\delta_{F.R.L}$ = Change in basic lift coefficient due to change in stabilizer angle from $\delta_{F.R.L}=0^\circ$. $\frac{dC_L}{d\delta}$ is plotted on page 2.0-17. The effectiveness factor for the

2.0 (Cont'd)

stabilizer (and elevators), K_α is plotted on page 4.0-19.

$K_\alpha \cdot \frac{dC_L}{d\delta_{E_I}} \cdot \delta_{E_I}$ = Change in basic lift coefficient due to change in inboard elevator angle from $\delta_{E_I} = 0°$. $\frac{dC_L}{d\delta_{E_I}}$ is plotted on page 2.0-18. (1)

$K_\alpha \cdot \frac{dC_L}{d\delta_{E_O}} \cdot \delta_{E_O}$ = Change in basic lift coefficient due to change in outboard elevator angle from $\delta_{E_O} = 0°$. $\frac{dC_L}{d\delta_{E_O}}$ is plotted on page 2.0-19. (1)

(1) The normal system stick free (rigged) elevator deflection is + 2° from the faired position.

$\Delta C_{L_{SPOILERS}}$ = Change in basic lift coefficient due to spoiler or speedbrake deflection. It should be noted that "spoilers" extended on one wing are used for lateral control, while symmetrically extended spoilers are used for "speed brakes."

$$\Delta C_{L_{SPOILERS}} = \sum_{\substack{\text{OPERATING} \\ \text{SPOILER} \\ \text{PANELS}}} (K_{\delta_{SP}}) \cdot (\Delta C_{L_{SP}})_{45} \cdot \frac{(C_{L_{SP}})_M}{(C_{L_{SP}})_{M=0}} \cdot \left(\frac{L_E}{L_{R/SP}}\right) \cdot F_{e_{GE}}$$

where $(\Delta C_{L_{SP}})_{45}$ is the change in basic lift coefficient due to deflecting the operating spoiler panels to 45°. The operating spoiler panels are determined from the hydraulic systems schematic on page 1.2-7. $(\Delta C_{L_{SP}})_{45}$ is plotted for spoilers and ground spoilers on page 2.0-21 and page 2.0-22

2.0 (Cont'd)

respectively. The spoiler effectiveness factor, $(K_{\delta_{SP}})_L$ is plotted on page 2.0-20. The Mach number effect, $(C_{L_{SP}})_M / (C_{L_{SP}})_{M=0}$ is plotted on page 2.0-23. The aeroelastic effect, $\left(\frac{L_E}{L_R}\right)_{SP}$ is plotted on pages 2.0-24, 2.0-25, and 2.0-26. The ground effect factor, $F_{\ell_{GE}}$ is obtained from page 5.0-29.

$\Delta C_{L_{\substack{\text{OUTBOARD} \\ \text{AILERONS}}}}$ = Change in basic lift coefficient due to outboard aileron deflection.

$$\Delta C_{L_{\substack{\text{OUTBOARD} \\ \text{AILERONS}}}} = \sum_{\substack{\text{LEFT AND RIGHT} \\ \text{OUTBOARD AILERONS}}} K_{\delta_{A_O}} \cdot \Delta C_{L_{A_O}} \cdot F_{\ell_{GE}}$$

where $\Delta C_{L_{A_O}}$ is the change in basic lift coefficient due to deflecting one outboard aileron up to 25° or the opposite outboard aileron down to 15°. $\Delta C_{L_{A_O}}$ is plotted on page 2.0-27. The outboard aileron effectiveness factor, $K_{\delta_{A_O}}$ is plotted on page 5.0-26. The ground effect factor, $F_{\ell_{GE}}$ is obtained from page 5.0-29.

$\Delta C_{L_{\substack{\text{LANDING} \\ \text{GEAR}}}}$ = Change in basic lift coefficient due to main and nose landing gear extension.

$$\Delta C_{L_{\substack{\text{LANDING} \\ \text{GEAR}}}} = K_{GEAR} \cdot \Delta C_{L_{GEAR}} \cdot \frac{(C_{L_{GEAR}})_M}{(C_{L_{GEAR}})_{M=0}}$$

where $\Delta C_{L_{GEAR}}$ is plotted on page 2.0-29. The Mach number effect, $(C_{L_{GEAR}})_M / (C_{L_{GEAR}})_{M=0}$ is plotted on page 2.0-30. The landing gear effectiveness factor, K_{GEAR} is plotted on page 2.0-28.

2.0 (Cont'd) $\Delta C_{L_{\substack{\text{GROUND}\\\text{EFFECT}}}}$ = Change in basic lift coefficient due to ground effect.

$$\Delta C_{L_{\substack{\text{GROUND}\\\text{EFFECT}}}} = K^{B}_{GE} \cdot \Delta C_{L_{GE}}$$

where $\Delta C_{L_{GE}}$ is plotted on page 2.0-32. The ground effect height factor, K^{B}_{GE}, is plotted on page 2.0-31.

$\Delta C_{L_{\text{FLAP FAILURE}}}$ = Change in basic lift coefficient due to flap extension or retraction from the flap position at which symmetric failure of both inboard or both outboard flaps occurs. For symmetric inboard or outboard flap failure,

$$\Delta C_{L\,\text{FLAP FAILURE}} = \left[(\Delta C_L)_{\alpha_{W.D.P.}=0^\circ}\right]_{\text{FLAP FAILURE}} + \Delta\left(\frac{dC_L}{d\alpha}\right)_{\text{FLAP FAILURE}} \cdot \alpha_{W.D.P.}$$

where $\left[(\Delta C_L)_{\alpha_{W.D.P.}=0^\circ}\right]_{\text{FLAP FAILURE}}$ is the change in basic lift coefficient at $\alpha_{W.D.P.} = 0^\circ$ due to symmetric inboard or outboard flap failure. $\left[(\Delta C_L)_{\alpha_{W.D.P.}=0^\circ}\right]_{\text{FLAP FAILURE}}$ is plotted on page 2.0-33. $\Delta\left(\frac{dC_L}{d\alpha}\right)_{\text{FLAP FAILURE}} \cdot \alpha_{W.D.P.}$ is the change in basic lift coefficient due to the effect of symmetric inboard or outboard flap failure on the rigid airplane basic lift coefficient curve slope. $\Delta\left(\frac{dC_L}{d\alpha}\right)_{\text{FLAP FAILURE}}$ is plotted on page 2.0-34. The above data is also applicable for asymmetric (monitor limited) inboard or outboard flap failure, e.g., one inboard flap failed and the opposite inboard flap at the monitor limited extension or retraction position.

AD 1546 D

2.0 (Cont'd)

$\Delta C_{L\ \text{FLAP FAILURE}}$ is to be added to total C_L computed for the inboard flap position. Note that inboard flap position should be used for all functions of flap in this document.

The angle of attack for stick shaker actuation is plotted on page 2.0-35. The angle of attack for initial buffet is plotted on page 2.0-36. Certification stall speeds are plotted on page 2.0-37. The initial buffet boundary and trimmed $C_{L\ \text{MAX.}}$ values are plotted on page 2.0-38.

LOW SPEED

NOTE 1 NO THRUST EFFECTS

2 $\Delta_{F.R.L.} = 0^\circ$, $\delta_{E_I} = \delta_{E_O} = 0^\circ$

3 GEAR UP, FREE AIR

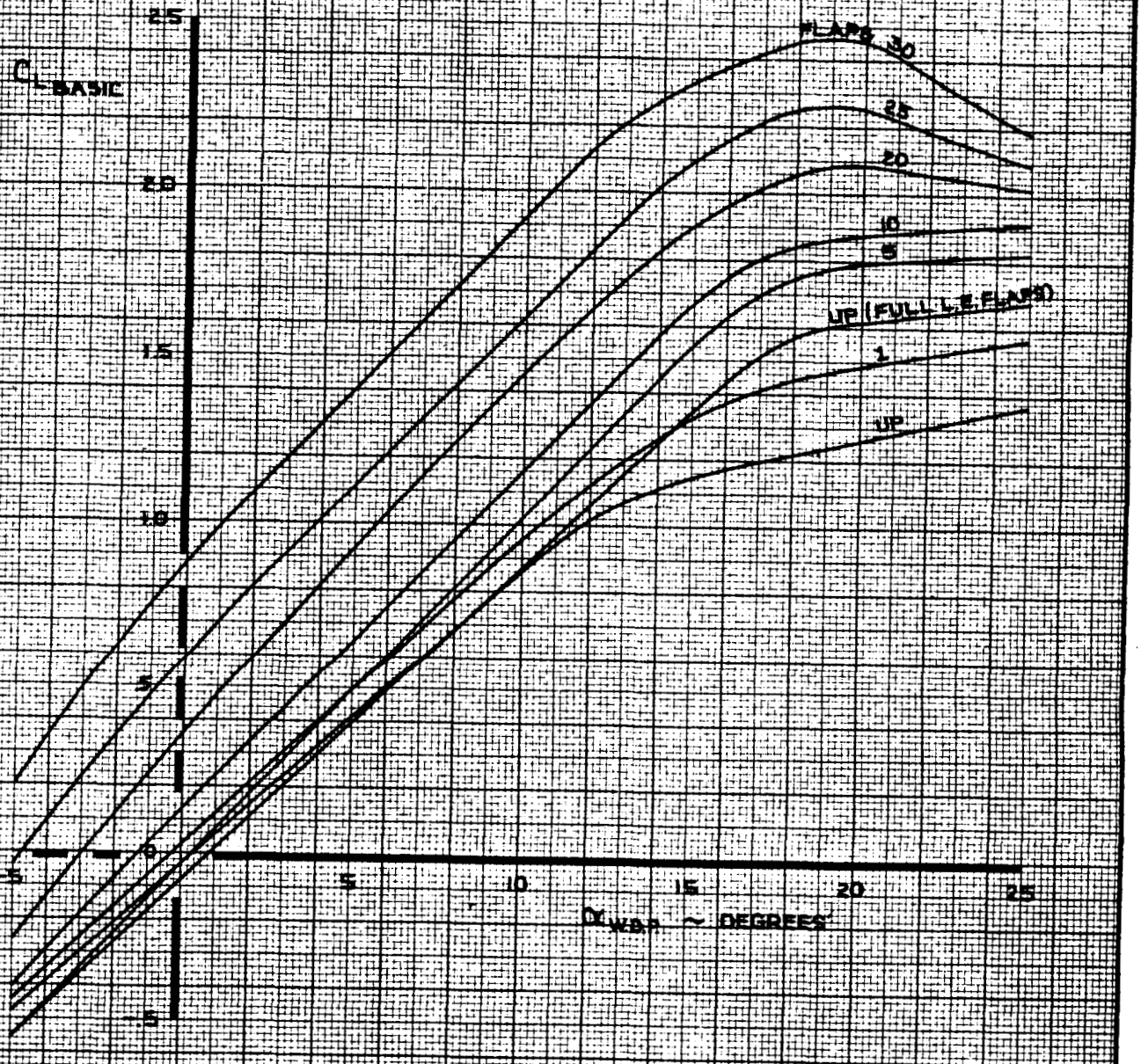

CALC	LOW	11·21·67	REVISED	DATE	LIFT COEFFICIENT EFFECT OF ANGLE OF ATTACK ON BASIC C_L
CHECK	FOSTER	1·24·68	LOW	2·15·68	
APR			BYSTROM	2·16·70	
APR					
INK	KINSMAN	2·18·70			THE BOEING COMPANY

747

D6-30643 Vol. II

PAGE 2.0-7

AD 461 C-R4

K-E ALBANENE 1961 TRACING PAPER REV. D

LOW SPEED

NOTE 1. USE FOR ALL ALTITUDES

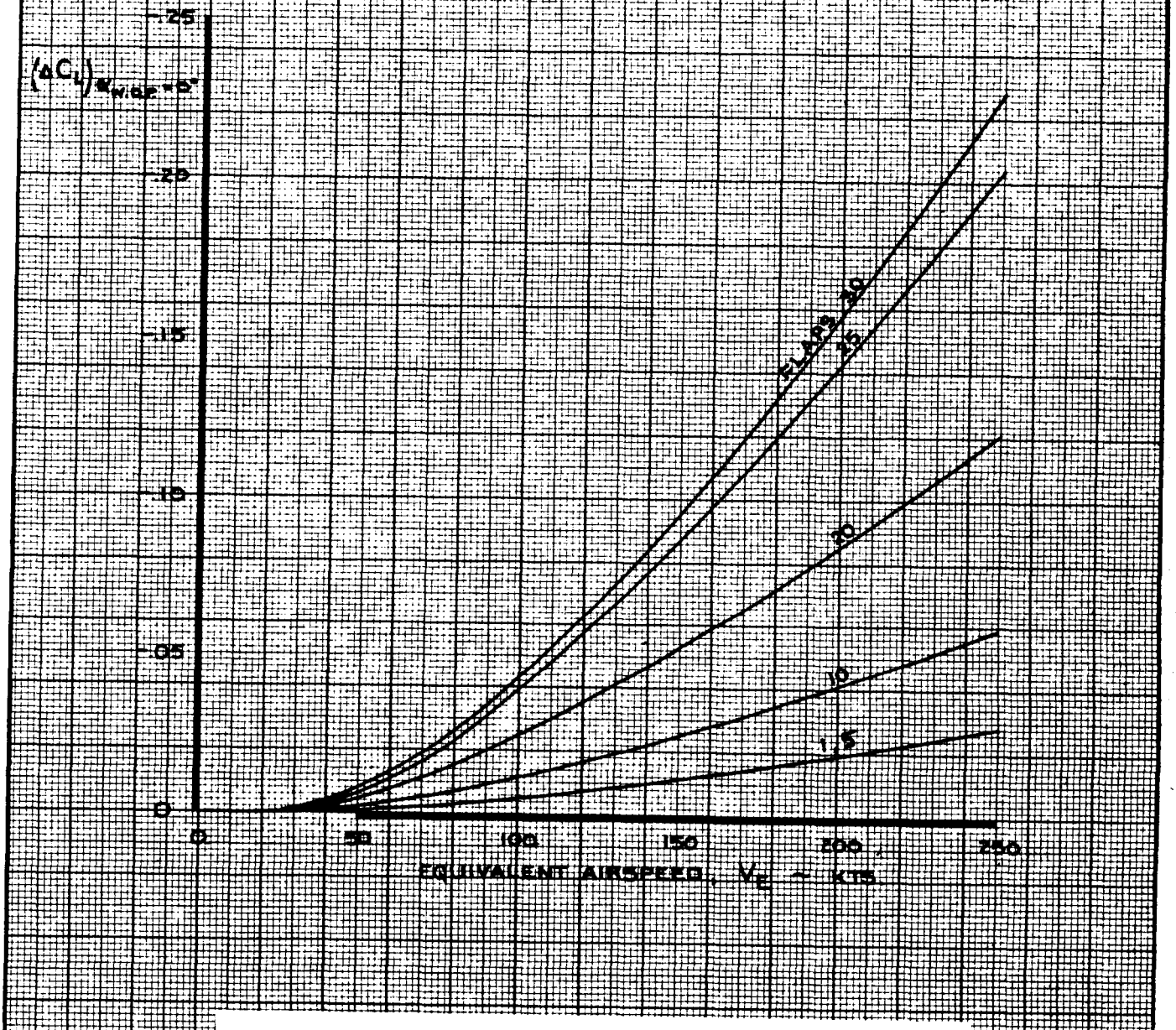

CALC	LOW	11/18/67	REVISED	DATE	LIFT COEFFICIENT EFFECT OF FLAPS ON $(\Delta C_L)_{\alpha_{W.D.P.}=0°}$	747
CHECK	FOSTER	1-24-68	LOW	1-23-70		D6-30643, Vol. II
APR						
APR					THE BOEING COMPANY	PAGE 2.0-9
INK	ODEGARD	11/18/67				

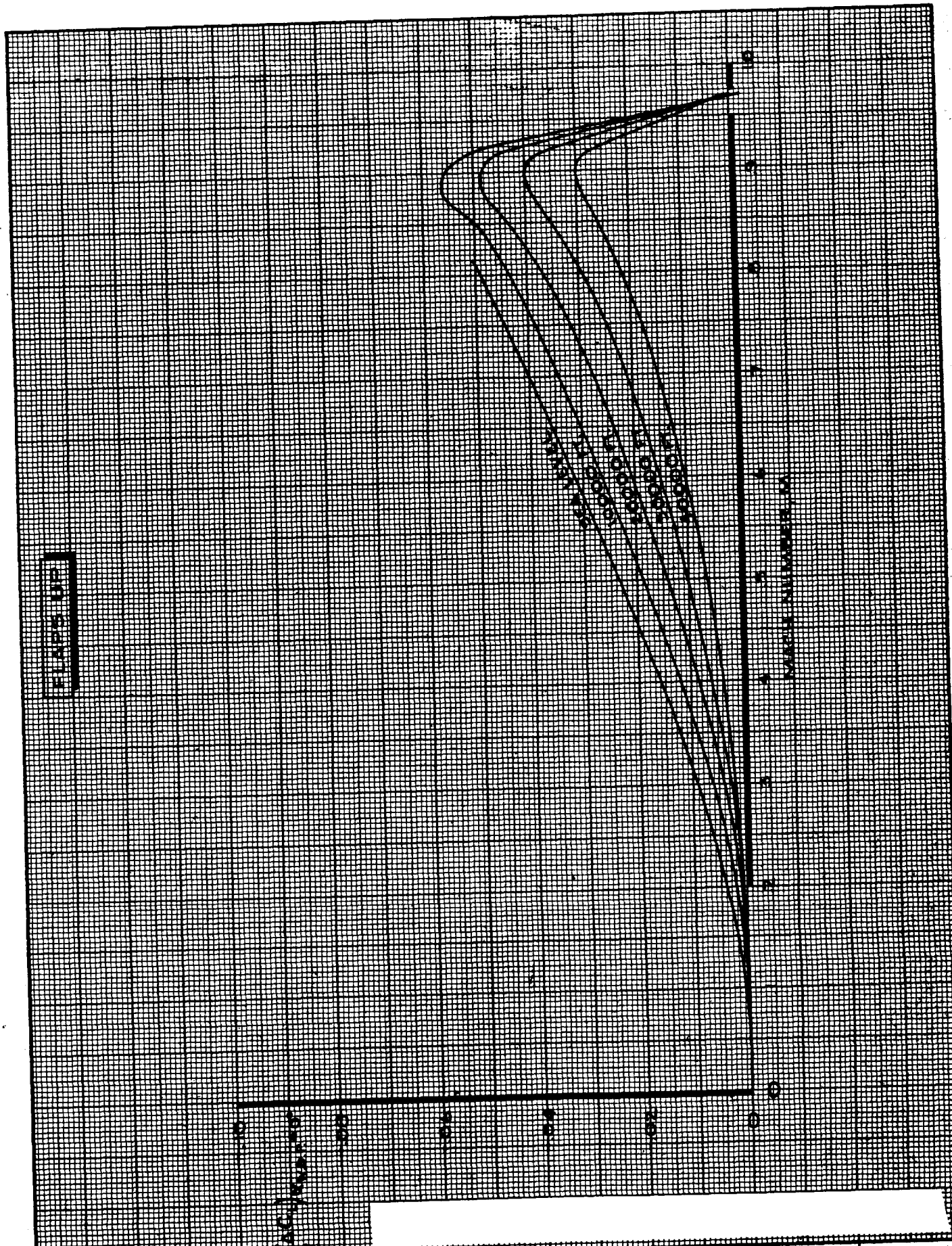

CALC	LOW	10/16/67	REVISED	DATE	LIFT COEFFICIENT	747
CHECK	FOSTER	1.24.68	LOW	6.14.69	AEROELASTIC EFFECT ON $(\Delta C_L)_{\alpha_{W.B.F.}=0^\circ}$	D6-30643 Vol. II
APR						PAGE
APR					THE BOEING COMPANY	2.0-10
INK	ODEGARD	10/16/67				REV. B

$C_{L\phi}$

TD 461 C-R4

LOW SPEED

NOTE 1. USE FOR ALL ALTITUDES

2. $\Delta C_L = \Delta\left(\frac{dC_L}{d\alpha}\right)_{\alpha \text{ W.O.F.}}$

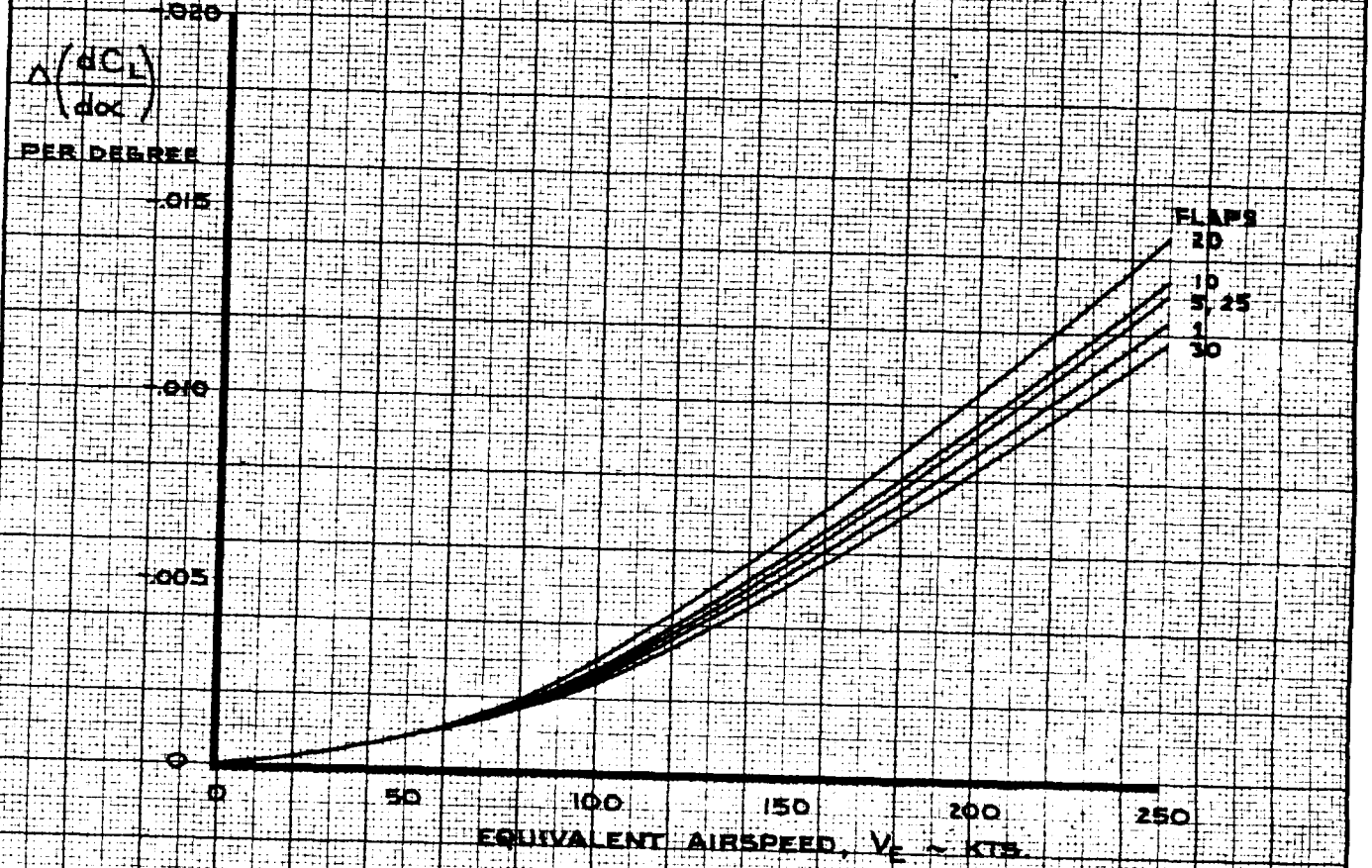

CALC	LOW	11/18/67	REVISED	DATE	LIFT COEFFICIENT EFFECT OF FLAPS ON $\Delta(dC_L/d\alpha)$
CHECK	FOSTER	1-24-68	LOW	1-23-70	
APR					
APR					
INK	ODEGARD	11/18/67			THE BOEING COMPANY

747

D6-30643, Vol. II

PAGE 2.0-11

REV. D

AD 461 C R4

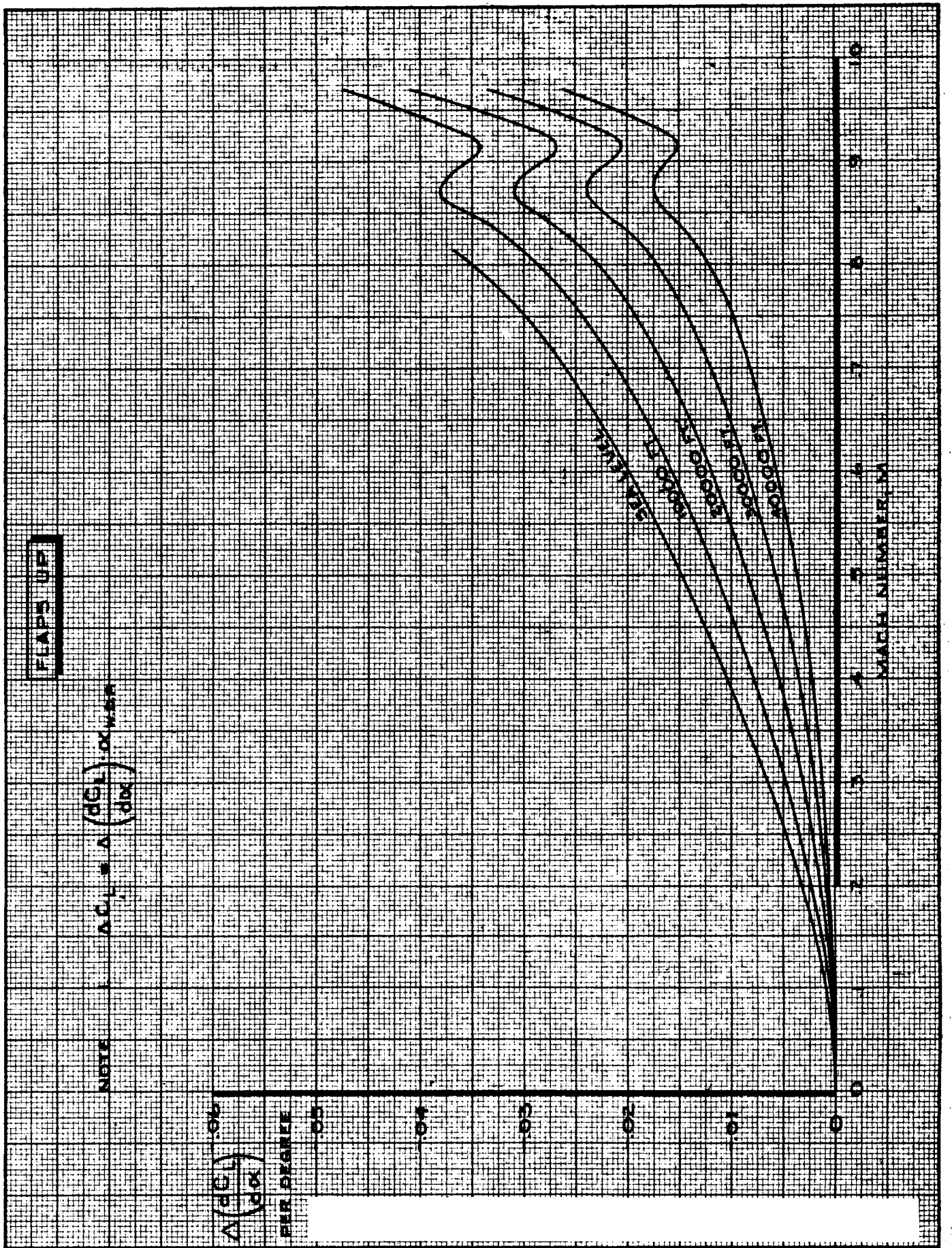

CALC	LOW	10/16/67	REVISED	DATE	LIFT COEFFICIENT AEROELASTIC EFFECT ON $\Delta(dC_L/d\alpha)$
CHECK	FOSTER	1-24-68	LOW	6-14-69	
APR					
APR					
INK	ODEGARD	10/16/67			THE BOEING COMPANY

747
D6-30643 Vol. II
PAGE 2.0-12
REV. B

AD 461 C R4

CLAL

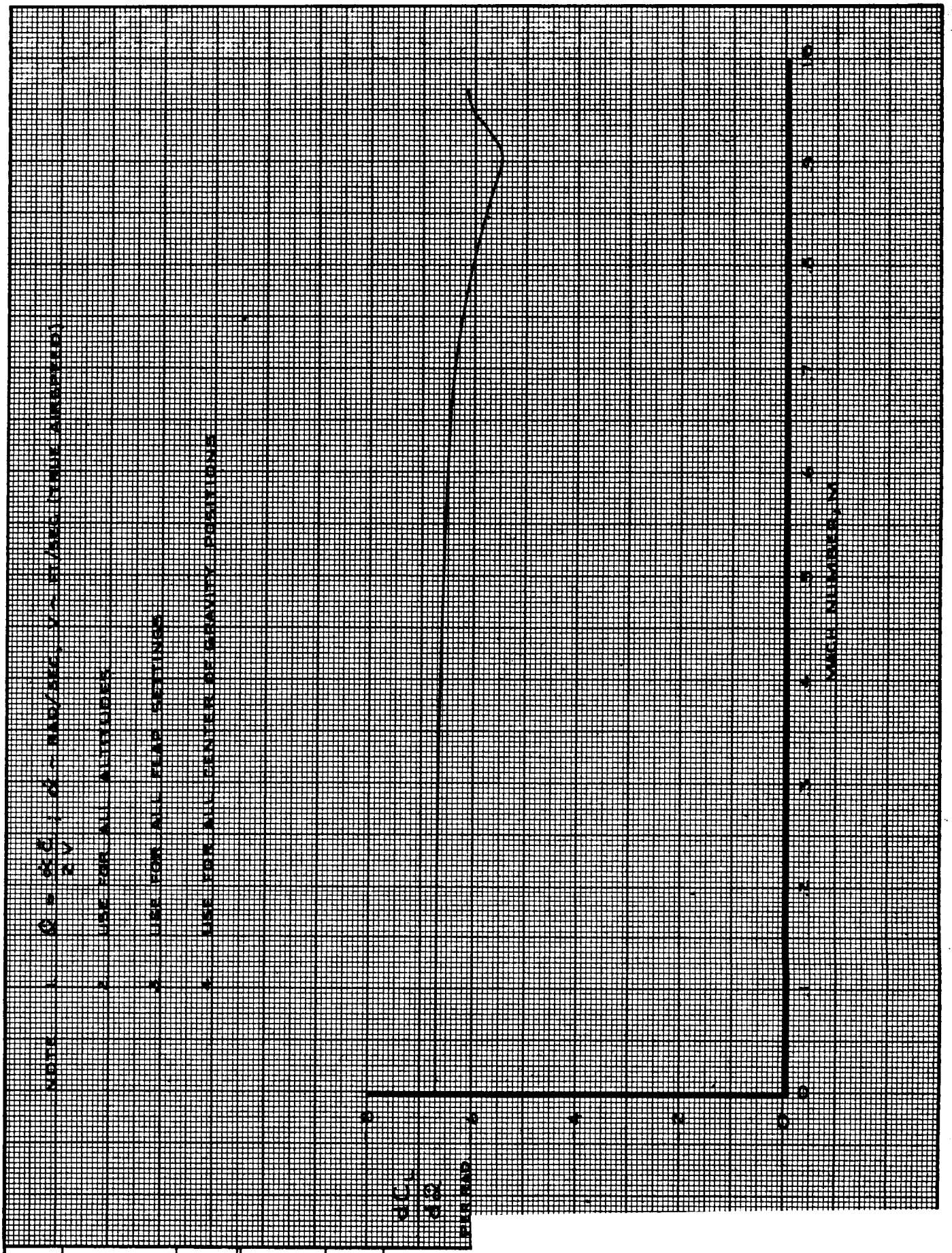

CALC	RICHARDSON	11/27/67	REVISED	DATE
CHECK	CURNUTT	11/29/67		
APR				
APR				
INK	ODEGARD	11/27/67		

LIFT COEFFICIENT
EFFECT OF $\hat{\alpha}$

747

D6-30643
Vol. II

THE BOEING COMPANY

PAGE
2.0-13

TD 461 C-R4

CLALD

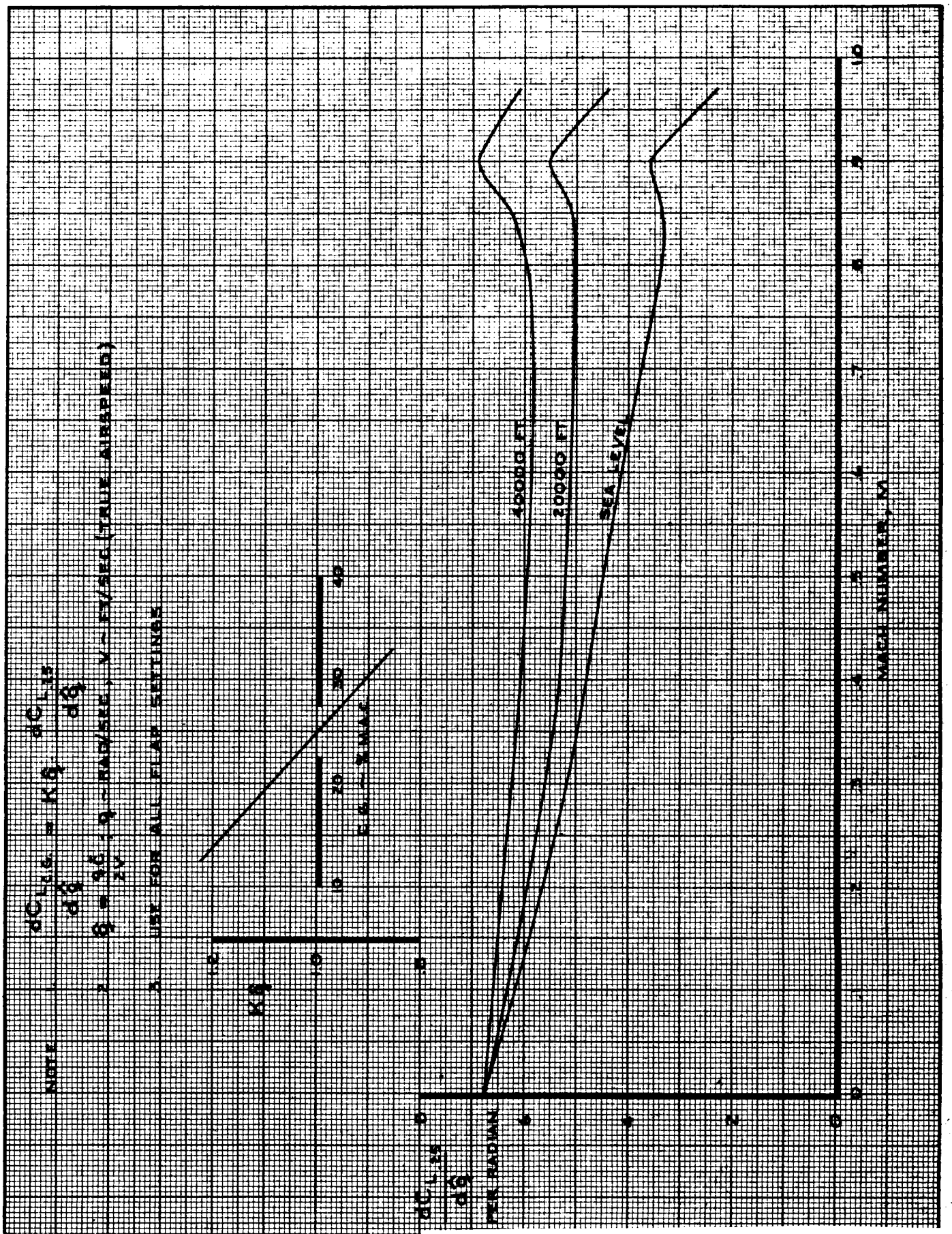

CALC	RICHARDSON	11/27/67	REVISED	DATE
CHECK	CURNUTT	11/29/67	LOW	6-14-69
APR				
APR				
INK	ODEGARD	11/27/67		

LIFT COEFFICIENT
EFFECT OF $\hat{q}$

747

D6-30643
Vol. II

THE BOEING COMPANY

PAGE
2.0-14

TD 461 C-R4

CL 00

REV. B

LOW SPEED

NOTE 1. USE FOR ALL ALTITUDES.

2. $\Delta C_L = \frac{dC_L}{dn_z} \cdot n_z$ ($n_z = 1$ FOR STEADY LEVEL FLIGHT)

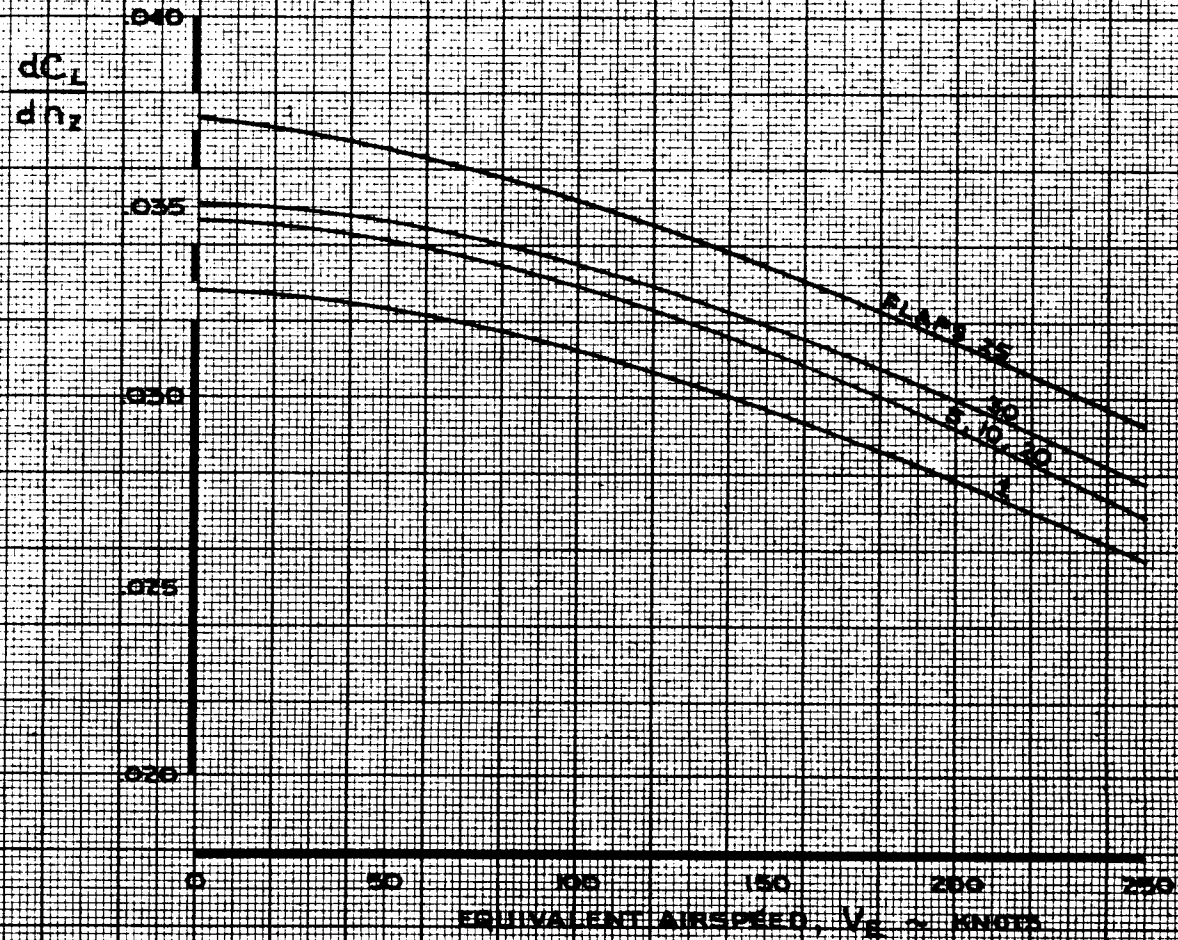

CALC	LOW	11/18/67	REVISED	DATE	LIFT COEFFICIENT EFFECT OF FLAPS ON dC_L/dn_z	747
CHECK	FOSTER	1-24-68	LOW	1-23-70		D6-30643 Vol. II
APR						
APR					THE BOEING COMPANY	PAGE 2.0-15
INK	ODEGARD	11/18/67				

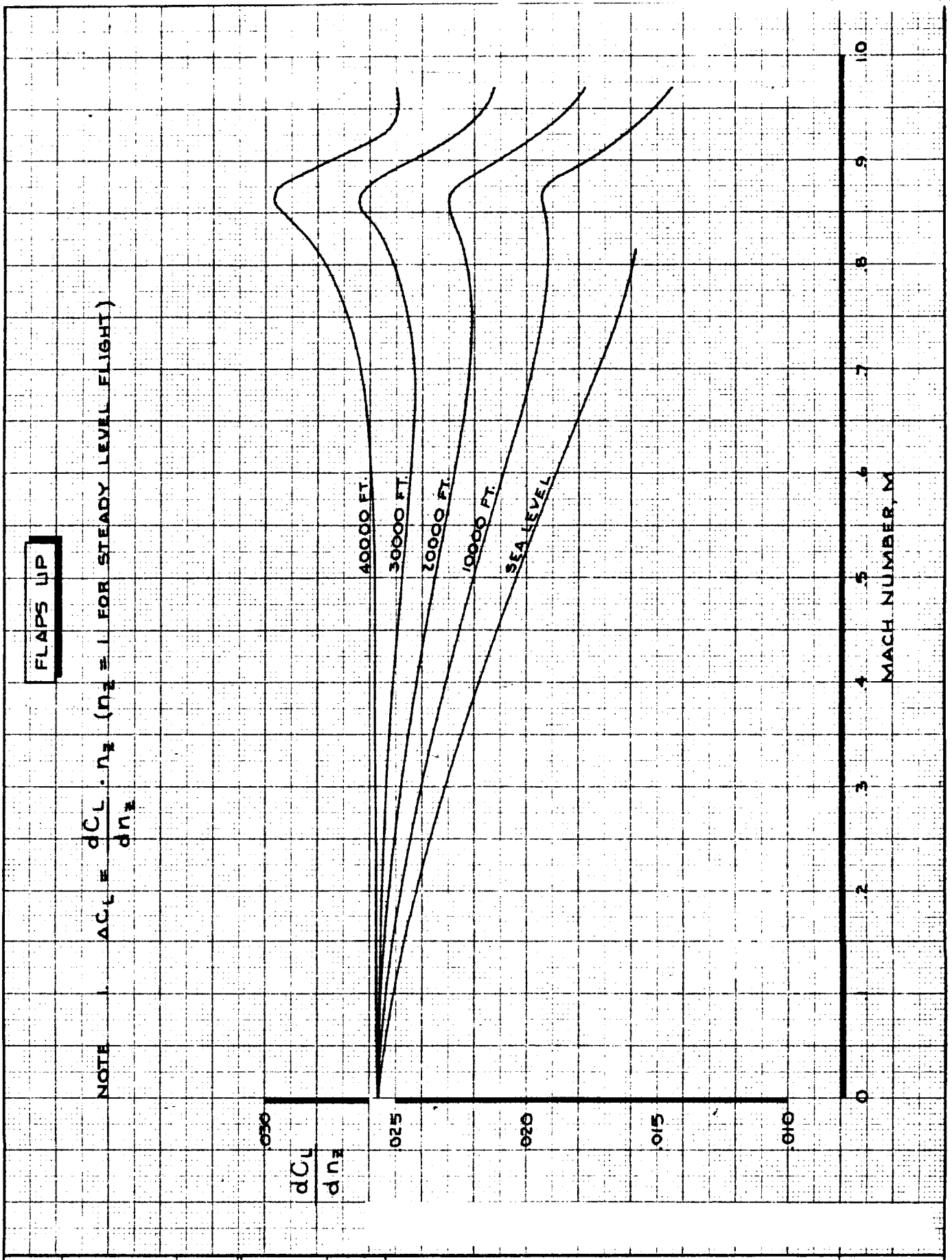

CALC	LOW	10/16/67	REVISED	DATE	LIFT COEFFICIENT EFFECT OF NORMAL LOAD FACTOR
CHECK	FOSTER	1-24-68	LOW	6-14-69	
APR					
APR					
INK	OREGARD	10/16/67			THE BOEING COMPANY

747
D6-30643 Vol. II
PAGE 2.0-16
REV. B

CLNZ

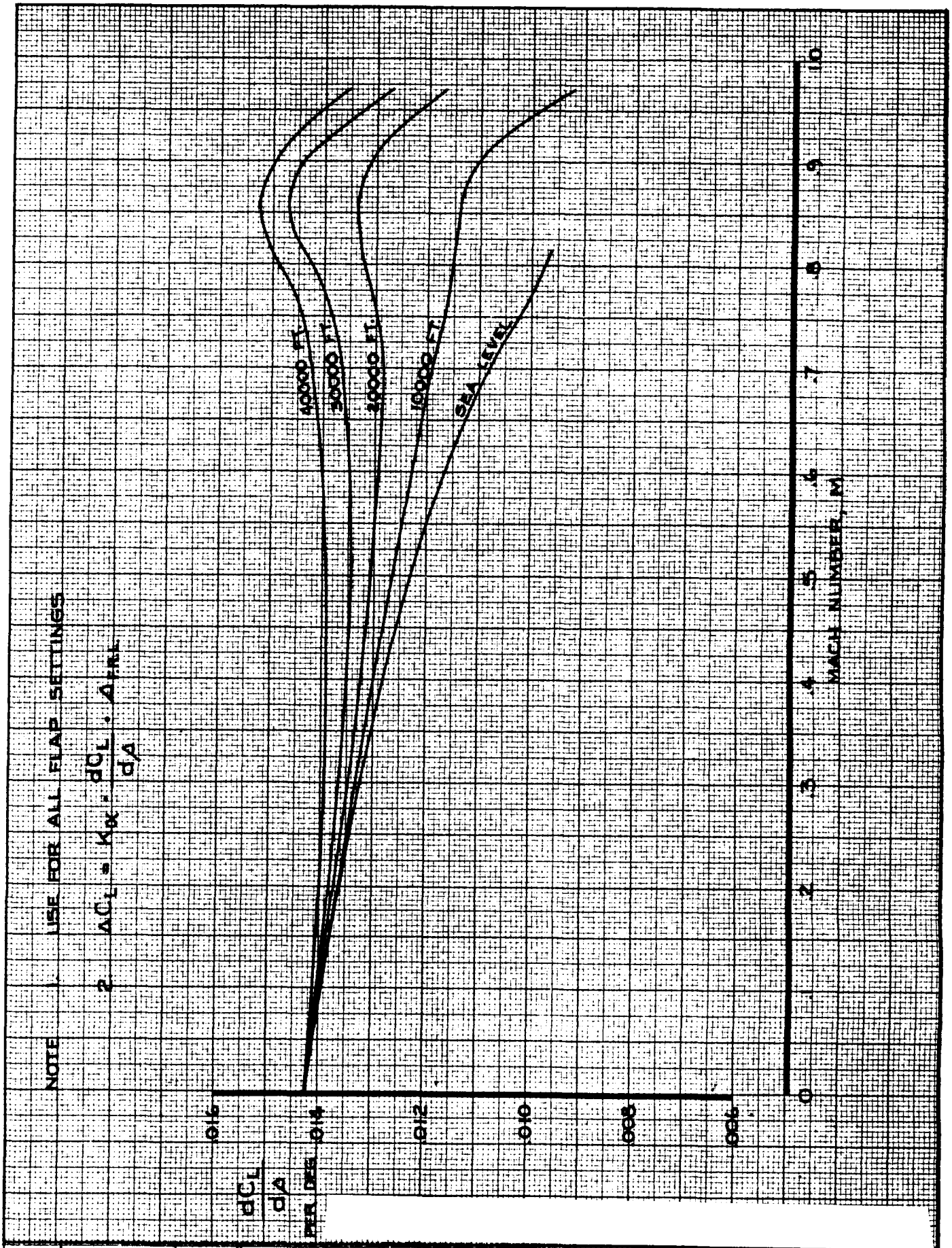

CALC	LOW	10-11-67	REVISED	DATE	LIFT COEFFICIENT EFFECT OF STABILIZER Δ
CHECK	FOSTER	1-24-68	FOSTER	9-25-69	
APR					
APR					
INK	ODEGARD	10-11-67			THE BOEING COMPANY

747
D6-30643 Vol. II
PAGE 2.0-17

AD 461 C-R4

USE: CLDS = -.2678 CMDS

K-E ALBANENE 1961 REV. D

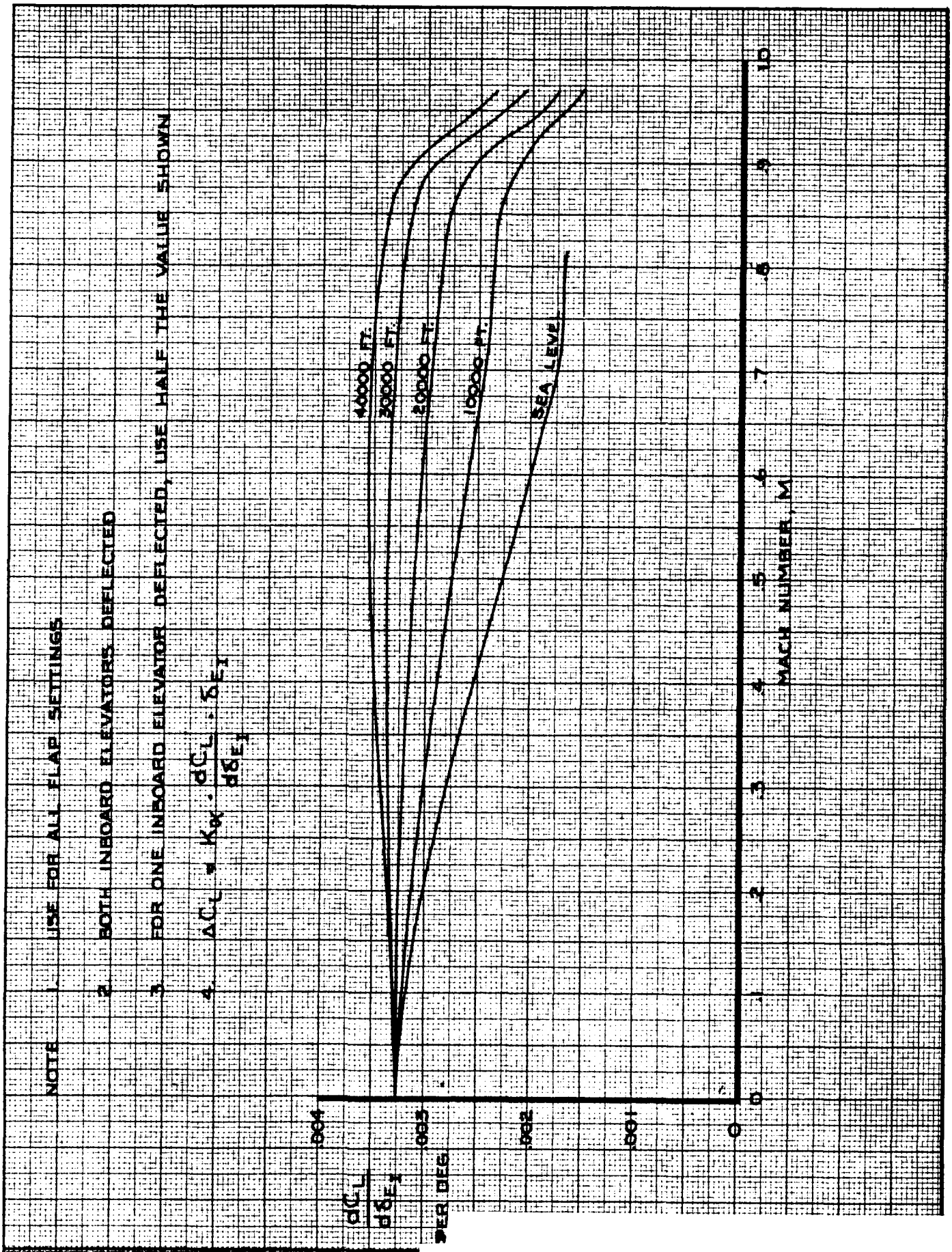

CALC	LOW	10-9-67	REVISED	DATE
CHECK	FOSTER	1-24-68	FOSTER	9-25-69
APR				
APR				
INK	ODEGARD	10-9-67		

LIFT COEFFICIENT
EFFECT OF INBOARD ELEVATORS

747

D6-30643, Vol. II

THE BOEING COMPANY

PAGE 2.0-18

AD 461 C-R4

USE: $C_{LDEI} = -.2538\ C_{MDEI}$

K-E ALBANENE 1961 TRACING PAPER REV. D

NOTE

1. USE FOR ALL FLAP SETTINGS
2. BOTH OUTBOARD ELEVATORS DEFLECTED
3. FOR ONE OUTBOARD ELEVATOR DEFLECTED, USE HALF THE VALUE SHOWN
4. $\Delta C_L = K_{\delta E} \cdot dC_L \cdot \delta_{E_0}$ $d\delta_{E_0}$

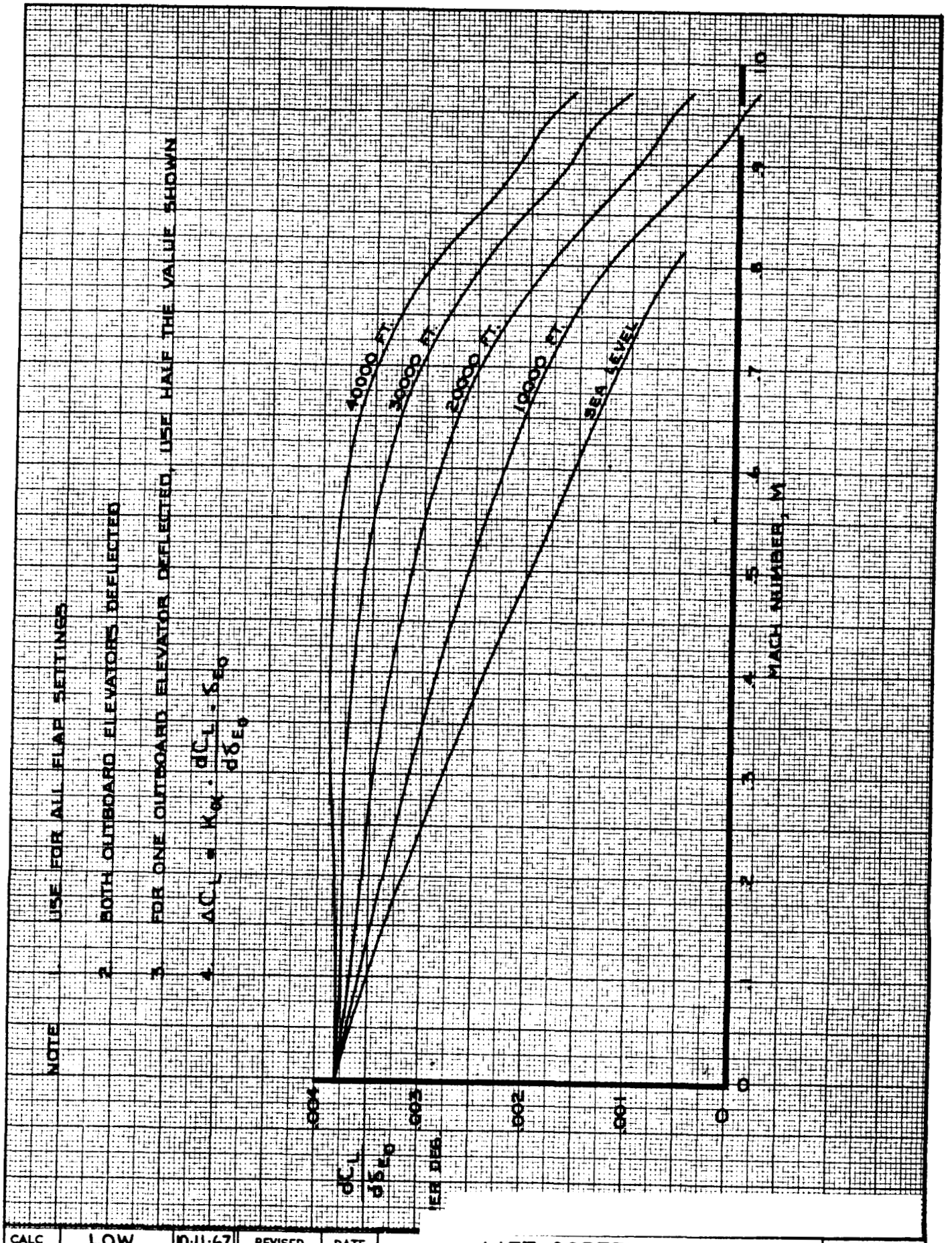

CALC	LOW	10-11-67	REVISED	DATE
CHECK	FOSTER	1-24-68	FOSTER	9-26-69
APR				
APR				
INK	ODEGARD	10-11-67		

LIFT COEFFICIENT
EFFECT OF OUTBOARD ELEVATORS

747

D6-30643
Vol. II

THE BOEING COMPANY

PAGE
2.0-19

AD 461 C-R4

USE : $CLD\delta = -.2538\ CMD\delta$

K-E ALBANENE 1961 TRACING PAPER REV. D

NOTE 1. USE FOR ALL SPOILER PANELS

2. PANELS 5, 6, 7 AND 8 LIMITED TO 20 DEG MAX DEFLECTION

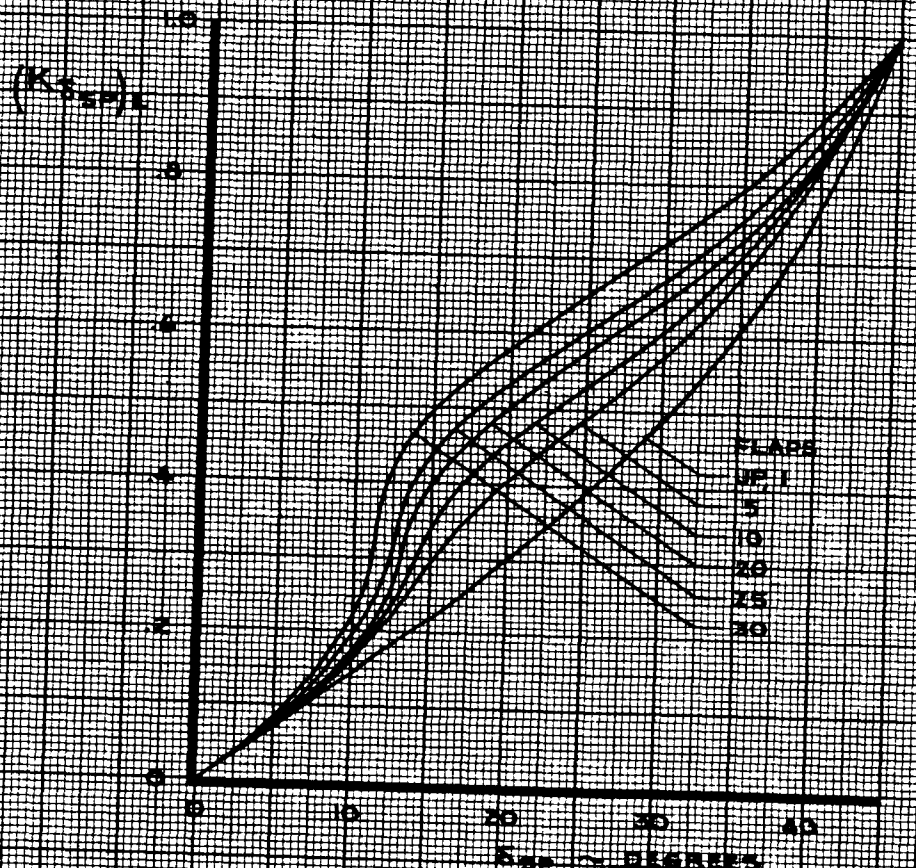

CALC	KUPCIS	12/26/67	REVISED	DATE	LIFT COEFFICIENT EFFECTIVENESS FACTOR SPOILERS	747
CHECK	FOSTER	1-24-68	KUPCIS	6-2-69		
APR			KUPCIS	8-22-69		D6-30643 Vol. II
APR			LOW	2-14-70		
INK	ODEGARD	12/26/67			THE BOEING COMPANY	PAGE 2.0-20

TD 461 C-R4

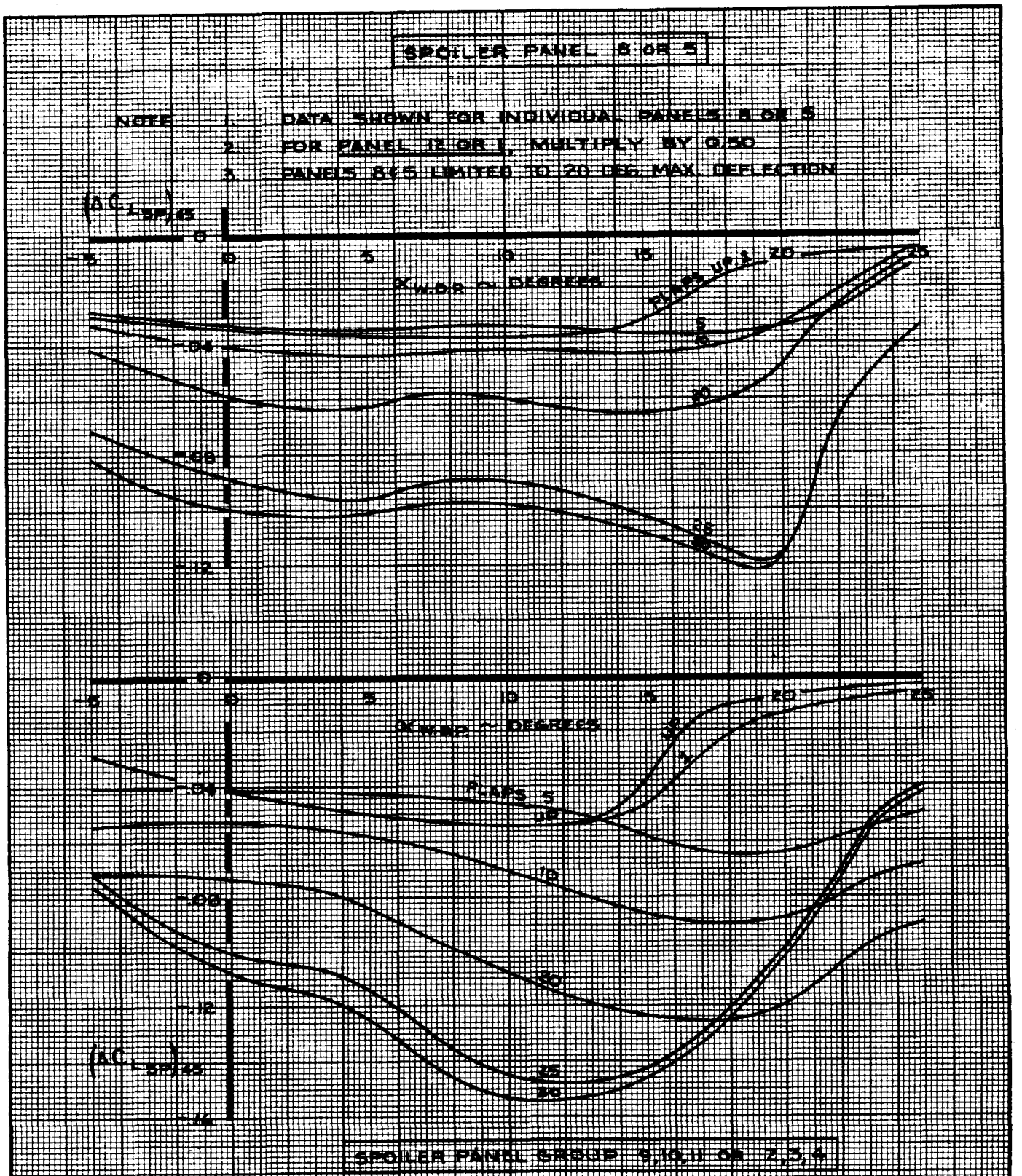

CALC	KUPCIS	12/21/67	REVISED	DAT
CHECK	FOSTER	1.24.68	KUPCIS	6.2.69
APR			LOW	2.14.70
APR				
INK	ODEGARD	12/21/67		

LIFT COEFFICIENT
EFFECT OF SPOILERS

747

D6-30643
Vol. II

THE BOEING COMPANY

PAGE 2.0-21

REV. D

SPOILER PANELS 6 AND 7

NOTE 1. DATA SHOWN FOR BOTH PANELS OPERATING

2. PANELS LIMITED TO 20 DEG. MAX. DEFLECTION

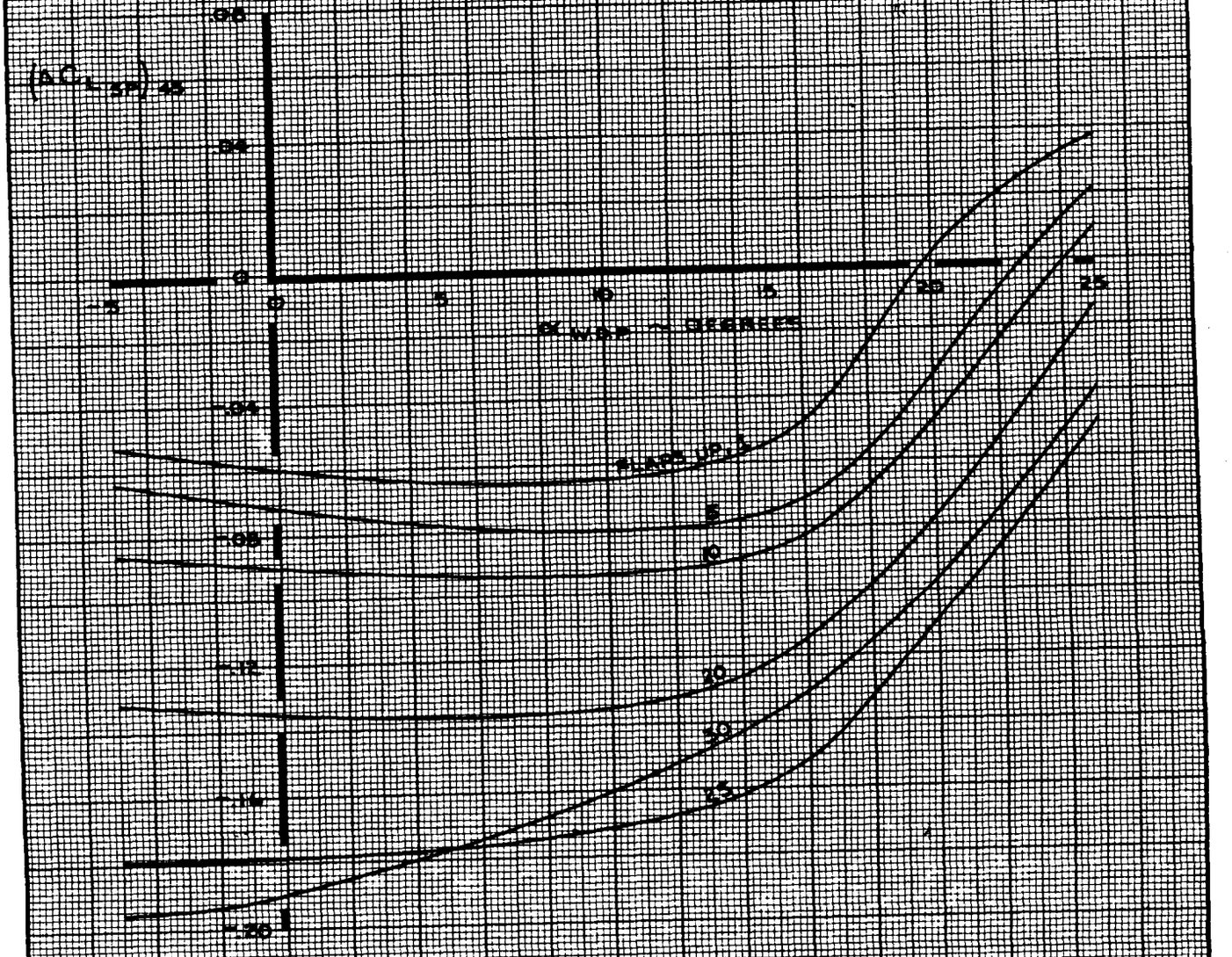

CALC	KUPCIS	12/26/67	REVISED	DATE	LIFT COEFFICIENT EFFECT OF SPOILERS (6 AND 7)
CHECK	FOSTER	1-24-68	KUPCIS	8-22-69	
APR			LOW	2-14-70	
APR					THE BOEING COMPANY
INK	ODEGARD	12/26/67			

747

D6-30643 Vol. II

PAGE 2.0-22

REV. D

CALC	KUPCIS	12/27/67	REVISED	DATE	LIFT COEFFICIENT EFFECT OF MACH NUMBER ON SPOILERS	747 D6-30643 Vol. II
CHECK	FOSTER	1-24-68				
APR						
APR					THE BOEING COMPANY	PAGE 2.0-23
INK	ODEGARD	12/27/67				

TD 461 C-R4

63

CLSPM

CALC	LOW	4/16/68	REVISED	DATE	LIFT COEFFICIENT AERODELASTIC EFFECT ON LIFT COEFFICIENT DUE TO SPOILERS (8ORS, 7 AND 6)
CHECK			LOW	6-18-69	
APR					
APR					
INK	Glenn	4-16-68			

747

D6-30643
Vol. II

THE BOEING COMPANY

PAGE 2.0-24

REV. C

AD 461 C R4

I.F.C.D.

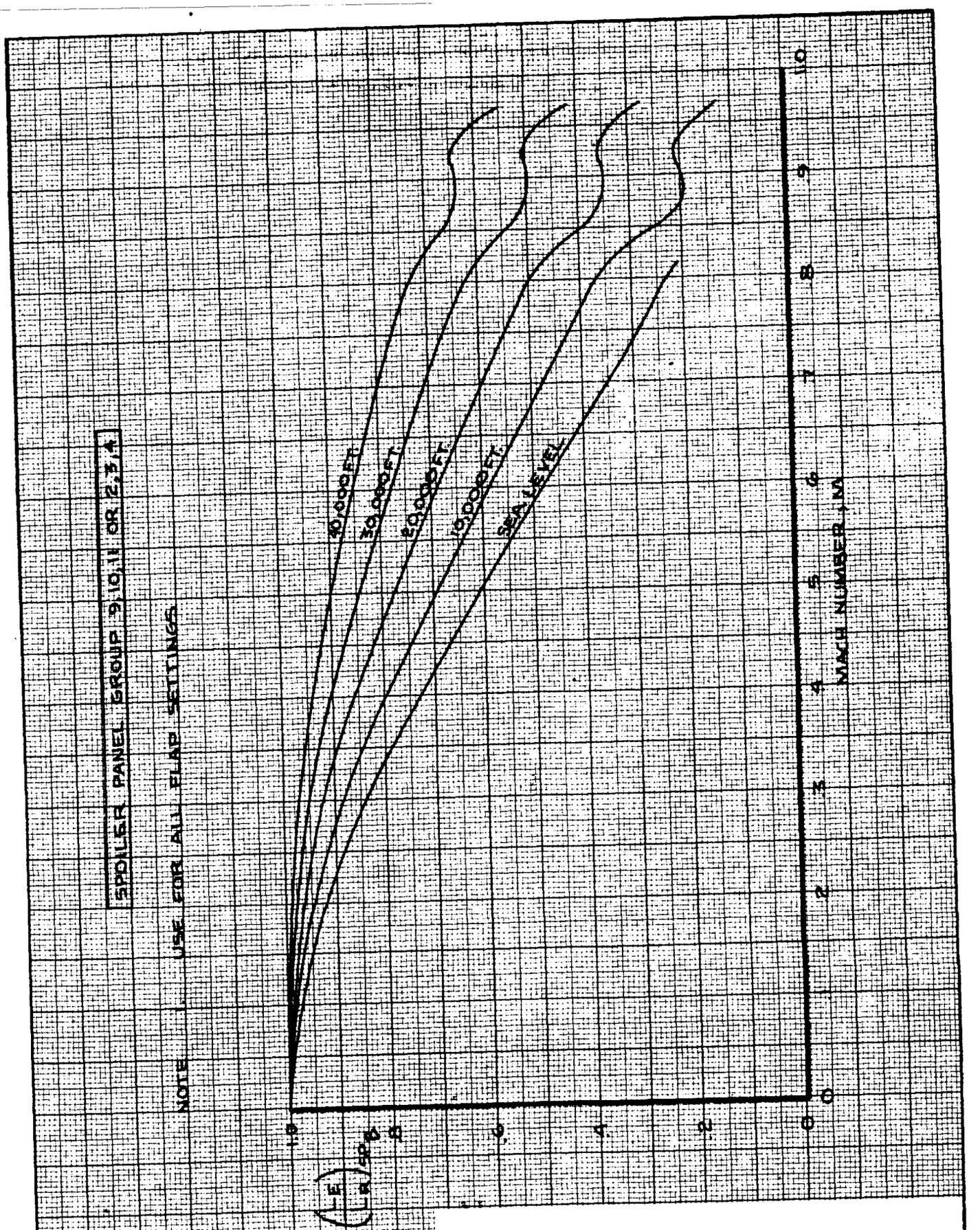

CALC	LOW	4/16/68	REVISED	DATE	LIFT COEFFICIENT	747
CHECK			LOW	6-14-69	AEROELASTIC EFFECT ON LIFT COEFFICIENT DUE TO SPOILERS (9,10,11 OR 2,3,9)	D6-30643 Vol. II
APR						
APR					THE BOEING COMPANY	PAGE 20-25
INK	Glenn	4-16-8				

AD 461 C R4

LESPB

REV. B

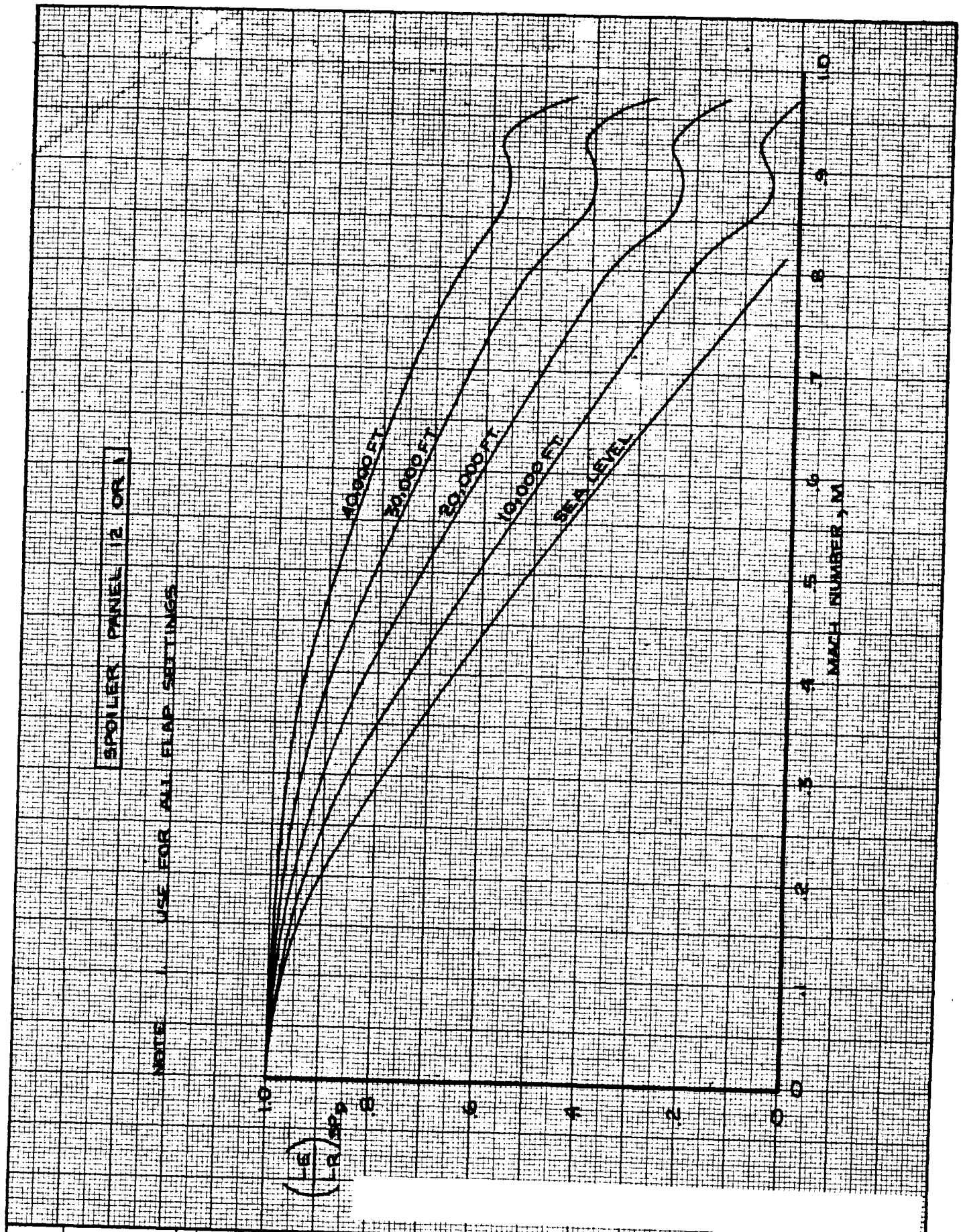

CALC	LOW	4/16/68	REVISED	DATE	LIFT COEFFICIENT	747
CHECK			LOW	6-14-69	AEROELASTIC EFFECT ON LIFT COEFFICIENT DUE TO SPOILERS (12 OR 1)	D6-30643 Vol. II
APR						
APR					THE BOEING COMPANY	PAGE 2.0-26
INK	Glenn	4-16-8				

AD 461 C R4

LESPD

REV. B

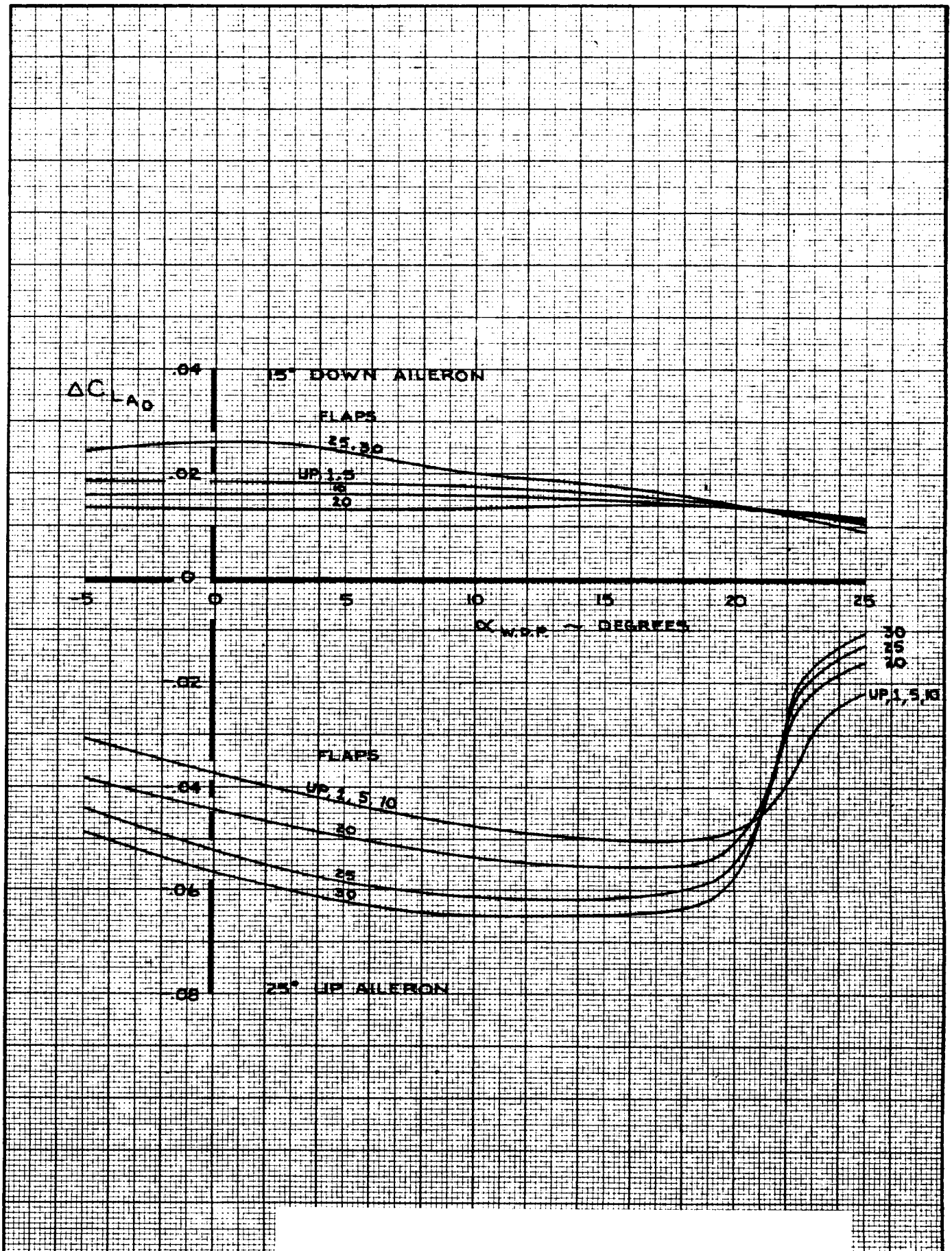

CALC	KUPCIS	11/16/67	REVISED	DATE	LIFT COEFFICIENT EFFECT OF OUTBOARD AILERON
CHECK	FOSTER	1-24-68	KUPCIS	4-2-68	
APR			LOW	2-14-70	
APR					
INK	ODEGARD	11/16/67			THE BOEING COMPANY

747
D6-30643, Vol. II
PAGE 2.0-27

LOW SPEED

NOTE 1. FREE AIR

2. FOR LANDING GEAR FAILURE, REPLACE $\Delta C_{L_{GEAR}}$ BY

$$\Delta C_{L_{GEAR\ FAILURE}} = K_{L_{GEAR}} \cdot \Delta C_{L_{GEAR}}$$

GEAR SELECTION	GEAR FAILURE	$K_{L_{GEAR}}$
DOWN	WING GEARS FAIL TO EXTEND	0.1
UP	WING GEARS FAIL TO RETRACT	0.9
✓	ONE WING GEAR FAILS TO RETRACT	0.45
✓	ONE BODY GEAR FAILS TO RETRACT	0.6
✓	ONE BODY GEAR DOOR FAILS TO RETRACT	0.3
✓	NOSE GEAR FAILS TO RETRACT	0

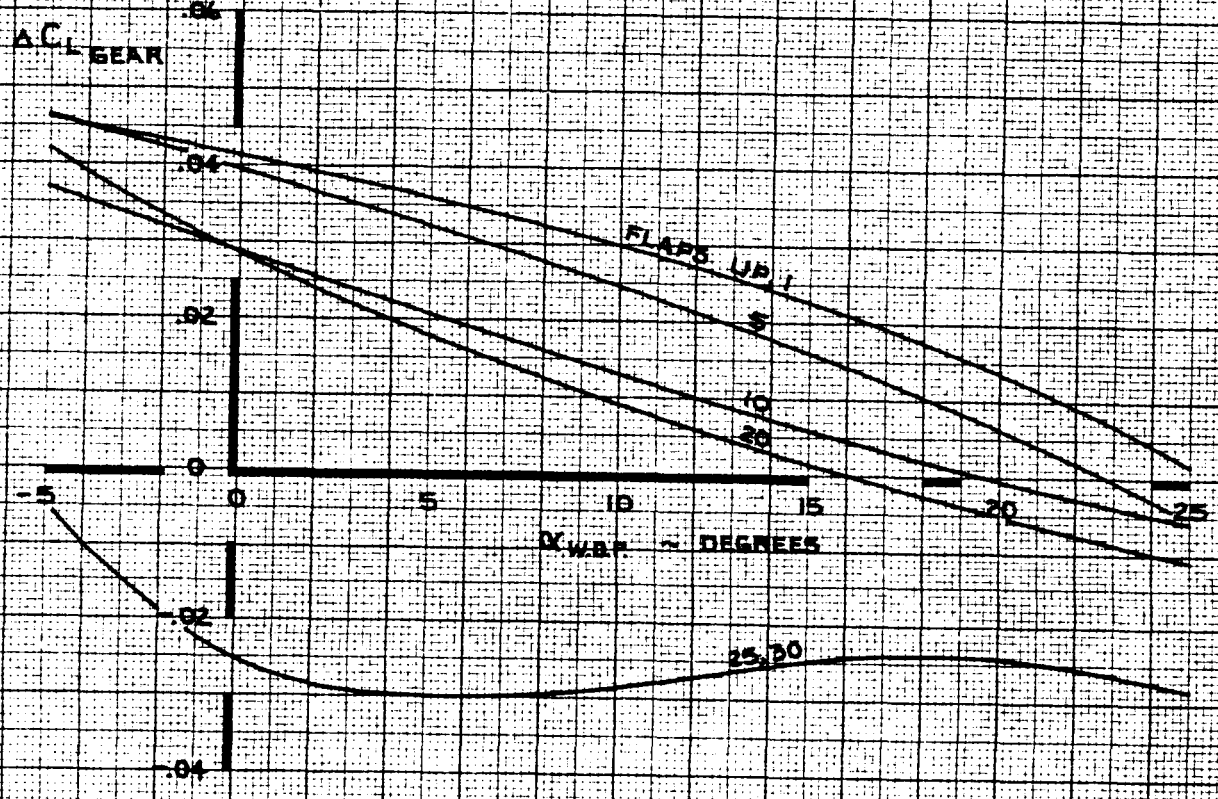

CALC	LOW	9-20-67	REVISED	DATE	LIFT COEFFICIENT EFFECT OF LANDING GEAR
CHECK	FOSTER	1-24-68	LOW	6-9-69	
APR			BYSTROM	2-16-70	
APR					
INK	ODEGARD	2-16-70			THE BOEING COMPANY

747
D6-30643 Vol. II
PAGE 2.0-29

AD 461 C-R4

K-E ALBANENE 1981 TRACING PAPER REV. D

NOTE 1. USE FOR ALL GEAR EFFECTS

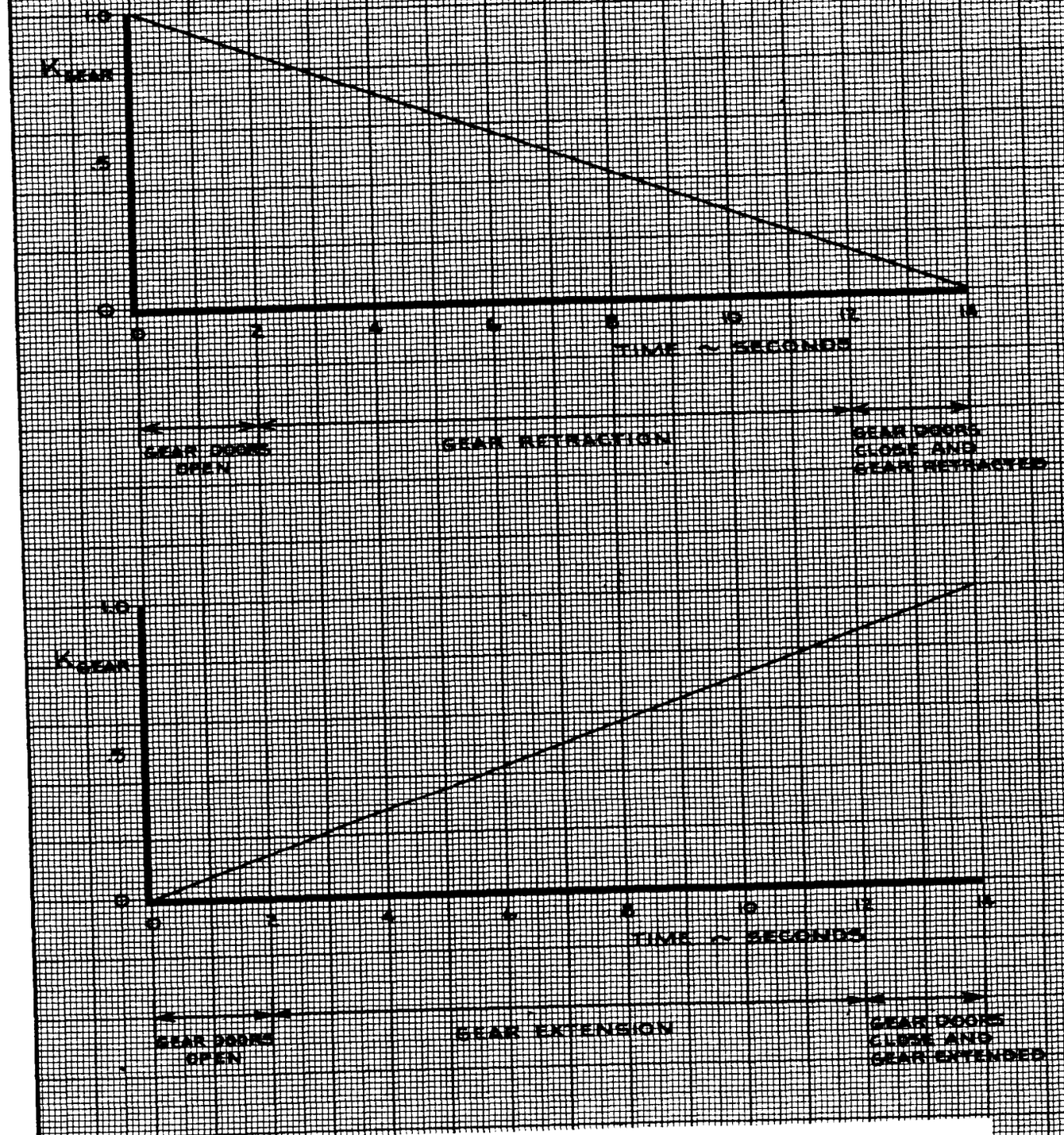

CALC	LOW	12/16/67	REVISED	DATE	LANDING GEAR EFFECTIVENESS FACTOR	747
CHECK	FOSTER	1-24-68				D6-30643 Vol. II
APR						
APR					THE BOEING COMPANY	PAGE 2.0-28
INK	ODEGARD	12/16/67				REV. A

TD 461 C-R4

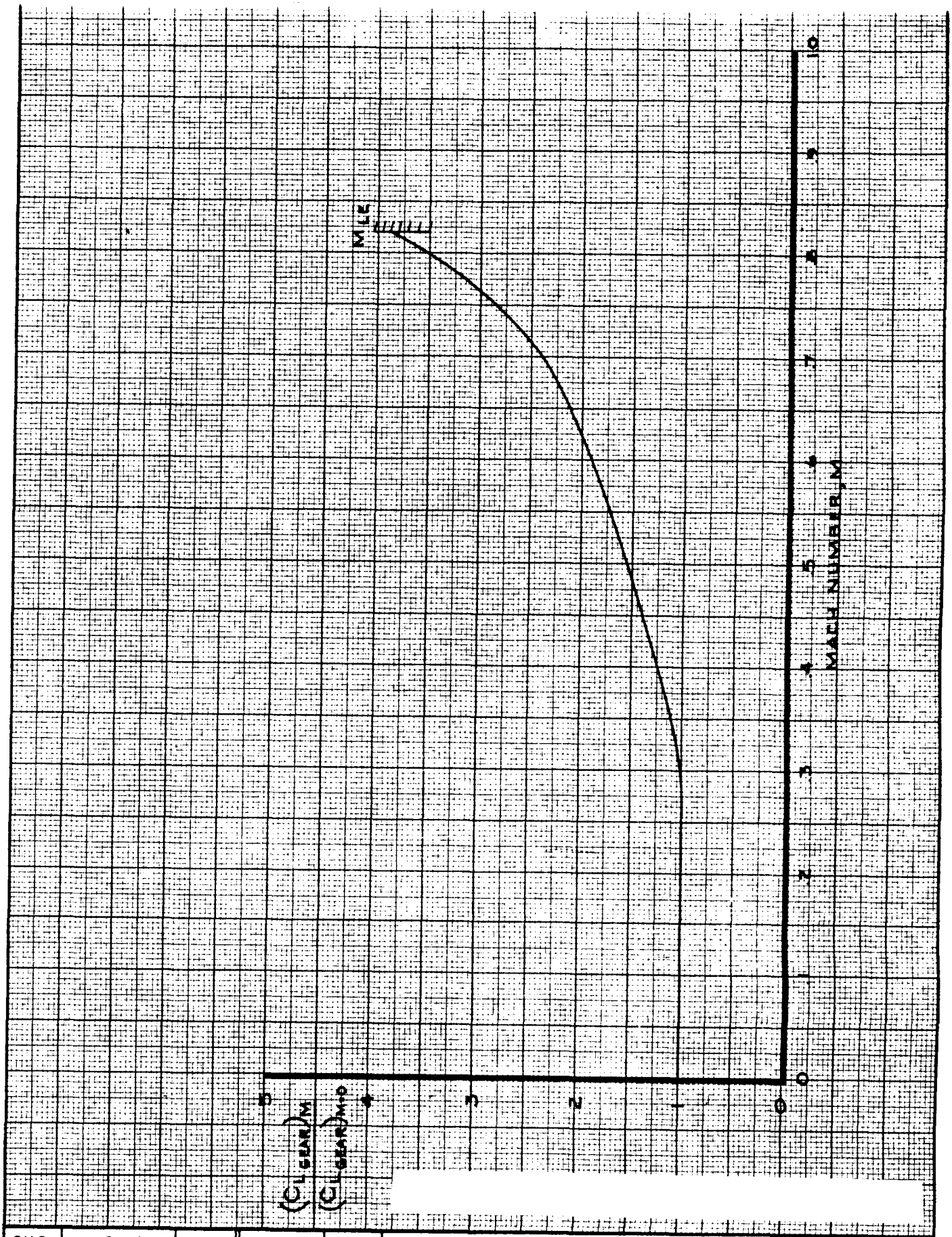

CALC	LOW	11·9·67	REVISED	DATE	LIFT COEFFICIENT EFFECT OF MACH NUMBER ON $\Delta C_{L_{GEAR}}$
CHECK	FOSTER	1·24·68			
APR					
APR					
INK	ODEGARD	11·9·67			THE BOEING COMPANY

747

D6-30643 Vol. II

PAGE 2.0-30

REV. A

AD 461 C R4

CLGM

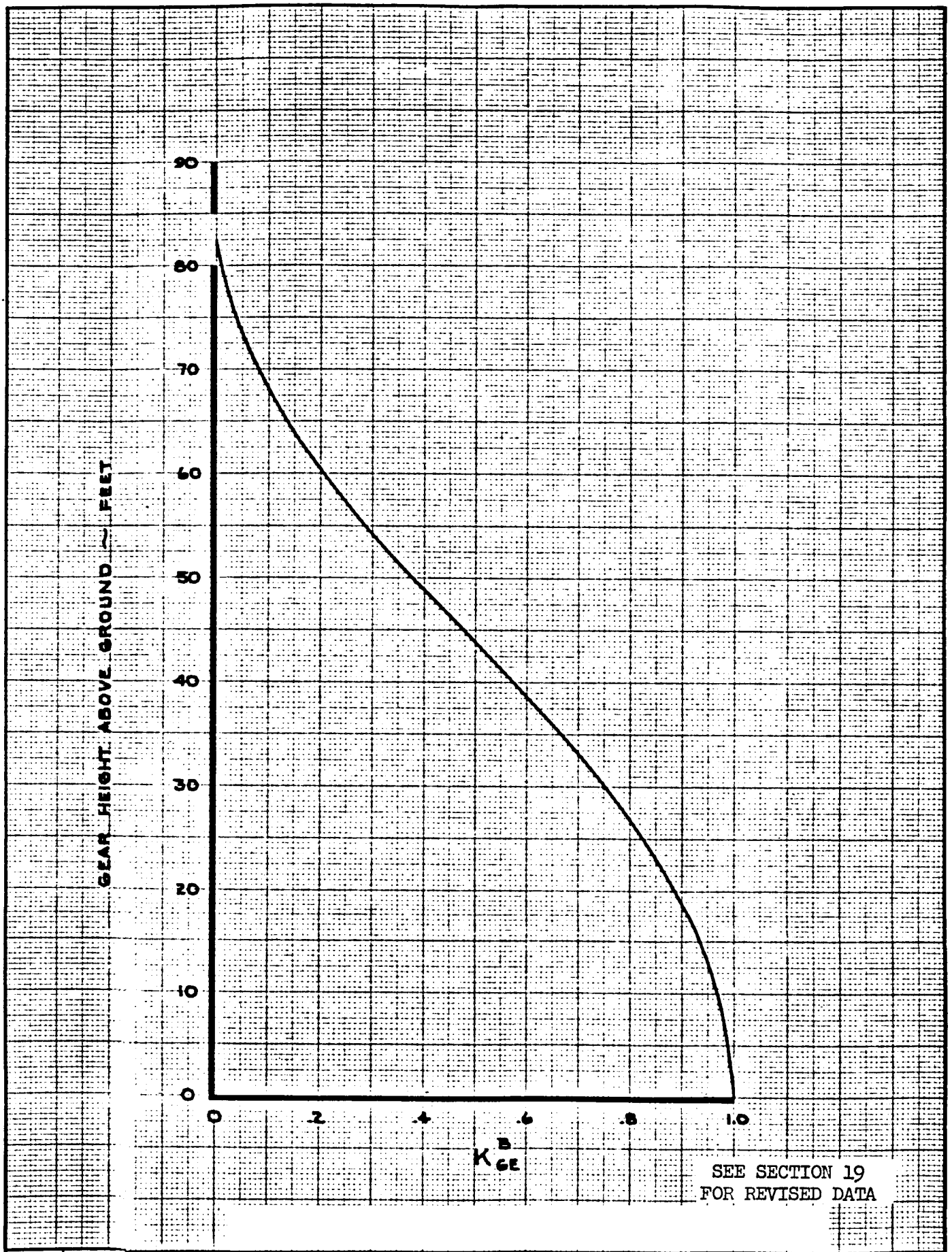

SEE SECTION 19
FOR REVISED DATA

CALC	CURNUTT	12/12/67	REVISED	DATE	GROUND EFFECT HEIGHT FACTOR, K^{B}_{GE}	747
CHECK	FOSTER	1-24-68				D6-30643 Vol. II
APR						
APR					THE BOEING COMPANY	PAGE 2.0-31
INK	ODEGARD	12/12/67				REV. A

TD 461 C-R4

NOTE 1. GEAR ON GROUND

2 $K^{B}_{GE} = 1.0$

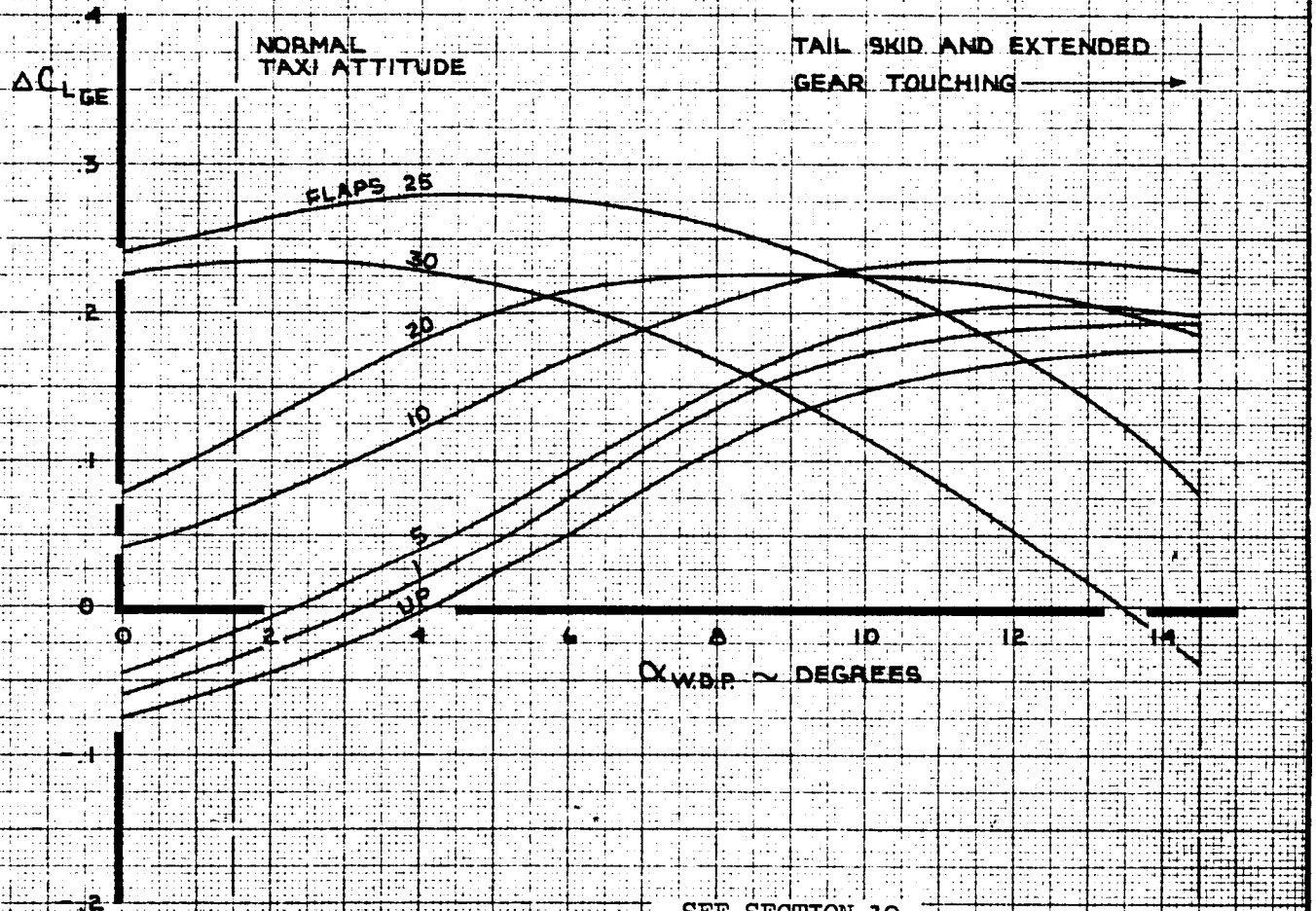

SEE SECTION 19
FOR REVISED DATA

CALC	CURNUTT	12-12-67	REVISED	DATE
CHECK	FOSTER	1-24-68	CURNUTT	3-5-70
APR				
APR				
INK	KINSMAN	3-5-70		

LIFT COEFFICIENT
GROUND EFFECT

THE BOEING COMPANY

747
D6-30643, Vol. II
PAGE 2.0-32

TD 461 C-R4

K-E ALBANENE 195L REV. D

NOTE 1. DATA APPLICABLE FOR SYMMETRIC OR ASYMMETRIC (MONITOR LIMITED) FLAP FAILURE.

THESE DATA NOT INCLUDED IN NASA SIMULATION

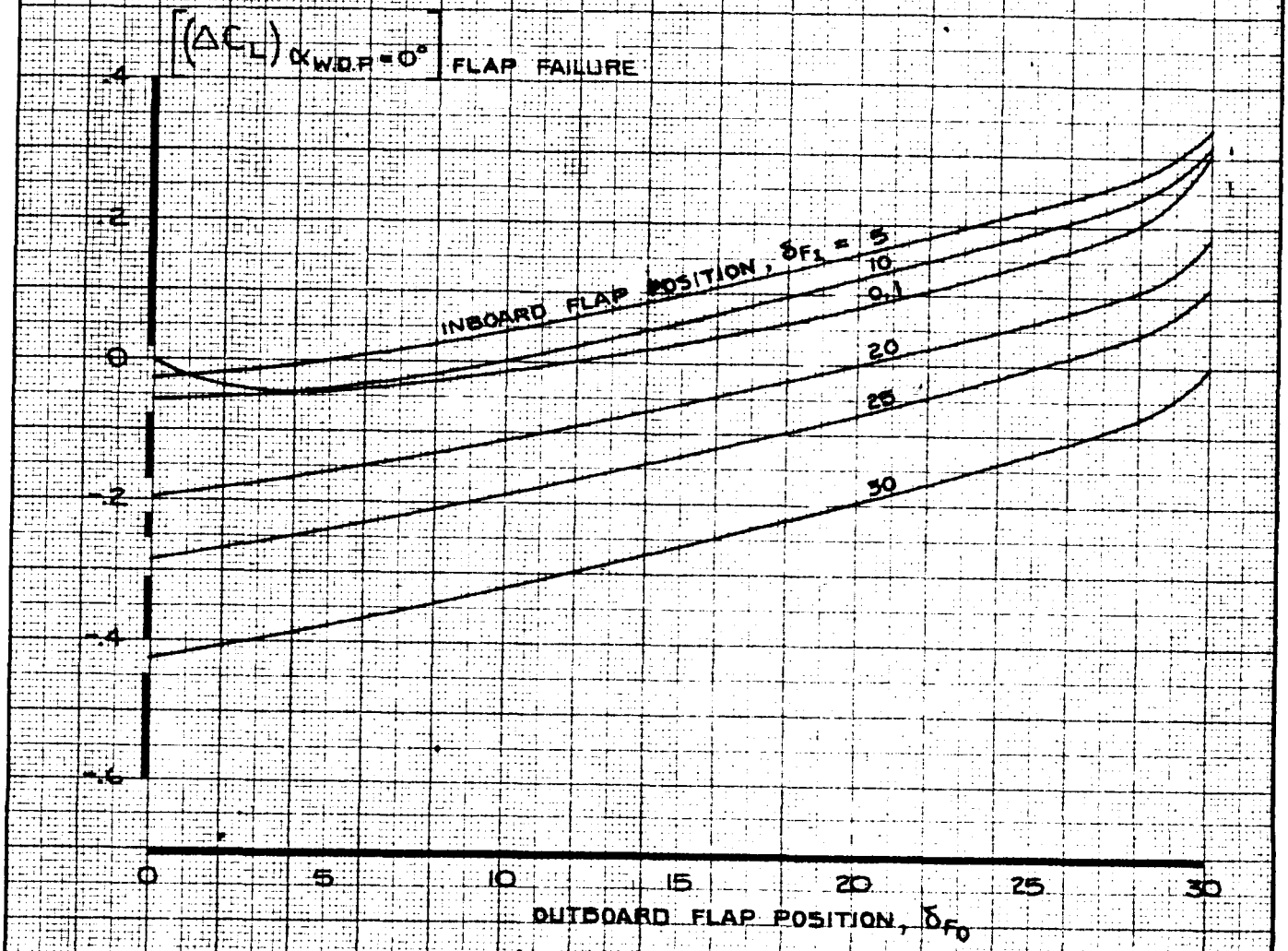

CALC	LOW	5-3-69	REVISED	DATE	LIFT COEFFICIENT EFFECT OF FLAPS ON $\left[(\Delta C_L)_{\alpha_{W.D.R=0^\circ}}\right]$ FLAP FAILURE
CHECK			LOW	2-17-70	
APR			LOW	6-25-70	
APR					
INK	ODEGARD	5-3-69			THE BOEING COMPANY

747
D6-30643 Vol. II
PAGE 2.0-33

TD 461 C-R4

K-E ALBANENE 1951 REV E

08

NOTE: DATA APPLICABLE FOR SYMMETRIC OR ASYMMETRIC (MONITOR LIMITED) FLAP FAILURE

THESE DATA NOT INCLUDED IN NASA SIMULATION

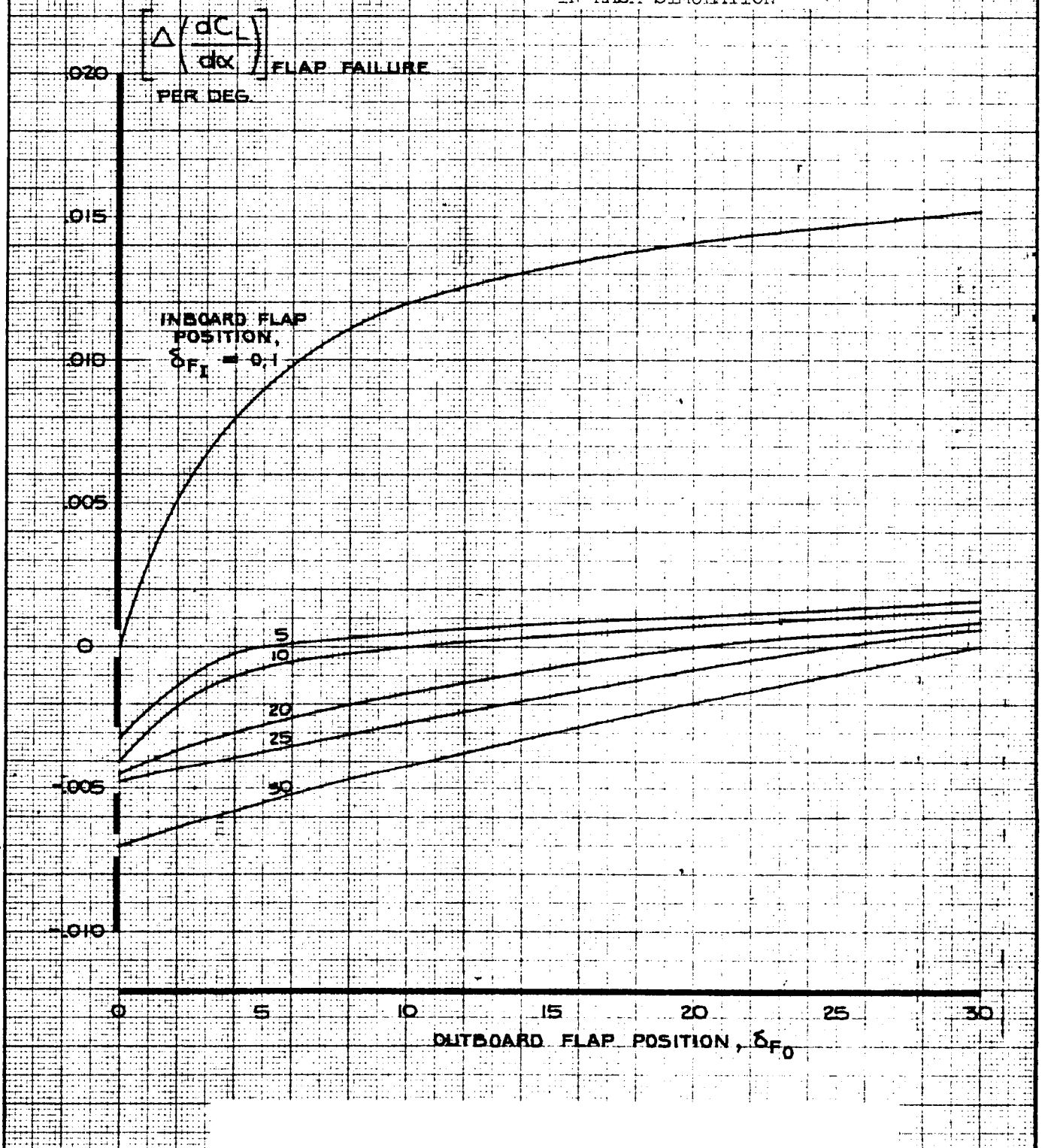

CALC	LOW	5-3-69	REVISED	DATE	LIFT COEFFICIENT EFFECT OF FLAPS ON $[\Delta(dC_L/d\alpha)]$ FLAP FAILURE
CHECK			LOW	2-17-70	
APR			LOW	6-25-70	
APR					
INK	ODEGARD	5-3-69			THE BOEING COMPANY

747

D6-30643 Vol. II

PAGE 2.0-34

TD 461 C-R4

K-E ALBANENE REV. E

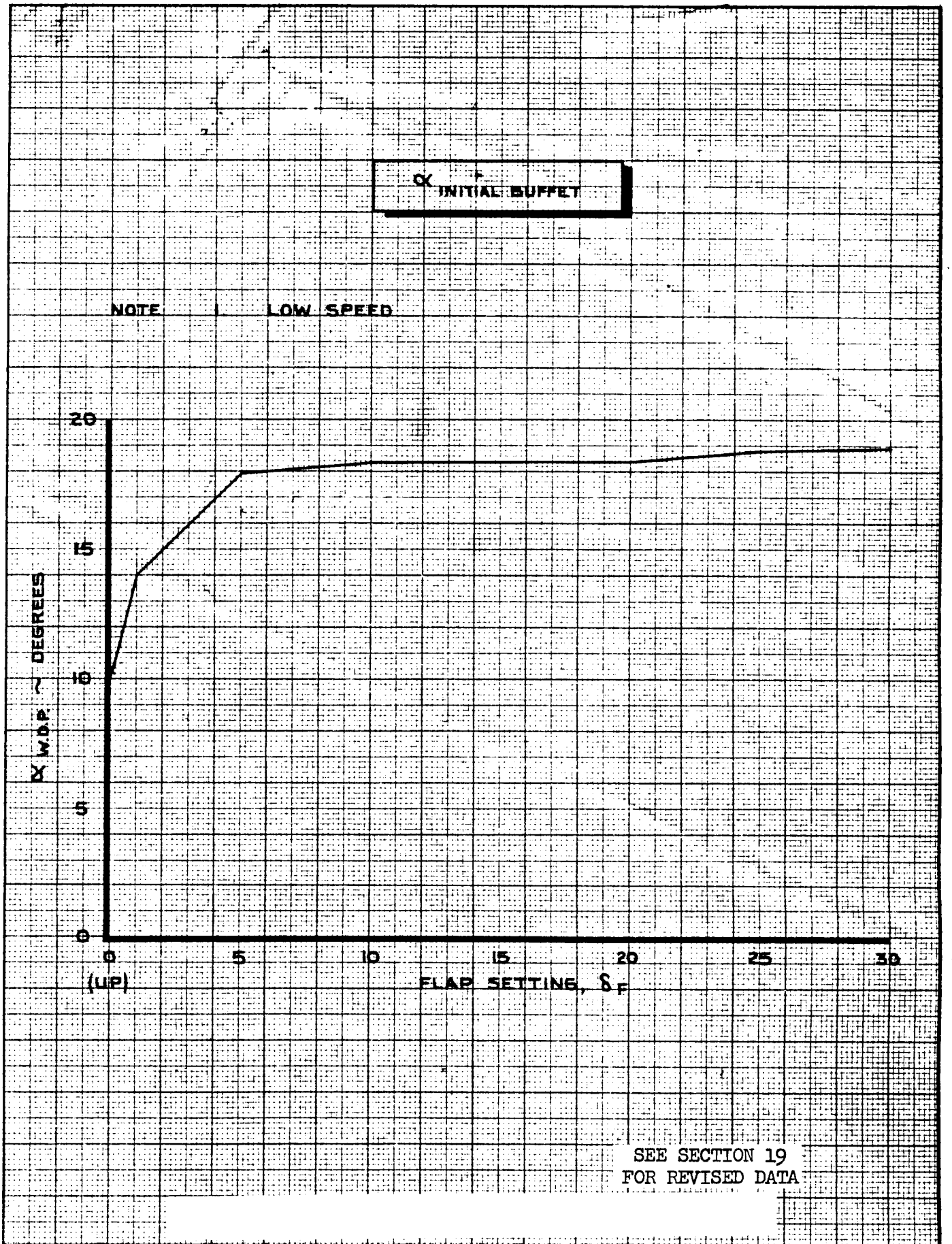

SEE SECTION 19
FOR REVISED DATA

CALC	LOW	1·19·68	REVISED	DATE
CHECK	FOSTER	1·24·68	LOW	6·4·69
APR			LOW	1·29·70
APR				
INK	ODEGARD	1·19·68		

ANGLE OF ATTACK
FOR INITIAL BUFFET

747

D6-30643
Vol. II

THE BOEING COMPANY

PAGE 2.0-36

AD 461 C-R4

K+E ALBANENE 1981 REV D

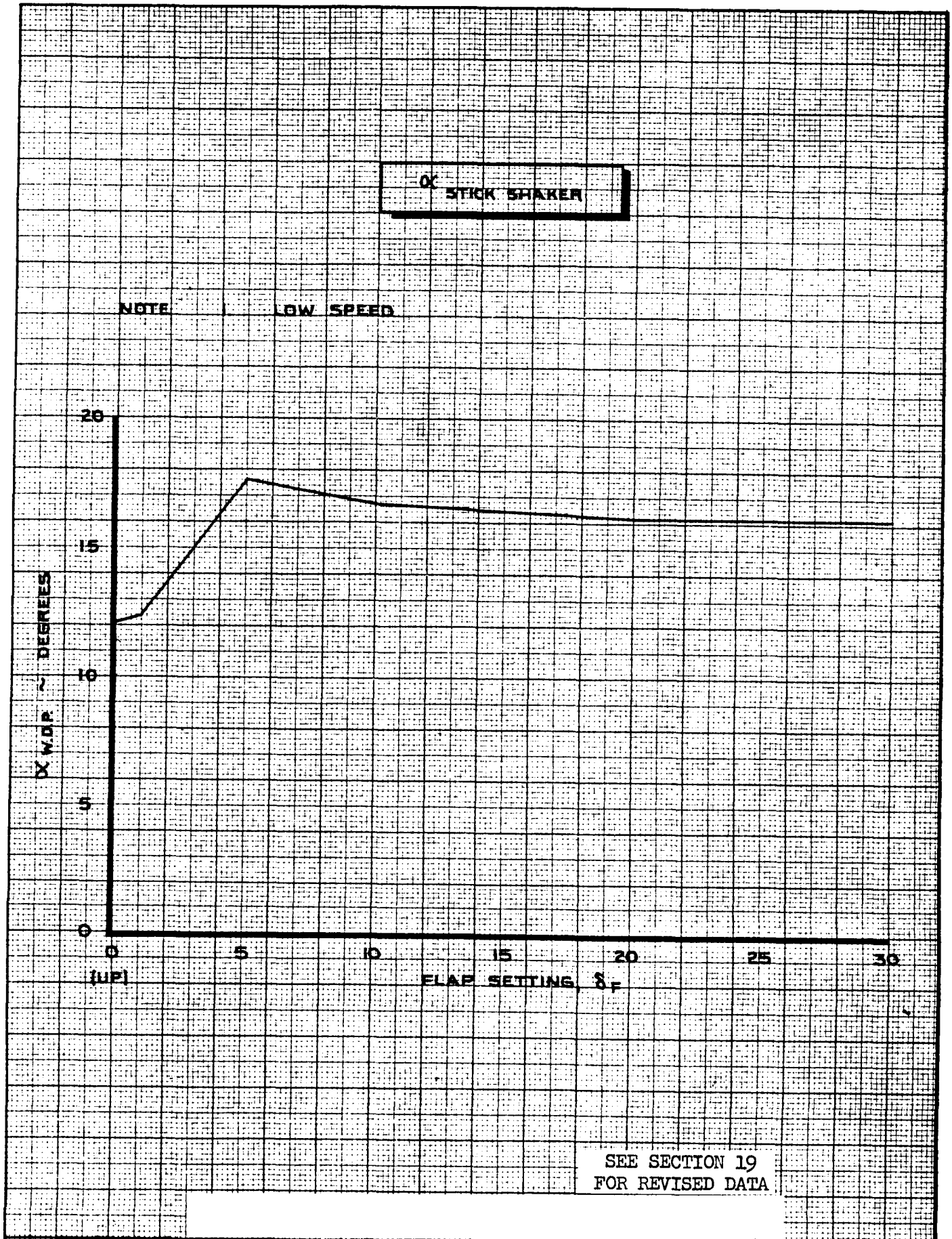

SEE SECTION 19
FOR REVISED DATA

CALC	LOW	1·19·68	REVISED	DATE
CHECK	FOSTER	1·24·68	LOW	6·4·69
APR			LOW	1·28·70
APR				
INK	ODEGARD	1·19·68		

ANGLE OF ATTACK
FOR STICK SHAKER ACTUATION

747

D6-30643
Vol. II

THE BOEING COMPANY

PAGE 2.0-35

AD 461 C-R4

K·E ALBANENE 1961 TRACING PAPER REV. D

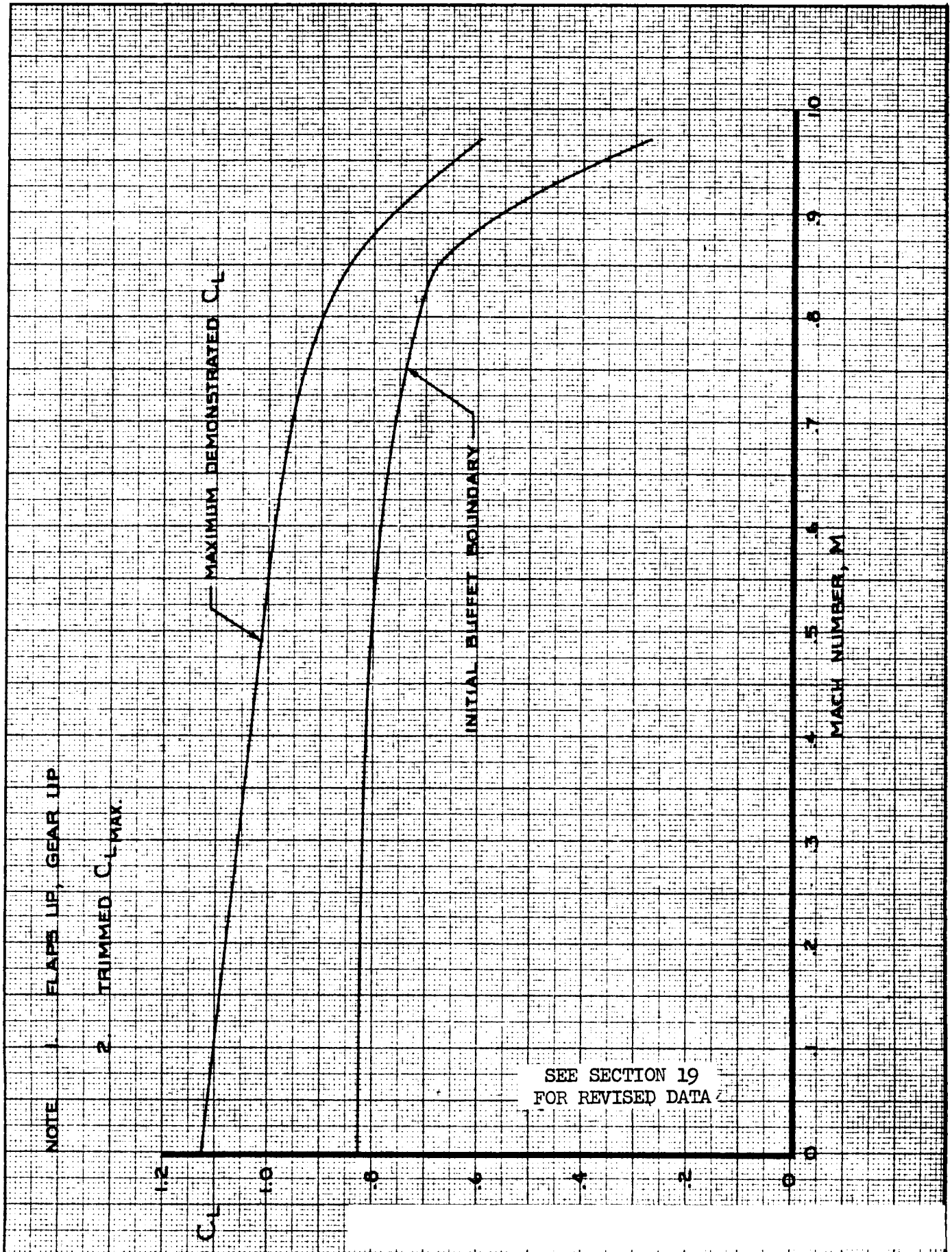

CALC	LOW	1-8-68	REVISED	DATE
CHECK	FOSTER	1-24-68	LOW	6-4-69
APR			LOW	1-20-70
APR				
INK	ODEGARD	1-8-68		

LIFT COEFFICIENT BUFFET BOUNDARY AND $C_{L_{MAX.}}$

747

D6-30643 Vol. II

THE BOEING COMPANY

PAGE 2.0-38

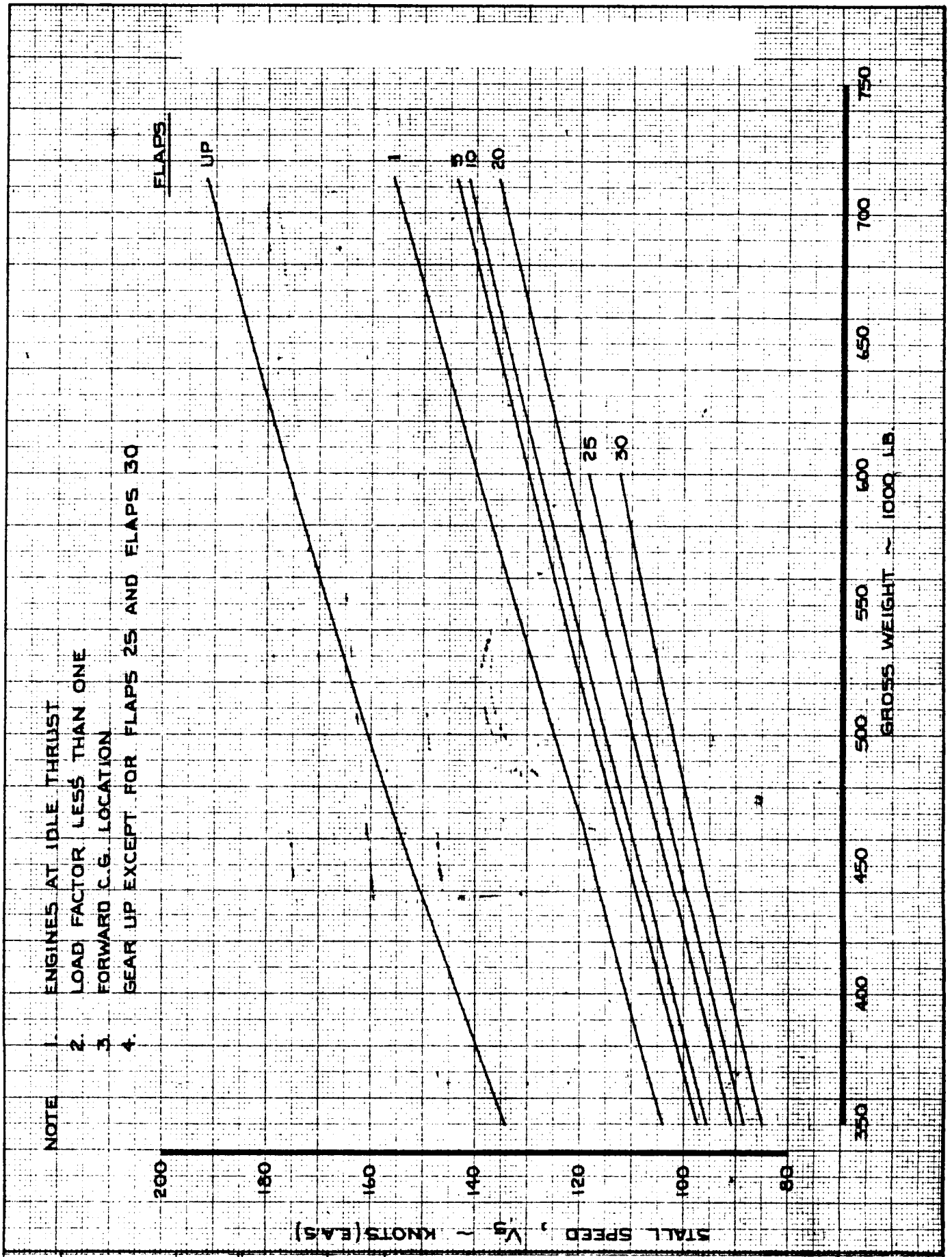

CALC	LOW	12-14-67	REVISED	DATE	CERTIFICATION STALL SPEEDS
CHECK	FOSTER	1-24-68	LOW	6-4-69	
APR			LOW	8-27-69	
APR			LOW	1-14-70	
INK	ODEGARD	12-14-67			THE BOEING COMPANY

747
D6-30643 Vol. II
PAGE 2.0-37

AD 461 C-R4

K-E ALBANENE 1961 TRACING PAPER REV. E

3.0 DRAG FORCE COEFFICIENT

The dimensionless aerodynamic drag force coefficient is given in terms of its significant components by the equation below:

At a given $\alpha_{W.D.P.}$,

$$C_D = K \cdot \left[C_{D_{BASIC}} + \frac{dC_D}{d\Delta} \cdot \Delta_{F.R.L.} \right] + [1-K][C_D]_M$$

$$+ \Delta C_{D_{SPOILERS}} + \Delta C_{D_{\substack{LANDING \\ GEAR}}} + \Delta C_{D_{\substack{GROUND \\ EFFECT}}}$$

$$+ \Delta C_{D_{SIDESLIP}} + \Delta C_{D_{RUDDERS}} + \left[\Delta C_{D_{FLAP\ FAILURE}} \right]^*$$

where,

$C_{D_{BASIC}}$ = Basic drag coefficient for the rigid airplane at $\Delta_{F.R.L.} = 0^\circ$, in free air and with the landing gear retracted. $C_{D_{BASIC}}$ is plotted on page 3.0-5.

K = 0 for flaps up. $K = 1$ for flaps 1, 5, 10, 20, 25 and 30.

$\frac{dC_D}{d\Delta} \cdot \Delta_{F.R.L.}$ = Change in basic drag coefficient due to change in stabilizer angle from $\Delta_{F.R.L.} = 0^\circ$. $\frac{dC_D}{d\Delta}$ is plotted on page 3.0-6 and page 3.0-7.

$[C_D]_M$ = Drag coefficient at Mach number, M. $[C_D]_M$ is plotted on page 3.0-8 and 3.0-9. $C_L{}^*$ is given by the first six terms of the lift force coefficient equation on page 2.0-1.

$[\ ]^*$ NOT IN NASA SIMULATION

3.0 $\Delta C_{D_{SPOILERS}}$ = Change in drag coefficient due to spoiler or speedbrake deflection.

(Cont'd)

$$\Delta C_{D_{SPOILERS}} = \Delta C_{D_{SP}} \left[1 + F_D \cdot K^{B}_{GE}\right] + .05 \cdot F_D \cdot K^{B}_{GE} \cdot \frac{1}{45n} \cdot \sum_{\substack{\text{OPERATING} \\ \text{SPOILER} \\ \text{PANELS}}} \delta_{SP}$$

where $\Delta C_{D_{SP}}$ is the change in drag coefficient due to spoiler or speedbrake deflection in free air.

$$\Delta C_{D_{SP}} = \sum_{\substack{\text{OPERATING} \\ \text{SPOILER} \\ \text{PANELS}}} \left[\left(\Delta C_{D_{SP}}\right)_{\alpha_{W.D.P.}=4^\circ} + \frac{d\left(\Delta C_{D_{SP}}\right)}{d\alpha} \cdot \left(\alpha_{W.D.P.} - 4^\circ\right) \right] \cdot \frac{\left(C_{D_{SP}}\right)_M}{\left(C_{D_{SP}}\right)_{M=0}}$$

where $\left(\Delta C_{D_{SP}}\right)_{\alpha_{W.D.P.}=4^\circ}$ is the change in drag coefficient at $\alpha_{W.D.P.}=4^\circ$ due to deflecting the operating spoiler panels. $\left(\Delta C_{D_{SP}}\right)_{\alpha_{W.D.P.}=4^\circ}$ is plotted for spoilers on page 3.0-10 and is tabulated for ground spoilers on page 3.0-12 . $\frac{d\left(\Delta C_{D_{SP}}\right)}{d\alpha}$ is the rate of change with angle of attack of drag coefficient due to deflecting the operating spoiler panels. $\frac{d\left(\Delta C_{D_{SP}}\right)}{d\alpha}$ is plotted for spoilers on page 3.0-11 and is tabulated for ground spoilers on page 3.0-12 . The Mach number effect, $\frac{\left(C_{D_{SP}}\right)_M}{\left(C_{D_{SP}}\right)_{M=0}}$, is plotted on page 3.0-13 . The ground effect lateral control factor, F_D , is plotted on page 3.0-14 . The ground effect height factor, K^{B}_{GE} is plotted on page 2.0-31 . n is the number of operating spoiler panels. δ_{SP} is the spoiler panel deflection

3.0 (Cont'd)

angle (degrees).

$\Delta C_{D_{\substack{\text{LANDING}\\\text{GEAR}}}}$ = Change in drag coefficient due to main and nose landing gear extension.

$$\Delta C_{D_{\substack{\text{LANDING}\\\text{GEAR}}}} = K_{GEAR} \cdot \Delta C_{D_{GEAR}} \cdot \frac{(C_{D_{GEAR}})_M}{(C_{D_{GEAR}})_{M=0}}$$

where $\Delta C_{D_{GEAR}}$ is plotted on page 3.0-15. The Mach number effect, $\frac{(C_{D_{GEAR}})_M}{(C_{D_{GEAR}})_{M=0}}$, is plotted on page 3.0-16. The landing gear effectiveness factor, K_{GEAR}, is plotted on page 2.0-28.

$\Delta C_{D_{\substack{\text{GROUND}\\\text{EFFECT}}}}$ = Change in drag coefficient due to ground effect.

$$\Delta C_{D_{\substack{\text{GROUND}\\\text{EFFECT}}}} = K^{A}_{GE} \cdot \Delta C_{D_{GE}}$$

where $\Delta C_{D_{GE}}$ is plotted on page 3.0-18. The ground effect height factor, K^{A}_{GE}, is plotted on page 3.0-17.

$\Delta C_{D_{SIDESLIP}}$ = Change in drag coefficient due to angle of sideslip, β. $\Delta C_{D_{SIDESLIP}}$ is plotted on page 3.0-19.

$\Delta C_{D_{RUDDERS}}$ = Change in drag coefficient due to rudder deflection.

$$\Delta C_{D_{RUDDERS}} = \Delta C_{D_{R_U}} + \Delta C_{D_{R_L}}$$

where $\Delta C_{D_{R_U}}$ and $\Delta C_{D_{R_L}}$ are the changes in drag coefficient due to deflection of the upper rudder and the lower rudder respectively. $\Delta C_{D_{R_U}}$ and $\Delta C_{D_{R_L}}$ are obtained from page 3.0-19.

3.0 $\Delta C_{D_{FLAP\ FAILURE}}$ = Change in basic drag coefficient due to flap extension or retraction from the flap position at which symmetric failure of both inboard or both outboard flaps occurs.

(Cont'd)

For symmetric inboard or outboard flap failure,

$$\Delta C_{D_{FLAP\ FAILURE}} = \left[(\Delta C_D)_{\alpha_{W.D.P.}=0^\circ}\right]_{FLAP\ FAILURE} + \Delta\left(\frac{dC_D}{d\alpha}\right)_{FLAP\ FAILURE} \cdot \alpha_{W.D.P.}$$

where $\left[(\Delta C_D)_{\alpha_{W.D.P.}=0^\circ}\right]_{FLAP\ FAILURE}$ is the change in basic drag coefficient at $\alpha_{W.D.P.} = 0^\circ$ due to symmetric inboard or outboard flap failure. $\left[(\Delta C_D)_{\alpha_{W.D.P.}=0^\circ}\right]_{FLAP\ FAILURE}$ is plotted on page 3.0-3. $\Delta\left(\frac{dC_D}{d\alpha}\right)_{FLAP\ FAILURE} \cdot \alpha_{W.D.P.}$ is the change in basic drag coefficient due to the effect of symmetric inboard or outboard flap failure on the airplane basic drag coefficient curve slope. $\Delta\left(\frac{dC_D}{d\alpha}\right)_{FLAP\ FAILURE}$ is plotted on page 3.0-11.

The above data is also applicable for asymmetric (monitor limited) inboard or outboard flap failure.

$\Delta C_{D_{FLAP\ FAILURE}}$ is to be added to total C_D corresponding to the lateral-directional condition.

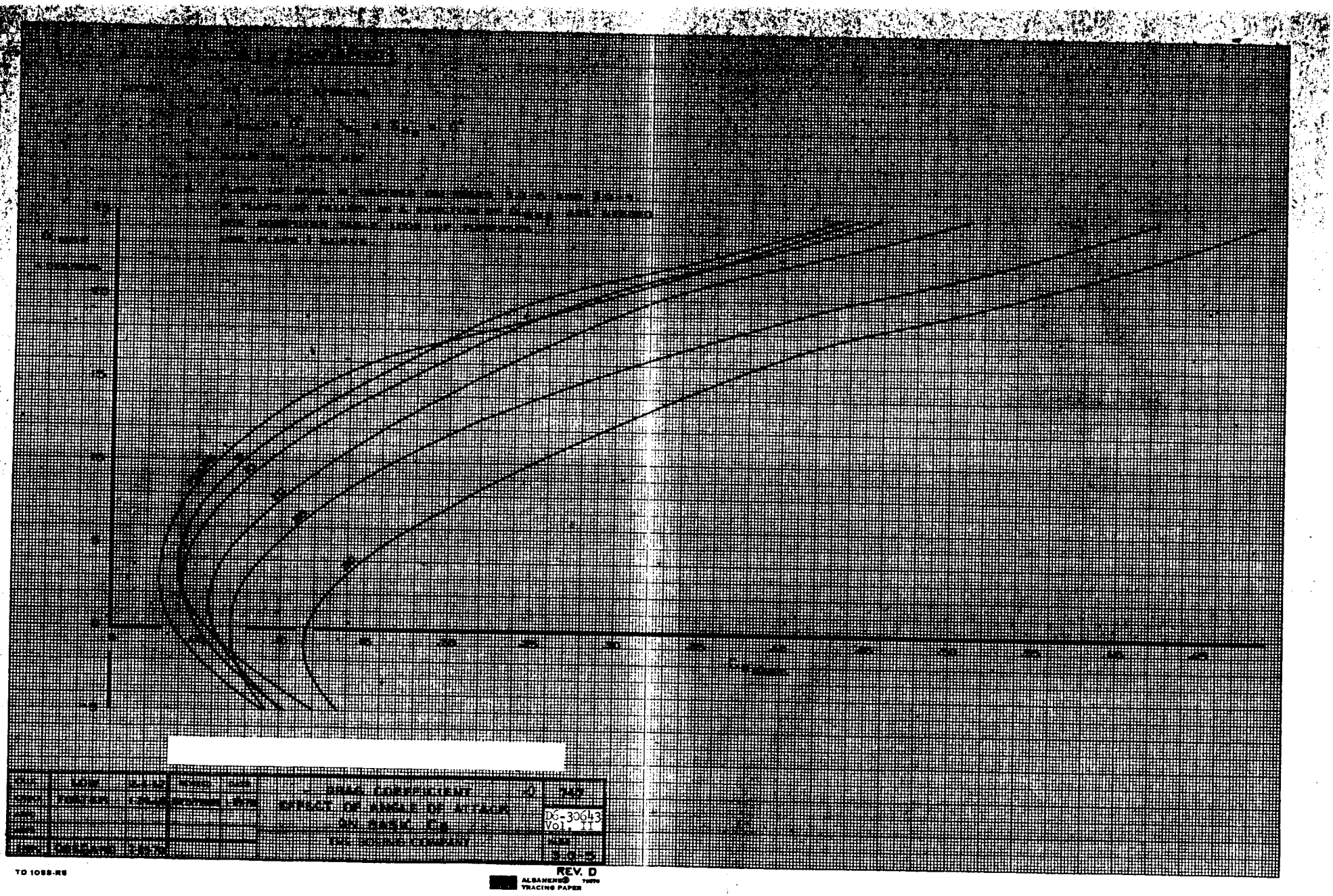
DRAG COEFFICIENT
EFFECT OF ANGLE OF ATTACK
ON BASIC C_D
DOUGLAS COMPANY
D6-30643
Vol. II
3-0-5
REV. D

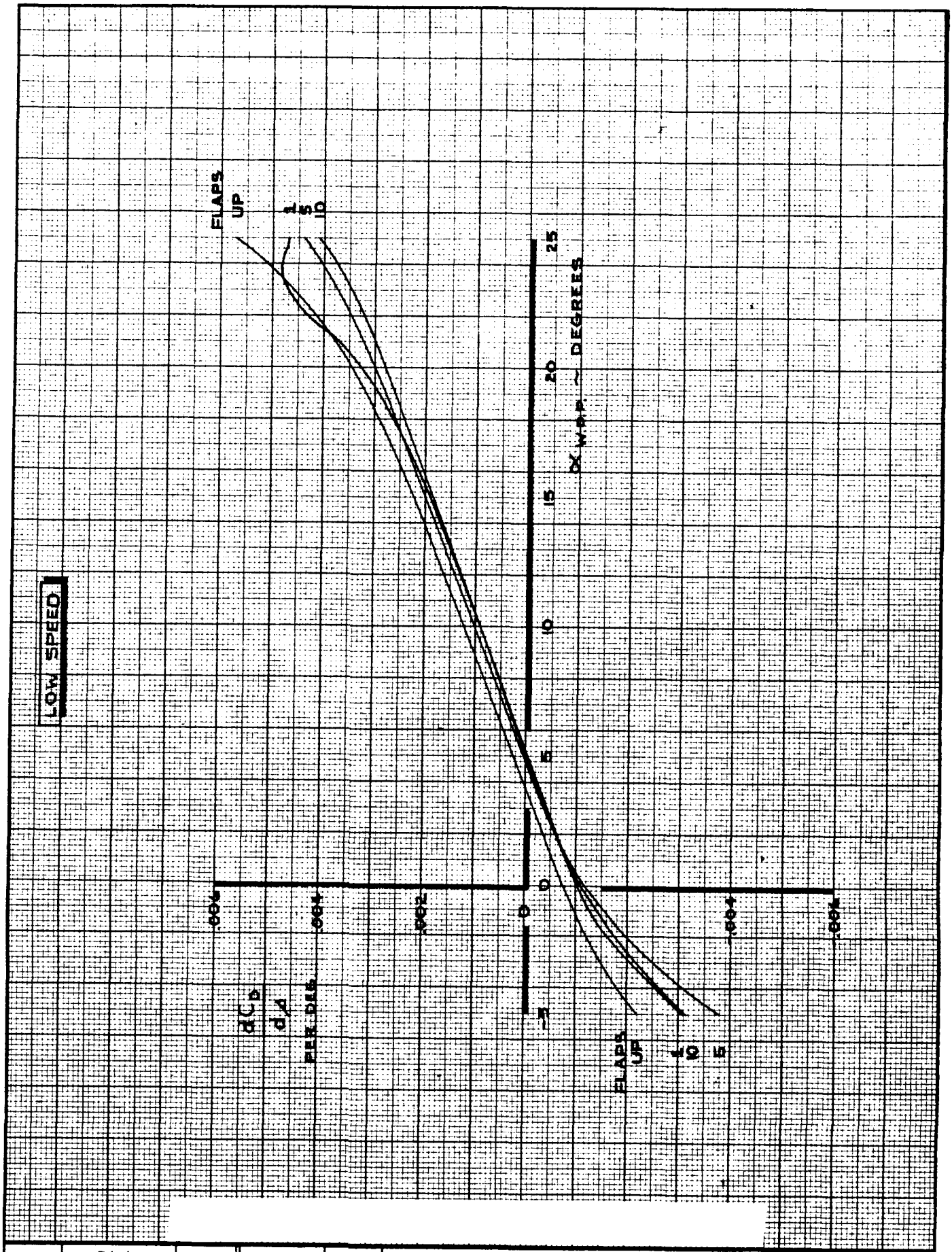

CALC	LOW	12/3/67	REVISED	DATE	DRAG COEFFICIENT EFFECT OF ANGLE OF ATTACK ON STABILIZER (FLAPS UP, 1, 5, 10)
CHECK	FOSTER	1-24-68	LOW	2-23-70	
APR					
APR					
INK	ODEGARD	12/3/67			THE BOEING COMPANY

747

D6-30643
Vol. II

PAGE
3.0-6

REV. D

TD 461 C-R4

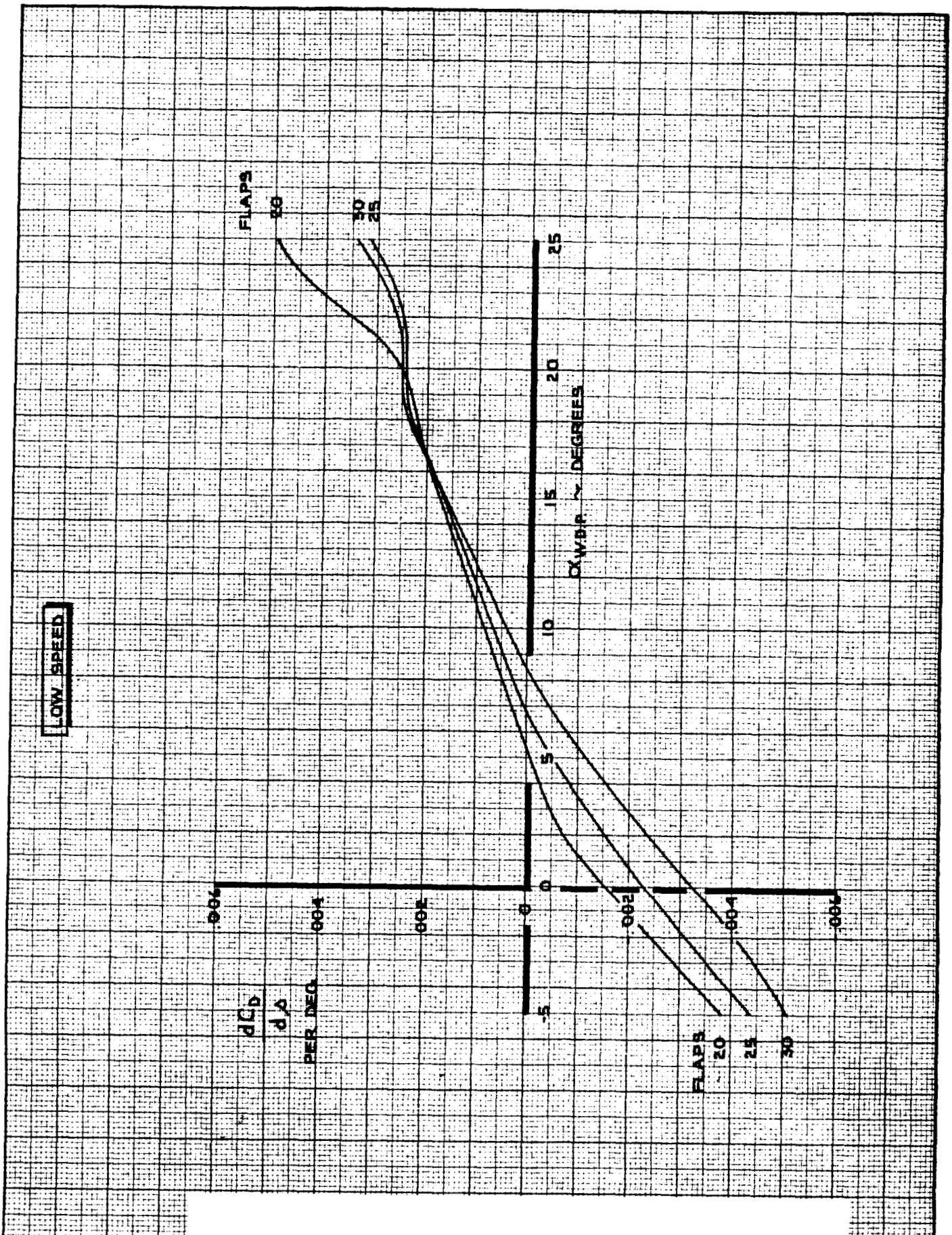

CALC	LOW	12-3-67	REVISED	DATE	DRAG COEFFICIENT EFFECT OF ANGLE OF ATTACK ON STABILIZER (FLAPS 20, 25, 30)
CHECK	FOSTER	1-24-68	LOW	2-26-70	
APR					
APR					
INK	KINSMAN	2-26-70			THE BOEING COMPANY

747

D6-30643, Vol. II

PAGE 3.0-7

AD 461 C-R4

K-E ALBANENE 1951 TRACING PAPER REV. D

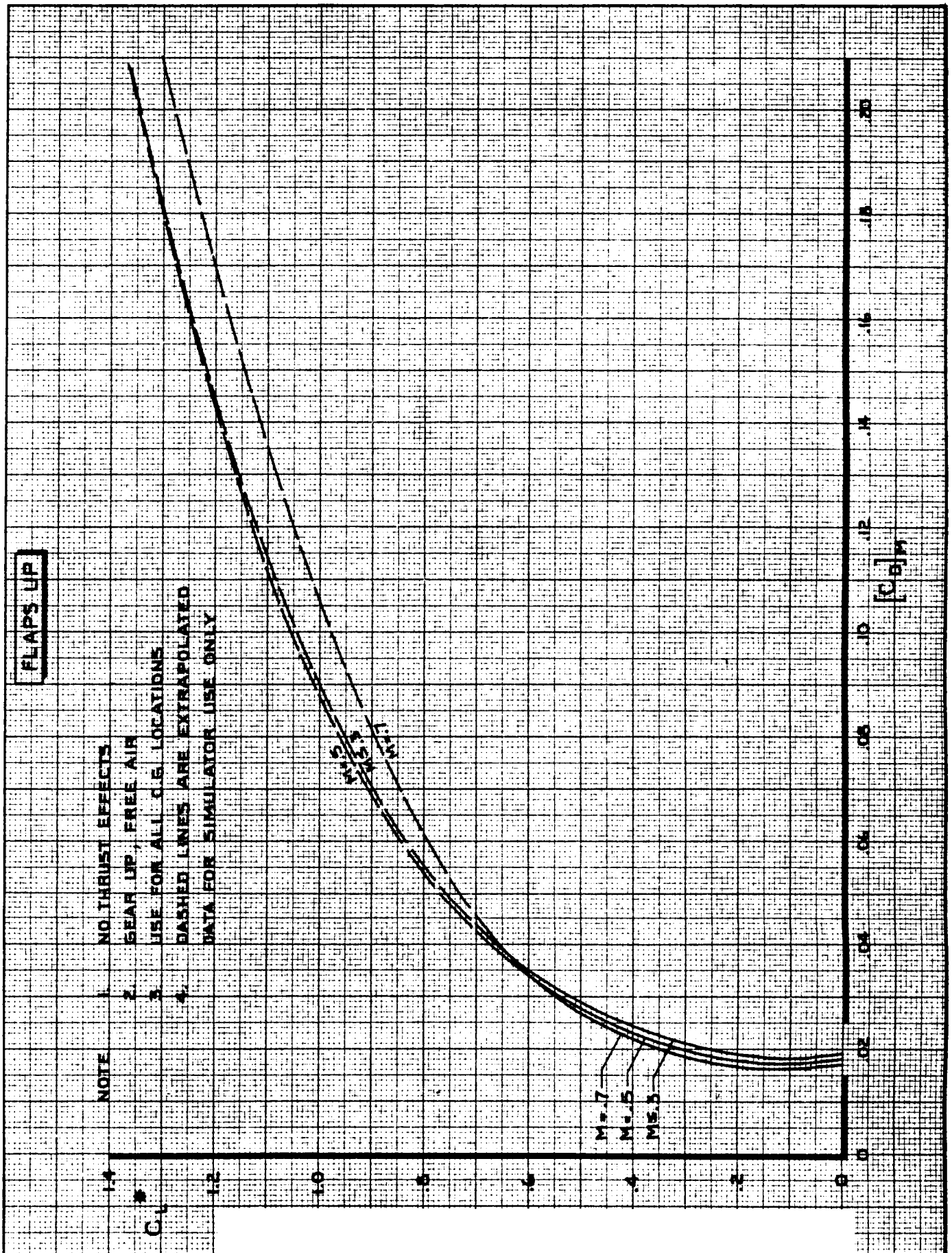

CALC	BYSTROM	2-13-70	REVISED	DATE	DRAG COEFFICIENT EFFECT OF MACH NUMBER M ≤ .7	747
CHECK						D6-30643 Vol. II
APR						
APR					THE BOEING COMPANY	PAGE 3.0-8
INK	ODEGARD	2-17-70				

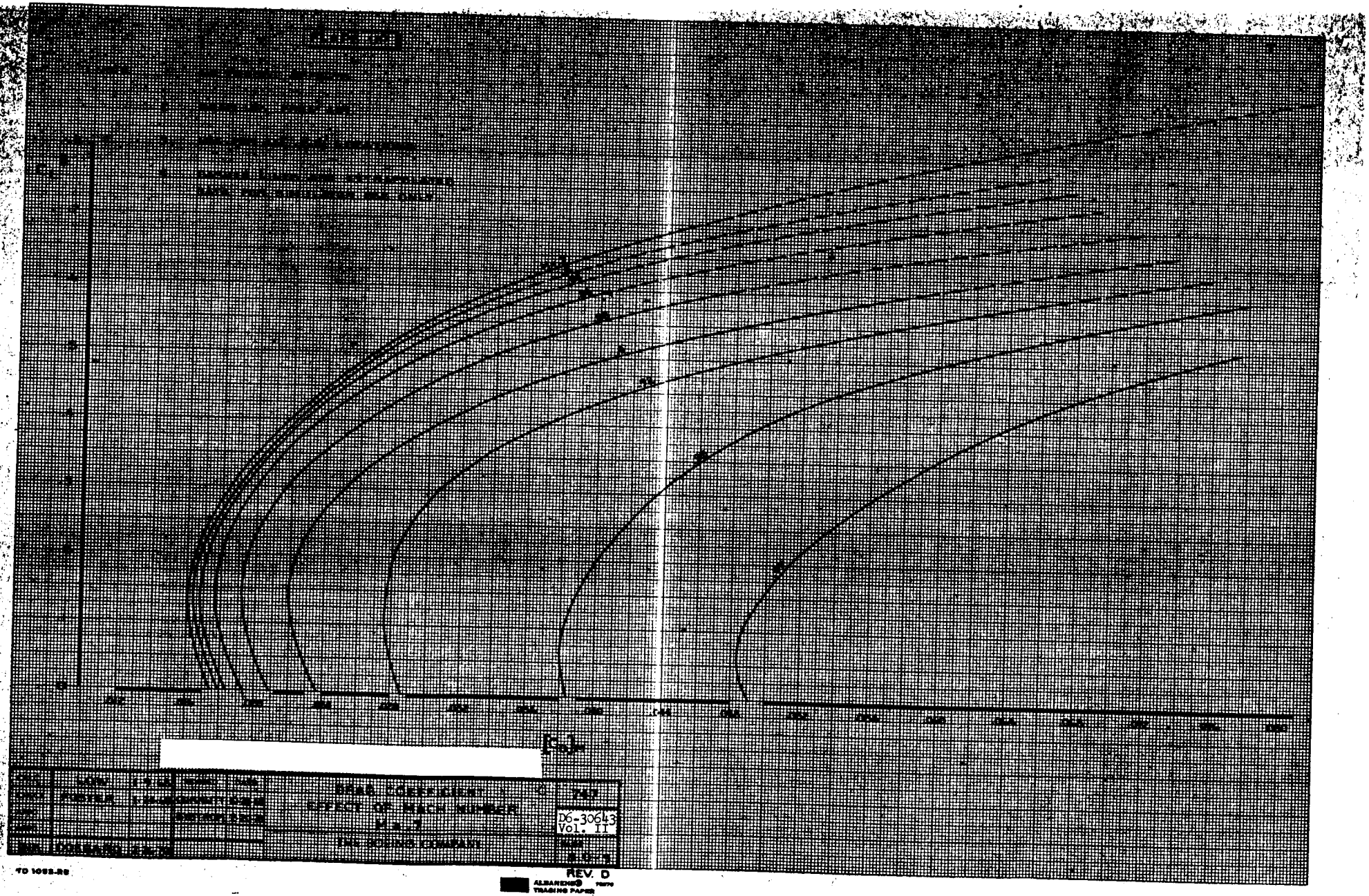
DRAG COEFFICIENT
EFFECT OF MACH NUMBER
M = .7
747
D6-30643
Vol. II
REV. D

SPOILER PANEL 8 OR 5

NOTE
1. DATA SHOWN FOR INDIVIDUAL PANELS 8 OR 5
2. FOR PANEL 12 OR 1, MULTIPLY BY 0.50
3. PANELS 8 & 5 LIMITED TO 20 DEG. MAX. DEFLECTION

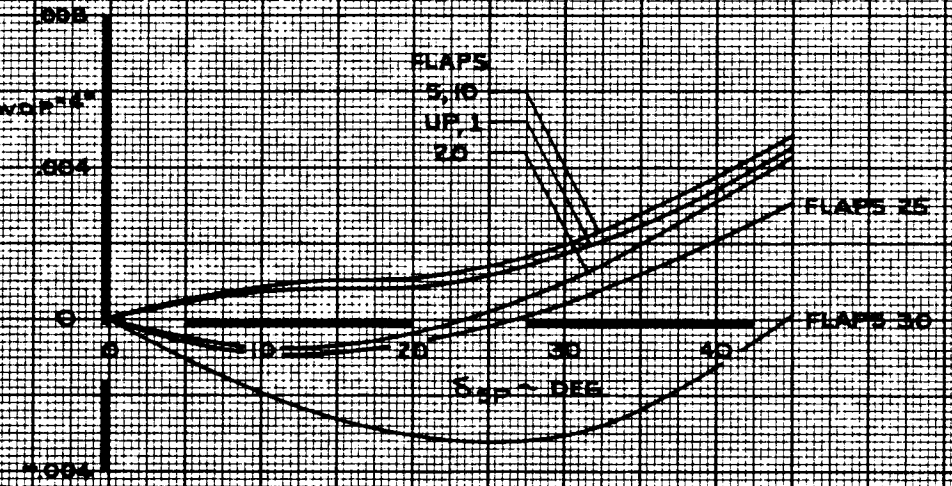

SPOILER PANEL GROUP 9,10,11 OR 2,3,4

NOTE
1. TOTAL EFFECT OF SPOILER GROUP 9,10,11 (OR 2,3,4) SHOWN
2. WITH HYDRAULIC SYSTEM NO. 2 OFF, MULTIPLY BY 0.30
3. WITH HYDRAULIC SYSTEM NO. 3 OFF, MULTIPLY BY 0.70
4. FOR SPOILER GROUP 9,10 (OR 3,4), MULTIPLY BY 0.66

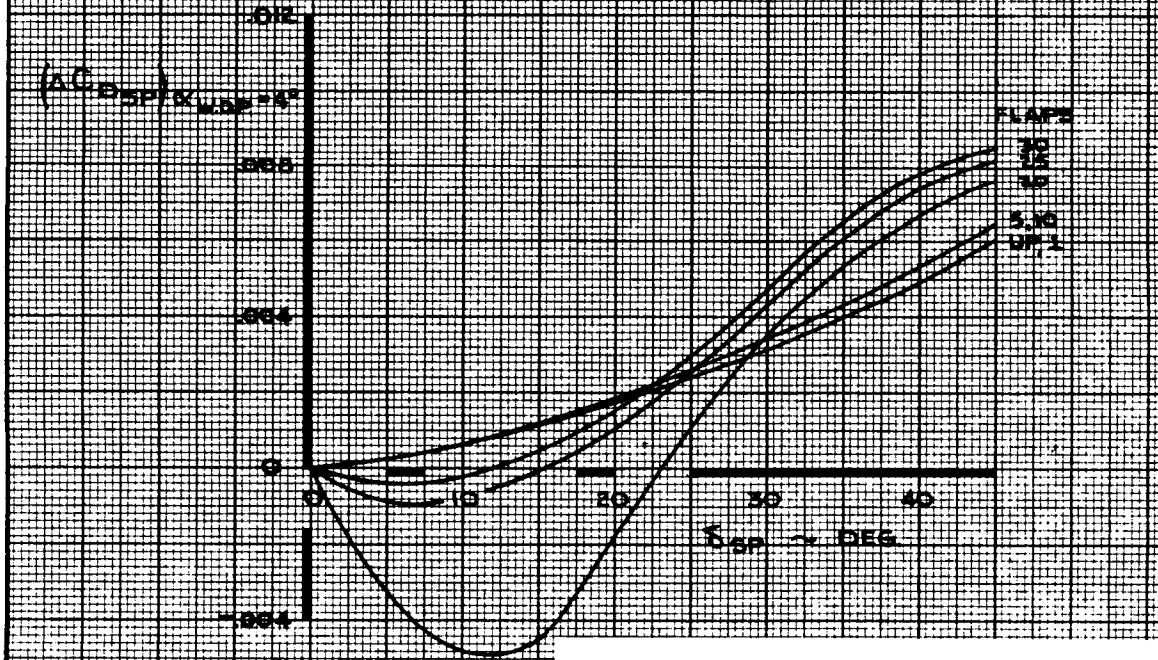

CALC	KUPCIS	1/2/68	REVISED	DATE
CHECK	FOSTER	1-24-68	KUPCIS	4-22-68
APR			KUPCIS	6-2-69
APR			LOW	2-14-70
INK	ODEGARD	1/2/68		

DRAG COEFFICIENT
EFFECT OF SPOILERS

747
D6-30643
Vol. II

THE BOEING COMPANY

PAGE 3.0-10
REV. D

TD 461 C-R4

SPOILER PANEL 8 OR 5

NOTE

DATA SHOWN FOR INDIVIDUAL PANELS 8 OR 5
FOR PANEL 12 OR 1, MULTIPLY BY 0.50
PANELS 8 & 5 LIMITED TO 20 DEG. MAX. DEFLECTION

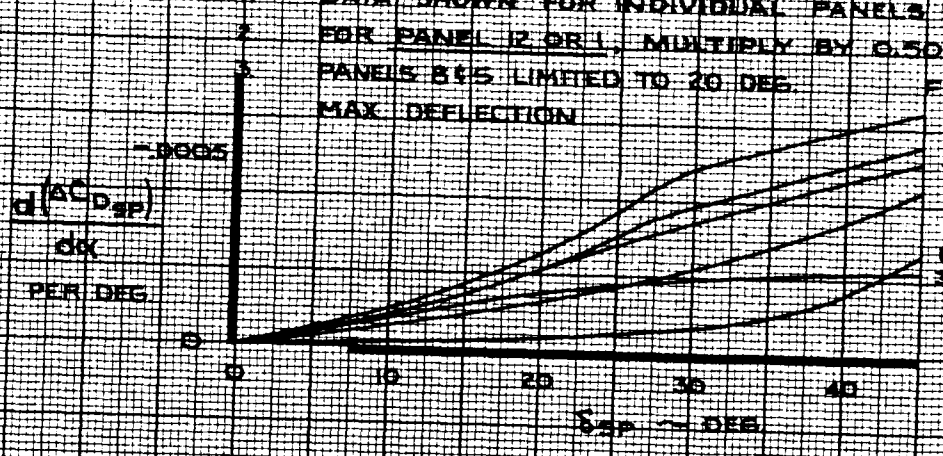

SPOILER PANEL GROUP 9,10,11 OR 2,3,4

NOTE

TOTAL EFFECT OF SPOILER GROUP 9,10,11 (OR 2,3,4) SHOWN
WITH HYDRAULIC SYSTEM NO. 2 OFF, MULTIPLY BY 0.30
WITH HYDRAULIC SYSTEM NO. 3 OFF, MULTIPLY BY 0.70
FOR SPOILER GROUP 9,10 (OR 3,4), MULTIPLY BY 0.65

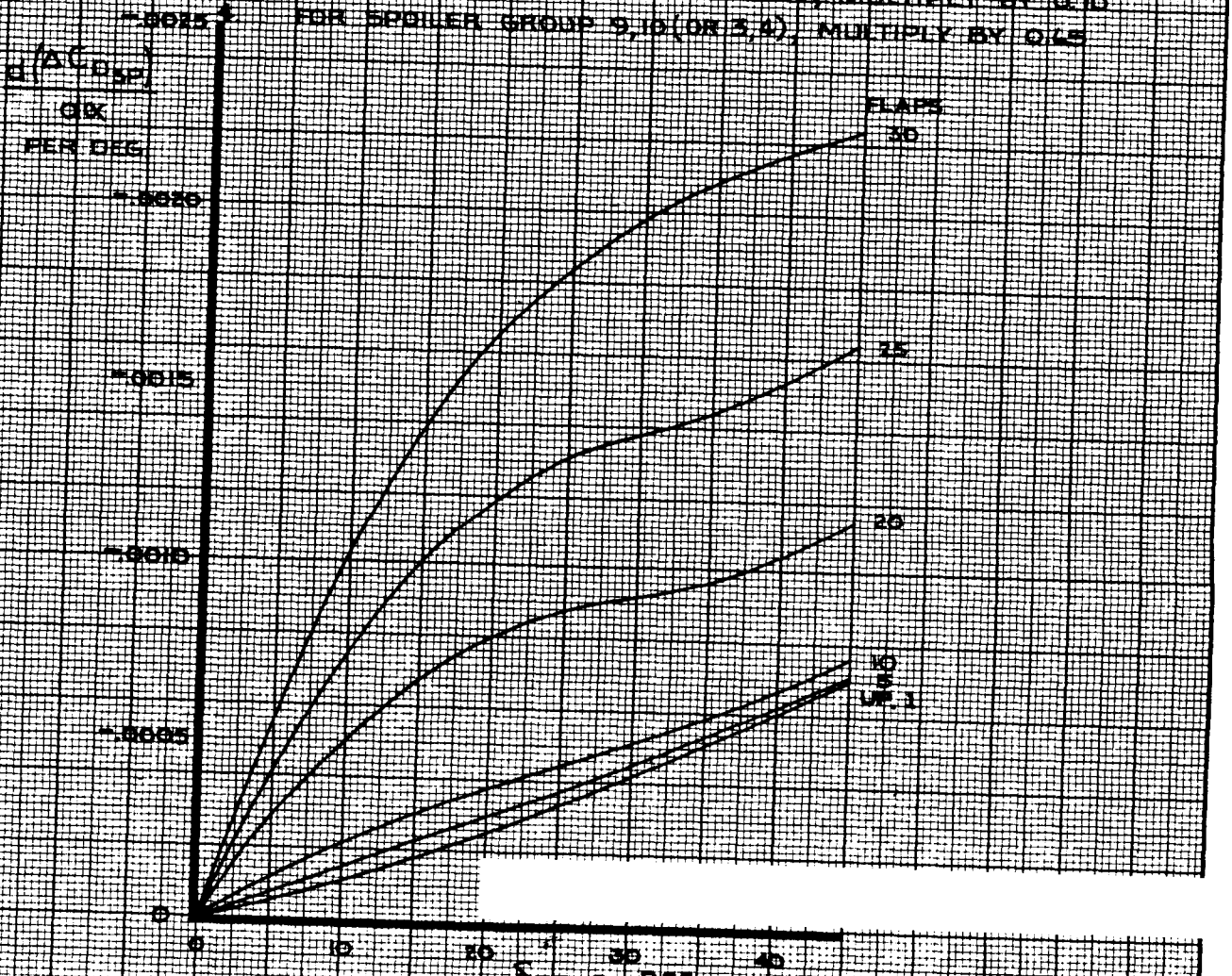

CALC	KUPCIS	1/2/68	REVISED	DATE	DRAG COEFFICIENT EFFECT OF ANGLE OF ATTACK ON SPOILERS
CHECK	FOSTER	1-24-68	KUPCIS	6-2-69	
APR			LOW	2-14-70	
APR					
INK	ODEGARD	1/2/68			THE BOEING COMPANY

747
D6-30643 Vol. II
PAGE 3.0-11
REV. D

TD 461 C-R4

SPOILER PANELS 6 AND 7

NOTE 1. DATA SHOWN FOR BOTH PANELS OPERATING AT 20°

FLAP SETTING	$(\Delta C_{D_{SP}})_{\alpha_{W.D.F.}=4^\circ}$	$\frac{d(\Delta C_{D_{SP}})}{d\alpha}$
UP	0.0008	− 0.00013
1	0.0008	− 0.00013
5	0.0020	− 0.00012
10	0.0020	− 0.00016
15	0.0016	− 0.00032
20	− 0.0008	− 0.00056
25	− 0.0036	− 0.00060
30	− 0.0054	− 0.00106

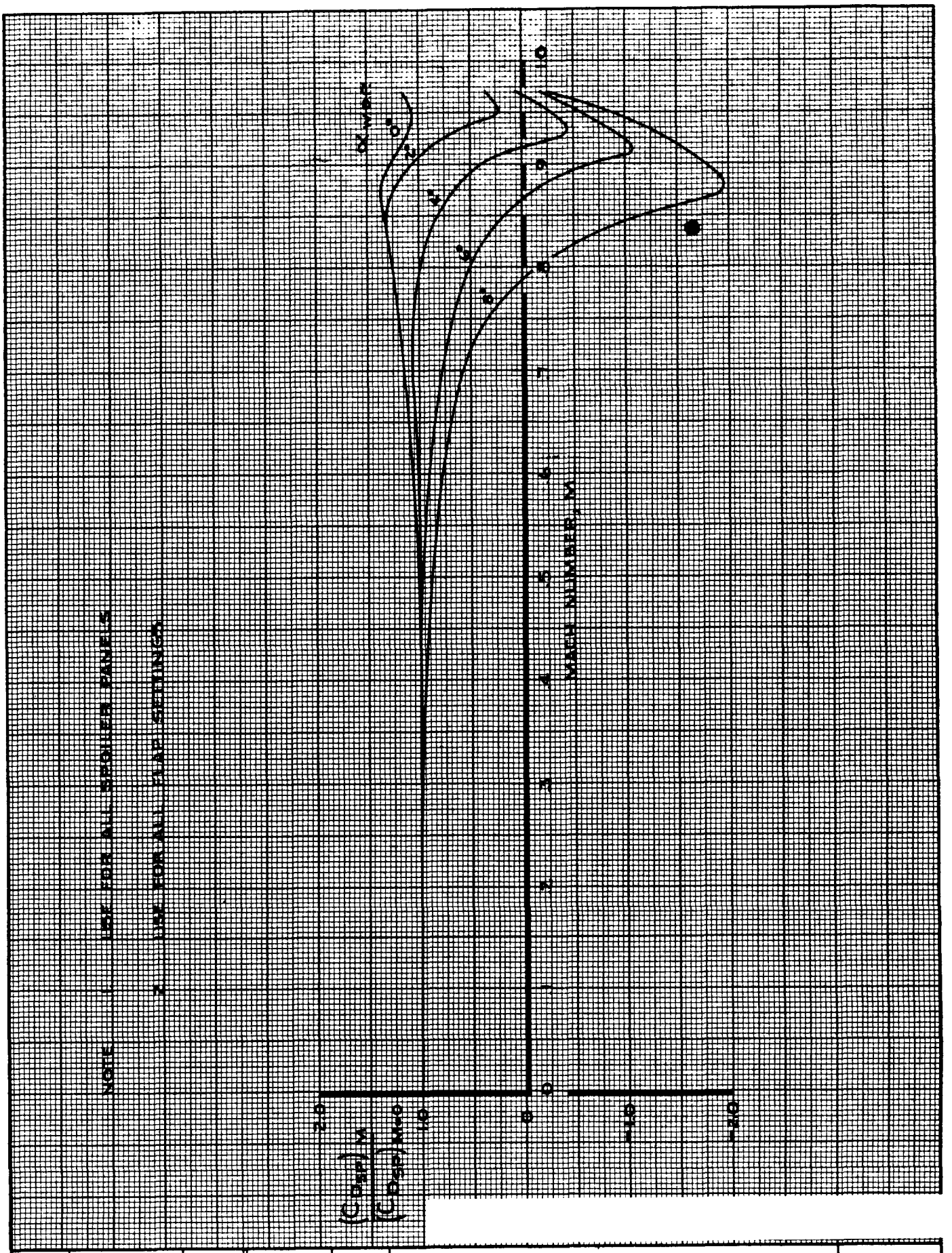

CALC	KUPCIS	1/4/68	REVISED	DATE	DRAG COEFFICIENT EFFECT OF MACH NUMBER ON SPOILERS
CHECK	FOSTER	1-24-68			
APR					
APR					
INK	ODEGARD	1/4/68			THE BOEING COMPANY

747
D6-30643 Vol. II
PAGE 3.0-13

TD 461 C-R4

CDSPM

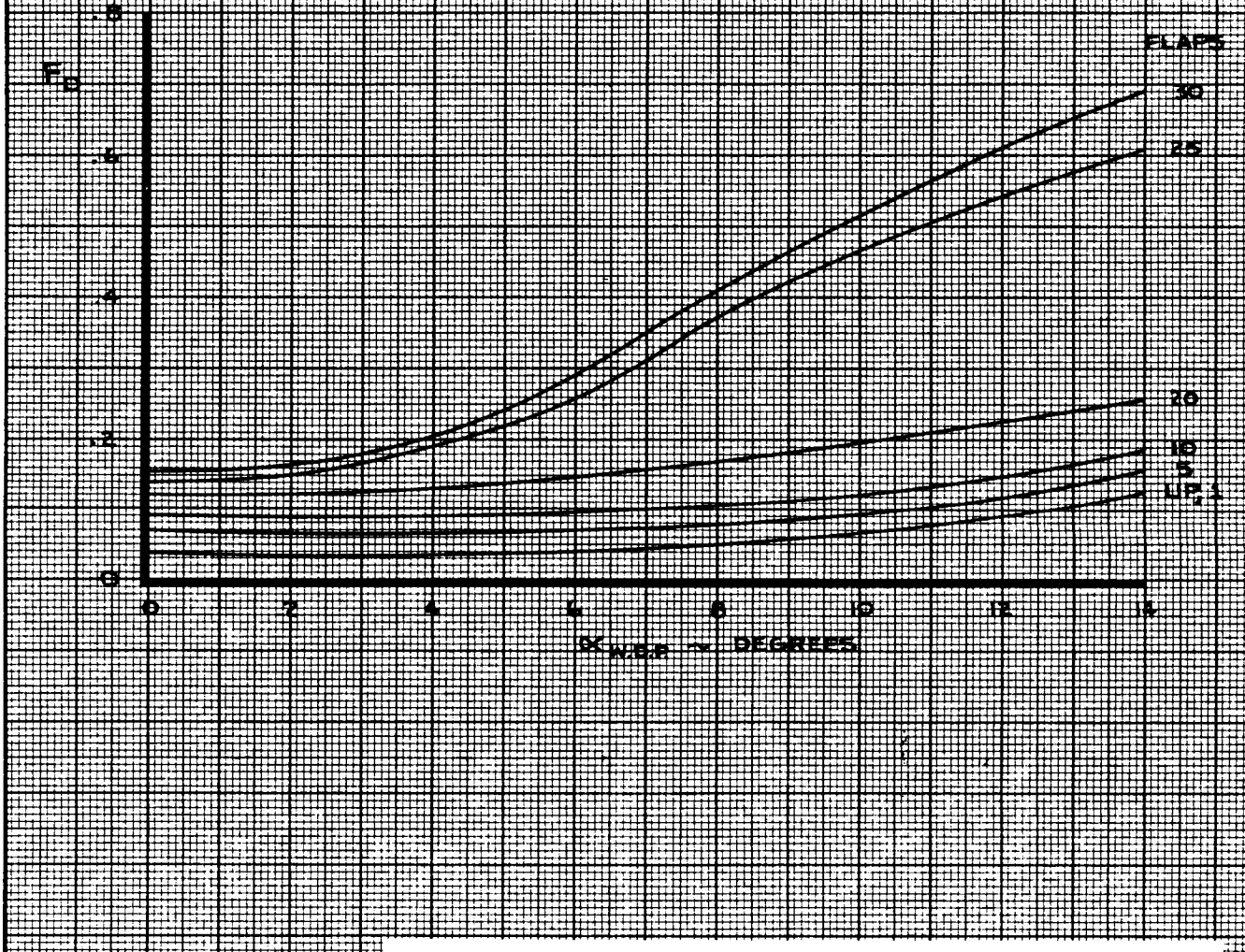

CALC	CURNUTT	12/18/67	REVISED	DATE	DRAG COEFFICIENT GROUND EFFECT LATERAL CONTROL FACTOR, F_D	747
CHECK	FOSTER	1-24-68	CURNUTT	10-28-68		D6-30643 Vol. II
APR			LOW	2-14-70		
APR					THE BOEING COMPANY	PAGE 3.0-14
INK	ODEGARD	12/18/67				

REV D

LOW SPEED

NOTE 1. FREE AIR

2. FOR LANDING GEAR FAILURE, REPLACE $\Delta C_{D_{GEAR}}$ BY

$$\Delta C_{D_{GEAR\ FAILURE}} = K_{D_{GEAR}} \cdot \Delta C_{D_{GEAR}}$$

GEAR SELECTION	GEAR FAILURE	$K_{D_{GEAR}}$
DOWN	WING GEARS FAIL TO EXTEND	0.4
UP	WING GEARS FAIL TO RETRACT	0.6
✓	ONE WING GEAR FAILS TO RETRACT	0.3
✓	ONE BODY GEAR FAILS TO RETRACT	0.1
✓	ONE BODY GEAR DOOR FAILS TO RETRACT	0.1
✓	NOSE GEAR FAILS TO RETRACT	0.1

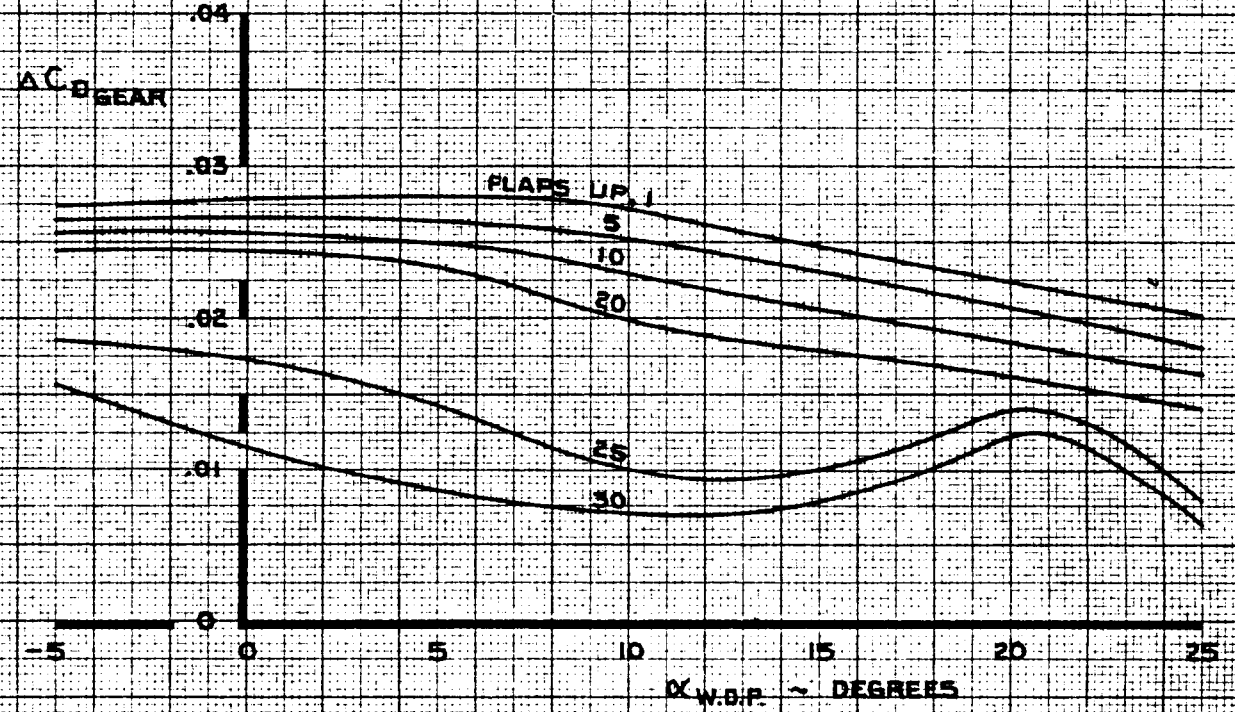

CALC	LOW	9-20-67	REVISED	DATE	DRAG COEFFICIENT EFFECT OF LANDING GEAR
CHECK	FOSTER	1-24-68	LOW	6-9-69	
APR			BYSTRÖM	2-18-70	
APR					
INK	ODEGARD	2-20-70			THE BOEING COMPANY

747
D6-30643 Vol. II
PAGE 3.0-15

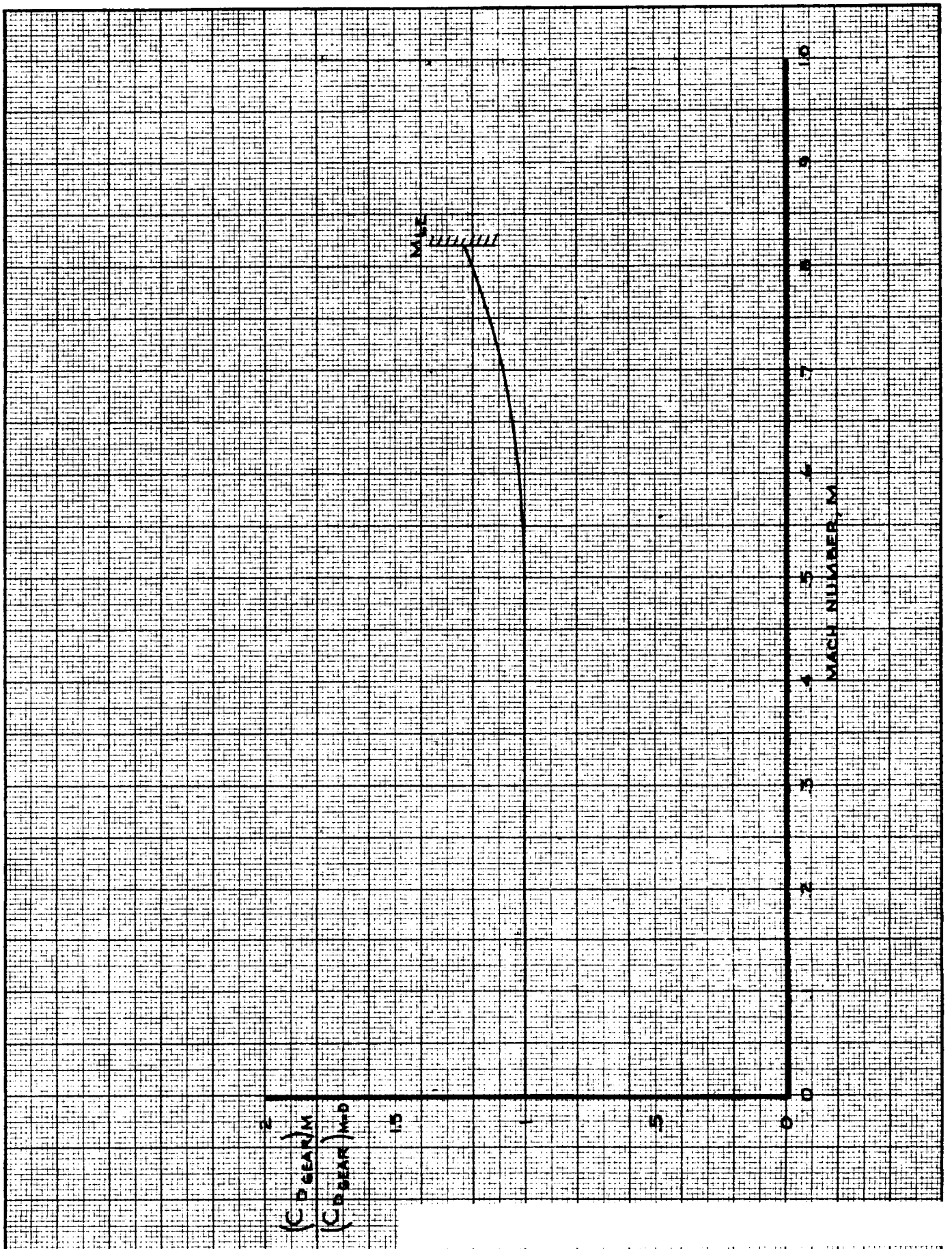

CALC	LOW	11-9-67	REVISED	DATE	DRAG COEFFICIENT EFFECT OF MACH NUMBER ON $\Delta C_{D_{GEAR}}$
CHECK	FOSTER	1-24-68			
APR					
APR					
INK	O'DEGARD	11-9-67			THE BOEING COMPANY

747
D6-30643 Vol. II
PAGE 3.0-16

AD 461 C R4

CD6M

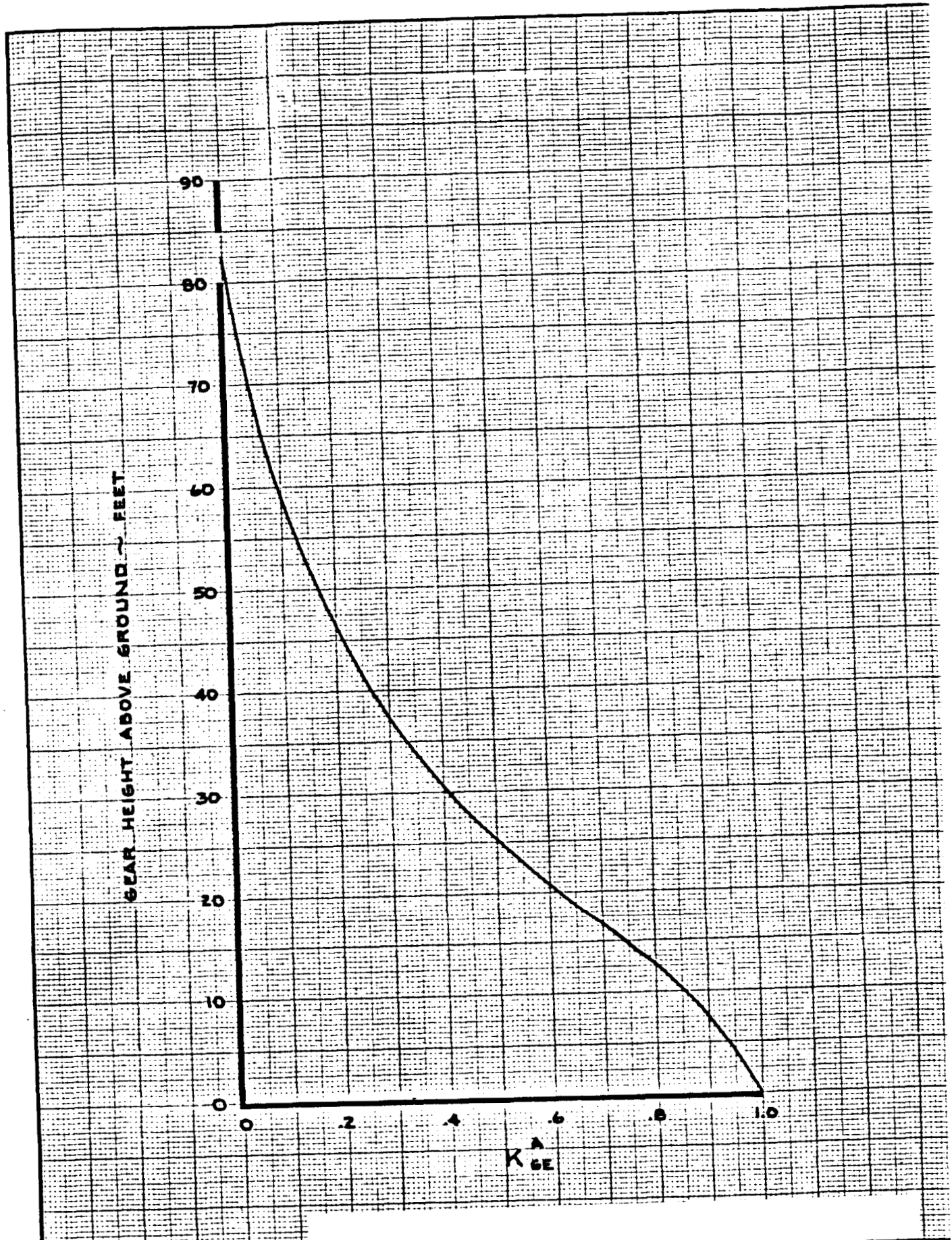

CALC	CURNUTT	12/20/67	REVISED	DATE	DRAG COEFFICIENT GROUND EFFECT HEIGHT FACTOR, K_{GE}^{A}
CHECK	FOSTER	1-24-68			
APR					
APR					
INK	ODEGARD	12/20/67			

747
D6-30606
Vol. I
PAGE 3.0-17

THE BOEING COMPANY

TD 461 C-R4

NOTE: 1 GEAR ON GROUND

2 $K^{A}_{GE} = 1.0$

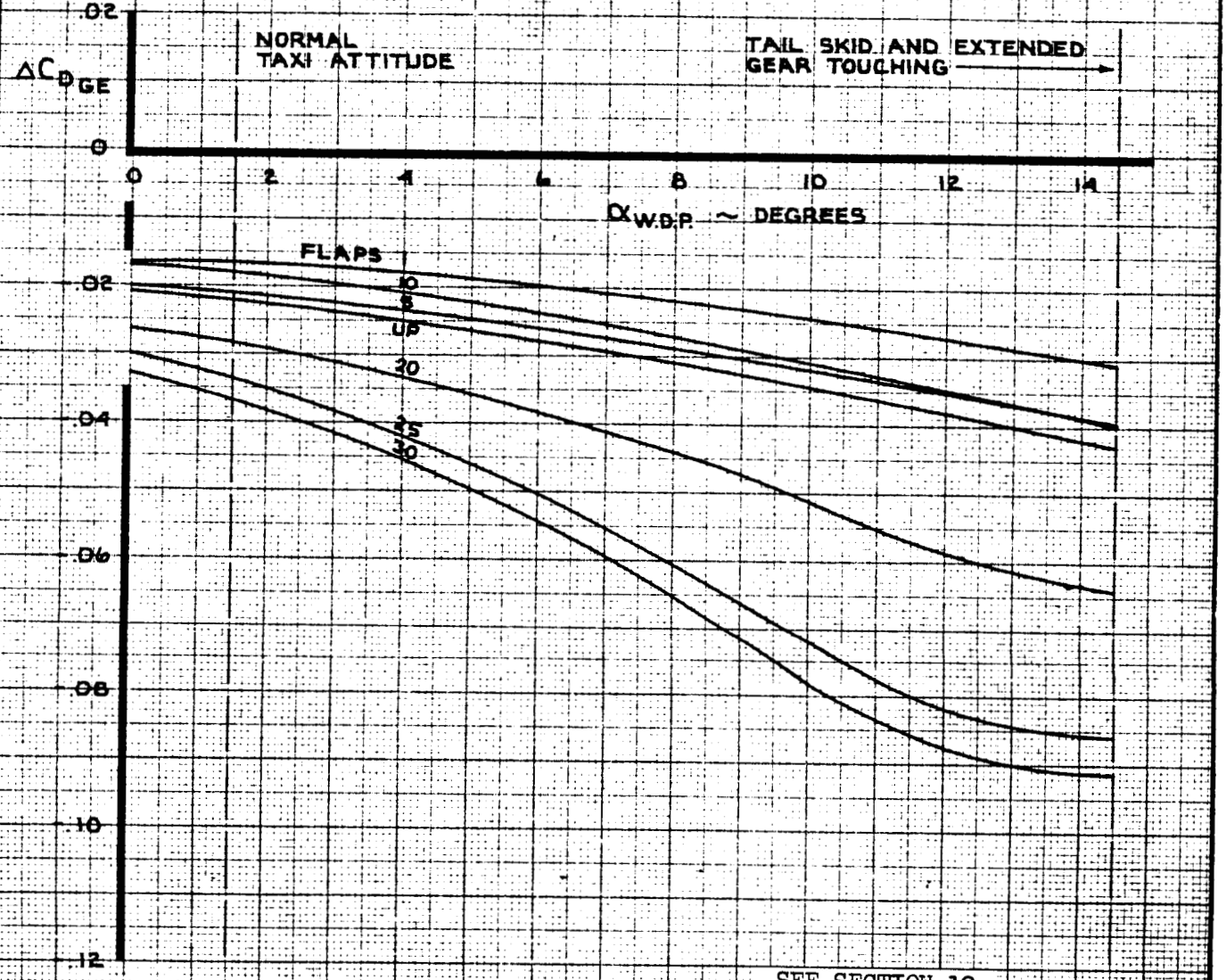

SEE SECTION 19
FOR REVISED DATA

CALC	CURNUTT	12-12-67	REVISED	DATE
CHECK	FOSTER	1-24-68	CURNUTT	3-5-70
APR				
APR				
INK	KINSMAN	3-6-70		

DRAG COEFFICIENT
GROUND EFFECT

747

D6-30643
Vol. II

THE BOEING COMPANY

PAGE 3.0-18

TD 461 C-R4

K-E ALBANENE 1951 REV.D

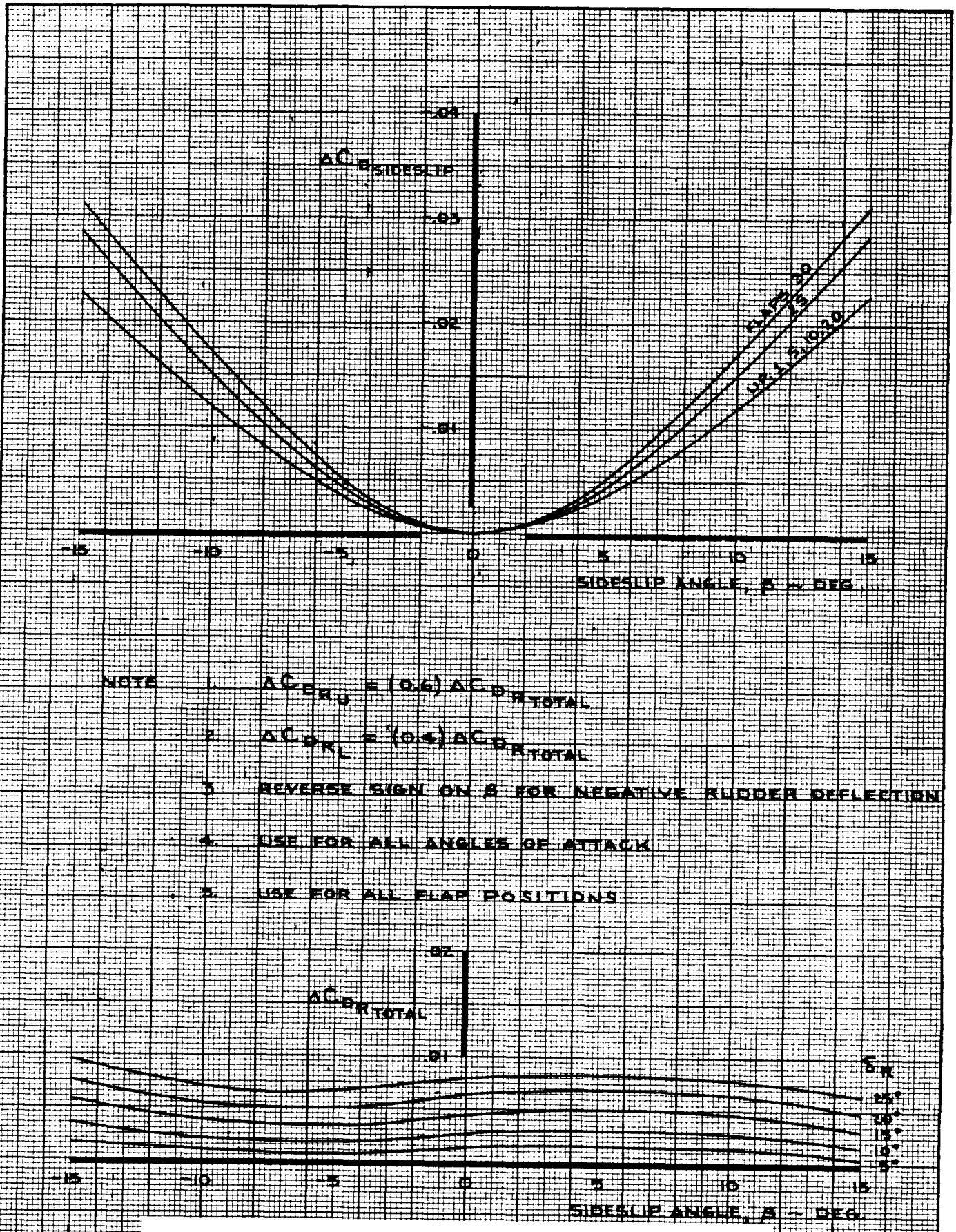

NOTE

1. $\Delta C_{D_{R_U}} = (0.4)\,\Delta C_{D_{R\,TOTAL}}$
2. $\Delta C_{D_{R_L}} = (0.4)\,\Delta C_{D_{R\,TOTAL}}$
3. REVERSE SIGN ON β FOR NEGATIVE RUDDER DEFLECTION
4. USE FOR ALL ANGLES OF ATTACK
5. USE FOR ALL FLAP POSITIONS

CALC	STIRLING	10/21/67	REVISED	DATE
CHECK	HOLTZNER	12/21/67	LOW:	2-17-70
APR			LOW	6-25-70
APR				
INK	ODEGARD	10/21/67		

DRAG COEFFICIENT
EFFECT OF SIDESLIP
AND RUDDER

747

D6-30643
Vol. II

THE BOEING COMPANY

PAGE
3.0-19

TD 461 C-R4

REV. E

NOTE 1. DATA APPLICABLE FOR SYMMETRIC OR ASYMMETRIC (MONITOR LIMITED) FLAP FAILURE

THESE DATA NOT INCLUDED IN NASA SIMULATION

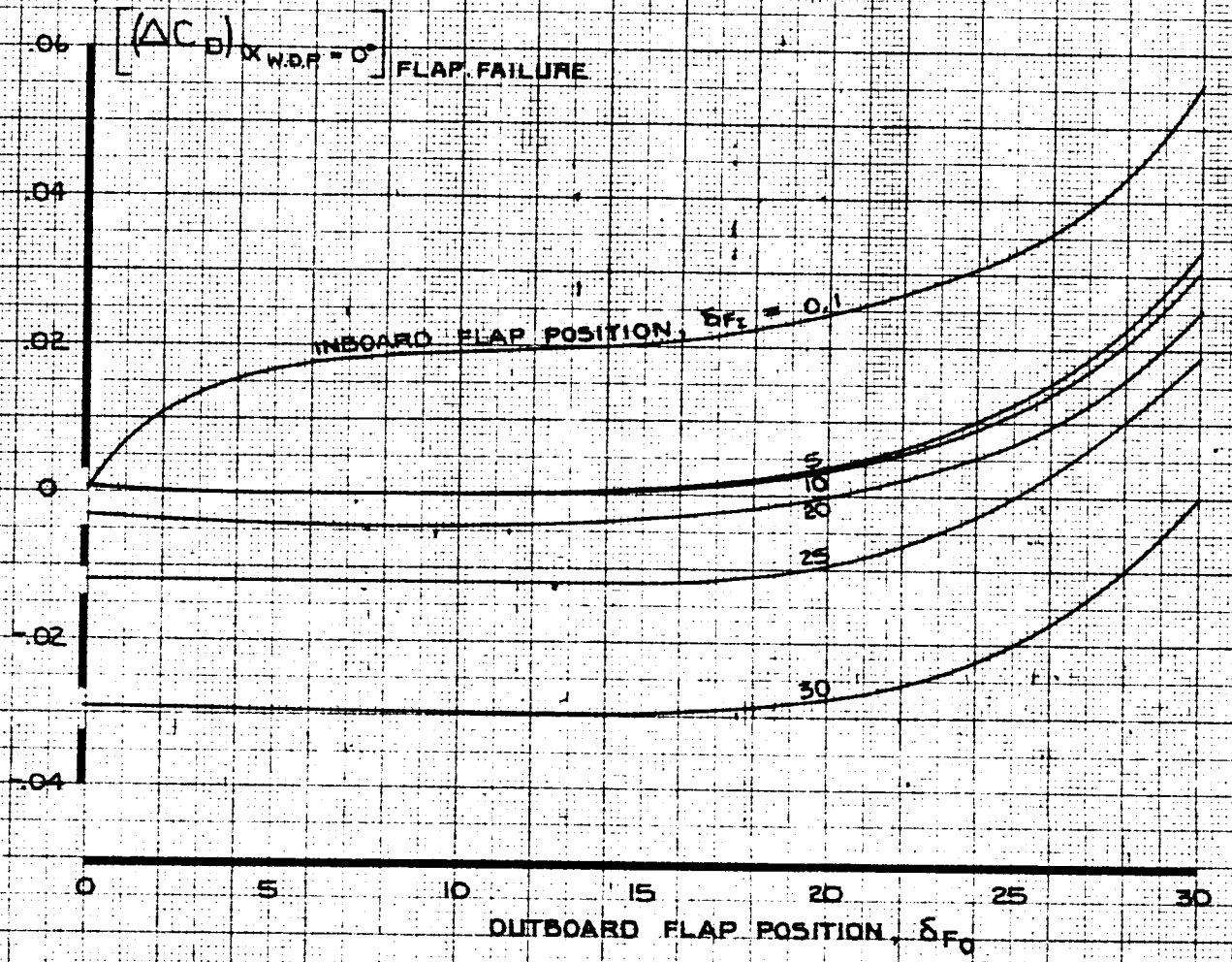

CALC	LOW	5-3-69	REVISED	DATE
CHECK			LOW	2-17-70
APR			LOW	6-25-70
APR				
INK	ODEGARD	5-3-69		

DRAG COEFFICIENT
EFFECT OF FLAPS ON
$[(\Delta C_D)_{\alpha\ W.D.P = 0^\circ}]$ FLAP FAILURE

THE BOEING COMPANY

747
D6-30643 Vol. II
PAGE 3.0-20

TD 461 C-R4

NOTE 1. DATA APPLICABLE FOR SYMMETRIC OR ASYMMETRIC (MONITOR LIMITED) FLAP FAILURE

THESE DATA NOT INCLUDED IN NASA SIMULATION

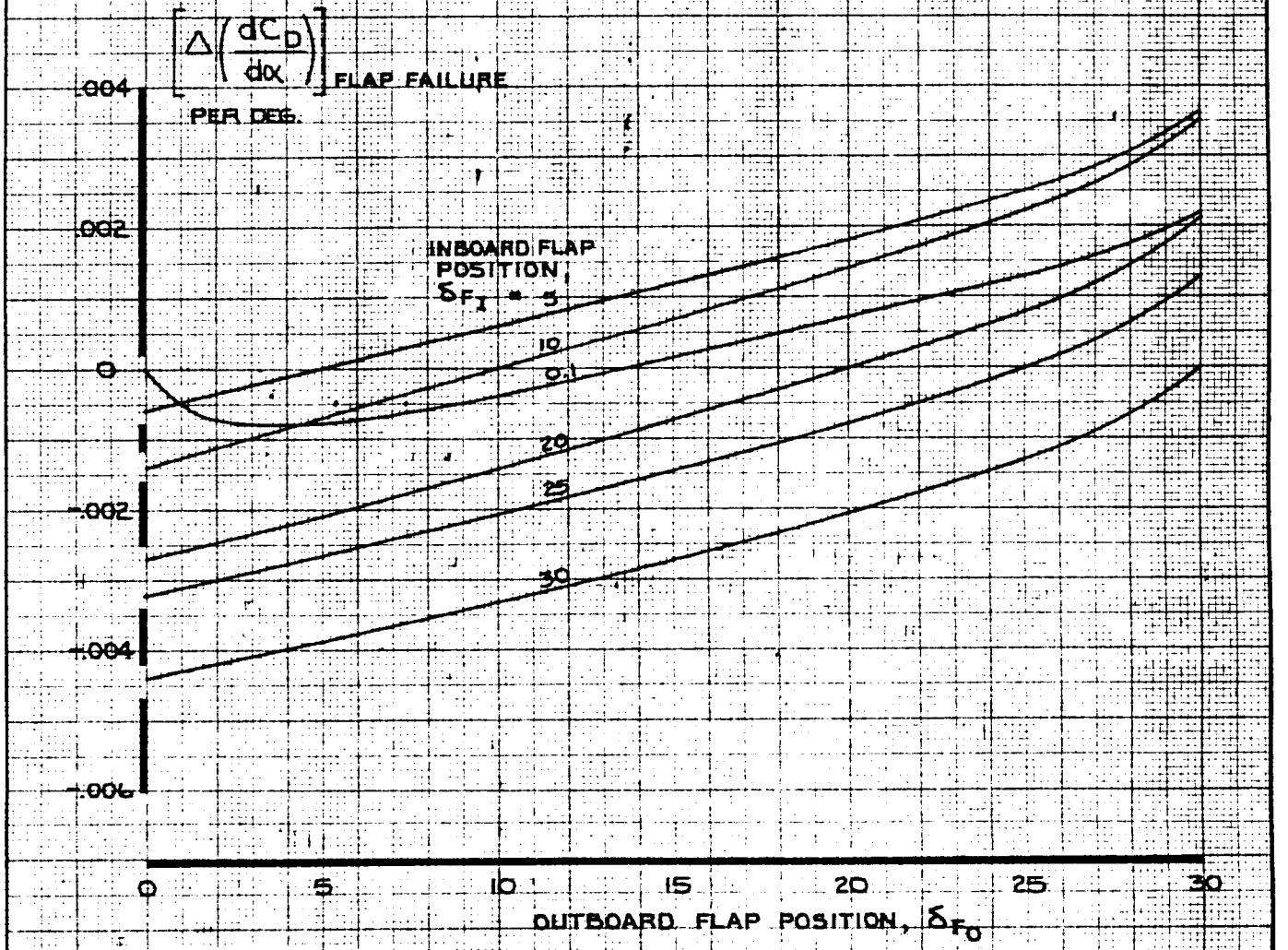

CALC	LOW	5-3-69	REVISED	DATE	DRAG COEFFICIENT EFFECT OF FLAPS ON $[\Delta(dC_D/d\alpha)]_{\text{FLAP FAILURE}}$
CHECK			LOW	2-17-70	
APR			LOW	6-25-70	
APR					
INK	ODEGARD	5-3-69			THE BOEING COMPANY

747
D6-30643 Vol. II
PAGE 3.0-21

4.0 PITCHING MOMENT COEFFICIENT

The dimensionless aerodynamic pitching moment coefficient is given in terms of its significant components by the equation below.

At a given $\alpha_{W.D.P.}$,

$$C_{m_{C.G.}} = C_{m_{.25\,BASIC}} + (\Delta C_{m.25})_{\alpha_{W.D.P.}=0^\circ} + \Delta\left(\frac{dC_{m.25}}{d\alpha}\right)\cdot\alpha_{W.D.P.}$$

$$+C_L(C.G.-.25) + \frac{dC_m}{d\hat{\alpha}}\cdot\left(\frac{\dot{\alpha}\bar{c}}{2V}\right) + \frac{dC_{m.25}}{d\hat{q}}\left(\frac{q\bar{c}}{2V}\right) + \frac{dC_{m.25}}{dn_z}\cdot n_z$$

$$+K_\alpha\cdot\frac{dC_{m.25}}{d\delta}\cdot\delta_{F.R.L.} + K_\alpha\cdot\frac{dC_{m.25}}{d\delta_{E_I}}\cdot\delta_{E_I} + K_\alpha\cdot\frac{dC_{m.25}}{d\delta_{E_O}}\cdot\delta_{E_O}$$

$$+\Delta C_{m.25_{SPOILERS}} + \Delta C_{m.25_{\substack{INBOARD\\AILERONS}}} + \Delta C_{m.25_{\substack{OUTBOARD\\AILERONS}}} + \Delta C_{m.25_{\substack{LANDING\\GEAR}}}$$

$$+\Delta C_{m.25_{\substack{GROUND\\EFFECT}}} + \Delta C_{m.25_{SIDESLIP}} + \Delta C_{m.25_{RUDDERS}} \left[+\Delta C_{m.25_{FLAP\ FAILURE}}\right]^*$$

where,

$C_{m.25_{BASIC}}$ = Basic pitching moment coefficient for the rigid airplane at $\delta_{F.R.L.} = 0^\circ$, in free air, with the landing gear retracted, and with the C.G. = 25% M.A.C. For low speed, $C_{m_{.25\,BASIC}}$ is plotted on pages 4.0-8 and 4.0-9. For flaps up, $C_{m_{.25\,BASIC}}$ is plotted on page 4.0-10.

$(\Delta C_{m.25})_{\alpha_{W.D.P.}=0^\circ}$ = Change in basic pitching moment coefficient at $\alpha_{W.D.P.}=0^\circ$ due to aeroelasticity. For low speed,

[ ]* NOT IN NASA SIMULATION

AD 1546 D

4.0 (Cont'd)

$(\Delta C_{m.25})_{\alpha_{w.a.p.}=0°}$ is plotted on page 4.0-11. For flaps up, $(\Delta C_{m.25})_{\alpha_{w.a.p.}=0°}$ is plotted on page 4.0-12.

$\Delta\left(\frac{dC_{m.25}}{d\alpha}\right)\cdot\alpha_{w.a.p.}$ = Change in basic pitching moment coefficient due to the aeroelastic effect on the rigid airplane basic pitching moment coefficient curve slope. For low speed, $\Delta\left(\frac{dC_{m.25}}{d\alpha}\right)$ is plotted on page 4.0-13. For flaps up, $\Delta\left(\frac{dC_{m.25}}{d\alpha}\right)$ is plotted on page 4.0-14.

$C_L\cdot(C.G.-.25)$ = Change in pitching moment coefficient due to center of gravity variation from 25% M.A.C. The total lift coefficient, C_L, is defined in Section 2.0.

$\frac{dC_m}{d\hat{\alpha}}\cdot\left(\frac{\dot{\alpha}\bar{c}}{2V}\right)$ = Change is basic pitching moment coefficient due to rate of change of angle of attack.

$$\frac{dC_m}{d\hat{\alpha}} = K_{\hat{\alpha}}\cdot\frac{dC_{m.25}}{d\hat{\alpha}}$$

where $\frac{dC_{m.25}}{d\hat{\alpha}}$ and the center of gravity factor, $K_{\hat{\alpha}}$ are plotted on page 4.0-15.

$\frac{dC_{m.25}}{d\hat{q}}\cdot\left(\frac{q\bar{c}}{2V}\right)$ = Change in basic pitching moment coefficient due to pitch rate. $\frac{dC_{m.25}}{d\hat{q}}$ is plotted on page 4.0-16.

$\frac{dC_{m.25}}{dn_z}\cdot n_z$ = Change in basic pitching moment coefficient due to aeroelastic inertia relief caused by normal load factor, n_z. For low speed, $\frac{dC_{m.25}}{dn_z}$ is plotted on page 4.0-17. For flaps up, $\frac{dC_{m.25}}{dn_z}$ is plotted

on page 4.0-18.

(Cont'd)

$K_\alpha \cdot \frac{dC_{m.25}}{d\delta} \cdot \delta_{F.R.L.}$ = Change in basic pitching moment coefficient due to change in stabilizer angle from $\delta_{F.R.L.} = 0°$. $\frac{dC_{m.25}}{d\delta}$ is plotted on page 4.0-20. The effectiveness factor for the stabilizer (and elevators), K_α, is plotted on page 4.0-19.

$K_\alpha \cdot \frac{dC_{m.25}}{d\delta_{E_I}} \cdot \delta_{E_I}$ = Change is basic pitching moment coefficient due to change in inboard elevator angle from $\delta_{E_I} = 0°$. $\frac{dC_{m.25}}{d\delta_{E_I}}$ is plotted on page 4.0-21. [1]

$K_\alpha \cdot \frac{dC_{m.25}}{d\delta_{E_O}} \cdot \delta_{E_O}$ = Change in basic pitching moment coefficient due to change in outboard elevator angle from $\delta_{E_O} = 0°$. $\frac{dC_{m.25}}{d\delta_{E_O}}$ is plotted on page 4.0-22. [1]

[1] The normal system stick free (rigged) elevator deflection is + 2° from the faired position.

$\Delta C_{m.25\ SPOILERS}$ = Change in basic pitching moment coefficient due to spoiler or speed brake deflection.

$$\Delta C_{m.25_{SPOILERS}} = \sum_{\substack{\text{OPERATING} \\ \text{SPOILER} \\ \text{PANELS}}} (K_{\delta_{SP}})_m \cdot (\Delta C_{m.25_{SP}})_{45} \cdot \frac{(C_{m.25_{SP}})_M}{(C_{m.25_{SP}})_{M=0}} \cdot \left(\frac{M_E}{M_R}\right)_{SP} \cdot Fm_{GE}$$

where $(\Delta C_{m.25\ SP})_{45}$ is the change in basic pitching moment coefficient due to deflecting the operating spoiler panels to 45°. $(\Delta C_{m.25\ SP})_{45}$ is plotted for spoilers and ground spoilers on page 4.0-24 and

4.0 (Cont'd)

4.0-25 respectively. The spoiler effectiveness factor, $(K_{\delta_{SP}})_m$ is plotted on page 4.0-23. The Mach number effect, $(C_{m_{.25_{SP}}})_M / (C_{m_{.25_{SP}}})_{M=0}$ is plotted on page 4.0-26. The aeroelastic effect, $\left(\frac{M_E}{M_R}\right)_{SP}$ is plotted on pages 4.0-27, 4.0-28, and 4.0-29. The ground effect factor, $F_{m_{GE}}$ is obtained as follows:

$$F_{m_{GE}} = \left[1 + (F_m \cdot K^B_{GE})\right]$$

where F_m is plotted on page 4.0-32. The ground effect height factor, K^B_{GE} is plotted on page 2.0-31.

$\Delta C_{m_{.25_{\substack{\text{INBOARD}\\\text{AILERONS}}}}}$ = Change in basic pitching moment coefficient due to inboard aileron deflection.

$$\Delta C_{m_{.25_{\substack{\text{INBOARD}\\\text{AILERONS}}}}} = K_{\delta_{A_I}} \cdot (\Delta C_{m_{.25_{A_I}}})_{20} \cdot \frac{(C_{m_{.25_{A_I}}})_M}{(C_{m_{.25_{A_I}}})_{M=0}} \cdot F_{m_{GE}}$$

where $(\Delta C_{m_{.25_{A_I}}})_{20}$ is the change in basic pitching moment coefficient due to deflecting one inboard aileron up to 20°. $(\Delta C_{m_{.25_{A_I}}})_{20}$ is plotted on page 4.0-30. The inboard aileron effectiveness factor, $K_{\delta_{A_I}}$ is to be obtained for the up inboard aileron deflection and is plotted on page 5.0-22. The Mach number effect, $(C_{m_{.25_{A_I}}})_M / (C_{m_{.25_{A_I}}})_{M=0}$ is plotted on page 4.0-30. The ground effect factor, $F_{m_{GE}}$ is obtained from page 4.0-32.

$\Delta C_{m_{.25_{\substack{\text{OUTBOARD}\\\text{AILERONS}}}}}$ = Change in basic pitching moment coefficient due to

4.0 (Cont'd)

outboard aileron deflection.

$$\Delta C_{m.25_{\substack{\text{OUTBOARD}\\\text{AILERONS}}}} = \sum_{\substack{\text{UP AND DOWN}\\\text{OUTBOARD}\\\text{AILERONS}}} K\delta_{A_O} \cdot \Delta C_{m.25A_O} \cdot Fm_{GE}$$

where $\Delta C_{m.25A_O}$ is the change in basic pitching moment coefficient due to deflecting one outboard aileron up to 25° or the opposite outboard aileron down to 15°. $\Delta C_{m.25A_O}$ is plotted on page 4.0-31. The outboard aileron effectiveness factor, $K\delta_{A_O}$, is plotted on page 5.0-26. The ground effect factor, Fm_{GE}, is obtained from page 4.0-32.

$\Delta C_{m.25_{\substack{\text{LANDING}\\\text{GEAR}}}}$ = Change is basic pitching moment coefficient due to main and nose landing gear extension.

$$\Delta C_{m.25_{\substack{\text{LANDING}\\\text{GEAR}}}} = K_{GEAR} \cdot \Delta C_{m.25_{GEAR}} \cdot \frac{(C_{m.25_{GEAR}})_M}{(C_{m.25_{GEAR}})_{M=0}}$$

where $\Delta C_{m.25_{GEAR}}$ is plotted on page 4.0-33. The Mach number effect, $(C_{m.25_{GEAR}})_M / (C_{m.25_{GEAR}})_{M=0}$, is plotted on page 4.0-34. The landing gear effectiveness factor, K_{GEAR}, is plotted on page 2.0-28.

$\Delta C_{m.25_{\substack{\text{GROUND}\\\text{EFFECT}}}}$ = Change in basic pitching moment coefficient due to ground effect.

$$\Delta C_{m.25_{\substack{\text{GROUND}\\\text{EFFECT}}}} = K_{GE}^{B} \cdot \Delta C_{m.25_{GE}}$$

where $\Delta C_{m.25_{GE}}$ is plotted on page 4.0-35.

4.0 (Cont'd)

The ground effect weight factor, K_{GE}^{β}, is plotted on page 4.0-31.

$\Delta C_{m_{.25\ SIDESLIP}}$ = Change in basic pitching moment coefficient due to angle of sideslip, β. $\Delta C_{m_{.25\ SIDESLIP}}$ is plotted on page 4.0-36.

$\Delta C_{m_{.25\ RUDDERS}}$ = Change in basic pitching moment coefficient due to rudder deflection.

$$\Delta C_{m_{.25\ RUDDERS}} = \Delta C_{m_{.25 R_U}} + \Delta C_{m_{.25 R_L}}$$

where $\Delta C_{m_{.25 R_U}}$ and $\Delta C_{m_{.25 R_L}}$ are the changes in basic pitching moment coefficient due to deflection of upper rudder and lower rudder respectively.

$\Delta C_{m_{.25 R_U}}$ and $\Delta C_{m_{.25 R_L}}$ are obtained from page 4.0-36.

$\Delta C_{m_{.25\ FLAP\ FAILURE}}$ = Increment in basic pitching moment coefficient due to flap deflection or retraction from the flap position at which symmetric failure of both inboard or both outboard flaps occurs.

For symmetric failure of outboard flap failure,

$$\Delta C_{m_{.25\ FLAP\ FAILURE}} = \left[(\Delta C_{m_{.25}})_{\alpha_{W.D.P.}=0^\circ}\right]_{FLAP\ FAILURE} + \Delta\left(\frac{dC_{m_{.25}}}{d\alpha}\right)_{FLAP\ FAILURE} \cdot \alpha_{W.D.P.}$$

where $\left[(\Delta C_{m_{.25}})_{\alpha_{W.D.P.}=0^\circ}\right]_{FLAP\ FAILURE}$ is the change in basic pitching moment coefficient at $\alpha_{W.D.P.} = 0^\circ$

4.0 (Cont'd)

due to symmetric inboard or outboard flap failure.

$\left[(\Delta C_{m_{.25}})_{\alpha_{W.D.P.}=0^\circ}\right]_{\text{FLAP FAILURE}}$ is plotted on page 4.0-37. $\Delta\left(\frac{dC_{m_{.25}}}{d\alpha}\right)_{\text{FLAP FAILURE}} \cdot \alpha_{W.D.P.}$ is the change in basic pitching moment coefficient due to the effect of symmetric inboard or outboard flap failure on the rigid airplane basic pitching moment coefficient curve slope.

$\Delta\left(\frac{dC_{m_{.25}}}{d\alpha}\right)_{\text{FLAP FAILURE}}$ is plotted on page 4.0-38.

The above data is also applicable for asymmetric (monitor limited) inboard or outboard flap failure.

$\Delta C_{m_{.25\ \text{FLAP FAILURE}}}$ is to be added to total $C_{m_{C.G.}}$ computed for the inboard flap position.

AD 1546 D

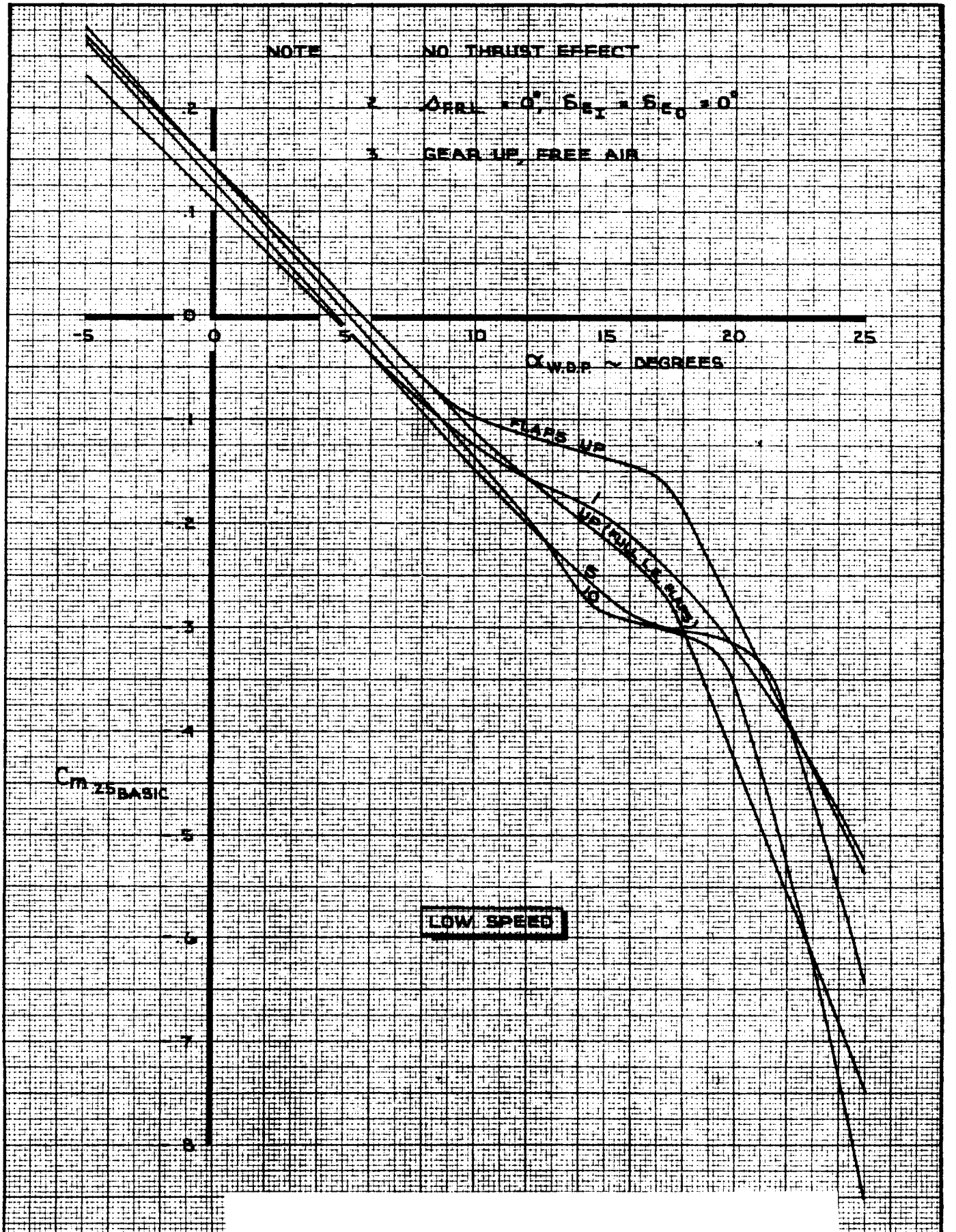

CALC	LOW	11·21·67	REVISED	DATE	PITCHING MOMENT COEFFICIENT EFFECT OF ANGLE OF ATTACK ON BASIC $C_{m.25}$ (FLAPS UP, 1, 5, 10)
CHECK	FOSTER	1·24·68	LOW	2·16·68	
APR			BYSTROM	2·9·70	
APR					
INK	KINSMAN	3·2·70			THE BOEING COMPANY

747

D6-30643 Vol. II

PAGE 4.0-8

AD 461 C-R4

K·E ALBANENE 1951 TRACING PAPER REV. D

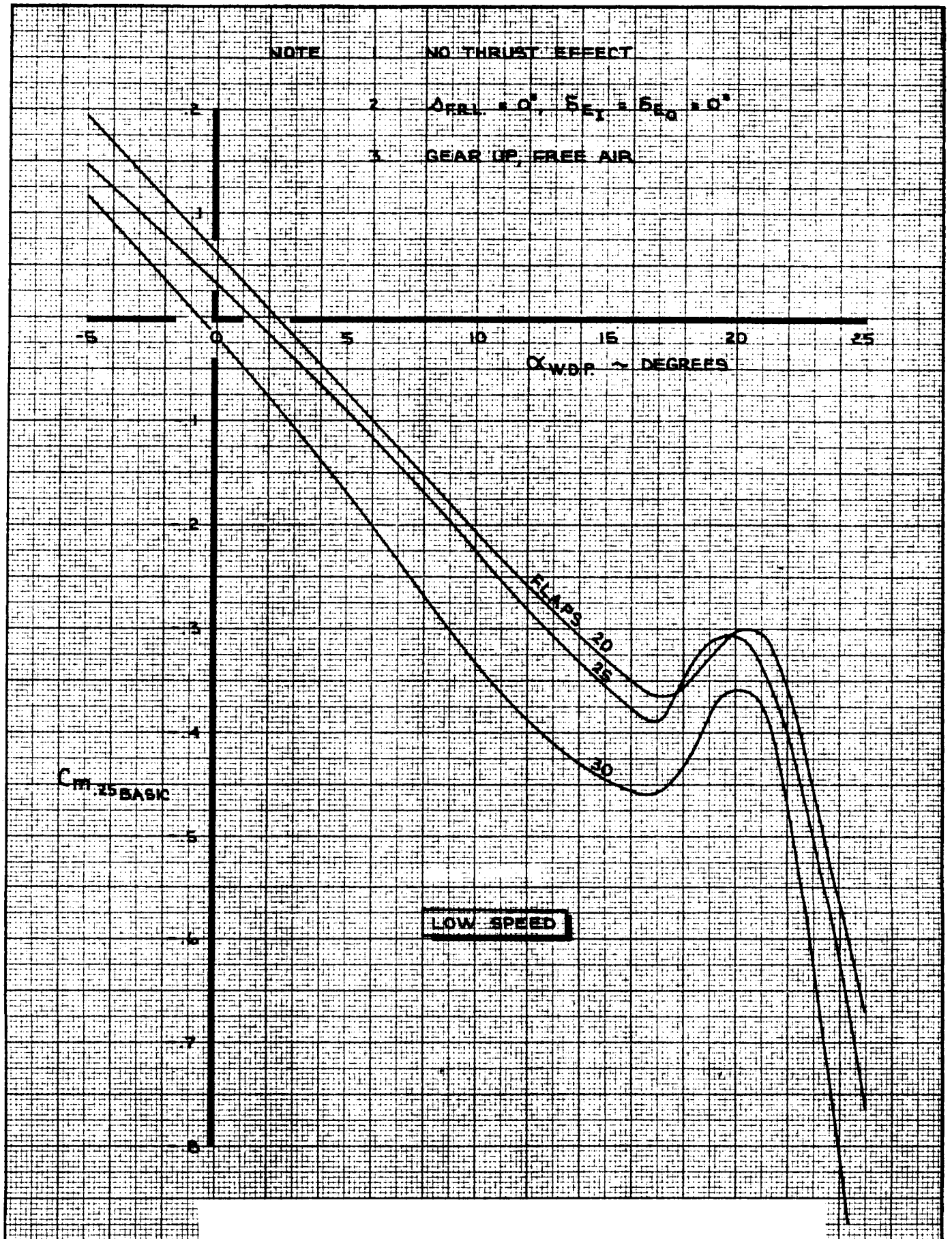

CALC	LOW	11-21-67	REVISED	DATE	PITCHING MOMENT COEFFICIENT EFFECT OF ANGLE OF ATTACK ON BASIC $C_{m.25}$ (FLAPS 20, 25, 30)
CHECK	FOSTER	1-24-68	LOW	2-16-68	
APR			BYSTROM	2-9-70	
APR					
INK	KINSMAN	3-2-70			THE BOEING COMPANY

747
D6-30643 Vol. II
PAGE 4.0-9

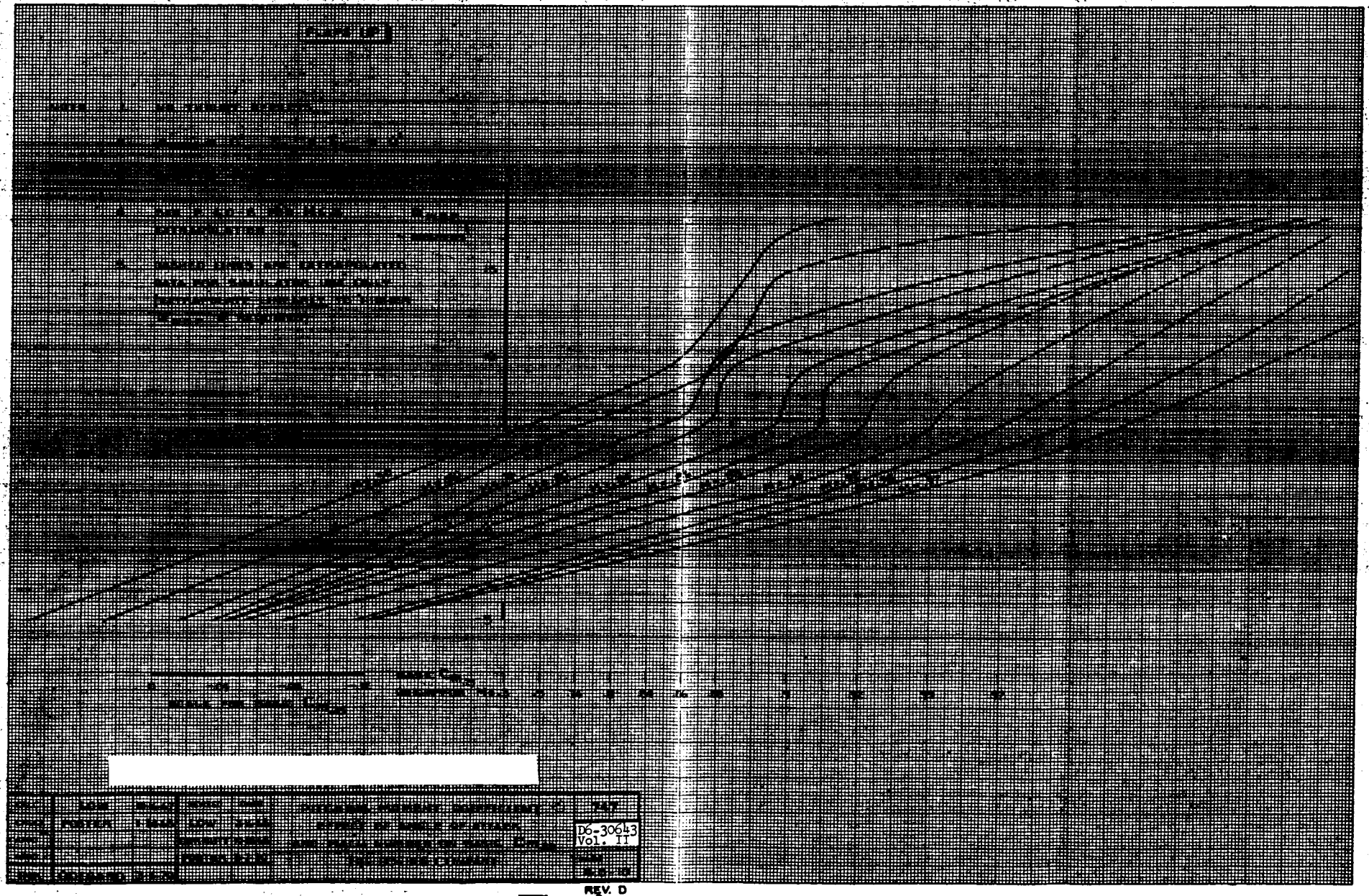

LOW SPEED

NOTE 1. USE FOR ALL ALTITUDES

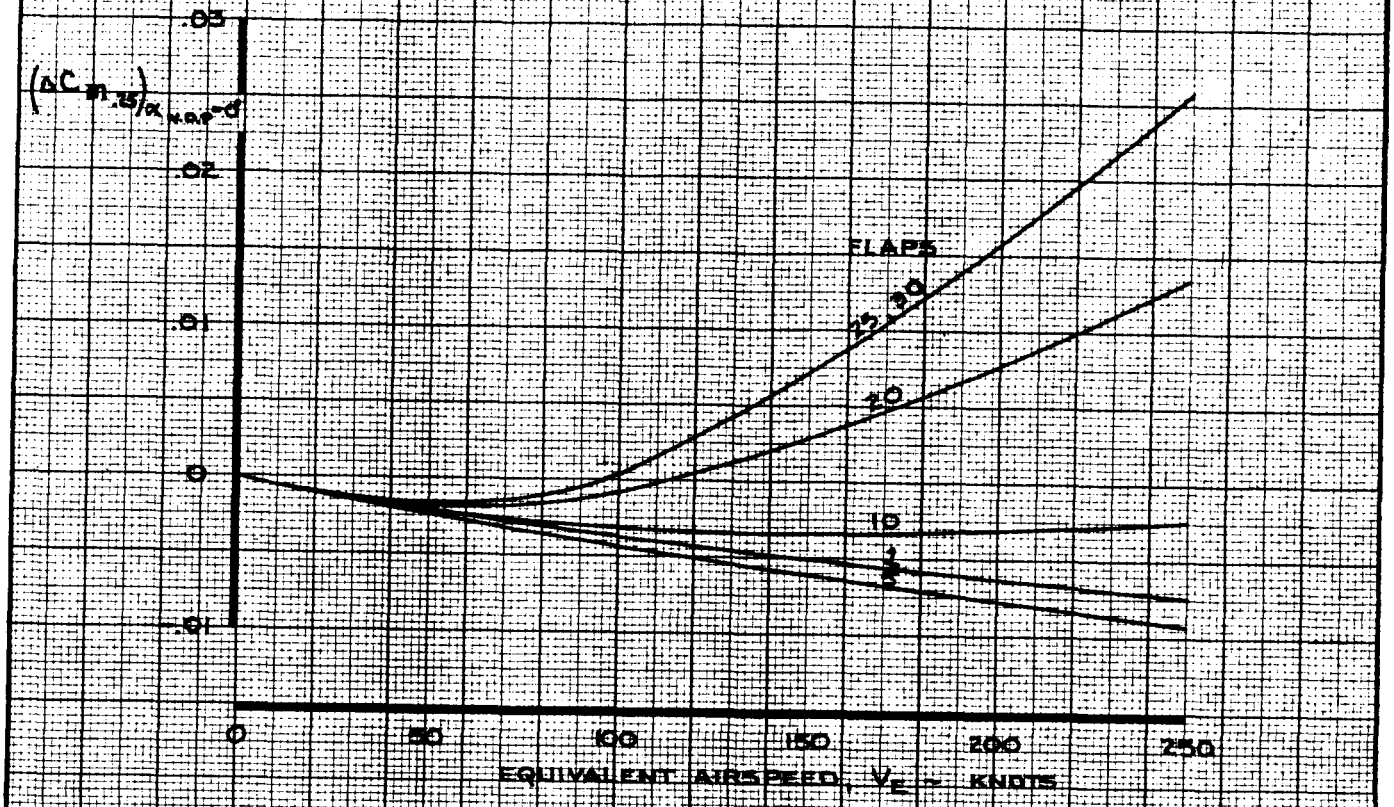

CALC	LOW	11/18/67	REVISED	DATE	PITCHING MOMENT COEFFICIENT EFFECT OF FLAPS ON $(\Delta C_{m_{.25}})_{\alpha_{W.B.P.}=0}$	747
CHECK	FOSTER	1-24-68	LOW	1-23-70		D6-30643 Vol. II
APR						
APR						
INK	ODEGARD	11/18/67			THE BOEING COMPANY	PAGE 4.0-11

TD 461 C-R4

REV D

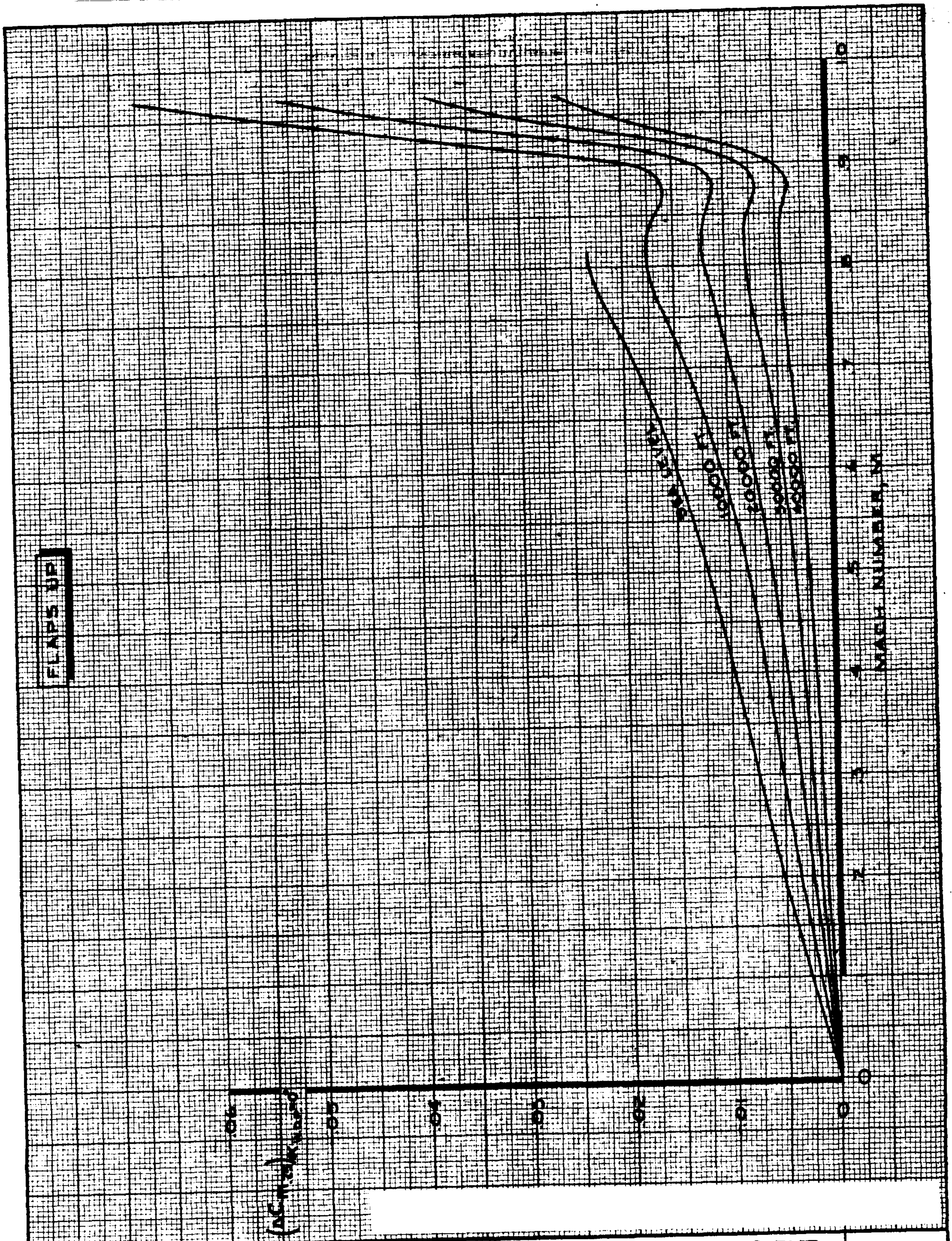

			REVISED	DATE
CALC	LOW	10/16/67		
CHECK	FOSTER	1-24-68	LOW	6-14-69
APR				
APR				
INK	ODEGARD	10/16/67		

AD 461 C R4

PITCHING MOMENT COEFFICIENT
AERODELASTIC EFFECT ON
$(\Delta C_{m.25})_{\alpha_{W.D.P.}=0°}$

THE BOEING COMPANY

747

D6-30643
Vol. II

CMØ

LOW SPEED

NOTE 1. USE FOR ALL ALTITUDES

2. $\Delta C_{m_{.25}} = \Delta\left(\frac{dC_{m_{.25}}}{d\alpha}\right) \cdot \alpha_{w.b.p.}$

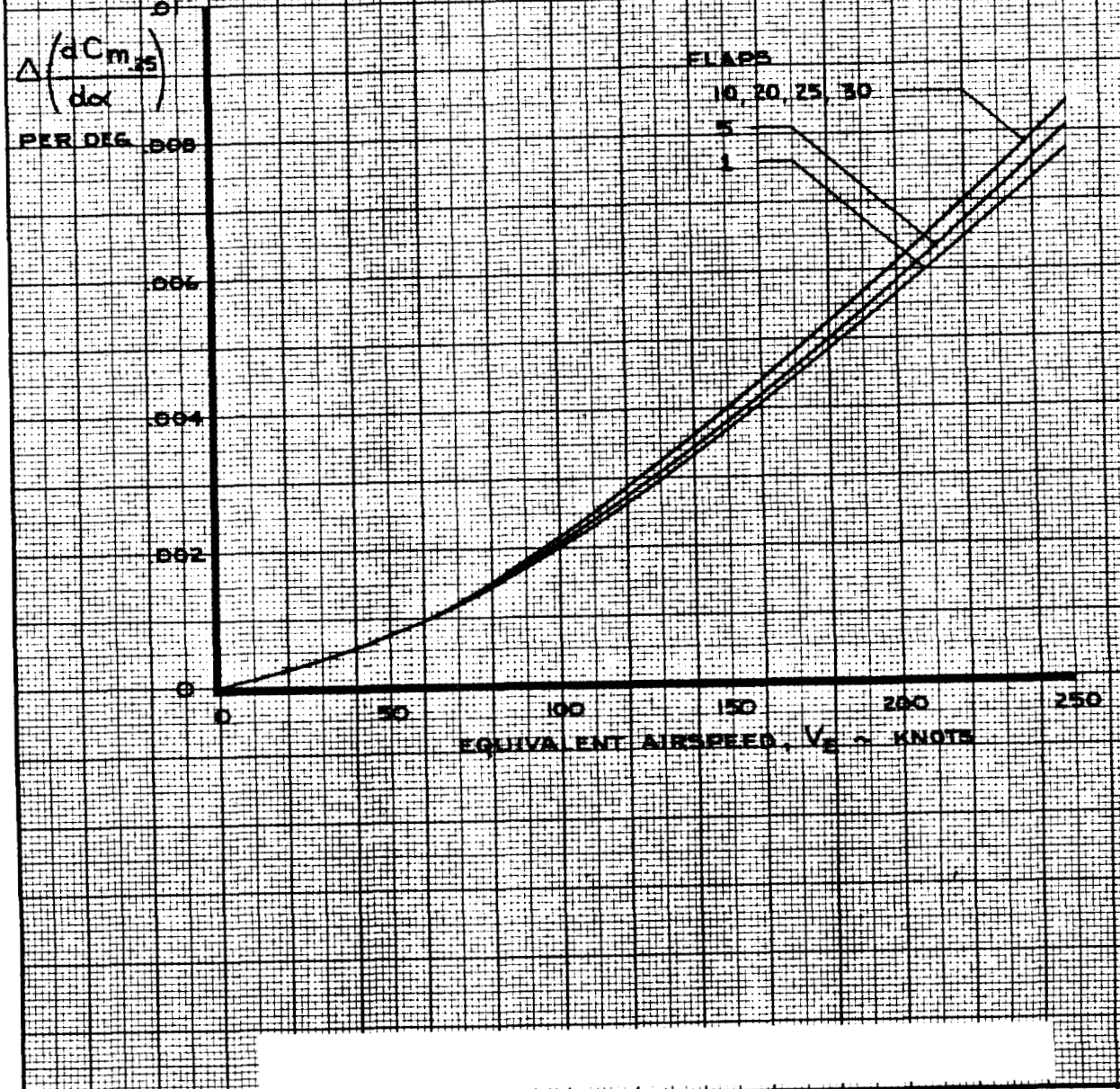

CALC	LOW	11/18/67	REVISED	DATE	PITCHING MOMENT COEFFICIENT EFFECT OF FLAPS ON $\Delta(dC_{m_{.25}}/d\alpha)$
CHECK	FOSTER	1-24-68	LOW	1-23-70	
APR					
APR					THE BOEING COMPANY
INK	ODEGARD	11/18/67			

747
D6-30643 Vol. II
PAGE 4.0-13
REV. D

TD 461 C-R4

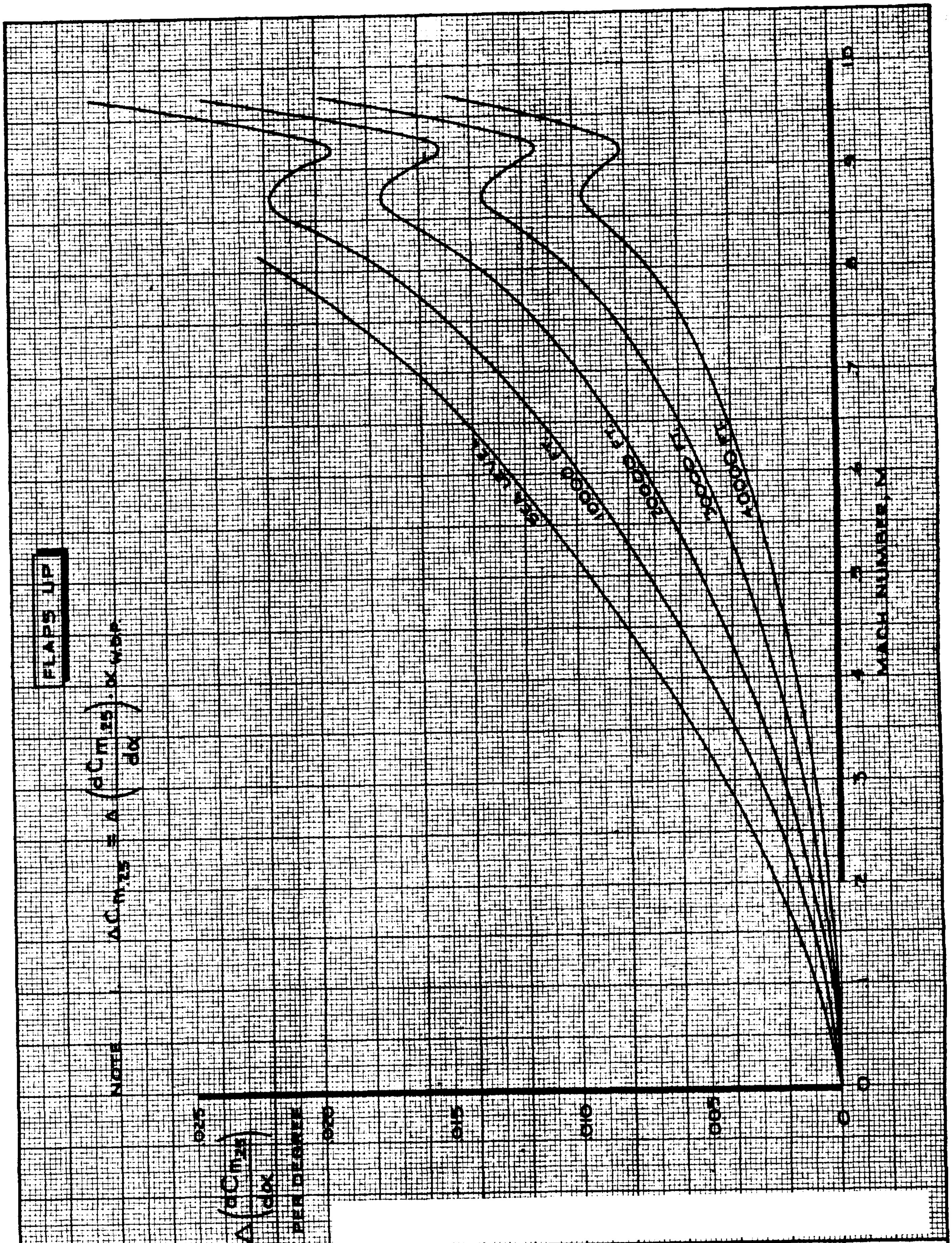

CALC	LOW	10/16/67	REVISED	DATE	PITCHING MOMENT COEFFICIENT AEROELASTIC EFFECT ON $\Delta(dC_{m_{.25}}/d\alpha)$	747
CHECK	FOSTER	1-24-68	LOW	6-14-69		D6-30643 Vol. II
APR						
APR					THE BOEING COMPANY	PAGE 4.0-14
INK	ODEGARD	10/16/67				

AD 461 C R4

CMAL

REV. B

72

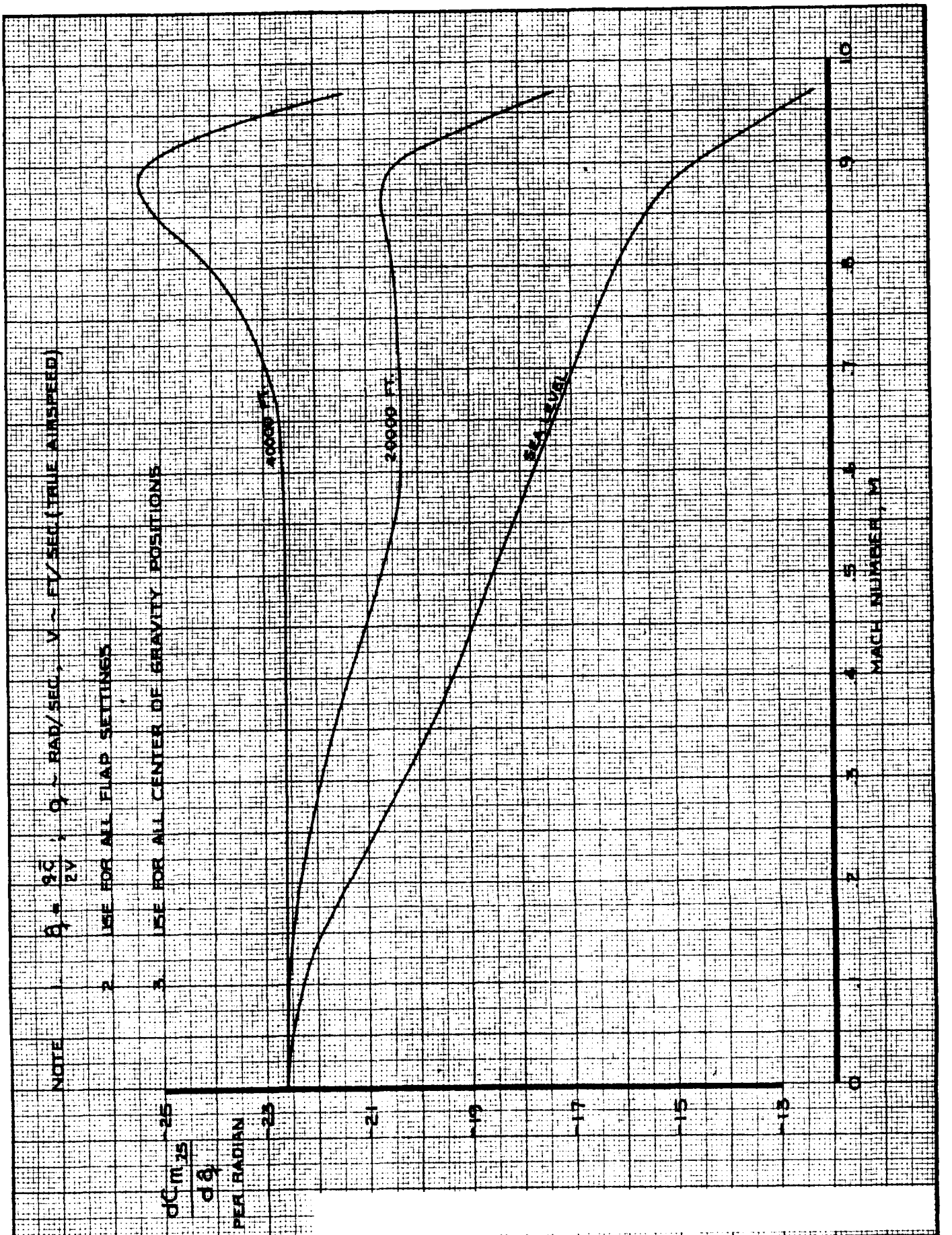

CALC	RICHARDSON	11-28-67	REVISED	DATE	PITCHING MOMENT COEFFICIENT EFFECT OF $\hat{q}$
CHECK	CURNUTT	11-30-67	LOW	6-14-69	
APR					
APR					
INK	ODEGARD	11-28-67			THE BOEING COMPANY

747

D6-30643 Vol. II

PAGE 4.0-16

TD 461 C-R4

CMO

K-E ALBANENE 1951 TRACING PAPER REV. B

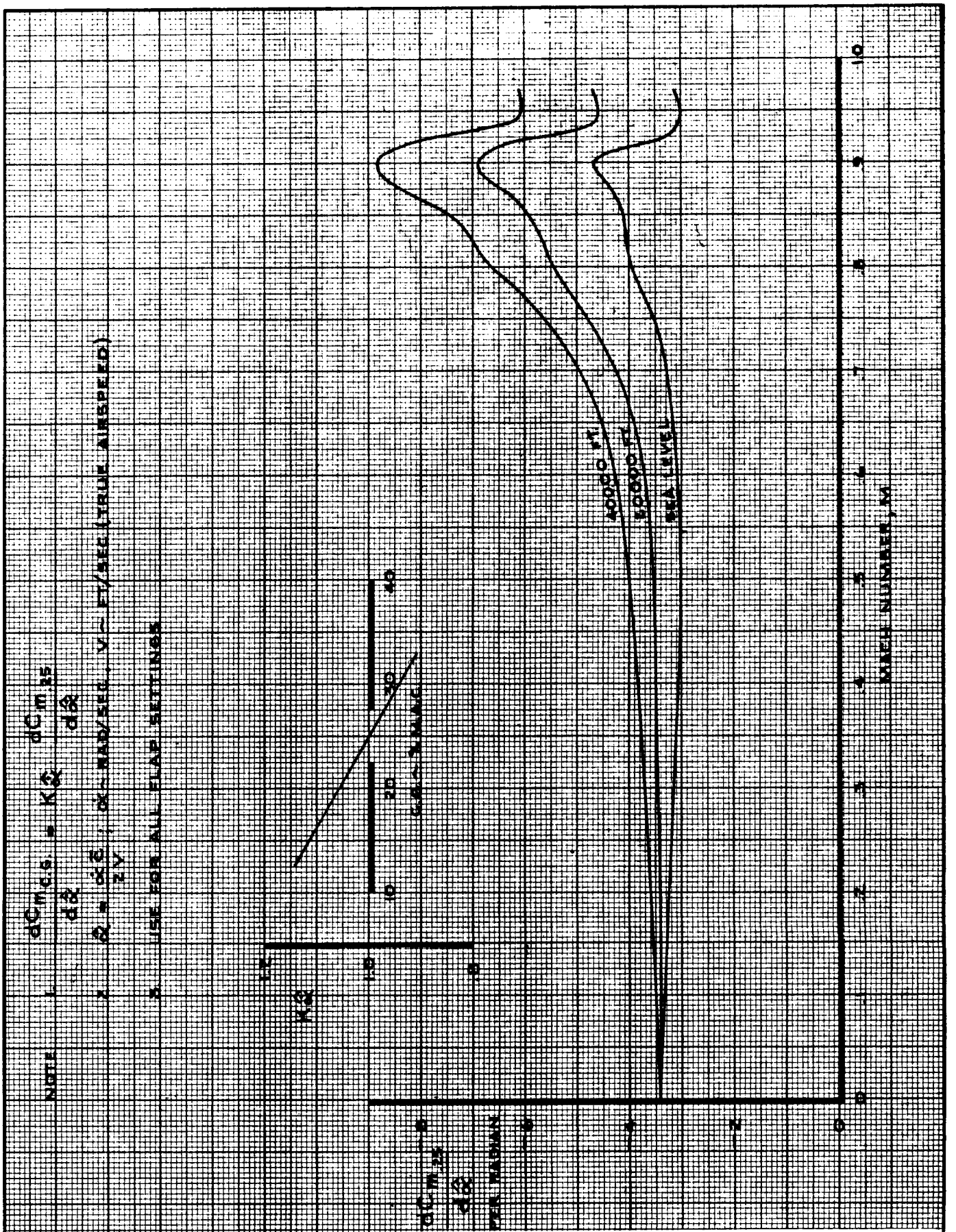

CALC	RICHARDSON	11/28/67	REVISED	DATE
CHECK	CURNUTT	11/30/67	LOW	6-14-69
APR				
APR				
INK	ODEGARD	11/28/67		

PITCHING MOMENT COEFFICIENT EFFECT OF $\hat{\alpha}$

747

D6-30643 Vol. II

THE BOEING COMPANY

PAGE 4.0-15

TD 461 C-R4

CMALD

REV. B

LOW SPEED

NOTE 1. USE FOR ALL ALTITUDES

2. $\Delta C_{m_{.25}} = \frac{dC_{m_{.25}}}{dn_z} \cdot n_z$ (n_z = 1 FOR STEADY LEVEL FLIGHT)

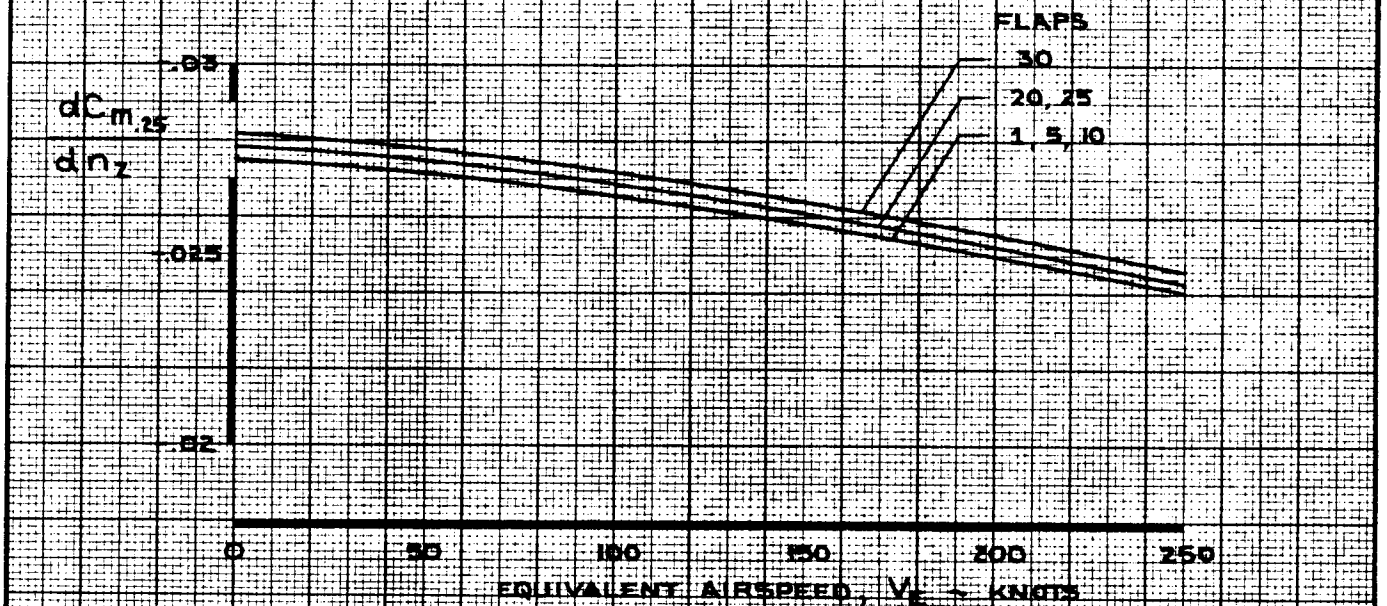

CALC	LOW	11/18/67	REVISED	DATE	PITCHING MOMENT COEFFICIENT EFFECT OF FLAPS ON $dC_{m_{.25}}/dn_z$
CHECK	FOSTER	1-24-68	LOW	1-23-70	
APR					
APR					
INK	ODEGARD	11/18/67			THE BOEING COMPANY

747
D6-30643 Vol. II
PAGE 4.0-17
REV D

TD 461 C-R4

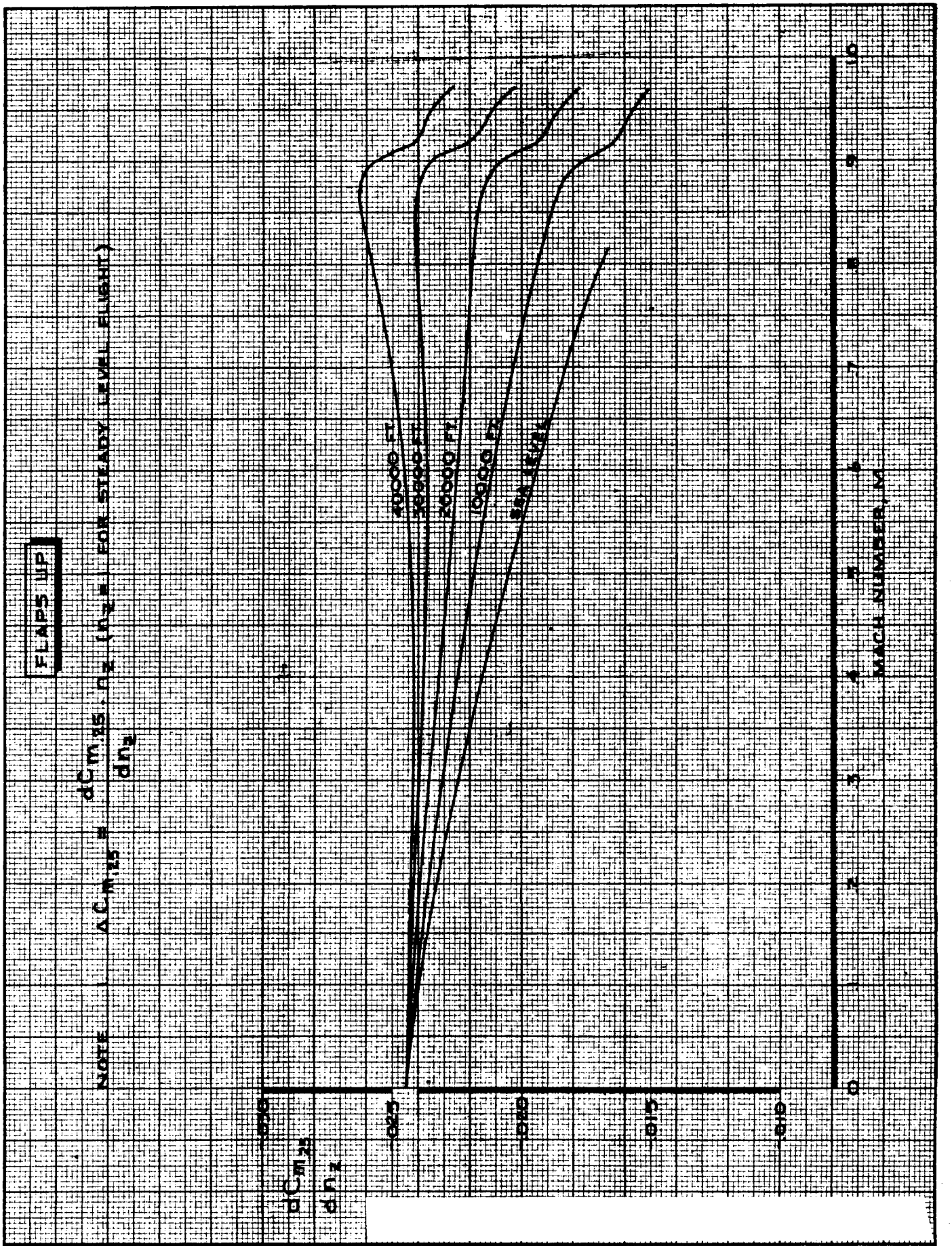

CALC	LOW	10/16/67	REVISED	DATE	PITCHING MOMENT COEFFICIENT EFFECT OF NORMAL LOAD FACTOR
CHECK	FOSTER	1-24-68	LOW	6-14-69	
APR					
APR					THE BOEING COMPANY
INK	ODEGARD	10/16/67			

747
D6-30643 Vol. II
PAGE 4.0-18
REV. B

AD 461 C R4

CMN7

451

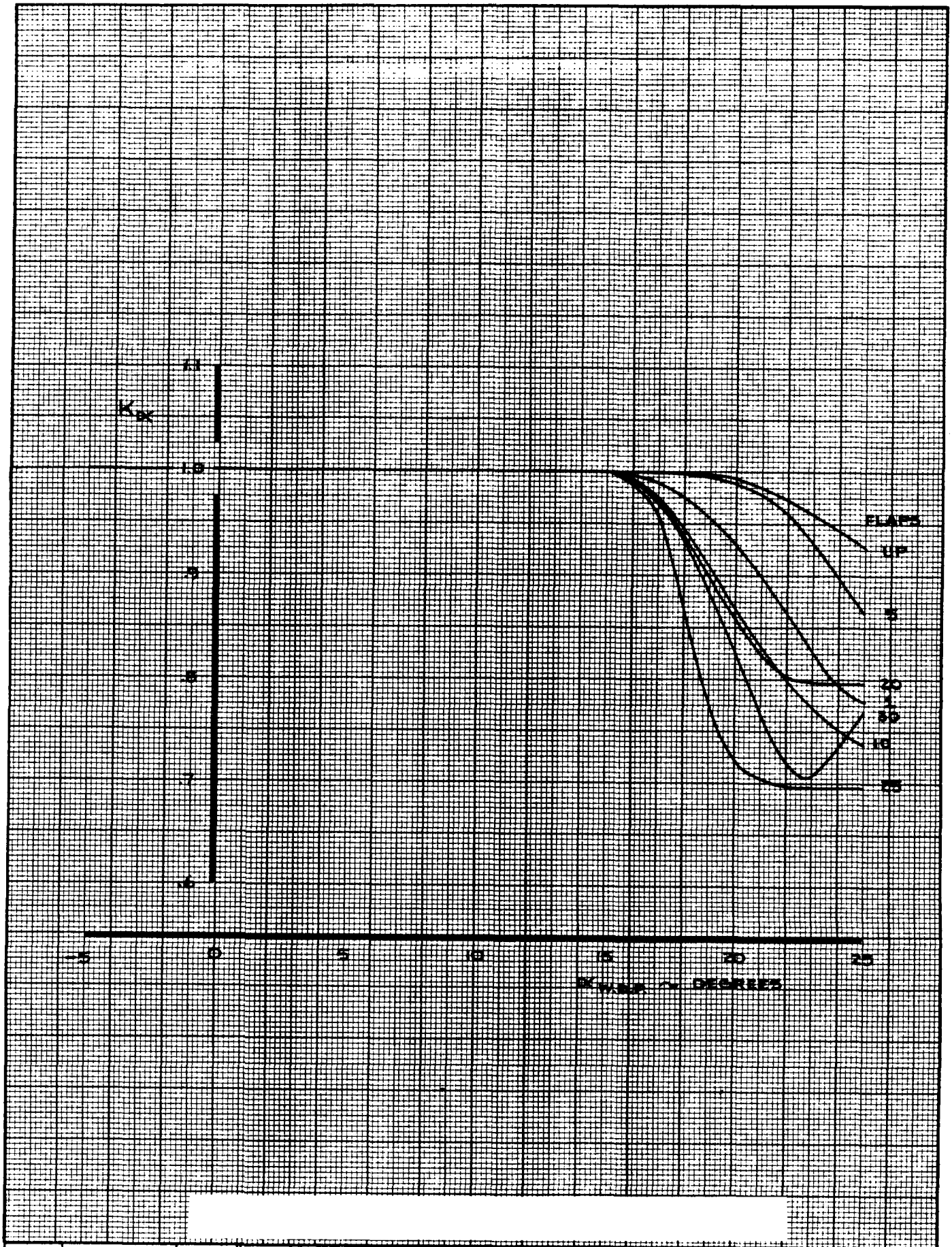

CALC	LOW	1/2/68	REVISED	DATE	EFFECTIVENESS FACTOR STABILIZER AND ELEVATORS
CHECK	FOSTER	1-24-68	LOW	2-14-70	
APR					
APR					
INK	ODEGARD	1/2/68			

747

D6-30643 Vol. II

THE BOEING COMPANY

PAGE 4.0-19

TD 461 C-R4

REV. D

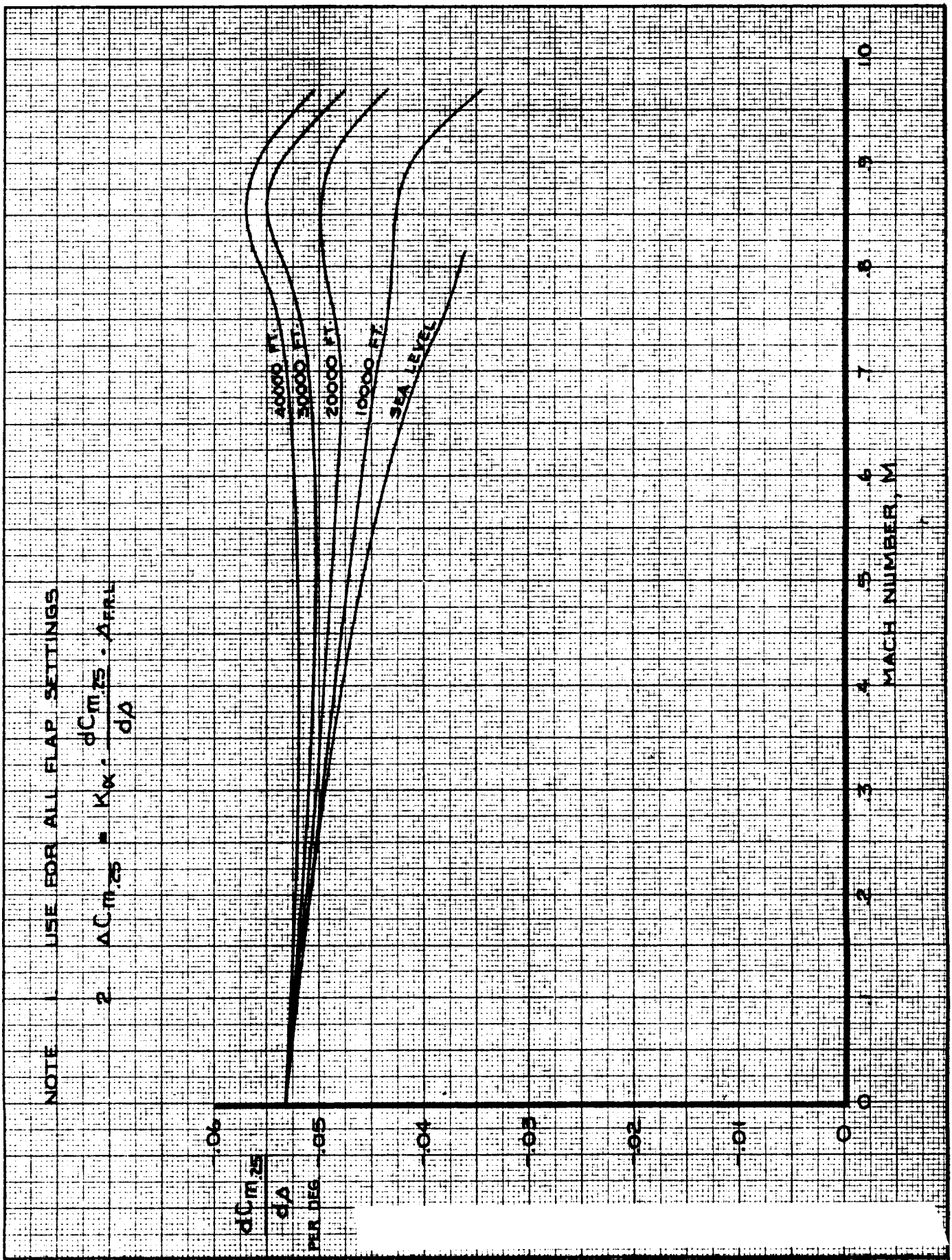

CALC	LOW	10-11-67	REVISED	DATE	PITCHING MOMENT COEFFICIENT, AEROELASTIC EFFECT ON STABILIZER EFFECTIVENESS
CHECK	FOSTER	1-24-68	BRYANT	8-17-69	
APR					
APR					
INK	ODEGARD	10-11-67			THE BOEING COMPANY

747

D6-30643 Vol. II

PAGE 4.0-20

AD 461 C-R4

K-E ALBANENE 1961 TRACING PAPER REV. D

NOTE

1. USE FOR ALL FLAP SETTINGS
2. BOTH INBOARD ELEVATORS DEFLECTED
3. FOR ONE INBOARD ELEVATOR DEFLECTED, USE HALF THE VALUE SHOWN
4. $\Delta C_{m.25} = K_K \cdot \frac{dC_{m.25}}{d\delta_{EI}} \cdot \delta_{EI}$

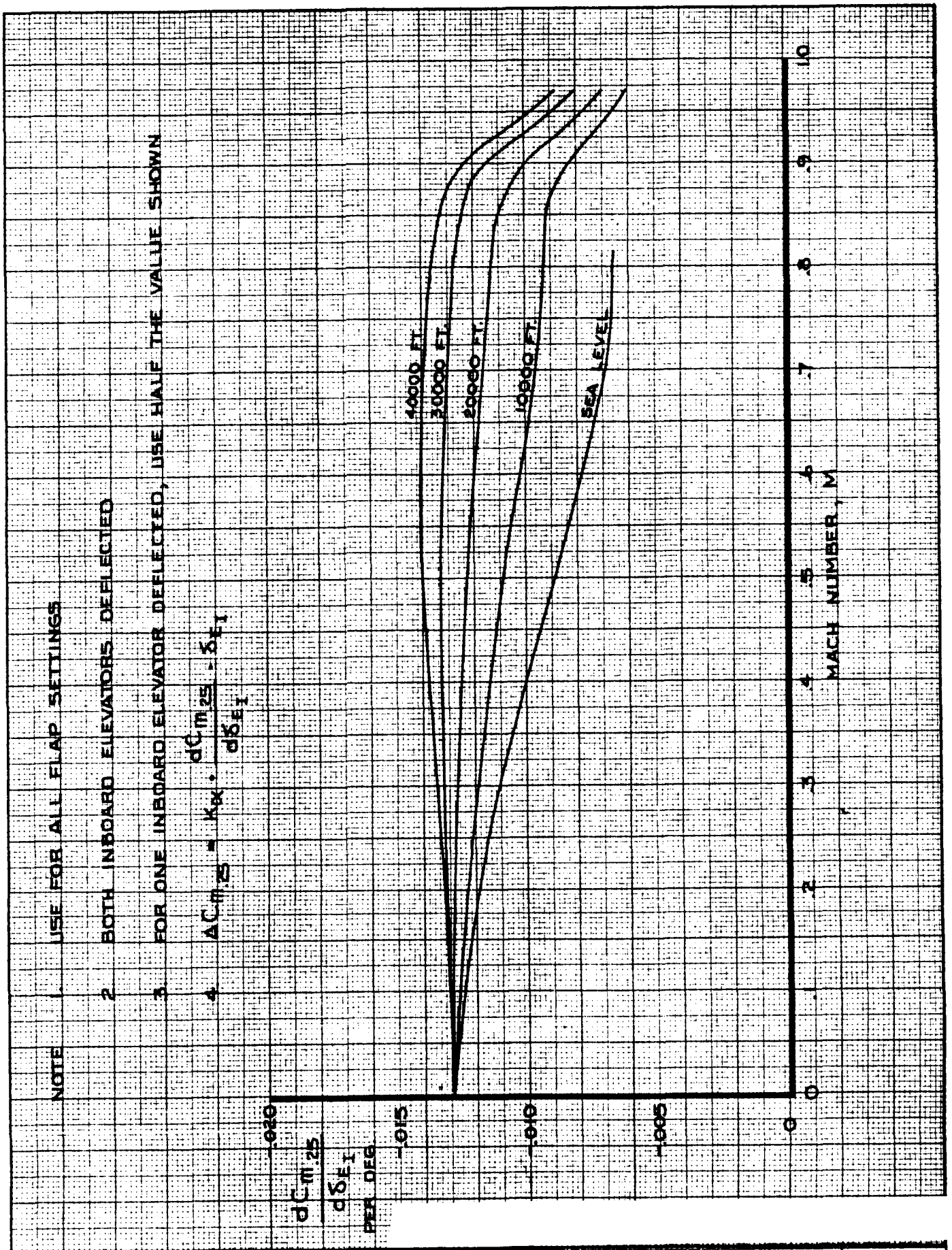

CALC	LOW	10-9-67	REVISED	DATE	PITCHING MOMENT COEFFICIENT AEROELASTIC EFFECT ON INBOARD ELEVATOR EFFECTIVENESS
CHECK	FOSTER	1-24-68	FOSTER	9-25-69	
APR					
APR					
INK	ODEGARD	10-9-67			

747

D6-30643 Vol. II

THE BOEING COMPANY

PAGE 4.0-21

AD 461 C-R4

K-E ALBANENE 1061 TRACING PAPER REV. D

NOTE
1. USE FOR ALL FLAP SETTINGS
2. BOTH OUTBOARD ELEVATORS DEFLECTED
3. FOR ONE OUTBOARD ELEVATOR DEFLECTED, USE HALF THE VALUE SHOWN
4. $\Delta C_{m.25} = K_{\delta E} \cdot \frac{dC_{m.25}}{d\delta E_o} \cdot \delta E_o$

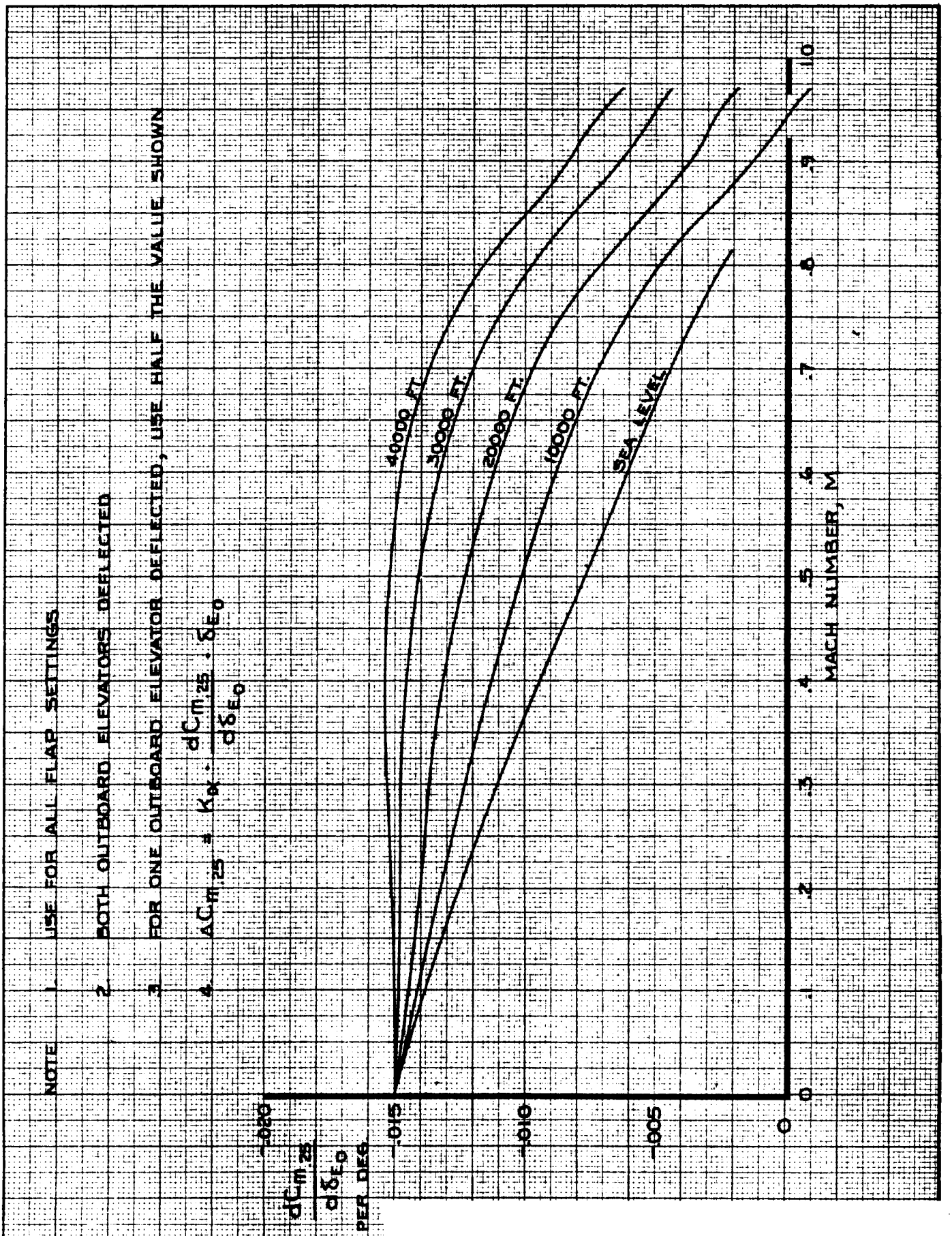

CALC	LOW	10-10-67	REVISED	DATE	PITCHING MOMENT COEFFICIENT AEROELASTIC EFFECT ON OUTBOARD ELEVATOR EFFECTIVENESS
CHECK	FOSTER	1-24-68	FOSTER	9-25-69	
APR					
APR					
INK	ODEGARD	10-10-67			THE BOEING COMPANY

747
D6-30643 Vol. II
PAGE 4.0-22

NOTE 1. USE FOR ALL SPOILER PANELS

2 PANELS 3, 5, 4, 7 AND 8 LIMITED TO 20° MAX DEFLECTION

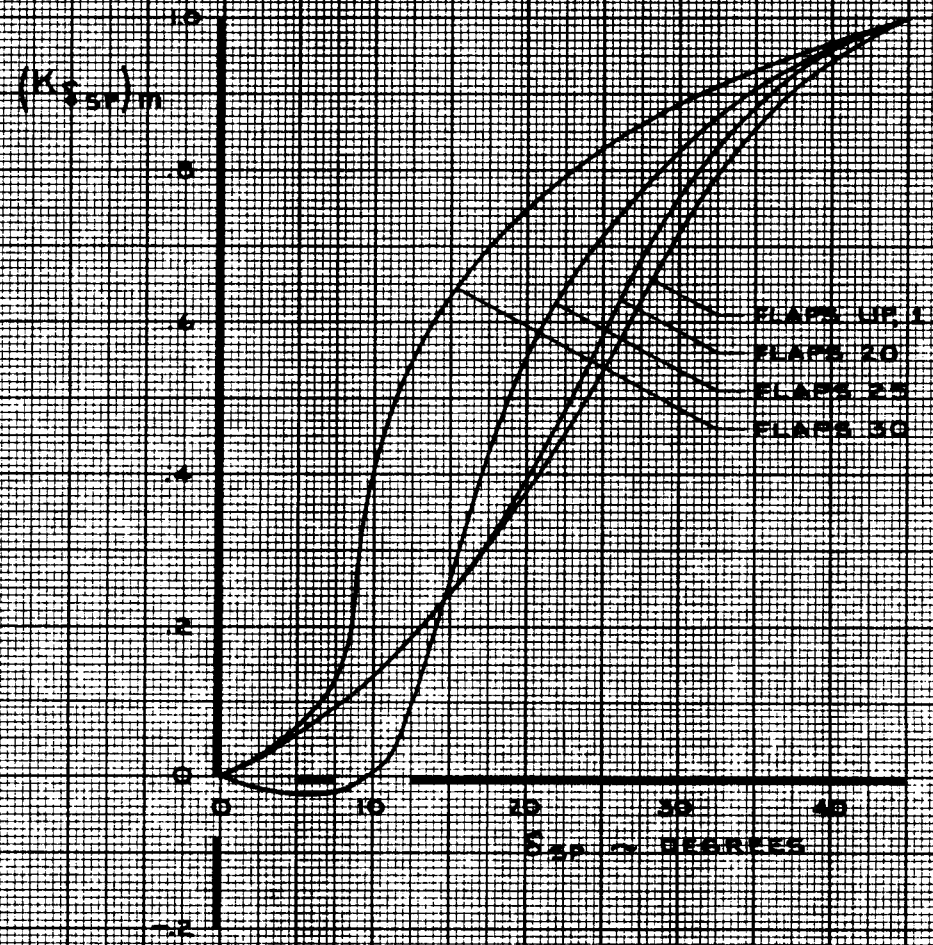

CALC	KUPCIS	12/16/67	REVISED	DATE	PITCHING MOMENT COEFFICIENT EFFECTIVENESS FACTOR SPOILERS	747
CHECK	FOSTER	1-24-68	KUPCIS	6-2-69		
APR			KUPCIS	8-22-69		D6-30643 Vol. II
APR			LOW	2-14-70		
INK	ODEGARD	12/16/67			THE BOEING COMPANY	PAGE 4.0-23

TD 461 C-R4

REV. D

SPOILER PANEL 8 OR 5

NOTE
1. DATA SHOWN FOR INDIVIDUAL PANELS 8 OR 5
2. FOR PANEL 12 OR 1, REVERSE SIGN
3. PANELS 8 & 5 LIMITED TO 20 DEG. MAX. DEFLECTION

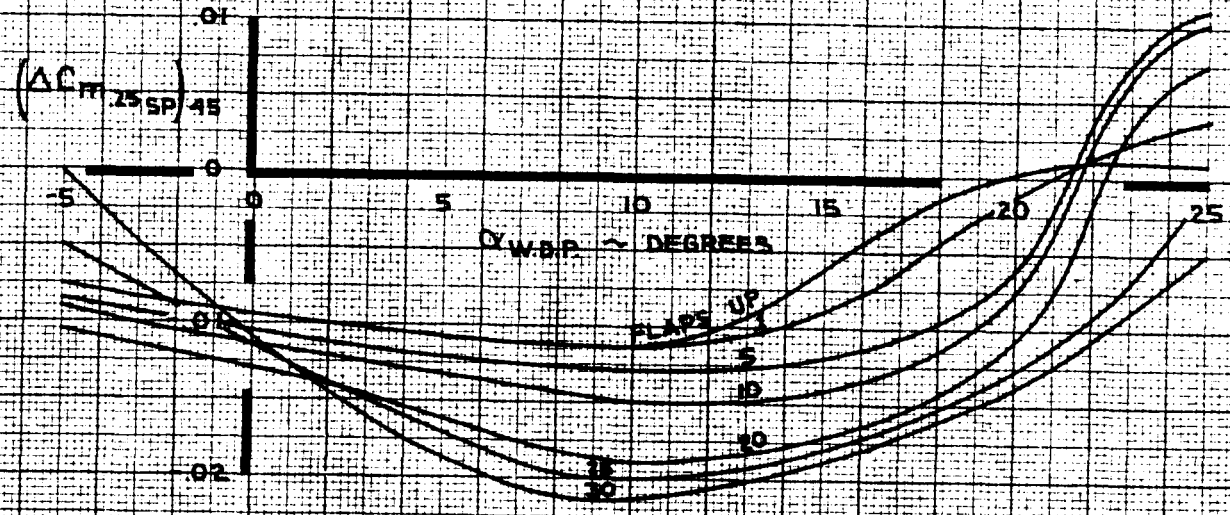

SPOILER PANEL GROUP 9,10,11 OR 2,3,4

NOTE
1. TOTAL EFFECT OF SPOILER GROUP 9, 10, 11 (OR 2, 3, 4) SHOWN
2. FOR SPOILER GROUP 9, 10 (OR 3, 4), MULTIPLY BY 0.67
3. WITH HYDRAULIC SYSTEM NO. 2 OFF, MULTIPLY BY 0.35
4. WITH HYDRAULIC SYSTEM NO. 3 OFF, MULTIPLY BY 0.67

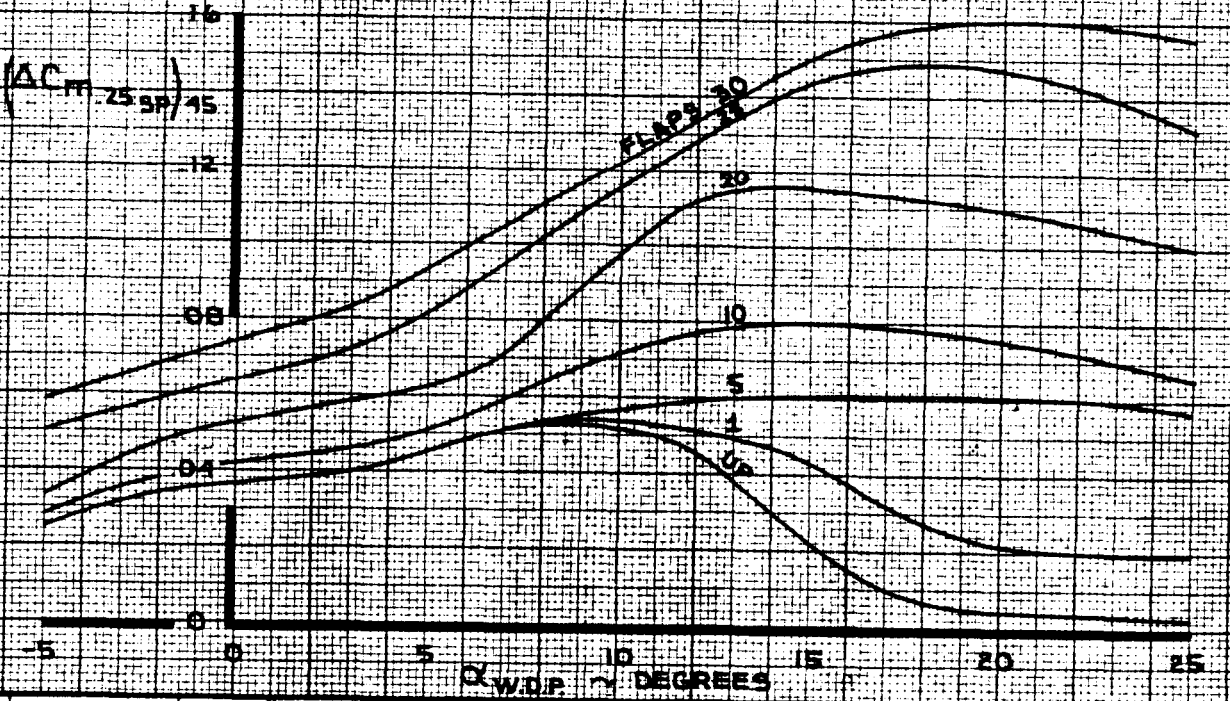

CALC	KUPCIS	12-16-67	REVISED	DATE	PITCHING MOMENT COEFFICIENT EFFECT OF SPOILERS
CHECK	FOSTER	1-24-68	KUPCIS	6-2-69	
APR			KUPCIS	2-14-70	
APR					
INK	KINSMAN	2-24-70			THE BOEING COMPANY

747

D6-30643 Vol. II

PAGE 4.0-24

AD 461 C-R4

K-E ALBANENE 1951 REV D

SPOILER PANELS 6 AND 7

NOTE 1. DATA SHOWN FOR BOTH PANELS OPERATING

2. PANELS LIMITED TO 20° MAX. DEFLECTION

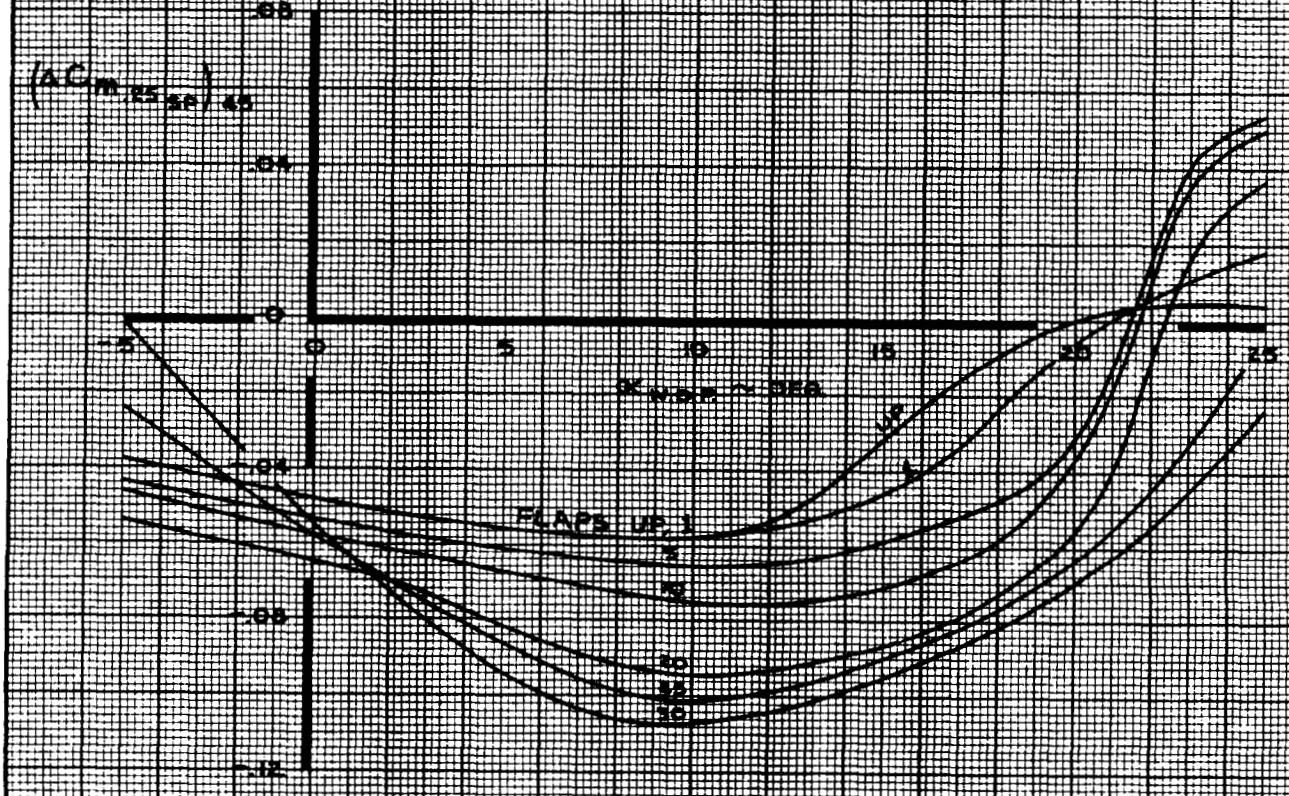

CALC	KUPCIS	12/16/67	REVISED	DATE	PITCHING MOMENT COEFFICIENT EFFECT OF SPOILERS (6 AND 7)
CHECK	FOSTER	1.24.68	KUPCIS	8.22.69	
APR			LOW	2.13.70	
APR					
INK	ODEGARD	12/16/67			THE BOEING COMPANY

747

D6-30643 Vol. II

PAGE 4.0-25

REV. D

TD 461 C-R4

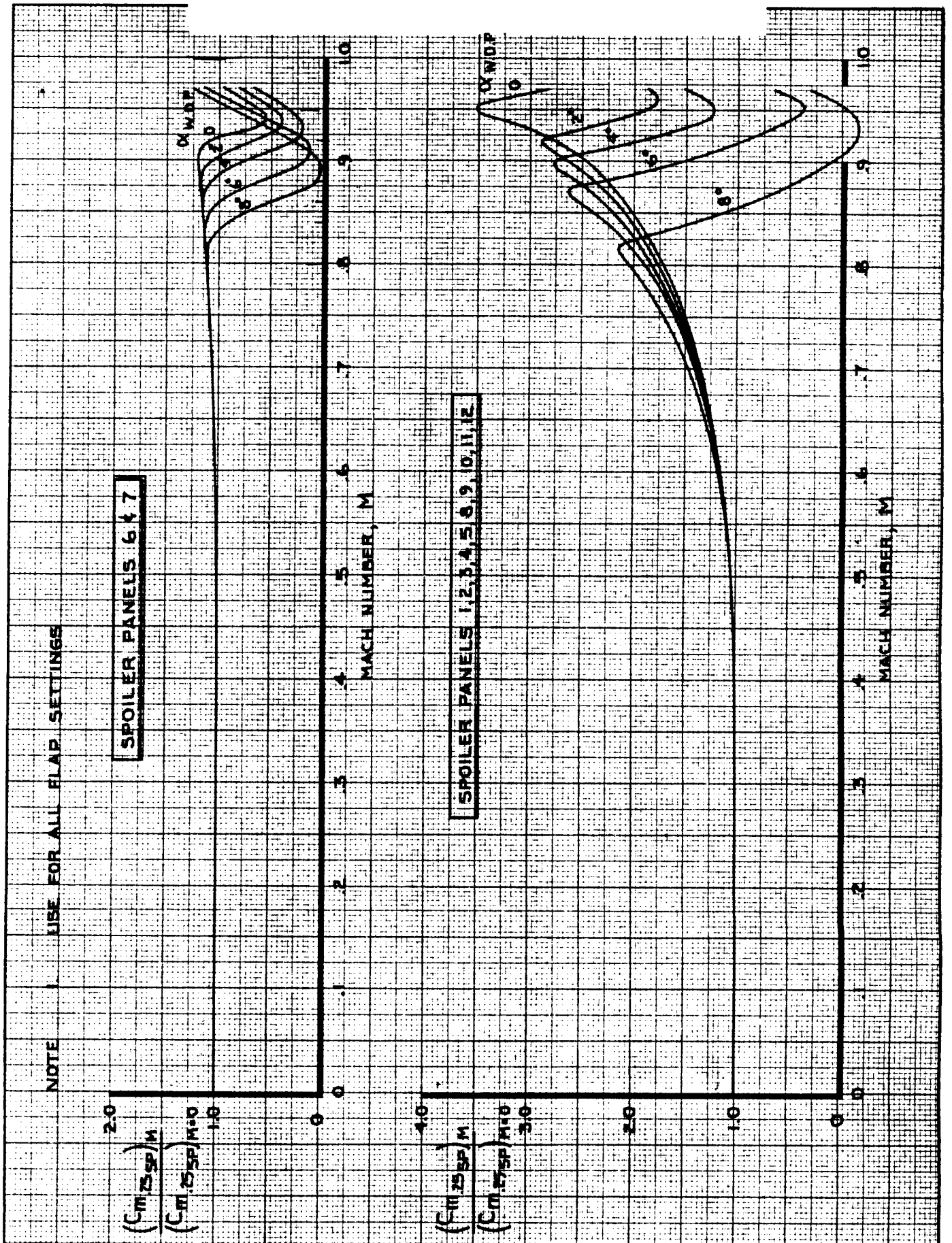

CALC	KUPCIS	12-18-67	REVISED	DATE	PITCHING MOMENT COEFFICIENT Δ EFFECT OF MACH NUMBER ON SPOILERS
CHECK	FOSTER	1-24-68	BYSTROM	2-19-70	
APR					
APR					
INK	ODEGARD	3-3-70			

747

D6-30643 Vol. II

THE BOEING COMPANY

PAGE 4.0-26

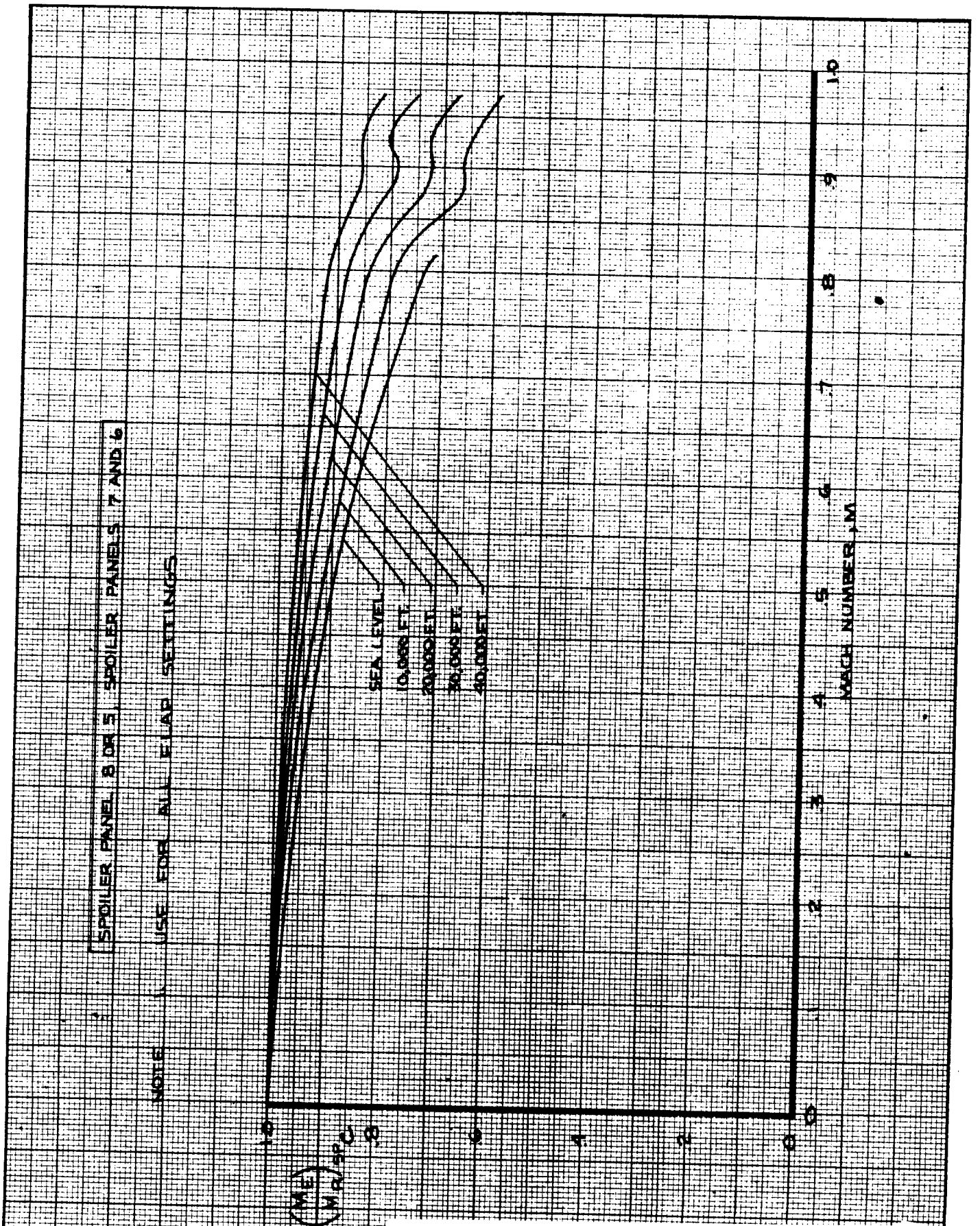

CALC	LOW	4/16/68	REVISED	DATE	PITCHING MOMENT COEFFICIENT
CHECK			LOW	6-14-69	AEROELASTIC EFFECT ON PITCHING MOMENT COEFFICIENT DUE TO SPOILERS (8 OR 5, 7 AND 6)
APR					
APR					
INK	Glenn	9/16/68			THE BOEING COMPANY

747

D6-30643 Vol. II

PAGE 4.0-27

AD 461 C R4

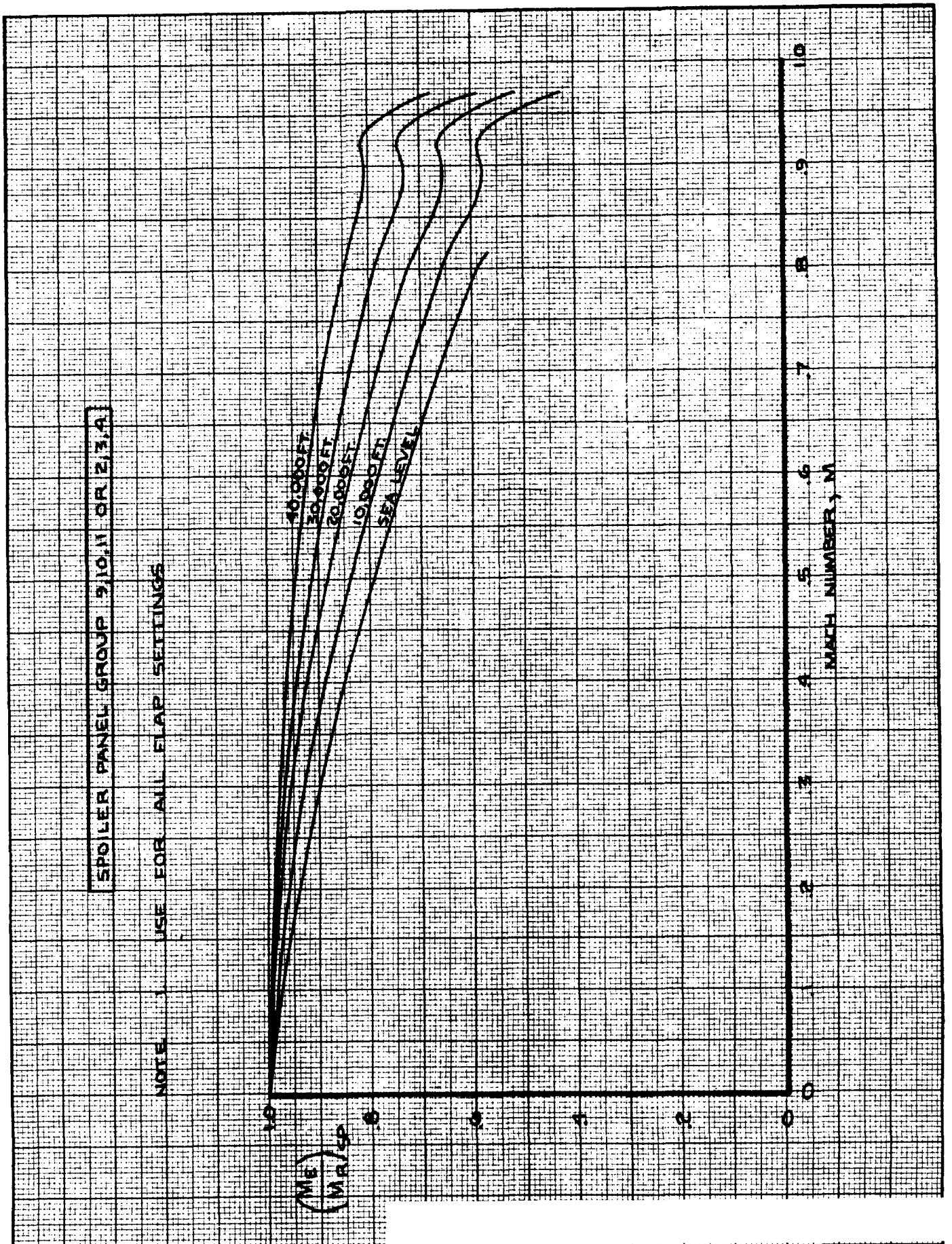

CALC	LOW	4/16/68	REVISED	DATE	PITCHING MOMENT COEFFICIENT	747
CHECK			LOW	6-14-69	AEROELASTIC EFFECT ON PITCHING MOMENT COEFFICIENT DUE TO SPOILERS (9,10,11 OR 2,3,4)	D6-30643 Vol. II
APR						
APR					THE BOEING COMPANY	PAGE 4.0-28
INK	Glenn	4-16-8				

AD 461 C R4

MESPB

REV. B

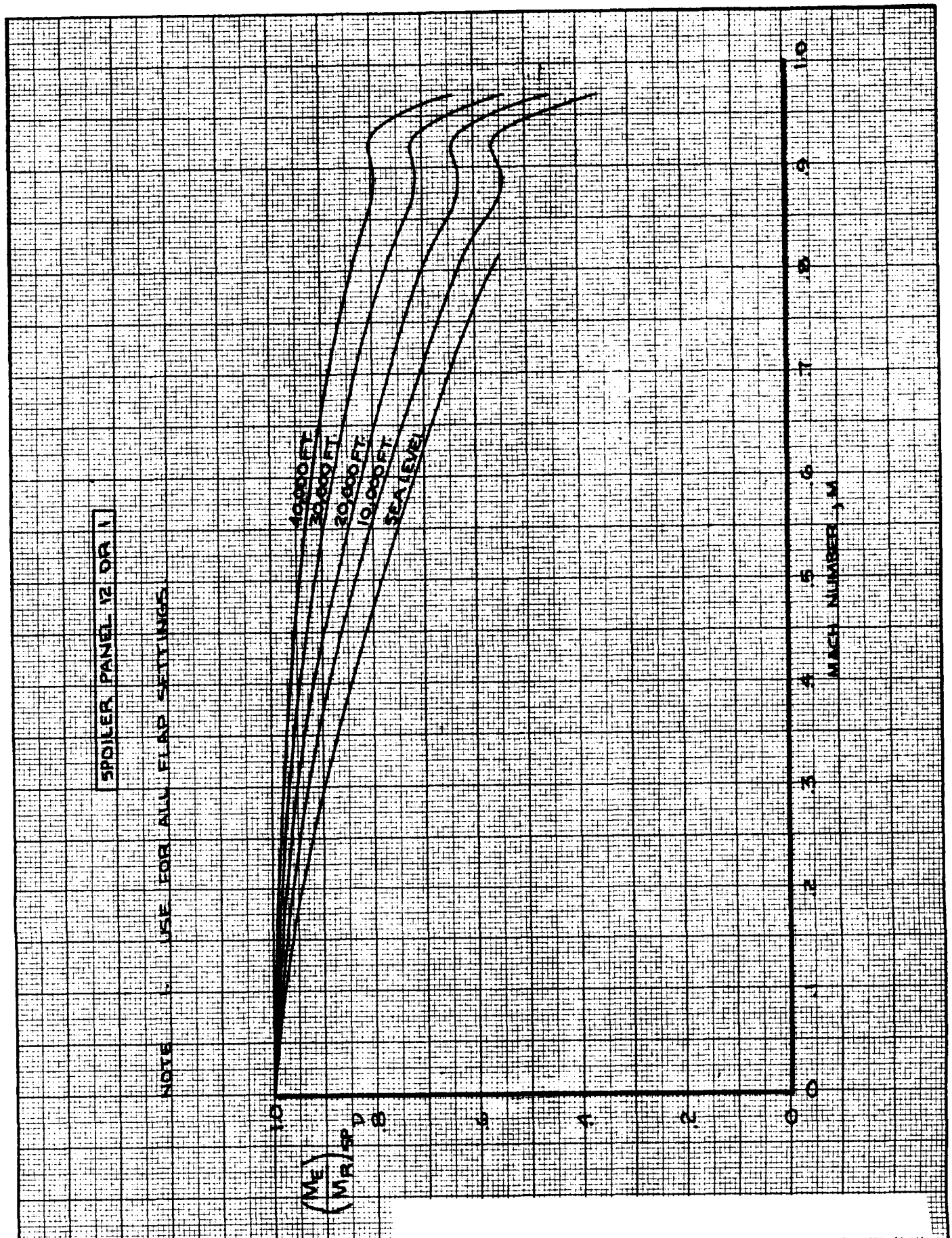

CALC	LOW	4/16/68	REVISED	DATE	PITCHING MOMENT COEFFICIENT AEROELASTIC EFFECT ON PITCHING MOMENT COEFFICIENT DUE TO SPOILERS (12 OR 1)
CHECK			LOW	6-14-69	
APR					
APR					THE BOEING COMPANY
INK	Glenn	4-16-68			

747

D6-30643 Vol. II

PAGE 4.0-29

REV. B

AD 461 C R4

NOTE 1 $\left(C_{m_{.25}A_I/2D}\right)$ IS SHOWN FOR UP AILERON ONLY

2 $\left(C_{m_{.25}A_I/2D}\right)$ FOR DOWN AILERON IS ZERO

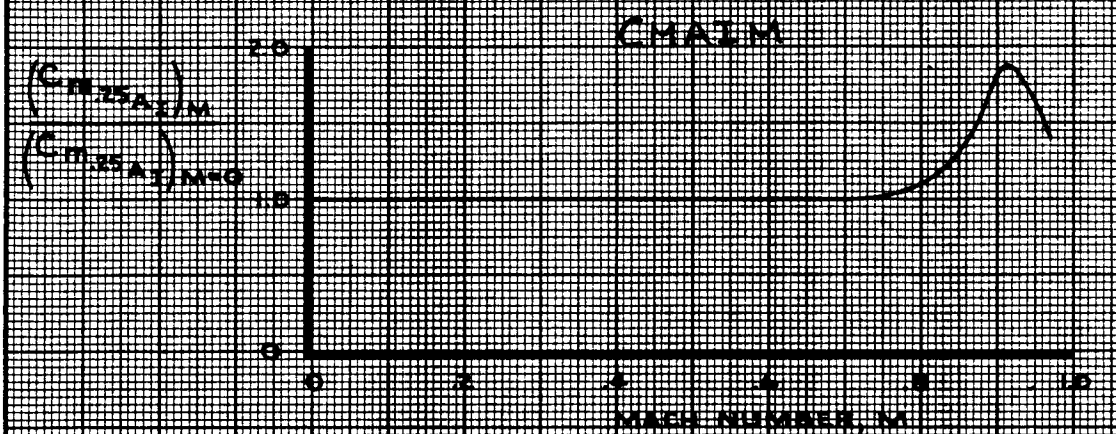

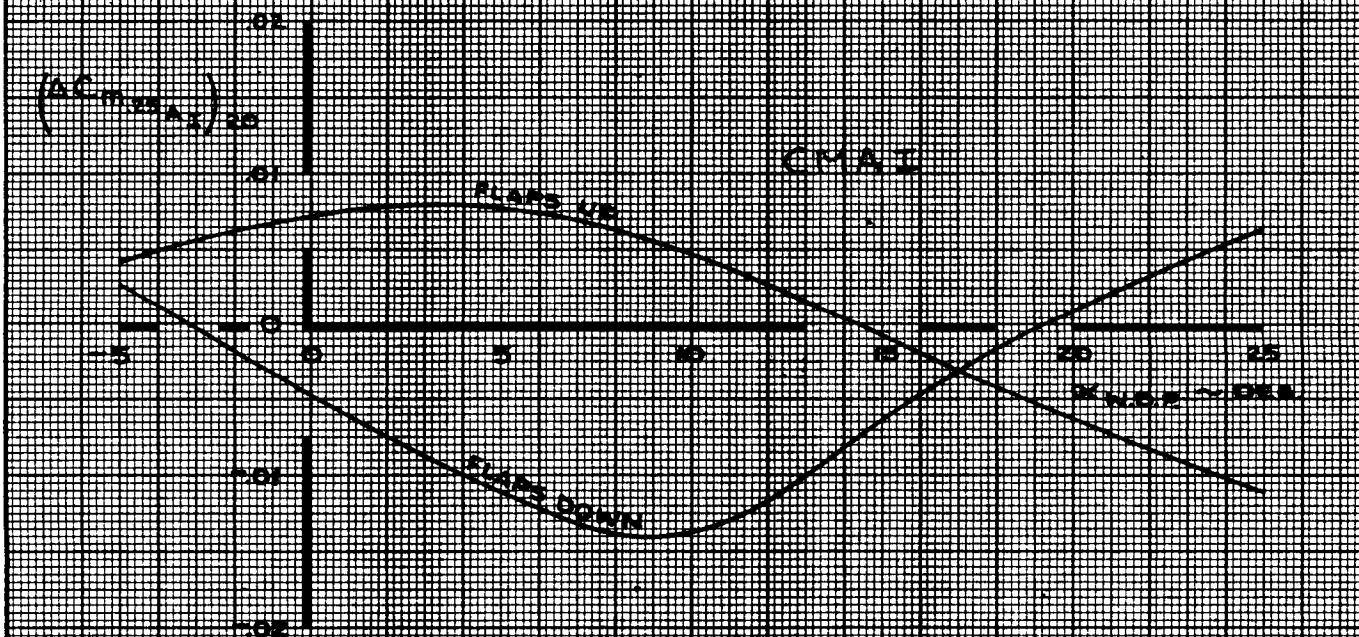

CALC	KUPCIS	11/8/67	REVISED	DATE	PITCHING MOMENT COEFFICIENT EFFECT OF INBOARD AILERON
CHECK	FOSTER	1-24-68			
APR					
APR					
INK	ODEGARD	11/8/67			

747

D6-30643 Vol. II

THE BOEING COMPANY

CMAIM/CMAI

PAGE 4.0-30

REV A

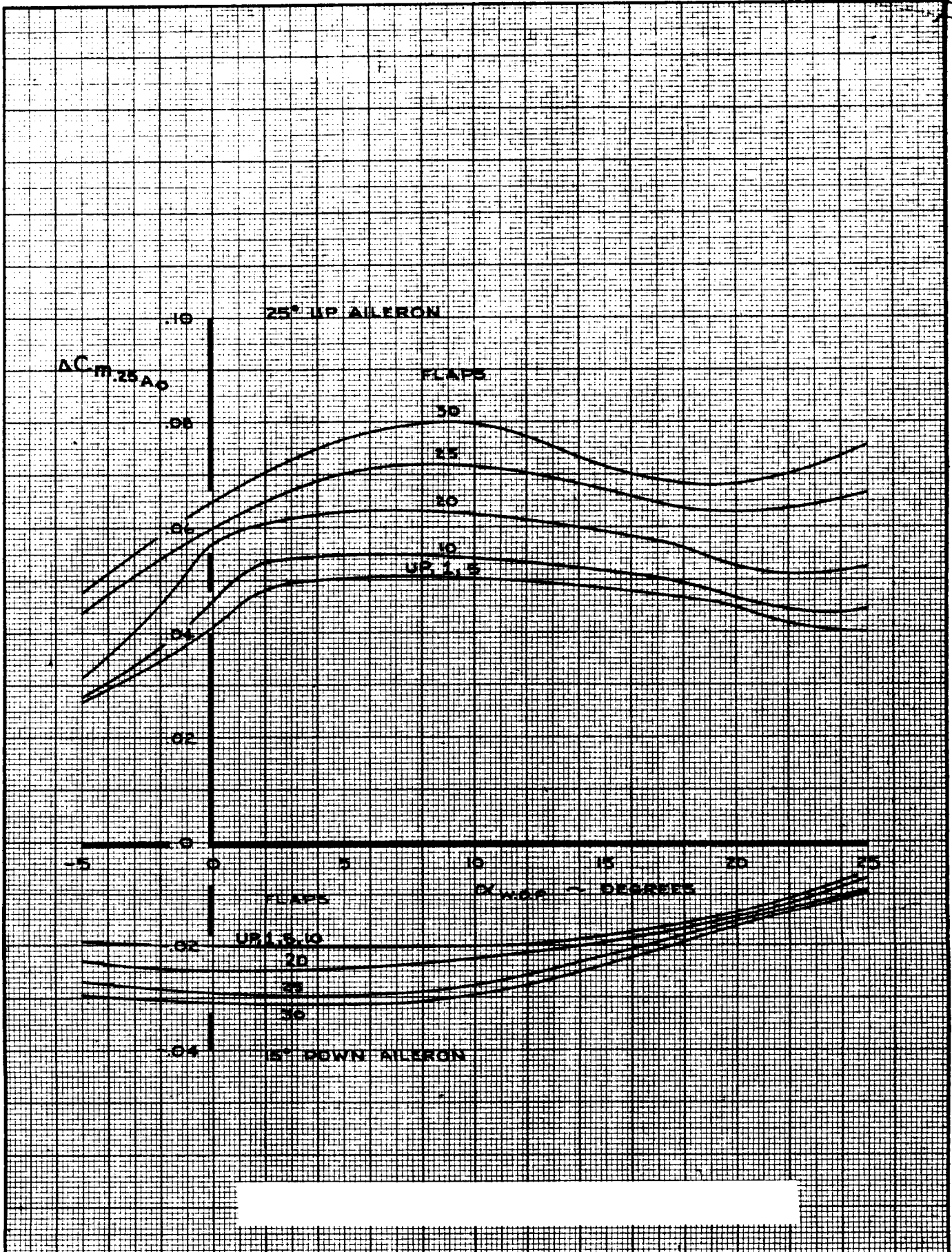

CALC	KUPCIS	11-15-67	REVISED	DATE	PITCHING MOMENT COEFFICIENT EFFECT OF OUTBOARD AILERON
CHECK	FOSTER	1-24-68	KUPCIS	4.22.68.	
APR			LOW	2-14-70	
APR					
INK	ODEGARD	11-15-67			THE BOEING COMPANY

747
D6-30643 Vol. II
PAGE 4.0-31

TD 461 C-R4

REV. D

NOTE 1. $F_{m_{GE}} = \left[1 + F_m \cdot K^{B}_{GE} \right]$

WHERE K^{B}_{GE} IS SHOWN ON PAGE 20-31.

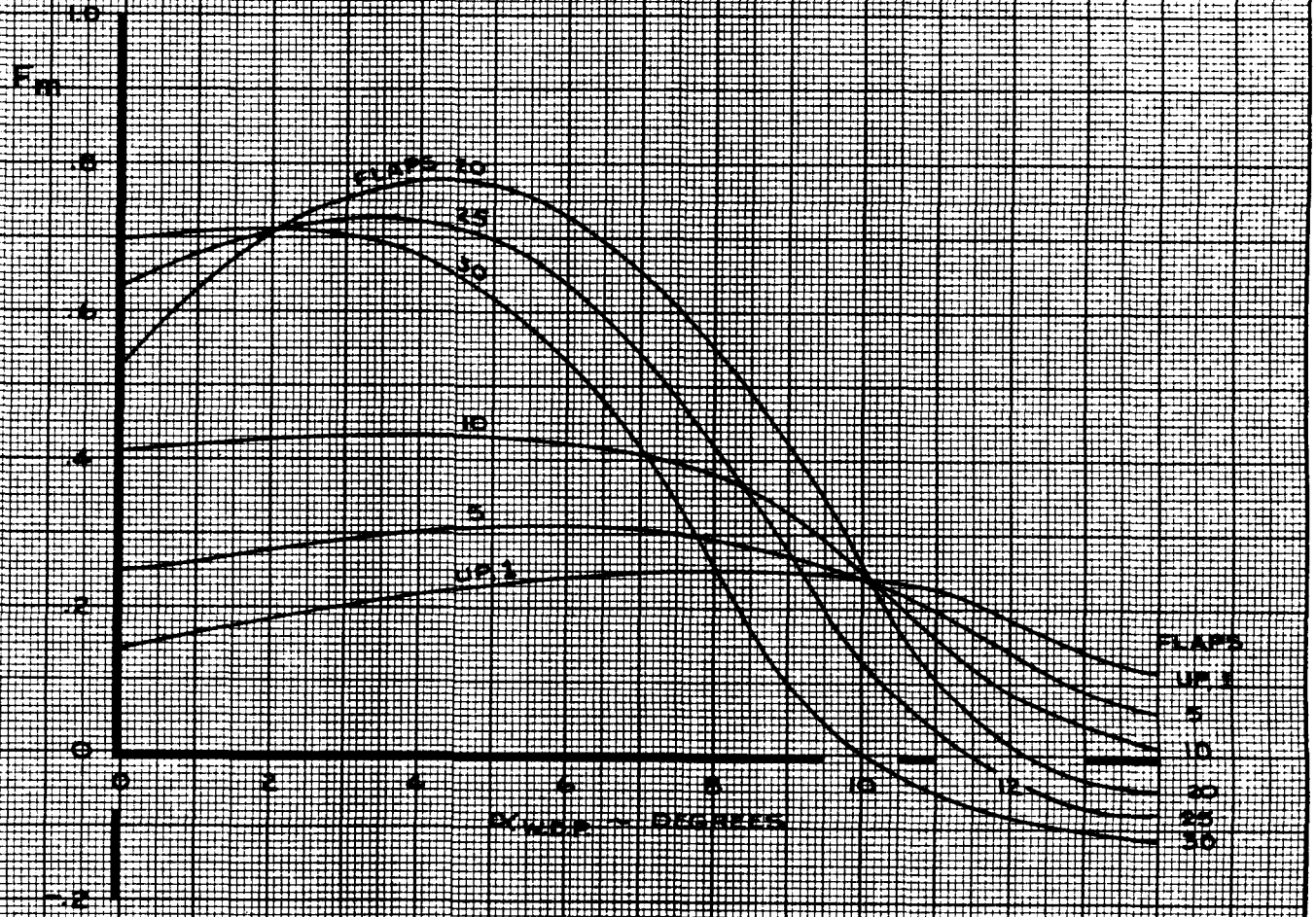

CALC	CURNUTT	12/18/67	REVISED	DATE	PITCHING MOMENT COEFFICIENT — GROUND EFFECT LATERAL CONTROL FACTOR, F_m
CHECK	FOSTER	1-24-68	LOW	2-14-70	
APR					
APR					
INK	ODEGARD	12/18/67			

747

D6-30643 Vol. II

THE BOEING COMPANY

PAGE 4.0-32

TD 461 C-R4

REV. D

LOW SPEED

NOTE 1 FREE AIR

2 FOR LANDING GEAR FAILURE, REPLACE $\Delta C_{m_{.25\,GEAR}}$ BY

$$\Delta C_{m_{.25\,GEAR\ FAILURE}} = K_{m_{GEAR}} \cdot \Delta C_{m_{.25\,GEAR}}$$

GEAR SELECTION	GEAR FAILURE	$K_{m_{GEAR}}$
DOWN	WING GEARS FAIL TO EXTEND	0.6
UP	WING GEARS FAIL TO RETRACT	0.4
✓	ONE WING GEAR FAILS TO RETRACT	0.2
✓	ONE BODY GEAR FAILS TO RETRACT	-0.4
✓	ONE BODY GEAR DOOR FAILS TO RETRACT	-0.4
✓	NOSE GEAR FAILS TO RETRACT	0.35

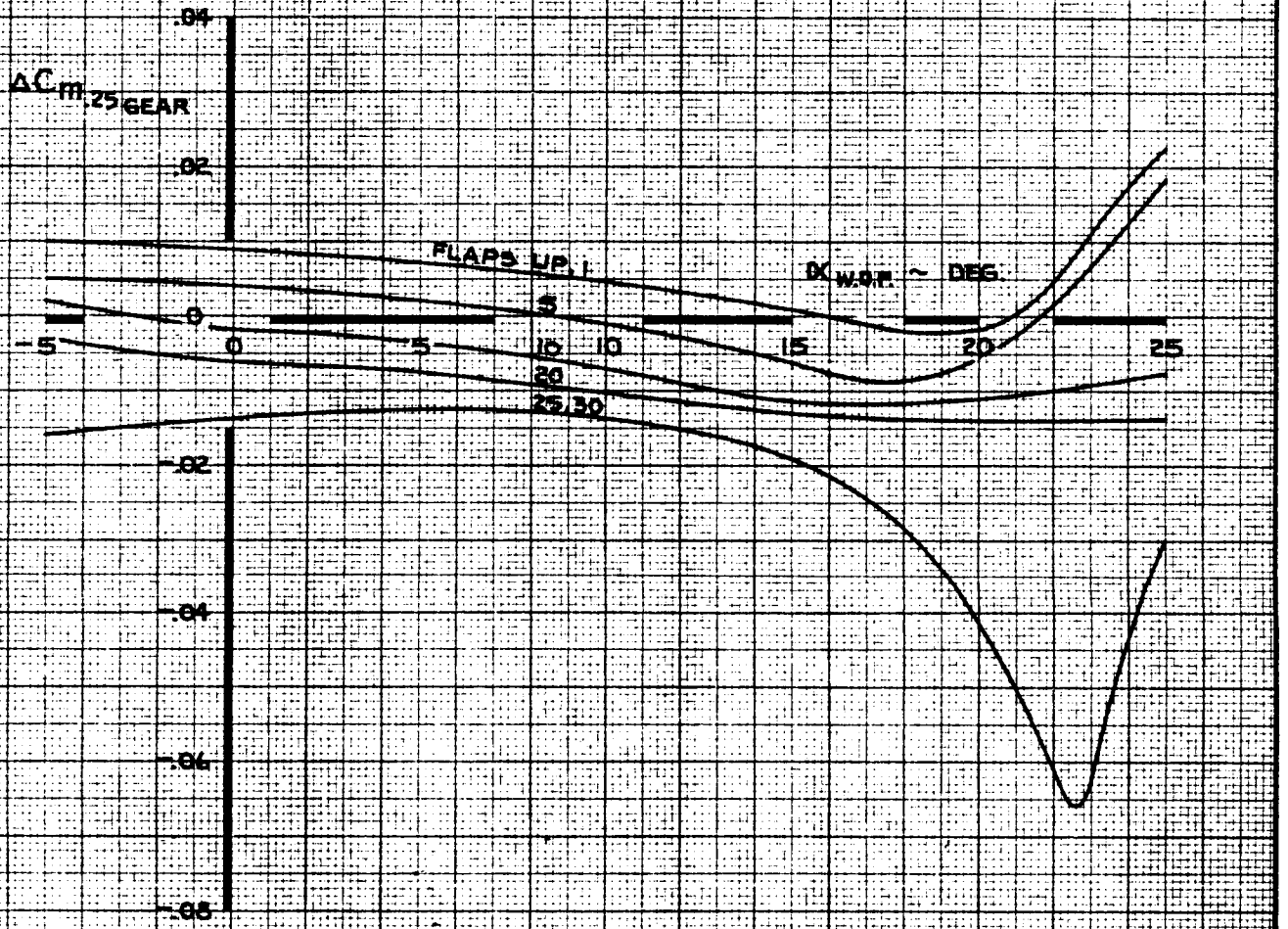

CALC	LOW	9-20-67	REVISED	DATE	PITCHING MOMENT COEFFICIENT EFFECT OF LANDING GEAR
CHECK	FOSTER	1-24-68	LOW	6-9-69	
APR			BYSTROM	2-23-70	
APR					
INK	ODEGARD	3-2-70			THE BOEING COMPANY

747
D6-30643 Vol. II
PAGE 4.0-33

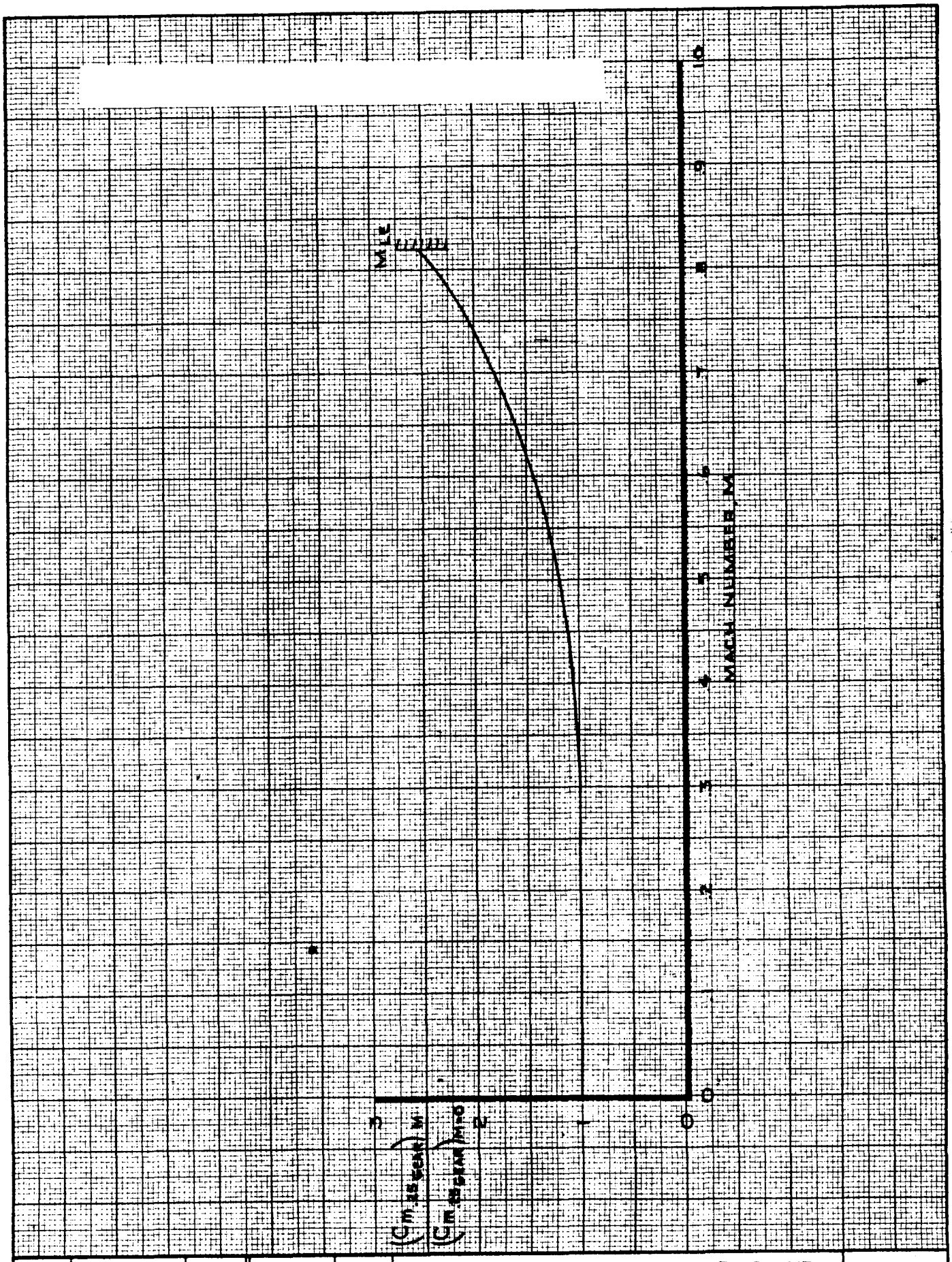

CALC	LOW	11-9-67	REVISED	DATE	PITCHING MOMENT COEFFICIENT EFFECT OF MACH NUMBER ON $\Delta C_{m_{.25\,GEAR}}$	747
CHECK	FOSTER	1-24-68				D6-30643 Vol. II
APR						
APR					THE BOEING COMPANY	PAGE 4.0-34
INK	ODEGARD	11-9-67				REV. A

NOTE 1. GEAR ON GROUND

2. $K_{GE}^{B} = 1.0$

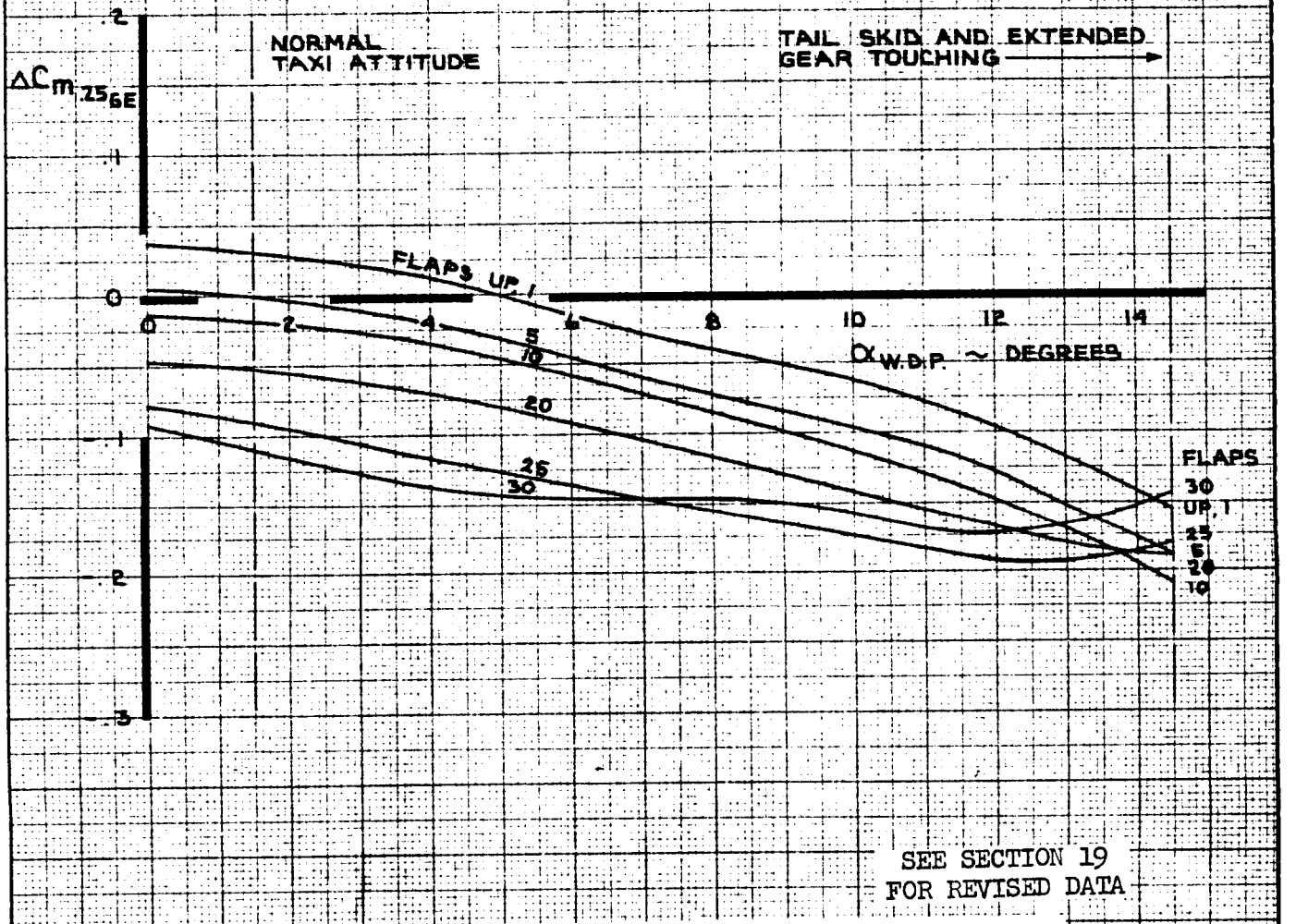

SEE SECTION 19
FOR REVISED DATA

CALC	CURNUTT	12-12-67	REVISED	DATE
CHECK	FOSTER	1-24-68	CURNUTT	3-6-70
APR				
APR				
INK	KINSMAN	3-6-70		

PITCHING MOMENT COEFFICIENT Δ
GROUND EFFECT

747

D6-30643
Vol. II

THE BOEING COMPANY

PAGE 4.0-35

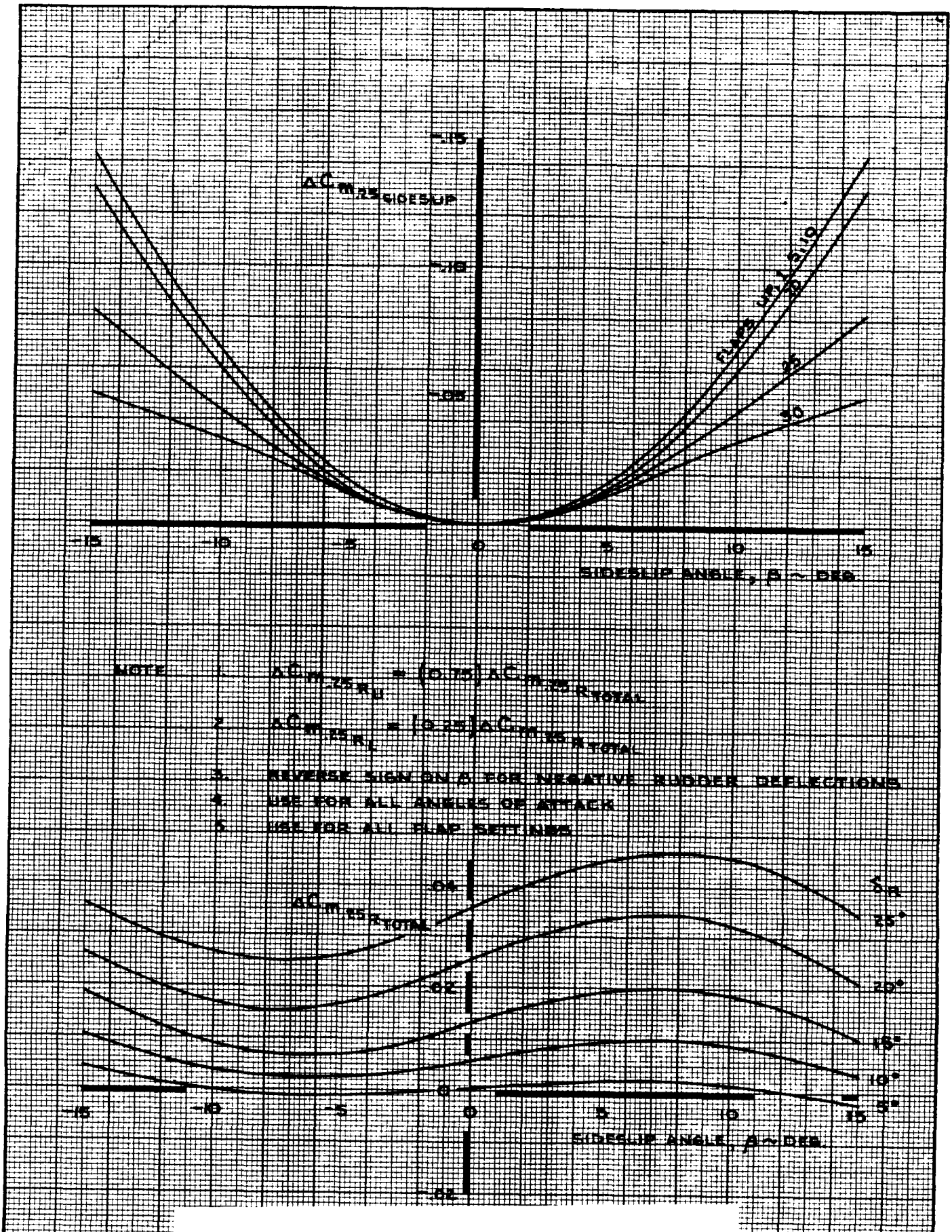

NOTE

1. $\Delta C_{m_{.25}R_U} = (0.75)\Delta C_{m_{.25}R_{TOTAL}}$
2. $\Delta C_{m_{.25}R_L} = (0.25)\Delta C_{m_{.25}R_{TOTAL}}$
3. REVERSE SIGN ON β FOR NEGATIVE RUDDER DEFLECTIONS.
4. USE FOR ALL ANGLES OF ATTACK
5. USE FOR ALL FLAP SETTINGS

CALC	STIRLING	10/20/67	REVISED	DATE
CHECK	RICHARDSON	12/26/67	LOW	2-14-70
APR				
APR				
INK	ODEGARD	12/26/67		

PITCHING MOMENT COEFFICIENT
EFFECT OF SIDESLIP
AND RUDDER

747

D6-30643
Vol. II

THE BOEING COMPANY

PAGE
4.0-36

TD 461 C-R4

REV. D

NOTE 1. DATA APPLICABLE FOR SYMMETRIC OR ASYMMETRIC (MONITOR LIMITED) FLAP FAILURE

THESE DATA NOT INCLUDED IN NASA SIMULATION

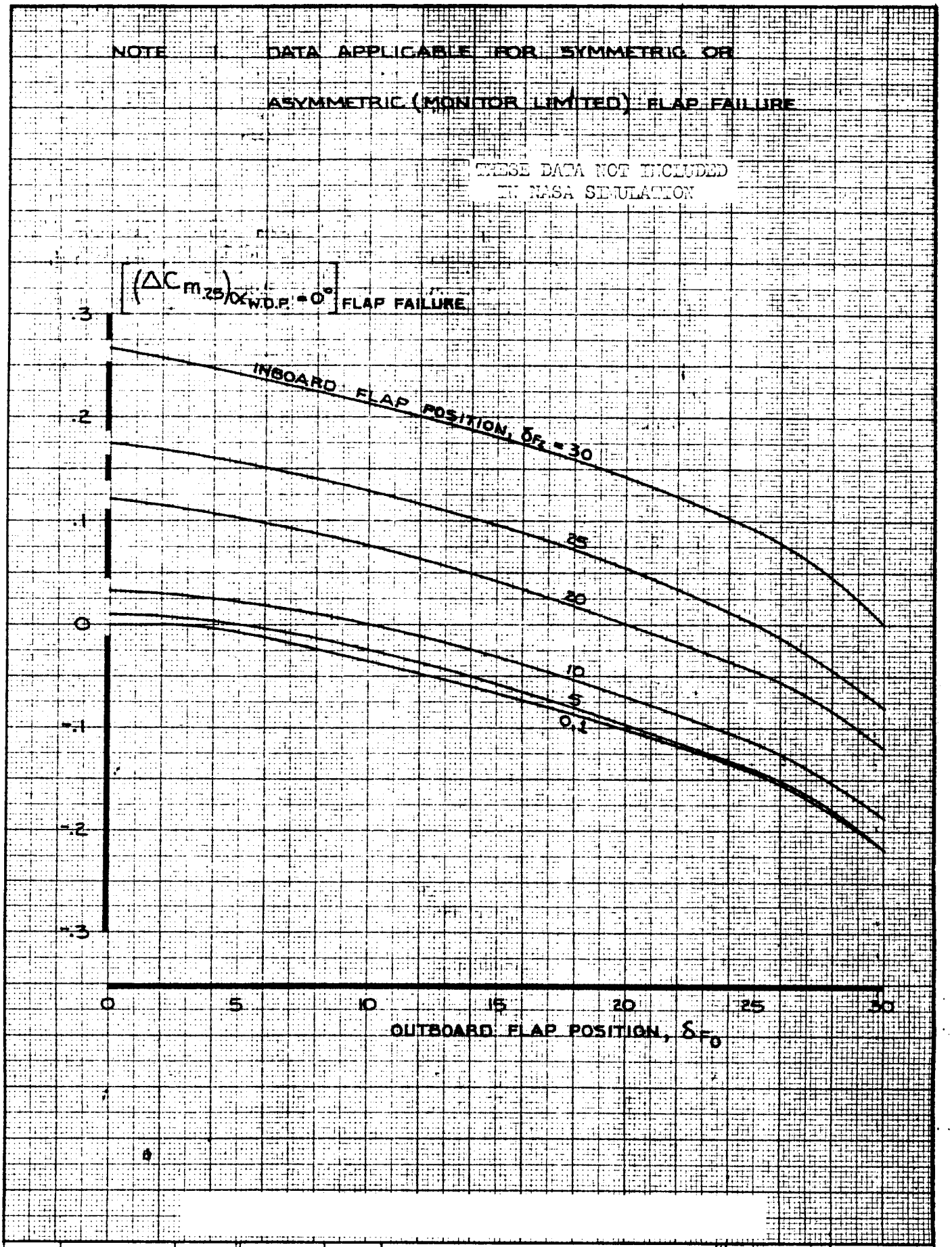

CALC	LOW	5-3-69	REVISED	DATE	PITCHING MOMENT COEFFICIENT EFFECT OF FLAPS ON $\left[(\Delta C_{m_{.25}})_{\alpha_{W.D.R.}=0^\circ}\right]$ FLAP FAILURE
CHECK			LOW	2-17-70	
APR			LOW	6-25-70	
APR					
INK	ODEGARD	5-3-69			THE BOEING COMPANY

747

D6-30643 Vol. II

PAGE 4.0-37

TD 461 C-R4

K+E ALBANENE 1851 (6) TRACING PAPER REV. E

NOTE DATA APPLICABLE FOR SYMMETRIC OR ASYMMETRIC (MONITOR LIMITED) FLAP FAILURE

THESE DATA NOT INCLUDED IN NASA SIMULATION

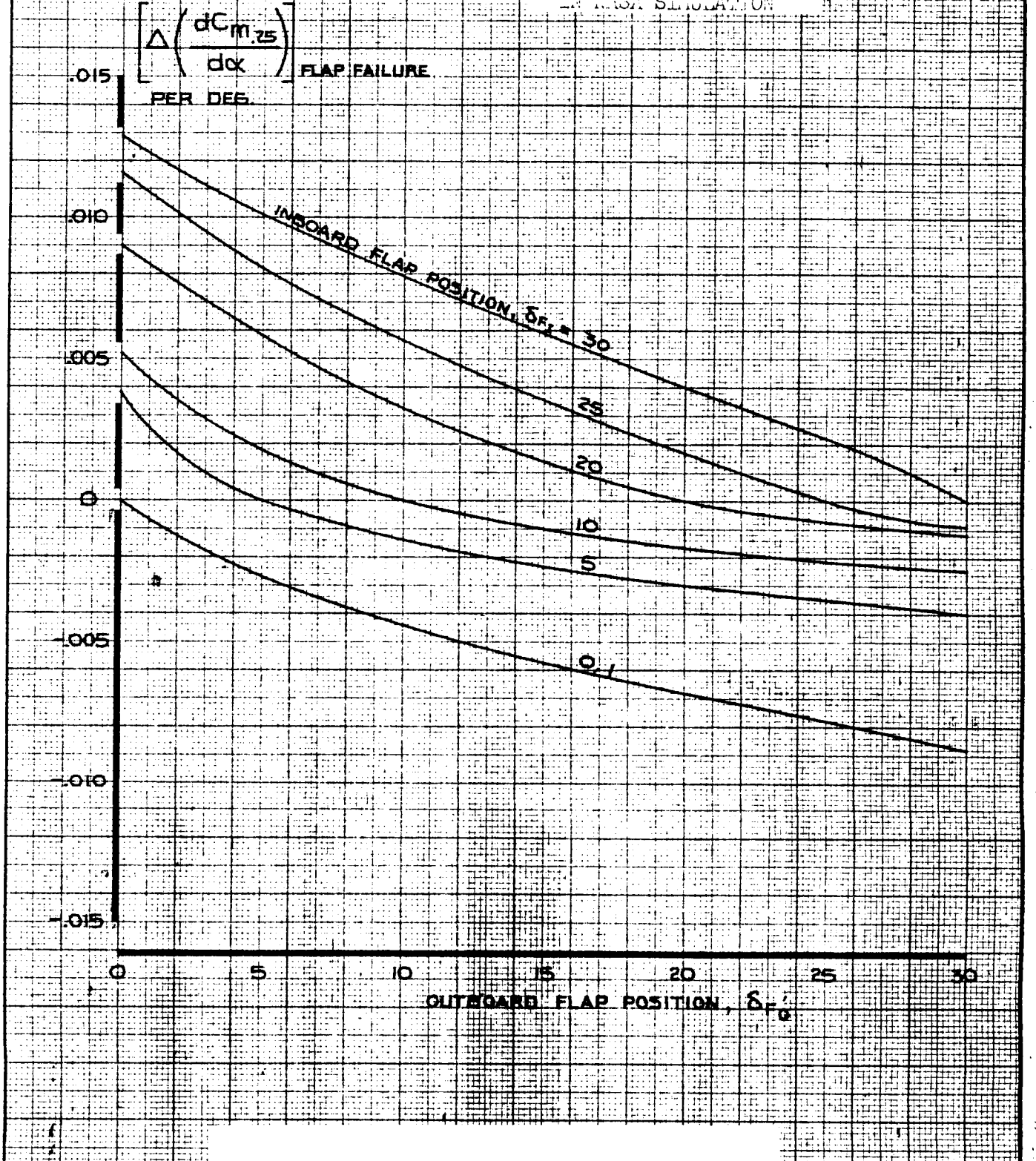

CALC	LOW	5-3-69	REVISED	DATE	PITCHING MOMENT COEFFICIENT EFFECT OF FLAPS ON $[\Delta(dC_{m_{.25}}/d\alpha)]$ FLAP FAILURE
CHECK			LOW	2-17-70	
APR			LOW	6-25-70	
APR					
INK	ODEGARD	5-3-69			THE BOEING COMPANY

747

D6-30643 Vol. II

PAGE 4.0-38

TD 461 C-R4

K+E ALBANENE 1961 TRACING PAPER REV. E

5.0 ROLLING MOMENT COEFFICIENT

The dimensionless aerodynamic rolling moment coefficient is given in terms of its significant components by the equation below.

At a given $\alpha_{W.D.P.}$,

$$C_\ell = \frac{dC_\ell}{d\beta}\cdot\beta + \frac{dC_\ell}{d\hat{p}}\cdot\frac{p_s b}{2V} + \frac{dC_\ell}{d\hat{r}}\cdot\frac{r_s b}{2V}$$

$$+ \Delta C_{\ell_{SPOILERS}} + \Delta C_{\ell_{\substack{INBOARD\\AILERONS}}} + \Delta C_{\ell_{\substack{OUTBOARD\\AILERONS}}}$$

$$+ \Delta C_{\ell_{RUDDERS}} + \left[\Delta C_{\ell_{FLAP\ FAILURE}} + \Delta C_{\ell_{L.E.\ FAILURE}}\right]^*$$

where,

$\frac{dC_\ell}{d\beta}\cdot\beta$ = Rolling moment coefficient due to angle of sideslip, β. The complete expression for $\frac{dC_\ell}{d\beta}$ is given as follows:

$$\frac{dC_\ell}{d\beta} = \left[\left(\frac{dC_\ell}{d\beta}\right)\cdot\frac{(C_{\ell_\beta})_\beta}{(C_{\ell_\beta})_{\beta=0}}\cdot\frac{(C_{\ell_\beta})_E}{(C_{\ell_\beta})_R} + K_{GEAR}\cdot\Delta\left(\frac{dC_\ell}{d\beta}\right)_{\substack{LANDING\\GEAR}}\right]\cdot F_{\ell_{\beta_{GE}}}$$

where $\left(\frac{dC_\ell}{d\beta}\right)$ is the basic rate of change of rolling moment coefficient due to angle of sideslip. For low speed, $\left(\frac{dC_\ell}{d\beta}\right)$ is plotted on page 5.0-7. For flaps up, $\left(\frac{dC_\ell}{d\beta}\right)$ is plotted on page 5.0-8. $\frac{(C_{\ell_\beta})_\beta}{(C_{\ell_\beta})_{\beta=0}}$ is plotted on page 5.0-9.

$[\ ]^*$ NOT IN NASA SIMULATION

AD 1346 D

5.0 (Cont'd)

The aeroelastic effect, $\frac{(C_{l_\beta})_E}{(C_{l_\beta})_R}$, is plotted on page 5.0-10. The effect of main and nose gear extension, $\Delta\left(\frac{dC_l}{d\beta}\right)_{\substack{\text{LANDING}\\\text{GEAR}}}$, is given by:

$$\Delta\left(\frac{dC_l}{d\beta}\right)_{\substack{\text{LANDING}\\\text{GEAR}}} = -.0003 \text{ PER DEGREE}$$

The landing gear effectiveness factor, K_{GEAR} is plotted on page 2.0-28. The ground effect factor, $F_{l_{\beta_{GE}}}$, is obtained as follows:

$$F_{l_{\beta_{GE}}} = \left[1 + F_{l_\beta} \cdot K^B_{GE}\right]$$

where the ground effect sideslip factor, F_{l_β}, is plotted on page 5.0-11. The ground effect height factor, K^B_{GE}, is plotted on page 2.0-31.

$\frac{dC_l}{d\hat{p}} \cdot \frac{p_s b}{2V}$ = Rolling moment coefficient due to roll rate about the stability axis, X_s. The complete expression for $\frac{dC_l}{d\hat{p}}$ is given as follows:

$$\frac{dC_l}{d\hat{p}} = \left(\frac{dC_l}{d\hat{p}}\right) \cdot \frac{(C_{l_\beta})_M}{(C_{l_{\hat{p}}})_{M=0}}$$

where $\left(\frac{dC_l}{d\hat{p}}\right)$ is plotted on page 5.0-12. The aeroelastic effect, $\frac{(C_{l_\beta})_M}{(C_{l_{\hat{p}}})_{M=0}}$, is plotted on page 5.0-13.

$\frac{dC_l}{d\hat{r}} \cdot \frac{r_s b}{2V}$ = Rolling moment coefficient due to yaw rate about the stability axis, Z_s. The complete expression for $\frac{dC_l}{d\hat{r}}$ is given as follows:

5.0

(Cont'd)

$$\frac{dC_\ell}{d\hat{p}} = \left(\frac{dC_\ell}{d\hat{p}}\right) \cdot \frac{(C_{\ell\hat{p}})_M}{(C_{\ell\hat{p}})_{M=0}}$$

where $\left(\frac{dC_\ell}{d\hat{p}}\right)$ is plotted on page 5.0-14. The aeroelastic effect, $\frac{(C_{\ell\hat{p}})_M}{(C_{\ell\hat{p}})_{M=0}}$, is plotted on page 5.0-15.

$\Delta C_{\ell_{SPOILERS}}$ = Rolling moment coefficient due to spoiler deflection.

$$\Delta C_{\ell_{SPOILERS}} = \sum_{\substack{\text{OPERATING} \\ \text{SPOILER} \\ \text{PANELS}}} (K_{\delta_{SP}})_\ell \cdot (\Delta C_{\ell_{SP}})_{45} \cdot \frac{(C_{\ell_{SP}})_M}{(C_{\ell_{SP}})_{M=0}} \cdot \left(\frac{R_E}{R_R}\right)_{SP} \cdot F_{\ell_{GE}}$$

where $(\Delta C_{\ell_{SP}})_{45}$ is the rolling moment coefficient due to deflecting the operating spoiler panels to 45°. $(\Delta C_{\ell_{SP}})_{45}$ is plotted on page 5.0-17. The spoiler effectiveness factor, $(K_{\delta_{SP}})_\ell$, is plotted on page 5.0-16. The Mach number effect, $\frac{(C_{\ell_{SP}})_M}{(C_{\ell_{SP}})_{M=0}}$, is plotted on page 5.0-18. The aeroelastic effect, $\left(\frac{R_E}{R_R}\right)_{SP}$, is plotted on pages 5.0-19, 5.0-20, and 5.0-21. The ground effect factor, $F_{\ell_{GE}}$, is obtained as follows:

$$F_{\ell_{GE}} = \left[1 + F_\ell \cdot K^B_{GE}\right]$$

where the ground effect lateral control factor, F_ℓ, is plotted on page 5.0-29. The ground effect height factor, K^B_{GE}, is plotted on page 2.0-31.

$\Delta C_{\ell_{\substack{\text{INBOARD} \\ \text{AILERONS}}}}$ = Rolling moment coefficient due to inboard aileron deflection.

5.0

(Cont'd)

$$\Delta C_{\ell_{\substack{\text{INBOARD}\\\text{AILERONS}}}} = \sum_{\substack{\text{LEFT AND RIGHT}\\\text{INBOARD}\\\text{AILERONS}}} K_{\delta_{A_I}} \cdot (\Delta C_{\ell_{A_I}})_{20} \cdot \frac{(C_{\ell_{A_I}})_M}{(C_{\ell_{A_I}})_{M=0}} \cdot \left(\frac{R_E}{R_R}\right)_{C_{\ell_{A_I}}} \cdot F_{\ell_{GE}}$$

where $(\Delta C_{\ell_{A_I}})_{20}$ is the rolling moment coefficient due to deflecting one inboard aileron up to 20° or the opposite inboard aileron down to 20°. $(\Delta C_{\ell_{A_I}})_{20}$ is plotted on page 5.0-**23.** The inboard aileron effectiveness factor, $K_{\delta_{A_I}}$, is plotted on page 5.0-**22.** The Mach number effect, $\frac{(C_{\ell_{A_I}})_M}{(C_{\ell_{A_I}})_{M=0}}$, is plotted on page 5.0-**24.** The aeroelastic effect, $\left(\frac{R_E}{R_R}\right)_{C_{\ell_{A_I}}}$, is plotted on page 5.0-**25.** The ground effect factor, $F_{\ell_{GE}}$, is obtained from page 5.0-**29.**

$\Delta C_{\ell_{\substack{\text{OUTBOARD}\\\text{AILERONS}}}}$ = Rolling moment coefficient due to outboard aileron deflection.

$$\Delta C_{\ell_{\substack{\text{OUTBOARD}\\\text{AILERONS}}}} = \sum_{\substack{\text{LEFT AND RIGHT}\\\text{OUTBOARD}\\\text{AILERONS}}} K_{\delta_{A_O}} \cdot \Delta C_{\ell_{A_O}} \cdot \left(\frac{R_E}{R_R}\right)_{C_{\ell_{A_O}}} \cdot F_{\ell_{GE}}$$

where $\Delta C_{\ell_{A_O}}$ is the rolling moment coefficient due to deflecting one outboard aileron up to 25° or the opposite outboard aileron down to 15°. $\Delta C_{\ell_{A_O}}$ is plotted on page 5.0-**27.** The outboard aileron effectiveness factor, $K_{\delta_{A_O}}$, is plotted on page 5.0-**26.** The aeroelastic effect, $\left(\frac{R_E}{R_R}\right)_{C_{\ell_{A_O}}}$, is plotted on page 5.0-**28.** The ground effect factor, $F_{\ell_{GE}}$, is obtained from page 5.0-**29.**

5.0 $\Delta C_{\ell_{RUDDERS}}$ = Rolling moment coefficient due to rudder deflection.

(Cont'd)

$$\Delta C_{\ell_{RUDDERS}} = K\delta_{R_U} \cdot (\Delta C_{\ell_{R_U}})_{25} \cdot \frac{(C_{\ell_{R_U}})_M}{(C_{\ell_{R_U}})_{M=0}} + K\delta_{R_L} \cdot (\Delta C_{\ell_{R_L}})_{25} \cdot \frac{(C_{\ell_{R_L}})_M}{(C_{\ell_{R_L}})_{M=0}}$$

where $(\Delta C_{\ell_{R_U}})_{25}$ and $(\Delta C_{\ell_{R_L}})_{25}$ are the rolling moment coefficients due to full deflection of the upper rudder and the lower rudder respectively.

$(\Delta C_{\ell_{R_U}})_{25}$ and $(\Delta C_{\ell_{R_L}})_{25}$ are plotted on page 5.0-30. The upper rudder effectiveness factor, $K\delta_{R_U}$, and the lower rudder effectiveness factor, $K\delta_{R_L}$, are plotted on pages 6.0-17 and 6.0-18 respectively. The aeroelastic effects, $\frac{(C_{\ell_{R_U}})_M}{(C_{\ell_{R_U}})_{M=0}}$ and $\frac{(C_{\ell_{R_L}})_M}{(C_{\ell_{R_L}})_{M=0}}$, for the upper rudder and the lower rudder, are plotted on page 5.0-31 and page 5.0-32 respectively.

$\Delta C_{\ell_{FLAP\ FAILURE}}$ = Rolling moment coefficient due to an asymmetric (monitor limited) inboard or outboard flap failure.

$$\Delta C_{\ell_{FLAP\ FAILURE}} = \Delta C_{\ell_{INB'D\ FAILURE}} \ \underline{OR} \ \Delta C_{\ell_{OUTB'D\ FAILURE}}$$

where $\Delta C_{\ell_{INB'D\ FAILURE}}$ is the rolling moment coefficient due to an asymmetric (monitor limited) inboard flap failure. $\Delta C_{\ell_{INB'D\ FAILURE}}$ for flap extension or retraction is plotted on pages 5.0-33 and 5.0-34 respectively.

$\Delta C_{\ell_{OUTB'D\ FAILURE}}$ for flap extension or retraction is plotted on pages 5.0-35 and 5.0-36 respectively.

5.0 (Cont'd) $\Delta C_{\ell_{L.E.\ FAILURE}}$ = Rolling moment coefficient due to asymmetric leading edge flap failure. $\Delta C_{\ell_{L.E.\ FAILURE}}$ is plotted on pages 5.0-37 and 5.0-38.

LOW SPEED

NOTE 1. GEAR UP, FREE AIR

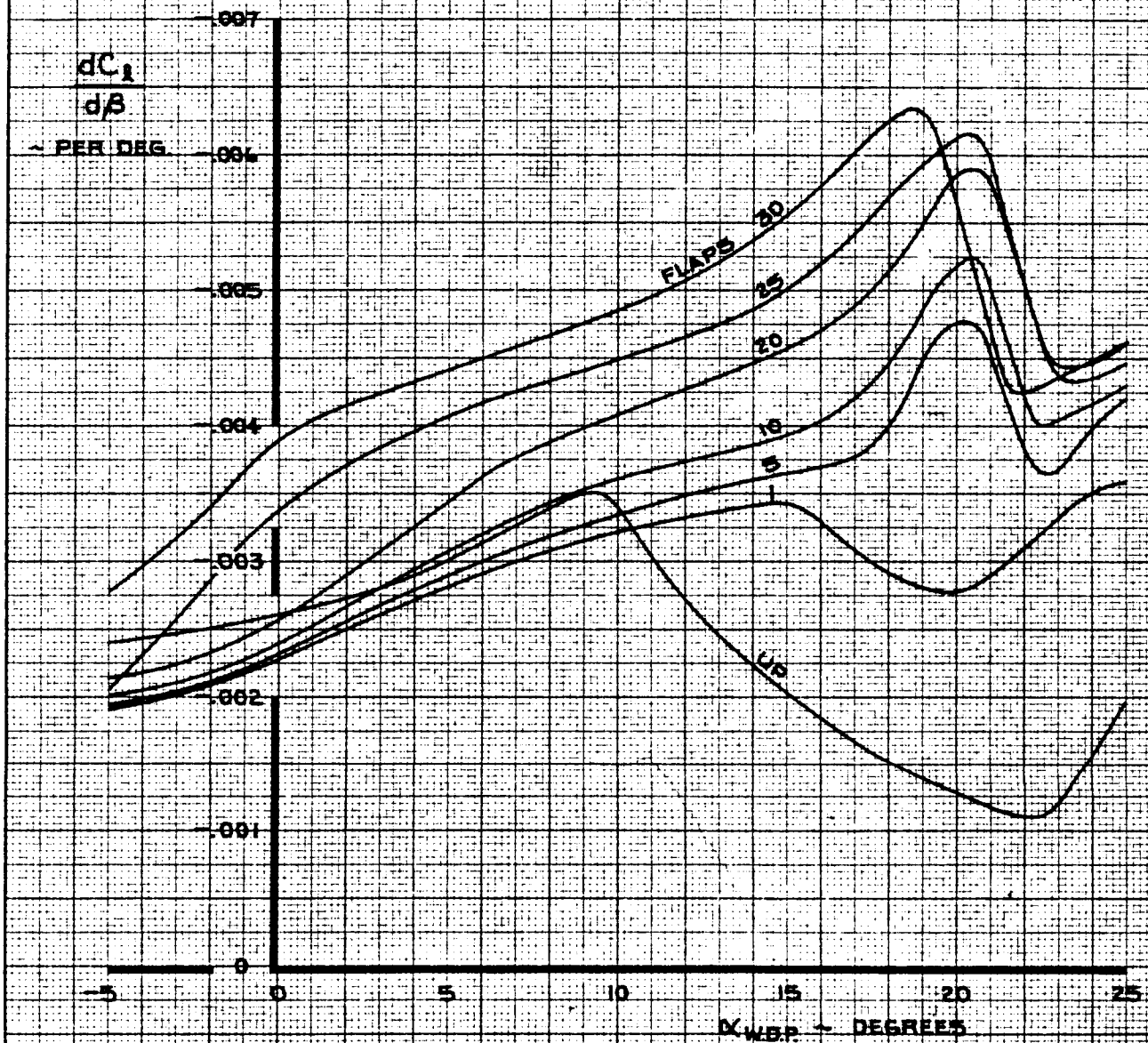

CALC	STIRLING	11-7-67	REVISED	DATE	ROLLING MOMENT COEFFICIENT DUE TO EFFECT OF SIDESLIP	747
CHECK	KUPCIS	11-7-67	LOW	6-4-69		D6-30643 Vol. II
APR			BECK	1-30-70		
APR					THE BOEING COMPANY	PAGE 5.0-7
INK	ODEGARD	2-9-70				

FLAPS UP

NOTE 1 GEAR UP

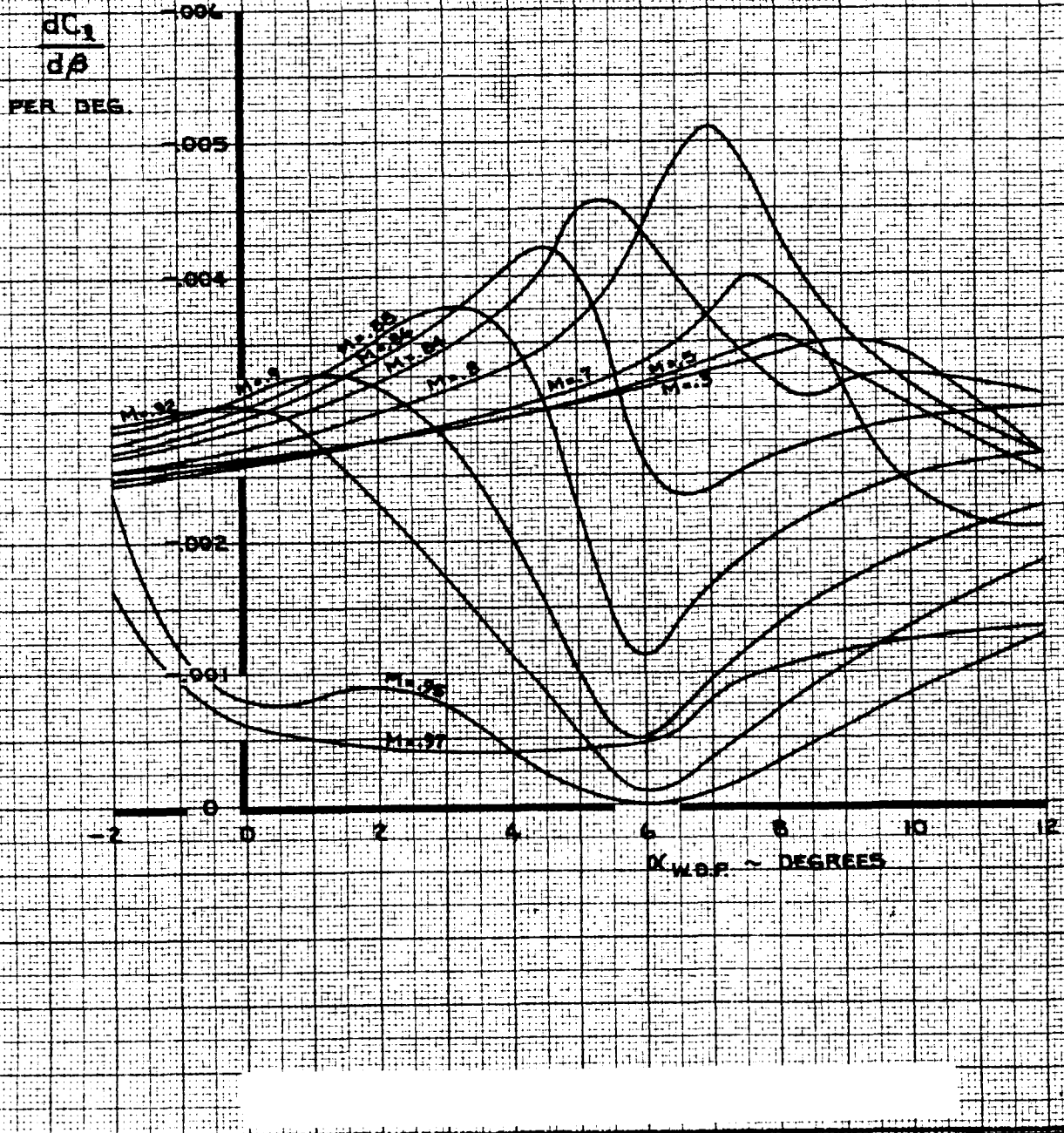

CALC	STIRLING	11·29·67	REVISED	DATE	ROLLING MOMENT COEFFICIENT EFFECT OF MACH NUMBER ON $dC_l/d\beta$	747
CHECK	KUPCIS	11·29·67	LOW	6·4·69		D6-30643 Vol. II
APR			BECK	1·30·70		
APR					THE BOEING COMPANY	PAGE 5.0-8
INK	ODEGARD	2·9·70				

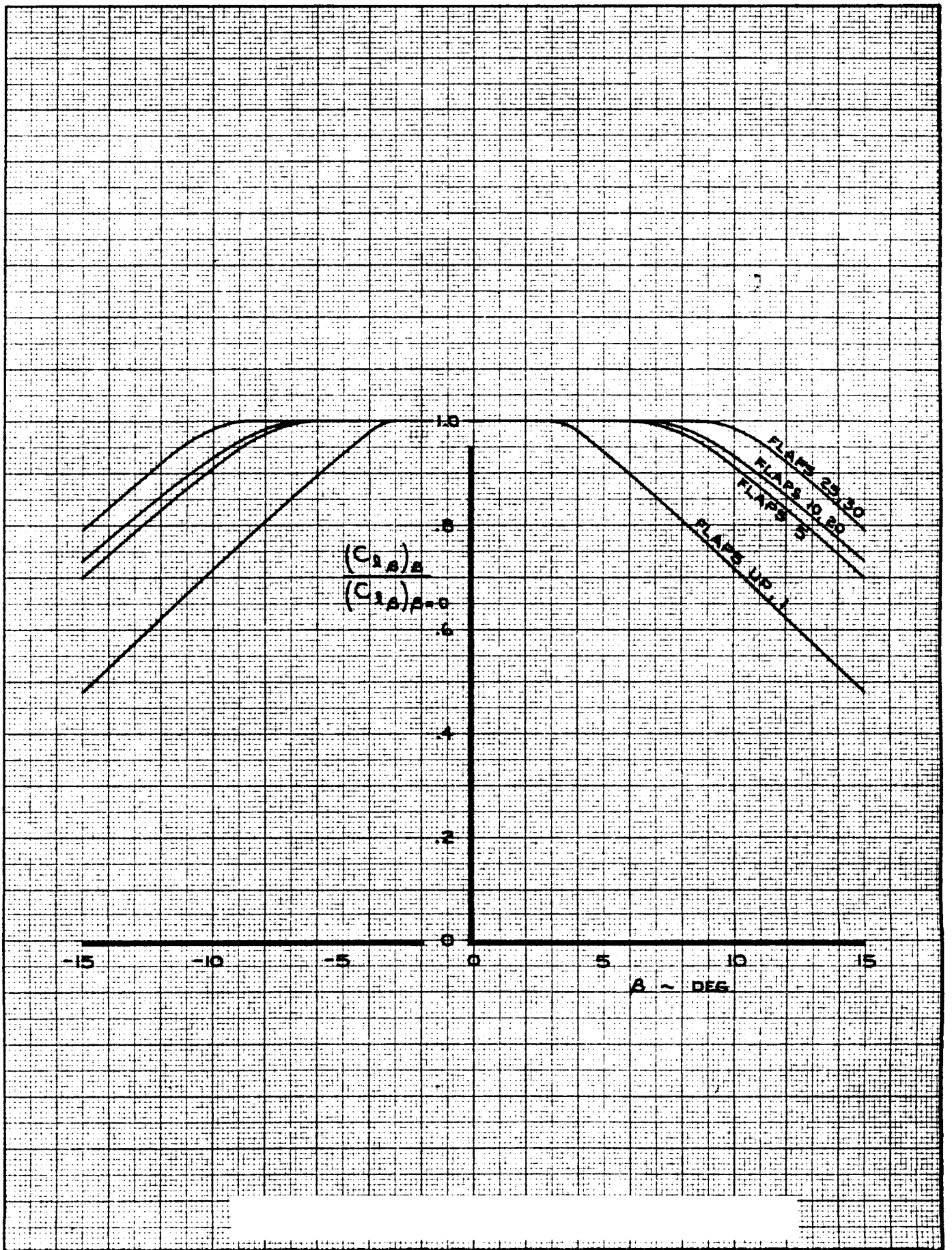

CALC	BECK	1-21-70	REVISED	DATE	ROLLING MOMENT COEFFICIENT SIDESLIP EFFECT ON $\frac{dC_l}{d\beta}$
CHECK					
APR					
APR					
INK	ODEGARD	1-30-70			

747

D6-30643 Vol. II

THE BOEING COMPANY

PAGE 5.0-9

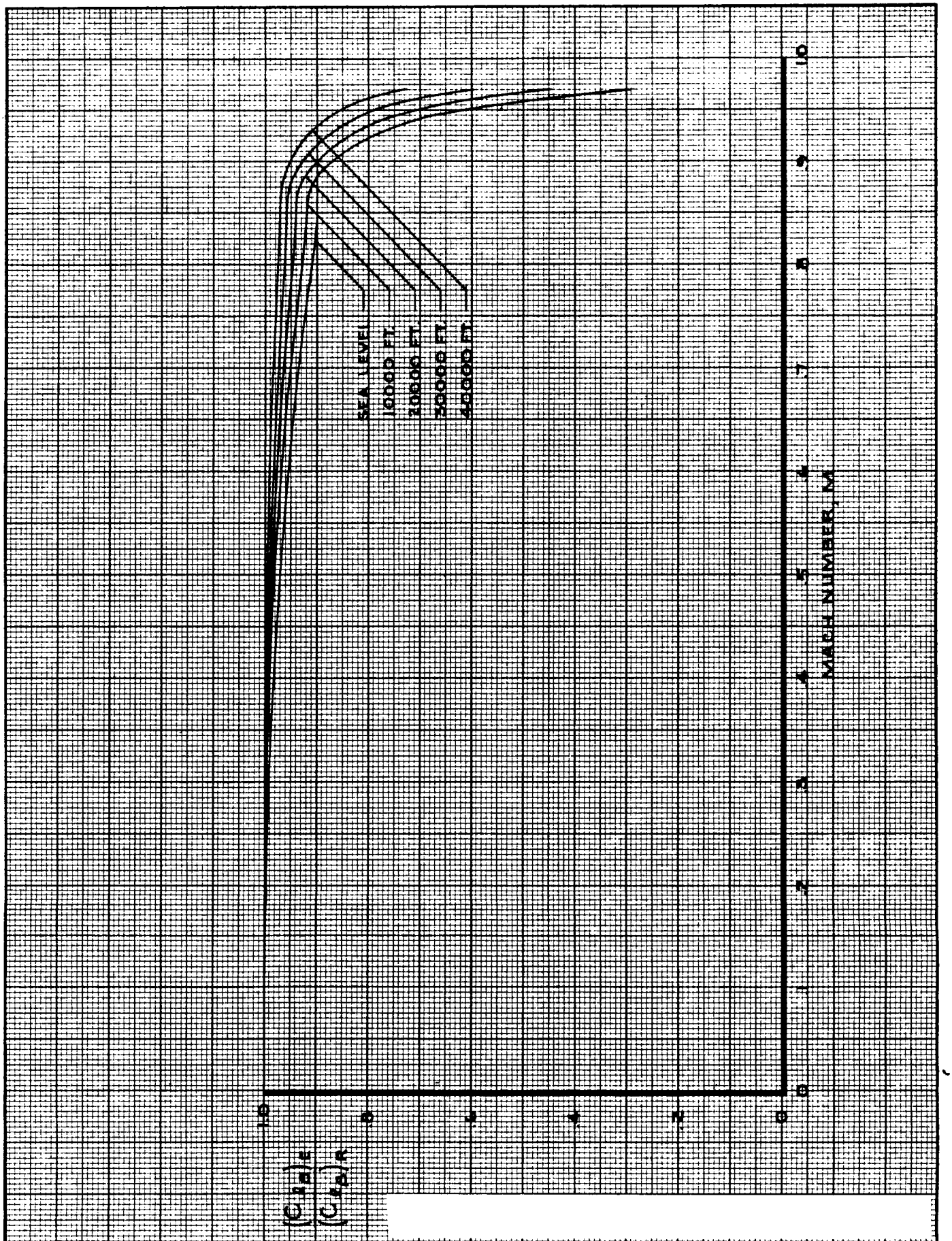

CALC	STIRLING	12/28/67	REVISED	DATE	ROLLING MOMENT COEFFICIENT AEROELASTIC EFFECT ON $\frac{dC_\ell}{d\beta}$
CHECK	FOSTER	1.24.68	LOW	6.4.69	
APR					
APR					
INK	ODEGARD	12/28/67			THE BOEING COMPANY

747
D6-30643
Vol. II
PAGE 5.0-10
REV. D

TD 461 C-R4

NOTE: $F_{\ell_{F_{GE}}} = \left[1 + F_{\ell_\beta} \cdot K^{B}_{GE}\right]$

WHERE K^{B}_{GE} IS SHOWN ON PAGE 2.0-51

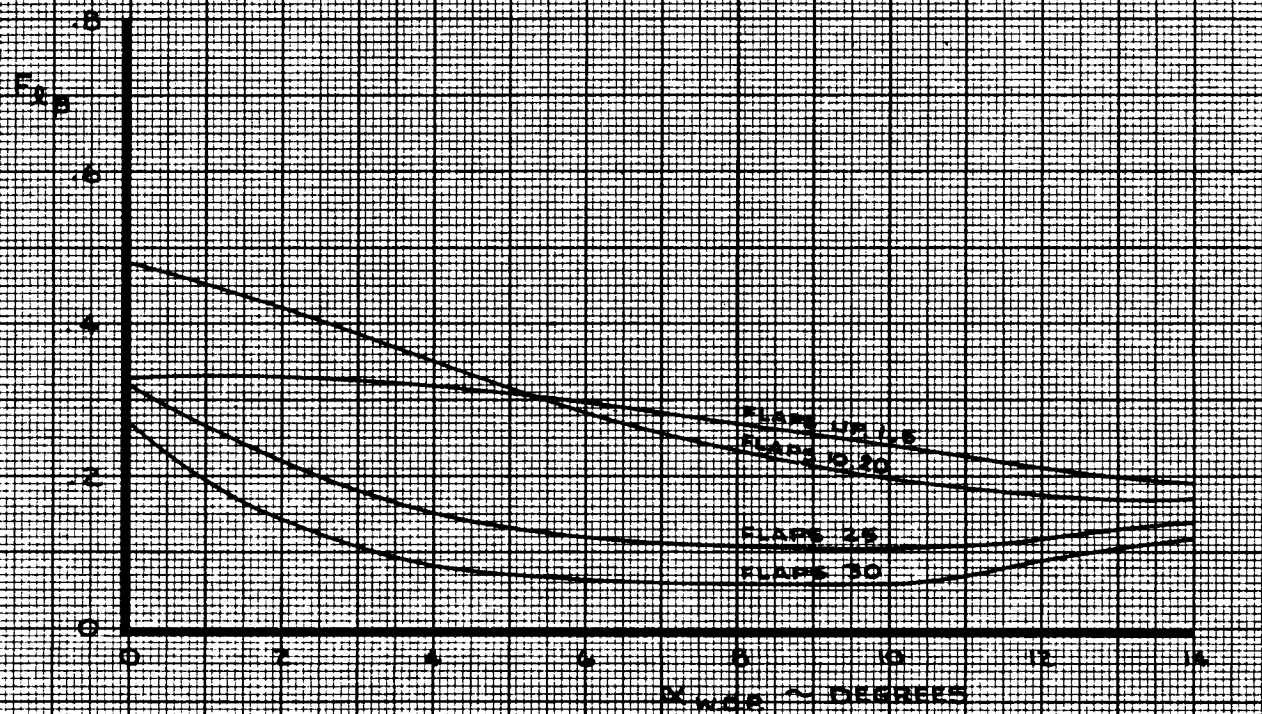

CALC	STIRLING	12/28/67	REVISED	DATE	ROLLING MOMENT COEFFICIENT GROUND EFFECT SIDESLIP FACTOR, F_{ℓ_β}
CHECK	FOSTER	1-24-68	LOW	6-4-69	
APR			LOW	2-14-70	
APR					
INK	ODEGARD	12/28/67			THE BOEING COMPANY

747

D6-30643 Vol. II

PAGE 5.0-11

REV. D

TD 461 C-R4

NOTE 1 $\hat{p} = \frac{p_s b}{2V}$; p_s ~ RAD/SEC, V ~ FT/SEC (TRUE AIRSPEED)

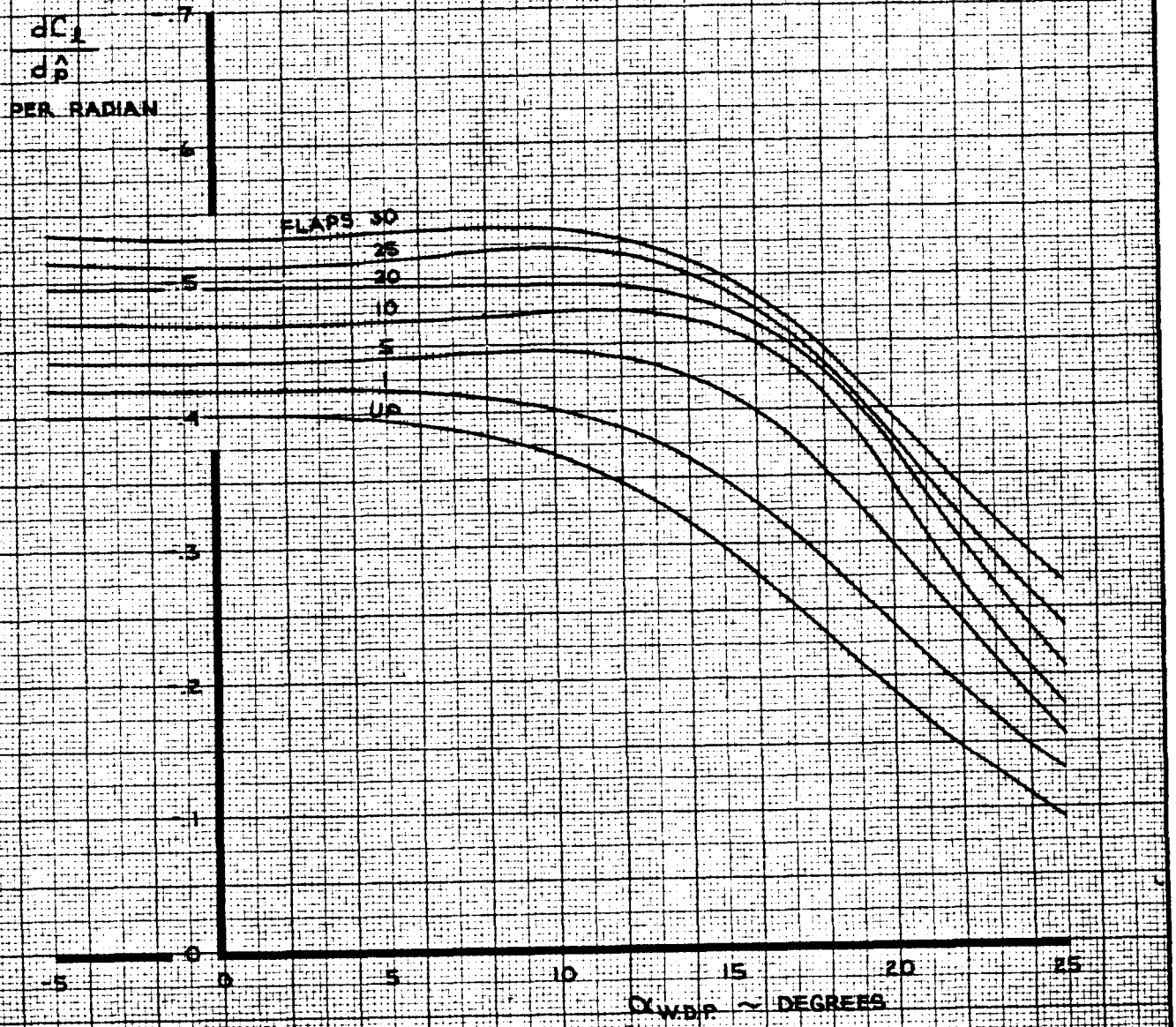

CALC	RICHARDSON	11-16-67	REVISED	DATE	ROLLING MOMENT COEFFICIENT EFFECT OF ROLL RATE
CHECK	CURNUTT	12-15-67	LOW	6-4-69	
APR			LUDWIG	11-3-69	
APR			CURNUTT	2-25-70	
INK	KINSMAN	3-4-70			

747

D6-30643 Vol. II

THE BOEING COMPANY

PAGE 5.0-12

AD 461 C-R4

K-E ALBANENE 1991 TRACING PAPER REV. D

NOTE 1. $\hat{r} = \frac{r_s b}{2V}$; r_s ~ RAD/SEC, V ~ FT/SEC (TRUE AIRSPEED)

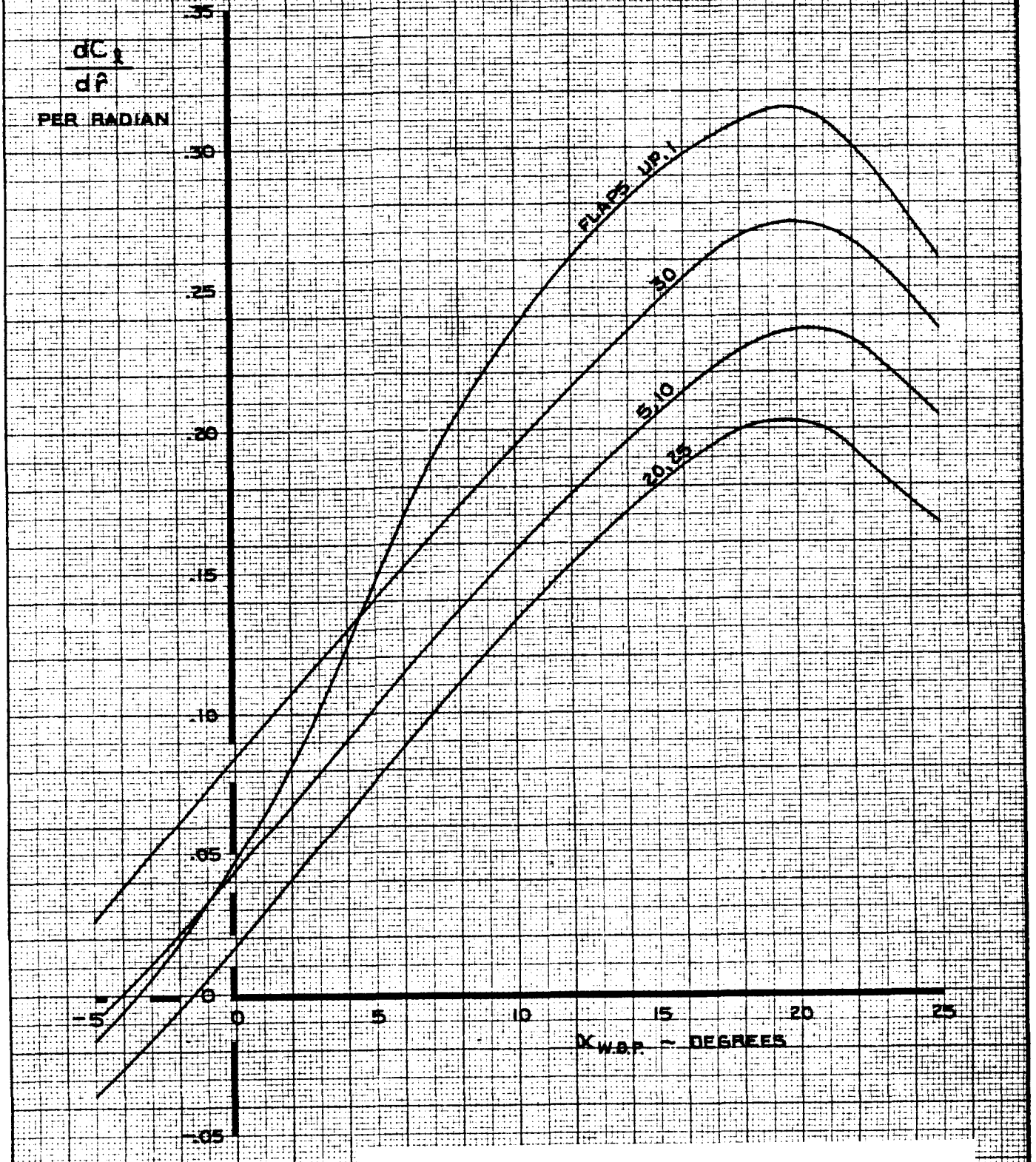

CALC	RICHARDSON	11-14-67	REVISED	DATE	ROLLING MOMENT COEFFICIENT EFFECT OF YAW RATE
CHECK	CURNUTT	11-16-67	LOW	6-4-69	
APR			CURNUTT	2-27-70	
APR					
INK	ODEGARD	3-3-70			

747

D6-30643 Vol. II

THE BOEING COMPANY

PAGE 5.0-14

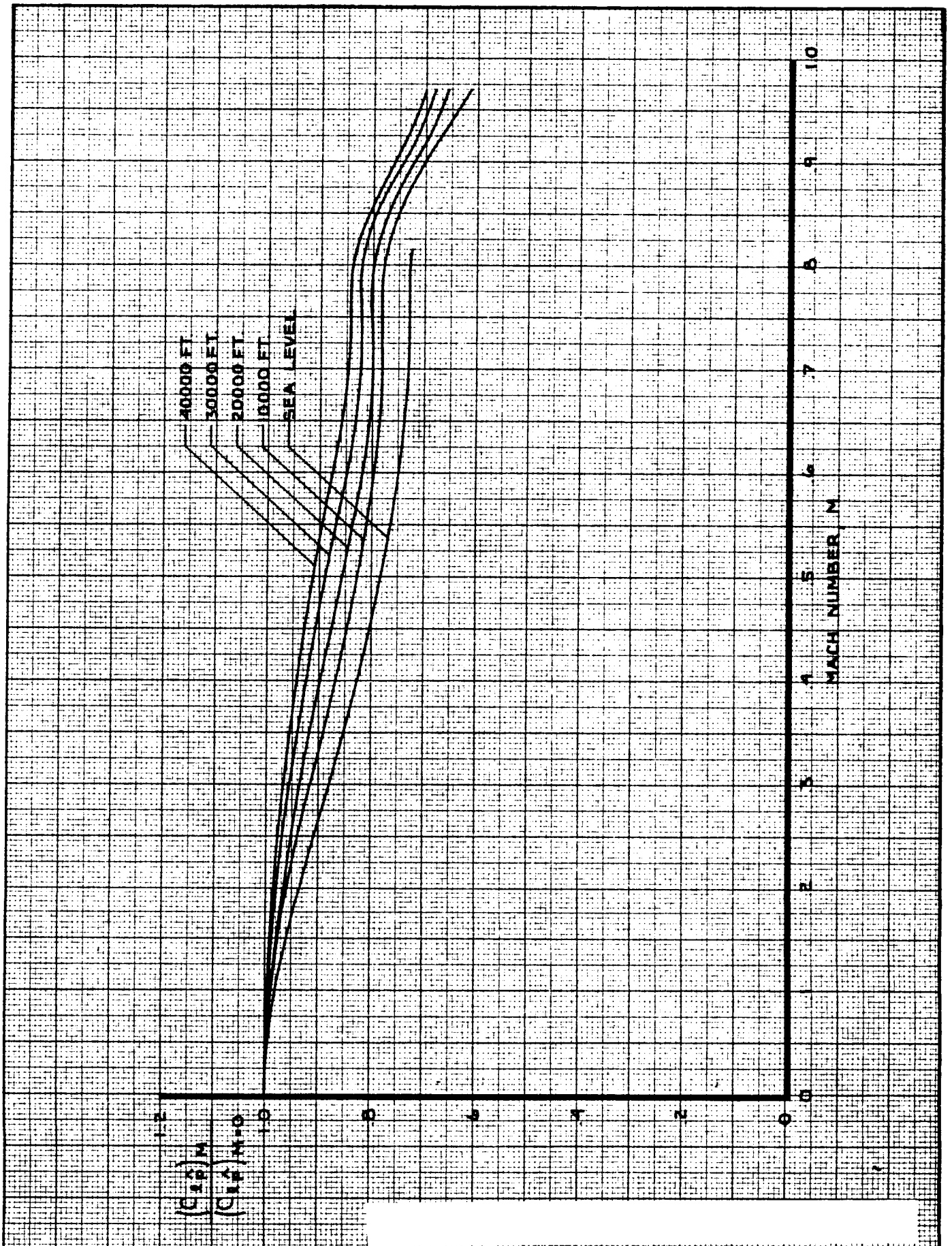

CALC	RICHARDSON	11·16·67	REVISED	DATE	ROLLING MOMENT COEFFICIENT ✓ AEROELASTIC EFFECT ON ROLLING MOMENT COEFFICIENT DUE TO ROLL RATE
CHECK	CURNUTT	11·16·67	LOW	6·4·69	
APR			CURNUTT	2·25·70	
APR					
INK	KINSMAN	3·4·70			THE BOEING COMPANY

747

D6-30643 Vol. II

PAGE 5.0-13

AD 461 C-R4

K·E ALBANENE 1951 TRACING PAPER REV. D

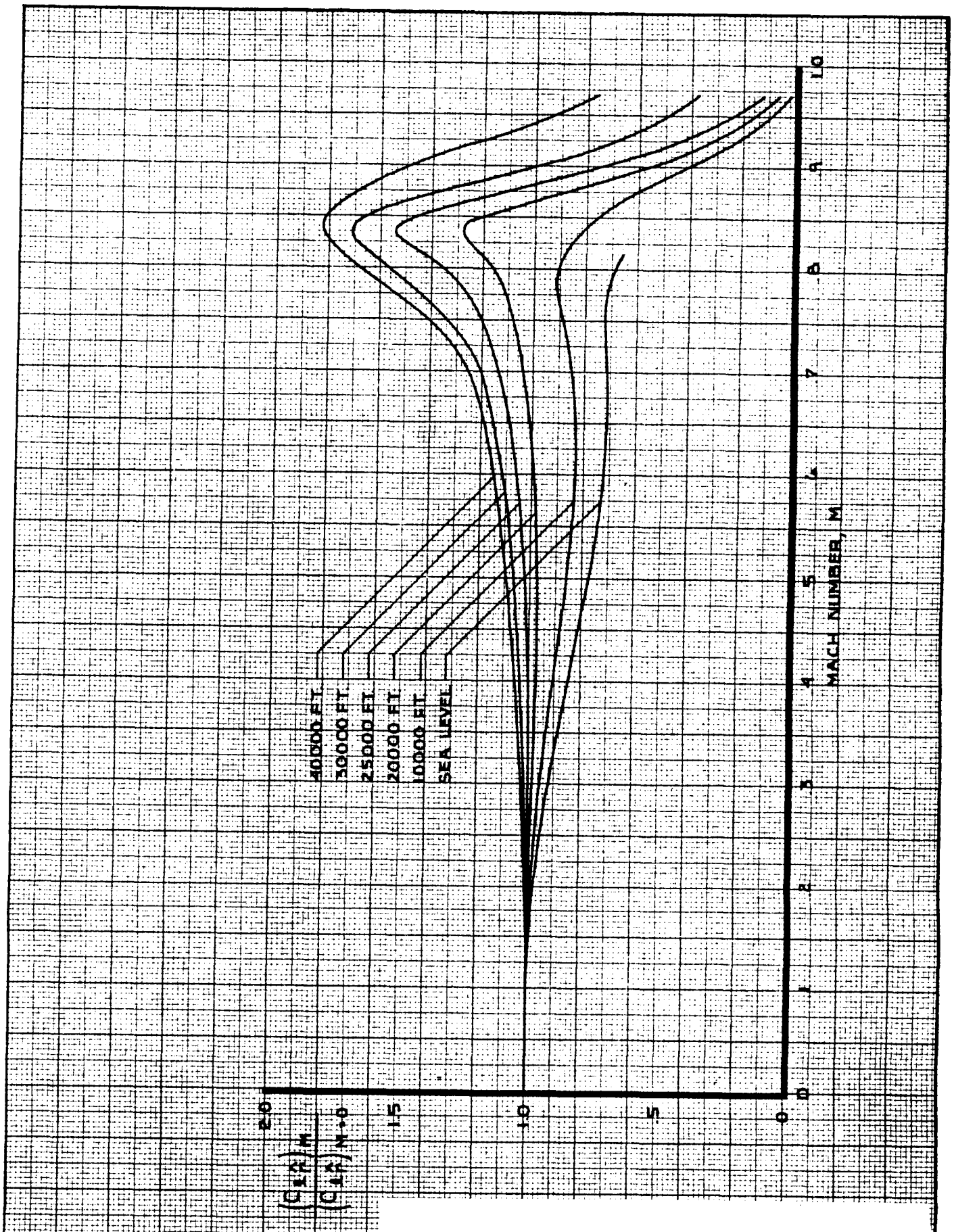

CALC	RICHARDSON	11-13-67	REVISED	DATE	ROLLING MOMENT COEFFICIENT AEROELASTIC EFFECT ON ROLLING MOMENT COEFFICIENT DUE TO YAW RATE
CHECK	CURNUTT	11-14-67	LOW	6-4-69	
APR			CURNUTT	2-25-70	
APR					
INK	KINSMAN	3-4-70			

747

D6-30643 Vol. II

THE BOEING COMPANY

PAGE 5.0-15

AD 461 C-R4

K-E ALBANENE 1951 REV. D

NOTE 1. USE FOR ALL SPOILER PANELS

2. PANELS 8 & 5 LIMITED TO 20 DEG. MAX DEFLECTION

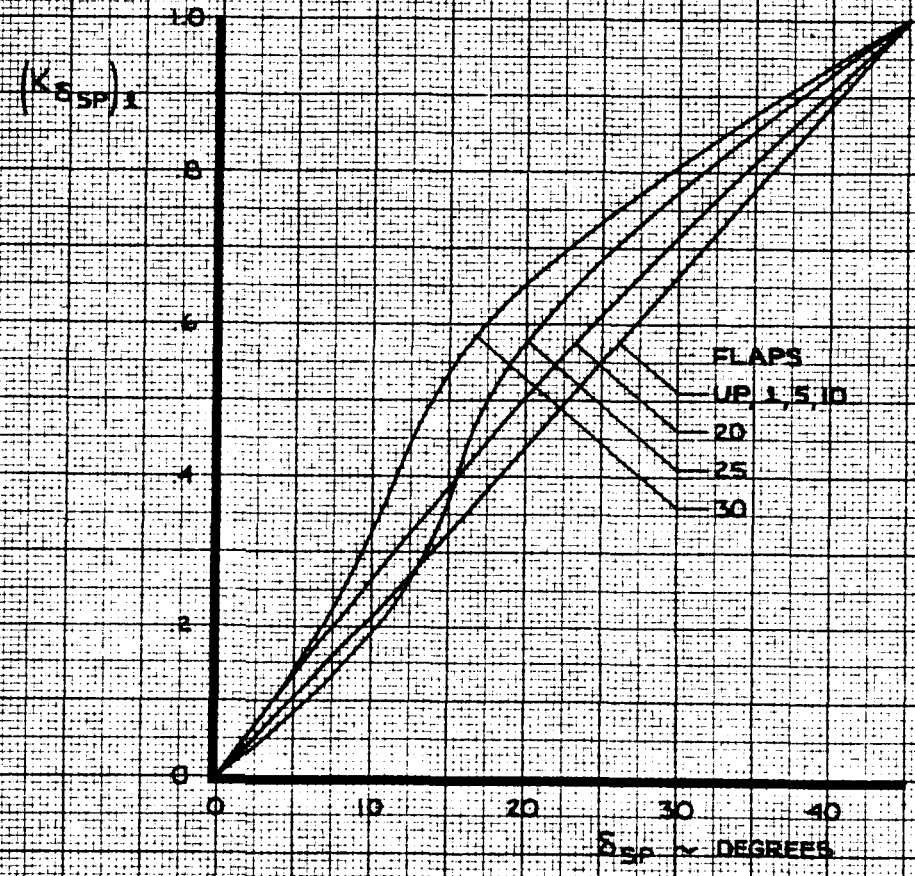

CALC	KUPCIS	1·30·67	REVISED	DATE	ROLLING MOMENT COEFFICIENT EFFECTIVENESS FACTOR SPOILERS	747
CHECK	FOSTER	1·24·68	KUPCIS	6·2·69		
APR			BECK	1·27·70		D6-30643 Vol. II
APR						
INK	KINSMAN	1·27·70			THE BOEING COMPANY	PAGE 5.0-16

TD 461 C-R4

SPOILER PANEL 8 OR 12

NOTE 1 DATA SHOWN FOR INDIVIDUAL PANELS 8 OR 12
2 FOR PANEL 1 OR 5, REVERSE SIGN
3 PANELS 8 & 5 LIMITED TO 20 DEG. MAX. DEFLECTION

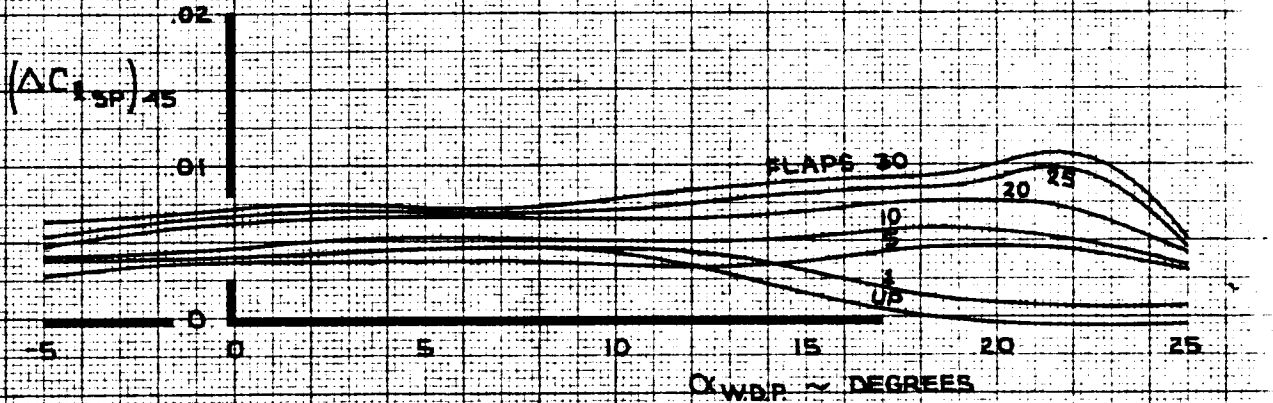

SPOILER PANEL GROUP 9, 10, 11

NOTE 1 TOTAL EFFECT OF SPOILER GROUP 9, 10, 11 SHOWN
2 FOR SPOILER GROUP 2, 3, 4, REVERSE SIGN
3 WITH HYDRAULIC SYSTEM NO. 2 OFF, MULTIPLY BY 0.32
4 WITH HYDRAULIC SYSTEM NO. 3 OFF, MULTIPLY BY 0.68

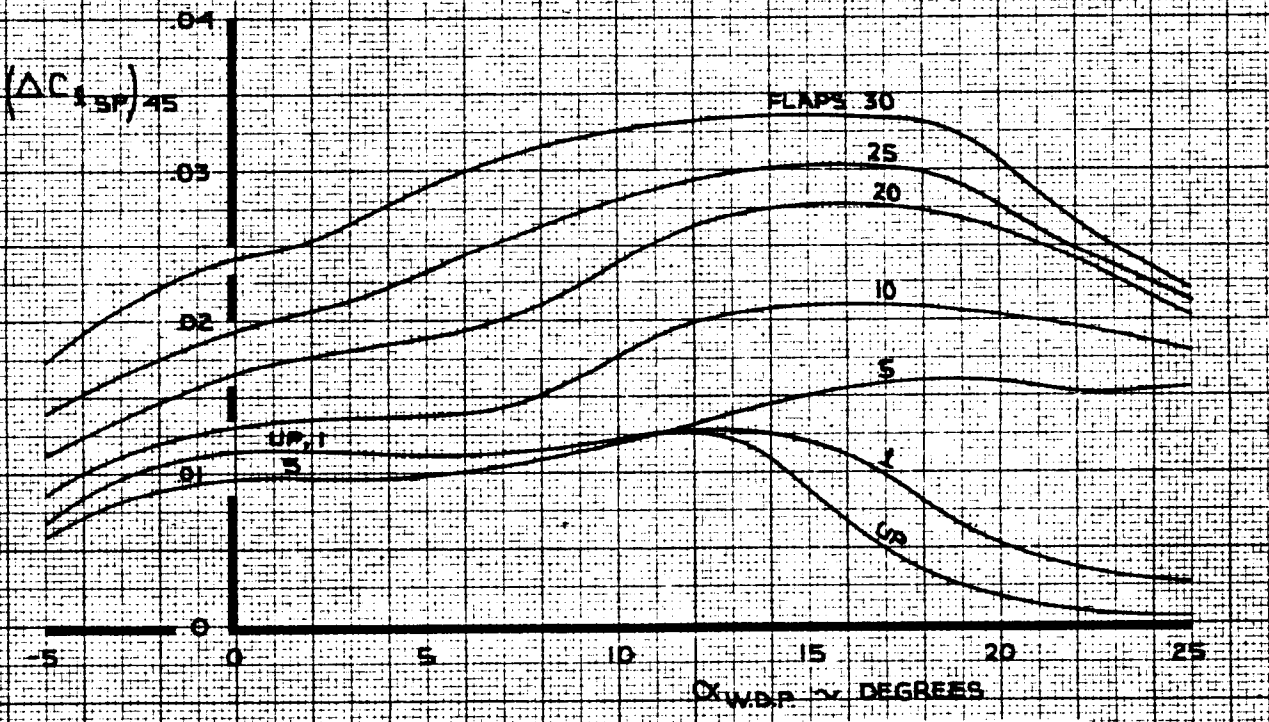

CALC	KUPCIS	11-29-67	REVISED	DATE
CHECK	FOSTER	1-24-68	KUPCIS	6-2-69
APR			KUPCIS	2-16-70
APR				
INK	KINSMAN	2-18-70		

ROLLING MOMENT COEFFICIENT
EFFECT OF SPOILERS

747

D6-30643 Vol. II

THE BOEING COMPANY

PAGE 5.0-17

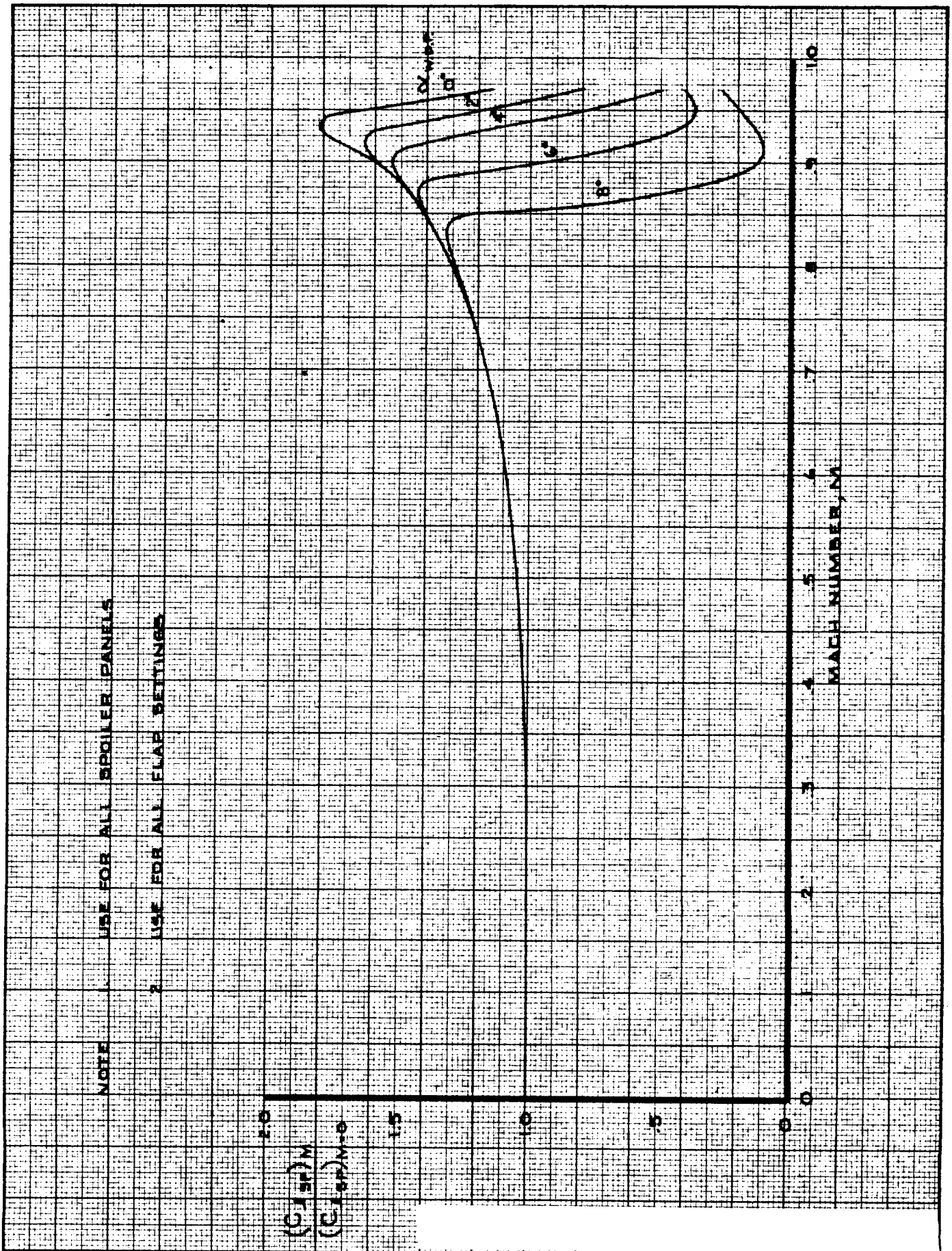

NOTE 1. USE FOR ALL SPOILER PANELS
2. USE FOR ALL FLAP SETTINGS

CALC	KUPCIS	10/23/67	REVISED	DATE	ROLLING MOMENT COEFFICIENT EFFECT OF MACH NUMBER ON SPOILERS
CHECK	FOSTER	1-24-68	LOW	6-4-69	
APR					
APR					
INK	ODEGARD	10/23/67			THE BOEING COMPANY

747
D6-30643 Vol. II
PAGE 5.0-18
REV. D

AD 451 C R4

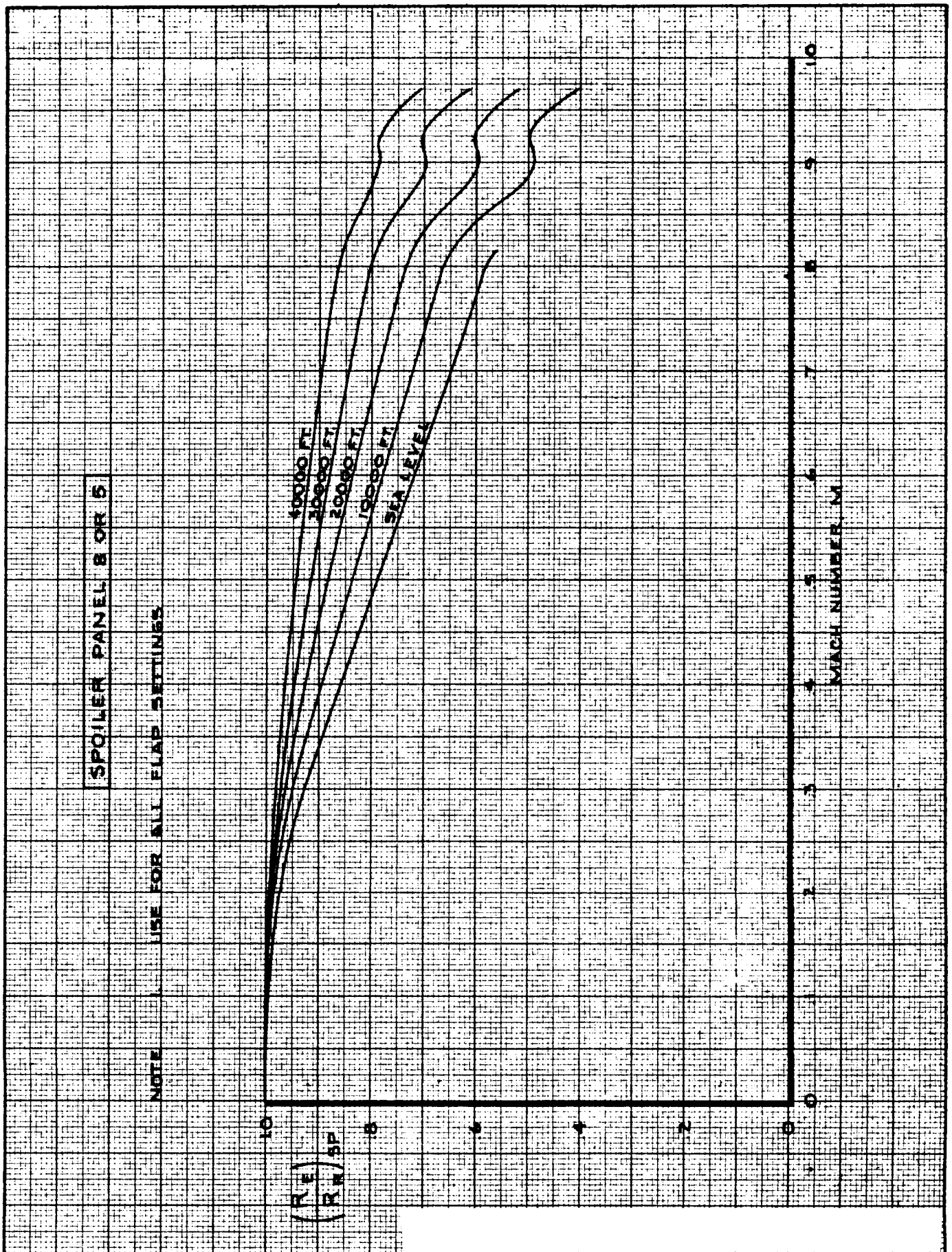

CALC	KUPCIS	10-30-67	REVISED	DATE	ROLLING MOMENT COEFFICIENT
CHECK	FOSTER	1-24-68	LOW	6-4-69	AEROELASTIC EFFECT ON ROLLING MOMENT COEFFICIENT DUE TO SPOILERS(8 OR 5)
APR					THE BOEING COMPANY
APR					
INK	ODEGARD	10-30-67			

747

D6-30643 Vol. II

PAGE 5.0-19

REV D

AD 461 C R4

102

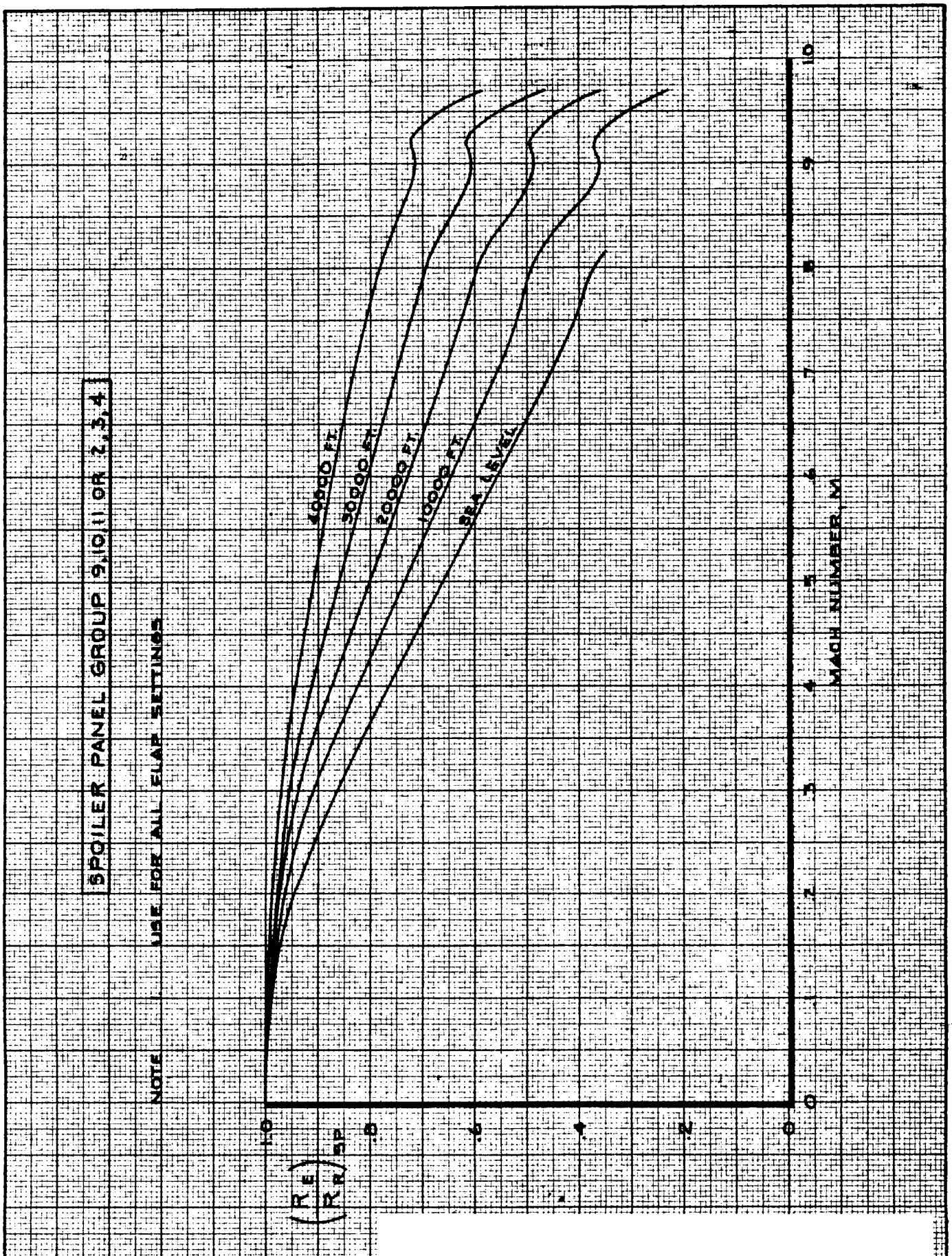

CALC	KUPCIS	10-30-67	REVISED	DATE	ROLLING MOMENT COEFFICIENT
CHECK	FOSTER	1-24-68	LOW	6-4-69	AEROELASTIC EFFECT ON ROLLING MOMENT
APR					COEFFICIENT DUE TO SPOILERS (9,10,11 OR 2,3,4)
APR					THE BOEING COMPANY
INK	ODEGARD	10-30-67			

747

D6-30643 Vol. II

PAGE 5.0-20

REV D

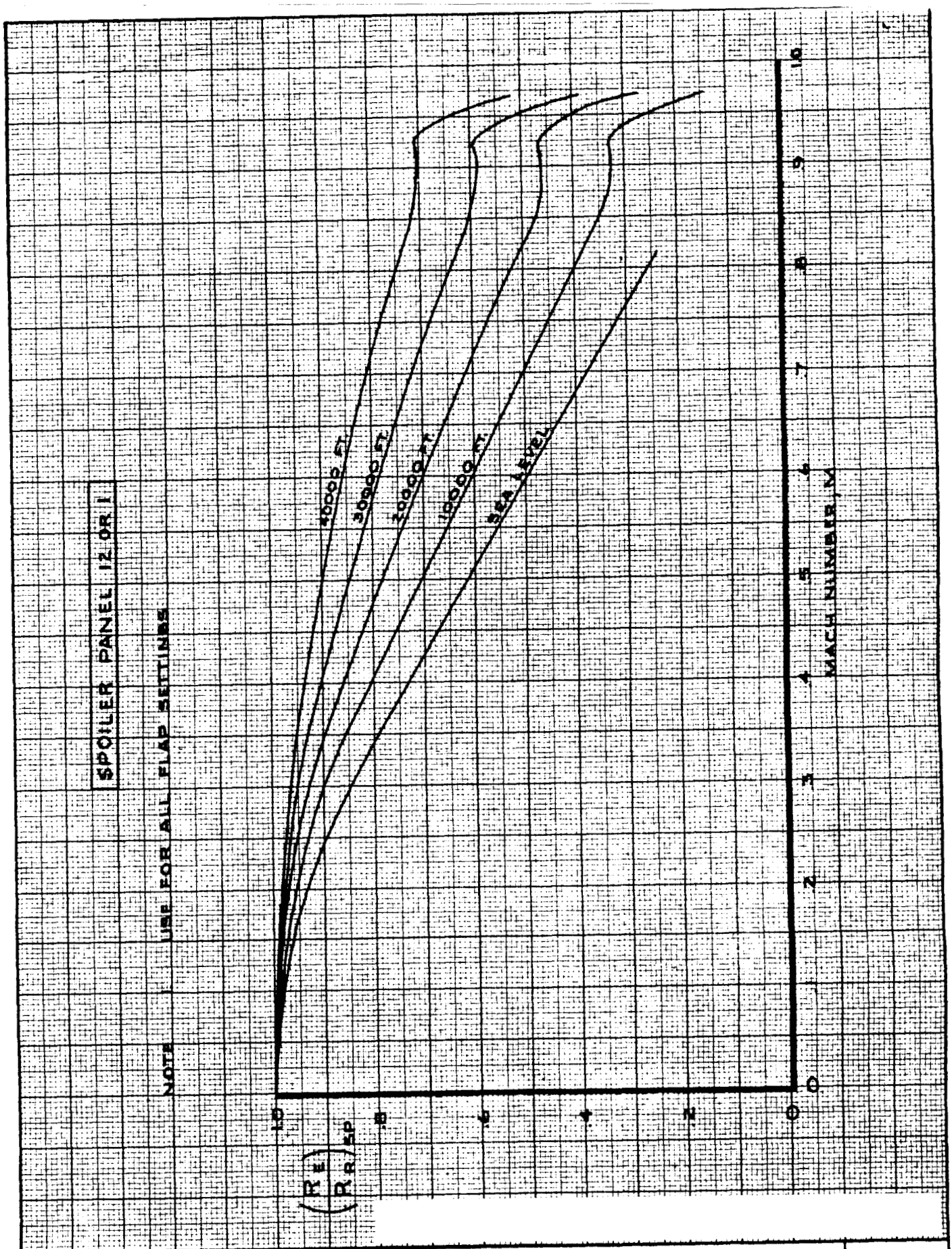

CALC	KUPCIS	10-30-67	REVISED	DATE	ROLLING MOMENT COEFFICIENT AEROELASTIC EFFECT ON ROLLING MOMENT COEFFICIENT DUE TO SPOILERS (12 OR 1)
CHECK	FOSTER	1-24-68	LOW	6-4-69	
APR					
APR					
INK	ODEGARD	10-30-67			THE BOEING COMPANY

747
D6-30643 Vol. II
PAGE 5.0-21
REV. D

AD 461 C R4

101

NOTE 1. SYMMETRIC FOR UP AND DOWN AILERON

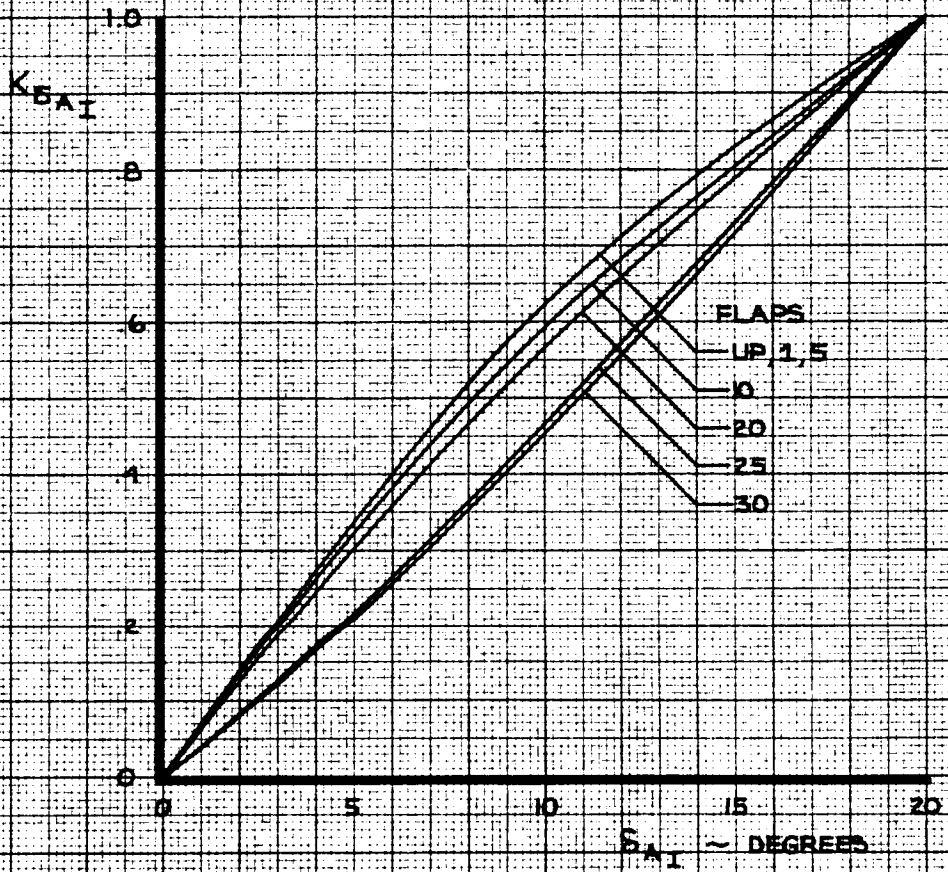

CALC	KUPCIS	11.6.67	REVISED	DATE	EFFECTIVENESS FACTOR INBOARD AILERONS	747
CHECK	FOSTER	1.24.68	LOW	6.4.69		D6-30643 Vol. II
APR			BECK	1.27.70		
APR					THE BOEING COMPANY	PAGE 5.0-22
INK	KINSMAN	1.27.70				

TD 461 C-R4

K-E ALBANENE 195L REV. D

NOTE 1. $(\Delta C_{l_{AI}})_{20}$ IS SHOWN FOR RIGHT AILERON UP ONLY

2. FOR FULL LATERAL CONTROL (RIGHT AILERON UP AND LEFT AILERON DOWN), USE 2 x $(\Delta C_{l_{AI}})_{20}$

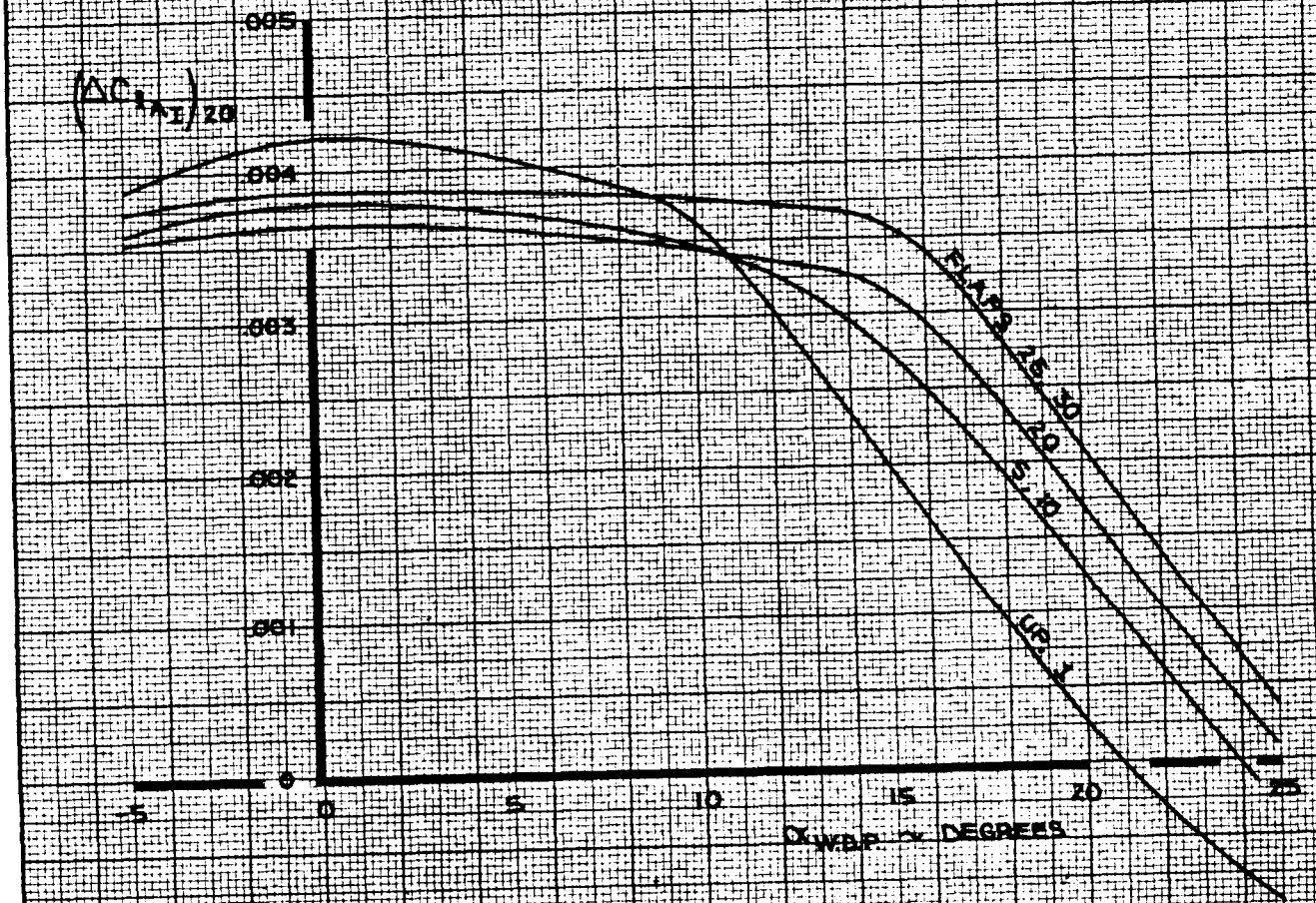

CALC	KUPCIS	11-6-67	REVISED	DATE	ROLLING MOMENT COEFFICIENT EFFECT OF INBOARD AILERON	747
CHECK	FOSTER	1-24-68	LOW	6-4-69		D6-30643 Vol. II
APR			KUPCIS	2-18-70		
APR					THE BOEING COMPANY	PAGE 5.0-23
INK	KINSMAN	2-1970				

K-E ALBANENE 1961 REV D

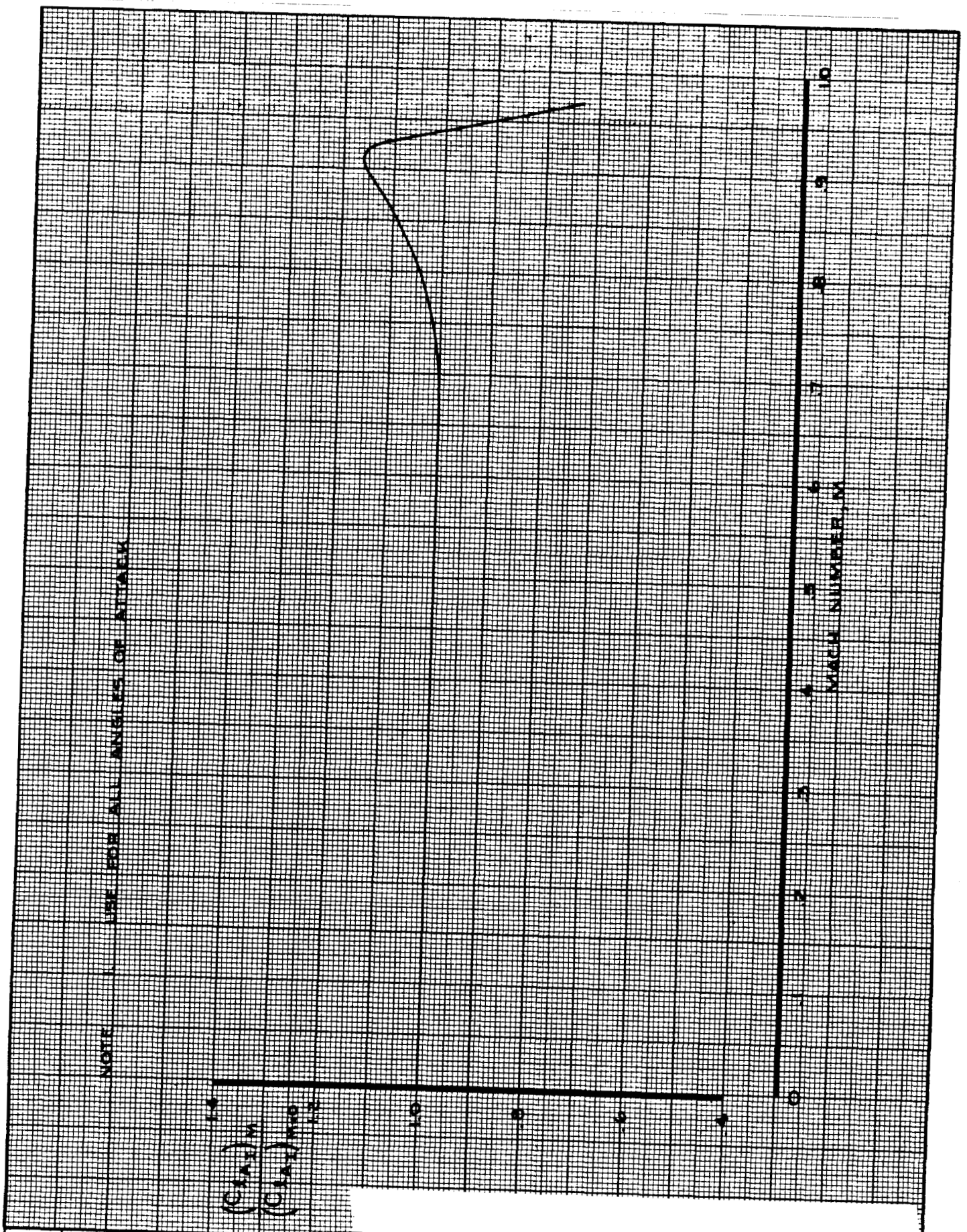

CALC	KUPCIS	11/1/67	REVISED	DATE	ROLLING MOMENT COEFFICIENT EFFECT OF MACH NUMBER ON INBOARD AILERONS
CHECK	FOSTER	1-24-68	LOW	6-4-69	
APR					
APR					
INK	ODEGARD	11/1/67			THE BOEING COMPANY

747

D6-30643 Vol. II

PAGE 5.0-24

REV. D

TD 461 C-R4

NOTE 1. USE FOR ALL FLAP SETTINGS.

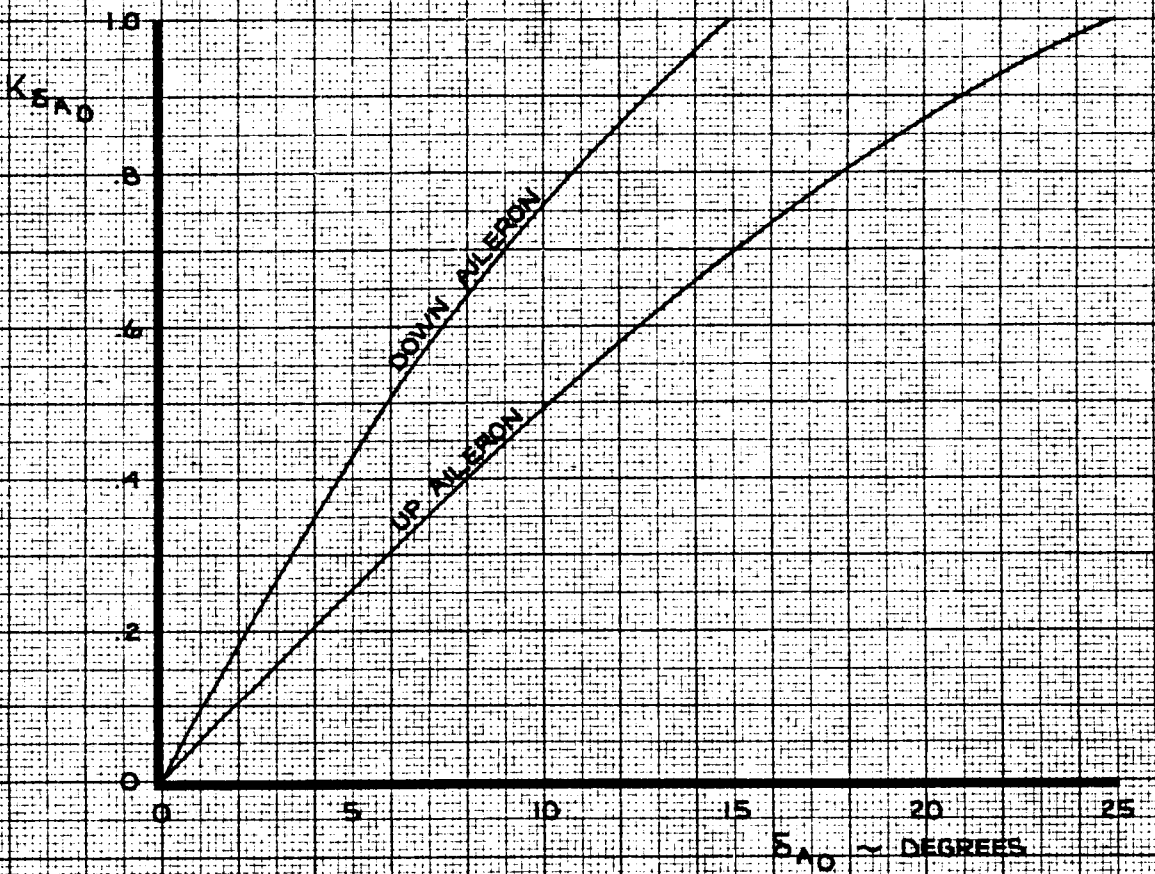

CALC	KUPCIS	11·16·67	REVISED	DATE	EFFECTIVENESS FACTOR OUTBOARD AILERONS	747
CHECK	FOSTER	1·24·68	LOW	6·4·69		D6-30643, Vol. II
APR			BECK	1·27·70		
APR					THE BOEING COMPANY	PAGE 5.0-26
INK	KINSMAN	1·27·70				

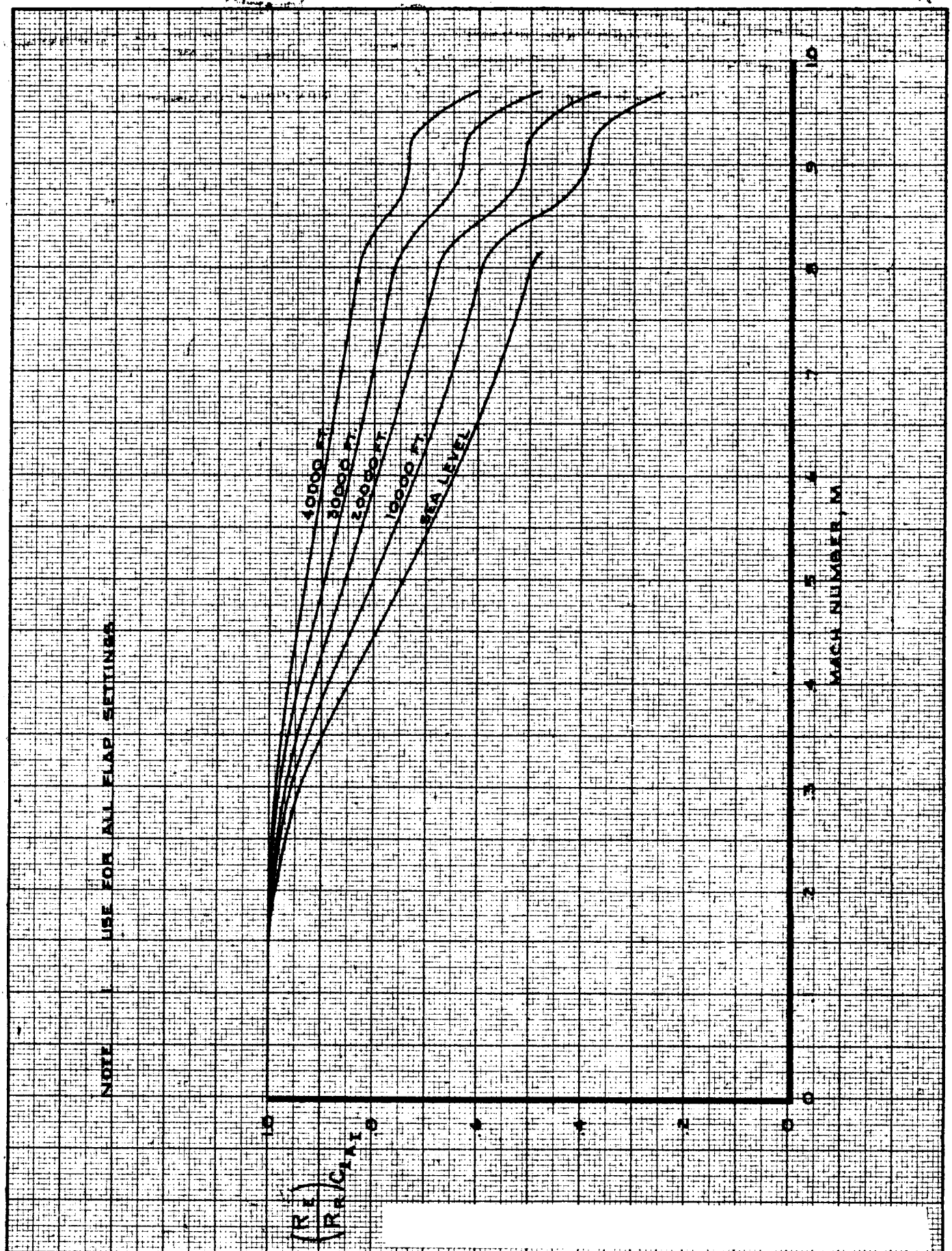

CALC	KUPCIS	10/31/67	REVISED	DATE	ROLLING MOMENT COEFFICIENT AEROELASTIC EFFECT ON ROLLING MOMENT COEFFICIENT DUE TO INBOARD AILERONS
CHECK	FOSTER	1-24-68	LOW	6-4-69	
APR					
APR					
INK	ODEGARD	10/31/67			

747

D6-30643 Vol. II

THE BOEING COMPANY

PAGE 5.0-25

AD 461 C R4

REV D

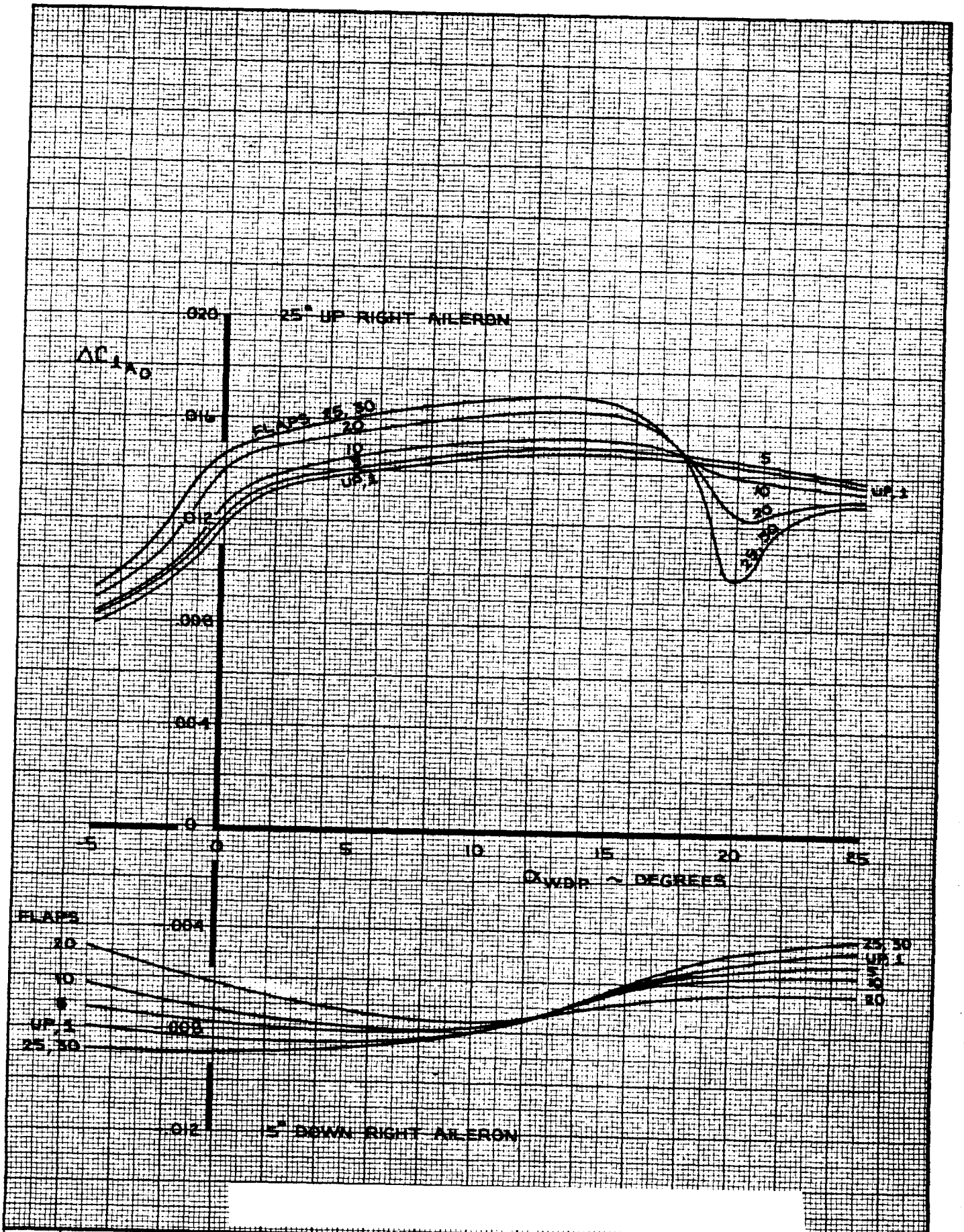

CALC	KUPCIS	11-13-67	REVISED	DATE	ROLLING MOMENT COEFFICIENT EFFECT OF OUTBOARD AILERON
CHECK	FOSTER	1-24-68	KUPCIS	9-22-68	
APR			KUPCIS	2-16-70	
APR					
INK	KINSMAN	2-20-70			THE BOEING COMPANY

747
D6-30643 Vol. II
PAGE 5.0-27

AD 461 C-R4

K-E ALBANENE 1951 TRACING PAPER REV. D

NOTE 1. USE FOR ALL FLAP SETTINGS

2. USE FOR ALL ALTITUDES

3. USE FOR UP OR DOWN AILERON

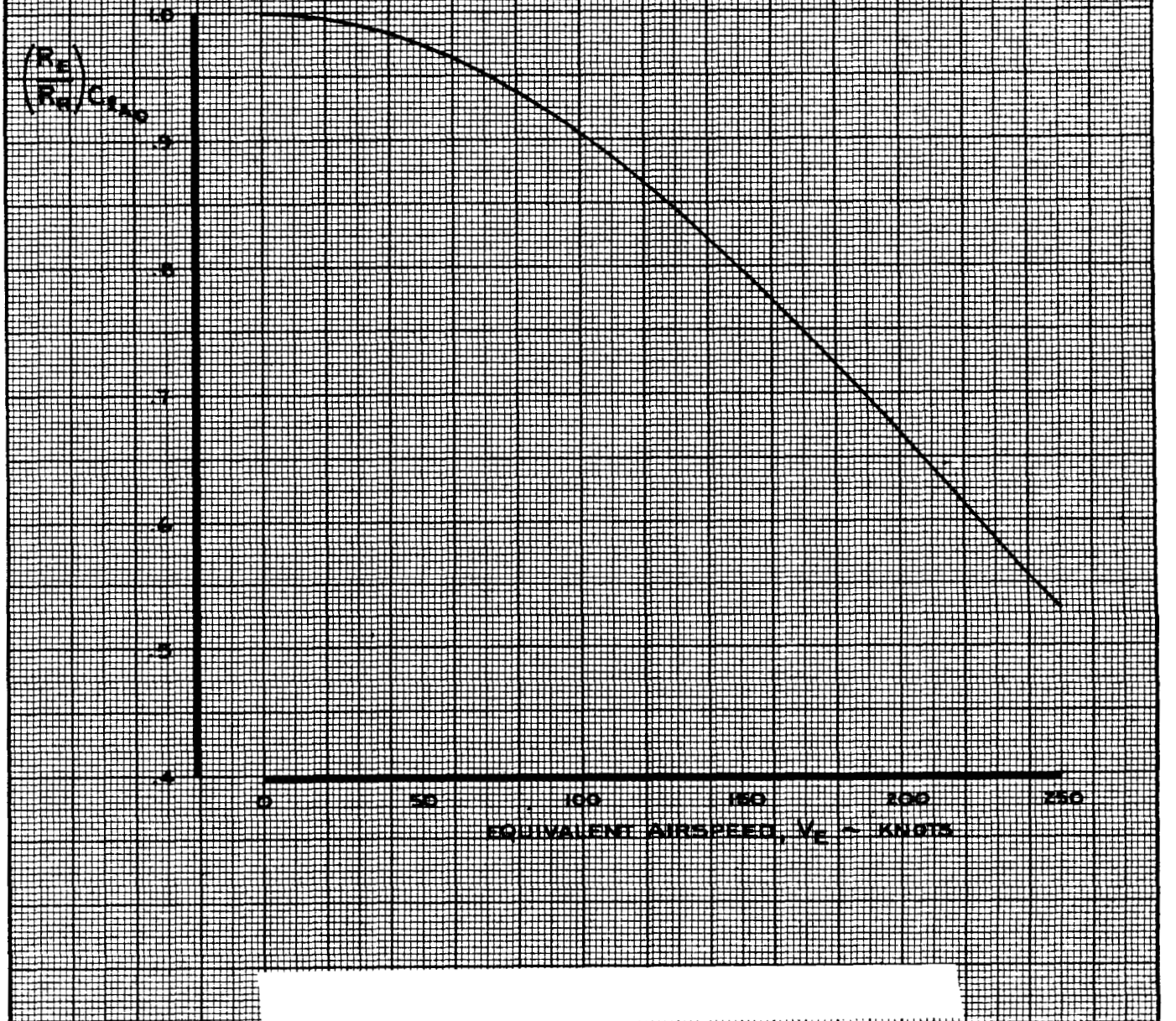

CALC	KUPCIS	1/22/68	REVISED	DATE	ROLLING MOMENT COEFFICIENT
CHECK	FOSTER	1-24-68	LOW	6-4-69	AEROELASTIC EFFECT ON ROLLING MOMENT
APR			LOW	1-23-70	COEFFICIENT DUE TO OUTBOARD AILERONS
APR					
INK	ODEGARD	1/22/68			THE BOEING COMPANY

747

D6-30643 Vol. II

PAGE 5.0-28

REV. D

NOTE 1. $F_{\ell_{GE}} = \left[1 + F_\ell - K^B_{GE}\right]$

WHERE K^B_{GE} IS SHOWN ON PAGE 2.0-31

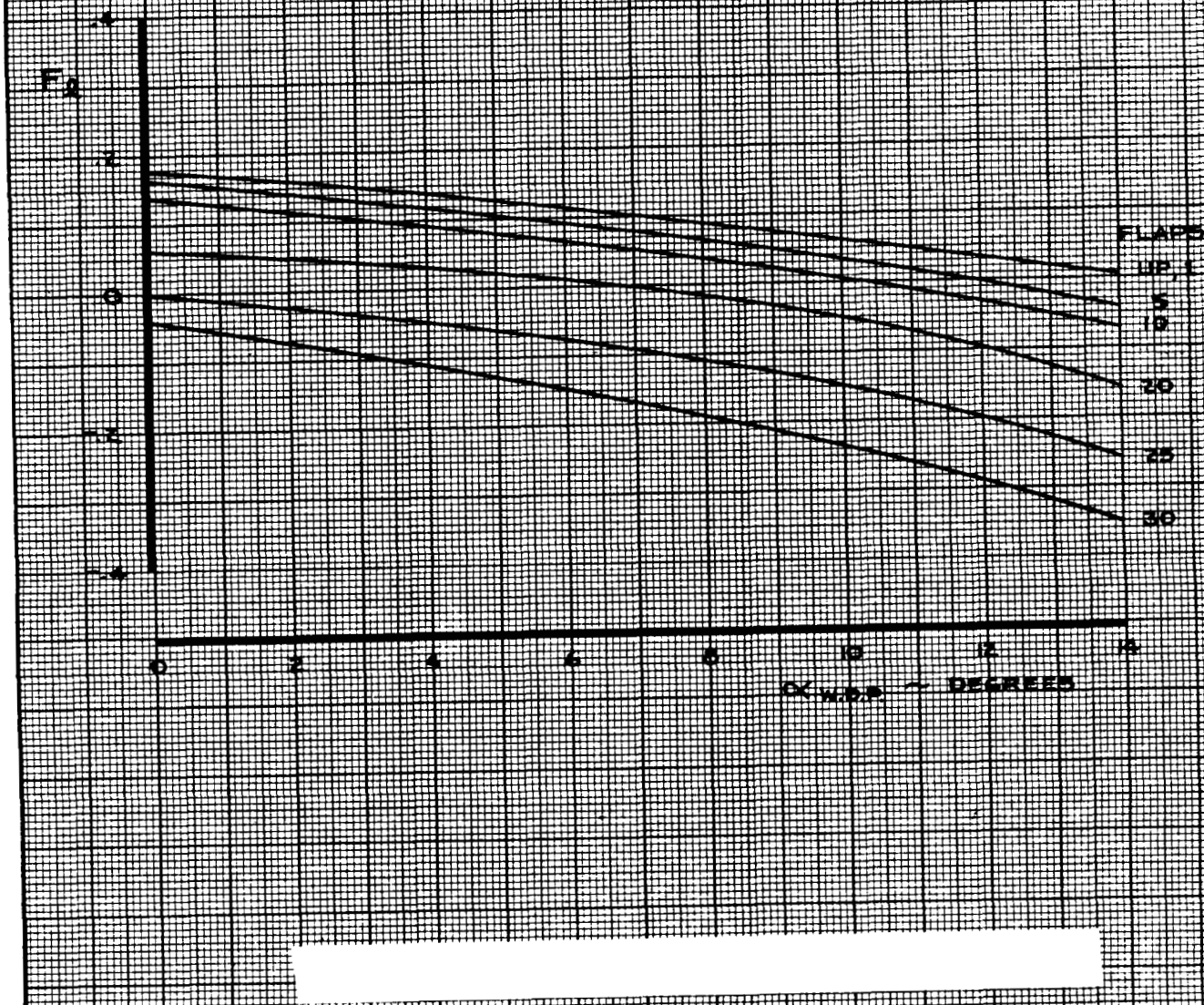

CALC	CURNUTT	12/18/67	REVISED	DATE	GROUND EFFECT LATERAL CONTROL FACTOR, F_ℓ	747
CHECK	FOSTER	1-24-68	LOW	6-4-69		D6-30643 Vol. II
APR			LOW	2-14-70		
APR					THE BOEING COMPANY	PAGE 5.0-29
INK	ODEGARD	12/18/67				REV. D

TD 461 C-R4

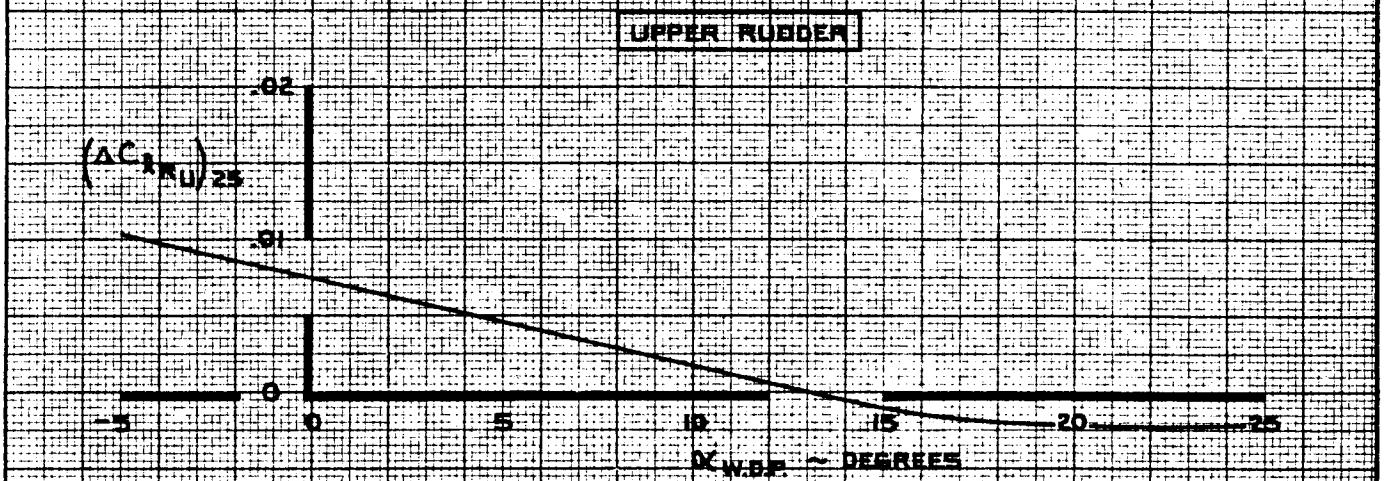

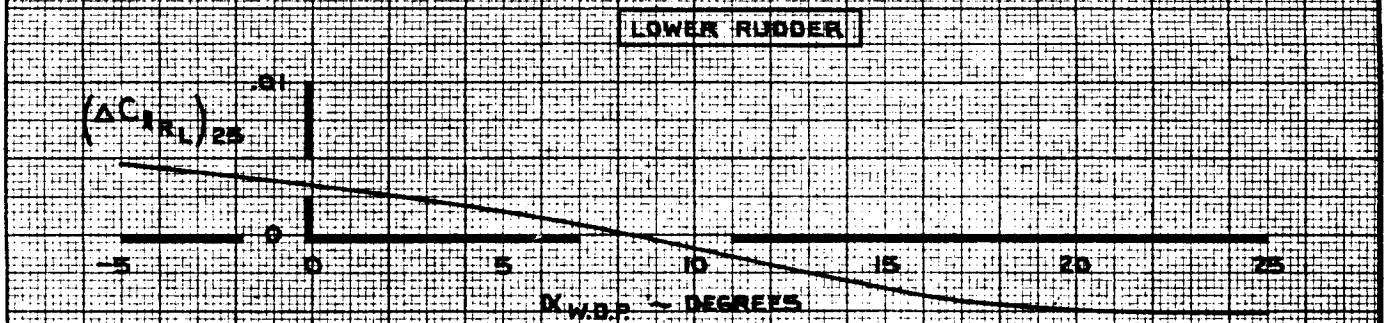

CALC	RICHARDSON	12-13-67	REVISED	DATE	ROLLING MOMENT COEFFICIENT Δ EFFECT OF RUDDERS	747
CHECK	FOSTER	1-24-68	LOW	6-4-69		
APR			BECK	1-27-70		D6-30643 Vol. II
APR						
INK	ODEGARD	2-3-70			THE BOEING COMPANY	PAGE 5.0-30

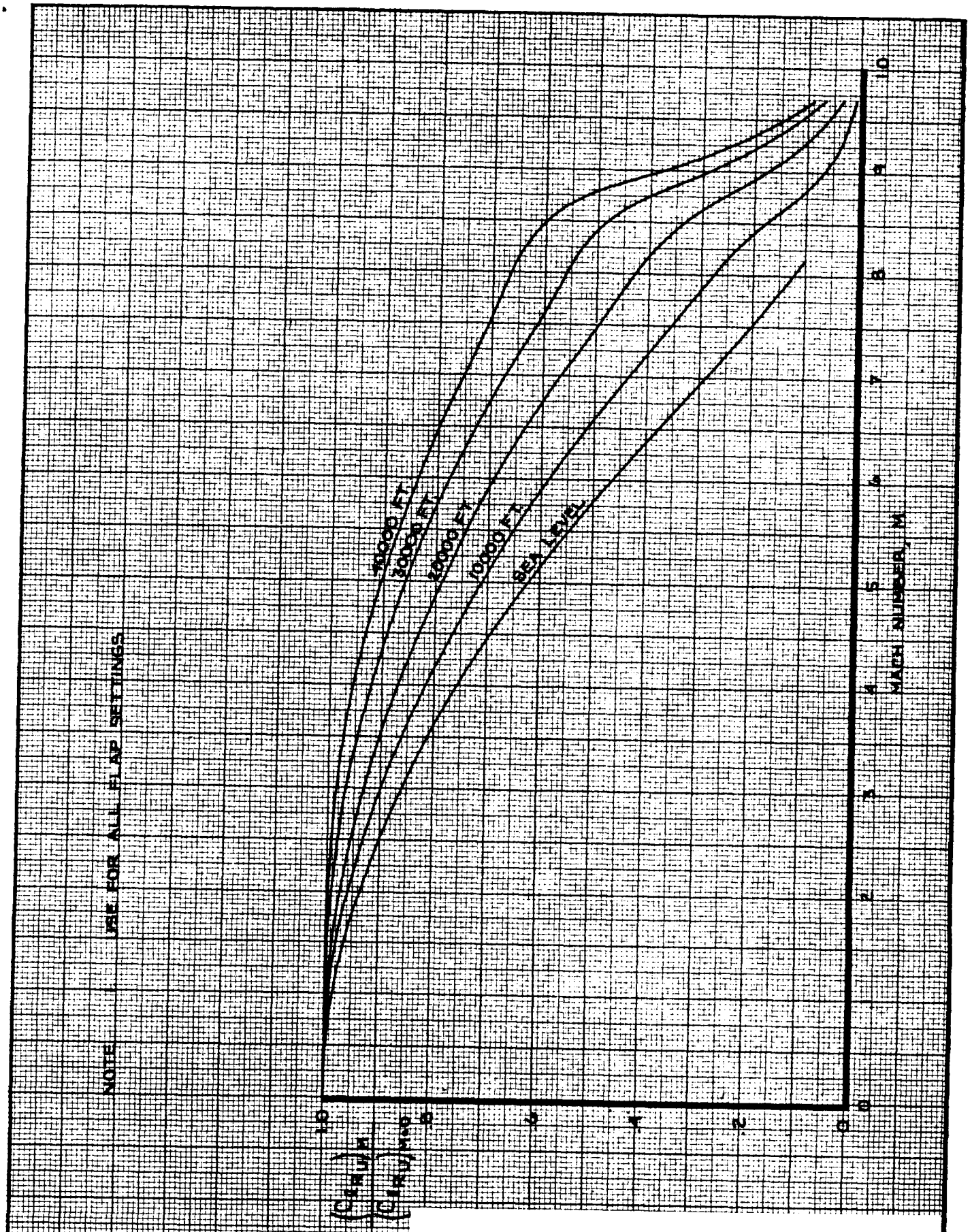

CALC	RICHARDSON	12-6-67	REVISED	DATE	ROLLING MOMENT COEFFICIENT △ AEROELASTIC EFFECT ON ROLLING MOMENT COEFFICIENT DUE TO UPPER RUDDER
CHECK	FOSTER	1-24-68	LOW	6-4-69	
APR			BECK	2-4-70	
APR					
INK	KINSMAN	2-4-70			

747

D6-30643 Vol. II

THE BOEING COMPANY

PAGE 5.0-31

AD 461 C-R4

K-E ALBANENE 1961 TRACING PAPER REV. D

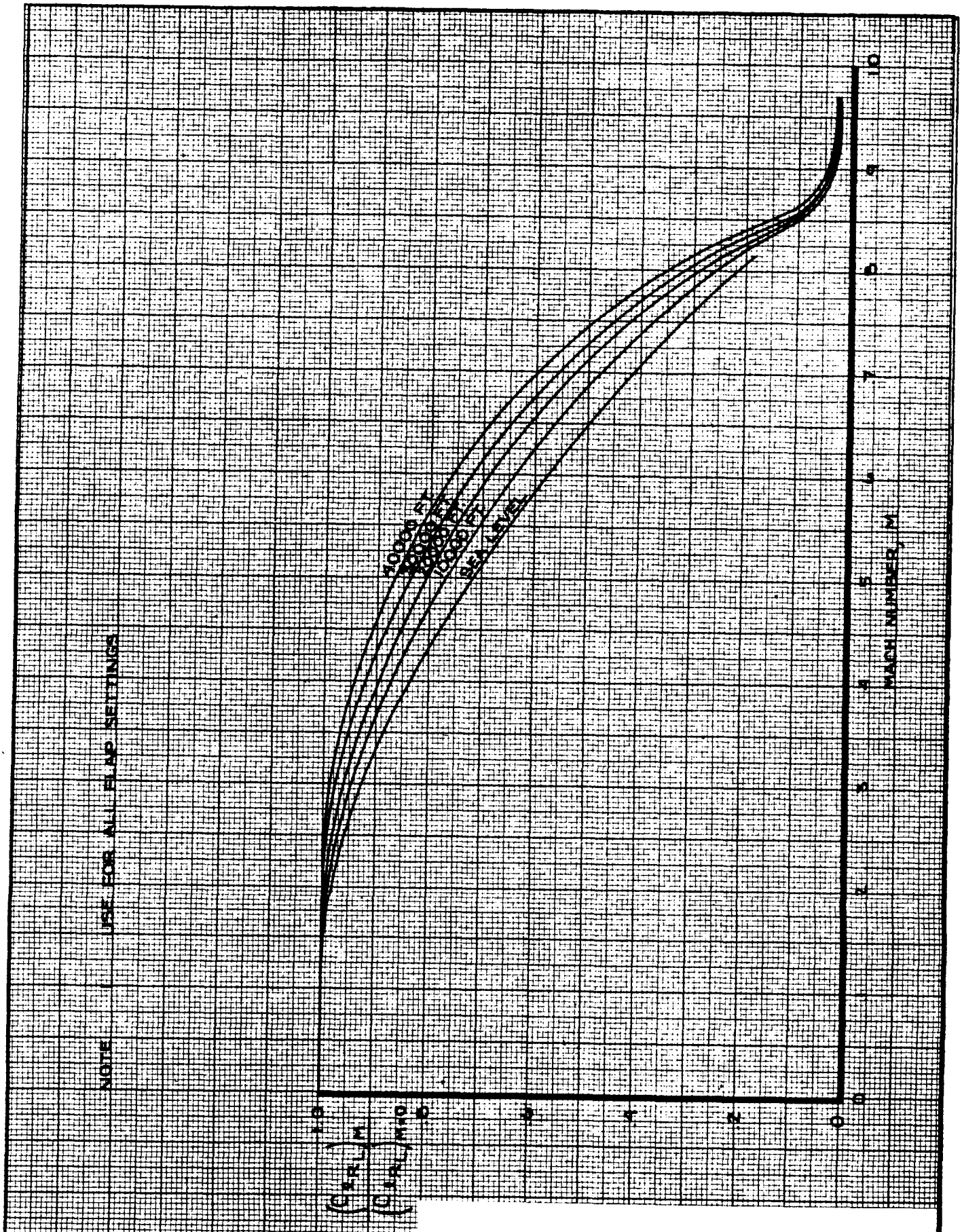

CALC	RICHARDSON	12·6·67	REVISED	DATE	ROLLING MOMENT COEFFICIENT △ AEROELASTIC EFFECT ON ROLLING MOMENT COEFFICIENT DUE TO LOWER RUDDER
CHECK	FOSTER	1·24·68	LOW	6·4·69	
APR			BECK	2·4·70	
APR					
INK	KINSMAN	2·4·70			THE BOEING COMPANY

747
D6-30643 Vol. II
PAGE 5.0-32

AD 461 C-R4

K·E ALBANENE 1951 TRACING PAPER REV. D

NOTE 1. RIGHT INBOARD FLAP AT MONITOR LIMITED EXTENSION POSITION CORRESPONDING TO LEFT INBOARD FLAP FAILURE POSITION

2. CHANGE SIGN FOR RIGHT INBOARD FLAP FAILURE

THESE DATA NOT INCLUDED IN NASA SIMULATION

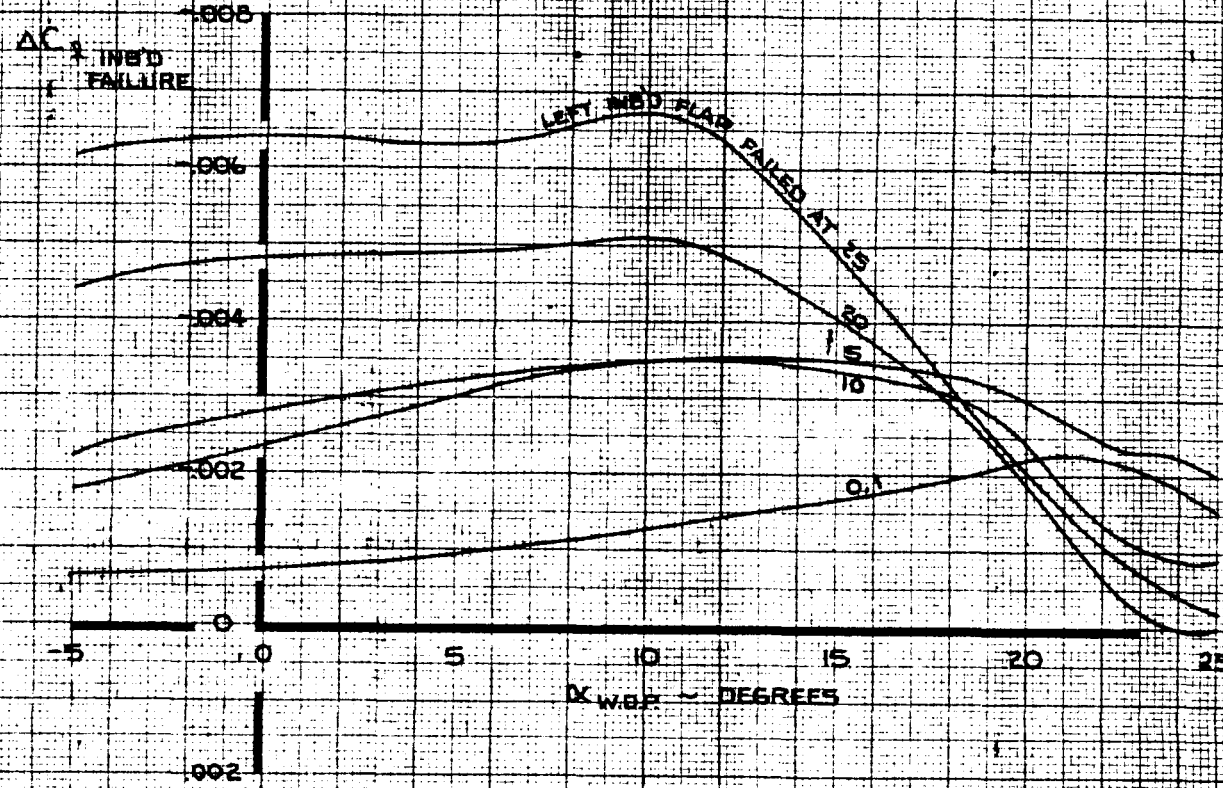

CALC	LOW	5-26-69	REVISED	DATE	ROLLING MOMENT COEFFICIENT EFFECT OF ASYMMETRIC INBOARD FLAP FAILURE FOR FLAP EXTENSION	747
CHECK			LOW	2-17-70		
APR			LOW	6-25-70		D6-30643 Vol. II
APR						
INK	ODEGARD	5-26-69			THE BOEING COMPANY	PAGE 5.0-33

TD 461 C-84

K•E ALBANENE 1961 TRACING PAPER REV. E

NOTE 1. RIGHT INBOARD FLAP AT MONITOR LIMITED RETRACTION POSITION CORRESPONDING TO LEFT INBOARD FLAP FAILURE POSITION

2. CHANGE SIGN FOR RIGHT INBOARD FLAP FAILURE

THESE DATA NOT INCLUDED IN NASA SIMULATION

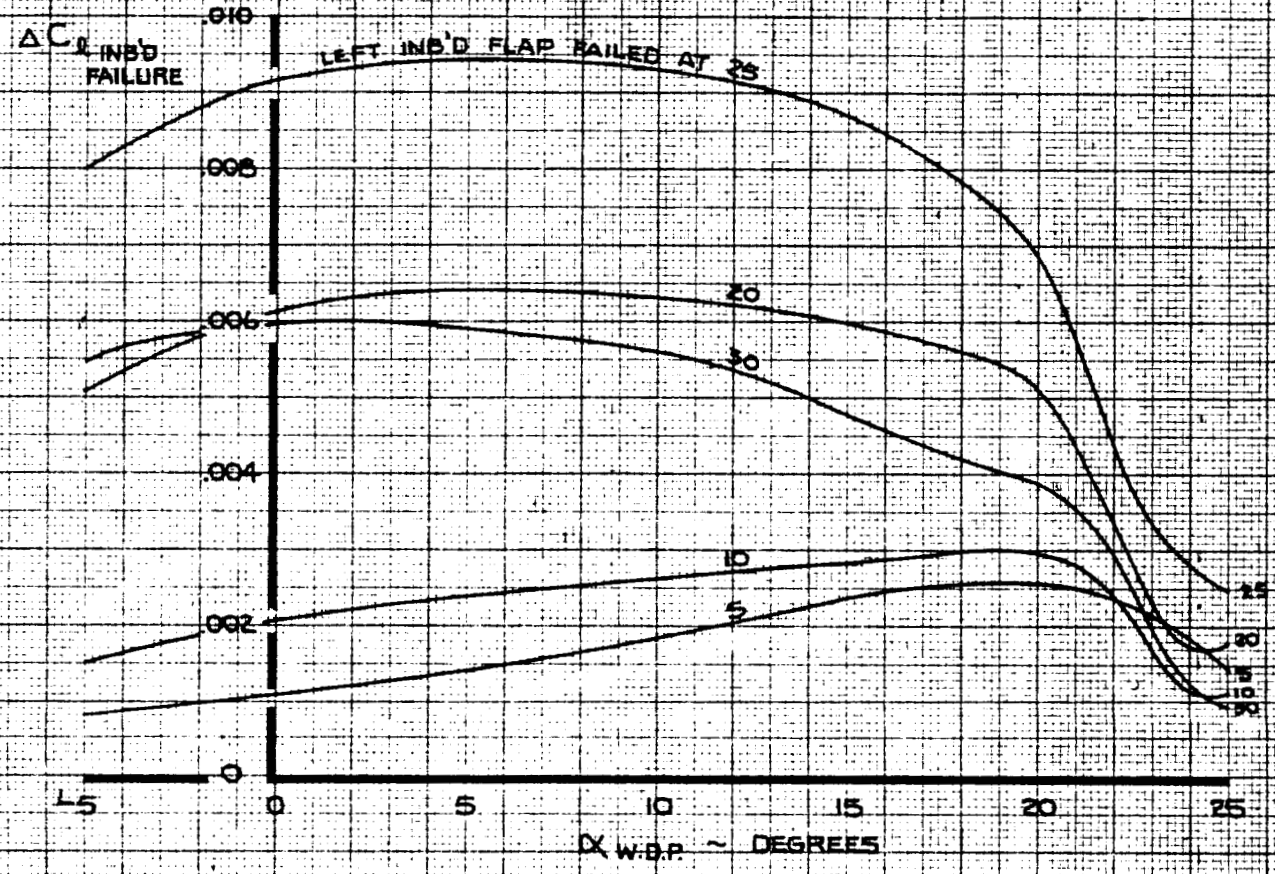

CALC	LOW	5-26-69	REVISED	DATE	ROLLING MOMENT COEFFICIENT EFFECT OF ASYMMETRIC INBOARD FLAP FAILURE FOR FLAP RETRACTION	747
CHECK	•		LOW	2-17-70		
APR			LOW	6-25-70		D6-30643 Vol. II
APR						
INK	ODEGARD	5-26-69			THE BOEING COMPANY	PAGE 5.0-34

NOTE 1 RIGHT OUTBOARD FLAP AT MONITOR-LIMITED EXTENSION POSITION CORRESPONDING TO LEFT OUTBOARD FLAP FAILURE POSITION

2 CHANGE SIGN FOR RIGHT OUTBOARD FLAP FAILURE

THESE DATA NOT INCLUDED IN NASA SIMULATION

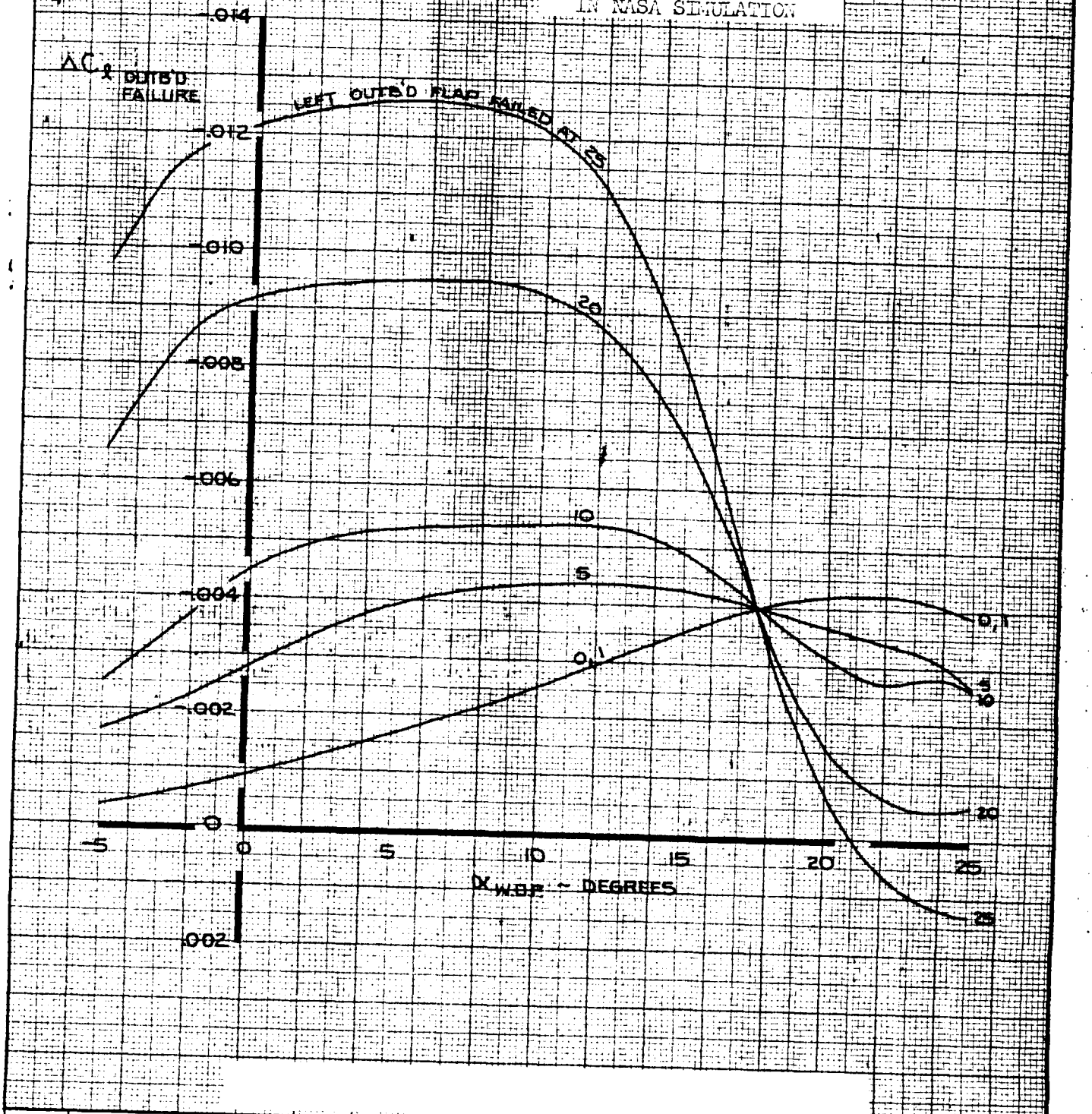

CALC	LOW	5-26-69	REVISED	DATE	ROLLING MOMENT COEFFICIENT EFFECT OF ASYMMETRIC OUTBOARD FLAP FAILURE FOR FLAP EXTENSION	747
CHECK			LOW	2-17-70		
APR			LOW	6-25-70		D6-30643 Vol. II
APR						
INK	ODEGARD	5-26-69			THE BOEING COMPANY	PAGE 6.0-35

TD 461 C-R4

NOTE 1. RIGHT OUTBOARD FLAP AT MONITOR LIMITED RETRACTION POSITION CORRESPONDING TO LEFT OUTBOARD FLAP FAILURE POSITION

2. CHANGE SIGN FOR RIGHT OUTBOARD FLAP FAILURE

THESE DATA NOT INCLUDED IN NASA SIMULATION

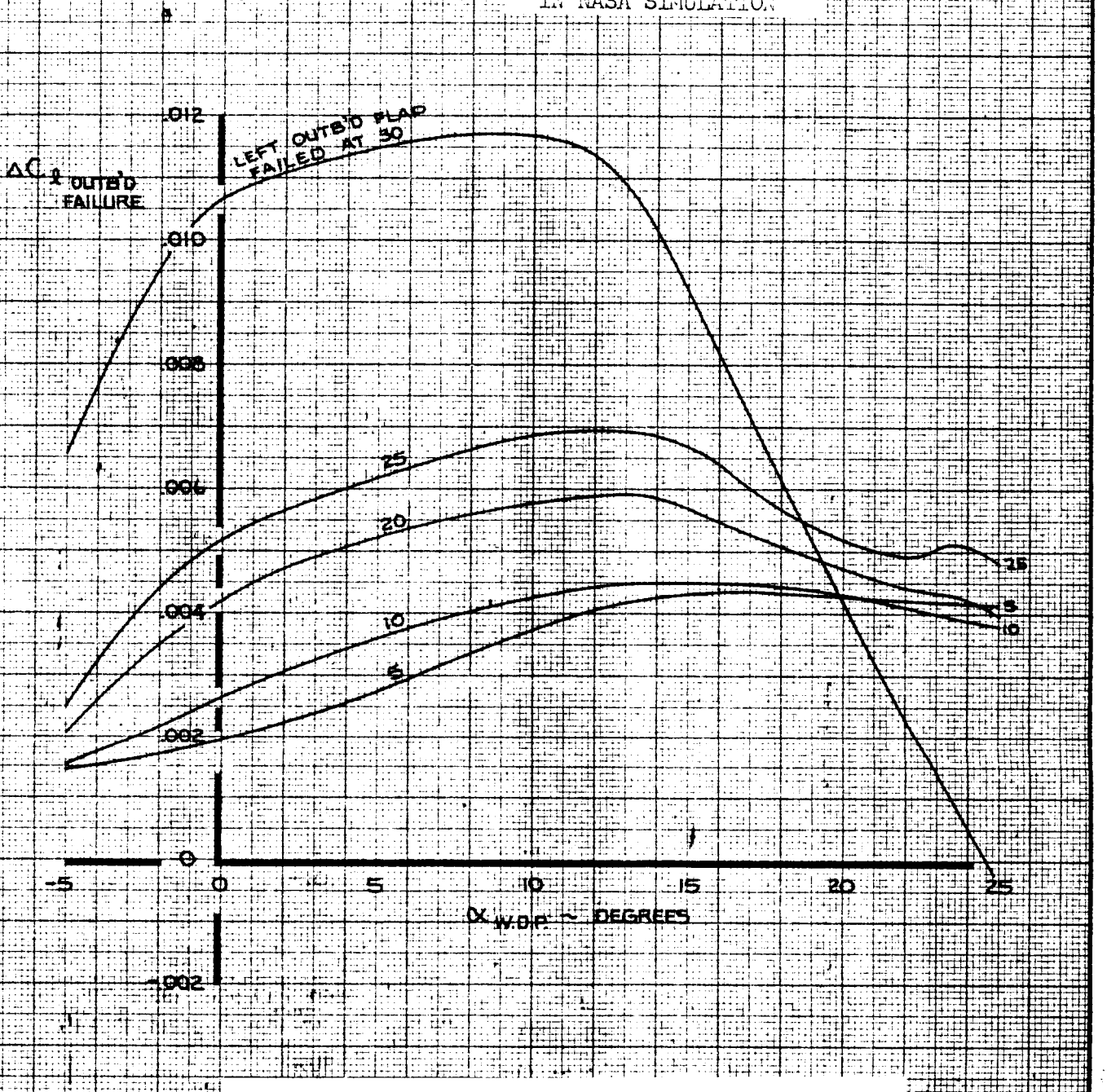

CALC	LOW	5-26-69	REVISED	DATE	ROLLING MOMENT COEFFICIENT EFFECT OF ASYMMETRIC OUTBOARD FLAP FAILURE FOR FLAP RETRACTION	747
CHECK			LOW	2-17-70		D6-30643 Vol. II
APR			LOW	6-25-70		
APR					THE BOEING COMPANY	PAGE 5.0-36
INK	ODEGARD	5-26-69				

TD 461 C-R4

K-E ALBANENE 1961 REV. E

NOTE: CHANGE SIGN FOR FAILURE OF L.E. FLAP SEGMENTS 22, 23, 24, 25, 26

THESE DATA NOT INCLUDED IN NASA SIMULATION

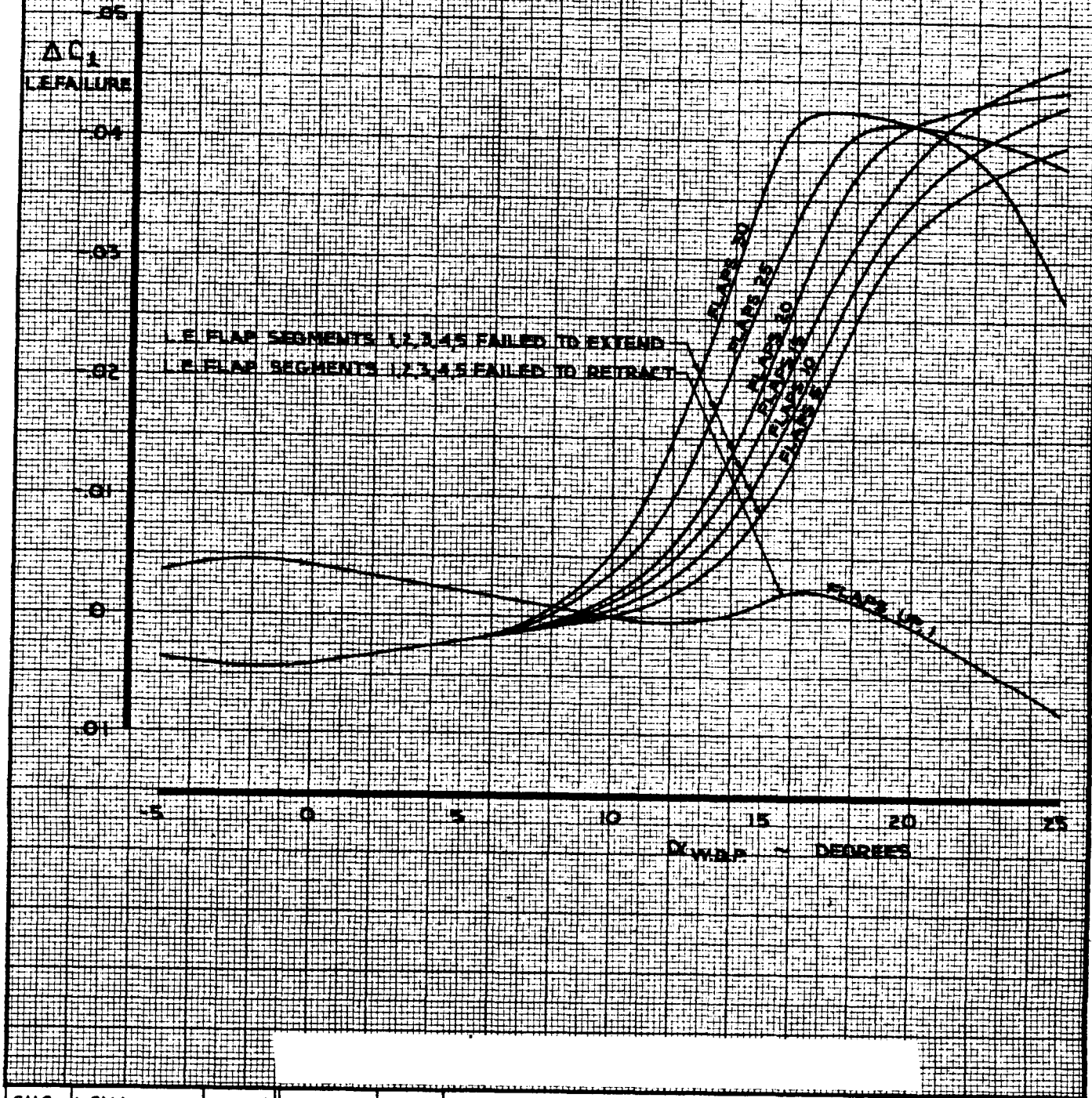

CALC	LOW	8-22-69	REVISED	DATE	ROLLING MOMENT COEFFICIENT EFFECT OF ASYMMETRIC L.E. FLAP SEGMENTS 1,2,3,4,5 OR 22,23,24,25,26	747
CHECK						D6-30643 Vol. II
APR						
APR						
INK	KINSMAN	8-22-69			THE BOEING COMPANY	PAGE 5.0-37

NOTE: CHANGE SIGN FOR FAILURE OF L.E. FLAP SEGMENTS 19, 20, 21

THESE DATA NOT INCLUDED IN NASA SIMULATION

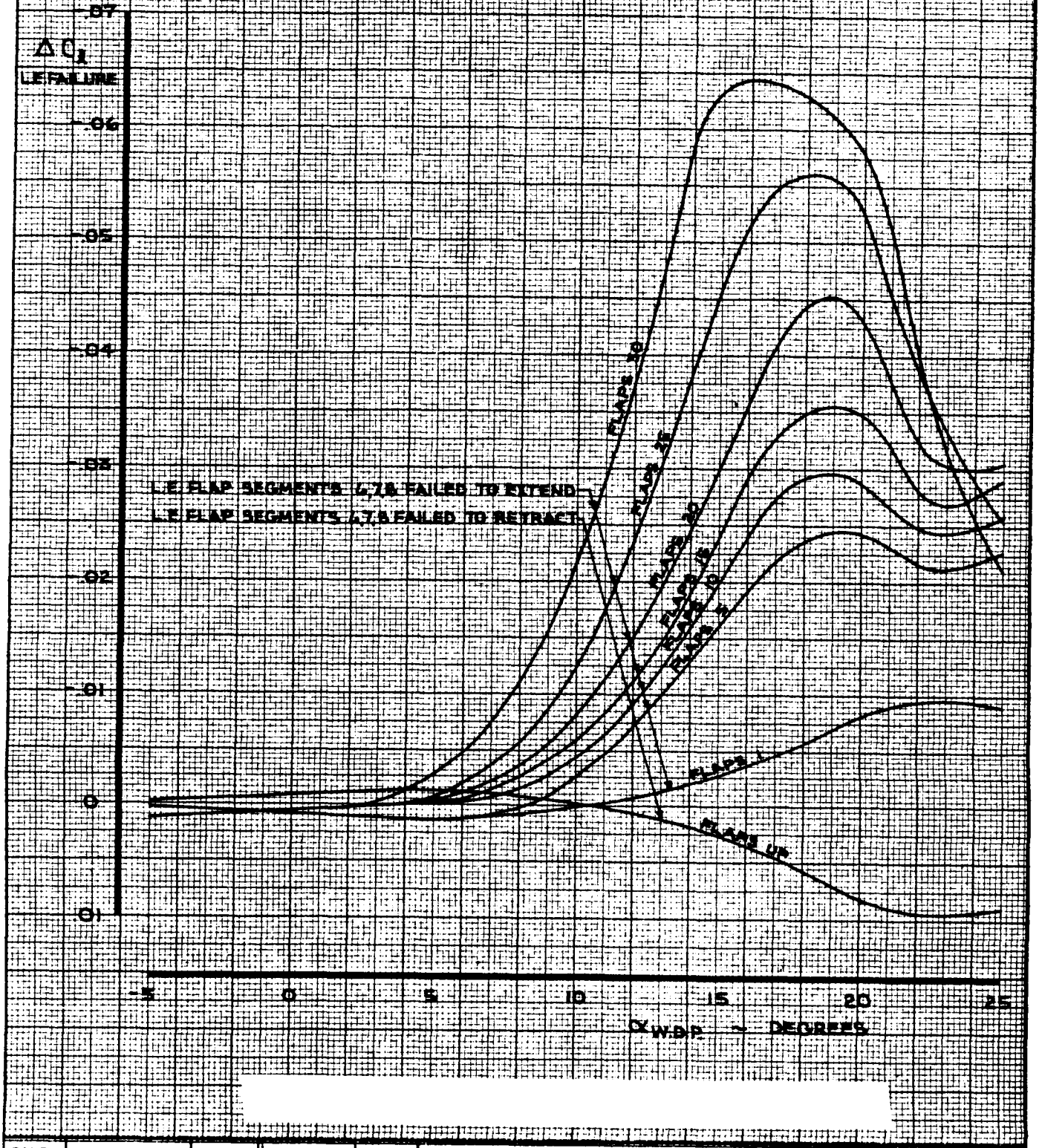

CALC	LOW	8-22-69	REVISED	DATE	ROLLING MOMENT COEFFICIENT EFFECT OF ASYMMETRIC L.E. FLAP SEGMENTS 6,7,8 OR 19, 20, 21
CHECK					
APR					
APR					
INK	KINSMAN	8-22-69			THE BOEING COMPANY

747

D6-30643 Vol. II

PAGE 5.0-38

AD 461 C-R4

K-E ALBANENE 1961 TRACING PAPER REV. D

6.0 YAWING MOMENT COEFFICIENT

The dimensionless aerodynamic yawing moment coefficient is given in terms of its significant components by the equation below.

At a given $\alpha_{W.B.P.}$,

$$C_{n_{C.G.}} = \frac{dC_n}{d\beta}\cdot\beta + \frac{dC_n}{d\hat{\dot{\beta}}}\cdot\frac{\dot{\beta}b}{2V} + \frac{dC_n}{d\hat{p}}\cdot\frac{p_s b}{2V} + \frac{dC_n}{d\hat{r}}\cdot\frac{r_s b}{2V}$$

$$+ \Delta C_{n_{SPOILERS}} + \Delta C_{n_{\substack{INBOARD\\AILERONS}}} + \Delta C_{n_{\substack{OUTBOARD\\AILERONS}}}$$

$$+ \Delta C_{n_{RUDDERS}} + \left[\Delta C_{n_{FLAP\ FAILURE}} + \Delta C_{n_{L.E.\ FAILURE}}\right]^*$$

where,

$\frac{dC_n}{d\beta}\cdot\beta$ = Yawing moment coefficient due to angle of sideslip, β. The complete expression for $\frac{dC_n}{d\beta}$ is given as follows:

$$\frac{dC_n}{d\beta} = \left(\frac{dC_n}{d\beta}\right)\frac{(C_{n_\beta})_M}{(C_{n_\beta})_{M=0}}\cdot Fn_{\beta_{GE}} + \frac{dC_Y}{d\beta}(C.G. - .25)\frac{\varepsilon}{b}$$

where $\left(\frac{dC_n}{d\beta}\right)$ is the basic rate of change of yawing moment coefficient due to angle of sideslip. For low speed, $\left(\frac{dC_n}{d\beta}\right)$ is plotted on page 6.0-6. The aeroelastic effect, $\frac{(C_{n_\beta})_M}{(C_{n_\beta})_{M=0}}$, is plotted on page 6.0-6. The ground effect factor, $Fn_{\beta_{GE}}$, is obtained as follows:

$[\ ]^*$ NOT IN NASA SIMULATION

6.0

(Cont'd)

$$F_{n_{\beta GE}} = \left[1 + F_{n_\beta} \cdot K^B_{GE}\right]$$

where the ground effect sideslip factor, F_{n_β}, is plotted on page 6.0-7. The ground effect height factor, K^B_{GE}, is plotted on page 2.0-31. $\frac{dC_Y}{d\beta}$ is obtained from page 7.0-1.

$\frac{dC_n}{d\hat{\beta}} \cdot \frac{\dot{\beta} b}{2V}$ = Yawing moment coefficient due to rate of change of sideslip angle. The complete expression for $\frac{dC_n}{d\hat{\beta}}$ is given as follows:

$$\frac{dC_n}{d\hat{\beta}} = \left(\frac{dC_n}{d\hat{\beta}}\right) \cdot \frac{(C_{n_{\hat{\beta}}})_M}{(C_{n_{\hat{\beta}}})_{M=0}}$$

where $\left(\frac{dC_n}{d\hat{\beta}}\right)$ is plotted on page 6.0-8. The aeroelastic effect, $\frac{(C_{n_{\hat{\beta}}})_M}{(C_{n_{\hat{\beta}}})_{M=0}}$, is plotted on page 6.0-8.

$\frac{dC_n}{d\hat{p}} \cdot \frac{p_s b}{2V}$ = Yawing moment coefficient due to roll rate about the stability axis, x_s. $\frac{dC_n}{d\hat{p}}$ is plotted on page 6.0-9.

$\frac{dC_n}{d\hat{r}} \cdot \frac{r_s b}{2V}$ = Yawing moment coefficient due to yaw rate about the stability axis, z_s. The complete expression for $\frac{dC_n}{d\hat{r}}$ is given as follows:

$$\frac{dC_n}{d\hat{r}} = K_{\hat{r}} \cdot \left(\frac{dC_{n_{.25}}}{d\hat{r}}\right) \cdot \frac{(C_{n_{\hat{r}}})_M}{(C_{n_{\hat{r}}})_{M=0}}$$

where $\left(\frac{dC_{n_{.25}}}{d\hat{r}}\right)$ and the center of gravity factor, $K_{\hat{r}}$,

AD 1546 D

6.0 (Cont'd)

are plotted on page 6.0-10. The aeroelastic effect, $\frac{(C_{n\hat{r}})_M}{(C_{n\hat{r}})_{M=0}}$, is plotted on page 6.0-10.

$\Delta C_{n_{SPOILERS}}$ = Yawing moment coefficient due to spoiler deflection.

$$\Delta C_{n_{SPOILERS}} = \sum_{\substack{\text{OPERATING} \\ \text{SPOILER} \\ \text{PANELS}}} (K\delta_{SP})_n \cdot (\Delta C_{n_{SP}})_{45} \cdot \frac{(C_{n_{SP}})_M}{(C_{n_{SP}})_{M=0}} \cdot F_{n_{GE}}$$

where $(\Delta C_{n_{SP}})_{45}$ is the yawing moment coefficient due to deflecting the operating spoiler panels to 45°. $(\Delta C_{n_{SP}})_{45}$ is plotted on page 6.0-12. The spoiler effectiveness factor, $(K\delta_{SP})_n$, is plotted on page 6.0-11. The Mach number effect, $\frac{(C_{n_{SP}})_M}{(C_{n_{SP}})_{M=0}}$, is plotted on page 6.0-13. The ground effect factor, $F_{n_{GE}}$, is obtained as follows:

$$F_{n_{GE}} = \left[1 + F_n \cdot K^{B}_{GE}\right]$$

where the ground effect lateral control factor, F_n, is plotted on page 6.0-14. The ground effect height factor, K^{B}_{GE}, is plotted on page 2.0-31.

$\Delta C_{n_{\substack{\text{INBOARD} \\ \text{AILERONS}}}}$ = Yawing moment coefficient due to inboard aileron deflection.

$$\Delta C_{n_{\substack{\text{INBOARD} \\ \text{AILERONS}}}} = \sum_{\substack{\text{LEFT AND RIGHT} \\ \text{INBOARD} \\ \text{AILERONS}}} K\delta_{A_I} \cdot (\Delta C_{n_{A_I}})_{20} \cdot \frac{(C_{n_{A_I}})_M}{(C_{n_{A_I}})_{M=0}} \cdot F_{n_{GE}}$$

where $(\Delta C_{n_{A_I}})_{20}$ is the yawing moment coefficient due to deflecting one inboard aileron up to 20° or

6.0 (Cont'd)

the opposite inboard aileron down to 20°. $(\Delta C_{n_{A_I}})_{20}$ is plotted on page 6.0-15. The inboard aileron effectiveness factor, $K_{\delta_{A_I}}$, is plotted on page 5.0-22. The Mach number effect, $\frac{(C_{n_{A_I}})_M}{(C_{n_{A_I}})_{M=0}}$, is plotted on page 6.0-15. The ground effect factor, $F_{n_{GE}}$, is obtained from page 6.0-14.

$\Delta C_{n_{\substack{\text{OUTBOARD}\\\text{AILERONS}}}}$ = Yawing moment coefficient due to outboard aileron deflection.

$$\Delta C_{n_{\substack{\text{OUTBOARD}\\\text{AILERONS}}}} = \sum_{\substack{\text{LEFT AND RIGHT}\\\text{OUTBOARD}\\\text{AILERONS}}} K_{\delta_{A_O}} \cdot \Delta C_{n_{A_O}} \cdot F_{n_{GE}}$$

where $\Delta C_{n_{A_O}}$ is the yawing moment coefficient due to deflecting one outboard aileron up to 25° or the opposite outboard aileron down to 15°. $\Delta C_{n_{A_O}}$ is plotted on page 6.0-16. The outboard aileron effectiveness factor, $K_{\delta_{A_O}}$, is plotted on page 5.0-26. The ground effect factor, $F_{n_{GE}}$, is obtained from page 6.0-14.

$\Delta C_{n_{\text{RUDDERS}}}$ = Yawing moment coefficient due to rudder deflection.

$$\Delta C_{n_{\text{RUDDERS}}} = K_{\delta_{R_U}} \cdot (\Delta C_{n_{R_U}})_{25} \cdot \frac{(C_{n_{R_U}})_M}{(C_{n_{R_U}})_{M=0}} + K_{\delta_{R_L}} \cdot (\Delta C_{n_{R_L}})_{25} \cdot \frac{(C_{n_{R_L}})_M}{(C_{n_{R_L}})_{M=0}}$$

$$+ \Delta C_{Y_{\text{RUDDERS}}} (\text{C.G.} - .25) \frac{\ell}{b}$$

where $(\Delta C_{n_{R_U}})_{25}$ and $(\Delta C_{n_{R_L}})_{25}$ are the yawing moment coefficients due to full deflection of the upper rudder and the lower rudder respectively.

AD 1346 D

6.0 (Cont'd)

$(\Delta C_{n_{R_U}})_{25}$ and $(\Delta C_{n_{R_L}})_{25}$ are plotted on page 6.0-19. The upper rudder effectiveness factor, $K_{\delta_{R_U}}$, and the lower rudder effectiveness factor, $K_{\delta_{R_L}}$, are plotted on page 6.0-17, and on page 6.0-18 respectively. The aeroelastic effects, $\frac{(C_{n_{R_U}})_M}{(C_{n_{R_U}})_{M=0}}$ and $\frac{(C_{n_{R_L}})_M}{(C_{n_{R_L}})_{M=0}}$, for the upper rudder and the lower rudder, are plotted on page 6.0-20 and page 6.0-21 respectively. It should be noted that for rudder deflection with one rudder inoperative, the appropriate rudder contribution should be multiplied by 1.12.

$\Delta C_{Y_{RUDDERS}}$ is obtained from page 7.0-3.

$\Delta C_{n_{FLAP\ FAILURE}}$ = Yawing moment coefficient due to an asymmetric (monitor limited) inboard or outboard flap failure.

$\Delta C_{n_{FLAP\ FAILURE}} = \Delta C_{n_{INB'D\ FAILURE}}$ OR $\Delta C_{n_{OUTB'D\ FAILURE}}$

where $\Delta C_{n_{INB'D\ FAILURE}}$ is the yawing moment coefficient due to an asymmetric (monitor limited) inboard flap failure. $\Delta C_{n_{INB'D\ FAILURE}}$ for flap extension or retraction is plotted on pages 6.0-22 and 6.0-23 respectively.

$\Delta C_{n_{OUTB'D\ FAILURE}}$ for flap extension or retraction is plotted on pages 6.0-24 and 6.0-25 respectively.

$\Delta C_{n_{L.E.\ FAILURE}}$ = Yawing moment coefficient due to asymmetric leading edge flap failure. $\Delta C_{n_{L.E.\ FAILURE}}$ is plotted on pages 6.0-26 and 6.0-27.

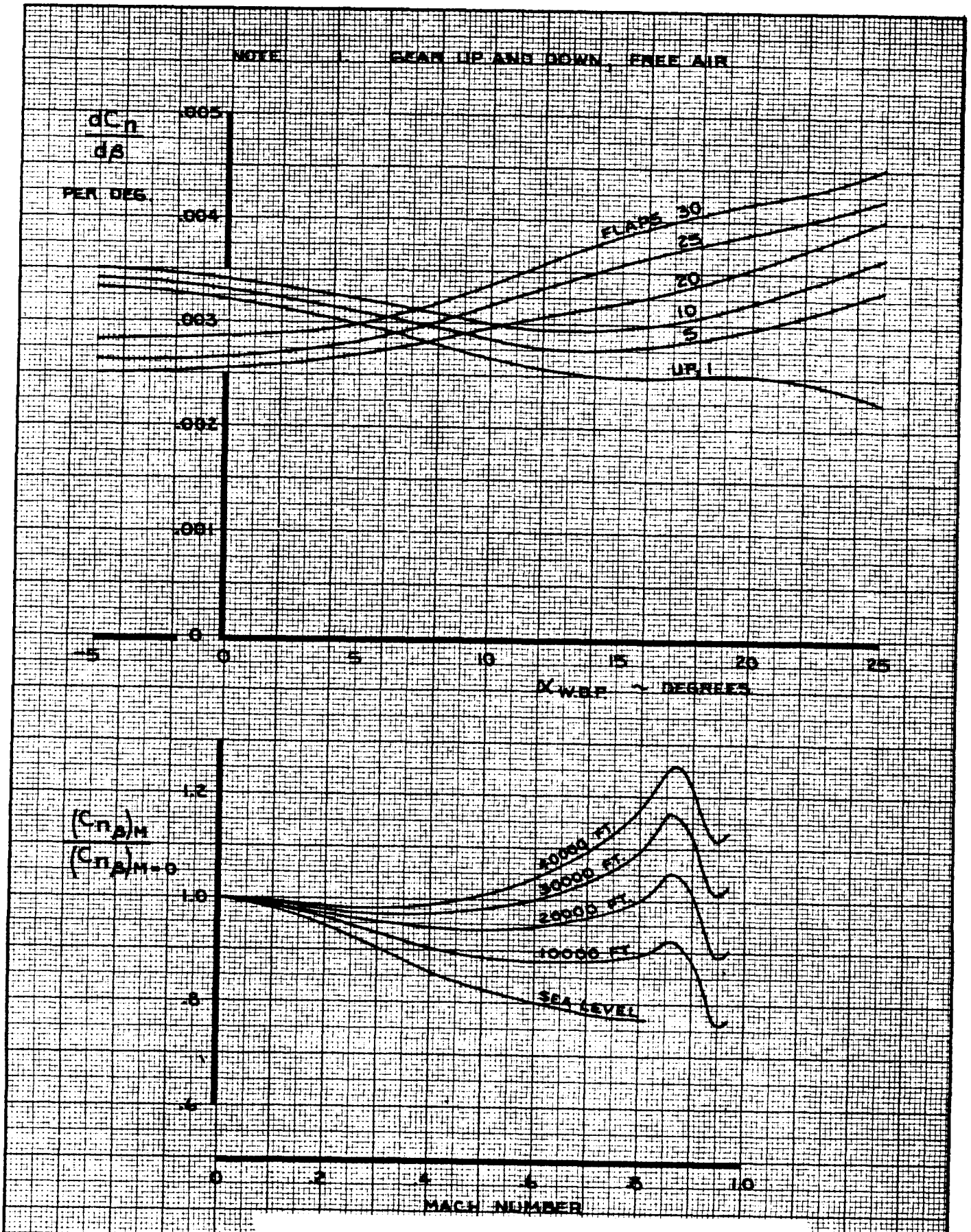

CALC	STIRLING	12-19-67	REVISED	DATE	YAWING MOMENT COEFFICIENT EFFECT OF SIDESLIP
CHECK	KUPCIS	12-19-67	BECK	2-3-70	
APR					
APR					
INK	ODEGARD	2-25-70			THE BOEING COMPANY

747

D6-30643 Vol. II

PAGE 6.0-6

AD 461 C-R4

K-E ALBANENE 1961 TRACING PAPER REV. D

NOTE: $F_{n_{\beta_{GE}}} = \left[1 + F_{n_\beta} K^{\beta}_{GE}\right]$

WHERE K^{β}_{GE} IS SHOWN ON PAGE 2.0-31

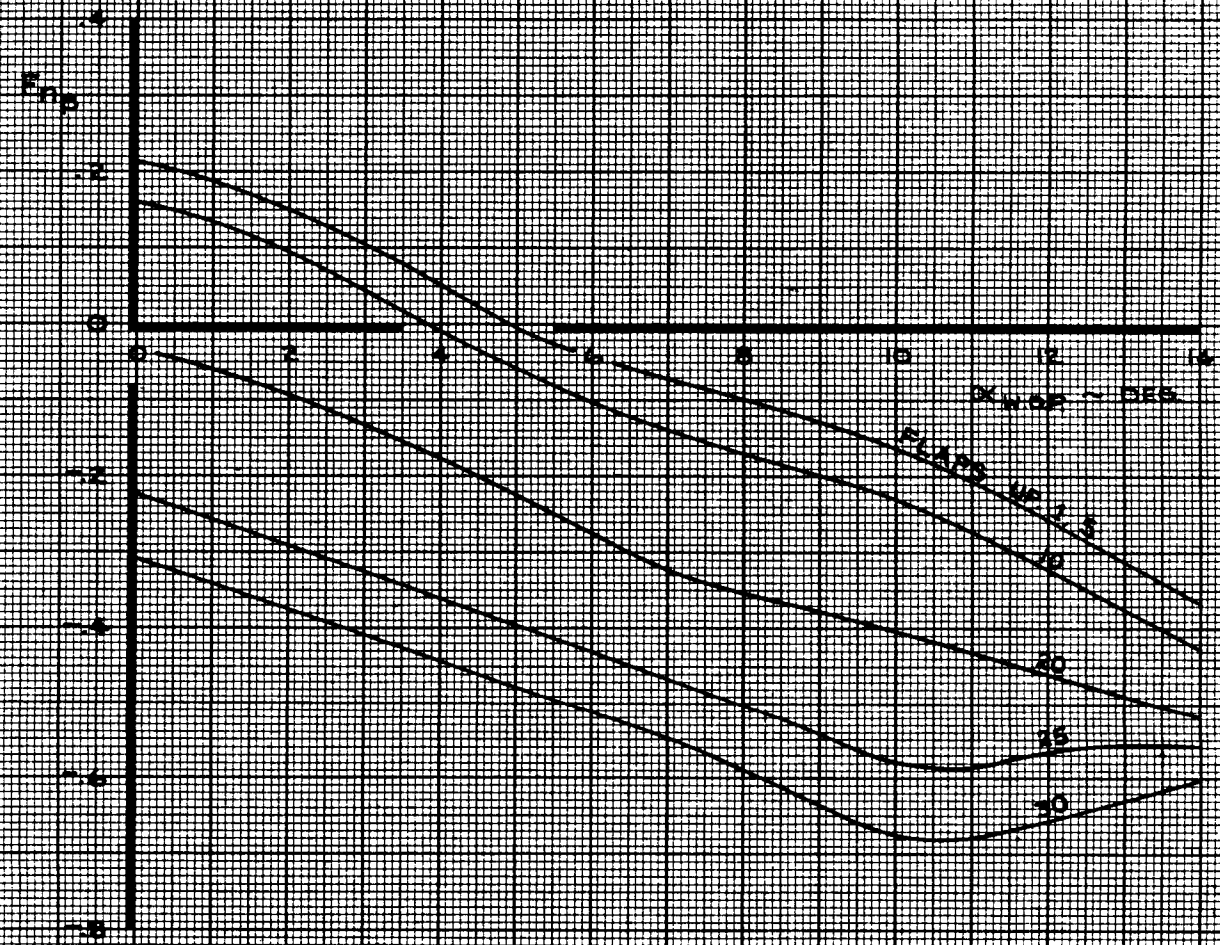

CALC	STIRLING	12/28/67	REVISED	DATE	YAWING MOMENT COEFFICIENT GROUND EFFECT SIDESLIP FACTOR, F_{n_β}
CHECK	KUPCIS	12/28/67	LOW	2-14-70	
APR					
APR					
INK	ODEGARD	12/28/67			

747

D6-30643 Vol. II

THE BOEING COMPANY

PAGE 6.0-7

REV. D

TD 461 C-R4

NOTE 1. $\hat{\beta} = \frac{\beta b}{2V}$; β ~ RAD/SEC, V ~ FT/SEC (TRUE AIRSPEED)

2. USE FOR ALL FLAP SETTINGS

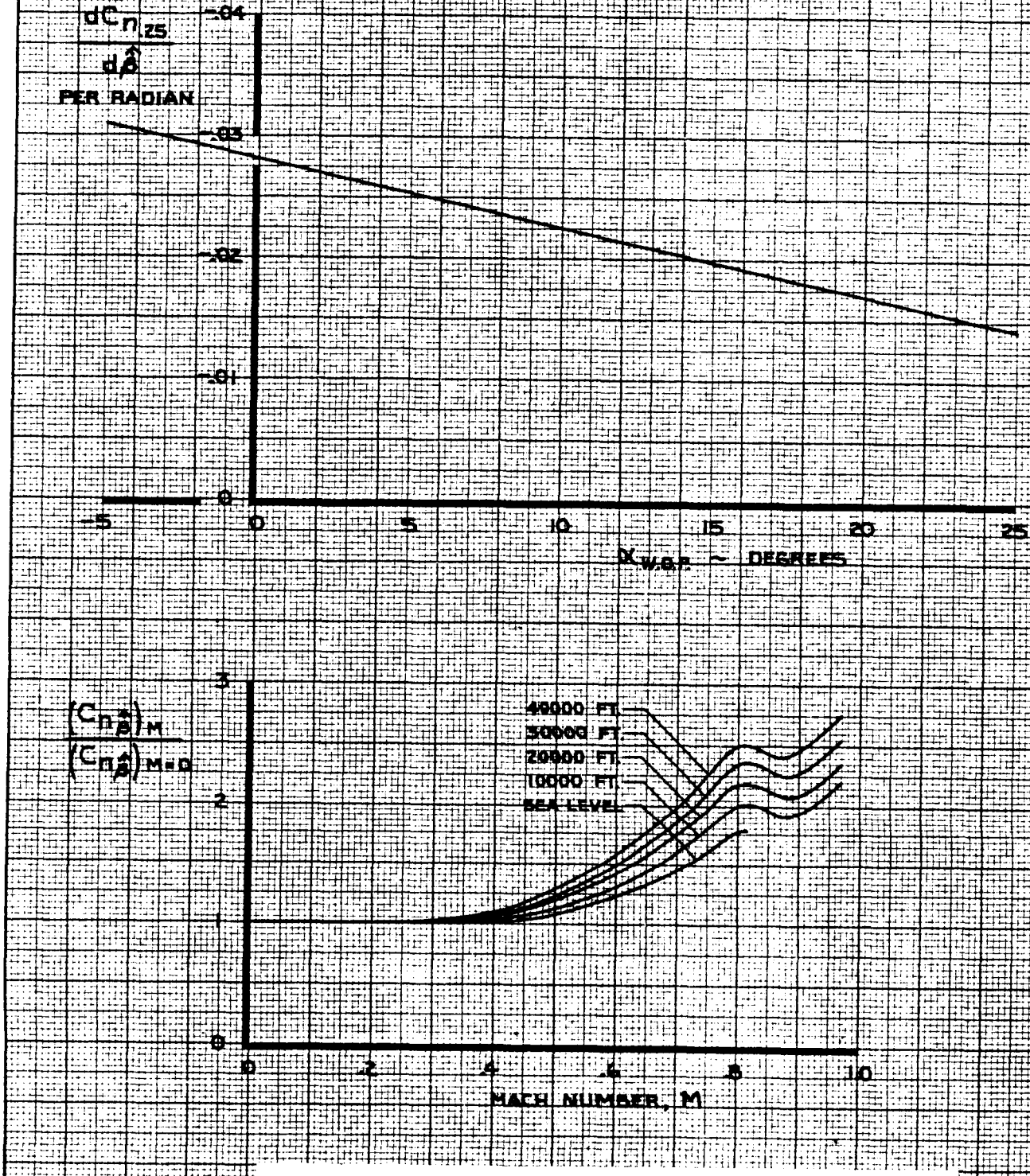

CALC	RICHARDSON	11-13-67	REVISED	DATE	YAWING MOMENT COEFFICIENT Δ EFFECT OF $\hat{\beta}$	747
CHECK	CURNUTT	11-14-67	LOW	6-14-69		
APR			LUDWIG	11-3-69		D6-30643, Vol. II
APR			CURNUTT	2-25-70		
INK	ODEGARD	3-3-70			THE BOEING COMPANY	PAGE 6.0-8

NOTE 1. $\hat{p} = \frac{p_s b}{2V}$; p_s ~ RAD/SEC, V ~ FT/SEC (TRUE AIRSPEED)

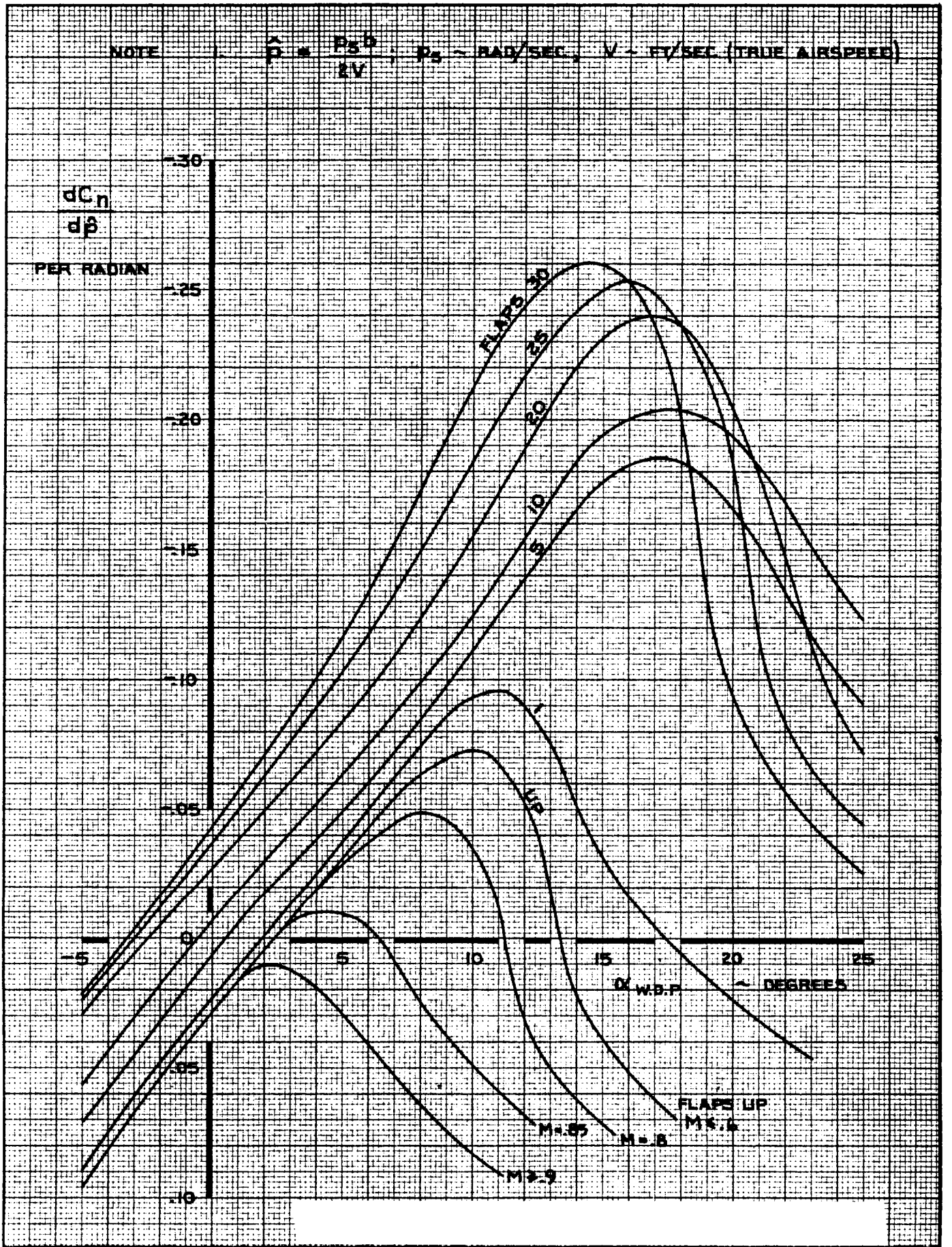

CALC	RICHARDSON	11-14-67	REVISED	DATE	YAWING MOMENT COEFFICIENT EFFECT OF ROLL RATE
CHECK	CURNUTT	11-16-67	LUDWIG	11-3-69	
APR			CURNUTT	2-25-70	
APR					
INK	ODEGARD	3-4-70			

747

D6-30643, Vol. II

THE BOEING COMPANY

PAGE 6.0-9

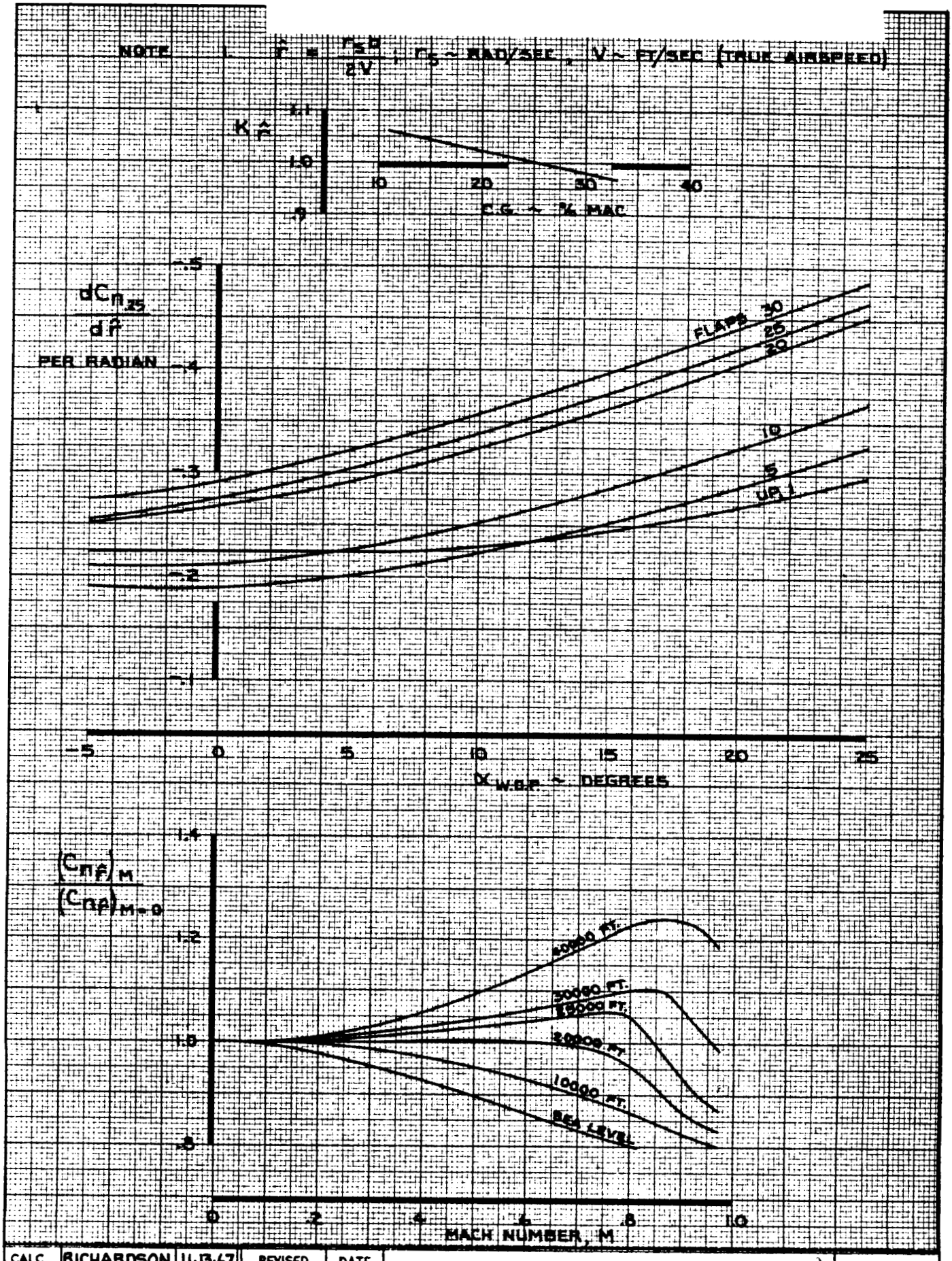

CALC	RICHARDSON	11-13-67	REVISED	DATE	YAWING MOMENT COEFFICIENT D EFFECT OF YAW RATE
CHECK	CURNUTT	11-16-67	LOW	6-14-69	
APR			CURNUTT	2-25-70	
APR					
INK	ODEGARD	3-2-70			THE BOEING COMPANY

747

D6-30643, Vol. II

PAGE 6.0-10

NOTE 1. USE FOR ALL SPOILER PANELS

2. PANELS 8 & 5 LIMITED TO 20 DEG. MAX. DEFLECTION

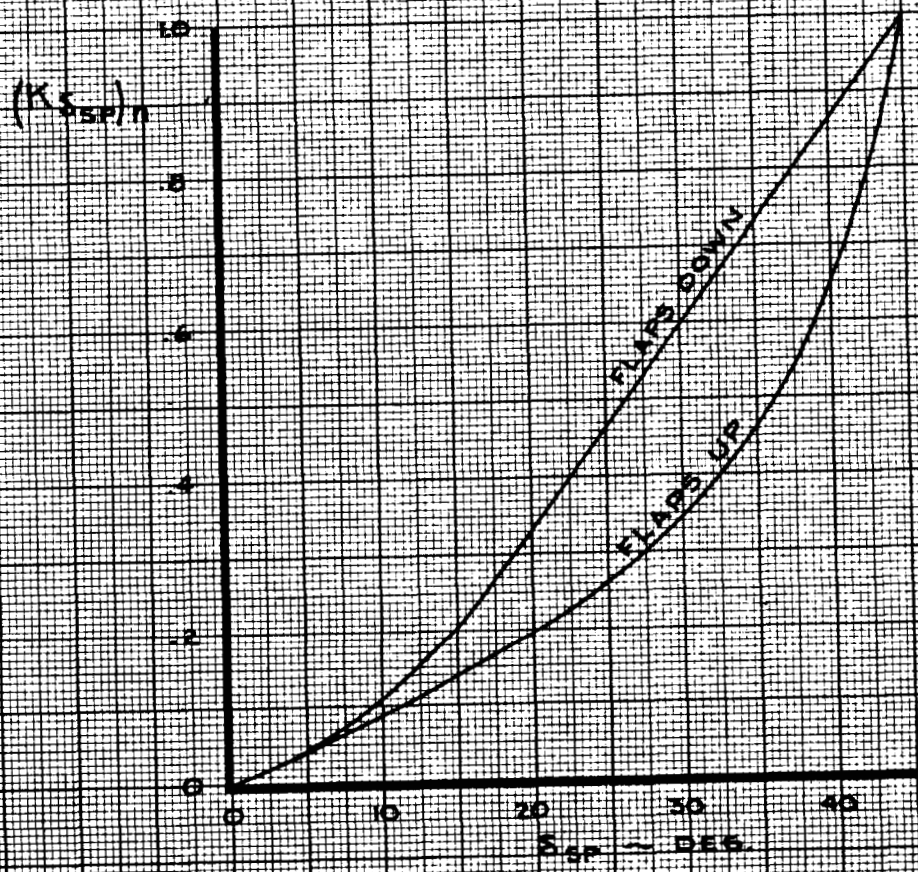

CALC	KUPCIS	12/6/67	REVISED	DATE	YAWING MOMENT COEFFICIENT EFFECTIVENESS FACTOR SPOILERS	747
CHECK	FOSTER	1-24-68	KUPCIS	6-2-69		D6-30643 Vol. II
APR						
APR					THE BOEING COMPANY	PAGE 6.0-11
INK	ODEGARD	12/6/67				REV. B

TD 461 C-R4

CDN1

SPOILER PANEL 8 OR 12

NOTE
1. DATA SHOWN FOR INDIVIDUAL PANELS 8 OR 12
2. FOR PANEL 1 OR 5, REVERSE SIGN
3. PANELS 8 & 5 LIMITED TO 20 DEG. MAX. DEFLECTION

SPOILER PANEL GROUP 9, 10, 11

NOTE
1. TOTAL EFFECT OF SPOILER GROUP 9, 10, 11 SHOWN
2. FOR SPOILER GROUP 2, 3, 4, REVERSE SIGN
3. WITH HYDRAULIC SYSTEM NO. 2 OFF, MULTIPLY BY 0.40
4. WITH HYDRAULIC SYSTEM NO. 3 OFF, MULTIPLY BY 0.60

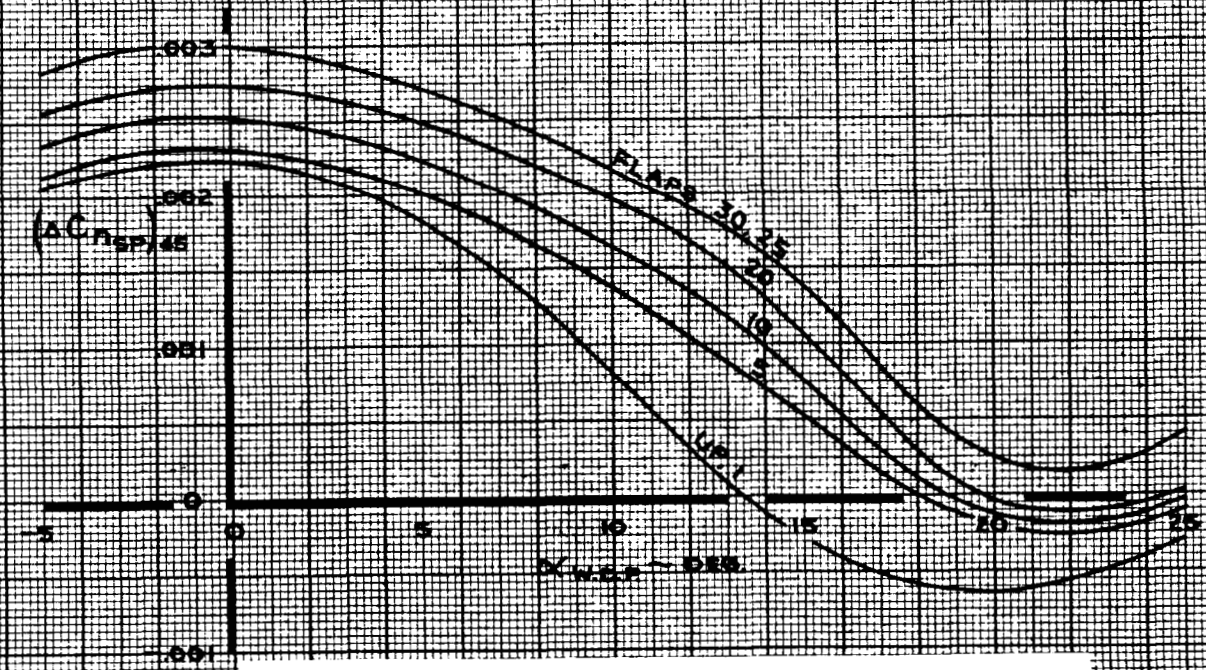

CALC	KUPCIS	12/5/67	REVISED	DATE	YAWING MOMENT COEFFICIENT EFFECT OF SPOILERS	747
CHECK	FOSTER	1-24-68	KUPCIS	6-2-69		D6-30643 Vol. II
APR			BECK	2-24-70		
APR					THE BOEING COMPANY	PAGE 6.0-12
INK	ODEGARD	12/5/67				

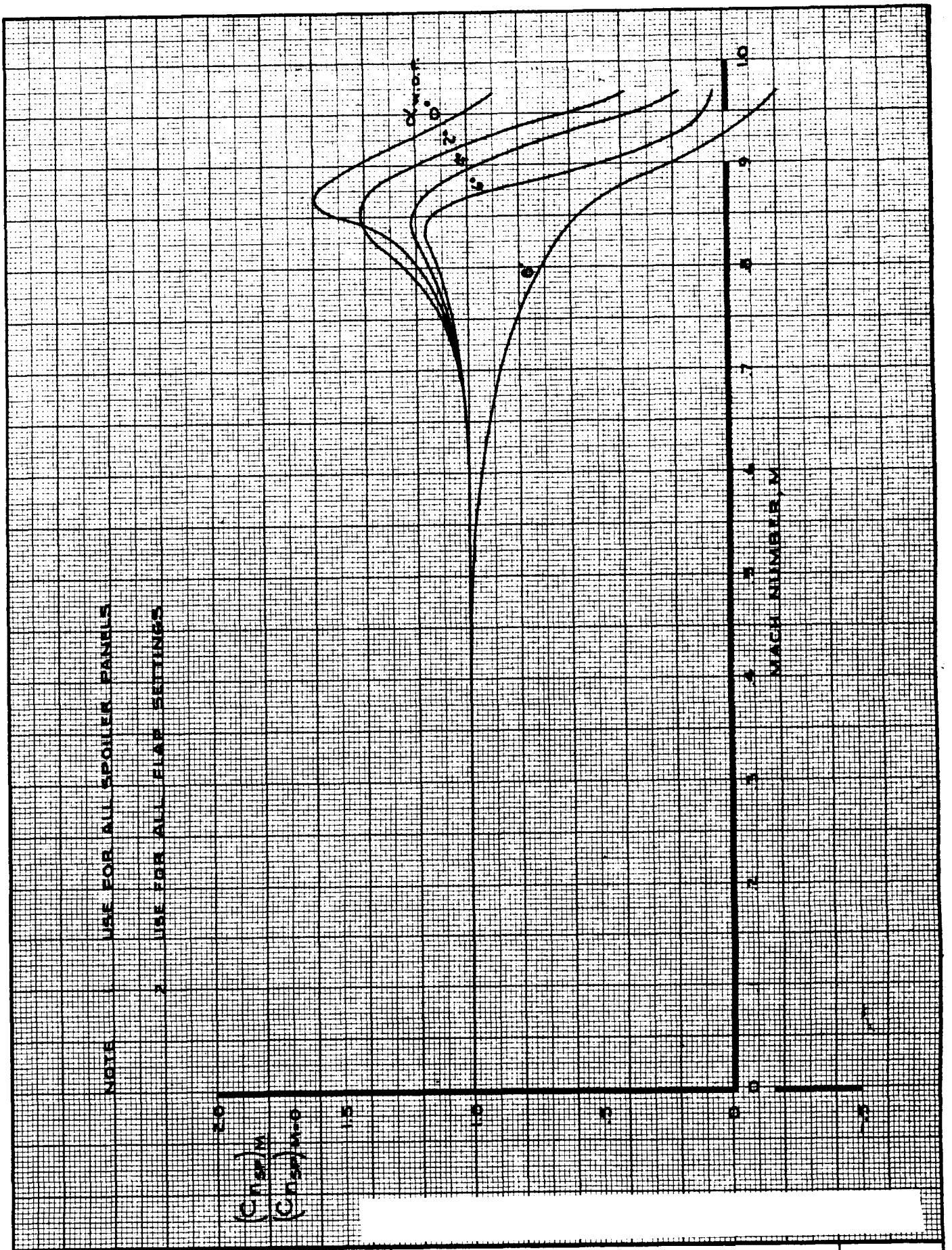

CALC	KUPCIS	12/1/67	REVISED	DATE	YAWING MOMENT COEFFICIENT EFFECT OF MACH NUMBER ON SPOILERS
CHECK	FOSTER	1-24-68			
APR					
APR					
INK	ODEGARD	12/1/67			

747

D6-30643, Vol. II

THE BOEING COMPANY

PAGE 6.0-13

TD 461 C-R4

$C_{N_{SPM}}$

NOTE 1. $F_{n_{GE}} = \left[1 + F_n - K^{B}_{GE}\right]$

WHERE K^{B}_{GE} IS SHOWN ON PAGE 2.0-51

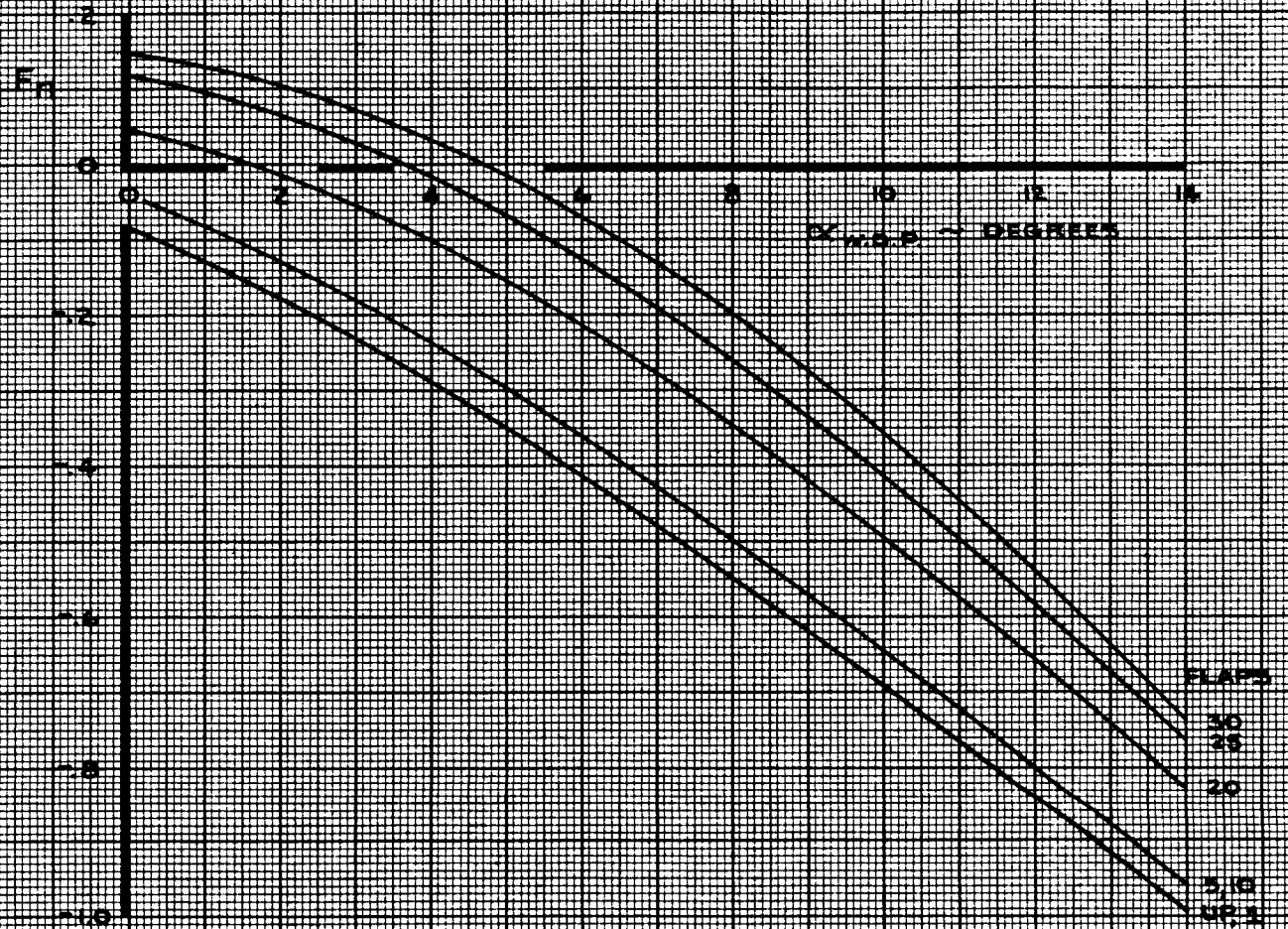

CALC	CURNUTT	12/18/67	REVISED	DATE	GROUND EFFECT LATERAL CONTROL FACTOR, Fn	747
CHECK	FOSTER	1-24-68	LOW	2-14-70		D6-30643, Vol. II
APR						
APR					THE BOEING COMPANY	PAGE 6.0-14
INK	ODEGARD	12/18/67				

NOTE 1. USE FOR ALL FLAP SETTINGS

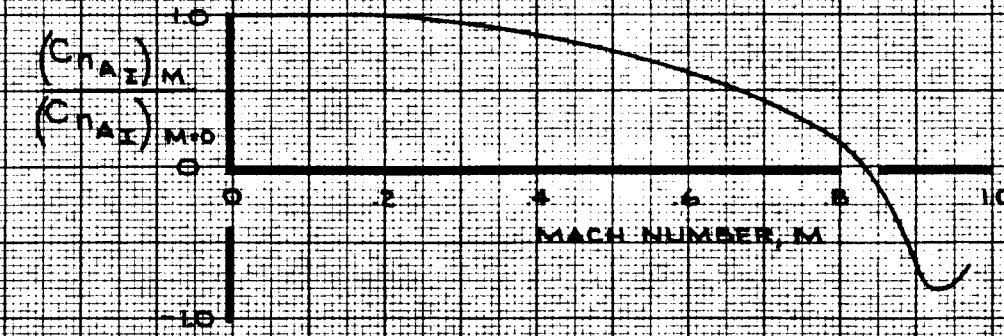

NOTE 1. $\left(\Delta C_{n_{A_I}}\right)_{20}$ IS SHOWN FOR RIGHT AILERON UP ONLY

2. FOR FULL LATERAL CONTROL (RIGHT AILERON UP AND LEFT AILERON DOWN), USE $2 \times \left(\Delta C_{n_{A_I}}\right)_{20}$

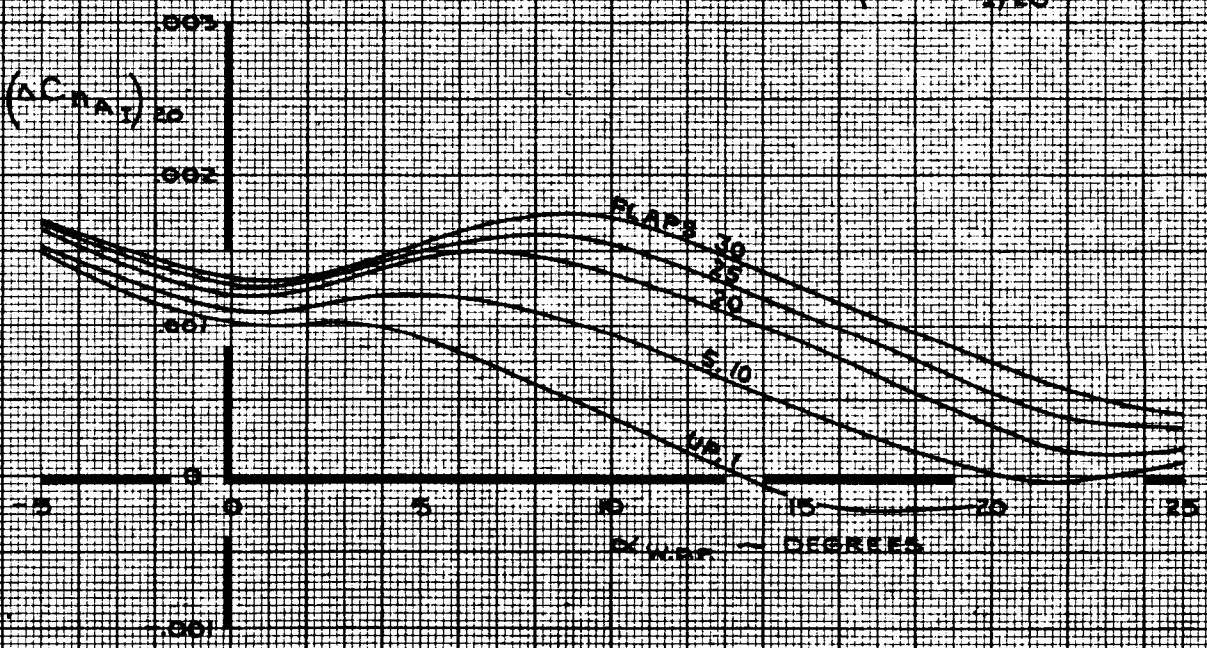

CALC	KUPCIS	11-6-67	REVISED	DATE	YAWING MOMENT COEFFICIENT EFFECT OF INBOARD AILERON
CHECK	FOSTER	1-24-68	LOW	2-14-70	
APR					
APR					
INK	W. ODEGARD	11-6-67			

747

D6-30643 Vol. II

THE BOEING COMPANY

PAGE 6.0-15

TD 461 C-R4

REV. D

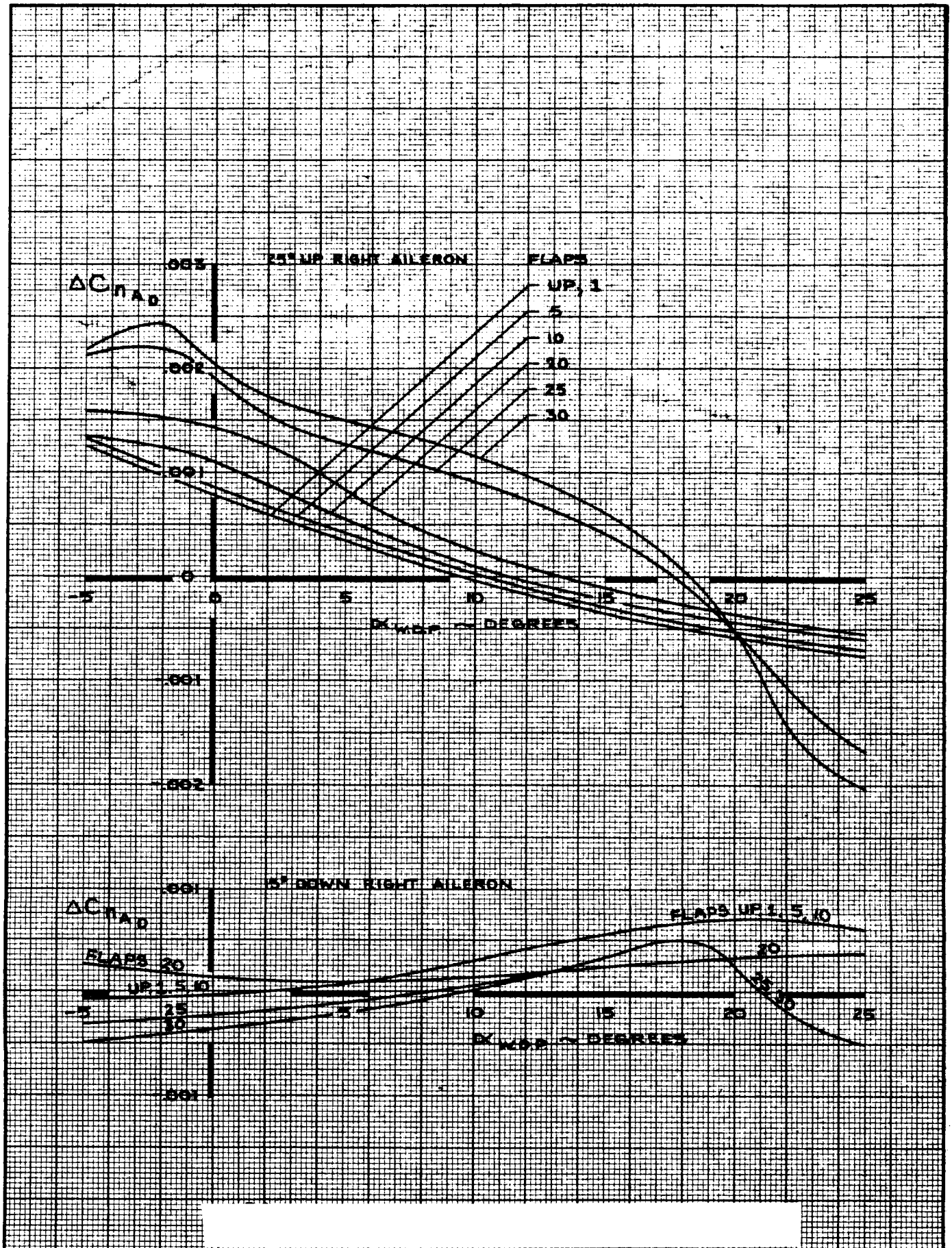

CALC	KUPCIS	11/14/67	REVISED	DATE	YAWING MOMENT COEFFICIENT EFFECT OF OUTBOARD AILERON
CHECK	FOSTER	1-24-68	KUPCIS	4-22-68	
APR			BECK	2-24-70	
APR					
INK	W. ODEGARD	11/14/67			THE BOEING COMPANY

747
D6-30643 Vol. II
PAGE 6.0-16
REV. D

TD 461 C-R4

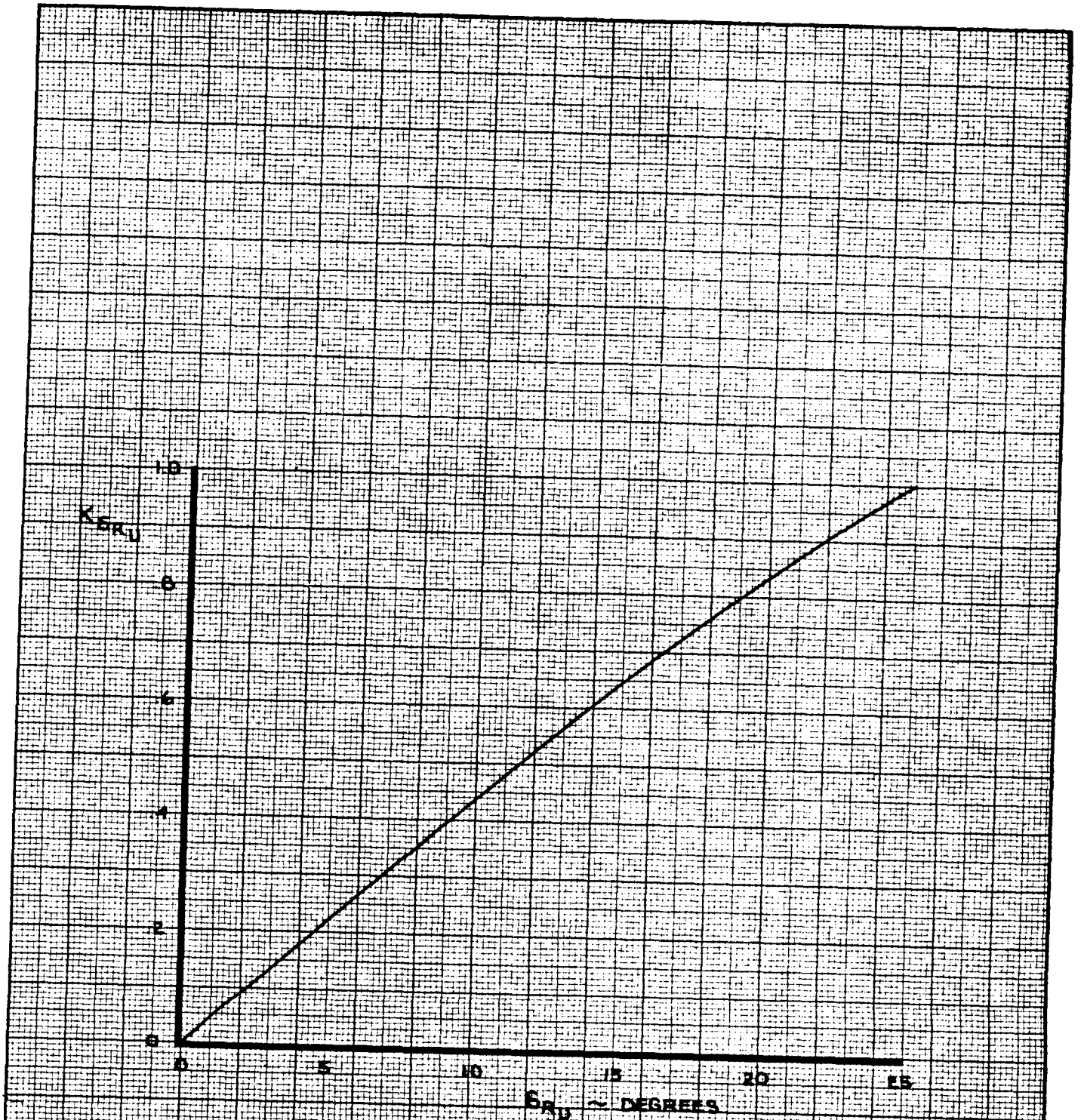

CALC	RICHARDSON	12-14-67	REVISED	DATE	EFFECTIVENESS FACTOR UPPER RUDDER	747
CHECK	FOSTER	1-24-68	BECK	2-26-70		D6-30643 Vol. II 3
APR						
APR						
INK	KINSMAN	2-27-70			THE BOEING COMPANY	PAGE 6.0-17

AD 461 C-R4

K-E ALBANENE 1951 TRACING PAPER REV. D

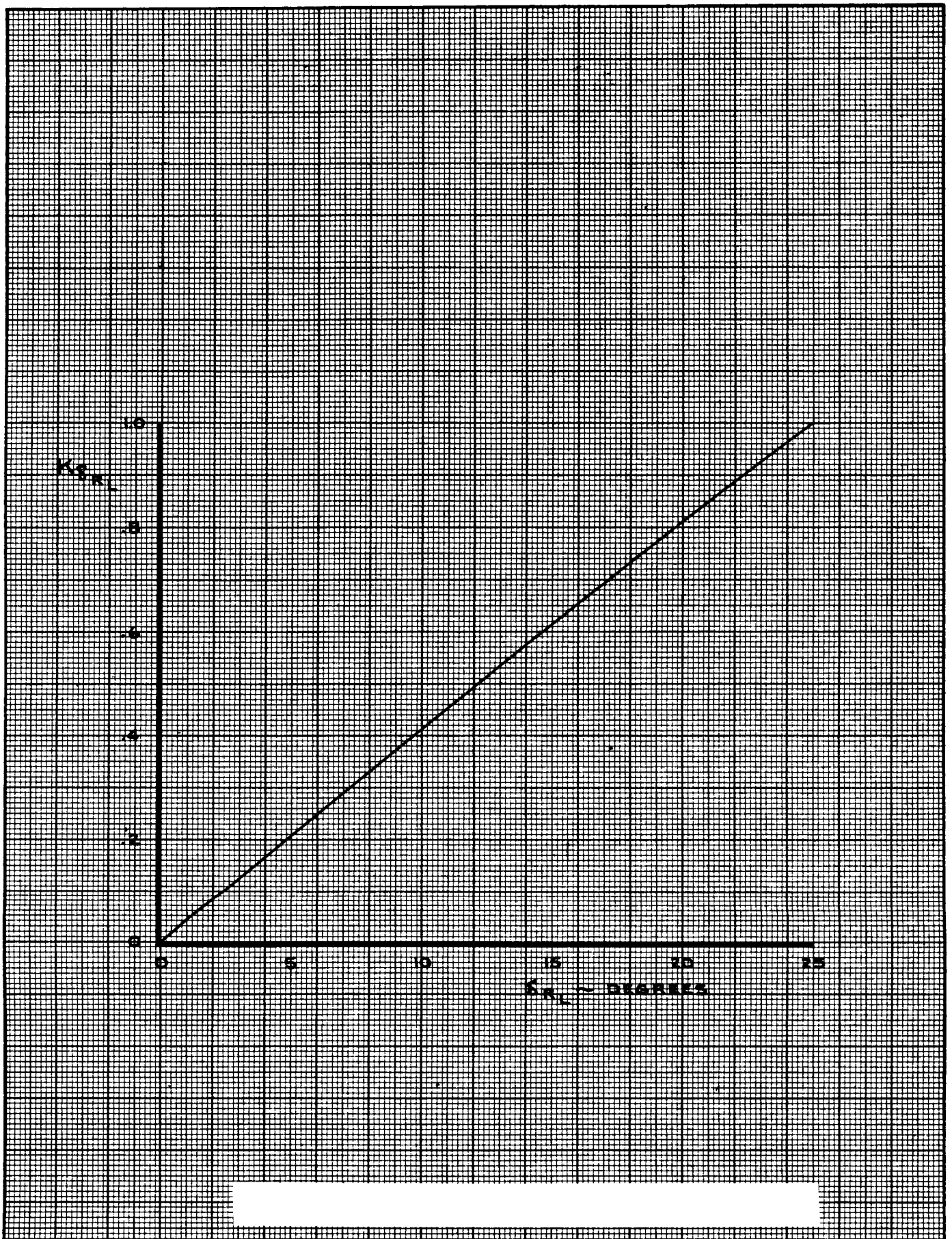

CALC	RICHARDSON	12/14/67	REVISED	DATE	EFFECTIVENESS FACTOR LOWER RUDDER	747
CHECK	FOSTER	1-24-68				D6-30643, Vol. II
APR						
APR					THE BOEING COMPANY	PAGE 6.0-18
INK	ODEGARD	12/14/67				

TD 461 C-R4

EDR1

UPPER RUDDER

NOTE 1. FOR LOWER RUDDER INOPERATIVE, MULTIPLY BY 1.12

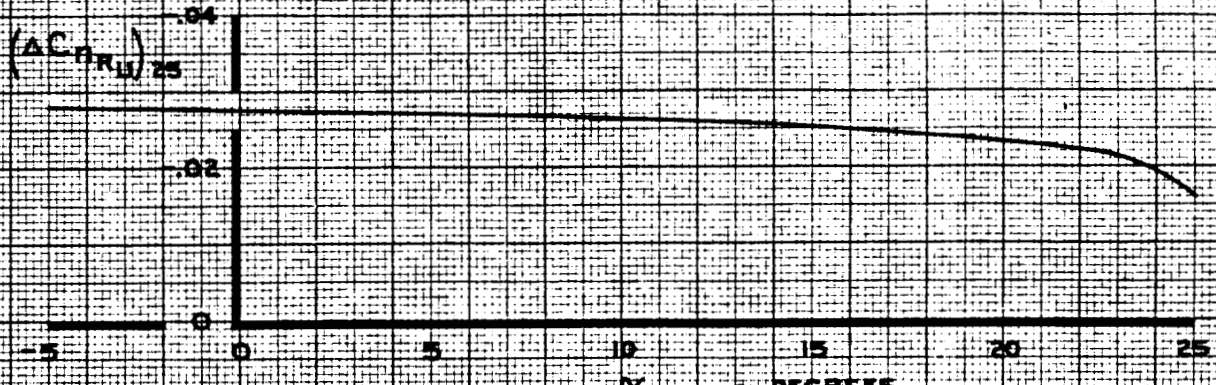

LOWER RUDDER

NOTE 1. FOR UPPER RUDDER INOPERATIVE, MULTIPLY BY 1.12

CALC	RICHARDSON	12-6-67	REVISED	DATE	YAWING MOMENT COEFFICIENT Δ EFFECT OF RUDDERS
CHECK	KUPCIS	12-6-67	RICHARDSON	4-8-68	
APR			BECK	1-28-70	
APR					
INK	ODEGARD	2-3-70			

747

D6-30643 Vol. II

THE BOEING COMPANY

PAGE 6.0-19

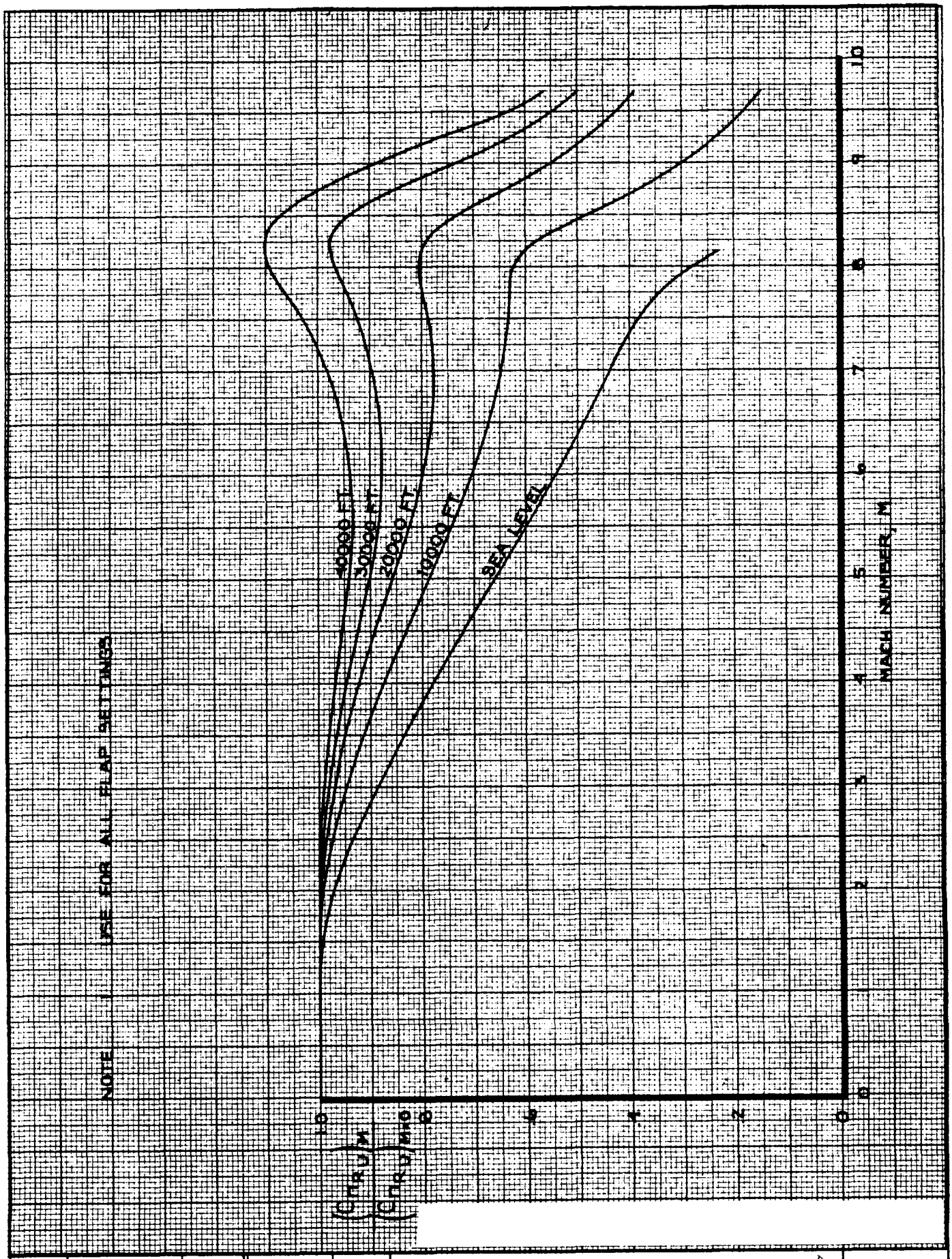

CALC	WILCOXEN	12·20·67	REVISED	DATE	YAWING MOMENT COEFFICIENT AEROELASTIC EFFECT ON YAWING MOMENT COEFFICIENT DUE TO UPPER RUDDER
CHECK	RICHARDSON	12·21·67	RICHARDSON	4·8·68	
APR			LOW	6·14·69	
APR			BECK	2·5·70	
INK	KINSMAN	2·5·70			THE BOEING COMPANY

747
D6-30643 Vol. II
PAGE 6.0-20

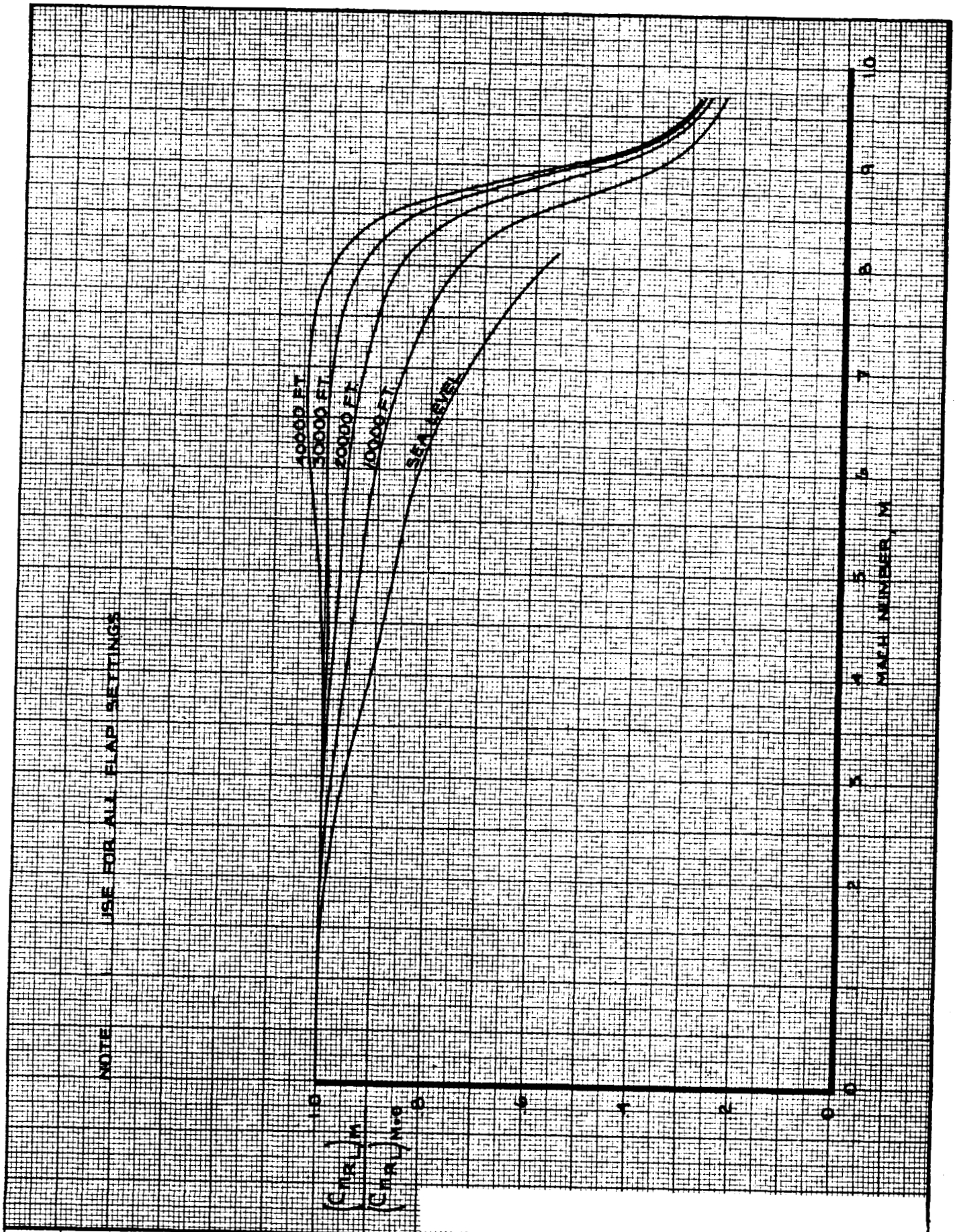

CALC	WILCOXEN	12-20-67	REVISED	DATE	YAWING MOMENT COEFFICIENT C_{N_β} AEROELASTIC EFFECT ON YAWING MOMENT COEFFICIENT DUE TO LOWER RUDDER
CHECK	RICHARDSON	12-21-67	RICHARDSON	4-8-68	
APR			LOW	6-14-69	
APR			BECK	2-5-70	
INK	KINSMAN	2-5-70			THE BOEING COMPANY

747
D6-30643 Vol. II
PAGE 6.0-21

AD 461 C-R4

K-E ALBANENE 1951 REV D

NOTE 1. RIGHT INBOARD FLAP AT MONITOR LIMITED EXTENSION POSITION CORRESPONDING TO LEFT INBOARD FLAP FAILURE POSITION

2. CHANGE SIGN FOR RIGHT INBOARD FLAP FAILURE

THESE DATA NOT INCLUDED IN NASA SIMULATION

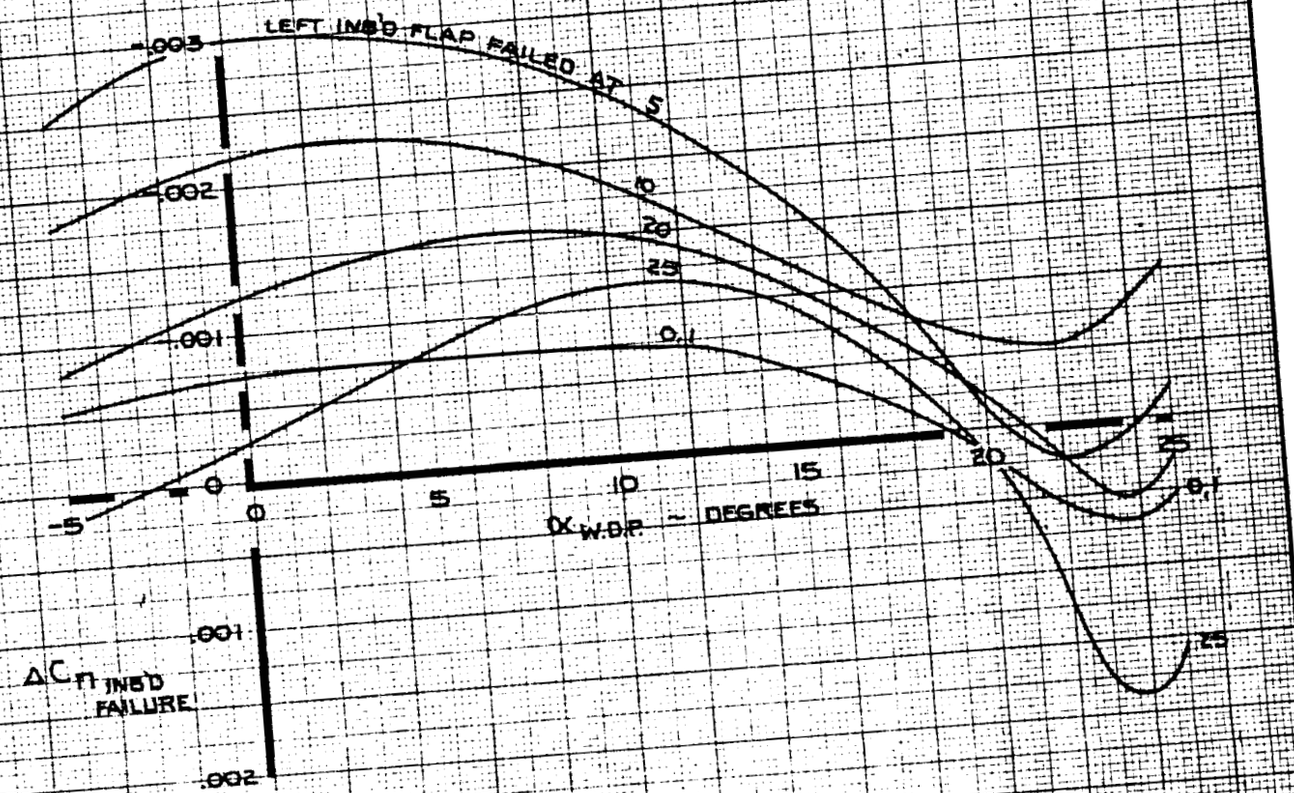

			REVISED	DATE
CALC	LOW	5-26-69	LOW	2-17-70
CHECK			LOW	6-25-70
APR				
APR				
INK	ODEGARD	5-26-69		

YAWING MOMENT COEFFICIENT
EFFECT OF ASYMMETRIC INBOARD FLAP FAILURE
FOR FLAP EXTENSION

THE BOEING COMPANY

747
D6-30643 Vol. II
PAGE 6.0-22

TD 461 C-R4

K-E ALBANENE 1951 REV E

NOTE 1. RIGHT INBOARD FLAP AT MONITOR LIMITED RETRACTION POSITION CORRESPONDING TO LEFT INBOARD FLAP FAILURE POSITION

2. CHANGE SIGN FOR RIGHT INBOARD FLAP FAILURE

THESE DATA NOT INCLUDED IN NASA SIMULATION

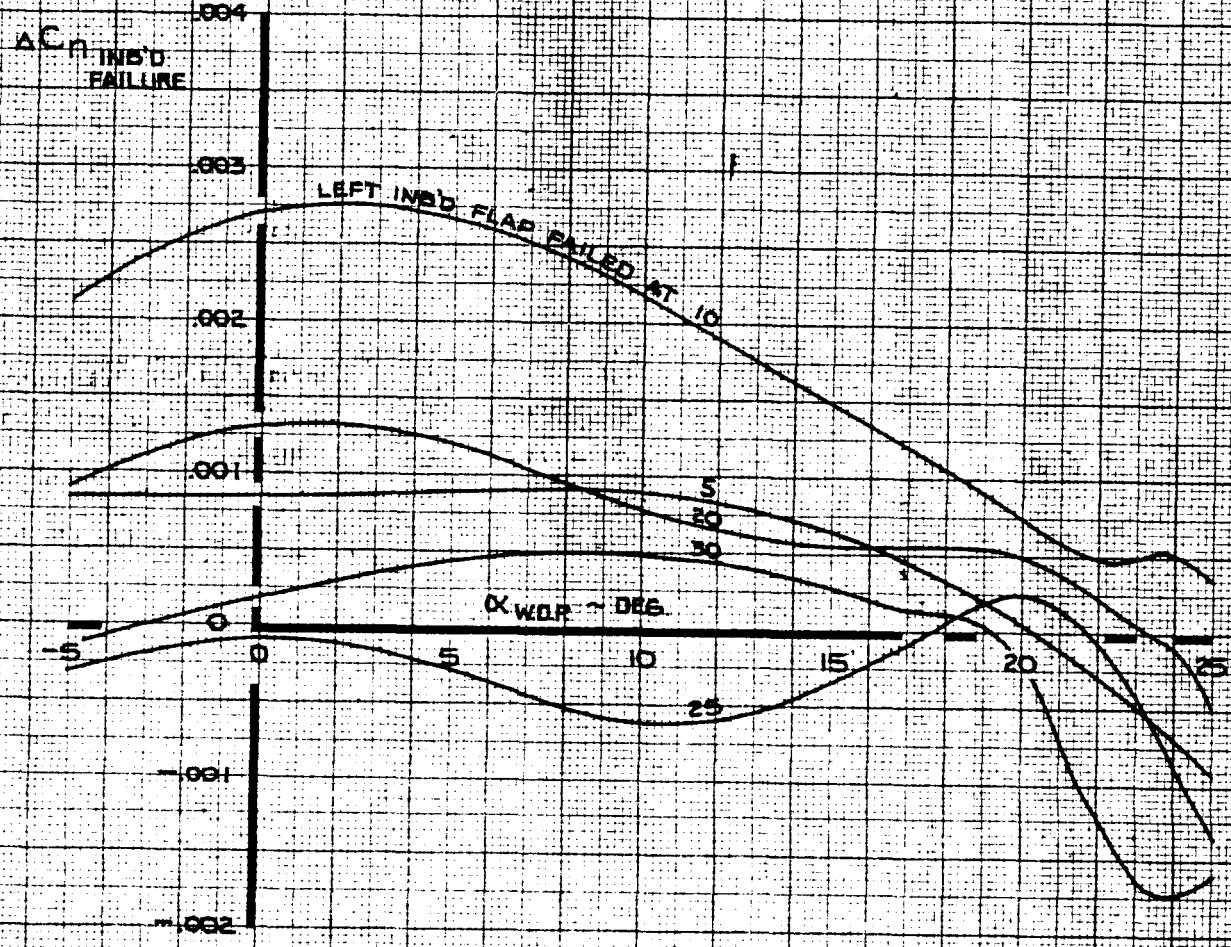

CALC	LOW	5-26-69	REVISED	DATE	YAWING MOMENT COEFFICIENT EFFECT OF ASYMMETRIC INBOARD FLAP FAILURE FOR FLAP RETRACTION	747
CHECK			LOW	2-17-70		
APR			LOW	6-25-70		D6-30643, Vol. II
APR						
INK	ODEGARD	5-26-69			THE BOEING COMPANY	PAGE 6.0-23

TD 461 C-R4

K-E ALBANENE 1951 REV. E

NOTE 1. RIGHT OUTBOARD FLAP AT MONITOR LIMITED EXTENSION POSITION CORRESPONDING TO LEFT OUTBOARD FLAP FAILURE POSITION

2. CHANGE SIGN FOR RIGHT OUTBOARD FLAP FAILURE

THESE DATA NOT INCLUDED IN NASA SIMULATION

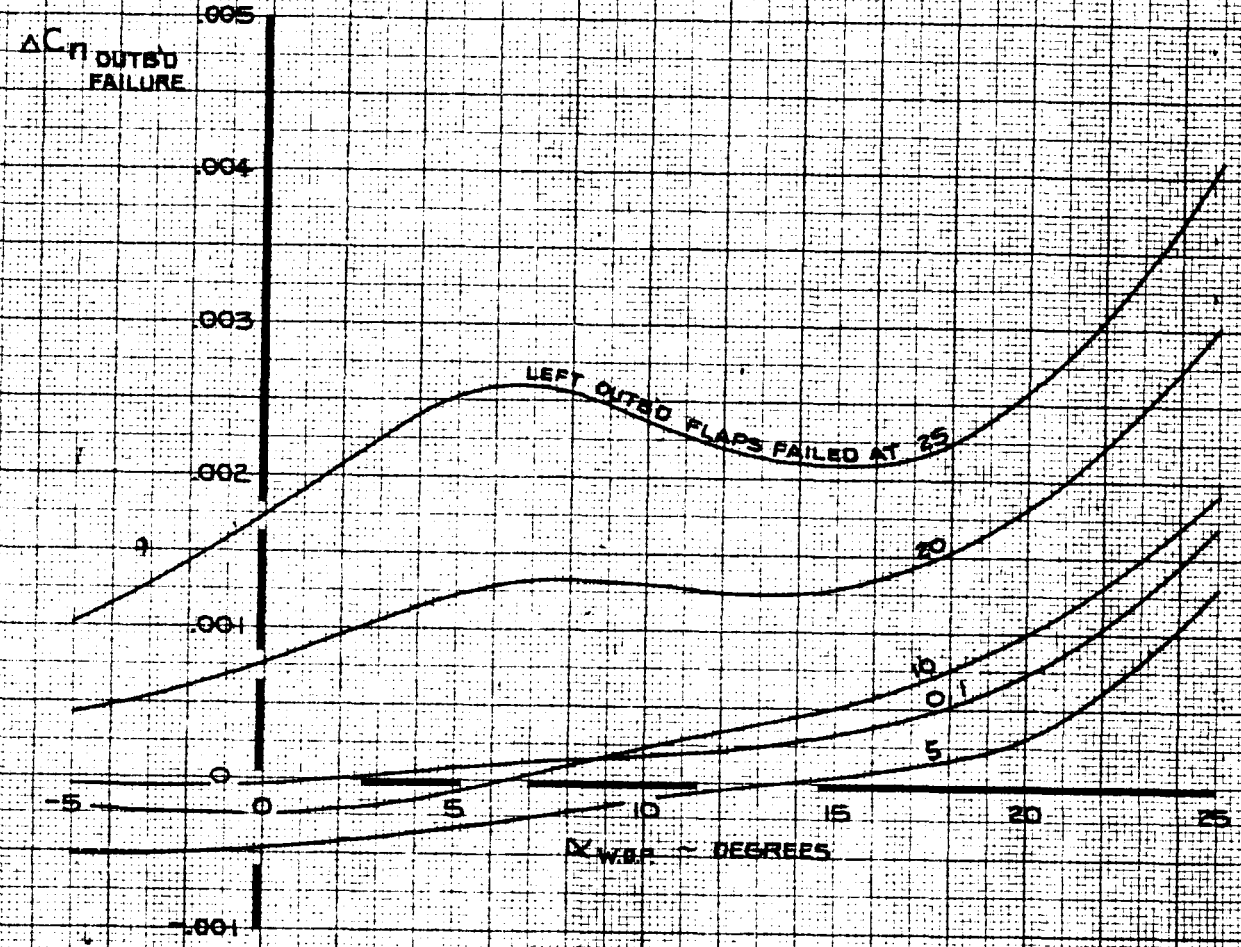

CALC	LOW	5-26-69	REVISED	DATE	YAWING MOMENT COEFFICIENT EFFECT OF ASYMMETRIC OUTBOARD FLAP FAILURE FOR FLAP EXTENSION	747
CHECK			LOW	2-17-70		D6-30643, Vol. II
APR			LOW	6-25-70		
APR						
INK	ODEGARD	5-26-69			THE BOEING COMPANY	PAGE 6.0-24

TD 461 C-R4

K-E ALBANENE 1961 REV E

NOTE: 1. RIGHT OUTBOARD FLAP AT MONITOR LIMITED RETRACTION POSITION CORRESPONDING TO LEFT OUTBOARD FLAP FAILURE POSITION

2. CHANGE SIGN FOR RIGHT OUTBOARD FLAP FAILURE

THESE DATA NOT INCLUDED IN NASA SIMULATION

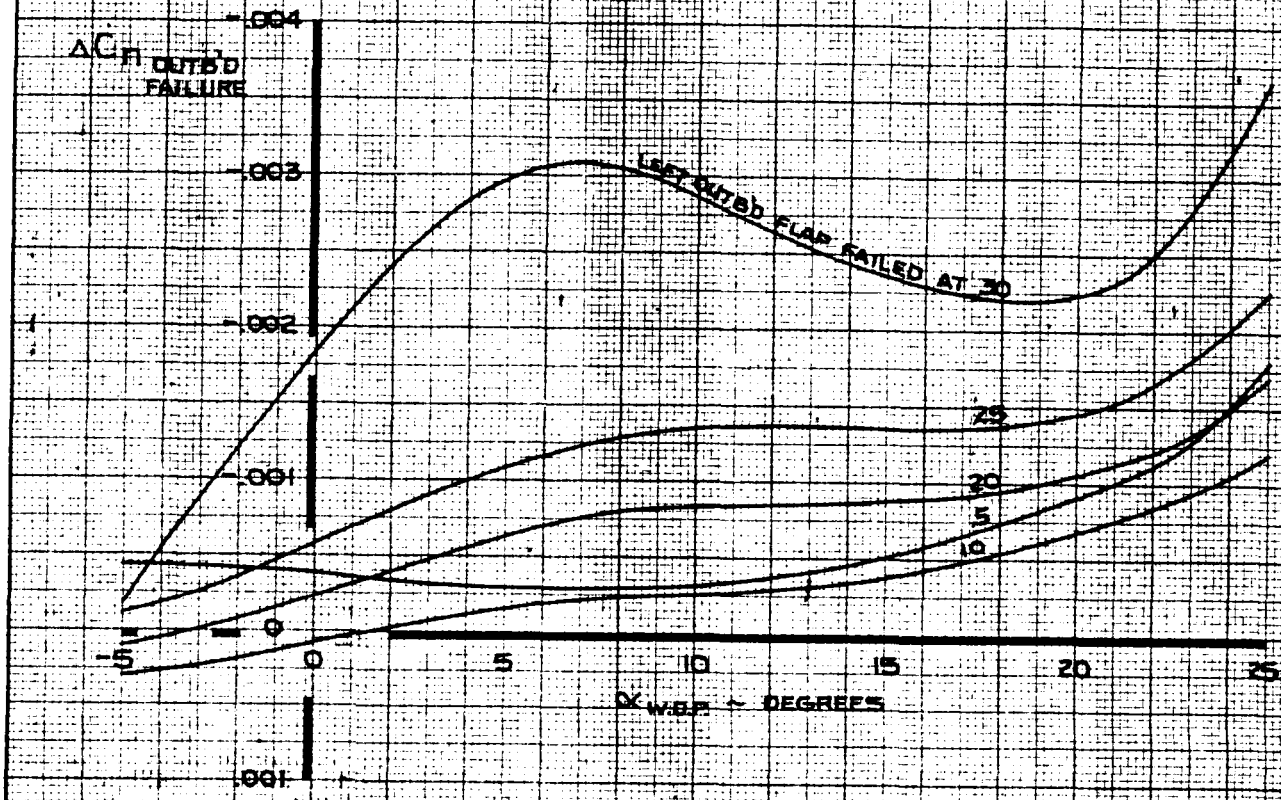

CALC	LOW	5-26-69	REVISED	DATE	YAWING MOMENT COEFFICIENT EFFECT OF ASYMMETRIC OUTBOARD FLAP FAILURE FOR FLAP RETRACTION	747
CHECK			LOW	2-17-70		
APR			LOW	6-25-70		D6-30643 Vol. II
APR						
INK	ODEGARD	5-26-69			THE BOEING COMPANY	PAGE 6.0-25

TD 461 C-R4

K+E ALBANENE 195L REV E

NOTE 1. CHANGE SIGN FOR FAILURE OF L.E. FLAP SEGMENTS 22, 23, 24, 25, 26

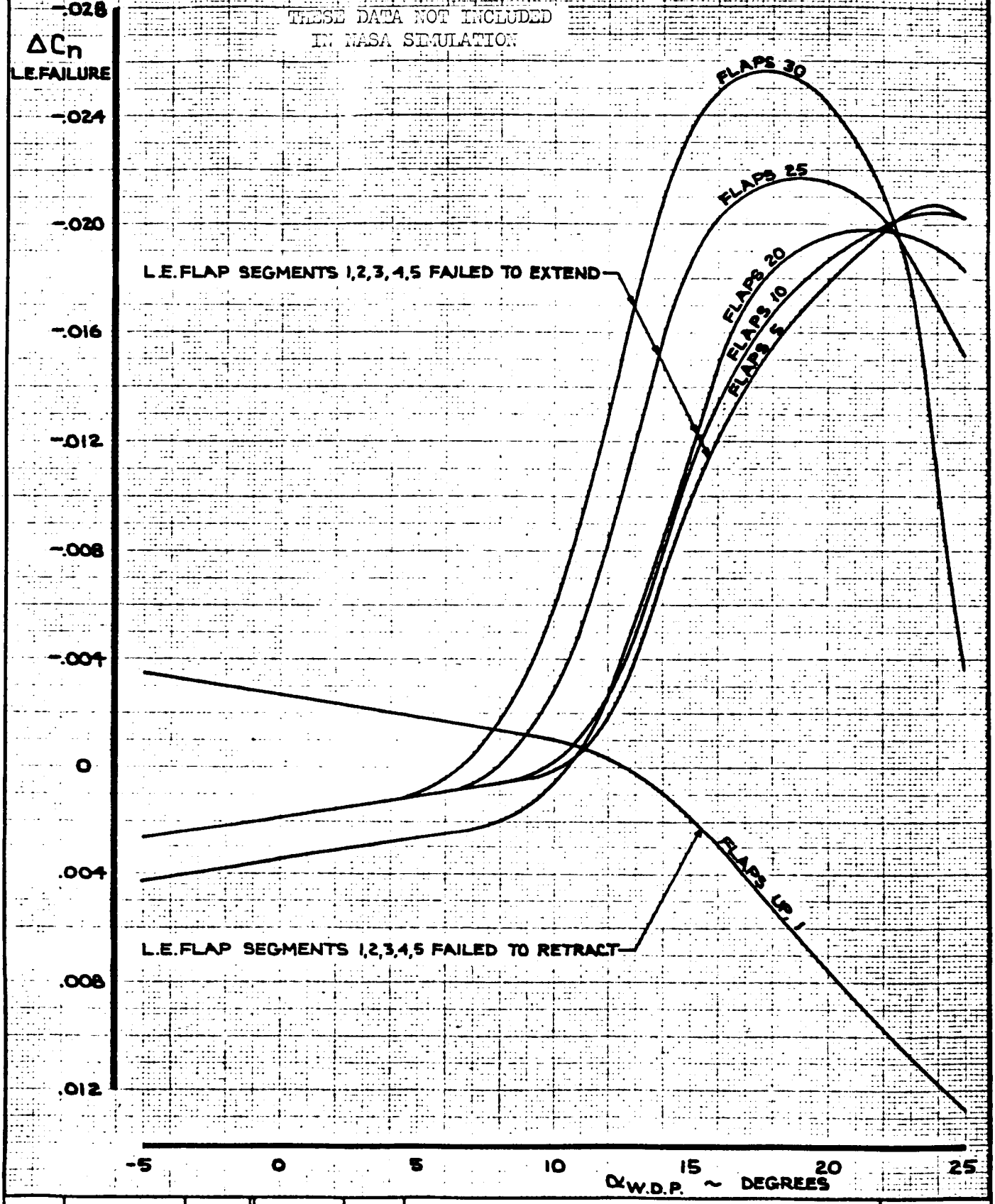

CALC	LOW	8-22-69	REVISED	DATE	YAWING MOMENT COEFFICIENT EFFECT OF ASYMMETRIC L.E. FLAP SEGMENTS 1,2,3,4,5 OR 22,23,24,25,26
CHECK			LOW	3-13-70	
APR					
APR					
INK	KINSMAN	8-22-69			THE BOEING COMPANY

747

D6-30643 Vol. II

PAGE 6.0-26

AD 461 L R4

ALBANENE 1964 REV. D

NOTE 1. CHANGE SIGN FOR FAILURE OF L.E. FLAP SEGMENTS 19, 20, 21

THESE DATA NOT INCLUDED IN NASA SIMULATION

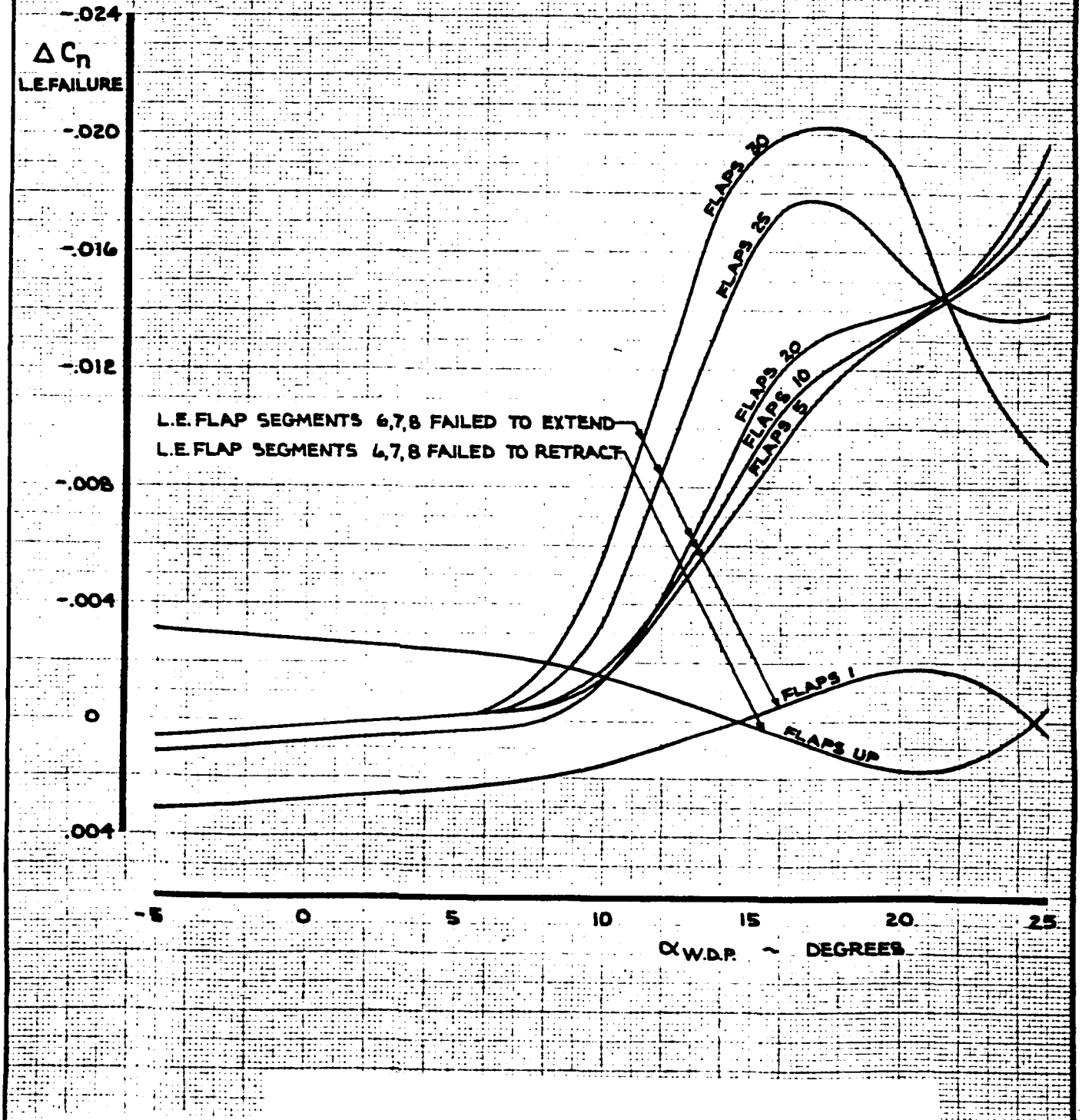

CALC	LOW	8-22-69	REVISED	DATE	YAWING MOMENT COEFFICIENT EFFECT OF ASYMMETRIC L.E. FLAP SEGMENTS 4,7,8 OR 19,20,21	747
CHECK			LOW	3-13-70		D6-30643 Vol. II
APR						
APR						
INK	KINSMAN	8-22-69			THE BOEING COMPANY	PAGE 4.0-27

7.0 SIDE FORCE COEFFICIENT

The dimensionless aerodynamic side force coefficient is given in terms of its significant components by the equation below.

At a given $\alpha_{W.B.P.}$,

$$C_Y = \frac{dC_Y}{d\beta}\cdot\beta + \frac{dC_Y}{d\hat{p}}\cdot\frac{p_s b}{2V} + \frac{dC_Y}{d\hat{r}}\cdot\frac{r_s b}{2V} + \Delta C_{Y_{SPOILERS}} + \Delta C_{Y_{RUDDERS}} + \left[\Delta C_{Y_{FLAP\ FAILURE}} + \Delta C_{Y_{L.E.\ FAILURE}}\right]^*$$

where,

$\frac{dC_Y}{d\beta}\cdot\beta$ = Side force coefficient due to angle of sideslip, β. The complete expression for $\frac{dC_Y}{d\beta}$ is given as follows:

$$\frac{dC_Y}{d\beta} = \left[\left(\frac{dC_Y}{d\beta}\right)\cdot\frac{(C_{Y_\beta})_M}{(C_{Y_\beta})_{M=0}} + K_{GEAR}\cdot\Delta\left(\frac{dC_Y}{d\beta}\right)_{LANDING\ GEAR}\right] F_{Y_{\beta_{GE}}}$$

where $\left(\frac{dC_Y}{d\beta}\right)$ is the basic rate of change of side force coefficient due to angle of sideslip. For low speed, $\left(\frac{dC_Y}{d\beta}\right)$ is plotted on page 7.0-5. The aeroelastic effect, $\frac{(C_{Y_\beta})_M}{(C_{Y_\beta})_{M=0}}$, is plotted on page 7.0-5. The effect of main and nose gear extension, $\Delta\left(\frac{dC_Y}{d\beta}\right)_{LANDING\ GEAR}$ is given by:

$$\Delta\left(\frac{dC_Y}{d\beta}\right)_{LANDING\ GEAR} = -0.002 \text{ PER DEGREE}$$

$[\ ]^*$ NOT IN NASA SIMULATION

AD 1546 D

7.0 (Cont'd)

The landing gear effectiveness factor, K_{GEAR} is plotted on page 2.0-28.

The ground effect factor, $F_{Y\beta_{GE}}$ is obtained as follows:

$$F_{Y\beta_{GE}} = \left[1 + F_{Y\beta} \cdot K^{B}_{GE}\right]$$

where the ground effect sideslip factor, $F_{Y\beta}$, is plotted on page 7.0-6. The ground effect height factor, K^{B}_{GE} .. is plotted on page 2.0-31.

$\frac{dC_Y}{d\beta} \cdot \frac{p_s b}{2V}$ = Side force coefficient due to roll rate about the stability axis, x_s. $\frac{dC_Y}{d\beta}$ is plotted on page 7.0-7.

$\frac{dC_Y}{d\hat{r}} \cdot \frac{r_s b}{2V}$ = Side force coefficient due to yaw rate about the stability axis, z_s . The complete expression for $\frac{dC_Y}{d\hat{r}}$ is given as follows:

$$\frac{dC_Y}{d\hat{r}} = \left(\frac{dC_Y}{d\hat{r}}\right) \cdot \frac{(C_{Y\hat{r}})_M}{(C_{Y\hat{r}})_{M=0}}$$

where $\left(\frac{dC_Y}{d\hat{r}}\right)$ is plotted on page 7.0-8. The aeroelastic effect, $\frac{(C_{Y\hat{r}})_M}{(C_{Y\hat{r}})_{M=0}}$, is plotted on page 7.0-9.

$\Delta C_{Y_{SPOILERS}}$ = Side force coefficient due to spoiler deflection.

$$\Delta C_{Y_{SPOILERS}} = \sum_{\substack{\text{OPERATING} \\ \text{SPOILER} \\ \text{PANELS}}} (K\delta_{SP})_Y \cdot (\Delta C_{Y_{SP}})_{45} \cdot \frac{(C_{Y_{SP}})_M}{(C_{Y_{SP}})_{M=0}} \cdot F_{n_{GE}}$$

where $(\Delta C_{Y_{SP}})_{45}$ is the side force coefficient due to deflecting the operating spoiler panels to 45°. $(\Delta C_{Y_{SP}})_{45}$ is plotted on page 7.0-11 . The spoiler

7.0 (Cont'd)

effectiveness factor, $(K\delta_{SP})_Y$, is plotted on page 7.0-10. The Mach number effect, $\frac{(C_{Y_{SP}})_M}{(C_{Y_{SP}})_{M=0}}$, is plotted on page 7.0-12. The ground effect factor, $F_{n_{GE}}$, is obtained from page 6.0-14.

$\Delta C_{Y_{RUDDERS}}$ = Side force coefficient due to rudder deflection.

$$\Delta C_{Y_{RUDDERS}} = K\delta_{R_U} \cdot (\Delta C_{Y_{R_U}})_{25} \cdot \frac{(C_{Y_{R_U}})_M}{C_{Y_{R_U}\,M=0}} + K\delta_{R_L} \cdot (\Delta C_{Y_{R_L}})_{25} \cdot \frac{(C_{Y_{R_L}})_M}{(C_{Y_{R_L}})_{M=0}}$$

where $(\Delta C_{Y_{R_U}})_{25}$ and $(\Delta C_{Y_{R_L}})_{25}$ are the side force coefficients due to full deflection of the upper rudder and the lower rudder respectively. $(\Delta C_{Y_{R_U}})_{25}$ and $(\Delta C_{Y_{R_L}})_{25}$ are plotted on page 7.0-13. The upper rudder effectiveness factor, $K\delta_{R_U}$, and the lower rudder effectiveness factor, $K\delta_{R_L}$, are plotted on pages 6.0-17 and 6.0-18 respectively. The aeroelastic effects, $\frac{(C_{Y_{R_U}})_M}{(C_{Y_{R_U}})_{M=0}}$ and $\frac{(C_{Y_{R_L}})_M}{(C_{Y_{R_L}})_{M=0}}$. for the upper rudder and the lower rudder, are plotted on pages 7.0-14 and 7.0-15 respectively.

$\Delta C_{Y_{FLAP\ FAILURE}}$ = Side force coefficient due to an asymmetric (monitor limited) inboard or outboard flap failure.

$$\Delta C_{Y_{FLAP\ FAILURE}} = \Delta C_{Y_{INB'D\ FAILURE}}\ \underline{OR}\ \Delta C_{Y_{OUTB'D\ FAILURE}}$$

where $\Delta C_{Y_{INB'D\ FAILURE}}$ is the side force coefficient due to an asymmetric (monitor limited) inboard flap failure. $\Delta C_{Y_{INB'D\ FAILURE}}$ for flap extension or retraction is plotted on pages 7.0-16 and 7.0-17

AD 1546 D

7.0 (Cont'd)

respectively.

$\Delta C_{Y_{OUTBD\ FAILURE}}$ for flap extension or retraction is plotted on pages 7.0-18 and 7.0-19 respectively.

$\Delta C_{Y_{L.E.\ FAILURE}}$ = Side force coefficient due to asymmetric leading edge flap failure. $\Delta C_{Y_{L.E.\ FAILURE}}$ is plotted on pages 7.0-20 and 7.0-21.

AD 1546 D

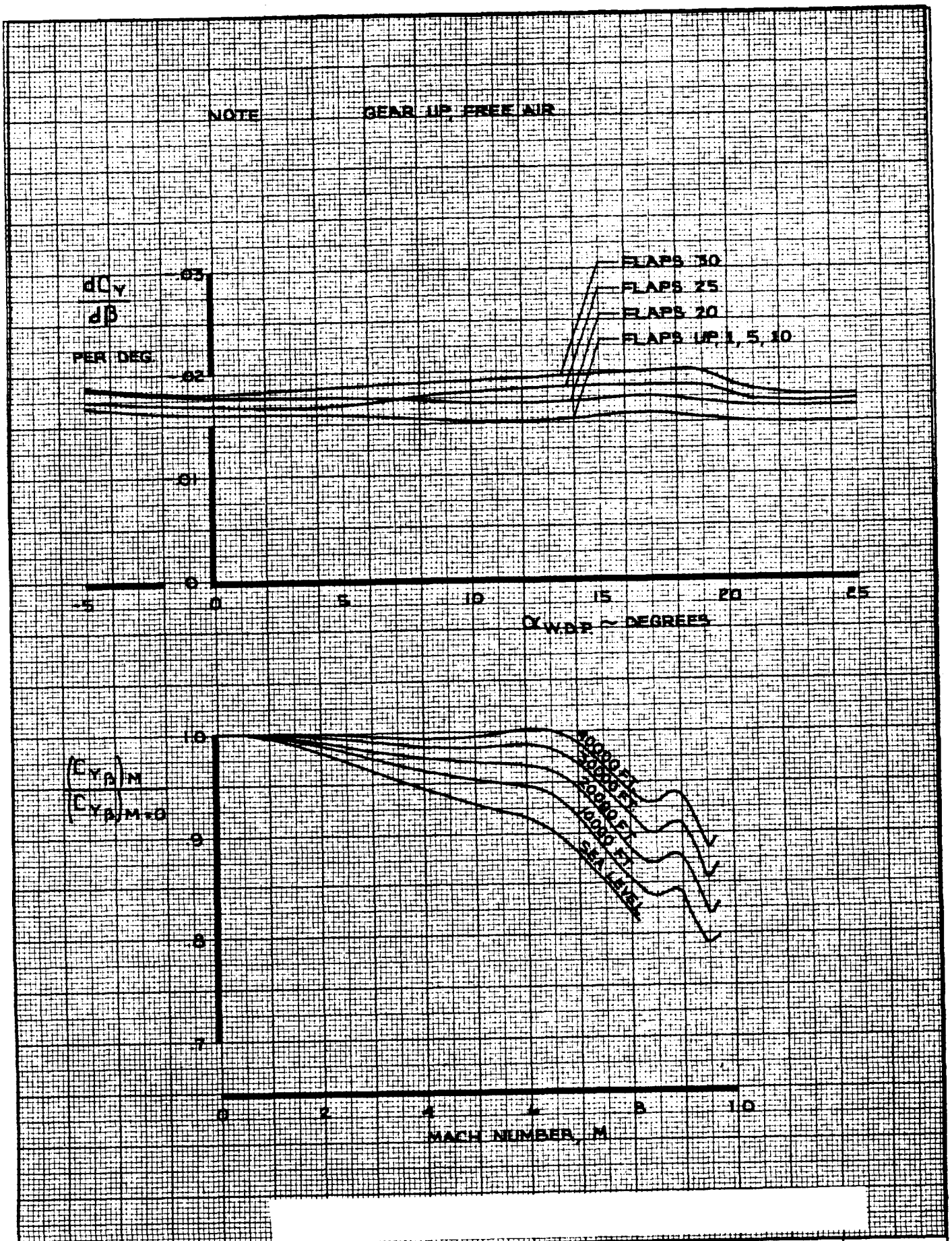

CALC	STIRLING	12-7-67	REVISED	DATE	SIDE FORCE COEFFICIENT EFFECT OF SIDESLIP	747
CHECK	FOSTER	1-24-68	BECK	2-3-70		D6-30643, Vol. II
APR						
APR					THE BOEING COMPANY	PAGE 7.0-5
INK	KINSMAN	2-14-70				

D

 REV D

NOTE 1. $F_{Y_{\beta_{GE}}} = \left[1 + F_{Y_\beta} K^{B}_{GE}\right]$

WHERE K^{B}_{GE} IS SHOWN ON PAGE 2.0-31

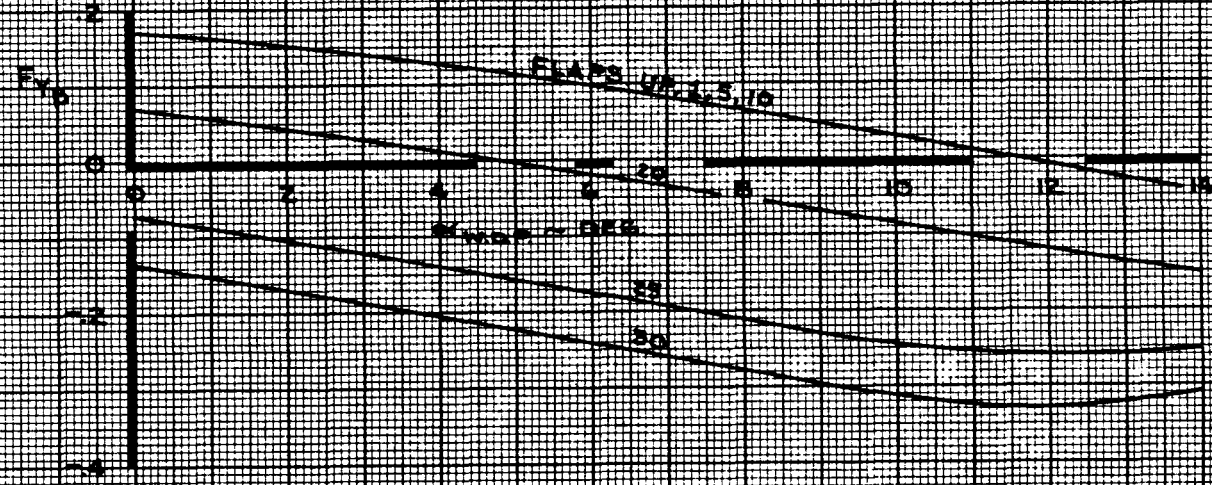

CALC	STIRLING	12/28/67	REVISED	DATE	SIDE FORCE COEFFICIENT GROUND EFFECT SIDESLIP FACTOR, F_{Y_β}
CHECK	FOSTER	1-24-68	LOW	2-14-70	
APR					
APR					
INK	ODEGARD	12/28/67			

747

D6-30643, Vol. II

THE BOEING COMPANY

PAGE 7.0-6

REV. D

TD 461 C-R4

NOTE $\hat{p} = \frac{p_s b}{2V}$; p_s — RAD/SEC, V — FT/SEC (TRUE AIRSPEED)

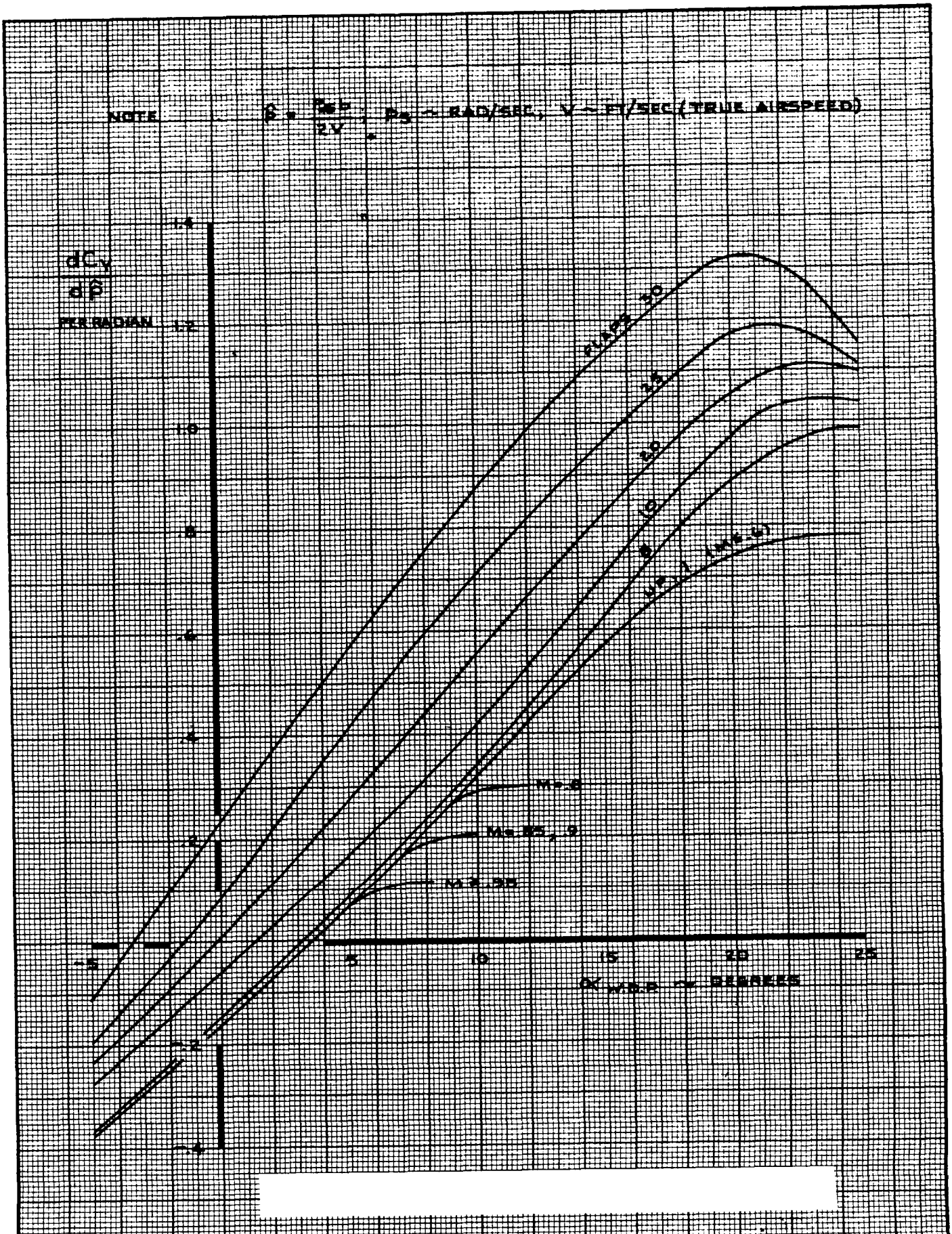

CALC	RICHARDSON	11/15/67	REVISED	DATE	SIDE FORCE COEFFICIENT EFFECT OF ROLL RATE
CHECK	CURNUTT	11/16/67	LOW	2-26-70	
APR					
APR					THE BOEING COMPANY
INK	ODEGARD	11/16/67			

747

D6-30643 Vol. II

PAGE 7.0-7

REV. D

TD 461 C-R4

NOTE: $\beta = \frac{r_s b}{2V}$; r_s ~ RAD/SEC, V ~ FT/SEC (TRUE AIRSPEED)

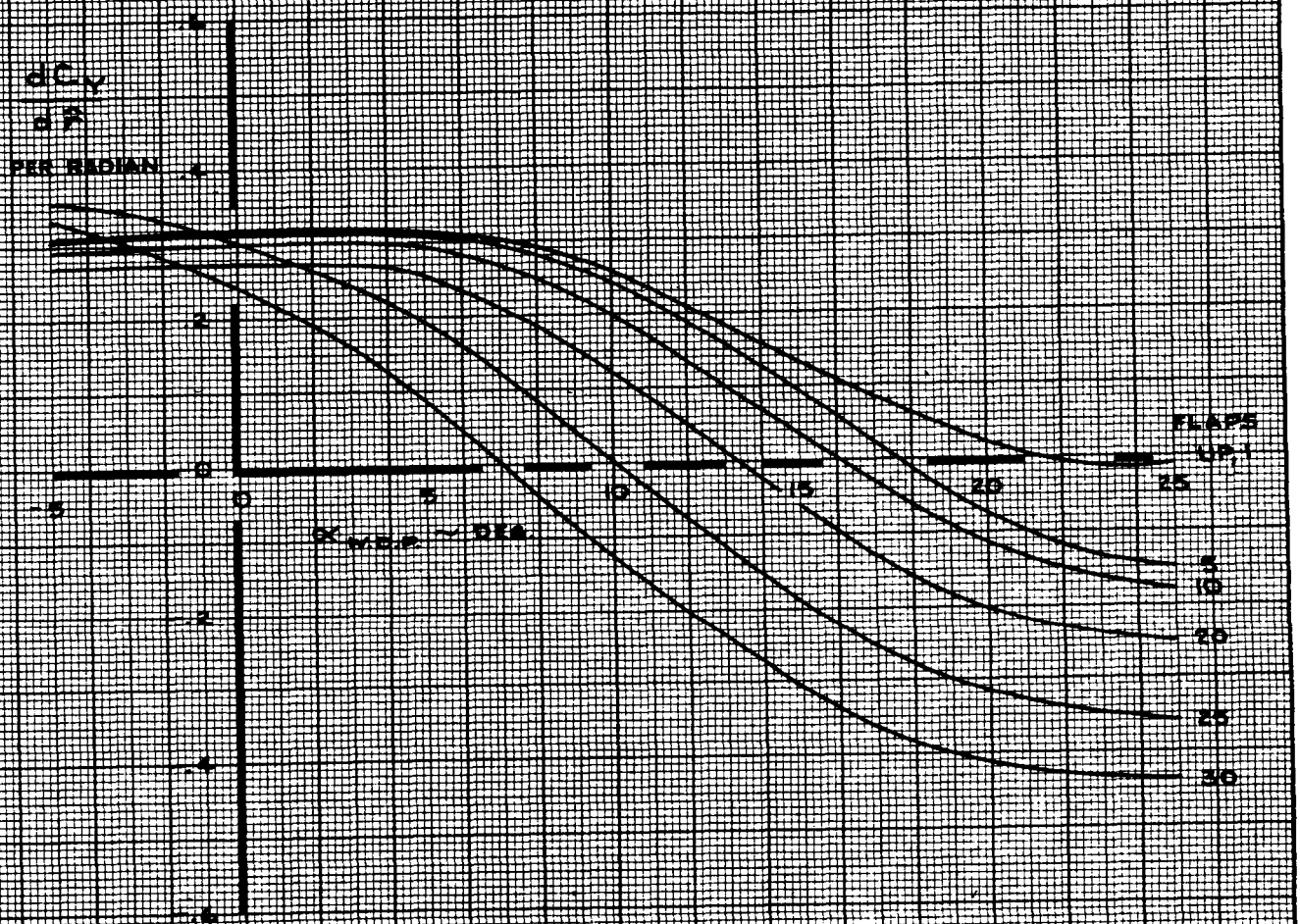

CALC	RICHARDSON	11/15/67	REVISED	DATE	SIDE FORCE COEFFICIENT EFFECT OF YAW RATE
CHECK	CURNUTT	11/16/67	LOW	2-26-70	
APR					
APR					THE BOEING COMPANY
INK	ODEGARD	11/15/67			

747

D6-30643, Vol. II

PAGE 7.0-8

REV. D

TD 461 C-R4

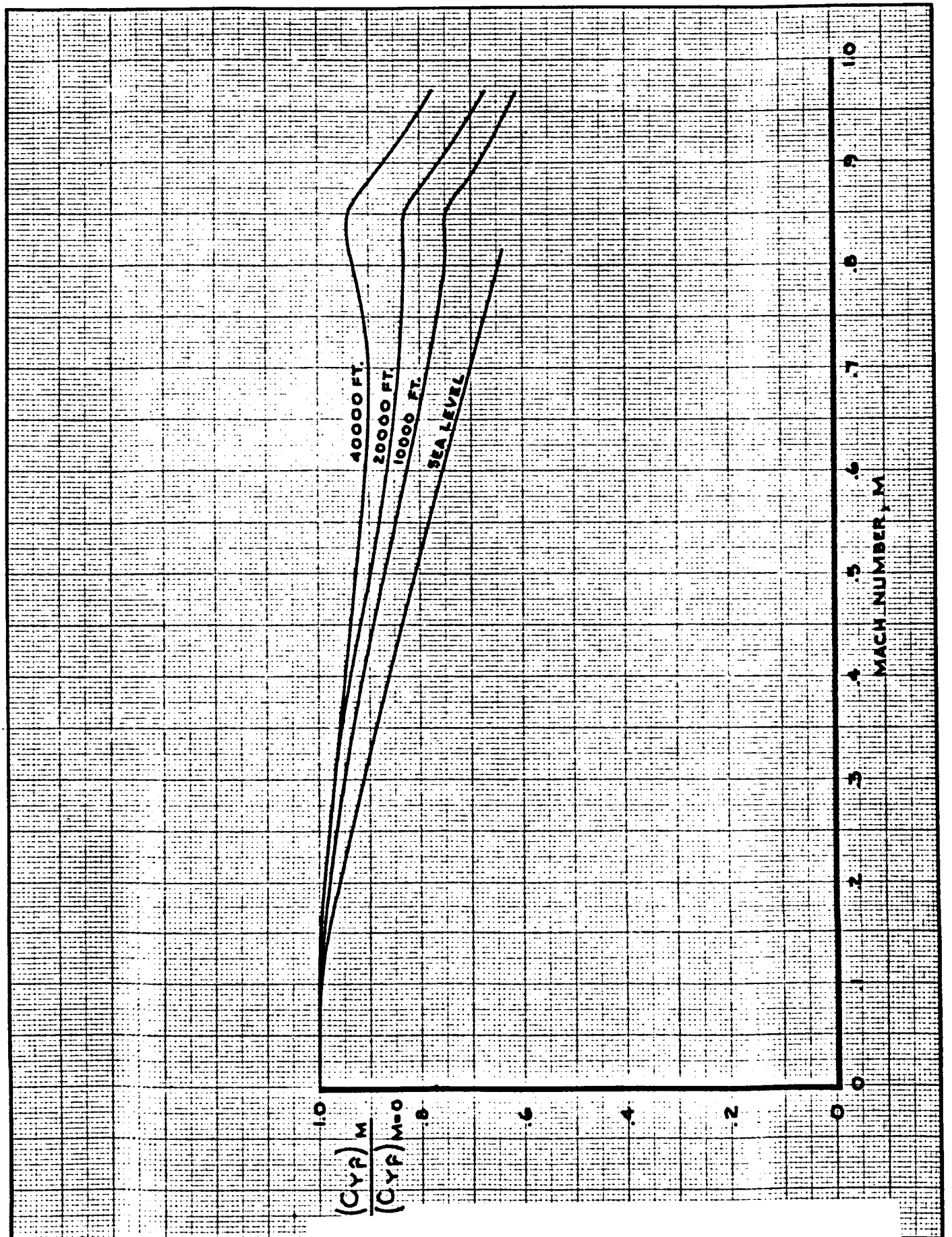

CALC	RICHARDSON	11/13/67	REVISED	DATE	SIDE FORCE COEFFICIENT AEROELASTIC EFFECT ON SIDE FORCE COEFFICIENT DUE TO YAW RATE
CHECK	CURNUTT	11/14/67	LOW	6-14-69	
APR					
APR					
INK	ODEGARD	11/14/67			

747

D6-30643 Vol. II

THE BOEING COMPANY

PAGE 7.0-9

TD 461 C-R4

REV. B

NOTE 1. USE FOR ALL SPOILER PANELS

2. PANELS 8 & 5 LIMITED TO 20 DEG MAX DEFLECTION

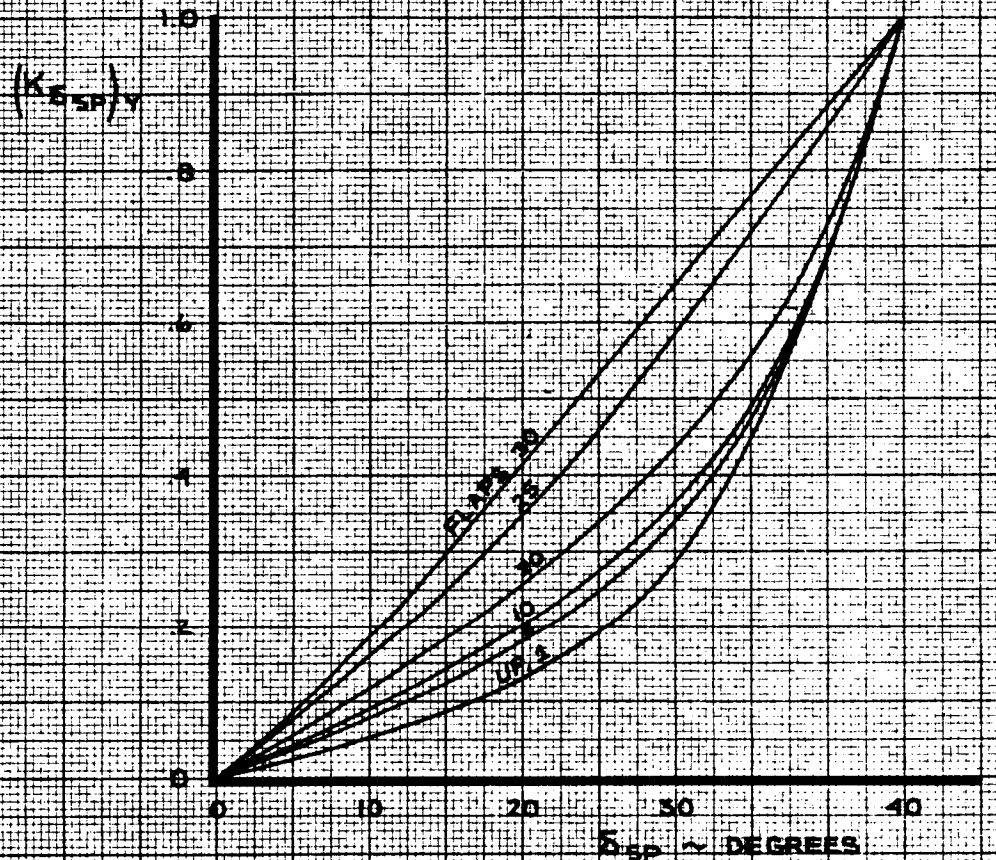

CALC	KUPCIS	12-11-67	REVISED	DATE	SIDE FORCE COEFFICIENT EFFECTIVENESS FACTOR SPOILERS	747
CHECK	FOSTER	1-24-68	KUPCIS	6-2-69		D6-30643 Vol. II
APR			KUPCIS	2-14-70		
APR					THE BOEING COMPANY	PAGE 7.0-10
INK	KINSMAN	2-20-70				

SPOILER PANEL 8 OR 12

NOTE
1. DATA SHOWN FOR INDIVIDUAL PANELS 8 OR 12
2. FOR PANEL 1 OR 5, REVERSE SIGN
3. PANELS 8 & 5 LIMITED TO 20 DEG MAX. DEFLECTION

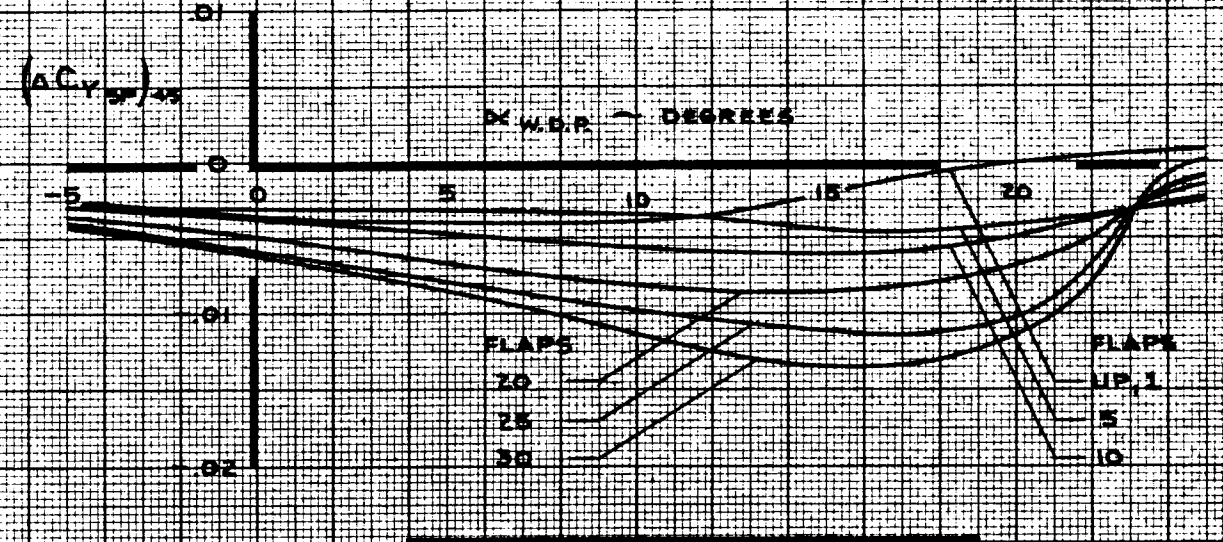

SPOILER PANEL GROUP 9, 10, 11

NOTE
1. TOTAL EFFECT OF SPOILER GROUP 9,10,11 SHOWN
2. FOR SPOILER GROUP 2,3,4, REVERSE SIGN
3. WITH HYDRAULIC SYSTEM NO. 2 OFF, MULTIPLY BY 0.40
4. WITH HYDRAULIC SYSTEM NO. 3 OFF, MULTIPLY BY 0.60

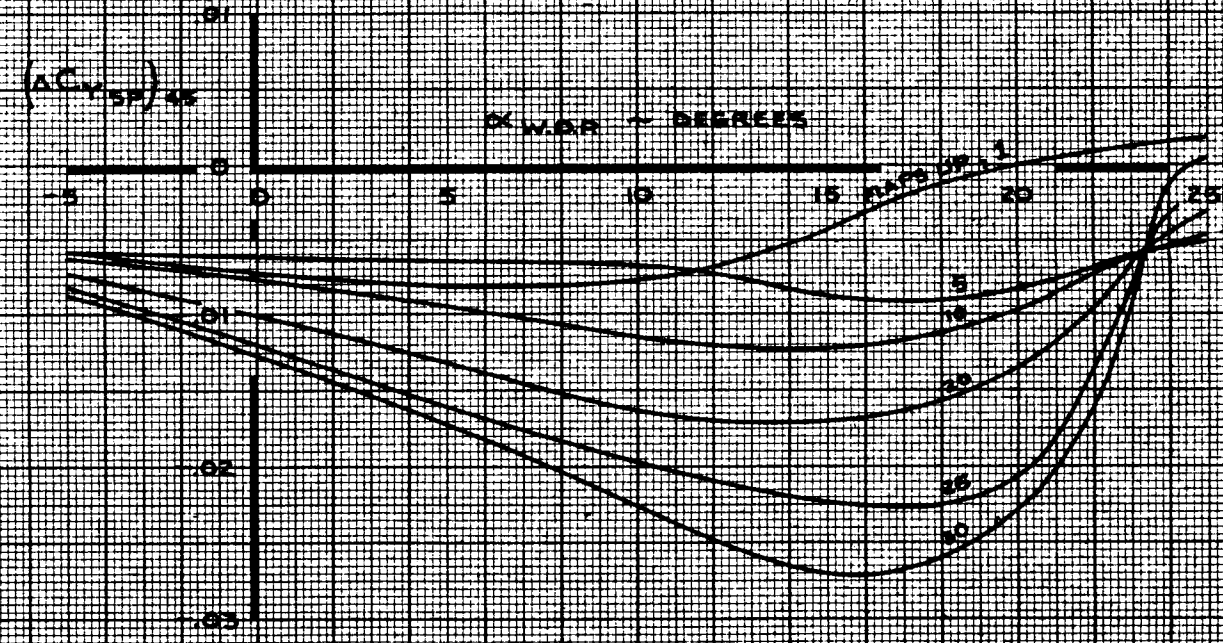

CALC	KUPCIS	12/11/67	REVISED	DATE	SIDE FORCE COEFFICIENT EFFECT OF SPOILERS	747
CHECK	FOSTER	1-24-68	KUPCIS	6-2-69		
APR			LOW	2-14-70		D6-20423
APR						
INK	ODEGARD	12/11/67			THE BOEING COMPANY	PAGE 7.0-11

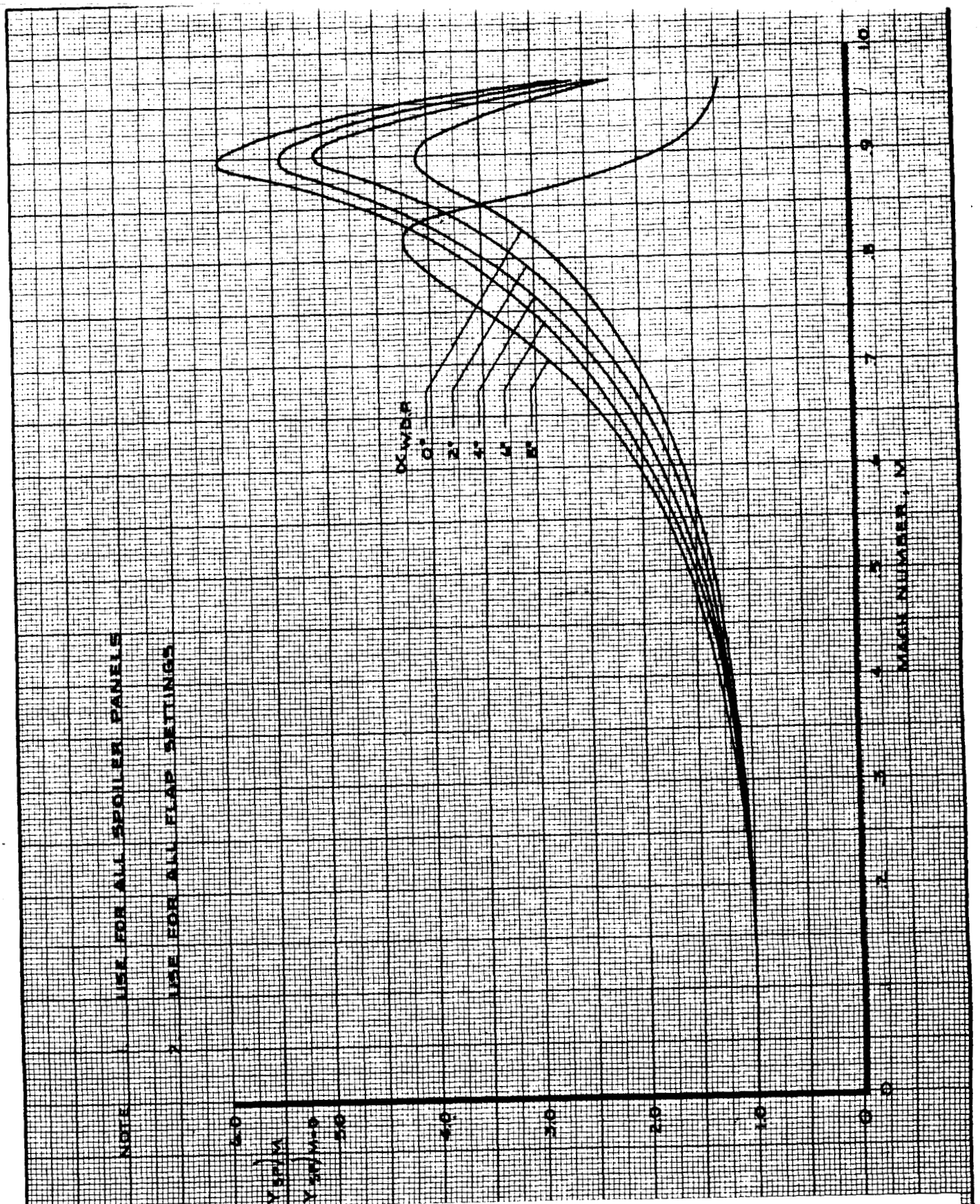

CALC	KUPCIS	12/12/67	REVISED	DATE	SIDE FORCE COEFFICIENT EFFECT OF MACH NUMBER ON SPOILERS	747
CHECK	FOSTER	1-24-68				D6-30643, Vol. II
APR						
APR					THE BOEING COMPANY	PAGE 7.0-12
INK	ODEGARD	12/12/67				

TD 461 C-R4

CYSPM

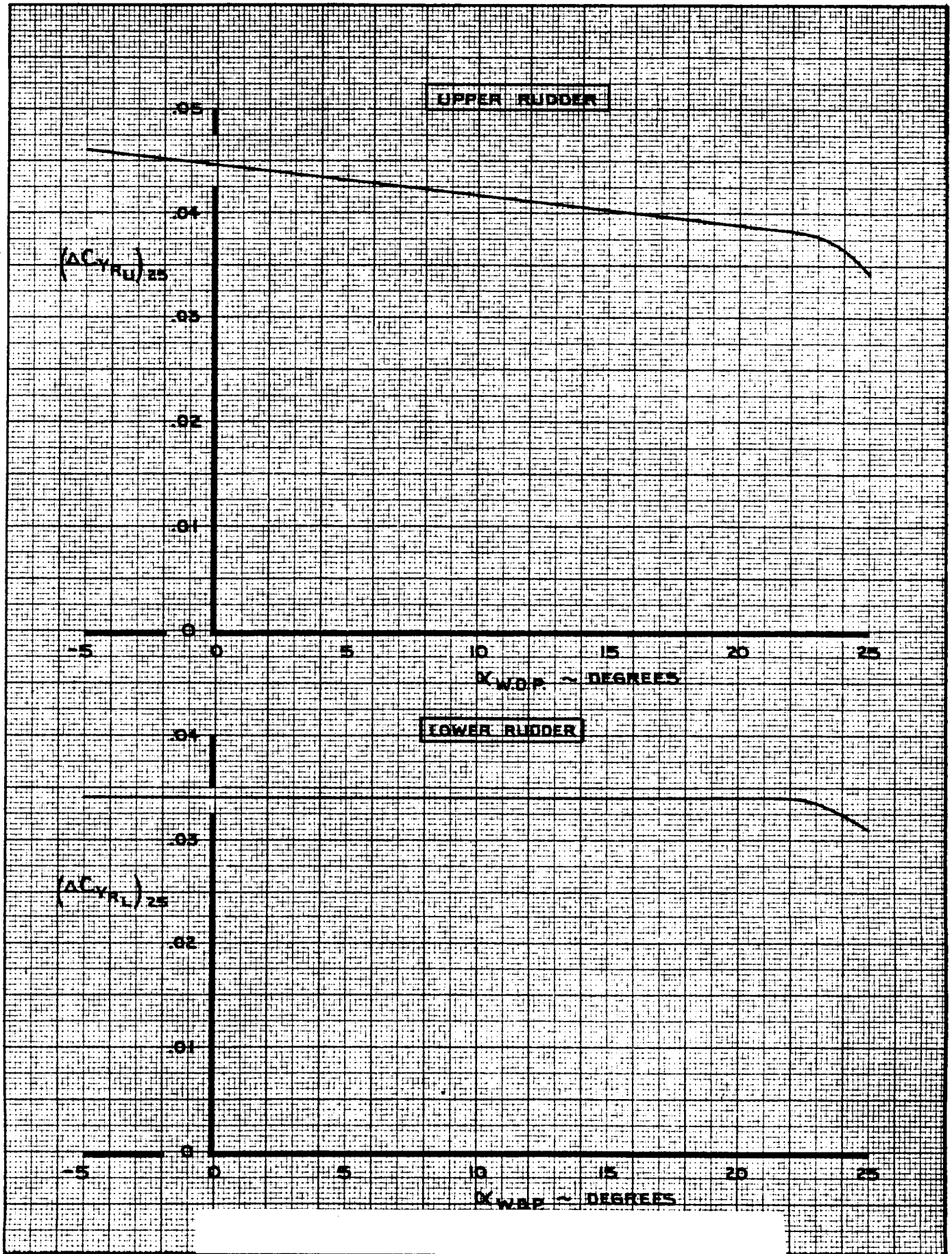

CALC	RICHARDSON	12-9-67	REVISED	DATE	SIDE FORCE COEFFICIENT EFFECT OF RUDDERS	747
CHECK	FOSTER	1-24-68	BECK	1-28-70		D6-30643 Vol. II
APR						
APR						
INK	ODEGARD	12-9-67			THE BOEING COMPANY	PAGE 7.0-13

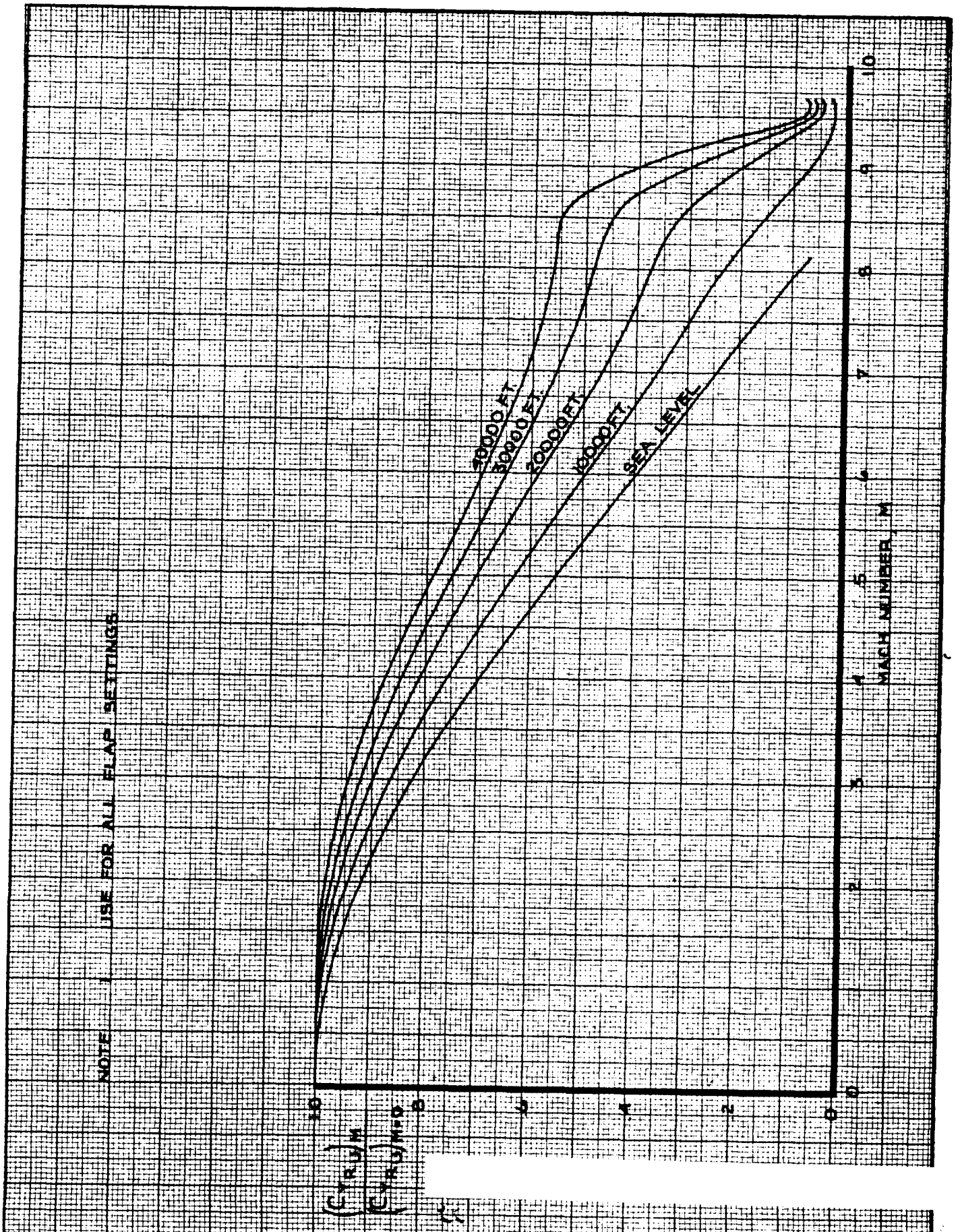

CALC	RICHARDSON	12-9-67	REVISED	DATE	SIDE FORCE COEFFICIENT △ AEROELASTIC EFFECT ON SIDE FORCE COEFFICIENT DUE TO UPPER RUDDER	747
CHECK	FOSTER	1-24-68	LOW	6-14-69		
APR			BECK	2-5-70		D6-30643, Vol. II
APR						
INK	KINSMAN	2-5-70			THE BOEING COMPANY	PAGE 7.0-14

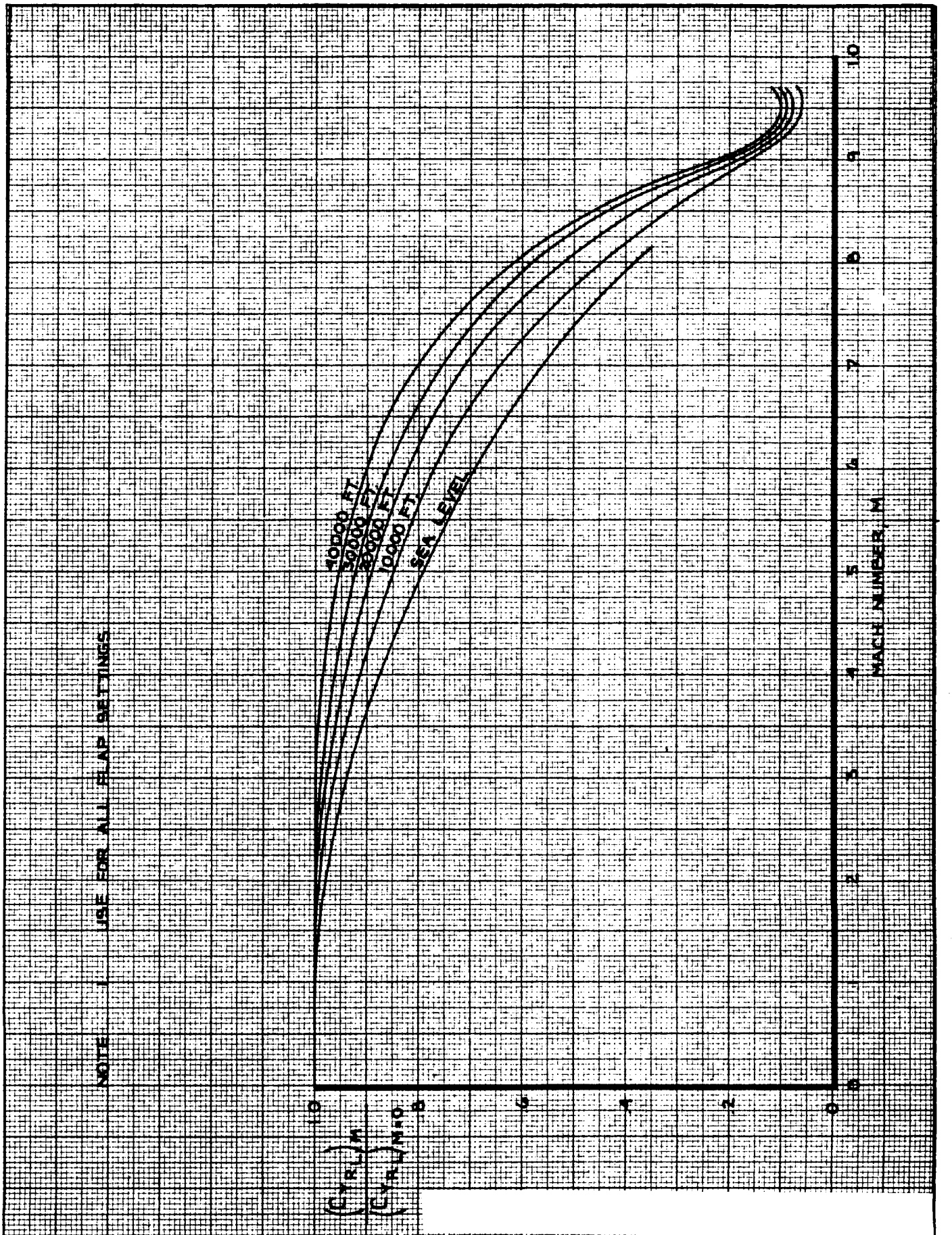

CALC	RICHARDSON	12·8·67	REVISED	DATE	SIDE FORCE COEFFICIENT AEROELASTIC EFFECT ON SIDE FORCE COEFFICIENT DUE TO LOWER RUDDER
CHECK	FOSTER	1·24·68	LOW	6·14·69	
APR			BECK	2·5·70	
APR					
	KINSMAN	2·5·70			

747

D6-30643 Vol. II

THE BOEING COMPANY

PAGE 7.0-15

NOTE 1. RIGHT INBOARD FLAP AT MONITOR LIMITED EXTENSION POSITION CORRESPONDING TO LEFT INBOARD FLAP FAILURE POSITION

2. CHANGE SIGN FOR RIGHT INBOARD FLAP FAILURE

THESE DATA NOT INCLUDED IN NASA SIMULATION

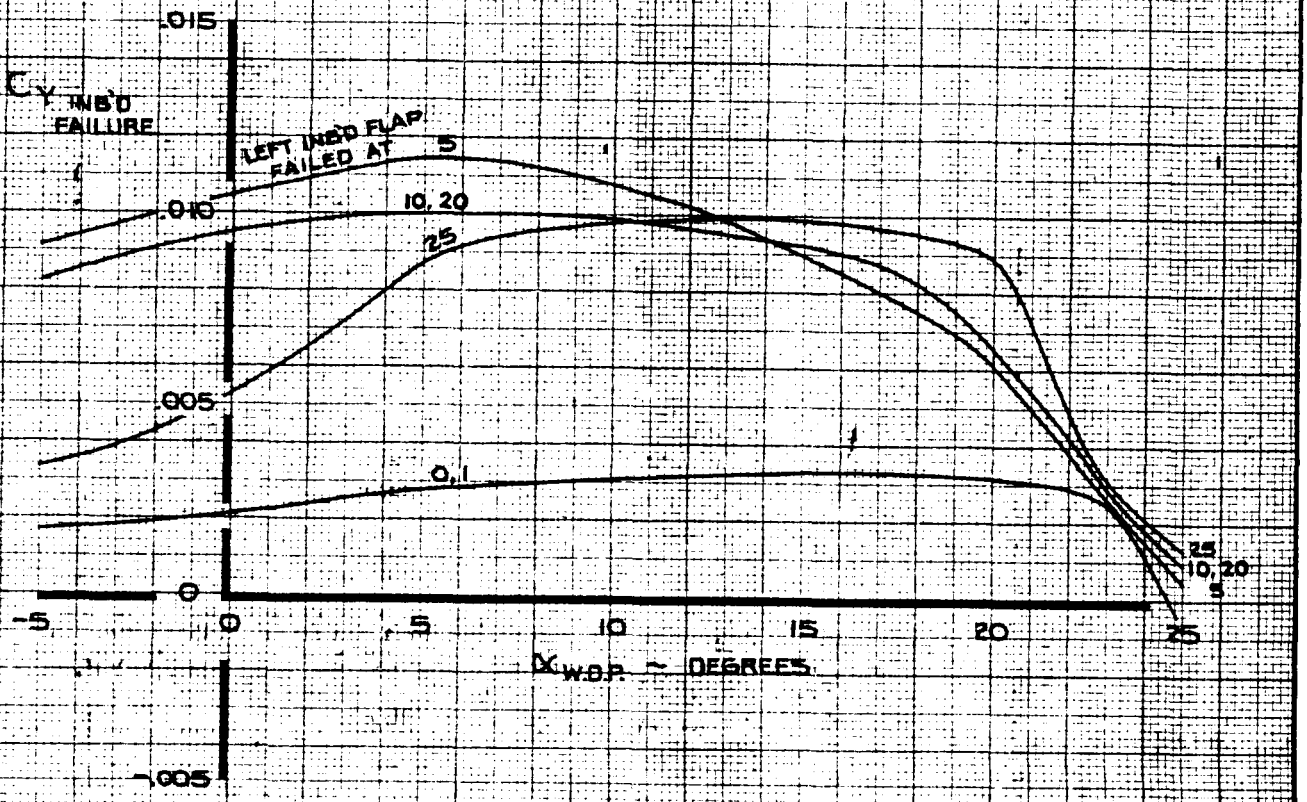

CALC	LOW	5-26-69	REVISED	DATE	SIDE FORCE COEFFICIENT
CHECK			LOW	2-17-70	EFFECT OF ASYMMETRIC INBOARD FLAP FAILURE
APR			LOW	6-25-70	FOR FLAP EXTENSION
APR					
INK	ODEGARD	5-26-69			THE BOEING COMPANY

747
D6-30643 Vol. II
PAGE 7.0-16

TD 461 C-R4

K-E ALBANENE 1961 REV. E

NOTE 1. RIGHT INBOARD FLAP AT MONITOR LIMITED RETRACTION POSITION CORRESPONDING TO LEFT INBOARD FLAP FAILURE POSITION

2. CHANGE SIGN FOR RIGHT INBOARD FLAP FAILURE

THESE DATA NOT [illegible] IN NASA SUMMARY [illegible]

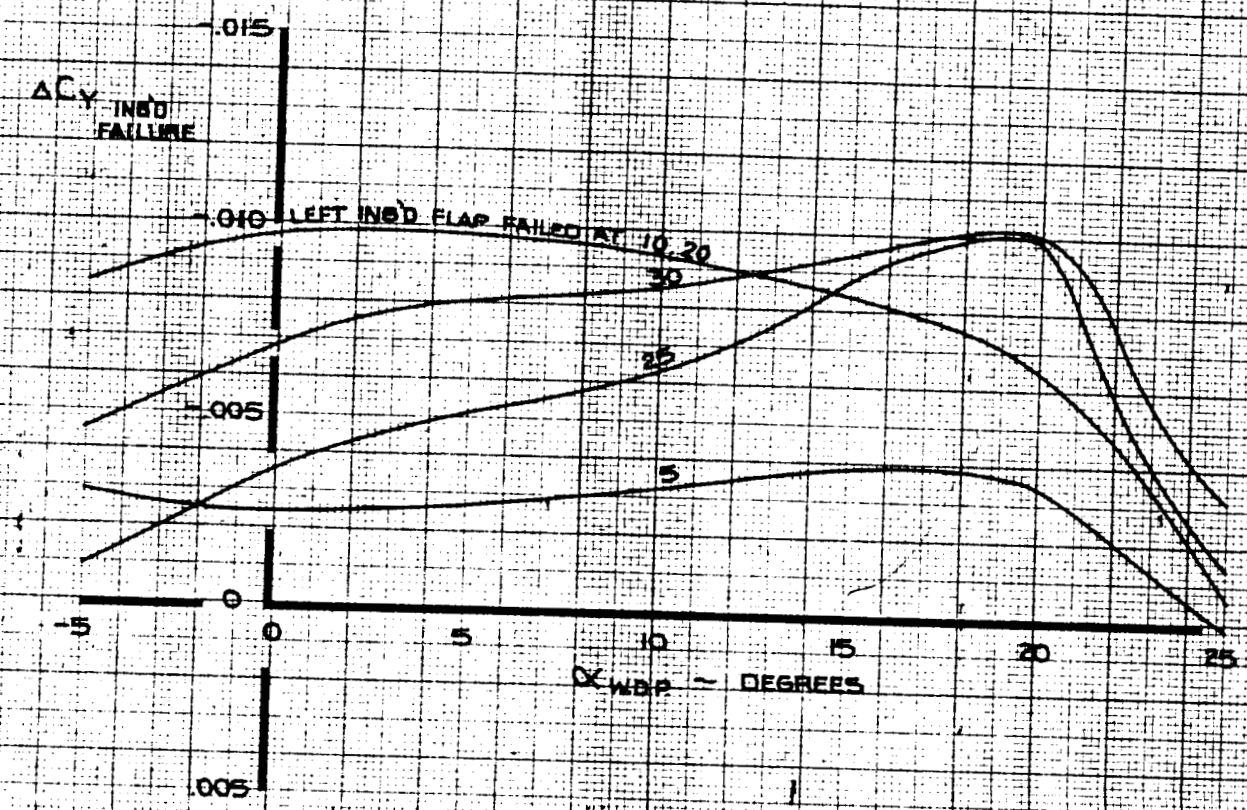

CALC	LOW	5-26-69	REVISED	DATE	SIDE FORCE COEFFICIENT EFFECT OF ASYMMETRIC INBOARD FLAP FAILURE FOR FLAP RETRACTION	747
CHECK			LOW	2-17-70		
APR			LOW	6-25-70		D6-30643, Vol. II
APR						
INK	ODEGARD	5-26-69			THE BOEING COMPANY	PAGE 7.0-17

TD 461 C-R4

K-E ALBANENE 1951 REV E

NOTE 1. RIGHT OUTBOARD FLAP AT MONITOR LIMITED EXTENSION POSITION CORRESPONDING TO LEFT OUTBOARD FLAP FAILURE POSITION

2. CHANGE SIGN FOR RIGHT OUTBOARD FLAP FAILURE

THESE DATA NOT FURNISHED BY NASA SPECIFICATION

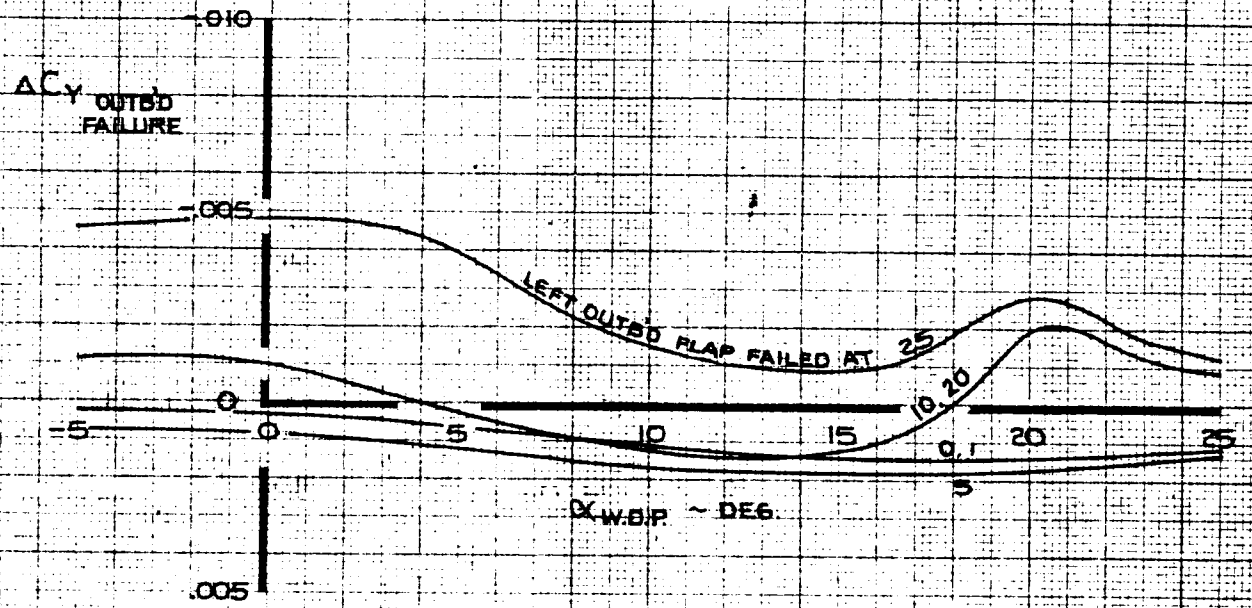

CALC	LOW	5-26-69	REVISED	DATE	SIDE FORCE COEFFICIENT EFFECT OF ASYMMETRIC OUTBOARD FLAP FAILURE FOR FLAP EXTENSION	747
CHECK			LOW	2-17-70		D6-30643 Vol. II
APR			LOW	6-25-70		
APR						
INK	ODEGARD	5-26-69			THE BOEING COMPANY	PAGE 7.0-18

NOTE 1. RIGHT OUTBOARD FLAP AT MONITOR LIMITED RETRACTION POSITION CORRESPONDING TO LEFT OUTBOARD FLAP FAILURE POSITION

2. CHANGE SIGN FOR RIGHT OUTBOARD FLAP FAILURE

THESE DATA NOT INCLUDED IN NASA SIMULATION

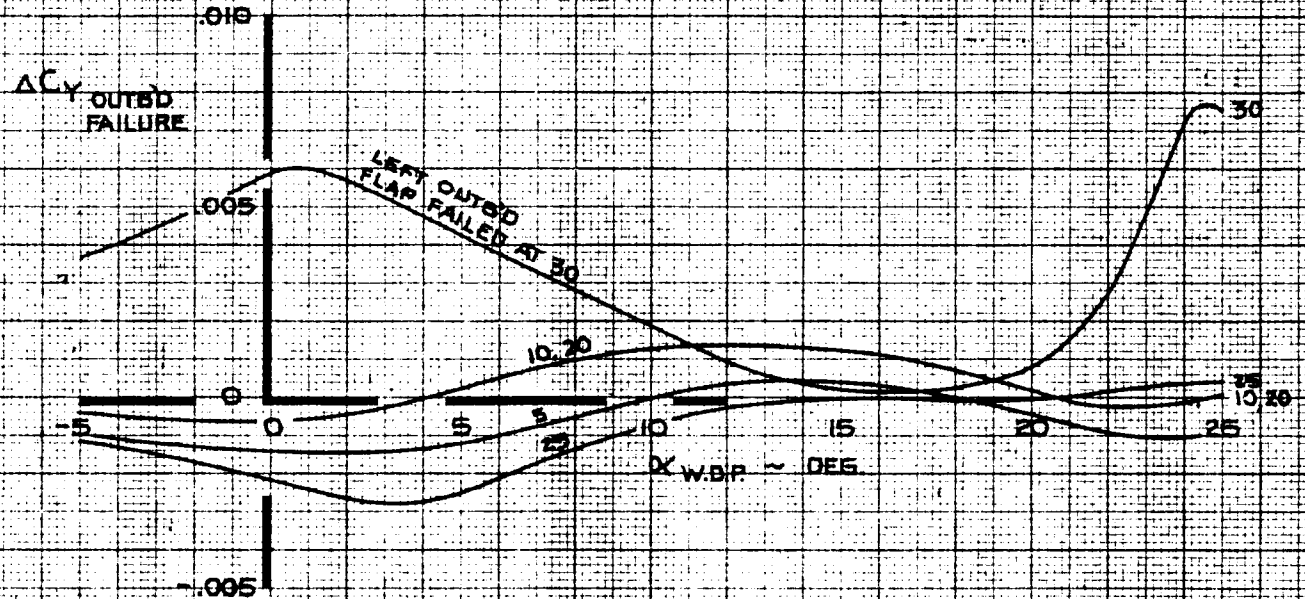

CALC	LOW	5-26-69	REVISED	DATE	SIDE FORCE COEFFICIENT EFFECT OF ASYMMETRIC OUTBOARD FLAP FAILURE FOR FLAP RETRACTION
CHECK			LOW	2-17-70	
APR			LOW	6-25-70	
APR					
INK	ODEGARD	5-26-69			THE BOEING COMPANY

747

D6-30643 Vol. II

PAGE 7.0-19

TD 461 C-R4

K-E ALBANENE 1981 TRACING PAPER REV. E

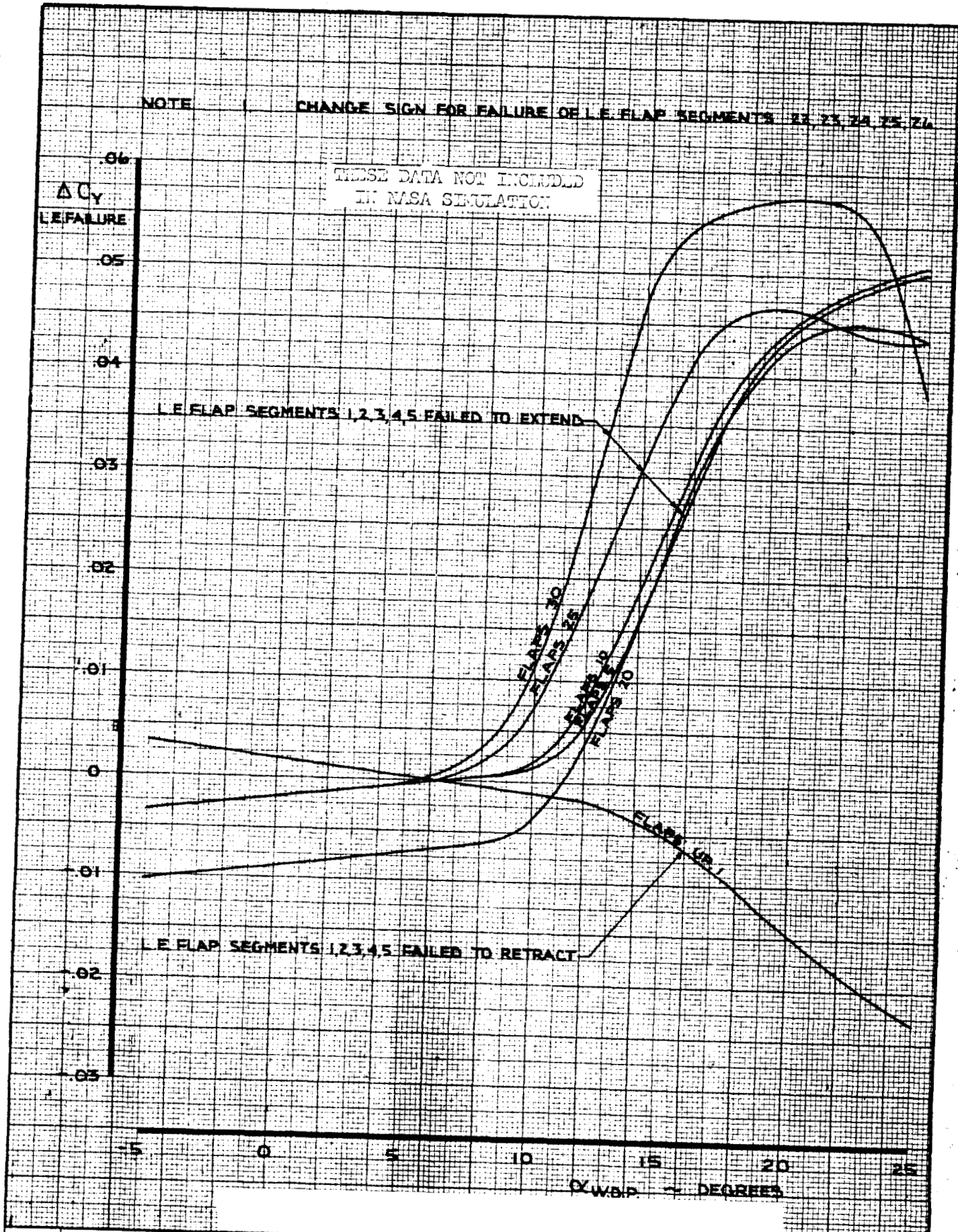

CALC	LOW	8-22-69	REVISED	DATE	SIDE FORCE COEFFICIENT EFFECT OF ASYMMETRIC L.E. FLAP SEGMENTS 1,2,3,4,5 OR 22,23,24,25,26	747
CHECK			LOW	3-13-70		
APR			LOW	6-26-70		D6-20423
APR						
INK	KINSMAN	8-22-69			THE BOEING COMPANY	PAGE 7.0-20

NOTE 1. CHANGE SIGN FOR FAILURE OF L.E. FLAP SEGMENTS 19, 20, 21

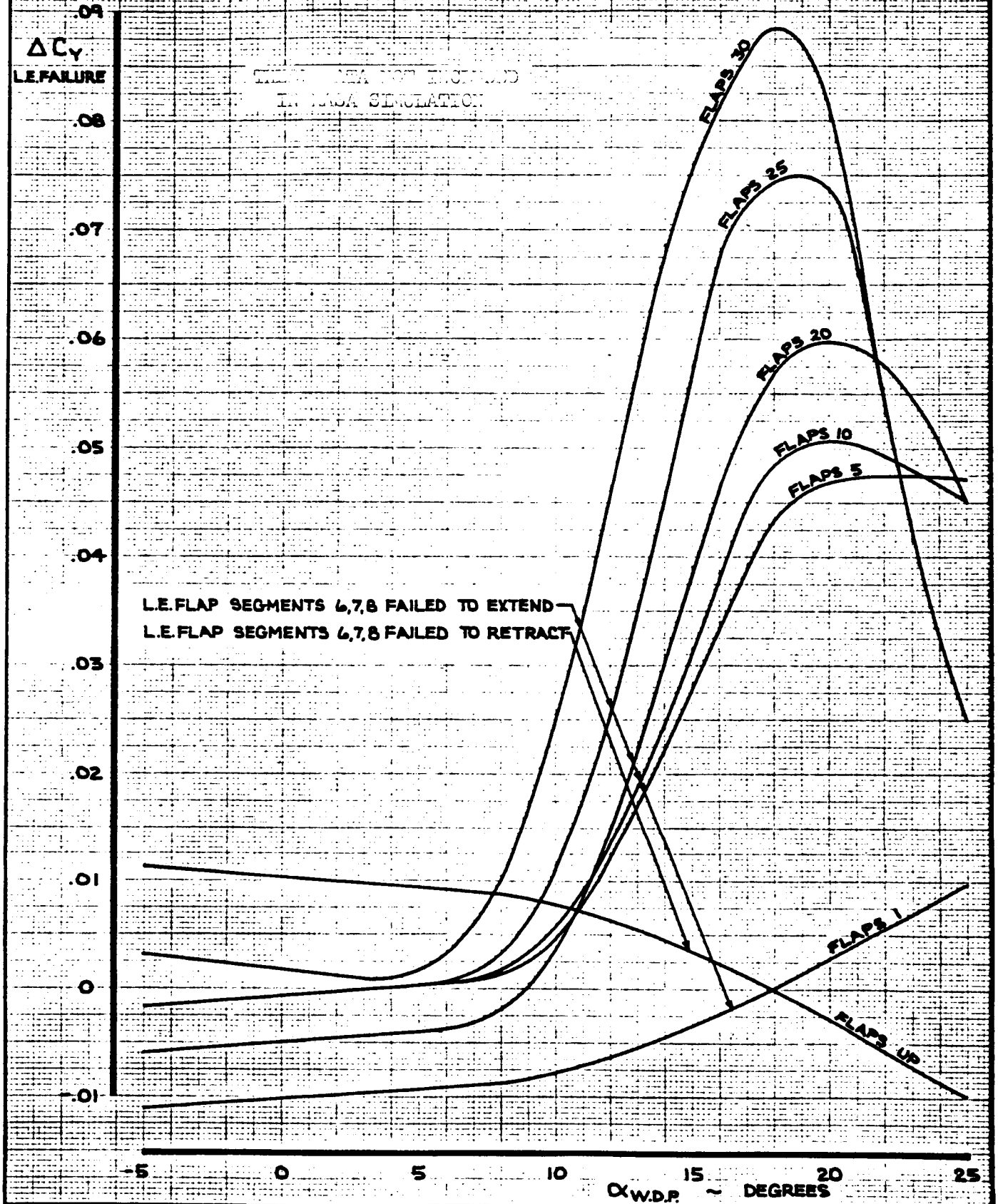

CALC	LOW	8-22-69	REVISED	DATE	SIDE FORCE COEFFICIENT EFFECT OF ASYMMETRIC L.E. FLAP SEGMENTS 6,7,8 OR 19,20,21	747
CHECK			LOW	3-13-70		D6-30643 Vol. II
APR						
APR					THE BOEING COMPANY	PAGE 7.0-21
INK	KINSMAN	8-22-69				

AD 461 C-R4

K-E ALBANENE 100L TRACING PAPER REV. D

236

8.0 LONGITUDINAL CONTROL SYSTEM

A general description of the longitudinal system is presented in the Introduction on Pages 1.2-1 and 1.2-2 and in Volume I. A block diagram of the simulated elevator control system and stick force program is shown on Page 8.1-3 . The data for each particular block can be found on the page numbers adjacent to the block.

8.1 Control Column Force and Elevator Deflection

The column travel in the 747 is 12.67° pull and -12.5° push. The column travel in the FSAA is $\pm 11^{\circ}$. The column deflection of the FSAA was scaled up by 1.15 (= 12.67/11) so that maximum column in the FSAA resulted in maximum column in the simulated 747.

The feel unit pressure, used in determining the feel unit torque, is

$$P_f = \frac{dFs}{d\delta e} \cdot (-120.9) \quad lb/in^2$$

where

$$\frac{dFs}{d\delta e} = \left[-.0025 \cdot q_c + \text{"Fs"}\right] \geq \text{"FQC"}$$

P_f = Feel unit pressure, lb/in^2

$\frac{dFs}{d\delta e}$ = Control column force gradient, lb/deg

"Fs" = Column force gradient at $q_c = 0$. This is plotted on Page 8.1-7

"FQC" = Column force gradient q_c limit. This is plotted on Page 8.1-8

The stick force due to the column mass unbalance is:

$$FS_{\substack{\text{mass} \\ \text{unbalance}}} = n_z \left[\theta_B + \delta_{column} - 5.4\right] \cdot (-.275) \text{ lb}$$

The FSAA control loader was programmed with a breakout force plus a constant gradient for zero computed stick force. The control loader preload characteristics recorded by an x-y plotter are shown on Page 8.1-9. The preload characteristics were subtracted from the computed stick force on the NASA digital computer. The control loader was commanded with an incremental stick force (computed stick force minus preload stick force).

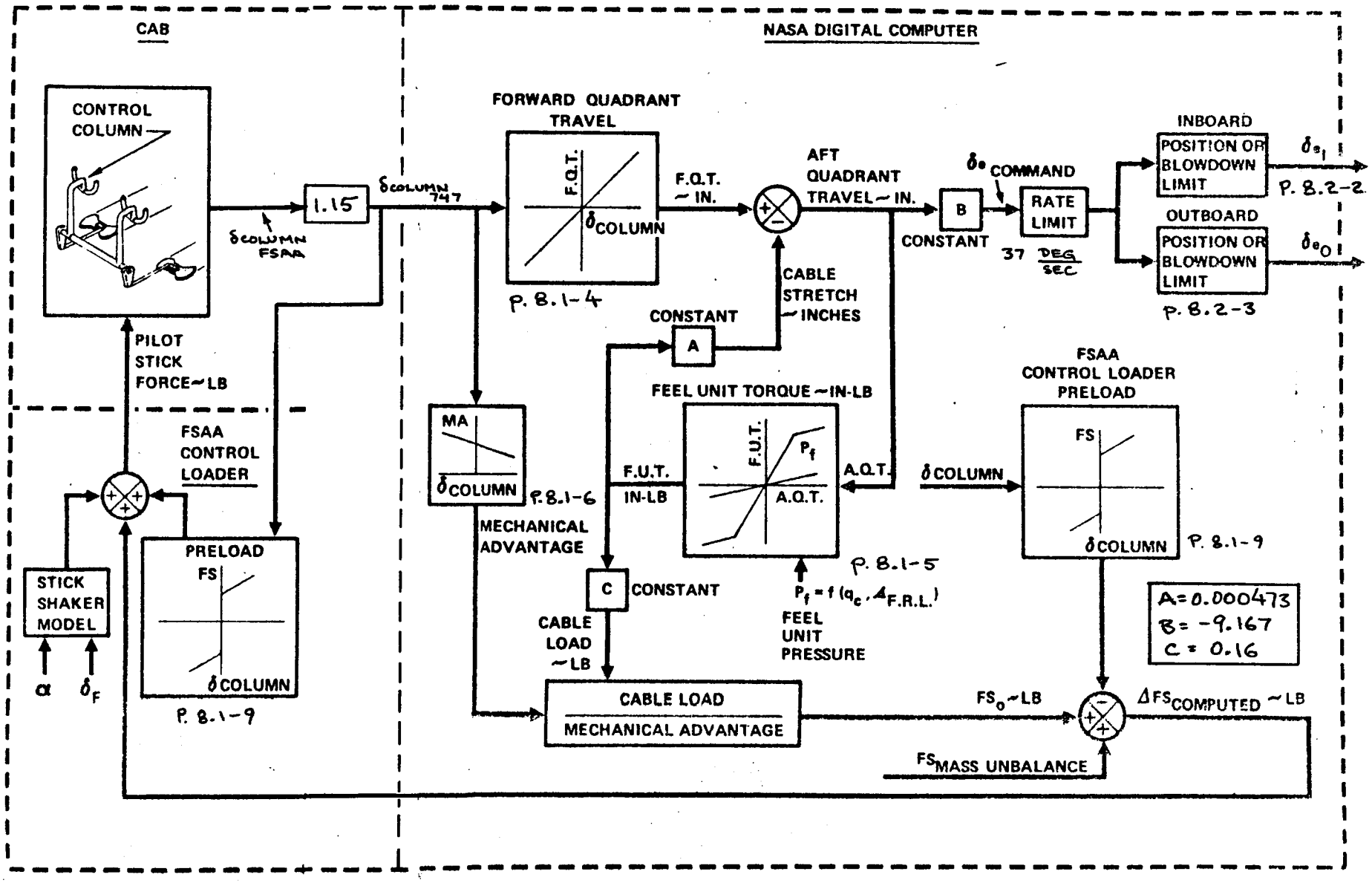

ELEVATOR AND STICK FORCE MODEL

δ_c	F.Q.T.
-12.5	-2.536
-10.0	-2.069
-7.5	-1.582
-5.0	-1.076
-2.5	-.549
0	0
2.5	.574
5.0	1.176
7.5	1.812
10.0	2.489
12.67	3.270

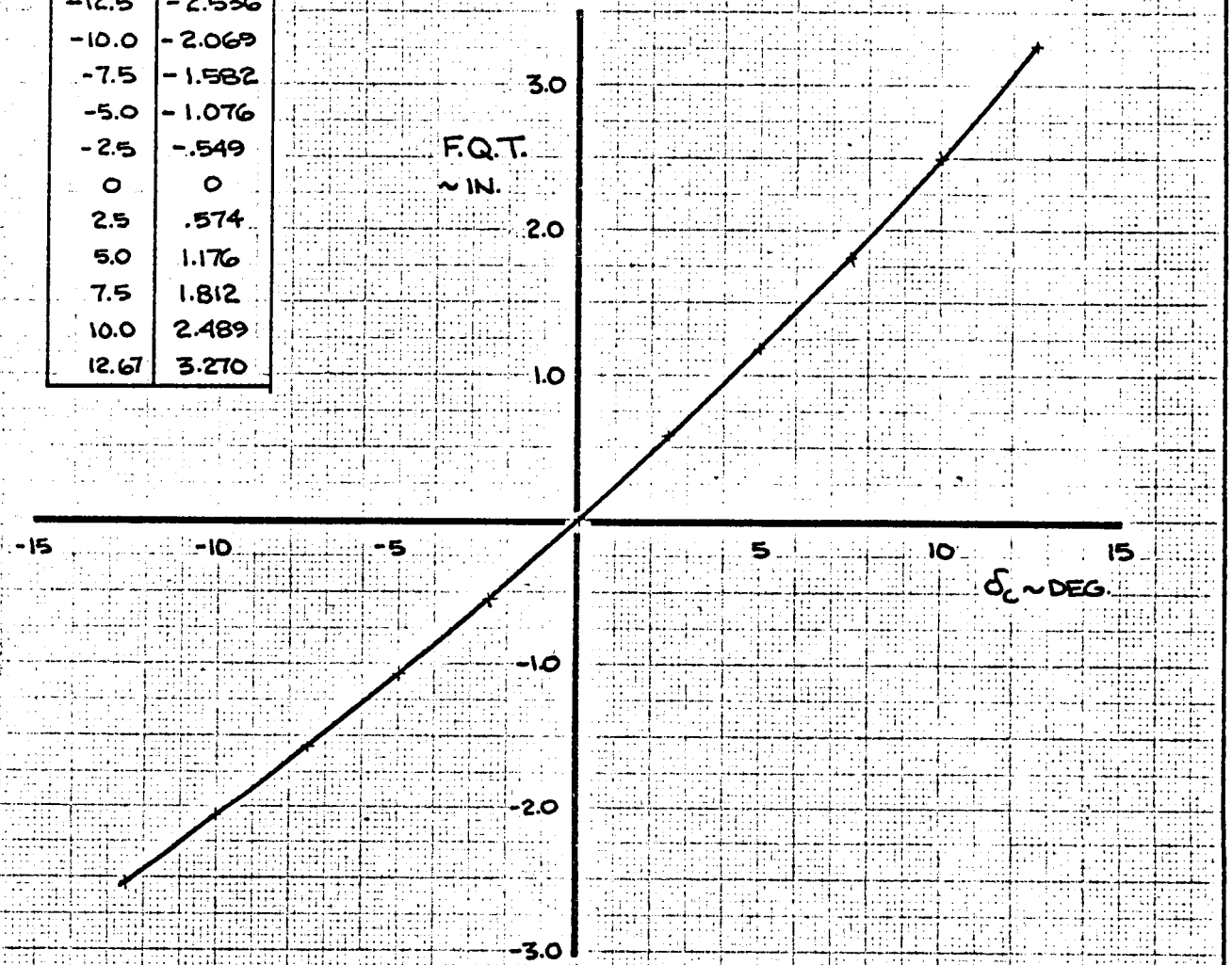

CALC	GLENN	1-14-9	REVISED	DATE
CHECK				
APR				
APR				

FORWARD QUADRANT TRAVEL VS. COLUMN DEFLECTION

THE BOEING COMPANY

747

D6-30643 Vol. II

PAGE 8.1-4

A.Q.T.	F.U.T. $P_f = 0$	F.U.T. $P_f = 2100$
2.727	293.7	2126.7
2.454	266.7	2043.0
2.182	237.6	1954.8
1.909	206.9	1862.7
1.636	175.3	1767.3
1.364	143.3	1669.2
1.091	111.7	1569.1
.818	80.9	1467.6
.573	54.5	1375.5
.436	40.5	1054.0
.218	19.3	531.7
0	0	0
-.218	-22.9	-543.9
-.436	-45.7	-1122.8
-.554	-58.1	-1450.0
-.818	-85.7	-1533.5
-1.091	-114.3	-1616.3
-1.364	-142.8	-1695.6
-1.636	-171.4	-1771.4

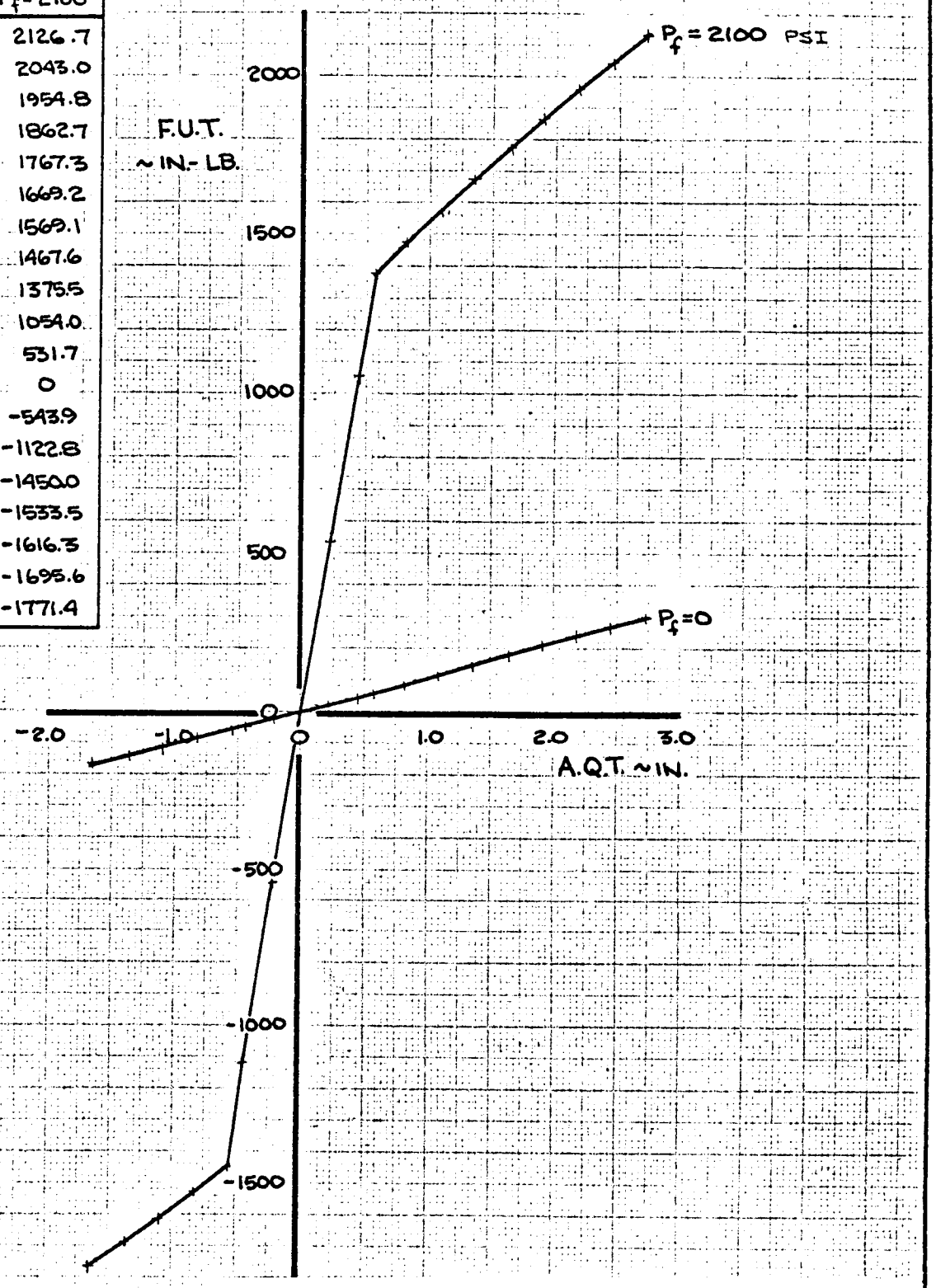

CALC	GLENN	1-15-60	REVISED	DATE
CHECK				
APR				
APR				

FEEL UNIT TORQUE vs. AFT QUADRANT TRAVEL

747

D6-30643 Vol. II

THE BOEING COMPANY

PAGE 8.1-5

TD 461 C-R4

K·E ALBANENE 1961 TRACING PAPER

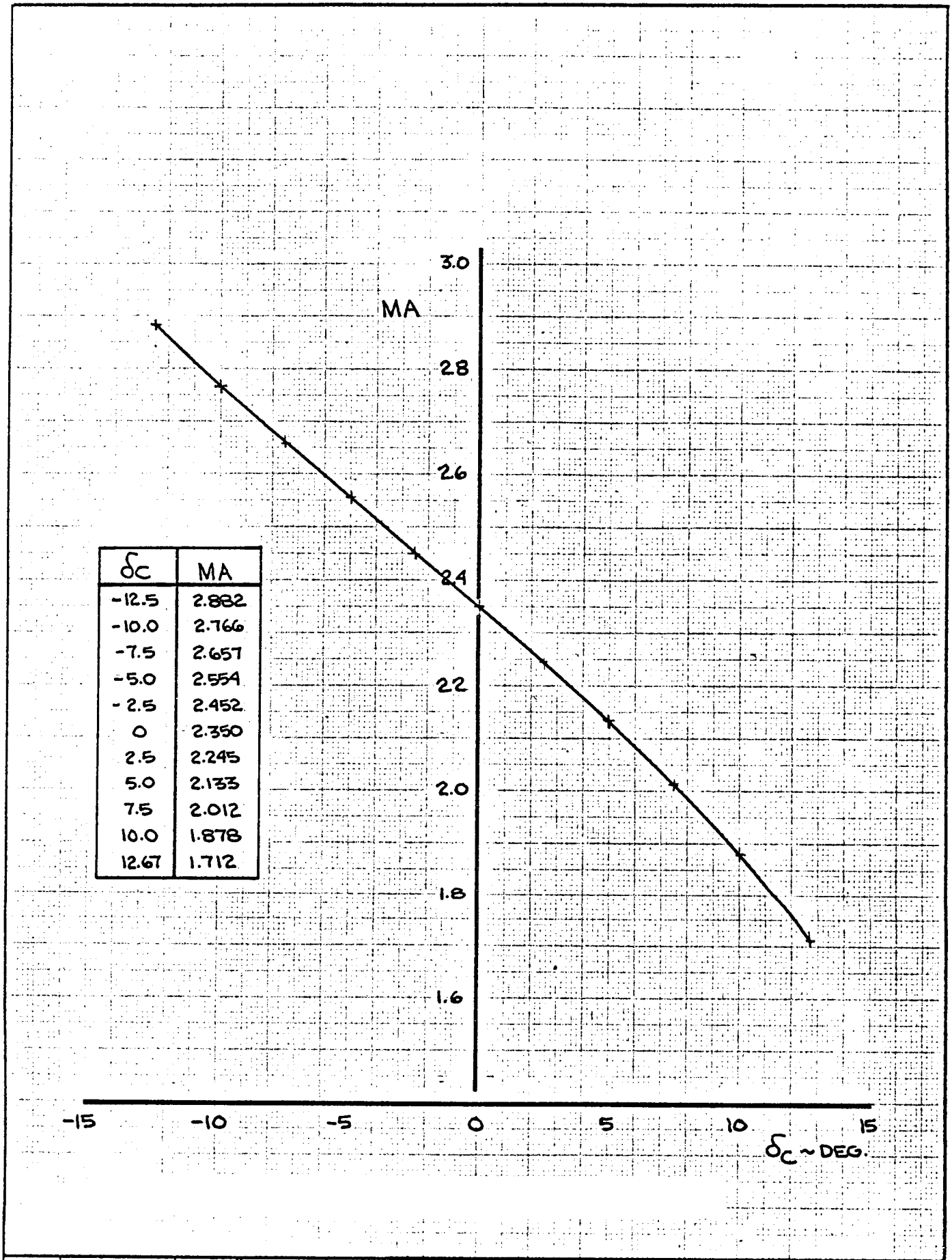

δc	MA
-12.5	2.882
-10.0	2.766
-7.5	2.657
-5.0	2.554
-2.5	2.452
0	2.350
2.5	2.245
5.0	2.133
7.5	2.012
10.0	1.878
12.67	1.712

CALC	GLENN	1-14-9	REVISED	DATE
CHECK				
APR				
APR				

MECHANICAL ADVANTAGE VS. COLUMN DEFLECTION

747

D6-30643 Vol. II

THE BOEING COMPANY

PAGE 8.1-6

TD 461 C-R4

K·E ALBANENE 1961

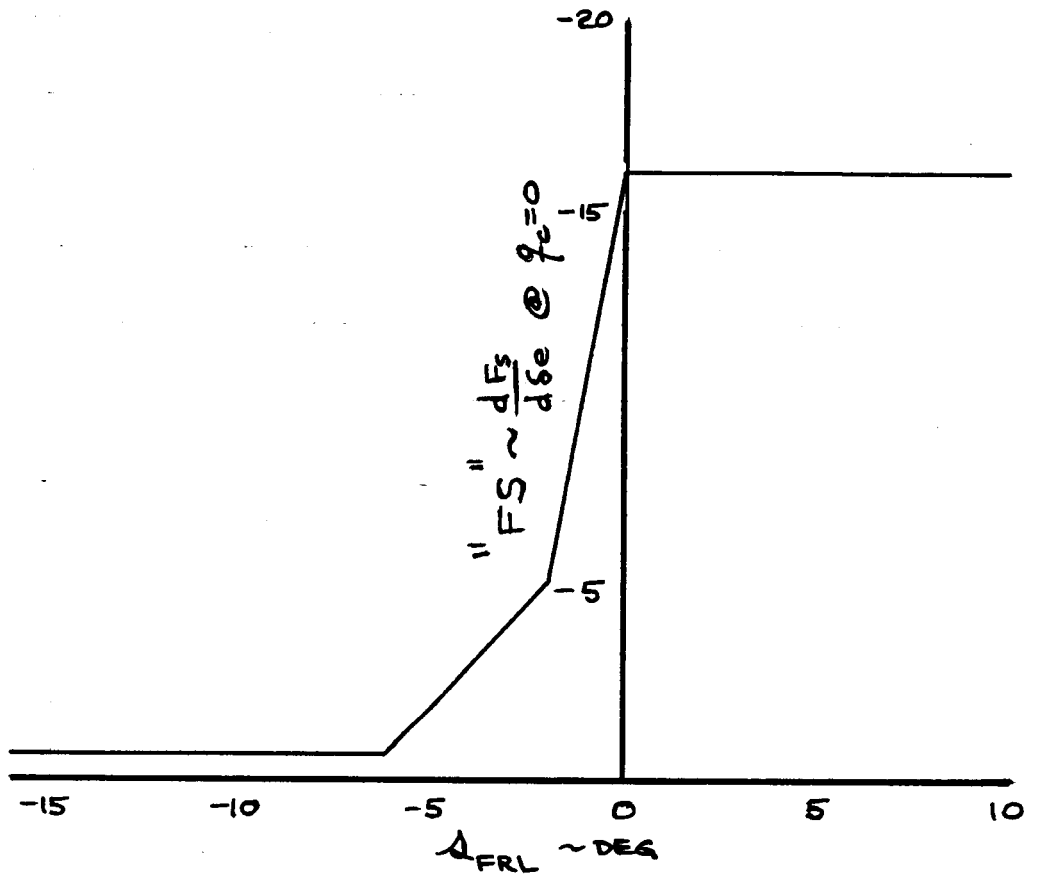

CALC			REVISED	DATE	CONTROL COLUMN FORCE GRADIENT AT $q_c = 0$	747
CHECK						
APR						D6-30643 VOL II
APR						
	NORDWALL	7-22-70			THE BOEING COMPANY	PAGE 8.1-7

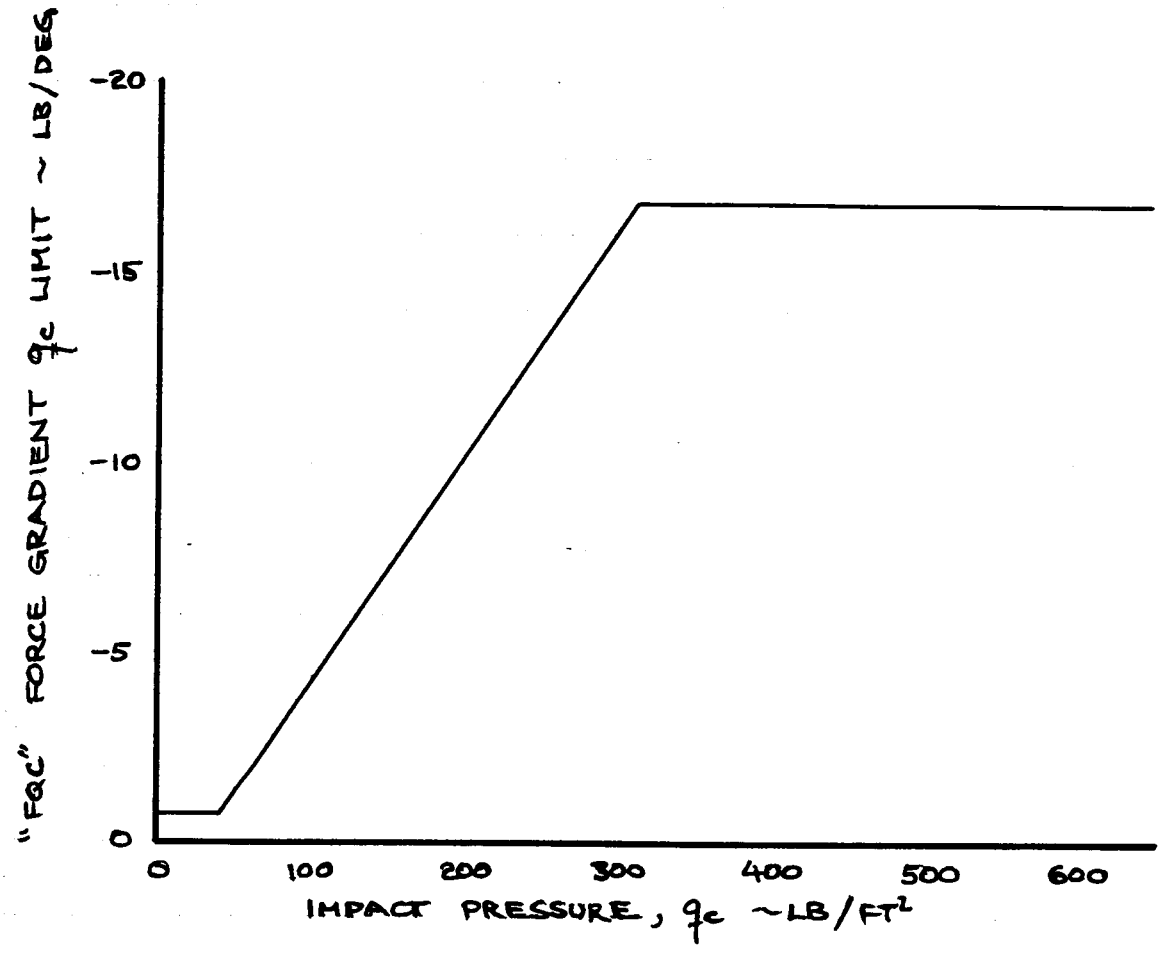

CALC			REVISED	DATE	CONTROL COLUMN FORCE GRADIENT q_c LIMIT	
CHECK						
APR						D6-30643 VOL II
APR						
	NORDWALL	7-22-70			THE BOEING COMPANY	PAGE 8.1-8

NASA
AMES RESEARCH CENTER

8.2 Elevator Control System

8.2.1 Elevator Limits - Boost On and Off

The maximum inboard and outboard elevator limits are shown on pages 8.2-2 and 8.2-3 for full and half boost operation, respectively.

An inboard or outboard elevator surface with both hydraulic systems off will trail at the float angles shown on pages 8.2-4 and 8.2-5, respectively.

8.2.2 Elevator Rigging

The elevator is downrigged at +2° from the faired position.

The outboard elevator angle is equal to the inboard elevator angle up to the blowdown angle of the outboard elevator.

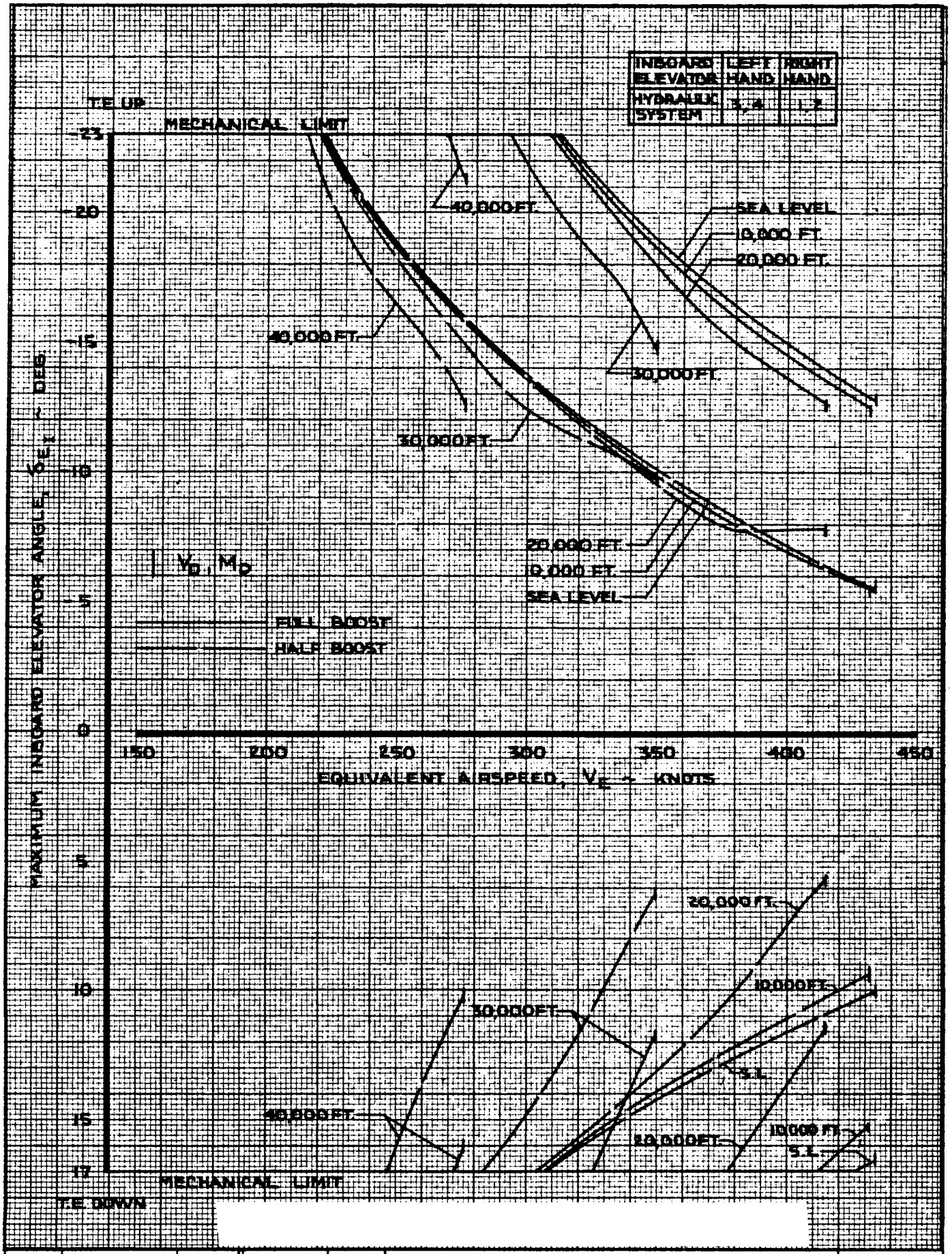

CALC	MOOIWEER	7-3-67	REVISED	DATE	LONGITUDINAL CONTROL △ INBOARD ELEVATOR BLOWDOWN
CHECK	FOSTER	12-14-67	LOW	6-14-69	
APR			HOLTZNER	8-22-69	
APR			LOW	1-21-70	
INK	ODEGARD	7-3-67			THE BOEING COMPANY

747

D6-30643; Vol. II

PAGE 8.2-2

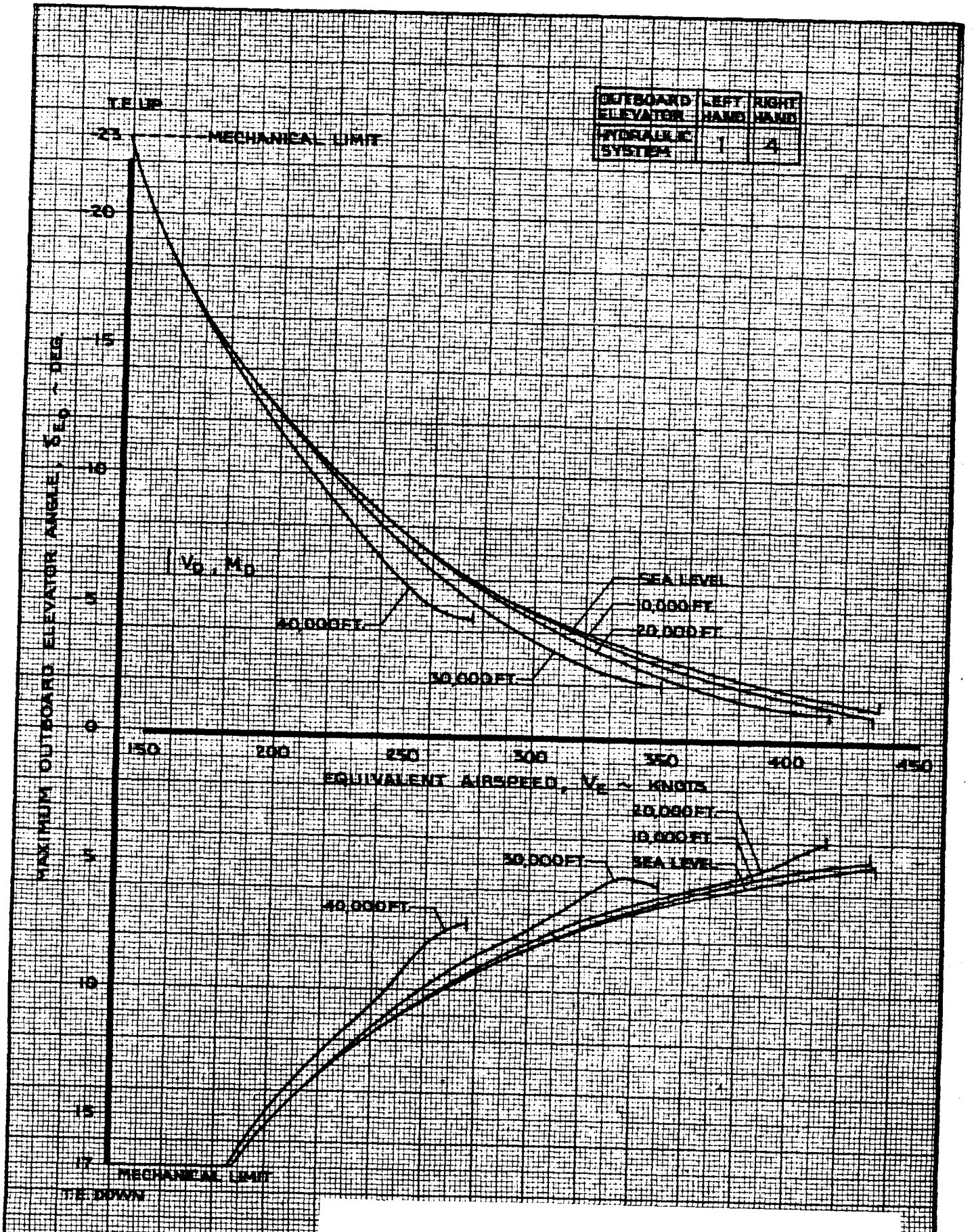

CALC	MOOIWEER	7-3-67	REVISED	DATE	LONGITUDINAL CONTROL △ OUTBOARD ELEVATOR BLOWDOWN
CHECK	FOSTER	12-14-67	LOW	6-14-69	
APR			HOLTZNER	8-22-69	
APR			LOW	1-21-70	
INK	ODEGARD	7-3-67			THE BOEING COMPANY

747

D6-30643, Vol. II

PAGE 8.2-3

AD 461 C-R4

K-E ALBANENE 1881 TRACING PAPER REV. D

NOTE 1. $\delta_{E_I\,FLOAT} = \left(\delta_{E_I\,FLOAT}\right)_{\Delta_{F.R.L.}=0^\circ} + \frac{d\delta_{E_I\,FLOAT}}{d\Delta} \cdot \Delta_{F.R.L.}$

OTHER DATA NOT INCLUDED IN NASA SIMULATION.

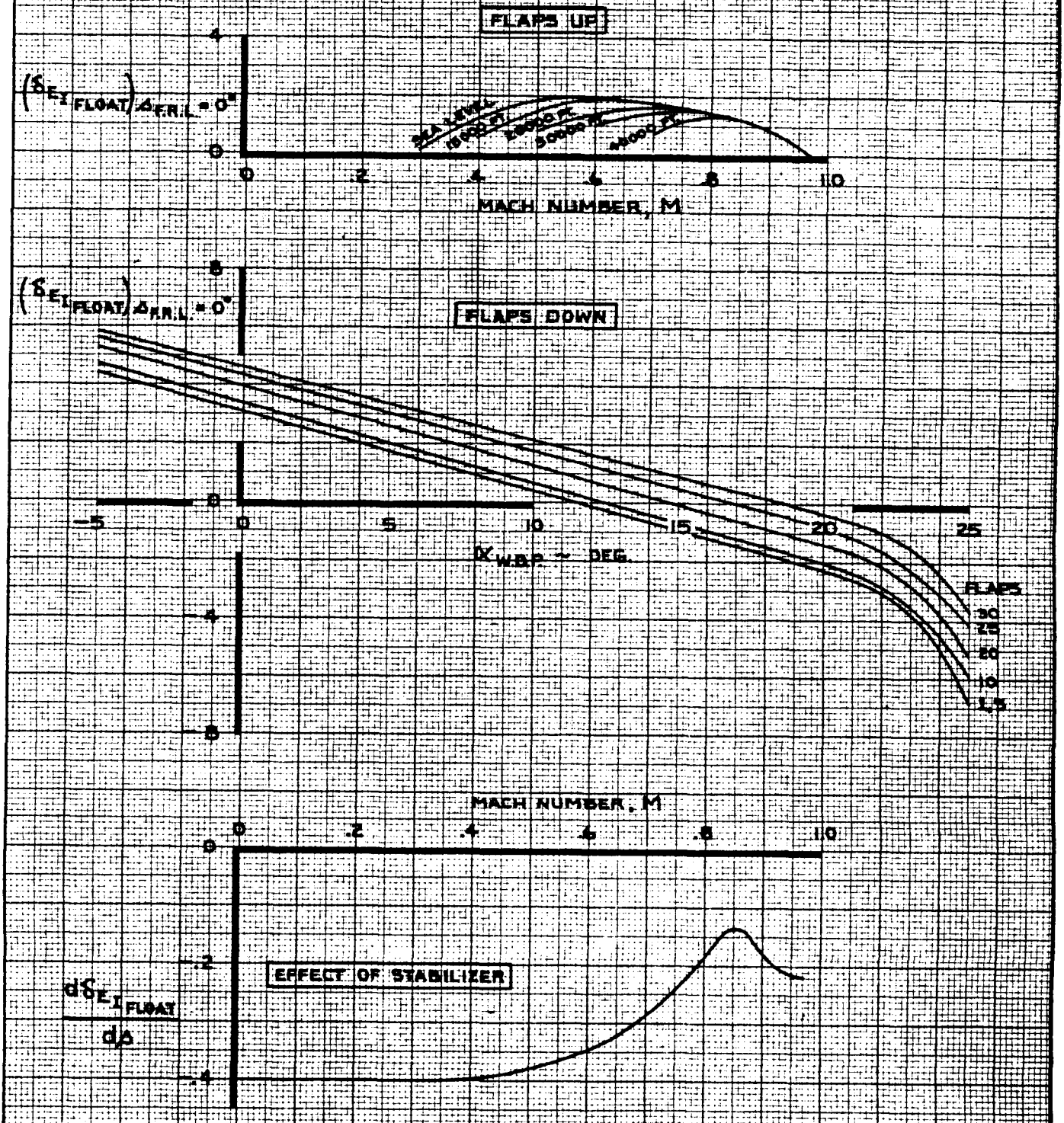

CALC	FOSTER	12-9-67	REVISED	DATE	LONGITUDINAL CONTROL INBOARD ELEVATOR FLOAT ANGLES
CHECK	HOLTZNER	1-15-68	LOW	2-6-70	
APR					
APR					
INK	ODEGARD	2-6-70			

747

D6-30643, Vol. II

THE BOEING COMPANY

PAGE 8.2-4

AD 461 C-R4

K-E ALBANENE 1961 TRACING PAPER REV. D

NOTE: $\delta_{E_{0_{FLOAT}}} = (\delta_{E_{0_{FLOAT}}})_{A_{F.R.L.}=0^\circ} + \frac{d\delta_{E_{0_{FLOAT}}}}{d\delta} \cdot A_{F.R.L.}$

THESE DATA NOT ENDORSED BY NASA SIMULATION

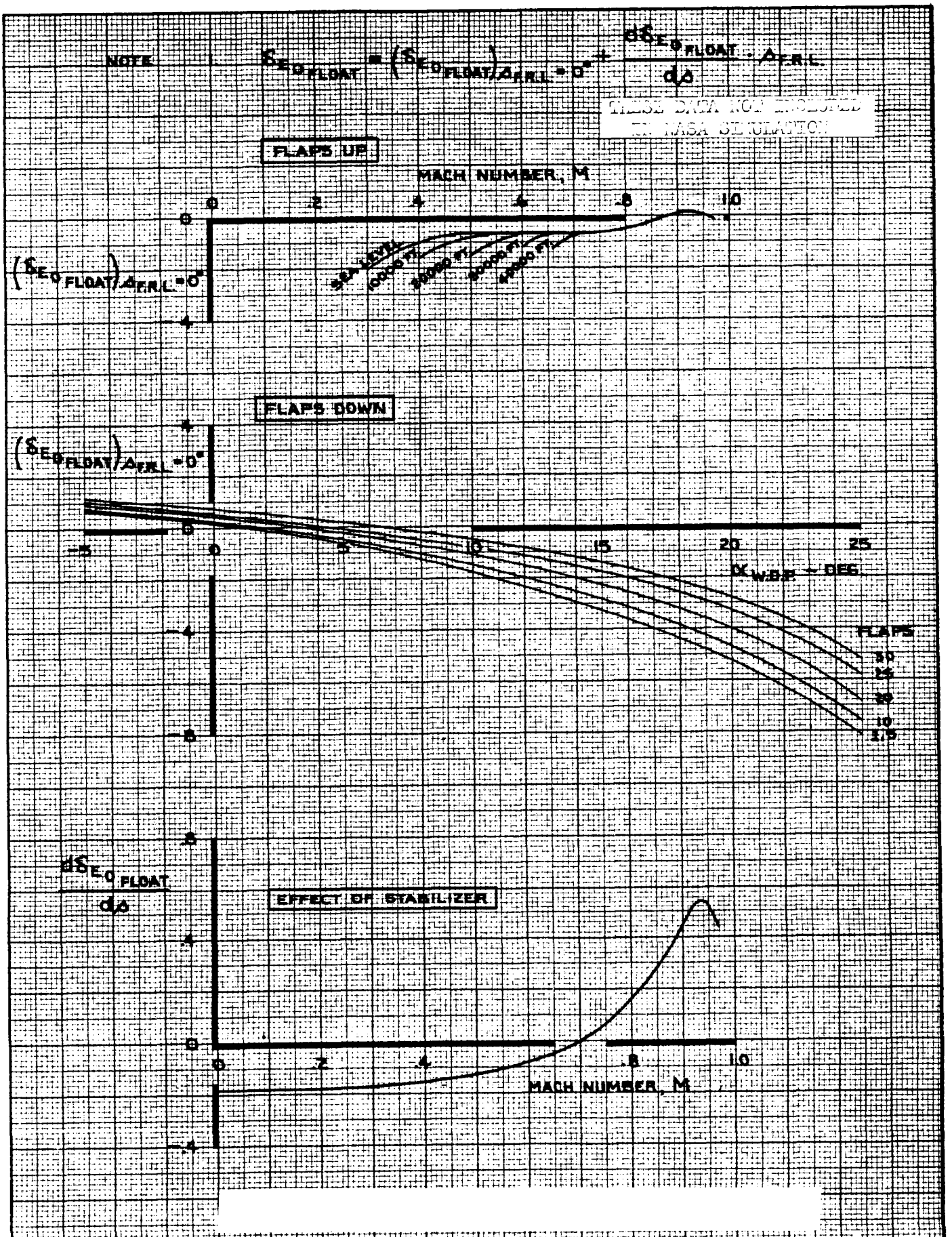

CALC	FOSTER	12-9-67	REVISED	DATE	LONGITUDINAL CONTROL OUTBOARD ELEVATOR FLOAT ANGLES	747
CHECK	HOLTZNER	1-15-68	LOW	2-6-70		D6-30643 Vol. II
APR						
APR					THE BOEING COMPANY	PAGE 8.2-5
INK	ODEGARD	2-6-70				

8.3 Stabilizer Trim System

8.3.1 Trim Rate

A block diagram of the simulated trim system is shown on Page 8.3-1. The stabilizer trim rate is programmed by impact pressure, q_c. Page 8.3-2 shows the pilot and autopilot trim rates.

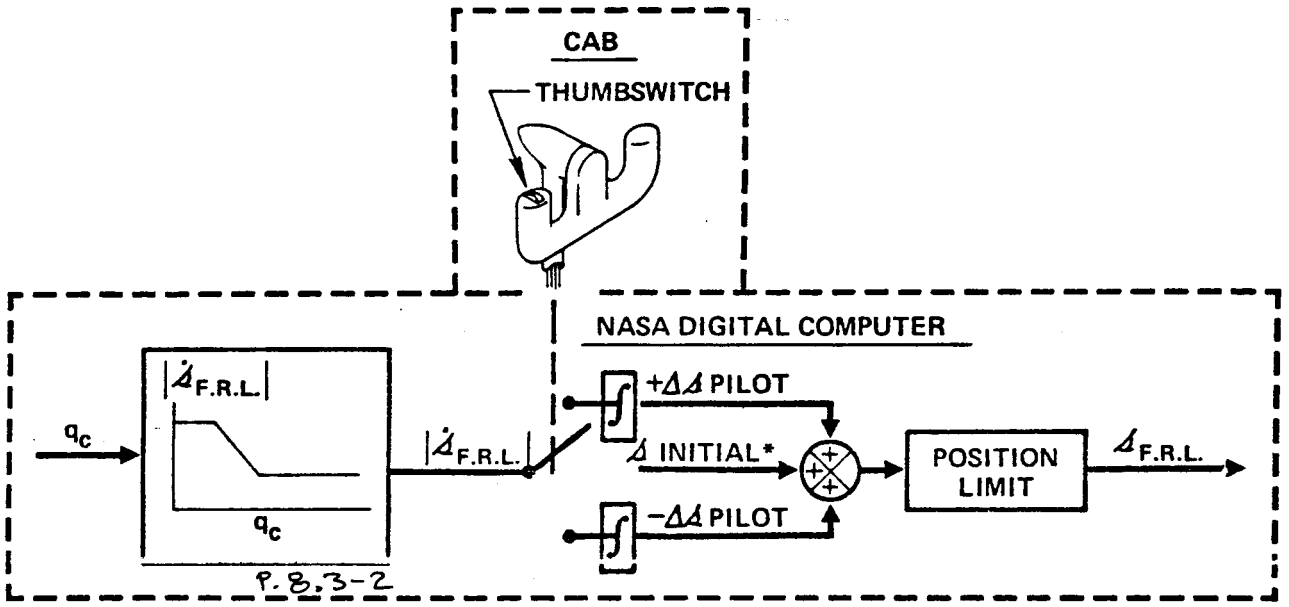

*SET BY COMPUTER TRIM PROGRAM

STABILIZER TRIM

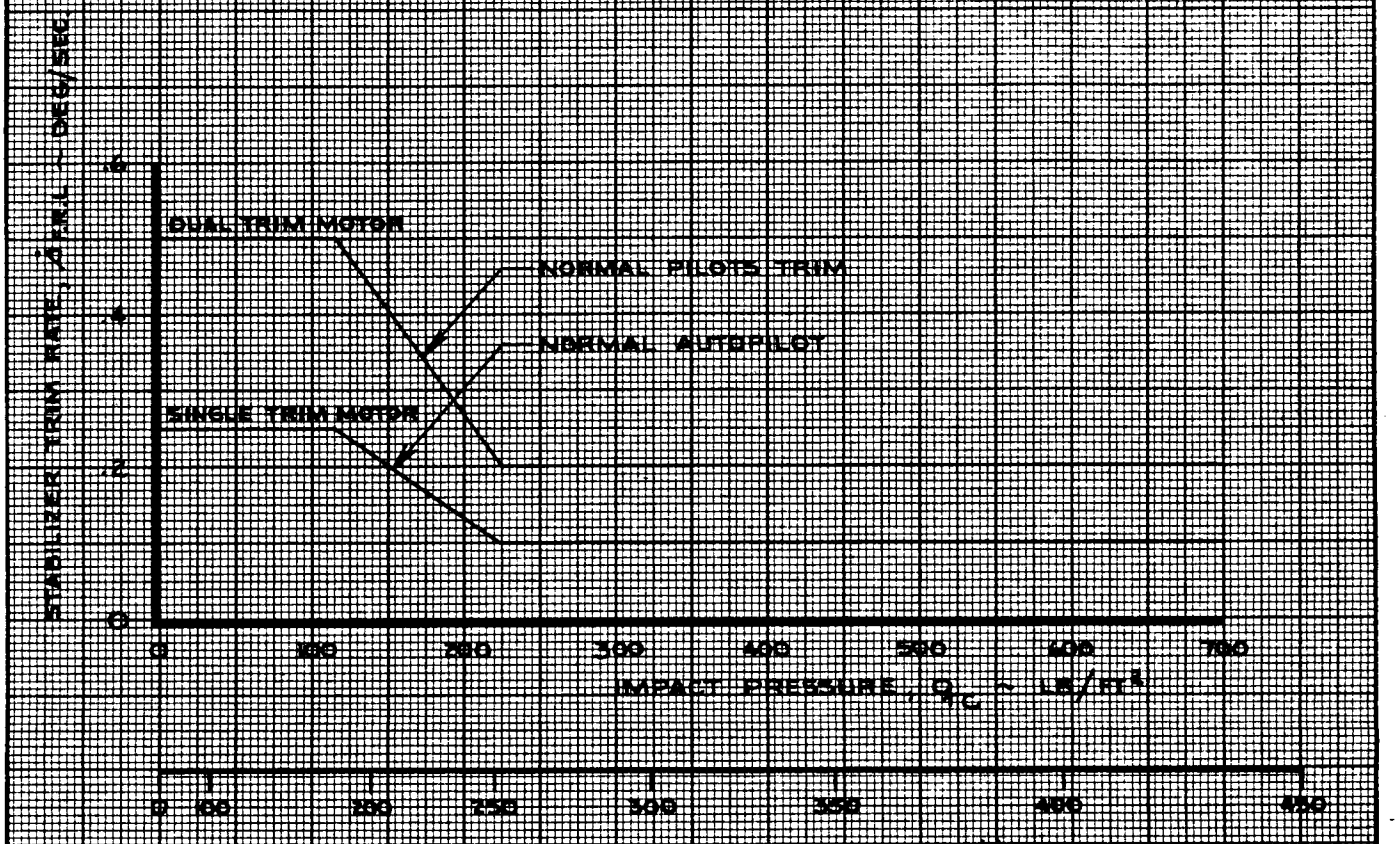

CALC	HOLTZNER	11/17/67	REVISED	DATE	LONGITUDINAL CONTROL STABILIZER TRIM RATE
CHECK	FOSTER	12/14/67	LOW	6-14-69	
APR			LOW	1-29-70	
APR					
INK	ODEGARD	11/17/67			

747

D6-30643 Vol. II

THE BOEING COMPANY

PAGE 8.3-2

TD 461 C-R4

REV. D

9.0 LATERAL CONTROL SYSTEM

A general description of the system is presented in the Introduction on Pages 1.2-2, 1.2-3 and 1.2-4 and in Volume I. A block diagram of the NASA simulated lateral control system is shown on Page 9.1-2a. The data for each particular block can be found on the page number adjacent to the block. The computer requirements for the simulation were reduced by applying an equivalent rate limit to the wheel rather than to each spoiler panel. The outboard aileron lockout program utilized in the simulation was a function of flap screw travel, Page 9.2-8, rather than a function of time, as shown on Page 9.2-4.

9.1 Control Wheel Force and Angle

9.1.1 Control Wheel Force

$$F_W = F_{W_S} \pm F_{W_{FR}}$$

where,

F_W = Control wheel force, positive for a clockwise wheel moment (lb).

F_{W_S} = Control wheel force due to the spring and cam mechanism (lb). This is plotted on page 9.1-3.

$F_{W_{FR}}$ = Friction force opposing control wheel motion (= 2.0 lb).

9.1.2 Control Wheel Angle

$$\delta_W = \delta_{W_{REF.}} + .35 F_W$$

where,

δ_W = Control wheel angle (degrees). The control wheel limits are $\delta_W = \pm 88$ degrees.

$\delta_{W_{REF.}}$ = Reference control wheel angle (degrees). This does not include the effect of cable stretch and is the input to the aileron and spoiler programs plotted on pages 9.2-3 and 9.2-5 respectively.

.35 = Cable stretch factor (deg/lb).

9.1.3 Lateral Trim

$\delta_{W_{TRIM}}$ = Zero force datum wheel angle due to trim (degrees). This is plotted on page 9.1-4. The trim shifts the wheel force datum but does not change the wheel limits. The trim limits are ± 6.27 units. The nominal trim rate is 2.5 degrees of control wheel per second.

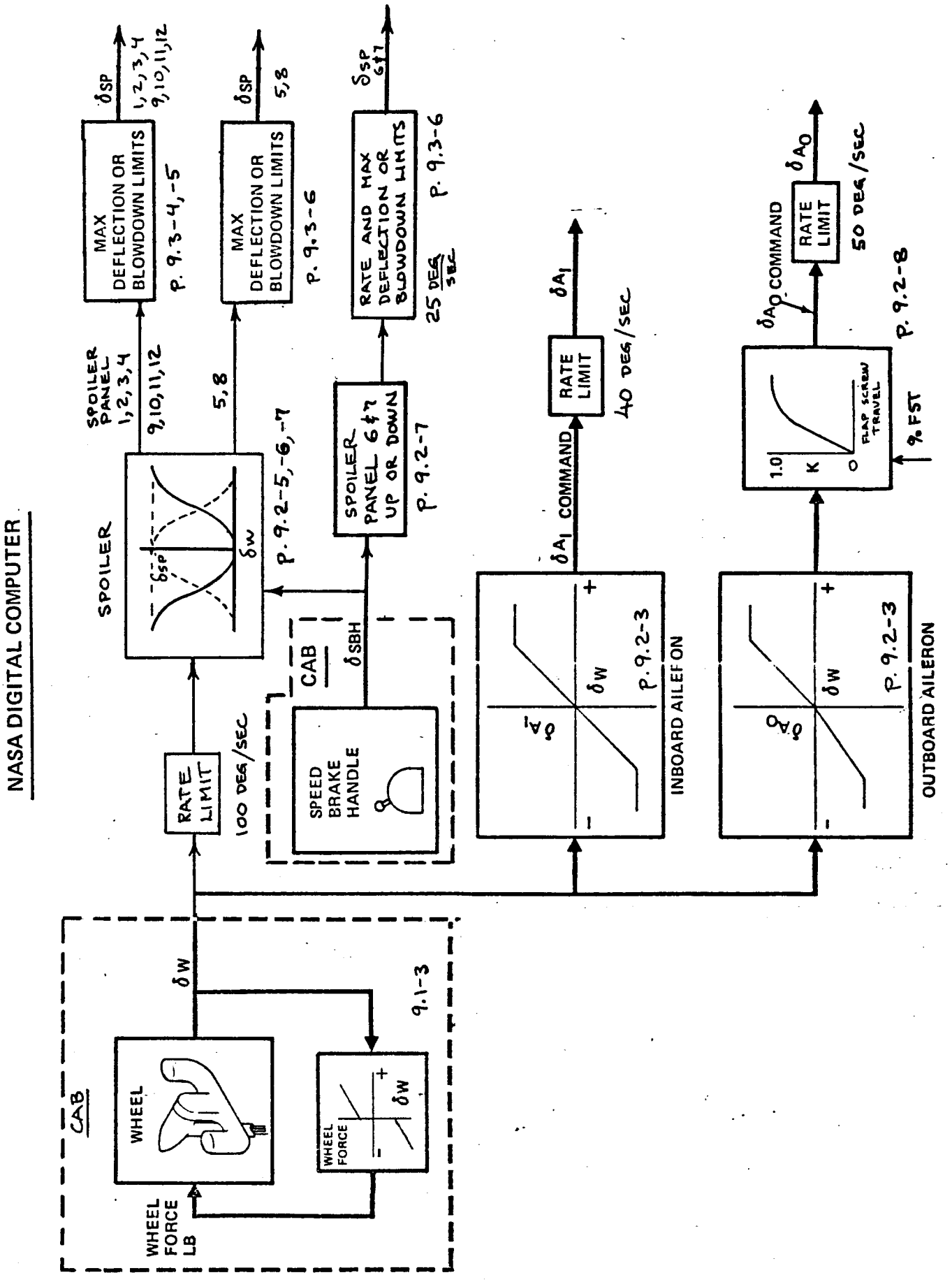

CALC	DRN	JULY 1970	REVISED	DATE
CHECK				
APPD				
APPD				

LATERAL CONTROL SYSTEM MODEL

BOEING NO. D6-30643 VOL II

REV LTR: SECT PAGE

NOTE 1. $F_W = F_{WS} + F_{WFR}$

2. $F_{W_{FR}} = 2.0$ LB.

3. SYMMETRIC FOR OPPOSITE WHEEL

4. CONTROL WHEEL LIMITS ARE $\delta_W = \pm 68°$

THESE DATA NOT INCLUDED IN NASA SIMULATION SEE P. 14.1-52

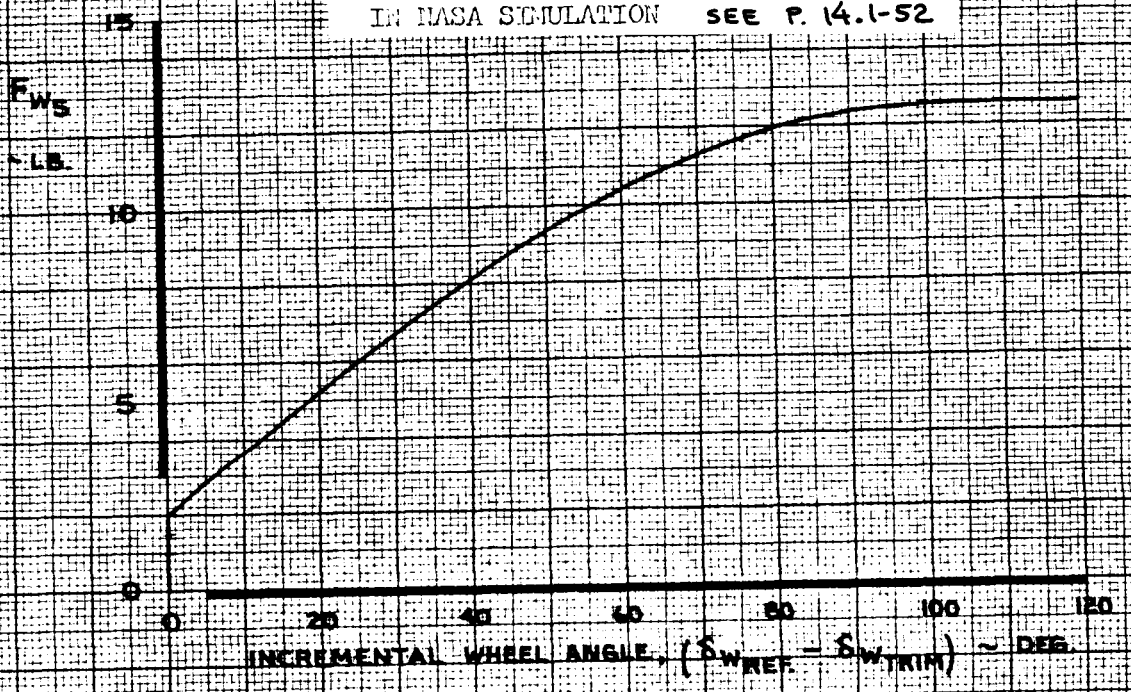

CALC	HOLTZNER	12-2-67	REVISED	DATE	LATERAL CONTROL	747
CHECK	FOSTER	12-14-67	HOLTZNER	4-19-68	FORCE DUE TO SPRING AND CAM MECHANISM	D6-30643 Vol. II
APR			KUPCIS	1-22-70		
APR					THE BOEING COMPANY	PAGE 9.1-3
INK	ODEGARD	2-10-70				

THESE DATA NOT INCLUDED
IN NASA SIMULATION

NOTE 1. SYMMETRIC FOR OPPOSITE TRIM

2. WHEEL FORCE DATUM SHIFTS WITH TRIM

3. TRIM LIMITS = ± 4.27 UNITS

4. TRIM RATE = 2.5° CONTROL WHEEL PER SECOND

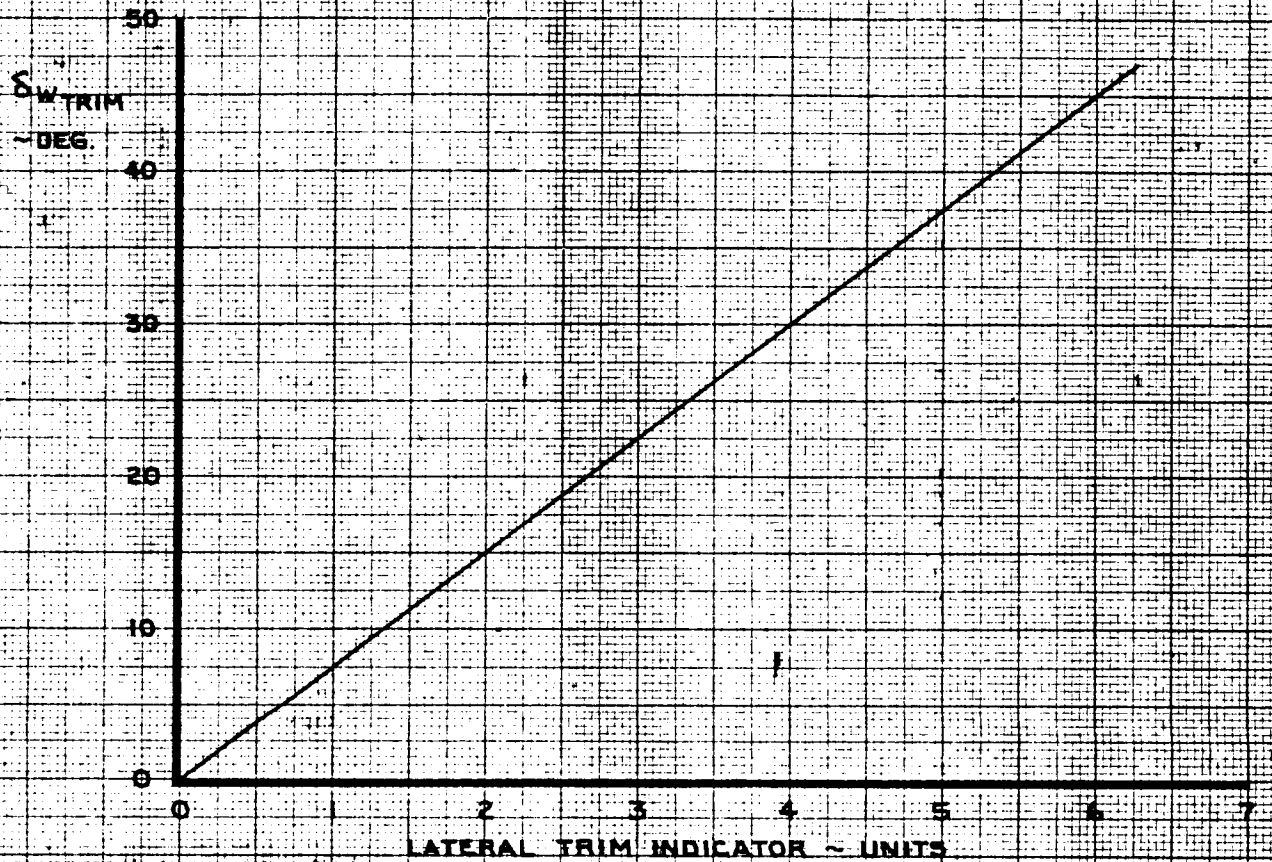

CALC	MOOIWEER	12-4-67	REVISED	DATE	LATERAL CONTROL LATERAL TRIM	747
CHECK	HOLTZNER	12-4-67	LOW	2-9-70		D6-30643 Vol. II
APR			KUPCIS	6-25-70		
APR						
INK	ODEGARD	2-10-70			THE BOEING COMPANY	PAGE 9.1-4

9.2 Aileron-Spoiler-Wheel Program

9.2.1 Lateral Control Only

The inboard aileron wheel program is plotted on page 9.2-3.

For fully unlocked outboard ailerons, the outboard aileron wheel program is plotted on page 9.2-3. Full outboard aileron authority is available at all times for flaps 5, 10, 20, 25 and 30.

Outboard aileron unlocking is started at outboard flap jackscrew extension to 0% of jackscrew travel and full unlocking takes about 15 seconds. After this time, full outboard aileron authority is available. Outboard aileron locking is started at outboard flap jackscrew retraction to 0% of jackscrew travel and full locking takes about 15 seconds. After this time, no outboard aileron authority is available. For intermediate outboard aileron authority

$$\delta_{A_O} = k_{\delta_{A_O}} \cdot \delta_{A_{O_{REF.}}}$$

where,

δ_{A_O} = Outboard aileron angle (degrees). The outboard aileron mechanical limits are 25° T.E. up and 15° T.E. down.

$k_{\delta_{A_O}}$ = Intermediate outboard aileron gain factor. This is a function of flap screw travel and is plotted on Page 9.2-4.

9.2.1 (Cont'd) $\delta_{A_{O_{REF.}}}$ = Reference outboard aileron angle (degrees) commanded from the aileron - wheel program, Page 9.2-3.

In the NASA simulation outboard ailerons are locked out when flaps are fully retracted.

The spoiler-wheel program is plotted on page 9.2-5.

9.2.2 Lateral Control With Speed Brake Operation

The aileron wheel program remains the same for all speed brake handle positions.

For intermediate and normal inflight speed brake handle positions, the spoiler wheel program is plotted on page 9.2-6.

9.2.3 Speed Brake Operation

The speed brake program with no lateral control inputs is plotted on page 9.2-7. Panels 3, 4, 5, 6, 7, 8, 9, 10 are used as inflight speed brakes (intermediate and inflight speed brake handle positions). The remaining panels 1, 2, 11, 12 operate only as ground speed brakes (ground speed brake handle position). Spoiler panels 6 and 7, which operate symmetrically as speed brakes only, cannot be modulated. These surfaces are either fully extended or fully retracted depending on the position of the speed brake handle.

NOTE 1. OUTBOARD AILERON PROGRAM IS FOR OUTBOARD AILERONS FULLY UNLOCKED

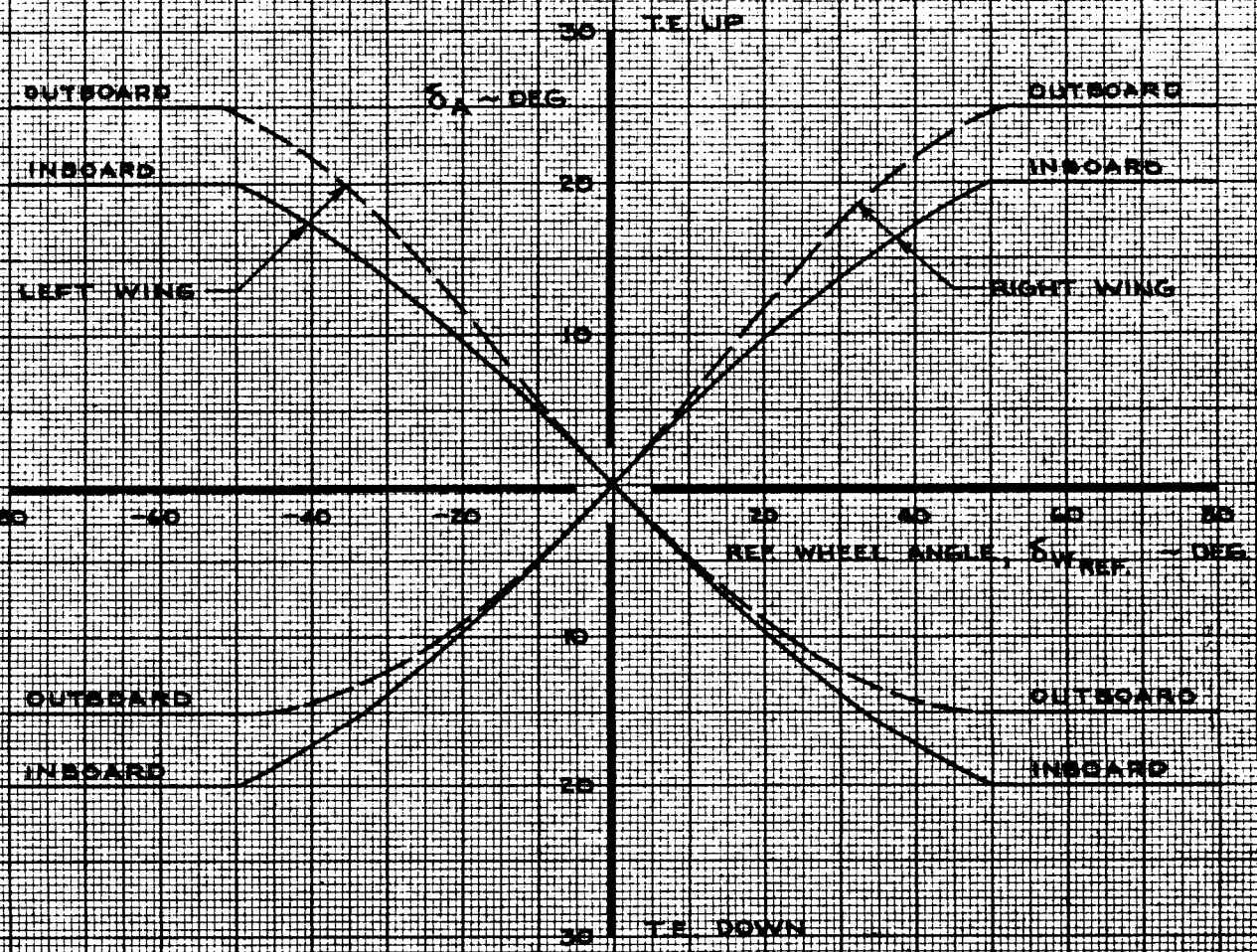

CALC	MOOIWEER	12/2/67	REVISED	DATE	LATERAL CONTROL AILERON-WHEEL PROGRAM	747
CHECK	HOLTZNER	12/2/67	HOLTZNER	4-22-8		D6-30643, Vol. II
APR			KUPCIS	1-31-70		
APR					THE BOEING COMPANY	PAGE 9.2-3
INK	ODEGARD	12/2/67				

OUTBOARD AILERON = OUTBOARD AILERON COMMANDED BY WHEEL × $k_{\delta_{A_O}}$

$(\delta_{A_O} = \delta_{A_O}{}_{REF} \cdot k_{\delta_{A_O}})$

REFER TO P. 9.2-3 FOR THE AILERON-WHEEL PROGRAM

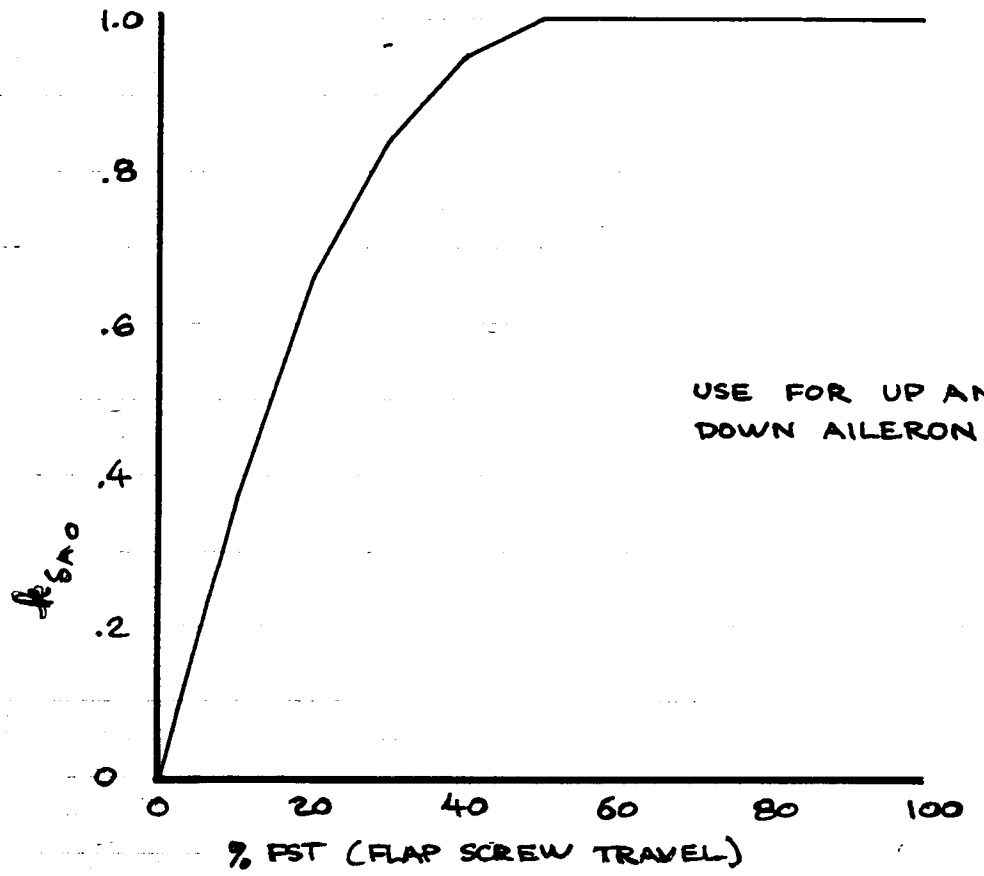

CALC			REVISED	DATE	LATERAL CONTROL INTERMEDIATE OUTBOARD AILERON GAIN FACTOR	747
CHECK						D6-30643 VOL II
APR						
APR					THE BOEING COMPANY	PAGE 9.2-4
	NORDWALL	3/25/74				

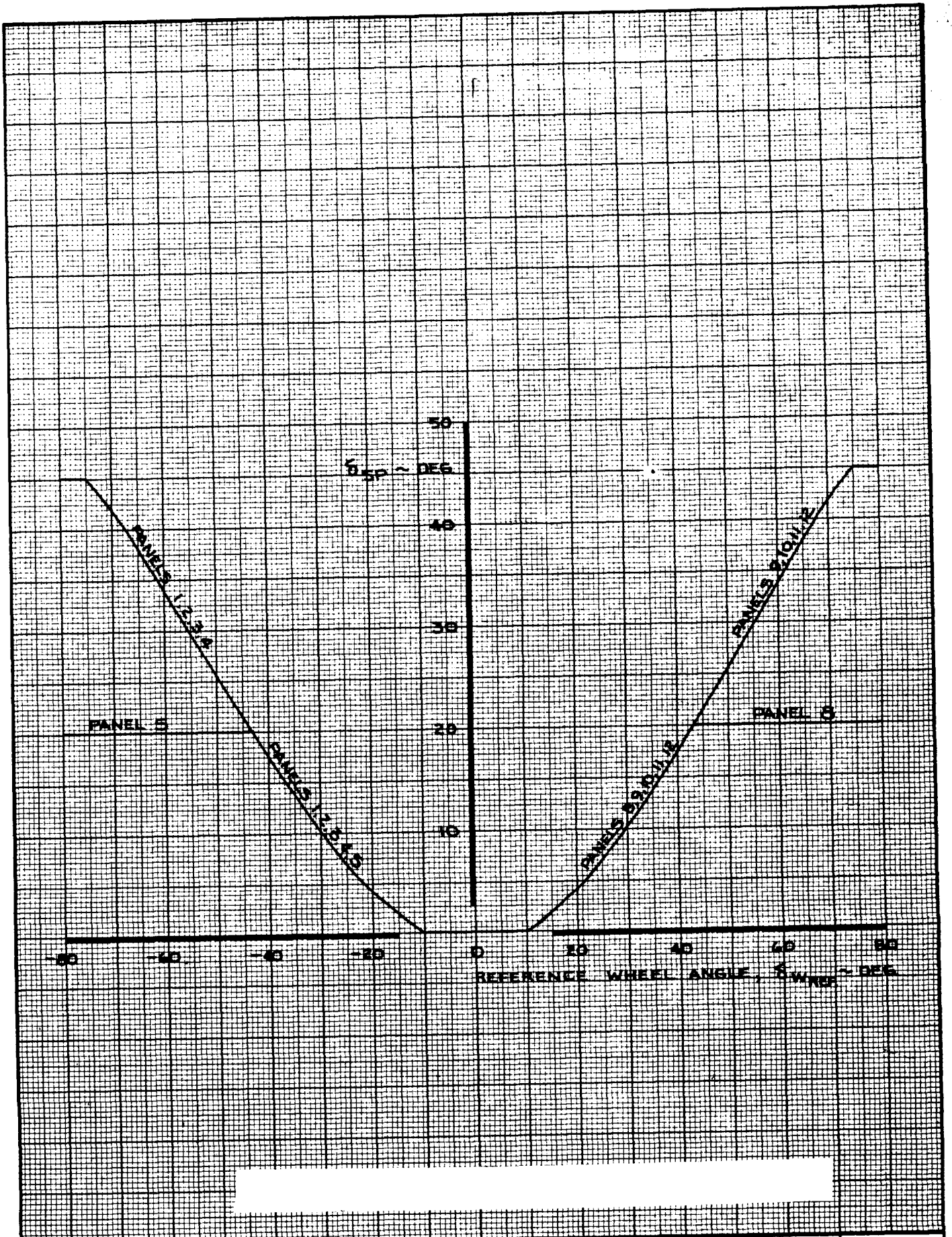

CALC	MOOIWEER	12/5/67	REVISED	DATE
CHECK	HOLTZNER	12/5/67	KUPCIS	6-2-69
APR				
APR				
INK	ODEGARD	12/5/67		

LATERAL CONTROL
FLIGHT SPOILER-WHEEL PROGRAM

747

D6-30643
Vol. II

THE BOEING COMPANY

PAGE
9.2-5

REV. B

TD 461 C-R4

NOTE . FOR SPEED BRAKES IN THE GROUND DETENT, USE THE IN-FLIGHT DETENT CURVES FOR PANELS 3,4,5 & 8,9,10. FOR PANELS 1&2 USE THE CURVE FOR PANELS 3,4. FOR PANELS 11 & 12 USE THE CURVE FOR PANELS 9,10. PANELS 6 & 7 REMAIN AT 20° FOR ALL WHEEL ANGLES

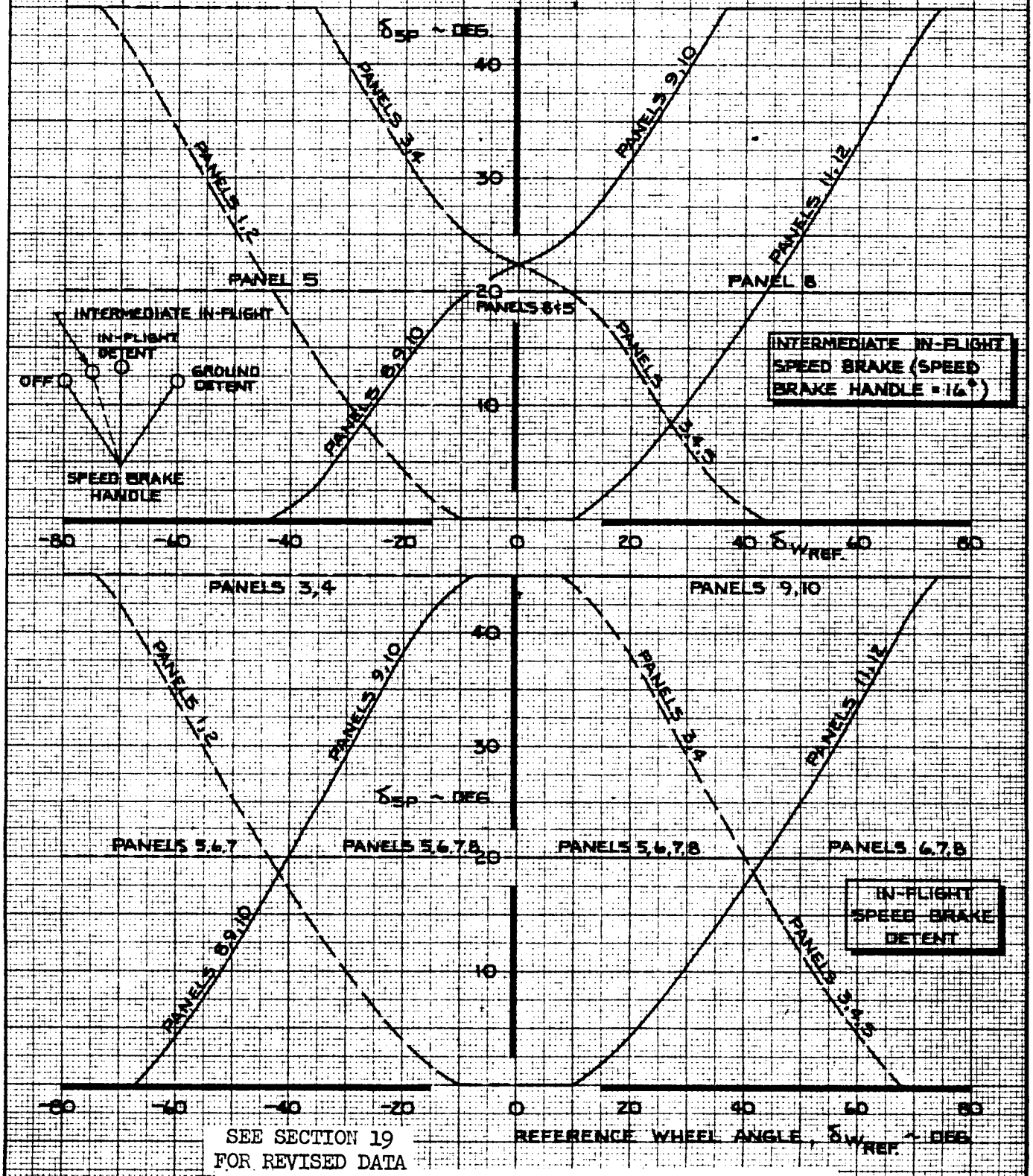

SEE SECTION 19
FOR REVISED DATA

CALC	MOOIWEER	12-5-67	REVISED	DATE
CHECK	HOLTZNER	1-15-68	KUPCIS	6-2-69
APR			KUPCIS	8-22-69
APR				
INK	ODEGARD	12-5-67		

LATERAL CONTROL
SPOILER PROGRAM AT COMBINED LATERAL CONTROL- SPEED BRAKES

THE BOEING COMPANY

747

D6-30643, Vol. II

PAGE 9.2-6

TD 461 C-R4

K-E ALBANENE 1961 REV. D

NOTE 1. SPEED BRAKE HANDLE FRICTION FORCE = 20 LB. PULL, 0 LB. PUSH

2. MAXIMUM AVAILABLE IN-FLIGHT SPEED BRAKE HANDLE POSITION = 34 DEG. (IN-FLIGHT DETENT)

3. SPEED BRAKES BEYOND THE IN-FLIGHT DETENT ARE AVAILABLE ONLY ON THE GROUND

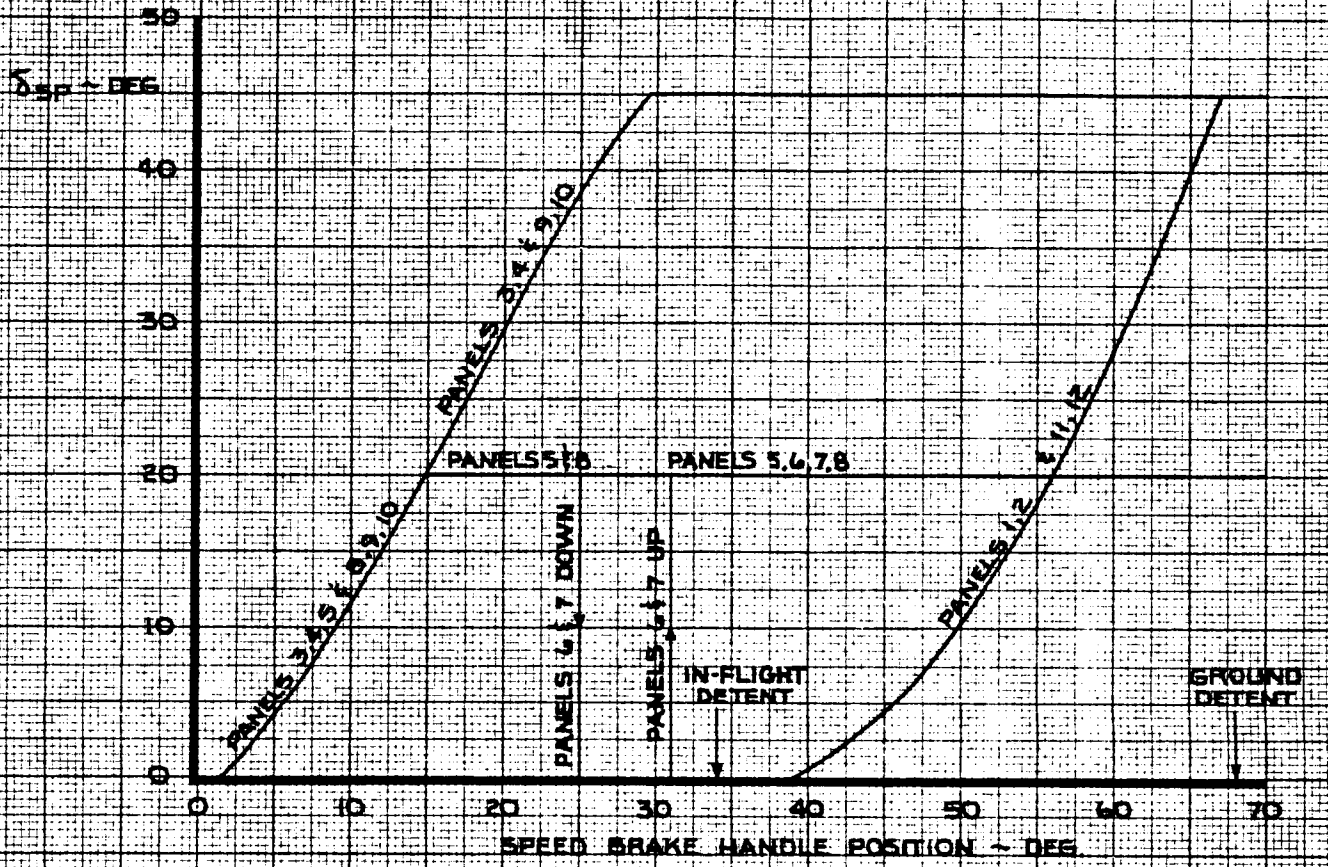

SEE SECTION 19
FOR REVISED DATA

CALC	MOOIWEER	12-5-67	REVISED	DATE	LATERAL CONTROL SPOILERS - SPEED BRAKE PROGRAM	747
CHECK	HOLTZNER	1-15-68	KUPCIS	6-2-69		D6-30643, Vol. II
APR			KUPCIS	8-22-69		
APR					THE BOEING COMPANY	PAGE 9.2-7
INK	ODEGARD	12-5-67				

TD 461 C-R4

K-E ALBANENE 1951 REV D

9.3 Control Surface Limits and Float Angles

The maximum inboard aileron and maximum outboard aileron angles for full boost and half boost are plotted on pages 9.3-2 and 9.3-3 respectively. The maximum spoiler angles are plotted on pages 9.3-4, 9.3-5 and 9.3-6.

Any inboard or outboard aileron surface with both hydraulic systems off, will trail at the float angles plotted on pages 9.3-7 and 9.3-8 respectively. The spoilers are held in a faired position, boost off, due to the hold down check valves.

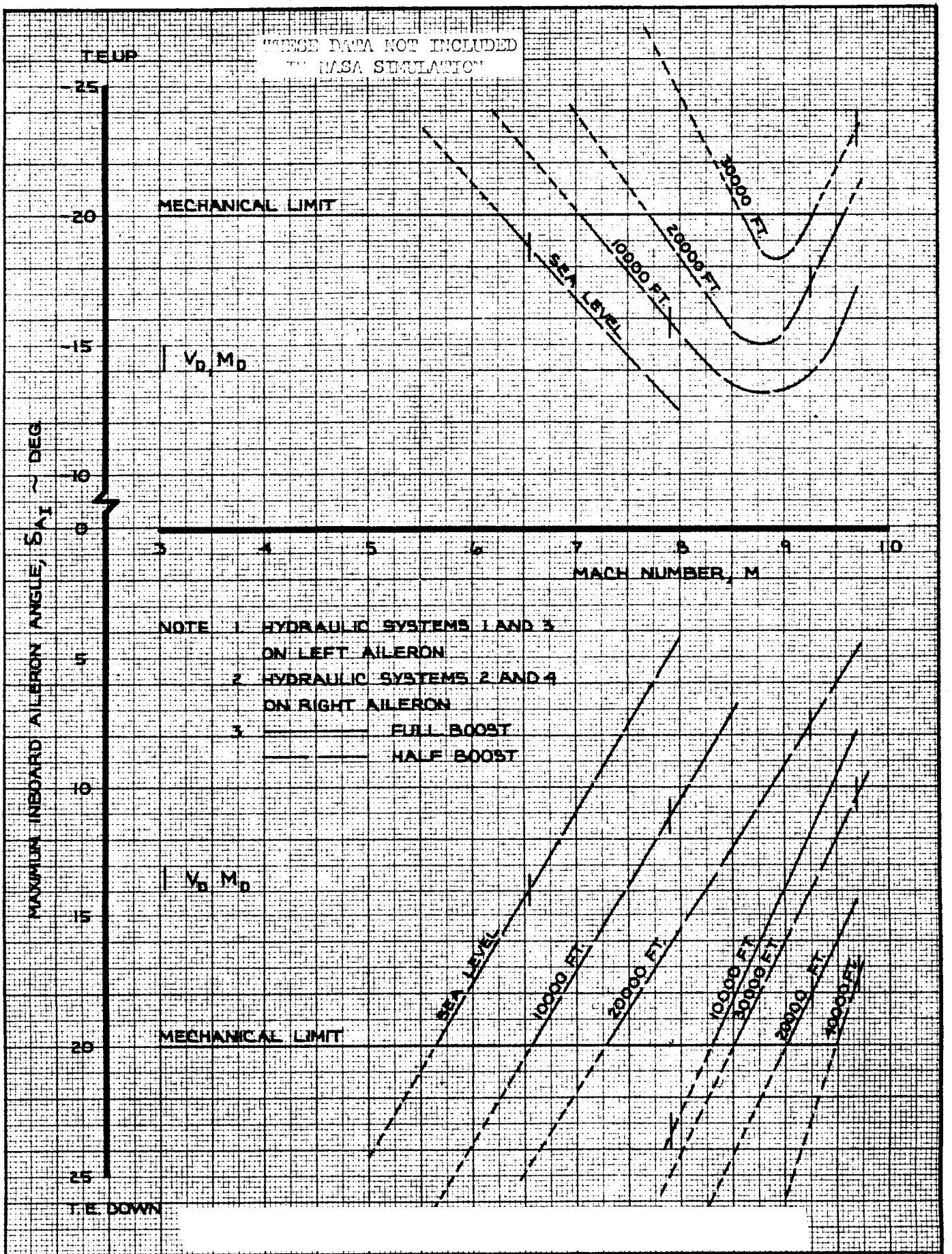

CALC	HOLTZNER	7-13-67	REVISED	DATE	LATERAL CONTROL INBOARD AILERON BLOWDOWN
CHECK	FOSTER	12-14-67	LAGREE	10-21-69	
APR					
APR					
INK	KINSMAN	10-21-69			

747

D6-30643, Vol. II

THE BOEING COMPANY

PAGE 9.3-2

TD 461 C-R4

K-E ALBANENE 1951 TRACING PAPER REV. D

THESE DATA NOT INCLUDED IN NASA SIMULATOR

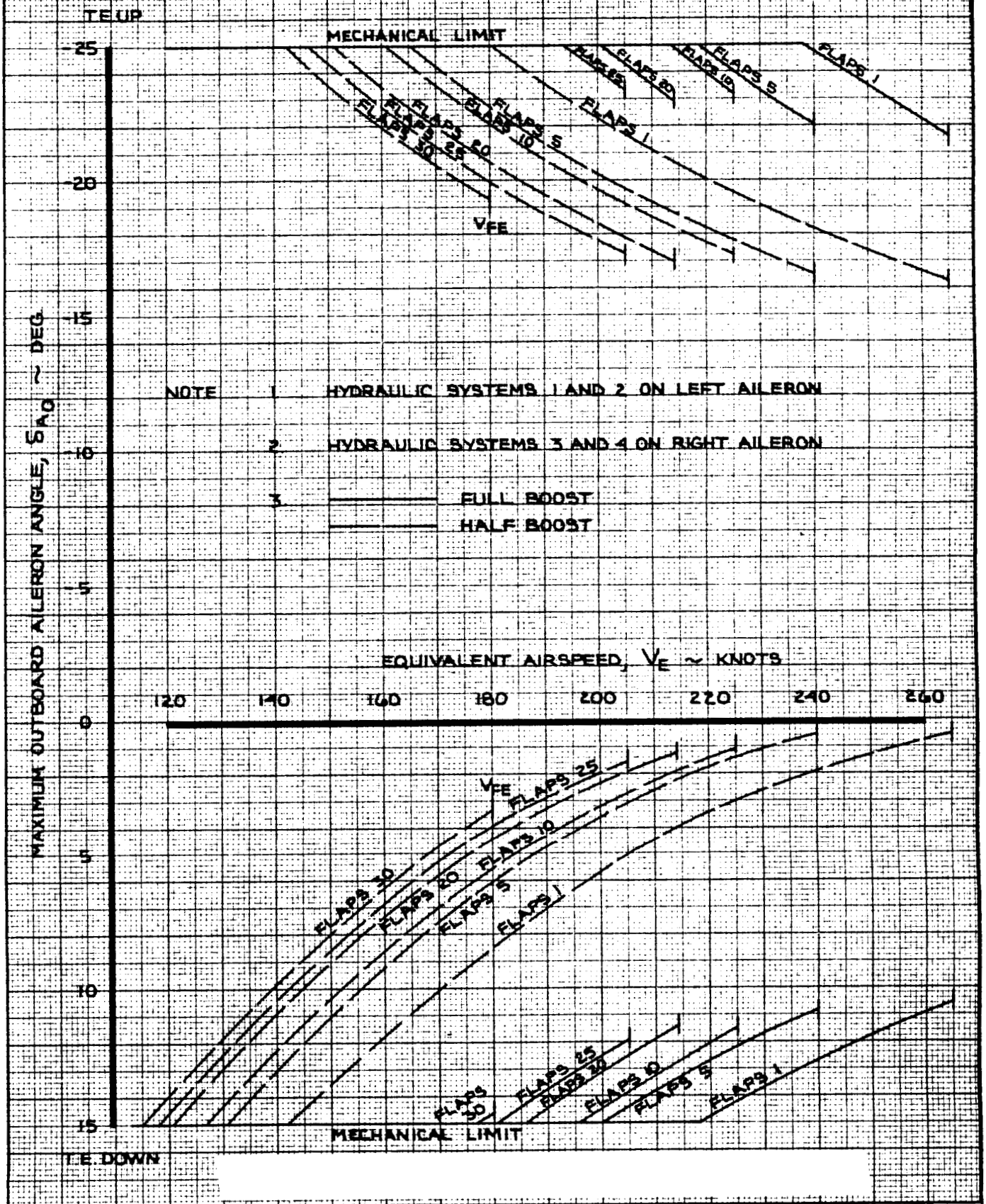

CALC	HOLTZNER	9-14-67	REVISED	DATE	LATERAL CONTROL Δ	747
CHECK	FOSTER	12-14-67	LAGREE	1-22-70	OUTBOARD AILERON BLOWDOWN	D6-30643-3 Vol. II
APR						
APR					THE BOEING COMPANY	PAGE 9.3-3
INK	ODEGARD	9-14-67				

TD 461 C-R4

K-E ALBANENE 1951 TRACING PAPER REV. D

PANEL 1 OR 12

HYDRAULIC SYSTEM NO. 3

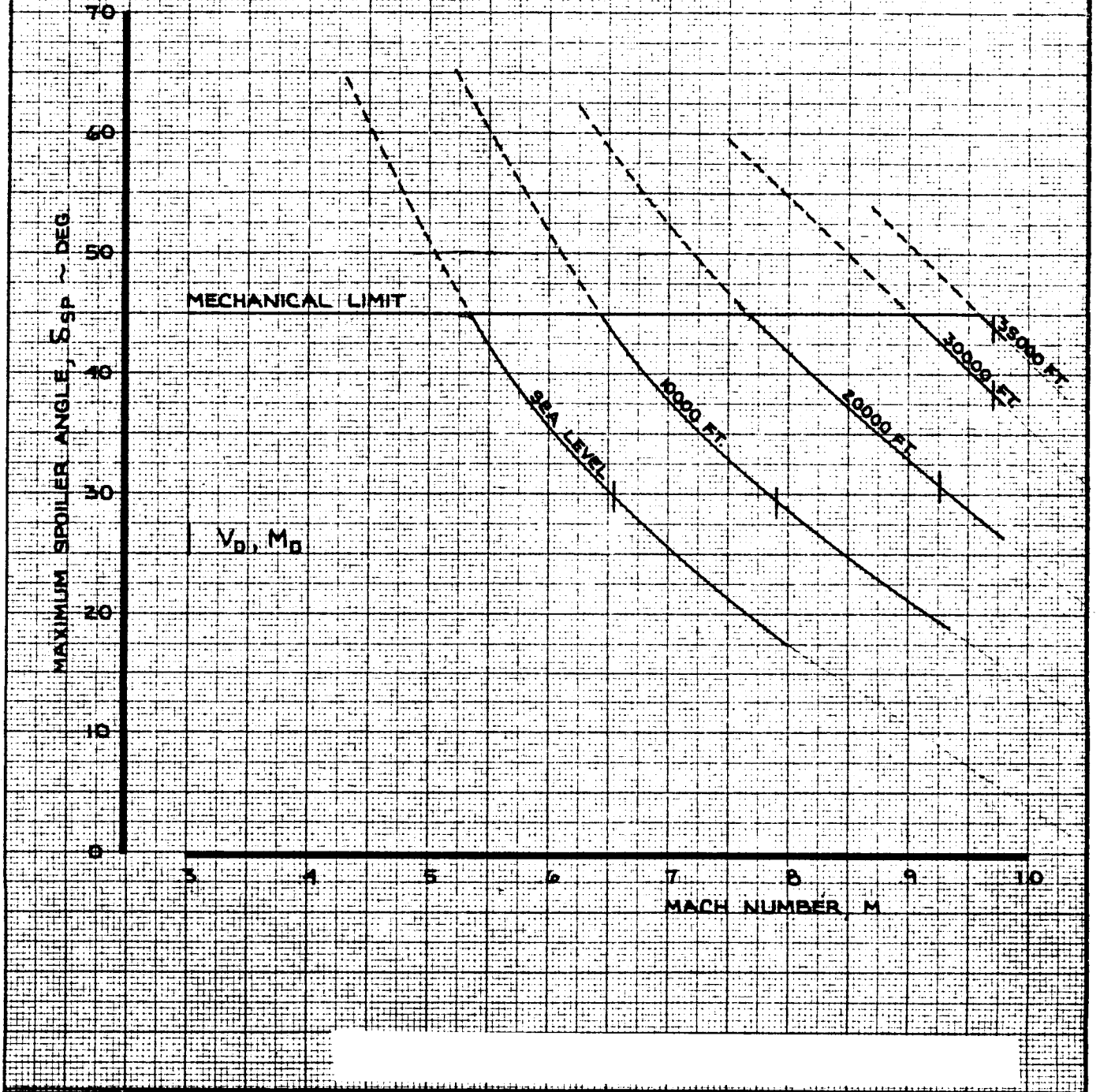

CALC	HOLTZNER	7-11-67	REVISED	DATE	LATERAL CONTROL SPOILER BLOWDOWN (PANEL 1 OR 12)	747
CHECK	FOSTER	12-14-67	KUPCIS	6-2-69		
APR			KUPCIS	8-22-69		D6-30643-5 Vol. II
APR			KUPCIS	1-8-70		
INK	KINSMAN	1-8-70			THE BOEING COMPANY	PAGE 9.3-4

AD 461 C-R4

K-E ALBANENE 1951 REV. D

PANELS 2,3,4
OR 9,10,11

HYDRAULIC SYSTEMS NO. 2 AND NO. 3

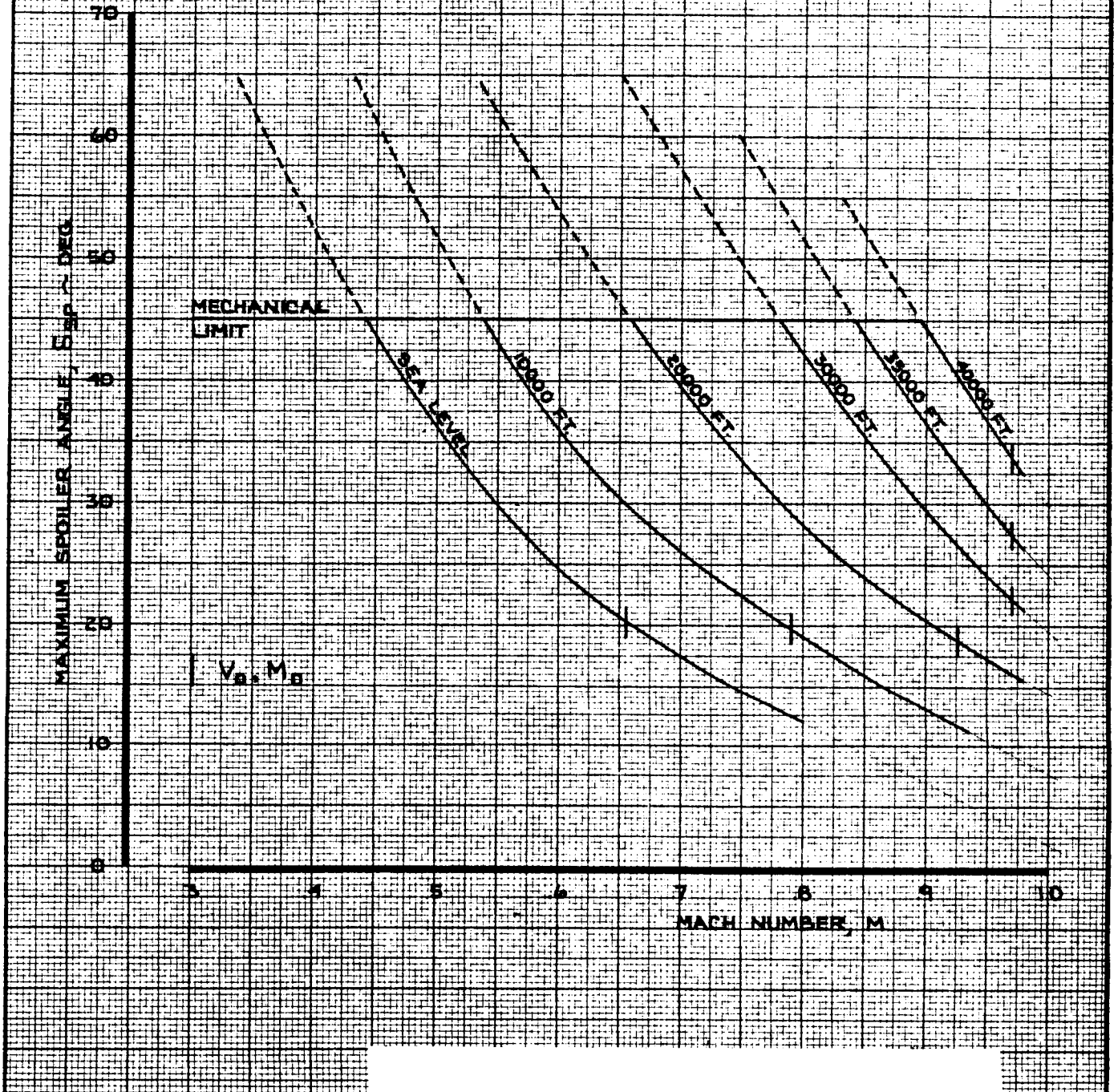

CALC	HOLTZNER	7-11-67	REVISED	DATE	LATERAL CONTROL SPOILER BLOWDOWN (PANELS 2, 3, 4 OR 9,10,11)
CHECK	FOSTER	12-14-67	KUPCIS	6-2-69	
APR			KUPCIS	8-22-69	
APR			KUPCIS	1-8-70	
INK	KINSMAN	1-8-70			THE BOEING COMPANY

747

D6-30643, Vol. II

PAGE 9.3-5

AD 461 C-R4

K-E ALBANENE 1961 REV. D

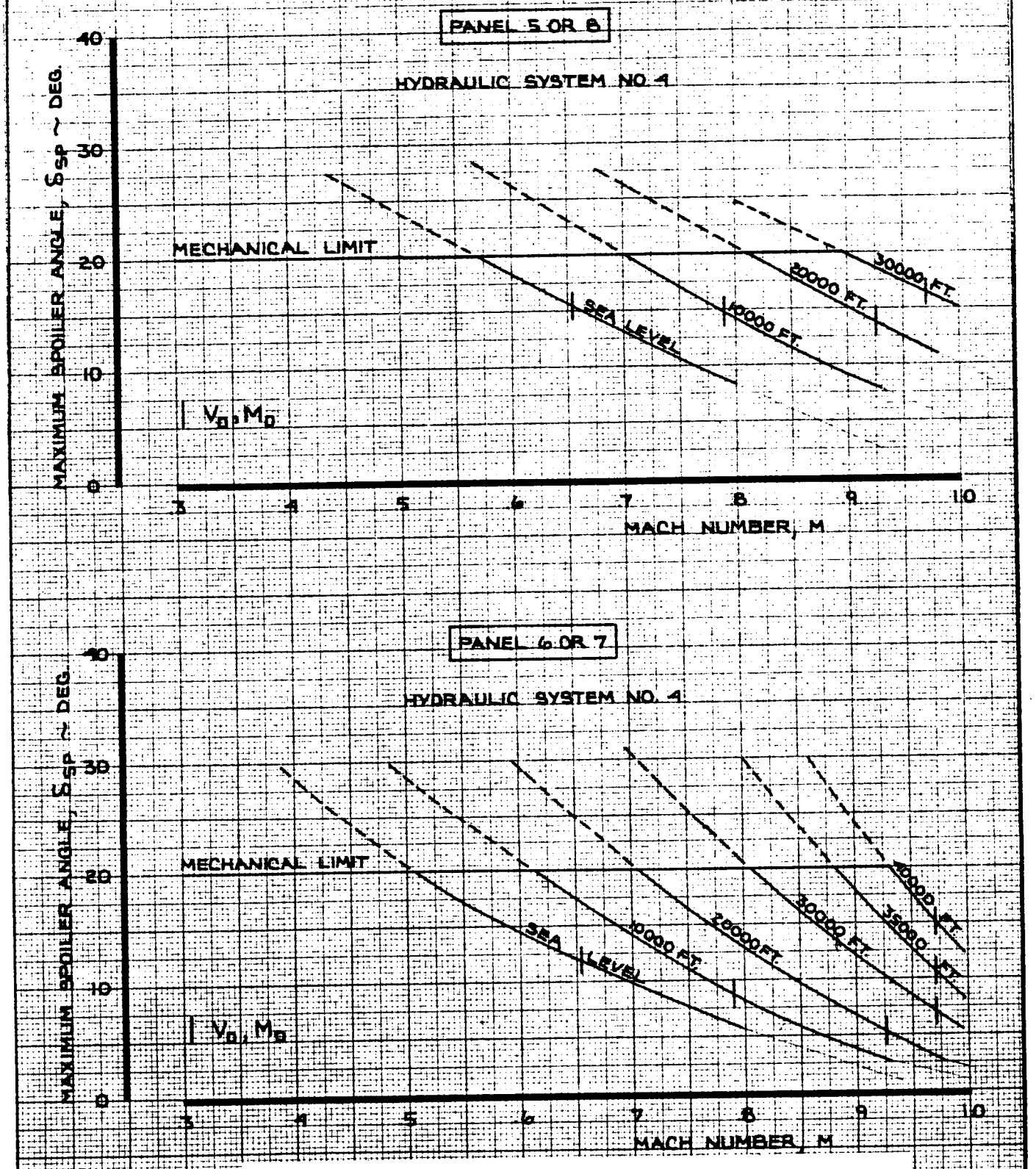

CALC	HOLTZNER	7-11-67	REVISED	DATE	LATERAL CONTROL SPOILER BLOWDOWN (PANELS 5, 6 OR 7, 8)	747
CHECK	FOSTER	12-14-67	KUPCIS	6-2-69		D6-30643-3 Vol. II
APR			KUPCIS	8-22-69		
APR			KUPCIS	1-9-70	THE BOEING COMPANY	PAGE 9.3-6
INK	KINSMAN	1-9-70				

NOTE 1. $\delta_{A_{I\,FLOAT}} = (\delta_{A_{I\,FLOAT}})_{\alpha_{W.B.P.}=0^\circ} + \frac{d\delta_{A_{I\,FLOAT}}}{d\alpha} \cdot \alpha_{W.B.P.}$

THESE DATA NOT INCLUDED IN NASA SIMULATION

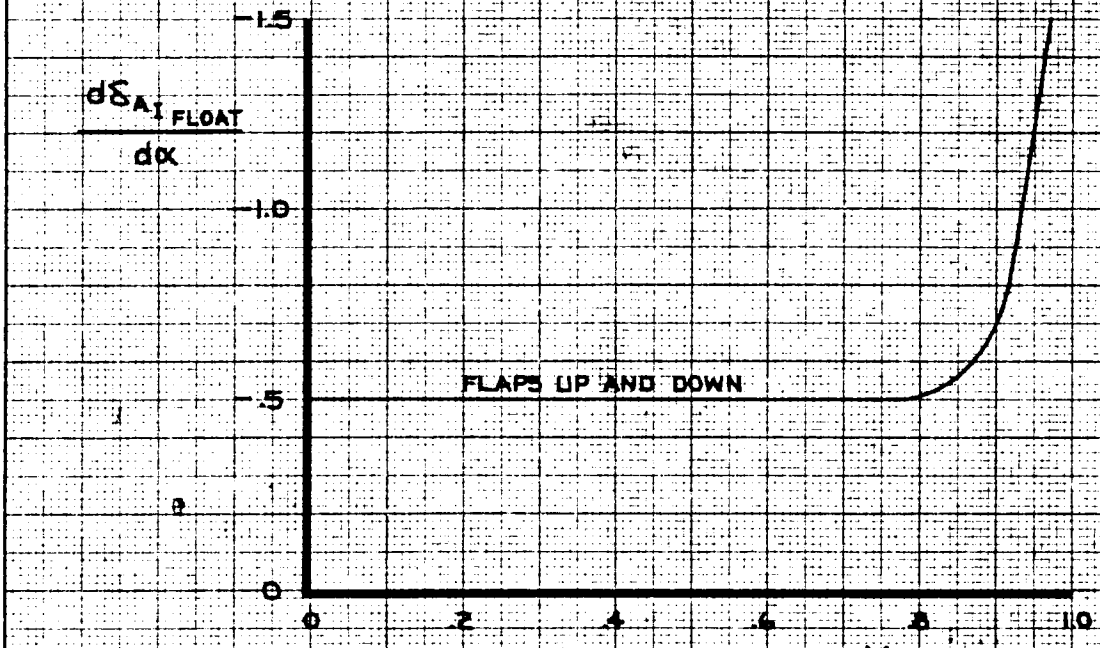

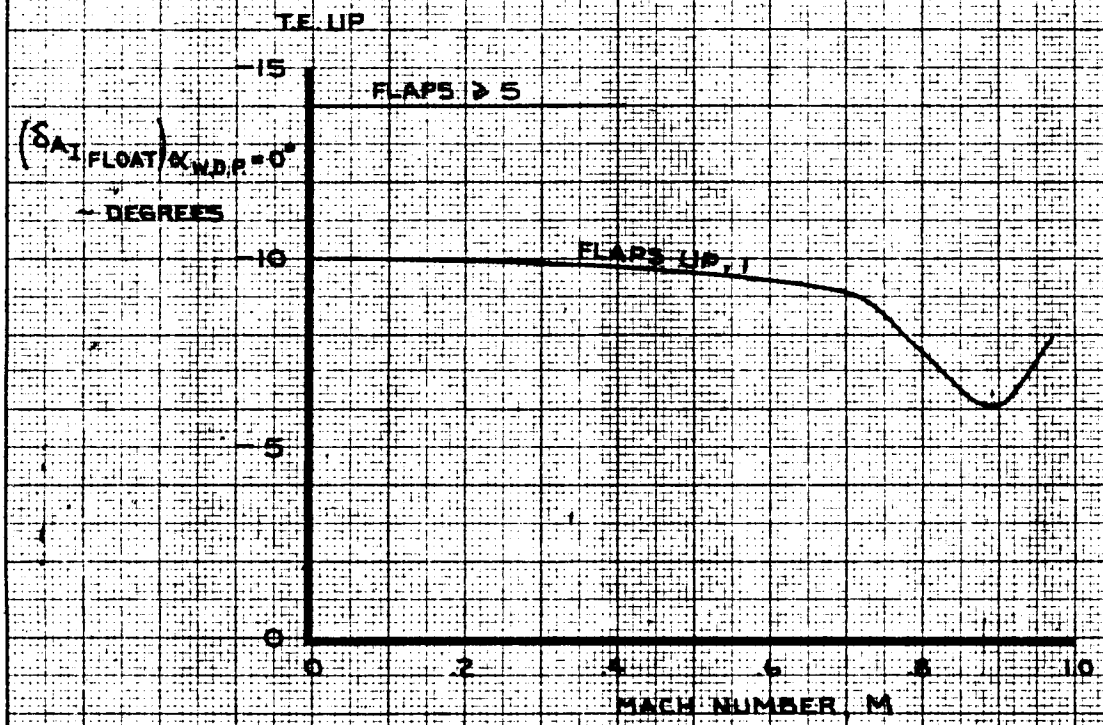

CALC	HOLTZNER	11-13-67	REVISED	DATE	LATERAL CONTROL INBOARD AILERON FLOAT ANGLES
CHECK	FOSTER	1-15-68	HOLTZNER	5-29-69	
APR			KUPCIS	1-29-70	
APR			KUPCIS	7-15-70	
INK	ODEGARD	11-13-67			THE BOEING COMPANY

747

D6-30643, Vol. II

PAGE 9.3-7

NOTE 1. $\delta_{A_{O_{FLOAT}}} = \left(\delta_{A_{O_{FLOAT}}}\right)_{\delta K_{W.D.P.}=0^{\circ}} + \frac{d\delta_{A_{O_{FLOAT}}}}{d\alpha} \cdot \delta K_{W.D.P.}$

2. INTERPOLATE LINEARLY FOR INTERMEDIATE FLAP SETTINGS

THESE DATA NOT INCLUDED IN AREA SELECTION

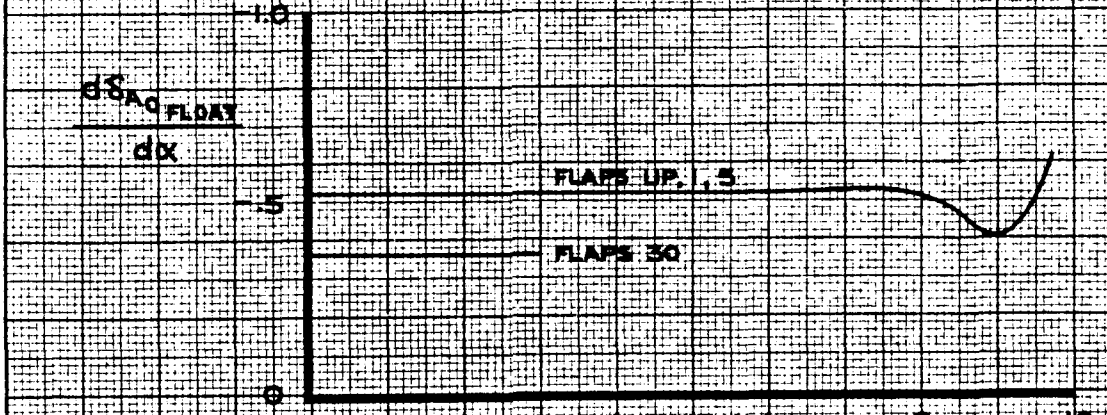

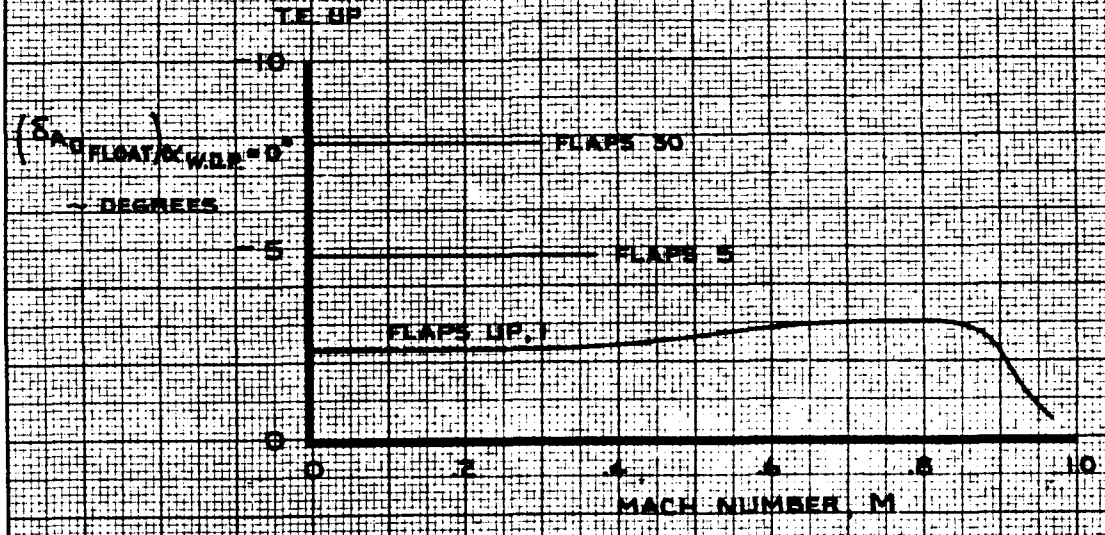

CALC	HOLTZNER	11-14-67	REVISED	DATE	LATERAL CONTROL OUTBOARD AILERON FLOAT ANGLES	747 D6-30643 Vol. II
CHECK	FOSTER	1-15-68	LOW	1-29-70		
APR						
APR					THE BOEING COMPANY	PAGE 9.3-8
INK	ODEGARD	11-14-67				

10.0 DIRECTIONAL CONTROL SYSTEM

A general description of the system is presented in the Introduction on Pages 1.2-4 and 1.2-5 and in Volume I. A block diagram of the simulated directional control system is shown on Page 10.1-2a. The data for each particular block can be found on the page number adjacent to the block.

10.1 Rudder Pedal Force and Angle

10.1.1 Rudder Pedal Force

$$F_P = F_{P_S} \pm F_{P_{FR}}$$

where,

F_P = Rudder pedal force, positive for a left rudder pedal force (lb).

F_{P_S} = Rudder pedal force due to the spring and cam mechanism (lb). This is plotted on page 10.1-3.

$F_{P_{FR}}$ = Friction force opposing rudder pedal motion (= 6.0 lb).

10.1.2 Rudder Pedal Angle

$$\delta_P = \delta_{P_{REF.}} + .023 F_P$$

where,

δ_P = Rudder pedal angle (degrees). The rudder pedal limits are $\delta_P = \pm 14$ degrees.

$\delta_{P_{REF.}}$ = Reference rudder pedal angle (degrees). This does not include the effect of cable stretch.

.023 = Cable stretch factor (deg/lb).

10.1.3 Rudder Trim

$\delta_{P_{TRIM}}$ = Zero force datum rudder pedal angle due to trim (degrees). This is plotted on page 10.1-4. The trim shifts the rudder pedal force datum but does not change the rudder limits. The trim limits are ± 10 units.

10.1.4 Rudder Limiter

$$\delta_R = \frac{\delta_R}{\delta_{R_{MAX.}}} \cdot \delta_{R_{MAX.}}$$

where,

$\frac{\delta_R}{\delta_{R_{MAX.}}}$ = Rudder angle ratio. This is plotted on page 10.1-5.

$\delta_{R_{MAX.}}$ = Maximum available rudder angle (degrees). This is plotted on page 10.1-6.

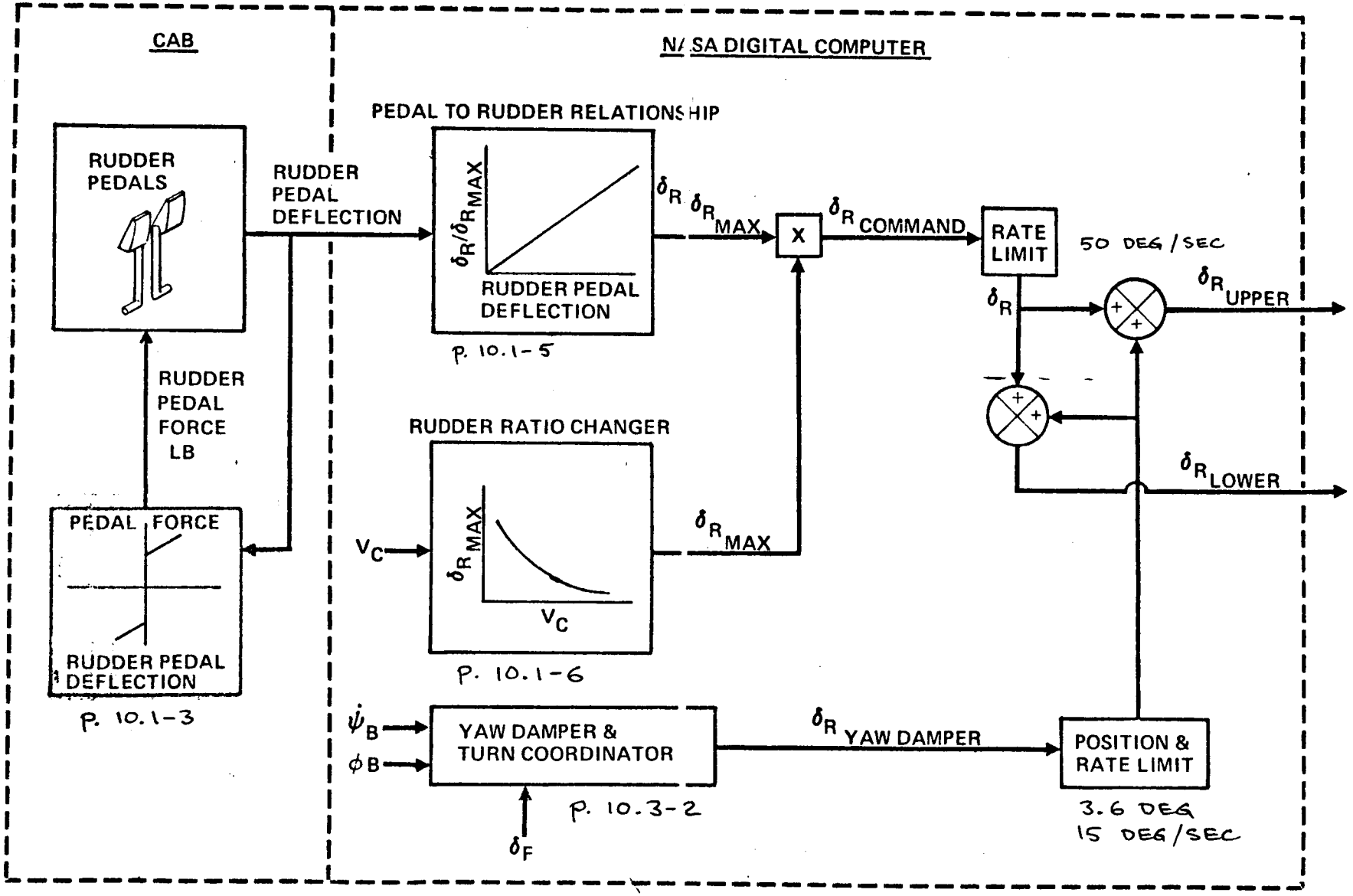

DIRECTIONAL CONTROL MODEL

NOTE 1. $F_P = F_{P_S} \pm F_{P_{FR}}$

2. $F_{P_{FR}} = 6.0$ LB.

3. SYMMETRIC FOR OPPOSITE RUDDER

4. RUDDER PEDAL LIMITS ARE $\delta_P = \pm 14°$

THESE DATA NOT INCLUDED IN NASA SIMULATION SEE P. 14.1-53

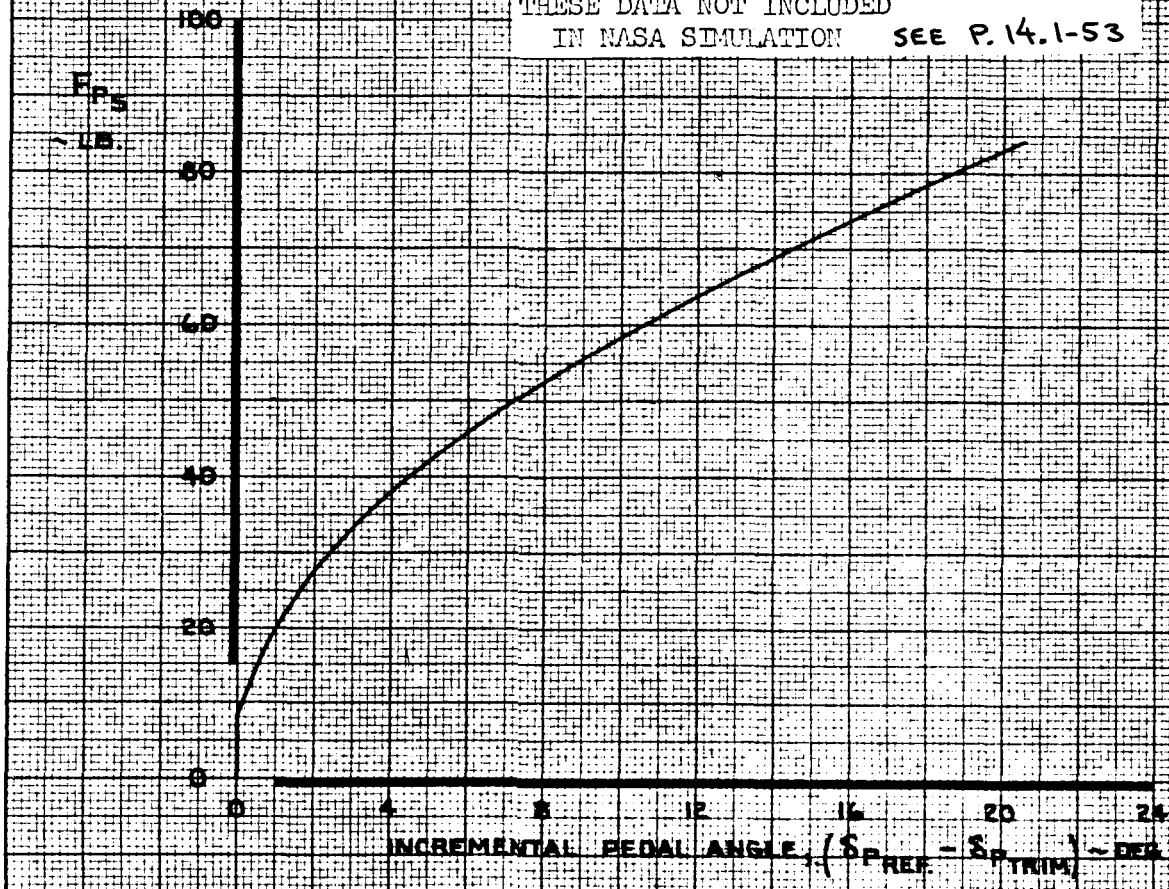

CALC	FOSTER	12-9-67	REVISED	DATE
CHECK	HOLTZNER	1-5-68	HOLTZNER	4-19-68
APR			LOW	2-9-70
APR				
INK	ODEGARD	2-13-70		

DIRECTIONAL CONTROL
FORCE DUE TO SPRING AND CAM MECHANISM

747
D6-30643 Vol. II

THE BOEING COMPANY

PAGE 10.1-3

THESE DATA NOT INCLUDED IN NASA SIMULATION

NOTE 1. SYMMETRIC FOR OPPOSITE TRIM

2. RUDDER PEDAL FORCE DATUM SHIFTS WITH TRIM

3. TRIM LIMITS = ±10 UNITS (± 4.36 TRIM WHEEL TURNS)

4. CLOCKWISE TRIM WHEEL ROTATION GIVES RIGHT RUDDER

5. TRIM WHEEL OPERATING TORQUE = 24 IN-LB
(TRIM WHEEL RADIUS = 2.07 IN.)

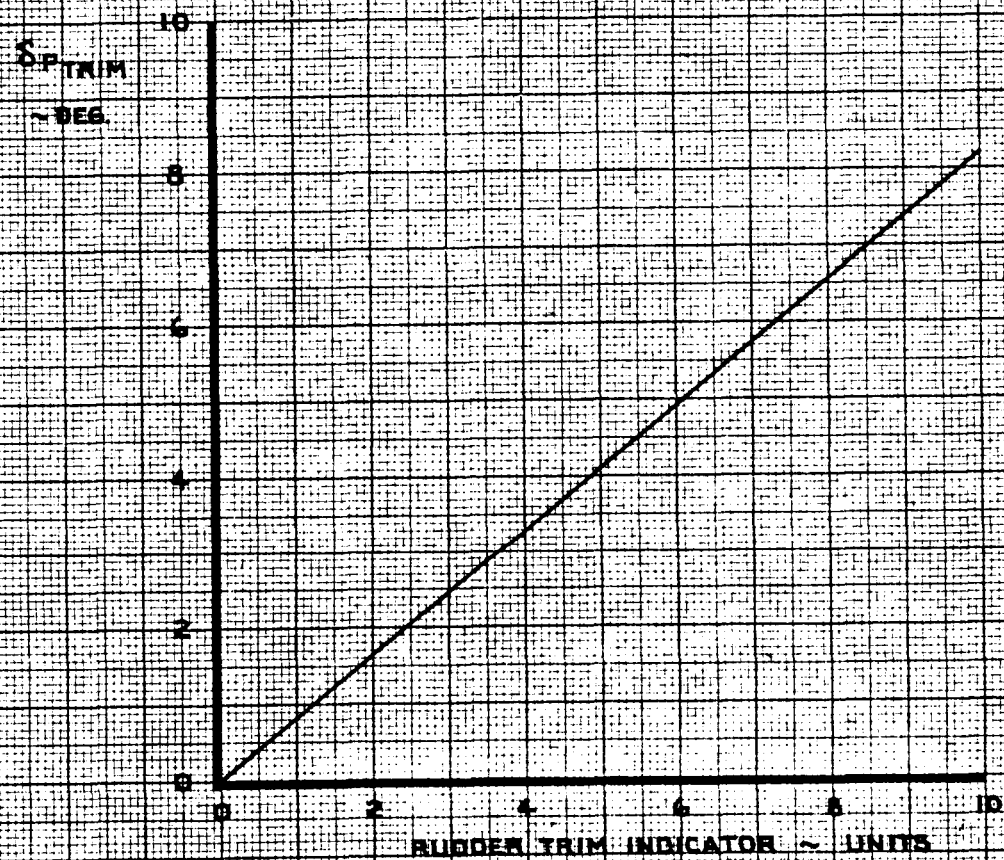

CALC	FOSTER	12-9-67	REVISED	DATE
CHECK	HOLTZNER	1-15-68	HOLTZNER	4-19-68
APR			LOW	2-9-70
APR				
INK	ODEGARD	2-13-70		

DIRECTIONAL CONTROL
RUDDER TRIM

747

D6-30643, Vol. II

THE BOEING COMPANY

PAGE 10.1-4

NOTE: 1. SYMMETRIC FOR OPPOSITE RUDDER

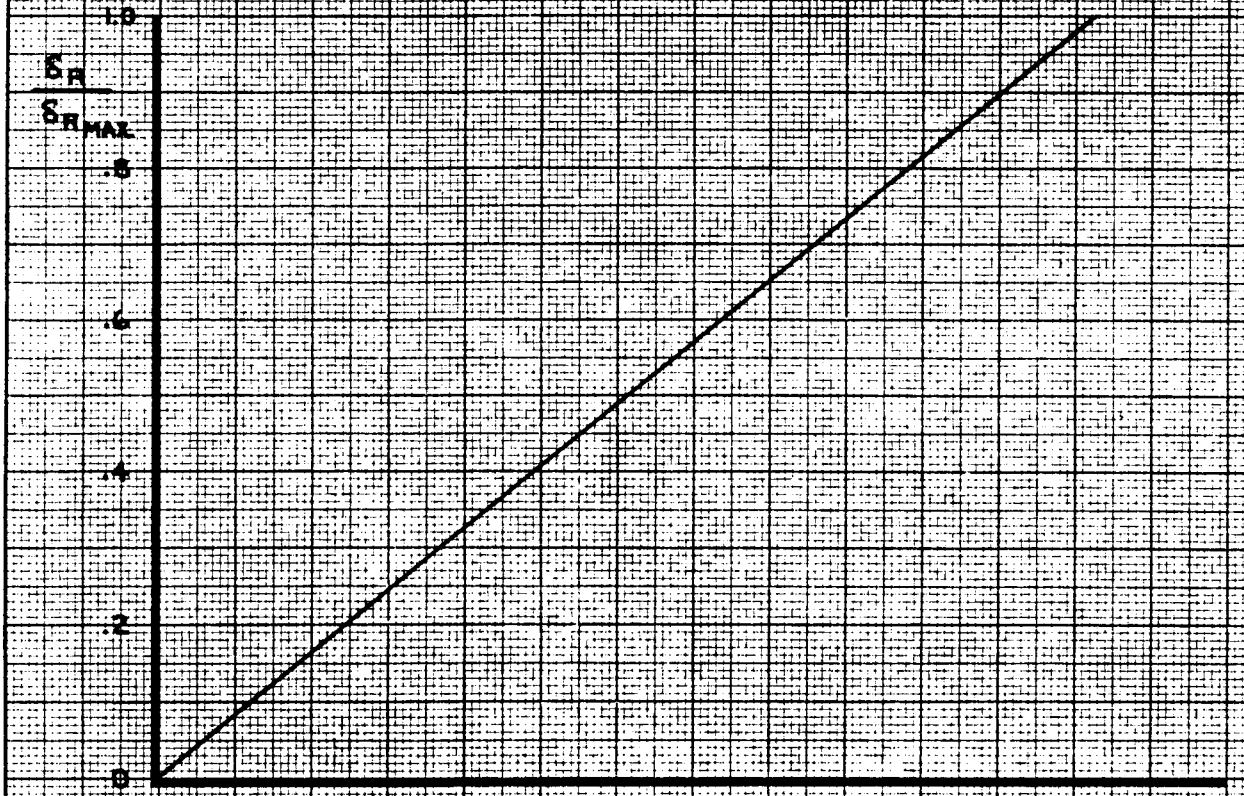

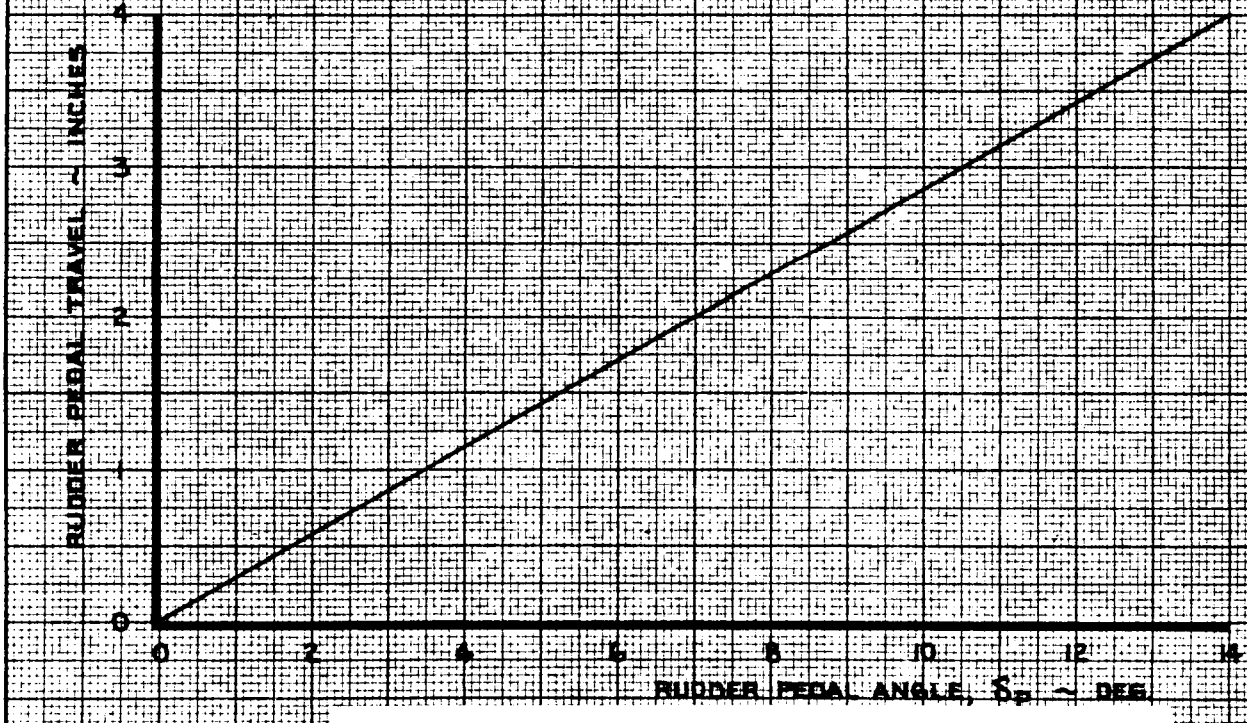

CALC	FOSTER	12·9·67	REVISED	DATE	DIRECTIONAL CONTROL RUDDER PEDAL MOTION	747
CHECK	HOLTZNER	1·5·68	FOSTER	4·22·68		
APR			LOW	2·9·70		D6-30643 Vol. II
APR						
INK	ODEGARD	2·13·70			THE BOEING COMPANY	PAGE 10.1-5

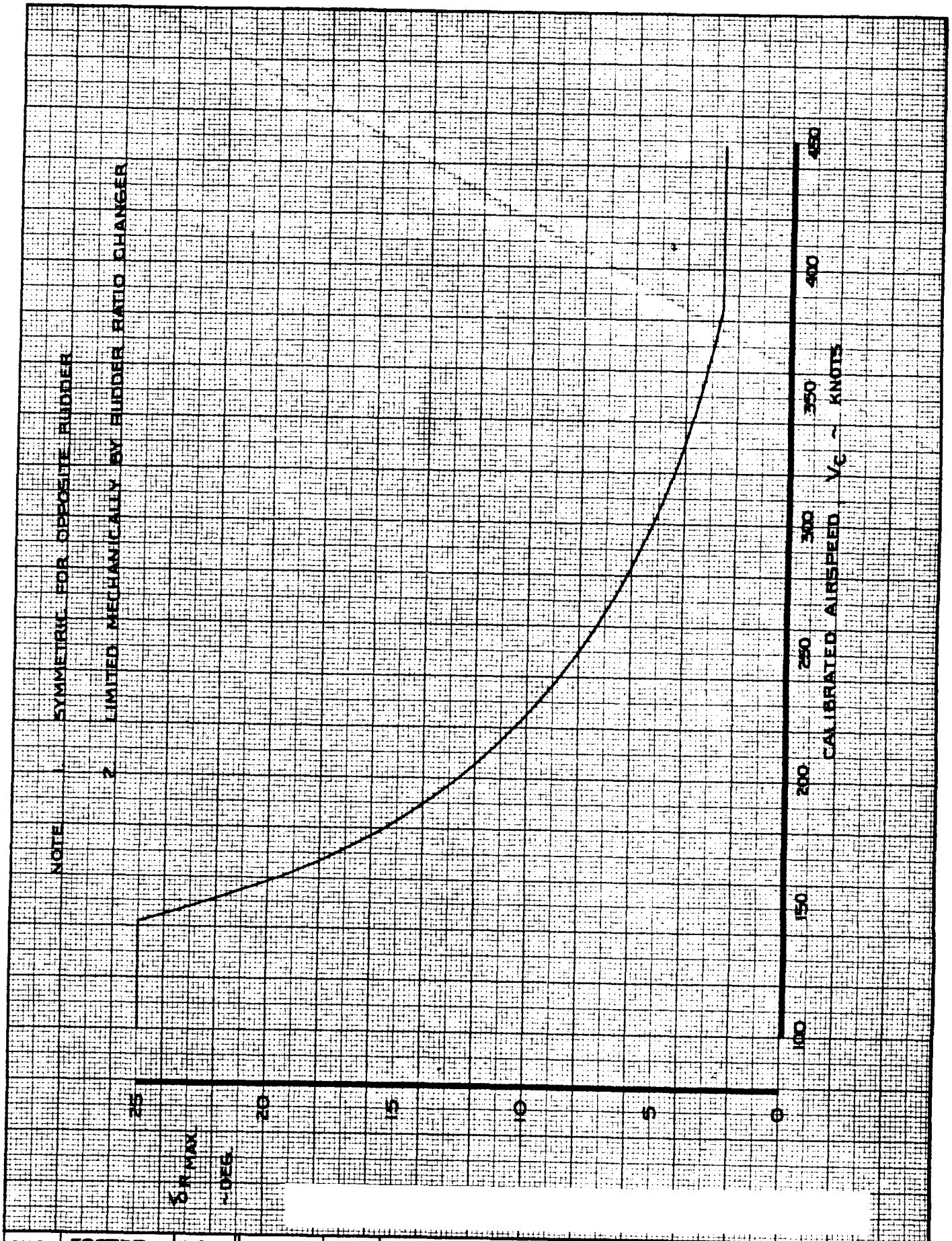

CALC	FOSTER	12-9-67	REVISED	DATE	DIRECTIONAL CONTROL ◇ RUDDER TRAVEL LIMITS	747
CHECK	HOLTZNER	1-5-68	KUPCIS	8-29-68		
APR			LOW	1-29-70		D6-30643 Vol. II
APR						
INK	ODEGARD	12-9-67			THE BOEING COMPANY	PAGE 10.1-6

TD 461 C-R4

K+E ALBANENE 1951 REV D

10.2 Rudder Blowdown

Rudder blowdown is not included in NASA Simulation.

The rudders are actuator force limited below the mechanically available rudder under some flight conditions. To determine these limits use the following equations:

$$HM \cos \delta_{R_U} = 955.2 \cdot C_{H_{R_U}} \cdot q$$

$$HM \cos \delta_{R_L} = 833.2 \cdot C_{H_{R_L}} \cdot q$$

where,

HM = ± 13,800 lb-ft. for each rudder with all hydraulic systems operative. This value is reduced by one-half if one of the two hydraulic systems on either rudder becomes inoperative.

The hinge moment coefficient can be calculated for any flight condition using the data on pages 10.2-2, 10.2-3, and 10.2-4 with the following equation:

$$C_{H_R} = \frac{(C_{H_R})_M}{(C_{H_R})_{M=0}} \cdot (C_{H_R})_{M=0}$$

Note that the hinge moments for rudders deflected separately are different from those with rudders deflected together. The rudders deflected separately curve is used only when one of the rudders is operating.

NOTE 1 REVERSE SIGNS FOR NEGATIVE RUDDER

2 USE FOR ALL FLAP SETTINGS

THESE DATA NOT INCLUDED IN NASA SIMULATION

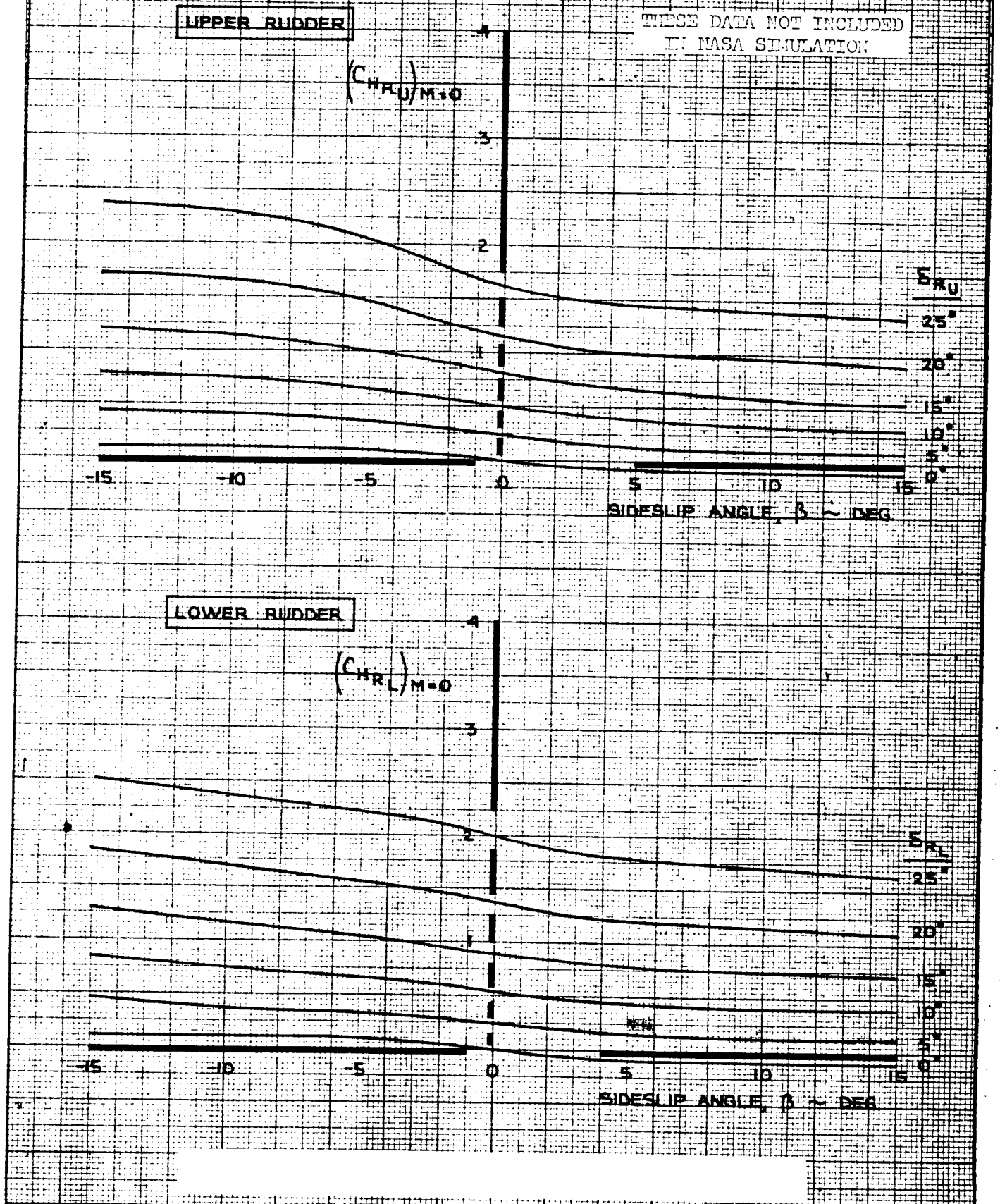

CALC	FOSTER	10-21-67	REVISED	DATE
CHECK	HOLTZNER	1-5-68	CURNUTT	10-29-68
APR			LAGREE	2-10-70
APR			BECK	6-25-70
INK	KINSMAN	2-16-70		

DIRECTIONAL CONTROL
RUDDER HINGE MOMENTS
SEGMENTS DEFLECTED TOGETHER

747

D6-30643
Vol. II

THE BOEING COMPANY

PAGE
10.2-2

AD 45[illegible] C-R4

H-E ALBANENE 1961 REV E

NOTE 1. REVERSE SIGNS FOR NEGATIVE RUDDER.
2. USE FOR ALL FLAP SETTINGS.

THESE DATA NOT INCLUDED IN NASA SIMULATION

UPPER RUDDER

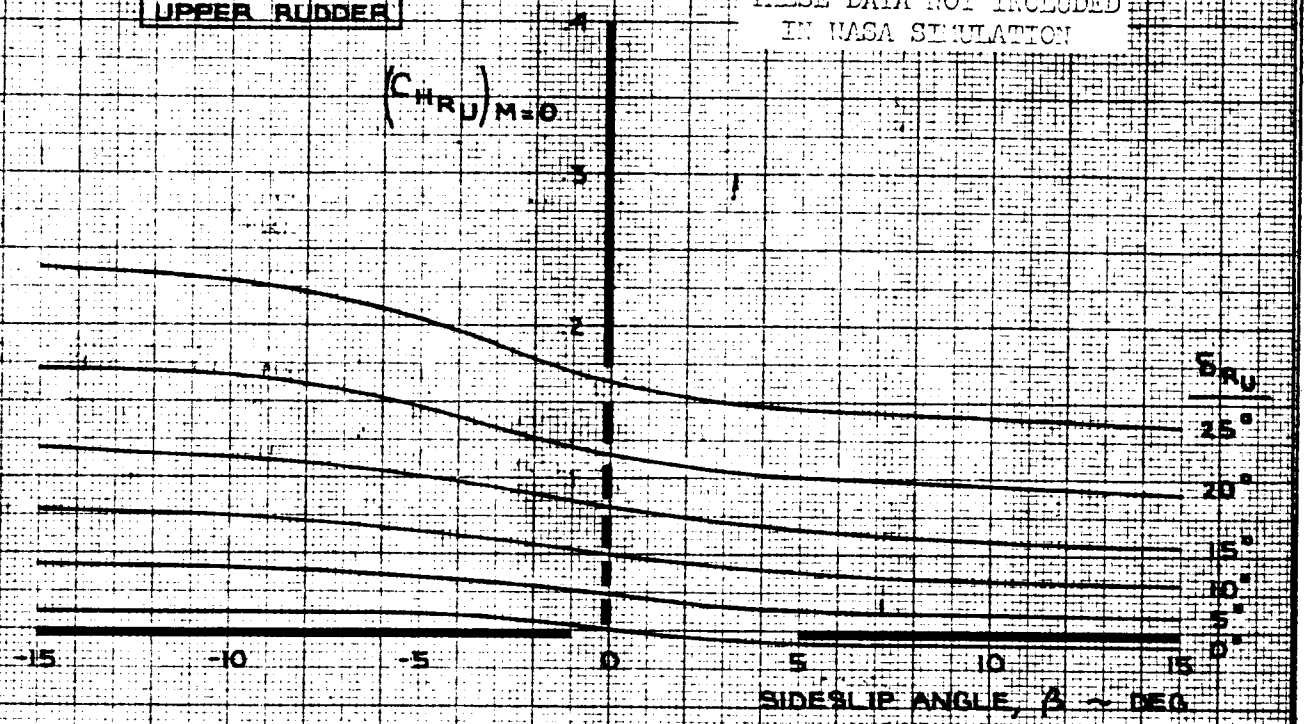

LOWER RUDDER

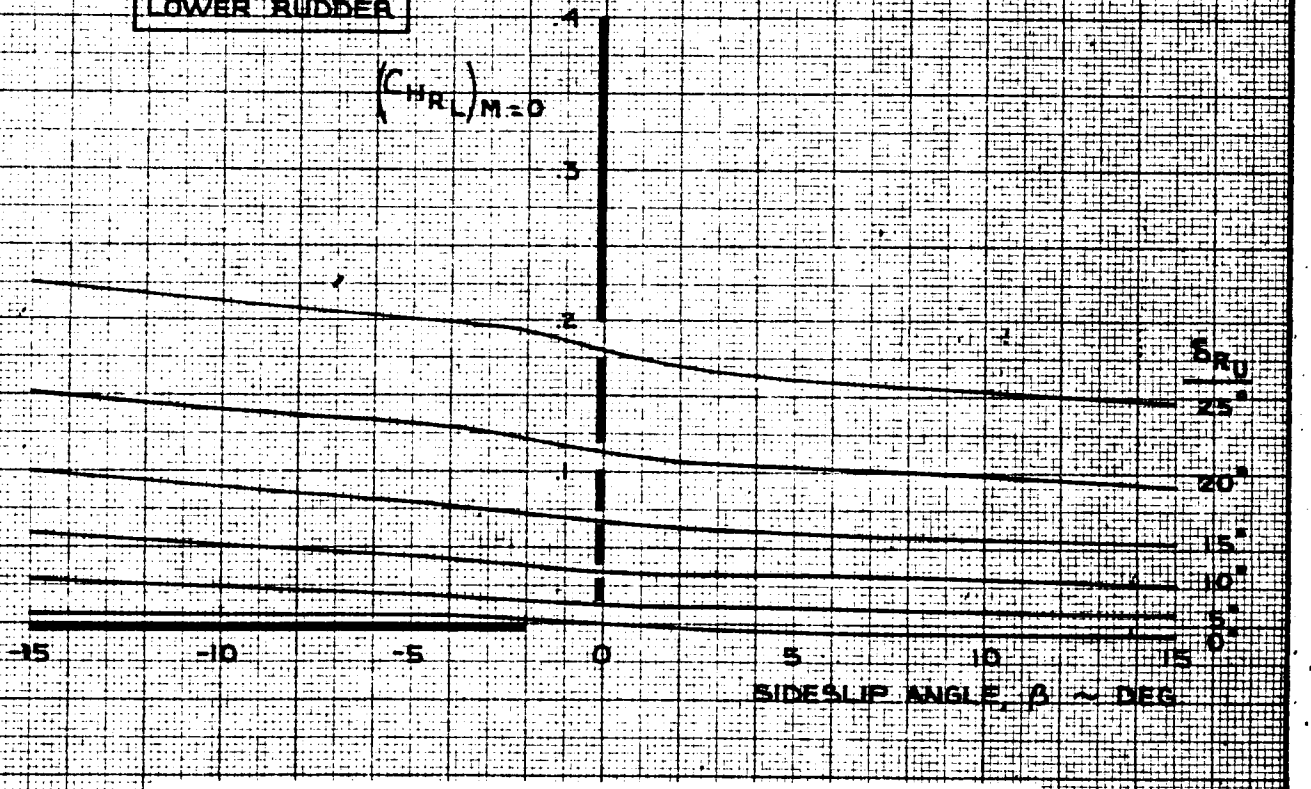

CALC	FOSTER	10-23-67	REVISED	DATE
CHECK	HOLTZNER	1-5-68	CURNUTT	10-29-68
APR			LAGREE	2-10-70
APR			BECK	6-25-70
INK	KINSMAN	2-17-70		

DIRECTIONAL CONTROL
RUDDER HINGE MOMENTS
SEGMENTS DEFLECTED SEPARATELY

THE BOEING COMPANY

747

D6-30643, Vol. II

PAGE 10.2-3

W-E ALBANENE 1951 REV E

THESE DATA NOT INCLUDED
IN NASA SIMULATION

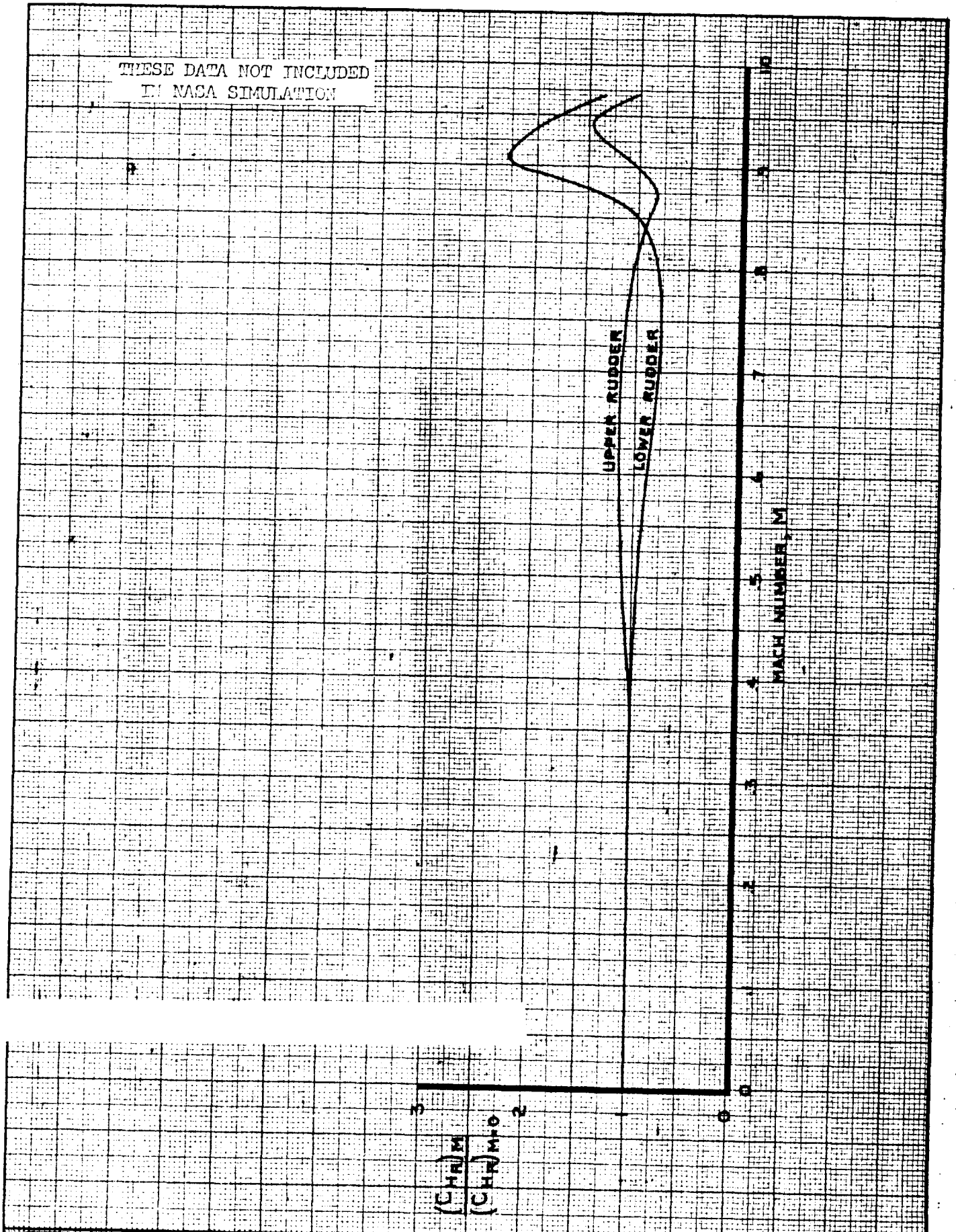

CALC	FOSTER	11-2-67	REVISED	DATE	DIRECTIONAL CONTROL RUDDER HINGE MOMENTS EFFECT OF MACH NUMBER
CHECK	HOLTZNER	1-5-68	LAGREE	2-2-70	
APR			BECK	6-25-70	
APR					
INK	ODEGARD	2-13-70			

747

D6-30643, Vol. II

THE BOEING COMPANY

PAGE 10.2-4

10.3 Yaw Damper/Turn Coordinator

Dutch roll oscillations on the 747 are attenuated by a series yaw damper which commands rudder proportional to yaw rate and bank angle. The yaw damper output signals are fed through shaping networks into the rudder actuator package, which drives the rudder. These rudder deflections do not result in any movement of the rudder pedals, nor do they affect normal operation of the rudder. The yaw damper is dualized in that both the upper and lower rudders have independent yaw damping systems. Deflection is limited to 3.6 degrees and the rate of deflection (for yaw damping) cannot exceed 15 degrees per second. A complete description of the yaw damper system is shown in the block diagram on page 10.3-2.

Turn coordination is achieved by deflecting the rudder, through the yaw damper actuator, proportional to roll rate. The input roll rate signal is actually a derived rate, as shown in the block diagram. The turn coordinator operates only when the flaps are down, having a gain of .69 degrees/degree per second.

An "easy-on" circuit has been incorporated with the flap switch to smooth transients in the bank attitude signals when the flap switch activates. (A warning light in the cockpit is provided to indicate improper operation of the flap switch).

747 YAW DAMPER TRANSFER FUNCTION & BLOCK DIAGRAM

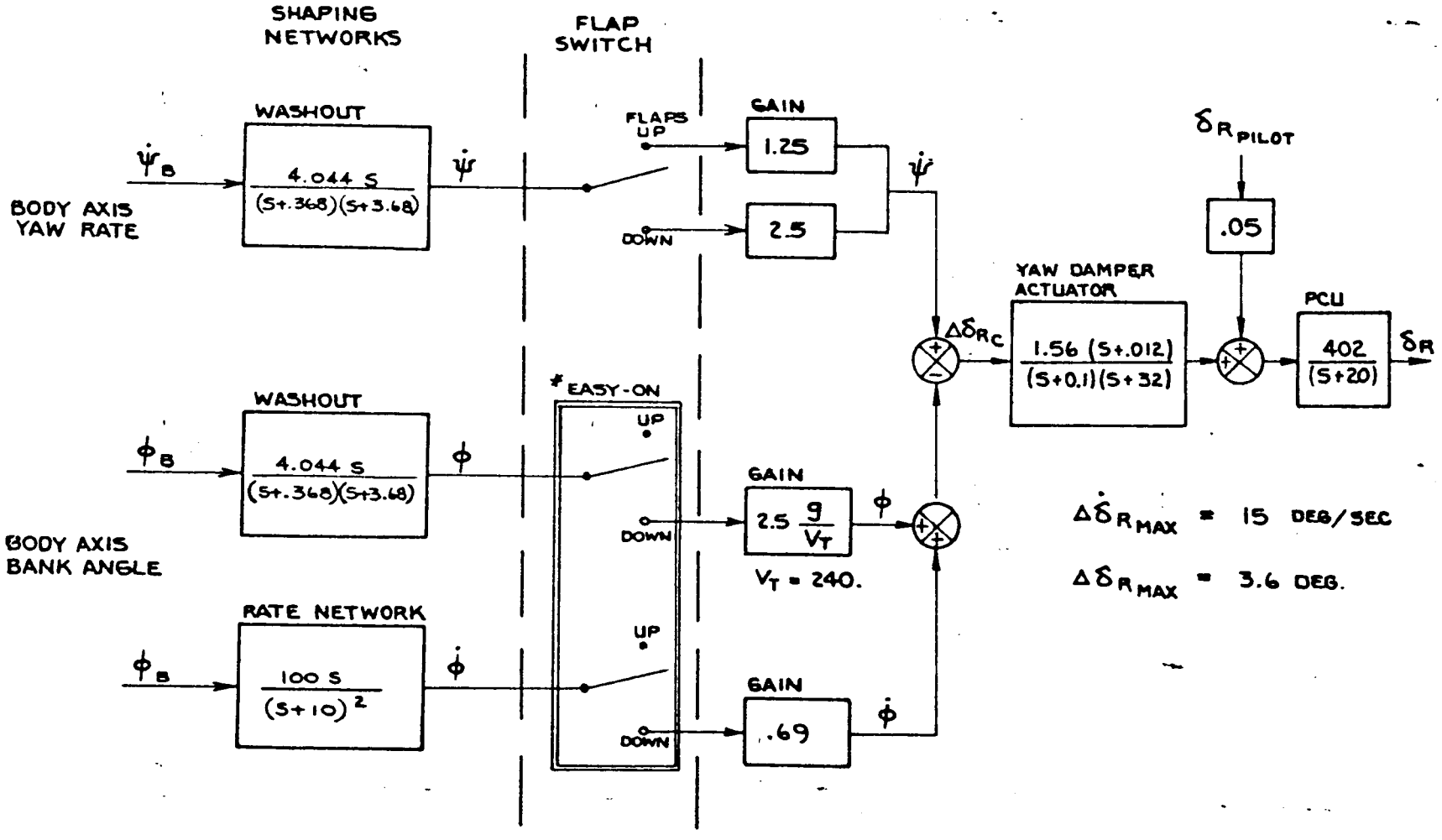

* EASY-ON/EASY-OFF SWITCHING NETWORK SMOOTHES TRANSIENTS DURING SWITCHING ONLY. TRANSITION BETWEEN SWITCH POSITIONS IS A LINEAR FUNCTION OF TIME, REQUIRING 10 SECONDS.

CALC	CURNUTT	12-29-67		
CHECK				
APPD			CURNUTT	2-14-70
APPD			CURNUTT	6-12-69
INK	ODEGARD	12-29-67		9-3-70

THE BOEING COMPANY RENTON, WASHINGTON

YAW DAMPER BLOCK DIAGRAM

747 D6-30643 Vol. II PAGE 10.3-2

REV. E

11.0 HIGH LIFT SYSTEM

A general description of the system is presented in the Introduction on Pages 1.2-5 and 1.2-6 and in Volume I. A block diagram of the simulated high lift model is shown on Page 11.0-2 . The data for each particular block can be found on the page number adjacent to the block.

A flap auto-retraction system is designed as part of the flap system. With the flap lever in the 30 detent and with aircraft speeds exceeding 169 knots, the flaps automatically drive back to the 25 position. The flaps automatically return to the original 30° setting when the airspeed is decreased to 164 knots.

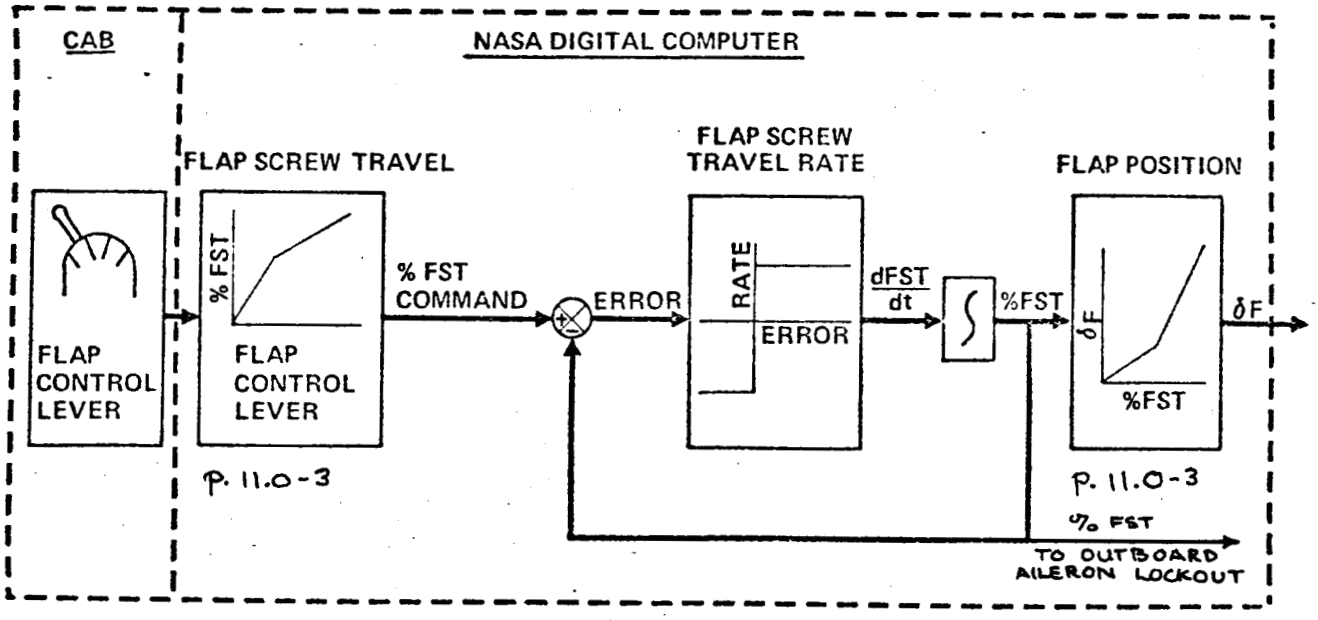

FLAP SCREW TRAVEL RATE $= \frac{d\,FST}{dt} = \pm 2.2$ DEG/SEC

HIGH LIFT MODEL

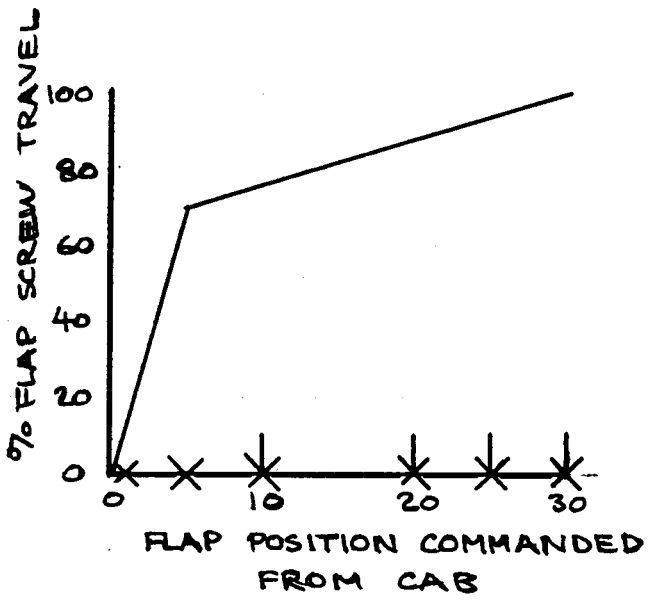

DETENT	% FST
0	0
5	70
30	100

| FSAA FLAP POSITION DETENT
X 747 FLAP POSITION DETENT

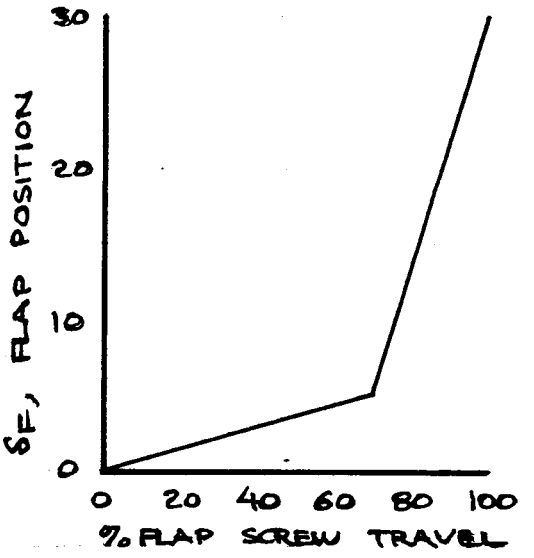

%FST	δ_F
0	0
70	5
100	30

CALC			REVISED	DATE	FLAP SCREW TRAVEL AND FLAP POSITION RELATIONSHIP	747
CHECK						D6-30643 Vol II
APR						
APR						
	NORDWALL	7/27/70			THE BOEING COMPANY	PAGE 11.0-3

12.0 PROPULSION SYSTEM

A general description of the system is presented in the Introduction on Pages 1.3-2 and 1.3-3 and in Volume I.

12.1 Engine Pressure Ratio

A block diagram of the engine pressure ratio simulation is shown on Page 12.1-2. The flight idle limit, occurring when the flap position is 25 or 30 and gear is down but not on the ground, was simulated by adding an incremental EPR of 0.015.

The NASA engine transient program, consisting of a transport delay and a lag, was modified to approximate the 747 engine dynamics shown on Pages 12.1-6 through 12.1-17.

The engine operating limitations are contained in Appendix A - Flight Manual.

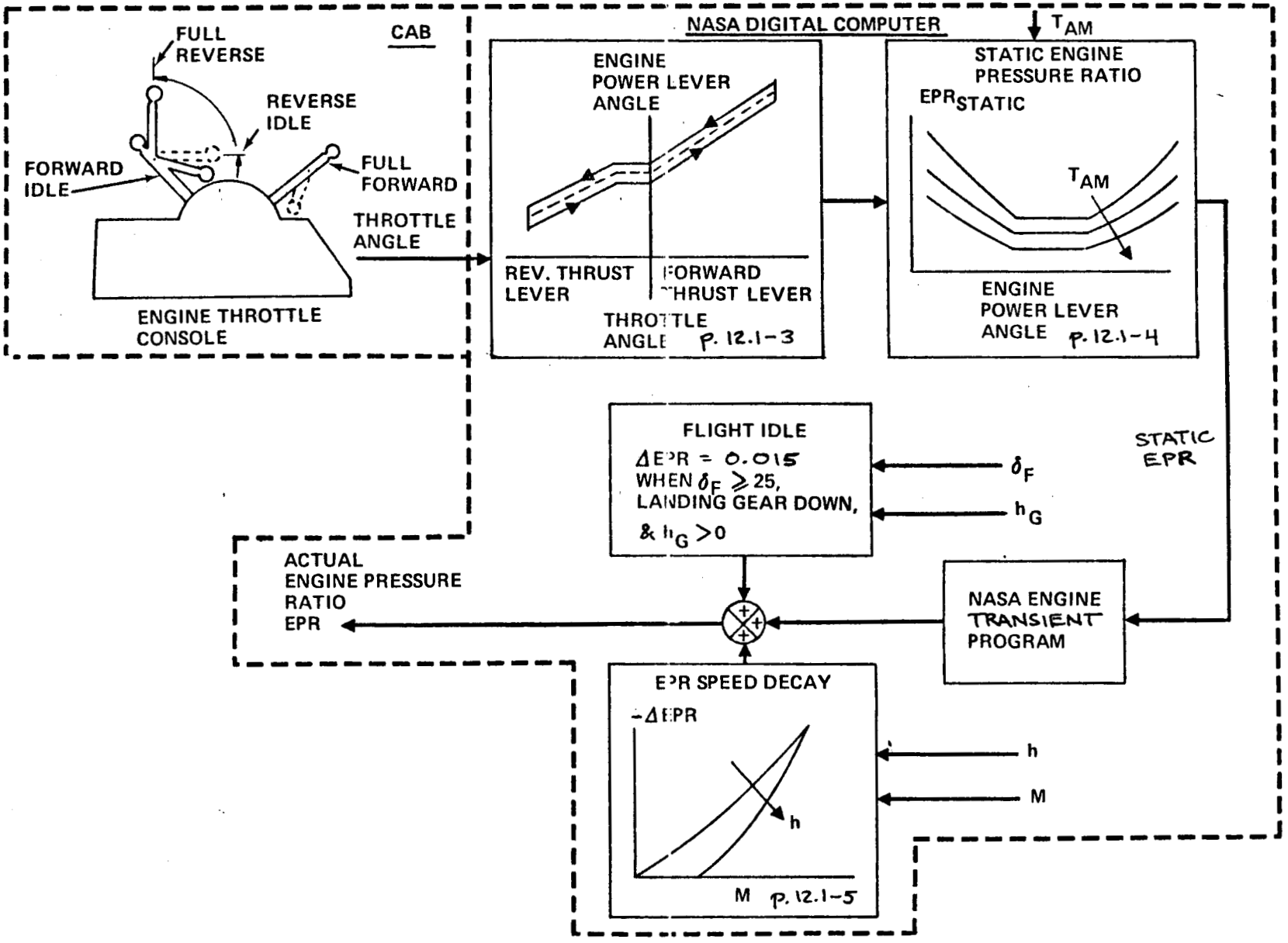

ENGINE PRESSURE RATIO SIMULATION

POWER LEVER ANGLE VS. THRUST LEVER ANGLE
ENGINE POWER LEVER STOP
THRUST REVERSER EXTEND PORT PRESSURIZED
THRUST REVERSER RETRACT PORT PRESSURIZED
FWD THRUST LOCKOUT STOP
REVERSE THRUST LOCKOUT STOP
REVERSE THRUST LEVER STOP (123°)
ENGINE POWER LEVER STOP
ENGINE POWER
LEVER ANGLE ~ DEGREES
WATER INJECTION PRESSURIZED
NOTE: THE AREA BETWEEN THE LINES ACCOUNTS FOR THE CABLE STRETCH AND BACKLASH OF THE SYSTEM.
MICROSWITCH LOCATIONS
RETRACTION OF LEADING EDGE FLAPS
LANDING GEAR WARNING HORN
FLAP SPEED BRAKE STABILIZER WARNING
AUTO THROTTLE LOW LIMIT SWITCH
2° TO OPEN
2° TO CLOSE
REVERSE THRUST LEVER TRAVEL ~ DEGREES
FORWARD THRUST LEVER TRAVEL ~ DEGREES
CALC JMMcNeill 8/29/68
CHECK
APP
APP
JMM 9/1/68
JMM 10/22/68
JMM 7/11/69
JMM 9/8/69
POWER LEVER ANGLE VS. THRUST LEVER ANGLE
JT3D-3 TURBOFAN ENGINE
THE BOEING COMPANY
ESTIMATED
747
D6-30643 Vol. II
PAGE 12.1-3

FOR FLIGHT SIMULATOR USE ONLY

TTJD-3, TURBOFAN ENGINE

ESTIMATED POWER LEVER ANGLE vs EPR RELATIONSHIP

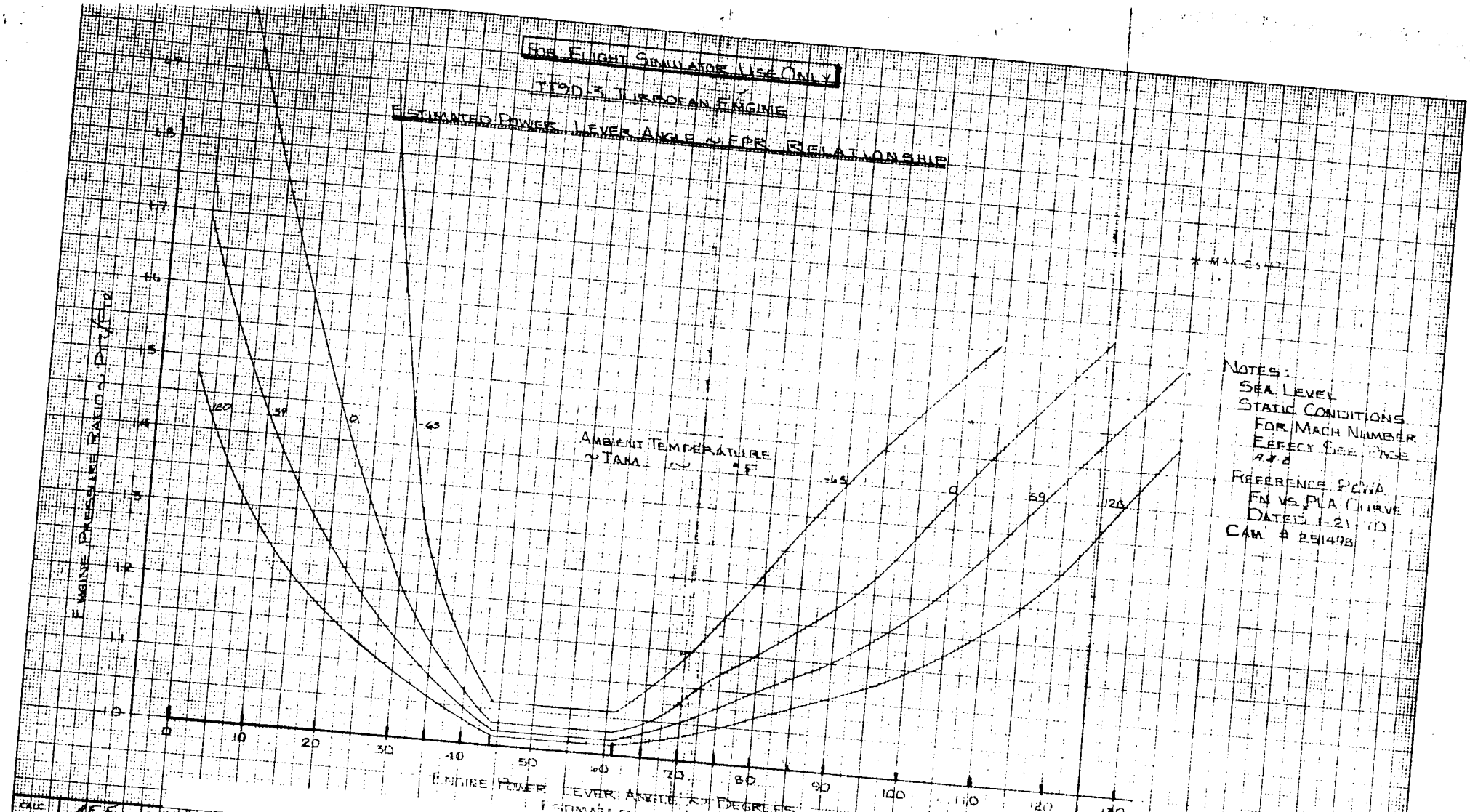

NOTES:
1. SEA LEVEL STATIC CONDITIONS FOR MACH NUMBER EFFECT SEE PAGE 12.1-2
2. REFERENCE P&WA FN VS PLA CURVES DATED 1-21-70 CAM # 25149B

CALC	A.E.F.	2-4-70	REVISED	DATE	POWER LEVER ANGLE vs EPR TTJD-3 TURBOFAN ENGINE THE BOEING COMPANY
CHECK					
APPD					
APPD					

7471
D6-30643 Vol. II
PAGE 12.1-4

TO 1065 R9 REV N

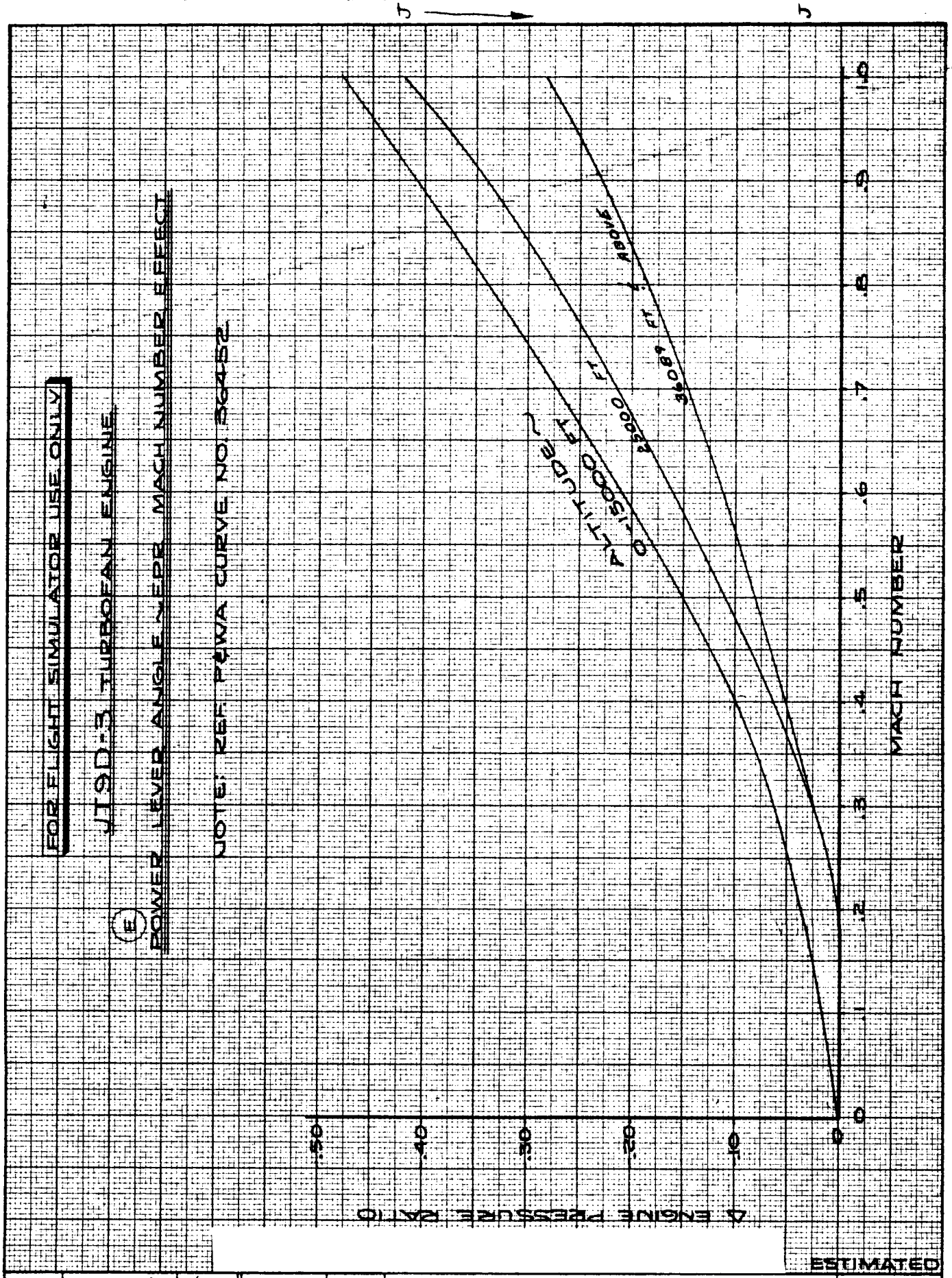

CALC	JMMcNeill	1/15/68	REVISED	DATE	POWER LEVER ANGLE ~ EPR MACH NUMBER EFFECT JT3D-3 TURBOFAN ENGINE
CHECK			JMM	7/15/68	
APR			JMM	7/11/9	
APR			JNS	5-8-70	
					THE BOEING COMPANY

747

D6-30643 Vol. II

PAGE 12.1-5

AD 461 C R4

SNAP ACCELERATION
SEA LEVEL STATIC JT9D-3

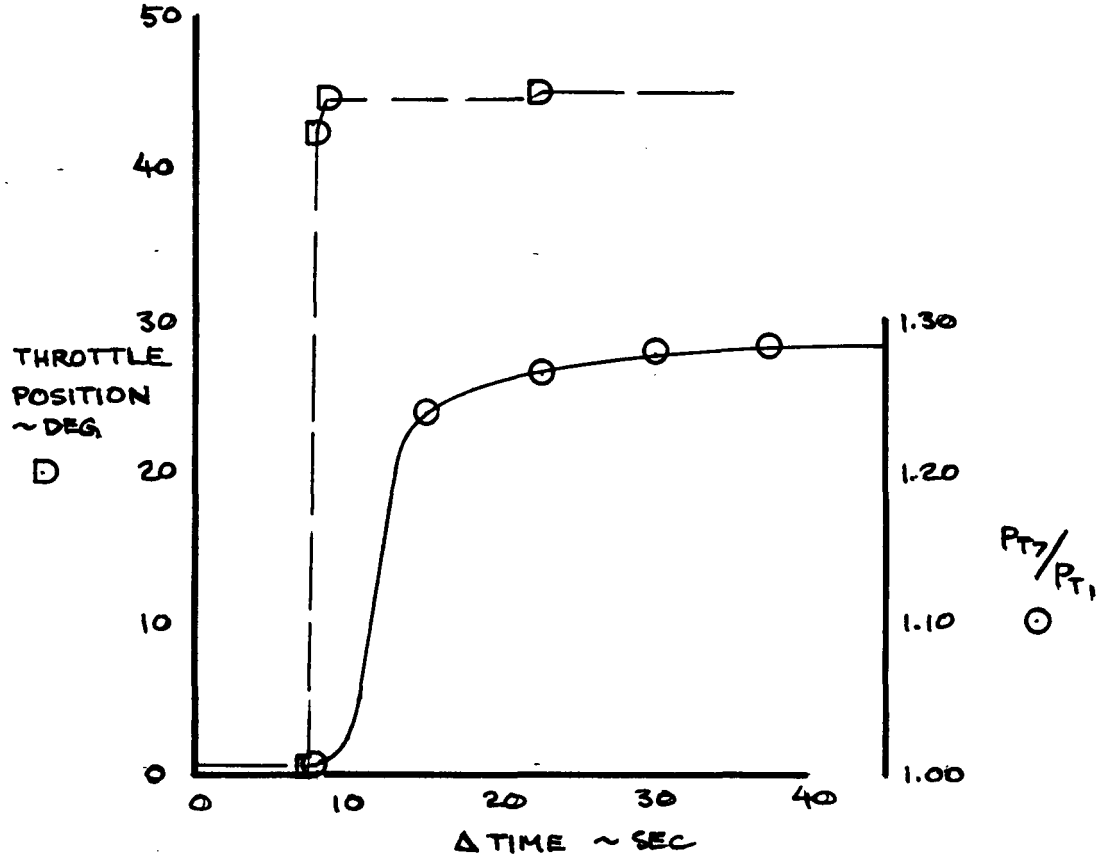

REF: D6-13302
P 6.2-1

CALC			REVISED	DATE	ENGINE TRANSIENT CHARACTERISTICS	747
CHECK						D6-30643 VOL II
APR						
APR					THE BOEING COMPANY	PAGE 12.1-6
	DRN	11/10/69				

SNAP ACCELERATIONS
SEA LEVEL STATIC JT9D-3

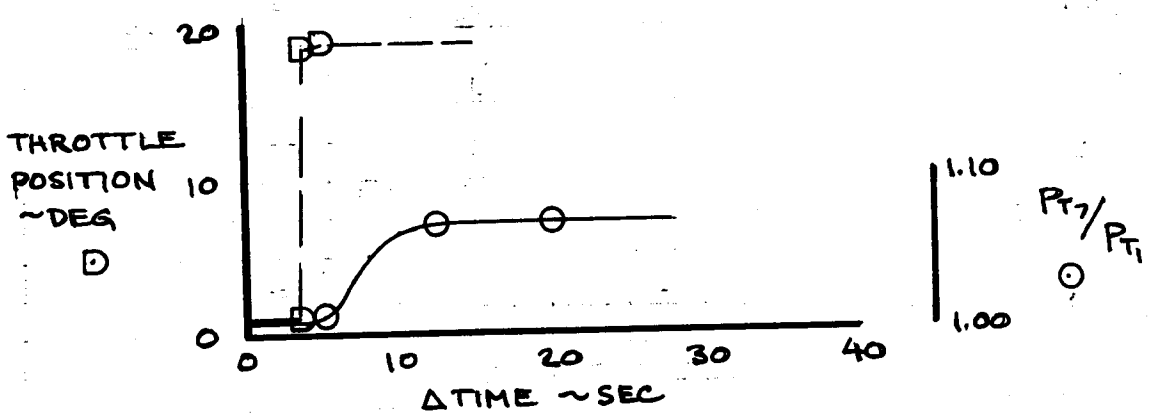

REF: D6-13302
P. 6.2-2

CALC			REVISED	DATE	ENGINE TRANSIENT CHARACTERISTICS	747
CHECK						D6-30643 VOL II
APR					THE BOEING COMPANY	PAGE 12.1-7
APR						
	DRN	11/10/69				

SNAP ACCELERATION – PARTIAL THROTTLE
SEA LEVEL STATIC JT9D-3

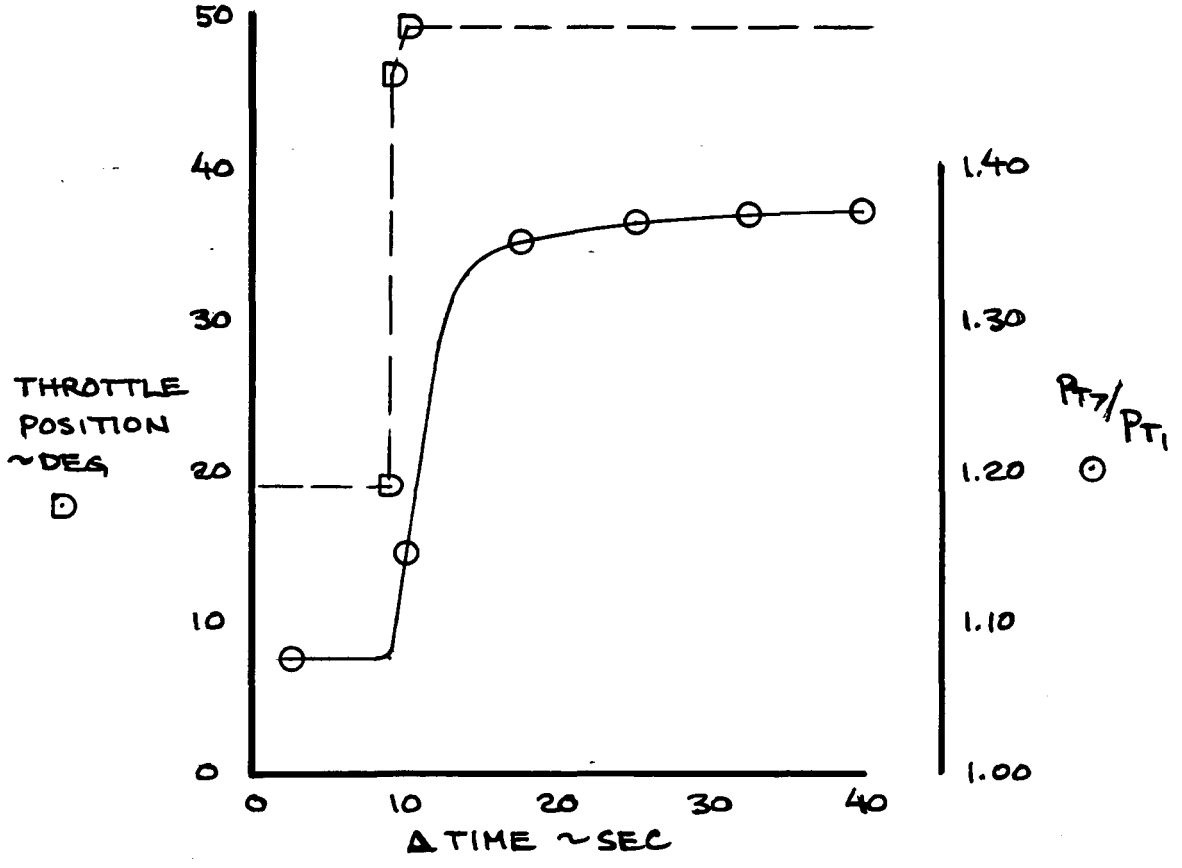

REF: D6-13302
P. 6.2-3

CALC			REVISED	DATE	ENGINE TRANSIENT CHARACTERISTICS	747
CHECK						D6-30643 VOL II
APR						
APR					THE BOEING COMPANY	PAGE 12.1-8
	DRN	11/10/69				

SNAP ACCELERATION – PARTIAL THROTTLE
SEA LEVEL STATIC JT9D-3

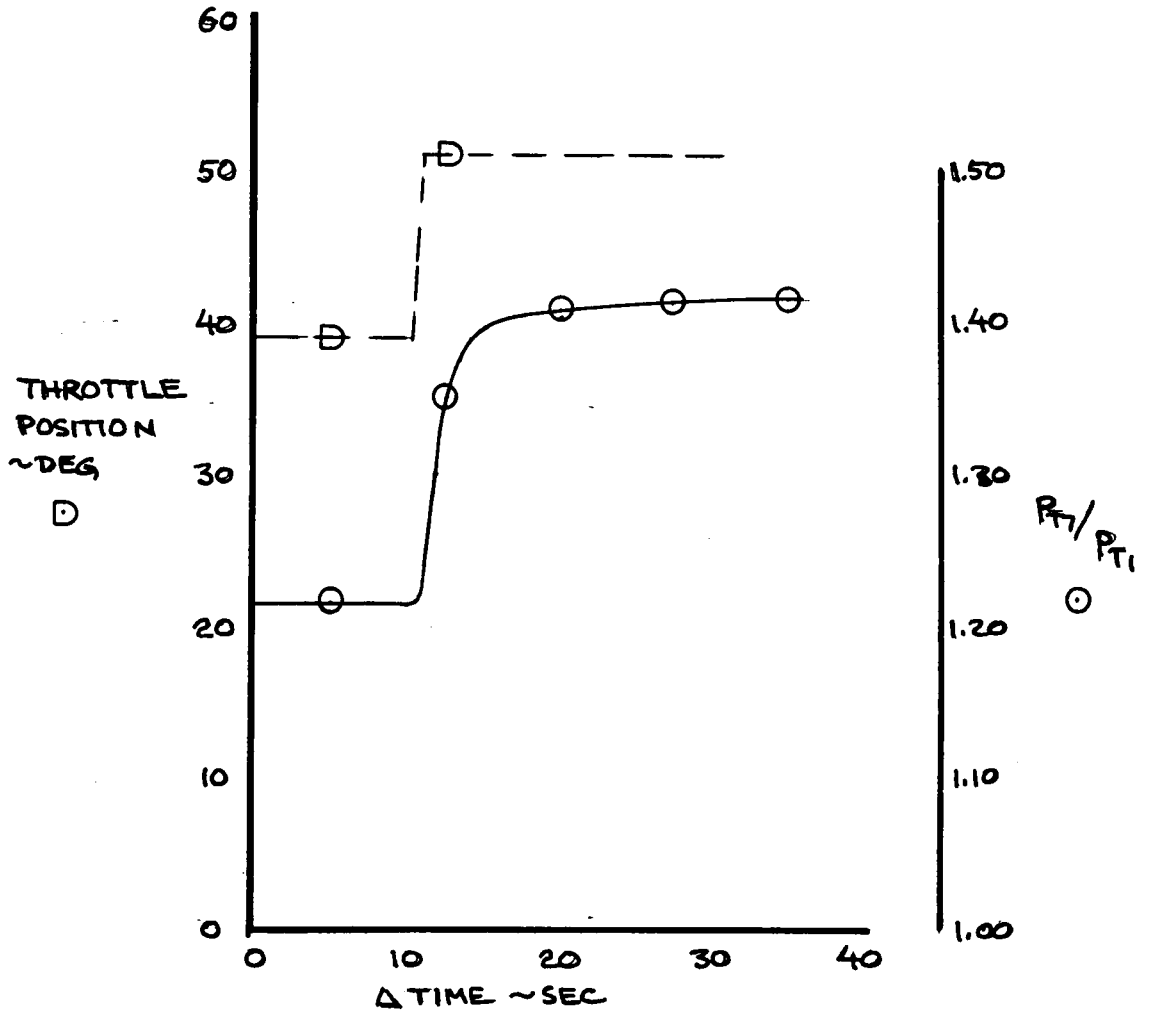

REF: D6-13302
P 6.2-4

CALC			REVISED	DATE	ENGINE TRANSIENT CHARACTERISTICS	747
CHECK						D6-30643 VOL II
APR						
APR					THE BOEING COMPANY	PAGE 12.1-9
	DRN	11/10/69				

SLOW DECELERATION - PARTIAL THROTTLE
SEA LEVEL STATIC JT9D-3

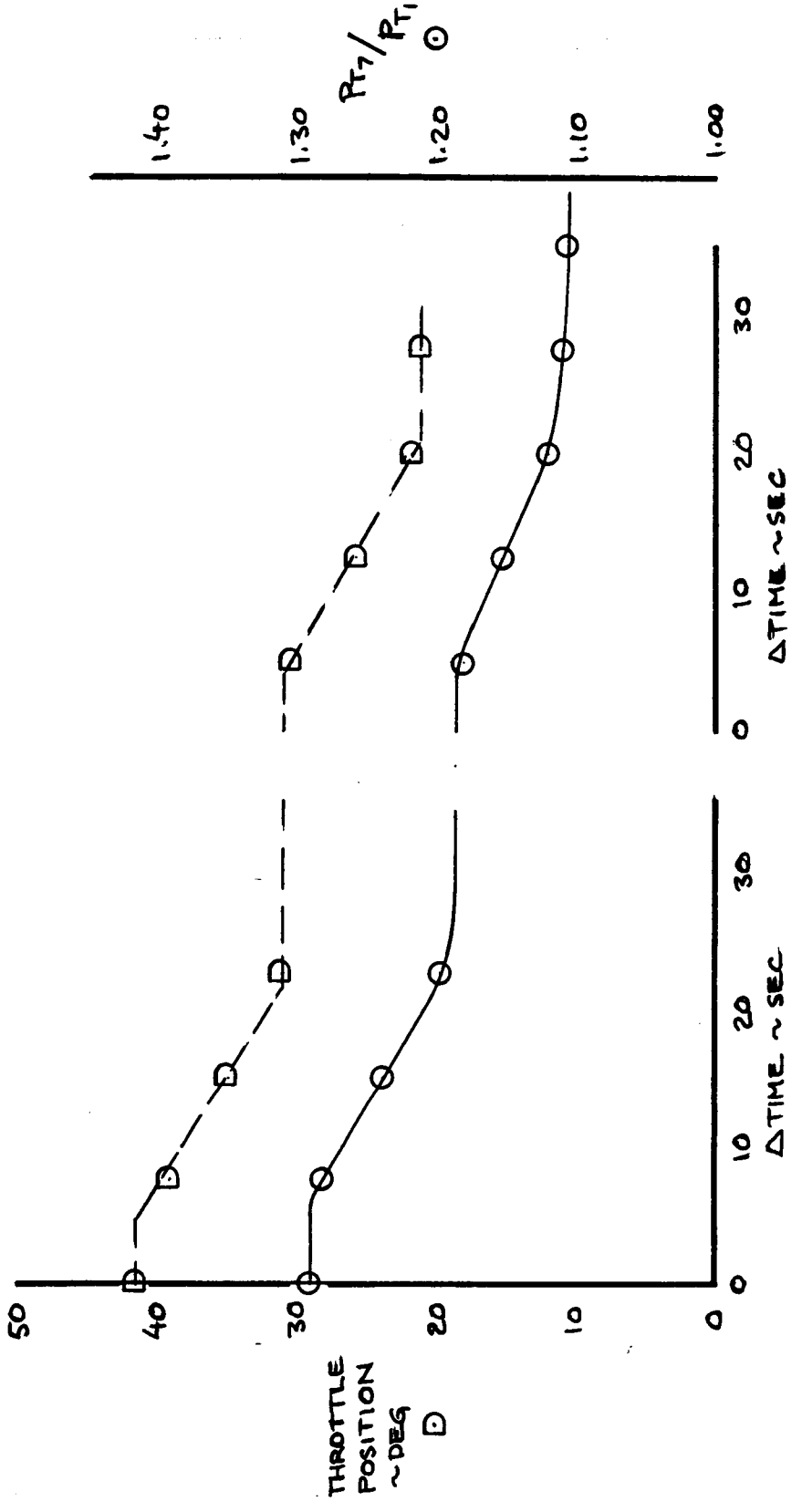

REF: D6-13302
P. 6.2-5, -6

CALC			REVISED	DATE
CHECK				
APR				
APR				
	DRN	11/10/69		

ENGINE TRANSIENT CHARACTERISTICS

747
D6-30643 VOL II

THE BOEING COMPANY

PAGE 12.1-10

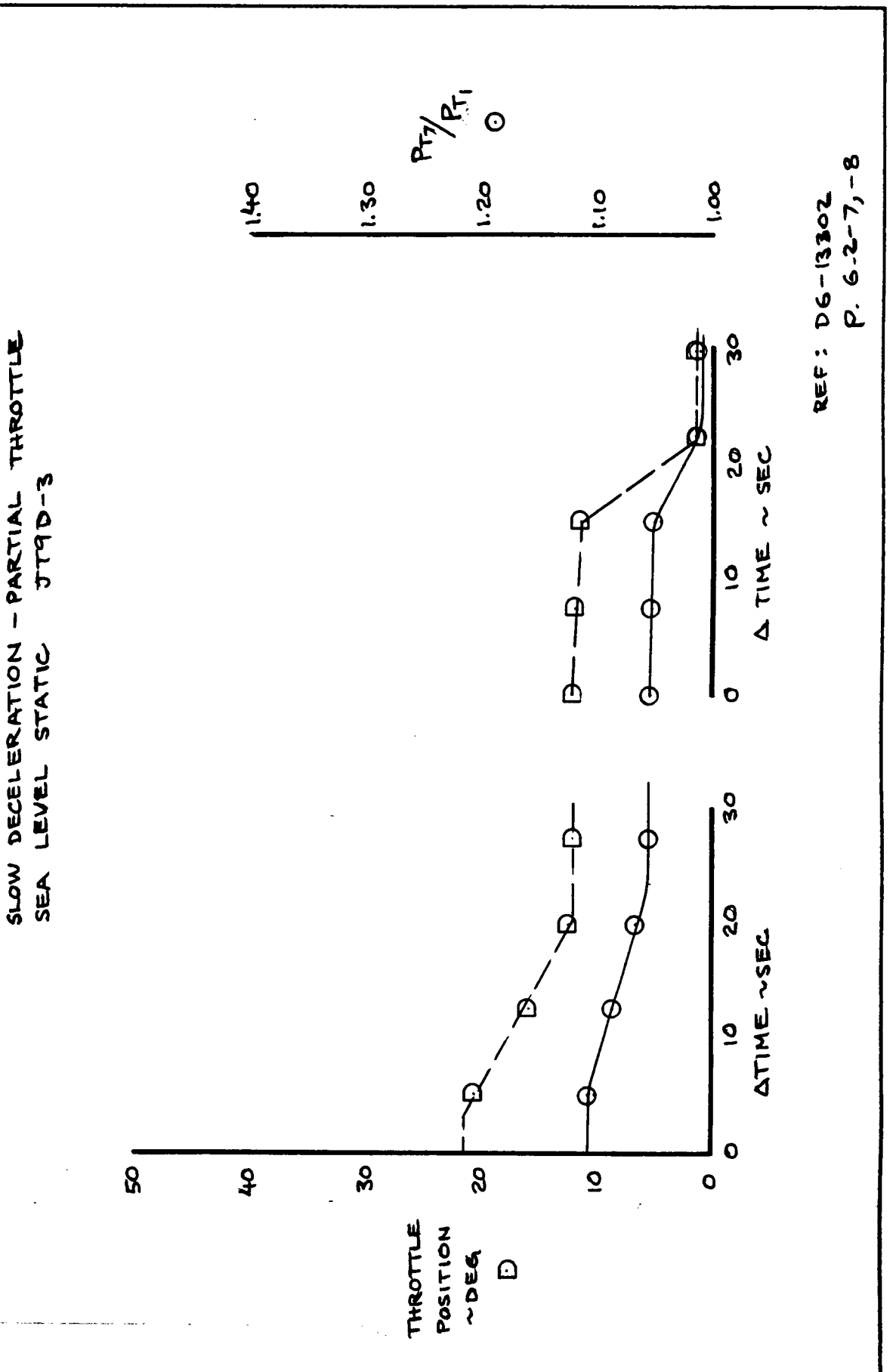

CALC			REVISED	DATE	ENGINE TRANSIENT CHARACTERISTICS	747
CHECK						D6-30643 VOL II
APR						
APR					THE BOEING COMPANY	PAGE 12.1-11
	DRN	11/10/69				

SNAP DECEL-ACCEL
20000 FT M=.80 JT9D-3

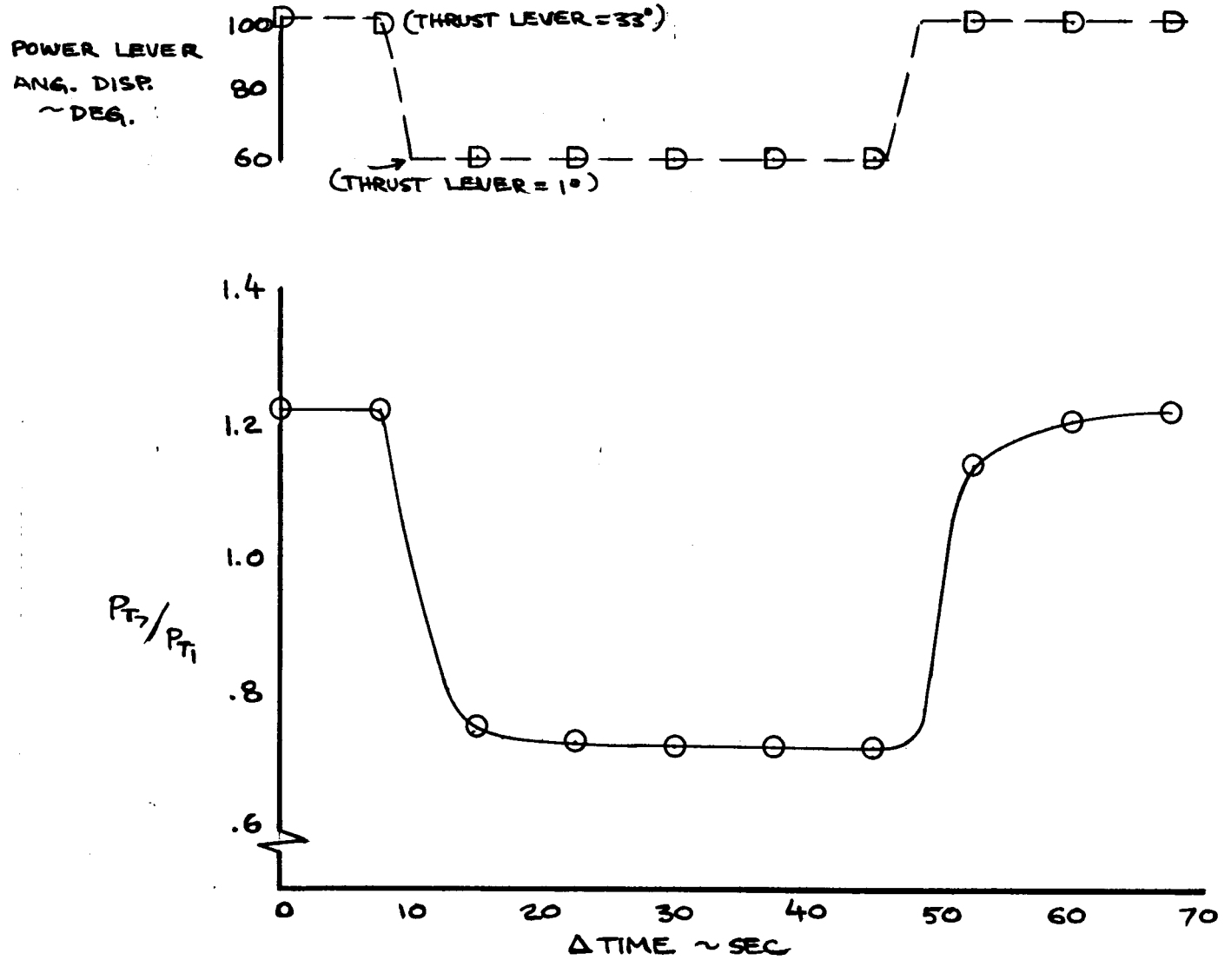

REF: D6-13302
P 6.2-9

CALC	CHECK	APR	APR	DRN
				11/10/69

REVISED	DATE

THE BOEING COMPANY

ENGINE TRANSIENT CHARACTERISTICS

747

D6-30643 VOL II

PAGE 12.1-12

AD 461 C-R4

K+E ALBANENE 1961 TRACING PAPER

SLOW DECEL-ACCEL
30000 FT M=.55 JT9D-3

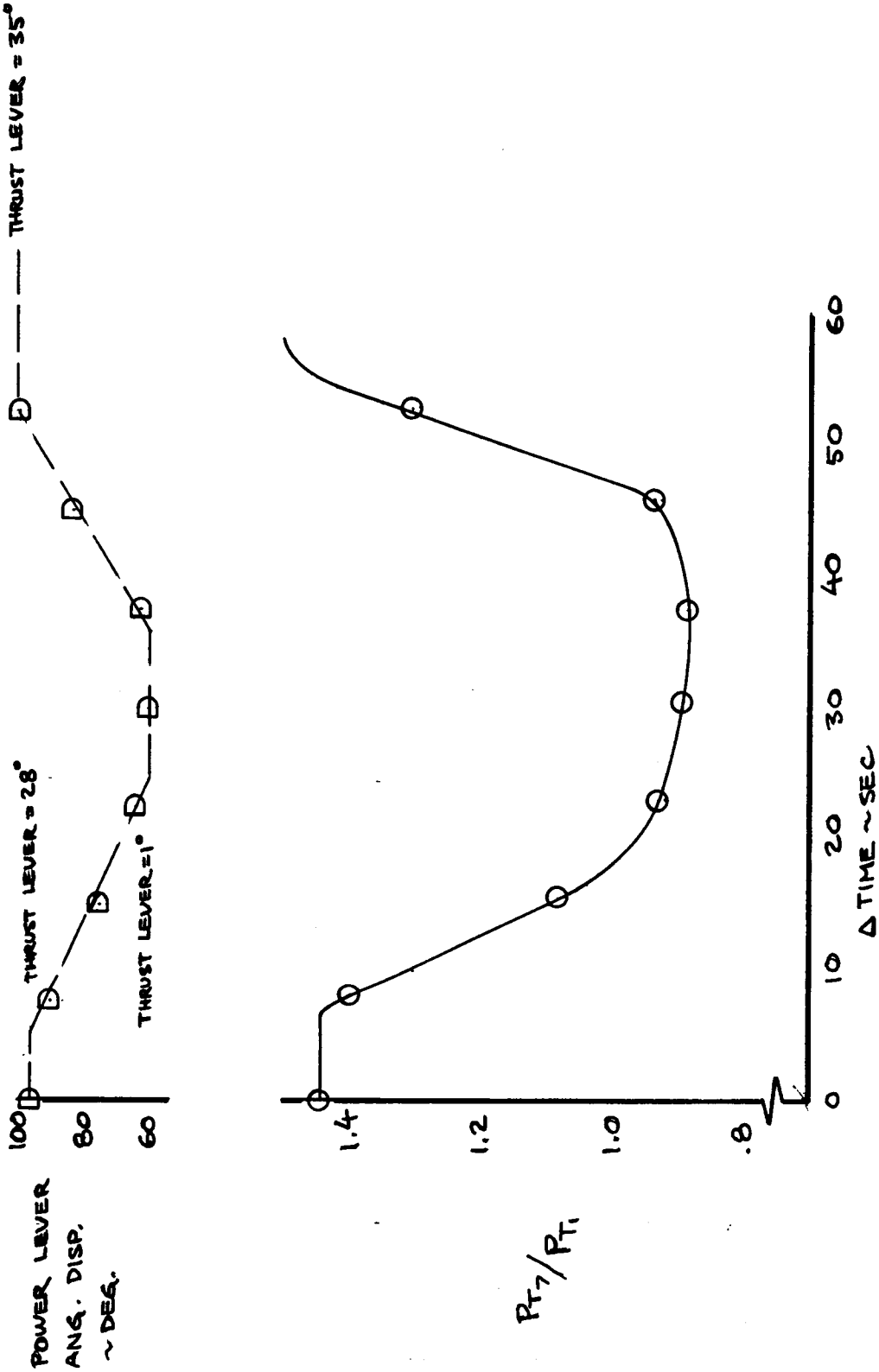

REF: D6-13302 P. 6.2-11

CALC			REVISED	DATE
CHECK				
APR				
APR				
	DRN	11/10/69		

ENGINE TRANSIENT CHARACTERISTICS

THE BOEING COMPANY

747
D6-30643 VOL II
PAGE 12.1-13

MEDIUM DECEL - SNAP ACCEL
30000 FT M=.55 JT9D-3

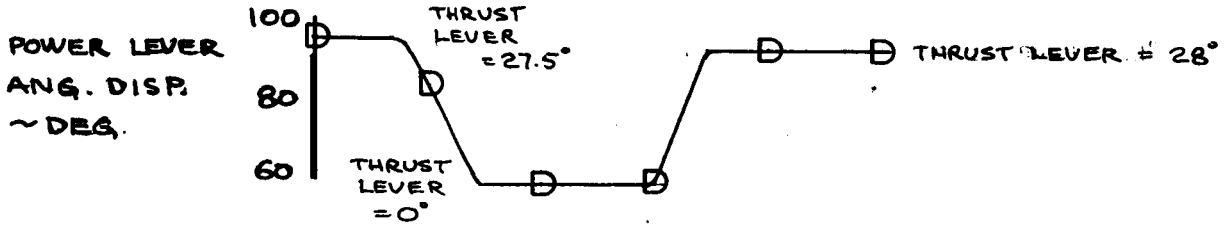

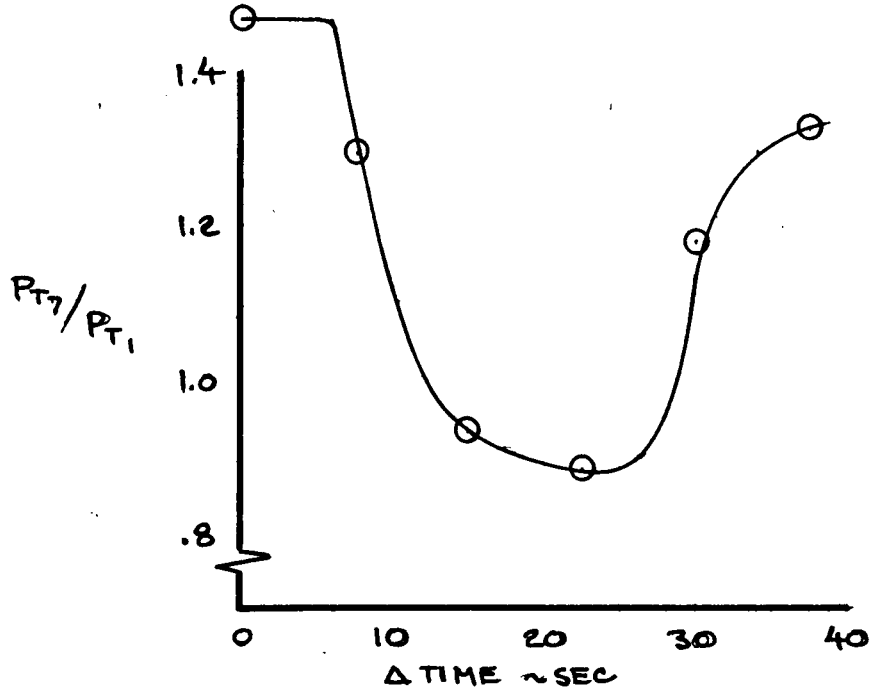

REF : D6-13302
P. 6.2-13

CALC	CHECK	APR	APR
			DRN
			11/10/69

REVISED	DATE

THE BOEING COMPANY

ENGINE TRANSIENT CHARACTERISTICS

747 | D6-30643 VOL II | PAGE 12.1-14

SNAP ACCEL - DECEL
30000 FT M=.85 JT9D-3

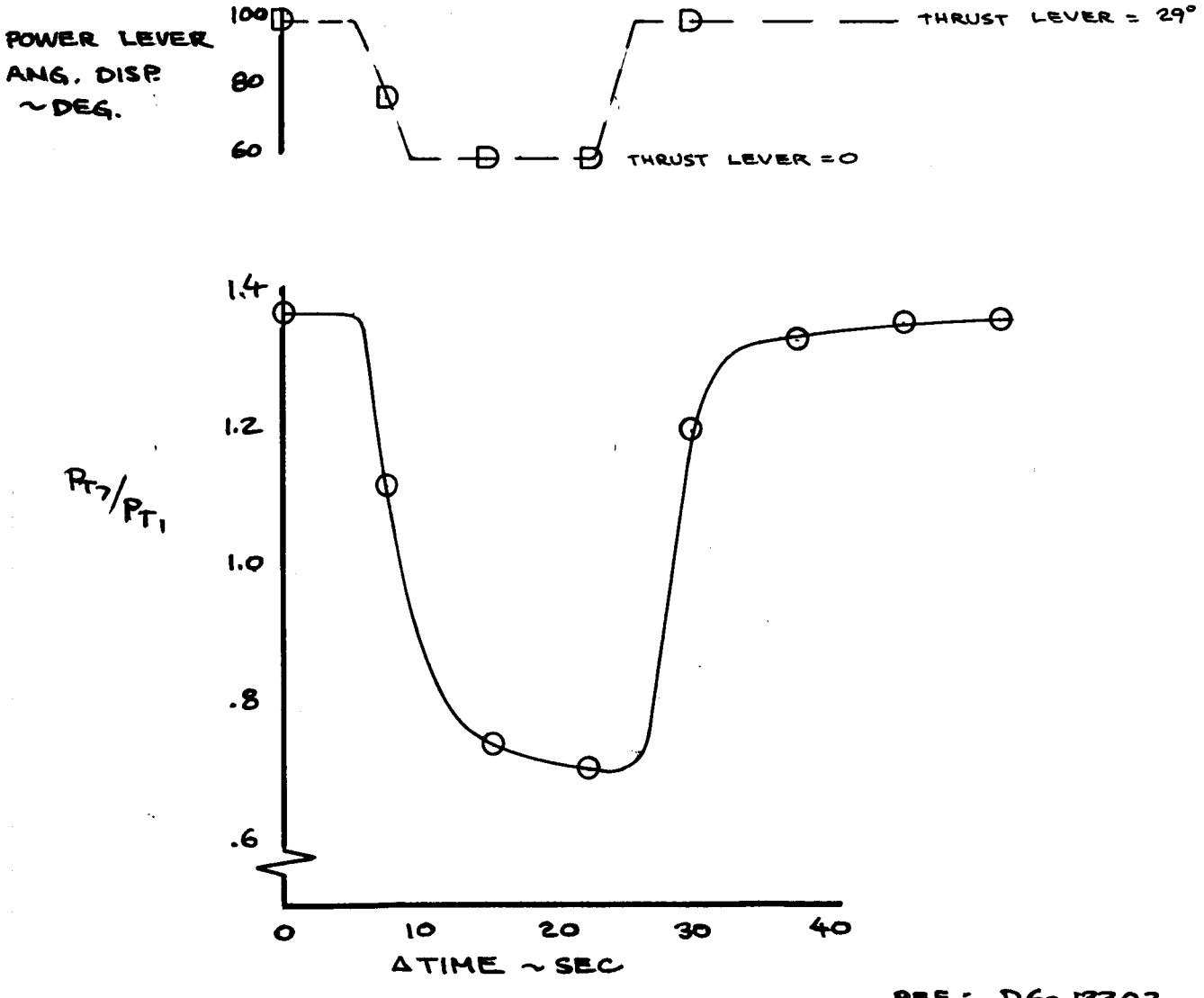

REF: D6-13302
P. 6.2-15

				CALC	
DRN				CHECK	
				APR	
1/10/69				APR	
			REVISED		
			DATE		

THE BOEING COMPANY

ENGINE TRANSIENT CHARACTERISTICS

747

D6-30613 VOL II

PAGE 12.1-15

AD 461 C-R4

K+E ALBANENE 1881 TRACING PAPER

SLOW DECEL - MEDIUM ACCEL
30000 FT M=.85 JT9D-3

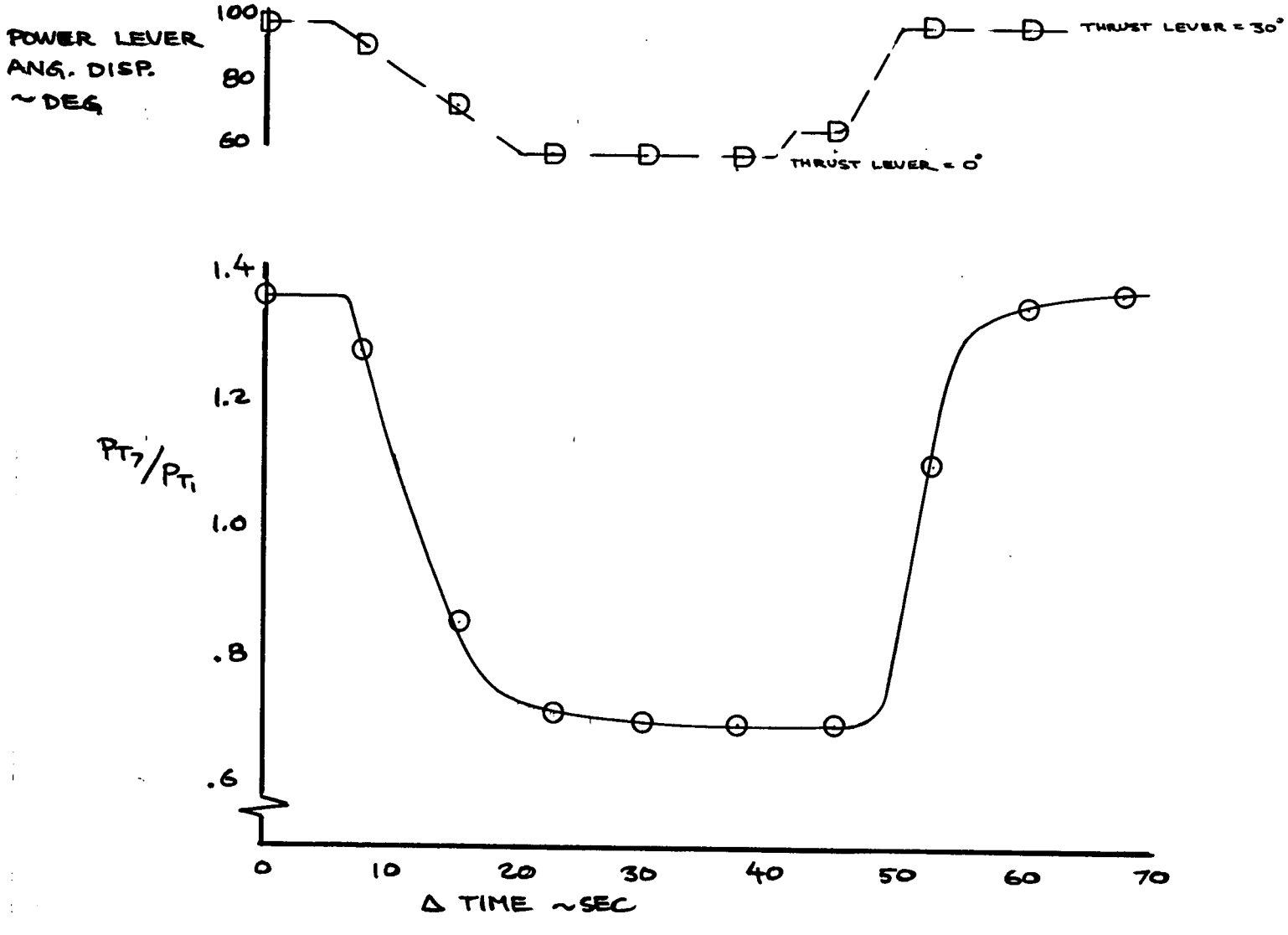

REF: DG-13302
P. 6.2-17

	CALC	CHECK	APR	APR
DRN				
11/10/69				

REVISED	DATE

THE BOEING COMPANY

ENGINE TRANSIENT CHARACTERISTICS

747 | DG-30613 VOL II | PAGE 12.1-16

AD 461 C-R4

K+E ALBANENE 1981 TRACING PAPER

MEDIUM DECEL - SNAP ACCEL
39000 FT M=.65 JT9D-3

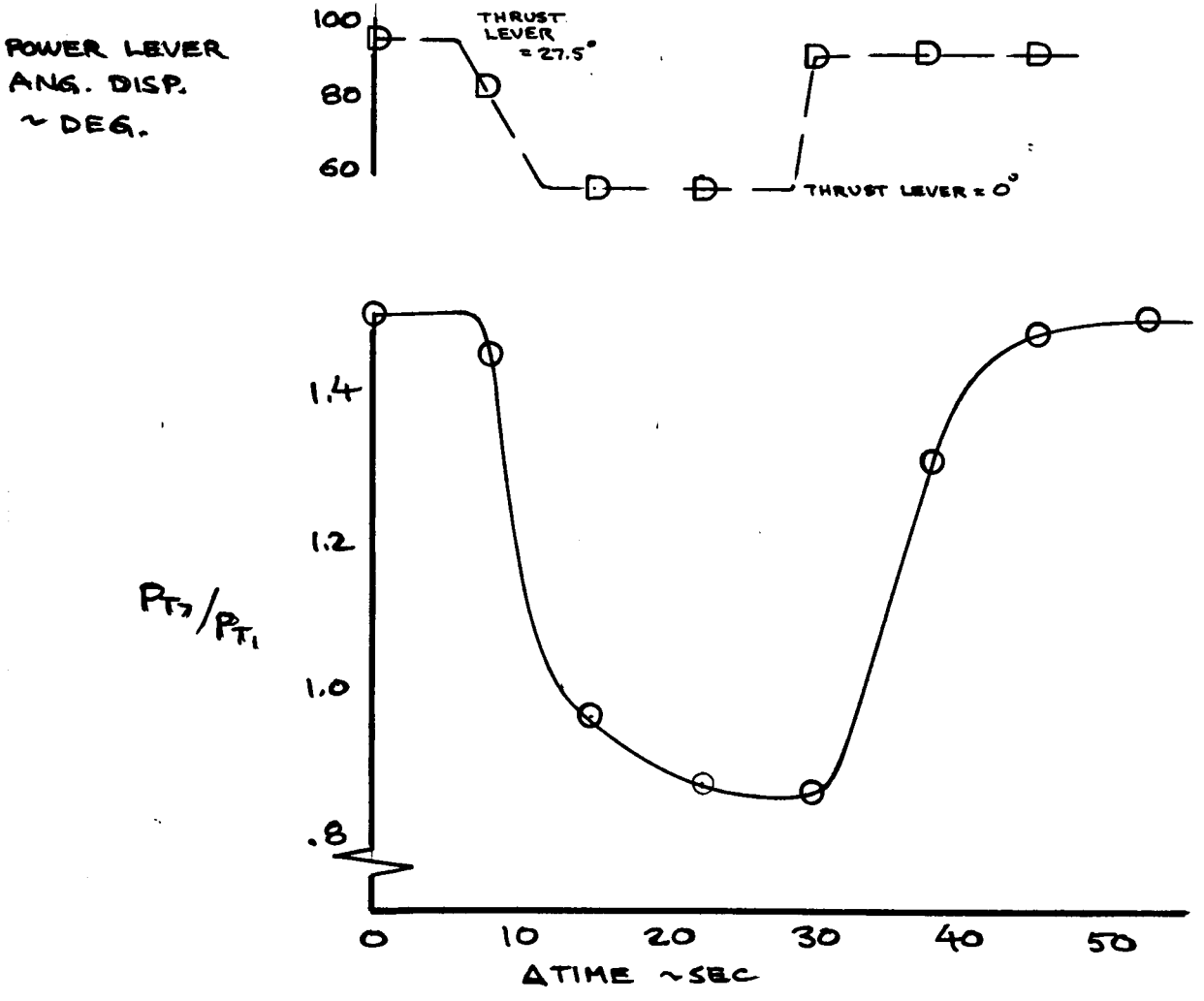

REF: DG-13302
P. 6.2-19

CALC					
CHECK					
APR					
APR.					
DRN	11/10/69				
DATE	REVISED				

ENGINE TRANSIENT CHARACTERISTICS

THE BOEING COMPANY

747

D6-30643 VOL II

PAGE 12.1-17

AD 461 C-R4

K+E ALBARENE 1981 TRACING PAPER

12.2 Engine Thrust

A block diagram of the engine thrust simulation is shown on Page 12.2-2.

The reverse thrust characteristics used in the simulation were a function of ambient pressure and EPR, Page 12.2-5 . This data was based on a Mach number of .2. Reverse thrust data as a function of Mach number is shown on Pages 12.2-6 , 12.2-7 and 12.2-8 .

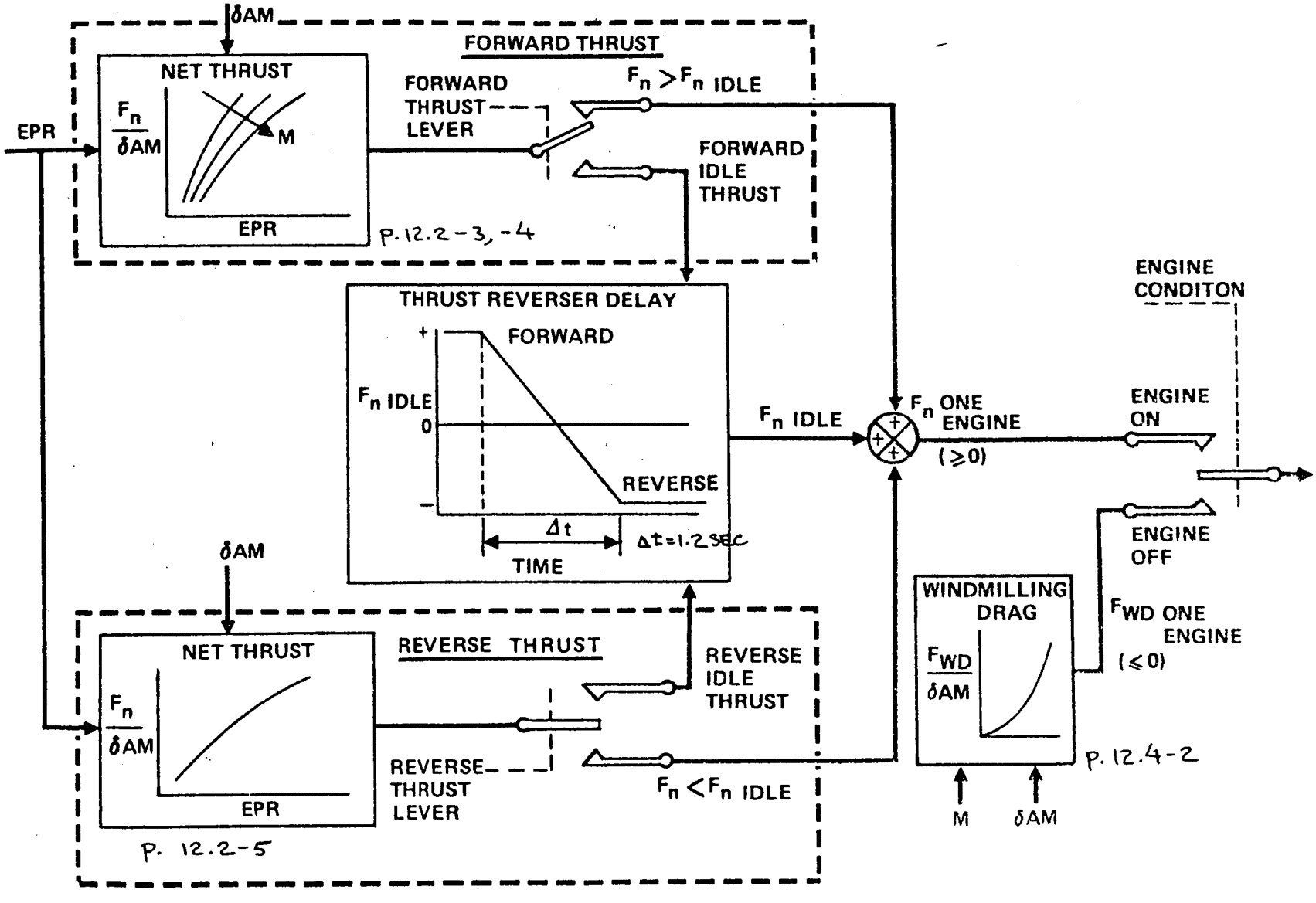

ENGINE THRUST SIMULATION

FOR FLIGHT SIMULATOR USE ONLY
INSTALLED GENERALIZED NET THRUST
JT9D-3 ENGINES
NOTE SCRUBBING EFFECT INCLUDED
INSTALLED CORRECTED NET THRUST ~ F_{n_c}/δ_{t_1} ~ 1000 LBS
INSTALLED CORRECTED NET THRUST ~ F_{n_c}/δ_{t_1} ~ 1000 LBS
ENGINE PRESSURE RATIO ~ P_{t_2}/P_{t_1}
O MACH
O MACH
CHKD
CHKD
APPD
APPD
REVISED
E.D.K
DATE
11/23/65
INSTALLED CORRECTED
GENERALIZED NET THRUST
JT9D-3 ENGINES
747
D6-30643
VOL. II
THE BOEING COMPANY
PAGE
12.2-3

FOR FLIGHT SIMULATOR USE ONLY
INSTALLED GENERALIZED NET THRUST
JT9D-3 ENGINES
NOTE SCRUBBING EFFECT INCLUDED
ENGINE PRESSURE RATIO ~ P_{t_2}/P_{t_2}
INSTALLED CORRECTED NET THRUST ~ F_N/δ_2 ~ 1000 LBS
CORRECTED NET THRUST ~ F_N/δ_2 ~ 1000 LBS
MACH
INSTALLED
CORRECTED
INSTALLED CORRECTED NET THRUST
JT9D-3 ENGINES
THE BOEING COMPANY
747
D6-30643 VOL. II
PAGE 12.2-4
REVISED
DATE
ENGR
CHECK
APPD
APPD

JT9D-3 ENGINE

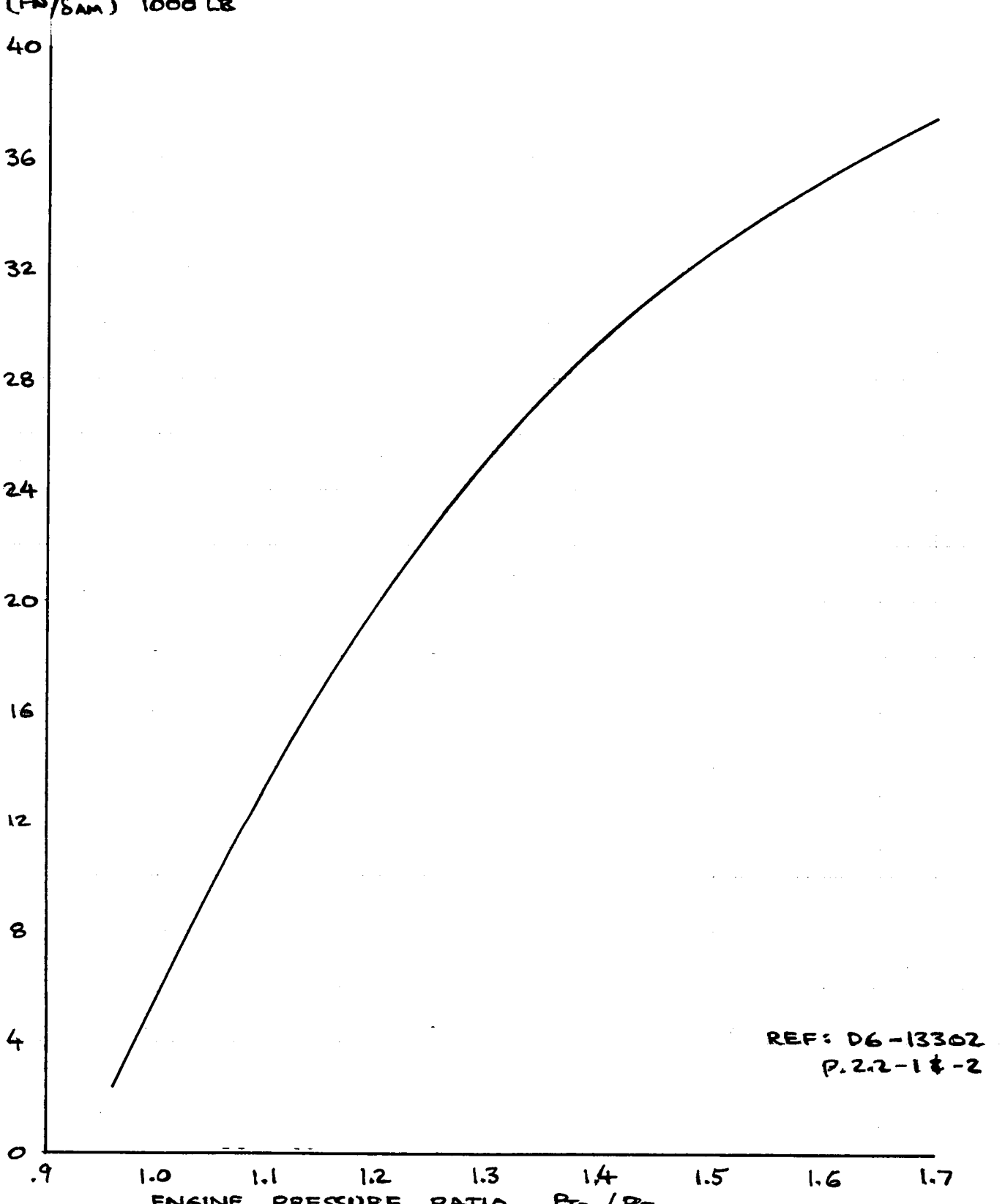

REF: D6-13302
P. 2.2-1 & -2

CALC			REVISED	DATE
CHECK				
APP				
APP				
		APRIL 1970		

REVERSE NET THRUST
PRIMARY + FAN REVERSER

747

D6-30643 VOL II

THE BOEING COMPANY

PAGE 12.2-5

JT9D-3 ENGINE

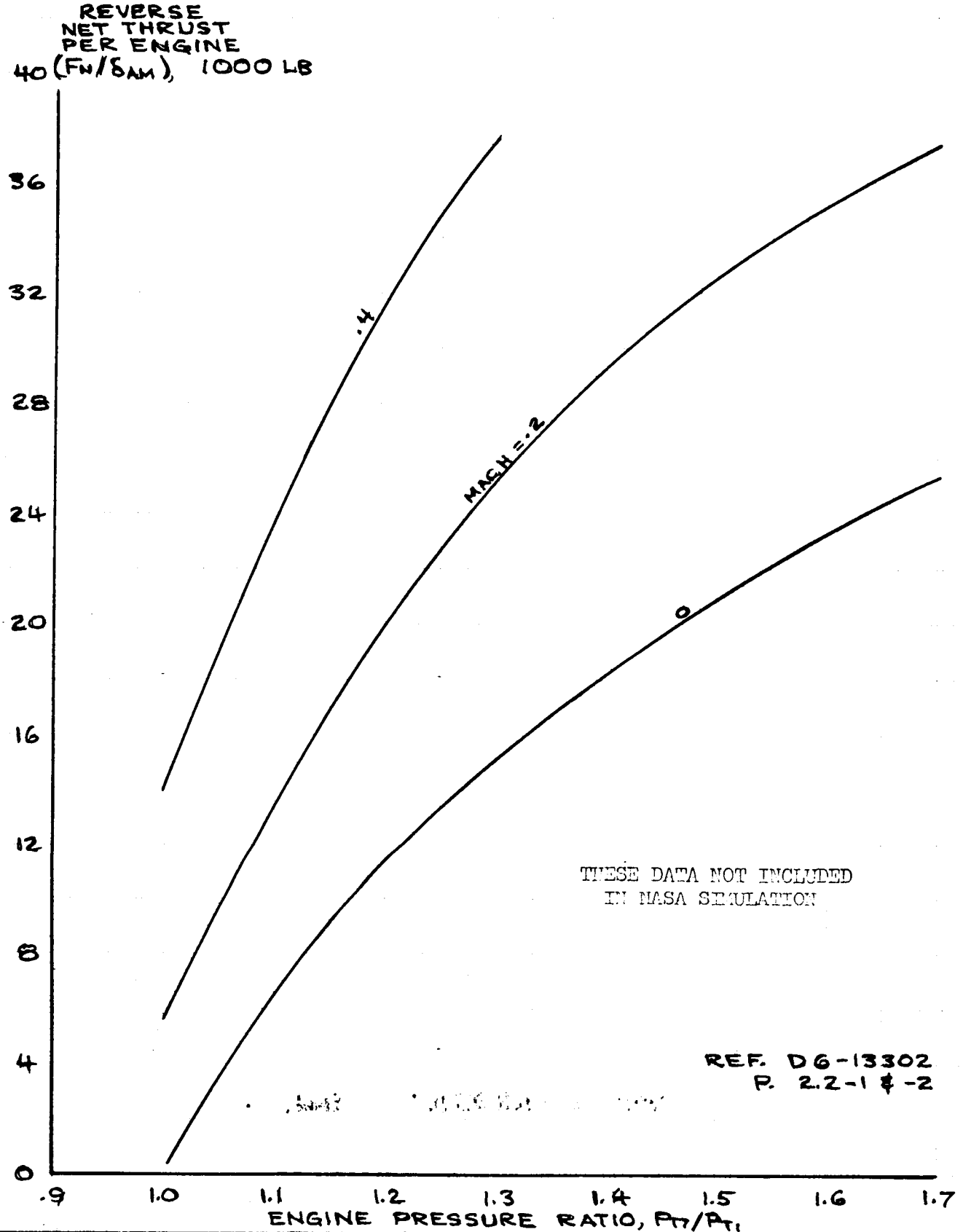

CALC			REVISED	DATE	REVERSE NET THRUST PRIMARY + FAN REVERSER
CHECK					
APP					
APP					
		APRIL 1970			THE BOEING COMPANY

747
D6-30648 VOL. II
PAGE 12.2-6

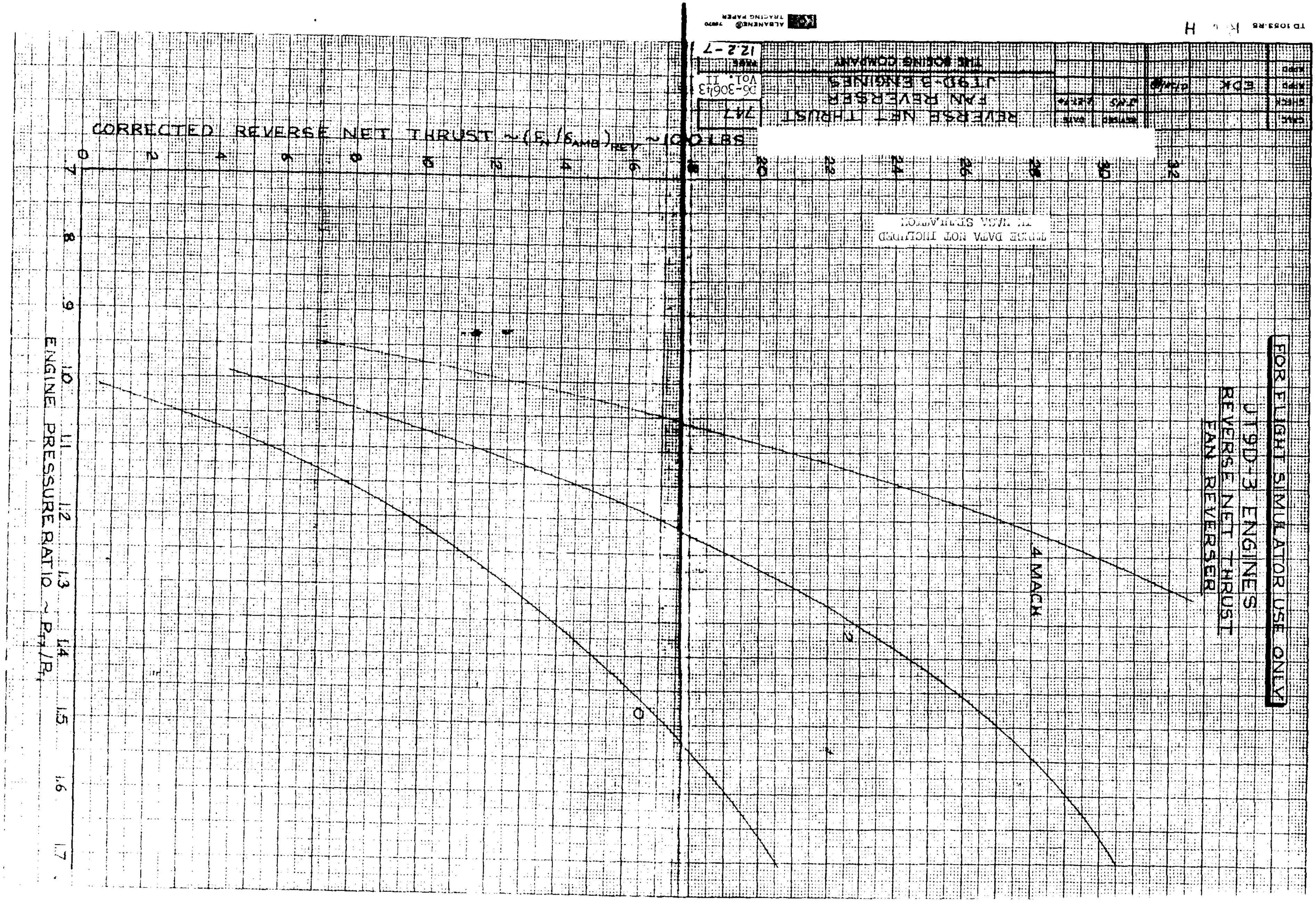

FOR FLIGHT SIMULATOR USE ONLY
JT9D-3 ENGINES
REVERSE NET THRUST
FAN REVERSER
CORRECTED REVERSE NET THRUST ~ $(F_N/\delta_{AMB})_{REV}$ ~ 1000 LBS
ENGINE PRESSURE RATIO ~ P_{T7}/P_{T1}
0
2
4
6
8
10
12
14
16
18
20
22
24
26
28
30
32
.7
.8
.9
1.0
1.1
1.2
1.3
1.4
1.5
1.6
1.7
0
.2
.4 MACH
THESE DATA NOT INCLUDED
IN NASA SIMULATION
REVERSE NET THRUST
FAN REVERSER
JT9D-3 ENGINES
THE BOEING COMPANY
747
D6-30643
Vol. II
12.2-7
EDK
ALBANENE TRACING PAPER
TD 1053-R5

FOR FLIGHT SIMULATOR USE ONLY

JT9D-3 ENGINES

REVERSE NET THRUST
PRIMARY REVERSER

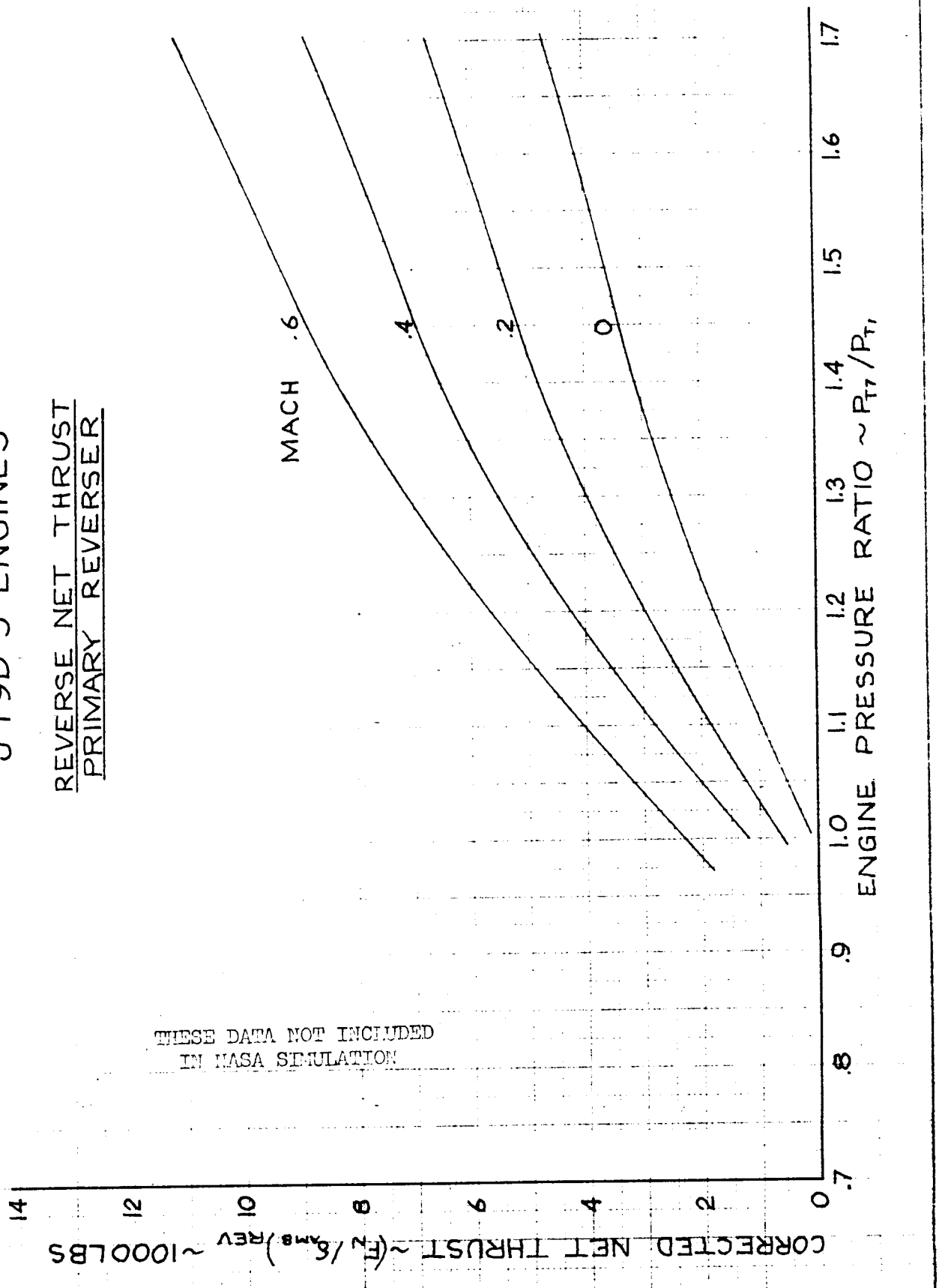

THESE DATA NOT INCLUDED
IN NASA SIMULATION

			REVISED	DATE
CALC				
CHECK			JNS	2-27-70
APP	EDK	12/20/69		
APP				

PRIMARY REVERSER
REVERSE NET THRUST
JT9D-3 ENGINES

747

D6-30643
Vol. II

THE BOEING COMPANY

PAGE
12.2-8

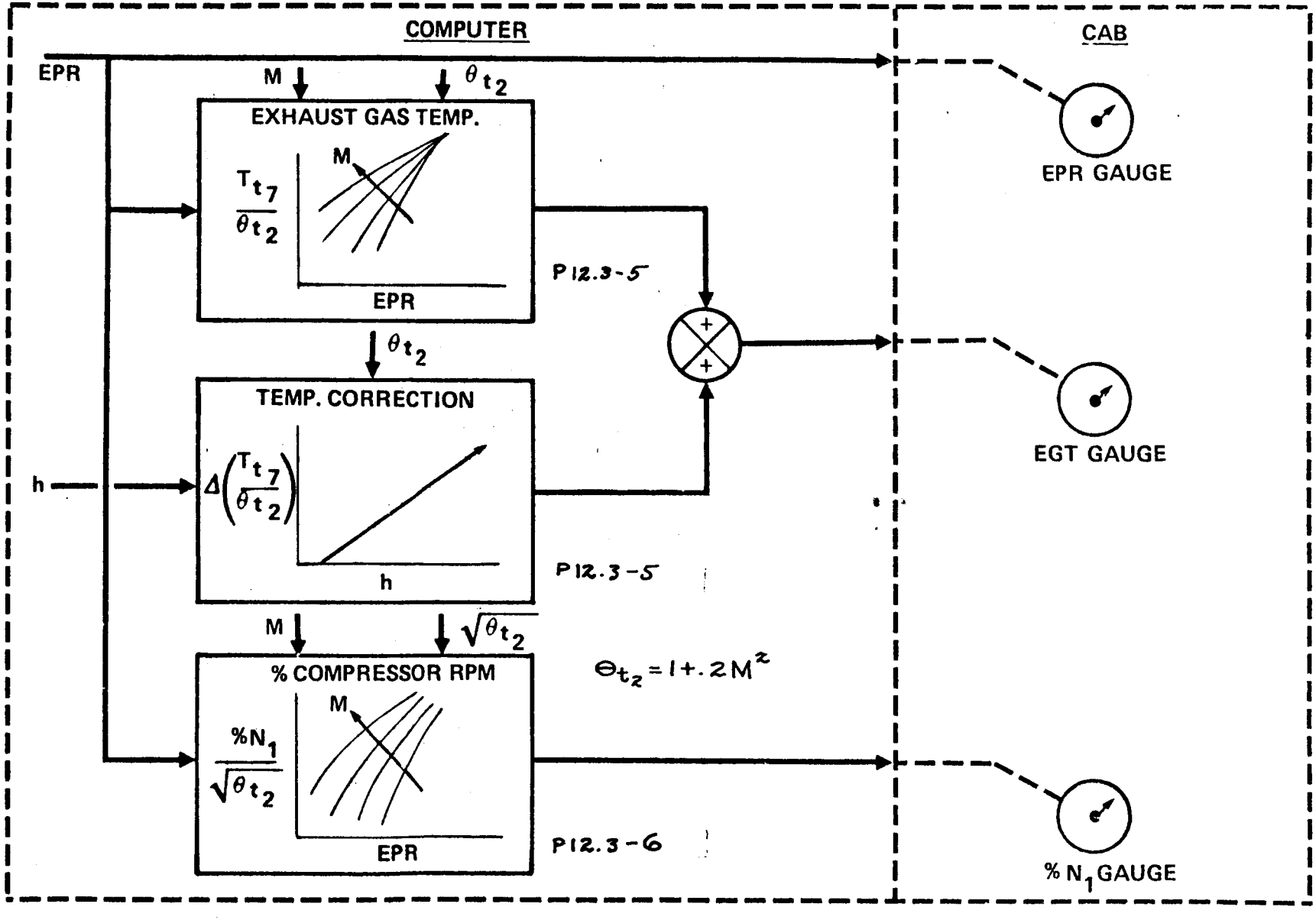

PARAMETERS FOR 747 ENGINE GAUGE DISPLAY

12.3 Engine Cockpit Display Parameters

A block diagram for engine display parameters is shown on Page 12.3-2 and the block diagram for the NASA engine gauge simulation is shown on Page 12.3- 3. The compressor RPM was scaled up by a factor of 8.8 to obtain the exhaust gas temperature in the simulation. The table on Page 12.3-4 shows the accuracy and the data points used in determining the scale factor.

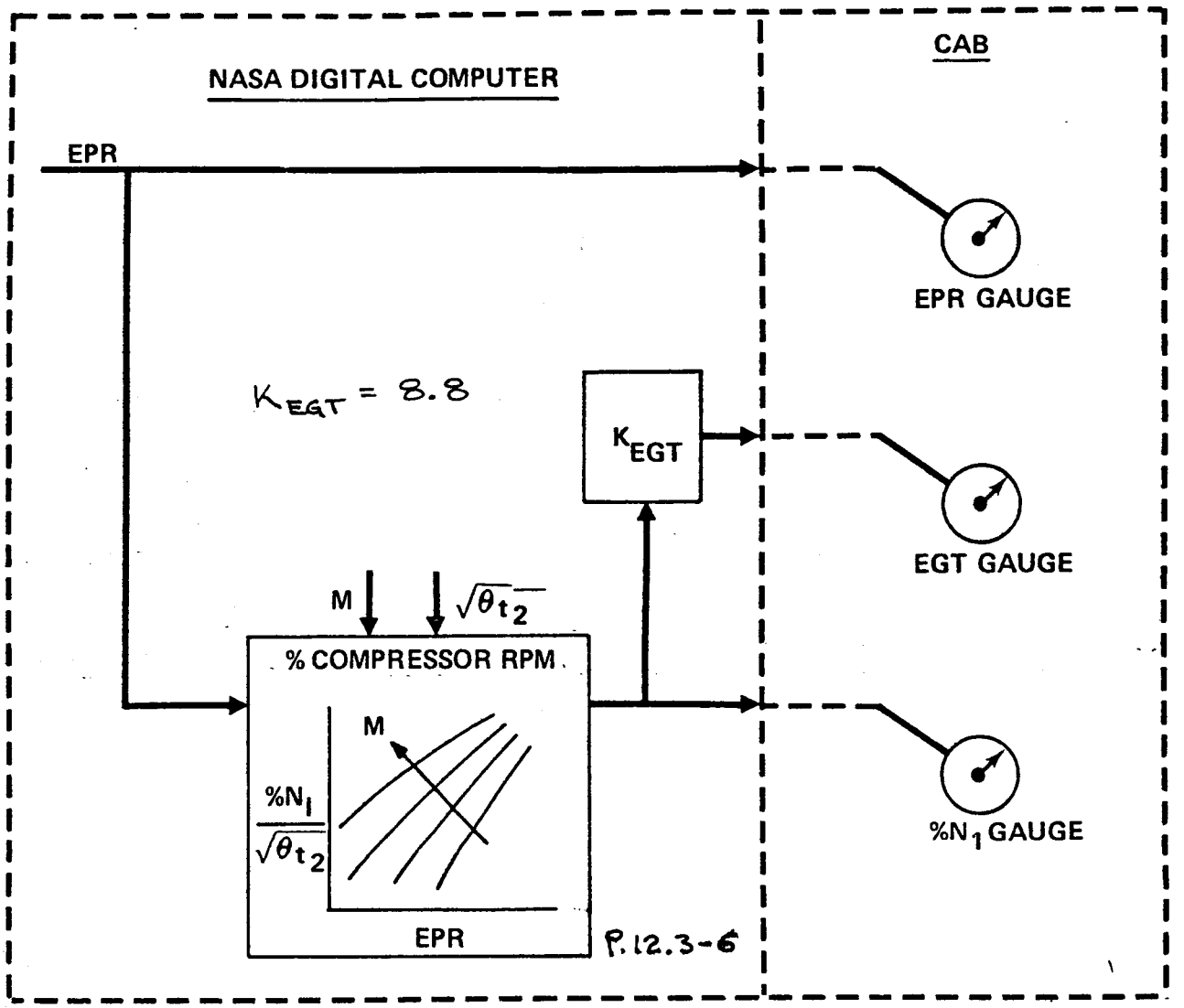

APPROXIMATIONS FOR NASA ENGINE GAUGE DISPLAY

EPR	M	θ_{T_2}	$\sqrt{\theta_{T_2}}$	$\frac{N_1}{\sqrt{\theta_{T_1}}}$ P. 12.3-6	N_1	$\frac{T_{T_6}}{\theta_{T_1}}$ P. 12.3-5	T_{T_6} °K	T_{T_6} °C	SF = $\frac{T_{T_6}\,°C}{N_1}$
1.0	.1	1.0	1.0	32.0	32.0	520	520	247	16.3
1.0	.8	1.128	1.061	80.5	85.4	892	1008	735	8.64
1.0	.5	1.05	1.025	67.5	69.2	785	825	555	8.03
1.5	.1	1.0	1.0	94.0	94.0	1097	1097	824	8.9
1.5	.8	1.128	1.061	99.5	105.8	1114	1253	980	9.3
1.5	.5	1.05	1.025	98.5	101.0	1110	1165	892	8.8
1.3	.1	1.0	1.0	83.5	83.5	967	967	694	8.3
1.3	.8	1.128	1.061	93.0	99.0	1041	1175	902	9.1
1.3	.5	1.05	1.025	90.0	92.2	1013	1065	792	8.6

$$\theta_{T_2} = 1 + .2M^2$$

$$\theta_{T_1} \approx \theta_{T_2}$$

$$SF = \frac{T_{T_6}\,°C}{N_1} \approx 8.8\ \frac{°C}{N_1}$$

THE BOEING COMPANY
12.3-5
D6-30613

FOR FLIGHT SIMULATOR USE ONLY

LOW PRESSURE COMPRESSOR ROTOR SPEED VS ENGINE PRESSURE RATIO

JT9D-3 BLOCK II ENGINE
INSTALLED ENGINE PERFORMANCE

VALID WITH OR WITHOUT AIRBLEED

100% N_1 = 3600 RPM
ALTITUDE -1000 TO 50000 FEET

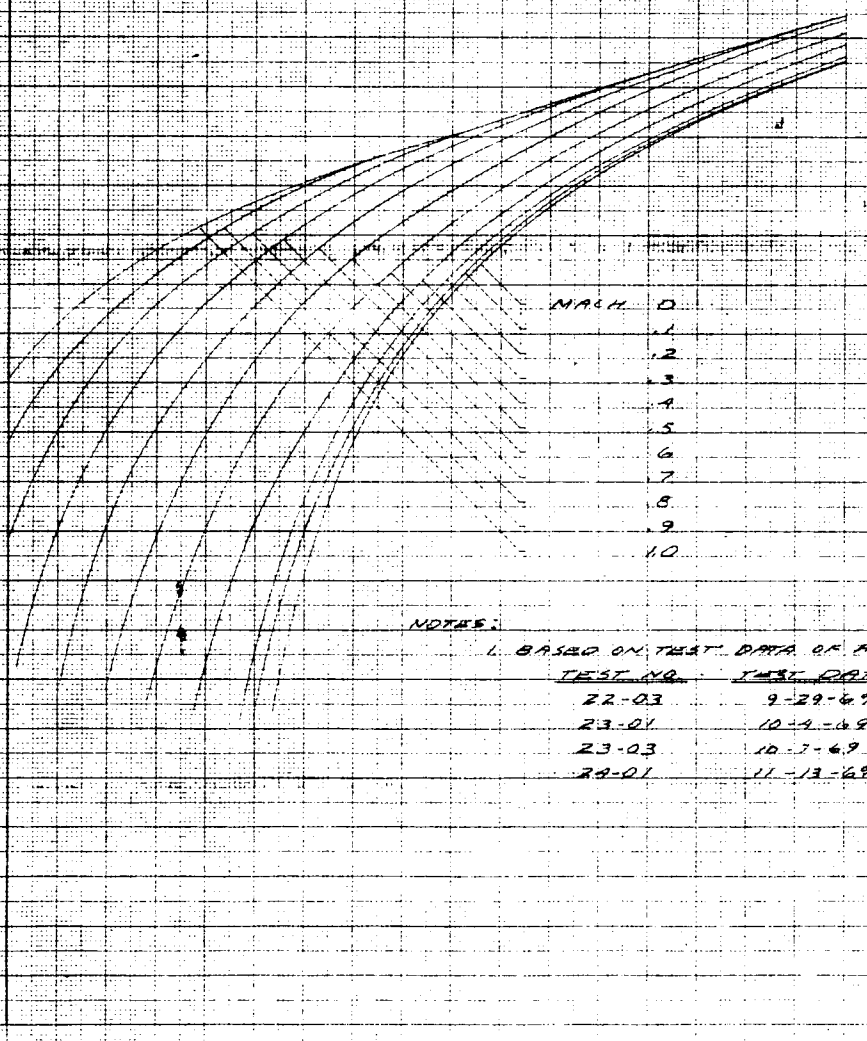

NOTES:

1. BASED ON TEST DATA OF R/A A9002

TEST NO.	TEST DATE
22-03	9-29-69
23-01	10-4-69
23-03	10-7-69
29-01	11-13-69

CORRECTED FAN SPEED $N_1/\sqrt{\theta_2}$ PERCENT

INDICATED ENGINE PRESSURE RATIO = P_{t_7}/P_{t_2}

CALC MLP 3/4/70
CHECK JWS 3-5-70
APPD
REVISED
DATE
BY
CHK
APPD

THE BOEING COMPANY

LOW SPEED COMPRESSOR ROTOR SPEED VS ENGINE PRESSURE RATIO
JT9D-3 BLOCK II ENGINE

D6-30613
Vol. II
PAGE 12.3-6

REV H

ALBANENE® TRACING PAPER 7970

12.4 Windmilling Drag

The windmilling drag characteristics on Page 12.4-2 were included in the simulation as a term in the engine equations.

For Flight Simulator only

JT9D-3 TURBOFAN ENGINE
WINDMILLING DRAG
REF: P&WA CURVE NO. 35819

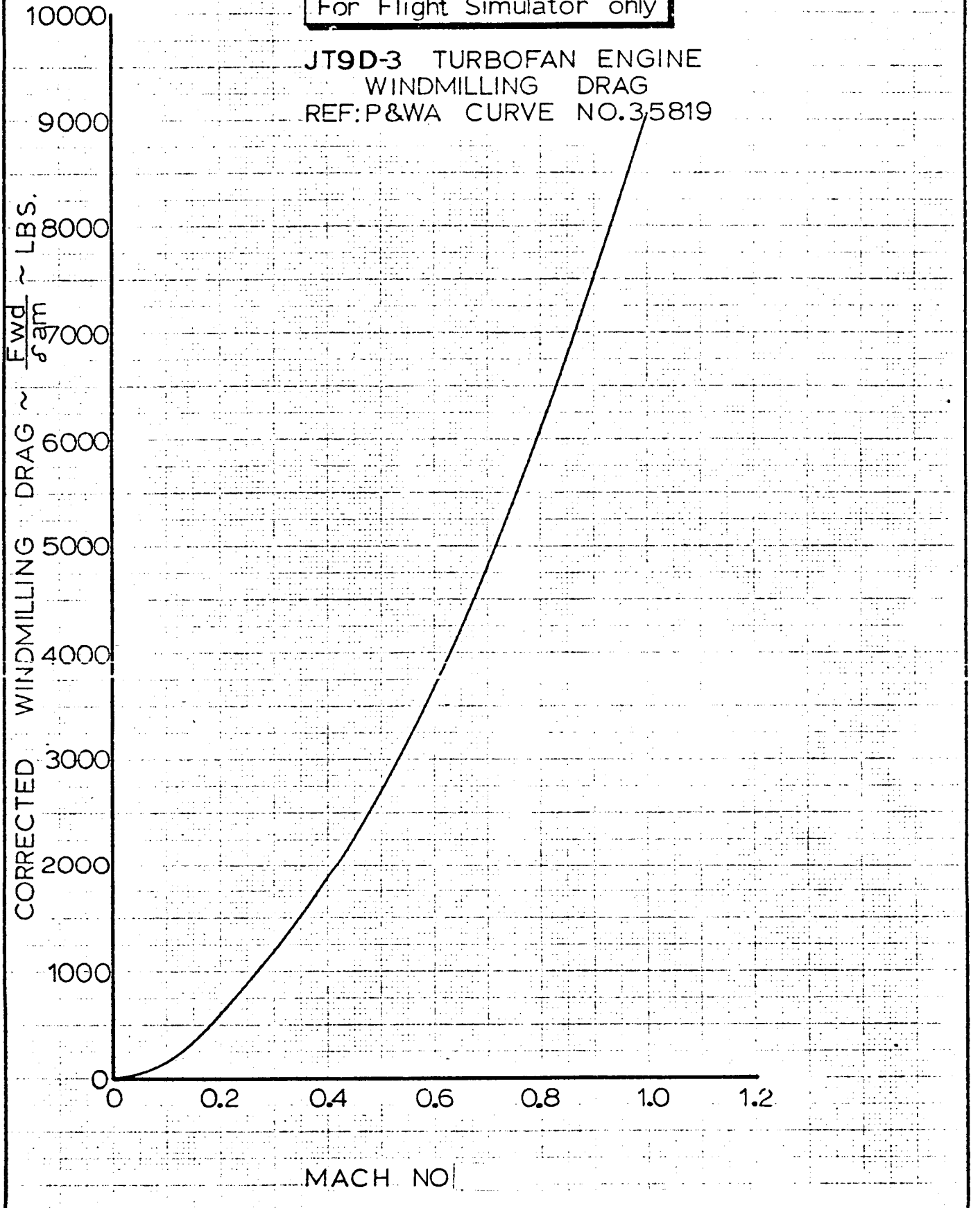

CALC	JMM	2/10/7	REVISED	DATE
CHECK	DLO	3/30/7	JMM	3/1/68
APR			E.C.R.	9/8/69
APR				

WINDMILLING DRAG

JT9D 3 TURBOFAN ENGINE

THE BOEING COMPANY

747

D6-30643 Vol. II

PAGE 12.4-2

12.5 Thrust Reverser Effects on Aerodynamic Coefficients

The thrust reverser effects on the lift, drag and pitching moment coefficients are presented on Page 12.5-2 . The approximations used in the simulation were made to conserve computer storage and justified because the thrust reversers are recommended to be in the idle reverse position by approximately 60 knots.

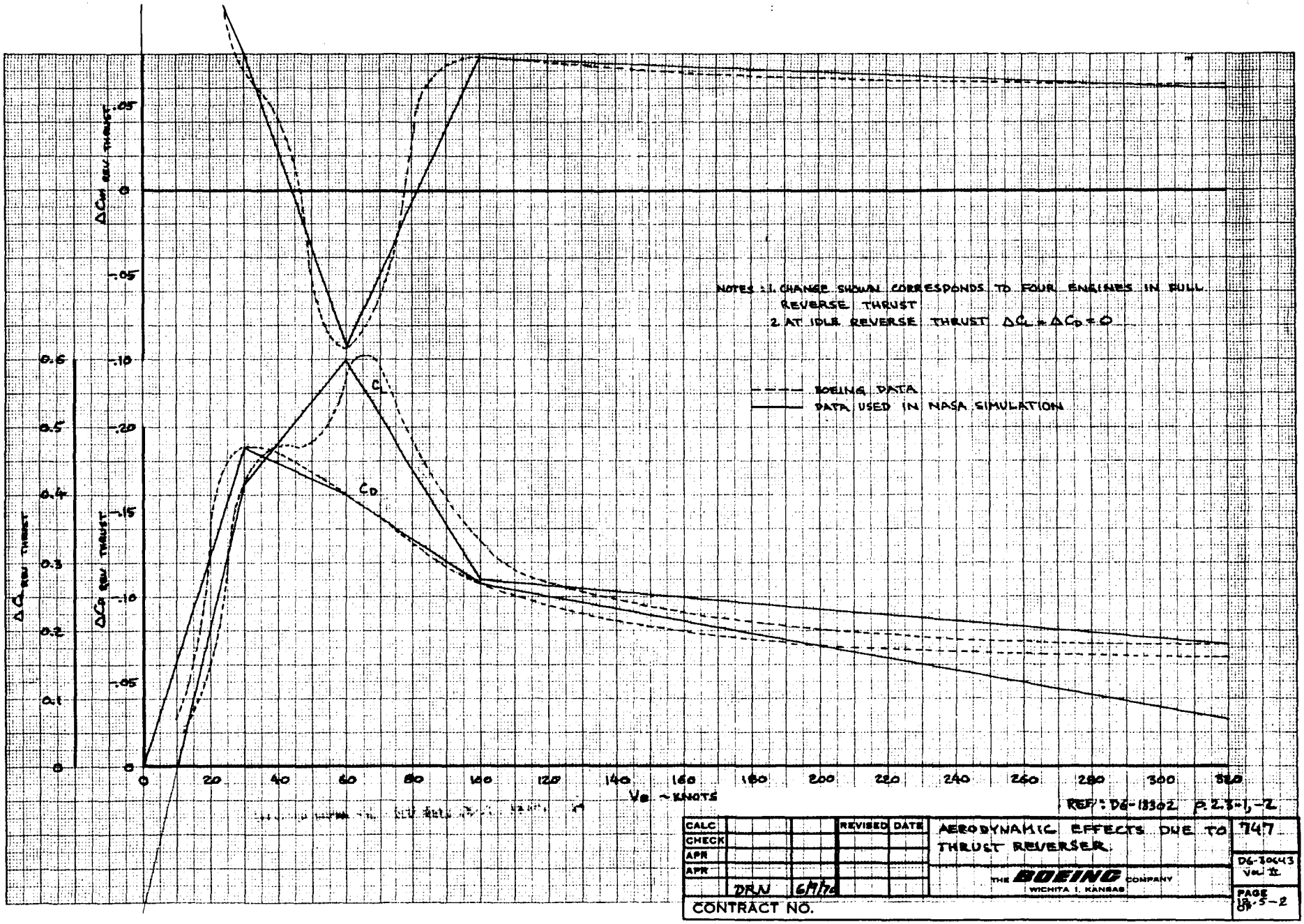

REF: D6-13302 p. 2.3-1, -2

CALC			REVISED	DATE	AERODYNAMIC EFFECTS DUE TO THRUST REVERSER
CHECK					
APR					
APR					THE BOEING COMPANY WICHITA 1, KANSAS
	DRN	6/9/76			
CONTRACT NO.					

747

D6-30643 Vol II

PAGE 18.5-2

K&E 10 X 10 TO THE CM KEUFFEL & ESSER CO. MADE IN U.S.A. 359-141-PC

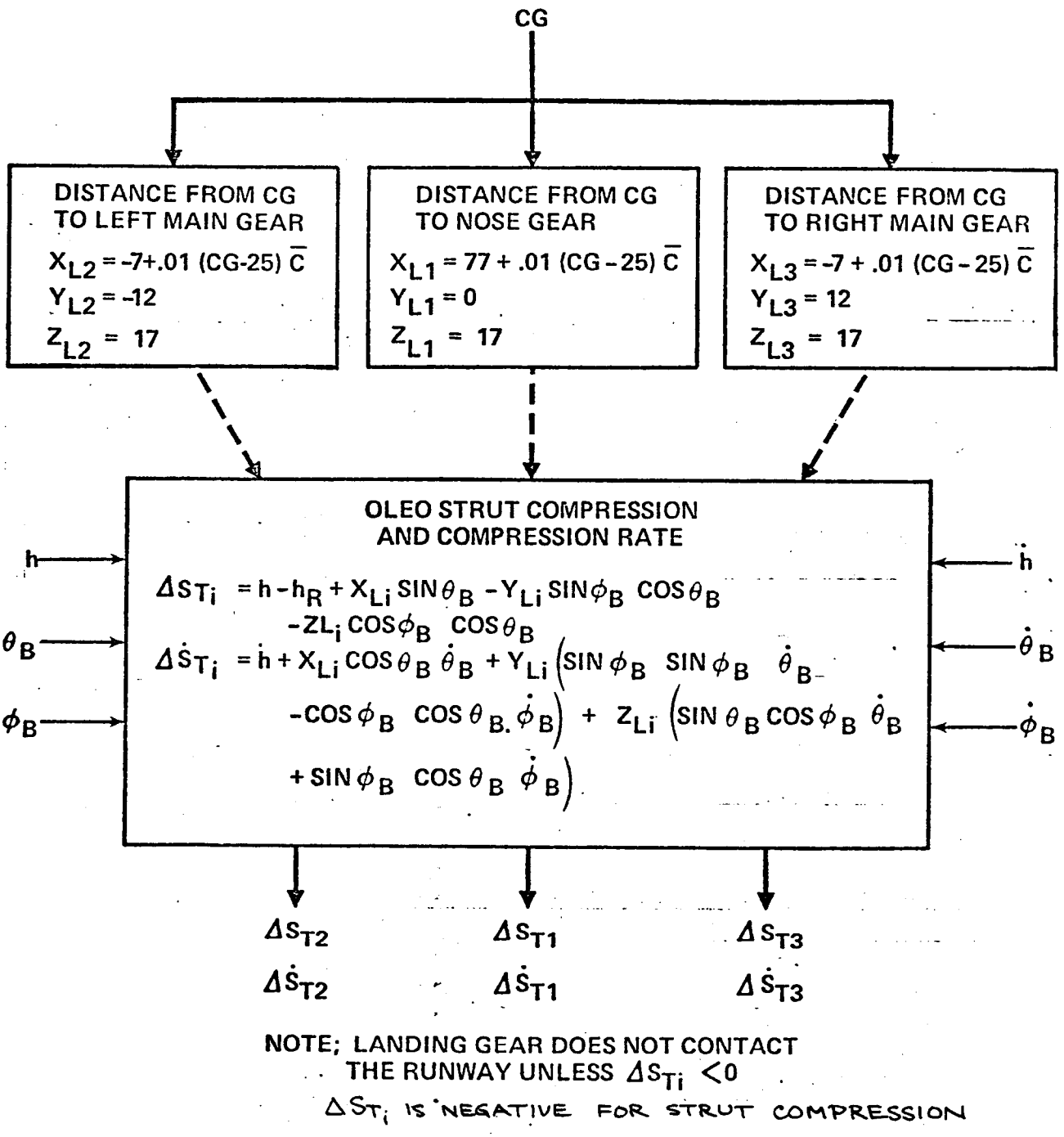

NOTE; LANDING GEAR DOES NOT CONTACT THE RUNWAY UNLESS $\Delta S_{Ti} < 0$

ΔS_{Ti} IS NEGATIVE FOR STRUT COMPRESSION

DETERMINATION OF OLEO STRUT COMPRESSION AND COMPRESSION RATE

13.0 LANDING GEAR

A general description of system and landing gear equations is included in Volume I of this report. A detailed derivation of the landing gear equations is contained in the Appendix to Volume I.

Block diagrams showing the method of calculating strut compression and force and wheel side and drag forces in the NASA simulation are shown on Pages 13.0-2 through 13.0-5. Refer to Volume I for the landing gear nomenclature.

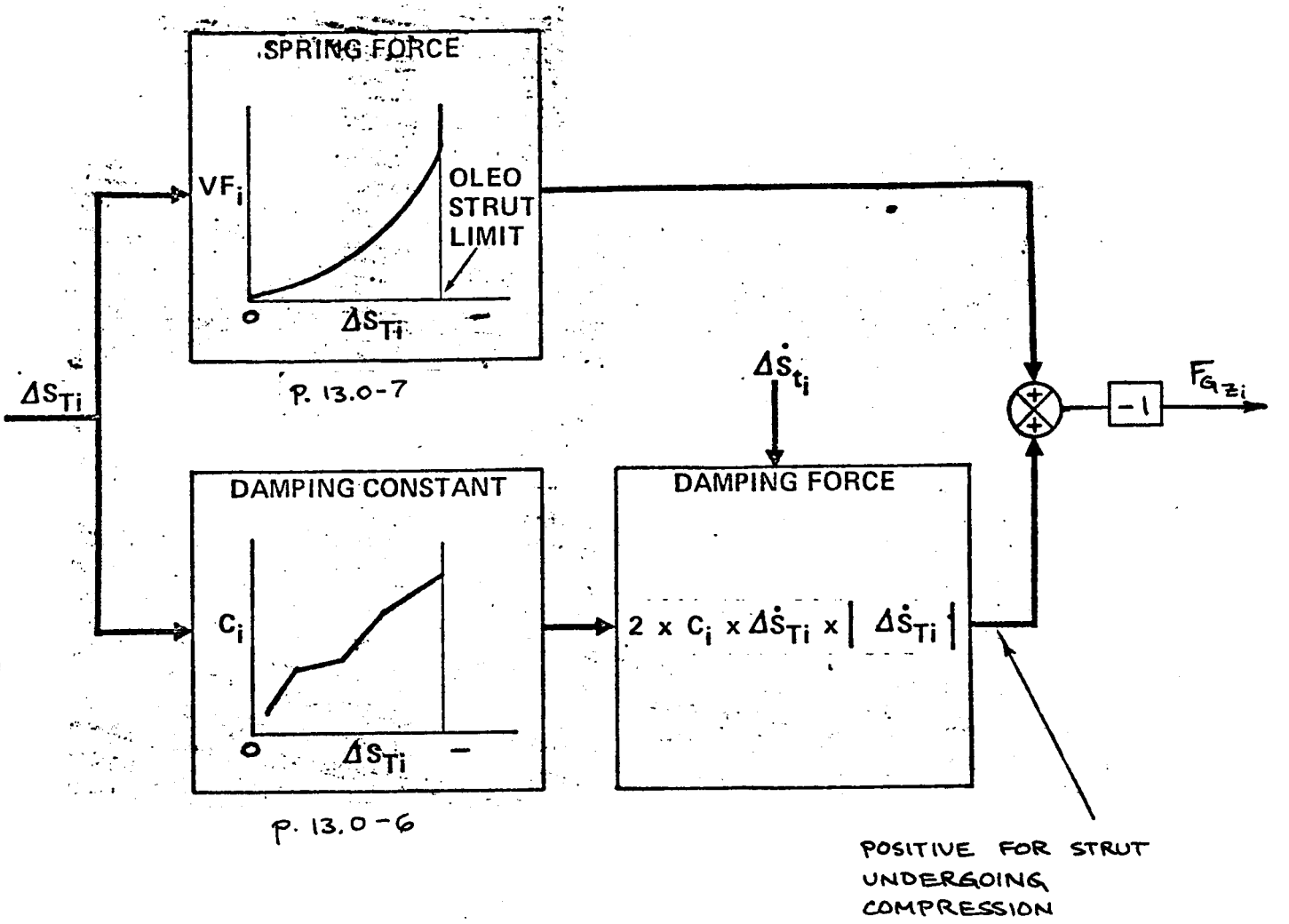

ΔS_{T_i} AND $F_{G_{Z_i}}$ ARE NEGATIVE FOR COMPRESSION

DETERMINATION OF OLEO STRUT FORCES

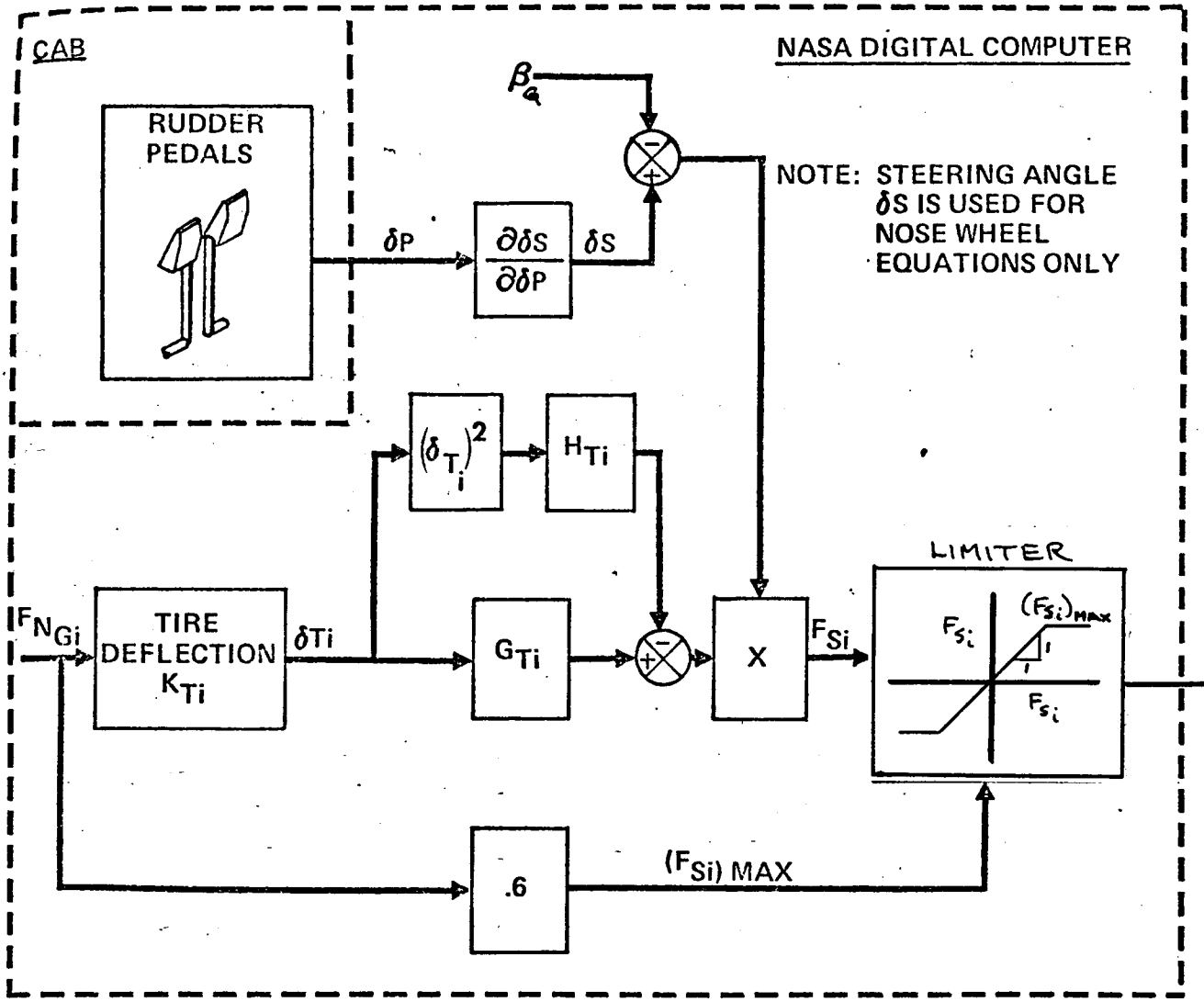

i = 1 NOSE GEAR
2 LEFT MAIN GEAR
3 RIGHT MAIN GEAR

10° STEERING, δ_S, FOR FULL PEDAL DEFLECTION, δ_P, 12.2°.

$$\frac{\partial \delta_S}{\partial \delta_P} = \frac{10}{12.2} = .82$$

$$K_{T_1} = -\frac{.093}{2(1000)} \frac{IN}{LB} \qquad K_{T_{2,3}} = \frac{-.077}{8(1000)} \frac{IN}{LB}$$

2 ← NO. OF WHEELS ON NOSE GEAR

8 ← NO. OF WHEELS ON EACH MAIN GEAR

$H_{T_1} = (2)(73730)(.0042) = 619$ $\quad H_{T_{2,3}} = 8(73730)(.0042) = 2477$

$G_{T_1} = 2(73730)(.026) = 3834$ $\quad G_{T_{2,3}} = 8(73730)(.026) = 15336$

DETERMINATION OF WHEEL SIDE FORCE

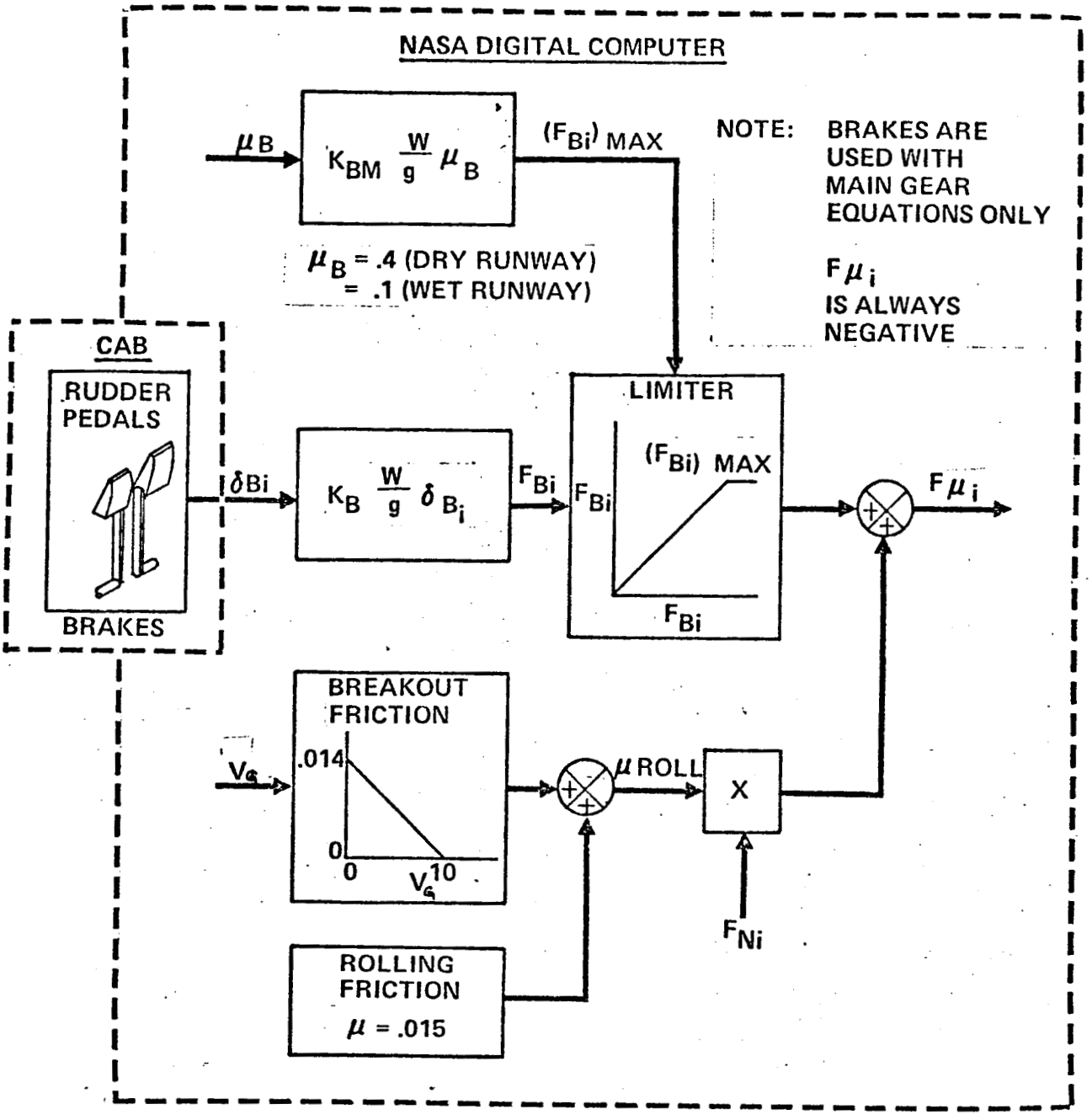

$$F_{B_i} = 2\left[.263 \cdot \frac{W}{g} \cdot \delta_{B_i}\right]$$

$$(F_{B_i})_{MAX} = 2(.834 + 4.167 \cdot \mu_B) \cdot \frac{W}{g}$$

MAXIMUM DECELERATION = 5 FT/SEC^2 FOR MAXIMUM BRAKING ON EACH MAIN GEAR

• DETERMINATION OF WHEEL DRAG FORCE

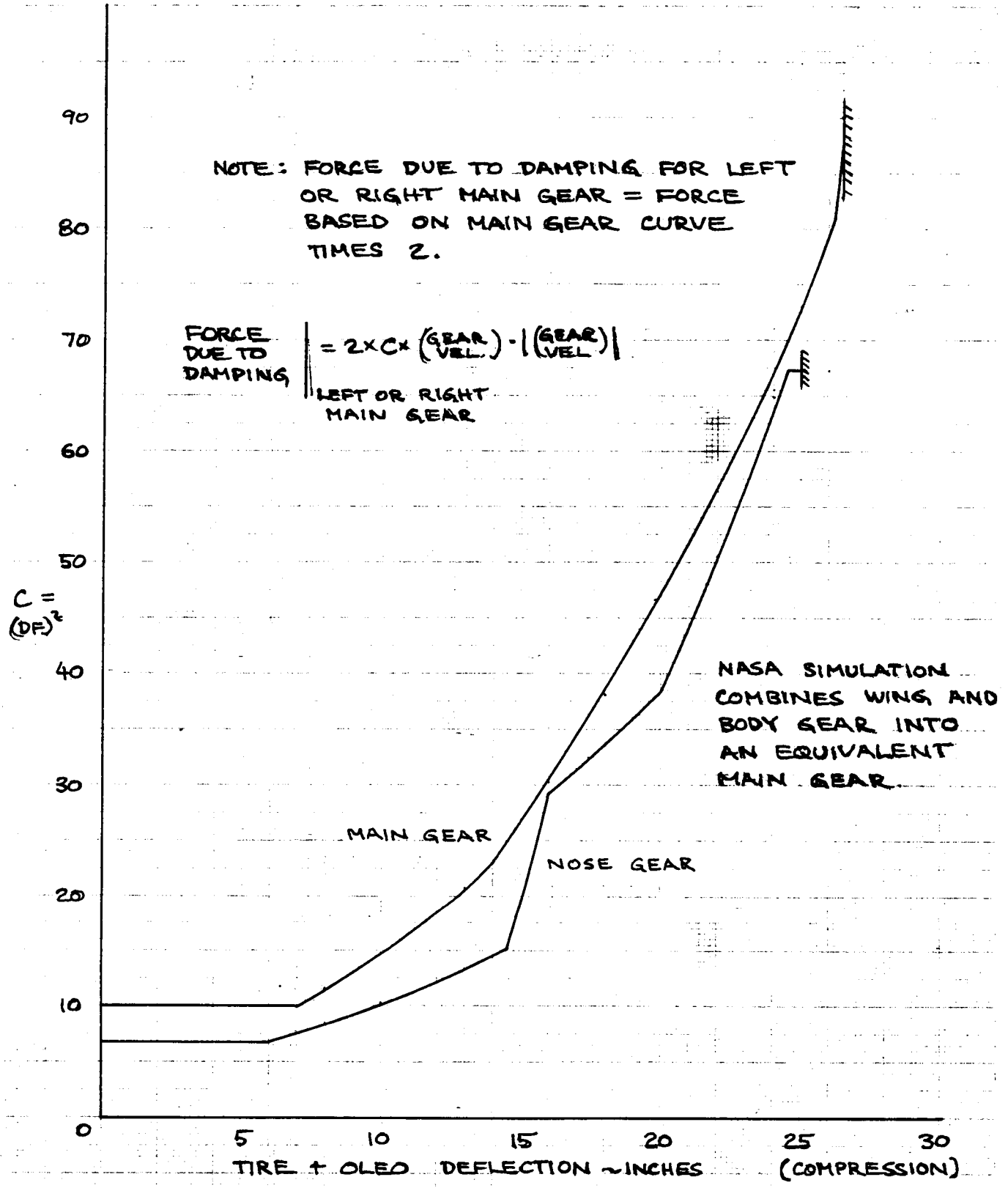

REF: D6-30437 P. 294

CALC	DRN	11/3/69	REVISED	DATE	OLEO DAMPING 747
CHECK					
APPD					
APPD					

E-3277 R2

REV LTR:

BOEING | NO. D6-30643 VOL II

SECT | PAGE 13.0-6

NOTE: FORCE DUE TO STRUT DEFLECTION FOR LEFT OR RIGHT MAIN GEAR = FORCE BASED ON MAIN GEAR CURVE TIMES 2.

NASA SIMULATION COMBINES WING AND BODY GEAR INTO AN EQUIVALENT MAIN GEAR.

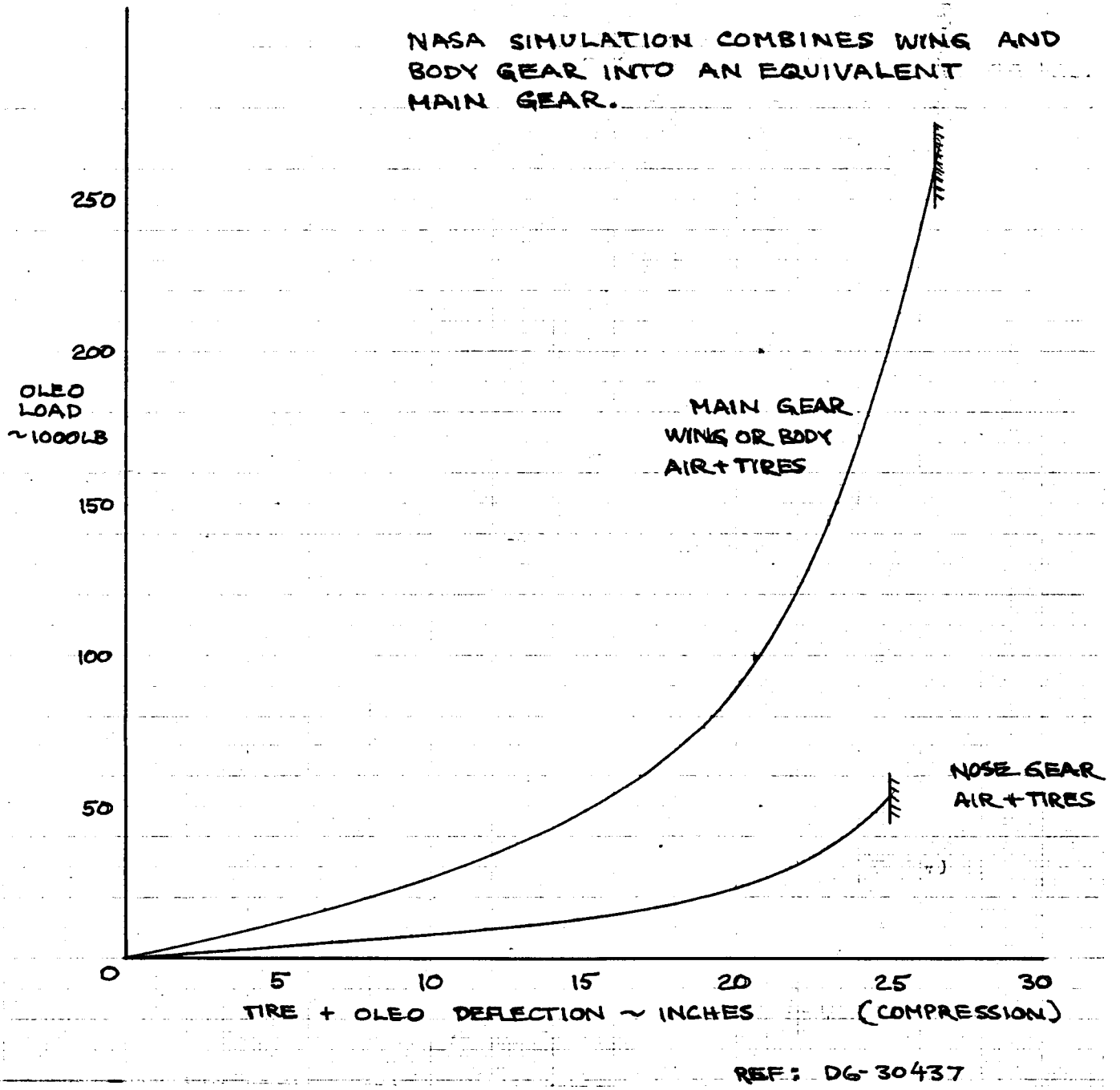

REF: D6-30437

CALC		11/5/69	REVISED	DATE	LANDING GEAR AIR CURVE 747
CHECK					
APPD					BOEING NO. D6-30643 VOL II
APPD					SECT PAGE 13.0-7

REV LTR:

E-3277 R2

14.1.1 COCKPIT INSTRUMENTS

The cockpit instruments were statically checked to assure that the piloted checkout could be conducted with confidence. Rudimentary checks were made of the following instruments:

1. Altimeter
2. Rate-of-climb-indicator
3. Airspeed indicator
4. Attitude indicator
5. Turn and bank indicator
6. Mach meter
7. Flap position indicator
8. Stabilizer position indicator

The checks were conducted by putting the computer in "hold" and comparing the instrument readings with the computer values. These comparisons were made a number of times throughout the simulation checkout and all of the instruments were in good agreement with the computed values. The instruments operated smoothly during the dynamic checks and piloted evaluation.

A comparison of digital values and cockpit instrument readings were tabulated during the four engine climb performance test. The comparison between the computed and indicated pitch attitude shows the largest discrepancy. However, the pitch attitude is difficult to read to a fraction of a degree. The differences are within the tolerances specified in the table on Page 14.2-10.

The stabilizer position indicator in the FSAA was programmed using stabilizer referenced to the fuselage reference line, δ_{FRL}. All of the aerodynamic data are in terms of δ_{FRL}. The 747 stabilizer indicator and stabilizer information used in the flight manual and D6-30833-1 is in stabilizer "pilot's units", δ_p. The conversion is given by:

$$\delta_p = 3^\circ - \delta_{FRL} .$$

14.1.2 ATMOSPHERE MODEL

The atmosphere model, presented in Volume I of this report, was checked for a number of altitude and airspeed conditions. Values of V_e for a number of altitudes were input to the computer. Output values of M, V_c (V_I), V, q . and q_c were checked with the data in the table on Page 14.1-5.

ATMOSPHERE CHECK

1. Standard Day, No Wind
2. Pilot's Airspeed V_I is equal to V_C

ALT. FT	V_I KTS	V_e KTS	V_{TRUE} FT/SEC	MACH NO.	q LB/FT^2	q_c LB/FT^2
0	100	100	169	.151	34	34
0	200	200	337.5	.302	135.5	138.5
0	300	300	506.5	.454	304.5	320.5
0	400	400	675	.605	541.5	593
10,000	150	149.5	294	.273	75.5	77
10,000	250	248	487.5	.452	208.5	219.5
10,000	350	345	677.5	.629	403	444.5
10,000	450	440	864.5	.803	656	768.5
20,000	250	245	567	.547	203.5	219.5
20,000	300	292	675.5	.651	289	320.5
20,000	350	338	781.5	.754	386.5	444.5
20,000	430	409	946	.913	576	695
30,000	200	195	538.5	.541	129	138.5
30,000	300	285	786.5	.791	275	320.5
30,000	350	327.5	904	.909	363.5	444.5
35,000	250	238	721	.741	191.5	219.5
35,000	295	276	837.5	.861	258	309.5
40,000	200	191.5	651	.672	124	138.5
40,000	250	234	796.5	.823	185.5	219.5

14.1.3 ENGINE CHARACTERISTICS

Static forward and reverse thrust characteristics were checked by comparing the computer output data with a manual calculation of the same condition. The comparisons are shown in the examples on Pages 14.1-7 and -8.

The transient engine characteristics are shown on Pages 14.1-9 and -10. A sea level static condition was set up and throttle changes were commanded. The resulting transient characteristics for EPR approximates the engine transient data shown in Section 12.

STATIC THRUST

ALTITUDE = 200 FT M= 0.2 STANDARD DAY

	MANUAL CALCULATION	DIGITAL OUTPUT
MAXIMUM FORWARD THRUST		
FORWARD THRUST LEVER ANGLE (INPUT)	61°	60.80°
POWER LEVER ANGLE	127°	127.0°
$T_{AMBIENT}$	58.3°F	58.39°F
EPR (f(POWER LEVER ANGLE))	1.509	
ΔEPR	-.036	-.0361
EPR (FINAL)	1.473	1.4737
F_N/δ	37500 LB	37444 LB.
δ	.9929	.9937
F_N	37234 LB.	37208 LB.
$N_1/\sqrt{\theta_{T_2}}$	93.1%	
N_1	93.6%	90.3%
IDLE FORWARD THRUST		
FORWARD THRUST LEVER ANGLE (INPUT)	0°	.19°
POWER LEVER ANGLE	57.5°	57.75°
EPR (f(POWER LEVER ANGLE))	1.02	
ΔEPR	-.036	-.0361
EPR (FINAL)	.984	.9839
F_N/δ	1250 LB	1264 LB.
F_N	1241 LB	1256 LB
$N_1/\sqrt{\theta_{T_2}}$	31 %	
N_1	31.1%	43.7%

CALC	DRN	JUNE 1970	REVISED	DATE
CHECK				
APPD				
APPD				

STATIC THRUST

REV LTR:

E 1196 R6

	MANUAL CALCULATION	DIGITAL OUTPUT
IDLE REVERSE THRUST		
REVERSE THRUST LEVER ANGLE (INPUT)	-34°	-31.07°
POWER LEVER ANGLE	45°	46.46°
EPR (f(POWER LEVER ANGLE))	1.02	
ΔEPR	-.036	-.0361
EPR (FINAL)	.984	.9839
$(F_N/\delta)_{REVERSE}$	4400 LB	4450 LB
$F_{N\ REVERSE}$	-4369 LB	-4422 LB
$N_1/\sqrt{\theta_{T_2}}$	31 %	
N_1	31.1 %	42.7 %
MAXIMUM REVERSE THRUST		
REVERSE THRUST LEVER ANGLE (INPUT)	-107°	-108.40°
POWER LEVER ANGLE	3.°	3.°
EPR (f(POWER LEVER ANGLE))	1.615	
ΔEPR	-.036	-.0361
EPR (FINAL)	1.579	1.5826
$(F_N/\delta)_{REVERSE}$	34700 LB	34646 LB
$F_{N\ REVERSE}$	-34454 LB	-34428 LB
$N_1/\sqrt{\theta_{T_2}}$	97.4 %	
N_1	97.8 %	95.06 %

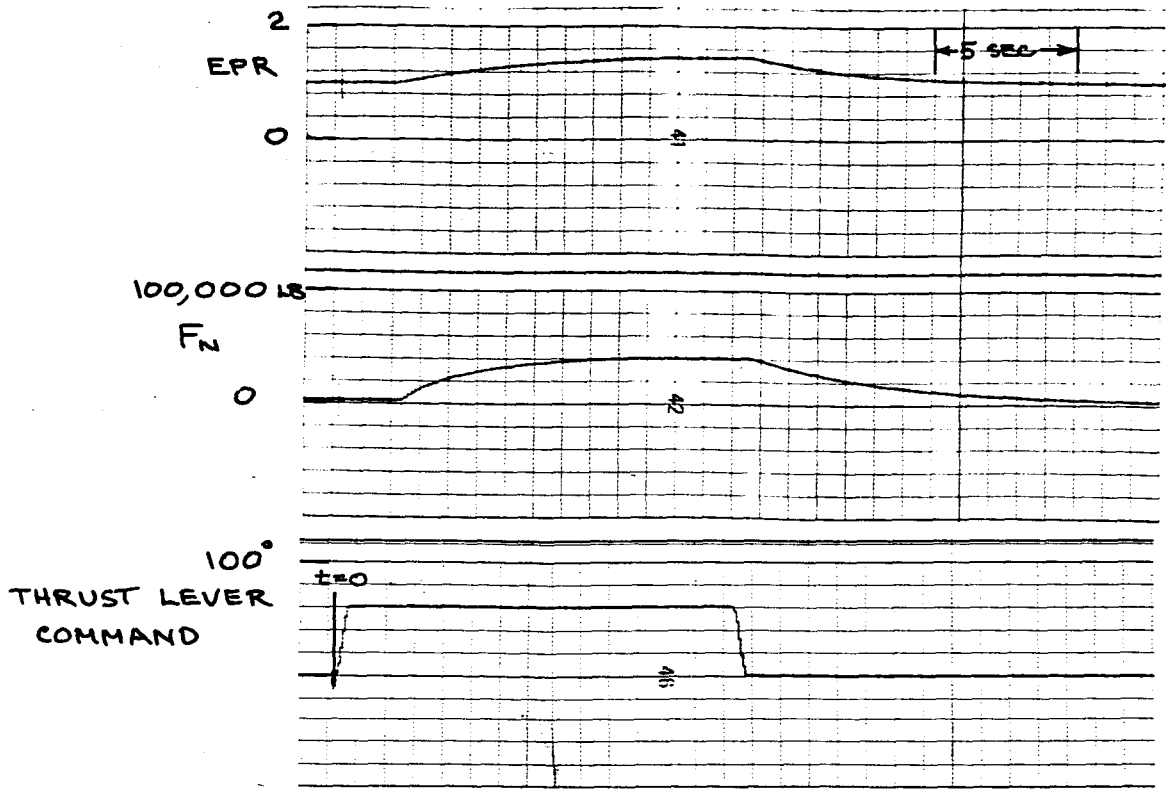

SEA LEVEL, STANDARD DAY, STATIC
IDLE TO MAXIMUM THRUST
SNAP ACCELERATION - DECELERATION

ENGINE TRANSIENTS

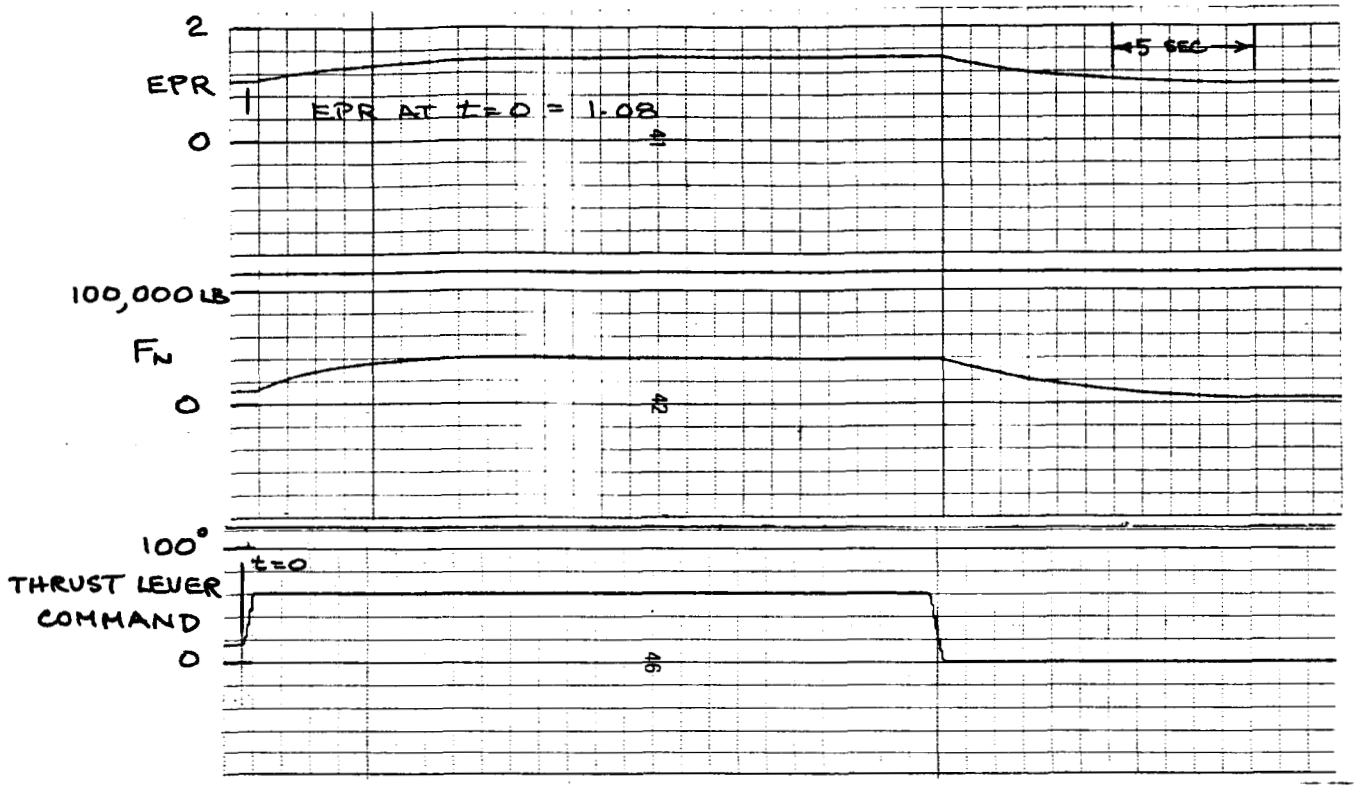

SEA LEVEL, STANDARD DAY, STATIC

EPR AT $t=0$ = 1.08

SNAP ACCELERATION - DECELERATION

ENGINE TRANSIENTS

14.1.4 LONGITUDINAL TRIM

The simulated airplane was statically trimmed at several variations of weight, c.g., altitude, speed, and flap positions. Computed values of δ_e, Θ_B, and EPR/F_n were compared to Boeing simulator and flight test results. Comparisons to simulator results are tabulated on Pages 14.1-12 and -13 and plotted on Pages 14.1-14 thru -18. Comparisons to flight test and simulator results are plotted on Pages 14.1-19 thru -21.

The effects of configuration changes, landing gear up and down and speed brakes up and down, were computed and the results are tabulated on Page 14.1-22.

The effect of ground effect on trim is tabulated on Page 14.1-12. The trim data are based on the ground effect curves on Pages 2.0-31, -32, 3.0-17, -18 and 4.0-35.

FLAP POSITION	GEAR	G.W. ~1000 LB	C.G. ~%MAC	ALTITUDE ~1000 FT	Ve KT	M	$\alpha_{W.D.P.}$ ~DEG		Δ_{FRL} ~DEG	
							BOEING	NASA	BOEING	NASA
0	UP	400	32	5	300	.497	2.64	2.61	.68	.67
					250	.414	4.07	4.06	.34	.33
				30	250	.694	2.90	2.84	.17	.20
					300	.832	1.26	1.21	.47	.49
				40	200	.703	4.96	4.86	-.48	-.43
					250	.879	2.19	2.13	-.112	-.094
		680	12.5	30	275	.763	4.80	4.73	-1.98	-1.91
					300	.832	3.55	3.50	-1.47	-1.46
		564	14	20	291	.65	3.66	3.60	-1.13	-1.08
			32		291	.65	3.44	3.41	.27	.30
					358	.80	1.61	1.56	.65	.67
			25	20	225	.502	7.08	7.00	-1.53	-1.49
					325	.725	2.41	2.36	.113	.131
				35	225	.703	5.96	5.88	-1.38	-1.34
					275	.859	3.09	3.03	-.68	-.66
30				.2	180	.272	1.62	1.52	-1.37	-1.34
					142	.215	6.99	6.83	-4.01	-3.96
	DN				142	.215	7.31	7.15	-4.36	-4.31
0	UP			5	250	.414	6.01	5.99	-.80	-.80

GROUND EFFECT

	GEAR ALT. ~FT	Δ_p UNITS	θ_8 ~DEG	EPR	THRUST ~LB
BOEING	100	4.89	5.0	1.190	76570
NASA		4.86	4.86	1.189	76237
BOEING	30	6.55	3.7	1.139	60750
NASA		6.51	3.55	1.139	60840
BOEING	10	7.11	3.3	1.106	50650
NASA		7.01	3.12	1.108	51132

564000 LB
c.g. = 33% V_I = 142 KT
FLAPS 30 GEAR DOWN

747

CALC	DRN	MAY 1970	REVISED	DATE
CHECK				
APPD				
APPD				

LONGITUDINAL TRIM

REV LTR:

AD 1546 D

LONGITUDINAL TRIM

COND. NO	FLAP POSITION	GEAR	G.W. ~ 1000 LB.	CG ~% MAC	ALTITUDE ~ 1000 FT	V_I	M	Δ_P ~UNITS		θ_B ~DEG		IEPR		F_N ~LB	F_N ~LB	Δ_{FRL} ~DEG	
								BOEING	NASA	BOEING	NASA	BOEING	NASA	BOEING	NASA	NASA	
4.0.1	UP	UP	650	12	20	373	.800	3.6	3.49	0.3	.214	1.124	1.125	43000	43303	-.49	
4.0.2	—	—	—	32	—	—	.800	2.4	2.37	0.1	.02	1.116	1.112	42300	42428	.634	
4.0.3	UP	UP	500	14	20	373	.800	3.1	3.05	-.7	-.67	1.089	1.093	39750	40309	-.05	
4.0.4	—	—	—	—	—	275	.600	4.3	4.24	2.0	1.96	1.065	1.065	28850	29022	-1.24	
4.0.5	UP	UP	500	14	35	253	.75	4.8	4.71	2.4	2.29	1.273	1.266	27440	27315	-1.71	
4.0.6	—	—	—	—	—	295	.86	4.3	4.20	0.7	.59	1.312	1.306	30970	30890	-1.2	
4.0.7	—	—	—	32	—	253	.75	3.1	3.09	2.1	2.01	1.243	1.235	26220	26060	-.092	
4.0.8	—	—	—	—	—	295	.86	3.1	3.00	0.5	.40	1.286	1.284	29950	30040	.001	
4.0.9	—	—	—	—	—	318	.92	3.0	2.92	-1.2	-1.48	1.447	1.40	37390	35900	.08	$\gamma = -1.7$
4.0.12	10	—	550	15	5	167	.277	7.8	7.72	8.1	8.05	1.120	1.118	46720	46354	-4.72	
4.0.13	20	—	—	—	—	159	.264	8.5	8.4	6.5	6.48	1.137	1.136	50800	50560	-5.4	
4.0.14	25	DN	—	—	—	155	.257	8.6	8.52	5.9	5.82	1.192	1.191	64540	64300	-5.52	
4.0.15	25	—	—	—	—	135	.224	10.9	10.85	9.7	9.59	1.214	1.212	69810	69310	-7.85	
4.0.16	30	—	—	—	—	150	.249	9.2	9.19	3.8	3.75	1.254	1.253	78670	78547	-6.19	
4.0.17	10	UP	710	11	5	190	.315	8.6	8.52	8.4	8.41	1.184	1.182	62820	62576	-5.52	
4.0.18	—	—	—	32	—	—	—	3.9	3.81	7.8	7.80	1.174	1.171	60380	59966	-.81	
4.0.19	30	DN	564	15	S.L.	142	.215	10.5	10.37	5.7	5.53	1.207	1.206	81760	81180	-7.37	
4.0.20	—	—	—	33	—	—	—	4.9	4.86	5.0	4.86	1.189	1.189	76460	76051	-1.86	
4.0.21	—	—	—	15	10	—	.259	10.6	10.44	5.7	5.52	1.352	1.347	81750	81070	-7.44	
4.0.22	—	—	—	—	—	180	.328	6.7	6.65	0.2	.207	1.415	1.408	89140	88377	-3.64	
4.0.23	25	DN	564	15	10	180	.328	6.8	6.79	3.1	3.1	1.278	1.276	68710	68410	-3.79	
4.0.24	30	DN	400	15	S.L.	120	.182	10.4	10.3	5.3	5.14	1.124	1.125	56510	56380	-7.3	
COMPUTATION TOLERANCE NASA VALUES ARE FROM COMPUTER OUTPUT								± .5 UNITS		± .5 DEG.		± .01		± 3%		± .25°	

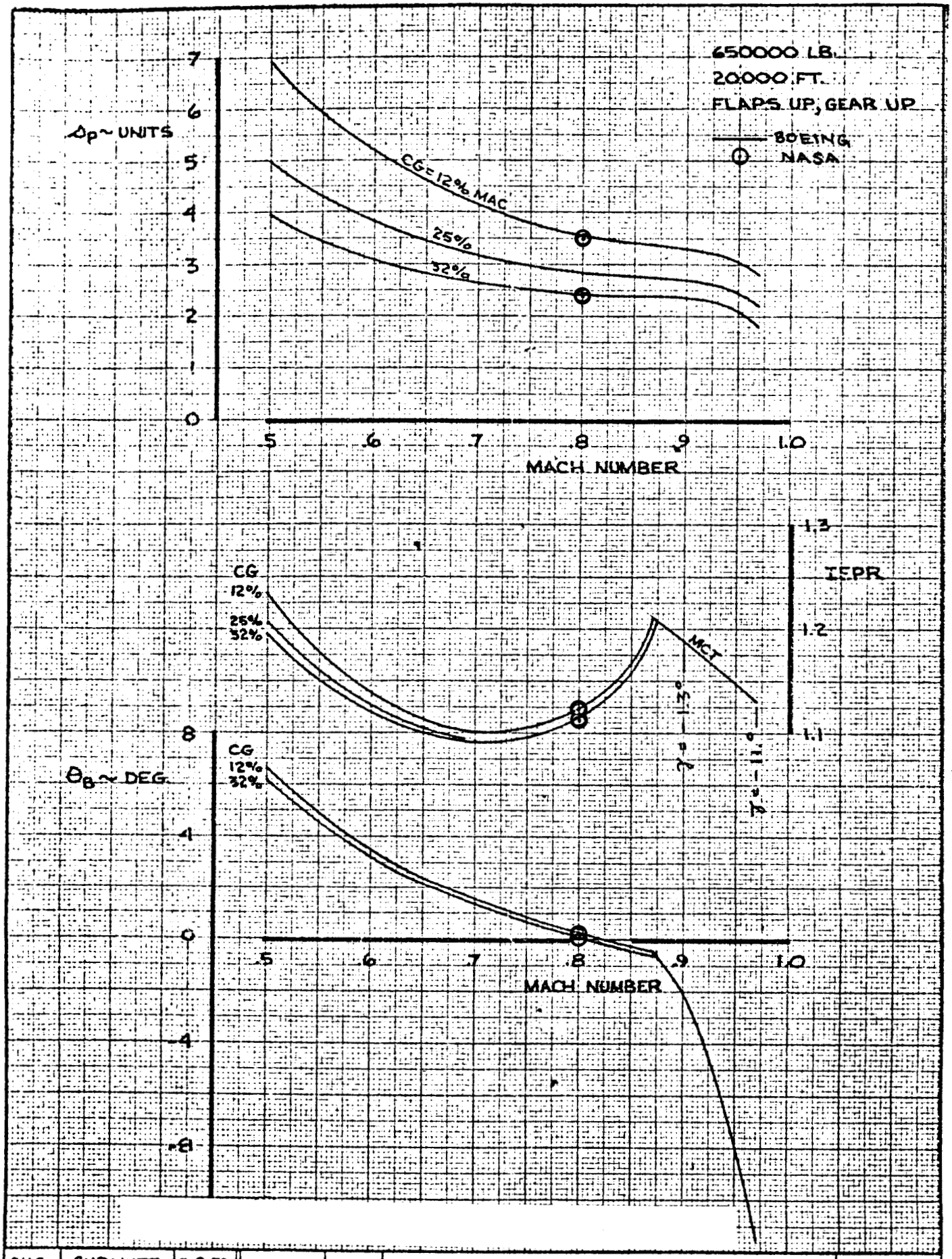

CALC	CURNUTT	5-8-70	REVISED	DATE
CHECK				
APR				
APR				
	GLENN	5-8-70		

LONGITUDINAL TRIM
ALT. = 20000 FT.

THE BOEING COMPANY

747
D6-30643
Vol. II
PAGE
14.1-14

500000 LB.
35000 FT.
FLAPS UP, GEAR UP

BOEING
NASA

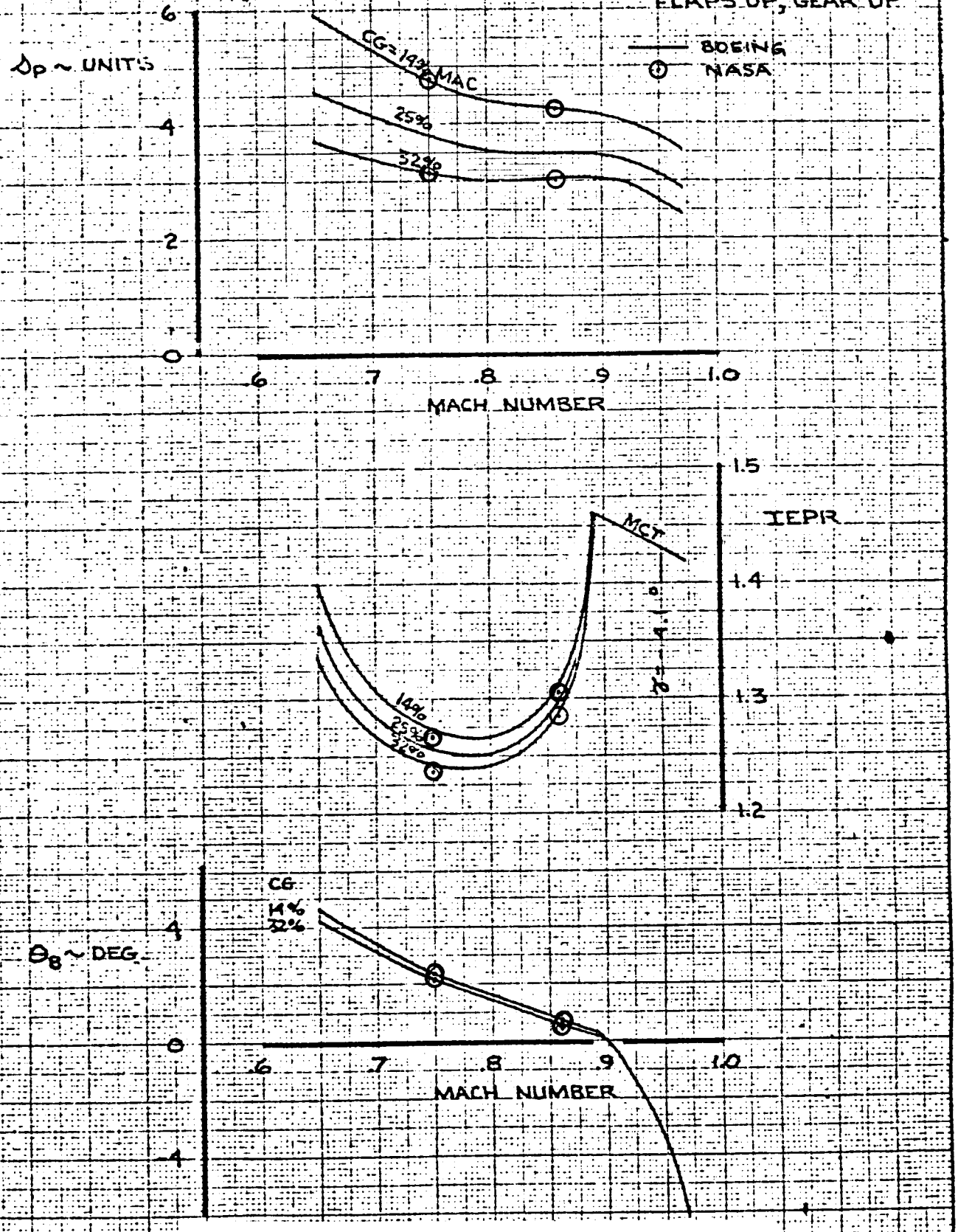

CALC	CURNUTT	5-13-70	REVISED	DATE	LONGITUDINAL TRIM ALT. = 35000 FT.	747 D6-30643 Vol. II
CHECK						
APR						
APR					THE BOEING COMPANY	PAGE 14.1 - 15
	GLENN	5-13-70				

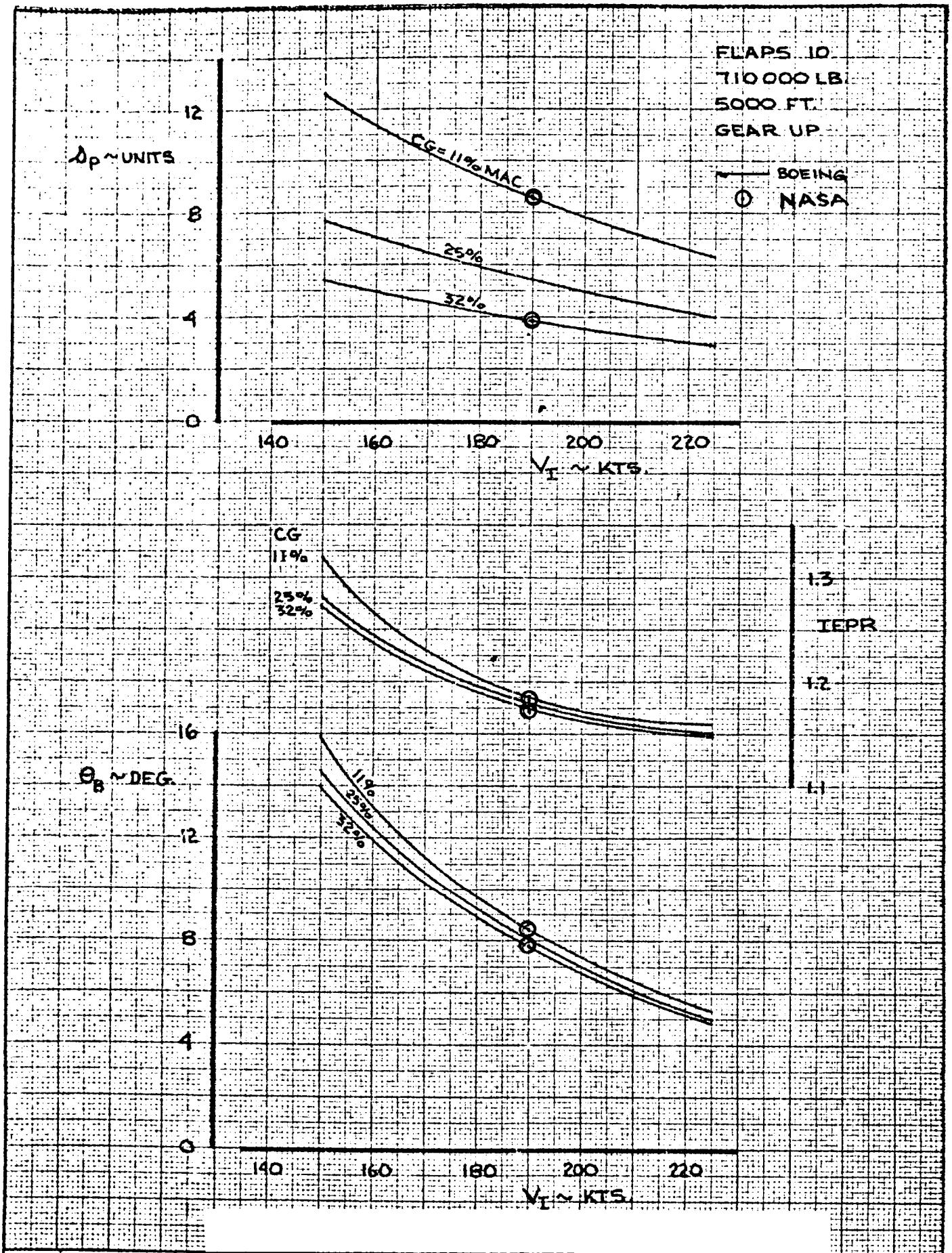

CALC	CURNUTT	5-9-70	REVISED	DATE	LONGITUDINAL TRIM FLAPS 10	747
CHECK						D6-30643 Vol. II
APR						
APR					THE BOEING COMPANY	PAGE 14.1-16
	GLENN	5-9-70				

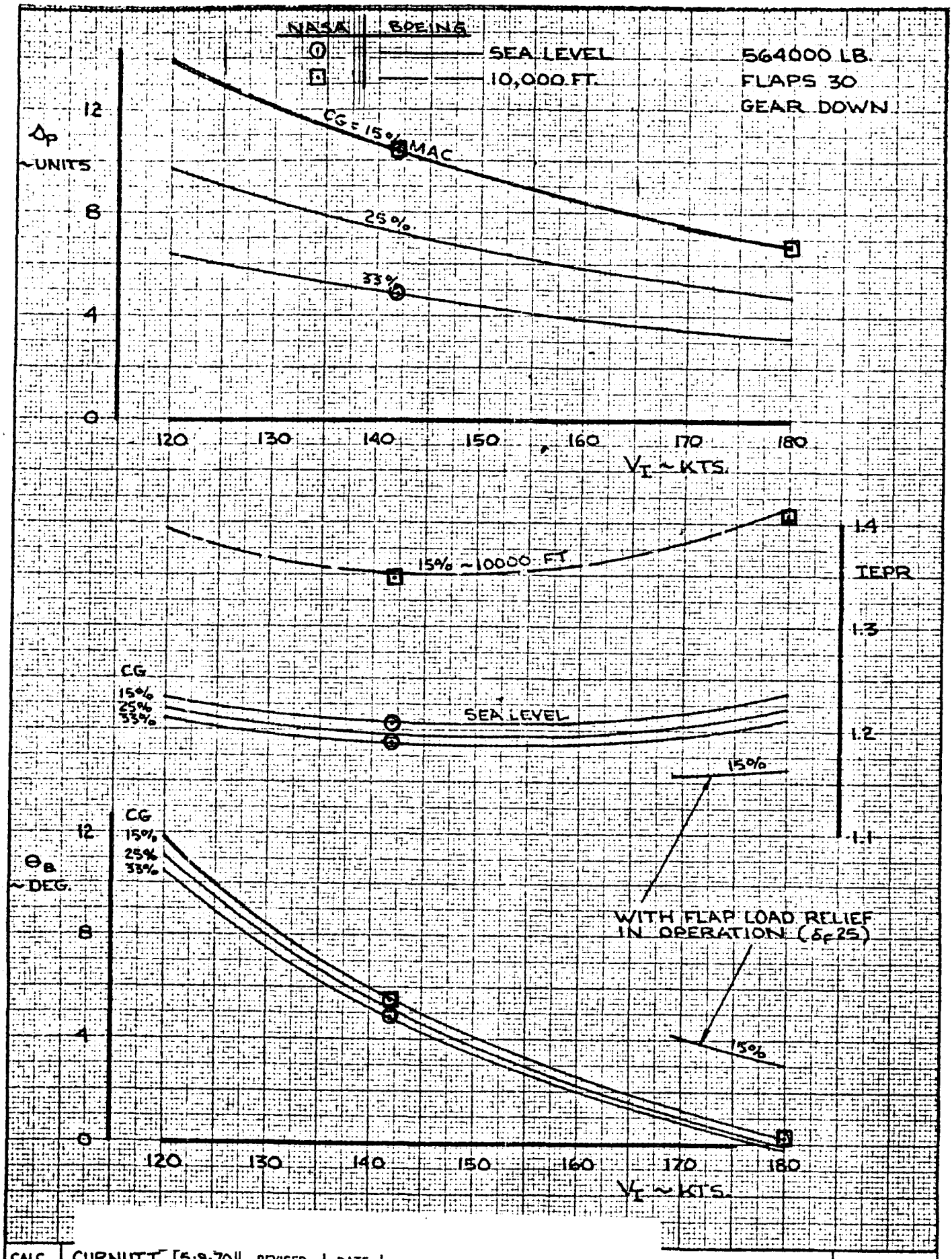

CALC	CURNUTT	5-9-70	REVISED	DATE
CHECK				
APR				
APR				
	GLENN	5-9-70		

LONGITUDINAL TRIM
FLAPS 30

747
D6-30643 Vol. II

THE BOEING COMPANY

PAGE 14.1-17

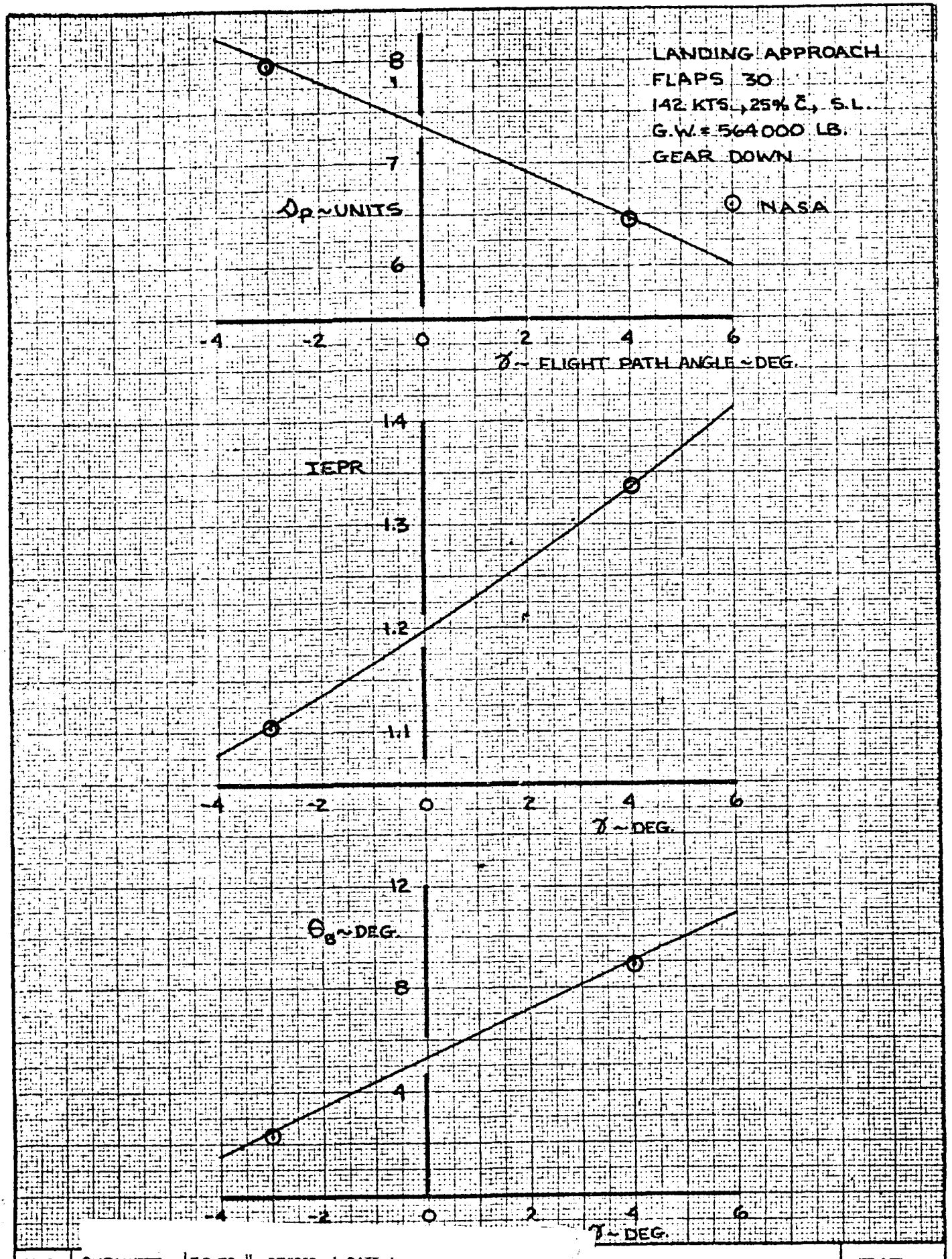

CALC	CURNUTT	5-9-70	REVISED	DATE
CHECK				
APR				
APR				
	GLENN	5-9-70		

EFFECT OF FLIGHT PATH ANGLE ON APPROACH TRIM CONDITIONS

747

D6-30643 Vol. II

THE BOEING COMPANY

PAGE 14.1-18

FLAPS UP
GEAR UP

SYM	A/P	FLT	C.G.~%MAC	G.W.~1000 LB.	ALT.~000FT
◇	RAJAI	3-5	12	654-656	24.5
○	✓	B-7	32	633-635	24.0-24.0
▽	✓	B-7	32	562-623	25.0
△	✓	10-2	12	647-654	23.0-25.0
□	✓	2-6	32	533	20.0
◺	✓	B-11	32	580	24.7
———	SIMULATOR (D6-20423, REV D)		12, 25, 32	650	20

○ NASA

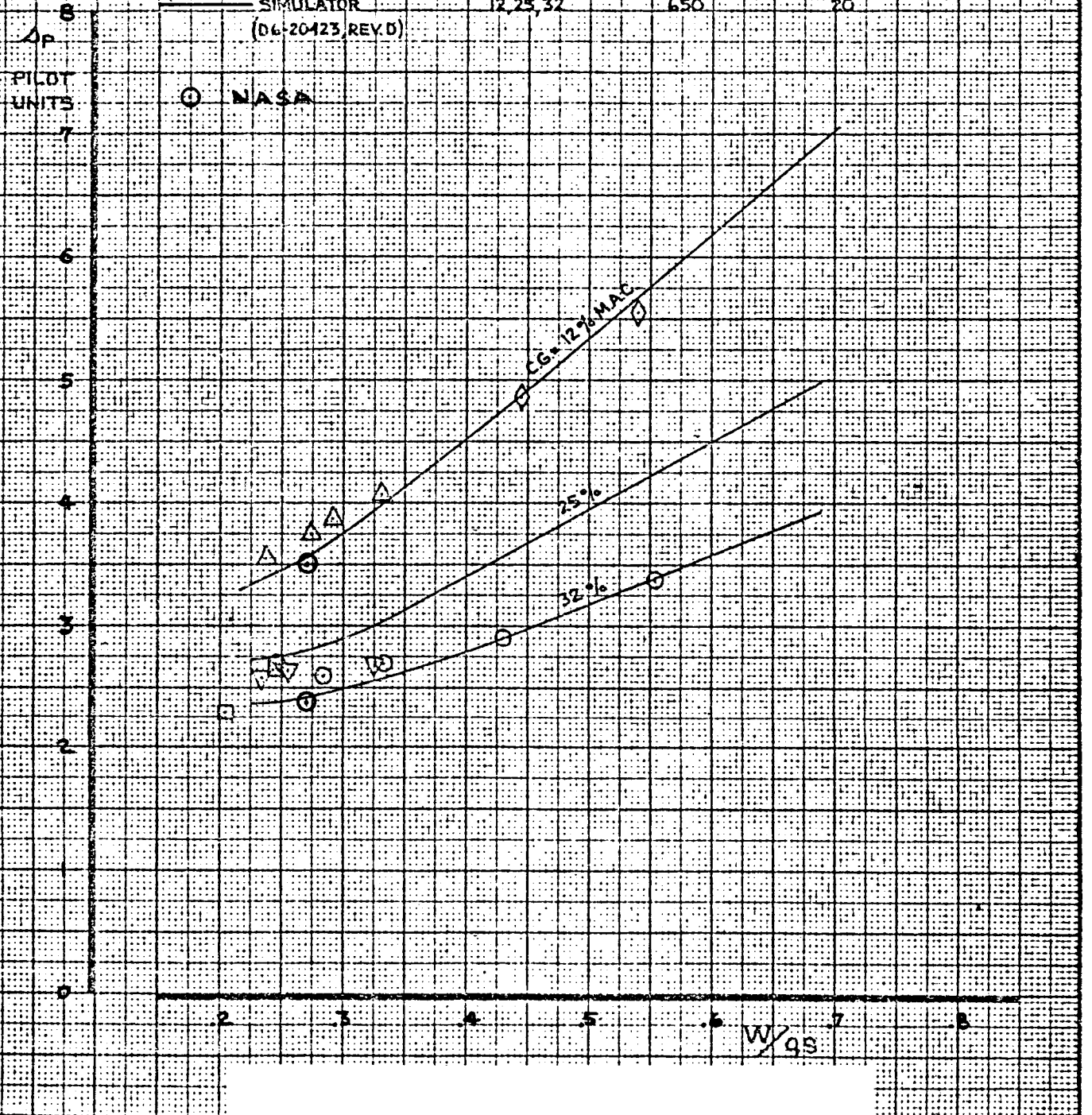

CALC	BYSTROM	3-18-70	REVISED	DATE	LONGITUDINAL TRIM ~ 20,000 FT.
CHECK			CURNUTT	5-20-70	
APR					
APR					
INK	KINSMAN	3-18-70			

747

D6-30643 Vol. II

THE BOEING COMPANY

PAGE 14.1-19

32

TD 441 C14

K-E ALBANENE 1000

FLAPS UP
GEAR UP

SYM	A/P	FLT.	C.G.~% M.A.C.	G.W.~1000 LB.	ALT.~1000 FT.
⊡	RAODI	30-2	14	537-569	34-35
◇	✓	31-6	32	542-561	34-35
⊙	✓	18-1	22	506-492	35
——	SIMULATOR (D6-20423, REV. D)		14, 25, 32	500	35

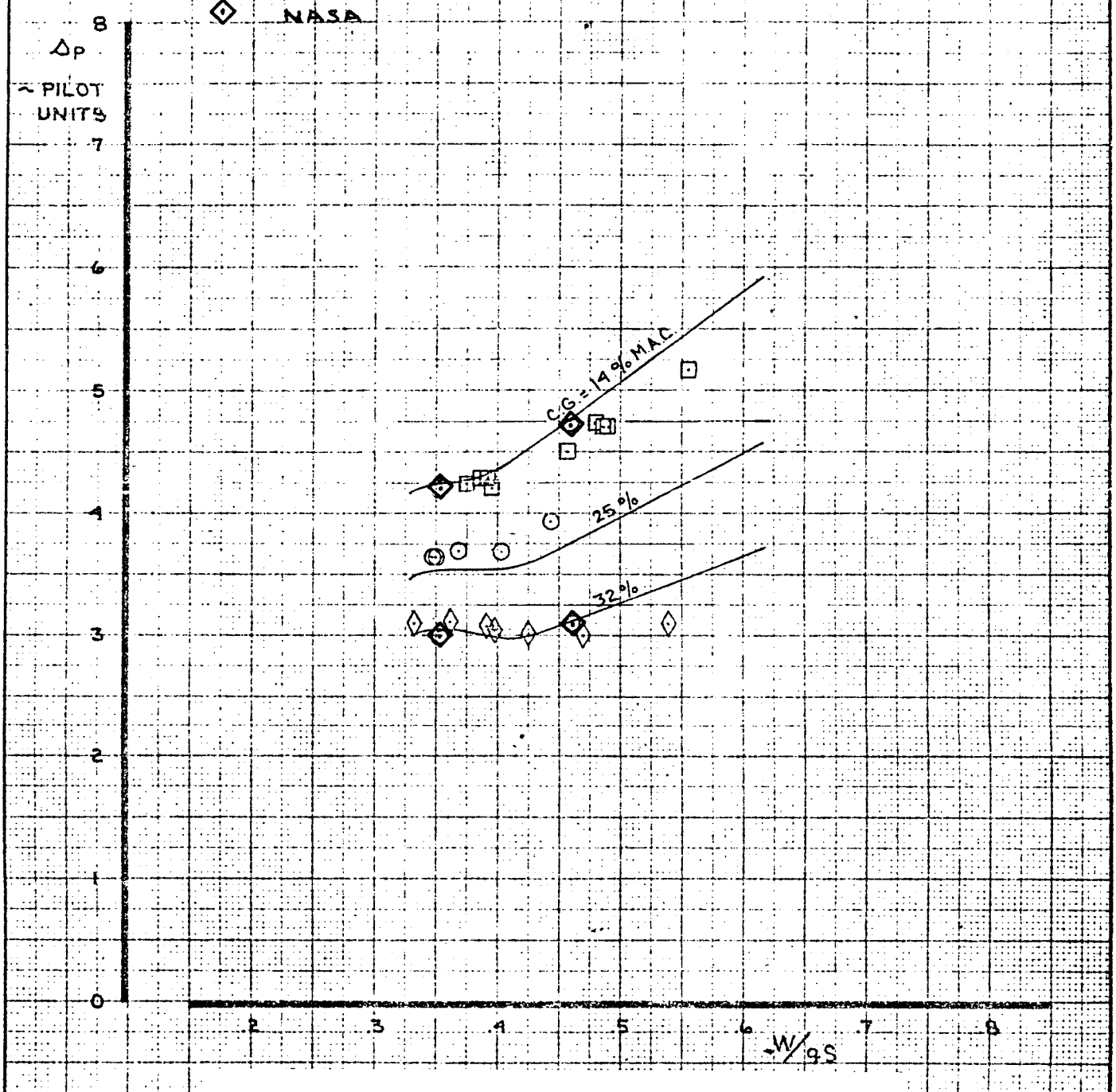

CALC	BYSTROM	3-18-70	REVISED	DATE	LONGITUDINAL TRIM ~ 35,000 FT.	747
CHECK			CURNUTT	5-20-70		
APR						D6-30643 Vol. II
APR						
INK	KINSMAN	3-18-70			THE BOEING COMPANY	PAGE 14.1-20

TD 461 C-R4

K-Σ ALBANENE TRACE

FLAPS 30
GEAR DOWN

SYM	A/P	FLT	C.G. % M.A.C.
▽	RA001	B-1	15
△	✓	B-1	31
⊙	✓	9-1	15
◺	✓	16-2	15
◇	✓	30-2	15
⊡	RA002	7-1	15

NOTE 1. FLAGGED SYMBOLS ARE IDLE THRUST
2. FLT 7-1 (RA002), FROM DRAG TESTING WITH AUTOPILOT ON, Δ_p CORRECTED TO $\delta_e = 2°$

——— SIMULATOR DATA (D6-20423, REV D) P.L.F.
– – – – IDLE THRUST (ZERO THROTTLE)
◇ NASA

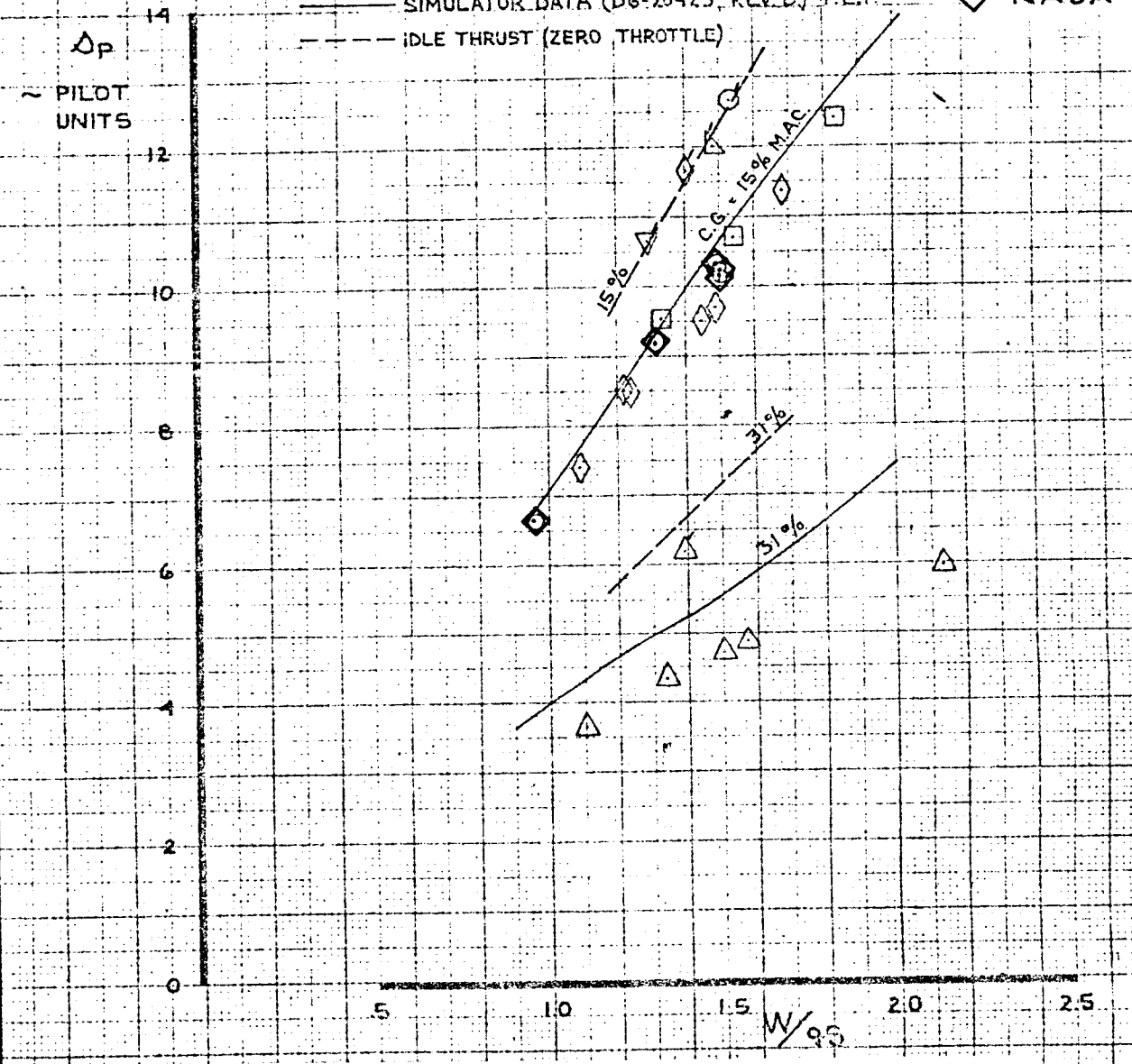

CALC	BYSTROM	3-25-70	REVISED	DATE	LONGITUDINAL TRIM ~ FLAPS 30
CHECK			GLENN	5-22-70	
APR					
APR					THE BOEING COMPANY
INK	KINSMAN	3-25-70			

747
D6-30643 Vol. II
PAGE 14.1-21

TABLE 6.5 CONFIGURATION CHANGES

TEST		FLAP POSITION	GEAR	G.W. ~ 1000 LB.	C.G. ~ % MAC	ALTITUDE ~ 1000 FT.	V_I/M	SPEED BRAKES	ΔP ~UNITS	F_S ~ LB.	δ_e ~DEG.	θ_B ~DEG.	γ ~DEG.	R/C ~FT/MIN.	IEPR	$F_{N_{TOTAL}}$ ~ LB.
GEAR EXTENSION	BOEING	30	UP	564	25	5	150	ZERO	6.3	0	2.0	3.5	0	0	1.225	72100
	NASA								6.38			3.61			1.225	72220
	BOEING	|	DN	564	25	5	150	ZERO	6.6	0	2.0	3.8	0	0	1.250	77710
	NASA								6.72			3.93			1.248	77546
	BOEING	UP	UP	564	32	5	250	ZERO	3.1	0	2.0	3.9	0	0	1.035	31500
	NASA								3.1			3.98			1.035	31414
	BOEING	UP	DN	564	32	5	250	ZERO	2.5	0	2.0	3.2	0	0	1.165	61200
	NASA								2.49			3.28			1.162	60563
SPEED BRAKES	BOEING	UP	UP	564	32	5	270	ZERO	2.8	0	2.0	3.0	0	0	1.028	32120
	NASA								2.82			3.05			1.028	32011
	BOEING	UP	UP	564	32	5	270	INFLT. DETENT	2.5	0	2.0	4.2	0	0	1.094	47800
	NASA								2.49			4.15			1.093	47454
	COMPUTATION TOLERANCE								± .25	±10%	± .5	± .3			± .01	± 3%

14.1.5 ELEVATOR-STABILIZER TRADES

The simulated airplane was initially trimmed for 1 g straight and level flight with zero column deflection. Values of δ_{col} were input and the airplane was retrimmed with stabilizer. The results are tabulated and plotted with Boeing simulation and flight test results on Page 14.1-24. This test provided a check on the column to elevator gearing, outboard elevator blowdown, and elevator and stabilizer effectiveness.

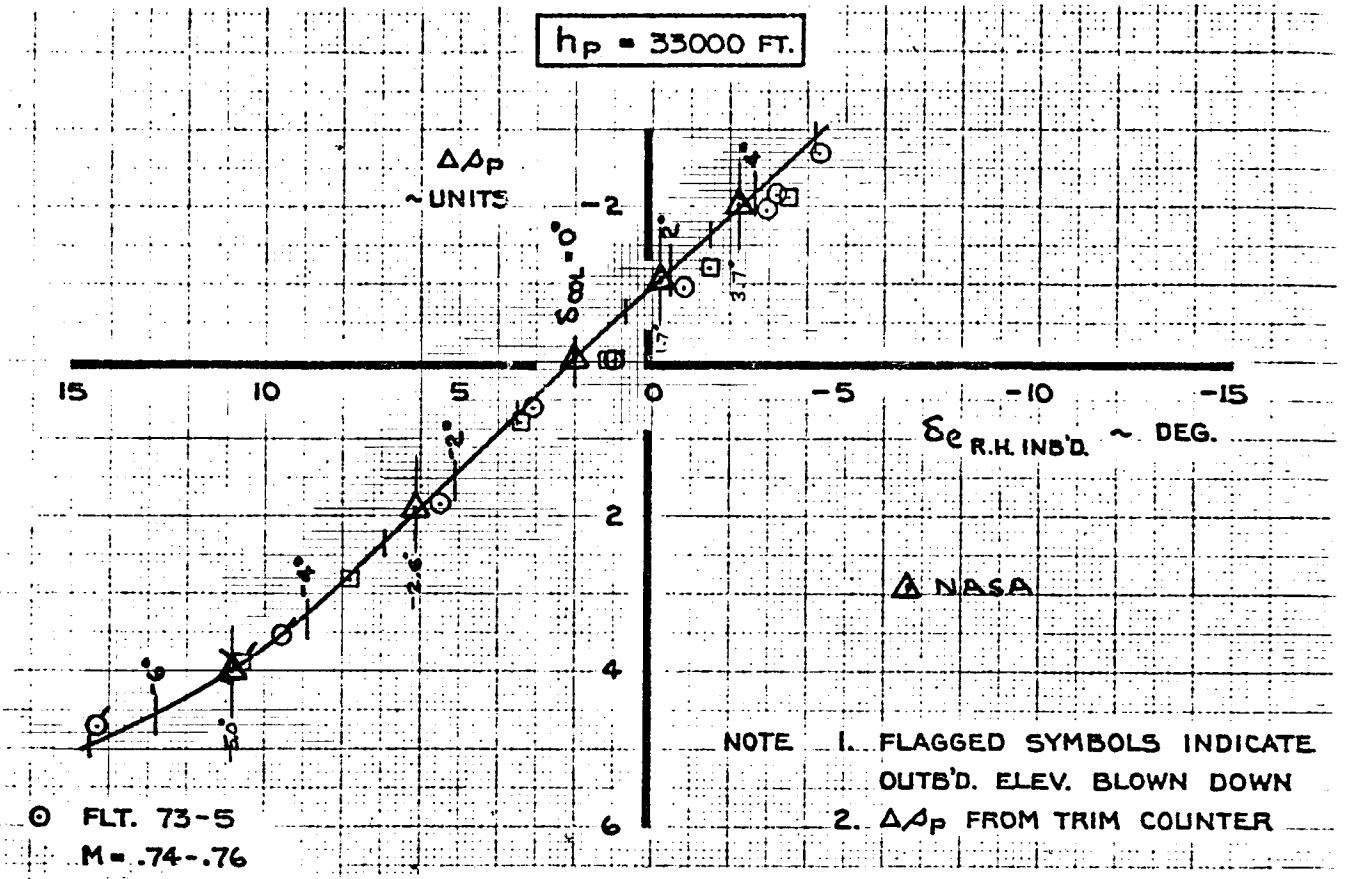

NOTE 1. FLAGGED SYMBOLS INDICATE OUTB'D. ELEV. BLOWN DOWN
2. $\Delta\mathcal{A}_P$ FROM TRIM COUNTER

⊙ FLT. 73-5
M = .74-.76
G.W. = 628000 LB.
C.G. = 11.7 % MAC
$\mathcal{A}_{P_{TRIM}}$ = 5.25 UNITS

⊡ FLT. 73-11
M = .74-.76
G.W. = 604000 LB.
C.G. = 12.1 % MAC
$\mathcal{A}_{P_{TRIM}}$ = 5.12 UNITS

—— SIMULATOR (D6-20423, REV. D DATA)
M = .75
G.W. = 628000 LB.
C.G. = 11.7 % MAC
$\mathcal{A}_{P_{TRIM}}$ = 5.4 UNITS

FLAPS UP
GEAR UP

$\mathcal{A}_P$ ~ UNITS		δ_e ~ DEG.		δ_{COL} ~ DEG.		$\Delta\delta_s$
BOEING TARGET	NASA TEST	BOEING TARGET	NASA TEST	BOEING TARGET	NASA TEST	~ DEG.
5.4	5.35	2.0	2.0	0	0	0
4.4	4.30	- .1	-.18	1.7	1.7	-1.05
3.4	3.36	-2.3	-2.22	3.7	3.7	-2.0
7.4	7.24	6.2	6.1	-2.6	-2.6	+1.9
9.4	9.32	10.8	10.95	-5.0	-5.0	+4.0
TOLERANCE		± .5°		± 1°		

747

			REVISED	DATE
CALC				
CHECK				
APPD				
APPD				JUNE 1970

STABILIZER - ELEVATOR TRADES
SIMULATOR - FLIGHT TEST COMPARISON

REV LTR:

BOEING | NO. D6-30643 VOL II
SECT | PAGE 14.1-24

E 1196 R6

14.1.6 AIRPLANE DYNAMICS

Dynamic responses were run to check the Dutch roll, short period, and phugoid modes of the simulated airplane.

14.1.6.1 Dutch Roll

The Dutch roll was initiated by releasing the airplane from an initial condition of sideslip. Responses were made with yaw damper on and off. Comparisons of the time histories between the NASA and Boeing simulations are shown on Pages 14.1-26 thru -36.

14.1.6.2 Short Period and Phugoid

The short period and phugoid modes were exited by an elevator input after the airplane had been trimmed for straight and level flight. An incremental elevator was input for a prescribed time and then removed. Comparisons of the time histories between the NASA and Boeing simulations are shown on Pages 14.1-37 thru -49.

NASA

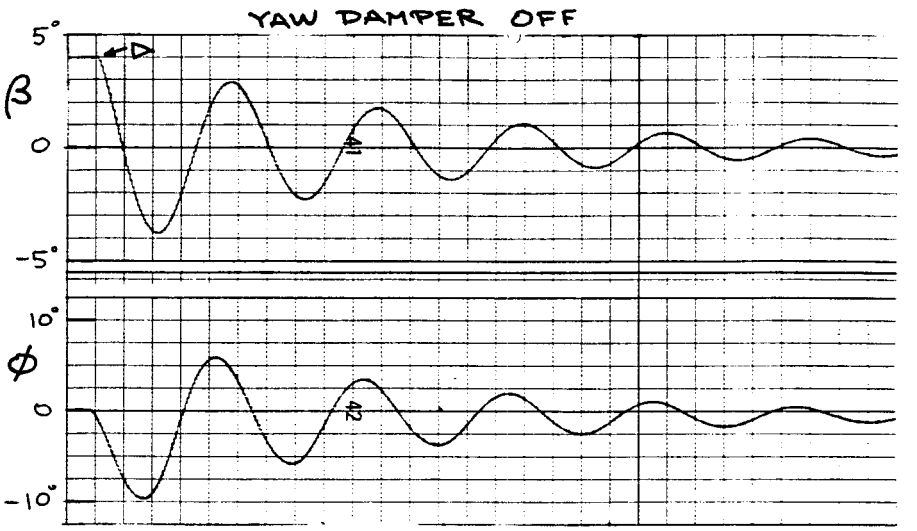

GW = 564000 LB
h = 20000 FT Ve = 325 KT
c.g. = 25 %

$\beta_{IC} = 5°$
(▷ NASA DAC LIMITED TO $\beta = 4°$ FOR TEST)

BOEING

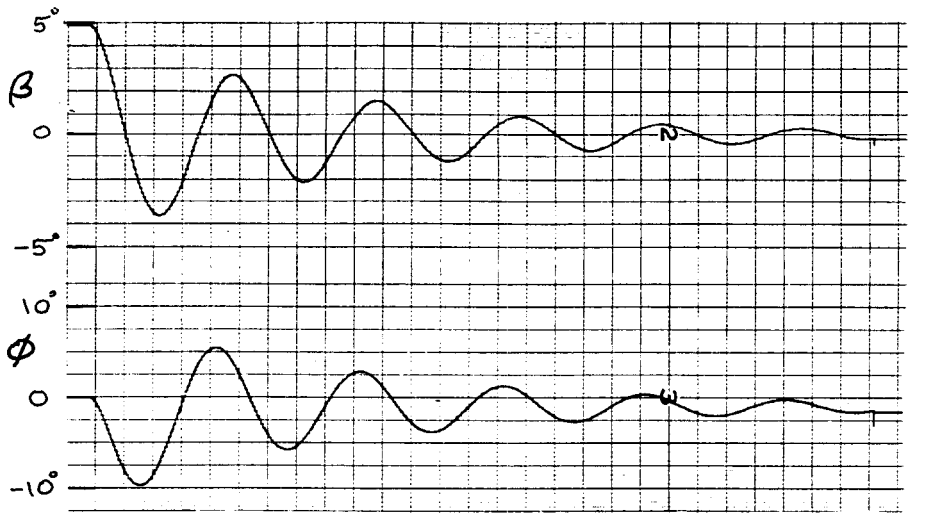

NASA-BOEING DUTCH ROLL COMPARISON

NASA

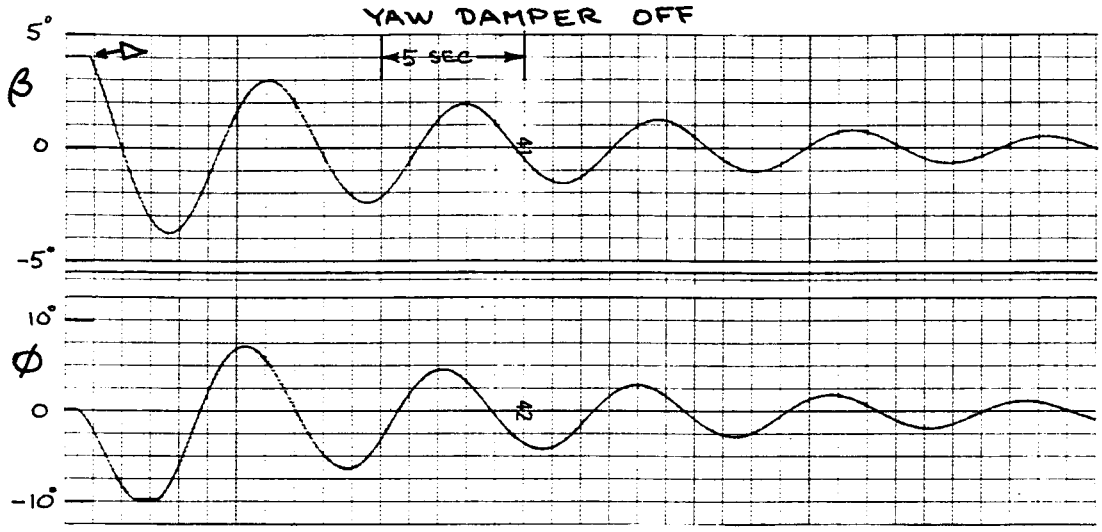

GW = 564000 LB
h = 20000 FT Ve = 225 KT
c.g. = 25%

$\beta_{IC} = 5°$
(▷ NASA DAC LIMITED TO $\beta = 4°$ FOR TEST)

BOEING

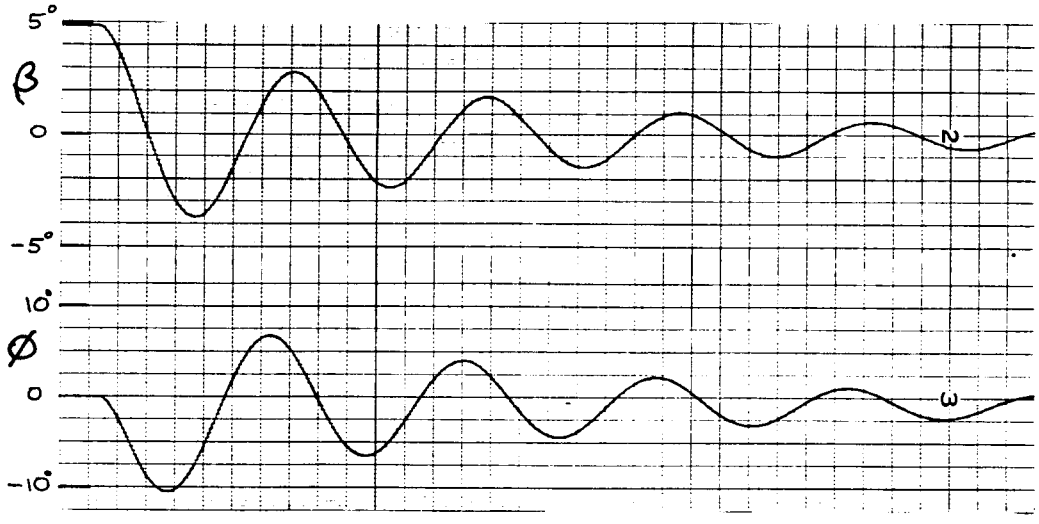

NASA-BOEING DUTCH ROLL COMPARISON

NASA

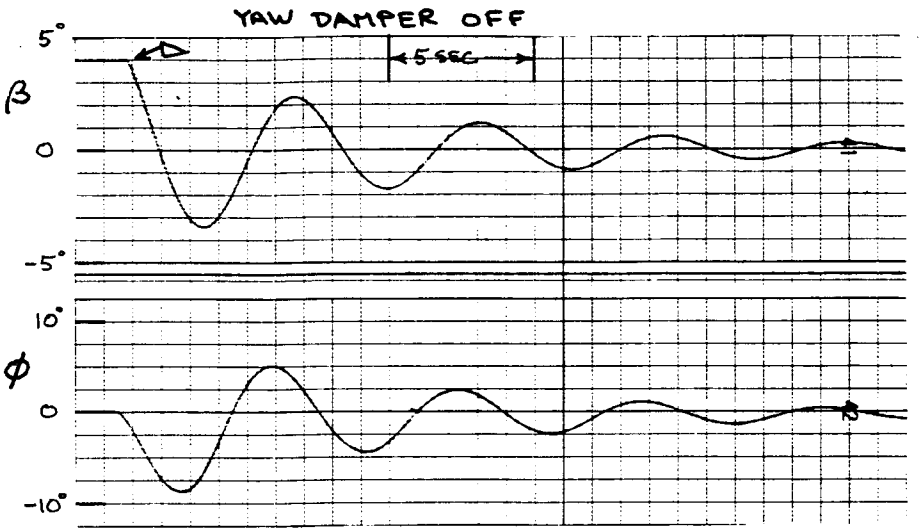

GW = 564000 LB
h = 5000 FT Ve = 250KT
c.g. = 25%

$\beta_{IC} = 5°$
(▷ NASA DAC LIMITED TO $\beta = 4°$ FOR TEST)

BOEING

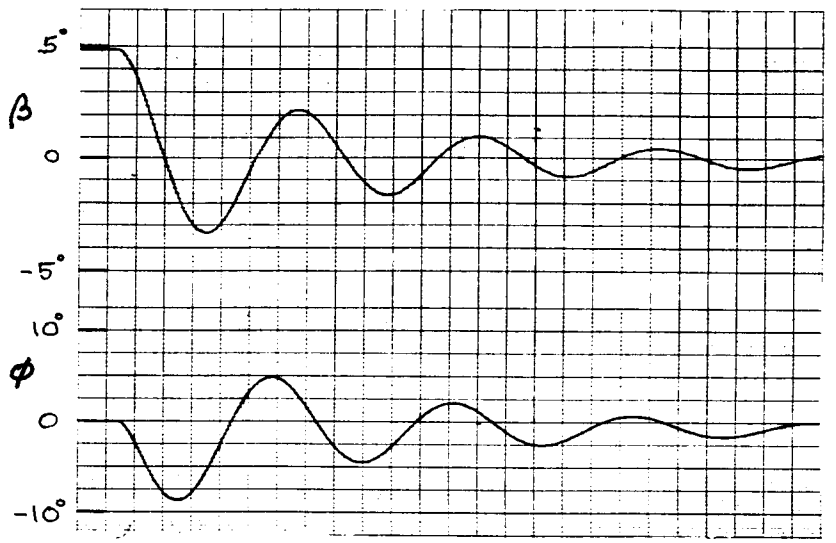

NASA-BOEING DUTCH ROLL COMPARISON

NASA

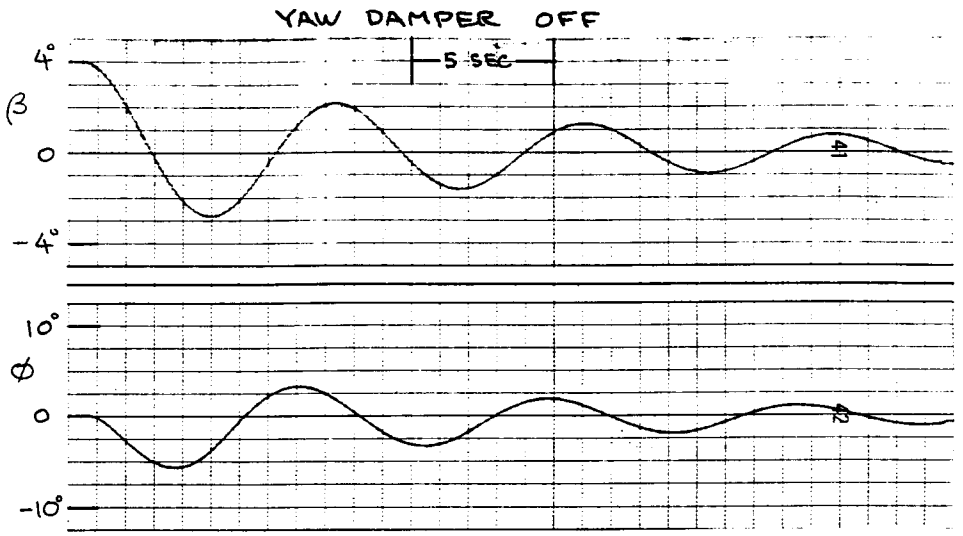

GW = 564000 LB
h = 200 FT Ve = 142 KT
c.g. = 25% δ_F = 30

BOEING

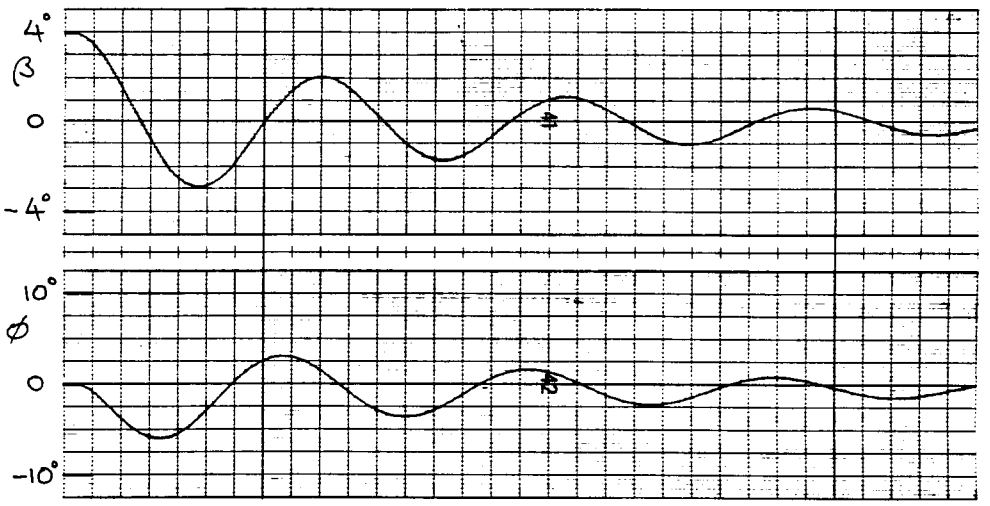

NASA-BOEING DUTCH ROLL COMPARISON

NASA

YAW DAMPER OFF

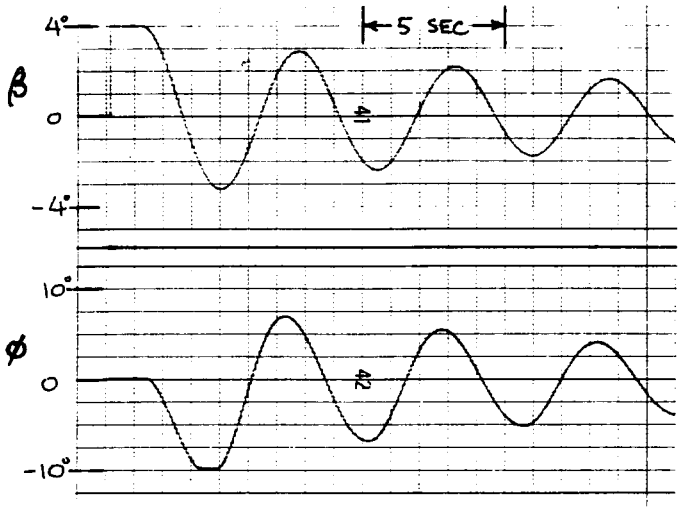

YAW DAMPER ON

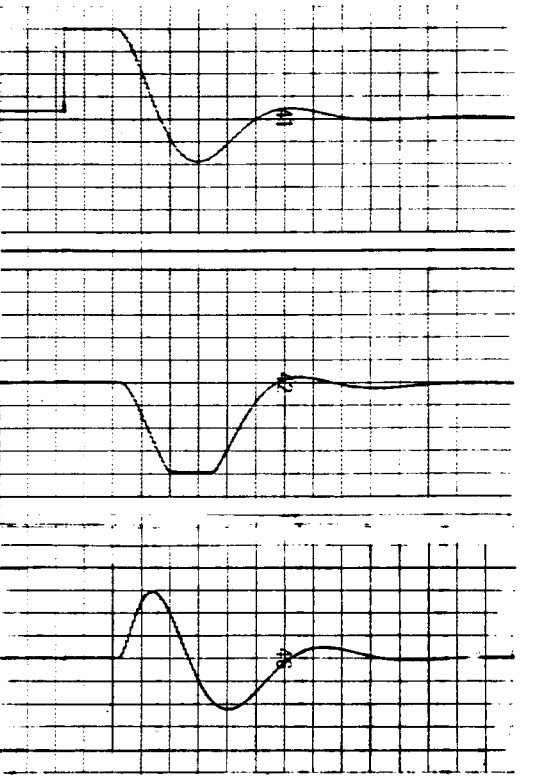

GW = 564000 LB
h = 35000 FT
Ve = 275 KT
c.g. = 25%

BOEING

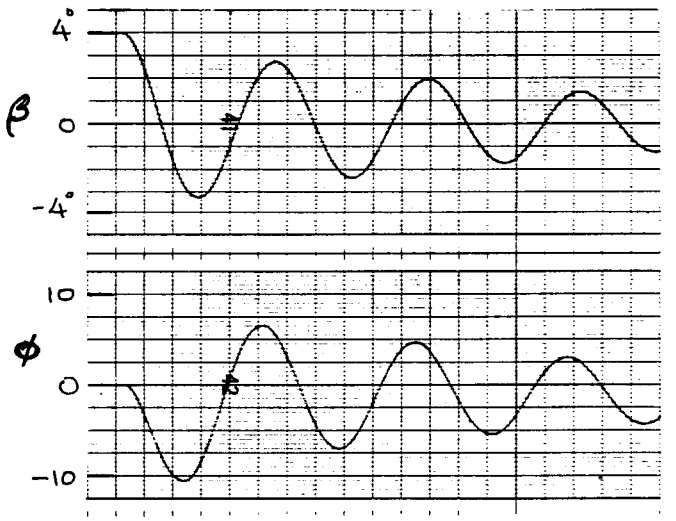

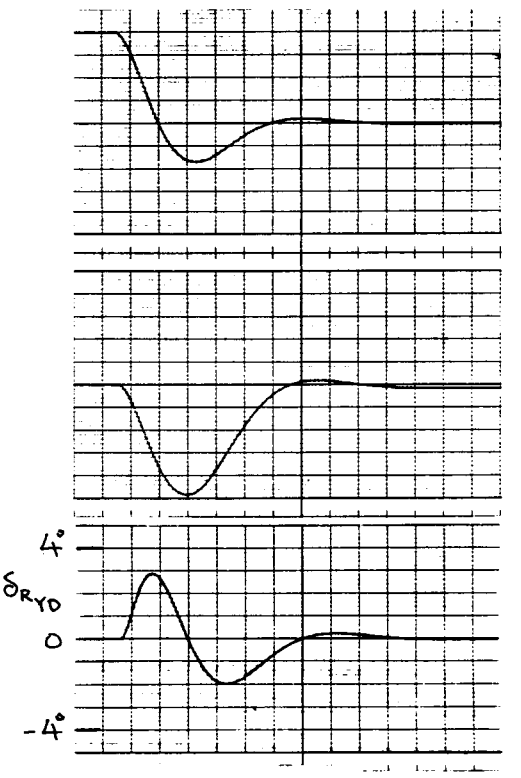

NASA-BOEING DUTCH ROLL COMPARISON

NASA

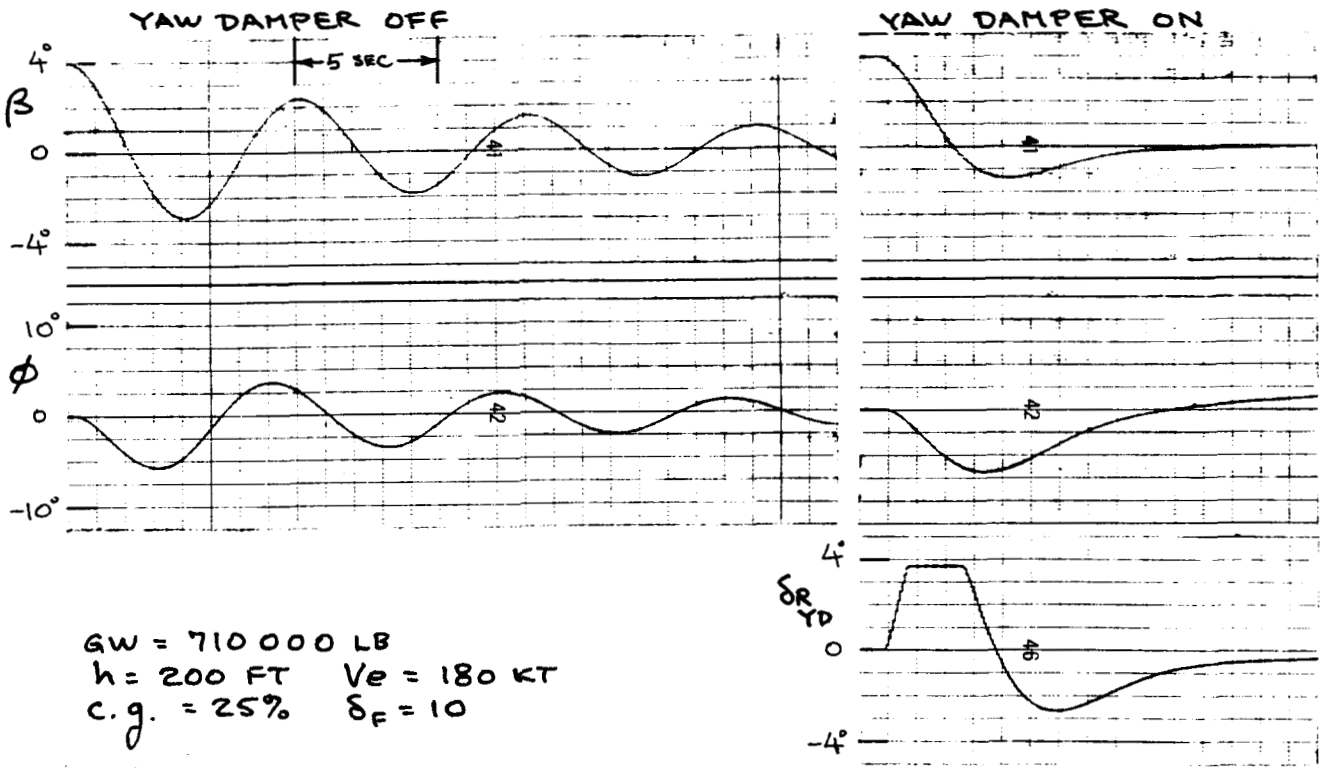

GW = 710 000 LB
h = 200 FT Ve = 180 KT
c.g. = 25% δ_F = 10

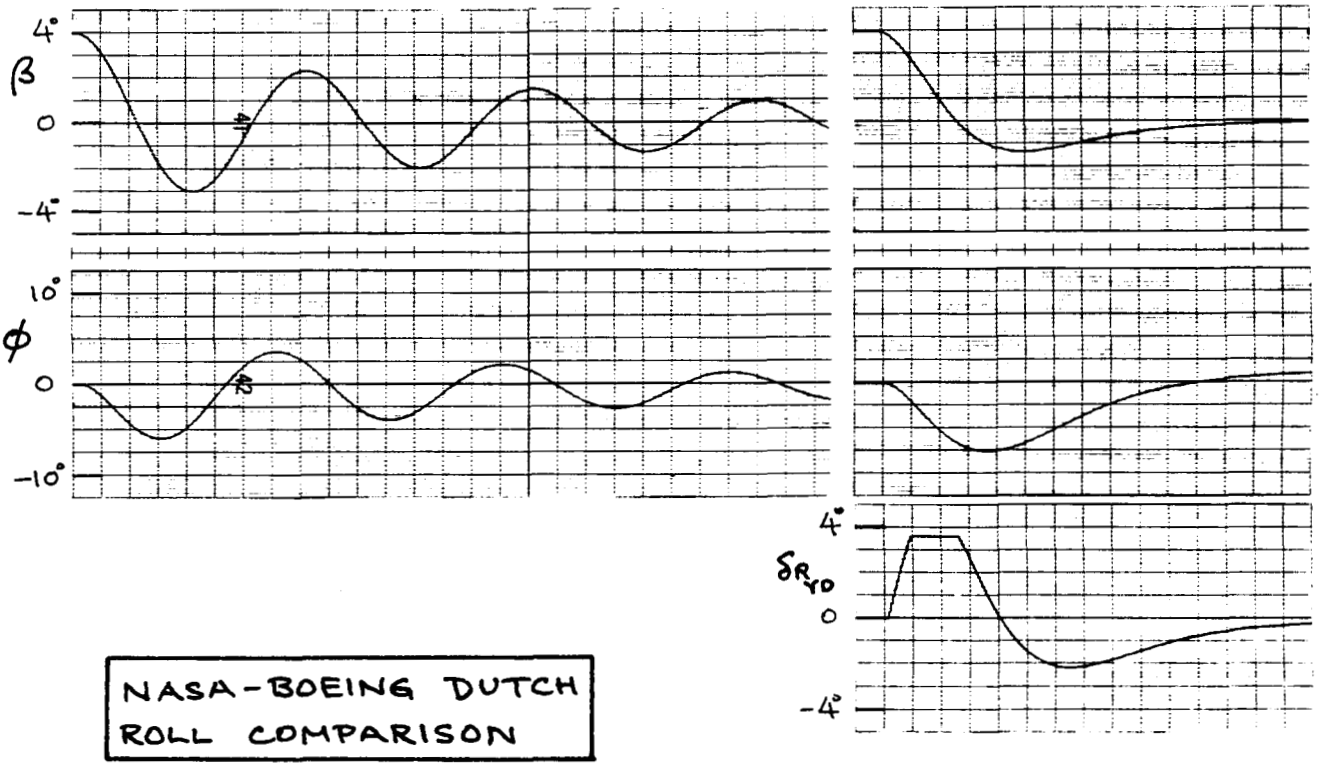

NASA-BOEING DUTCH ROLL COMPARISON

NASA

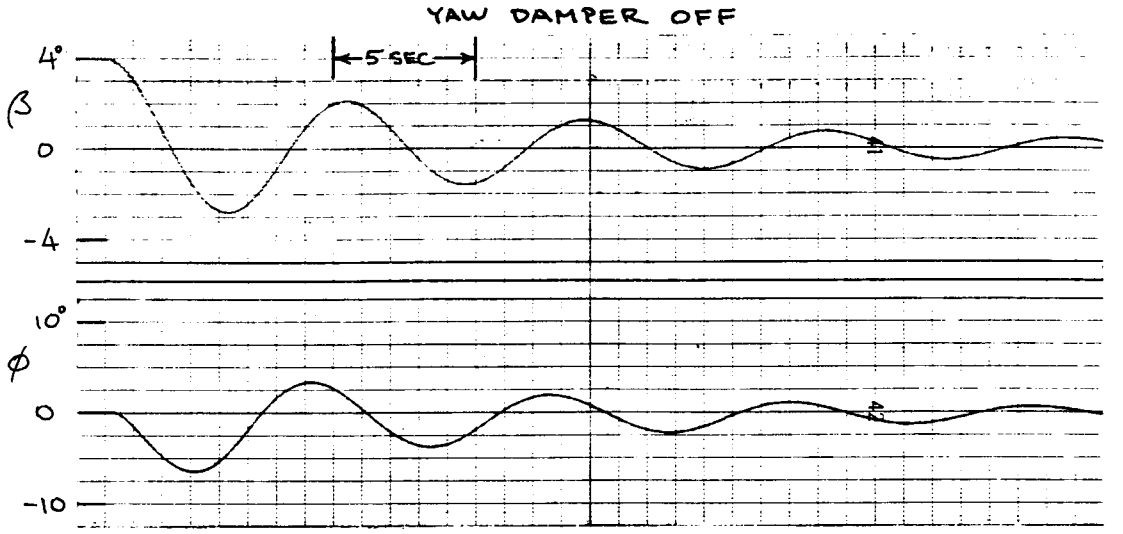

GW = 564000 LB
h = 200 FT Ve = 180 KT
c.g. = 25% δ_F = 30

BOEING

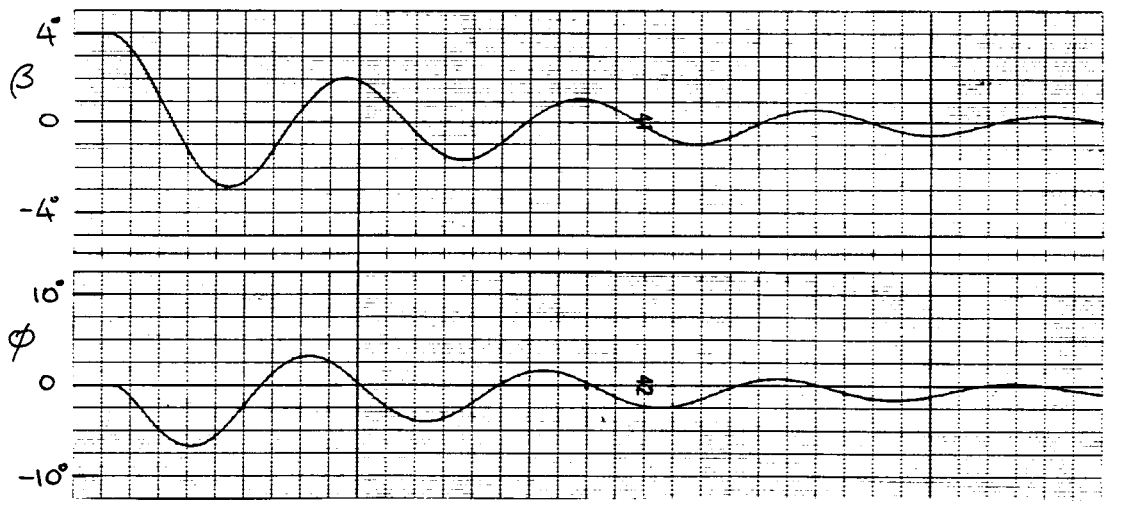

NASA-BOEING DUTCH ROLL COMPARISON

NASA

YAW DAMPER ON

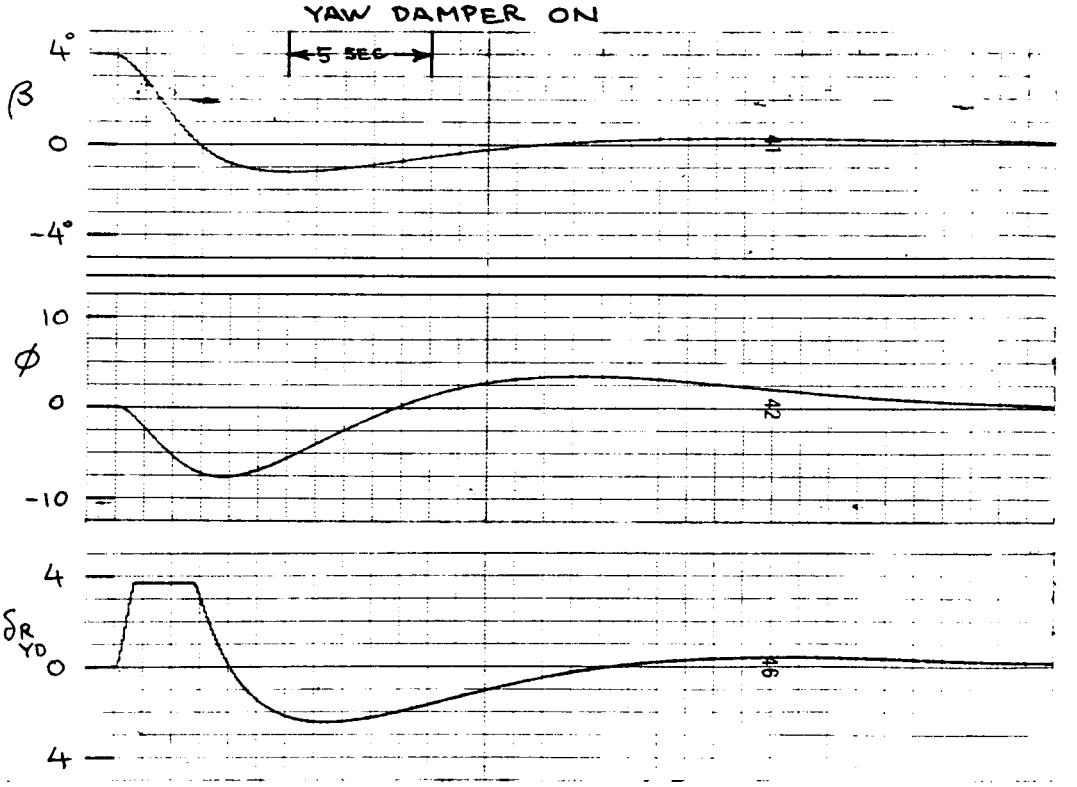

BOEING

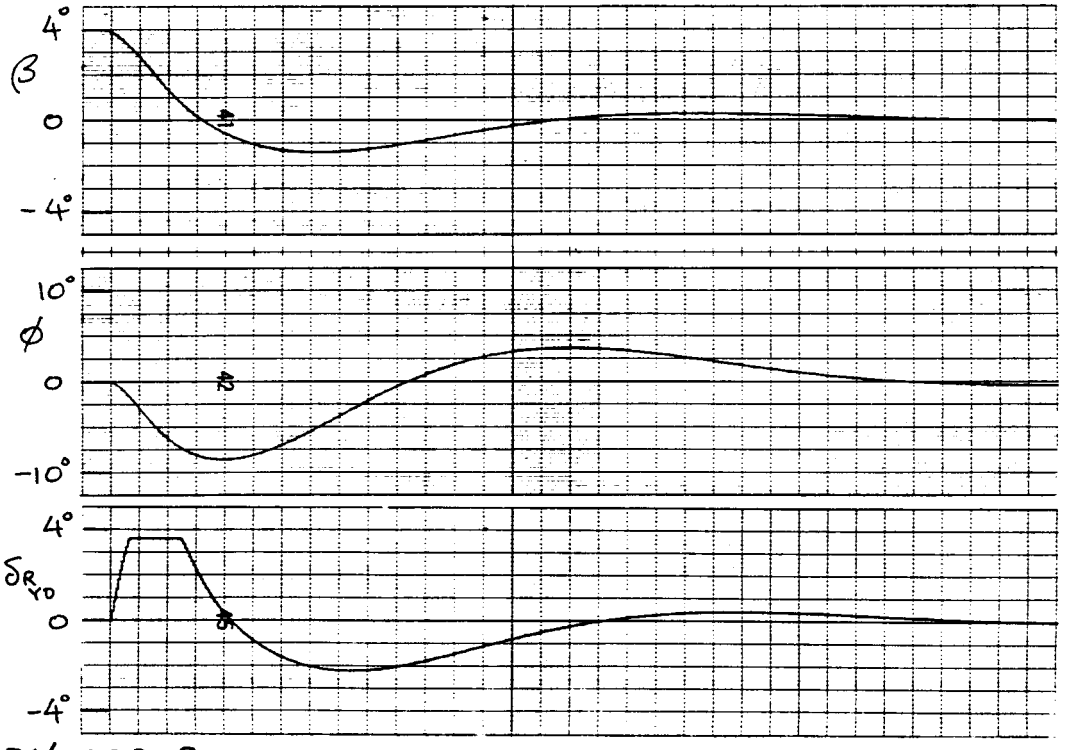

GW = 564 000 LB
h = 200 FT Ve = 180 KT
c.g. = 25% δ_F = 30

NASA-BOEING DUTCH ROLL COMPARISON

NASA

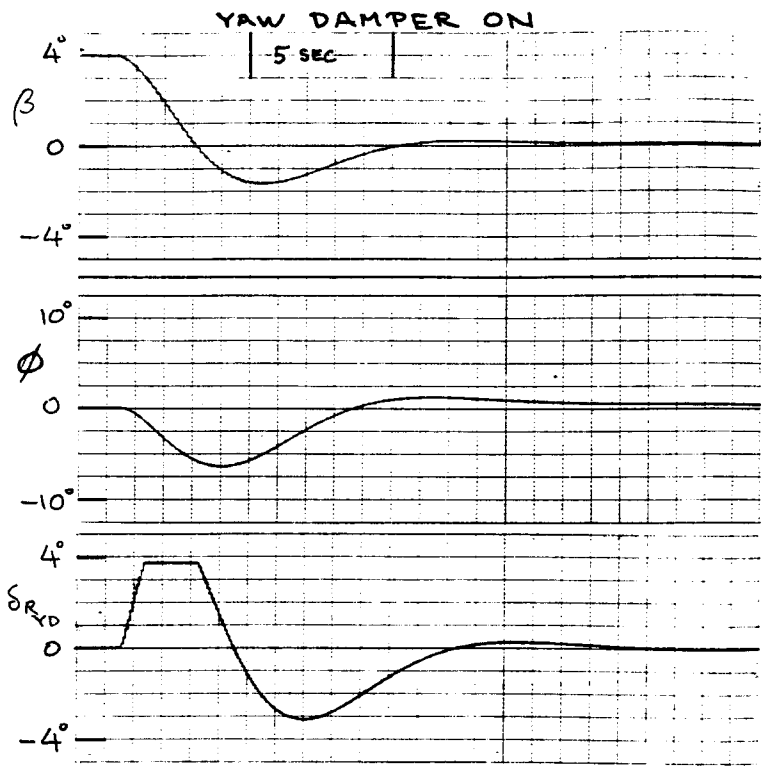

BOEING

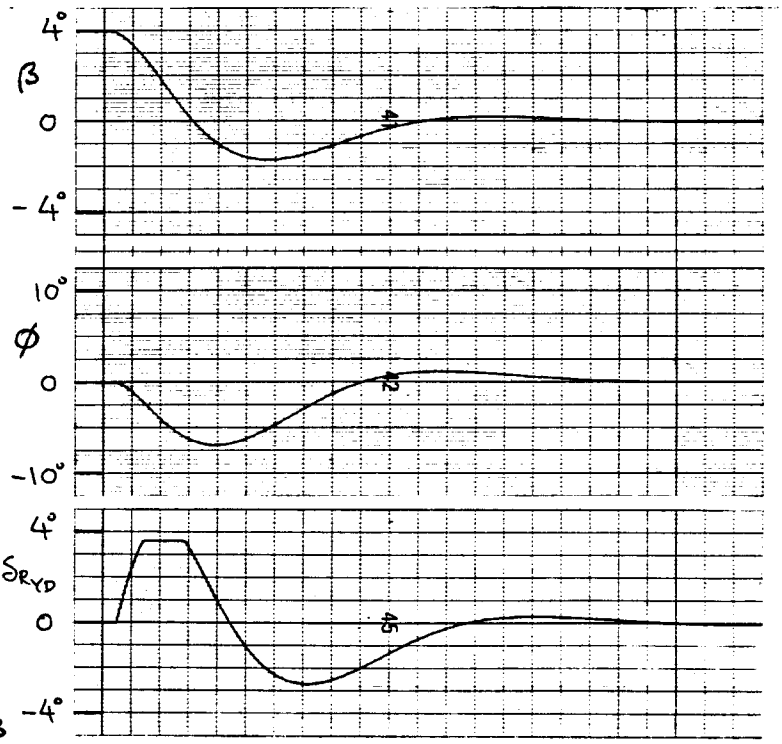

GW = 564 000 LB
h = 200 FT Ve = 142 KT
c.g. = 25 % δ_F = 30

NASA-BOEING DUTCH ROLL COMPARISON

NASA

YAW DAMPER OFF

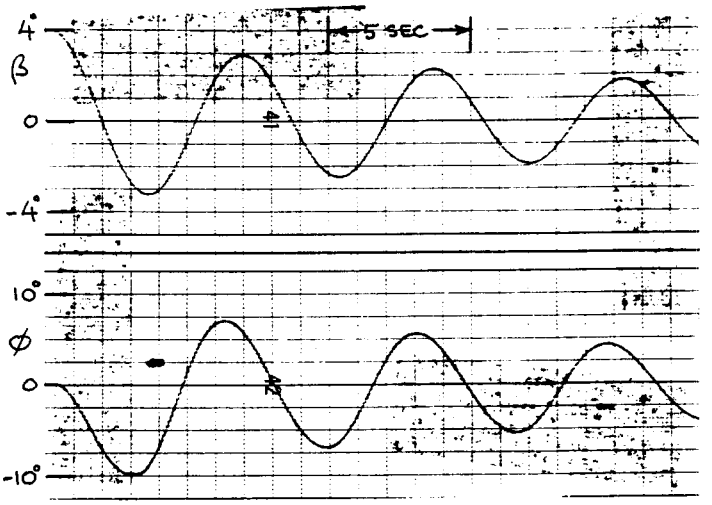

YAW DAMPER ON

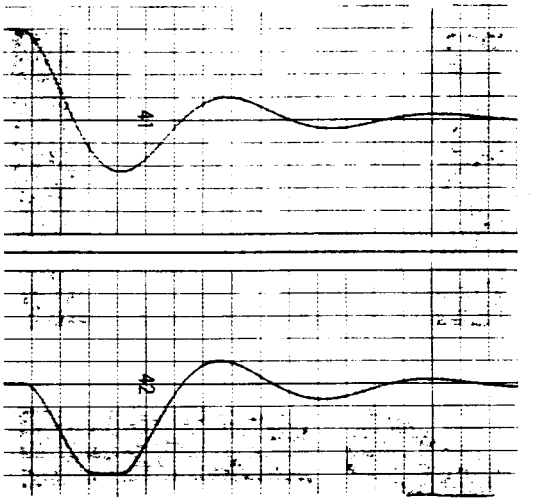

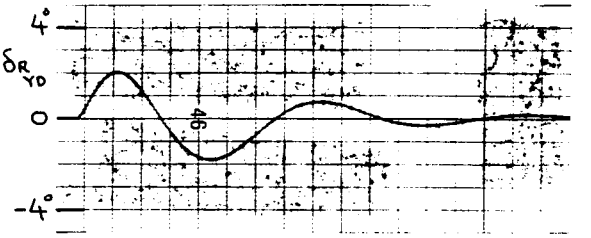

GW = 564 000 LB
h = 35000 FT
Ve = 225 KT
c.g. = 25%

BOEING

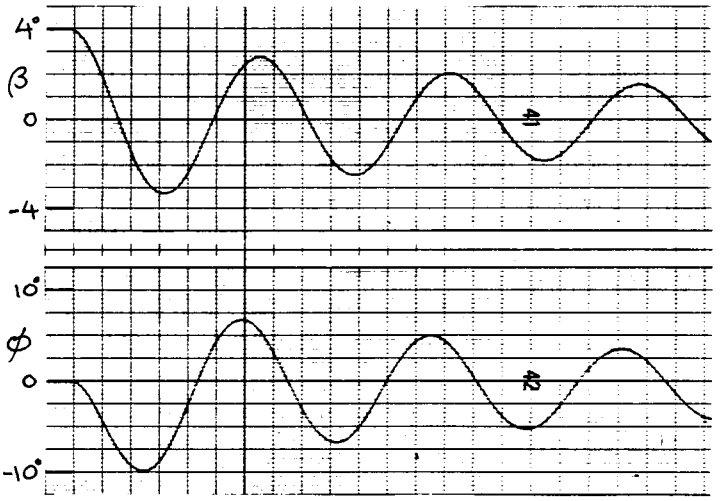

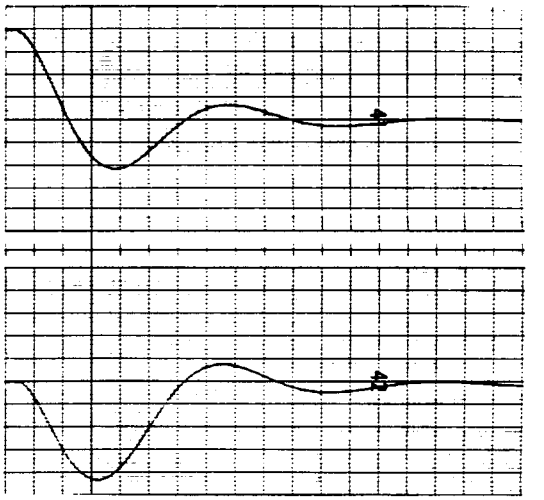

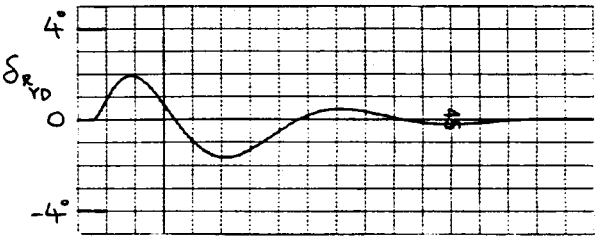

NASA-BOEING DUTCH ROLL COMPARISON

NASA

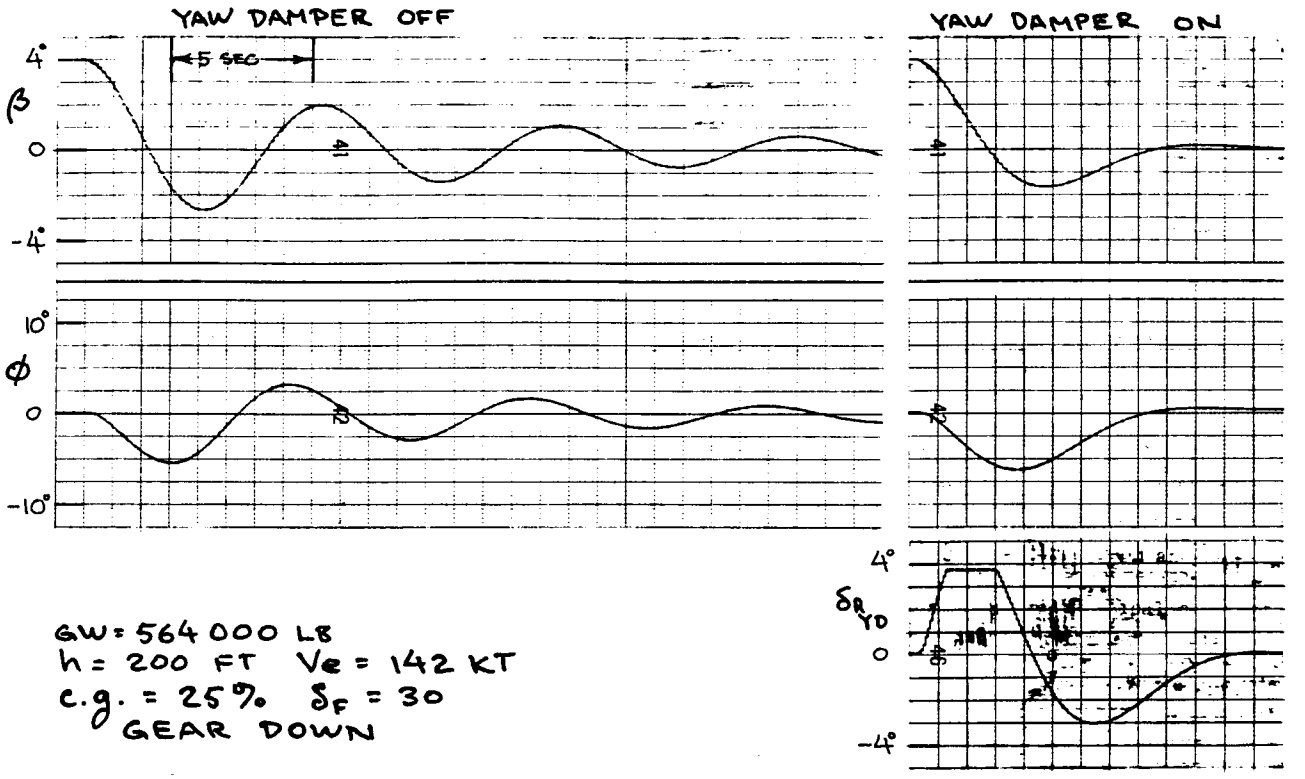

GW = 564 000 LB
h = 200 FT Ve = 142 KT
c.g. = 25% δ_F = 30
GEAR DOWN

BOEING

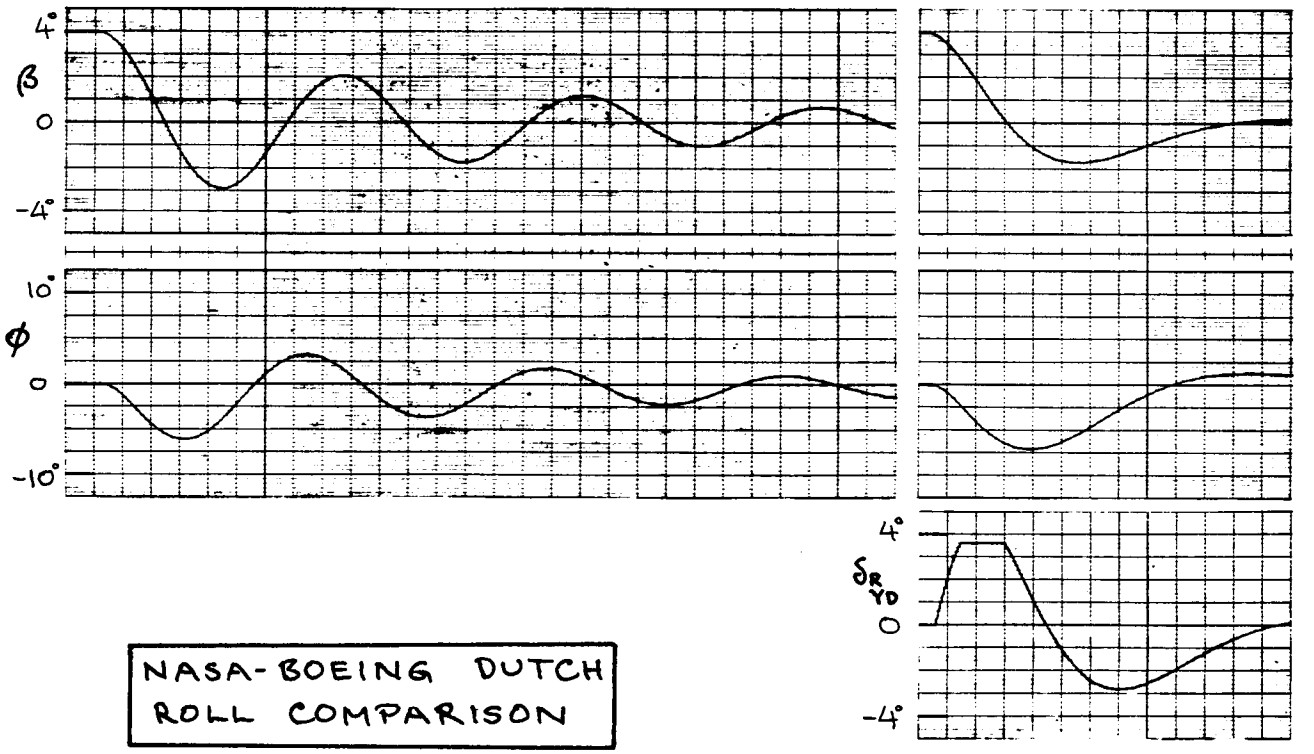

NASA-BOEING DUTCH ROLL COMPARISON

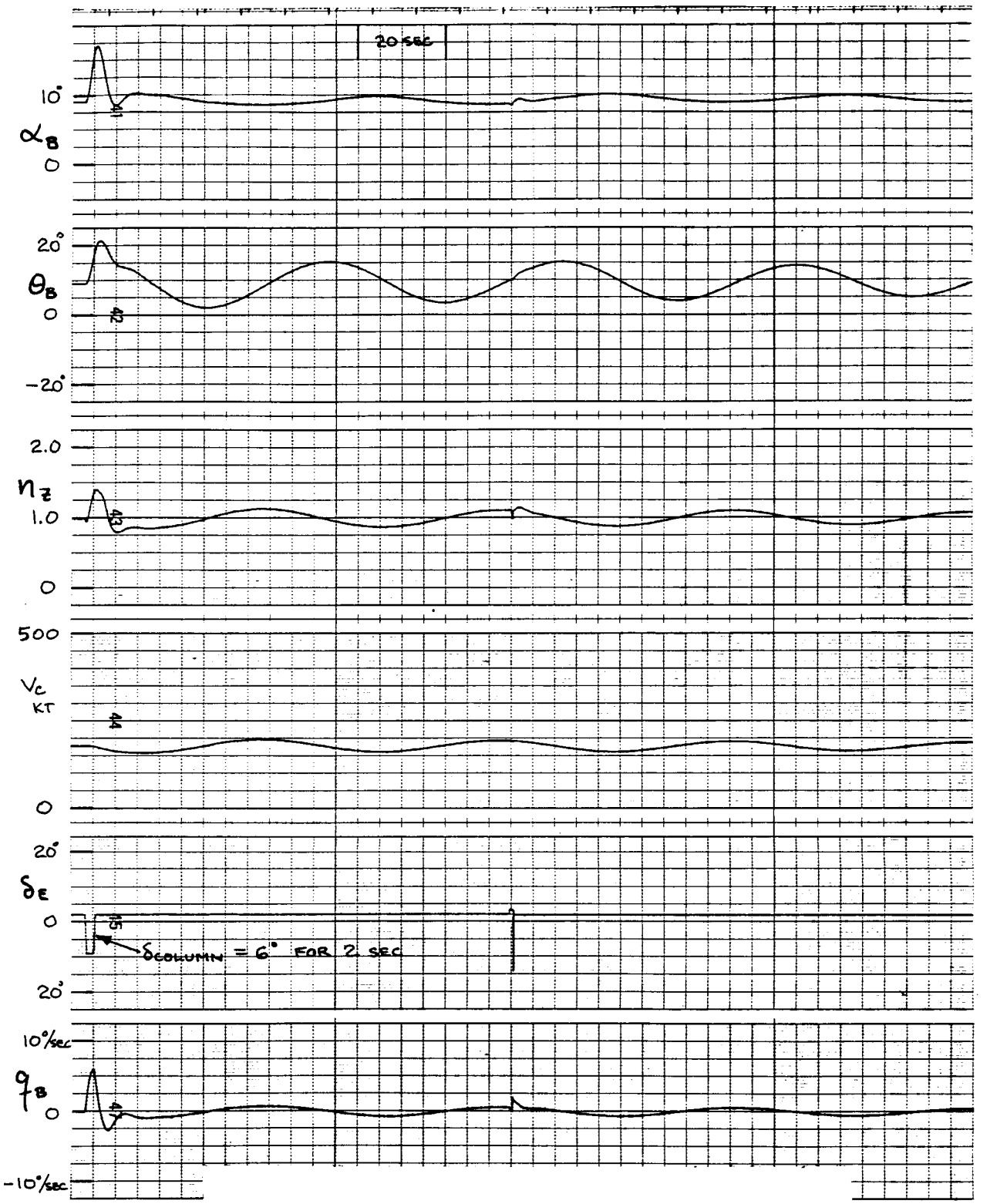

GW = 710 000 LB h = 5000 FT
V_I = 180 KT c.g. = 25 %
δ_F = 10 GEAR UP

LONGITUDINAL DYNAMICS

NASA

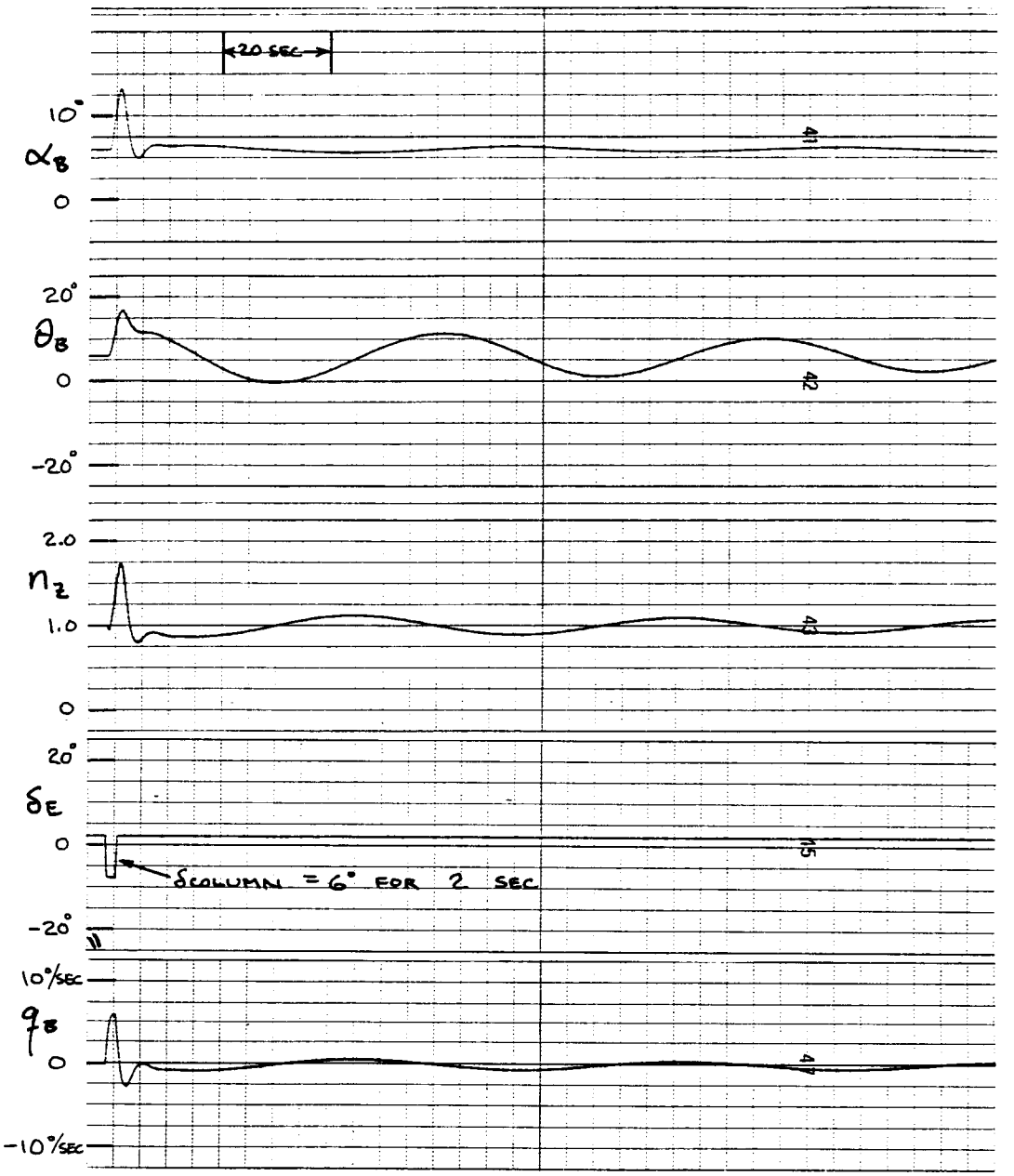

GW = 710 000 LB h = 5000 FT
V_I = 210 KT C.g. = 25%
δ_F = 10 GEAR UP

LONGITUDINAL DYNAMICS

NASA

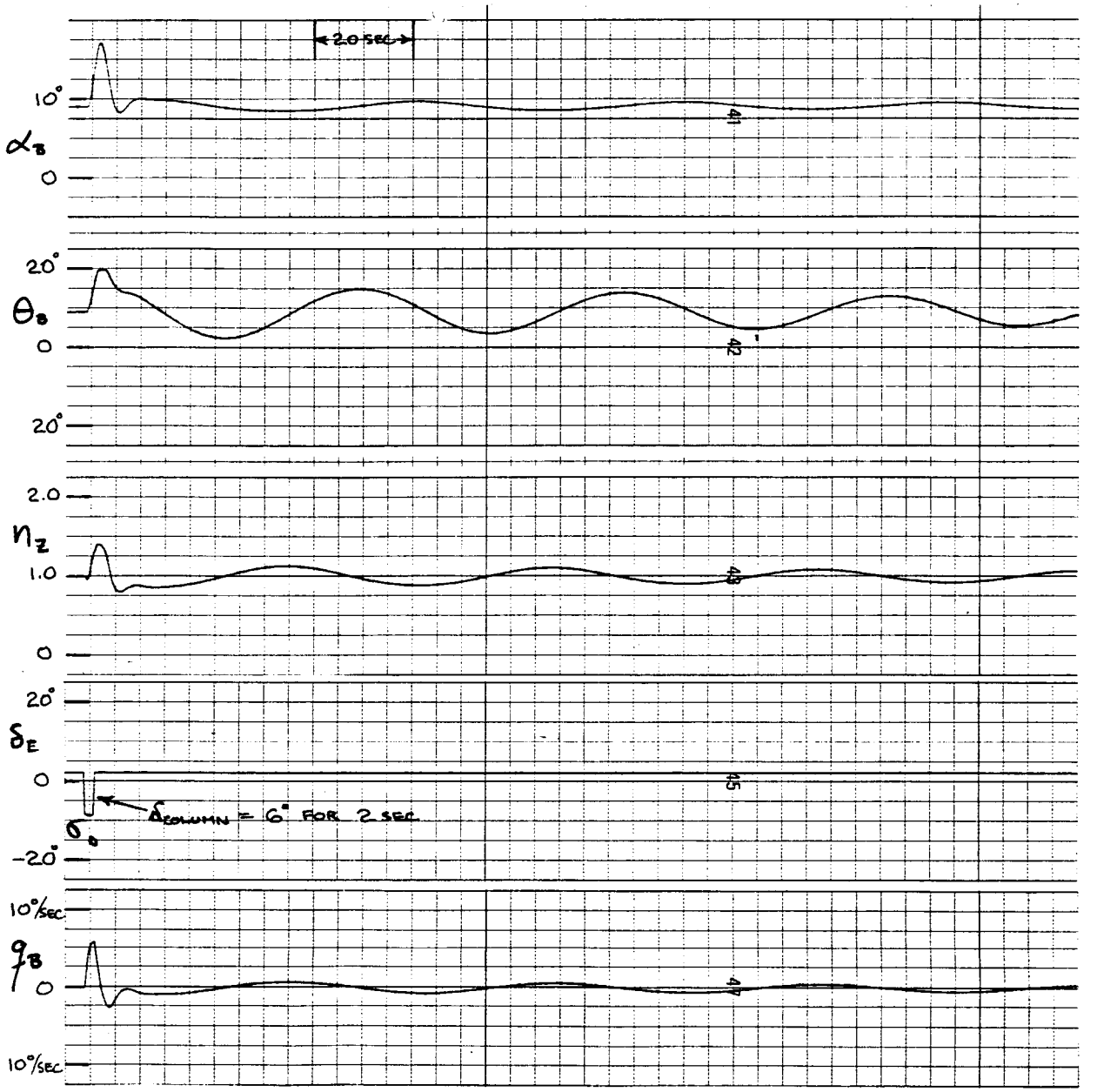

GW = 710 000 LB h = 5000 FT
V_I = 180 KT c.g. = 25%
δ_F = 10 GEAR UP

LONGITUDINAL DYNAMICS

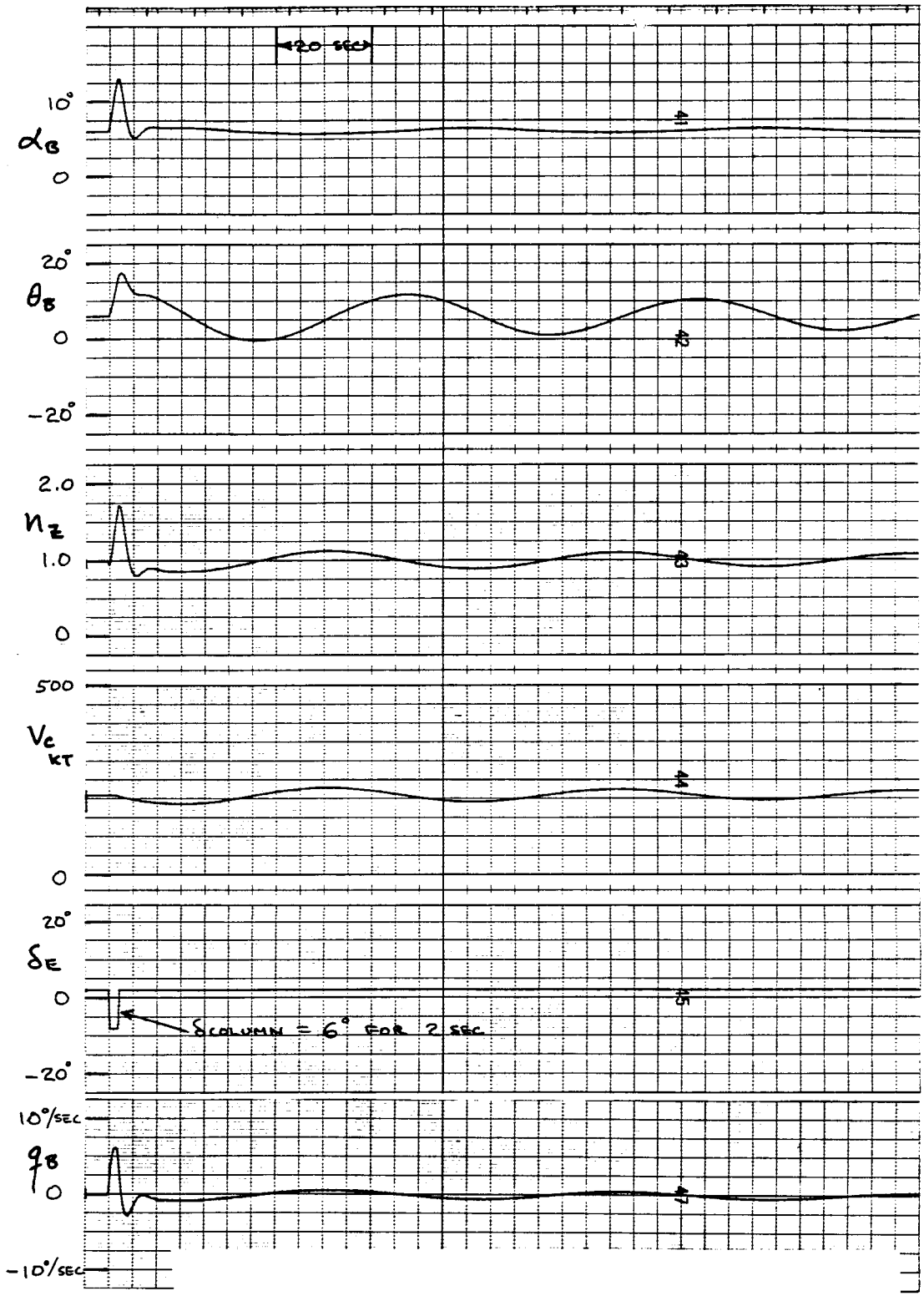

GW = 710 000 LB h = 5000 FT
V_I = 210 KT c.g. = 25 %
δ_F = 10 GEAR UP

LONGITUDINAL DYNAMICS

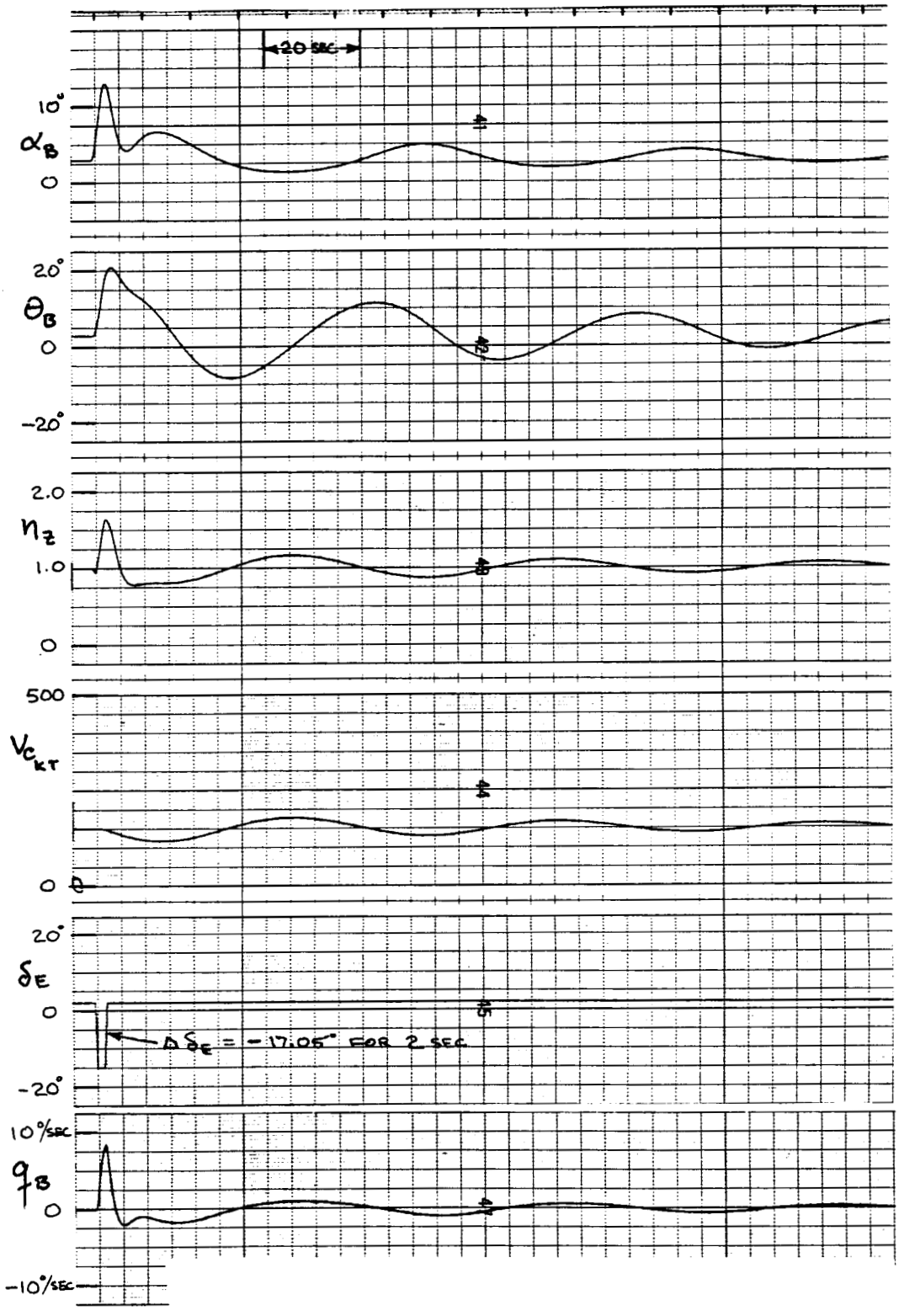

GW = 564000 LB h = 5000 FT
V_I = 153 KT C.g. = 33%
δ_F = 30 GEAR DOWN

LONGITUDINAL DYNAMICS

NASA

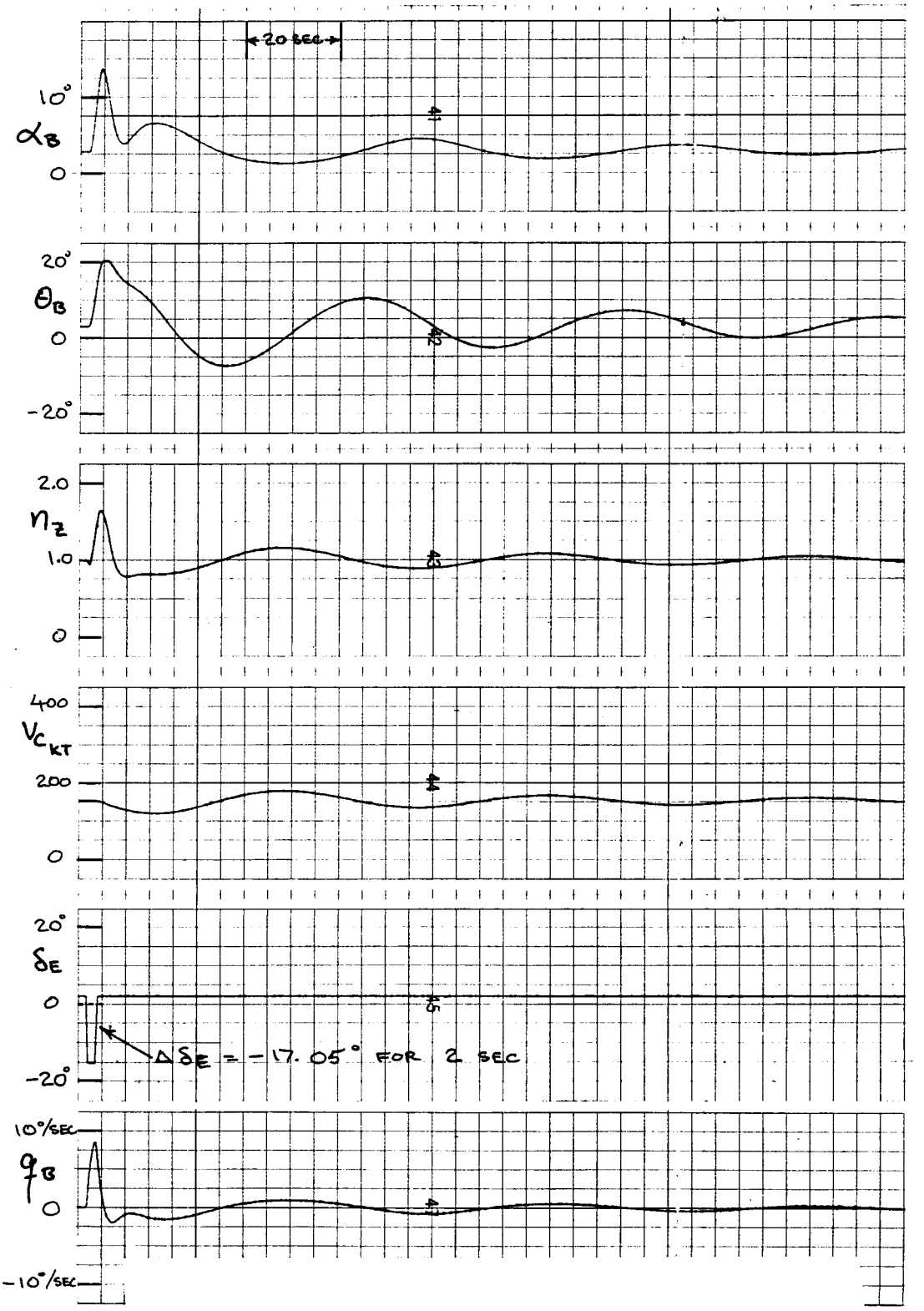

GW = 564 000 LB h = 5000 FT
V_I = 153 KT C.G = 33%
δ_F = 30 GEAR DOWN

LONGITUDINAL DYNAMICS

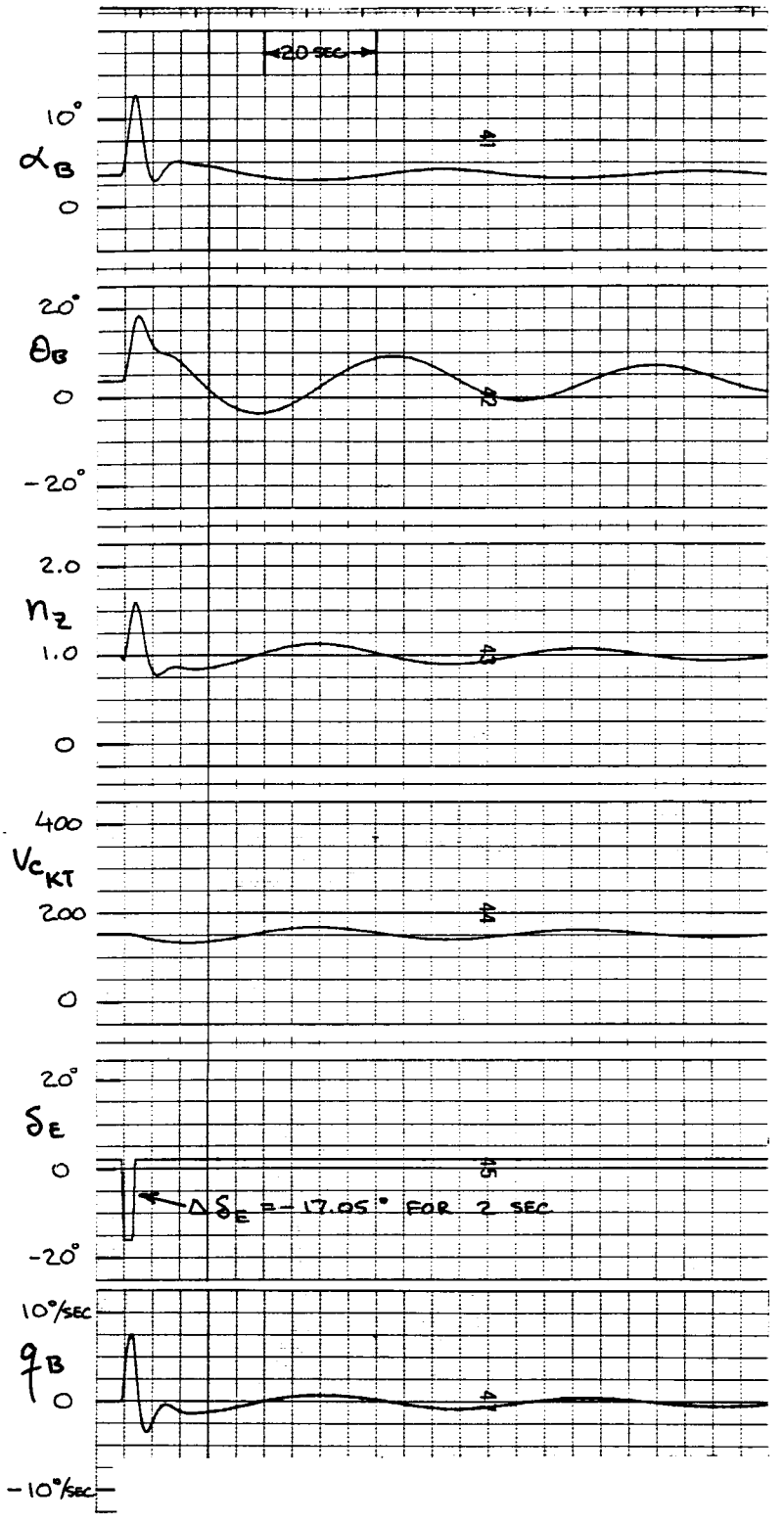

GW = 564 000 LB h = 5000 FT
V_I = 153 KT C.g. = 15 %
δ_F = 30 GEAR DOWN

LONGITUDINAL DYNAMICS

NASA

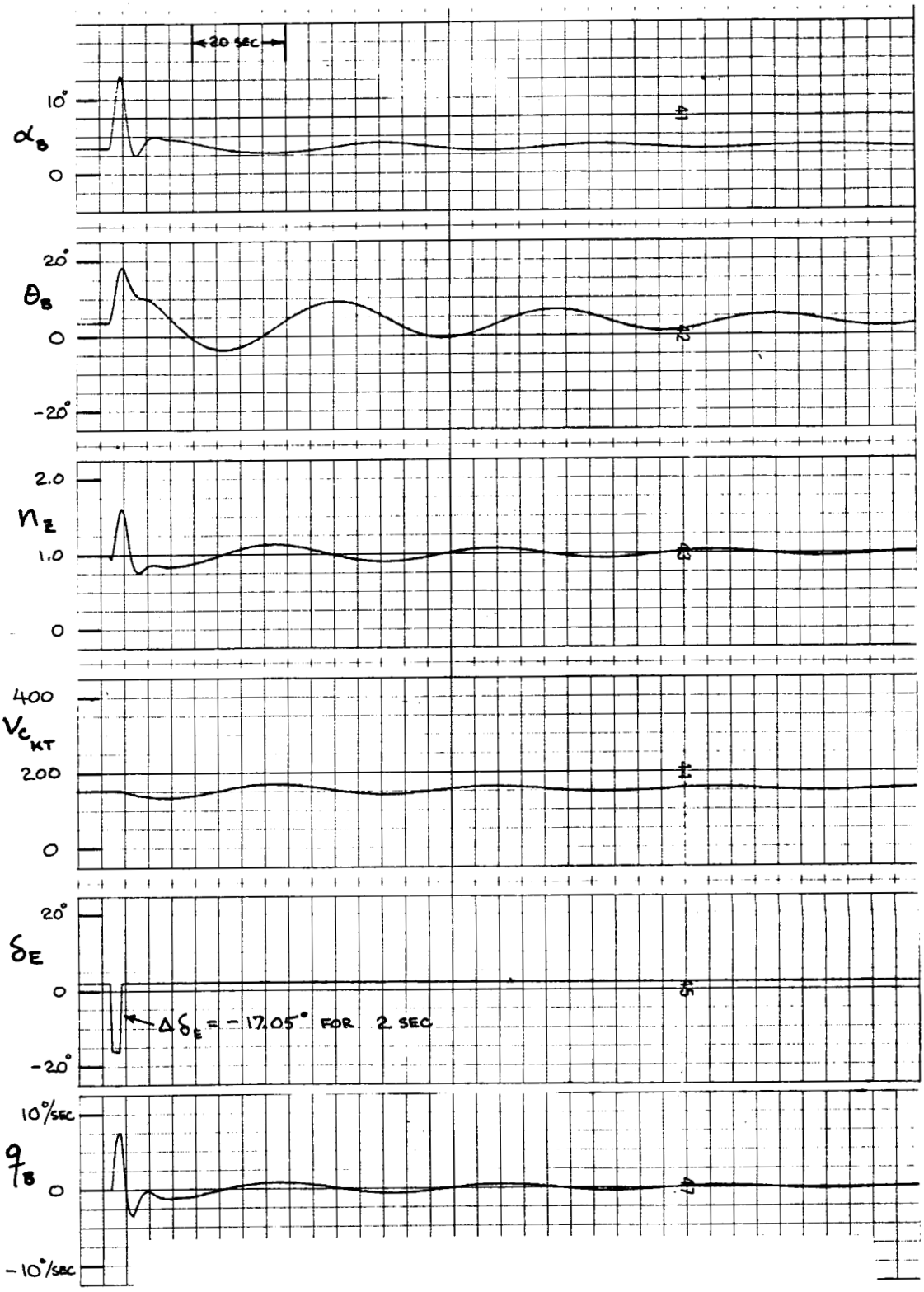

G.W = 564 000 LB h = 5000 FT
V_I = 153 KT c.g. = 15%
δ_F = 30 GEAR DOWN

LONGITUDINAL DYNAMICS

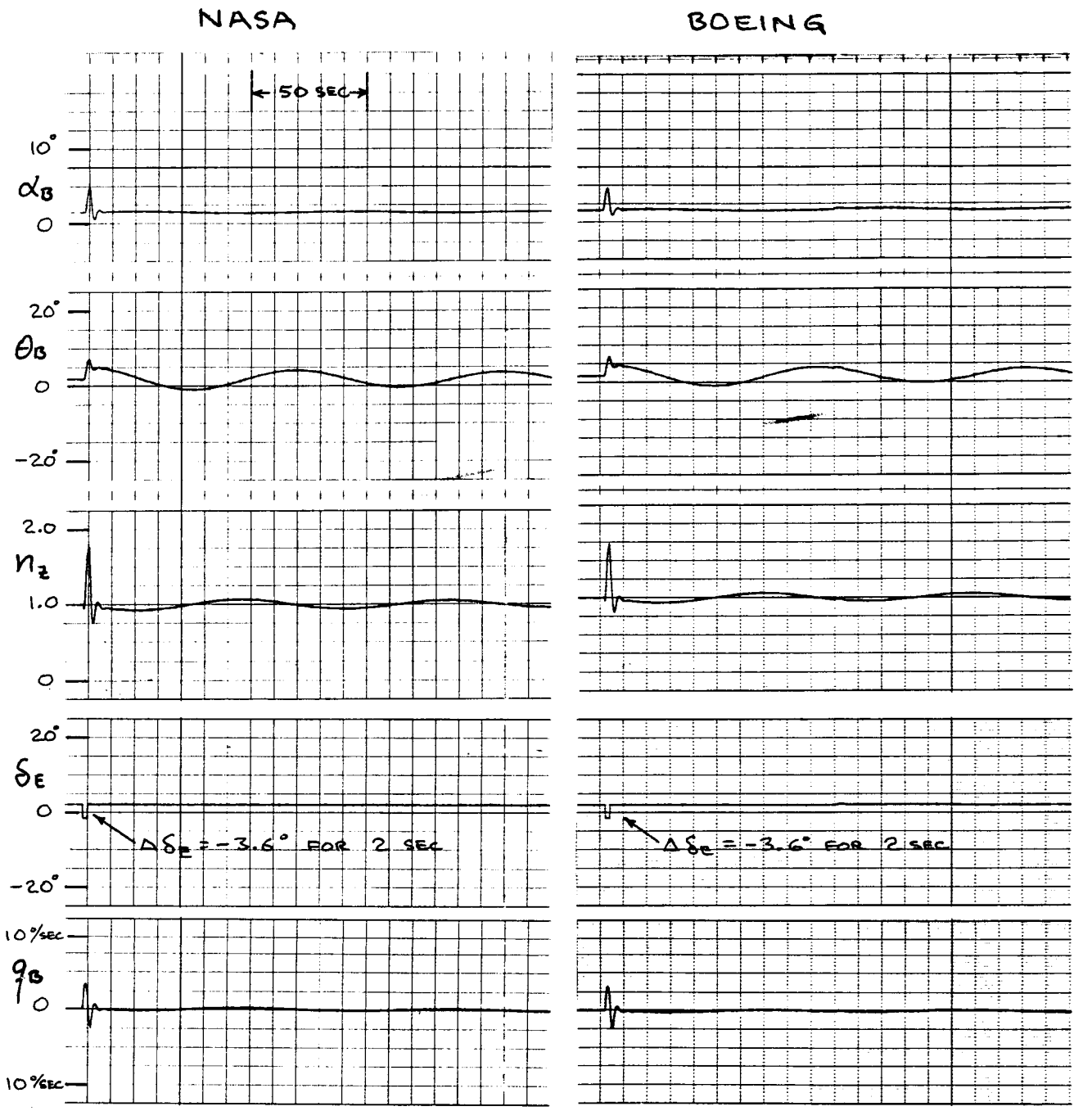

GW = 564000 LB h = 20000 FT
M = .65 c.g. = 14%

LONGITUDINAL DYNAMICS

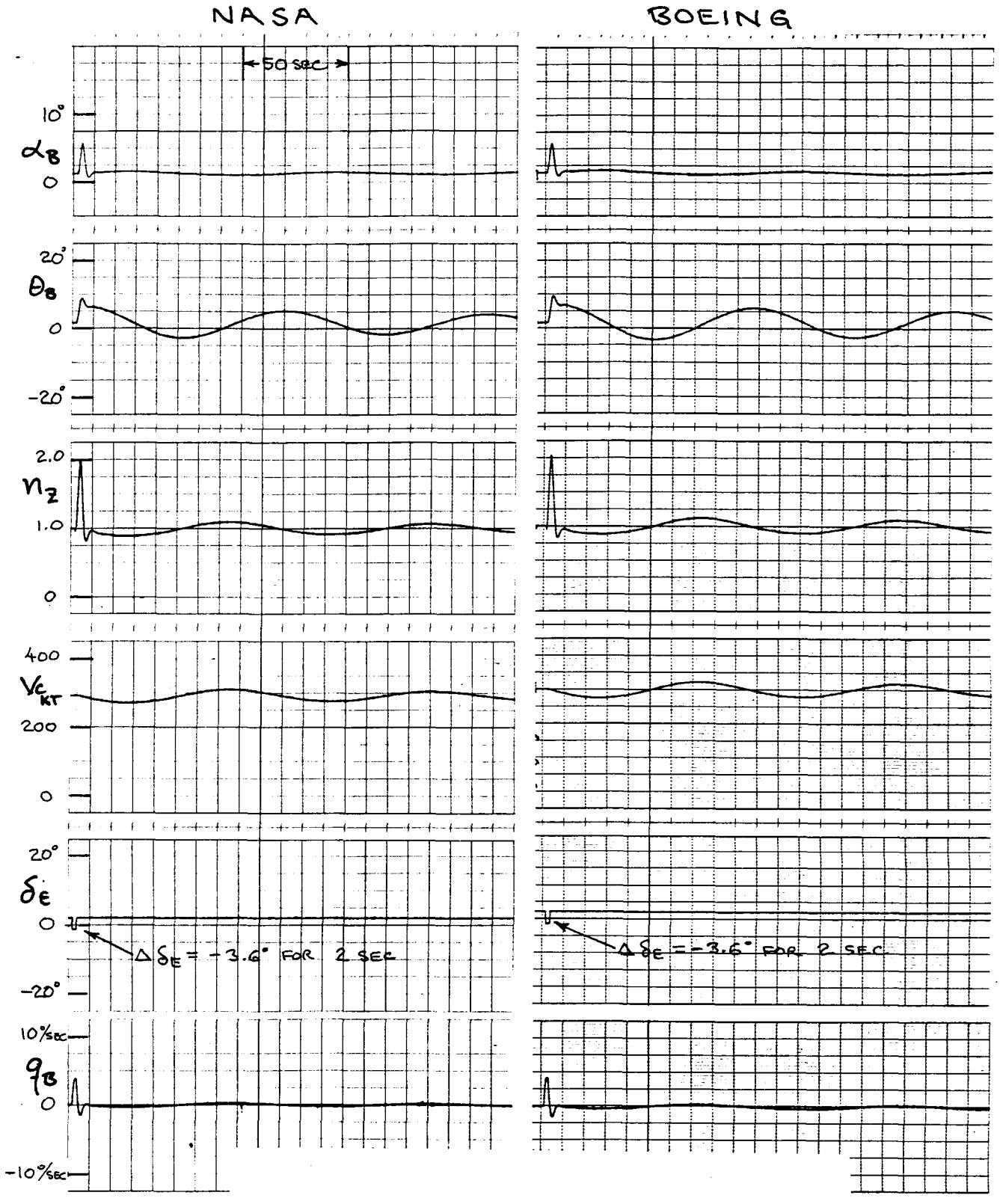

GW = 564 000 LB h = 20000 FT
M = .65 c.g. = 32%

LONGITUDINAL DYNAMICS

NASA

BOEING

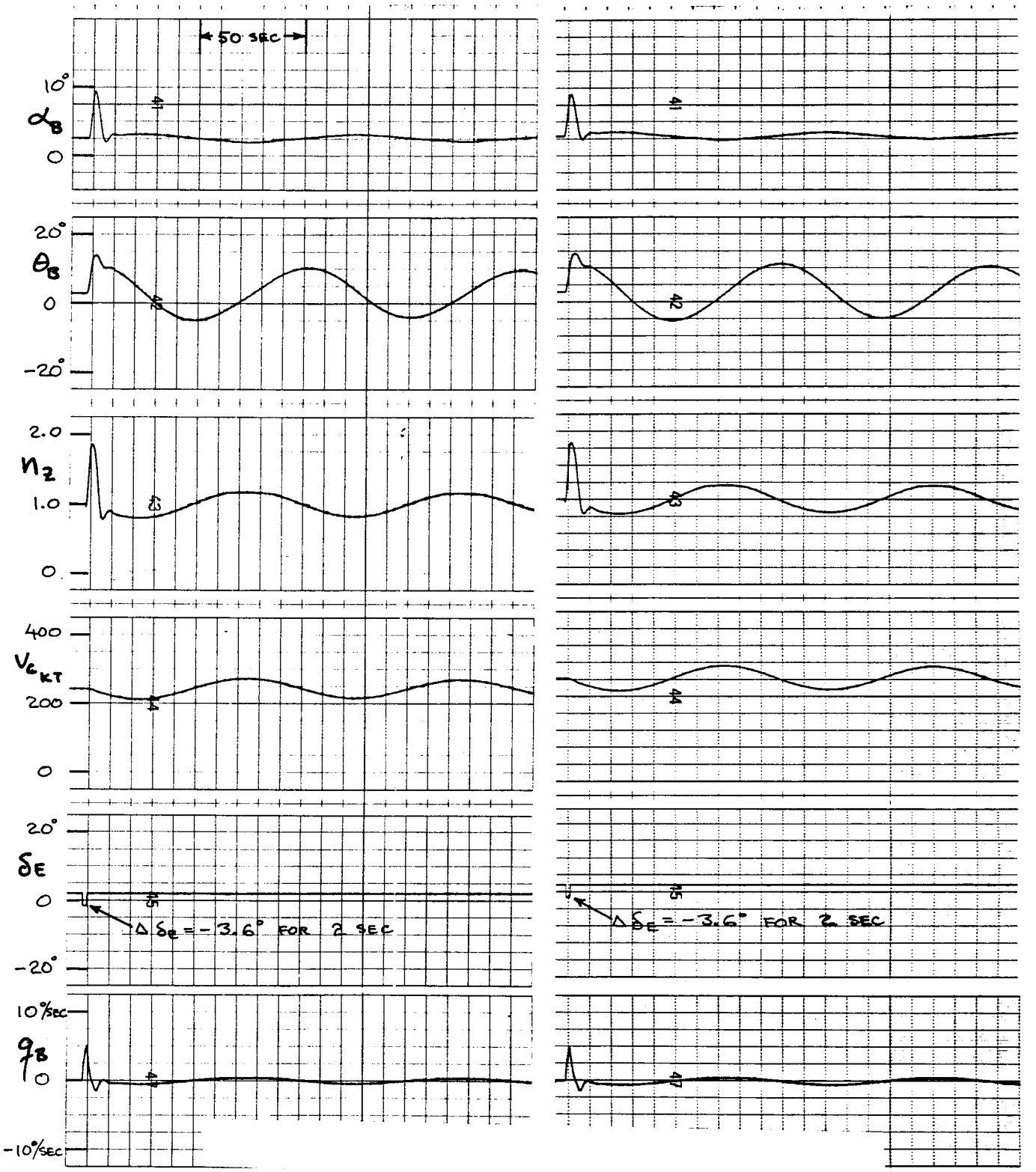

GW = 564000 LB h = 35000 FT
M = .75 c.g. = 32%

LONGITUDINAL DYNAMICS

NASA

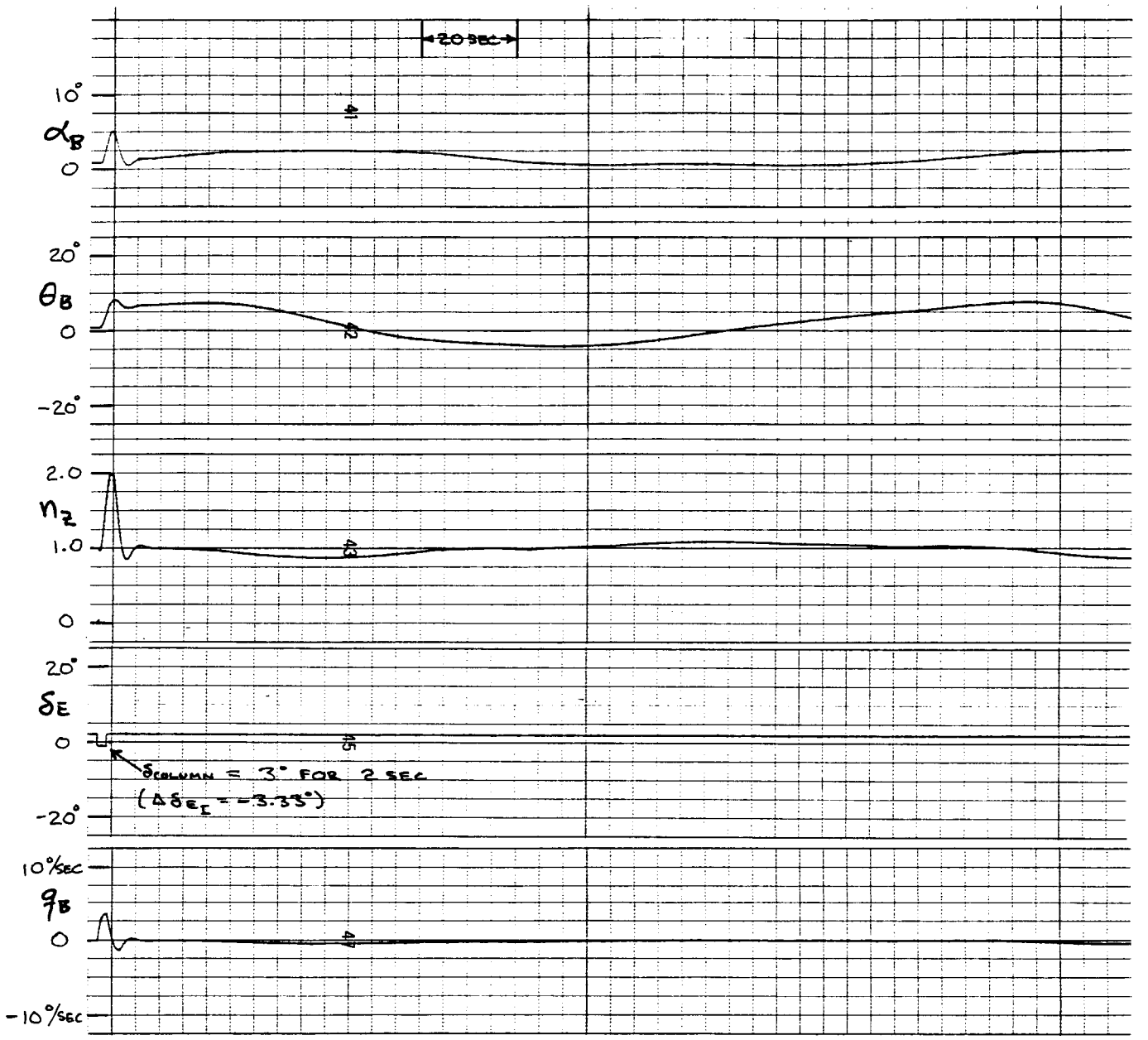

GW = 564000 LB h = 35000 FT
M = .87 C.g. = 32%

LONGITUDINAL DYNAMICS

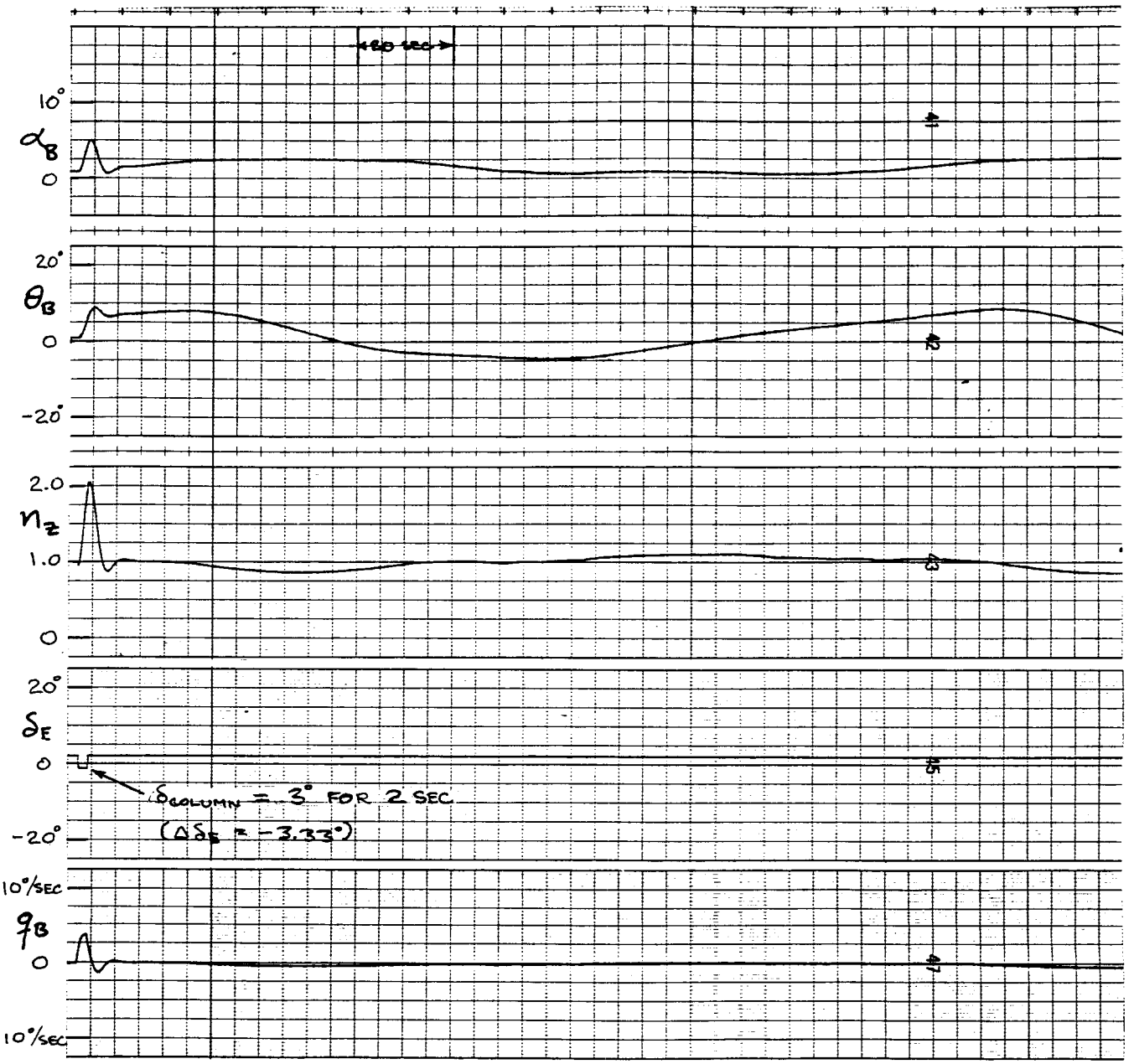

GW = 564000 LB h = 35000 FT
M = .87 C.g. = 32%

LONGITUDINAL DYNAMICS

14.1.7 FLIGHT CONTROLS

14.1.7.1 Force and Displacement

The force and displacement curves for the wheel and rudder are shown on Pages 14.1-52 and 14.1-53. These curves were obtained from the control loader in the FSAA cab. The wheel force in the cab should be compared to the force characteristics on Page 9.1-3. The rudder force in the cab should be compared to the force characteristics on Page 10.1-3. Wheel and rudder forces were not calculated in the computer.

The column force was calculated in the computer and a modified force increment was input to the control loader to augment the constant stick force gradient initially set in the column control loader. Tests were made to verify the computed and cab column force.

A condition was set up in the computer to check the δ_{col} to δ_e relationship and the resulting forces for two c.g. positions. The tabulated comparisons between Boeing and NASA simulations are on Pages 14.1-54, 55. The data is plotted on Page 14.1-56. Column force and displacement data in the FSAA cab was also obtained for this condition. The control column was deflected to a position and the computed values of stick force, δ_e, and δ_{col} were obtained. Column stick force and δ_{col} were also obtained from the column control loader through a calibrated x-y plotter. The results are tabulated on Page 14.1-55 and plotted on Page 14.1-57.

Similar computed stick force data was obtained from the elevator stabilizer trade condition. The results are tabulated on Page 14.1-54 and plotted on Page 14.1-58.

Maneuvering column force data was obtained during the piloted checkout.

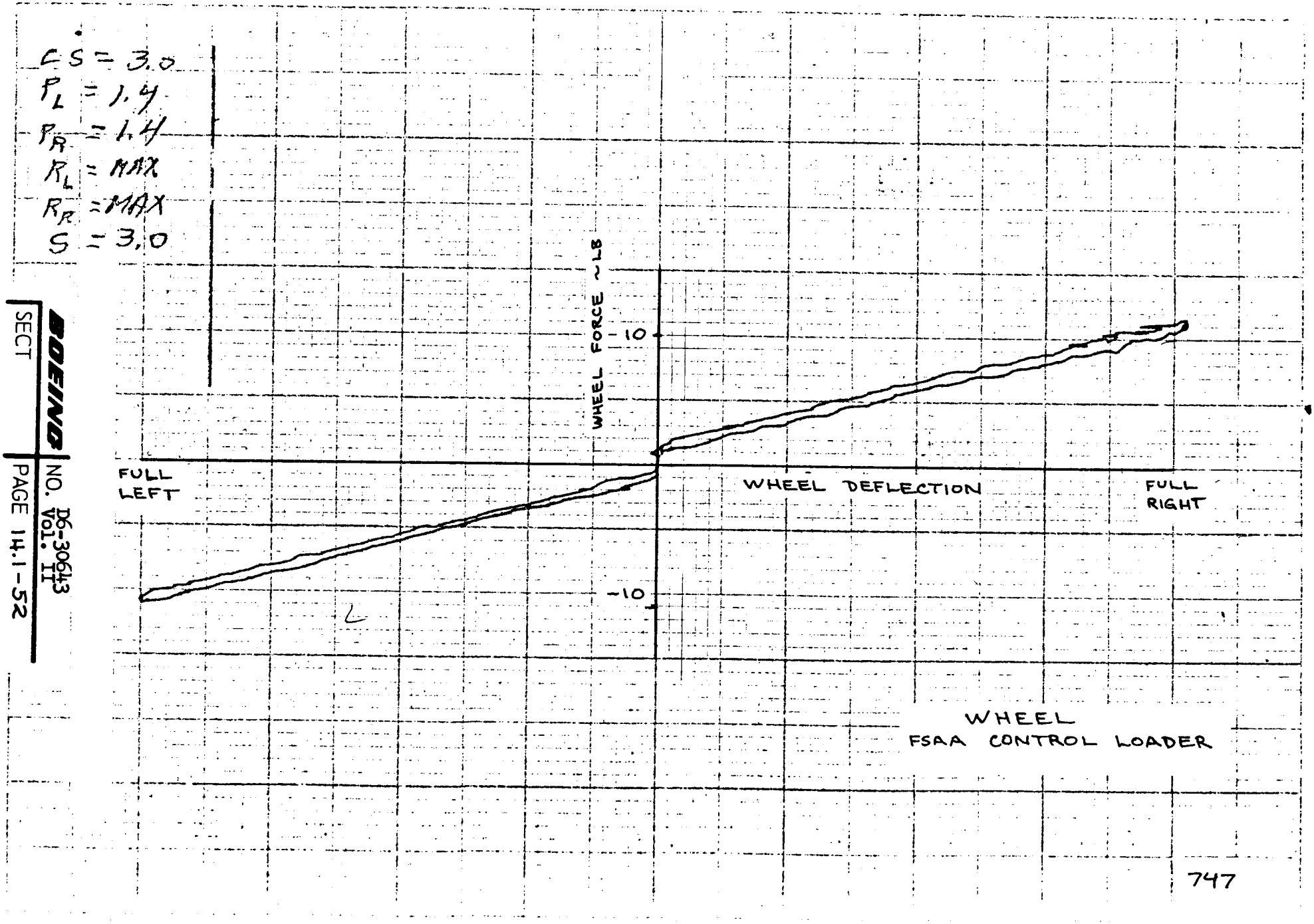
CS = 3.0
P_L = 1.4
P_R = 1.4
R_L = MAX
R_R = MAX
S = 3.0
WHEEL FORCE ~ LB
10
-10
FULL LEFT
WHEEL DEFLECTION
FULL RIGHT
L
WHEEL
FSAA CONTROL LOADER
747

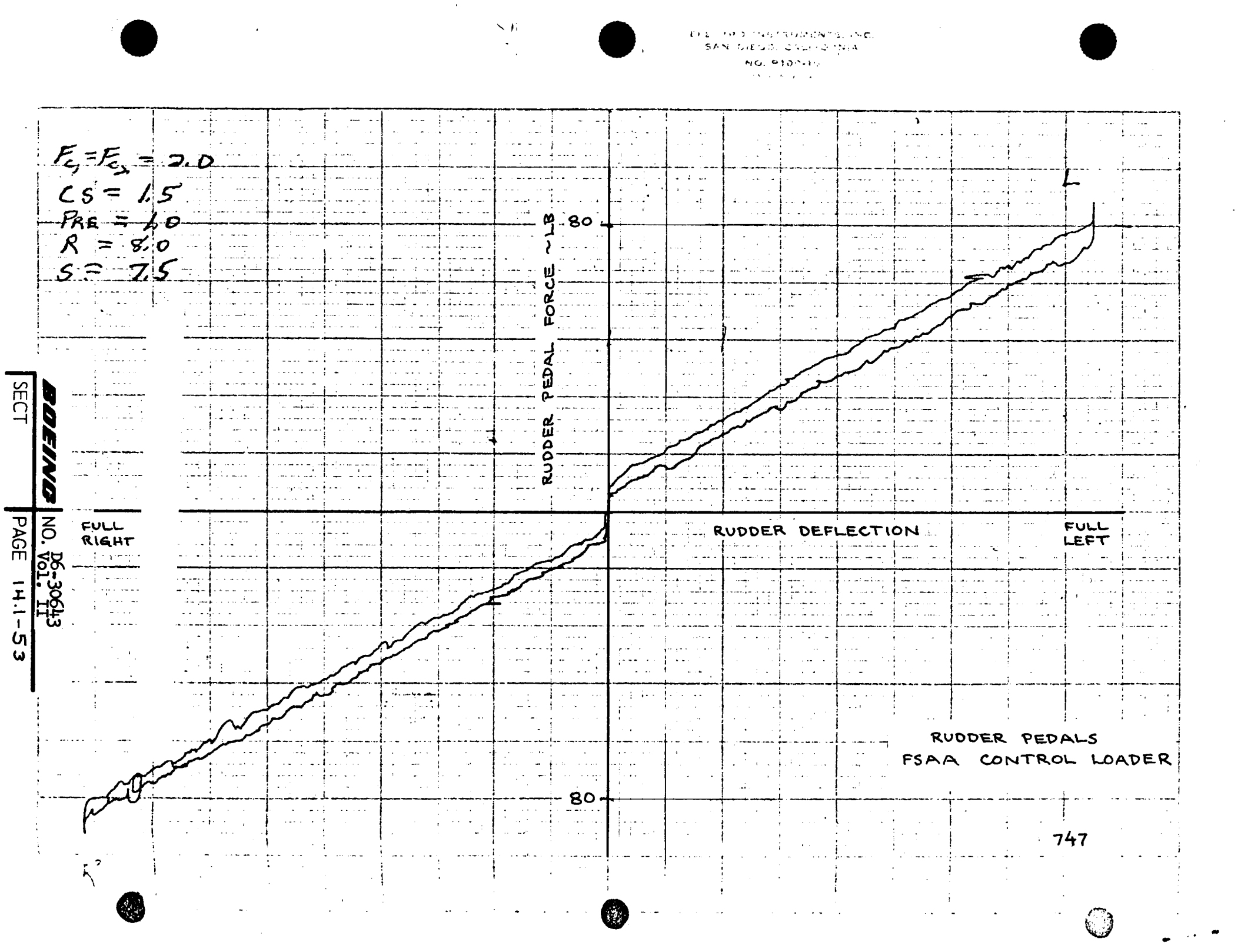
$F_{c_1} = F_{c_2} = 2.0$
CS = 1.5
PRE = 4.0
R = 8.0
S = 7.5
L
80
RUDDER PEDAL FORCE ~LB
FULL RIGHT
RUDDER DEFLECTION
FULL LEFT
80
RUDDER PEDALS
FSAA CONTROL LOADER
747

LONGITUDINAL CONTROL FORCES

		COND. NO.	FLAP POSITION	GEAR	G.W. ~ 1000 LB.	C.G. ~ % MAC	ALTITUDE ~ 1000 FT.	M	δ_P ~ UNITS		F_S ~ LB.		δ_e ~ DEG.		δ_{COL} ~ DEG.		DIGITAL OUTPUT $\Delta\delta$ ~ DEG.
									BOEING	NASA	BOEING	NASA	BOEING	NASA	BOEING	NASA	
②	STAB.-ELEV. TRADES	6.1.1a	UP	UP	628	11.7	33	.75	5.4	5.35	0	0 ①	2.0	2	0	0	0
		.1b							4.4	4.30	24	25.3	- .1	-.18	1.7	1.7	-1.05
		.1c							3.4	3.36	64	63.3	-2.3	-2.22	3.7	3.7	-2.0
		.1d							7.4	7.24	-19	-19.03	6.2	6.1	-2.6	-2.6	+1.9
		.1e							9.4	9.32	-14	-15.3	10.8	10.95	-5.0	-5.0	+4.0
③	COLUMN FORCES	6.1.2a	UP	UP	600	11.0	35	.8	5.1	5.05	0	0	2.	2.	0	0	
		.2b									36	36	- 3.	-2.83	3.2	3.2	
		.2c									70	72.1	-18.	-18.26	10.3	10.3	
		.2d									-33	-34.7	7.	7.	-3.6	-3.6	
		.2e									-38	-38.2	12.	11.9	-6.4	-6.4	
		6.1.3a				32.0			3.2	3.12	0	0	2.	2	0	0	
		.3b									80	82.4	- 3.	-3.12	4.5	4.5	
		.3c									101	101.3	- 8.	-7.96	6.9	6.9	
		.3d									-70	-73.6	7.	7.07	-5.0	-5.0	
		.3e									-77	-78.2	12.	12.34	-8.2	-8.2	
COMPUTATION TOLERANCE											± 10%		± .5°		± 1°		

① COMPUTED VALUES - INCLUDES 2.5 LB BREAKOUT FORCE IN PULL DIRECTION AND 3.0 LB IN PUSH DIRECTION.

② GRAPHICAL RESULTS ON PAGE 14.1-58

③ GRAPHICAL RESULTS ON PAGE 14.1-56

600,000 LB M = 0.8 h = 35,000 FT

c.g. = 11% Δ_{FRL} = −2.1 DEG

INPUT $\delta_{COLUMN\ FSAA}$ ② ③ ~DEG	δ_{COLUMN} COMPUTED ~DEG	δ_{E_I} COMPUTED ~DEG	δ_{E_O} COMPUTED ~DEG	FSAA STICK FORCE ~LB ②	COMPUTED STICK FORCE ~LB ①
3.75	3.77	−3.96	−3.96	40	40.7
12.5	12.73	−23.0	−5.87	81	86.3
−4.4	−4.38	8.41	8.41	−38	−35.15
−12.3	−12.3	17.0	9.33	−37	−37.05

c.g. = 32% Δ_{FRL} = −.2 DEG

4.4	4.43	−3.0	−3.0	79	80.0
8.3	8.37	−11.1	−5.87	108	114.1
−4.94	−4.93	6.95	6.95	−69	−71.2
−12.5	−12.52	17.0	9.33	−75	−77.3
−12.1	−12.1	17.0	9.33	−76	−78.0

① INCLUDES 2.5 LB BREAKOUT FORCE IN PULL DIRECTION AND 3.0 LB IN PUSH DIRECTION

② $\delta_{COLUMN\ FSAA}$ & FSAA STICK FORCE OBTAINED FROM X-Y PLOTTER OUTPUT OF CONTROL LOADER.

③ ASSUME 7 IN. OF FSAA COLUMN DEFLECTION = 12.67 DEG. OF 747 COLUMN DEFLECTION.

GRAPHICAL RESULTS ON PAGE 14.1-56

747

CALC	DRN	JUNE 1970	REVISED	DATE
CHECK				
APPD				
APPD				

COMPARISON BETWEEN COMPUTED AND FSAA STICK FORCE

REV LTR:

F 1196 R6

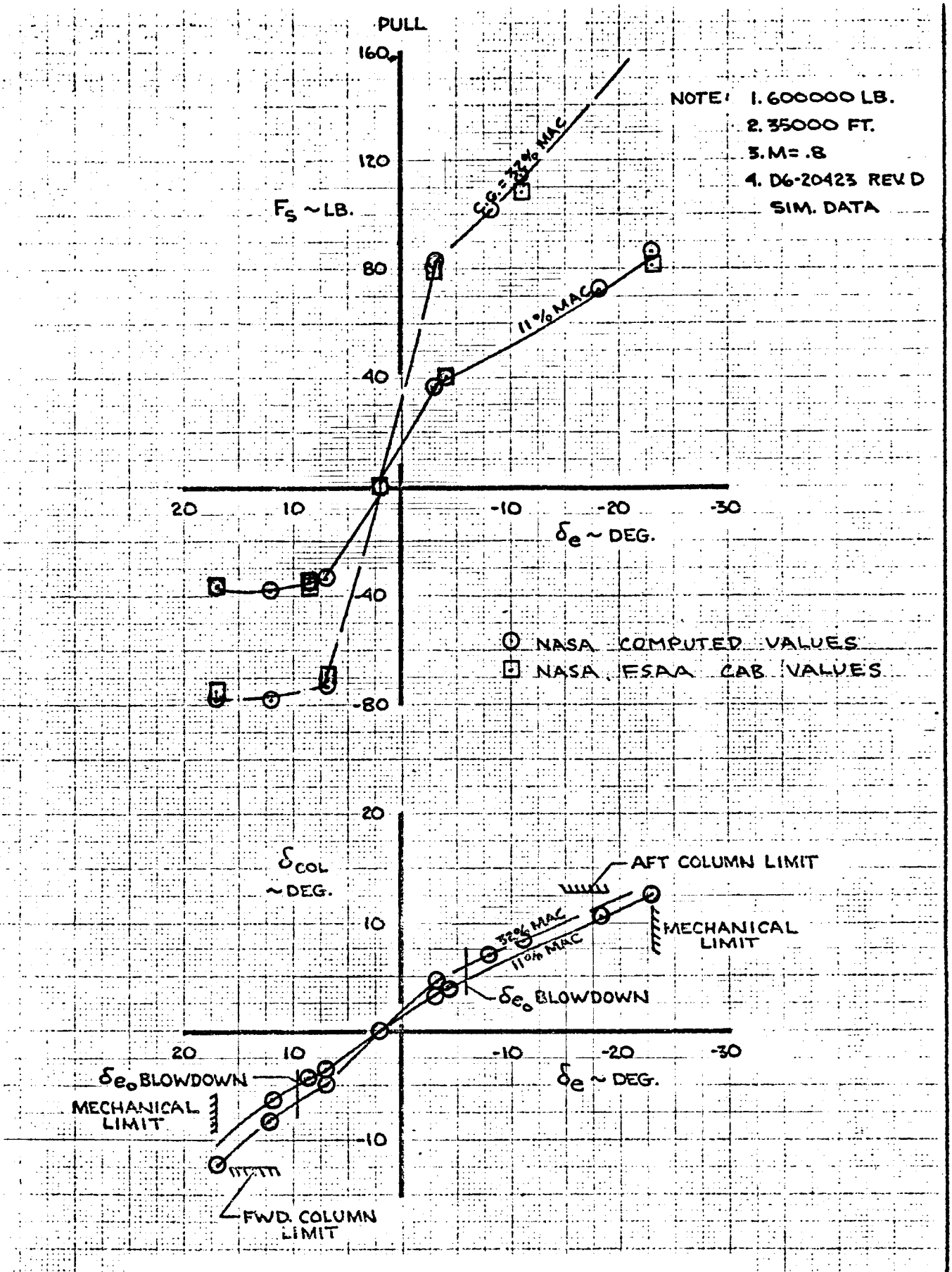

CALC	CURNUTT	5-26-70	REVISED	DATE
CHECK				
APR				
APR				
	GLENN	5-27-70		

COLUMN FORCES
LONGITUDINAL AXES FROZEN
35000 FT. ~ M=.80 ~ 600000 LB.

747

D6-30643 Vol. II

THE BOEING COMPANY

PAGE 14.1 56

AD 461 C-R4

ALBANENE 1686

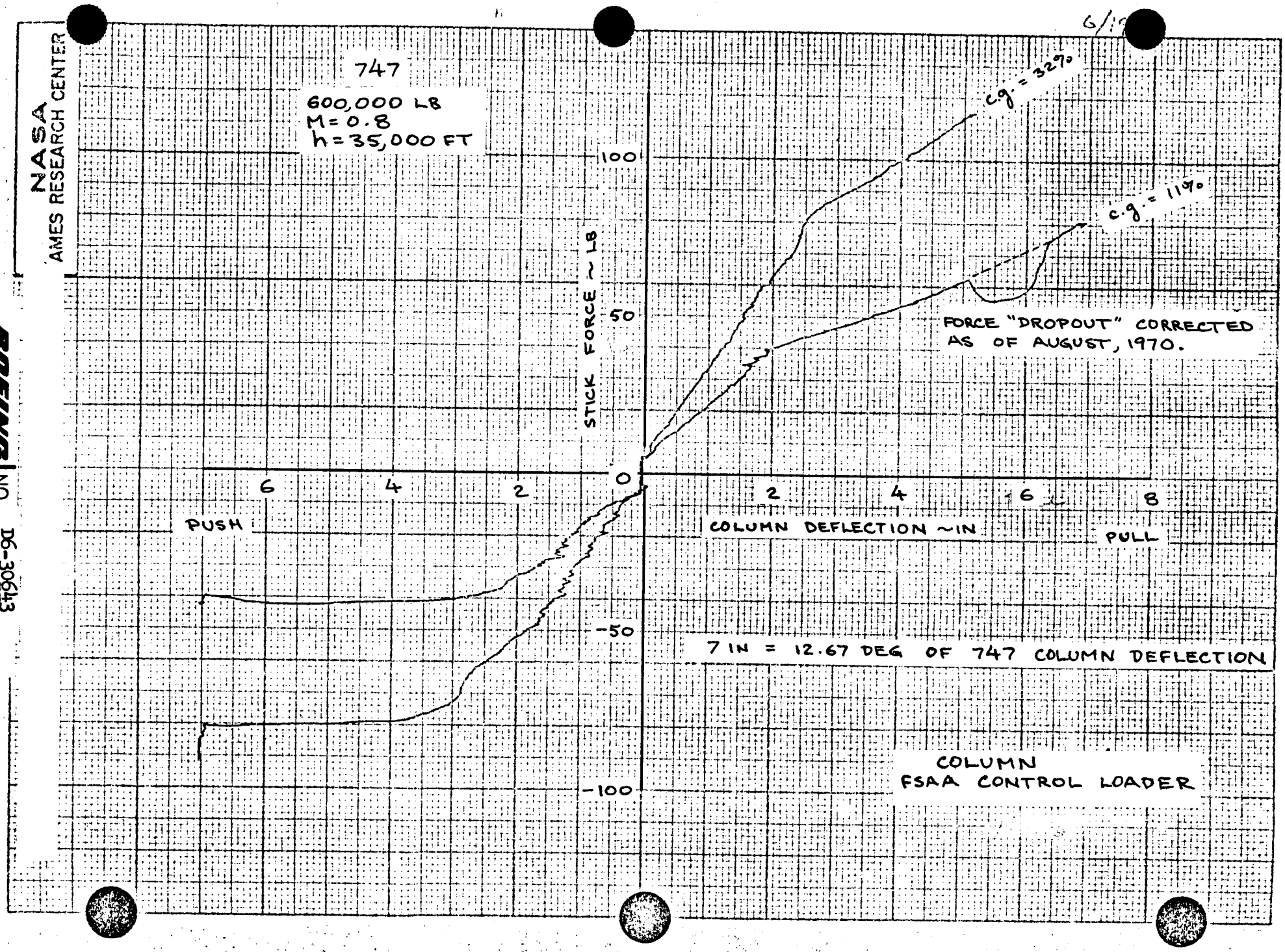
NASA
AMES RESEARCH CENTER
747
600,000 LB
M=0.8
h=35,000 FT
c.g. = 32%
c.g. = 11%
FORCE "DROPOUT" CORRECTED
AS OF AUGUST, 1970.
STICK FORCE ~ LB
100
50
0
-50
-100
6
4
2
0
2
4
6
8
PUSH
COLUMN DEFLECTION ~IN
PULL
7 IN = 12.67 DEG OF 747 COLUMN DEFLECTION
COLUMN
FSAA CONTROL LOADER

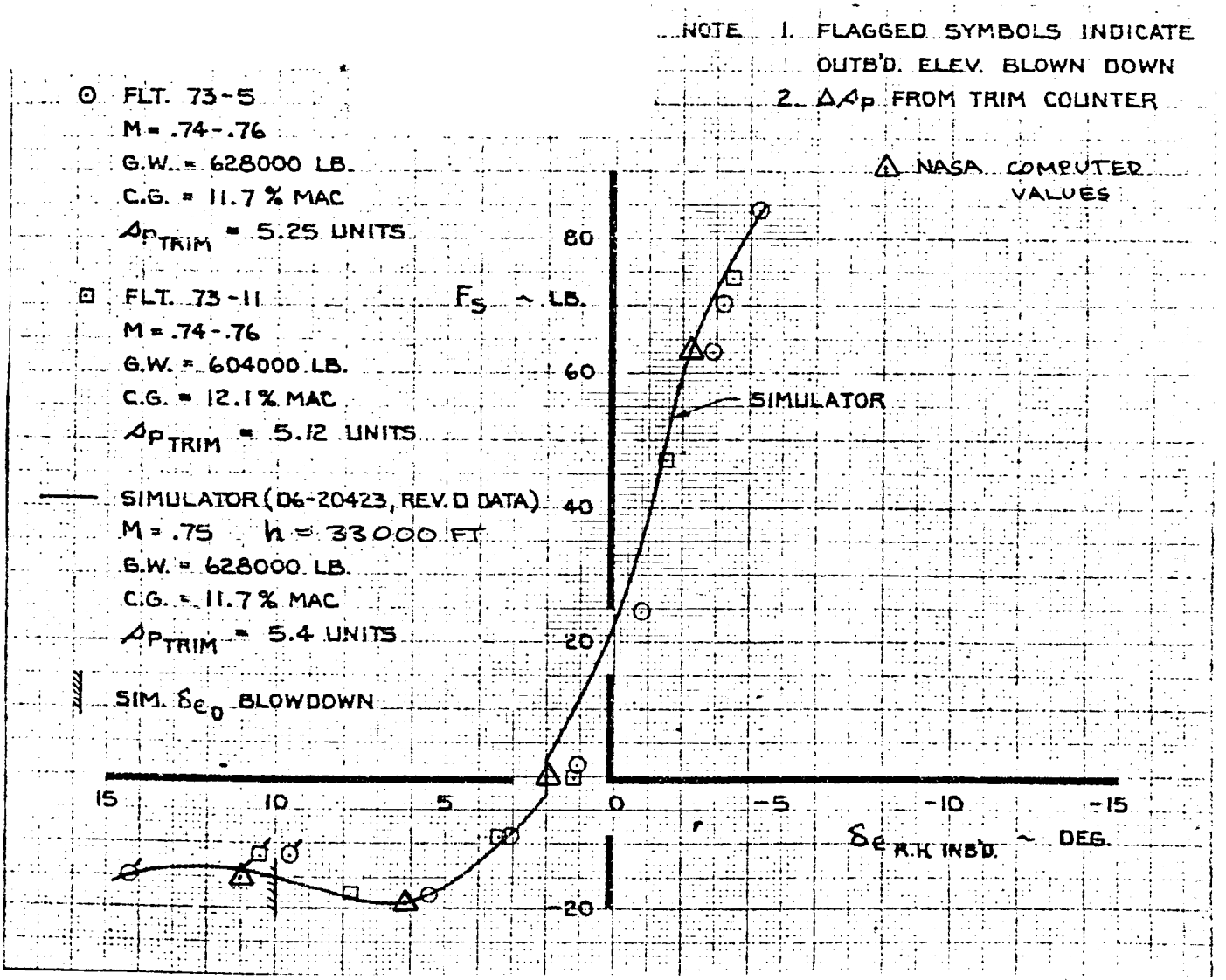

ELEVATOR STABILIZER TRADES

COLUMN FORCES
SIMULATOR - FLIGHT TEST COMPARISON

14.1.7.2 RIGGING

The lateral control rigging was checked at high speed. The table on Page 14.1-60 shows a comparison of Boeing and NASA simulation results for various combinations of wheel and speed brake inputs.

REV SYM

LATERAL CONTROL RIGGING

V_I = 350 KTS.
ALT. = 5000 FT.
G.W. = 400000 LB.

	δ_{WHEEL} ~DEG.	SPEED BRAKE HANDLE	δ_{AI} L.H. ~ DEG.		δ_{AI} R.H. ~ DEG.		δ_{AO} F/L ~ DEG.		δ_{SP} 1/12 ~ DEG.		δ_{SP} 2,3,4 9,10,11 ~ DEG.		δ_{SP} 5/8 ~ DEG.		δ_{SP} 6,7 ~ DEG.	
			BOEING	NASA	BOEING	NASA	BOEING	NASA	BOEING	NASA	BOEING	NASA	BOEING	NASA	BOEING	NASA
	-10	ZERO	- 5.0	5.0	- 5.0	5.0	0	0	0	0	0	0	0	0	0	0
	-30	|	-13.7	13.63	-13.7	13.63	|	0	10.4	10.4/0	10.4	10.4/0	10.4	10.4/0	0	0
	-50	|	-20.0	20.	-20.0	20.	|	0	25.6	25.6/0	25.6	25.6/0	20.0	20./0	0	0
	-75	|	-20.0	20.	-20.0	20.	|	0	44.1	43.9/0	32.9	32.8/0	20.0	20./0	0	0
	10	|	5.0	5.0	5.0	5.0	|	0	0	0	0	0	0	0	0	0
	50	|	20.0	20.	20.0	20.	|	0	25.7	0/25.6	25.7	0/25.6	20.0	0/20.	0	0
	80	INFLIGHT DETENT	20.0	20.	20.0	20.	|	0	44.1	0/43.9	32.9	0/32.8	20.0	0/20.	18.9	18.9
	0	INFLIGHT DETENT	0	0	0	0	|	0	0/0	0/0	$\delta_{SP_{2,11}}=0$ / $\delta_{SP_{3,9,10}}=32.9$	0/32.8	20.0/20.0	20./20.	18.9	18.9
COMPUTATION TOLERANCE			± 1.0 DEG.						± 1.0 DEG.							

14.1.7.3 BLOWDOWN

The blowdown for elevator and spoiler and the ratio changer limit value for rudder was verified at different times throughout the simulation checkout. The elevator stabilizer trade test provided a data point for elevator blowdown and the lateral rigging check provided spoiler blowdown data.

A further check on blowdown was a comparison of initial accelerations with full control inputs. The tabulation on Page 14.1-62 is a comparison of initial accelerations and control surface positions between Boeing and NASA simulations.

FLIGHT CONDITION: $h = 20000$ FT $M = 0.800$ c.g. = 32%
GW = 564000 LB $\delta_F = 0$ GEAR UP
TRIM: $\alpha_B = 1.61$, $\delta_{FRL} = -.66$ Ve = 358.51KT

			DIGITAL OUTPUT			
			BOEING	NASA	BOEING	NASA
INPUT	WHEEL	DEG	80.06	80.00	-80.0	-80.0
	COLUMN	DEG	12.67	12.67	-12.5	-12.5
	RUDDER PEDAL	DEG	12.2	12.2	-12.2	-12.2
	β_{IC}	DEG	4.994	5.0	4.995	5.0
OUTPUT						
	C_L		.1221	.1268	.2489	.251
	C_D		.0221	.0226	.0237	.0224
	C_ℓ		.0032	.0033	-.0291	-.0292
	C_m		.2700	.2735	-.1767	-.1760
	C_n		.0127	.0126	.0176	.0175
	C_Y		-.0822	-.0828	-.0579	-.0579
	a_y	FT/SEC^2	-11.242	-11.348	-7.921	-7.943
	n_z		.522	.549	1.060	1.083
	$\dot{p}_B$	DEG/SEC^2	6.735	6.823	-53.95	-54.09
	$\dot{q}_B$	DEG/SEC^2	32.105	32.557	-19.80	-19.76
	$\dot{r}_B$	DEG/SEC^2	7.632	7.603	9.512	9.470
	INBOARD ELEVATOR	DEG	-16.97	-17.05	16.99	17.00
	OUTBOARD ELEVATOR	DEG	-2.04	-2.06	6.03	6.02
	STICK FORCE	LB	181.19	181.30	-87.81	-89.14
	INBOARD AILERON	DEG	20.0	20.0	20.0	20.0
	RUDDER	DEG	2.86	2.85	-2.86	-2.85
	SPOILER PANEL 1/12	DEG	0/41.84	0/41.8	41.84/0	41.71/0
	2/11	DEG	0/28.29	0/28.27	28.30/0	28.22/0
	3/10	DEG	0/28.29	0/28.27	28.30/0	28.22/0
	4/9	DEG	0/28.29	0/28.27	28.30/0	28.24/0
	5/8	DEG	0/20.0	0/20.0	20.0/0	20.0/0

CALC	6/19/70	DRN	REVISED	DATE
CHECK				
APPD				
APPD				

COMPARISON OF INITIAL VALUES (t=0) FOR VARIOUS CONTROL INPUTS

REV LTR:

E 1196 R6

14.1.8 LANDING GEAR

The landing gear was static checked by allowing the airplane to settle on the ground and verifying the amount of strut compression. Dynamic responses were made by releasing the airplane from Δh and $\Delta\theta$ initial conditions.

In consideration of the computer limitations and the overall simulation, the landing gear simulation was run at a computational frame time of 39 milliseconds. The time histories on Page 14.1-64 shows the response to a Δh initial condition for two different computation times. The increase in computation speed, frame time to 13 ms, results in a smoother response than the "normal" frame time of 39 ms. Neglecting the limit cycle, the response with the 39 ms frame time appears to have the same frequency and slightly increased damping over the 13 ms response.

The time histories on Page 14.1-65 shows the response to a $\Delta\theta$ initial condition. The comments on the Δh response are applicable to the $\Delta\theta$ responses.

The effects of slowing the computation speed, or increasing the frame time, are shown in the responses on Page 14.1-66. The amplitude of the limit cycle increased as the computation speed decreased.

The aircraft response due to landing gear deflections felt realistic to the Boeing test pilot in the moving base simulation. Even though a limit cycle existed in the computed response with a 39 ms frame time the amplitude of the computed limit cycle was low and the frequency was high enough (3 cps) that no objectionable characteristics were noted by the pilot.

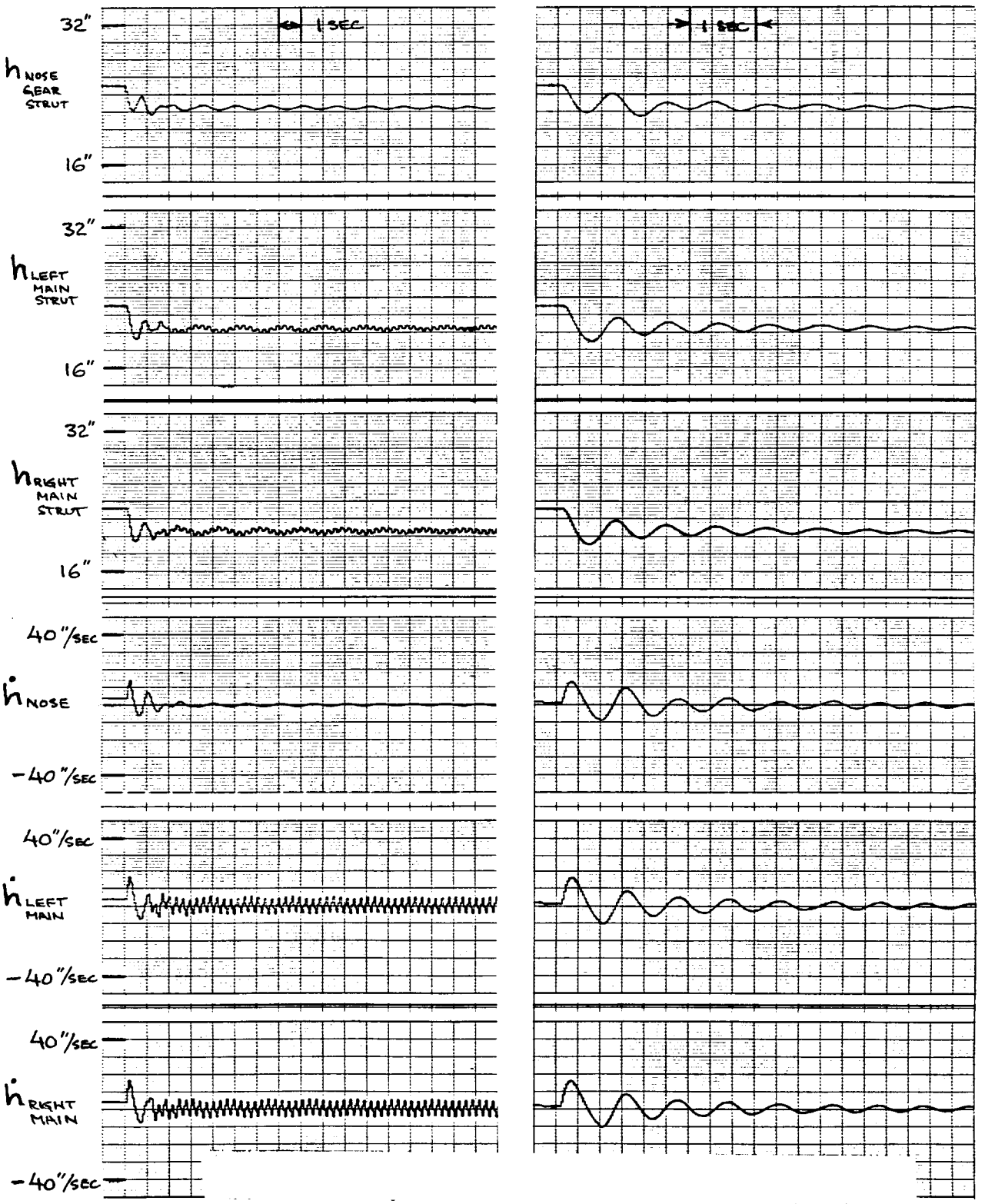

FRAME TIME = 39 MS (REAL TIME)

FRAME TIME = 13 MS (TIME SCALED)

Δh_{IC} = 2.5" COMPRESSION

GW = 436 000 LB C.g. = 25%

LANDING GEAR RESPONSE

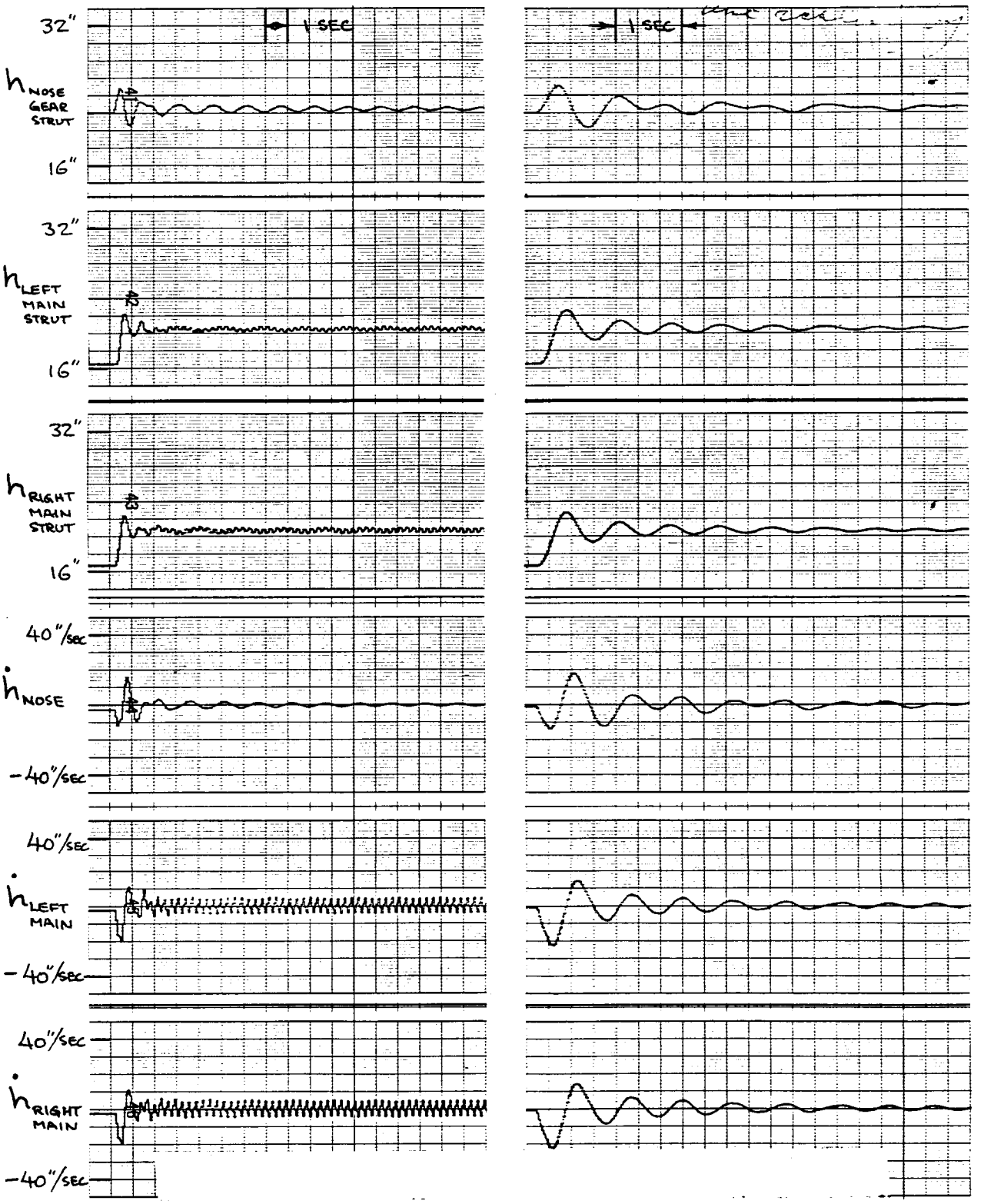

FRAME TIME = 39 MS (REALTIME)

FRAME TIME = 13 MS (TIME SCALED)

$\Delta\theta_{1c} = -.2°$

GW = 436000 LB C.G. = 25%

LANDING GEAR RESPONSE

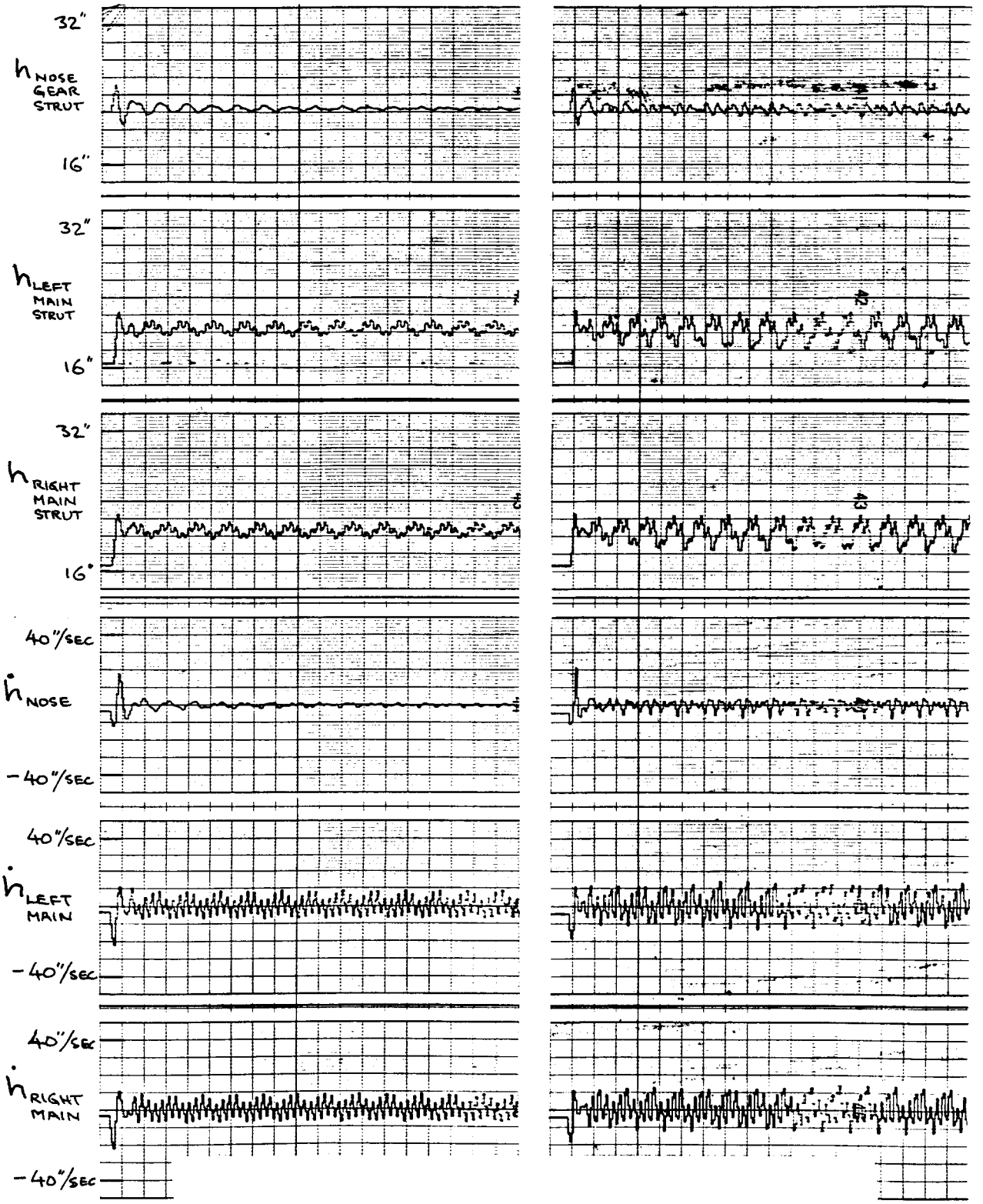

FRAME TIME = 50 MS (TIME SCALED)

FRAME TIME = 65 MS (TIME SCALED)

$\Delta\theta_{IC} = -.2°$

GW = 436000 LB c.g. = 25%

LANDING GEAR RESPONSE

14.2 PILOTED CHECKOUT

The piloted checkout provided an overall assessment of the simulation as well as quantitative data. Jack Waddell, Boeing 747 project pilot, flew the motion simulator for a total of 5 hours in 3 sessions. He qualitatively evaluated the following characteristics:

1. Airplane handling characteristics
    a. Dutch roll mode
    b. Spiral mode
    c. Short period mode
    d. Phugoid mode
    e. Roll rate
    f. Climb performance
    g. Flap extension and retraction
    h. Speed brakes
2. Engine response
3. Ground effect
4. Control forces
5. Takeoff (3 and 4 engine)
6. Landing
7. Stall
8. Air minimum control speed
9. Buffet
10. Stick shaker

The ground effect characteristics were modified during the approach and landing evaluation. The ground effect data on Pages 2.0-31, -32,

3.0-17, -18, and 4.0-35 were modified by the following factors:

.7 times the pitching moment increment

.3 times the drag increment

.9 times the lift increment

The above changes to the ground effect data were substantiated by additional piloted testing on the Boeing 747 simulation. The resulting Boeing revisions are included in Section 19.

The buffet and stick shaker amplitude and frequency characteristics were tailored to the satisfaction of the pilot. His overall comments substantiated the validity of the simulation.

Rapid roll inputs resulted in lateral acceleration which the pilot felt were greater than in the airplane. The pilots vertical location above the c.g. (10 feet) was reduced to an effective distance of 6 feet in the simulator drive equations. The pilot felt the resulting simulator motion comparable to the airplane. The lateral acceleration due to the pilot location above the c.g. is attributed to aircraft flexibility.

Quantitative data were obtained with NASA pilots. The following pages contain the results of the piloted tests.

14.2.1 TAKEOFF

Two takeoffs at different gross weights were performed to verify the takeoff acceleration. The simulation of basic drag characteristics, thrust lapse rate, ground effect in taxi attitudes, rolling coefficient of friction and inertia effects are indirectly checked by timing takeoff acceleration.

The time to obtain rotation and lift-off speeds were determined by the airspeed indicator and a stop watch. Comparisons between Boeing and NASA simulations are shown in the table on Page 14.2-4 . The NASA simulated takeoff started with V = 15 kt (at t = 0) and takeoff thrust while the Boeing takeoff data started at V = 0 (t = 0) and takeoff thrust. To compare the two, the time to accelerate from 0 to 15 knots must be added to the NASA data. This time is equal to 15 kt divided by the average acceleration. The average acceleration was determined from the curves on Pages 14.2-7 and 14.2-8 .

Time histories from the NASA takeoff are shown on Pages 14.2-5 and -6 . Velocity versus time data from the NASA test are plotted with the Boeing results on Pages 14.2-7 and -8 .

TAKEOFF ACCELERATION

	FLAP POSITION	GEAR	G.W. ~ 1000 LB.	C.G. ~ % MAC	ALTITUDE ~ 1000 FT.	ΔP ~UNITS	T/O IEPR	ROTATION		LIFTOFF			h = 35 FT	
								V_I ~KTS	TIME ~SEC	V_{IO} ~KTS	TIME ~SEC	DISTANCE ~ FT	V_{35} ~ KTS	TIME ~SEC
BOEING	10	DN	707.2	14.0	S.L.	8.4	1.420	161	47.5	168	50.0	7500	171	54.0
NASA									45 ①		47.5 ①			
BOEING	20	DN	527.2	15.6		6.8	1.380	131	30.0	140	33.0	4200	142	35.0
NASA									27 ②		30 ②			
COMPUTATION TOLERANCE									±2 Sec		±2 Sec	± 100 Ft		

① ADD 3.5 SEC. TO ACCOUNT FOR STARTING AT 15 KT (V=15 KT AT t=0)

② ADD 3.0 SEC TO ACCOUNT FOR STARTING AT 15 KT

NASA-BOEING TAKE-OFF ACCELERATION COMPARISON

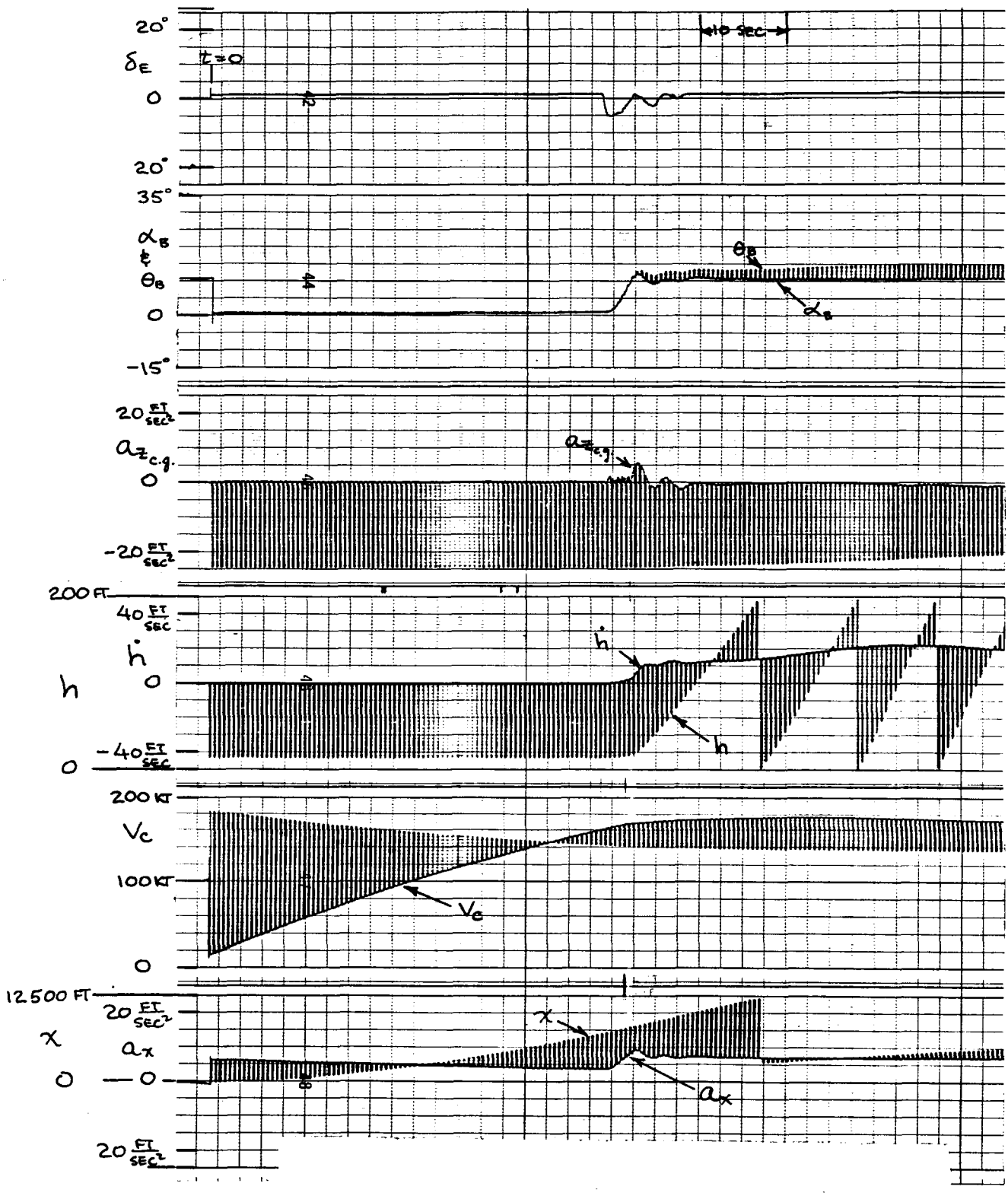

GW = 707 200 LB SEA LEVEL
δ_F = 10 c.g. = 14%
$\Delta_{F.R.L}$ = − 5.4

TAKE-OFF

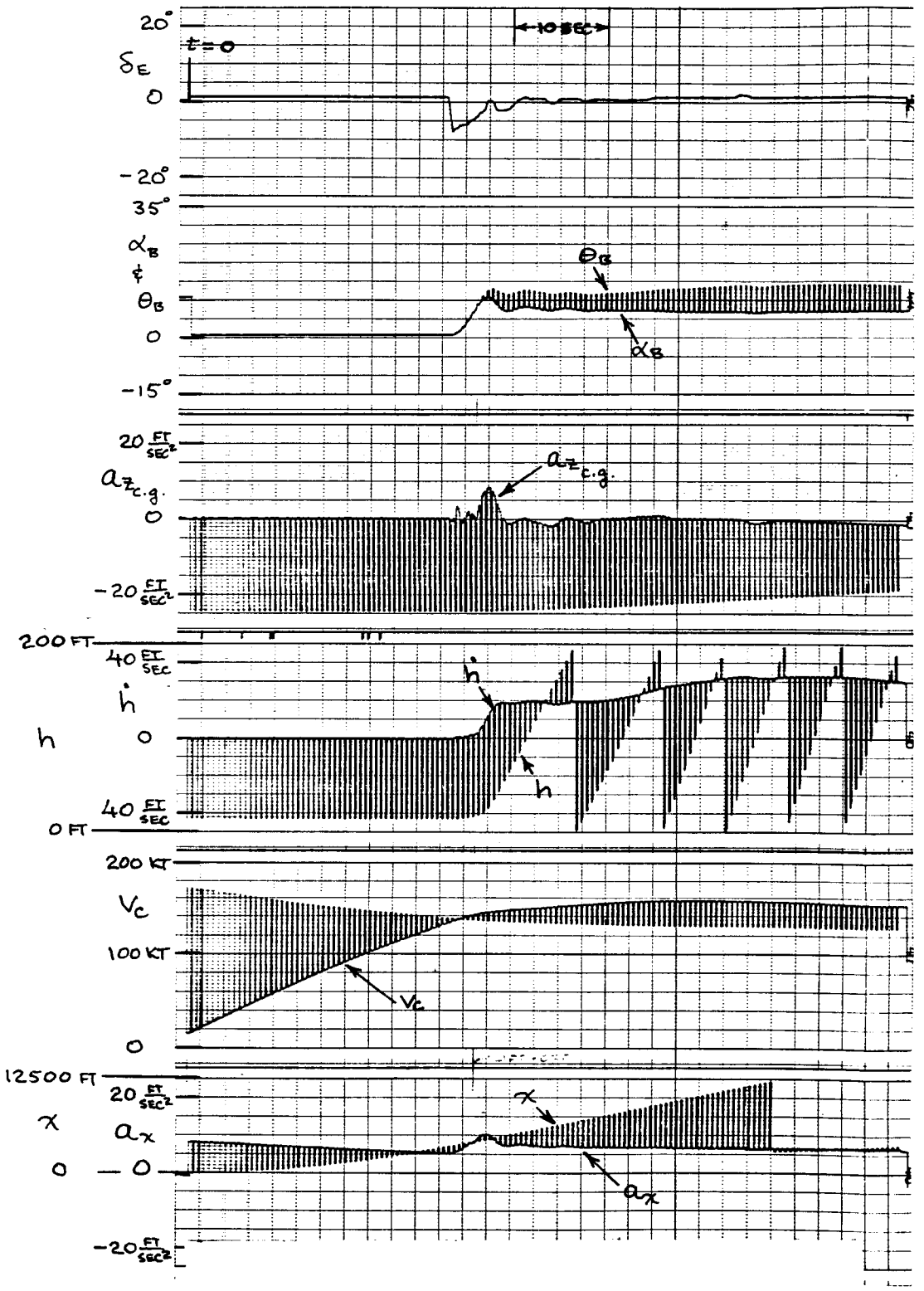

GW = 527200 LB SEA LEVEL
δ_F = 20 c.g. 15.6%
$\alpha_{FRL.}$ = -3.8

TAKE OFF

TAKEOFF ACCELERATION
FLAPS 10
G.W. = 707200 LB.
C.G. = 14% MAC
TEST 61-2 CERT.
COND. 1.06.051.007.0

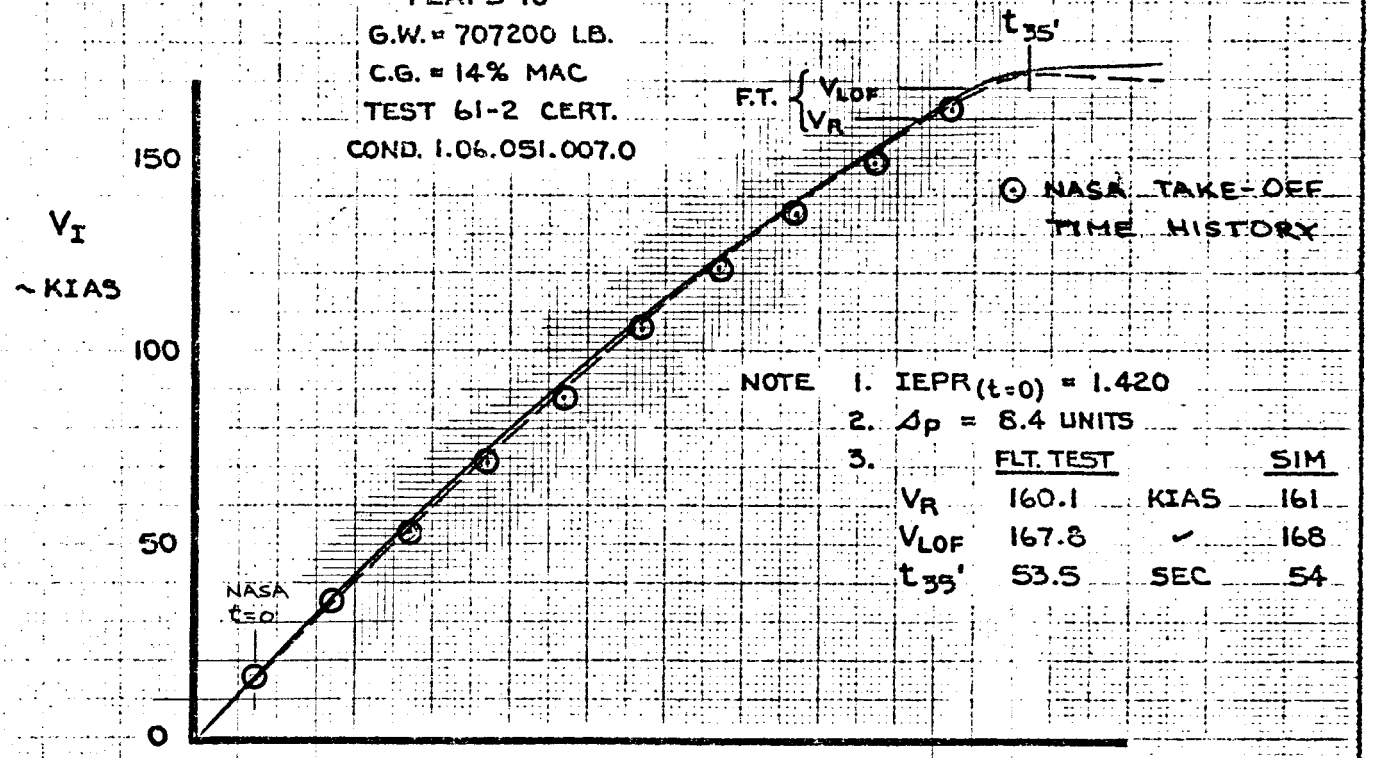

NOTE 1. $IEPR_{(t=0)}$ = 1.420
2. Δp = 8.4 UNITS
3.

	FLT. TEST		SIM
V_R	160.1	KIAS	161
V_{LOF}	167.8	✓	168
$t_{35'}$	53.5	SEC	54

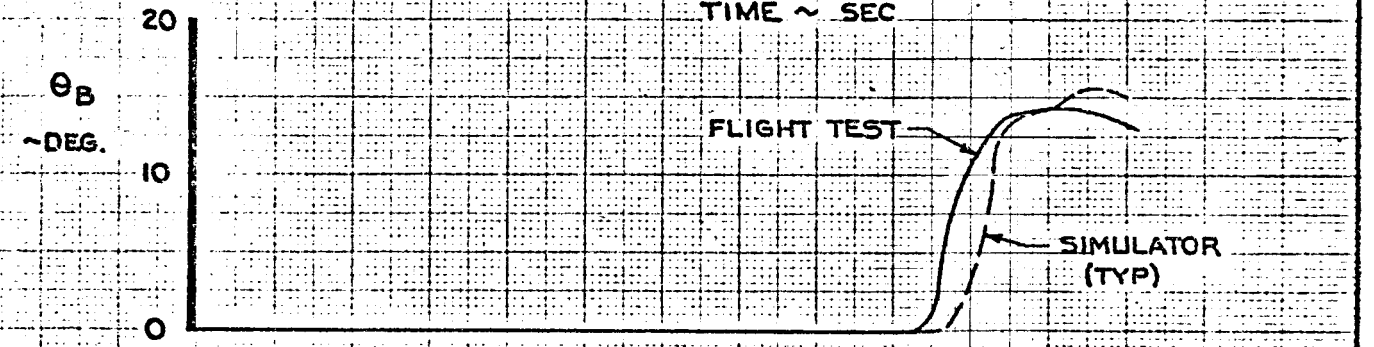

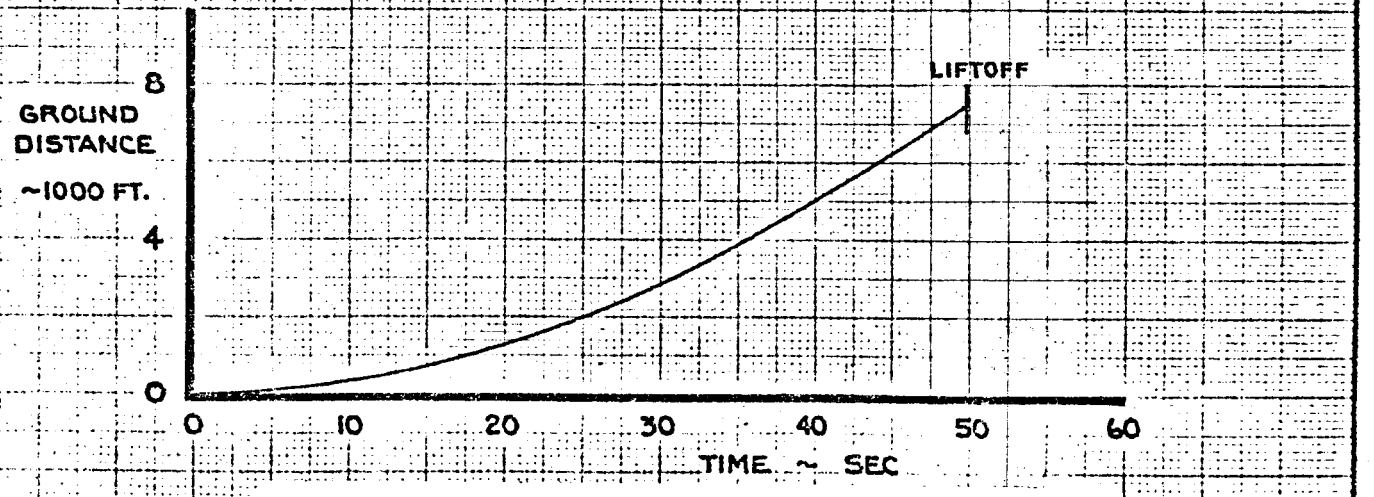

CALC	CURNUTT	5-16-70	REVISED	DATE	TAKEOFF ACCELERATION FLAPS 10 707200 LB.
CHECK					
APR					
APR					
	ODEGARD	5-18-70			THE BOEING COMPANY

747
D6-30643 Vol. II
PAGE 14.2-7

AD 461 C-84

K+E ALBANENE 1895 TRACING PAPER

TAKEOFF ACCELERATION
FLAPS 20
G.W. = 527200 LB.
C.G. = 15.6% MAC
TEST 59-10 CERT.
COND. 1.06.051.015.0

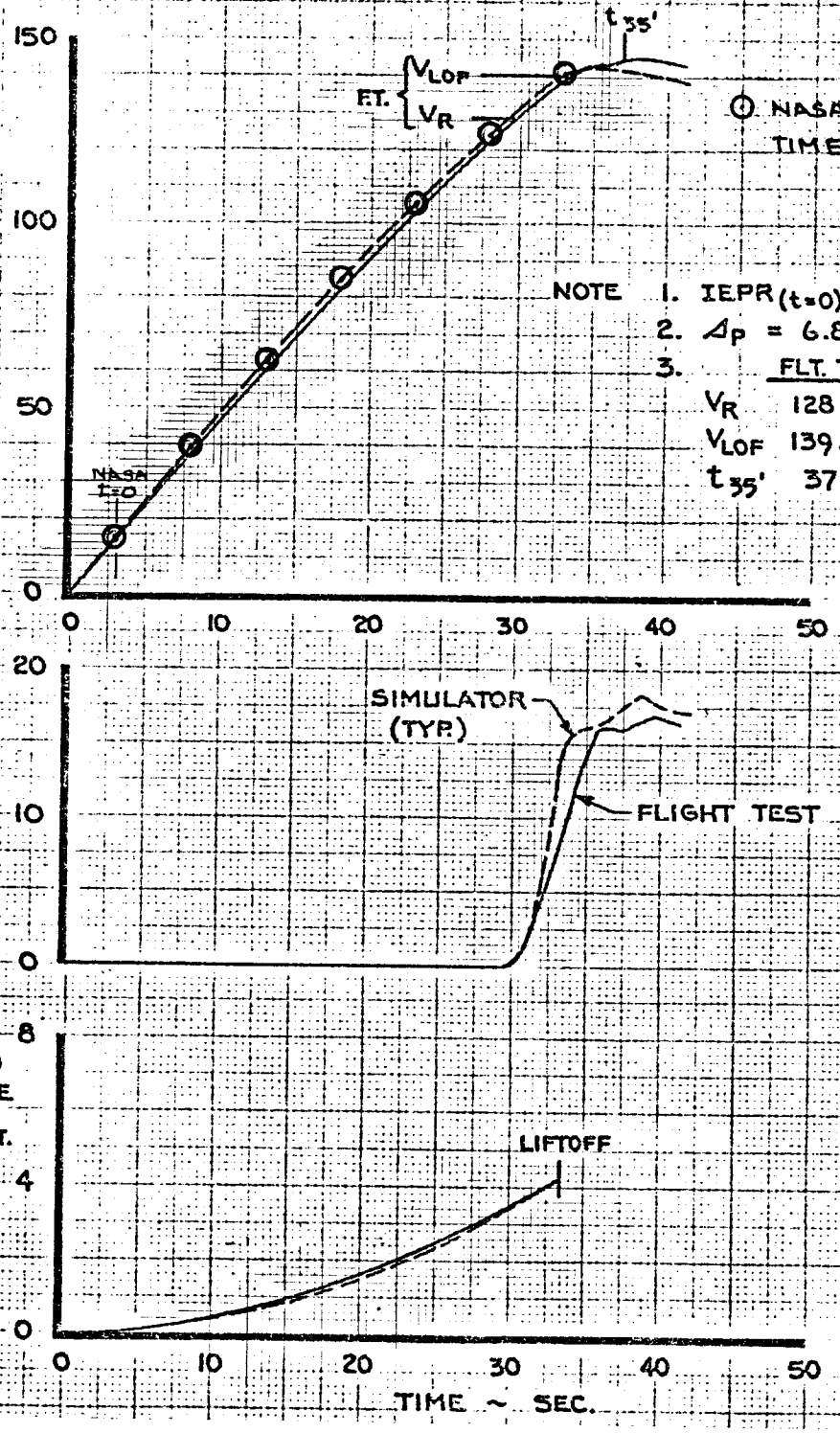

⊙ NASA TAKE-OFF TIME HISTORY

NOTE 1. $IEPR_{(t=0)}$ = 1.380
2. Δ_P = 6.8 UNITS
3.

	FLT. TEST		SIM
V_R	128.6	KIAS	131
V_{LOF}	139.7	"	140
$t_{35'}$	37	SEC.	35

CALC	CURNUTT	5-16-70	REVISED	DATE	TAKEOFF ACCELERATION FLAPS 20 527200 LB.	747
CHECK						D6-30643 Vol. II
APR						
APR						
	ODEGARD	5-18-70			THE BOEING COMPANY	PAGE 14.2-8

AU 461 C-R4

14.2.2 CLIMB PERFORMANCE

The purpose of this test was to verify the climb performance simulation. The pilot started the test near sea level and his task was to fly the air speed and EPR schedule prescribed for this condition, Page 14.2-10. At the check altitudes, the computer was put in "hold" and data was obtained from the cockpit instruments and the computer. The comparison between Boeing and NASA simulator results is tabulated on Page 14.2-10 and plotted on Page 14.2-11. The difficulty in performing this task is to have the airplane stabilized when putting the computer to "hold".

FOUR-ENGINE CLIMB PERFORMANCE

CLIMB CONDITION	FLAP POSITION	GEAR	G.W. ~1000 LB.	C.G. ~% MAC	ALTITUDE ~1000 FT.	V_I/M	IEPR		Θ_B ~DEG.		R/C ~FT/MIN.		F_N ~LB/ENG
							BOEING	NASA	BOEING	NASA	BOEING	NASA	
CLIMB TO ALT.	UP	UP	650	14	5	340	1.187	1.187	4.3	4.4	1770	1800	18200
					10		1.225	1.235	3.8	4.0	1660	1750	16900
					15		1.265	1.27	3.2	3.1	1500	1400	15500
					20①		1.309	1.32	2.5	2.8	1220	1100	14000
					25		1.345	1.345	1.7	1.5	760	500	12300
					30	.81	1.417	1.425	2.3	2.5	460	500	10700
					34.3	.81	1.47-		2.7		0		9300
COMPUTATION TOLERANCE							± .01		± .5 DEG.		± 5%		

NASA DATA WAS OBTAINED FROM COCKPIT INSTRUMENTS

① NASA DATA AT 21700 FT.

	CALC	CHECK	APR	APR
	CURNUTT	ZIELINSKI		
	5-18-70	5-18-70		
JDEGARD	5-18-70	5-18-70		

REVISED	DATE

4 - ENGINE ENROUTE CLIMB

G.W. = 650000 LB.

C.G. = 14% MAC

NOTE
1. MAX. CLIMB THRUST (A/C AIRBLEED ON)
2. STANDARD DAY
3. NO FUEL BURNOFF
4. SEE TABLE (PAGE 5.2-3) FOR THRUST, IEPR, AND ATTITUDE INFORMATION

NASA
⊙ COCKPIT DATA
⊡ DIGITAL DATA

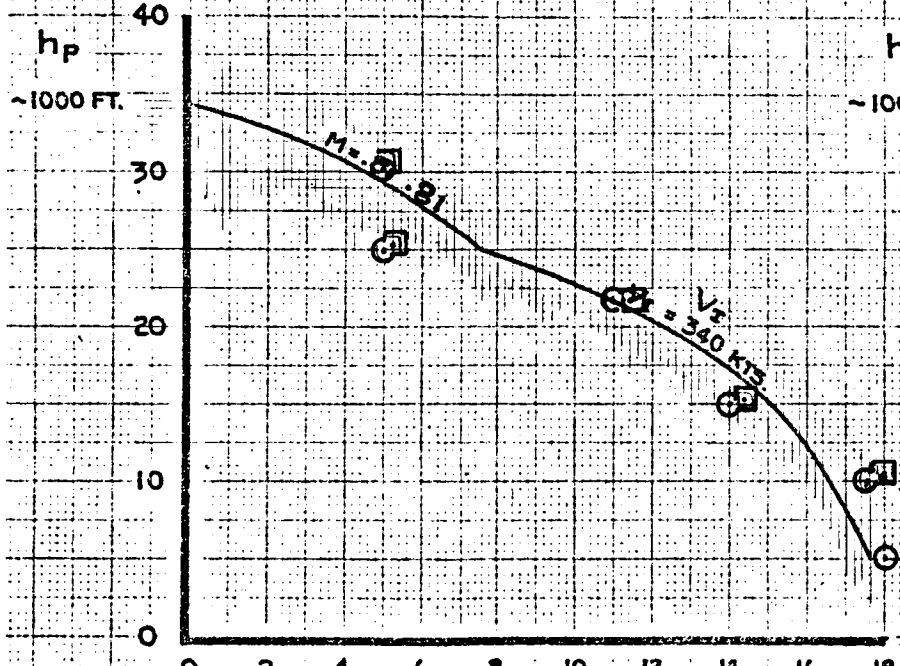

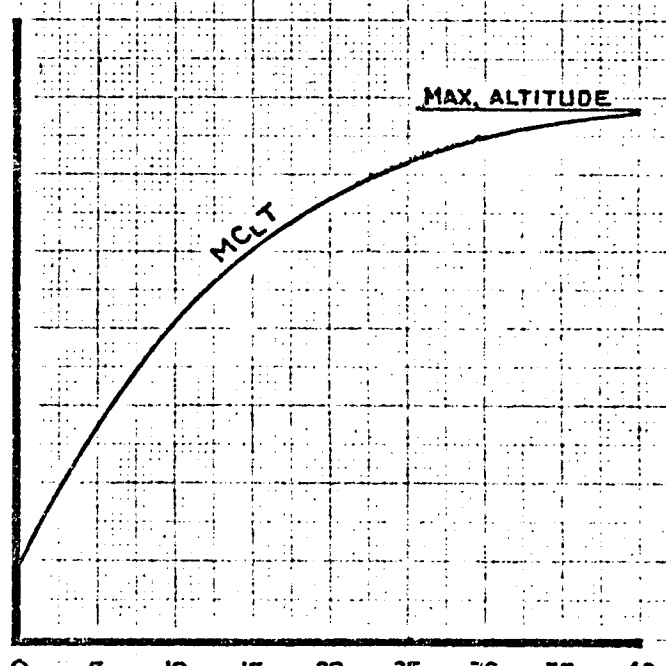

FOUR-ENGINE ENROUTE CLIMB

G.W. = 650000 LB.

THE BOEING COMPANY

747

D6-30643 Vol. II

PAGE 14.2-11

14.2.3 INFLIGHT ACCELERATION AND DECELERATION

The acceleration condition was performed by starting at M = .65 with maximum continuous thrust and accelerating to the maximum speed. Speed and time data were obtained from the cockpit. The comparison between Boeing and NASA simulations is shown on Page 14.2-13.

The deceleration check was performed with speed brakes and idle power, starting at M = .85. The NASA simulation results are plotted on Page 14.2-14. The differences in the NASA and Boeing data are the result of a difference in idle EPR. The Boeing test utilized a revised Mach and altitude correction to EPR which affected the idle thrust at high altitude and Mach number. The trend of the results, accounting for the higher idle thrust, appeared correct. The adjustment to the idle EPR was made in the NASA simulation after the checkout data were obtained.

GW = 450000 LB.
ALT = 35000 FT.
CG = 25% MAC

© NASA

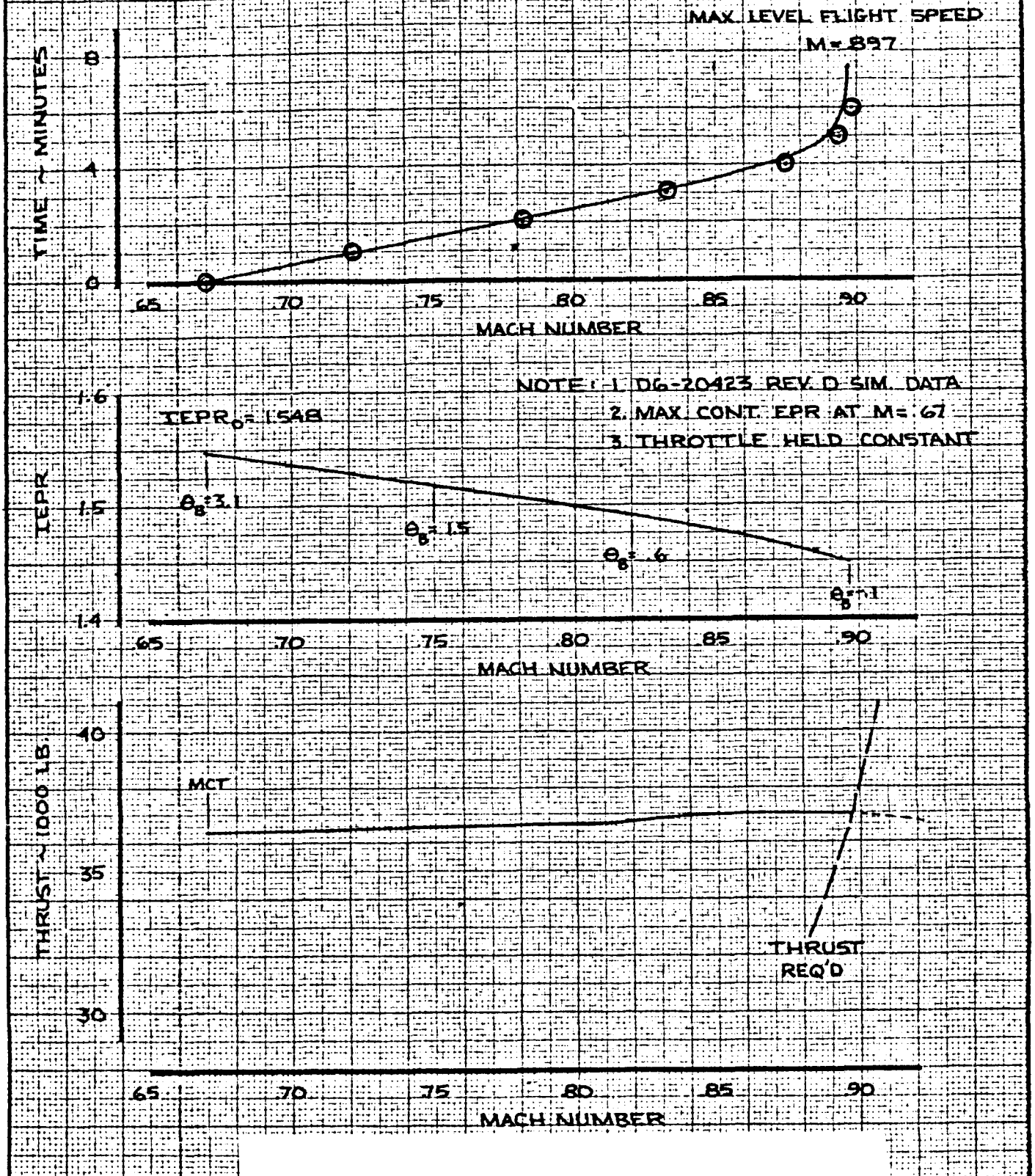

CALC	BRYANT	5/15/70	REVISED	DATE	LEVEL FLIGHT ACCELERATION FLAPS UP
CHECK					747
APR					450000 LB. 35000 FT. D6-30643 Vol. II
APR					THE BOEING COMPANY
	GLENN	5/15/70			PAGE 14.2-13

G.W. = 450000 LB.
ALT. = 35000 FT.
CG = 25% MAC

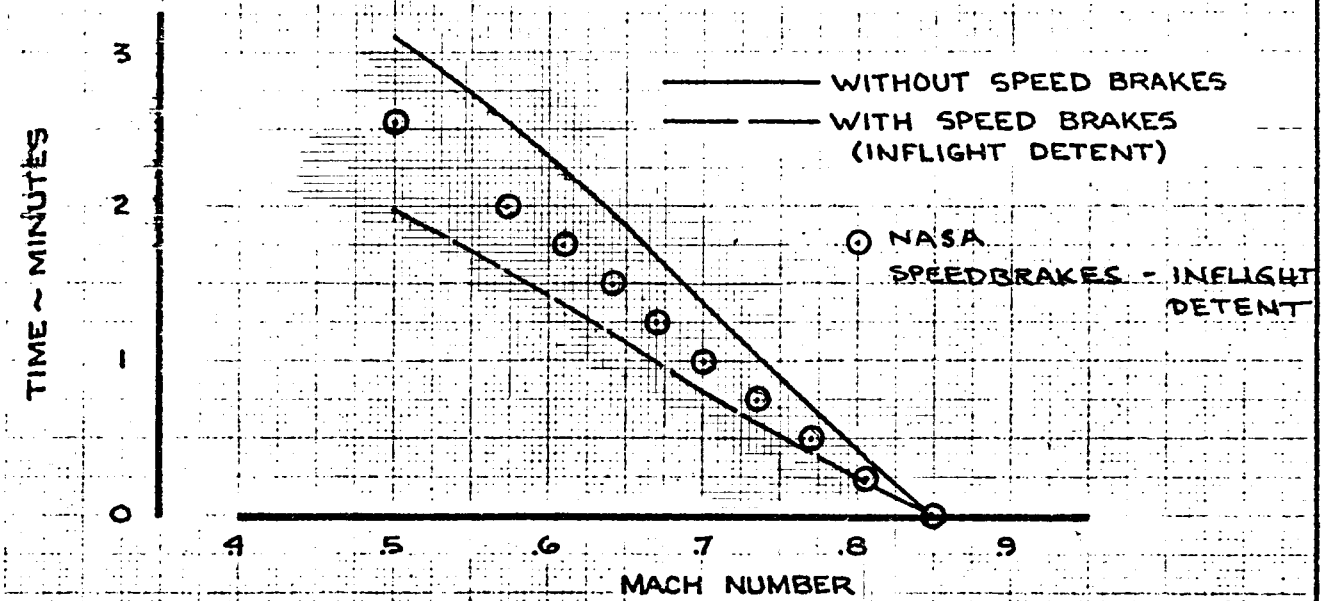

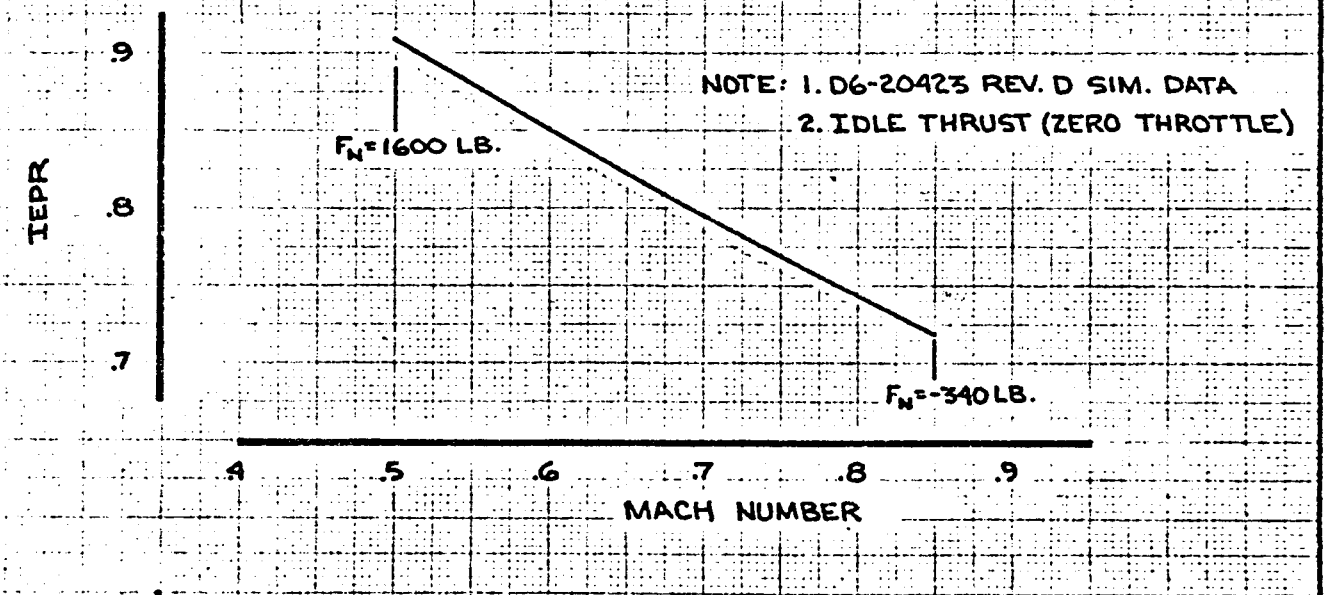

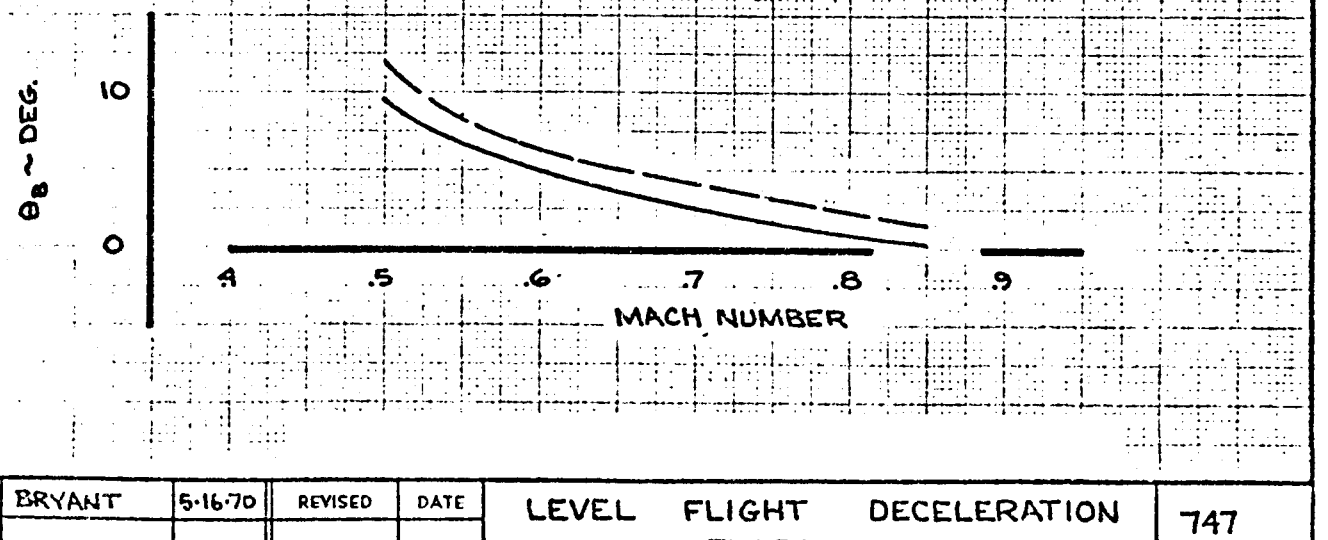

CALC	BRYANT	5-16-70	REVISED	DATE
CHECK				
APR				
APR				
	GLENN	5-19-70		

LEVEL FLIGHT DECELERATION
FLAPS UP
450000 LB. 35000 FT.

747

D6-30643
Vol. II

THE BOEING COMPANY

PAGE 14.2-14

AD 461 C-R4

K-E ALBUQUERQUE 1956

14.2.4 STEADY TURNS

This test was conducted to check the stick force and elevator required to hold a bank angle, or load factor. The pilot trimmed the airplane for straight and level flight and then rolled into a steady coordinated turn at a specified bank angle. The airplane was allowed to descend in order to maintain a constant airspeed. When the condition was stabilized, the computer was put in "hold" and the computed values of F_s, ϕ_B, and δ_e were obtained. The results are tabulated with the Boeing simulation results on Page 14.2-16. The data are plotted, along with flight test results, on Pages 14.2-17 and -18. The data scatter is a result of the difficulty in having a stabilized condition when going to "hold". A calculated value of $n_z = 1/\cos\phi_B$ was used in plotting the data.

STEADY COORDINATED TURNS

FLAP POSITION	GEAR	G.W. ~ 1000 LB.	C.G. ~ % MAC	ALTITUDE ~ 1000 FT.	V_I/M	Δ_P ~UNITS	BANK ANGLE, ϕ_B ~DEG		F_S ~LB.		δ_e ~DEG		n_Z	
							BOEING	NASA	BOEING	NASA	BOEING	NASA	BOEING	n_Z NASA
UP	UP	540	31	34	.86	3.1	30 45 55*	30.6 47/47.5	15.0 33.0 52.0	14 38/32.5	1.3 .3 - .8	1.39 -.06/.3	1.15 1.41 1.74	1.16 1.47/1.43
UP	UP	560	14	34	.86	4.4	30 50 58*	28 50.7	14.5 44.0 61.5	14.5 47	1.0 -1.8 -3.2	.84 -2.2	1.15 1.55 1.89	1.13 1.58
30	DN	459	30.8	11	127	5.7	30 40 45	31.1 45.9/44.7	11.5 17.0 19.5	11.7 19.9/18.1	-1.8 -5.2 -7.6	-2.5 -7.1/-6.65	1.15 1.30 1.41	1.17 1.44/1.41
COMPUTATION TOLERANCE									± 10%		± .5 DEG.			

* INITIAL BUFFET

$n_z = 1/\cos\phi_B$

FLAPS UP
GEAR UP

NASA	SYM	A/P	FLT.	COND. NO.	C.G. ~ % MAC	G.W. ~ 1000 LB.	ALT. ~ FT.	M
⊙	⊙	RA001	31-6	1.21.003.005.0, .6-.7	31	540	34000	.86
⊡	⊡	″	30-2	1.21.003.047.0-.9	14	560	″	″

═══ SIMULATOR (D6-20423, REV. D DATA)

NOTE: 1. CONSTANT THROTTLE (P.L.F. @ n_z = 1.0)
2. SIMULATOR F_S INCLUDES 2.5 LB. BREAKOUT FORCE

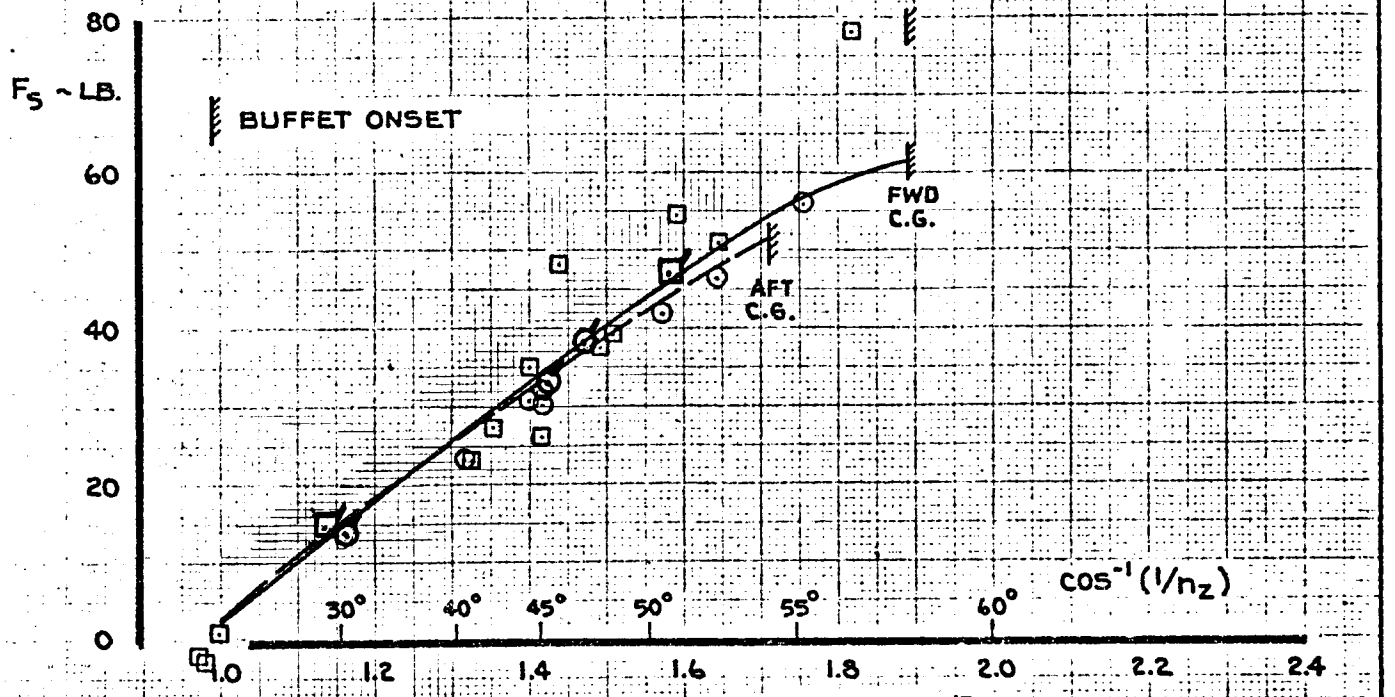

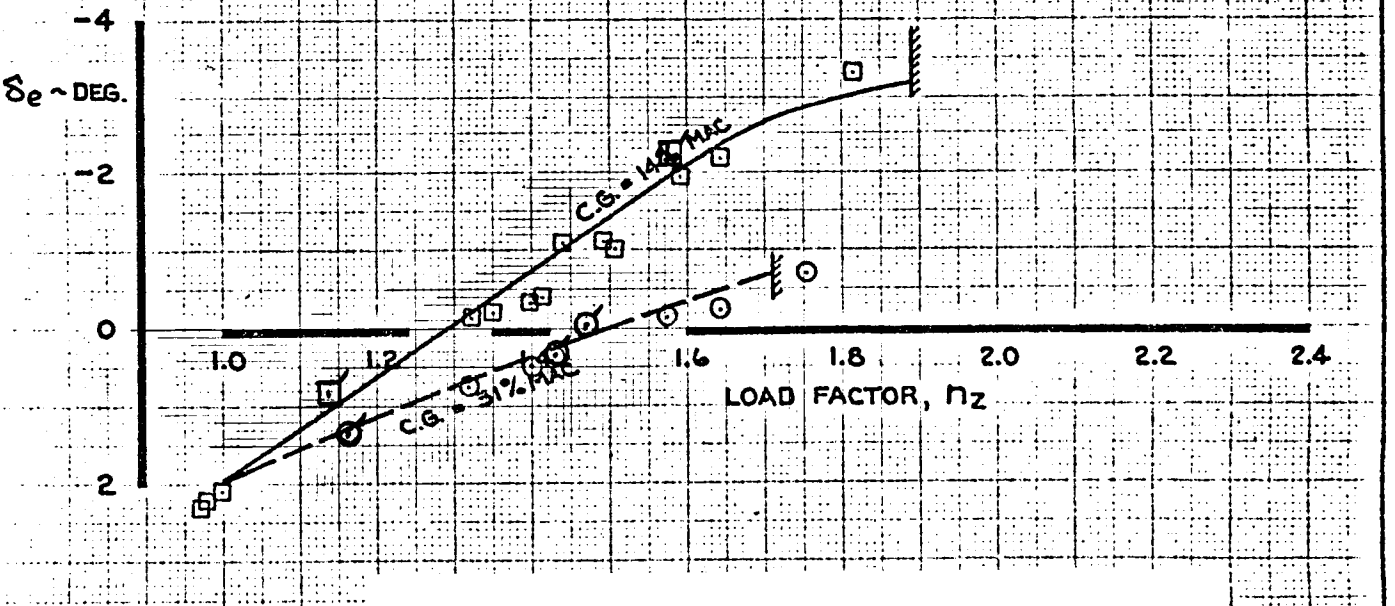

CALC	BYSTROM	4-4-70	REVISED	DATE	STEADY COORDINATED TURN 35000 FT. M = .86
CHECK			CURNUTT	5-18-70	
APR					
APR					
	ODEGARD	5-20-70			THE BOEING COMPANY

747
D6-30643 Vol. II
PAGE 14.2-17

FLAPS 30
GEAR DOWN

NASA	SIM	A/P	FLT.	COND. NO.	C.G. ~ % MAC	G.W. ~ 1000 LB.	ALT. ~ FT.	V_I ~ KTS	M
⊙	⊙	ON	8-1	1.00.002.034.0	30.8	459	11000	127	.24
	⊡	~	~	1.00.002.035.0-1	30.7	460	~	150	.28

═══ SIMULATOR (D6-20423, REV. D DATA)

NOTE 1. CONSTANT THROTTLE (P.L.F. @ n_z = 1.0)
2. SIMULATOR F_S INCLUDES 2.5 LB. BREAKOUT FORCE

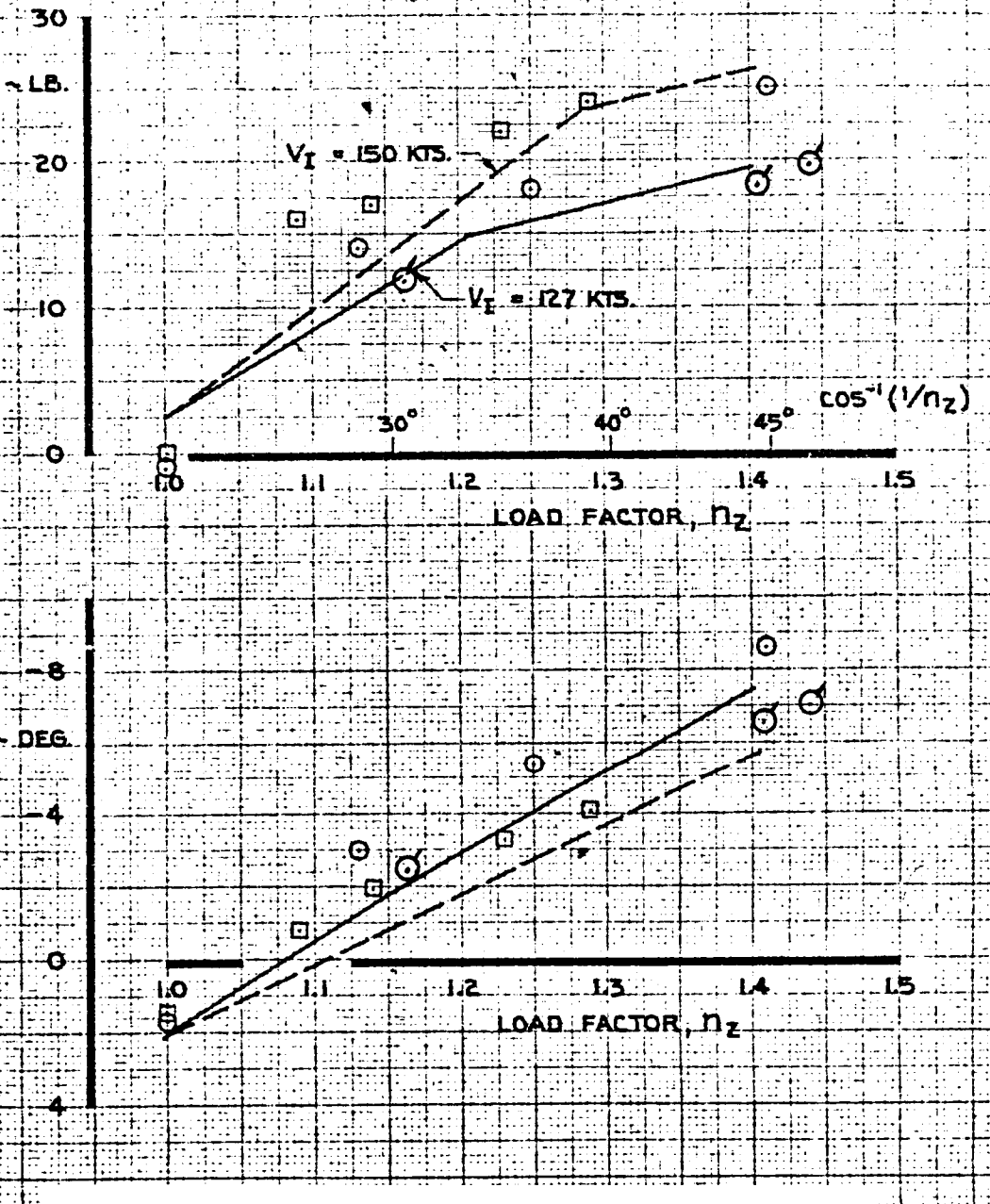

CALC	BYSTROM	4-1-70	REVISED	DATE
CHECK			CURNUTT	5-18-70
APR				
APR				
	ODEGARD	5-20-70		

STEADY COORDINATED TURN
FLAPS 30 AFT C.G.

747

D6-30643 Vol. II

THE BOEING COMPANY

PAGE 14.2-18

14.2.5 LONGITUDINAL STATIC STABILITY

The airplane was trimmed for straight and level flight. Without changing the stabilizer or throttle, the pilot slowly changed the speed using the elevator. The thrust discrepancy was allowed to generate a rate of climb or descent. Computed values of δ_e, F_s, and θ_B were recorded when the airplane was stabilized at the prescribed speed. The column was then released to see if the airplane would return to the trim speed. The results are plotted on Page 14.2-20.

FLAPS 20
GEAR UP

NASA	SYM	A/P	FLT.	COND. NO.	CG %MAC	GW LB.	ALT. FT.	TRIM IEPR
⊙	□	RA101	4-3 CERT.	1.22.051.001-.009	32	562000	10000	1.172

$\alpha_{FRL} = -1.26°$ ——— SIMULATOR (D6-20423 REV. D DATA)

NOTE: 1. SHADED SYMBOL INDICATES TRIM POINT
2. FLAGGED SYMBOLS INDICATE RETURN TO TRIM
3. THRUST FOR LEVEL FLIGHT AT THE TRIM SPEED
4. MASS UNBALANCE EFFECTS INCLUDED IN BREAKOUT

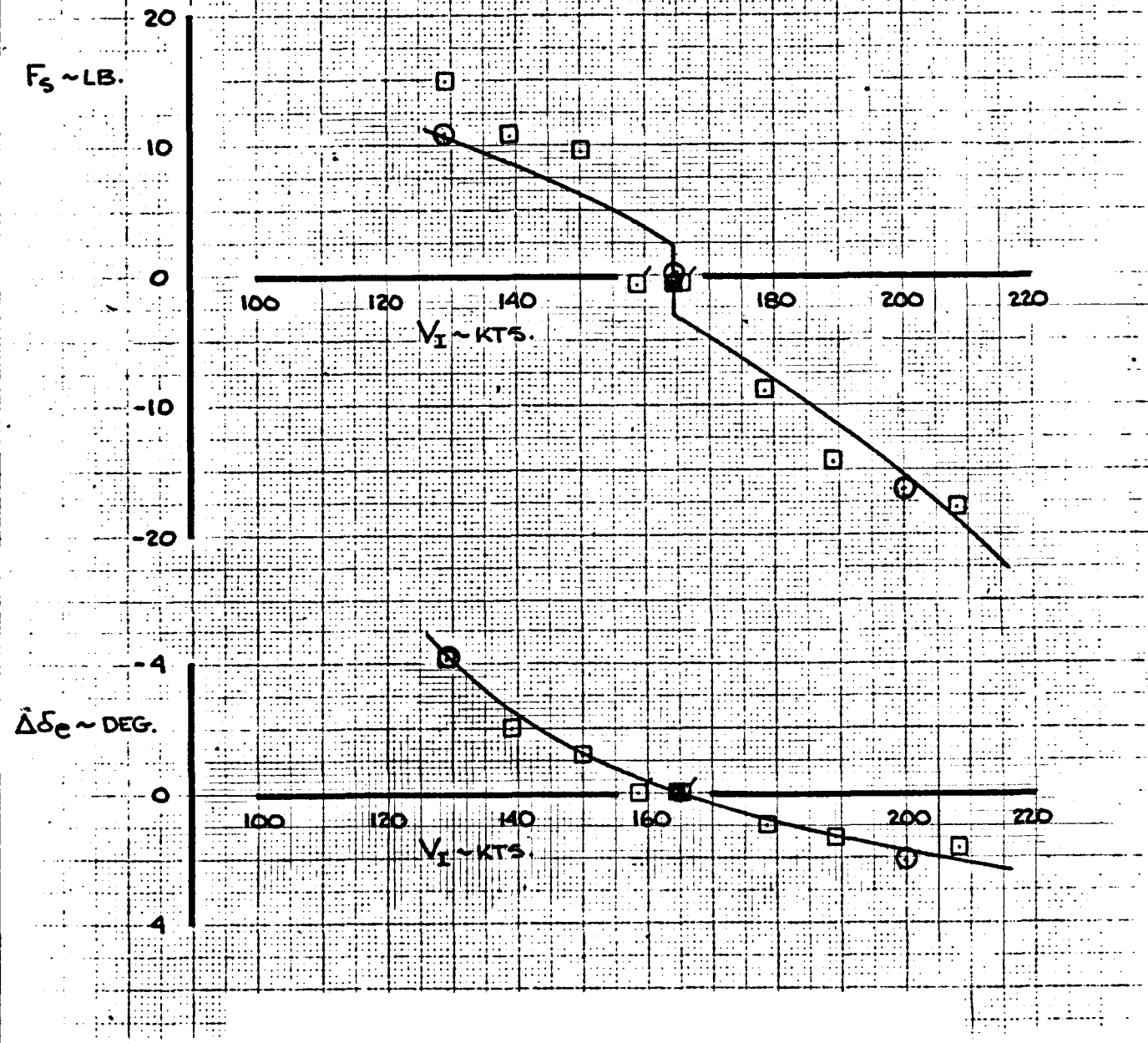

CALC	HOLTZNER	3-30-7	REVISED	DATE	APPROACH STABILITY
CHECK			CURNUTT	5-19-70	
APR					
APR					
	GLENN	5-20-70			THE BOEING COMPANY

747
D6-30643
Vol. II
PAGE 14.2-20

14.2.6 STEADY SIDESLIPS

After a trimmed flight condition was set up, the pilot slowly applied rudder to hold a steady sideslip. A combination of lateral control and bank angle was used to maintain a straight and level flight path. When the airplane was stabilized, computed values of β, δ_R, δ_w, and ϕ_B were recorded. Comparisons between NASA and Boeing simulations and flight test are shown on Pages 14.2-22 and -23.

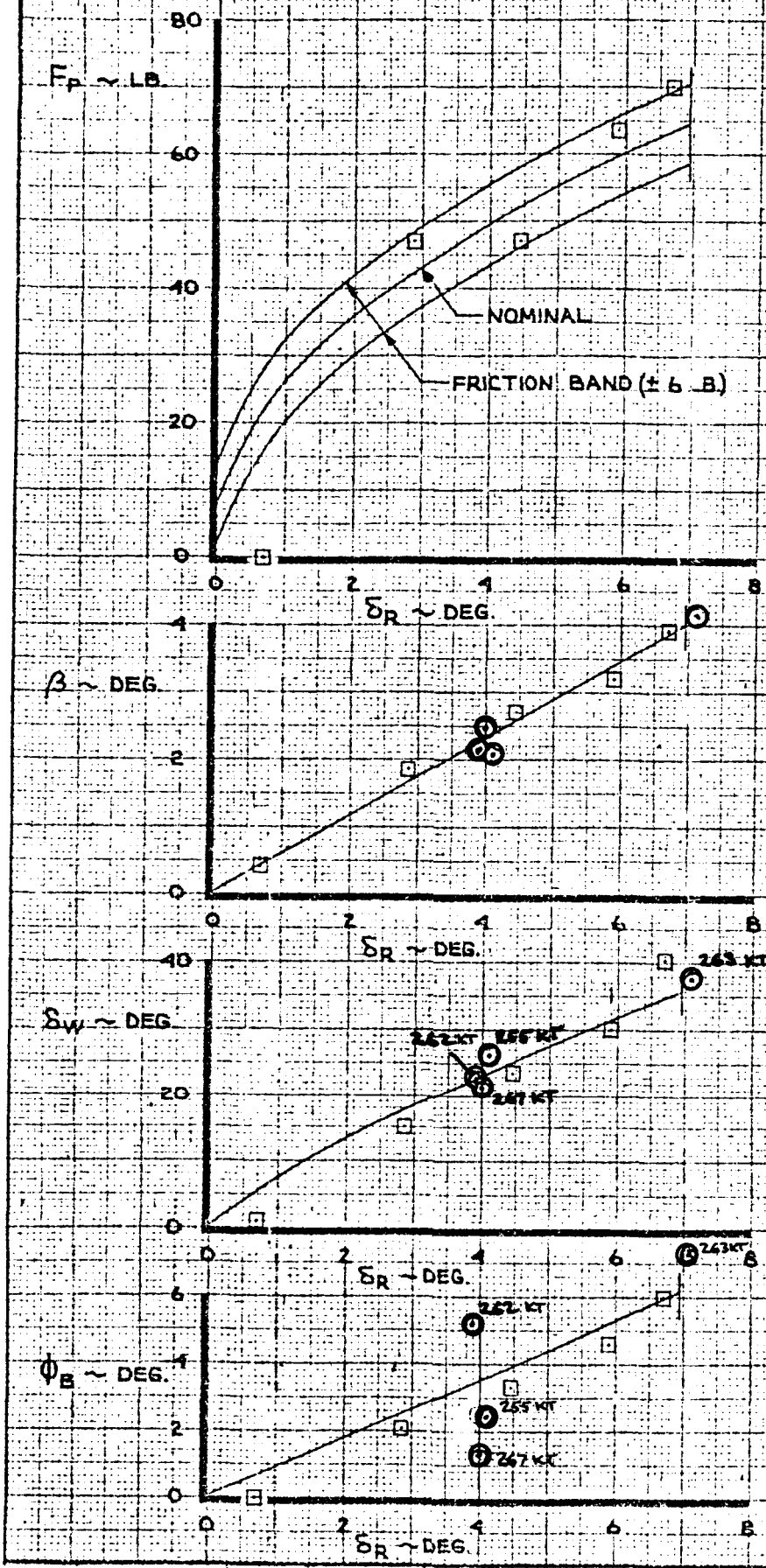

FLAPS UP

GEAR UP

G.W. = 556,600 LB.

h_p = 36,000 FT.

C.G. = 31.0 % M.A.C.

V_c = 265.75 KNOTS

D6-20423 REV. D SIM. DATA

MAXIMUM RUDDER (RATIO CHANGER LIMIT)

SYMMETRIC FOR POSITIVE & NEGATIVE RUDDER

□ FLT. 39-1, A/P RADDI COND. NO. 1.27.001.DD3 (.0-.4)

⊙ NASA

CALC	BECK	5-19-70	REVISED	DATE
CHECK				
APR				
APR				
INK	KINSMAN	5-20-70		

STEADY SIDESLIP

M = .80 h_p = 36,000 FT.

747

D6-30643 Vol. II

THE BOEING COMPANY

PAGE 142-22

FLAPS 20

D6-20423 REV. D SIM. DATA
MAXIMUM RUDDER
(RATIO CHANGER LIMIT)

SYMMETRIC FOR POSITIVE & NEGATIVE RUDDER

GEAR UP
G.W. = 558,000 LB.
h_p = 9850 FT.
C.G. = 31.9 % M.A.C.
V_I = 143.4 KNOTS

⊙ NASA
⊡ FLIGHT 4-1, A/P RAIOL
COND. 1.25.051.002
(β BASED ON MANUAL NOTES)

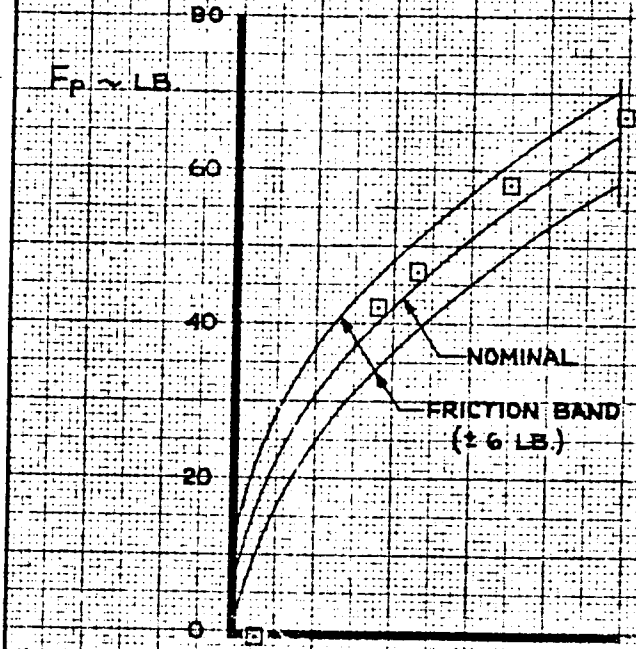

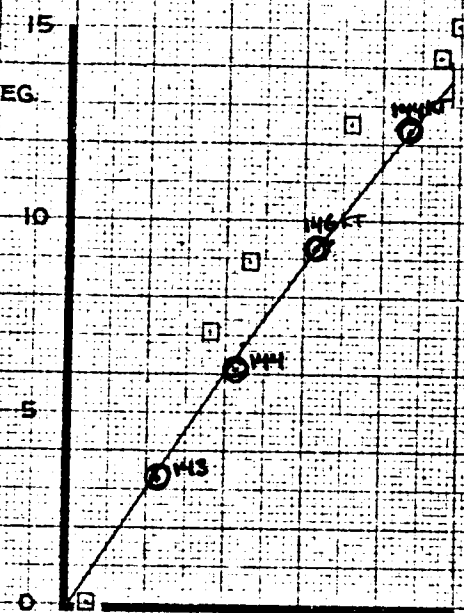

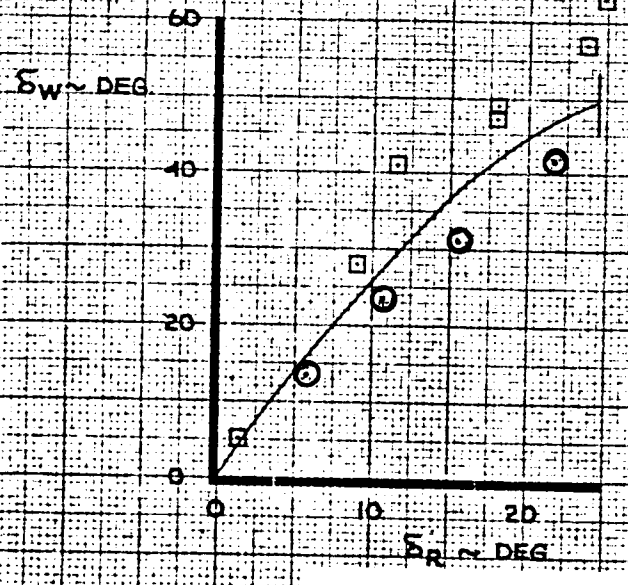

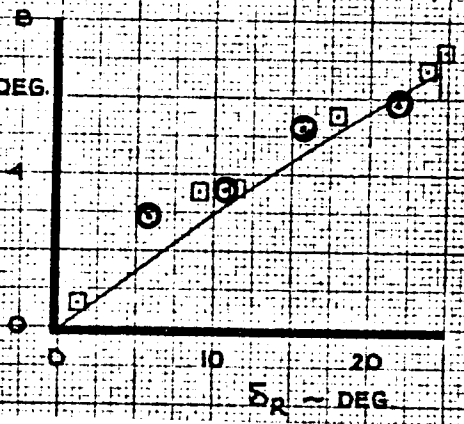

CALC	BECK	5-18-70	REVISED	DATE	STEADY SIDESLIP
CHECK					V_I = 143.4 KNOTS FLAPS 20
APR					
APR					
INK	KINSMAN	5-22-70			THE BOEING COMPANY

747
D6-30643
Vol. II
PAGE 14.2-23

AE 461 C-R4

K-E ALBANENE 1951

14.2.7 ROLL RATES

The pilot trimmed the airplane for straight and level flight and then rolled into a 30° bank. The yaw damper was on and the rudder pedals were not used. After the bank angle was established, a wheel input was rapidly applied and held until the airplane banked to 30° in the opposite direction. The time to bank through the 60° was obtained with a stop watch and the maximum roll rate and magnitude of wheel input were obtained from the computed time histories. The average roll rate was determined by dividing the change in bank angle, 60°, by the time required to bank 60°. The NASA simulator data is compared to Boeing results in the table on Page 14.2-25 and to the plotted data on Pages 14.2-26 thru -28.

ROLL RATES

FLAP POSITION	GEAR	G.W. ~1000 LB.	ALTITUDE ~1000 FT.	$V_{I/M}$	HYD. SYS. INOPERATIVE	YAW DAMPER	$\delta_{W_{TRIM}}$ ~DEG. ($\delta_A = 30^{\circ}_L$)	δ_W ~DEG.		$t_{-30/30}$ ~SEC.		$P_{AVG.}$ ~DEG/SEC.		P_{MAX} ~DEG/SEC	
								BOEING	NASA	BOEING	NASA	BOEING	NASA	BOEING	NASA
10	UP	710	10	200	—	ON	-3.4	25 50 80	32° 80	7.5 5. 4.1	7. 4.8/4.5	8. 12. 14.5	8.6 12.5/13.4	9.5 16. 19.	11 19/17
0	UP	550	35	.86	—	ON	- .8	25 50 80	41° 80	8.6 4. 3.5	5.1 3.2/3.5	7. 15. 17.	11.8 18.8/17	9. 19. 23.	15.5 24/25
30	DN	564	S.L.	180 142	— —	ON	-7.6 -11.6	80 25 50 80	35 80	3.8 12. 7.1 5.5	9 5.8	16. 5.0 8.5 10.8	6.7 10.3	21.5 7.5 14. 15.5	11.5 16.5

FLAPS 10
10000 FT.
** 564000 LB.

NOTE: 1. TRIM AT -30° BANK AND ROLL THROUGH +30° BANK
2. GEAR UP; YAW DAMPER ON
3. I_{XX} = 14.3 x 10^6 SLUG-FT^2
**4. REDUCE ROLL RATES 1 DEG/SEC. FOR 710000 LB.
(I_{XX} = 20.3 x 10^6 SLUG-FT^2)

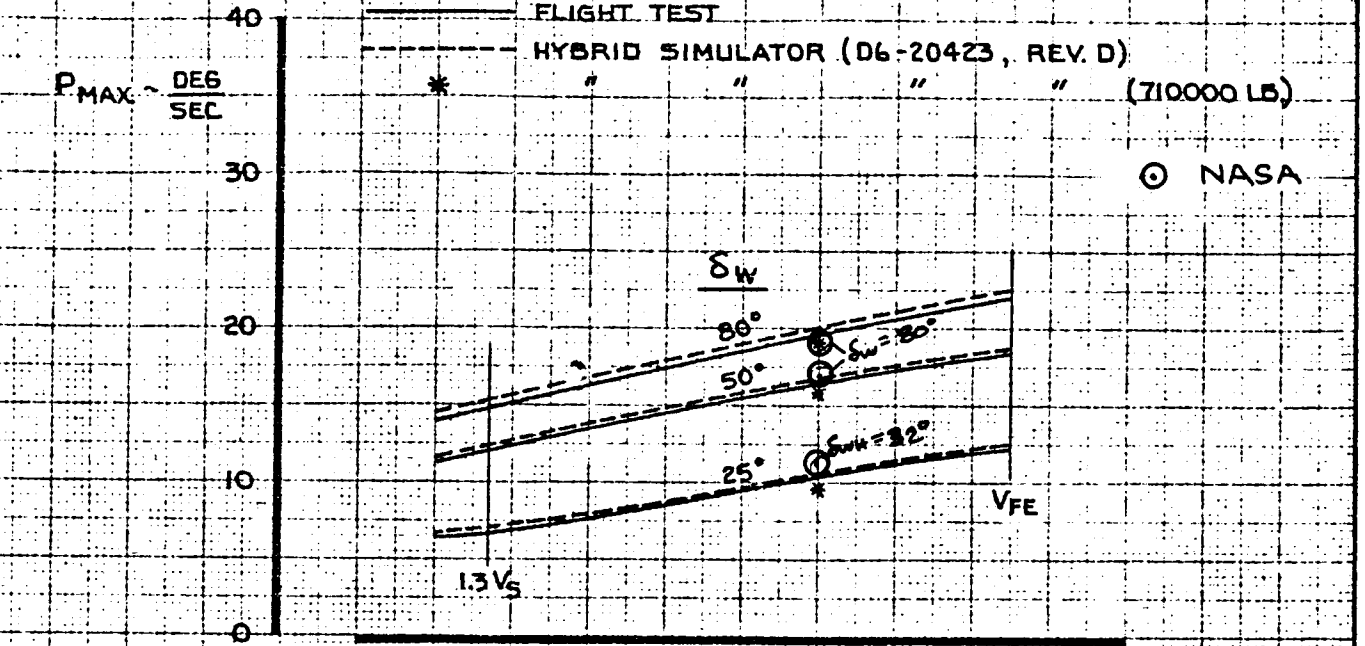

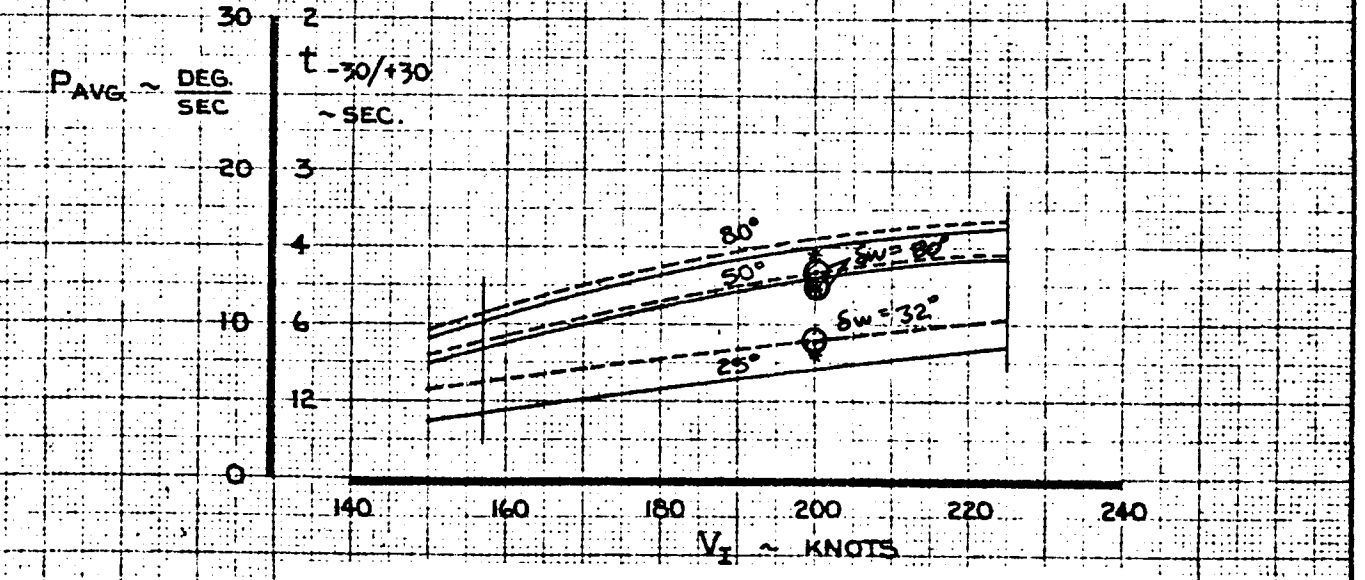

CALC	KUPCIS	5-1-70	REVISED	DATE
CHECK				
APR				
APR				
	ODEGARD	5-14-70		

ROLL RATE CAPABILITY
FLAPS 10

747

D6-30643
Vol. II

THE BOEING COMPANY

PAGE 14.2-26

FLAPS UP
35,000 FT.
550,000 LB.

NOTE: 1. TRIM AT -30° BANK AND ROLL THROUGH +30° BANK
2. YAW DAMPER ON
3. I_{XX} = 14.0 x 10^6 SLUG FT.^{2}
4. WHEEL EFFECT APPLIES TO TEST CONDITIONS (I_{XX} = 17.8 x 10^6 SLUG·FT^2)

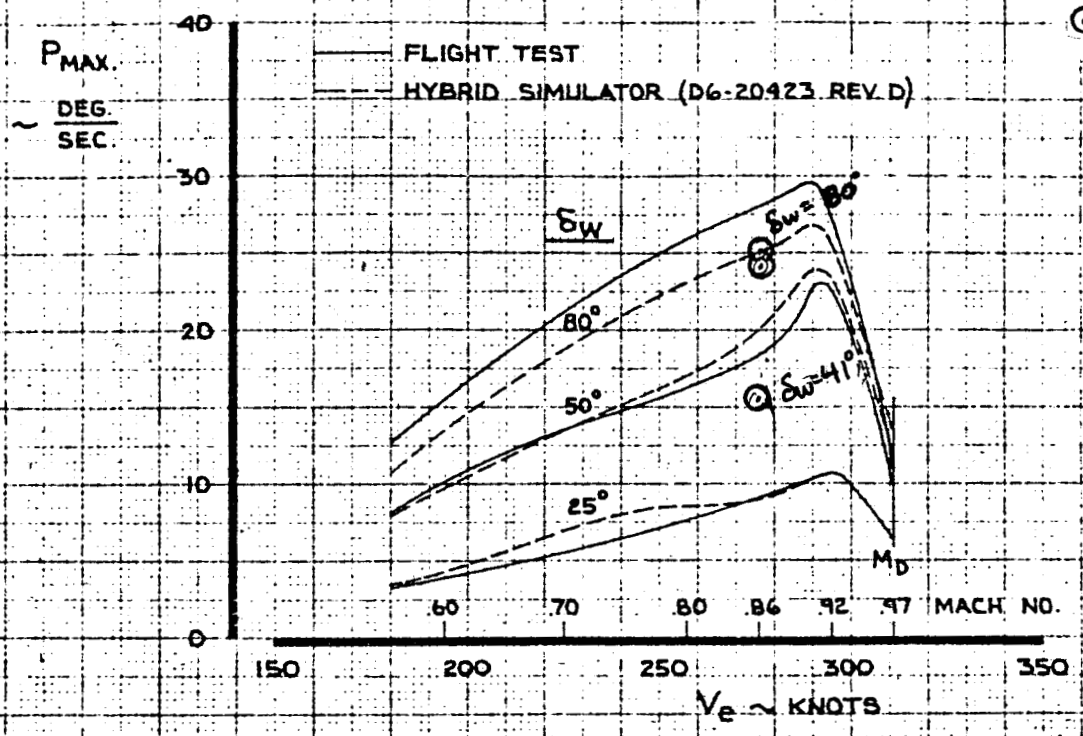

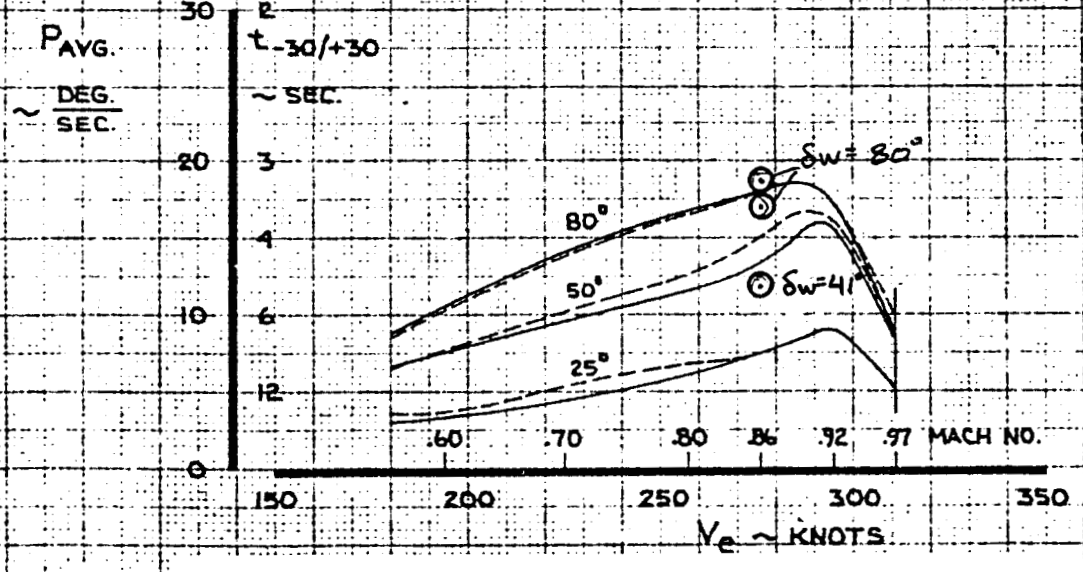

CALC	KUPCIS	5-4-70	REVISED	DATE	ROLL RATE CAPABILITY FLAPS UP ~ 35,000 FT.
CHECK			CURNUTT	5-12-70	
APR					
APR					
INK	KINSMAN	5-13-70			THE BOEING COMPANY

747
D6-30643 Vol. II
PAGE 14.2-27

FLAPS 30
SEA LEVEL
564,000 LB

NOTE 1. TRIM AT -30° BANK AND ROLL THROUGH +30° BANK.
2. GEAR DOWN; YAW DAMPER ON
3. $I_{XX} = 1.43 \times 10^6$ SLUG FT.^{2}
4. WHEEL EFFECT APPLIES TO TEST CONDITIONS ($I_{XX} = 18.1 \times 10^6$ SLUG FT.^{2})

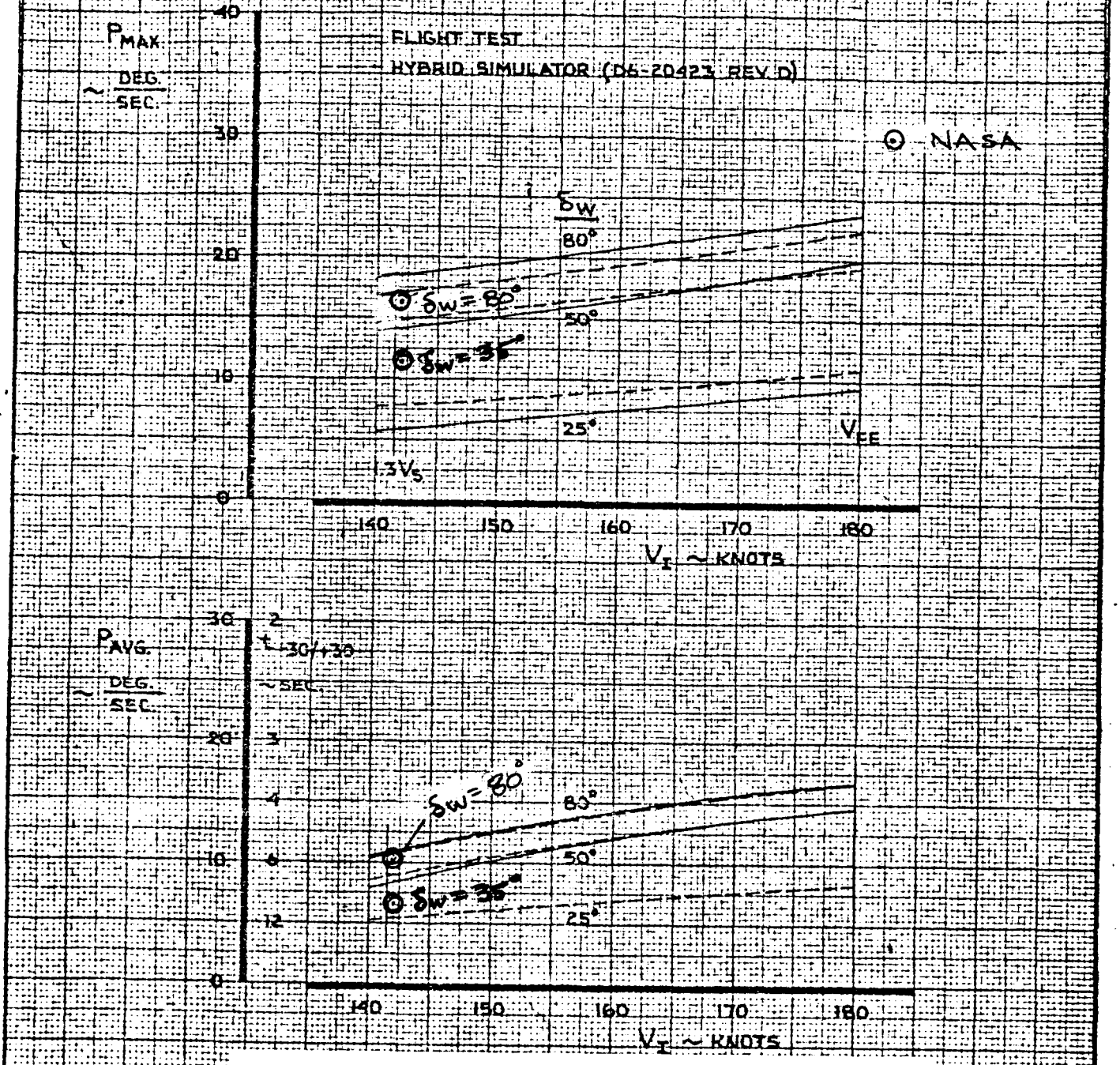

CALC	KUPCIS	4-30-70	REVISED	DATE	ROLL RATE CAPABILITY FLAPS 30
CHECK					
APR					
APR					
INK	KINSMAN	5-14-70			THE BOEING COMPANY

747
D6-30643 Vol. II
PAGE 14.2-28

AD 461 C-R4

K+E ALBANY, N.Y. 1961

14.2.8 AIR MINIMUM CONTROL SPEED

Minimum control speed in the air is defined as the lowest speed at which an airplane can maintain straight flight with a critical engine failed, rudder at full deflection, and bank angle at 5 degrees (dead engine high). The results from the NASA test are plotted on Page 14.2-30.

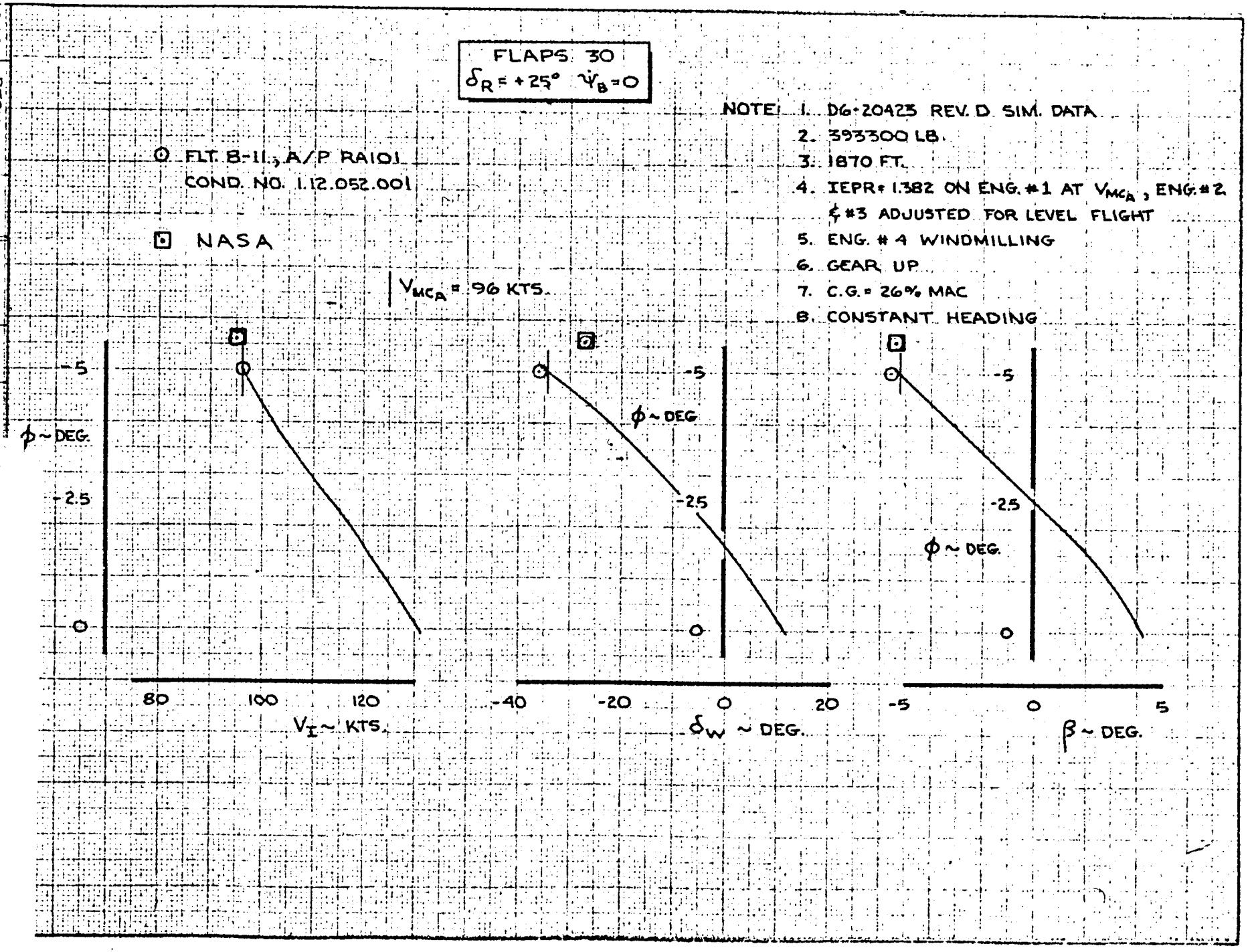

	CALC	CHECK	APR	APR
BECK				
GLENN				
5-26-70				
5-27-70				

REVISED	DATE

THE BOEING COMPANY

MINIMUM CONTROL SPEEDS

V_{MC_A}

747

D6-30643 Vol. II

PAGE 14.2-30

15.0 APPENDIX A - FLIGHT MANUAL

Selected pages from the performance section of the FAA approved airplane flight manual are contained in this section. This information will allow the simulation to be operated in compliance with the appropriate performance criteria and certification requirements of FAR Part 25 and Part 36.

BOEING 747

FAA APPROVED

AIRPLANE FLIGHT MANUAL

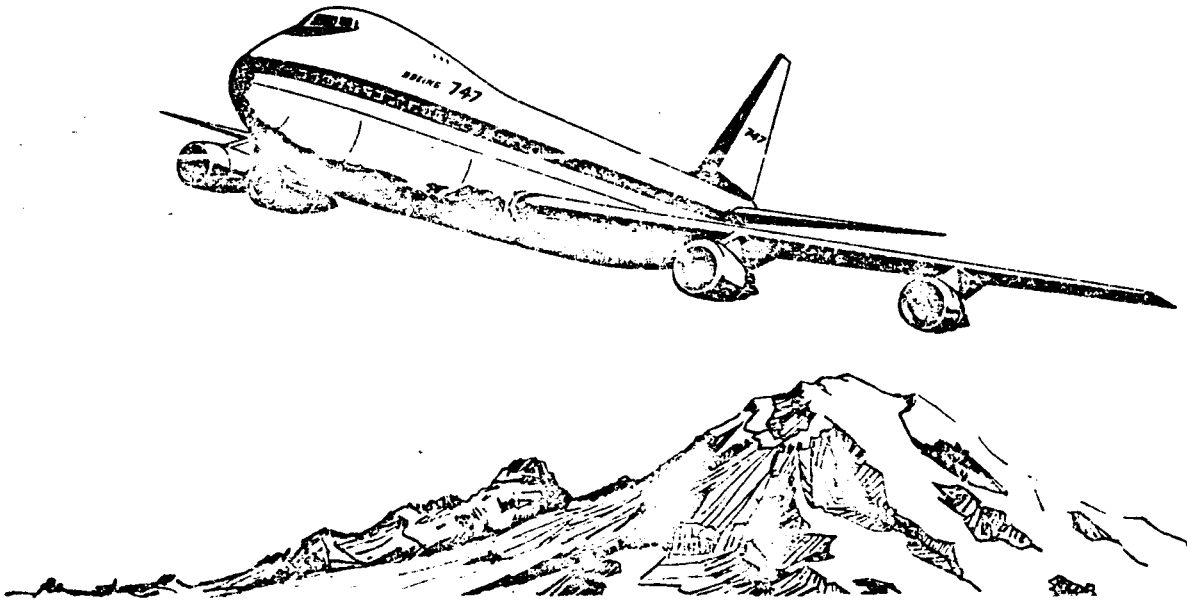

THIS AIRPLANE MUST BE OPERATED IN COMPLIANCE WITH THE PRESCRIBED CERTIFICATE LIMITATIONS IN SECTION 1 HEREIN

Approved by: Robert H. Johnson

Chief, Aircraft Engineering Division,
FAA, WESTERN REGION

Date December 30, 1969

D6-13703

PUBLISHED BY THE BOEING COMPANY, COMMERCIAL AIRPLANE GROUP, RENTON, WASHINGTON U.S.A.

SECTION 4 - PERFORMANCE

GENERAL

REGULATORY COMPLIANCE

The information in this section is presented for compliance with the appropriate performance criteria and certification requirements of FAR Part 25 and Part 36.

STANDARD PERFORMANCE CONDITIONS

All performance in this section is based on the following:

1. Approved engine thrust ratings less installation losses, airbleed and accessory losses.
2. Full temperature accountability within the operational limits, except for landing distance, which is based on standard day temperatures.
3. Trailing edge flaps positions as follows:

	Trailing Edge Flaps
Takeoff	10, 20
Transition Flap Setting	1, 5
Enroute	0
Approach	20
Landing	25, 30

4. Leading edge devices in the appropriate position for trailing edge flap position.

VARIABLE FACTORS AFFECTING PERFORMANCE

Details of the variable factors affecting performance are given under performance configuration, but certain assumptions relating to all performance data are as follows:

ICING PROTECTION

The effect of anti-icing systems operation is shown on applicable charts.

HUMIDITY

Humidity has no appreciable effect on the thrust of the engines; therefore, it has not been considered in the performance data.

WIND

The wind velocity used in calculations is factored to assure compliance with the relevant operating regulations. All charts should be entered with actual tower-reported wind components.

GENERAL

DEFINITIONS

AIRSPEEDS

All airspeed and Mach values in this manual assume a zero instrument error.

All Indicated Airspeeds are based on normal static source position error.

Position error is the instrument indication error due to location of static ports.

Equivalent Airspeed, EAS - Airspeed indicator reading, as installed in the airplane, corrected for static source position error and compressibility.

Calibrated Airspeed, CAS - Airspeed indicator reading, as installed in the airplane, corrected for static source position error.

Indicated Airspeed, IAS - Airspeed indicator reading, as installed in the airplane, uncorrected for static source position error.

True Mach Number, M - Machmeter reading, as installed in the airplane, corrected for static source position error.

Critical Engine Failure Speed, V1 - The speed at which, when an engine failure is recognized, the distance to continue the takeoff to a height of 35 feet will not exceed the usable takeoff distance; or, the distance to bring the airplane to a full stop will not exceed the accelerate-stop distance available. V1 must not be less than the Ground Minimum Control Speed, VMCG, or greater than the rotation speed, VR, or greater than the maximum brake energy speed, VMBE.

Engine Failure Speed Ratio, V1/VR - The ratio of the engine failure speed, V1, for actual runway dimensions and conditions, to the rotation speed, VR.

Maximum Brake Energy Speed, VMBE - The maximum speed on the ground from which a stop can be accomplished within the energy capabilities of the brakes.

GENERAL

DEFINITIONS

AIRSPEEDS (Continued)

Rotation Speed, VR - The speed at which rotation is initiated during the takeoff.

Takeoff Safety Speed, V2 - The scheduled target speed to be attained at the 35 foot height with one engine inoperative.

Air Minimum Control Speed, VMCA - The minimum flight speed at which the airplane is controllable with a maximum of 5° bank when the critical engine suddenly becomes inoperative with the remaining engines at takeoff thrust.

Ground Minimum Control Speed, VMCG - The minimum speed on the ground at which the takeoff can be continued, utilizing aerodynamic controls alone, when the critical engine suddenly becomes inoperative with the remaining engines at takeoff thrust.

Landing Reference Speed, VREF - The minimum speed at the 50 foot height in a normal landing. This speed is equal to 1.3 times the stall speed in the landing configuration.

Design Maneuvering Speed, VA - The maximum speed at which application of full available aileron, rudder or elevator will not overstress the airplane.

G E N E R A L

DEFINITIONS (Continued)

TEMPERATURE

ISA - International Standard Atmosphere, as accepted by the International Civil Aviation Organization.

OAT - Outside Air Temperature - the free air static (ambient) temperature.

SAT - Static Air Temperature - outside air (ambient) temperature as computed by the Air Data Computer and presented on the Static Air Temperature indicator.

TAT - Total Air Temperature - static air temperature plus adiabatic compression (ram) rise as indicated on the Total Air Temperature indicator.

WIND

Wind Velocity - The actual wind velocity at a 50 foot height reported from the tower and corrected by the wind component chart to a headwind or tailwind component parallel to the flight path.

HEIGHT

Gross Height - The geometric height attained at any point in the takeoff flight path using gross climb performance. Gross height is used for calculating actual pressure altitudes at which obstacle clearance procedures and wing flap retraction are initiated, and level-off-height scheduled.

Net Height - The geometric height attained at any point in the takeoff flight path using net climb performance. Net height is used to determine the net flight path which must clear any obstacles by at least 35 feet to comply with the regulations.

ICING

Icing Conditions - Icing may develop when visible moisture such as fog, rain, or wet snow is present with Static Air Temperature below 8°C (46°F).

TAKEOFF DATA

Balanced Field Length - The condition where V1 is selected to make the takeoff distance equal to the accelerate-stop distance.

Unbalanced Field Length - The condition where V1 is selected to make the takeoff distance and accelerate-stop distance unequal.

GENERAL

GRADIENT OF CLIMB

Gross Gradient - The demonstrated ratio, expressed as a percentage, of:

$$\frac{\text{Change in Height}}{\text{Horizontal Distance Traveled}}$$

The gradients shown on the charts are true gradients, i.e., they are based on true, not pressure, rates of climb.

Net Gradient - The demonstrated gross gradient reduced by the increment as required by regulation.

BUFFET ONSET CHARACTERISTICS

The buffet boundary is a basic characteristic of the airplane that is defined by angle of attack and Mach numbers. Below approximately 0.85 M, the buffet is related to the wing maximum lift capability (therefore to true airplane stall). In the range above 0.85 M, buffet is related to the growth of shock waves on the wing.

At any flight condition, it is possible to determine the altitude, low-speed, high-speed, and maneuvering margins before buffet onset occurs. (See Cruise Maneuvering Capability chart.)

CROSSWIND VALUES (Takeoff and Landing)

The maximum demonstrated crosswind component is 30 knots reported wind at 50 foot height. This component is not considered to be limiting.

For performance scheduling, the full headwind component may be used provided that the corresponding crosswind component does not exceed 30 knots.

MINIMUM CONTROL SPEEDS

The Air Minimum Control Speeds (VMCA), and the Ground Minimum Control Speeds (VMCG), of this airplane are shown on a chart in this Section, and on the takeoff Speeds charts where applicable.

PERFORMANCE CONDITIONS AND PROCEDURES

Takeoff field length performance shown in this section accounts for 115 percent of the all-engines operating distance, or the total distance considering an engine failure recognition at V1, whichever is greater. These distances are based on a smooth, dry, hard-surfaced runway.

The appropriate airplane configuration, outlined under Performance Configurations, was used.

The conditions and procedures used in establishing the performance data in this manual are presented under each phase of operation. Procedures are guidance material only. R

TAKEOFF

Conditions

Prior to takeoff, a review was made of stabilizer and flap settings, takeoff speeds, and that sufficient field length was available for the gross weight and ambient conditions. Corrections were applied, when necessary, for significantly altered ambient conditions or loading.

Procedures

Thrust was set to 1.1 EPR prior to brake release, or as the airplane was aligned with the runway. With no wind, or a direct headwind, EPR was advanced prior to brake release. Thrust levers were adjusted as necessary to obtain target EPR values by approximately 40 to 80 knots on the takeoff roll.

Rudder pedals were used for directional control through the nose wheel and rudder.

Rotation to takeoff attitude was initiated at VR. A speed not less than V2 was obtained at a height of 35 feet. The landing gear was retracted after a positive rate of climb was established.

A smooth positive rotation was used to the initial climb attitude (approximately 13 to 22 degrees depending upon gross weight and thrust available). Minor attitude variations were made after liftoff to achieve the initial climb speed. Engine failure results in approximately 2 to 2-1/2 degrees lower attitude than normal climb.

NOTE: With center of gravity at or near the aft limit, avoid sudden brake release and maintain forward pressure on the control column to approximately 80 knots to increase nose wheel steering effectiveness.

PERFORMANCE CONDITIONS AND PROCEDURES

REFUSED TAKEOFF (Anti-Skid On)

Conditions

Calculated accelerate-stop distances account for demonstrated recognition and reaction times, plus arbitrary time delays.

Reverse thrust was not used.

Procedures

When an engine failure occurred, the takeoff was refused when the failure was recognized prior to V1.

If the takeoff was refused for any reason, prior to V1, the following procedure was accomplished as rapidly as possible:

Wheel Brakes - MAXIMUM BRAKING APPLIED
All Thrust Levers - IDLE
Speed Brakes - UP

CLIMB-OUT (3 or 4 Engines)

Conditions

Climb gradient and obstacle clearance flight path performance is based on the most critical engine inoperative at V1.

Procedures

Takeoff flap setting and V2 speed were maintained to at least the height selected for initiation of flap retraction. R

Flaps were retracted according to the Flap Retraction Speed Schedule, in this section.

Enroute procedures were followed after climbing to at least 1500 feet above runway elevation, or after all takeoff flight path obstacles had been cleared.

PERFORMANCE CONDITIONS AND PROCEDURES

OBSTACLE CLEARANCE

Conditions

With all engines operating, a speed not greater than V2 + 10 knots was maintained until either the scheduled flap retraction height, or the minimum gross height for obstacle clearance (whichever was lower), was reached.

When engine failure occured prior to V2, and the takeoff weight was obstacle limited, V2 was maintained up to the gross height required for obstacle clearance.

If an engine failure occured after V2, speed at engine failure (V2 + 10 knots maximum) was maintained up to the gross height required for obstacle clearance.

Procedures

When the height selected for initiation of flap retraction was limited due to distant-obstacle considerations, the procedure was to initiate flap retraction and accelerate to final takeoff climb speed while maintaining constant altitude and initial takeoff thrust setting.

Final takeoff climb was continued to 1500 feet above runway elevation, or to the minimum gross height required for obstacle clearance, at final takeoff climb speed and maximum continuous thrust.

NOTES: The airplane should be levelled off, and flaps retracted at the selected level-off height, only if the limiting obstacle is beyond the Third Segment and an engine failure has occurred.

The height selected for initiation of flap retraction may be limited by available performance as described under Takeoff Flight Path, this section. Vertical clearance of either close-in or distant obstacles in the intended flight path must be established by reference to the appropriate obstacle clearance charts.

PERFORMANCE CONDITIONS AND PROCEDURES

LANDING FIELD LENGTH

Conditions

All landing field lengths shown in this section are based on standard day temperatures on a smooth, level, hard-surfaced runway. Dry landing field lengths are demonstrated landing distances, from a 50 foot height at VREF, divided by a factor 0.6. Wet landing field lengths are determined by multiplying the dry landing field length by a factor of 1.15.

Procedures

Approach and landing were made with landing gear down, flaps in landing position, thrust reduced to flight-idle on all engines before touch-down, and automatically set to ground-idle on all engines after touch-down.

When the landing was made with anti-skid operating, full speed brakes and maximum wheel braking were applied 2 seconds or less after touch-down.

When the landing was made with anti-skid inoperative, speed brakes were raised immediately upon touch-down and steady, light braking was used if gross weight was approximately 500,000 lb (226,800 kg.) or less. Steady, light to moderate braking was used if landing weight was over 500,000 lbs (226,800 kg.). Brakes were modulated as necessary to prevent skidding. R

NOTE: Landing field lengths are not based on use of reverse thrust.

FLAP RETRACTION SPEED SCHEDULE

Maximum level-off heights, Third Segment distances and Final Segment climb performance shown in this manual are based upon retracting the wing flaps during Third Segment acceleration using the schedule below. This schedule is recommended for all normal flap retraction operations.

During acceleration, select flap positions at the following initiation speeds:

TAKEOFF FLAPS POSITION 10 OR 20

Initiation Speed, Knots	Select Flap Position
V2 + 20	10
V2 + 40	5
V2 + 60	1
V2 + 80	0

Final Segment Climb Speed: V2 + 80 Knots.

When flaps are being retracted at a constant altitude due to engine failure, with a critical final segment obstacle, begin climbing when V2 + 80 knots is achieved, maintaining takeoff thrust setting until flaps are completely retracted. R

PERFORMANCE CONFIGURATION

The airplane configuration associated with the performance data in this manual is shown below. Performance conditions not shown below are on the appropriate charts.

	THRUST	FLAPS	GEAR
TAKEOFF	Takeoff on all engines to V1, and three engines subsequent to V1.	Takeoff setting. Noted on charts.	Down
1st SEGMENT CLIMB	Takeoff on operating engines (3).	Same as takeoff.	Down
2nd SEGMENT CLIMB	Same as 1st segment.	Same as takeoff.	Up
3rd SEGMENT	Same as 1st segment.	Takeoff setting to flaps up, according to schedule.	Up
FINAL TAKEOFF CLIMB	Maximum continuous on operating engines (3).	Up	Up
ENROUTE CLIMB	Maximum continuous on operating engines (3 or 2).	Up	Up
APPROACH CLIMB	Takeoff on operating engines (3).	Approach setting. Noted on chart.	Up
LANDING CLIMB	Maximum available in 8 seconds on all engines.	Landing setting. Noted on chart.	Down
LANDING	Ground idle on all engines after touchdown.	Landing setting. Noted on chart.	Down

Anti-skid is on for takeoff and landing with up to two brakes deactivated, unless anti-skid inoperative braking performance is used.

One or three Air Conditioning Packs are on for all takeoff thrust operations. R

All three Air Conditioning packs are on for final takeoff climb. For enroute climb the number of the Air Conditioning packs on is noted on the charts. R

Wing anti-icing is off during all flaps-extended operations.

NOISE CHARACTERISTICS R

No determination has been made by the Federal Aviation Administration that the noise levels in this manual are, or should be, acceptable or unacceptable for operation at, into, or out of, an airport.

The noise levels tabulated below are the result of Federal Aviation Regulations, Part 36 certification tests:

GROSS WEIGHT		FLAPS	NOISE LEVEL (EPNdB)		
Pounds	Kilograms	Position	Takeoff	Sideline	Approach
			3.5 nautical miles	0.35 nautical mile	1.0 nautical mile
710,000	322,056	10	115.0	101.9	---
673,000	305,273	20	114.5	101.9	---
564,000	255,830	30	---	---	113.6

The traded noise level is 112.0 EPNdB

Normal all engines takeoff procedures were used, with a climb-out at V2 + 10 knots at Takeoff Thrust with no thrust cut-back. The landing approach was made at VREF + 10 knots.

ENVIRONMENT ENVELOPE

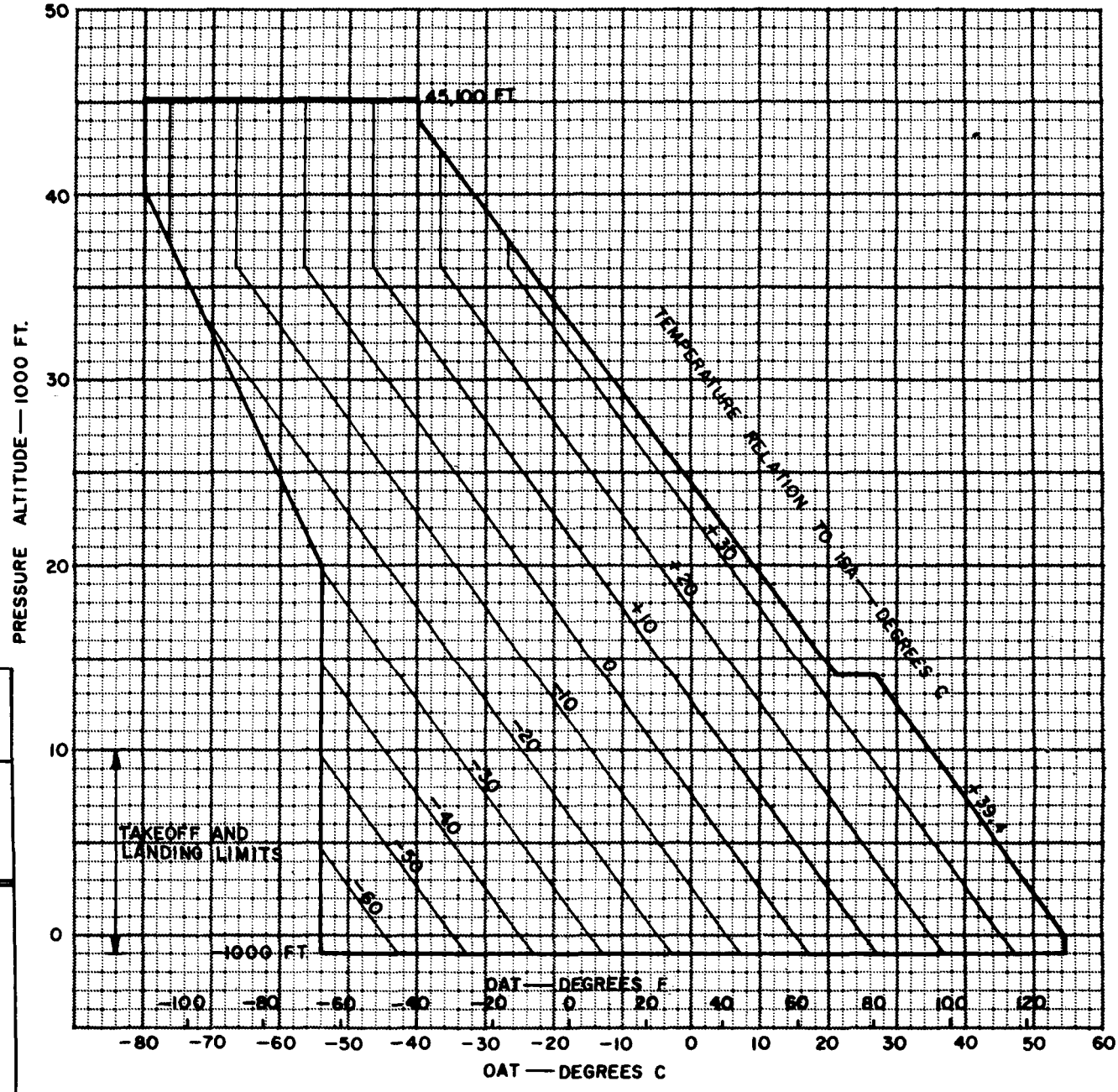

CHART APPLICABLE TO	APPROVED	DATE
747	FAA LA-274	12-23-69

12

WIND COMPONENT

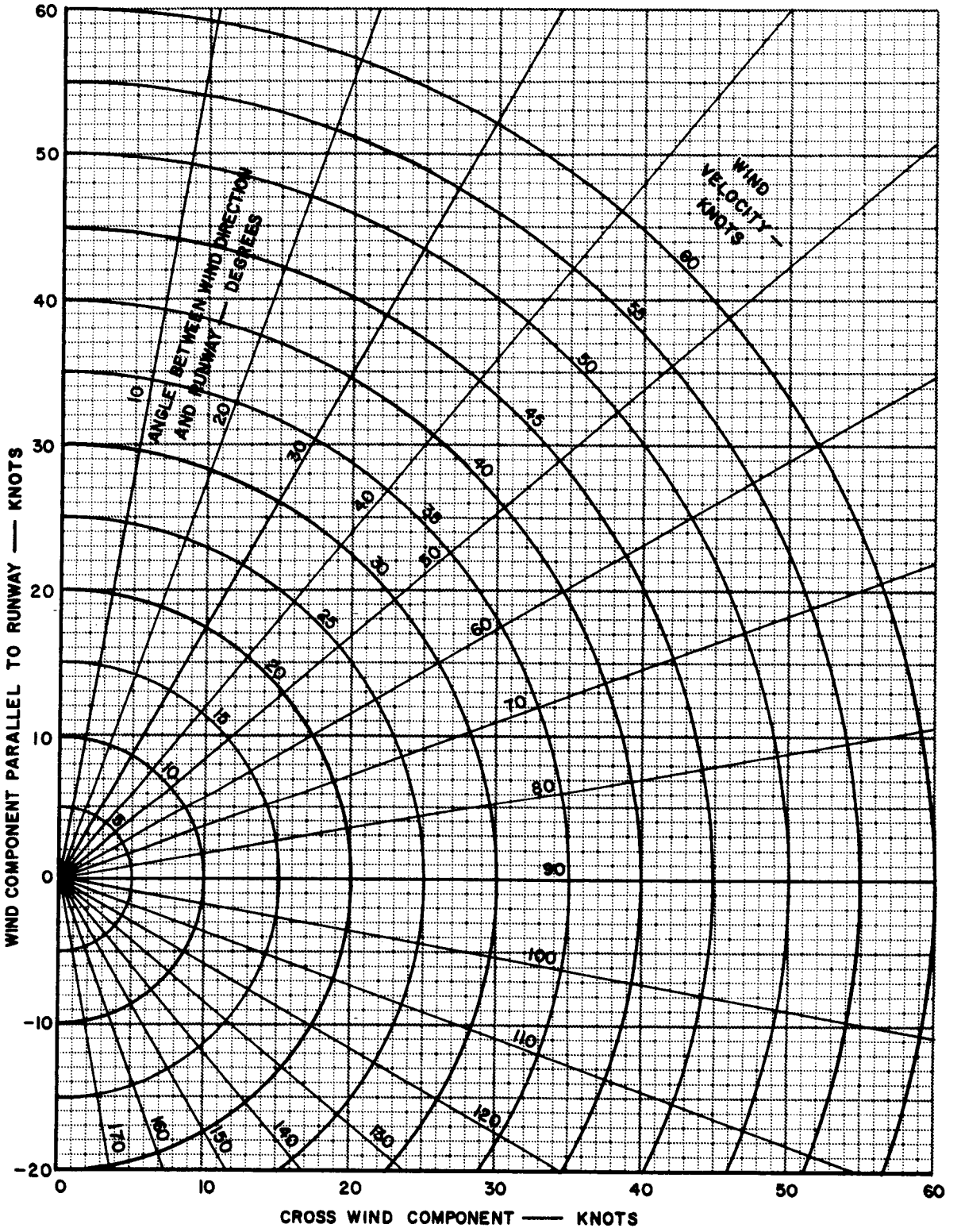

SCHOEN 1-7-69

FAA APPROVED 12-30-69

PERFORMANCE

TAKEOFF EPR

40-80 KNOTS

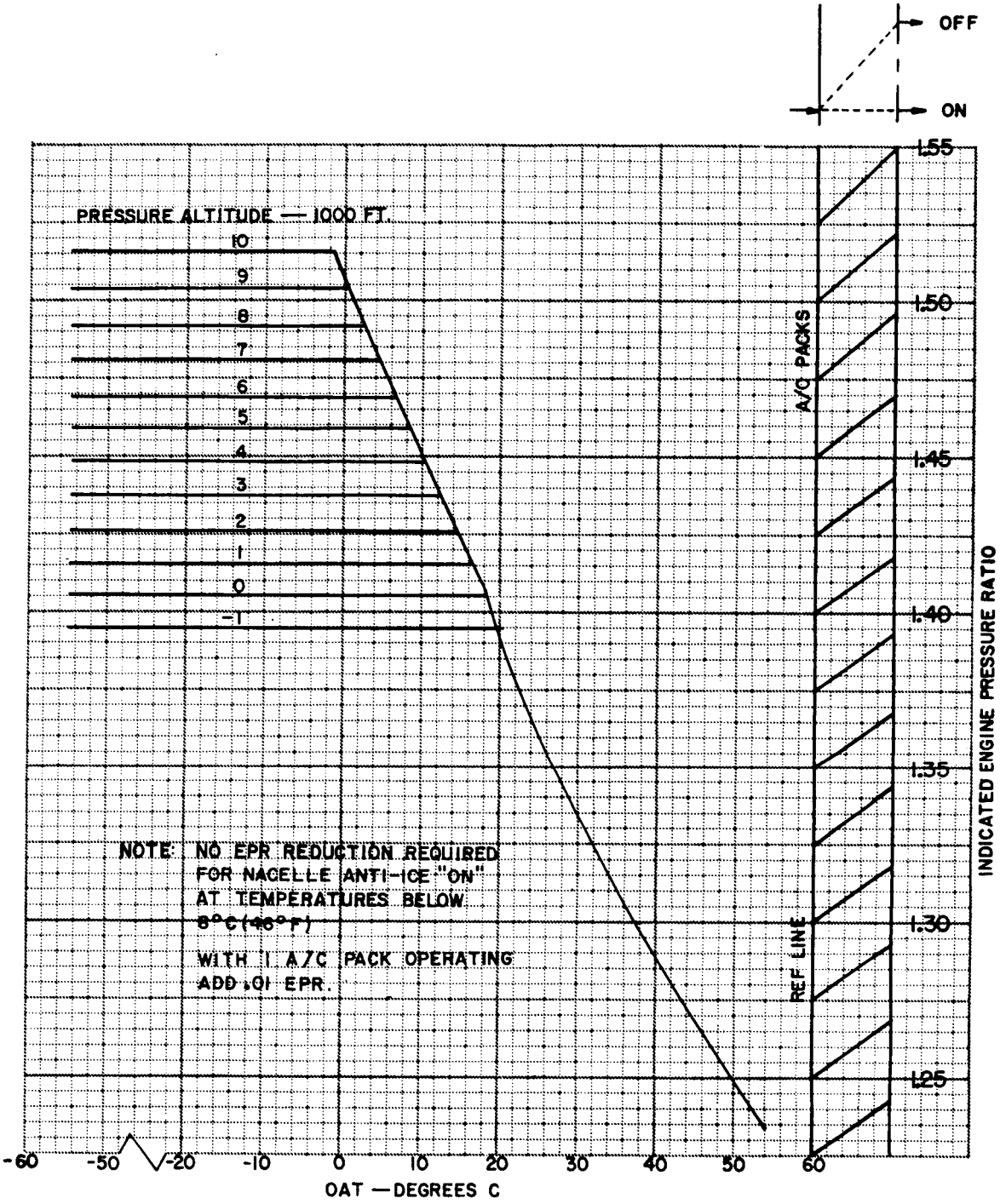

CHART APPLICABLE TO	APPROVED	DATE
747-100 JT9D-3	H.Y. Chow LA-377	12/10/69

PERFORMANCE

TAKEOFF EPR

GO-AROUND

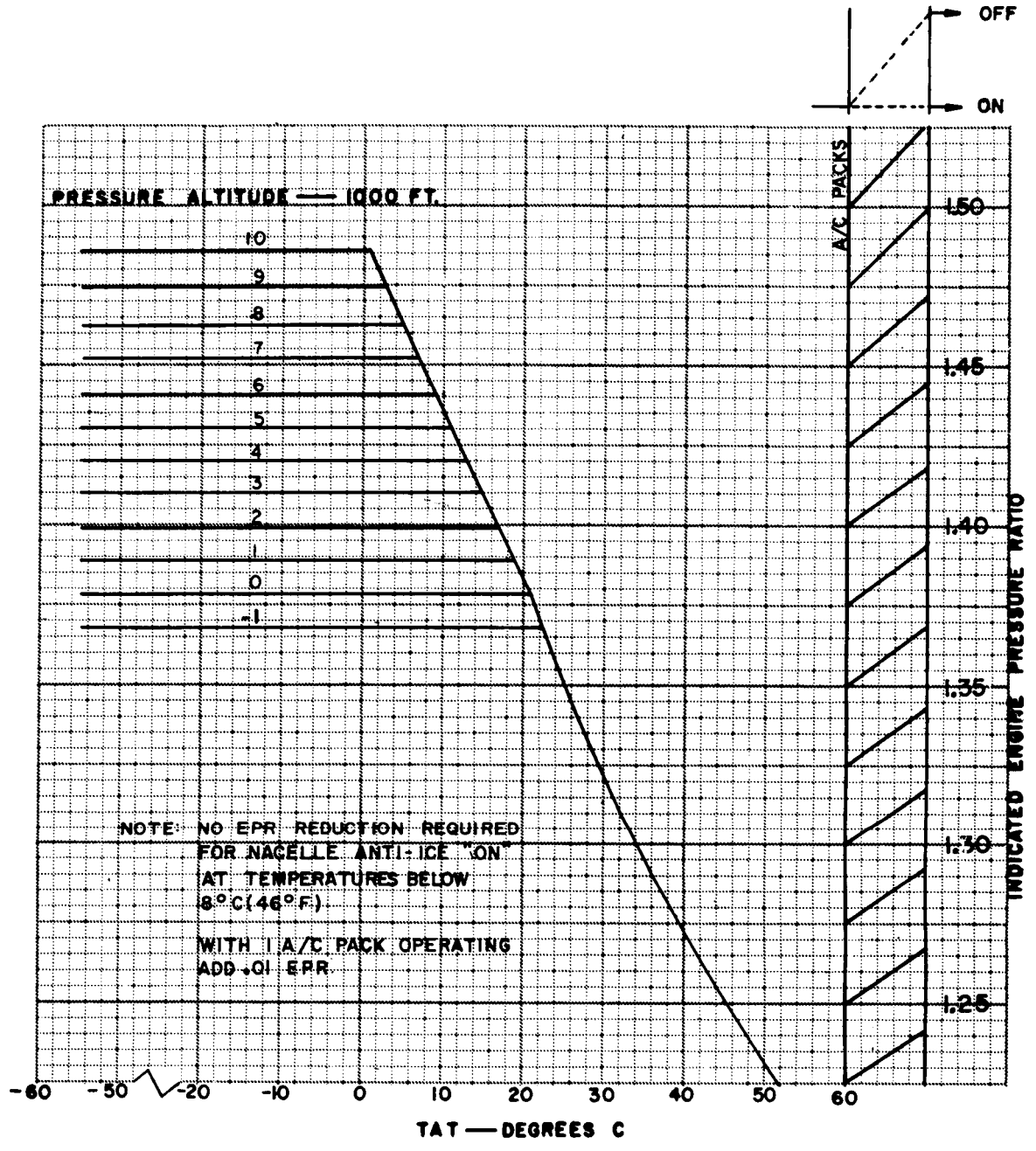

CHART APPLICABLE TO	APPROVED	DATE
747-100 JT9D-3	H.Y. Chdw LA-377	12/10/69

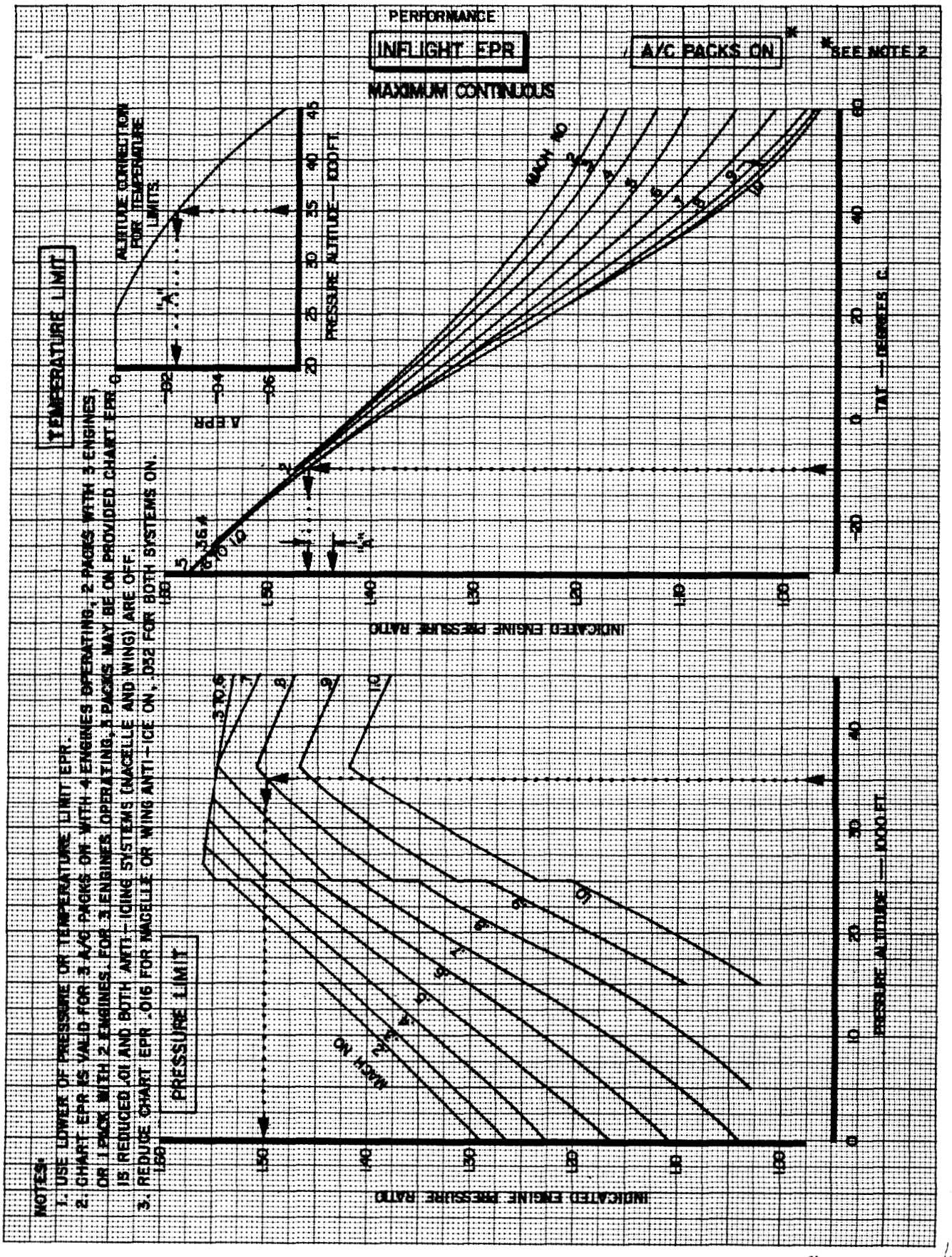

CHART APPLICABLE TO	APPROVED	DATE
747-100 JT9D-3	OBS LA	4/14/69

BASSETT 11-18-69

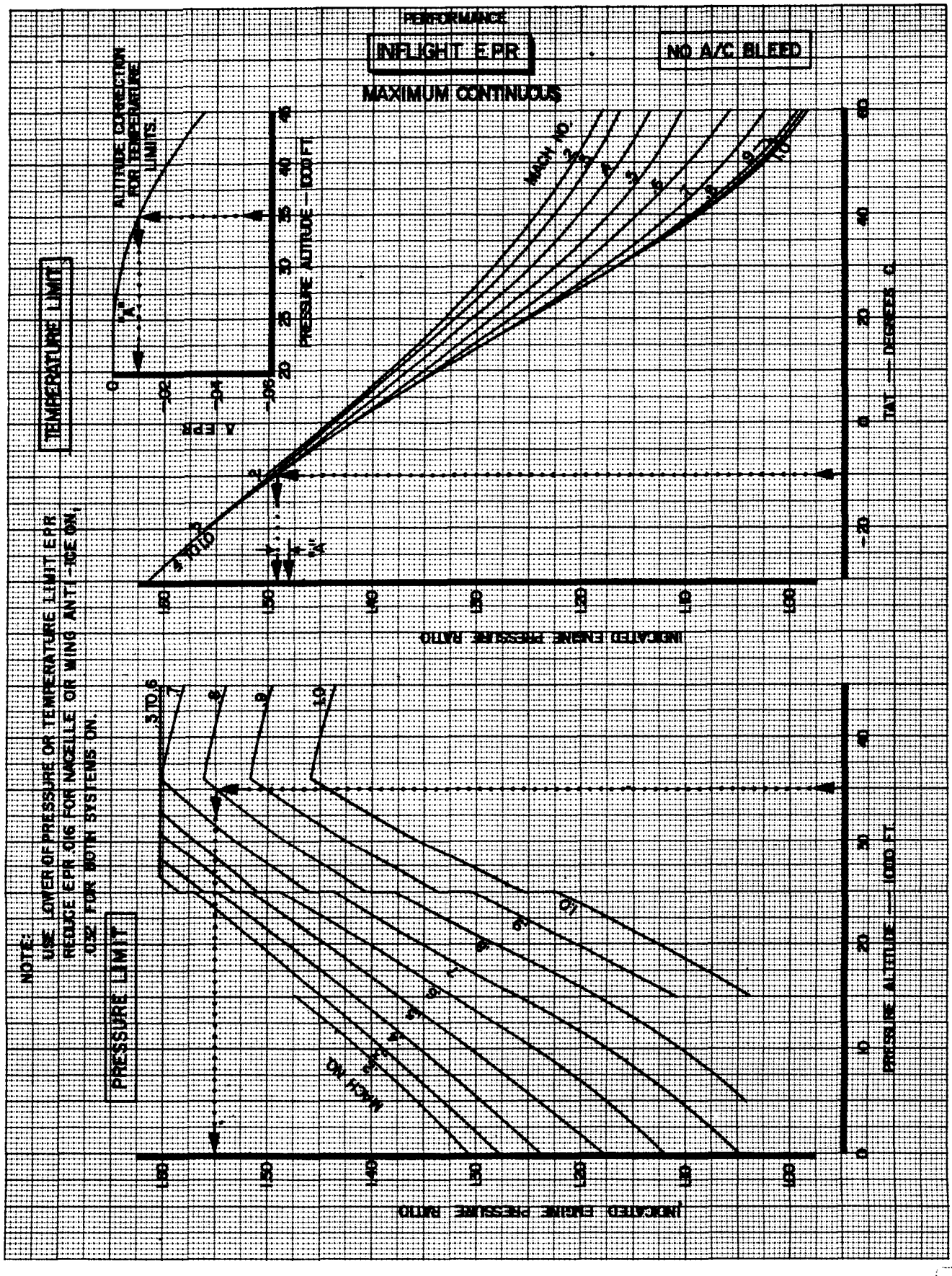

BASSETT 11-18-69

CHART APPLICABLE TO	APPROVED	DATE
747-100 JT9D-3	ORIG LA 457	4/27/65

RECOMMENDED TAKEOFF STABILIZER SETTING

USE FOR ALL TAKEOFF FLAP SETTINGS

SET STABILIZER FOR TAKEOFF CENTER OF GRAVITY DETERMINED BY CALCULATED OR GRAPHICAL METHOD, WITH GEAR DOWN AND WITH TAKEOFF FLAPS.

$\Delta_p = 3 - \Delta_{FRL}$ $\Delta_{FRL} = 3 - \Delta_p$

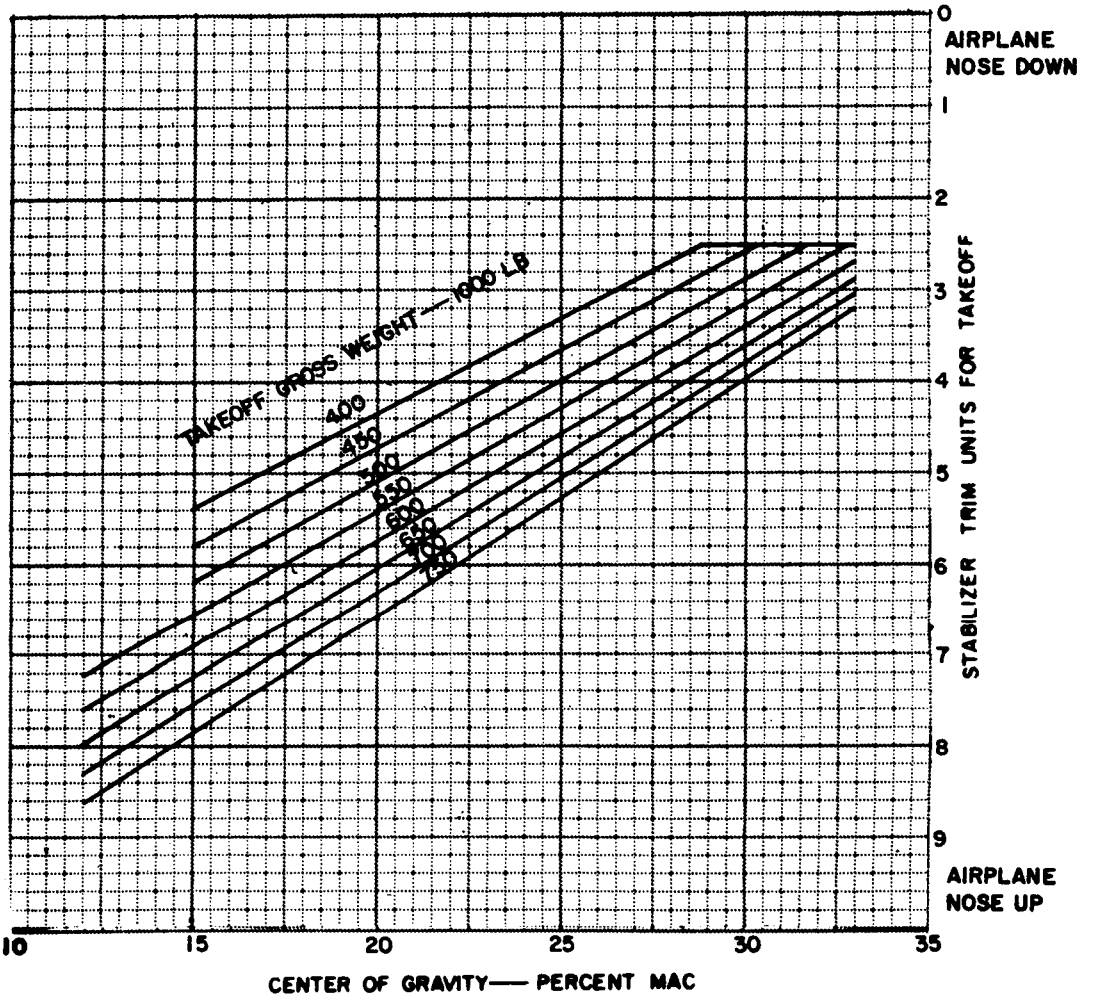

CHART APPLICABLE TO	APPROVED	DATE
747-100		2-10-70

PERFORMANCE

TEMPERATURE CONVERSION

TOTAL AIR — STATIC AIR

HEATED ROSEMOUNT PROBE

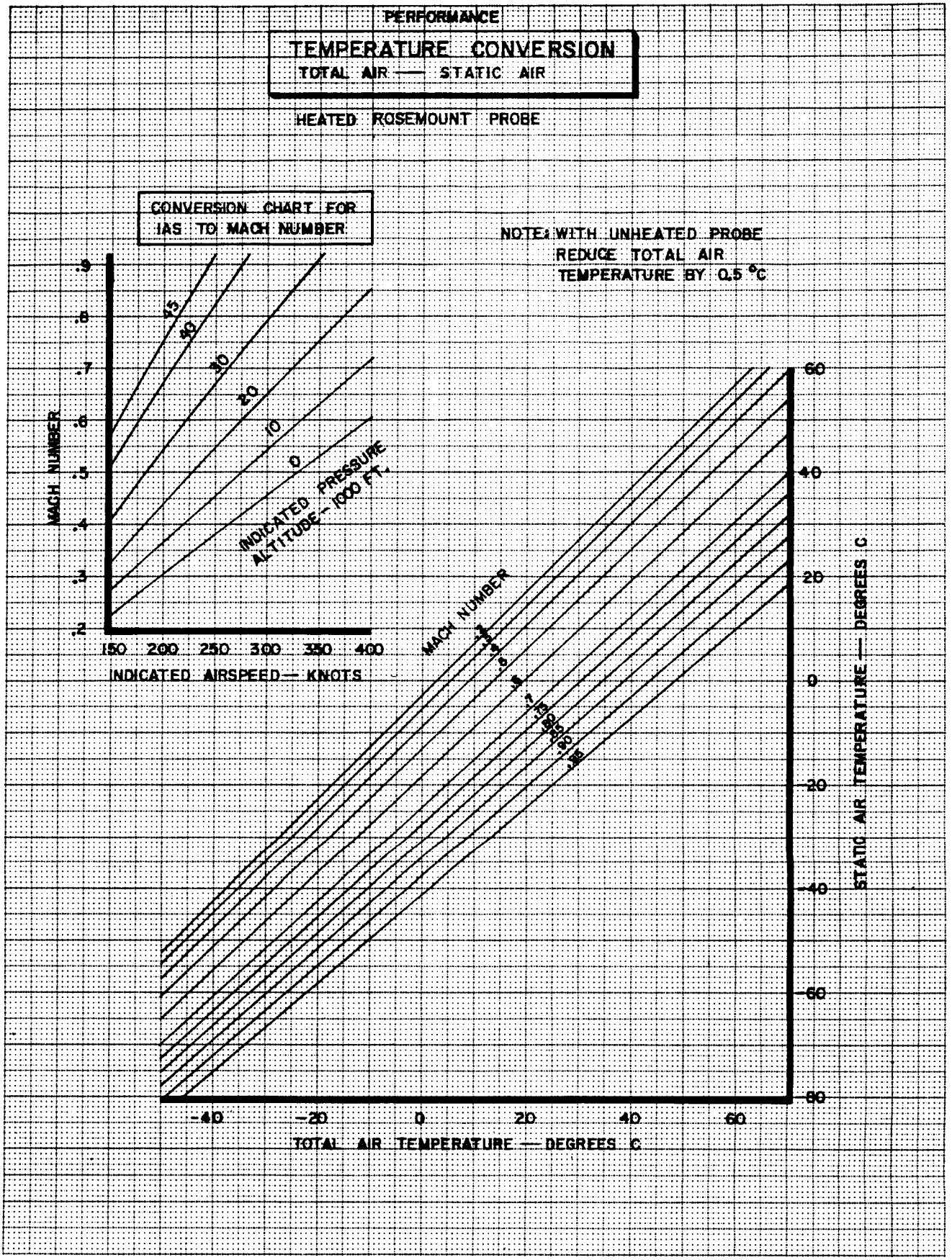

CHART APPLICABLE TO	APPROVED	DATE
747	FAA LA-411	3-27-70

PERFORMANCE

MINIMUM CONTROL SPEEDS

V_{MCG}

1 ENGINE INOPERATIVE

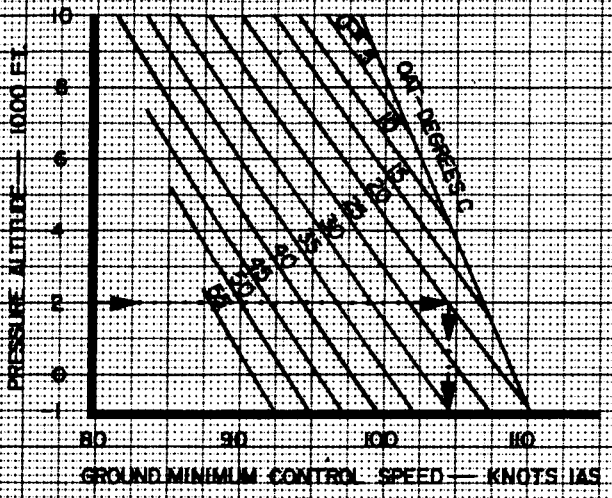

V_{MCA}

1 ENGINE INOPERATIVE

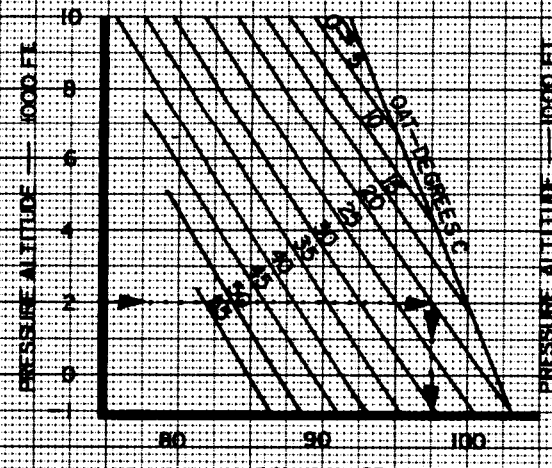

2 ENGINES INOPERATIVE

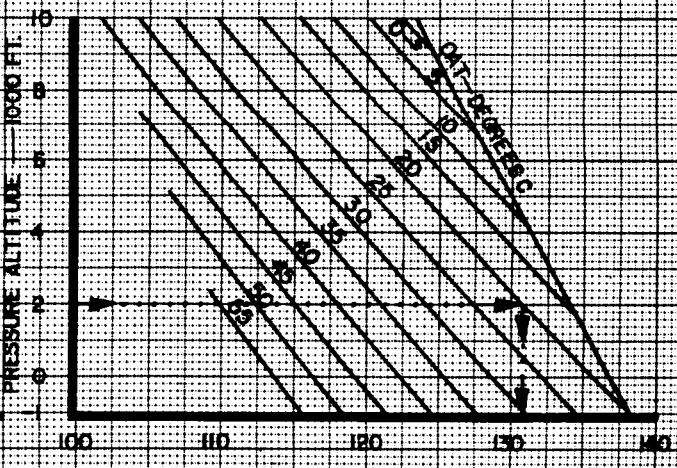

CHART APPLICABLE TO	APPROVED	DATE
747-100 JT9D-3	B² LA-274	12-9-69

BEER 12·9·69

STALL SPEEDS

NOTE APPLICABLE FOR TAKEOFF AND LANDING ALTITUDES ONLY.

GEAR UP EXCEPT AS NOTED

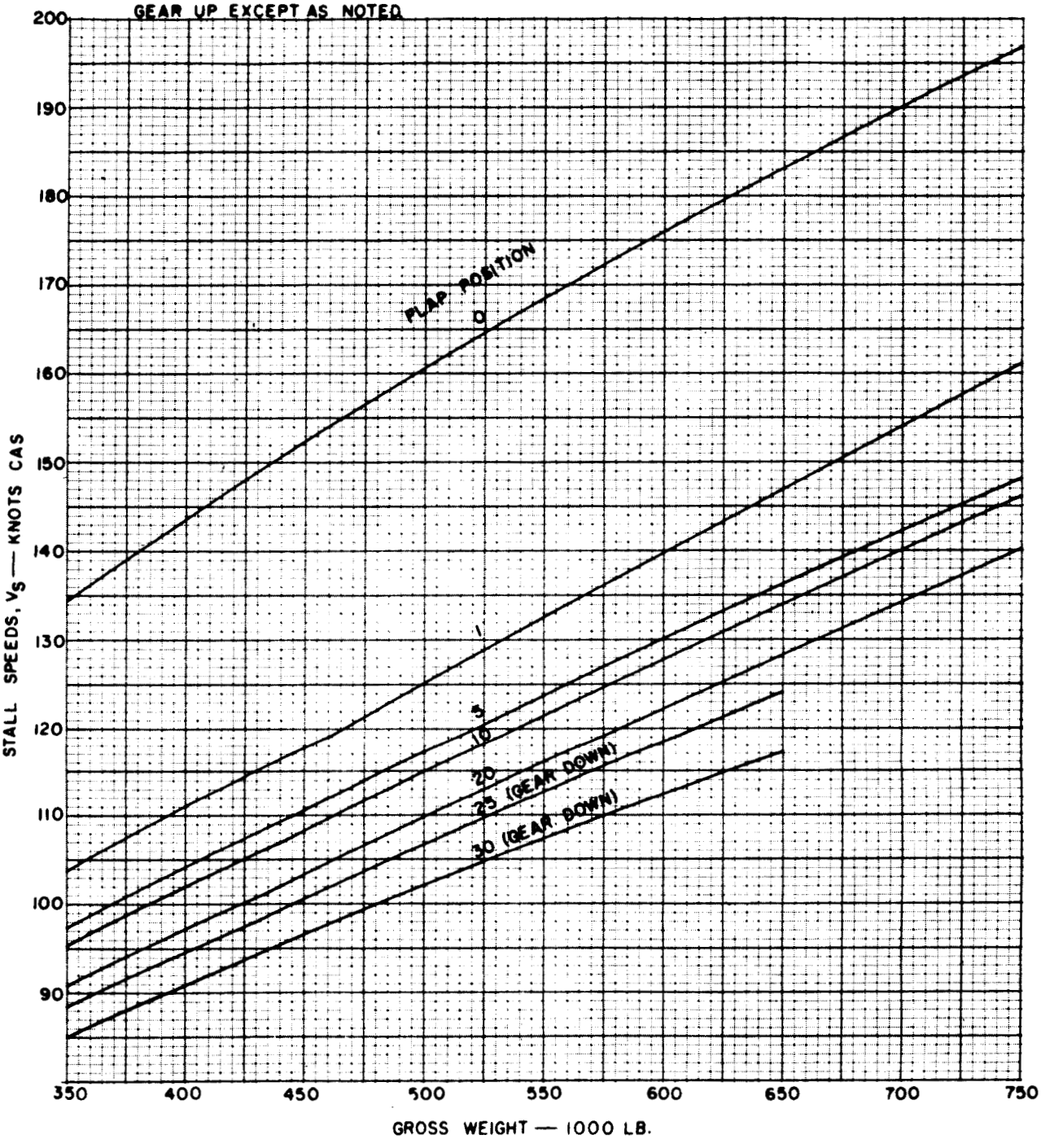

CHART APPLICABLE TO	APPROVED	DATE
747-100	LA-274	11-22-69

PERFORMANCE

CRUISE MANEUVERING CAPABILITY

FLAPS AND GEAR UP

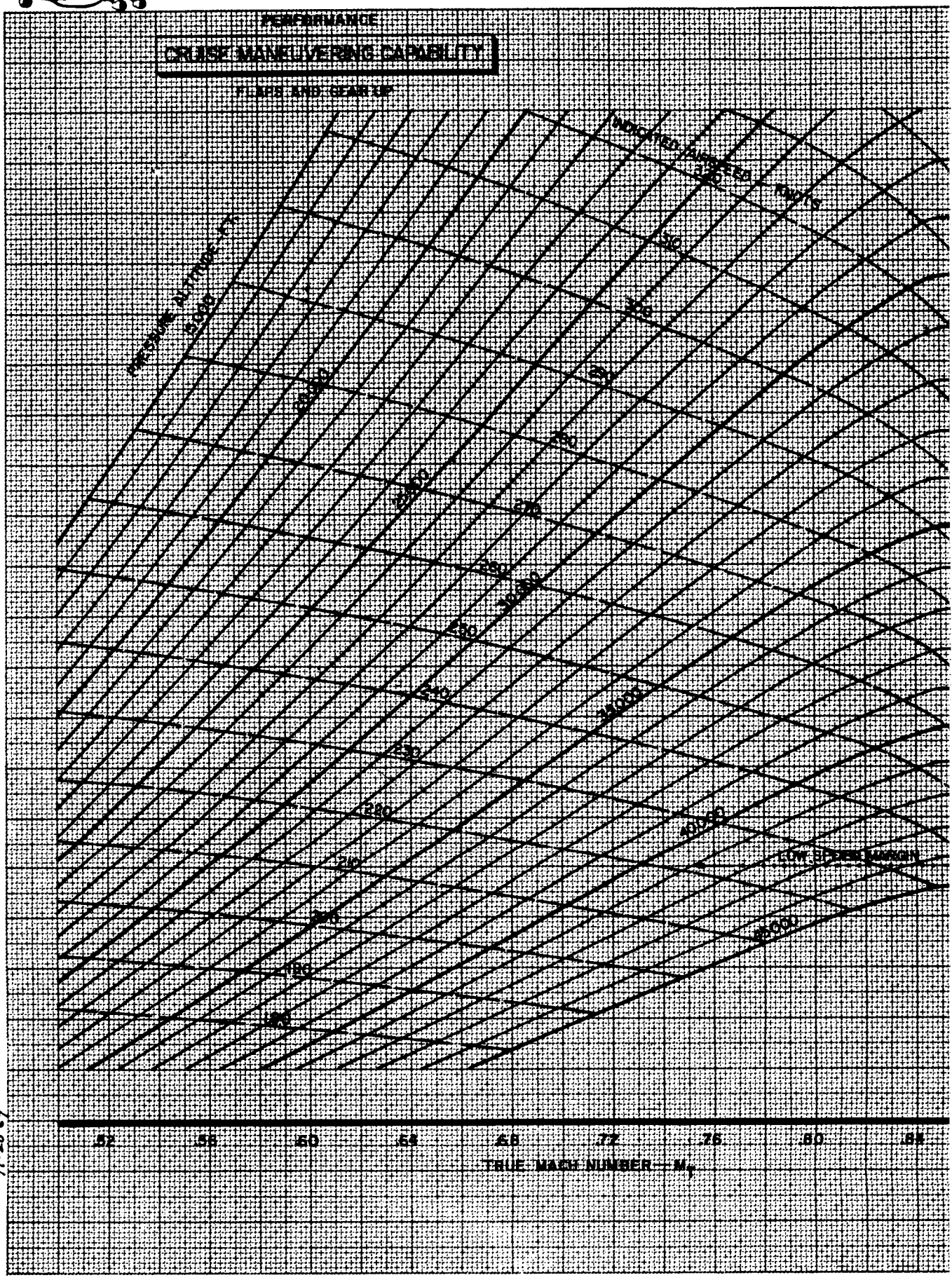

CALC	HORN	11-25-69	REVISED	DATE
CHECK	H. GINTER	11-26-69		
747-100	JT9D-3			

BL LA-274 11-28-69

MAXIMUM ALLOWABLE TAKEOFF WEIGHT

NORMAL TAKEOFF WEIGHT ANALYSIS

CHART READING PROCEDURE

The following steps will be adequate for most takeoff situations. The dotted guide-lines on typical charts and the Illustrative Examples are for guidance purposes.

1. Select most probable takeoff flap setting.

2. Runway Length Corrections (All Engines) chart - Enter with actual runway length available. Make slope and wind corrections. Read corrected runway length.

3. Runway Length and V1 Adjustments chart - Enter with actual runway length available on both the Runway Length, and Accelerate-Stop Distance scales. Make slope and wind corrections from the respective reference lines. Where the two corrected distances intersect on the "web" portion of the chart, read V1/VR, and corrected runway length.

4. Maximum Takeoff Weight, Field Length Limits chart - Enter with the lesser of the corrected runway lengths from Step 2 or Step 3, airport pressure altitude, and temperature. Read gross weight.

5. Maximum Takeoff Weight, Climb Limits chart - Enter with airport pressure altitude and temperature. Read gross weight.

6. IF 200 MPH TIRES ARE INSTALLED, USE:
   Maximum Takeoff Weight, Tire Speed chart - Enter with airport pressure altitude and temperature. Make wind correction. Read gross weight.

NOTE: If obstacles are present, proceed with Steps 7 through 10.

MAXIMUM ALLOWABLE TAKEOFF WEIGHT

NORMAL TAKEOFF WEIGHT ANALYSIS

CHART READING PROCEDURE (Continued)

7. Takeoff Climb chart - Enter with least gross weight determined by Steps 4, 5, 6, structural limits, or operational requirements, then proceed to temperature and airport pressure altitude. Read Second Segment gradient. Correct the gradient for wind, if applicable, using Gradient Corrections chart.

8. Obstacle Clearance (Close-in Obstacles) chart - Enter with obstacle distance from end of takeoff distance required. Correct the distance for wind. Proceed vertically to zero-wind gradient available, from Step 7.

   (a) If this exceeds obstacle height, obstacle is cleared.
   (b) If obstacle height is not exceeded, follow dashed field-length-trade guide lines to obstacle height. Read gradient required for obstacle clearance. This gradient accounts for the shorter takeoff distances required when gross weight is reduced. (See SLOPED RUNWAY EFFECT ON OBSTACLE CLEARANCE).

9. Obstacle Clearance (Distant Obstacles) chart - Enter with obstacle distance from end of takeoff distance required. Proceed vertically to wind-corrected gradient available, from Step 7.

   (a) If this exceeds obstacle height, obstacle is cleared. However, now drop back down to obstacle height, then move left (horizontally) to wind-corrected gradient available. Read gross height.
   (b) If obstacle is not cleared at wind-corrected gradient available, follow dashed field-length-trade lines to the obstacle height. Read gross height and gradient required for obstacle clearance. Correct the gradient required to zero-wind gradient, on the Gradient Corrections chart. (See OBSTACLE IN THIRD SEGMENT, and OBSTACLE IN FINAL SEGMENT.)

MAXIMUM ALLOWABLE TAKEOFF WEIGHT

NORMAL TAKEOFF WEIGHT ANALYSIS

CHART READING PROCEDURE (Continued)

10. Takeoff Climb chart - Enter gradient scale with the largest zero-wind gradient required for obstacle clearance as determined from Step 8 or 9. Proceed to airport pressure altitude, and temperature. Read gross weight.

11. Takeoff Speeds chart - Enter with airport pressure altitude, temperature, and the least gross weight determined by Steps 4, 5, 6, 10, structural limits, or operating requirements. Read VR, and V2. Read V1 at the V1/VR ratio from Step 3. The resulting V1 must exceed the minimum V1 (VMCG), (See V1 Less than VMCG), and the resulting VR must exceed the VMCA limit. (See VR Less than VMCA Limit).

12. Maximum Brake Energy Limit Speed chart - Enter with airport pressure altitude, temperature, and gross weight used in Step 11. Correct for runway slope, and wind. Read VMBE. This speed must exceed V1 of Step 10. (See V1 Greater than VMBE).

13. Gross Height - Pressure Altitude Conversion chart - Enter with gross height obtained from Step 9. Correct for temperature and altitude. Read pressure altitude increment. Add this value to the airport pressure altitude. Acceleration and flap retraction should not be scheduled below this altimeter reading.

14. Determine flap retraction and final climb speeds from the FLAP RETRACTION SPEED SCHEDULE.

MAXIMUM ALLOWABLE TAKEOFF WEIGHT

TAKEOFF WEIGHT ANALYSIS WITH IMPROVED CLIMB PERFORMANCE

The following steps describe the procedure for finding the maximum allowable takeoff weight when using Improved Climb Performance. Improved Obstacle Clearance with speed increase is considered under a separate paragraph heading. The term, "normal", refers to the weights and speeds based on no increase in takeoff speeds.

1. Steps 1 through 6 of the Normal Takeoff Analysis are unchanged.

2. Maximum Takeoff Weight and Speeds (Improved Climb Performance) chart - Enter the weight portion of this chart with normal field length and climb limited gross weights. Follow the guidelines until they intersect. At the intersection, read gross weight and speed increase. Repeat, using tire speed and climb limited gross weights if 200 MPH tires are installed. Use lesser weight and speed increase.

3. Takeoff Speeds chart - Enter this chart, as in Normal Analysis, with pressure altitude and temperature, and with the gross weight determined from Step 2 above. Read VR, V2, and V1 for the V1/VR ratio in Step 3 of Normal Analysis.

4. Maximum Takeoff Weight and Speeds (Improved Climb Performance) chart - Enter the speed correction portion with the VR, V2 and V1 speeds determined in Step 3 above. Follow the guidelines to the speed increase determined in Step 2 above. Read Corrected VR, V2, and V1. V1 must be less than VMBE. (See V1 Greater than VMBE).

5. Determine flap-retraction speeds based on the V2 speed derived from Step 3 above.

MAXIMUM ALLOWABLE TAKEOFF WEIGHT

SELECTION OF V1

When the calculated or scheduled takeoff weight is not field-length limited, V1 may be raised or lowered to suit operating conditions within the restrictions imposed by the available runway length, VMCG, VR, and VMBE. Even when takeoff weight is field-length limited, a small reduction in V1 is available if the 3-engine field length requirement is shorter than the all-engine requirement. This is generally true for this airplane.

The following additional Steps are required in the Normal Takeoff Weight Analysis to determine the V1 limits:

1. Maximum Takeoff Weight (Field Length Limits) chart - Enter with airport pressure altitude, temperature, and actual scheduled takeoff weight. Read corrected runway length required.

2. Runway Length and V1 Adjustments chart - Enter, in upper right portion of the chart, with the corrected runway length obtained from Step 1. Where this runway length intersects the slope and wind corrected takeoff distance available line as determined in Step 3 of the Normal Analysis procedure, read minimum V1/VR. Where this runway length intersects the slope and wind corrected accelerate-stop distance line as determined in Step 3 of the Normal Analysis procedure, read maximum V1/VR.

   If either intersect occurs off the limits of the chart, use minimum or maximum values shown on the chart.

3. Takeoff Speed chart - At the actual scheduled takeoff weight, and the V1/VR ratios determined in Step 2 above, read minimum V1 and maximum V1.

4. Choose a suitable, single value of V1 between the limits determined in Step 3 above. The speed selected must be greater than VMCG, and less than the VR and VMBE determined in Steps 11 and 12 of the Normal Analysis procedure.

MAXIMUM ALLOWABLE TAKEOFF WEIGHT

V1 LESS THAN VMCG

Usually this will only occur when the takeoff weight is not field-length limited:

Takeoff Speeds chart - Read V1 at the field-length limited gross weight obtained from Step 4 of Normal Analysis procedure, and at the V1/VR ratio obtained from Step 3 of Normal Analysis. Use a V1 between VMCG and the maximum V1 so determined, but not exceeding VR.

V1 GREATER THAN VMBE

If the minimum V1, as determined by Steps 1 through 3 under SELECTION OF V1, still exceeds the brake energy speed, the takeoff weight will have to be reduced:

Maximum Brake Energy Limit Speed chart - Determine ΔV1, as defined on the chart. Reduce gross weight as indicated and redetermine VR, V1 and V2 for the lower weight.

VR LESS THAN VMCA LIMIT

On this airplane, VMCG is greater than 1.05 VMCA; therefore, minimum VR is equal to VMCG. This implies that the available runway length must be sufficient to permit a V1 equal to VR. This condition will be satisfied if the slope - and wind-corrected accelerate-stop distance exceeds 4500 feet on the Runway Length and V1 Adjustments chart.

OPERATION WITH ONE AIR CONDITIONING PACK ON R

Performance limited takeoff weights and takeoff climb gradients available can be increased by scheduling takeoff with only one air conditioning pack on. Performance increments are shown on the Takeoff With 1 A/C Pack On chart; these increments are applied to the weights and gradients obtained in steps 4, 5 and 7 of the Normal Takeoff Weight Analysis procedure. The gradient increment must be subtracted from the gradient required for use in step 10 to find an obstacle limited weight.

MAXIMUM ALLOWABLE TAKEOFF WEIGHT

SLIPPERY RUNWAY

Wet or icy runway conditions have the same effect on takeoff field length requirements as an inoperative anti-skid system; namely, reduced braking effectiveness. This makes the one engine inoperative condition critical.

The operator must review the existing runway conditions, decide how much additional stopping distance is desired, then proceed with the following steps to determine the changes in the field length limited takeoff weight, and V1 speed:

1. Omit Step 2 of the Normal Takeoff Weight Analysis procedure.

2. Runway Length and V1 Adjustments chart - Determine V1/VR as usual, except that the accelerate-stop distance must be reduced by an arbitrary amount equal to the desired extra stopping margin before making corrections for slope and wind. At the intersection of the corrected takeoff distance available and corrected accelerate-stop distance lines in the "web" portion of the chart, read corrected runway length and V1/VR.

3. Maximum Takeoff Weight chart - Enter the appropriate chart with the corrected runway length from Step 2 above. Read gross weight.

NOTE: If the V1, determined by using the V1/VR ratio from Step 2 above, is greater than the minimum V1 as determined under SELECTION OF V1, no reduction in field length limited takeoff weight is necessary. In fact, the use of minimum V1 in this case will give a greater stopping distance margin.

MAXIMUM ALLOWABLE TAKEOFF WEIGHT

EXAMPLES

Example lines shown on the charts do not necessarily reflect these examples.

ILLUSTRATIVE EXAMPLE 1

Given: Airport Conditions R

Runway Length Available = 12,000 ft.
Runway Slope = 0.5% (Uphill)
Airport Elevation (Pressure Altitude) = 2000 ft.
Obstacles: 120 ft. high at 3400 ft.
500 ft. high at 25,000 ft.

Atmospheric Conditions

Reported Wind (at 50 ft.) = 10 kt. (Headwind)
OAT = 20°C (68°F)

Airplane Conditions

Takeoff flap position 10
This example illustrates the general use of the charts, and the obstacle clearance charts in particular, and is restricted to normal speed operation.
See example 5 for improved obstacle clearance with speed increase method.
See chart reading procedure for chart titles and methods of use.

1. From Runway Length Corrections (All Engines) chart, corrected runway length = 12,070 ft.

2. From Runway Length and V1 Adjustments chart, corrected runway length = 12,570 ft. and V1/VR = .970

3. From Maximum Takeoff Weight (Field Length Limits) chart, using the lesser of the corrected runway length from Steps 1 and 2, field length limited takeoff weight = 683,000 lb.

4. From Maximum Takeoff Weight (Climb Limits) chart, climb limited takeoff weight = 649,000 lb.

5. From Maximum Takeoff Weight (Tire Speed Limits) chart, 200 MPH tire speed limited takeoff weight = 743,000 lb. Maximum Takeoff weight = 649,000 lb.

6. From Takeoff Climb chart, using field length limited weight of 683,000 lb, second segment gross gradient at 400 ft. = 2.30%
Using Gradient Corrections chart, gradient corrected for wind = 2.37%

(Continued)

MAXIMUM ALLOWABLE TAKEOFF WEIGHT

EXAMPLES

ILLUSTRATIVE EXAMPLE 1 (Continued)

7. From Close-in Obstacle Clearance chart, second segment gross gradient required for close-in obstacle clearance = 4.50%. Obstacle is not cleared with gradient available (uncorrected for wind). Change in reference zero = 5100 - 3400 = 1700 ft. due to the decrease in field length required for the reduced takeoff weight. R

   In this distance, reference zero shifts 1700 x .005 = 8.5 ft. (vertical) due to runway slope.

   The obstacle height is now 128.5 ft. at 5100 ft. from reference zero and the required gradient is 3.08%.

8. From Distance Obstacle Clearance chart determine gross gradient required and minimum gross height.

   Gradient capability (from Step 6) = 3.08% (corrected for wind = 3.17%)
   Corrected obstacle distance = 25,000 + 1700 = 26,700 ft.
   Required gross gradient = 2.89% (less than gradient available).
   Distance from reference zero to reach obstacle height of 500 ft. is 23,300 ft.
   Minimum gross height for flap retraction is 770 ft.

9. From Takeoff Climb chart, obstacle limited weight = 638,500 lb. at a gross gradient of 3.08%. R

10. From Distance Obstacle Clearance chart, maximum level-off height is 940 ft. Therefore extended final segment climb is unnecessary in this case.

11. From Gross Height - Pressure Altitude Conversion chart, the pressure altitude increment for a gross height of 770 ft. is 750 ft. Therefore, the minimum pressure altitude for level-off and flap retraction is 2750 ft.

12. From Takeoff Speeds chart for V1/VR = .970 and 638,500 lb.
    VR = 152.5 kt. V1 = 147.5 kt. V2 = 159 kt.

13. Determine flap retraction and final climb speeds.

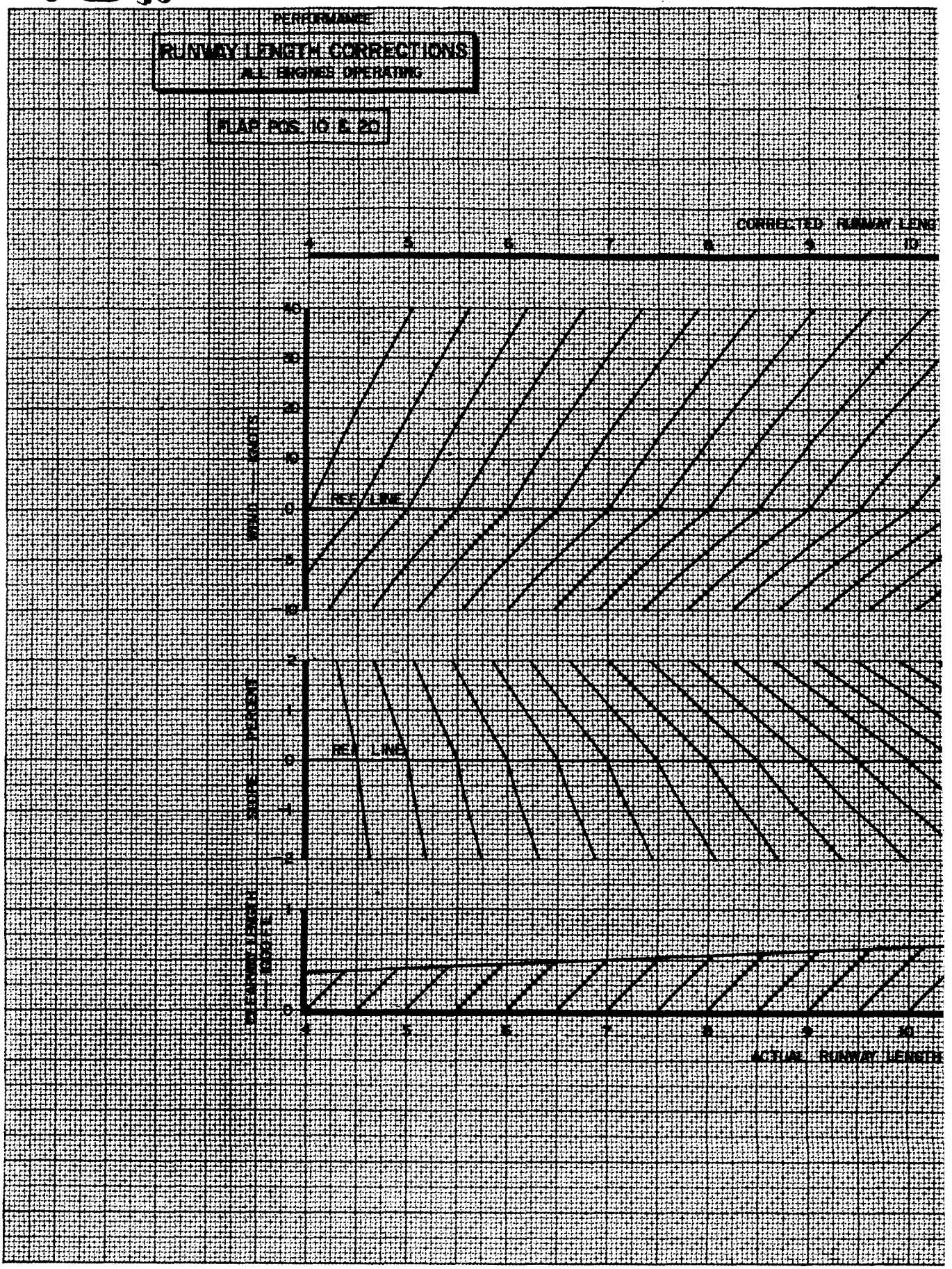

CHART APPLICABLE TO	APPROVED	DATE
747-100 JT9D-3	B¹ LA-274	12-8-69

BASSETT 12.7.69

PERFORMANCE

RUNWAY LENGTH & V_1 ADJUSTMENTS

FLAP POS. 10 & 20

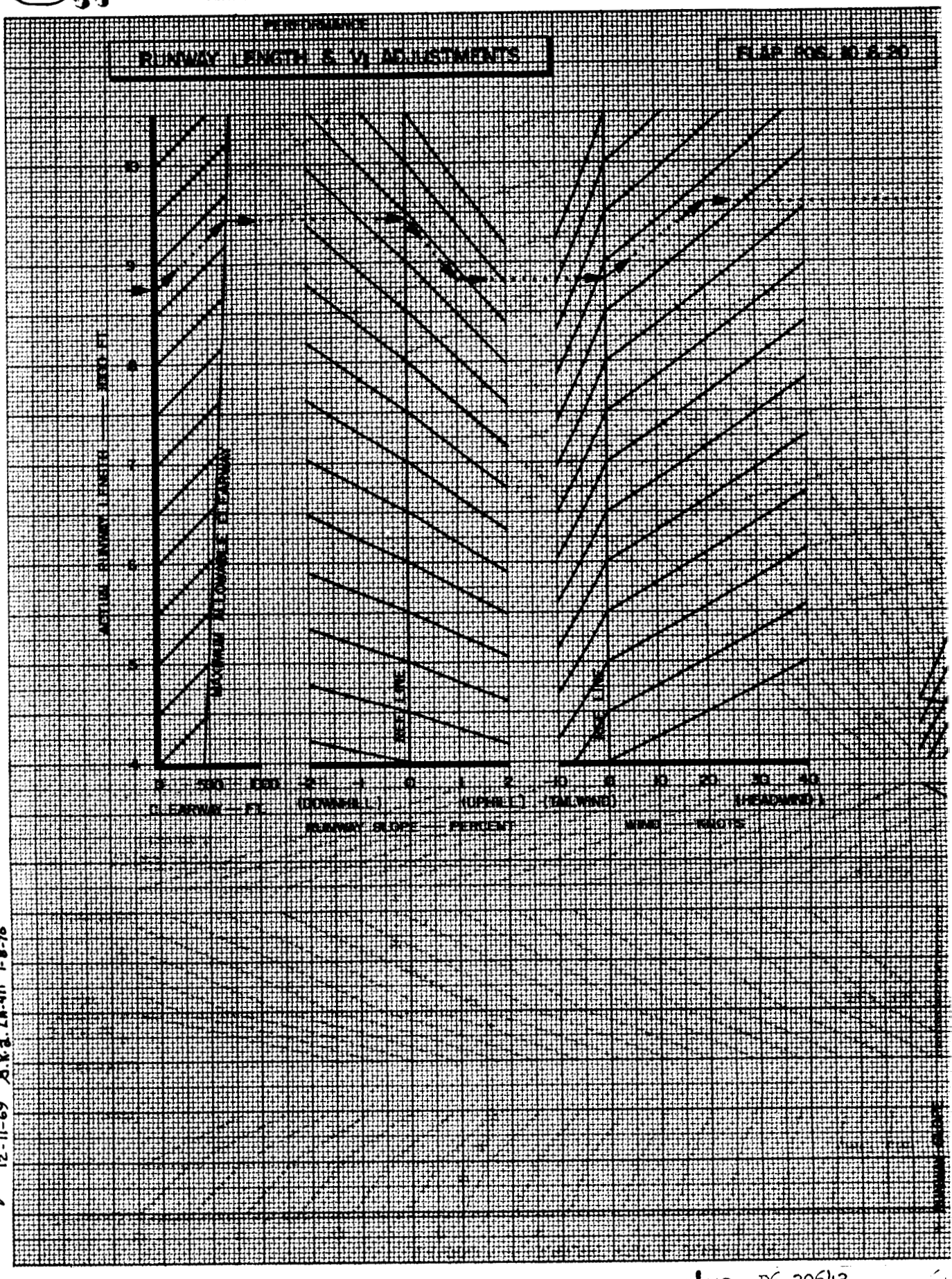

CALC	SCOTT	12-9-69	REVISED	DATE
CHECK	747—100			

A.R.S. LA-411 1-8-70

AJS LA-177 12-11-69

PERFORMANCE

RUNWAY LENGTH & V_1 ADJUSTMENTS

FLAP POS. 10 & 20

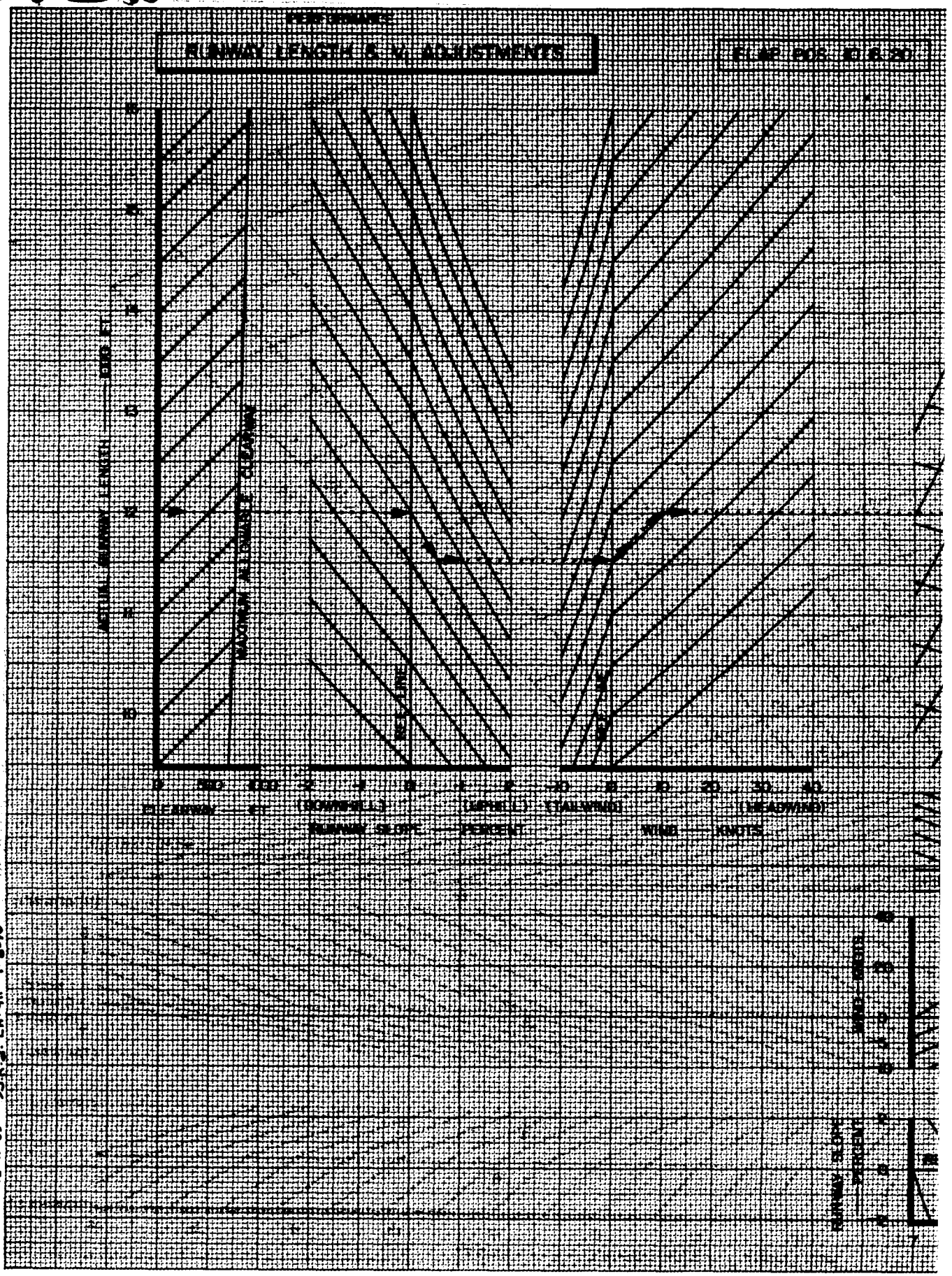

CALC	SCOTT	12-9-69	REVISED	DATE
CHECK	747-100			

S.R.S. LA-411 1-8-70

AMS LA-177 12-11-69

FAA APPROVED 1-20-70

PERFORMANCE

MAXIMUM TAKEOFF WEIGHT
FIELD LENGTH LIMITS

FLAP POS 10

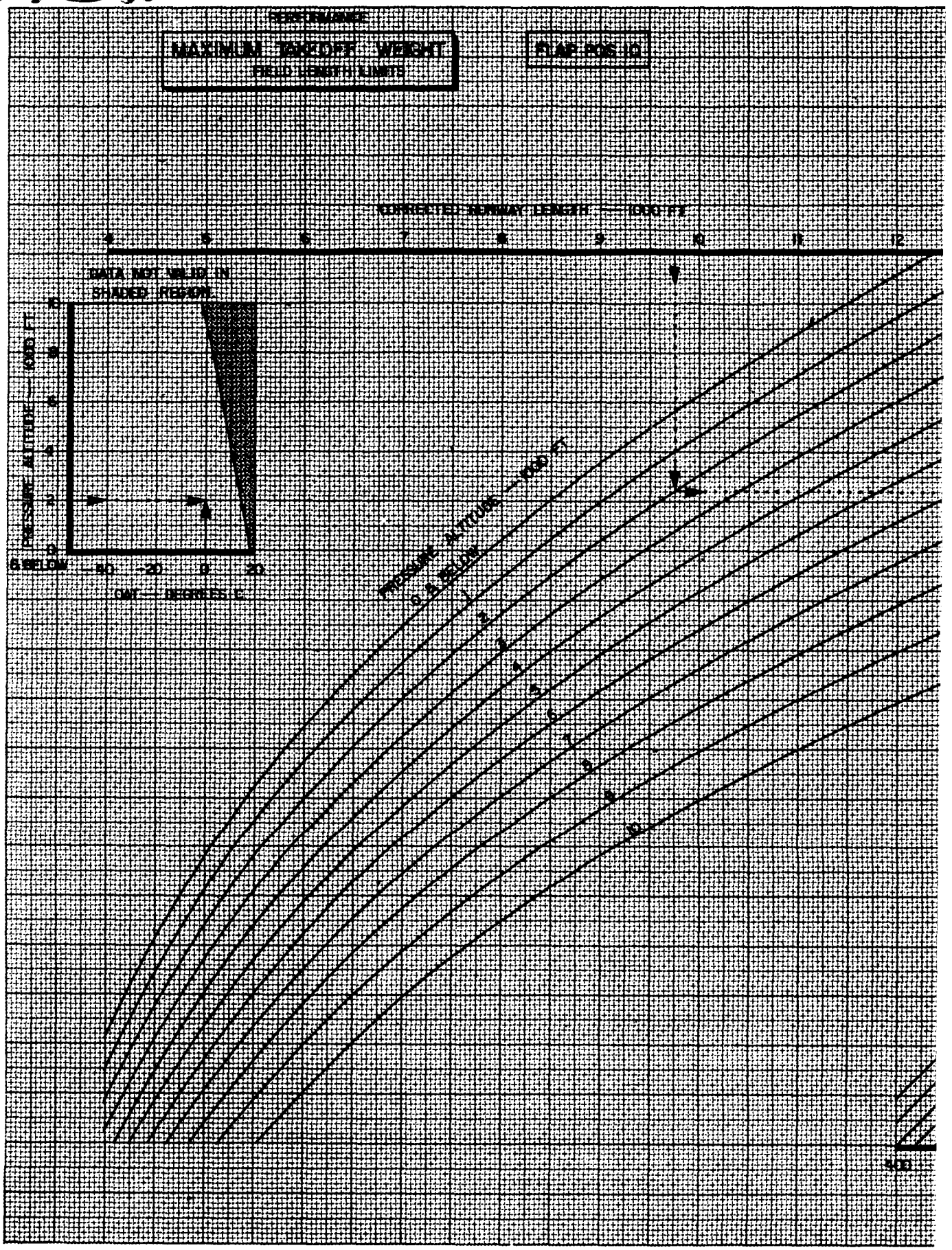

CALC	SCOTT	12-16-69	REVISED	DATE
CHECK				
747-100	JT9D-3			

LA-177
12-17-69

PERFORMANCE

MAXIMUM TAKEOFF WEIGHT
FIELD LENGTH LIMITS

FLAP POS 10

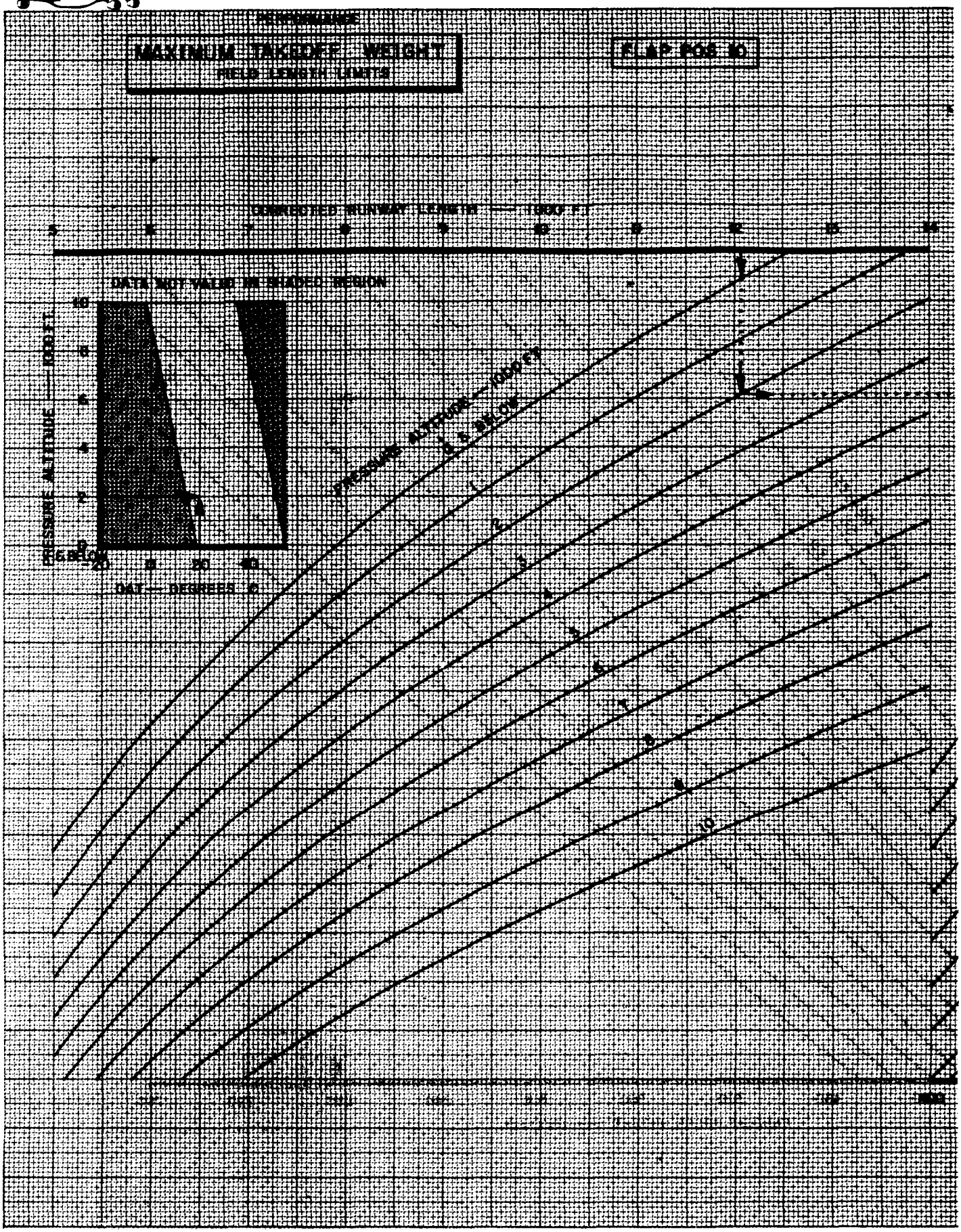

CALC	D GIUS	12-9-69	REVISED	DATE
CHECK			G.R.J. LA-411	12-10-69
747-100 JT9D-3				

PERFORMANCE

MAXIMUM TAKEOFF WEIGHT
CLIMB LIMITS

FLAP POS. 10

NOTE:
HIGHER WEIGHTS ARE ALLOWED WITH IMPROVED CLIMB PERFORMANCE. SEE TEXT.

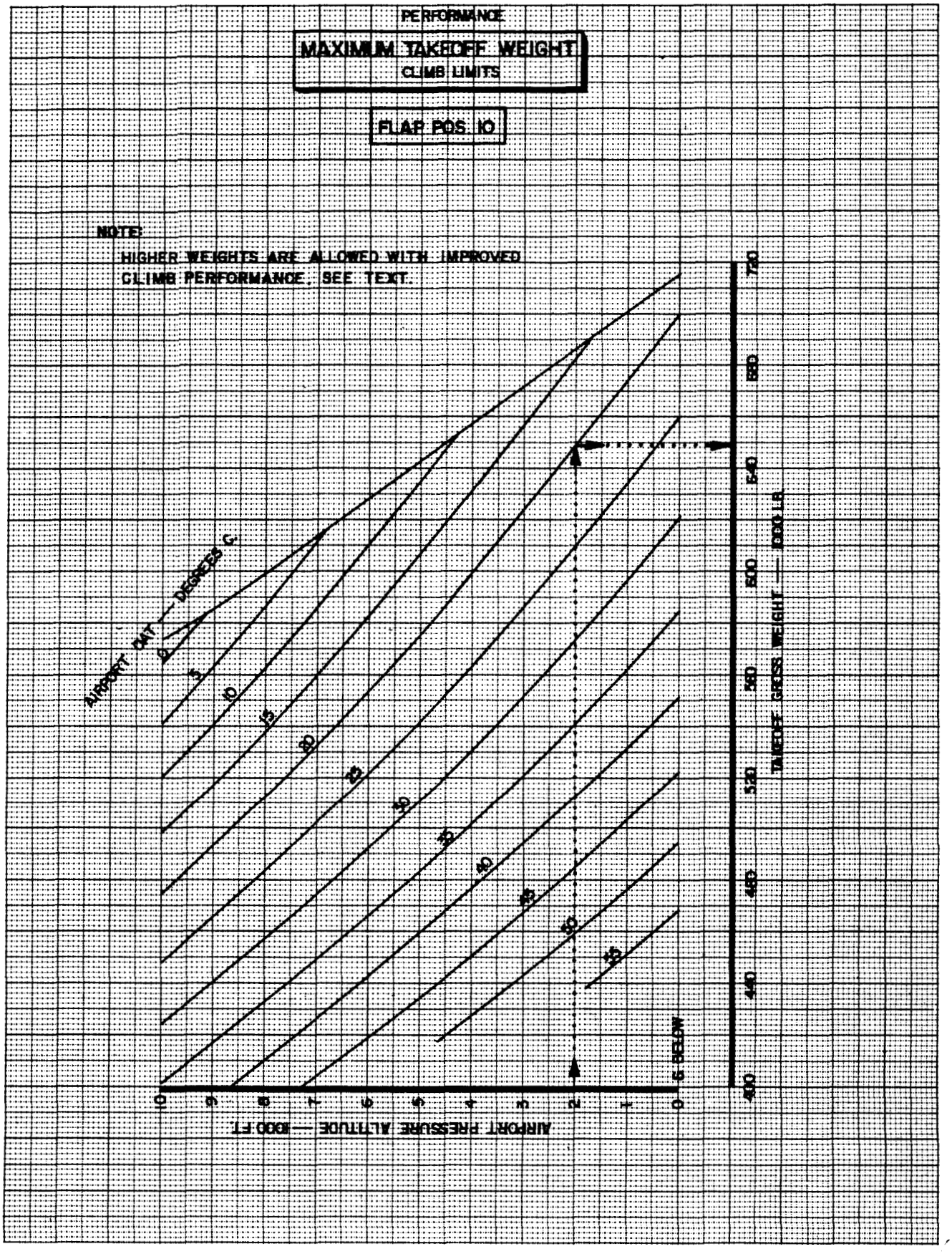

BASSETT 12-6-69

CHART APPLICABLE TO	APPROVED	DATE
747-100 JT9D-3	D.R.P. LA-411	12-7-69

PERFORMANCE

MAXIMUM TAKEOFF WEIGHT
FOR TIRE SPEED OF 200 MPH

FLAP POS 10

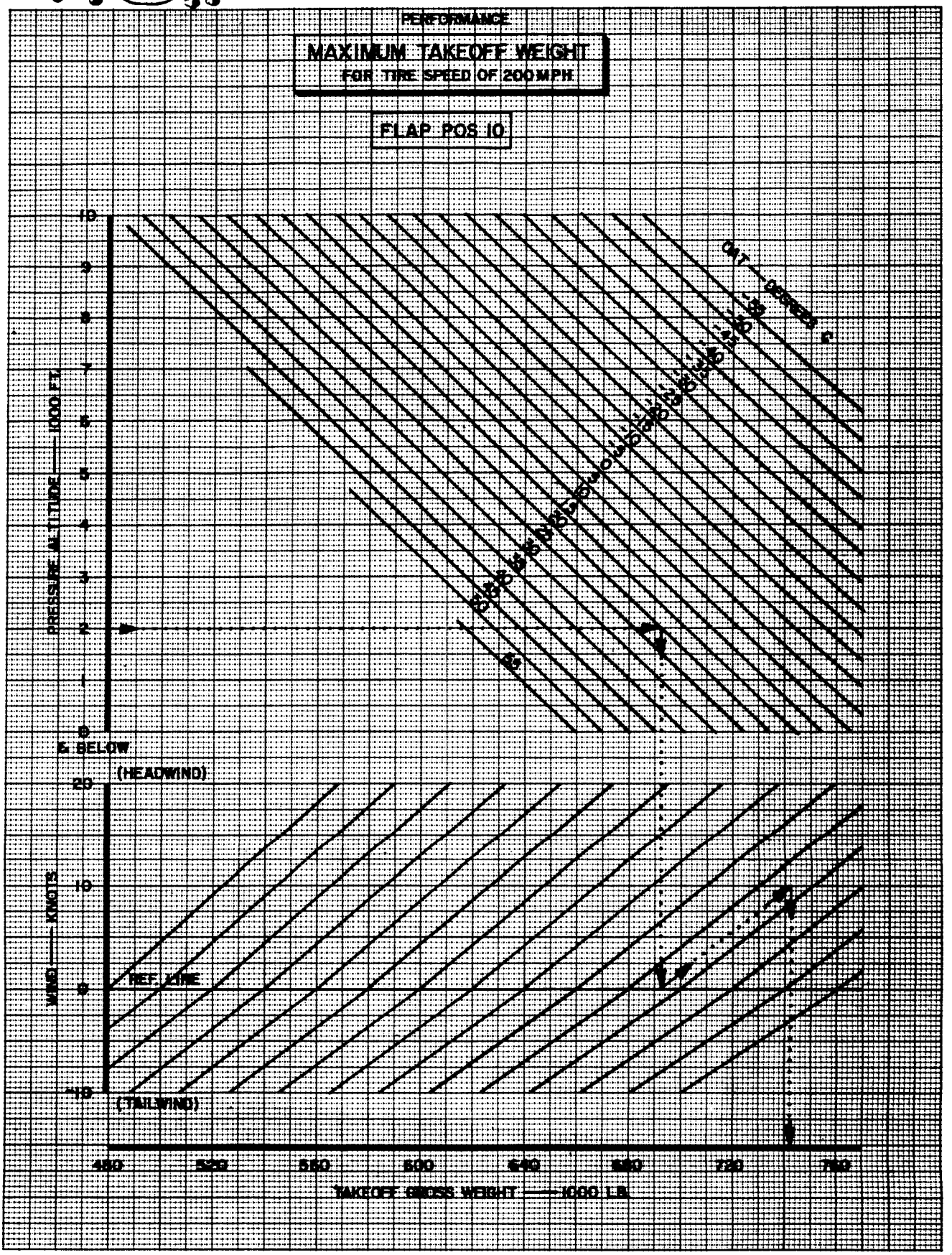

CHART APPLICABLE TO	APPROVED	DATE
747-100 JT9D-3	FAA LA-411	12-10-69

LEE 12-7-69

PERFORMANCE

MAXIMUM TAKEOFF WEIGHT AND SPEEDS

IMPROVED CLIMB PERFORMANCE

FLAP POS 10

WEIGHT LIMITS

TIRE LIMITS

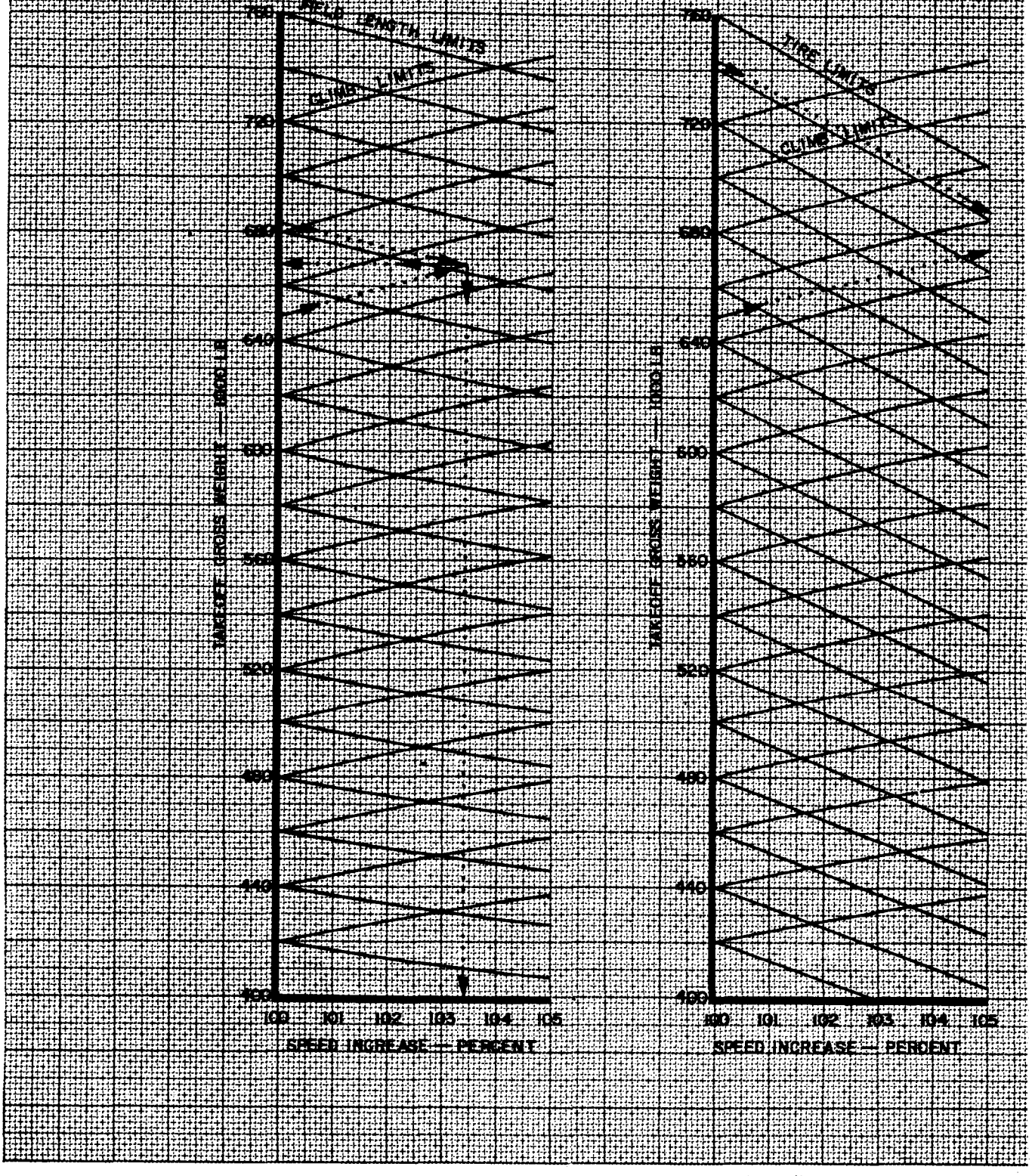

CHART APPLICABLE TO	APPROVED	DATE
747-100 JT9D-3	B² LA-274	12-11-69

PERFORMANCE

TAKEOFF SPEEDS

FLAP POS. 10

NOTE: THE EFFECT OF ENGINE AIR BLEED ON TAKE OFF SPEEDS IS NEGLIGIBLE

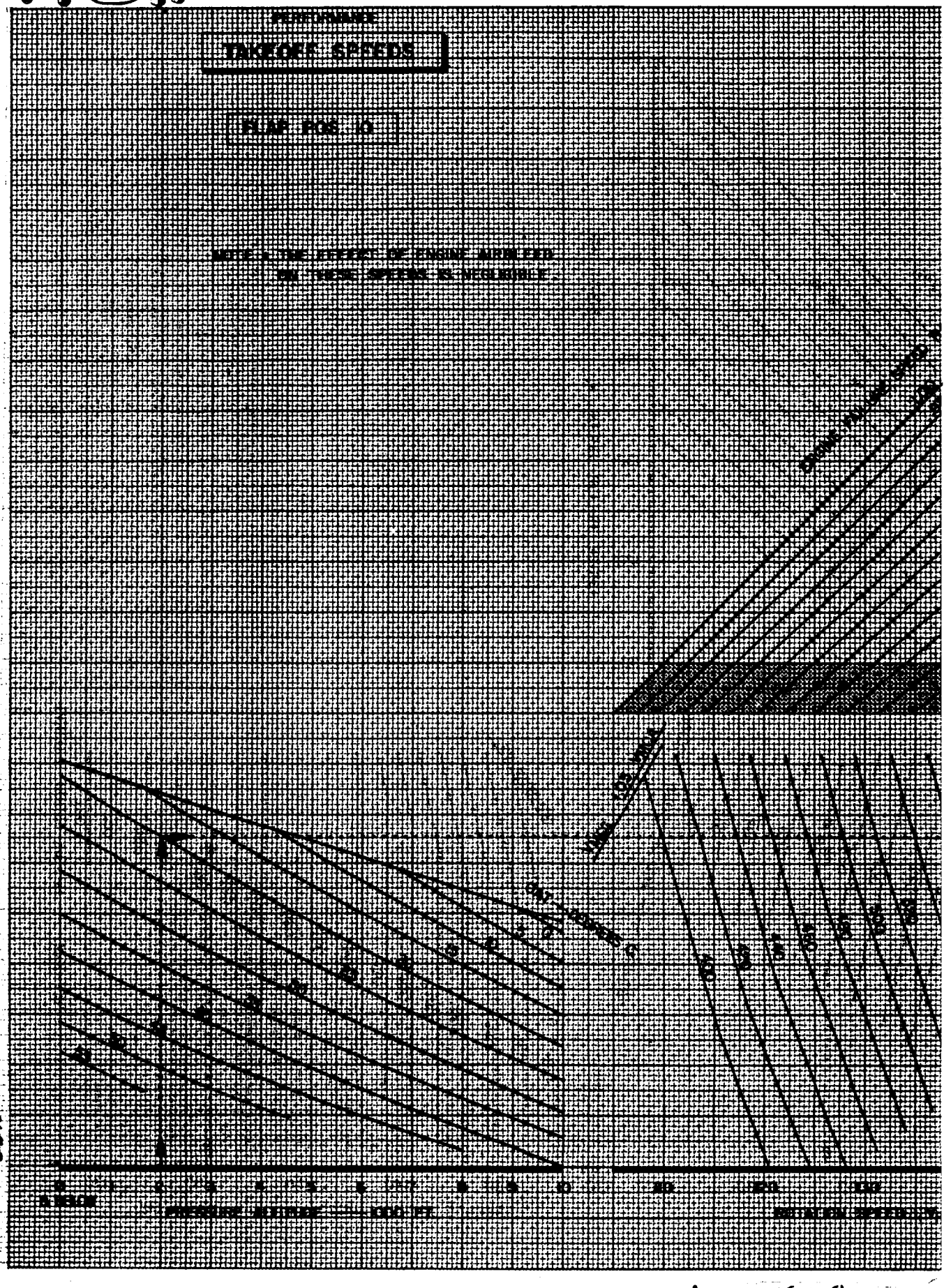

CALC	SCOTT	11-26-69	REVISED	DATE
CHECK	747—100 JT9D-3			

AJS LA-17 2-4-70

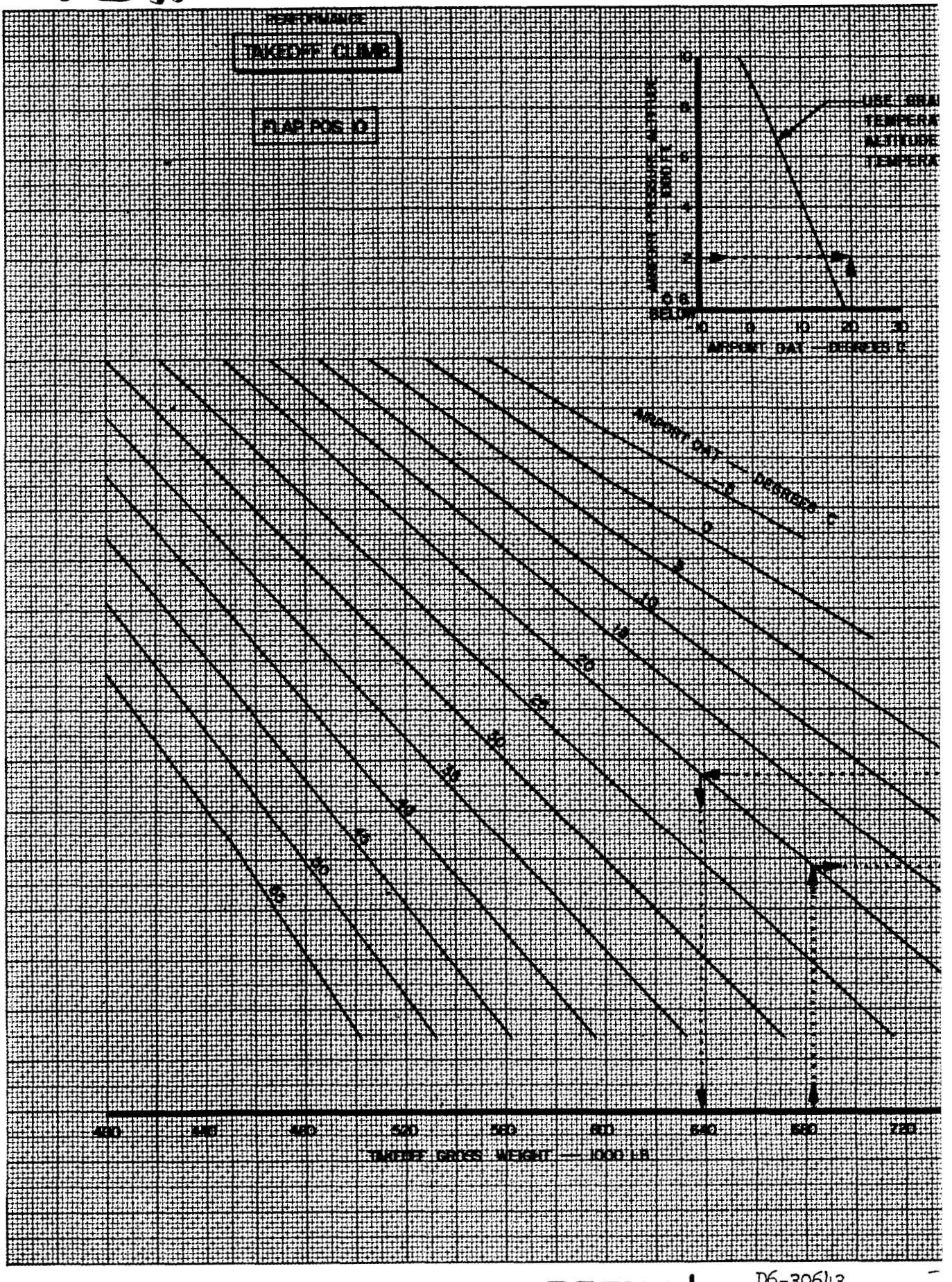

CHART APPLICABLE TO	APPROVED	DATE
747-100 JT9D-3	LA-ITT	12-9-69

BASSETT 11-28-69

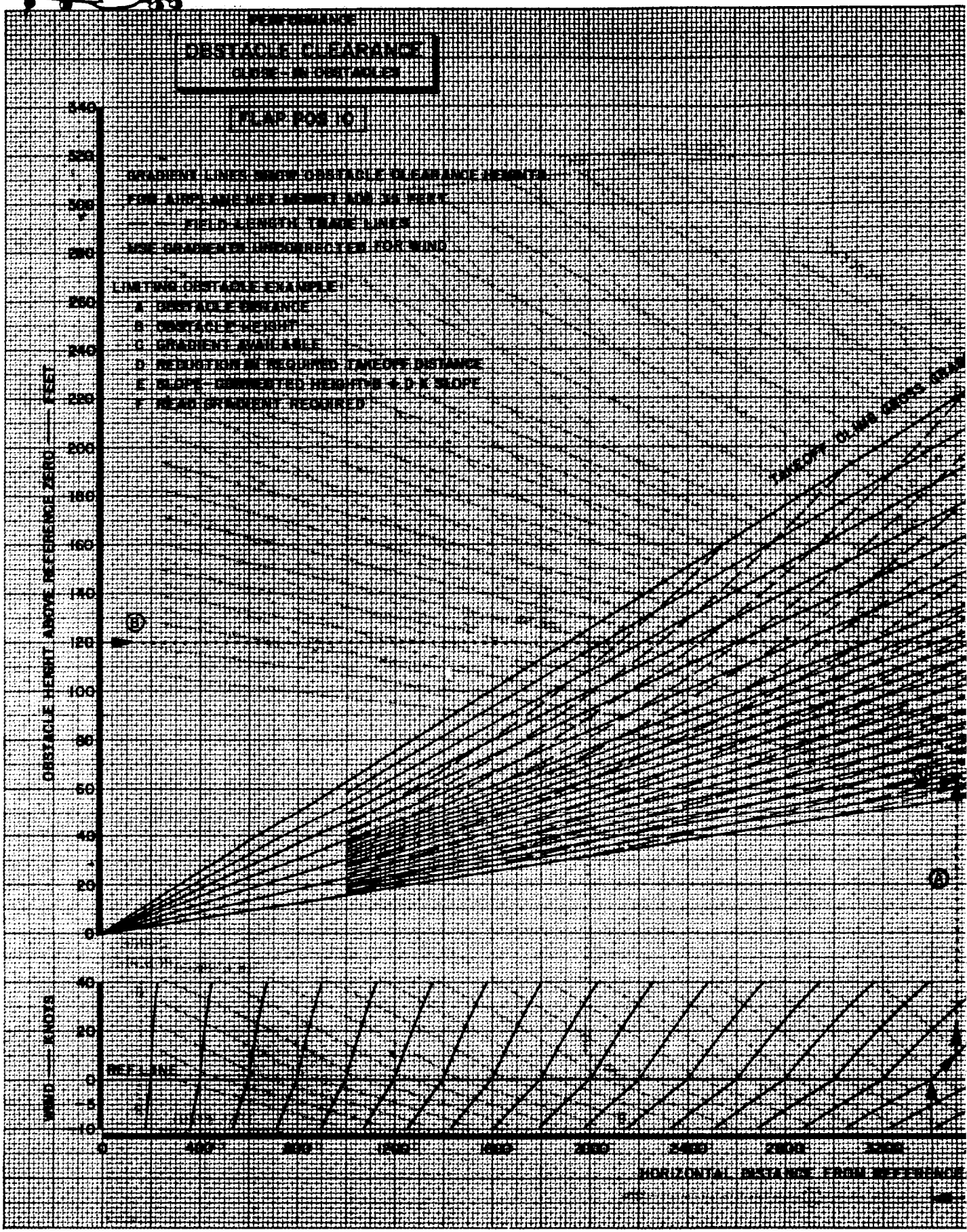

CHART APPLICABLE TO	APPROVED	DATE
747-100 JT9D-3	S.R.d. FAA 411	12-12-69

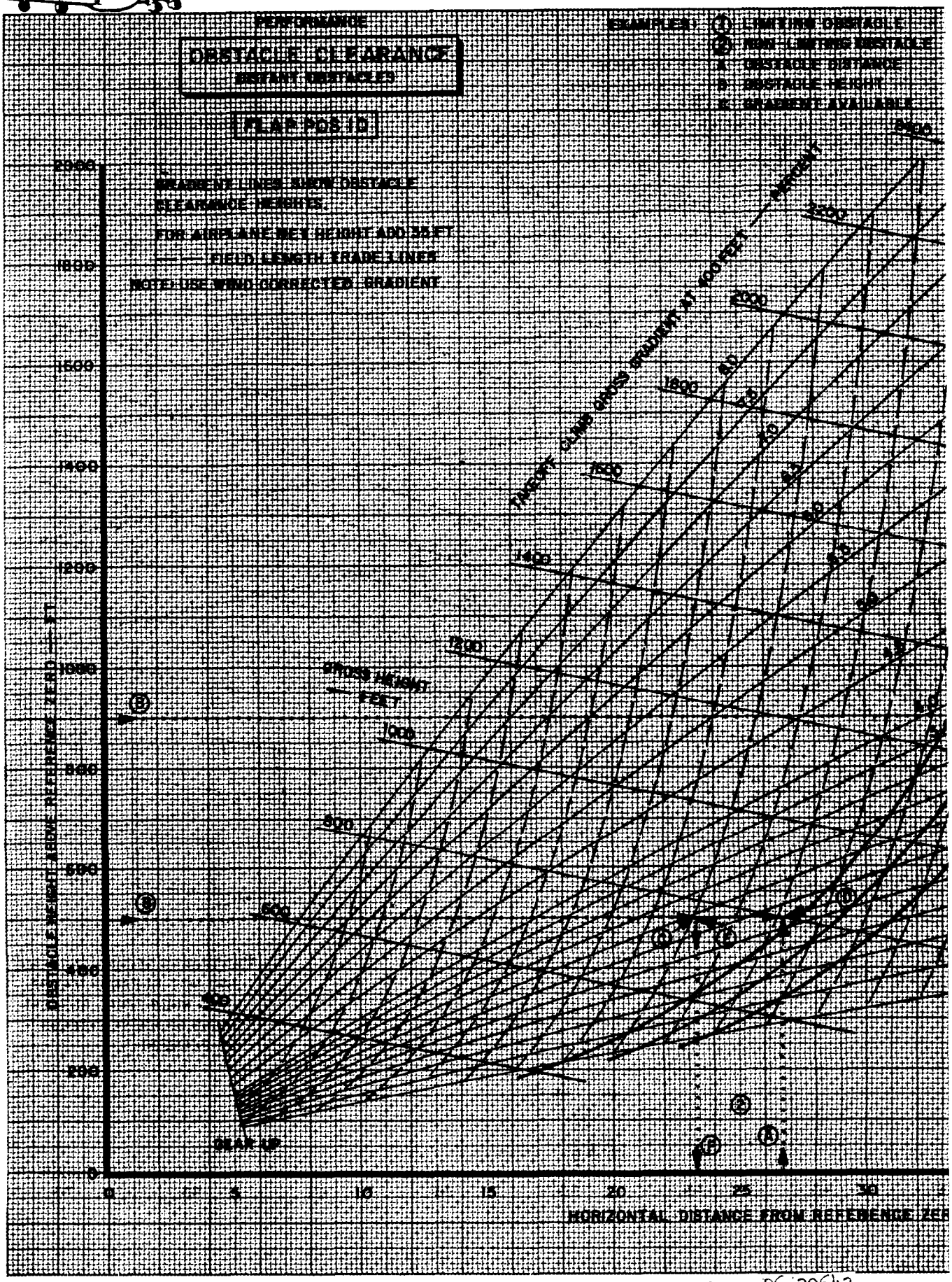

CHART APPLICABLE TO	APPROVED	DATE
747-100 JT9D-3	B.R.S. LAW	12-12-69

PERFORMANCE

THIRD SEGMENT DISTANCE

FLAP POS 10

NOTE: ENTER CHART WITH TAKEOFF CLIMB GRADIENT CORRECTED FOR WIND AND LEVEL-OFF HEIGHT ABOVE 400 FT.

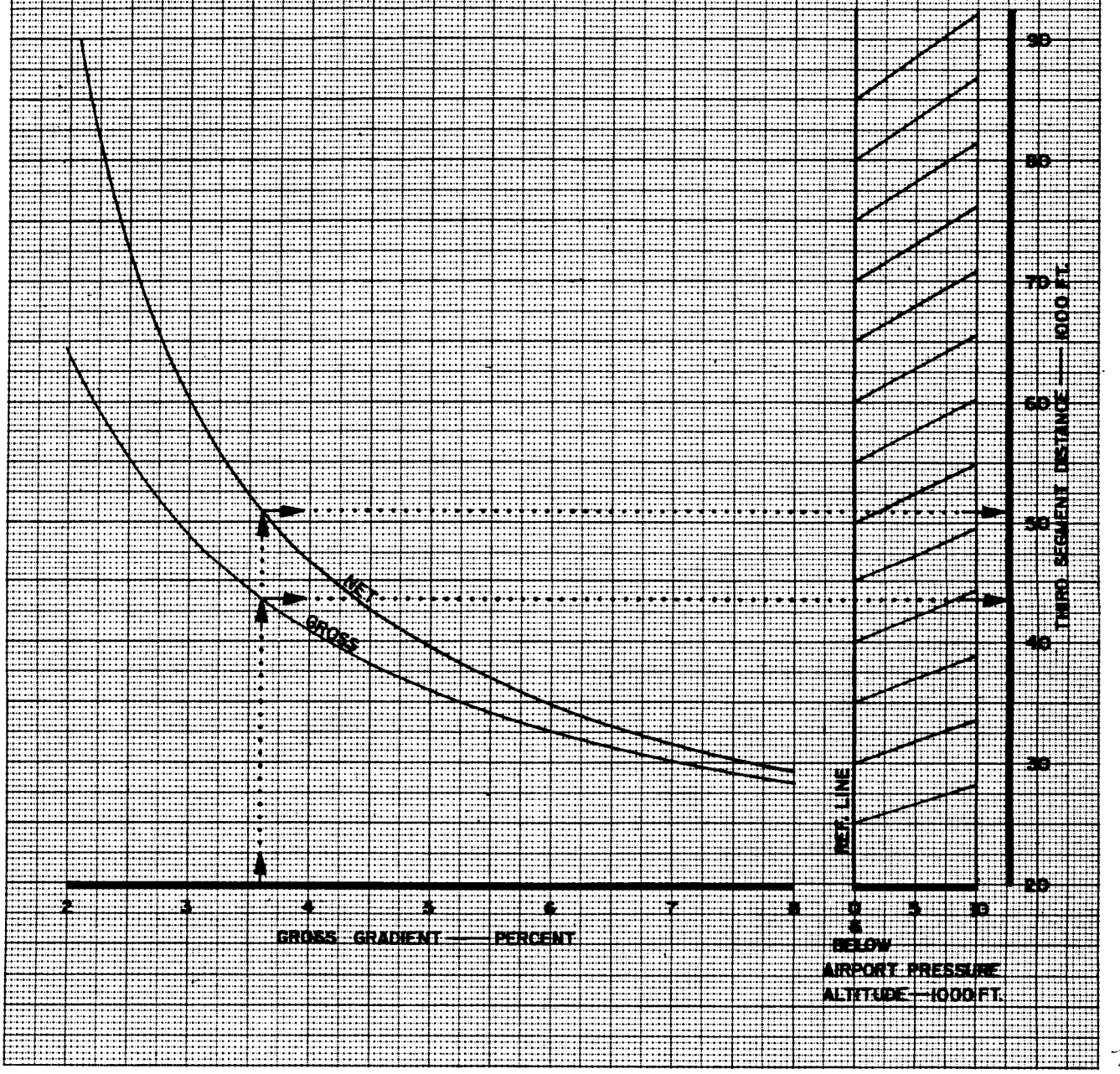

CHART APPLICABLE TO	APPROVED	DATE
747-100 JT9D-3	B² CA-274	12-9-69

PERFORMANCE

TAKEOFF SPEEDS

FLAP POS. 20

MODEL 747-100
JT9D-3

CHART APPLICABLE TO	APPROVED	DATE
747-100 JT9D-3	BCZ LA-274	1-10-70
	AJS LA-111	2-10-70

BASSETT 12-11-69

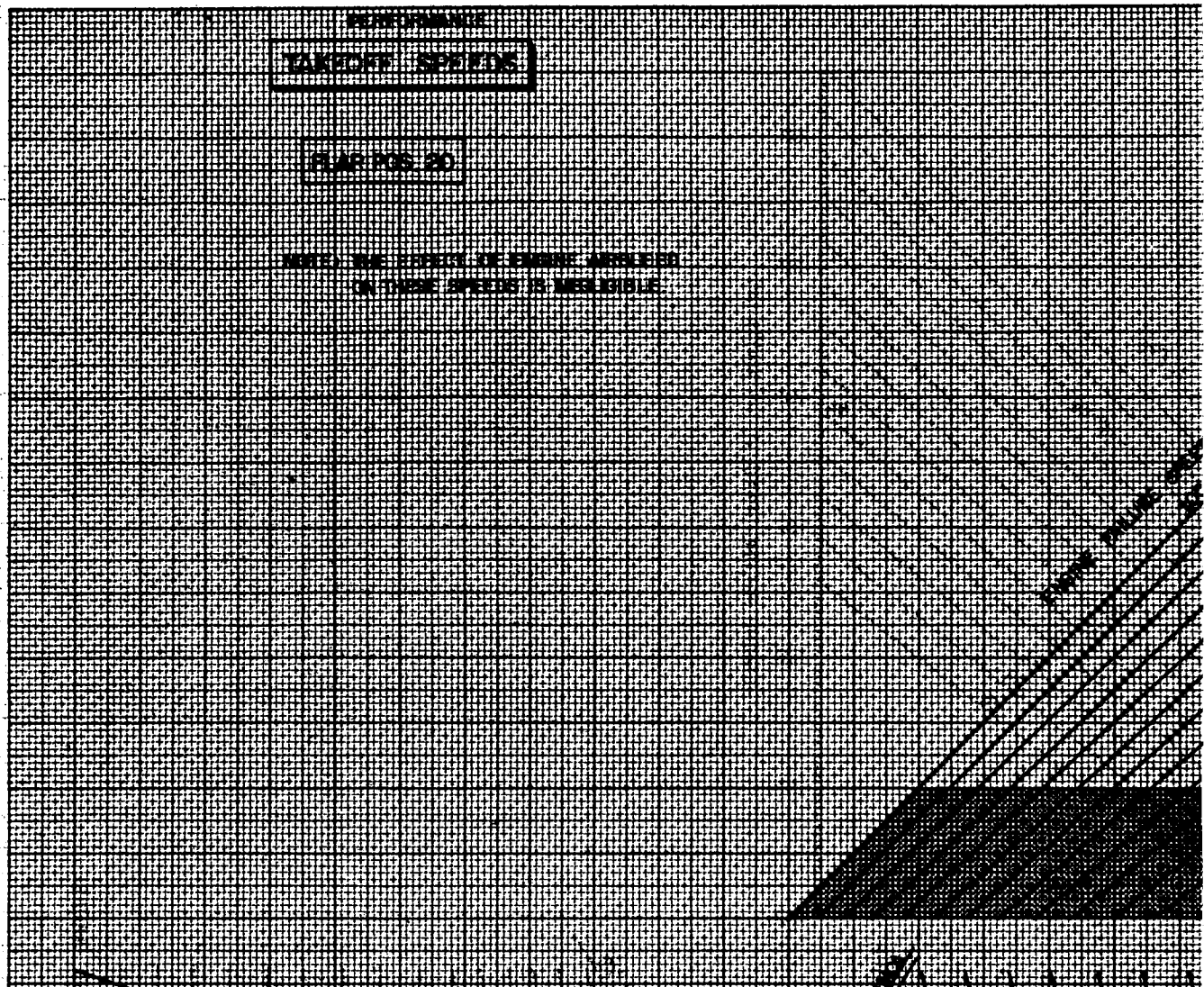

PERFORMANCE

TAKEOFF CLIMB

FLAP POS. 20

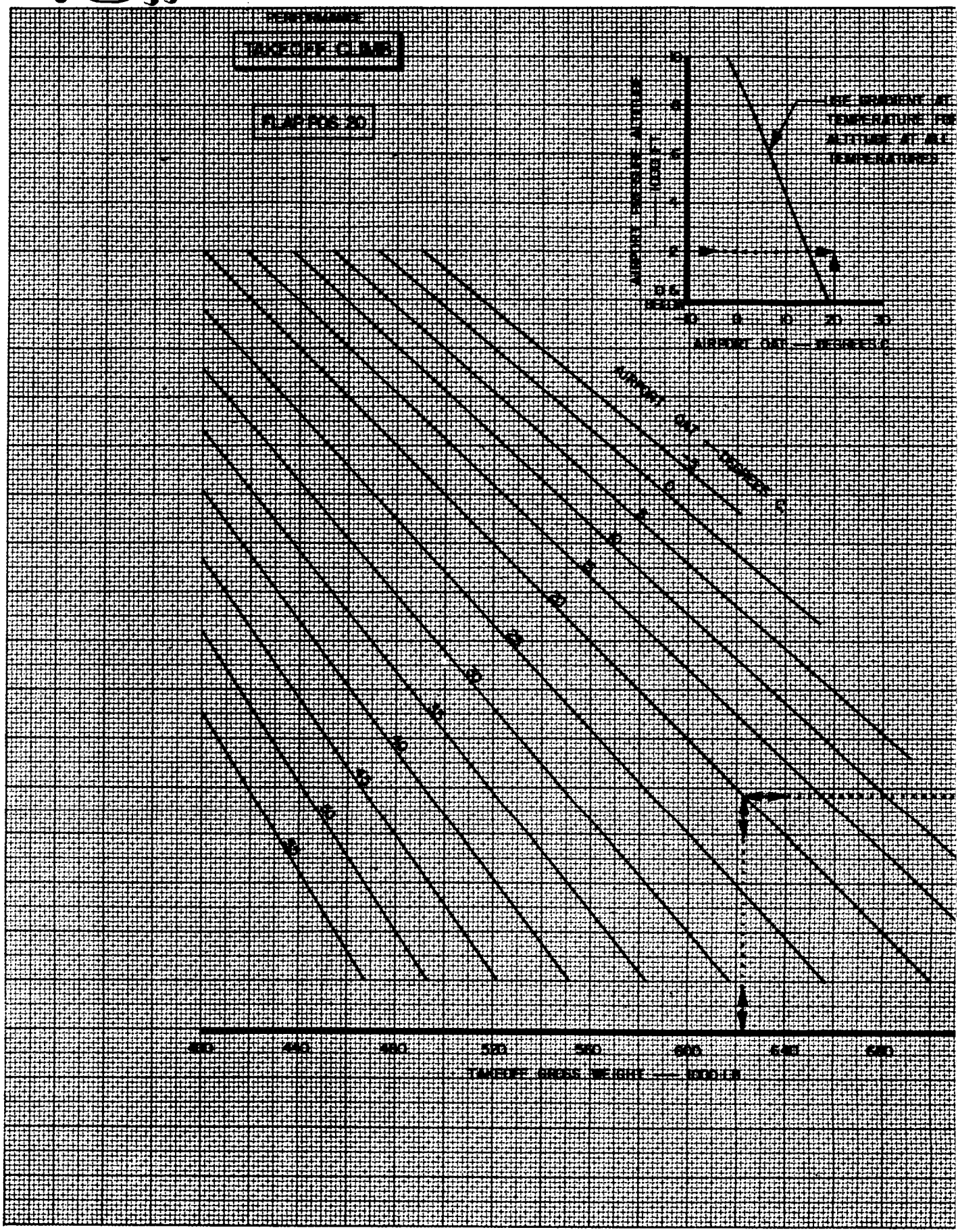

BASSETT 12-13-69

CHART APPLICABLE TO	APPROVED	DATE
747-100 JT9D-3	LA-177	12-13-69

GROSS HEIGHT – PRESSURE ALTITUDE CONVERSION

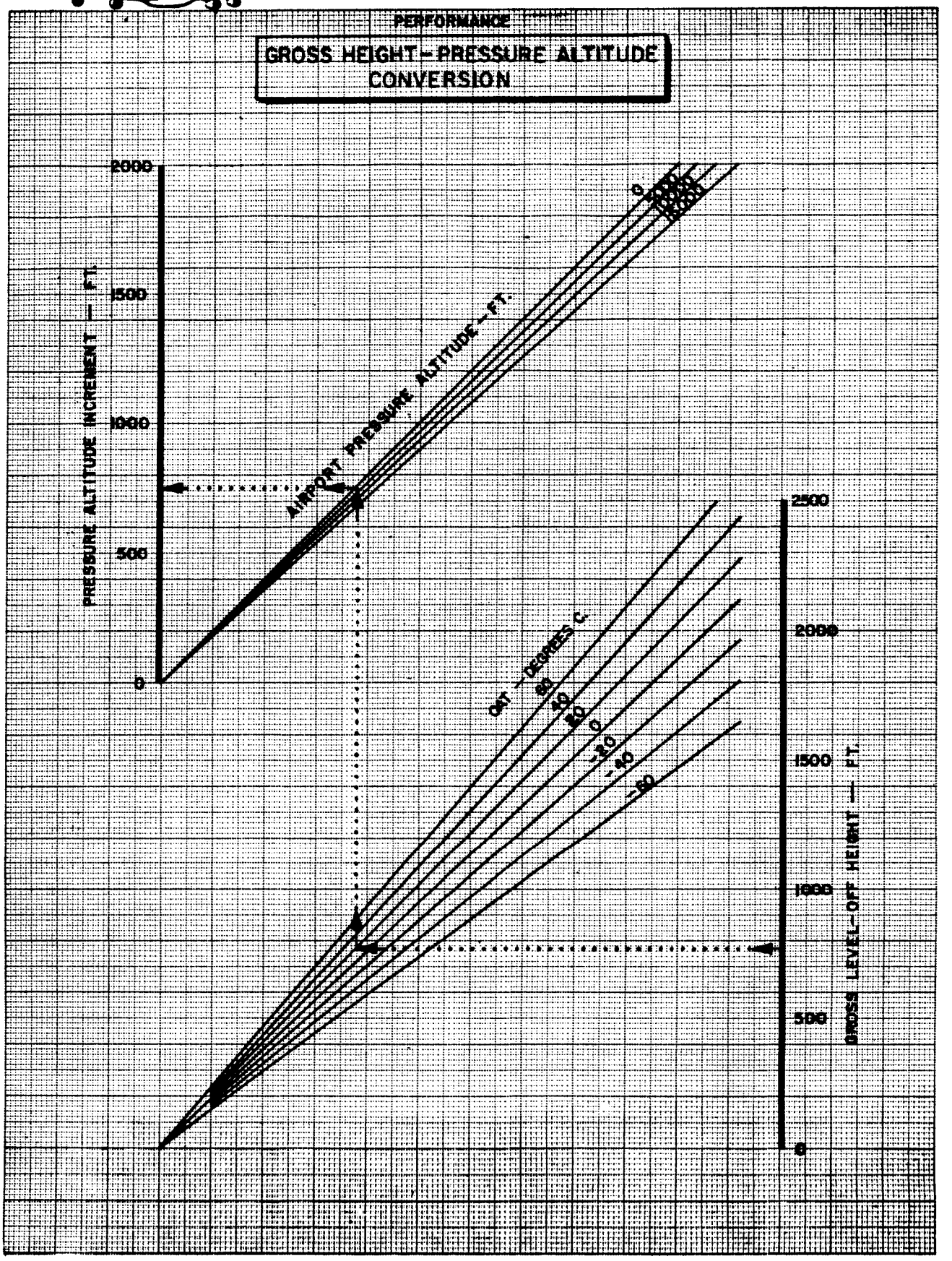

CHART APPLICABLE TO	APPROVED	DATE
ALL MODELS	D.R.S. LA-YU	12-15-69

ASSETT 9.30.69 104

PERFORMANCE

FINAL TAKEOFF CLIMB

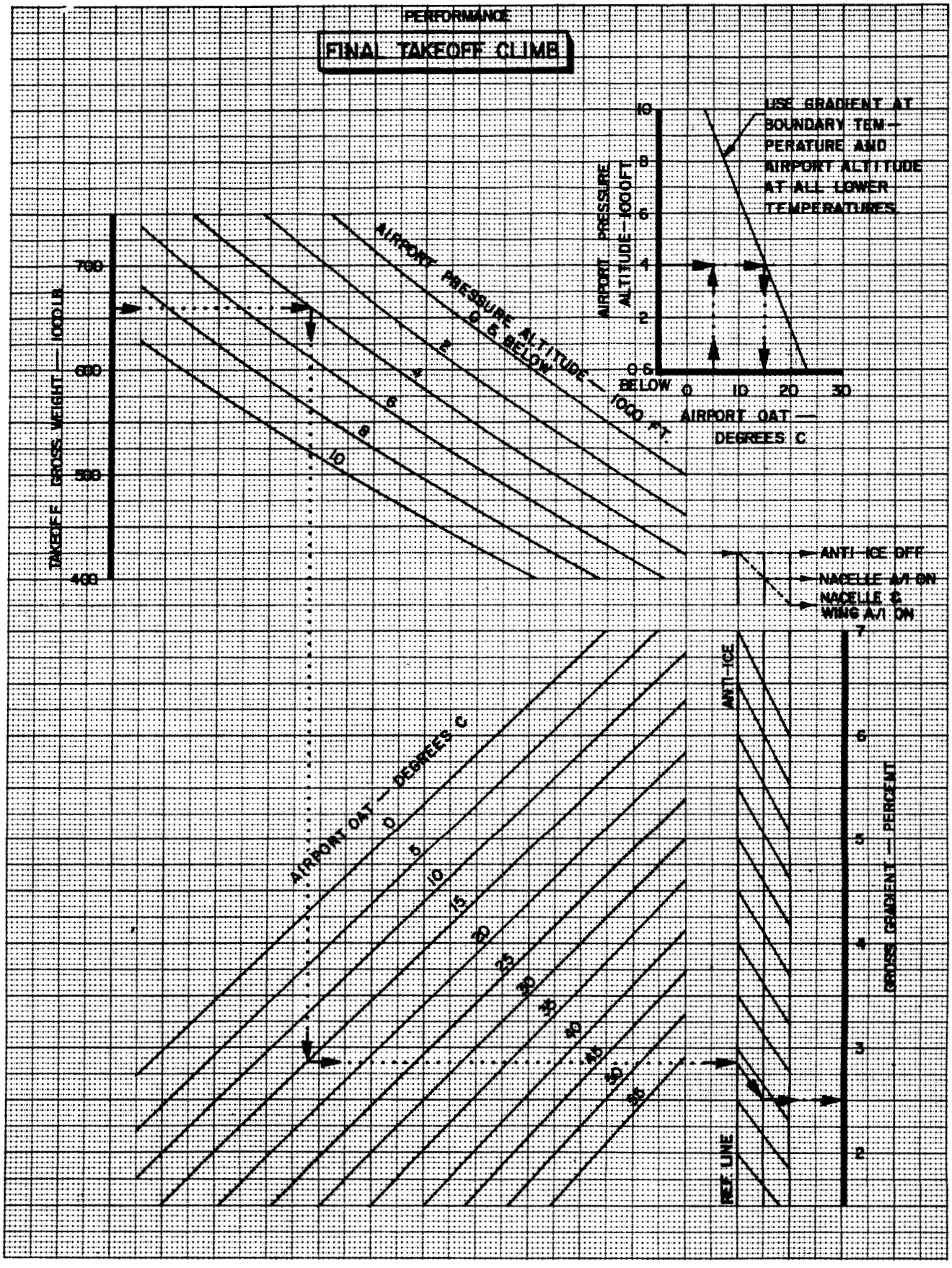

CHART APPLICABLE TO	APPROVED	DATE
747-100 JT9D-3	B² LA-274	12-10-69

BASSETT 11-29-69

PERFORMANCE

GRADIENT CORRECTIONS

GRADIENT DECREMENT (%) IN BANKED TURN		
BANK ANGLE DEGREES	FLAP POS. 0	FLAP POS. 10 & 20
5	.02	.07
10	.10	.27
15	.25	.63

TAKEOFF CLIMB

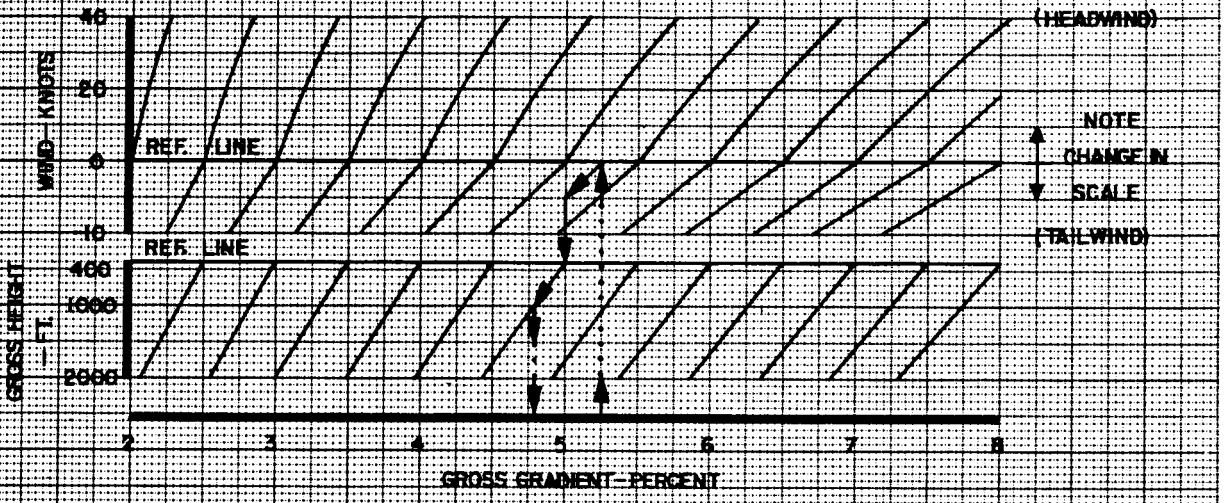

FINAL TAKEOFF CLIMB

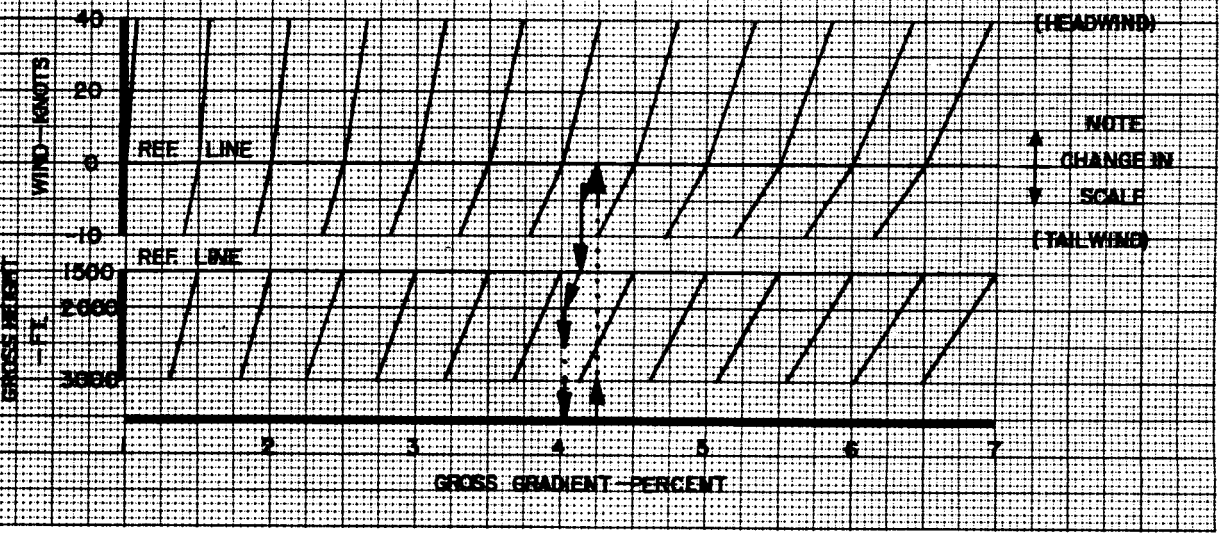

CHART APPLICABLE TO	APPROVED	DATE
747—100 JT9D-3	FAA LA-274	12-16-69

PERFORMANCE

ENROUTE CLIMB WEIGHTS
FOR POSITIVE NET GRADIENT

ENGINE INOPERATIVE

FOR ENROUTE CLIMB SPEED SCHEDULE SEE ENROUTE CLIMB, ENGINE INOPERATIVE CHART.

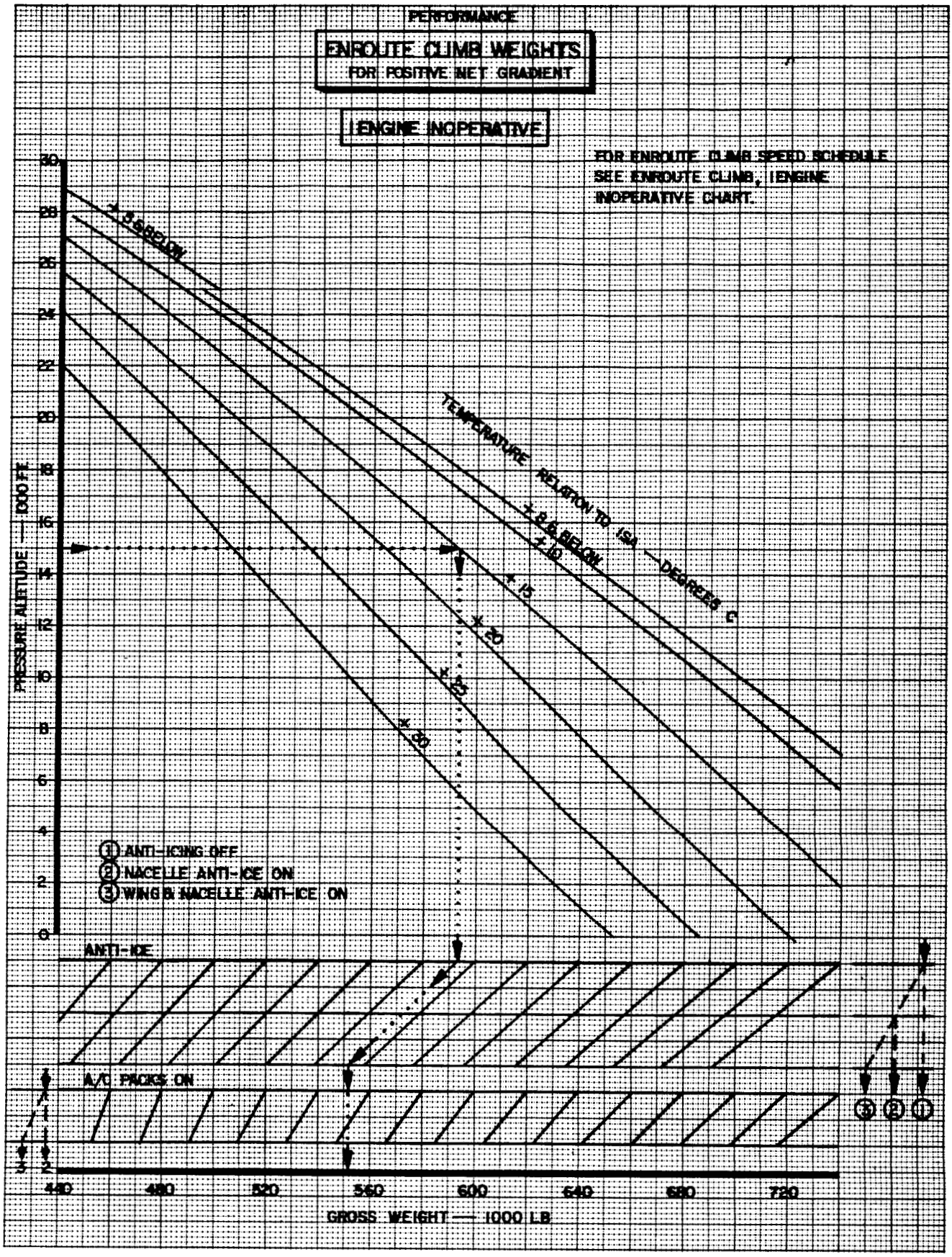

CHART APPLICABLE TO	APPROVED	DATE
747-100 JT9D-3	LR-411	12-10-69

MC LAUGHLIN 12-8-69

PERFORMANCE

ENROUTE CLIMB WEIGHTS
FOR POSITIVE NET GRADIENT

2 ENGINES INOPERATIVE

1 A/C PACK ON

FOR ENROUTE CLIMB SPEED SCHEDULE SEE ENROUTE CLIMB, 2 ENGINE INOPERATIVE CHART.

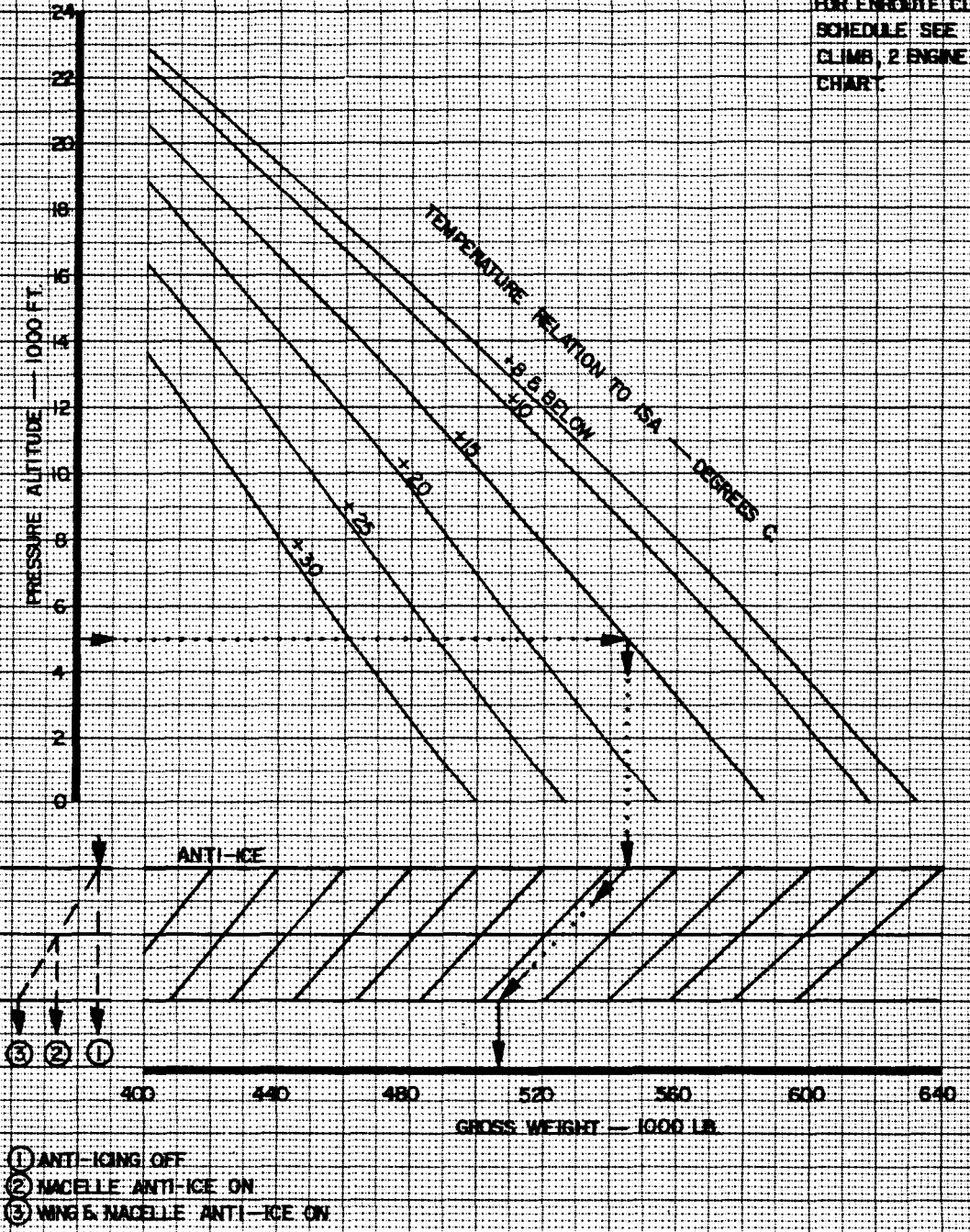

① ANTI-ICING OFF
② NACELLE ANTI-ICE ON
③ WING & NACELLE ANTI-ICE ON

CHART APPLICABLE TO	APPROVED	DATE
747-100 JT9D-3	A.R.J. LA-411	12-7-69

BASSETT 12.3.69

APPROACH AND LANDING

Charts on the following pages present approach and landing gradients, maximum landing weights as limited by approach and landing performance, landing field length requirements, and landing weights for the maximum brake energy at which wheel thermal plugs will remain intact.

The speed schedules shown on the Approach and Landing Climb charts are those at which the gradients were calculated in accordance with FAR 25.121(d) and 25.119, and have no operational significance. The minimum landing approach speeds are shown on the Landing Field Length and Speed charts.

The ICE CORRECTION on the charts accounts for maximum probable performance effects of ice remaining on the airplane surfaces without anti-ice protection. The correction applies when operating in icing conditions during any part of the flight, unless the forecast temperature at the destination airport is high enough (above 8°C or 46°F) to ensure that the ice will melt off prior to approach and landing.

The Maximum Landing Weight, Climb Limits, can be increased for one air conditioning pack on operation. This information is included to permit a showing of compliance with FAR 25.1001 (c) at the increased allowable takeoff weight. R

This information may also be used to schedule higher allowable landing weights provided approach and landing procedures are modified to have only one air conditioning pack on prior to the point where a go-around might be initiated. See Normal Procedures. R

PERFORMANCE

APPROACH CLIMB

FLAP POS 20

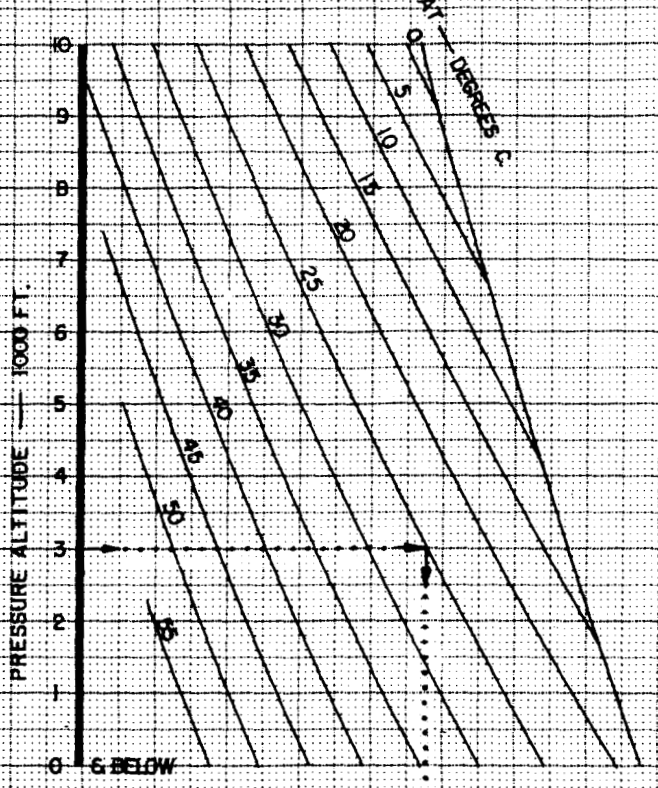

SPEED SCHEDULE

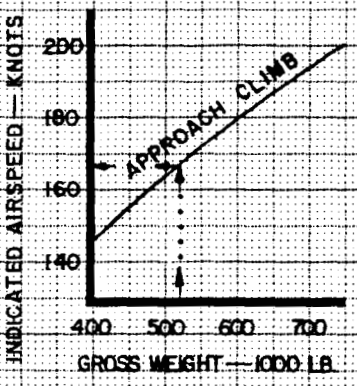

APPROACH CLIMB
GROSS GRADIENT LIMIT = 2.7%

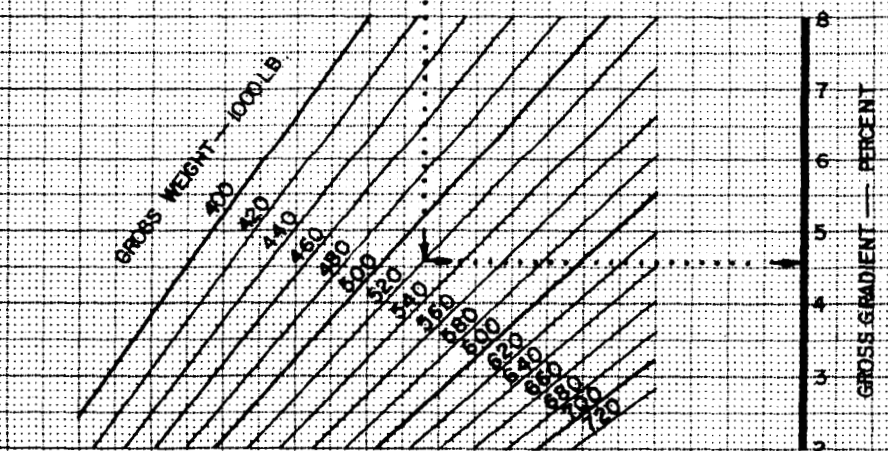

REDUCE GRADIENT BY 0.15 % FOR ICE ACCUMULATION WHEN OPERATING IN ICING CONDITIONS DURING ANY PART OF THE FLIGHT WITH FORECAST LANDING TEMPERATURE BELOW 8°C

CHART APPLICABLE TO	APPROVED	DATE
747-100 JT9D-3	B.R.J. LA-411	12-11-69

DURINGER 12-10-69

PERFORMANCE

LANDING CLIMB

FLAP POS. 25 & 30

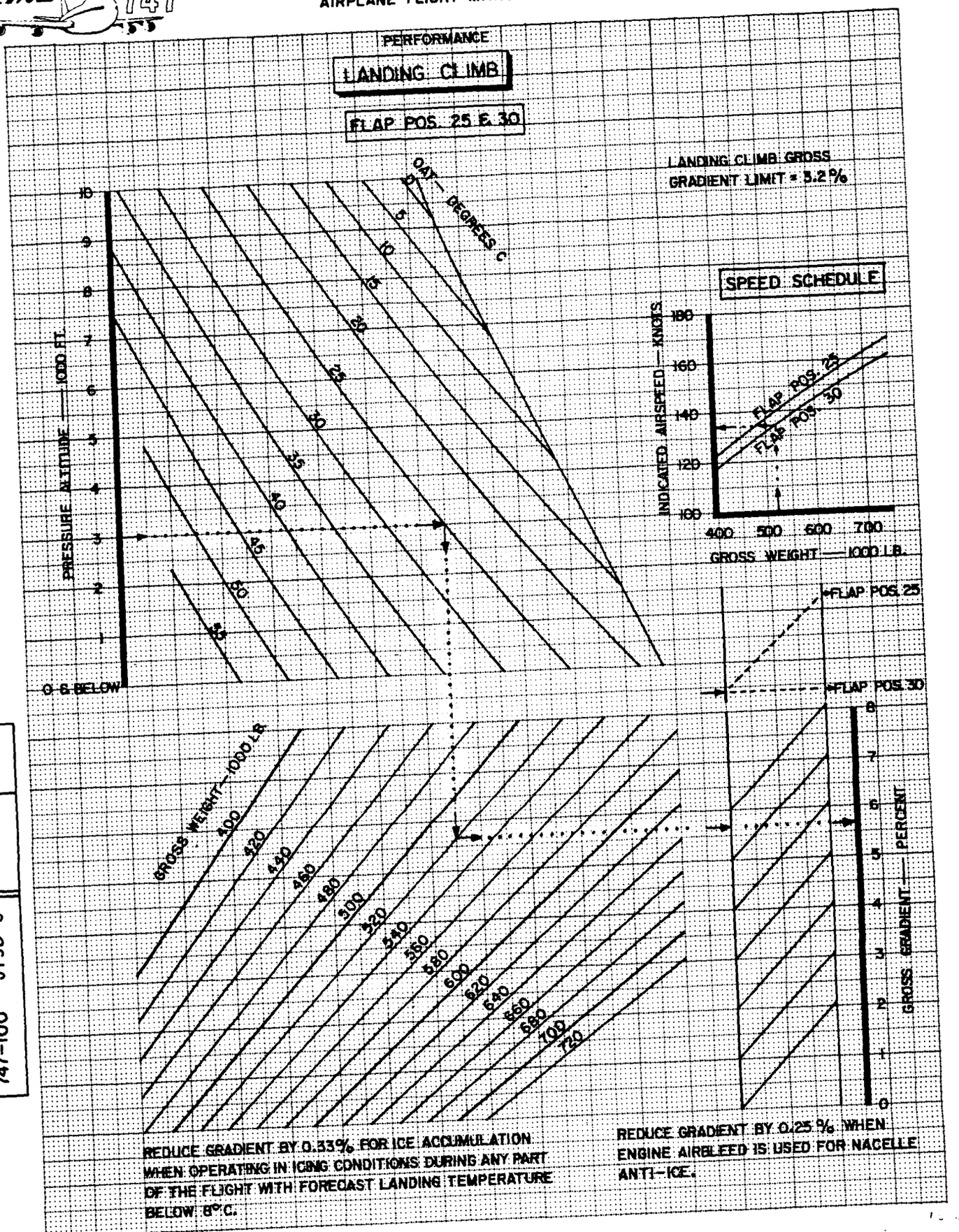

REDUCE GRADIENT BY 0.33% FOR ICE ACCUMULATION WHEN OPERATING IN ICING CONDITIONS DURING ANY PART OF THE FLIGHT WITH FORECAST LANDING TEMPERATURE BELOW 8°C.

REDUCE GRADIENT BY 0.25 % WHEN ENGINE AIRBLEED IS USED FOR NACELLE ANTI-ICE.

CHART APPLICABLE TO	APPROVED	DATE
747-100 JT9D-3	A.R.B. 4/11	12-12-69

SCOTT 12-10-69

PERFORMANCE

MAXIMUM LANDING WEIGHT
CLIMB LIMITS

APPROACH FLAP POS. 20
LANDING FLAP POS. 30

NOTE: USE ICE CORRECTION WHEN OPERATING IN ICING CONDITIONS DURING ANY PART OF THE FLIGHT WITH FORECAST LANDING TEMPERATURE BELOW 8°C

CORRECTION FOR 1 A/C PACK OPERATION

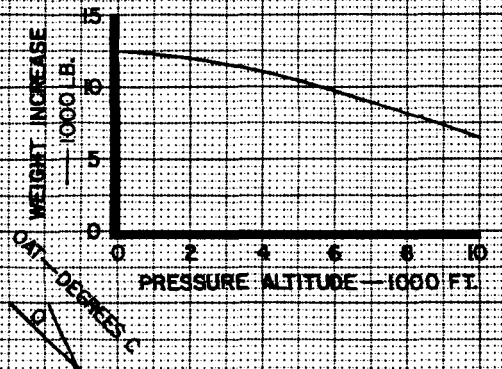

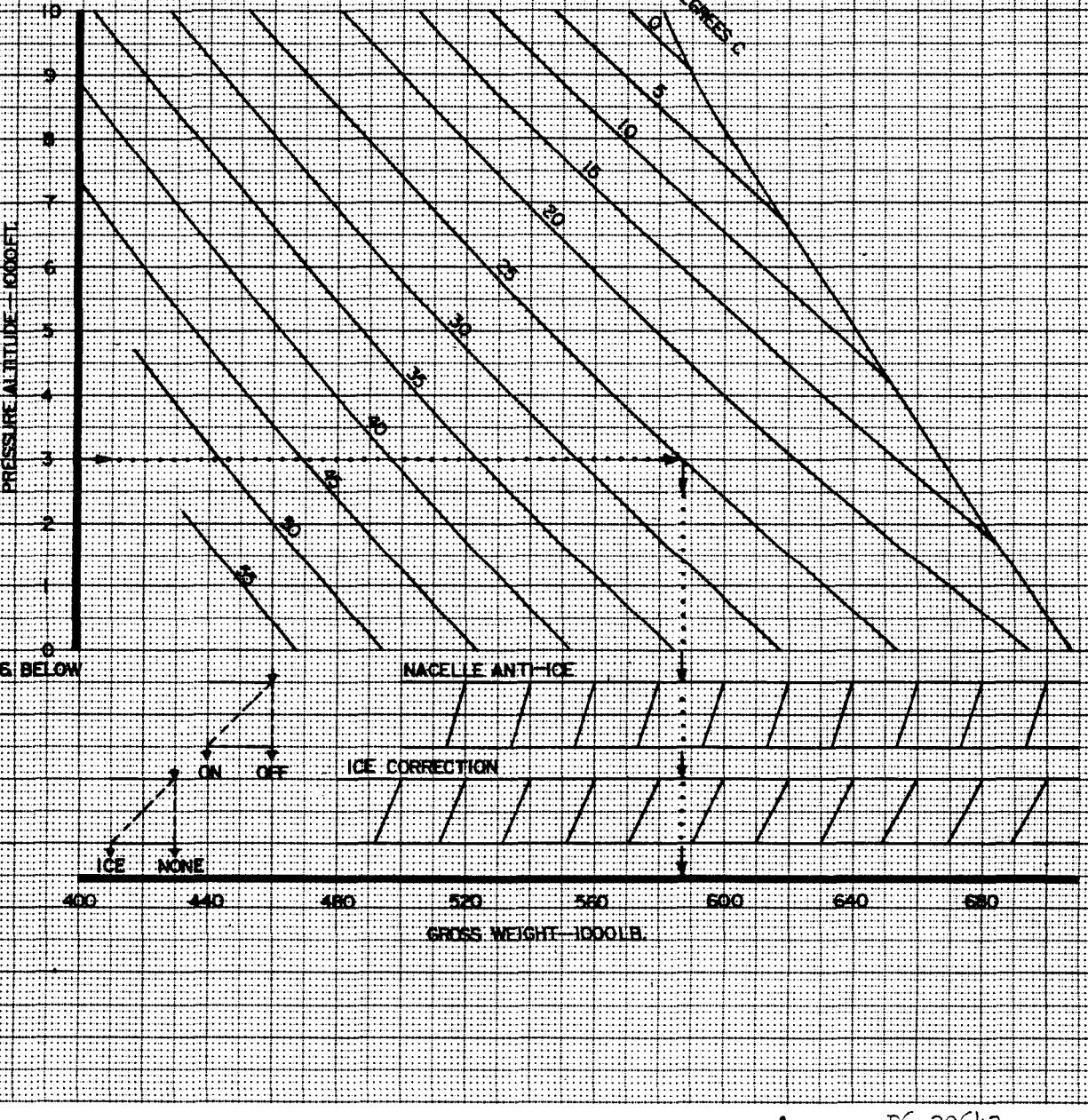

CHART APPLICABLE TO	APPROVED	DATE
747-100 JT9D-3	B.R.P. LA-411	12-11-69
	AJS LA-177	5-20-70

PERFORMANCE

MAXIMUM LANDING WEIGHT
CLIMB LIMITS

APPROACH FLAP POS. 20
LANDING FLAP POS. 25

NOTE: USE ICE CORRECTION WHEN OPERATING IN ICING CONDITIONS DURING ANY PART OF THE FLIGHT WITH FORECAST LANDING TEMPERATURE BELOW 8°C.

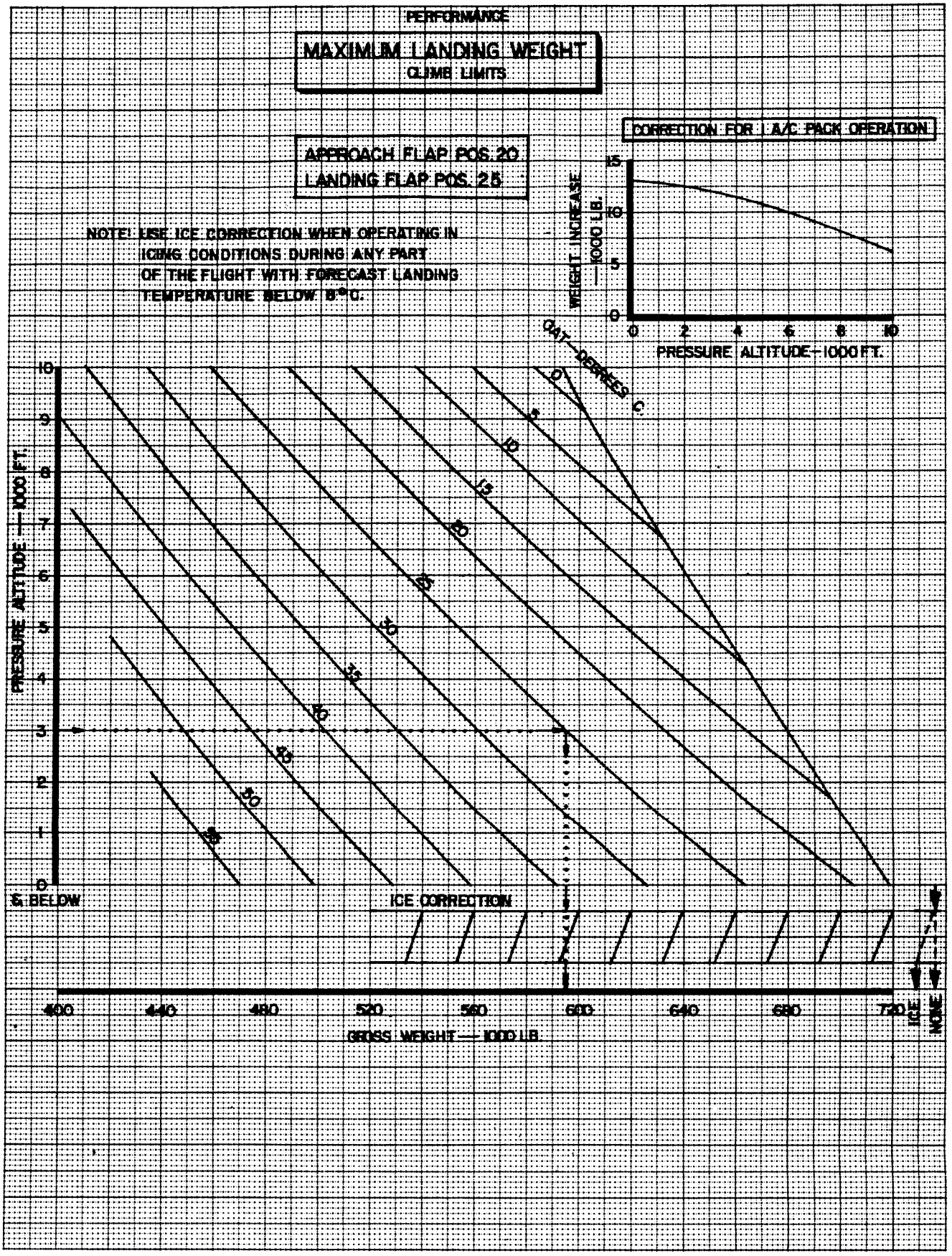

BASSETT 12.069

CHART APPLICABLE TO	APPROVED	DATE
747-100 JT9D-3	B.R.P. LA-411	12-11-69
	LA-477	5-22-70

PERFORMANCE

LANDING FIELD LENGTH AND SPEED

FLAP POS. 30

NOTE: WHEN EITHER INBOARD REVERSER IS INOPERATIVE ADD 150 FT TO FIELD LENGTH REQUIRED.

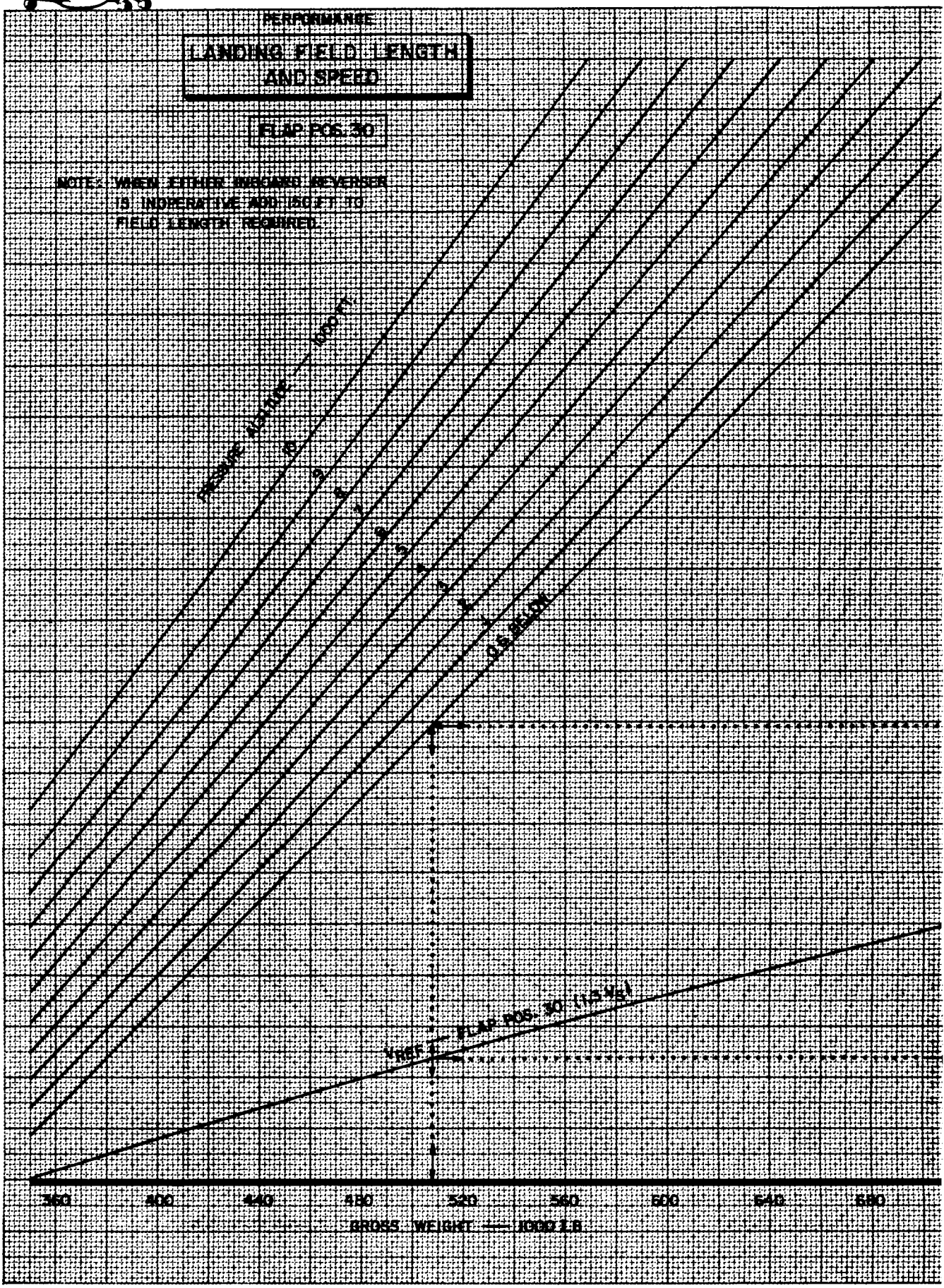

CHART APPLICABLE TO	APPROVED	DATE
747-100 JT9D-3	J.R.S. LA-411	1-8-70
	AJS LA-171	1-26-70

PERFORMANCE

LANDING FIELD LENGTH CORRECTIONS
ANTI-SKID INOPERATIVE

FLAP POS 30

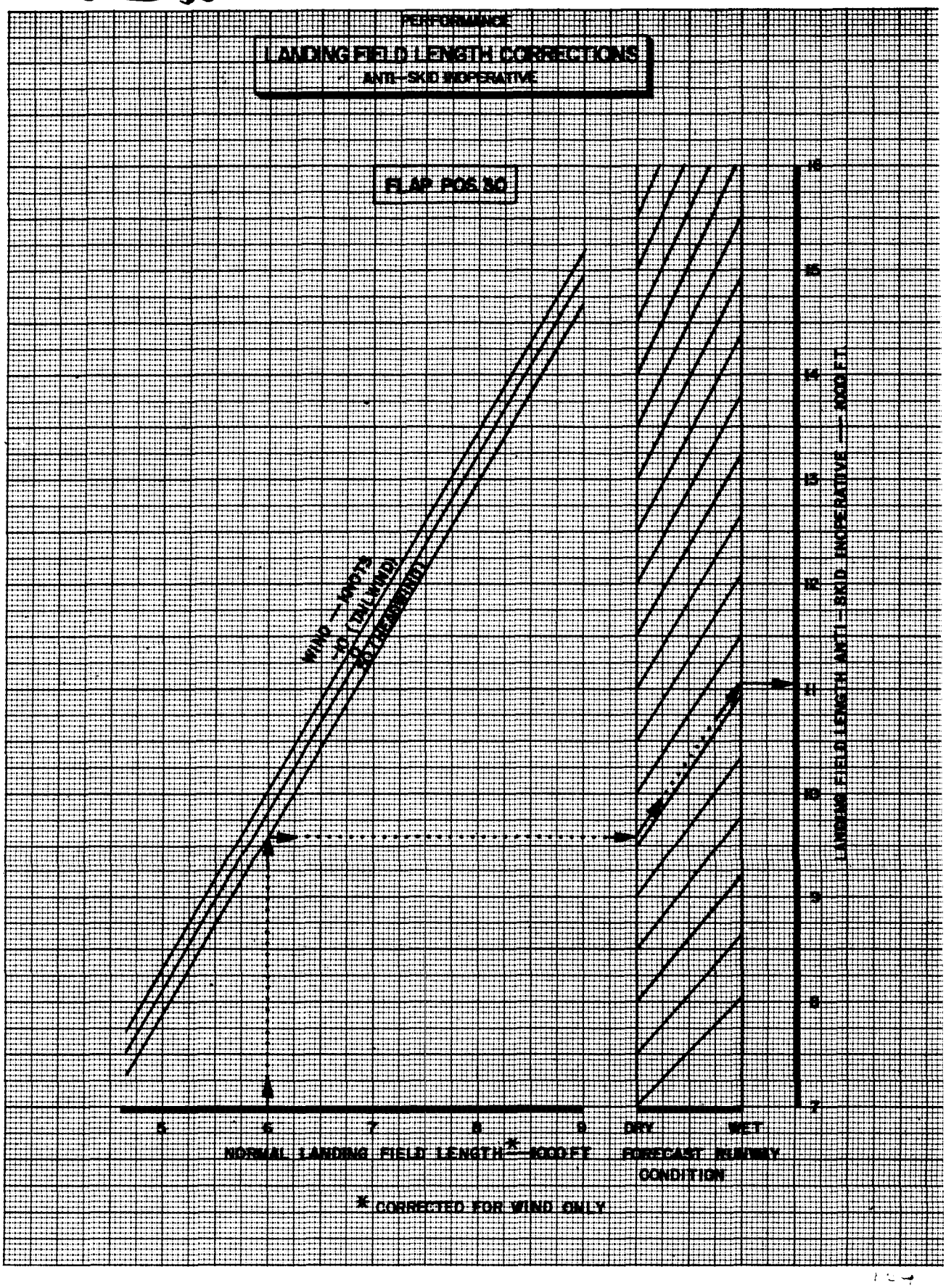

CHART APPLICABLE TO	APPROVED	DATE
747-100 JT9D-3	R. d. LA- 4/11	1-8-70

PERFORMANCE

LANDING FIELD LENGTH AND SPEED

FLAP POS. 25

NOTE: WHEN EITHER INBOARD REVERSER IS INOPERATIVE ADD 150 FT. TO FIELD LENGTH REQUIRED.

NOTE CHANGE IN SCALE

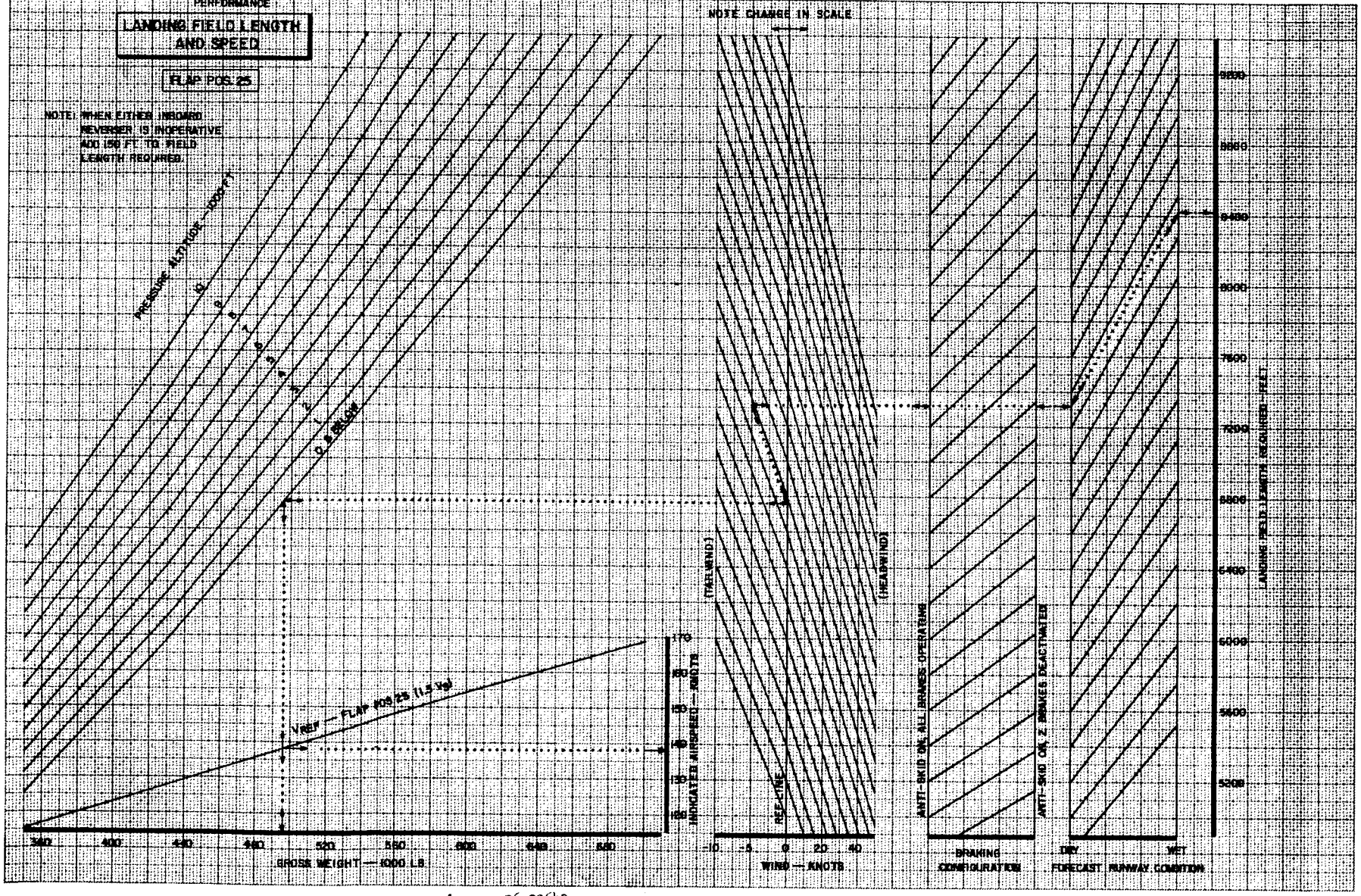

CHART APPLICABLE TO	APPROVED	DATE
747-100 JT9D-3	A.E. Lay Mgr. LA-177	1-8-70 1-26-70

PERFORMANCE

LANDING FIELD LENGTH CORRECTIONS
ANTI — SKID INOPERATIVE

FLAP POS 25

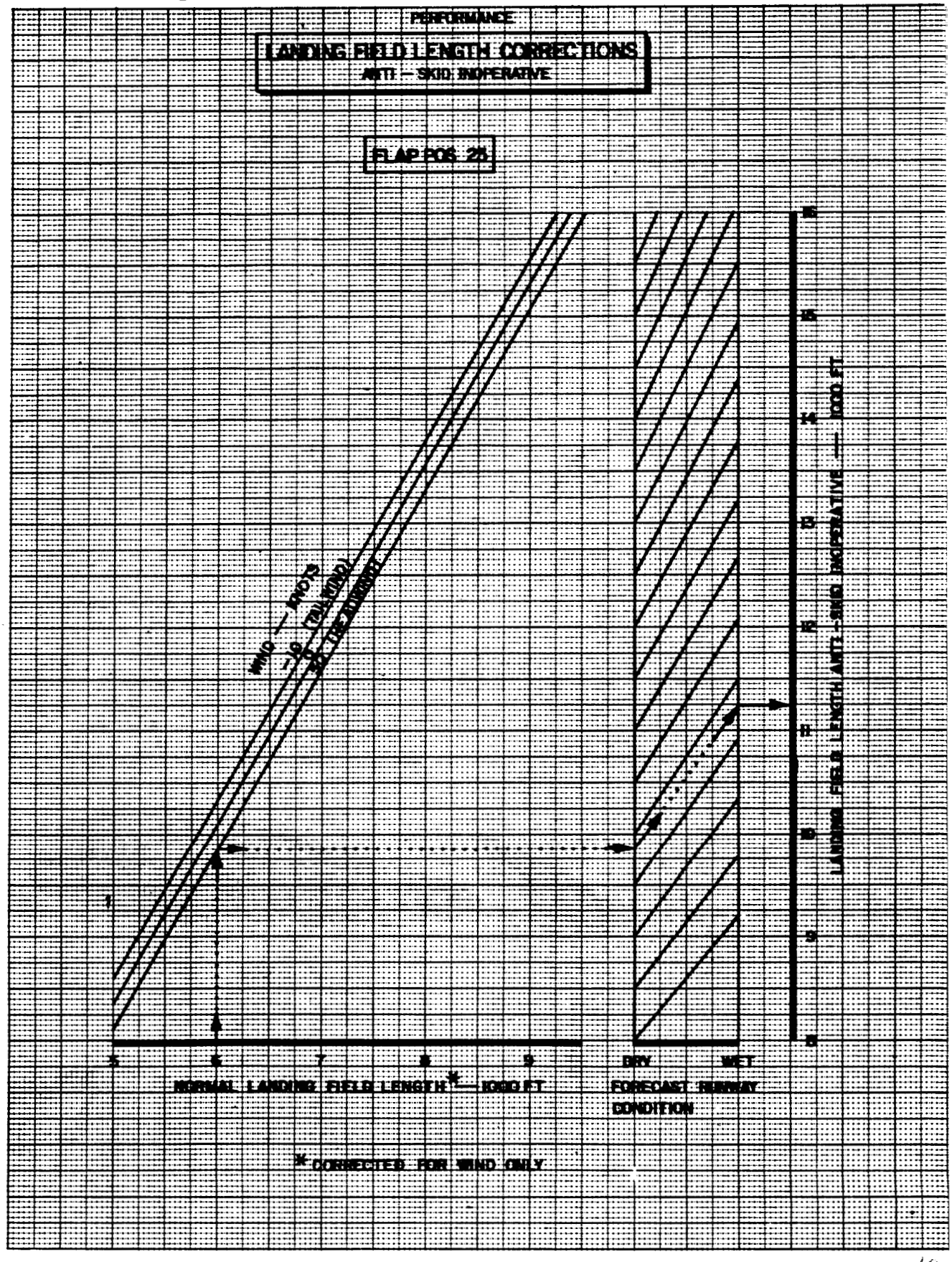

CHART APPLICABLE TO	APPROVED	DATE
747-100 JT9D-3	A.R. Lyn	1-8-70

BASSETT 12-19-69

16.0 APPENDIX B - BUFFET CHARACTERISTICS

The buffet frequency was estimated for the conditions listed in the table on Page 16.0-2. These conditions include stall buffet for each flap detent and compressibility buffet for M_D and V_D conditions. From this investigation it was concluded that:

Average buffet frequency = 3.0—3.5 CPS

Buffet amplitude range = $\pm$.1g—$\pm$.6g

For illustration, flight data is attached for the following five conditions.

COND.	V_C ~KT INITIAL BUFFET	ALTITUDE ~1000FT	G.W ~1000 LB	FLAPS/GEAR	C.G. ~%MAC	PAGE
M_D	—	32	464	UP / UP	27	16.0-3,-4
V_D	447	15.5	490	UP / UP	25	16.0-5,-6
CLEAN STALL	190	18.7	552	UP / UP	32	16.0-7,-8
STALL	128	12.0	536	10 / UP	32	16.0-9,-10
STALL	107	13.4	525	30 / DOWN	33.3	16.0-11,-12

COND	Vc ~KT	ALTITUDE ~1000 FT	G W ~1000LB	FLAPS / GEAR	C.g ~% MAC	BUFFET FREQ ~CPS
M_D		32	464	UP / UP	27	2.9 - 3.1
V_D	447	15.5	490	UP / UP	25	3.1 - 3.3
CLEAN STALL	190	18.7	552	UP / UP	32	3.0 - 5.0
STALL	137	16.5	538	5 / UP	32	3.0 - 4^+
STALL	128	12.0	536	10 / UP	32	3.0 - 4^+
STALL	117	10.9	530	20 / UP	32.5	2.8 - 3.5
STALL	114	15.65	525	25 / DOWN	33	2.8 - 3.5
STALL	107	13.4	525	30 / DOWN	33.3	2.8 - 4^+

INITIAL BUFFET = $\pm .1g \rightarrow \pm .5 \rightarrow .75\,g$

REFERENCE : D6-30642 "747-100 SIMULATOR FLIGHT DECK VIBRATION ENVIRONMENT"

17.0 APPENDIX C - AUTOTHROTTLE

The block diagram on Page 17.0-2 is a simplified autothrottle block diagram for use in small perturbation 747 control simulation. This data is provided for information purposes and was not incorporated in the simulation.

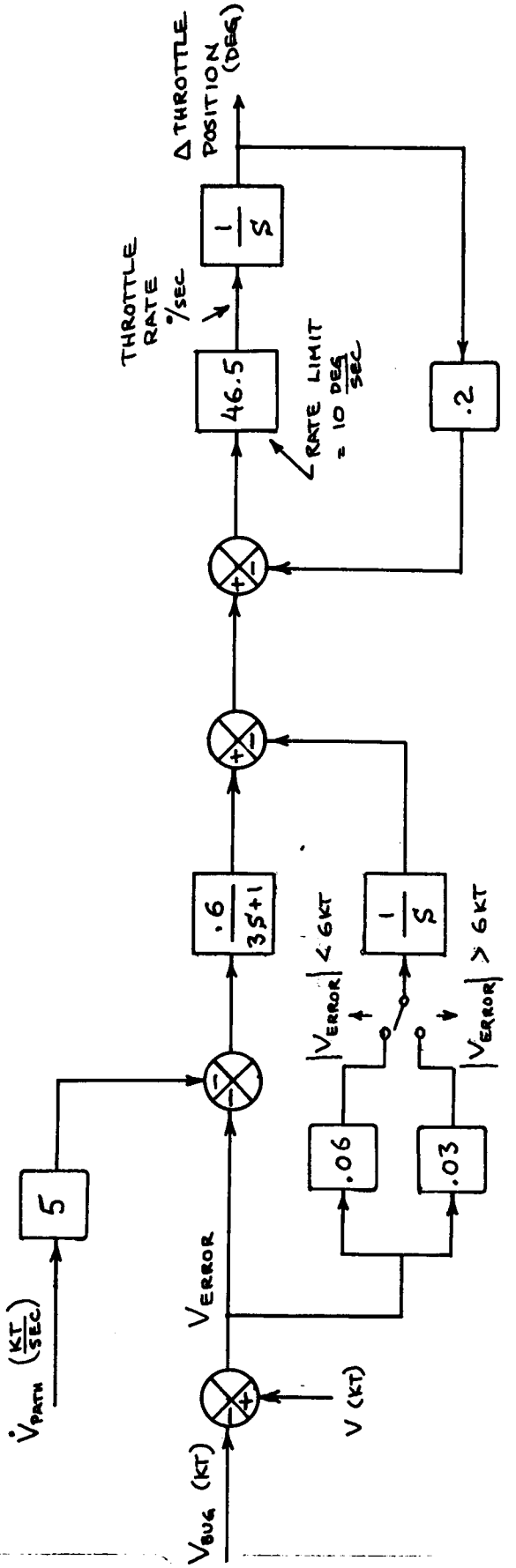

747

CALC		7/24/70	REVISED	DATE	SIMPLIFIED AUTOTHROTTLE BLOCK DIAGRAM
CHECK					
APPD					
APPD					

REV LTR:

E 1196 R6

18.0 APPENDIX D - AUTOPILOT

This section contains a description of the automatic pilot, flight director, yaw damper, and autothrottle systems for the 747 aircraft. This data is provided for information purposes. The autopilot and autothrottle were not incorporated in the simulation.

PAGES 3 - 4 OMITTED

SUMMARY

This document provides a description of the Automatic Pilot, Flight Director, Yaw Damper, and Autothrottle Systems for the 747 aircraft. It contains block diagrams, pictorials, and tables to describe operation of each of these systems as they are planned for incorporation in the aircraft.

Two autopilots give the flight crew a choice of fail-safe systems, each of which can provide all manual and path modes except LAND. Both autopilot channels are used to give "fail passive" control at low altitudes during the automatic landing sequence. Two separate dual-channel automatic pilot pitch trim systems and two yaw dampers give a high level of system integrity.

LIST OF ILLUSTRATIONS

LIST OF TABLES

I. 747 INTEGRATED AUTOPILOT AND FLIGHT DIRECTOR

A. GENERAL

The Sperry SPZ-1 integrated autopilot flight director system was developed for the Boeing 747. The autopilot is used for path or manual control via the pitch wheel and turn knob.* Flight director commands are provided and may be used to monitor autopilot operation, or to be tracked with the autopilot manual mode, or to be tracked manually.

The basic 747 is equipped with a dual autopilot system and a triple flight director system. Each pitch or roll computer contains all of the circuitry necessary to compute the respective pitch or roll autopilot and flight director commands. Each autopilot or flight director channel consists of two computers: one roll, and one pitch.

The general autopilot flight director system layout and interconnects used on the basic Boeing 747 are shown in Figure 1. A dual set of sensors provide navigational and performance signals to the autopilot flight director computers.

Only autopilot computers of channel A and B are connected to hydraulic servos. Computer C is used only for computing flight director commands and cannot be switched in as an autopilot. The number 1 sensor group serves both the A and C computers while sensor group 2 supplies information to the B computers.

Instrument switching allows either the pilot or co-pilot to select any one of the three flight director computer signals for display on his ADI.

The autopilot can be used as a single-channel system in the navigation, cruise, and manual modes of operation. Either channel A or B can be selected for these single-channel modes.

For automatic landing only, fail passive operation is obtained with the dual channel system. Both A and B autopilot channels must be engaged for this mode of operation.

The cockpit location of the controls and indicators for the autopilot/Flight Director, as well as the other systems of the IEFCS, are shown in Figure 1A.

*Maneuvering control for certain airlines will be via control wheel steering instead of turn and pitch knob.

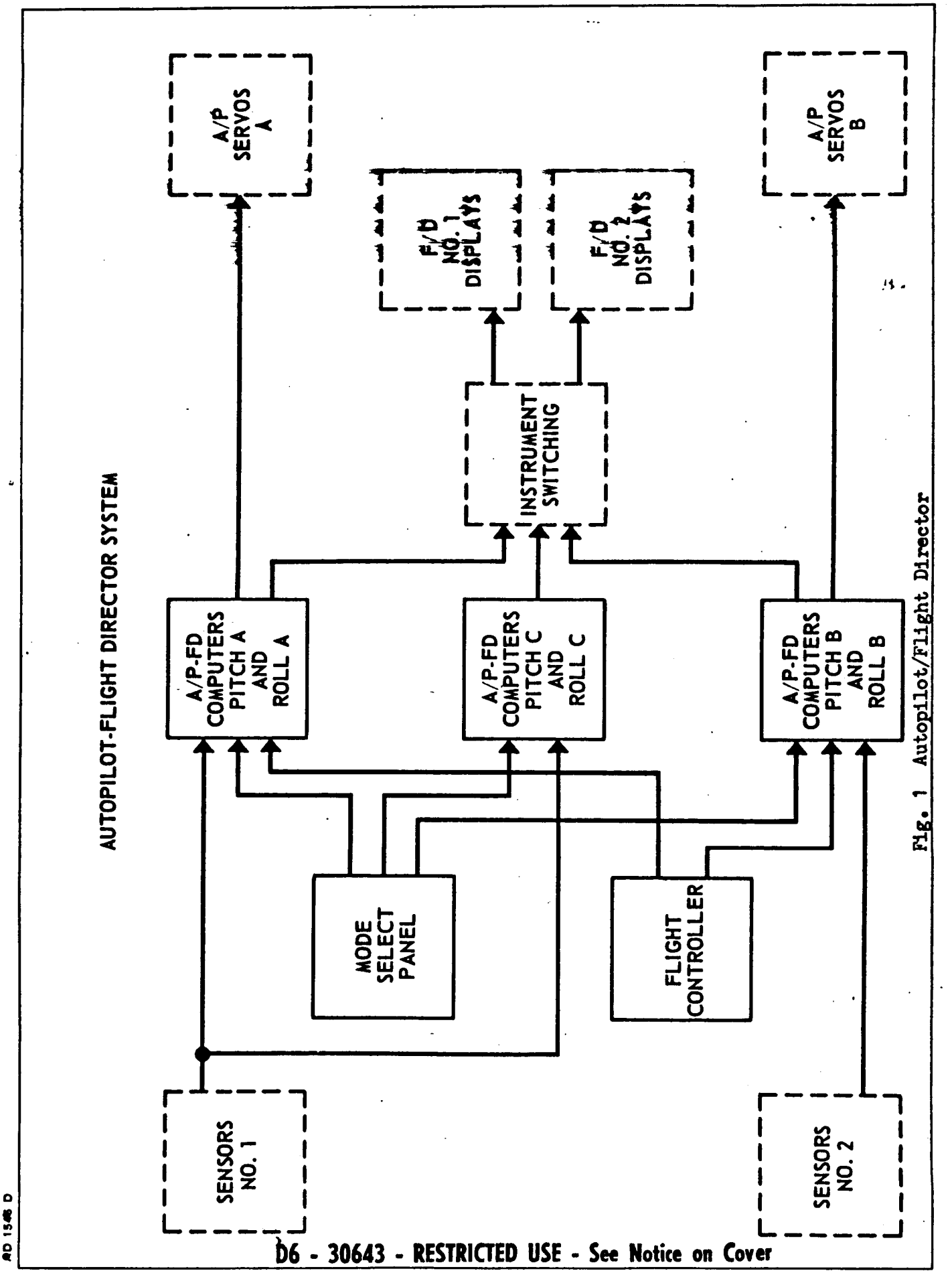

Fig. 1 Autopilot/Flight Director

AD 1546 D

B. SYSTEM INTRODUCTION

All components associated with each flight axis of each channel are packaged in separate computer units. The elements which comprise a basic autopilot/flight director system are:

1) One mode selector panel
2) One flight controller or optionally 3 force sensors.
3) Two flight mode annunciators
4) One monitor and logic unit
5) Three accessory boxes
6) Three roll computers
7) Three pitch computers
8) One automatic stabilizer trim unit

1. Mode Select Panel

The mode select panel contains the switches and logic for mode selection and control of all the autopilot/flight director computer channels. Figure 2 shows the mode select panel. The controls shown shaded in are for optional modes.

The engage switches are solenoid held in MAN and COMMAND with locking provisions at OFF. Each engage switch controls both the pitch and roll computer associated with that channel. Either channel A or B may be engaged in Manual or Command by choice of engage switches. Once one engage switch has been placed into the Manual or Command position, the other switch is locked off and cannot be moved from the OFF position except when LAND has been selected and a monitor check has been satisfactorily completed.

The course select switch may be placed in either the course 1 or course 2 position without regard to which channel of the autopilot has been selected. It is solenoid held in both positions. The switch drops to the dual position when the LAND mode has been selected. Course 1 position feeds the No. 1 VOR/LOC receiver output and No. 1 course error signal to all three A/P - F/D roll computers. and course 2 does likewise for the No. 2 VOR/LOC and No. 2 course error. In the dual position, LOC No. 1 and Course error No. 1 are fed to computers A and C while LOC No. 2 and course error No. 2 are fed to the B computer. Figure 3 is a pictorial diagram of the above switching functions and indicates the isolation and independence achieved for single and dual channel modes of autopilot operation.

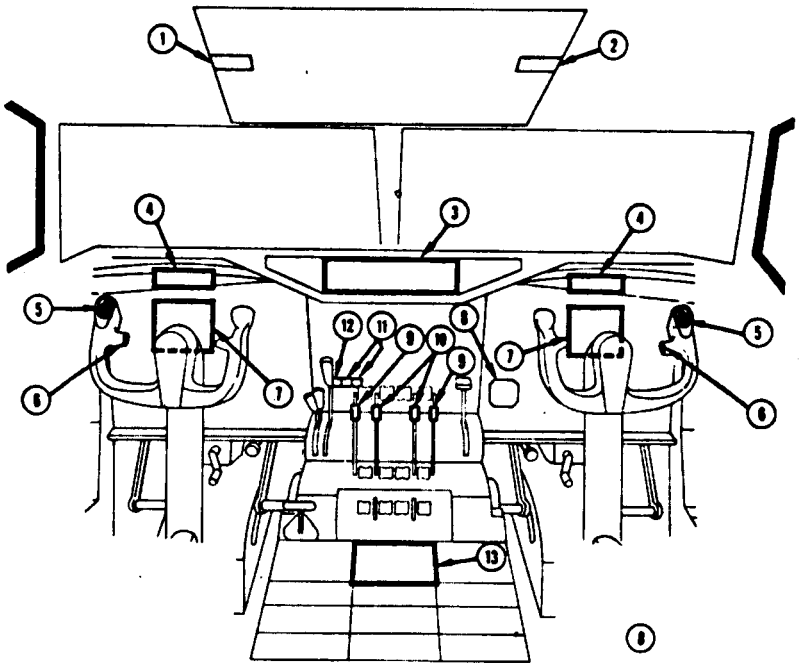

① YAW DAMPER CONTROL PANEL
② (FUNCTION DELETED)
③ MODE SELECT PANEL
④ FLIGHT MODE ANNUNCIATOR
⑤ STABILIZER TRIM DUAL SWITCHES
⑥ AUTOPILOT DISENGAGE SWITCH
⑦ ATTITUDE DIRECTOR INDICATOR
⑧ CONTROL SURFACE POSITION INDICATOR
⑨ AUTOTHROTTLE DISCONNECT SWITCH
⑩ GO-AROUND SWITCHES
⑪ AUTOMATIC STABILIZER TRIM LIGHTS
⑫ (FUNCTION DELETED)
⑬ FLIGHT CONTROLLER

Figure 1a

747 COCKPIT FLIGHT CONTROLS AND INDICATORS

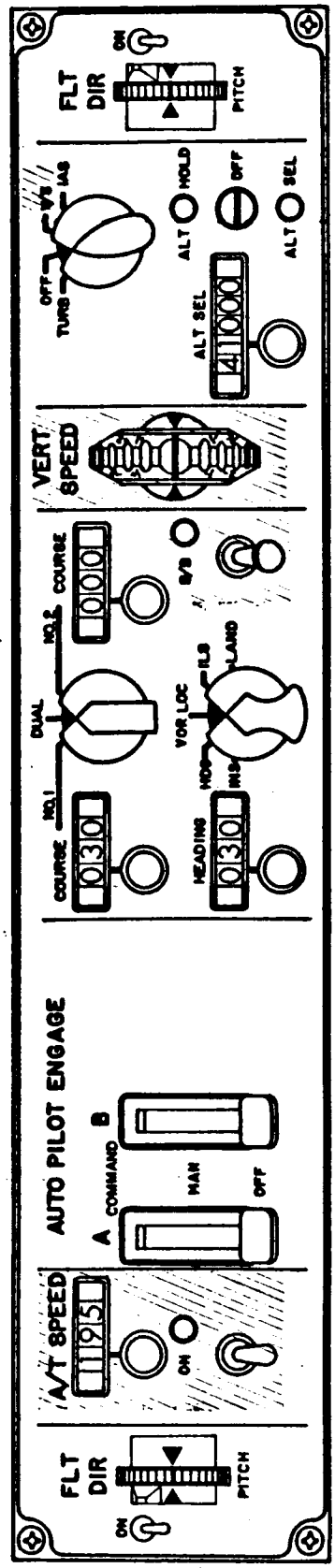

Fig. 2 Mode Select Panel

AD 1546 D

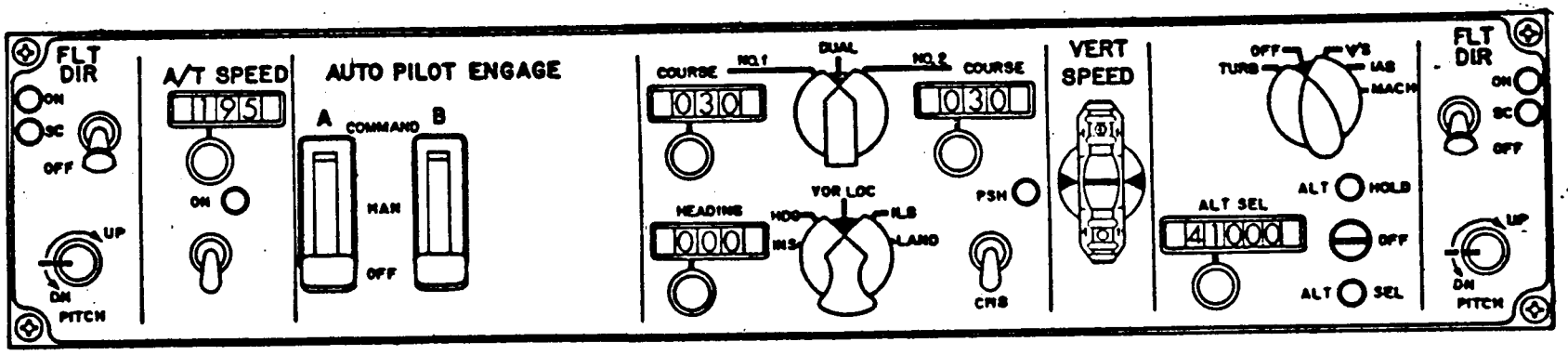

FIG. 2a

MODE SELECT PANEL

(WITH CONTROL WHEEL STEERING AND MACH HOLD OPTION)

PRESET COURSE SWITCHING

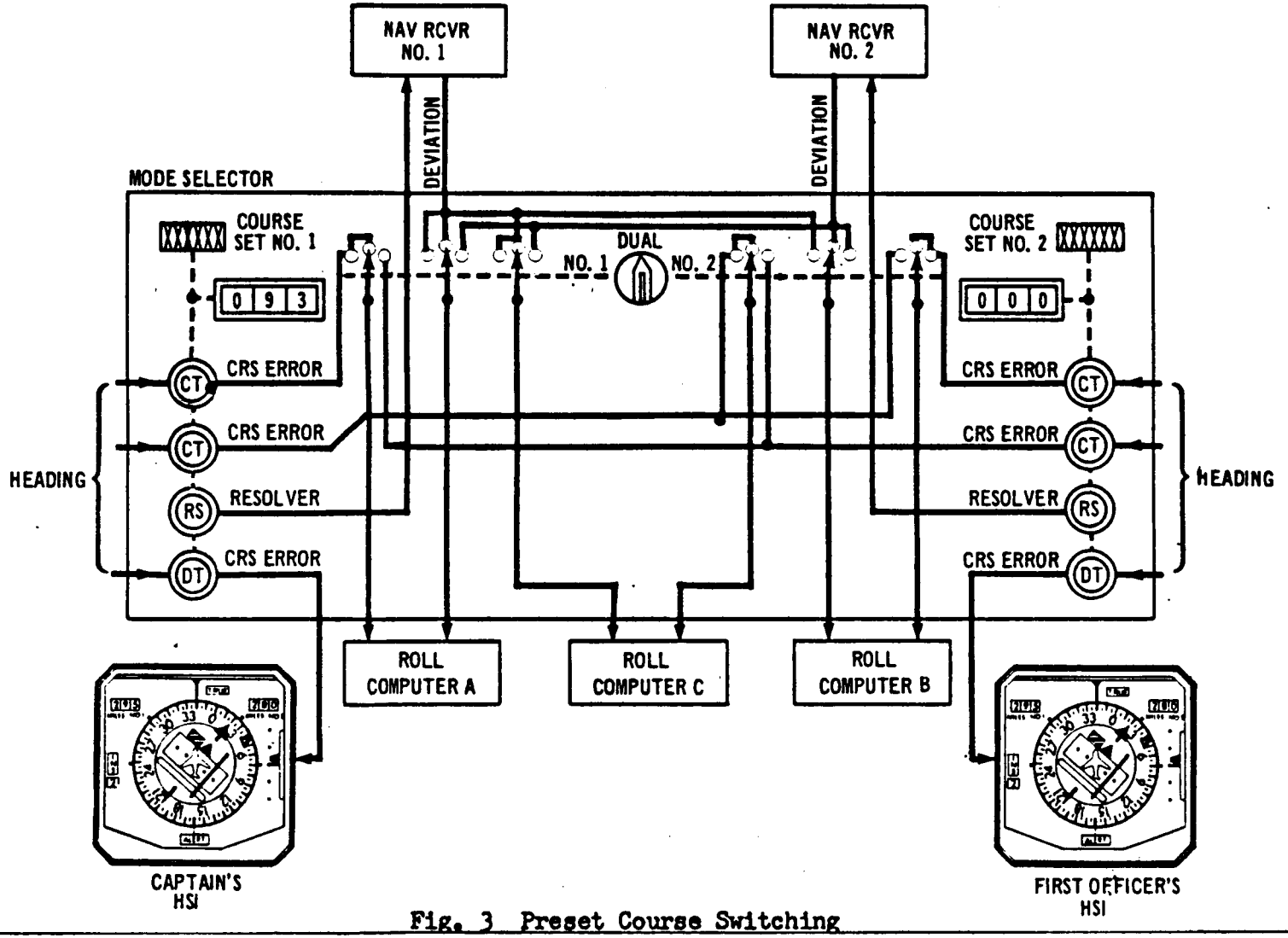

Fig. 3 Preset Course Switching

Heading select is accomplished for all three channels through a single set knob which positions two synchros fed from two separate magnetic heading reference units to maintain heading isolation.

The lateral navigation modes (INS, HDG, VOR/LOC), as well as the landing approach control modes ILS and LAND, are selected by the main mode selector switch. This is a simple rotary type switch without holding or centering devices. A second selector switch, also rotary type, allows selection of the Turbulence mode, V/S (vertical speed), IAS hold, or Mach hold. This second switch is solenoid held in each mode select position. The V/S and IAS modes may be selected alone or during the arm phases of ALT. Select, ILS, and LAND. When used during the armed phases of another mode, the switch will drop to OFF when the mode goes into the capture phase.

The switch will not hold in Turb. if the autopilot is not engaged. Also, if the switch is moved to Turb while the altitude select is engaged, the altitude select switch will drop to OFF. Further, if Turb. is engaged and ALT hold is selected, the Turb. switch will drop to OFF.

The Back Beam switch is designed to mechanically preclude accidental turn on and is solenoid held in the ON position. It will hold only if VOR/LOC is selected on the mode selector switch. Also available on the mode select panel are the ON/OFF switches and pitch trim controls for flight directors.

The mode selection and mode compatibility interlocks related to the position of the switches on the Mode Select Panel are shown in Table 1. (Pitch channel) and Table 2 (Roll channel) for both the autopilot and the Flight Director.

2. Flight Controller

The Flight Controller which contains the autopilot pitch wheels and turn knob is shown in Figure 4. The pitch wheel and turn knob provide attitude commands proportional to their respective rotations. The outputs for channels A and B of the autopilot are electrically independent. The potentiometers used with the pitch wheels are unclutched electrically from the wheels during all pitch path modes.

For customers who order the control wheel steering option the flight controller is not used. Instead three force transducers shown in Figure 4a are provided to maneuver the aircraft via the normal control column and control wheel with autopilot engaged.

AUTOPILOT-FLIGHT DIRECTOR MODE CHART - PITCH MODES

PITCH MODES / A/P ENGAGE SWITCH	ALL OFF		ALT HOLD		ALT SELECT ARMED		ALT SELECT CAPTURE		IAS HOLD		MACH HOLD [SPECIAL FEATURE]		VERT SPEED [OPTION]		ILS (GLIDE SLOPE) ARMED		ILS (GLIDE SLOPE) CAPTURE		LAND (GS & FLARE) ARMED		LAND (GS & FLARE) CAPTURE		G/A (FIXED ATTITUDE)		TURBULENCE (NOT AVAIL. IN ILS OR LAND MODES)	
	A/P	FD	A/P	FD	A/P	FD	A/P	FD	A/P	FD	A/P	FD	A/P	FD	A/P	FD	A/P	FD	A/P	FD	A/P	FD	A/P	FD	A/P	FD
COMMAND	PW	PTW	X	X	PW OR ▷1	PTW OR ▷1	X	X	X	X	X	X	X	X	PW OR ▷2	PTW OR ▷2	X	X	PW OR ▷2 *	PTW OR ▷2	X *	X	NOT APPL ▷4		NOT APPL ▷4	
MANUAL	PW	PTW	X	X	PW	PTW OR ▷1	PW	X	PW	X	PW	X	PW	X	ALT HOLD OR PW	PTW OR ▷2	PW	X	ALT HOLD OR PW*	PTW OR ▷2	PW *	X ▷3	NOT APPL ▷4		PW	PTW
OFF	0	PTW	0	X	0	PTW OR ▷1	0	X	0	X	0	X	0	X	0	PTW OR ▷2	0	X	* 0	PTW OR ▷2	* 0	X ▷3	0	X	TURB SWITCH WILL NOT HOLD	

0 NOT ENGAGED

X ENGAGED OR OPERATIVE

PW PITCH CONTROL WHEEL (OR CWS)

PTW PITCH TRIM WHEEL

▷1 SELECTED COMPATIBLE MODE, THAT IS: IAS HOLD, MACH HOLD, VERT SPEED, ILS ARMED OR LAND ARMED.

▷2 SELECTED COMPATIBLE MODE, THAT IS: ALT HOLD, ALT SEL, IAS HOLD, OR VERT SPEED.

▷3 NOT CERTIFIED BEYOND CATEGORY II.

▷4 AUTOPILOT ENGAGE SWITCH WILL NOT HOLD IN THIS POSITION.

* A/P WARNING LIGHT "FLASHING AMBER" UNLESS BOTH A/P ENGAGE SWITCHES ARE IN "COMMAND" POSITION.

Table 1 Autopilot/Flight Director Mode Chart - Pitch Modes

AUTOPILOT-FLIGHT DIRECTOR MODE CHART - ROLL MODES

ROLL MODES / A/P ENGAGE SWITCH	INS		HDG (SELECT)	VOR/LOC		VOR/LOC BACK BEAM [OPTION]		ILS (LOC)		LAND (LOC)		G/A (WING LEVEL)	TURBULENCE (NOT AVAIL. IN ILS OR LAND MODES)
	ARMED	CAPTURE		ARMED	CAPTURE	ARMED	CAPTURE	ARMED	CAPTURE	ARMED	CAPTURE		
	A/P FD	A/P FD	A/P FD	A/P FD	A/P FD	A/P FD	A/P FD	A/P FD	A/P FD	A/P FD	A/P FD	A/P FD	A/P FD
COMMAND	HDG SEL HDG SEL	X X	X X	HDG SEL HDG SEL	X X	NOT APPL ④	NOT APPL ④	HDG SEL HDG SEL	X X	HDG SEL * HDG SEL	X * X	NOT APPL ④	NOT APPL ④
MANUAL	TK HDG SEL	TK X	TK X	TK HDG SEL	TK X	TK HDG SEL	TK X	TK HDG SEL	TK X	TK * HDG SEL	TK * X ③	NOT APPL ④	TK SEL MODE
OFF	0 HDG SEL	0 X	0 X	0 X	0 X	0 HDG SEL	0 X	0 HDG SEL	0 X	* 0 HDG SEL	* 0 X ③	0 X	TURB SWITCH WILL NOT HOLD

0 NOT ENGAGED

X ENGAGED OR OPERATIVE

TK TURN CONTROL KNOB (OR CWS)

③ NOT CERTIFIED BEYOND CATEGORY II.

④ AUTOPILOT ENGAGE SWITCH WILL NOT HOLD IN THIS POSITION

* A/P WARNING LIGHT "FLASHING AMBER" UNLESS BOTH A/P ENGAGE SWITCHES ARE IN "COMMAND" POSITION.

Table 2 Autopilot/Flight Director Mode Chart - Roll Modes

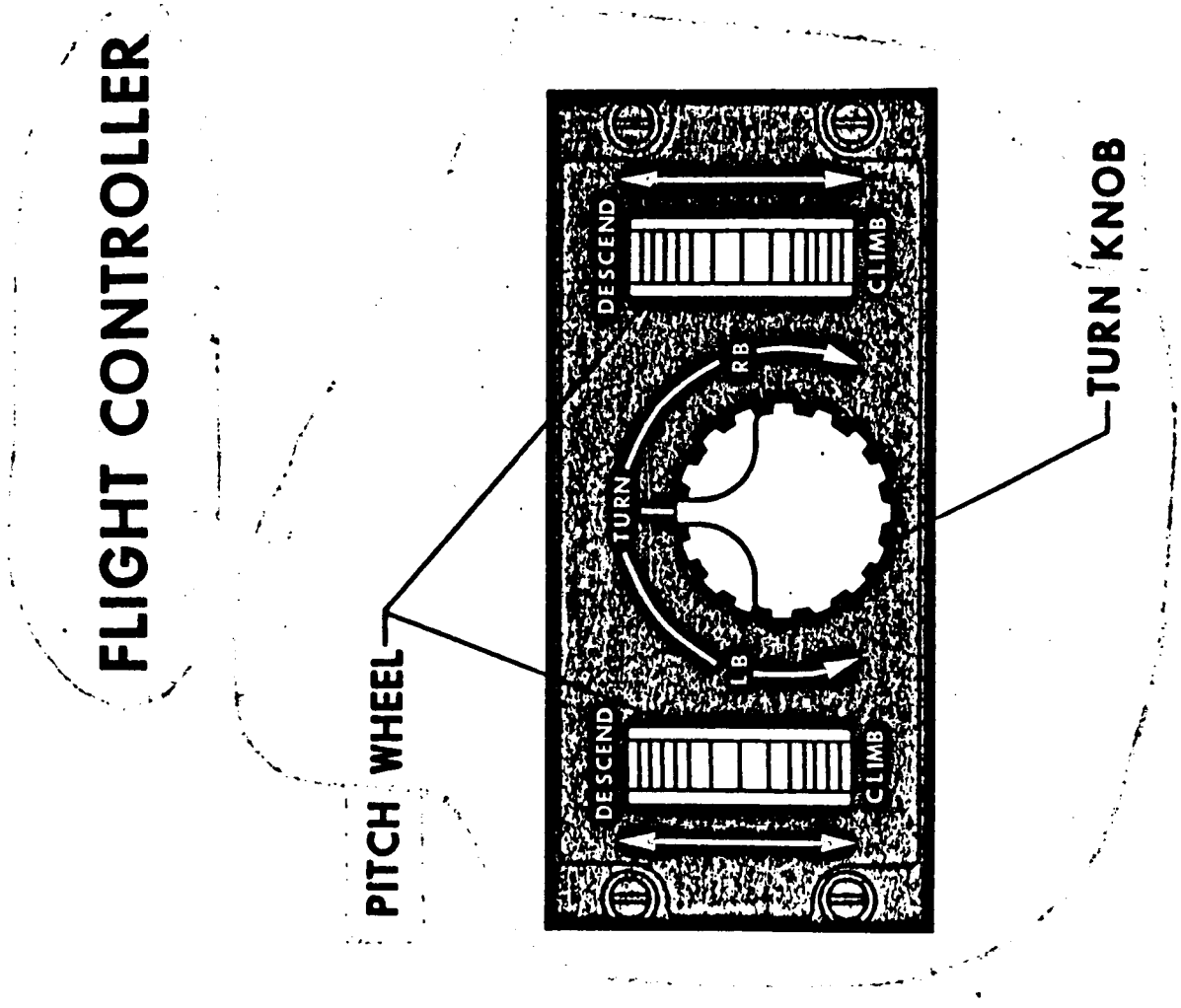

Fig. 4 Flight Controller

AD 1546 D

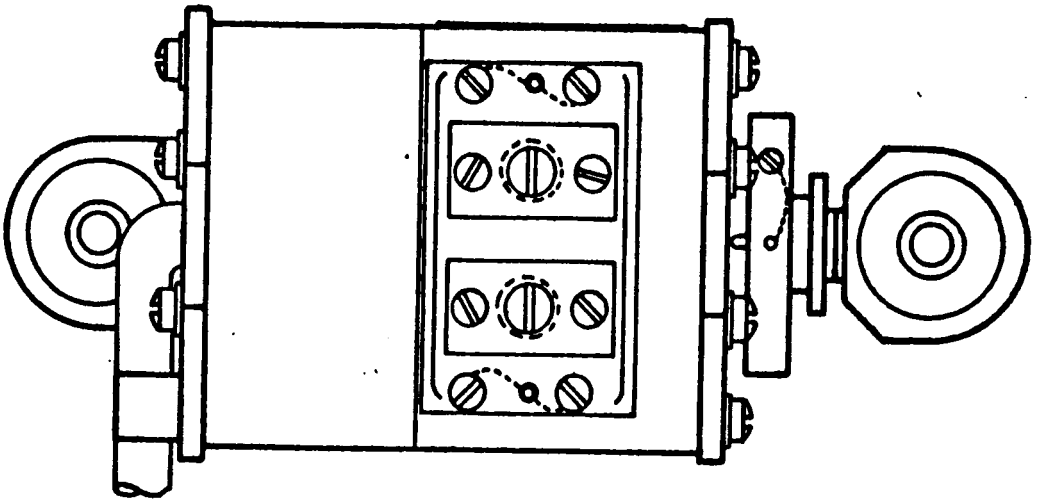

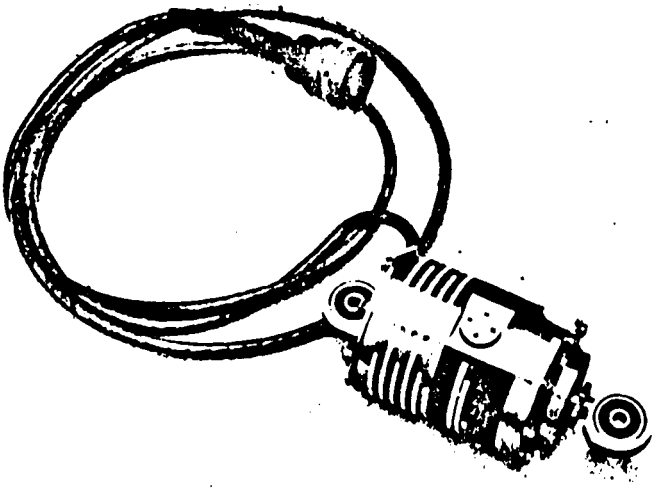

CONTROL WHEEL STEERING
FORCE TRANSDUCER

AD 1546 D

D6 - 30643 - RESTRICTED USE - See Notice on Cover

3. Flight Mode Annunciation

Dual flight mode annunciators are provided on the 747. Flight director modes and autopilot modes are displayed side by side on each annunciator panel as shown in Figure 4a.

The basic modes annunciated are:

- o ALT SEL (Altitude Select)
- o NAV (Navigation)
- o GS (Glide Slope)
- o FLARE
- o GO AROUND

In each mode the annunciator displays an amber light when the particular mode is armed and switches to a green light when the mode is initiated. Table 3 shows each autopilot and Flight Director mode as it will be displayed on the mode annunciator.

Also displayed on the annunciator panel are the autopilot and autothrottle warning and disengage lights.

A press-to-test feature is included in the flight mode annunciator. All amber lights are tested by depressing the left hand section of the panel. All green lights as well as the red warning lights of the autopilot and autothrottle are tested by depressing the right hand section of the panel.

4. Monitor and Logic Unit

The monitor and logic unit is a separate package which contains much of the autopilot/Flight Director engage interlock logic, dual-channel monitoring logic, mode annunciation logic, and the warning light circuits. The physical and electrical arrangement of the monitor and logic unit provides complete channel isolation.

5. Accessory Boxes

The accessory boxes are Boeing supplied units which provide the switching and interconnect functions necessary to interface the autopilot and flight director systems to other airplane systems.

6. Pitch and Roll Computers

The A/P - F/D pitch and roll computers include the computing and logic circuitry necessary to receive data from the aircraft sensors and produce autopilot servo and flight director commands for all modes of operation.

FLIGHT MODE ANNUNCIATOR

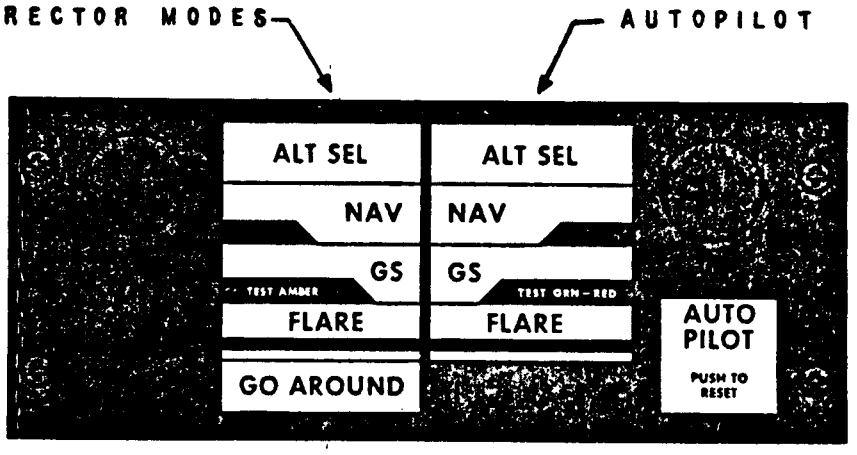

BASIC

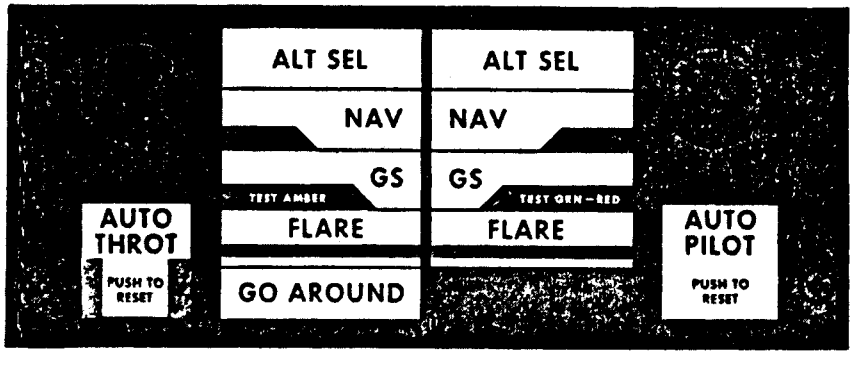

WITH AUTOTHROTTLE OPTION

Figure 46

FLIGHT MODE ANNUNCIATOR

MODE	CONDITION	FLIGHT MODE ANNUNCIATOR									
		AUTOPILOT AND FLIGHT DIRECTOR								F/D ONLY	
		ALT. SEL.		NAV.		GS		FLARE		GO AROUND	
		AMBER	GREEN	AMBER	GREEN	AMBER	GREEN	AMBER	GREEN	AMBER	GREEN
LOC	ARM			X							
	CAPTURE & CONTROL				X						
VOR	ARM			X							
	CAPTURE & CONTROL				X						
INS	ARM			X							
	CAPTURE & CONTROL				X						
ILS	ARM			X		X					
	CAPTURE & CONTROL				X		X			X	
LAND	ARM			X		X					
	CAPTURE & CONTROL				X		X	X		X	
	FLARE				X		X		X	X	
ALT. SEL.	ARM	X									
	CAPTURE & CONTROL		X								
GO AROUND F/D ONLY	ARM									X	
	CAPTURE & CONTROL										X

Table 3 Flight Mode Annunciator Chart

7. Automatic Stabilizer Trim Unit

The automatic stabilizer trim unit (ASTU) contains the computational circuitry necessary to provide automatic stabilizer trim whenever the autopilot is engaged. The ASTU contains two independent self monitored trim channels. One channel provides trim operation while the other is in standby. Automatic transfer is provided to the standby channel in the event that the trim monitor detects a malfunction.

8. Self-Test and Maintenance Monitoring

Self-test of the pitch and roll computers, the automatic stabilizer trim unit and the monitor and logic unit is performed with a go/no-go readout by means of the Built-In-Test-Equipment (BITE).

The BITE switches and lights, located on the front panels of each of the above units, permit the rapid isolation of a faulty unit, while the complete system is installed on the airplane.

A typical BITE test is shown in Figure 4b. The BITE sets up input signals and sensors to adjust two or more signal path gains in the unit under test (UUT) as required to achieve a null summation of the signal path outputs, if all circuits are normal. The null condition is sensed by BITE null detection logic. Simultaneously, specific portions of the unit logic are addressed by BITE. The status of the unit logic circuits and the output of the BITE signal null detector are combined in BITE logic to produce a go/no-go output to the BITE readout lights.

Maintenance monitoring has been included in the system as a basic feature to help in isolating the cause of autopilot warning or disengagement during dual-channel autopilot operation.

The maintenance monitoring circuits and readouts are included in the Monitor and Logic Unit. The readout is located in the top portion of the Monitor and Logic Unit front panel, above the BITE readout lights. The maintenance monitor readout consists of four latching indicators which trip to indicate that autopilot warning or disengagement occurred for one of the following reasons:

1. Power loss to channel A (single or dual channel operation)
2. Power loss to channel B (single or dual channel operation)
3. Pitch channel camout monitoring trip (dual channel operation)
4. Roll channel camout monitoring trip (dual channel operation)

The above faults are monitored and displayed permanently by the latched indicators, until these are manually reset.

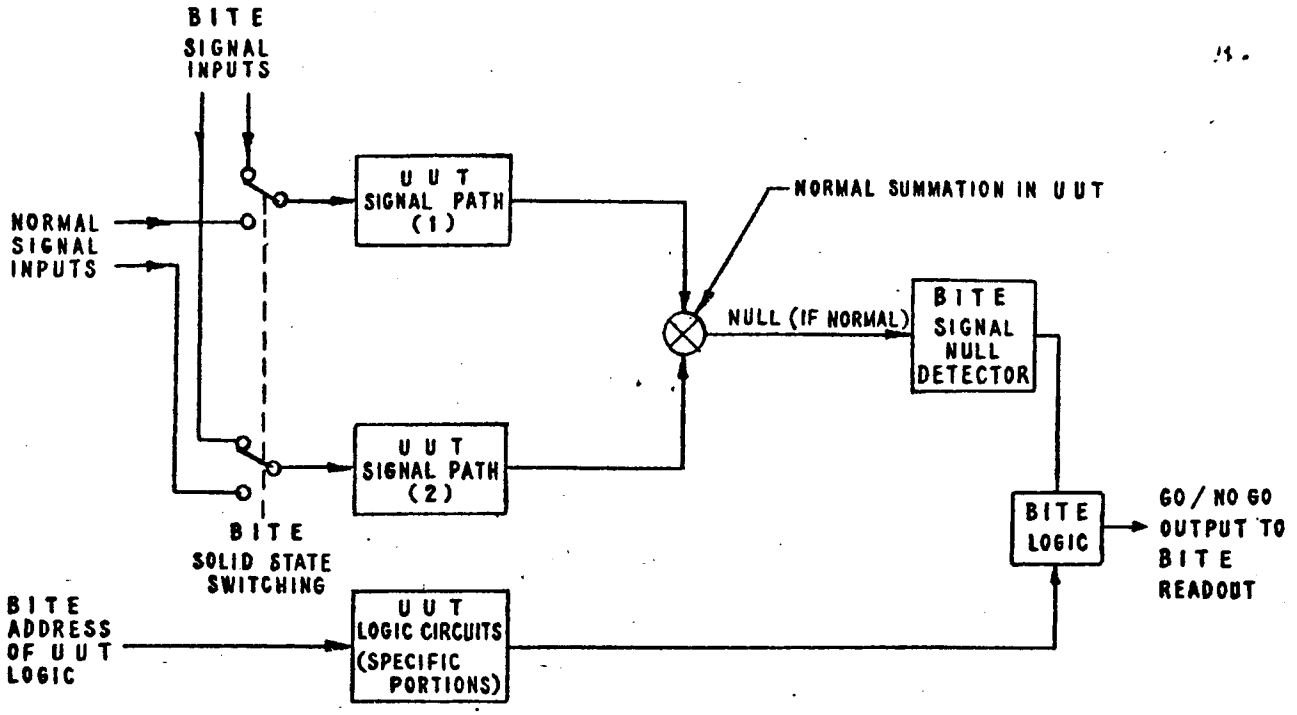

NOTE : UUT = UNIT UNDER TEST

FIG. 4b — TYPICAL BITE TEST

9. ILS Deviation Warning System (Optional)

The Deviation Warning System is a dual system, monitoring the Captain's and First Officer's navigation receiver outputs. (See Figure 4d)

The system warns the pilots when the outputs of the navigation receivers exceed 20 ua from the localizer beam centerline or 75 ua from the Glide Slope beam centerline with a delay time of 2.2 seconds. The warning system is in operation when the autopilot is engaged in the ILS or LAND mode and the radio altitude is below 500 feet altitude. From 500 feet to 200 feet the system provides a warning if the receiver output exceeds either GS or LOC thresholds. If the nav. receiver signal causing the warning is reduced below the detection threshold, the warning light will be turned off. However, below 200 feet altitude the system becomes latching and once the warning system has been tripped the warning light will remain on even though the signal error has been reduced below the threshold. Below Flare altitude (53 feet) the warning system monitors only LOC deviation signal errors.

The two monitor systems are independent. However, to provide greater redundancy the deviation warning signals are cross fed such that if one monitor is tripped it will also switch on the warning light driver stage of the second monitor, thus illuminating all warning lamps associated with the ILS deviation warning system.

Confidence tests of the system can be performed either on the ground or in flight. The confidence tests are pilot activated and monitored. The tests are activated by proper mode selection and engagement of the A/P and F/D and the deflection of the VHF NAV test switch.

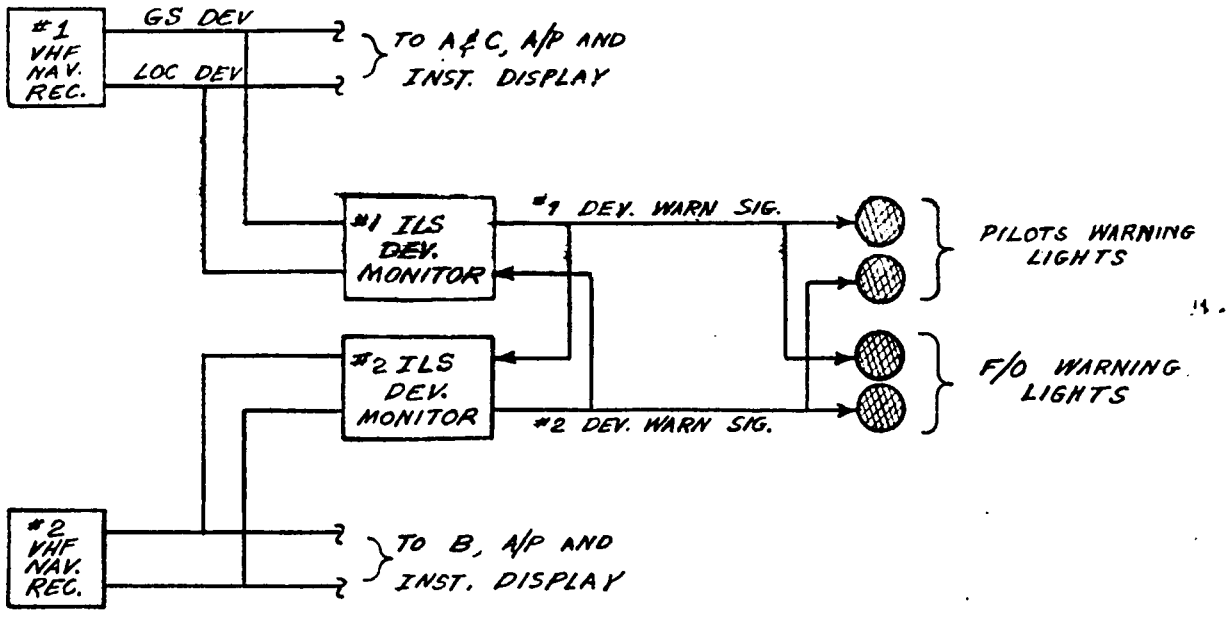

ILS DEVIATION WARNING
SYSTEM BLOCK DIAGRAM

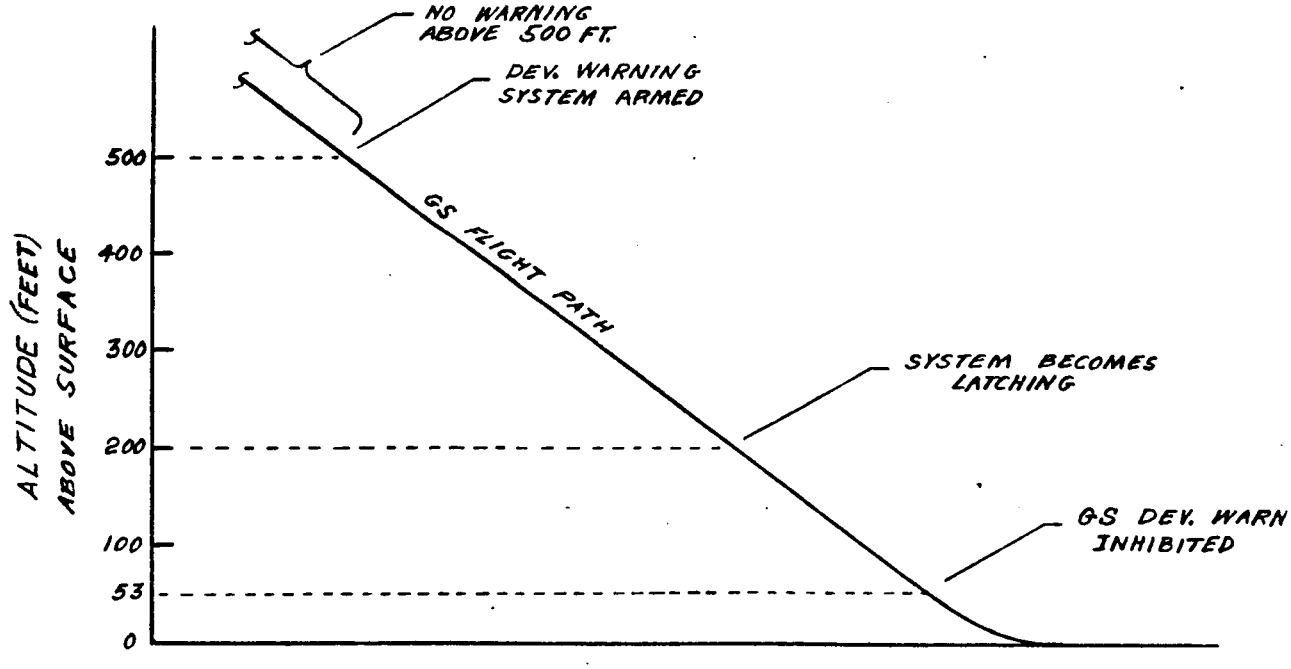

ENGR.	[illegible]	2/24/[illegible]	REVISED	DATE	ILS DEVIATION WARNING SYSTEM (OPTIONAL)	D6-30643 Vol. II
CHECK						FIG 4d
APR						
APR					THE BOEING COMPANY RENTON, WASHINGTON	Page 21d
					18	

AD 1017-R6

Rev d

C. DESCRIPTION OF THE AUTOPILOT ACTUATOR SYSTEM

When the autopilot is engaged, autopilot commands are coupled into the primary flight control system via parallel servo actuators. Thus, the control wheel and column, as well as the control surfaces, move in response to autopilot commands.

The lateral control system of the 747 utilizes a pair of hydraulic central control actuators which control the hydraulic-powered surface actuators. These central control actuators accept commands from either the autopilot or the manual control system. During all manual or autopilot operation, the two central control actuators are slaved together through a cross link.

The 747 lateral autopilot servo system is mechanized as shown in Figure 5. The pitch axis autopilot servo mechanization is similar in concept to the lateral system.

The mechanization of the servo makes the system fail safe for all single-channel operation and fail passive for all dual-channel (LAND) operation.

1. Single-Channel Operation

Single-channel autopilot operation is used in all modes except LAND. In single-channel operation, either the A channel or B channel autopilot may be selected. The autopilot drives an autopilot servo actuator integral with the central control package. The servo actuator output displacements are proportional to the autopilot command signals. The autopilot actuator drives the manual controls via a force detent. When either autopilot is engaged, both central control packages are driven from the engaged autopilot actuator.

Autopilot authority in the lateral axis is stroke limited to the equivalent of twenty-five degrees of control wheel displacement. In the pitch axis, authority is limited by reacting the force detent against the manual feel pressure system.

The pilot can overpower the autopilot at any time by applying approximately fourteen pounds at the control wheel in the lateral axis and about twenty-seven pounds in the longitudinal axis.

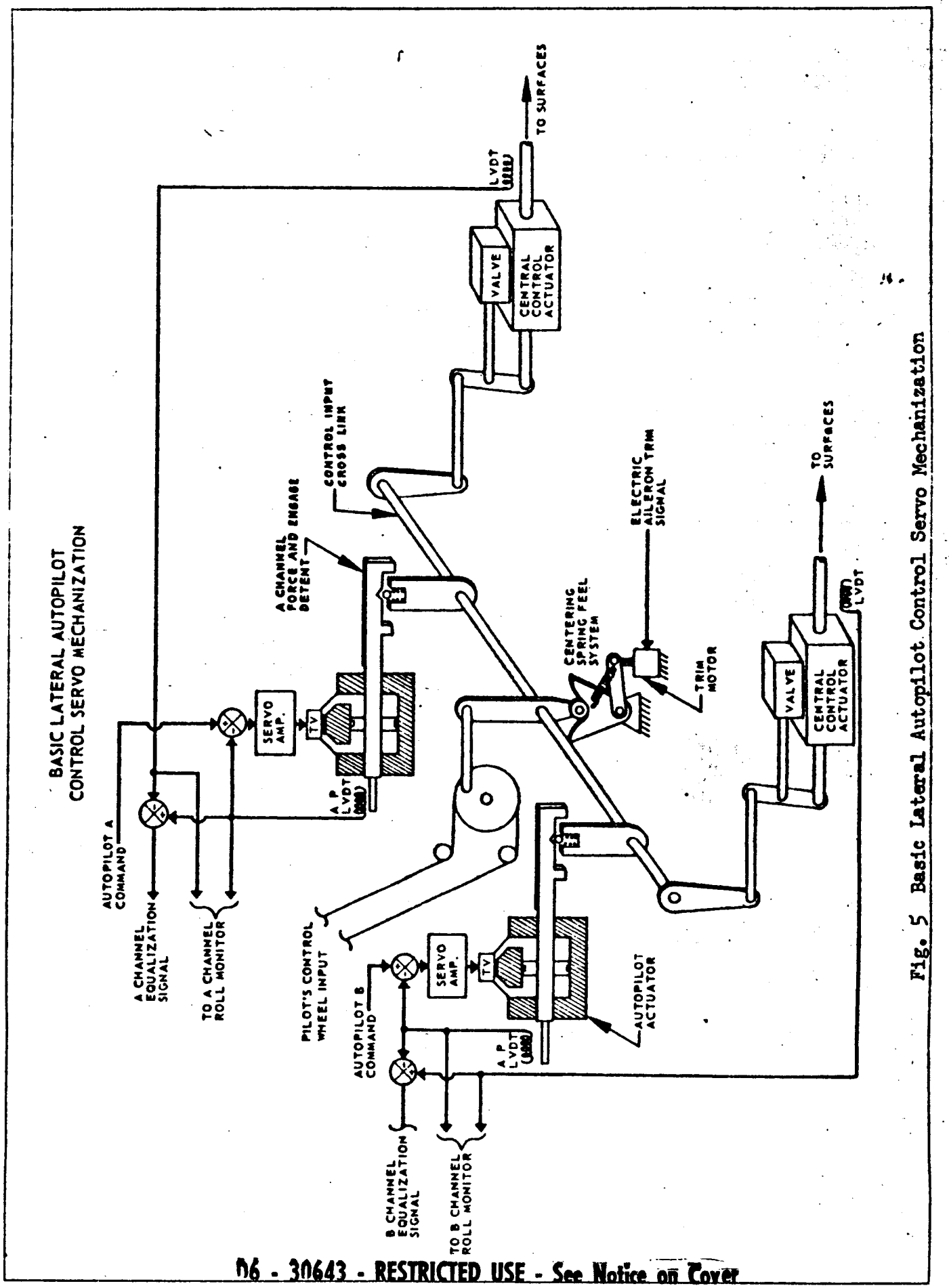

Fig. 5 Basic Lateral Autopilot Control Servo Mechanization

2. Engage Synchronization

Synchronization loops are provided to eliminate engage transients.

When the autopilot is disengaged, the autopilot actuator is hydraulically de-energized and caged to the null position. The synchronizer loop around the servo amplifier holds the servo amplifier output near null. As soon as the autopilot is engaged, hydraulic pressure builds up first in the force detent mechanism moving the autopilot actuator, which is still not pressurized, to a position matching that of the control wheel. Since the autopilot LVDT is active, the voltage resulting from a change in autopilot actuator position will be fed back to the servo amplifier and synchronized within 0.25 sec.

Additional loops are included in the roll autopilot and the pitch autopilot, to synchronize the attitude commands.

3. Dual-Channel Operation

During dual-channel operation, both autopilot actuators are coupled to the manual controls via their respective force detents as shown in Figure 5. The force detents are mechanized to give the characteristics shown in Figure 6a.

To reach equilibrium, the forces applied to the cross link must sum to zero. The forces applied to the cross link are from the two force detents, feel system and control system friction. Since the initial force gradients of the detents are steep, disagreement between the two autopilot actuator positions of more than approximately 0.5° aileron will cause one or both of the detents to reach its maximum force level.

If one channel fails hardover, the second channel and the feel system will keep airplane controls in the trim position. If the second channel should command in the same direction as the hardover, the surfaces will correctly respond to the second channel as illustrated in Figure 6b.

Except in the case of rather precise agreement between autopilot channels, the resultant dual-channel autopilot command is the lesser of the two autopilot commands. Several pertinent points can be concluded:

(a) A hardover command results in a passive failure with negligible surfaces deflection.

(b) If the two autopilot commands are opposing, the output is zero and the airplane remains in trim.

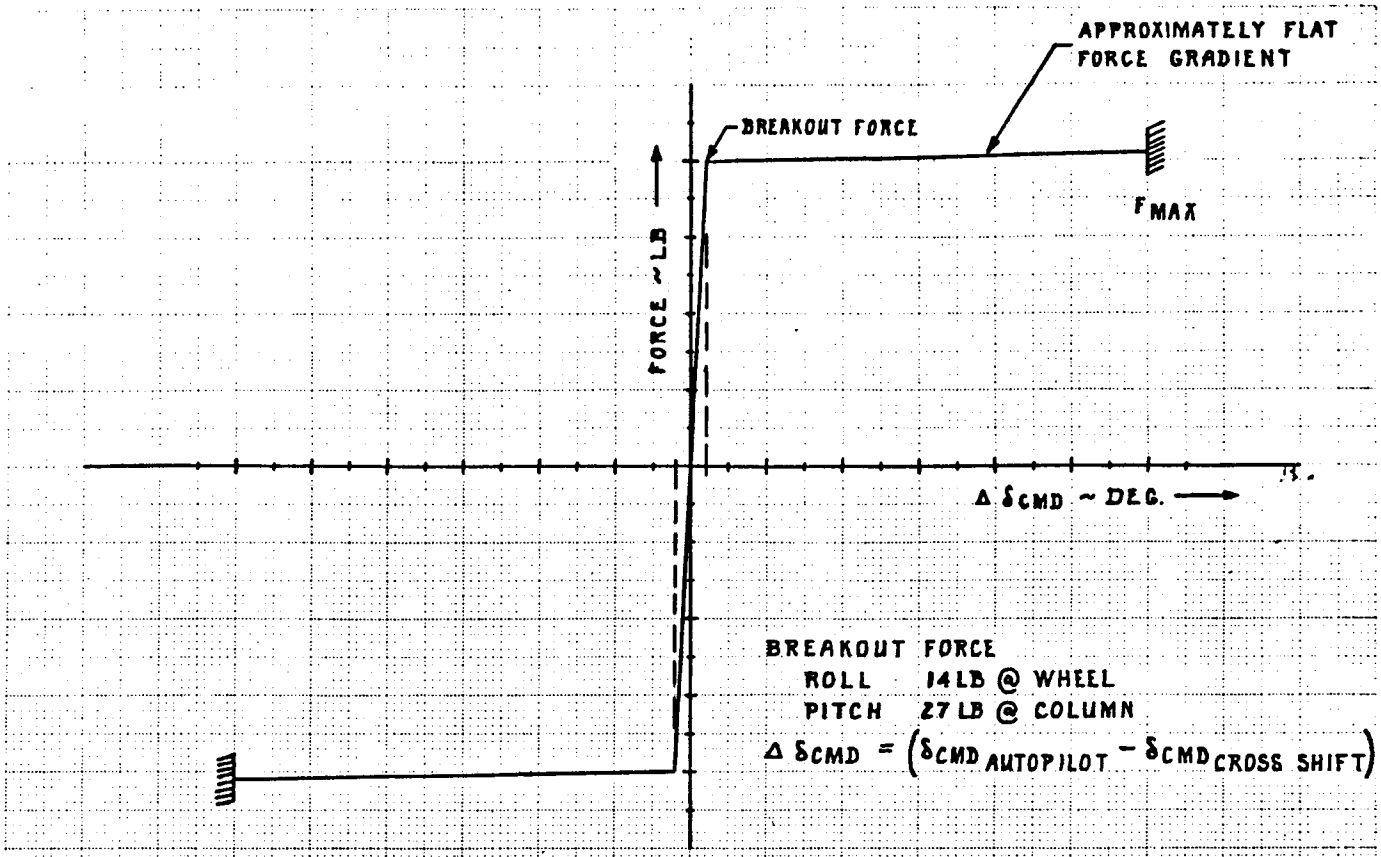

FIG. 6a GENERAL FORCE DETENT CHARACTERISTICS

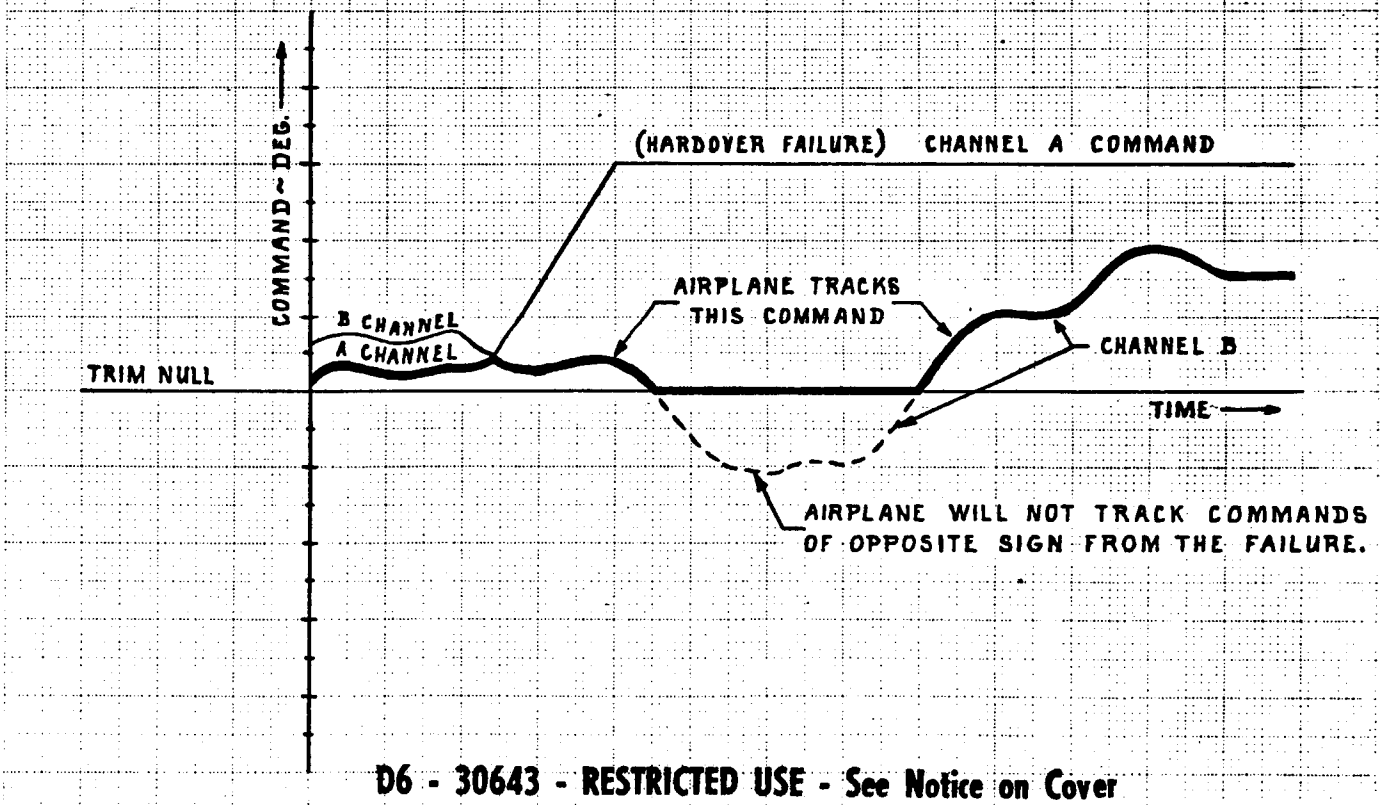

FIG. 6b GENERAL OPERATING CHARACTERISTICS OF DUAL CHANNEL SERVO SYSTEM

CALC			REVISED	DATE	FORCE DETENT AND SERVO OPERATING CHARACTERISTICS	D6-30643 Vol. II
CHECK						FIG. 6
APR						
APR					THE BOEING COMPANY	PAGE 18-25

(c) During normal operation, the airplane will track the autopilot command having the lesser value. If one autopilot fails passive, the resultant output is nearly zero. Thus, the dual-channel servo actuator system provides true "Fail Passive" operation for use in the LAND mode.

D. FLIGHT DIRECTOR OPERATION AND MODES

The flight director and autopilot computation paths become separate just prior to the autopilot path integrator as shown in the roll axis and pitch axis computer block diagrams. Command and rate limits are incorporated into the separate autopilot and flight director computer circuits. These limits are switched as a function of the mode selected and the associated submodes. The Flight Director system characteristics are summarized in Table 5 on page 38 for the roll axis and Table 6 on page 45a for the pitch axis.

As shown in the autopilot-Flight Director mode charts (Tables 1 and 2 on pages 17 and 18), the flight director computes and displays the navigational and vertical path data even when the autopilot engage switches are in the OFF position. When the autopilot is off, the pilots can fly the displayed flight director commands using the primary flight controls. When the autopilot is engaged in MANUAL, the flight director commands can be followed using the pitch wheel and turn knob. All modes of the autopilot except turbulence are also provided for the flight director.

There are two control modes which are exclusively flight director modes. These are go-around and back beam (optional). Go-around provides a wings leveling command in the lateral axis and a fixed pitch attitude climb command in the pitch axis. The go-around mode is initiated by the pilot operating either of two go-around switches located on the inboard throttle levers. Operating a go-around switch will cause the autopilot engage switch to drop to the OFF position from either MANUAL or COMMAND.

The back beam mode is initiated by selecting the VOR/LOC mode, then placing the solenoid held back beam switch in ON. In this mode, the flight director provides localizer back beam intercept, capture and track commands which can be flown by the pilot using either the turn knob with the autopilot in MANUAL, or the primary flight controls with the autopilot off. During back beam, any one of several pitch control modes can be chosen to provide flight director pitch commands.

E. ROLL AUTOPILOT

The lateral autopilot computer block diagram is shown in Figure 11 on Page 42. Gains, transfer functions, special gain programs, mode engage and switching logic are summarized in Table 4 and Figures 8, 9 and 10 on Page 37 and following. Finally, a block diagram of the lateral flight control system is shown in Figure 12 on Page 43.

The roll attitude and rate loops (see Figure 11) are basic for all modes of operation. These loops provide both roll mode damping and spiral mode stabilization.

The rate signals are sensed by the gyros installed in each roll autopilot computer. The roll attitude signals are from the Inertial Navigation System. Fixed attitude and rate gains of

$$\frac{\delta_{AIL}}{\phi} = 3.2 \frac{\text{Deg}}{\text{Deg}} \quad \text{and} \quad \frac{\delta_{AIL}}{\dot{\phi}} = 3.6 \frac{\text{Deg}}{\text{Deg/Sec}}$$ are employed.

When engaged in MANUAL, the roll autpilot responds to bank commands inserted via the turn knob. When zero bank is commanded (turn knob in detent), wings leveling occurs after which the autopilot holds airplane heading. When engaged in COMMAND, the pilot has the option of control by any of the following modes: Heading Select, VOR/Localizer, INS, ILS, or LAND.

Prior to the autopilot engagement, either in the single channel or the dual channel mode, synchronization loops operate to eliminate autopilot engage transients.

1. Engage Synchronization

In addition to the servo amplifier output synchronization mentioned earlier (See page 24), a second loop (command synchronizer) holds the servo amplifier input near zero by synchronizing the attitude command, prior to autopilot engagement in any single channel mode.

A third loop, used only for the dual channel mode, synchronizes the attitude command by nulling the servo amplifier input through feedback to the lateral path integrator of the channel yet to be engaged. This loop operates only after both autopilot switches are in the command position and until the second autopilot channel becomes engaged. During the operation of this loop, the previously mentioned command synchronizer loop is inhibited.

2. Manual

The manual mode is engaged by placing the autopilot engage switch in the MANUAL position. The autopilot cannot be engaged with the

turn knob out of detent. When the turn knob is in its center detent position, wings leveling occurs and the autopilot flys to hold heading. The heading reference is established by the Magnetic Heading Reference Unit (MHRU).

The turn knob produces a bank angle command proportional to turn knob displacement. The turn knob output is generated by a shaped pot with a dead-zone in the center equivalent to ± 16° of knob rotation. The maximum range of rotation of the turn knob is ±128° which commands ±30° bank angle. Maximum roll rate for the Manual Mode is ±4°/sec. Provisions are available for a 7 degrees/second rate limit.

When the magnetic heading clutch in the MHRU is engaged, the heading error synchro is clutched to a magnetic heading repeater and provides a heading error signal. When the turn knob is in detent, the clutch automatically engages.

Proportional and integral heading error signals produce the bank angle command necessary to maintain the airplane heading. The integral of heading error reduces heading errors to zero in the presence of thrust assymmetry or other lateral control system mis-trim. Both gains are scheduled as a function of true airspeed to maintain consistent system performance throughout the flight regime.

Certain airline customers will have control wheel steering incorporated instead of a turn knob. The control wheel steering option will be usable at all times when the autopilot is engaged in Manual Mode. In addition, when the autopilot is engaged in "Command" roll control wheel steering is available in the arm phase of lateral path modes such as LOC, VOR, or INS. Thus the control wheel steering will be available to establish the intercept angle desired prior to the capture maneuver on these modes. A special switch is included on the Mode Select Panel as shown in Figure 2a. This switch allows either CWS or Heading Select to be used for the above mentioned arm phases.

The roll control wheel steering block diagram is shown in figure 11a. Force on the control wheel commands roll rate via an integral path. The integrator is bypassed with a displacement or "boost" path to minimize the velocity error or overshoot which results when force is abruptly removed from the wheel. Constant CWS gains are used over the speed range of the 747 so that light feel forces are present at all times in roll.

Two electronic detents are used. The lower detent activates the CWS mode and is equivalent to the turn knob detent. The higher value detent is used in the autopilot to disconnect path modes and drop the engage switch from command to manual. This action overrides these modes and provides the CWS function.

3. Turbulence Mode

The turbulence mode may be engaged at any time except when the nav. mode selector is on ILS or LAND.

If the autopilot engage switch is in COMMAND when the turbulence mode is engaged, the switch will revert from COMMAND to MANUAL.

The system configuration in turbulence is identical with the MANUAL configuration except that the gains are reduced by approximately one half and the heading hold signal is removed.

4. Command

a. Heading Select Mode

The heading select mode allows the pilot to use the autopilot to fly on a desired heading.

The desired heading is selected by means of the heading knob on the Mode Select Panel. The heading select mode is engaged by placing the Nav. mode select switch in HDG and positioning the autopilot engage switch in COMMAND.

The command signal is the Heading Selector error (instantaneous heading of the airplane minus the selected heading). The gain is scheduled as a function of true airspeed to maintain consistent system performance throughout the flight regime.

The attitude command limit for the Heading Select mode is ±30° with the option for change to ±10° for TAS above 500 feet/sec. The roll rate limit is variable from 1.5deg/sec to ±3 deg/sec as a function of the amount of heading select error. C

b. Localizer Mode

Use of this mode requires the following pilot procedures:

(1) Tune in the localizer receivers.

(2) Dial in the runway heading with the course selectors on the mode select panel.

(3) Position the mode select switch in VOR/LOC.

(4) Dial in the desired localizer beam intercept heading displayed on the Heading Select window.

(5) Position the Automatic pilot engage switch in COMMAND.

The autopilot is in the Heading Select mode until the localizer capture sensor operates and the capture mode is initiated.

AD 1546 D

After capture, the system switches to the localizer on-course mode when the on-course logic is satisfied.

The basic damping signal in the localizer mode is ground heading, obtained by summing drift angle with course error.

The use of ground heading is contingent upon receipt of a drift angle valid signal (DAV) from the INS. If this signal is lost, the roll computer automatically reverts to the use of derived beam rate, washed out heading, and lagged roll for localizer mode damping. The beam displacement and integral parameters are the same for the drift angle valid and non-valid conditions.

The localizer system has three submodes of operation; namely: capture, on-course, and on-course approach. The circuit implementation of the system is such that it will automatically switch to the proper submode configuration when predetermined requirements are satisfied.

(1) LOC Capture

The localizer capture is initiated when a summed combination of intercept angle and derived beam rate becomes equal to or less than the instantaneous beam error or when beam error is less than one degree. The exact capture and on-course logic and gains are shown in Table 4.

When the drift angle valid signal is present, the displacement command is the localizer beam error and damping is provided by the derived ground heading signal. If the drift angle valid signal is lost, the ground heading signal is removed and derived beam rate and course error are substituted.

(2) LOC On-Course

The LOC on-course submode is initiated when predetermined conditions of bank angle, beam displacement and beam rate are satisfied, as summarized in Table 4.

The localizer on-course configuration is similar to the capture configuration, with the following modifications:

a signal proportional to the integral of beam error is introduced to reduce the steady state error in presence of thrust asymmetry and lateral mistrim conditions,

a thirty-three second time constant high pass filter in the ground heading and course error path washes out steady state errors due to INS and course error signals offsets, as well as heading errors due to crosswinds in the drift angle non-valid condition,

a signal proportional to lagged roll is added for increased damping in the drift angle non-valid condition.

(3) LOC On-Course Approach

The autopilot switches from the on-course submode to on-course approach submode at 1500 feet of altitude.

Mechanization of this submode is similar to that of the on-course submode when the drift angle is valid. When the drift angle is not valid, the washed out course error signal is removed to improve wind shear performance. The beam displacement and integral gains are scheduled linearly with radio altitude to compensate for beam convergence while the damping parameter gains are increased to improve close-in performance.

The submode gains, command limits and engage logic are summarized in Table 4.

C. VOR Mode

The procedure for the pilot to engage this mode is identical to that of the localizer except that the VOR frequency has to be selected rather than the LOC frequency. The VOR mode has three submodes; namely: capture, on-course, and over the station. The basic damping parameter is ground heading. If the drift angle valid signal is lost, the INS drift angle signal is removed, leaving the course heading error as the system damping signal. The displacement command is the beam error for both drift angle valid and non-valid conditions. System gains are scheduled as a function of TAS to maintain good performance throughout the flight regime. The system gains, limits and mode initiation logic are summarized in Table 4.

(1) Capture

When the VOR mode is first selected and the aircraft is outside the capture threshold, the autopilot is in the heading select mode which steers the airplane to the desired intercept angle established with the heading select control on the Mode Select Panel. The capture sensor is armed.

The variable engage point logic used for VOR capture is shown in Table. 4. For intercept angles between 90 degrees and 10 degrees, the capture starts at beam error between 1.8 and 0.2 dots. The greater the intercept angle, the earlier the capture maneuver is initiated.

A 34 degrees course cut limit is provided.

(2) On-Course

The on-course submode is initiated when the bank angle is less than 3 degrees and the course error is less than 15 degrees.

The beam displacement gain is reduced to one-half the value used during capture. A beam integral signal is introduced to reduce the beam error in presence of thrust asymmetry and lateral control surface mistrims. A 200-second washout of the ground heading signal is also introduced to eliminate INS drift angle and course error static offsets. In the drift angle non-valid condition, this washout improves the system performance under cross wind conditions.

Maximum position and rate commands are limited to ± 10 degrees and ± 1.5 degrees/second respectively during the VOR on-course submode.

(3) Over the Station

The VOR over-the-station sensor initiates this submode upon detection of beam rates higher than 0.5 degrees/second. The system automatically reverts to the on-course mode, after passing the station, when the beam rate signal has decreased below 0.5 degrees/second for 20 seconds.

During the time that the airplane is over the station, the VOR beam signal is removed and the autopilot command signal is either ground heading for the drift angle valid condition, or course error for drift angle non-valid condition. If the pilot desires to make a course change while over the station, he may dial in the change in course setting and the system will track outbound on the new radial.

d. INS Mode

The autopilot may be used to capture and track any of the great circle routes that have been programmed into the INS computer.

The INS mode is armed by placing the Nav. mode selector switch of the autopilot mode select panel in the INS position. Figure 7 shows a typical control sequence. If the aircraft is further than 7.5 nautical miles off the desired great circle course, the autopilot is in the heading select mode, and steers the airplane to the desired intercept angle established with the heading select knob. In order for the Heading Select mode to operate on those airplanes with remote set preselect heading where the heading error signal is developed in the HSI, the INS-RADIO switch must be left in RADIO position until the INS capture point is reached. When the 7.5 mile point is reached, the INS mode is initiated.

Cross-track deviation and track angle error outputs of the INS are used to compute the desired steering command.

INS MODE

SEQUENCE:

① INS MODE SELECTED
- HDG SEL MODE IN CONTROL
- ARMED FOR INS CAPTURE
- NAV ANNUNCIATOR – AMBER

② INS CAPTURE
- INS MODE IN CONTROL TO CAPTURE DESIRED TRACK
- NAV ANNUNCIATOR – GREEN

③ INS ON COURSE
- INS MODE IN CONTROL TO MAINTAIN DESIRED TRACK
- REDUCED ROLL RATE AND BANK ANGLE LIMITS
- NAV ANNUNCIATOR – GREEN

④ INS AUTOMATIC WAYPOINT SWITCHING
- DISCRETE SIGNAL FROM INS TO RECYCLE CAPTURE MODE IF NECESSARY TO ACQUIRE NEW DESIRED TRACK
- NAV ANNUNCIATOR – GREEN

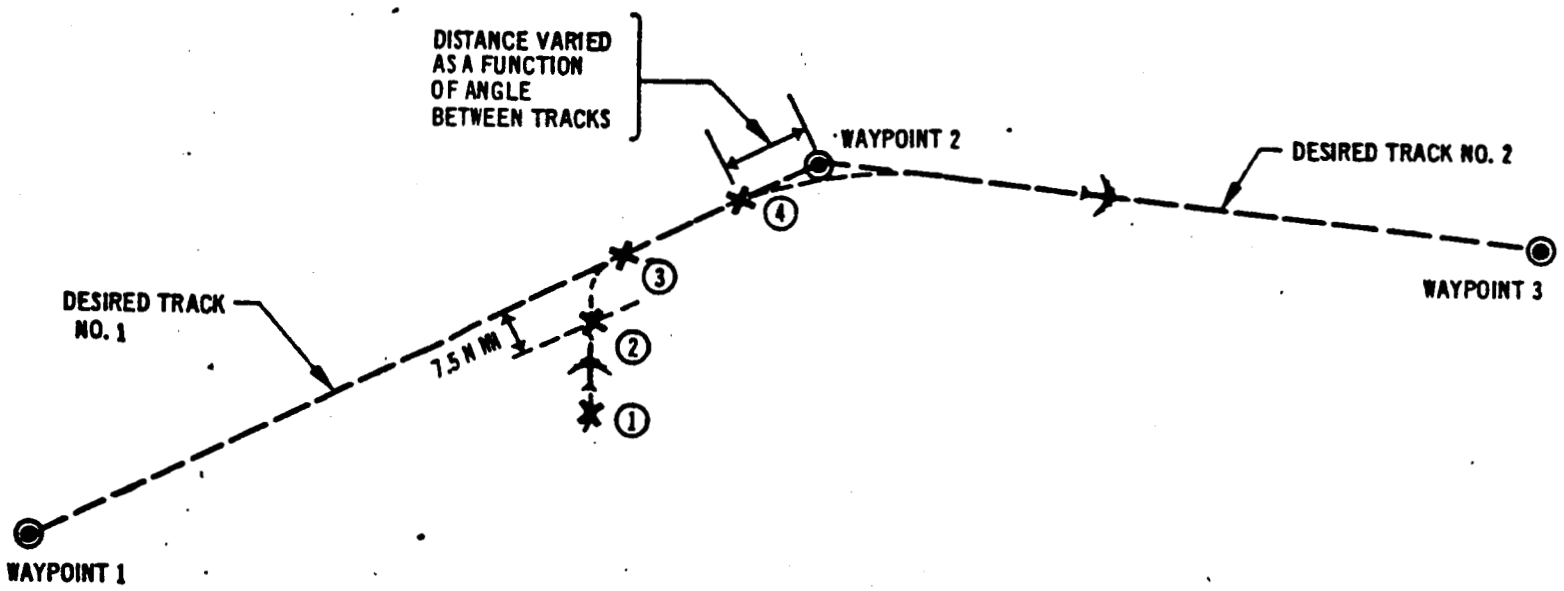

Fig. 7 – INS Mode Sequence

Control is similar to VOR control with the following exceptions:

a. Since the INS provides the equivalent of a non-convergent beam, the distance from destination does not effect system performance.

b. The damping signal, track angle error, is not susceptible to cross-wind effects which would result in lateral displacement from the desired course.

(1) INS Capture

The capture maneuver is automatically initiated at 7.5 nautical miles from the desired INS course. The bank angle command is limited to 30 degrees and bank rate is limited to 4 degrees per second during capture. The system gains are summarized in Table 4. A 25-degree course cut limiter is employed.

(2) INS On-Course

The capture is complete and on-course control is initiated when the cross-track deviation is reduced below 1,070 feet and track angle is below 3 degrees. The same gains are employed in the autopilot as during capture. The on-course sensor downshifts the bank and bank rate limiters to 10 degrees and 1.5 degrees per second respectively.

(3) Waypoint switching

Automatic switching from one great circle courseto another is provided. On the INS system Control and Display Unit, the "Auto-Manual" switch must be set to the "Auto" position to use this feature. If this is not done, the autopilot will overfly the waypoint and continue on the extension of the great circle. If the "Auto" sequence is used, switching of the autopilot to the next route occurs a short distance before the waypoint is reached. (See Table 4) It will occur at 3.5 nautical miles for cases where the angular change between successive courses is small. Restoration of the capture bank limits is provided automatically. When the on-course conditions are again satisfied, the reduced bank and bank rate limits are automatically reinstated.

e. ILS Mode

The ILS mode is identical to the Localizer Mode for the roll autopilot. Glideslope control is armed by this mode and the autopilot continues to fly toward the glideslope beam on either pitch attitude, vertical speed, altitude or IAS hold (optional mode) until a predetermined glideslope signal level is reached. (See pitch axis system description).

f. Land Mode

The autopilot LAND mode provides the Boeing 747 with a fail-passive dual-channel automatic approach and landing system. The LAND mode features dual ILS and flare coupling.

The LAND mode is properly selected when the following prerequisites are satisfied:

1) Nav. Mode Selector switch in LAND
2) Both course controls set to the runway heading
3) Heading select control set for the desired intercept angle with the localizer
4) VHF/NAV receivers set to the proper localizer frequency
5) Both autopilot engage switches in the command position.

Upon selection of this mode, single-channel operation, identical to that for ILS mode, is initiated. Dual-channel operation does not begin until after the autopilot is on Loc. approach, glide slope capture is completed, and the airplane is less than 1,500 feet altitude above the surface. The second channel synchronizes to the controlling channel until it is engaged; at this point, the flare computer is armed and equalization and monitoring of both channels begins.

(1) Equalization

Equalization is accomplished by taking the difference of the central control actuator and the autopilot actuator LVDT signals and feeding this signal back to the autopilot path integrator.

The output position of the central control actuator will be equal to the output position of the autopilot actuator having the least value (see Section C). Thus, the channel having the greater command will be different from the central control actuator output by the difference between the A and B autopilot commands.

The channel with the lower command signal receives no equalization signal since the difference between commanded and output position is zero, while the channel having the higher signal receives an equalization that tends to reduce its output signal to match that of the controlling channel. It should be noted that each channel has an independent equalization system and that there are no cross ties between channels.

The equalization signal in the lateral axis is limited, so that ramp faults of relatively low values may be detected. The equalization signal is also gain scheduled as a function of radio altitude from 1 to 0.5. Thus, equalization is decreased as the airplane approaches touchdown.

(2) Monitoring

The monitoring system on the 747 dual-channel autopilot acts on the measured difference between the output position of each autopilot actuator and the output position of the central control actuator associated with that autopilot actuator. A block diagram of the monitoring system is shown in Figure 13. The two actuator position sensors used in the equalization circuit also feed the monitor. Each channel has a pair of monitors: one for pitch and one for roll. A failure is indicated by the monitor if an autopilot channel disagrees with the central control actuator output by a given amount for a set length of time. These values are presently set at six degrees and two seconds in the roll channel. A steady red cockpit warning light is initiated any time a monitor is tripped. Thus, early warning of any potential problems is brought quickly to the pilot's attention without disconnecting the autopilots. Should the warning light be activated by noise or radio beam masking, it is not latched to the ON condition; and thus, goes out at the conclusion of these temporary disturbances.

SUMMARY OF AUTOPILOT ROLL AXIS

	MODE	SUBMODE	CONDITION	COMMAND: DESCRIPTION	COMMAND: SYMBOL	GAIN: VALUE	GAIN: UNIT	GAIN: FILTER	GAIN: FUNCTION OF	ROLL ANGLE COMMAND LIMIT	ROLL RATE COMMAND LIMIT	REMARKS
MANUAL	ROLL ATTITUDE HOLD	---	---	ROLL ANGLE	$\Delta\phi/\phi$	3.2	DEG/DEG	---	---	12 DEG AILERON	20 DEG/SEC AILERON	THESE TWO SIGNALS WILL BE ON FOR ALL LATERAL AUTOPILOT MODES; IN THE TURBULENCE MODE THE GAINS ARE REDUCED BY 50%
				ROLL RATE	$\Delta\omega/\phi$	3.6	DEG/DEG/SEC	$\frac{1}{.25\Delta s+1}$	---			
				TURN KNOB	ϕ_c/TK	0.234	DEG/DEG	---	---	30 DEG	4 DEG/SEC	7 DEG/SEC LIMIT OPTIONAL
	HEADING HOLD	---	---	MAGNETIC HDG	ϕ_c/ϕ_{mh}	2.84	DEG/DEG	---	TAS	30 DEG	4.0 DEG/SEC	TURN KNOB IN DETENT AND BANK ANGLE LESS THAN 3 DEG
				HEADING INTEGRAL	$\phi_c/\int\phi_{mh}\,dt$	.020	DEG/DEG SEC	---	TAS			
	TURBULENCE	---	---	ROLL ANGLE	$\Delta\omega/\phi$	1.6	DEG/DEG	---	---	12 DEG AILERON	20 DEG/SEC AILERON	---
				ROLL RATE	$\Delta\omega$	1.8	DEG/DEG	$\frac{1}{.1765+1}$	---			
	CONTROL WHEEL STEERING (OPTION)	---	---	CONTROL WHEEL STEERING	ϕ_c/LB WHEEL FORCE	2.4	DEG/LB	$\tau = 1.7$	---	30 @ 56	7.6 DEG/SEC	SYSTEM WILL BE IN THE HEADING HOLD MODE WHEN BANK ANGLE IS LESS THAN 3 DEG SYSTEM HAS DEAD ZONE OF 4 LB.
				CONTROL WHEEL STEERING INTEGRAL	ϕ_c/INTEG WHEEL FORCE	3	DEG/SEC/LB	$\tau = 1.7$				
COMMAND	HEADING SELECT	---	---	HEADING SELECTOR	ϕ_c/ψ_{ss}	2.83	DEG/DEG	---	TAS	FUNCTION OF TAS	1.5-8 DEG/SEC AS FN OF ϕ_c	---
	INS	CAPTURE	INS NAV MODE VALID	CROSS TRACK DEVIATION	ϕ_c/CTD	8.85	DEG/1000 FT	$\frac{1}{25+1}$	TAS	30 DEG	4 DEG/SEC	CAPTURE LOGIC: CTD < 7.5 N MILES; COURSE CUT LIMIT: 20° TAE
				TRACK ANGLE ERROR	ϕ_c/TAE	3.16	DEG/DEG	$\frac{1}{5+1}$	TAS			
		ON-COURSE	INS NAV MODE VALID	CROSS TRACK DEVIATION	ϕ_c/CTD	8.85	DEG/1000 FT	$\frac{1}{5+1}$	TAS	10 DEG	1.5 DEG/SEC	ON-COURSE LOGIC: CTD ≤ 1070 FEET AND TAE ≤ 3.0 DEG; WAYPOINT SWITCHING AT DIST. TO GO = 2.1 + |10 sin Δψ| NMI for |Δψ| = 0 to 6 = 5.25°; for |Δψ| = .875 (|Δψ| − 25) for |Δψ| > 25°
				TRACK ANGLE ERROR	ϕ_c/TAE	3.16	DEG/DEG	$\frac{1}{5+1}$	TAS			
	LOC NLS OR LAND	CAPTURE	INS NAV MODE VALID	BEAM ERROR	ϕ_c/η	23.3	DEG/DEG	---	---	30 DEG	7 DEG/SEC	LOC. CAPTURE LOGIC: $\dot\eta^2 < 2.20 \sin\phi_{ss} + 0.372\ \dot\eta^2$/SEC (3 SEC. Delay) or $\eta < 0.8°$; COURSE CUT LIMIT: INS 25° ϕ_{ss}, IMS 30° ϕ_{ss}
				GROUND HEADING	ϕ_c/ψ_{ss}	1.5	DEG/DEG	---	---			
			INS NAV MODE NON-VALID	BEAM ERROR	ϕ_c/η	23.3	DEG/DEG	---	---			
				BEAM RATE	$\phi_c/\dot\eta$	75.0	DEG/DEG/SEC	---	---			
				COURSE ERROR	ϕ_c/ψ_{ss}	0.96	DEG/DEG	---	---			
		ON COURSE	INS NAV MODE VALID	BEAM ERROR	ϕ_c/η	23.3	DEG/DEG	---	---	10 DEG	4 DEG/SEC	LOC. ON-COURSE LOGIC: $\phi < 3°$; $\eta < 0.8°$ AND $\dot\eta < 0.027°$/SEC.
				BEAM INTEGRAL	$\phi_c/\int\eta\,dt$	.35	DEG·DEG SEC	---	---			
				GROUND HEADING	ϕ_c/ψ_{ss}	1.5	DEG/DEG	$\frac{.335}{.335+1}$	---			
			INS NAV MODE NON-VALID	BEAM ERROR	ϕ_c/η	23.3	DEG/DEG					
				BEAM RATE	$\phi_c/\dot\eta$	75.0	DEG·DEG/SEC	---	---			
				BEAM INTEGRAL	$\phi_c/\int\eta\,dt$	.35	DEG·DEG·SEC	---	---			
				COURSE ERROR	ϕ_c/ψ_{ss}	0.96	DEG/DEG	$\frac{.335}{.335+1}$				
				LAGGED ROLL	ϕ_c/ϕ_{ss}	1.886	DEG/DEG	---	---			
		ON-COURSE APPROACH	INS NAV MODE VALID	BEAM ERROR	ϕ_c/η	23.3	DEG/DEG	-	ALTITUDE	10 DEG AT FLARE 5 DEG	4 DEG/SEC AT FLARE 4 DEG/SEC	LOC. ON-COURSE APPROACH LOGIC: $h_r \le 1000$ FEET
				BEAM INTEGRAL	$\phi_c/\int\eta\,dt$	.35	DEG·DEG SEC	---	ALTITUDE			
				GROUND HEADING	ϕ_c/ϕ_{ss}	2.5	DEG/DEG	$\frac{.335}{.335+1}$	---			
			INS NAV MODE NON-VALID	BEAM ERROR	ϕ_c/η	23.3	DEG/DEG	---	ALTITUDE			
				BEAM RATE	$\phi_c/\dot\eta$	75.0	DEG/DEG/SEC	---	ALTITUDE			
				BEAM INTEGRAL	$\phi_c/\int\eta\,dt$	.35	DEG·DEG SEC	---	ALTITUDE			
				LAGGED ROLL	ϕ_c/ϕ_{ss}	2.33	DEG/DEG	---	---			
		DUAL CHANNEL (LAND ONLY)	---	EQUALIZATION	$\Delta\delta_a/\Delta\phi^{dt}$	.0672	DEG/DEG SEC	---	ALTITUDE	$\Delta\delta_a$ IS LIMITED TO 2 DEG AILERON	---	DUAL CHANNEL OPERATION BEGINS WHEN SYSTEM AT LOC. APPROACH/GLIDE SLOPE CAPTURE COMPLETED AND RADIO ALTITUDE LESS THAN 1000 FEET.
	VOR	CAPTURE	INS NAV VALID	BEAM ERROR	ϕ_c/η	18.5	DEG/DEG	$\frac{1}{(4.4s+1)^2}$	TAS	30 DEG	4 DEG/SEC	VOR CAPTURE LOGIC: $\eta \le 0.8 \sin\phi_{ss}$ OR $\eta < 2°$; COURSE CUT LIMIT: $5\phi_{ss}$
				GROUND HEADING	ϕ_c/ϕ_{ss}	2.52	DEG/DEG	---	TAS			
			INS NAV NON-VALID	BEAM ERROR	ϕ_c/η	18.5	DEG/DEG	$\frac{1}{(4.4s+1)^2}$	TAS			
				COURSE ERROR	ϕ_c/ψ_{ss}	2.52	DEG/DEG	---	TAS			
		ON-COURSE	INS NAV VALID	BEAM ERROR	ϕ_c/η	9.5	DEG/DEG	$\frac{1}{(4.4s+1)^2}$	TAS	10 DEG	1.5 DEG/SEC	VOR ON-COURSE LOGIC: $\phi < 3°$ AND $\psi_{ss} \le 10°$
				BEAM INTEGRAL	$\phi_c/\int\eta\,dt$	.0063	DEG·DEG SEC	---	TAS			
				GROUND HEADING	ϕ_c/ϕ_{ss}	2.52	DEG/DEG	$\frac{.2005}{.2005+1}$	TAS			
			INS NAV MODE NON-VALID	BEAM ERROR	ϕ_c/η	9.5	DEG/DEG	$\frac{1}{(4.4s+1)^2}$	TAS			
				BEAM INTEGRAL	$\phi_c/\int\eta\,dt$	.0063	DEG/DEG SEC	---	TAS			
				COURSE ERROR	ϕ_c/ϕ_{ss}	2.52	DEG/DEG	$\frac{.2005}{.2005+1}$	TAS			
		OVER STATION	INS NAV	GROUND HEADING	ϕ_c/ϕ_{ss}	2.52	DEG/DEG	$\frac{.2005}{.2005+1}$	TAS	10 DEG	1.5 DEG/SEC	OVER STATION LOGIC: $\eta \ge 0.5°$/SEC REVERT TO ON-COURSE 20 SECONDS AFTER $\eta \le 0.5°$/SEC
			INS NAV	COURSE ERROR	ϕ_c/ϕ_{ss}	2.52	DEG/DEG	$\frac{.2005}{.2005+1}$	TAS			

NOTES

1. CROSS TRACK DEVIATION IS LIMITED TO 9000 FEET
2. GROUND HEADING (ψ_{GI}) + COURSE ERROR (ψ_{CEI}) + DRIFT ANGLE (ψ_{DA})
3. $\frac{1}{(.208+1)(.1765+1)}$ °/SEC
4. $\frac{1}{.208+1}\phi_{ss}$
5. TAS < 500 FT/SEC ϕ_c LIMIT = 30°; TAS > 500 FT/SEC ϕ_c LIMIT = 20°; WITH A/C WIRING OPTION GND OR OPEN; TAS > 500 FT/SEC ϕ_c LIMIT = 10°; WITH A/C WIRING OPTION TO CMD
6. TAS SEE FIGURE 8 FOR GAIN SCHEDULING
7. ALTITUDE SEE FIGURE 9 FOR GAIN SCHEDULING. TIME BASE SCHEDULING IS USED AS BACKUP. SEE FIGURE 10 (SINGLE CHANNEL ONLY).
8. MONITOR LIGHT WILL BE ON WHEN $\Delta\delta_a > 8°$ FOR 2 SECONDS.
9. YAW DAMPER INVALID AND TAS ABOVE 296 KNOTS; ROLL ANGLE AND PATH CMD GAINS REDUCED TO HALF.
10. YAW DAMPER INVALID AND TAS ABOVE 296 KNOTS; ROLL ANGLE GAIN REDUCED TO 1.1 $\frac{s_p}{p}$

				REVISED	DATE	TABLE 4	D6-13645
CALC				~~Rev B~~	~~9/19/69~~	SUMMARY OF AUTOPILOT ROLL AXIS	
CHECK				Rev C	10-10-69		
APPD				Rev d	2/23/70	THE BOEING COMPANY	PAGE 37
APPD							

MODE	COMMAND		GAIN		DISPL LIMIT	RATE LIMIT	REMARKS
	DESCRIPTION	SYMBOL	VALUE	UNIT			
GO-AROUND	ROLL ANGLE	CMDBAR/ϕ	0.032	IN/DEG	—	—	THIS SIGNAL IN "ON" ALL F/D MODES
	ROLL RATE	$\phi c/\dot{\phi}$	0.6	DEG/DEG/SEC.	—	—	THIS SIGNAL IN "ON" AT F/D LOC O/C MODES
HEADING SELECT	SAME AS AUTOPILOT					9°/SEC	THE SUBMODES ENGAGED LOGICS ARE IDENTICAL TO THAT OF AUTOPILOT
INS	SAME AS AUTOPILOT					INS CAP 4°/SEC INS O/C 1.5°/SEC	
12 LOC, ILS OR LAND	SAME AS AUTOPILOT EXCEPT THAT PATH INTEGRAL IS DELETED NOTE: WITH AUTOPILOT IN MAN. OR OFF, FLIGHT DIRECTOR GAIN ON LOC IS REDUCED TO $\frac{1}{2}$					LOC CAP 9°/SEC LOC O/C 4.0°/SEC	
VOR	SAME AS AUTOPILOT EXCEPT THAT PATH INTEGRAL IS DELETED					VOR CAP 4°/SEC VOR O/C 1.5°/SEC	

12 BACK BEAM IS AVAILABLE IN FLIGHT DIRECTOR ONLY (OPTION)

Table 5

SUMMARY OF FLIGHT DIRECTOR ROLL AXIS

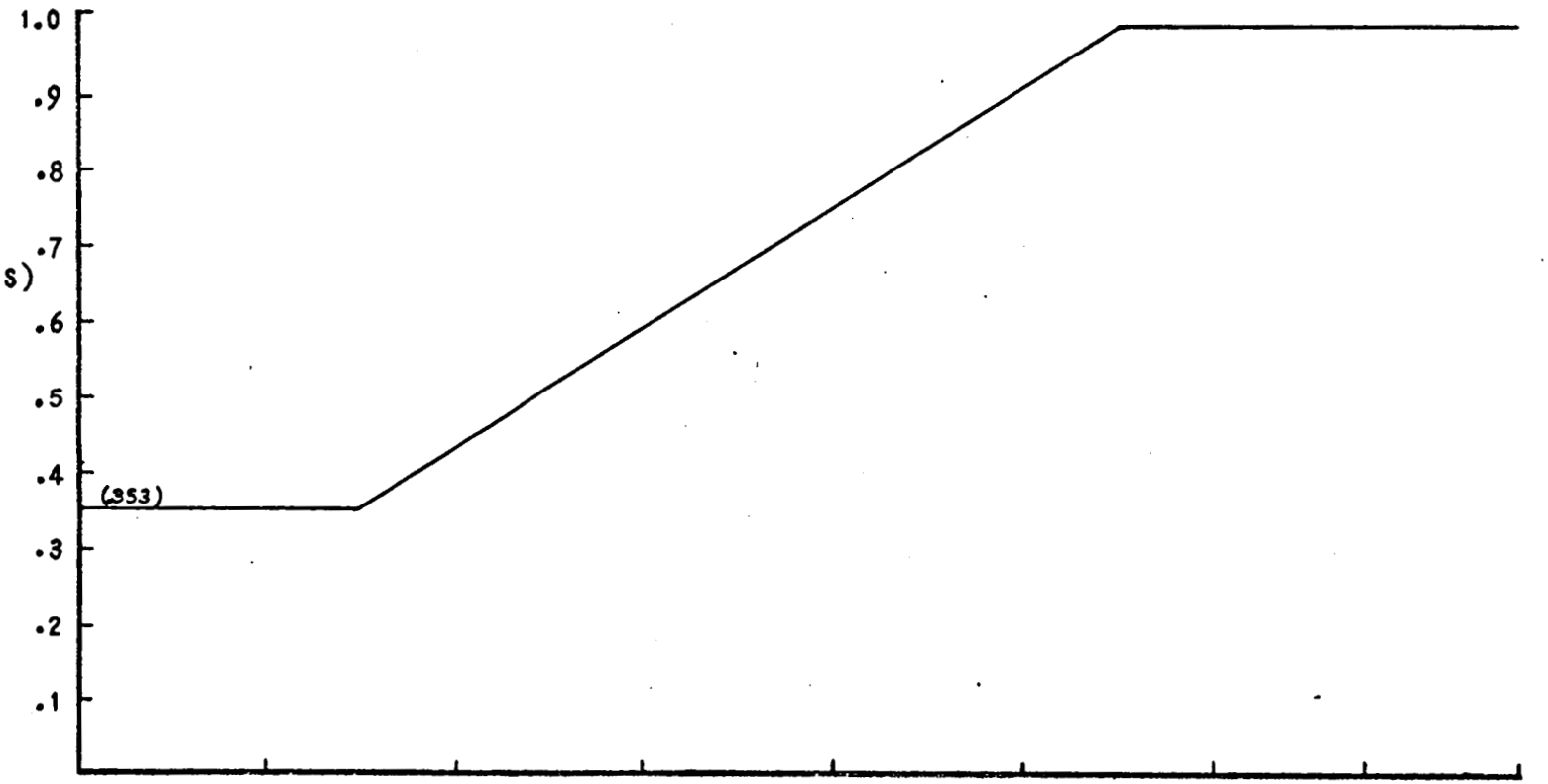

FIG. 8 TRUE AIRSPEED GAIN PROGRAM

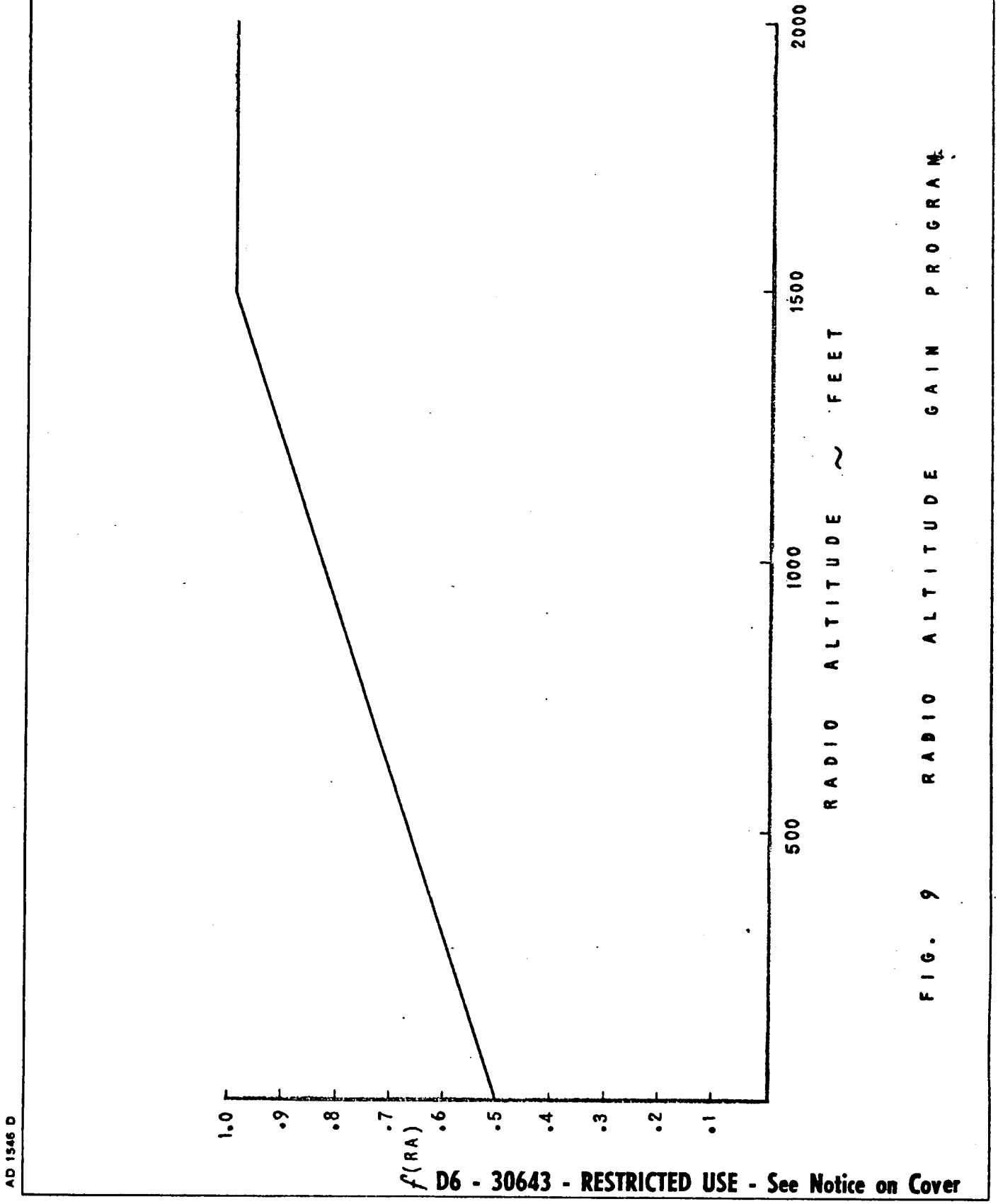

FIG. 9 RADIO ALTITUDE GAIN PROGRAM

AD 1546 D

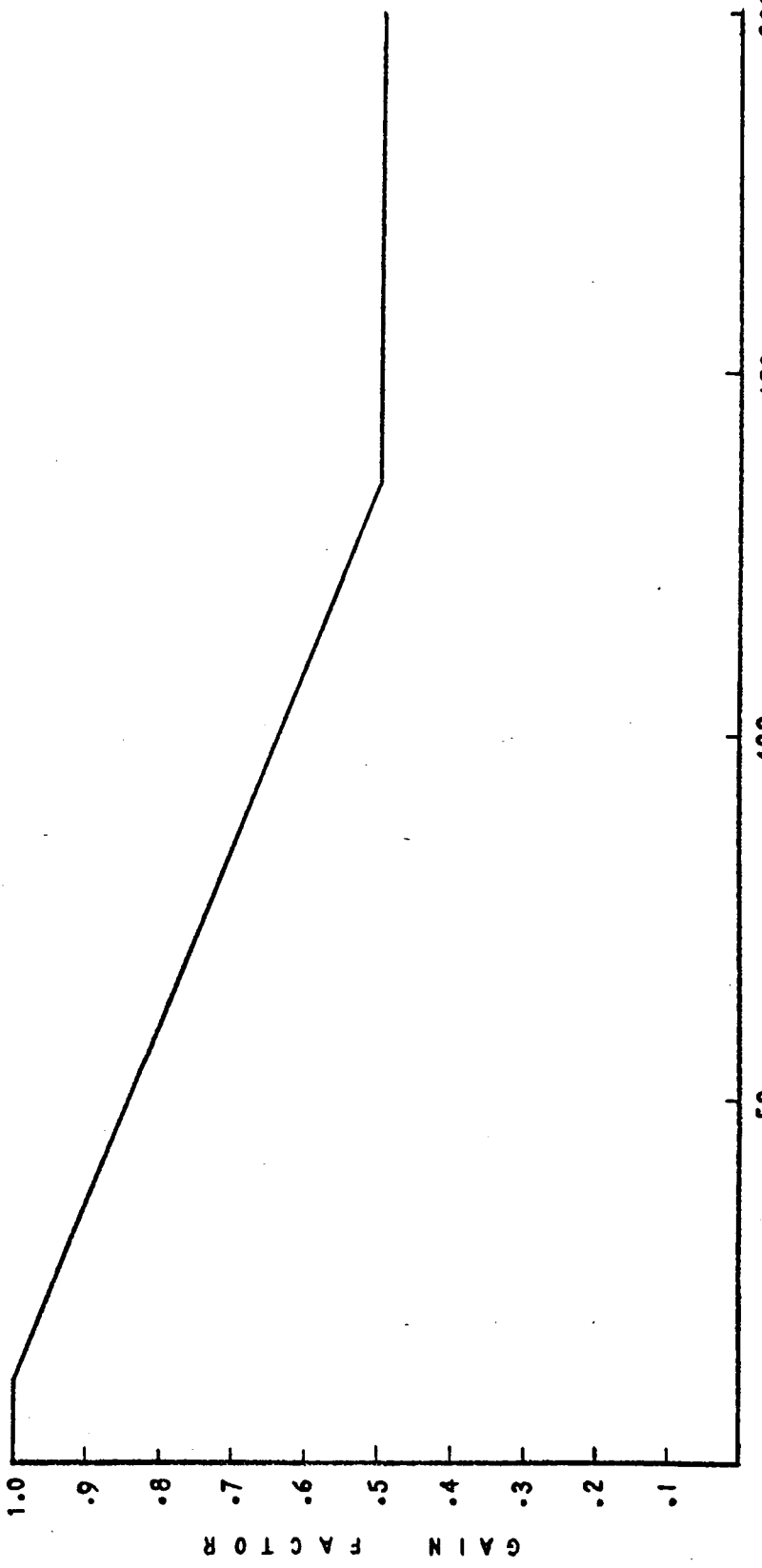

FIG. 10 TIME-BASED GAIN PROGRAM

AD 1546 D

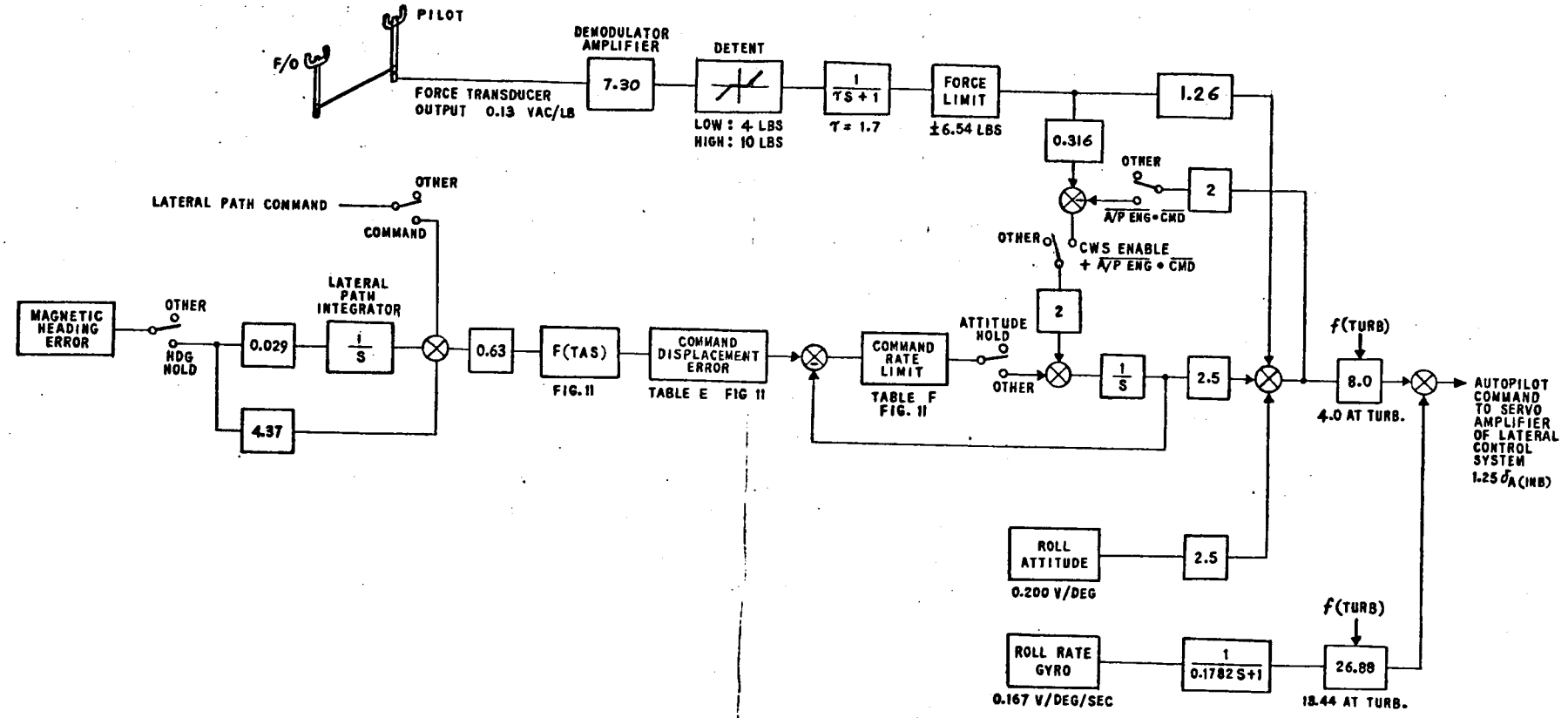

FIG. 11a

747 ROLL CONTROL WHEEL STEERING BLOCK DIAGRAM

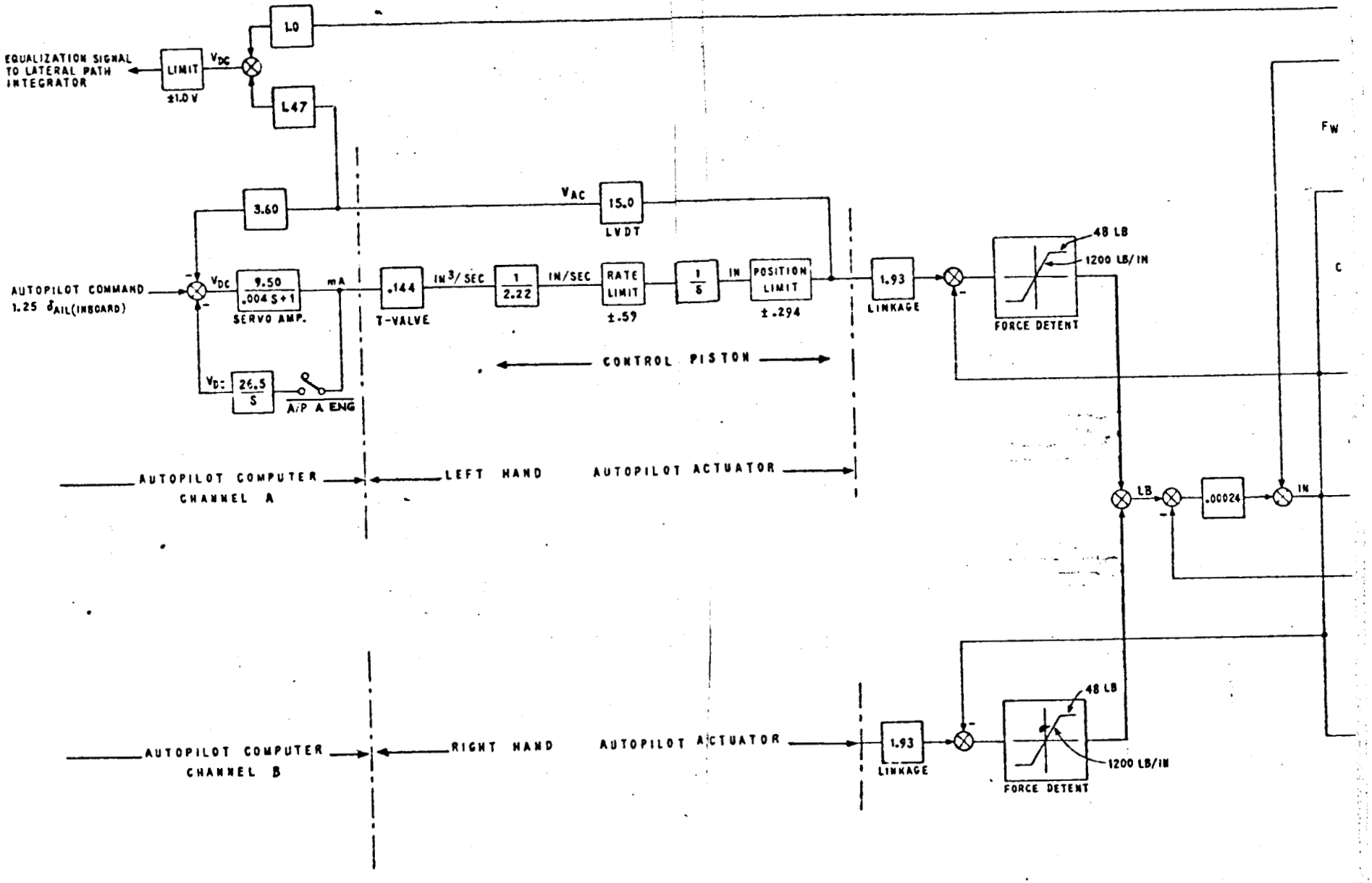
EQUALIZATION SIGNAL TO LATERAL PATH INTEGRATOR
LIMIT
±1.0 V
V_{DC}
1.0
1.47
3.60
V_{AC}
15.0
LVDT
AUTOPILOT COMMAND
1.25 $\delta_{AIL(INBOARD)}$
V_{DC}
9.50
.004 S+1
SERVO AMP.
mA
.144
T-VALVE
IN³/SEC
1
2.22
IN/SEC
RATE LIMIT
±.59
1
S
IN
POSITION LIMIT
± .294
1.93
LINKAGE
48 LB
1200 LB/IN
FORCE DETENT
CONTROL PISTON
V_{DC}
26.5
S
A/P A ENG
AUTOPILOT COMPUTER CHANNEL A
LEFT HAND AUTOPILOT ACTUATOR
LB
.00024
IN
AUTOPILOT COMPUTER CHANNEL B
RIGHT HAND AUTOPILOT ACTUATOR
1.93
LINKAGE
48 LB
1200 LB/IN
FORCE DETENT
F_W
C

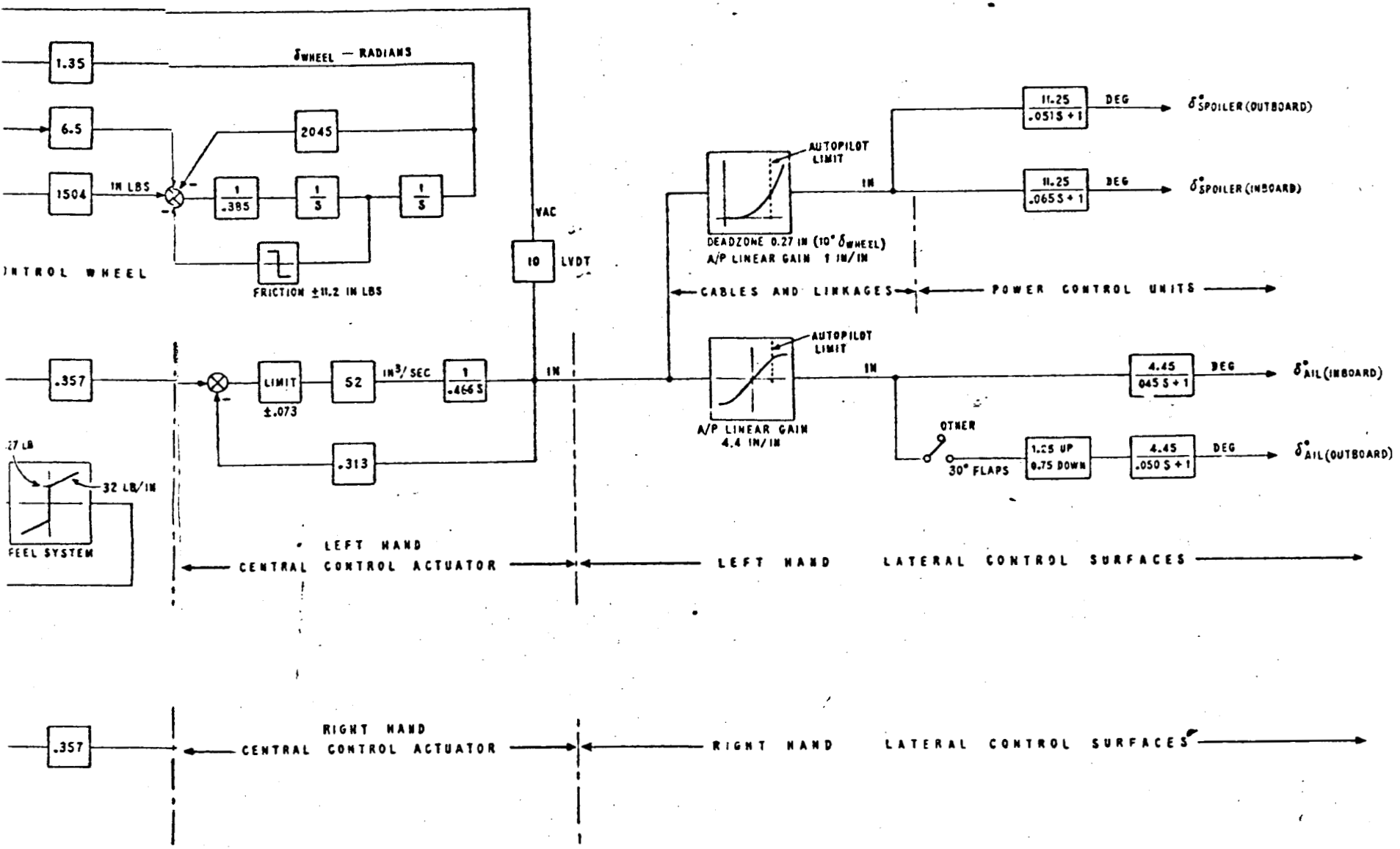

CALC			REVISED	DATE	747 LATERAL FLIGHT CONTROL SYSTEM	D6-30643 Vol. II
CHKR			Rev. A			FIG. 12
AP	E.H		REV B	3/11/68		
APR					THE BOEING COMPANY RENTON WASHINGTON	PAGE 18-43

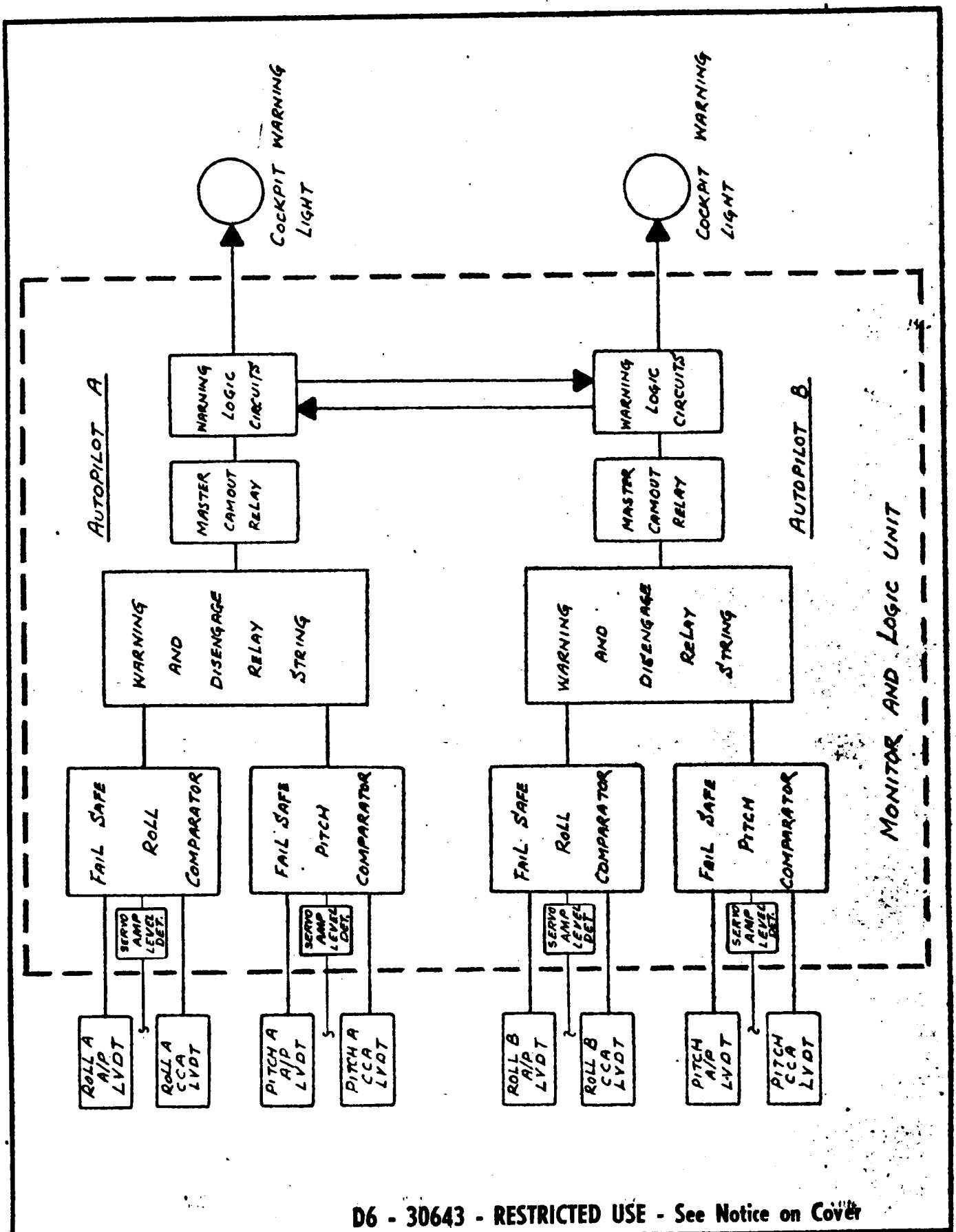

D6 - 30643 - RESTRICTED USE - See Notice on Cover

			REVISED	DATE
CALC				
CHECK			Rev a	2/23/70
APPD				
APPD				

LAND MODE MONITORING BLOCK DIAGRAM

D6-30643 Vol. II

FIG. 13

THE BOEING COMPANY RENTON, WASHINGTON

PAGE 18 - 44

TD 973 D-83

Rev d

F. PITCH AUTOPILOT

A summary of Autopilot/Flight Director pitch axis characteristics is contained in Tables 6 and 7.

The 747 autopilot operates through a parallel servo system. Thus all actuator response due to a command from the autopilot is also fed back to the control column. The feedback path is the primary elevator control system. At the frequencies which the autopilot system normally operates, the control column can be assumed to be directly proportional to the elevator surface motion. Figure 23a shows the linearized transfer functions for the Autopilot servo and elevator power control unit. The normal gain between δ column and δ elev. is .478 degrees of column per degree of elevator displacement about surface neutral. The full column to elevator curve is shown in Figure 23b.

Figure 14 is the block diagram of the basic pitch autopilot control system. Pitch attitude and rate loops are basic for pitch modes of operation. These loops provide both short and long period stabilization and damping. The rate signals are sensed by gyros installed in each autopilot computer. Attitude signals are from Inertial Navigation System (INS). Fixed attitude and rate gains of $\frac{\delta e}{\theta} = 3.5 \frac{\text{Deg}}{\text{Deg}}$ and $\frac{\delta e}{\theta} = 2.2 \frac{\text{Deg}}{\text{Deg/Sec}}$ are employed for flaps up flight. Rate damping is increased from 2.2 to 3.5 for flaps down flight. The pitch rate is passed through a $1/(.1s+1)$ lag for higher frequency suppression, a $1/(.05s + 1)$ lag for structural mode decoupling and a washout $ts/(ts + 1)$ where $t = 2$ for flaps up and to provide roll compensation. The compensation signal $(1-\cos\phi)$ is gain scheduled as a function of airspeed.

When the autopilot is on, the automatic trim system maintains pitch trim of the airplane. This is true for all autopilot modes except turbulence. When this mode is engaged, pitch trim is not active.

When engaged in MANUAL, the pitch autopilot responds to commands inserted via the pitch knob. When engaged in COMMAND, the pilot has the option of control by any of the following modes: ALT. HOLD, ALT. SELECT, IAS HOLD, V/S (Vertical Speed Control), MACH HOLD, ILS, or LAND.

1. Engage Synchronization

Before the autopilot is engaged, the output of the servo amplifier is fed back to the path integrator at a high gain. This loop maintains the output of the servo amplifier at zero in order to obtain transient-free elevator when the A/P is engaged. At engagement, the synchronizing path is opened. The integrator hold circuit tracks airplane attitude which serves as the reference for attitude hold, the initial mode of the A/P.

2. Manual

The MANUAL mode is engaged by placing the autopilot engage switch in the MANUAL position. Synchronization is provided so there is no attitude transient when the mode is engaged.

a. PITCH WHEEL: If the pilot desires to change the airplane pitch attitude, the pitch wheel on the flight controller is used. The pitch wheel produces an attitude command proportional to wheel displacement.

b. CONTROL WHEEL STEERING (CWS): (CWS is alternative to Pitch Wheel.) CWS enables the pilot, by applying a force to the column to insert a command signal into the A/P to change the airplane attitude. The force signal is processed as in Figure 14a. Force on the control column commands pitch rate via an integral path, the gain of which is programmed with True Airspeed to give uniform performance over the flight regime. When the force is removed, the path integrator is synchronized to the airplane attitude at the time of force release.

When the A/P is in MANUAL or in COMMAND and not in any path mode, the A/P will be in the CWS mode. If in COMMAND and in a path mode and the high detent force (19 pounds) is exceeded, the path mode drops off and the A/P drops to MANUAL except when in Altitude Hold. When in CWS and the deadzone (low detent) is exceeded, the automatic trim is inhibited. Whenever an attitude of ± 25 degrees is reached and the pilot applies a force in the direction to increase this attitude, the rate path is inhibited (MANEUVER LIMIT CONTROL).

3. Turbulence

In a turbulent environment TURB. may be engaged on the Turb/Speed mode select switch when the NAV mode switch is not in ILS or LAND. With TURB engaged, the autopilot is automatically switched from COMMAND to MANUAL and the flight director pitch trim control becomes effective. The pitch attitude and pitch rate gains are reduced by one-half. The automatic stabilizer trim is off in the turbulence mode.

PITCH FLIGHT DIRECTOR MODE	GAIN							REMARKS
	PARAMETER	SYMBOL	SUBMODE	VALUE	UNITS	SHAPING	PROGRAM	
ATTITUDE HOLD	BAR SENSITIVITY			.059	IN/DEG			
	RATE DAMPING	$\theta_c/\dot{\theta}$		.90	DEG/DEG/SEC	$\frac{2S}{(2S+1)(.1S+1)(.05S+1)}$	6)	FLAPS DOWN FILTER AS IN AUTOPILOT
	LIFT COMP PTK GRADIENT	$\theta_c/(1-\cos\phi)$		18.8	$\frac{\text{DEG}}{\text{FCN OF DEG}}$	$\frac{1}{.08S+1}$	CAS	$\frac{2.5^\circ\theta_c}{30^\circ\phi}$
ALTITUDE HOLD	ALT HOLD	$\theta_c/\Delta h_B$	—	-.016	DEG/FT	$\frac{1}{.08S+1}$ PATH FILTER AND LIMITER AT 8° θ_c COMMON TO ALL MODES SHOWN	CAS	
	ALT HOLD RATE	$\theta_c/\dot{h}$	—	.032	DEG/FT/SEC			d
	ALT HOLD ATTITUDE	θ_c/θ		1	DEG/DEG $\frac{20S}{20S+1}$			
IAS HOLD	ATTITUDE	θ_c/θ	—	1	DEG/DEG	$\frac{20S}{20S+1}$		
	AIRSPEED HOLD	$\theta_c/\Delta V$		.13	DEG/KT	3)		
MACH HOLD	ATTITUDE	θ_c/θ	—	1	DEG/DEG	$\frac{20S}{20S+1}$		
	MACH ERROR	$\theta_c/\Delta M$	—	95	DEG/MACH	3)		
VERTICAL SPEED HOLD	ATTITUDE	θ_c/θ	—	1	DEG/DEG	$\frac{1.5S}{1.5S+1}$		
	VERTICAL SPEED ERROR	$\theta_c/\Delta\dot{h}$	—	.05	DEG/FT/SEC	3)	CAS	d
ALTITUDE SELECT	ATTITUDE	θ_c/θ	CAPTURE	1	DEG/DEG	$\frac{8S}{8S+1}$		
			HOLD	1		$\frac{20S}{20S+1}$		
	ALTITUDE ERROR GAIN	$\theta_c/\Delta h_T$	CAPTURE	.0035	DEG/FT	3)	CAS	d
			HOLD	.018				
	ALTITUDE RATE	$\theta_c/\dot{h}$	CAPTURE	.05	$\frac{\text{DEG}}{\text{FT/SEC}}$	3)		d
			HOLD	.092				
GLIDE SLOPE	ATTITUDE	θ_c/θ	CAPTURE	1	DEG/DEG	$\frac{1.5S}{1.5S+1}$		
			HOLD	1		$\frac{14S}{14S+1}$		
	CAPTURE GAIN	$\theta_c/\dot{h}_B$		.21	DEG/FT/SEC	—		SINK RATE BIAS 12 FT/SEC
	BEAM ERROR	θ_c/ϵ		28	DEG/DEG	3)	RA OR[4] TIME	
	PATH DAMPING	$\theta_c/\ddot{h}$	CAPTURE AND HOLD	2.5	DEG/FT/SEC^2	$\frac{28S}{28S+1}\frac{1}{.85S+1}\frac{1}{10S+1}$		
FLARE	SINK RATE ERROR	$\theta_c/\dot{h}_c$		.03	DEG/FT/SEC	$\frac{1}{.3S+1}$		
	SINK RATE INTEGRAL	$\theta_c/\int\dot{h}_c$		.26	$\frac{\text{DEG/SEC}}{\text{FT/SEC}}$	$\frac{1}{.3S+1}$		
	FLARE RATIO	$\dot{h}/h$	—	.167	$\frac{\text{DEG/SEC}}{\text{FT/SEC}}$	$\dot{h} = \frac{\dot{h}}{S+1}\frac{h}{S+1}$		GAIN COMMON TO AUTOPILOT
	DAMPING	$\theta_c/\int\ddot{h}$	—	.12	DEG SEC/FT	$\frac{1}{.2S+1}\frac{28S}{28S+1}\frac{1}{.33S+1}$		
		$\theta_c/\dddot{h}$		.2	DEG SEC^2/FT			
	PITCH RATE	θ_c/θ		.9	DEG/DEG/SEC	$\frac{10S}{(10S+1)(.1S+1)}$		
	PITCH ATTITUDE	θ_c/θ		1	DEG/DEG	$\frac{4S}{4S+1}$		
GO-AROUND	NOSEUP BIAS	θ_c	—	12	DEG	—	—	

1) AUTOMATIC STABILIZER TRIM IS INHIBITED DURING THESE MODES.

2) SEE DIAGRAM 1 FOR CAS GAIN PROGRAM.

3) THE GAIN PATH INCLUDES THE $\frac{1}{.08S+1}$ PATH FILTER AS WELL AS AN 8 DEG θ_c AMPLITUDE LIMIT.

4) WITH THE RADIO ALTIMETER, VALID SIGNAL PRESENT GAINS ARE PROGRAMMED AS PER DIAGRAM 2 WITH RADIO ALTITUDE, OTHERWISE, THEY ARE PROGRAMMED WITH THE TIME BASE PROGRAM SHOWN IN DIAGRAM 4.

5) SEE DIAGRAM 3 FOR TAS GAIN PROGRAM.

6) IN FOR GLIDE SLOPE CAPTURE, TRACK; FLARE; GO AROUND ONLY.

REV SYM d

Table 6
Flight Director Pitch Axis

AUTOPILOT PITCH AXIS

	PITCH AUTOPILOT MODE	GAIN								REMARKS
		PARAMETER	SYMBOL	SUBMODE	VALUE	UNITS	SHAPING	PROGRAM		
MANUAL	ATTITUDE HOLD	ATTITUDE	$\delta e/\theta$	OTHER	3.2	DEG/DEG	$\frac{1}{(.05S+1)}$	---		
				GLIDE SLOPE AND FLARE			$\frac{1}{(.05S+1)}$			
		DAMPING	$\delta e/\dot{\theta}$	FLAPS UP	1.4	$\frac{DEG}{DEG/SEC}$	$\frac{2S}{(.1S+1)(2S+1)(.05S+1)}$	---	d	BODE LOSS AT MID-BAND NOT INCLUDED.
				FLAPS DOWN	3.5		$\frac{10S}{(.1S+1)(10S+1)(.05S+1)}$			
		LIFT COMP	$\theta o/(1-\cos\phi)$	---	18.9	$\frac{DEG}{FCN\ OF\ DEG}$	$\frac{1}{.05S+1}$	CAS[2]		$\frac{2.5^\circ\theta c}{30^\circ\phi}$
		PITCH KNOB	θc/STROKE	---	1	DEG/STROKE	---	---		STROKE IS THE AMOUNT KNOB CAN BE MOVED WITHOUT REMOVAL OF HAND.
	TURBU-LENCE[1]	ALL ABOVE GAINS	$\delta e/\theta c$	---	½ THE ABOVE	DEG/DEG	---	---		LIFT COMP REMAINS UNCHANGED
	CONTROL WHEEL STEERING (OPTIONAL)[1]	CWS GAIN	θc/ LB STICK FORCE	---	0	DEG/LB				τ = .35 SEC
		CWS INTEGRAL GAIN	$\theta c/\int$FORCE	---	.32	$\frac{DEG/SEC}{LB}$	$\frac{1}{\tau S+1}$	TAS 5		THIS MODE IS ALTERNATIVE TO PITCH KNOB
	ALT HOLD	ALT HOLD	$\theta c/\Delta h_B$	---	.029	DEG/FT	$\frac{1}{.65S+1}$ 3)	CAS[2]		
		ALT HOLD INTEGRAL	$\frac{\theta c/\int\Delta h_B}{\theta c/\Delta h_B}$	---	.067	$\frac{INTEGRAL}{DISPLACEMENT}$	PATH FILTER AND LIMITER AT 8°θc COMMON TO ALL MODES SHOWN			
		ALT HOLD RATE	$\theta c/\dot{h}$	---	.05	DEG/FT/SEC			d	
COMMAND	IAS	AIRSPEED HOLD	$\theta c/\Delta V$	---	.2	DEG/KT		NO GAIN PROGRAM		
		AIRSPEED HOLD INTEGRAL	$\frac{\theta c/\int\Delta V}{\theta c/\Delta V}$	---	.05	$\frac{INTEGRAL}{DISPLACEMENT}$				
	MACH HOLD (OPTIONAL)	MACH HOLD GAIN	θc/MACH	---	120	DEG/MACH NO.				
		MACH HOLD INTEGRAL	$\frac{\theta c/\int MACH}{\theta c/MACH}$		.05	$\frac{INTEGRAL}{DISPLACEMENT}$				
	VERTICAL SPEED	VERTICAL SPEED	$\theta c/\Delta\dot{h}$	---	.09	DEG/FT/SEC		CAS[2]	d	COMMAND IS RATE LIMITED TO 4 FT/SEC[2]
		VERTICAL SPEED INTEGRAL	$\frac{\theta c/\int\Delta\dot{h}}{\theta c/\dot{h}}$	---	.2	$\frac{INTEGRAL}{DISPLACEMENT}$				
	ALTITUDE SELECT	ALTITUDE ERROR GAIN	$\theta c/\Delta h_f$	CAPTURE AND HOLD	.006 / .029	DEG/FT			d	
		ALTITUDE RATE	$\theta c/\dot{h}$	CAPTURE	.09	$\frac{DEG}{FT/SEC}$				COMMAND RATE LIMIT 133 FT/SEC
				HOLD	.05				d	AS ABOVE BUT LIMIT MAY BE 30 FT/SEC FOR $\dot{h}$ <30'/S IN HOLD.
		ALTITUDE SEL INTEGRAL	$\frac{\theta c/\int\Delta h}{\theta c/\Delta h}$	CAPTURE	.125	$\frac{INTEGRAL}{DISPLACEMENT}$				
				HOLD	.05					
	GLIDE SLOPE	CAPTURE GAIN	$\theta c/\int\Delta\dot{h}$	CAPTURE	.064	$\frac{DEG/SEC}{FT/SEC}$	THROUGH PATH INTEGRATOR ONLY			12.5 FT/SEC BIAS
		BEAM ERROR	$\theta c/\varepsilon$	CONTROL	45	DEG/DEG	3) 3.5 DEG/SEC ELEV EASY-ON	R.A. 4) OR TIME BASE		MAY BE TIME BASE GAIN PROGRAMMED FOR LOSS OF VALID
		BEAM INTEGRAL	$\frac{\theta c/\int\varepsilon}{\theta c/\varepsilon}$	CONTROL	.042	$\frac{INTEGRAL}{DISPLACEMENT}$			d	
		PATH DAMPING	$\theta c/\ddot{h}$	CAPTURE AND CONTROL	4.0	2) DEG/FT/SEC	$\frac{28S}{28S+1}\cdot\frac{1}{.65S+1}\cdot\frac{1}{10S+1}$	---		THIS PATH ALSO FEEDS TO THE PATH INTEGRATOR AT 1/15 GAIN
	FLARE	SINK RATE ERROR	$\theta c/\dot{h}_c$	---	.43	DEG/FT/SEC	---	---		T/D BIAS = 2 FT/SEC
		SINK RATE INTEGRAL	$\frac{\theta c/\int\dot{h}_c}{\theta c/\dot{h}_c}$	---	.64	$\frac{INTEGRAL}{DISPLACEMENT}$	---	---		
		FLARE RATIO	$\dot{h}/h$	--	.167	$\frac{FT/SEC}{FT}$	$\dot{h}=\frac{Sh}{S+1}+\frac{\dot{h}'}{S+1}$	---		
		DAMPING	$\theta c/\int\dot{h}$	--	.12	DEG SEC/FT	$\frac{1}{2S+1}\cdot\frac{28S}{28S+1}$	---		
			$\theta c/\dot{h}'$	--	.20	DEG SEC²/FT	4) 6)			
	DUAL CHANNEL EQUALIZATION	GLIDE SLOPE	$\theta c/\Delta\delta e$	---	.163	$\frac{DEG/SEC}{DEG}$	MINIMUM GAIN .055	---		7)
		FLARE	$\theta c/\Delta\delta e$	---	.102	$\frac{DEG/SEC}{DEG}$		---		
	DISENGAGE SYNCHRONIZATION		$\dot{\theta}c/\theta c$	---	20	$\frac{DEG/SEC}{DEG}$	RATE LIMITED TO 6.7 DEG/SEC	---		
	FLARE SYNCHRONIZATION			---	7.24	$\frac{DEG/SEC}{DEG}$		---		
	ATTITUDE MEMORY SYNCHRONIZATION			---	30	$\frac{DEG/SEC}{DEG}$		---		

1) AUTOMATIC STABILIZER TRIM IS INHIBITED DURING THESE MODES.
2) SEE DIAGRAM 1 FOR CAS GAIN PROGRAM.
3) THE GAIN PATH INCLUDES THE $\frac{1}{.65S+1}$ PATH FILTER AS WELL AS AN 8 DEG θc AMPLITUDE LIMIT.
4) WITH THE RADIO ALTIMETER, VALID SIGNAL PRESENT GAINS ARE PROGRAMMED AS PER FIGURE 18 WITH RADIO ALTITUDE, OTHERWISE, THEY ARE PROGRAMMED WITH THE TIME BASE PROGRAM.
5) SEE FIGURE 16 FOR TAS GAIN PROGRAM.
6) LIMITED AT 3.0 DEGREES ELEVATOR DIFFERENCE.
7) CAM OUT LEVEL 6.0 DEGREES ELEVATOR DIFFERENCE, WARNING LIGHT DELAY 1 SECOND.

TABLE 7
AUTOPILOT PITCH AXIS

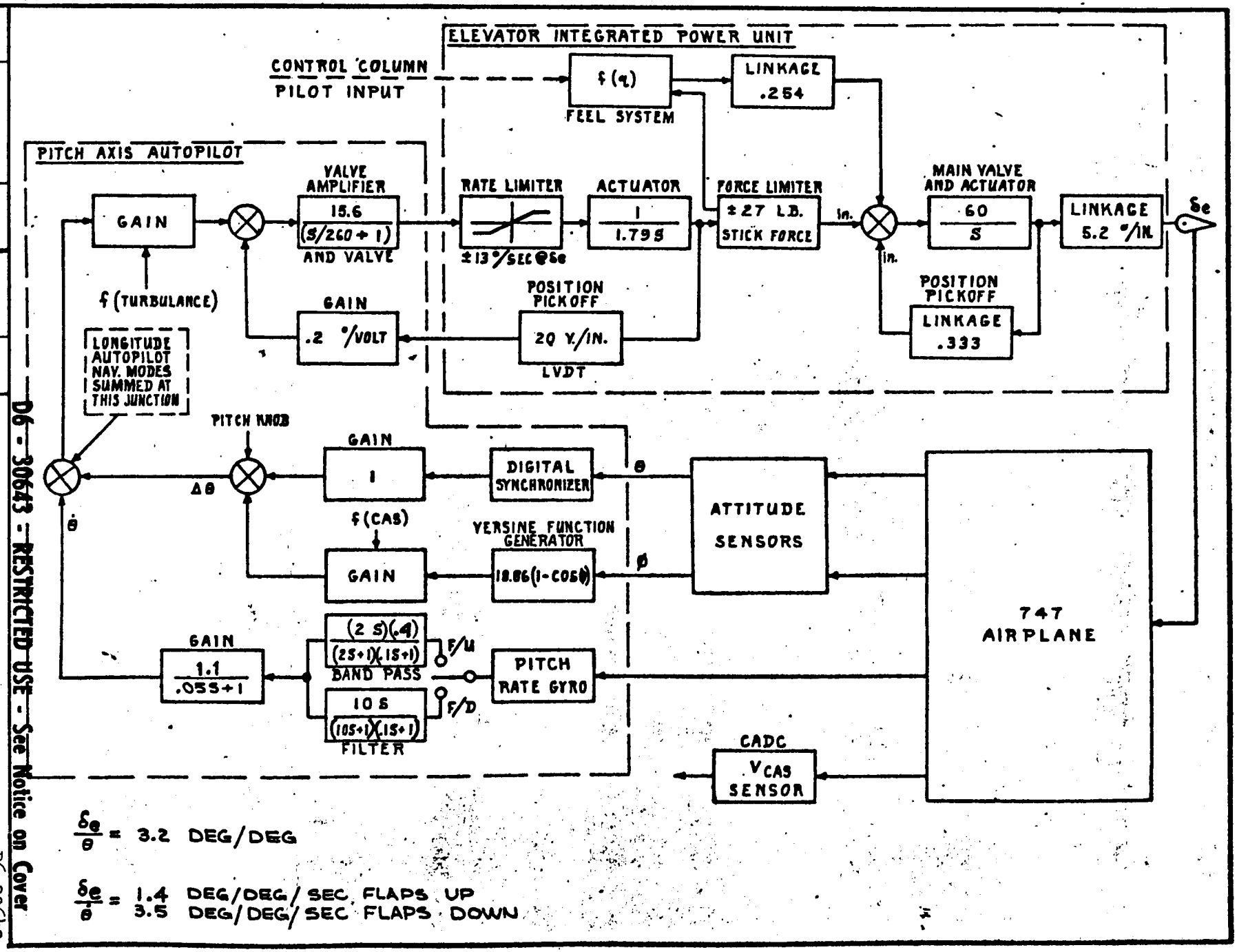

	CALC	CHECK	APPD	REVISED	DATE
				REV B	8/8/69
			Rev C		2/24/70

D6 - 30643 - RESTRICTED USE - See Notice on Cover

THE BOEING COMPANY
RENTON, WASHINGTON

ATTITUDE HOLD MODE
PITCH AUTOPILOT

D6-30643
Vol. II

FIG. 14

PAGE 18-16

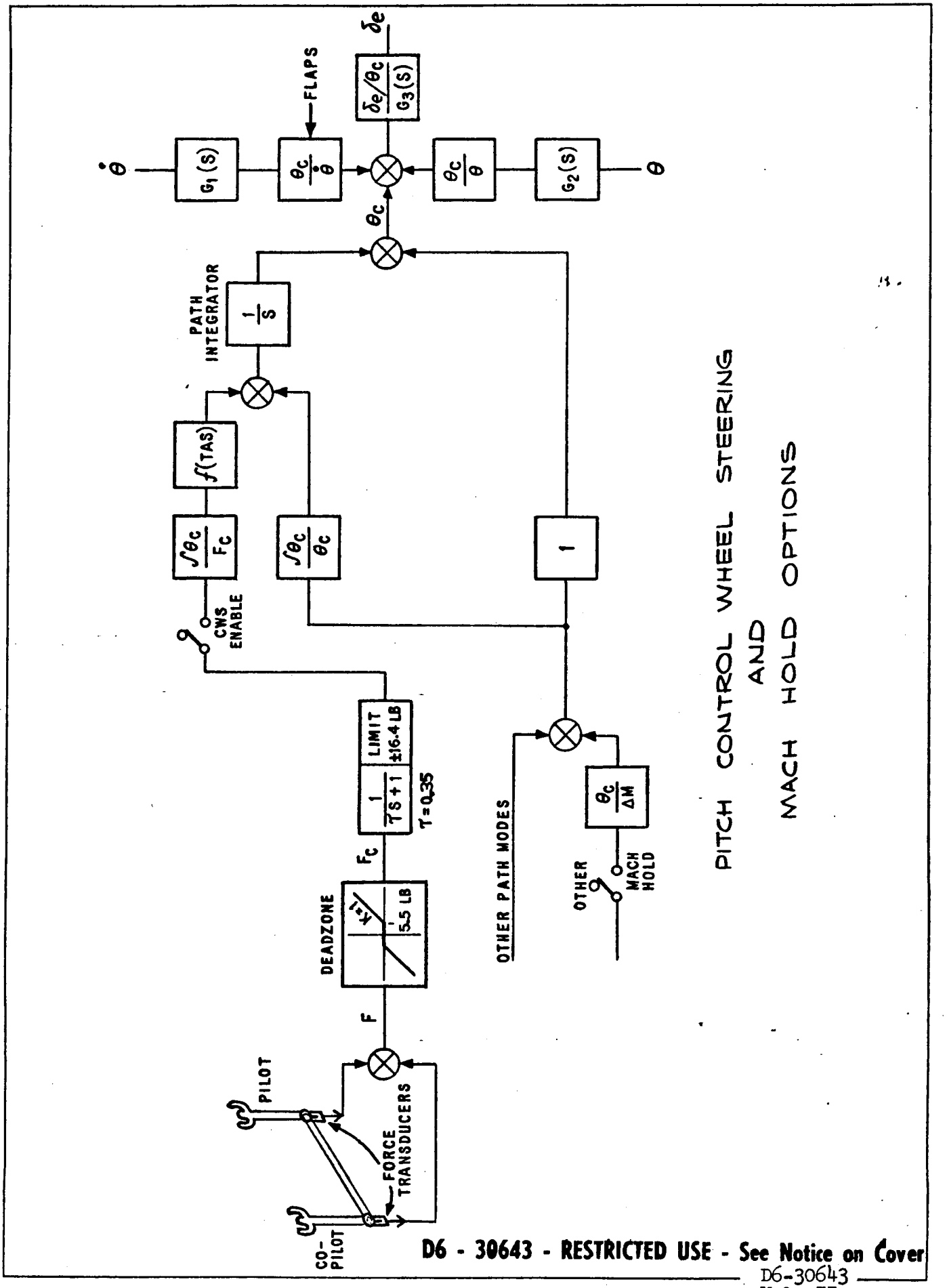

AD 1546 D

4. Command

When engaged in COMMAND and no other pitch mode is selected, the A/P is in pitch attitude hold and the pitch knob is operative.

a. Altitude Hold

The altitude Hold mode holds the airplane at the altitude existing when the mode is engaged. This mode can be engaged in either MANUAL or COMMAND. If the mode is engaged with the airplane climbing or descending at a reasonable rate, the airplane returns to and holds the engage altitude.

The Air Data Computer provides the reference signal for this mode. This altitude error signal is provided after clutching a mechanically nulled synchro to the altitude shaft at mode engage. Aircraft altitude rate (or vertical speed) is also sensed and provided by the Air Data Computer.

The block diagram and gains for the Altitude Hold mode are included as part of Figure 15.

The altitude error signal commands attitude changes required to maneuver the airplane toward zero altitude error. Altitude rate is added to improve damping. Integral control on the altitude error removes standoffs. The gains used are programmed down at high speeds to about 1/3 of the low speeds. (See Figure 16.)

b. Altitude Select

The Altitude Select mode allows the pilot to select a desired flight altitude. If the selected altitude is more than 1200 feet from actual altitude, the pilot also selects the desired mode of climb or descent. With these selections made and the mode engaged, the autopilot maneuvers the airplane to smoothly capture and hold the selected altitude. This mode is particularly useful when a number of successive altitude changes are required.

Altitude Select has three submodes: arm, capture, and track. (See Figures 15 and 17.)

(1) Arm

In the arm submode, the pilot selects some other pitch mode of the autopilot, such as vertical speed, IAS hold, or pitch knob, to command the aircraft to climb or descend toward the desired altitude. In this submode, the altitude select switch is engaged and the capture logic is armed.

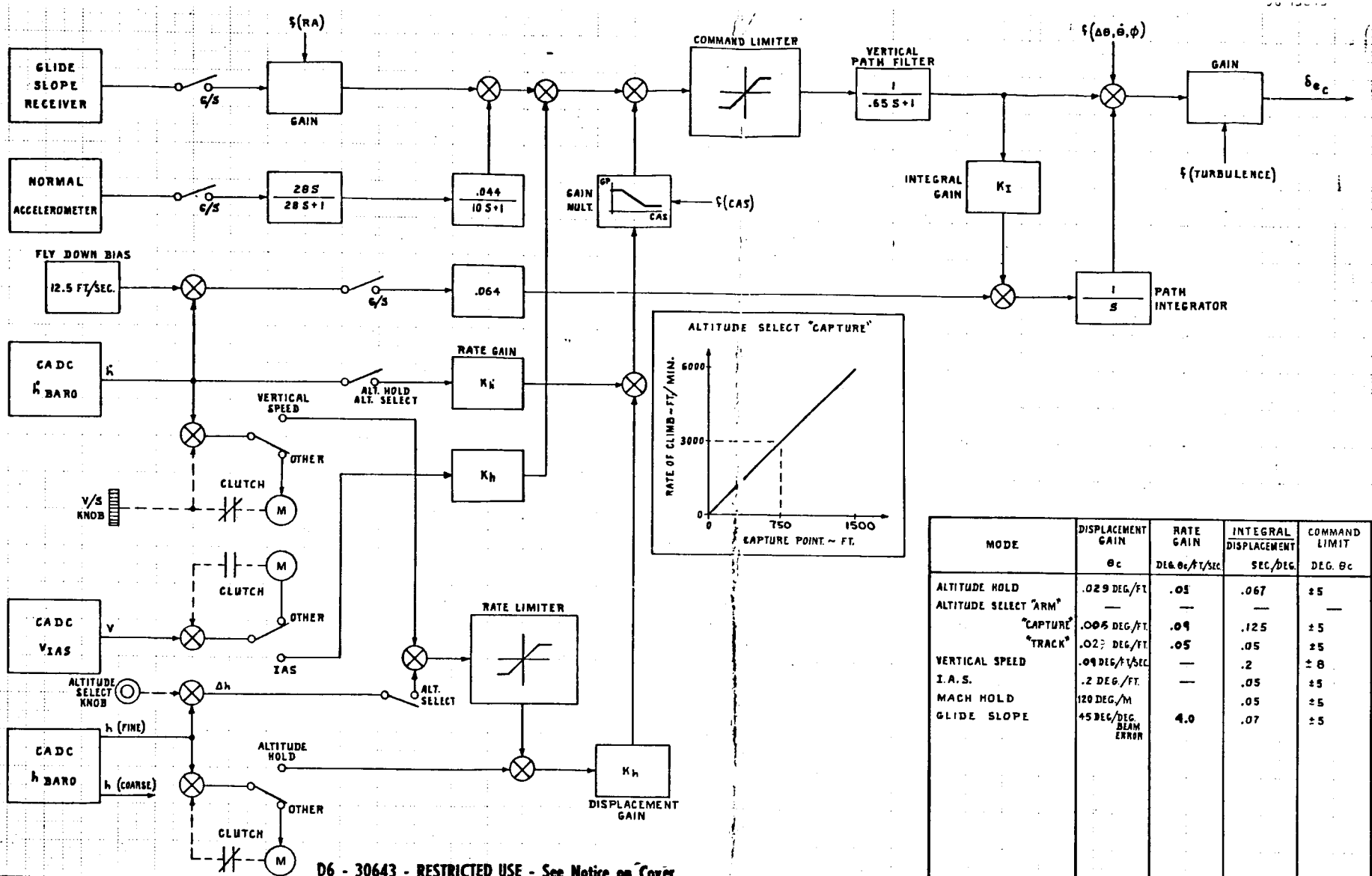

MODE	DISPLACEMENT GAIN θc	RATE GAIN DEG. θc/FT/SEC	INTEGRAL DISPLACEMENT SEC/DEG.	COMMAND LIMIT DEG. θc	RATE LIMIT
ALTITUDE HOLD	.029 DEG./FT.	.05	.067	±5	—
ALTITUDE SELECT "ARM"	—	—	—	—	—
"CAPTURE"	.006 DEG./FT.	.09	.125	±5	30 FT./SEC.
"TRACK"	.029 DEG./FT.	.05	.05	±5	30 FT./SEC.
VERTICAL SPEED	.09 DEG./FT/SEC.	—	.2	±8	4 FT/SEC.²
I.A.S.	.2 DEG./FT.	—	.05	±5	—
MACH HOLD	120 DEG./M		.05	±5	—
GLIDE SLOPE	45 DEG/DEG. BEAM ERROR	4.0	.07	±5	—

d

D6 - 30643 - RESTRICTED USE - See Notice on Cover

			REVISED	DATE
CALC			REV B	6/13/67
CHECK			REV C	10/10/67
APR			REV D	2/23/72
APR				

ATTITUDE CONTROL - PATH MODES

D6-30643 Vol. II

FIG. 15

THE BOEING COMPANY

PAGE 18-48

Rev. d

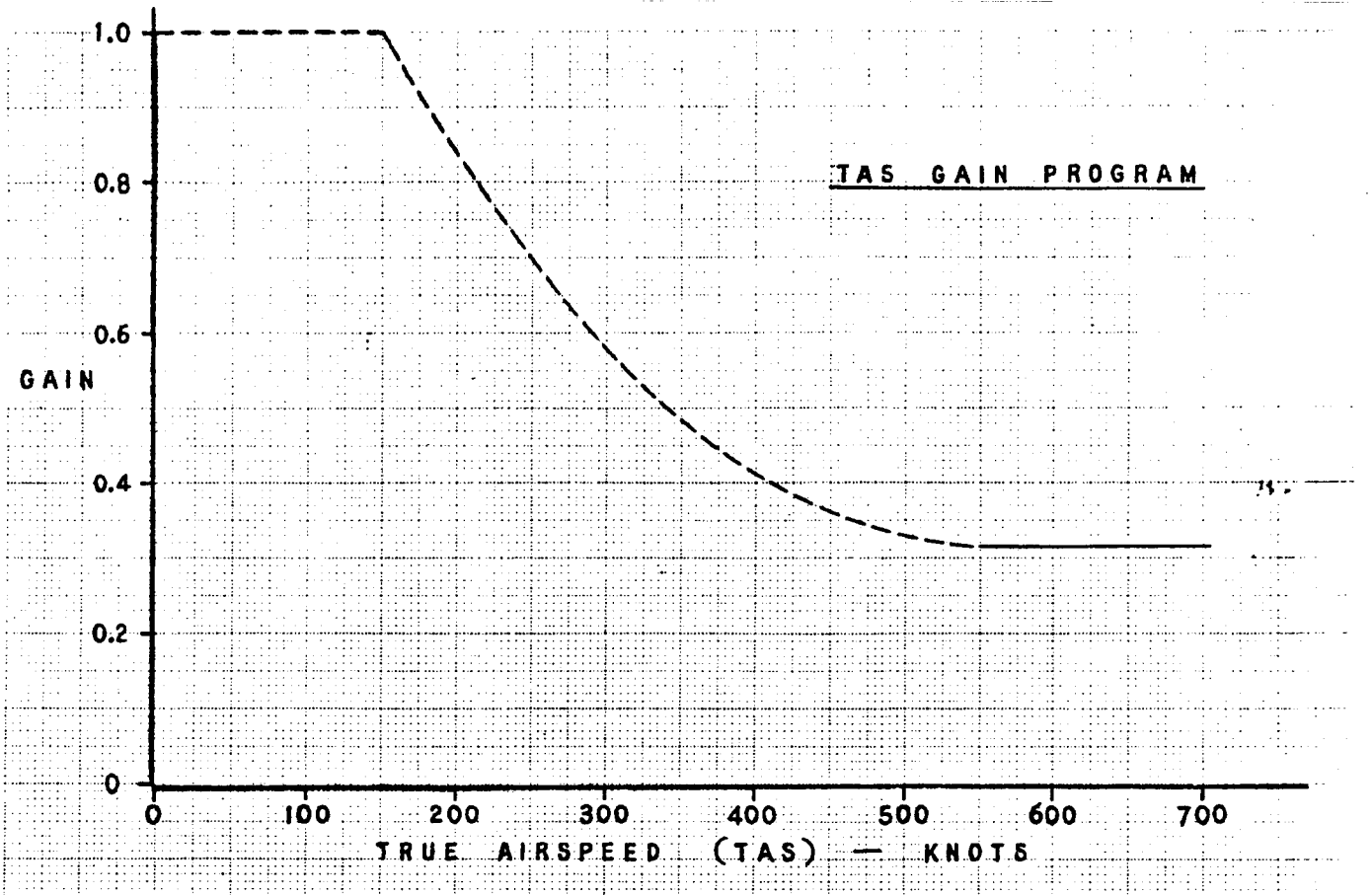

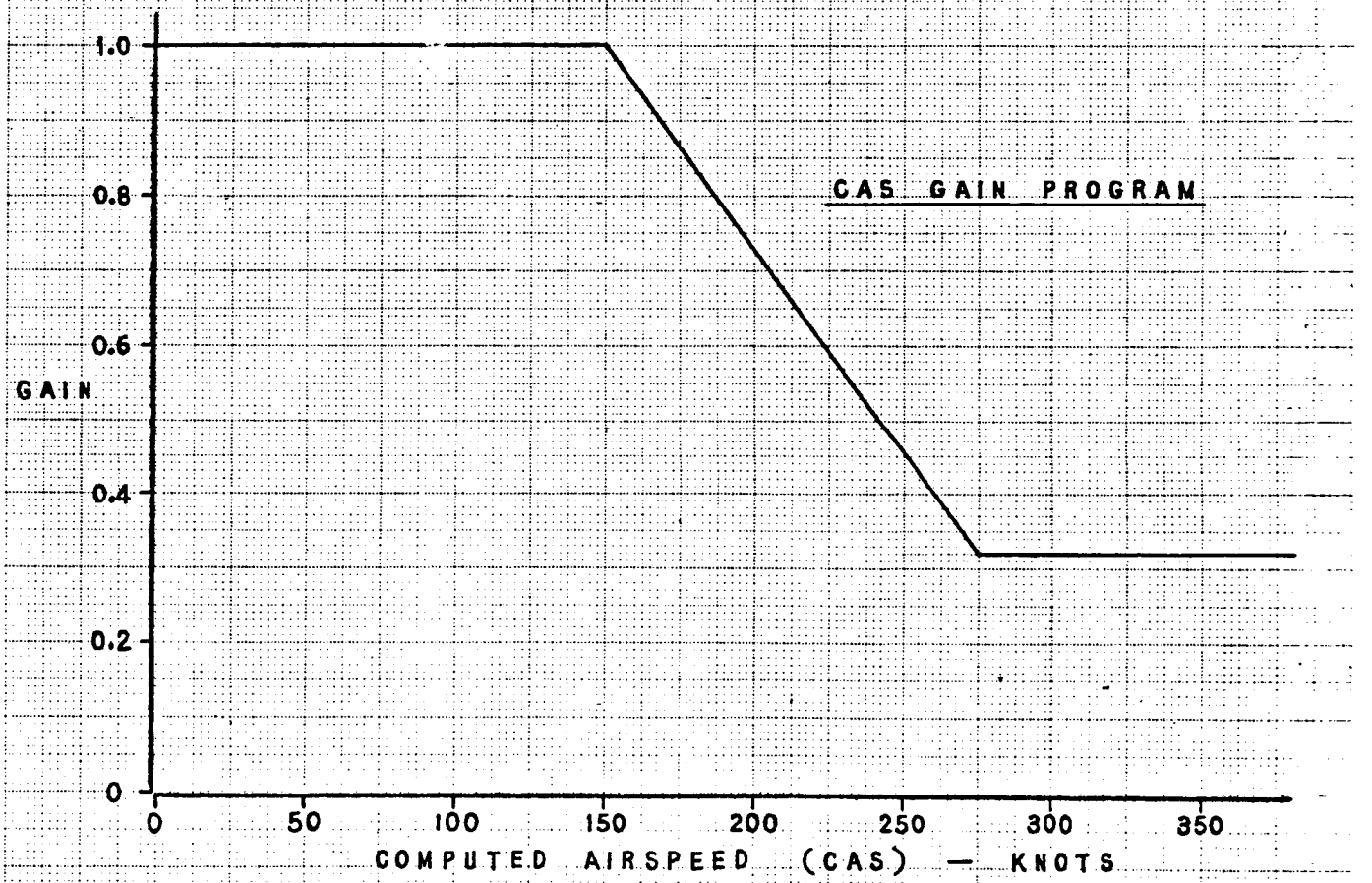

CALC			REVISED	DATE
CHECK			Rev. C	10-10-69
APR				
APR				

PITCH PATH MODE
GAIN SCHEDULE

FIG. 16

D6-30643
Vol. II

THE BOEING COMPANY

ALTITUDE SELECT MODE

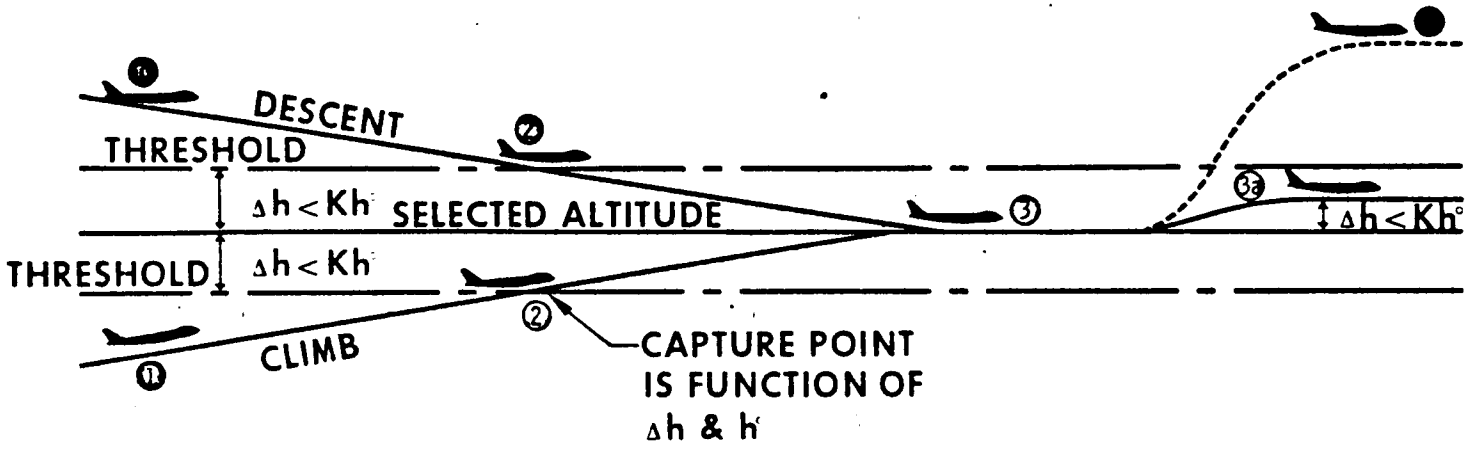

SEQUENCE:

(1) DESIRED ALTITUDE SELECTED

- ALT SELECT ARMED
- PITCH MODE CONTROL IN DIRECTION OF ATTITUDE
  - PITCH KNOB
  - IAS HOLD
  - VERTICAL SPEED
  - MACH HOLD
- ALT SEL ANNUNCIATOR — AMBER

(2) SELECTED ALTITUDE CAPTURED

- ALT SELECT MODE IN CONTROL PITCH MODE SWITCH MOVES TO OFF
- ALT SEL ANNUNCIATOR — GREEN

(3) CHANGE IN SELECTED ALTITUDE

(3a) < Kh° CHANGE - ALT SELECT MODE IN CONTROL

- ALT SEL ANNUNCIATOR — GREEN

● > Kh° CHANGE-PITCH MODE SWITCH IN CONTROL

- ALT SEL ANNUNCIATOR — AMBER

Fig. 17 Altitude Select Mode

(2) Capture

Capture is initiated when the aircraft's altitude approaches the selected altitude to within 1200 feet, and the altitude error (in feet) is less than 15 times the altitude rate (in feet/sec.) as sensed by the coincidence detector. The detector uses course altitude and rate data from the CADC to determine the switching point. When the detector is satisfied, it switches off the previously used climb or descent mode and initiates capture. During capture, the fine altitude data from the CADC and altitude rate information are summed as indicated by the following control equation to command the aircraft to maneuver and capture the selected altitude:

$$\Delta\Theta_c = G_M(.006\Delta h + .09\dot{h}) \quad d$$

where: G_M is the gain program with computed airspeed (unity at low speed)

$\Delta\Theta_c$ is pitch attitude command in degrees

Δh is altitude error in feet

$\dot{h}$ is rate of climb in feet per second

This produces a flare toward the selected attitude which is rate limited to reduce "g" forces if initiated from steep climbs or descents.

(3) Track

The track phase is initiated when the airplane approaches within 100 feet of the selected attitude, with a rate not exceeding 5 feet/seconds. The control equation is as follows:

$$\Delta\Theta_c = G_M(.029\Delta h + .05\ \dot{h}) \quad d$$

with the units defined as above.

c. Vertical Speed

The vertical speed mode is selected by the Turb/Speed switch on the Mode Select Panel. Prior to selection, the vertical speed wheel on the Mode Select Panel is synchronized to aircraft

AD 1546 D

vertical speed. It is driven by an electro-mechanical servo follow-up to accomplish this repeating function. Upon engagement of this mode, the motor of this follow-up de-activates to provide the reference required to generate a vertical speed error signal. Should the pilot desire to operate at a different vertical speed, the command wheel is moved to establish a new reference. The vertical speed wheel has 1000 ft/minute graduations between the limits of operation which are +4000 ft/minute to -8000 ft/minute.

The block diagram and gains used for the vertical speed mode are shown in Figure 15. An acceleration limiter provides smooth system response to command changes. Gain scheduling is included to allow good performance over the speed range of the 747.

d. IAS Hold

This mode gives the pilot automatic Indicated Airspeed hold capability.

A clutched synchro on the computed airspeed shaft of the CADC provides an IAS error signal which is the difference between actual IAS and the IAS at the time of mode engage. The error signal commands pitch attitude required to hold the reference airspeed. The block diagram and gains used are shown in Figure 15.

3. Mach Hold

The Mach Hold mode provides the capability to automatically hold the airplane Mach existing when the mode is engaged. The mode is selected by the Turb/Speed select switch on the Mode Select Panel. The Mach error signal is generated in the CADC by a clutched synchro. The error signal commands the airplane pitch attitude required to zero the Mach error signal. The block diagram and gains are shown in Figure 15.

f. ILS Mode

The pitch axis control system for dual channel automatic landing is shown in Figure 19. The ILS mode uses part of one channel, that is, glide slope capture and control. Upon selection of ILS, glide slope capture is armed and the glide slope indicator light on the mode annunciator panel is amber. During the glide slope arm phase, a glide slope intercept path from above or below the glide path can be flown on ALT. HOLD, ALT. SELECT, MANUAL, MACH, IAS, or V/S. When the glide slope receiver is within ± 30 mv (±.14°) of beam center, the vertical beam sensor is tripped and glide slope capture begins. A sink rate error signal, barometric altitude rate plus a 12.5 fps bias, is switched into the path integrator for 10 seconds to produce a pitch angle approximately equal to that needed to fly the glide slope.

Normal acceleration, through a washout to eliminate steady state accelerometer outputs and filtered through a 10 second lag to pseudo-integrate, is switched in for beam damping. During the 10 second pitch down, beam error is synchronized by a limited integrator at the integrator's high rate. At the end of the 10 seconds, the sink rate error signal is switched off and glide slope control begins.

Beam error minus the synchronized signal stored on the rate-limited integrator is switched in, with this stored value bleeding down at the low rate of the integrator to give an easing on of the signal. On glide slope, beam error is programmed with radio altitude to provide a nearly constant elevator deflection per foot of beam error. The gain programmer is shown in Figure 18. In the event of a radio altimeter failure, a time-based gain program is also provided. (Figure 18-2).

g. Land Mode

The LAND Mode is shown in Figure 19. It is selected on the NAV mode selector when dual-channel, fail passive localizer, glide slope, and flare is planned. Sequencing during the LAND mode is shown in Figure 20.

Upon selecting of the LAND mode and with one channel in COMMAND, the autopilot is in single channel operation. The mode is the same as ILS except that the autopilot warning light flashes amber and the autopilot will automatically disengage at 150 ft. if the second channel is not engaged.

The second channel is locked in OFF until the automatic confidence test of the dual-channel camout monitor is completed. This takes about 1 second after LAND is selected and the first channel is engaged in COMMAND. Upon moving the second channel engage switch to COMMAND, the flashing amber warning light is extinguished and the second channel is armed. The system will operate in this configuration until the dual channel engage interlock logic is satisfied.

The autopilot remains in single channel operation until all of the following conditions are met:

LOC on-course
Rad. Altitude less than 1,500 ft.
Glide Slope control
Rad. Altitude valid

When these conditions are met, dual-channel operation begins and is annunciated after a three second delay by an amber A/P FLARE ARM light on the Mode Annunciator Panel. The non-latching autopilot camout monitor gives the pilot a steady red warning light on the Mode Annunciator Panel if a

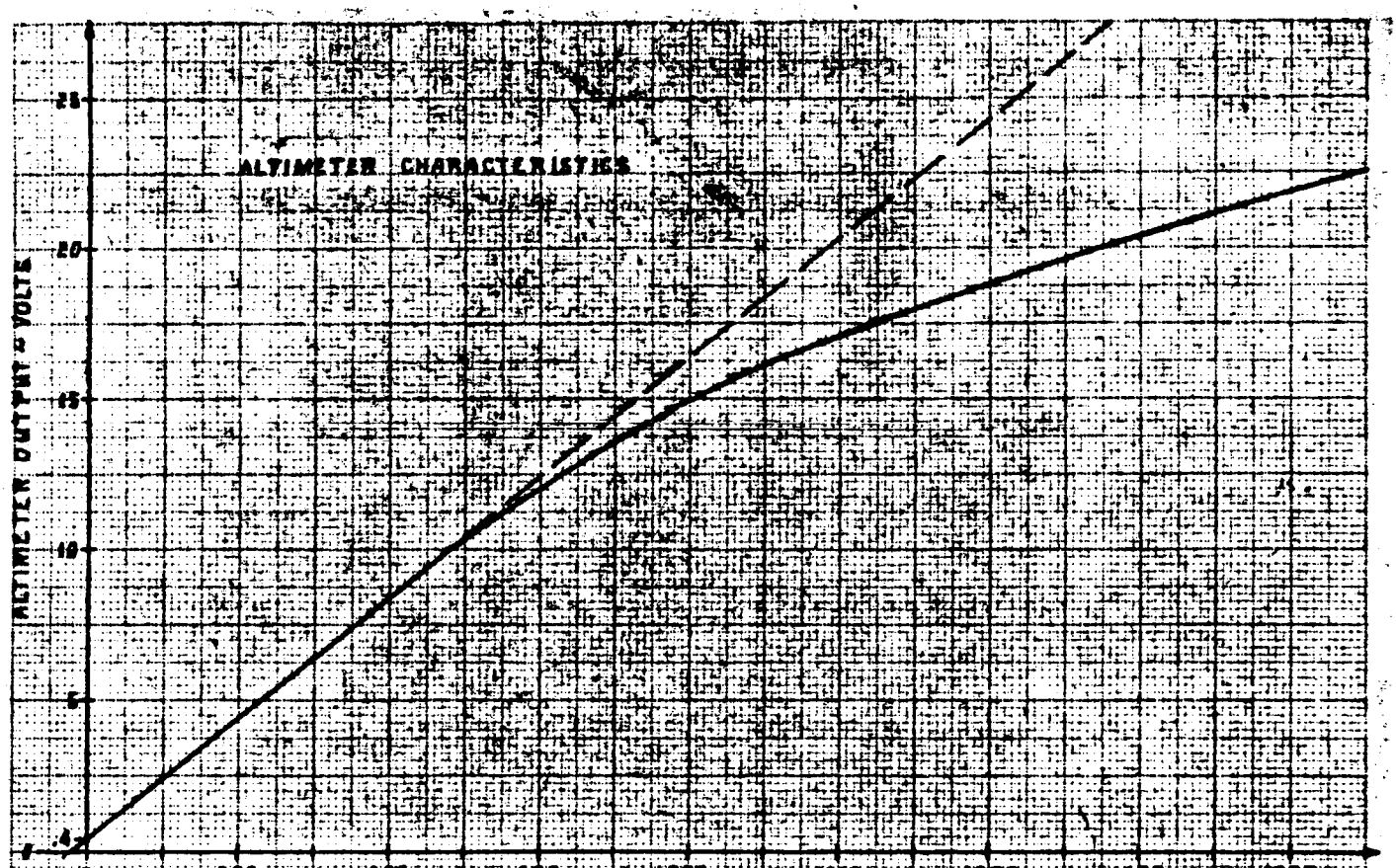

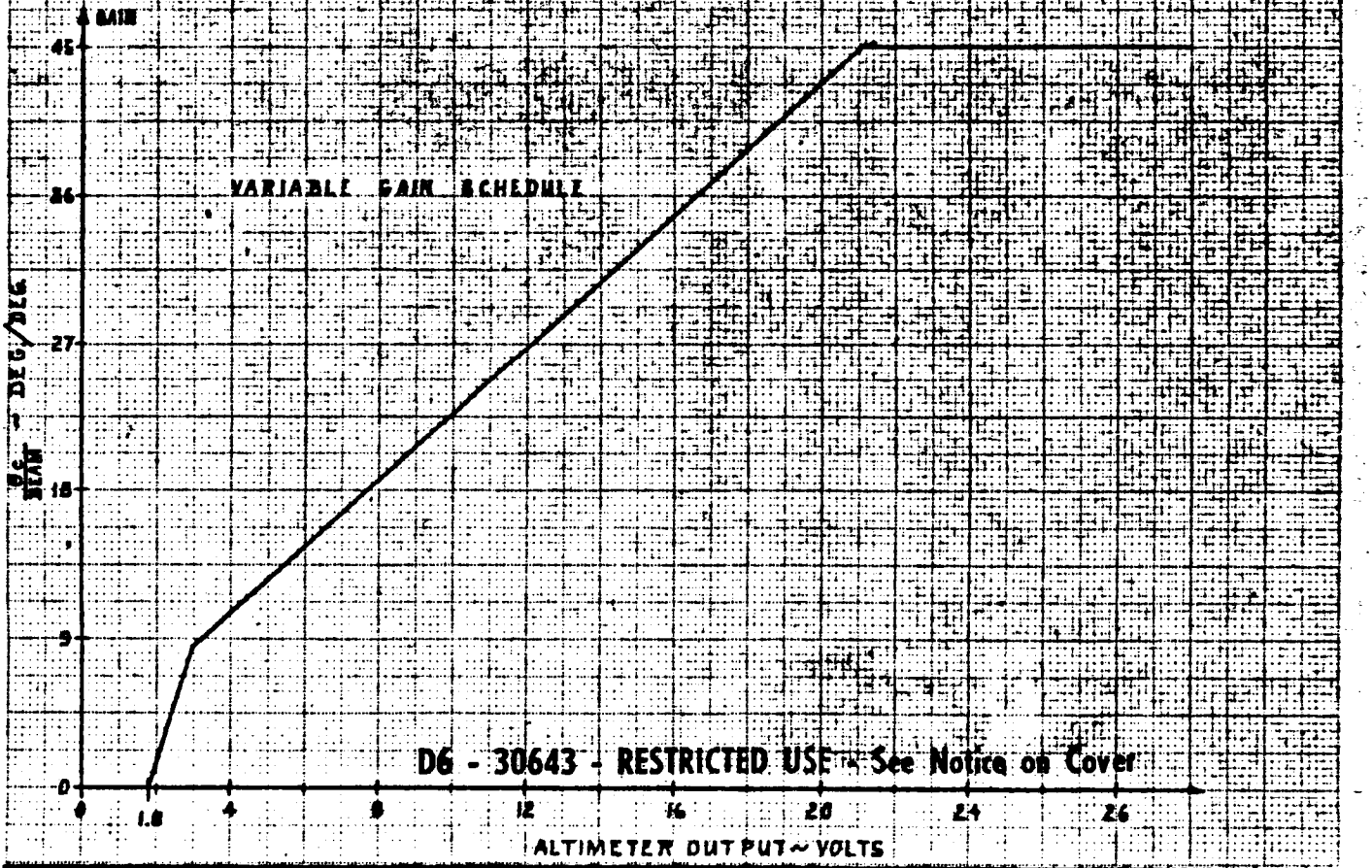

CALC			REVISED	DATE
CHECK				
APR				
APR				

GLIDE SLOPE MODE
GAIN SCHEDULE

D6-30643
Vol. II

FIG. 18

THE BOEING COMPANY

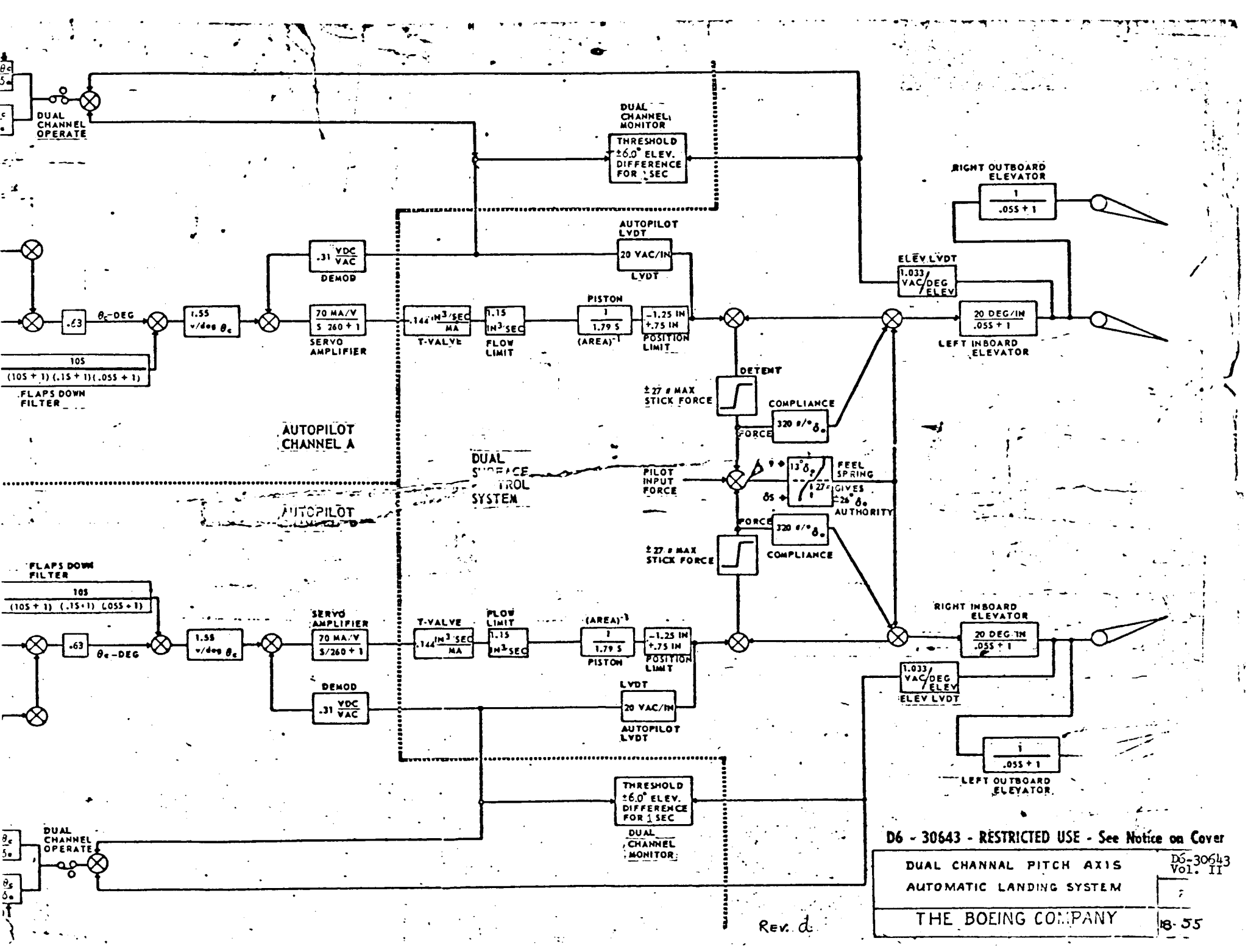

D6 - 30643 - RESTRICTED USE - See Notice on Cover

DUAL CHANNAL PITCH AXIS AUTOMATIC LANDING SYSTEM

D6-30643 Vol. II

THE BOEING COMPANY

18-55

Rev. d

LAND MODE (GLIDE SLOPE)

SEQUENCE:

① ILS OR LAND SELECTED

- PITCH MODE SWITCHES IN CONTROL
  - PITCH WHEEL (OR CWS)
  - IAS HOLD
  - V/S
  - ALT HOLD
  - ALT SEL
- ANNUNCIATOR
  GS – AMBER

② GLIDE SLOPE CAPTURED

- GS MODE IN CONTROL
- PITCH MODE SWITCHES MOVE TO OFF
- ANNUNICATOR
  GS–GREEN
  FLARE – AMBER *

③ FLARE INITIATED *

- FLARE MODE IN CONTROL
- ANNUNICATOR
  GS–GREEN
  FLARE–GREEN

④ TOUCHDOWN *

- A/P OFF

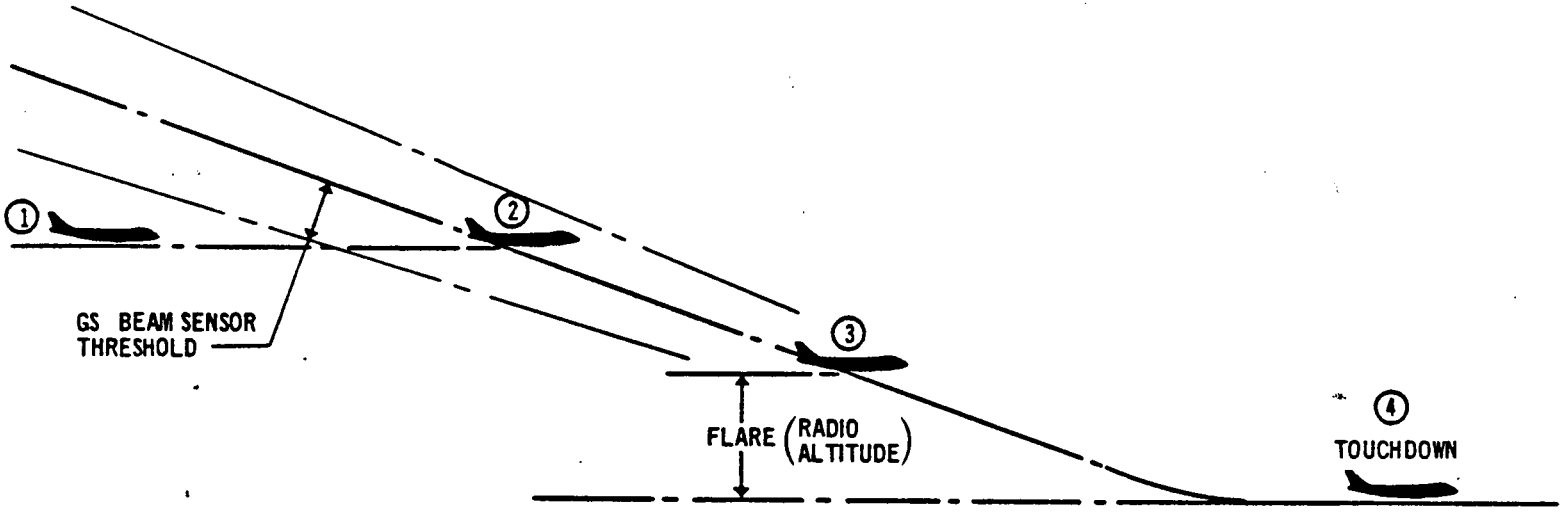

*LAND MODE ONLY

Fig. 20 Land Mode Sequence

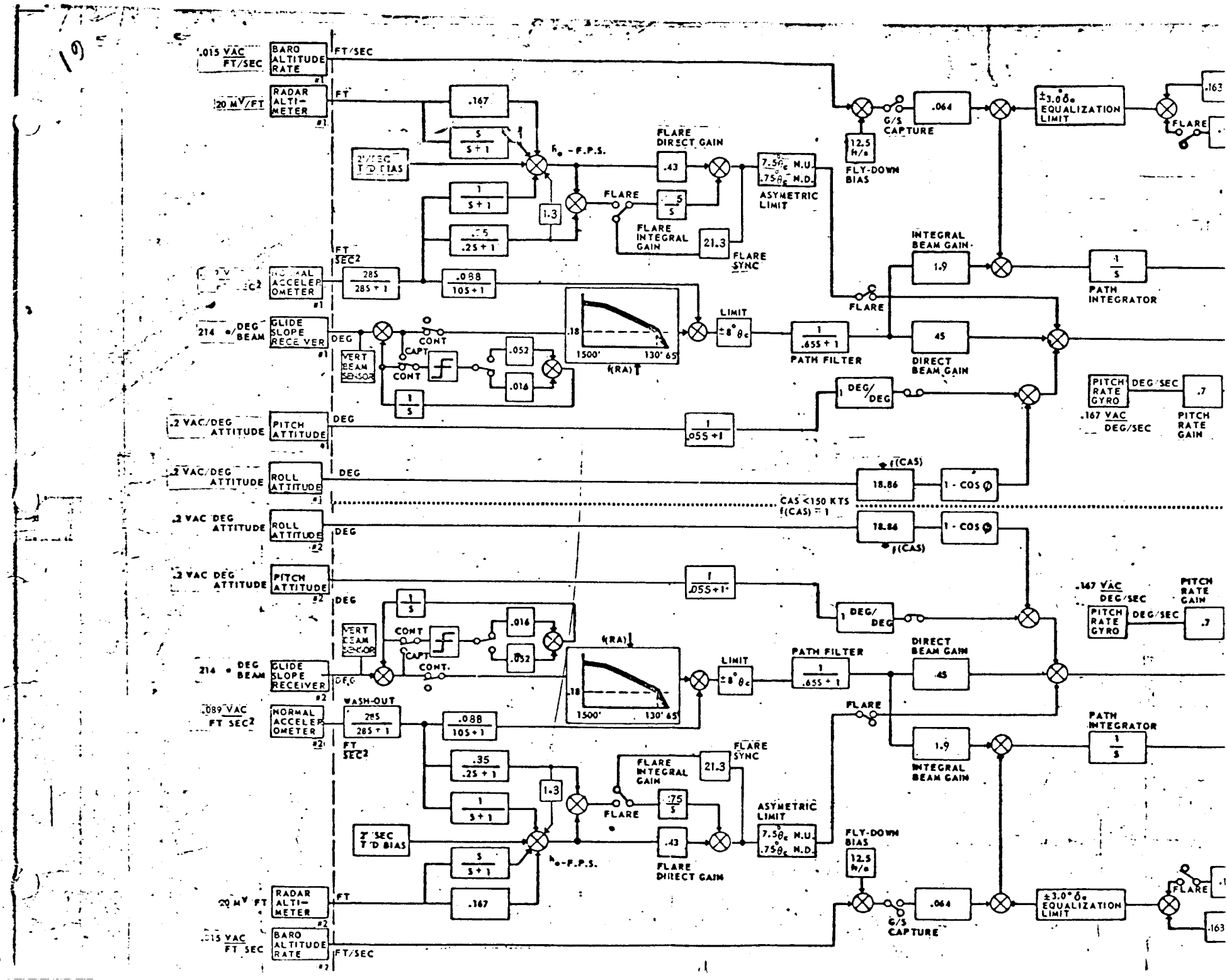
.015 VAC FT/SEC
BARO ALTITUDE RATE #1
FT/SEC
20 MV/FT
RADAR ALTI-METER #1
FT
.167
S/S+1
1/S+1
.5/.25+1
1.3
h_o - F.P.S.
FLARE DIRECT GAIN
.43
FLARE
.5/S
FLARE INTEGRAL GAIN
21.3
FLARE SYNC
ASYMETRIC LIMIT
7.5θc N.U.
.75θc M.D.
12.5 h/a
FLY-DOWN BIAS
G/S CAPTURE
.064
±3.0° δe EQUALIZATION LIMIT
FLARE
.163
FT/SEC²
NORMAL ACCELER-OMETER #1
.285/.285+1
.088/.10S+1
INTEGRAL BEAM GAIN
1.9
1/S
PATH INTEGRATOR
214 μ/DEG BEAM
GLIDE SLOPE RECEIVER #1
DEG
VERT BEAM SENSOR
CONT
CAPT
.052
.016
1/S
.18
1500'
130' 65
f(RA)
LIMIT
±8° θc
1/.65S+1
PATH FILTER
45
DIRECT BEAM GAIN
FLARE
.2 VAC/DEG ATTITUDE
PITCH ATTITUDE #1
1/.05S+1
1 DEG/DEG
PITCH RATE GYRO
DEG/SEC
.7
.167 VAC DEG/SEC
PITCH RATE GAIN
ROLL ATTITUDE #1
f(CAS)
18.86
1 - COS Φ
CAS <150 KTS f(CAS) = 1
ROLL ATTITUDE #2
PITCH ATTITUDE #2
.089 VAC FT SEC²
WASH-OUT
.285/.285+1
.35/.25+1
2° SEC T'D BIAS
.167
RADAR ALTI-METER #2
.015 VAC FT SEC
BARO ALTITUDE RATE #2

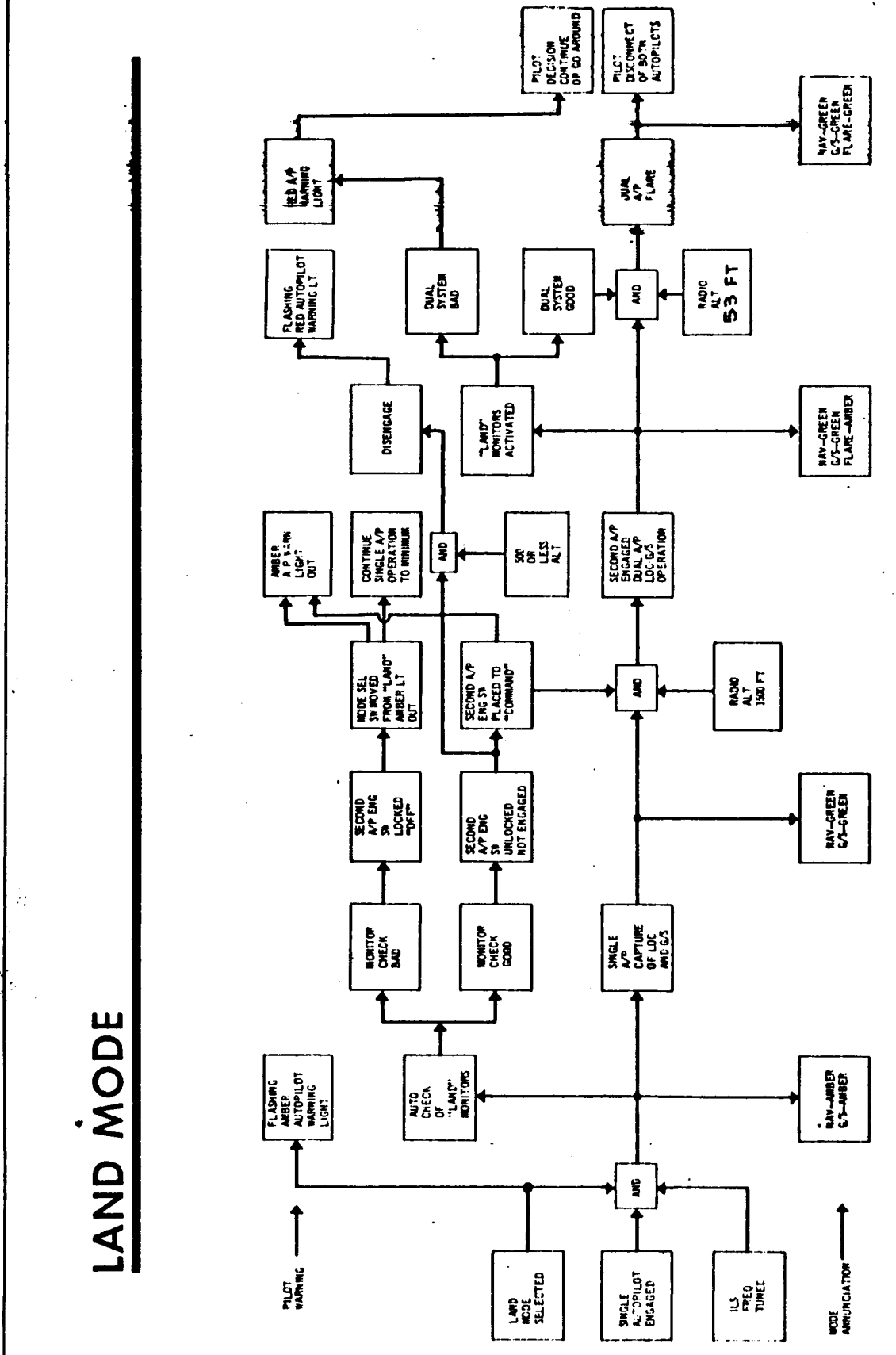

Fig. 21 Land Mode Interlocks

AD 1546 D

camout exists (Page 61) in either channel for two seconds. Interlocks for the LAND mode are shown in flow diagram, Figure 21.

(2) Synchronization

When in LAND with both channel engage switches in COMMAND, but still flying single channel, the second channel actuator is in the caged position and its servo amplifier output is being nulled by the path integrator by means of the synchronization loop. At A/P FLARE ARM, the hydraulic pressure builds up first in the force detent mechanism moving the autopilot actuator to a position matching that of the elevator. The LVDT signal generated when the autopilot actuator is moved into position is fed back to the servo amplifier, and is nulled out by the synchronization loop. The actuator is then pressurized and the synchronization loop is opened. Since the servo amp was held to zero, the actuator does not move until it is commanded from the autopilot.

(3) Glide Slope

The glide slope control law for each channel is the same as that of ILS. Figure 19 shows all switches in position for glide slope control.

During dual-channel operation, equalization is in effect, without signal intertie between channels. An equalization command proportional to the difference, if any, between the autopilot actuator and the elevator is fed back to the path integrator. The equalizer signal to the path integrator is limited. The equalization gain is programmed down as a function of altitude since the requirement for equalization to reduce null offsets is likewise reduced.

(4) Flare

At the flare point, the FLARE light on the mode annunciator changes from amber to green. The camout monitor remains active.

Since the gain programmer is zero, beam error and the gain programmed portion of equalization are not applied during flare. However, a small fixed gain equalization signal remains on throughout flare.

The flare law:

$$\dot{h}_e = \dot{h}_{DER} + \frac{h}{6} + 2; \quad \dot{h}_{DER} = h \frac{S}{S+1} + a \frac{1}{S+1}$$

commands an airplane descent rate, linearly decreasing with altitude, from the descent rate at flare to 2 feet/second.

AD 1546 D

The descent rate is derived from the radio altitude and vertical accelerometer signals. The descent rate error is summed with filtered acceleration for damping and then passed through direct and integral paths to produce an attitude command. A synchronizer loop maintains the command to zero until flare.

$$\theta_{CF} = K_D h_e + K_{DA} a_Z + \frac{1}{S}(K_I h_e + K_{I_A} a_z + BIAS)$$

The flare command is limited to 7.5° nose up and .75° nose down pitch attitude.

(5) Fail-Passive Actuators

The autopilot actuators are located on the two inboard elevator control packages. Figures 22 and 23 show the autopilot elevator control configuration.

The feel computer provides a centering force for all autopilot and manual control commands. Feel force is programmed as a function of dynamic pressure and stabilizer position and provides authority limitation to the autopilot. The autopilot actuators are tied to the main valve inputs through force limited detents. In single-channel operation, only one detent is engaged and both main valves follow the engaged autopilot actuator.

Figure 5 shows a schematic of the detents and servo system mechanization for the roll axis. Pitch mechanization is similar. In dual-channel operation, both autopilot actuatios are powered and the detents are engaged. If the autopilot actuator positions disagree, the elevators will follow the command nearer zero. The detent monitors associated with each autopilot channel measure the disagreement of the autopilot actuators with the output. A disagreement of 6.0° elevator will give a camout and a consequent pilot warning light after a one-second delay. Dual-channel elevator authority is double the single-channel authority or approximately +10, -30 degrees at final approach speed. The detent authority remains constant at 27 pounds stick force, maximum. At maximum q conditions, elevator single-channel authority diminishes to ± 1.5 degrees elevator.

C
d

ELEVATOR CONTROL SYSTEM

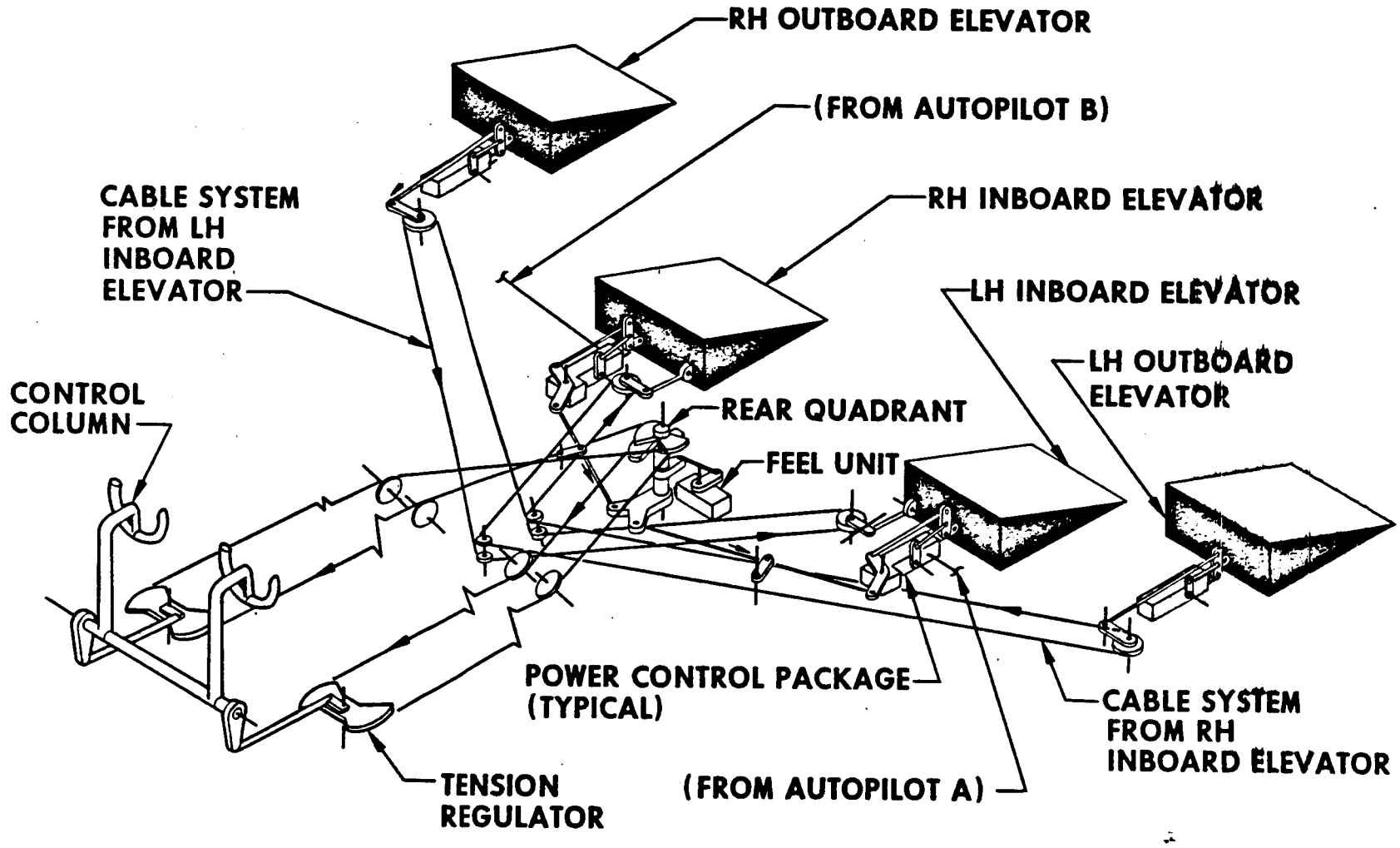

Fig. 22 Elevator Control System

AUTOPILOT ELEVATOR SCHEMATIC

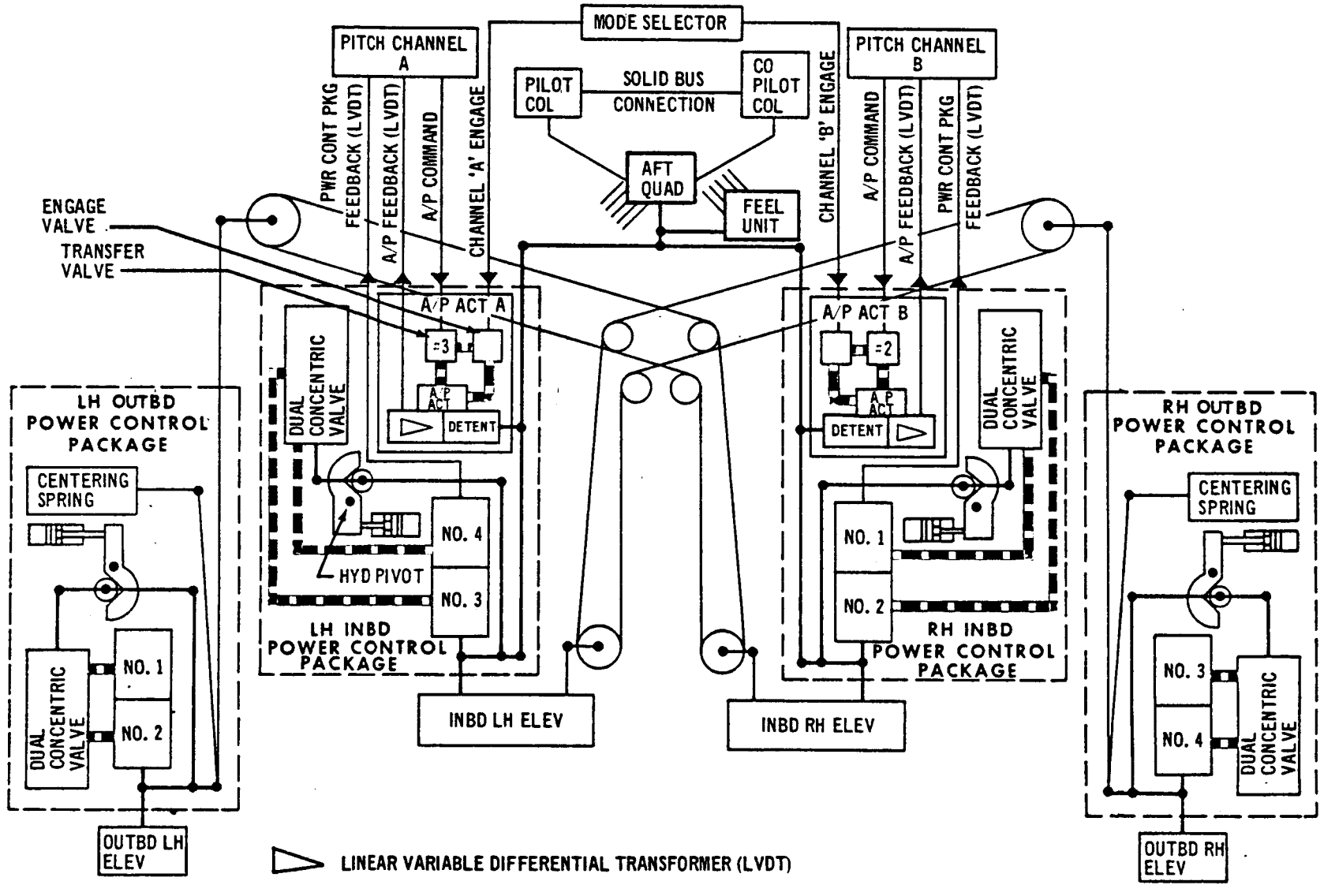

Fig. 23 Autopilot Elevator Schematic

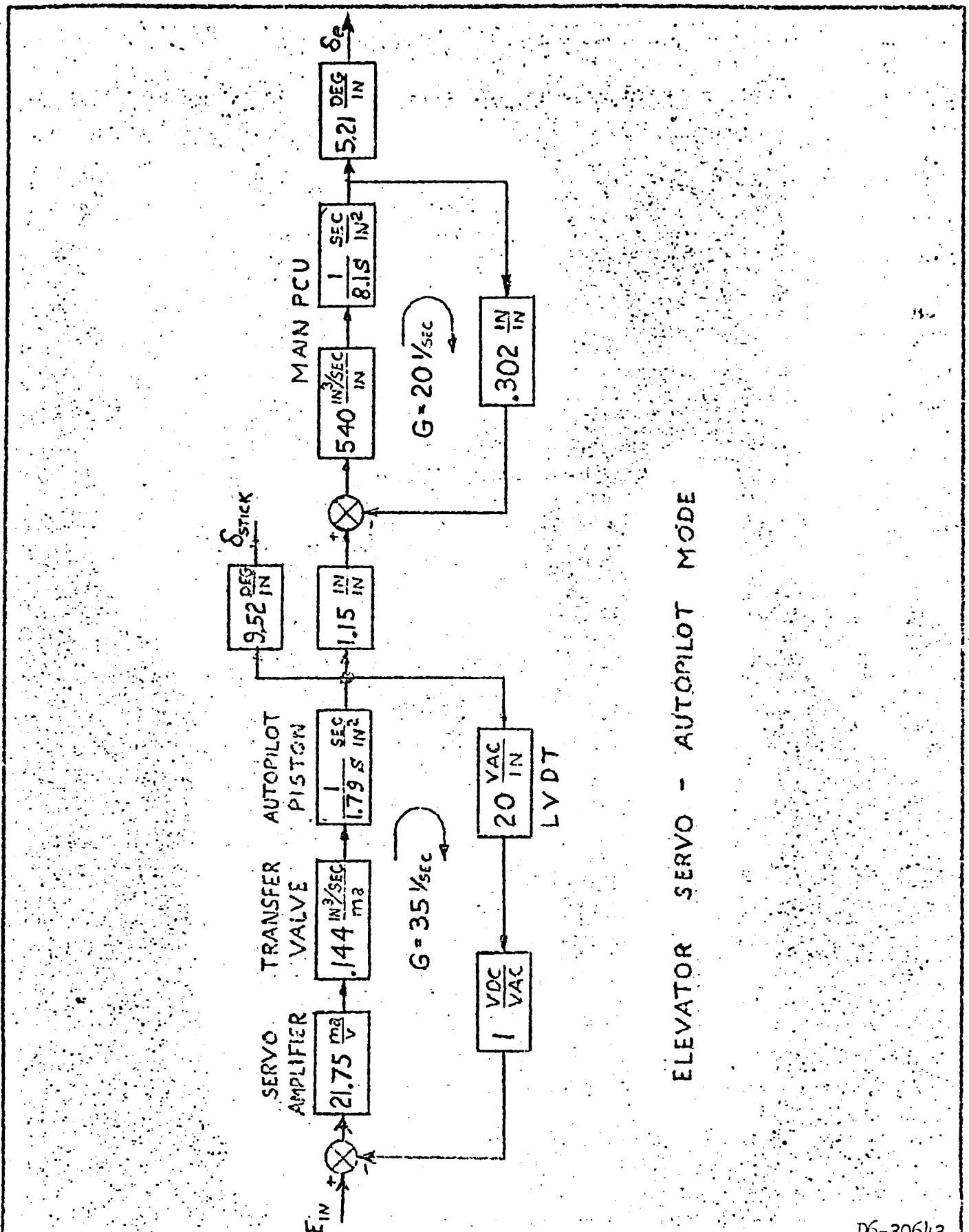

CALC	O. J.	5-28-9	REVISED	DATE	BLOCK DIAGRAM ELEVATOR - AUTOPILOT MODE	747
CHECK						FIG. 23a
APPD					THE BOEING COMPANY SEATTLE, WASHINGTON	PAGE 18-60a
APPD						

AD 973 D-R3

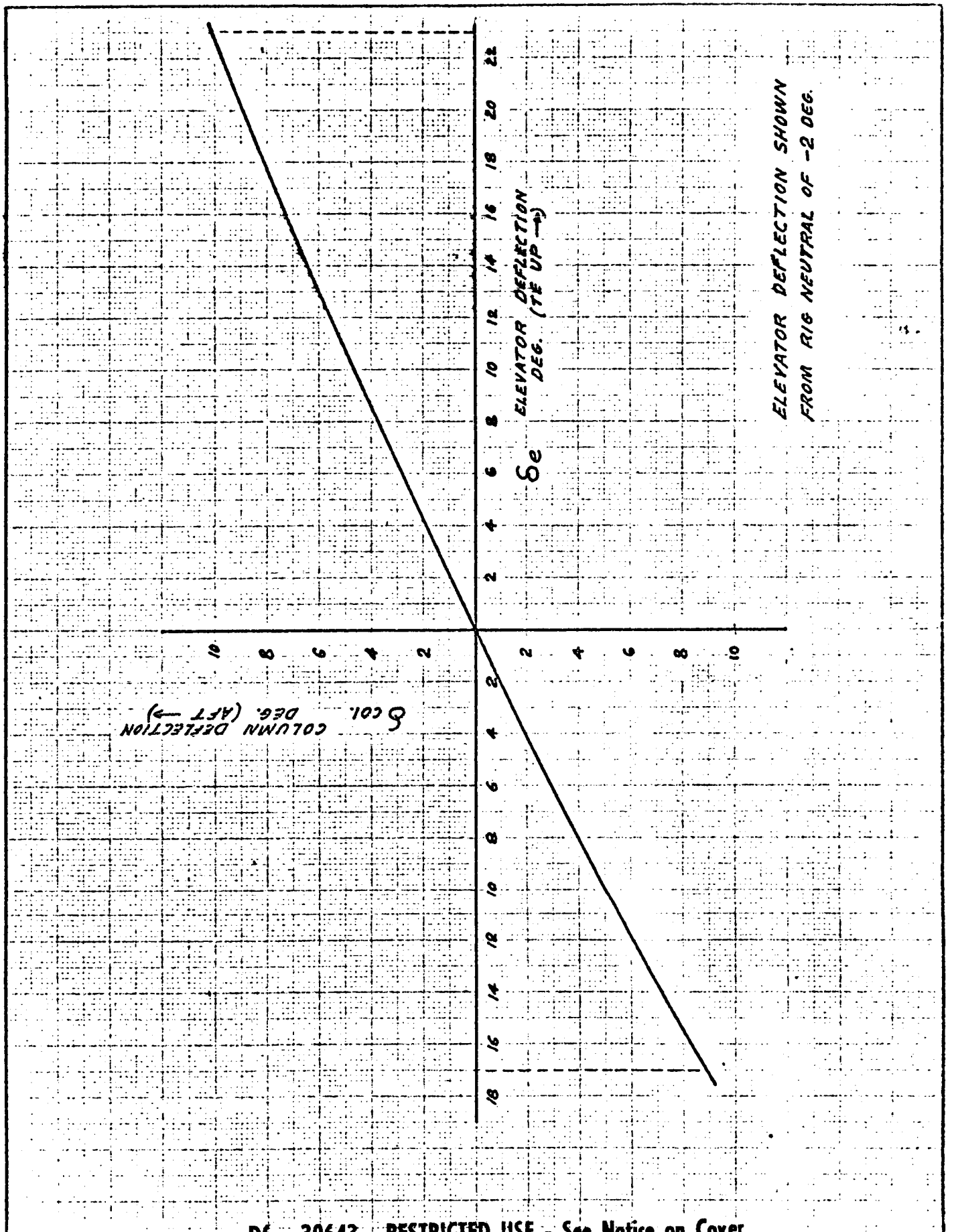

CALC	DFJ	5/27/70	REVISED	DATE
CHECK				
APR				
APR				

ELEVATOR TO COLUMN GEARING

THE BOEING COMPANY

D6-30643 Vol. II

FIG. 23b

PAGE 18-60b

G. AUTOPILOT AUTOMATIC STABILIZER TRIM

The autopilot is provided with two separate stabilizer trim systems. During single-channel cruise operation of the autopilot, the A trim system is utilized with the "A autopilot" and the B trim system is utilized with the "B autopilot". During dual-channel operation of the autopilot, both trim systems are capable of operation. One of the two is utilized and the other is armed and in a standby state. Suitable monitoring and logic is included to effect an automatic transfer to the standby trim, should a malfunction occur in the active channel of trim.

The auto-trim unit drives the stabilizer to reduce steady state elevator displacement from neutral when the autopilot is engaged. This reduces to a low level the transient which occurs when autopilot is disengaged. Auto-trim is obtained during all autopilot modes except Turbulence.

The stabilizer has no direct connection with the primary control system. Thus, motions of the stabilizer show up on the column only as the amount of elevator surface which must be held on the column to maintain airplane trim. When the autopilot is engaged the autopilot commands the amount of elevator needed to maintain the desired flight path and airplane trim. When the autopilot is commanding an elevator position greater than the trim threshold (Figure 24) the trim system will drive the stabilizer until the elevator required to maintain the desired flight path is reduced below .185 degrees of elevator. The effect of automatic trim as seen on the column is a smooth return of the column to near neutral as the trim system operates. The rate of stabilizer trim is inversely proportional to the impact pressure ($\bar{q}$). Thus, the column rate of return is similarly reduced.

Autopilot Stabilizer Trim Unit (ASTU) channel is shown in Figure 24. The arm and control circuits are identical. Trim is effected by the presence of discretes from both arm and control when there is hydraulic pressure to operate the brake pressure switch. When the elevator exceeds the trim threshold for five seconds, the stabilizer is driven until the elevator decreases to 0.185 degrees. The trim rate and thresholds are variable with feel pressure as indicated in Figures 24b and 24c.

The trim warning monitor is activated 8.5 seconds after an active or passive failure of the arm or control circuits or brake pressure switch. A warning is also obtained for an out-of-trim condition sustained for 12 seconds.

Dual-Channel Autopilot Mode (Autoland)

One auto-trim channel is engaged in this condition; and in the event of failure, this channel is automatically disengaged and the other standby channel is engaged by the changeover switches in the Boeing accessory box. Thus, "fail operational" trim is provided during automatic landing. Should a camout occur, the ASTU is inhibited from moving the stabilizer.

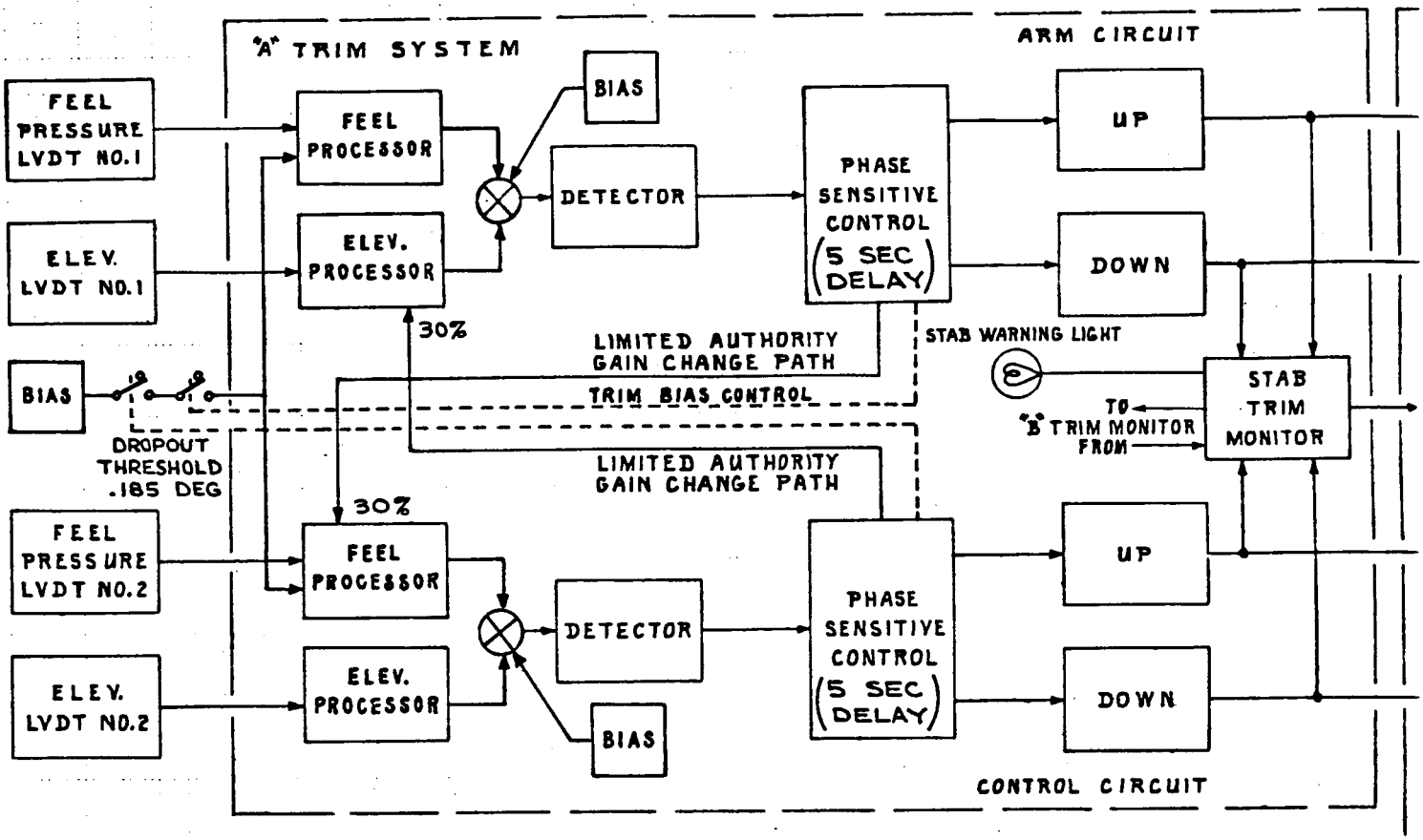

"B" TRIM SYSTEM
IDENTICAL TO
"A" TRIM SYSTEM

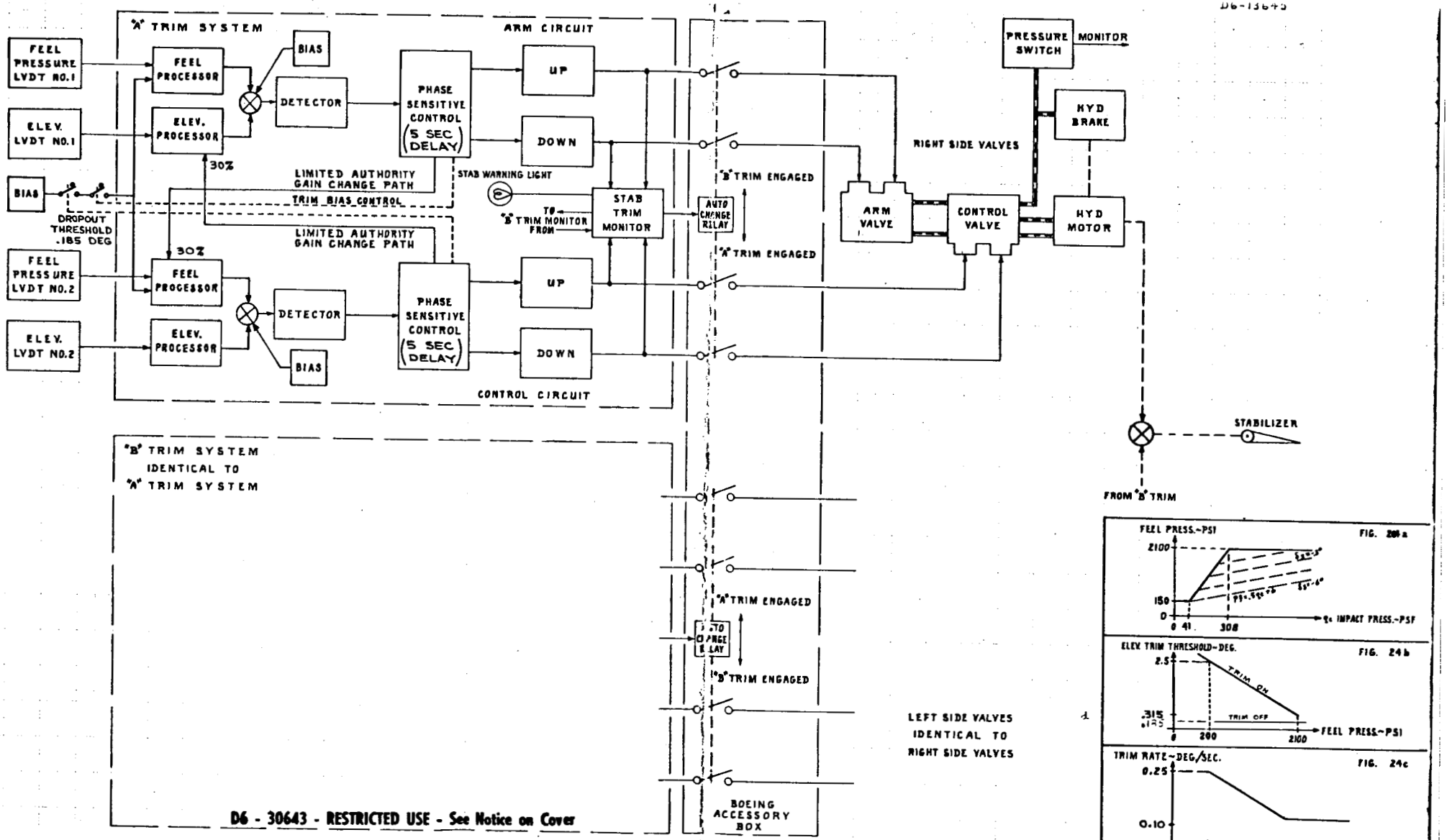

D6 - 30643 - RESTRICTED USE - See Notice on Cover

			REVISED	DATE
CALC			REV B	6/15/62
CHECK			REV C	2/23/71
APR				
APR				

AUTOMATIC STABILIZER TRIM

THE BOEING COMPANY

D6-30643 Vol. II

FIG. 24

PAGE 18-62

Rev. d

II. MACH TRIM SYSTEM

(SYSTEM NOT INSTALLED ON 747 AIRPLANE)

Pages 63 - 68 deleted.

AD 1346 D

III. YAW DAMPER SYSTEM

A. GENERAL

The 747 directional control system comprises dual rudders, each independently powered by a dual tandem hydraulic actuator. Dual redundant yaw damping is provided on the 747 by incorporating an independent electro-hydraulic augmentation system with each rudder segment.

Yaw damping signals are connected to the rudder actuators in a series fashion such that the pilot's rudder pedals are not displaced by yaw damper commands. This feature permits the yaw dampers to be operative at all times through take-off, cruise, and landing without interferring with normal pilot rudder control.

A preflight cockpit operated confidence test is provided to check each yaw damper system prior to departure from the ramp area. Disengage switches mounted on the pilot's overhead panel are provided to enable the flight crew to shut off either yaw damper system should a malfunction occur. Figure 27 is a pictorial diagram of the lower rudder yaw damper system.

In addition to providing additional damping of basic airframe lateral directional oscillations (dutch roll), the 747 yaw damper system has an added feature designed to improve airplane response to turning maneuvers in flap down flight conditions. This system is called the "turn coordinator" and deflects rudders proportional to roll rate in a "turn coordinating" sense, thereby improving roll control response.

Due to a favorable phase relationship, the turn coordinator feature has the added benefit of further improving basic dutch roll damping beyond that available from the yaw damping mode alone.

The "turn coordinator" system is used at flaps down condition only. An "easy on/off" circuit is implemented in the "turn coordinator" command path to eliminate transient rudder kicks resulting from the flap switching should the aircraft not be at zero roll attitude.

The design objective is to provide additional dutch roll damping and turn coordination with a system which provides no potentially hazardous failure conditions. (See document D6-13647, IEFCS Failure Analysis).

B. SYSTEM DESCRIPTION

Figure 28 is the block diagram of the 747 dutch roll damper and turn coordination system. Its mathematical model is shown in Figure 29.

1. Dutch Roll Damping Signals

Dutch roll damping is provided by a yaw rate ($\dot{\Psi}$) signal. At flaps down condition, additional bank angle signal is provided to increase system damping. Yaw rate is sensed by a rate gyro, mounted in the yaw damper chassis. Bank angle is obtained from the Inertial Navigation System (INS). These signals are independently demodulated.

2. Band Pass Filter

At flaps up condition, the yaw rate signal passes through a band pass filter into the servo amplifier. The band pass filter is composed of R-C components and operational amplifiers. The transfer function of the filter can be expressed in Laplace form as the following:

$$\frac{2.72S}{(2.72S+1)\ (.272S+1)}$$

At flaps down condition, roll attitude signal passes through a similar band pass filter and is summed with the filtered yaw rate signal into the servo amplifier. This additional filtered roll attitude signal provides additional dutch roll damping.

The functions of the band pass filter are:

(1) To washout the steady yaw rate and roll attitude signals and to eliminate null offset of sensors.

(2) To provide dutch roll damping signals with minimum phase shift at dutch roll frequencies, in order to achieve optimum damping.

(3) To reduce high frequency signal amplitudes so as to minimize possible coupling with structural modes.

The Bode and phase angle plots of the band pass filter are shown in Figures 31 and 32.

3. Dutch Roll Damper Gain

At flaps down condition, the yaw rate and the roll attitude gains are $2.5\ \frac{\delta_R\ (\text{degree})}{\dot{\Psi}\ (\text{degrees/sec})}$ and $.076\ \frac{\delta R\ (\text{degree})}{\emptyset\ (\text{degree})}$ respectively.

At flaps up condition, the yaw rate gain is 1.25 $\frac{\delta R \text{ (degree)}}{\dot{\psi} \text{ (degree/sec)}}$. For detail information, refer to Figure 33 root loci plot.

4. Turn Coordination

A shaping circuit is used to derive a roll rate signal from the roll angle input. The rate circuit used has a transfer function of $\frac{.1s}{(.1s+1)^2}$ which yields a derived roll rate signal from roll angle at turn entry frequencies, but cuts off at frequencies above 1.4 cps in order to minimize the effects of system noise.

The turn coordinator system operates at flaps down flight conditions only. Switching is accomplished by a flaps switch.

The system gain is 0.693 $\frac{\delta R \text{ (degree)}}{\phi \text{ (degree/sec)}}$.

5. Easy On-Off Circuit

An easy on-off circuit is implemented in the filtered roll attitude signals path to eliminate transient rudder kicks when the roll attitude signal is turned off or on by the flap actuated switches.

6. Yaw Damper Electro-Hydraulic Servo

The servo valve amplifier accepts dutch roll damper, turn coordinator, and servo feedback inputs and provides an output to the electro-hydraulic transfer valve. The transfer valve controls motion of the yaw damper actuator which is linked to the main power control unit valve via a summing link. The electro-hydraulic transfer valve is supplied system pressure via a solenoid operated shut-off valve when the yaw damper is engaged. The yaw damper servo actuator is self-centered by caging springs when the system is de-energized. This preserves the integrity of manual commands when the yaw damper is not energized.

The maximum rudder rate which the yaw damper can command is controlled by the area of the servo actuator orifice and by the area of the piston and is $\pm$ 15 deg/sec at no load. The maximum rudder displacement is controlled by the summing lever stops and is $\pm$ 3.6 degrees.

AD 1546 D

There are two feedback paths in the yaw damper. The first path directly feeds back yaw damper actuator position. This feedback is required so that yaw damper servo output will follow command inputs. The second path feeds back yaw damper actuator position via a $\frac{8}{85S + 1}$ in parallel with the normal position feedback. When the yaw damper system is disengaged, the servo amplifier output is fed back through this lag to provide synchronization.

7. Self-Test and Confidence Test

The yaw damper computer provides self-test circuitry for the two categories of fault isolation testing: Line Replaceable Unit test (electronic components) and system test (electronic components plus the actuator loop). The self-tests are performed by positioning the test switch and momentarily depressing the press-to-test switch on the yaw damper front panel. The monitor light on the front panel will indicate the test results (go or no go).

Confidence Test is a pilot actuated and monitored system test. Channel confidence tests can be initiated singularly or simultaneously by use of the cockpit mounted test switches. By observing the upper and lower rudder surfaces position indicator located on the pilot's instrument panel, the operating status of the systems can be assessed.

The confidence test and self-test are interlocked to prevent test initiation in flight.

Separate confidence tests are provided for the dutch roll damping and the turn coordinator functions.

8. Performance

Analog computer simulation and digital computer root locus analysis were conducted to investigate yaw damper system performance. Results indicate that the system performs well at all flight conditions. The lowest augmented airplane dutch roll damping ratio is 0.30 at the landing approach 33 degrees flaps down condition. System performance for various flight conditions are summarized in root loci plots in Figure 33.

9. Tolerance

Phase shifts and gain variations affect system performance. Root locus analysis were conducted to investigate the effect of tolerances on performance. The Bode plot and phase angle plot for the nominal and the maximum time constants of the rudder to sensors input transfer function are shown in Figures 31 and 32 respectively. The two flight conditions, which describe the lower and upper bound of the unaugmented dutch roll frequency

were investigated.. They are the landing approach 33 degrees flaps down and maximum dynamic pressure conditions where the dutch roll frequencies are 0.12 cps and 0.20 cps respectively.

The yaw damper system performance for the above two conditions is summarized in Figures 34 and 35. If the system components are within the design tolerances, the system performances as described by the envelope in the figures is satisfactory. The upper and lower bounds of the envelope are the gain tolerance limits while the left and right bounds are the phase angle tolerance limits.

10. Failure Mode Design Features

At flaps down condition, three sensed signals are used in the yaw damper. The yaw rate, roll angles, and derived roll rate signals each provide an increment of dutch roll damping. If failures occur in any of these signal chains such that one or more of the signals is not driving the rudder, the remaining signals will continue to provide some dutch roll damping. All three of these signals are washed out and thus cannot command a continuous steady-state rudder position.

At flaps up condition, roll angle and derived roll rate signals are removed by the easy on-off circuit and the delayed flaps energized switch. Monitoring circuitry is implemented to detect failure of this flap actuated switching. A red light is illuminated on the yaw damper control panel if flap switching failure occurs.

Any type of malfunction causing a no-signal condition or a sustained large signal will not cause more than a modest transient airplane response. Control excursions are positively limited by hydraulic system velocity and force limits, plus displacement stops effective at all speeds.

YAW DAMPER DIAGRAM
SHOWN FOR LOWER RUDDER (CHANNEL NO. 2)

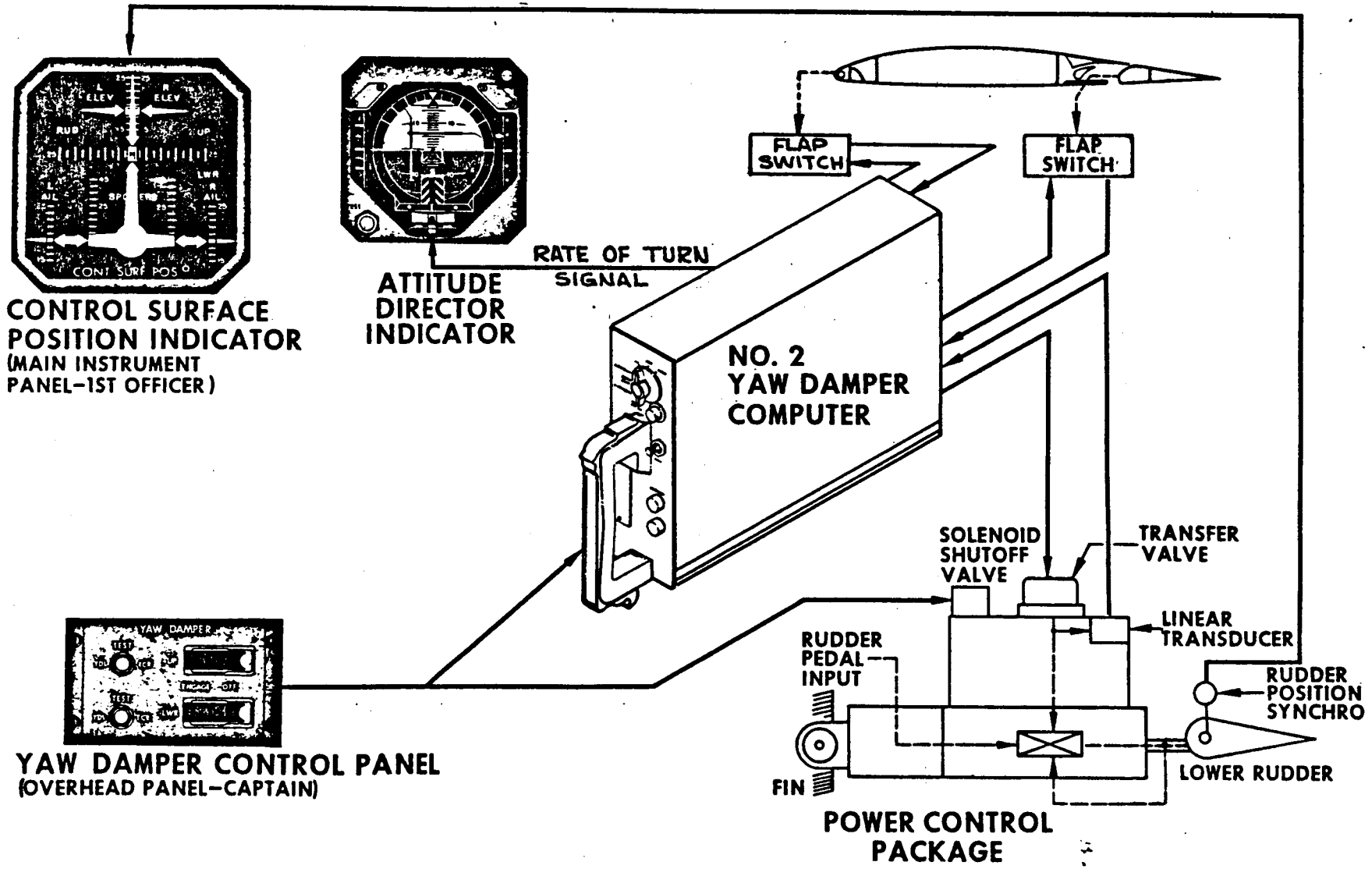

Fig. 27 Yaw Damper Pictorial Diagram

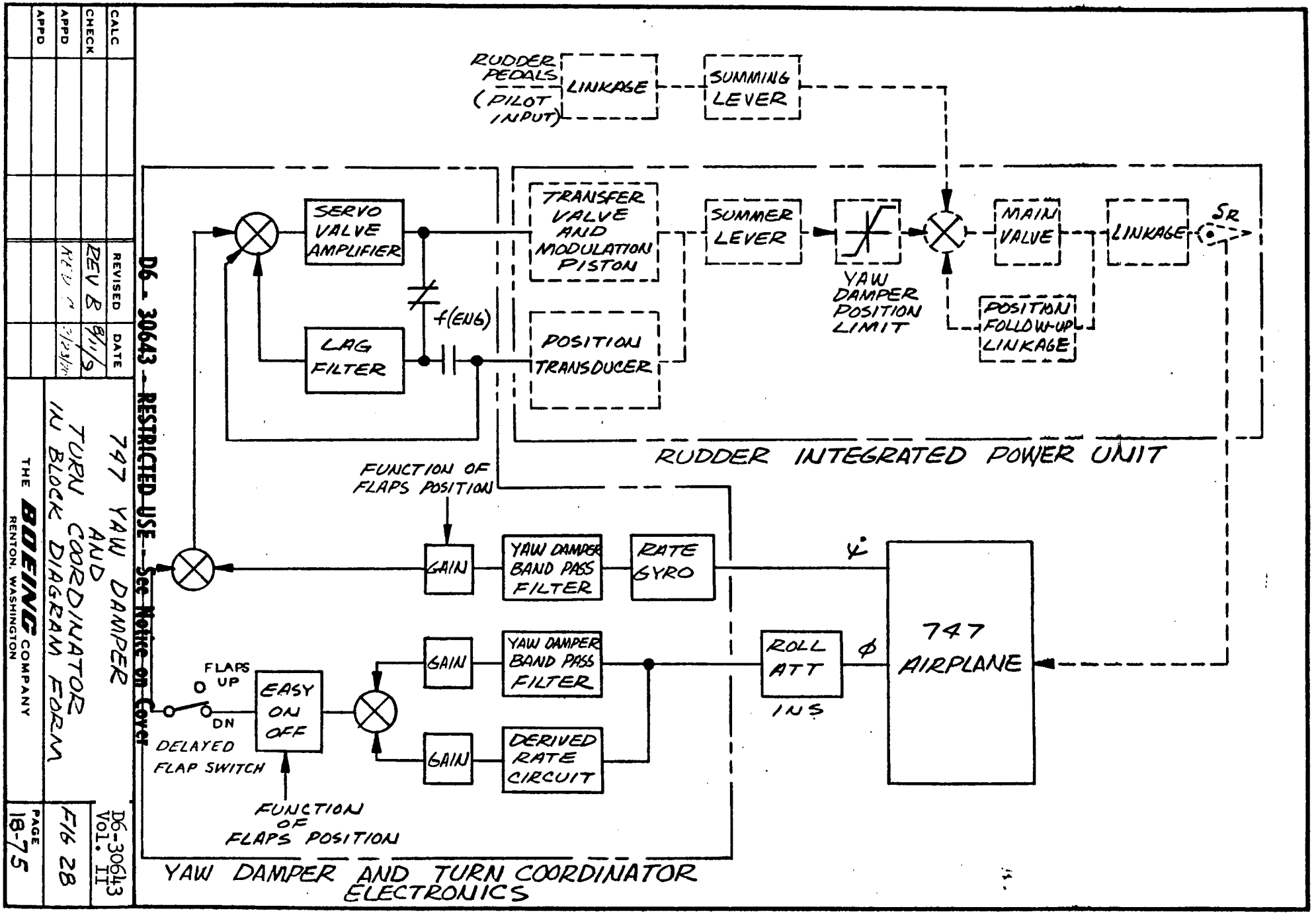

D6 - 30643 - RESTRICTED USE - See Notice on Cover

	CALC	CHECK	APPD	APPD
REVISED		REV B	REV A	
DATE		8/1/9	2/23/9	

747 YAW DAMPER AND TURN COORDINATOR IN BLOCK DIAGRAM FORM

THE BOEING COMPANY RENTON, WASHINGTON

D6-30643 Vol. II

FIG 2B

PAGE 18-75

TD 873 D-R3

S-7000

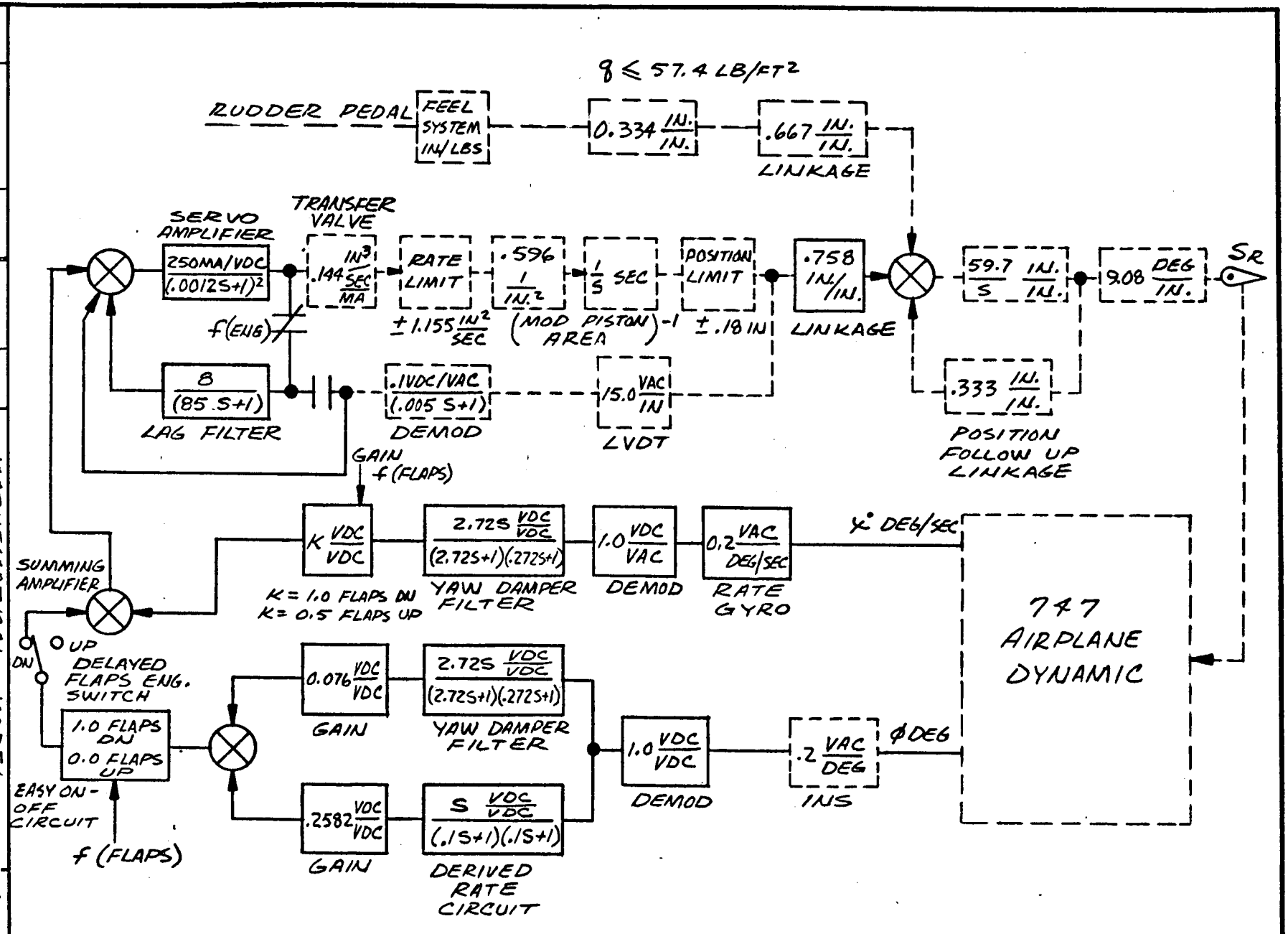

	CALC	CHECK	APPD	REVISED	DATE
				REV B	8/11/72

MATHEMATICAL MODEL OF THE 747 YAW DAMPER AND TURN COORDINATOR SYSTEMS

THE BOEING COMPANY RENTON, WASHINGTON

D6-30643 Vol. II

F/G 29

PAGE 18-76

TD 973 D-R3

D6 - 30643 - RESTRICTED USE - See Notice on Cover

8-7000

Page 77 Omitted

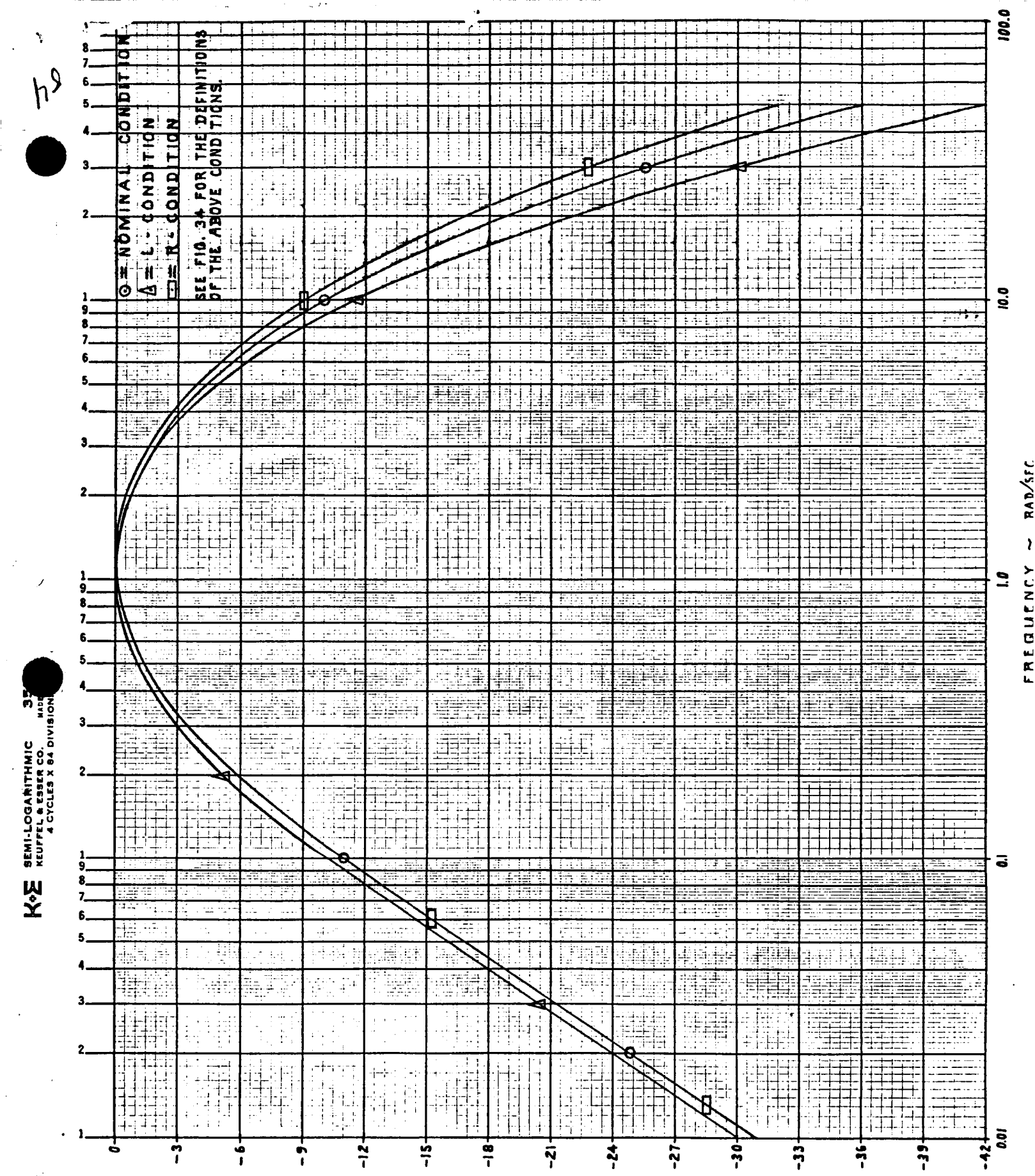

			REVISED	DATE
CALC				
CHECK				
APR				
APR				

FREQUENCY RESPONSE OF
YAW DAMPER
BANDPASS FILTER

THE BOEING COMPANY

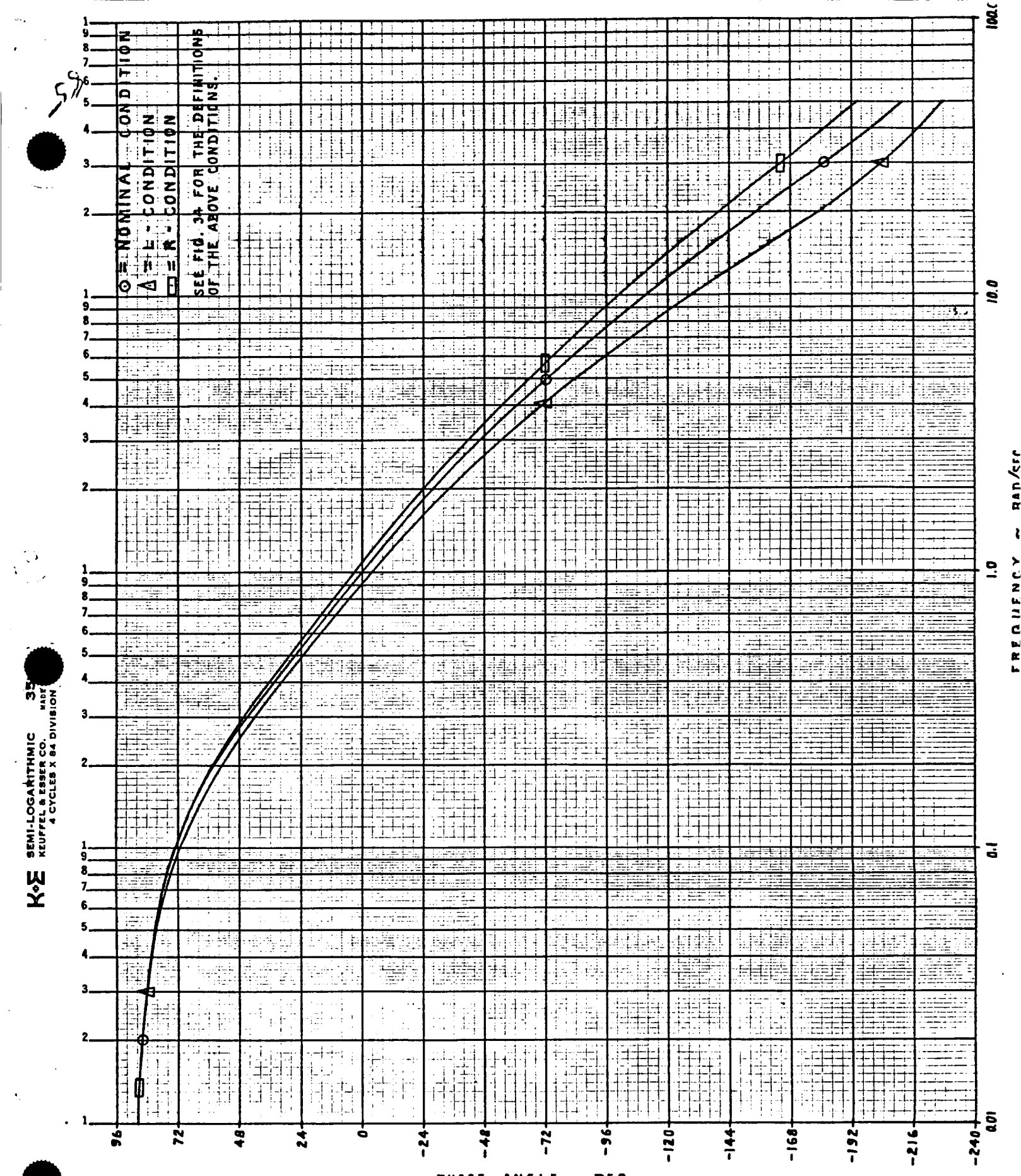

CALC			REVISED	DATE
CHECK				
APR				
APR				

PHASE ANGLE PLOT OF
YAW DAMPER
BANDPASS FILTER

THE BOEING COMPANY

D6-30643
Vol. II

FIG. 32

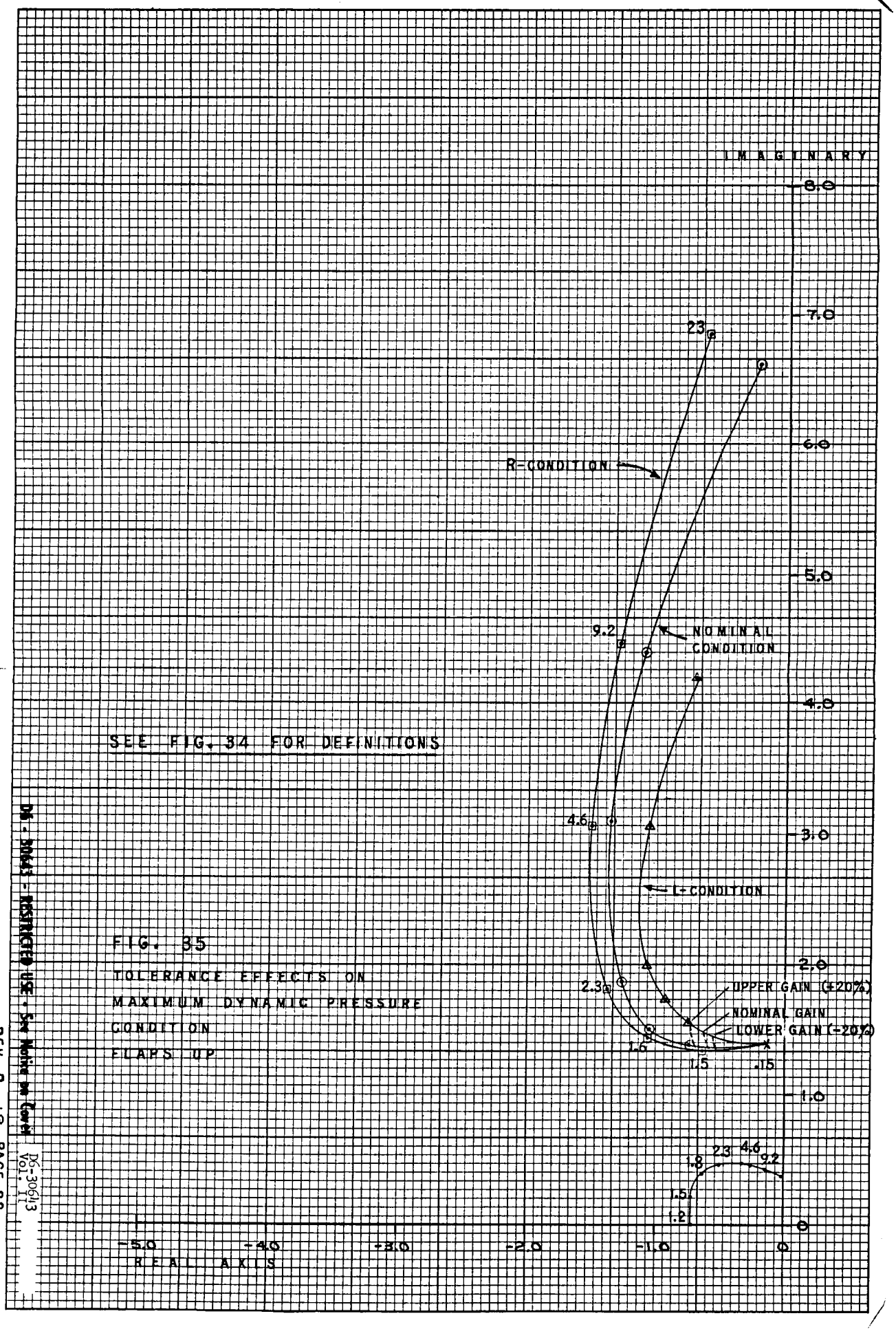

SEE FIG. 34 FOR DEFINITIONS

FIG. 35

TOLERANCE EFFECTS ON
MAXIMUM DYNAMIC PRESSURE
CONDITION
FLAPS UP

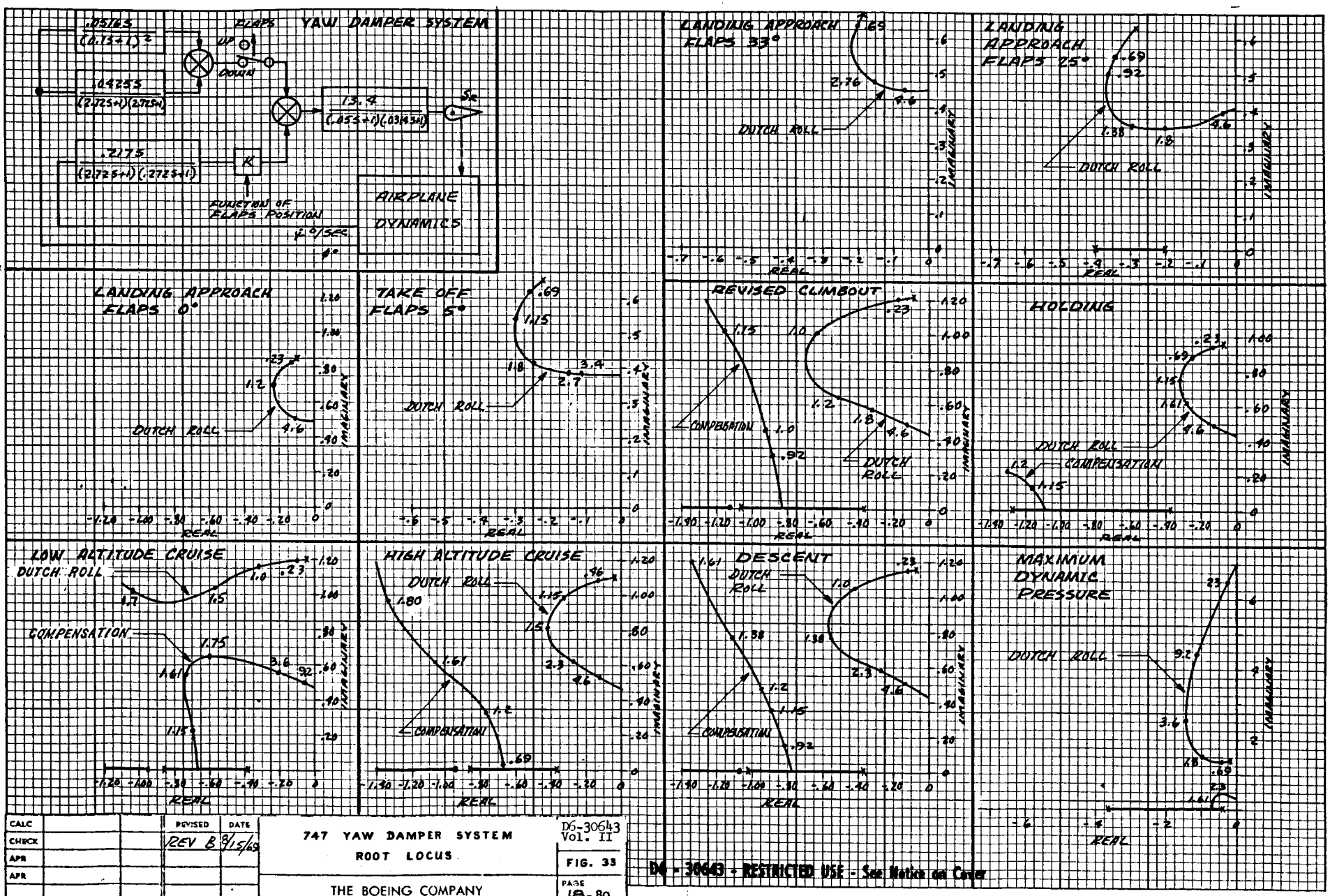

CALC			REVISED	DATE
CHECK			REV B	8/15/69
APR				
APR				

747 YAW DAMPER SYSTEM
ROOT LOCUS

D6-30643
Vol. II

FIG. 33

THE BOEING COMPANY

PAGE 18-80

FIG. 34

TOLERANCE EFFECTS ON
LANDING APPROACH CONDITION
FLAPS DOWN 33°

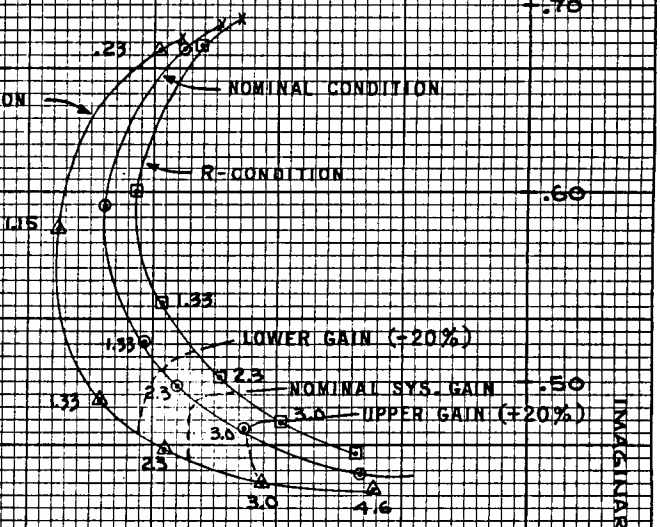

NOMINAL CONDITION

$$\frac{\delta_{R_C}^{\circ}}{\dot{\psi}\ ^{\circ}/SEC} = \frac{K(0.224)S}{(2.72S+1)(0.272S+1)} \qquad \frac{\delta_R^{\circ}}{\delta_{R_C}^{\circ}} = \frac{13.4}{(0.05S+1)(0.0314S+1)}$$

L-CONDITION

$$\frac{\delta_{R_C}^{\circ}}{\dot{\psi}\ ^{\circ}/SEC} = \frac{K(0.224)S}{(2.892S+1)(0.2892S+1)} \qquad \frac{\delta_R^{\circ}}{\delta_{R_C}^{\circ}} = \frac{14.2}{(0.062S+1)(0.054S+1)}$$

R-CONDITION

$$\frac{\delta_{R_C}}{\dot{\psi}\ ^{\circ}/SEC} = \frac{K(0.224)S}{(2.655S+1)(0.2655S+1)} \qquad \frac{\delta_R^{\circ}}{\delta_{R_C}^{\circ}} = \frac{12.9}{(0.0413S+1)(0.01967S+1)}$$

K ≙ YAW DAMPER SYSTEM GAIN

$$\frac{\delta_{R_C}}{\phi} = \left[\frac{0.0413S}{(2.72S+1)(0.272S+1)} + \frac{0.0516S}{(0.1S+1)^2}\right]$$

FOR ALL FLAPS DOWN CONDITIONS

$\frac{\delta_{R_C}}{\phi} = 0$ FOR FLAPS UP CONDITION

IV. AUTOTHROTTLE SYSTEM

A. GENERAL

The 747 is equipped with a single-channel autothrottle system. This system is designed to capture and hold a selected indicated airspeed during terminal area maneuvering, and approach and landing flight regimes by automatically positioning the throttles. It may be used for indicated airspeeds up to 400 kts. Figures 36 and 37 pictorially describe the system. Salient features of the autothrottle are:

1. Clutches in the mechanical drive to the throttles enable the pilot to override the action of the system at any time.

2. The system is operable during manual flight control or while the Autopilot is engaged.

3. The system limits the rate of change of commanded airspeed so that throttle motions occur smoothly.

4. Thrust changes following pitch maneuvering are minimized, and the magnitude of transient thrust changes arising from wind gusts are limited by a gust filter.

5. A throttle retard function, interlocked with the Autopilot Land Mode, is provided to automatically retard the throttles during an autopilot flare.

B. SYSTEM DESCRIPTION

A block diagram of the autothrottle system is shown in Figure 38. A more detailed description is provided below.

1. Command and Airspeed Error Signals

The system engage switch and the speed control knob are situated on the AFCS Mode Select Panel.

The Autothrottle computer receives an airspeed error control signal from the Captain's airspeed indicator. Whenever a difference exists between the pilot-selected airspeed command, indicated in digital form on the AFCS Mode Select Panel, and the actual captain's airspeed, throttle action to reduce the error is commanded. The servo-motor is geared to the throttle levers via clutches which allow the pilot to easily override the system.

AUTOTHROTTLE SPEED CONTROL SEQUENCE

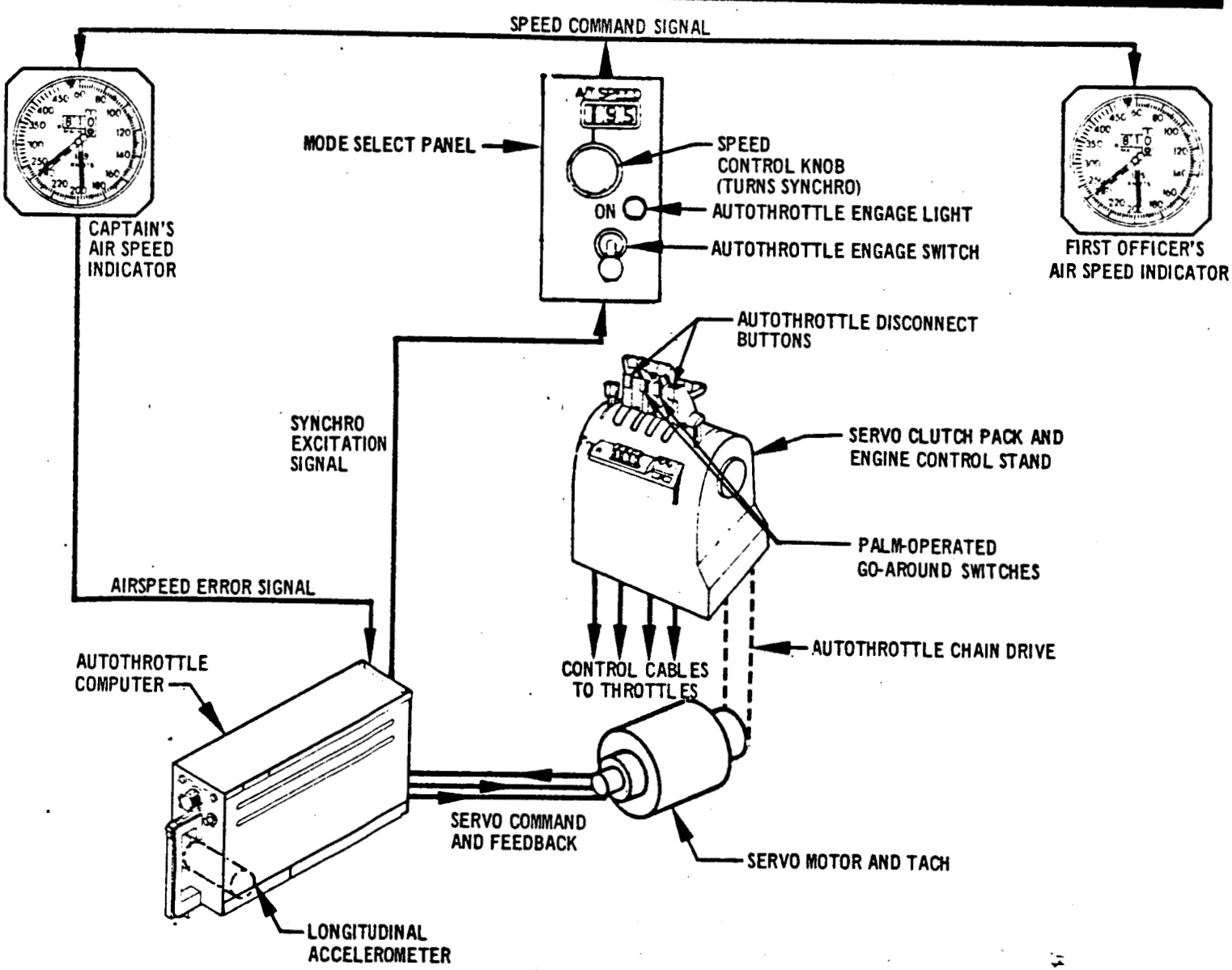

Fig. 36 Autothrottle Speed Control System

AUTOTHROTTLE CONTROLS AND MONITORS
(MAIN INSTRUMENT PANEL)

FLIGHT MODE ANNUNCIATOR LIGHT SET (CAPTAIN)

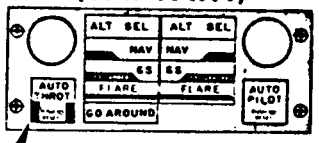

AUTOTHROTTLE WARNING LIGHT

LIGHT GOES RED FOR FAILURE WARNING AND AMBER FOR EXCESSIVE AIRSPEED ERROR. THE RED LIGHT HAS PRIORITY OVER THE AMBER.

MODE SELECT PANEL

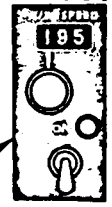

AUTOTHROTTLE ENGAGE AND SPEED SELECTION

FLIGHT MODE ANNUNCIATOR LIGHT SET (FIRST OFFICER)

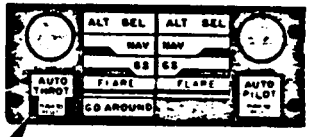

AUTOTHROTTLE WARNING LIGHT

LIGHT GOES RED FOR FAILURE WARNING AND AMBER FOR EXCESSIVE AIRSPEED ERROR. THE RED LIGHT HAS PRIORITY OVER THE AMBER.

FAST-SLOW INDICATION

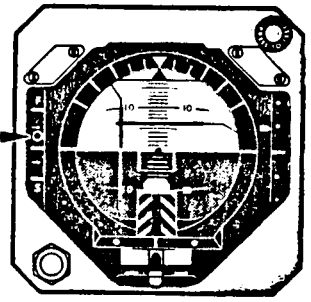

ATTITUDE DIRECTOR INDICATOR (CAPTAIN)

FAST-SLOW INDICATION

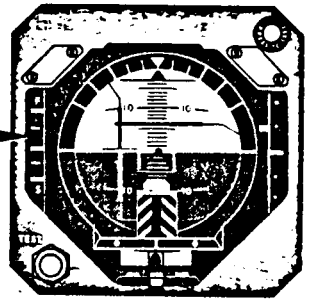

ATTITUDE DIRECTOR INDICATOR (FIRST OFFICER)

Fig. 37 Autothrottle Controls and Monitors

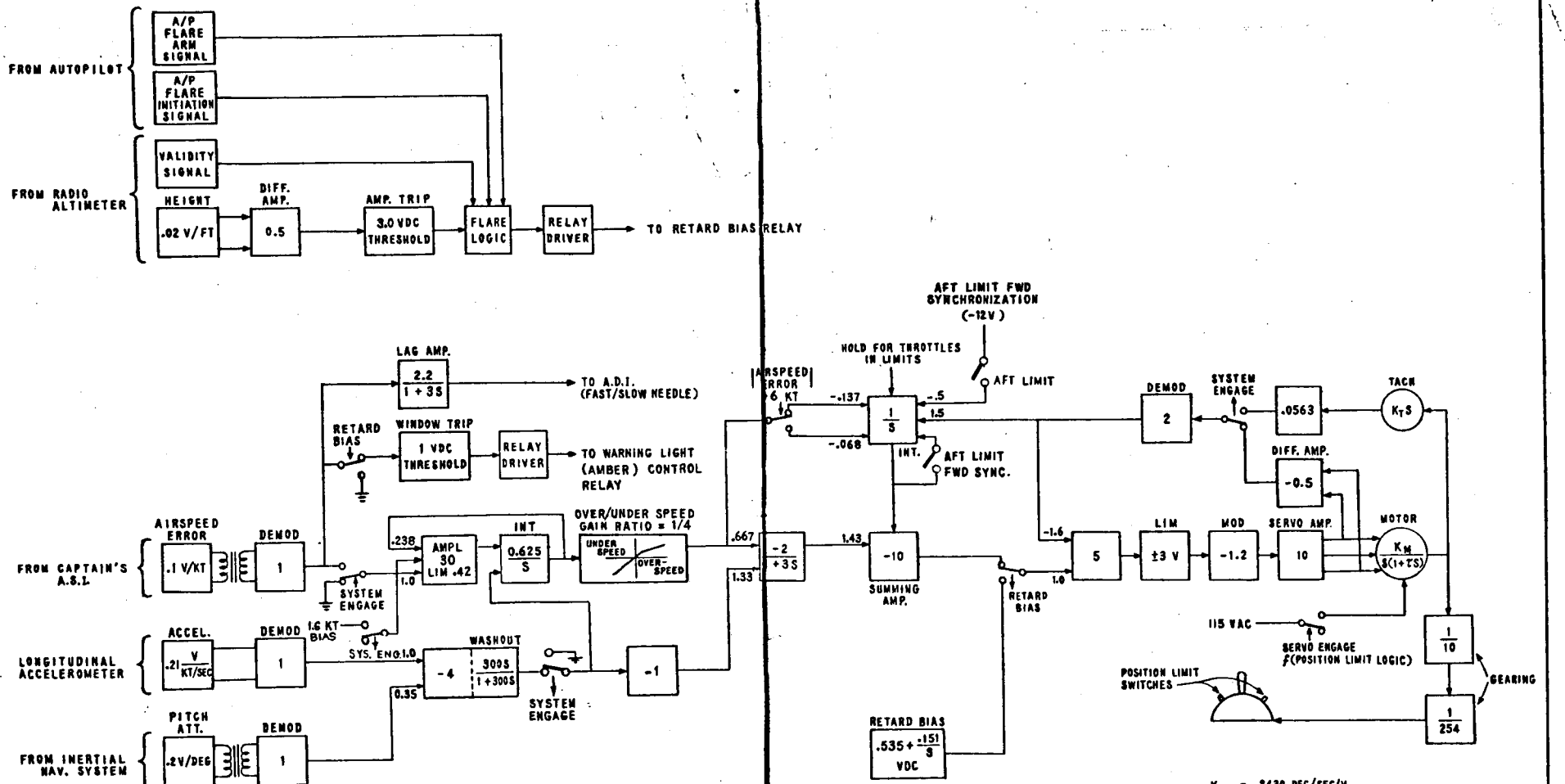

FIG. 38 — AUTOTHROTTLE SYSTEM BLOCK DIAGRAM

2. Accelerometer, Attitude, and Elevator Signals

The longitudinal accelerometer, which is an integral part of the computer, provides rate of change of speed information.

The pitch attitude input, obtained from the Inertial Navigation System, cancels the attitude component of the accelerometer output.

3. Computation

The computer utilizes transformer coupling for the A.C. input signals. A differential amplifier is used for the D.C. radio altimeter signal to provide isolation and noise rejection.

All A.C. signals are demodulated prior to shaping, filtering, and error level detection. The processed D.C. signals are summed and modulated for use in the A.C. power amplifier which drives the servo-motor. Prior to engagement, the system is synchronized for inputs other than airspeed error. See block diagram Figure 38.

The basic airspeed error input signal is processed through an acceleration limiting circuit. This circuit assymmetrically limits the airspeed command rate. The rate limited command signal is passed through an asymmetric gain program which reduces the gain for overspeed errors larger than 2 kt to .25 of its value. This gain reduction for large overspeed errors compensates for the fast deceleration of the engine and the higher authority of the throttle in the aft direction. The IAE signal is summed with the compensated longitudinal accelerometer signal and passed through the gust filter to suppress the effects of air turbulence on system activity.

4. Throttle Control and Limits

Control of the throttle levers is accomplished by a proportional plus integral servo configuration. The servo proportional response is obtained by integrating the tachometer output.

Switches are provided to limit forward and aft throttle motion. The forward limit position is set to avoid exceeding the maximum allowable engine pressure ratio or temperature; the aft position closely corresponds to the flight idle thrust value. Whenever

the throttles are driven to either limit position, the integrator is put into a "hold" condition to prevent it from computing an erroneous throttle position. The system remains engaged and will drive the throttles out of the limit position when the appropriate signal is developed.

5. ADI Signal

The demodulated output from the airspeed indicator, filtered by a 3-second lag, is supplied to fast-slow indicators on the two Attitude Director Indicators in the cockpit.

6. Airspeed Error Warning

When the Autothrottle is engaged, an airspeed error greater than ten knots causes the amber Flight Mode Annunicator light to illuminate.

7. Disengage

A pilot can disengage the system by means of any of the following:

(a) The engage switch on the AFCS mode selector panel.

(b) Disconnect switches on throttle levers 1 and 4.

(c) Go-around switches on throttle levers 2 and 3.

8. Flare

In conjunction with the Land Mode of the Autopilot, the system provides automatic throttle retard during the flare maneuver. The conditions necessary to activate this function are that the Autopilot must have been armed for flare, the Autopilot flare must have commenced, and the radio altimeter signal must be below the trigger altitude. The logic requirements prevent inadvertent operation of the retard function.

9. Test

Incorporated in the computer is an automatic test arrangement which can isolate a failure to the computer or servo-motor without requiring the use of supplementary ground-test equipment. This test is accomplished by means of a rotary switch and a push-button switch located on the front panel of the computer. The rotary switch is used to select the unit to be tested (i.e., the computer or the servo-motor) and the push-button initiates the test. The rotary switch will remain in the selected

position until it is manually returned to the "OFF" position. The Autothrottle system cannot be engaged, and a steady red warning light shows on the front panel (and in the cockpit) when the switch is not in the "OFF" position.

The test results are indicated by lights located on the computer's front panel. A "test-in-progress" light is illuminated on initiation of a test; and a "go" light is illuminated upon successful completion. A failure is indicated by the "test-in-progress" light being extinguished without a "go" indication.

The equipment functionally tests the entire Autothrottle system in approximately one minute. The testing is performed by injecting test signals into the various computer inputs while monitoring both the input and output of the feedback integrator in the servo loop. If each of these monitoring devices yields the proper indication, then the test step is completed and the next step is performed. If each test step is successful, the program will proceed to the last step and yield a "go" indication is withheld.

19.0 APPENDIX E - REVISED SIMULATION DATA

The data in this section contains revisions that Boeing recommends incorporating in the NASA simulation.

SUMMARY OF AREAS AND DIMENSIONS

ITEM	VALUE	DIMENSION
Wing Area (S)	5500	$Ft.^2$
Wing Mean Aerodynamic Chord (MAC)	27.31	Ft.
Wing Span (b)	195.68	Ft.
Wheel Base		
Wing Gear	78.96	Ft.
Body Gear	88.96	Ft.
Wheel Tread		
Wing Gear	36.16	Ft.
Body Gear	12.5	Ft.
Effective Engine Moment Arms		
Inboard		
Y_{E_I}	39.6	Ft.
Z_{E_I}	8.3 (air)	Ft.
	8.5 (ground)	Ft.
Outboard		
Y_{E_O}	69.4	Ft.
Z_{E_O}	3.1 (air)	Ft.
	4.8 (ground)	Ft.

Note The transition between the ground and air values for the effective engine pitching arms, Z_{E_I} and Z_{E_O}, is a function of the averaged main landing gear compression ratio, η.

For $0 \leq \eta \leq 1$. $Z_{E_O} = Z_{E_{O_{AIR}}} + \eta \cdot \Delta Z_{E_O}$

$Z_{E_I} = Z_{E_{I_{AIR}}} + \eta \cdot \Delta Z_{E_I}$

where $\Delta Z_{E_O} = Z_{E_{O_{GROUND}}} - Z_{E_{O_{AIR}}} = 1.7$ FT.

$\Delta Z_{E_I} = Z_{E_{I_{GROUND}}} - Z_{E_{I_{AIR}}} = 0.2$ FT.

and $\eta = \frac{1}{18n} \sum_{n=1}^{4}$ Main Landing Gear Oleo Compression (inches)

where n = number of main landing gears.

REF: P. 1.1-3

AD 1546 D

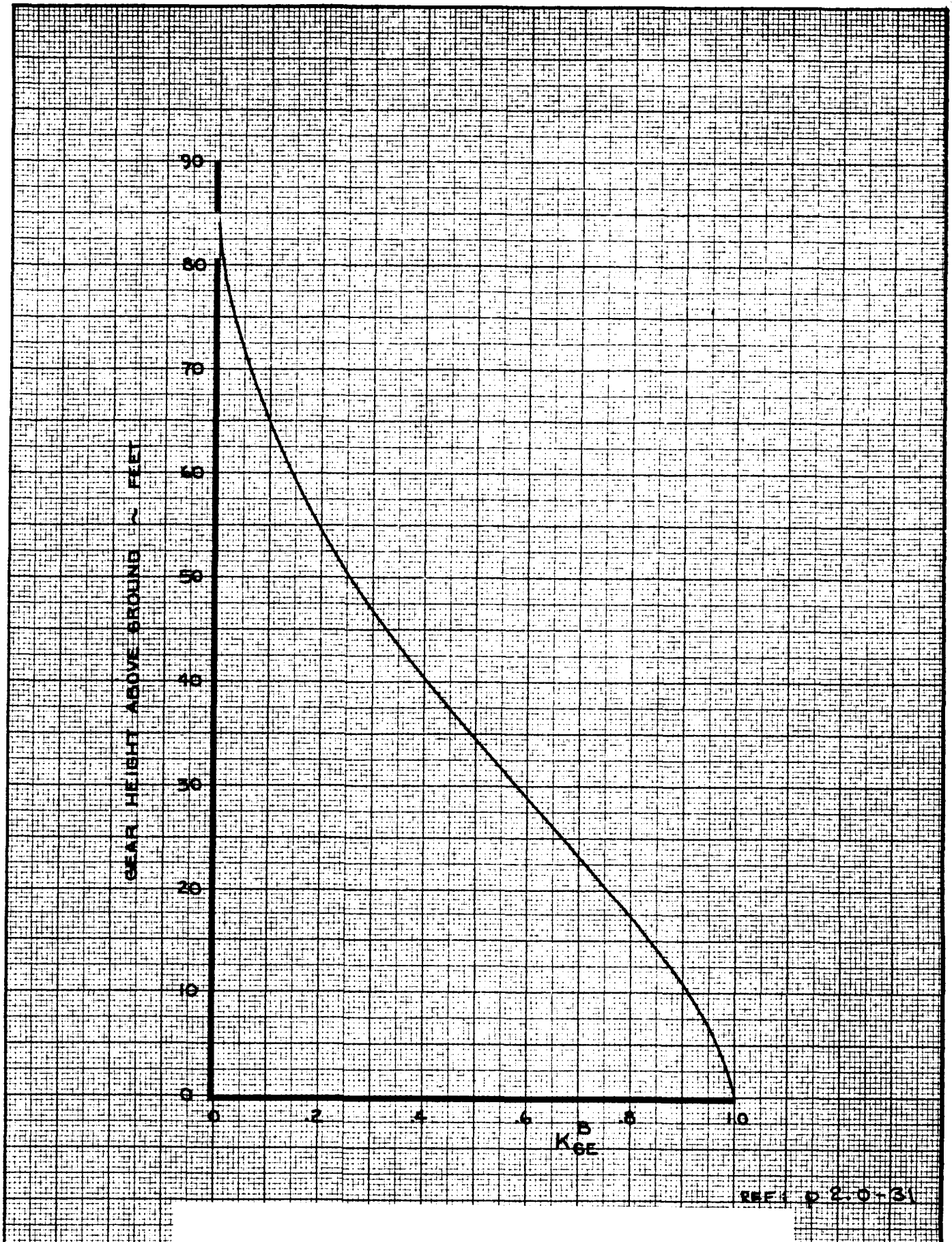

CALC	CURNUTT	12-12-67	REVISED	DATE	GROUND EFFECT HEIGHT FACTOR, K_{GE}^{B}	747
CHECK	FOSTER	1-24-68	CURNUTT	9-1-70		D6-30643 Vol. II
APR						
APR					THE BOEING COMPANY	PAGE 19.0-3
INK	ODEGARD	9-1-70				

NOTE 1 GEAR ON GROUND

2 $K_{GE}^{B} = 1.0$

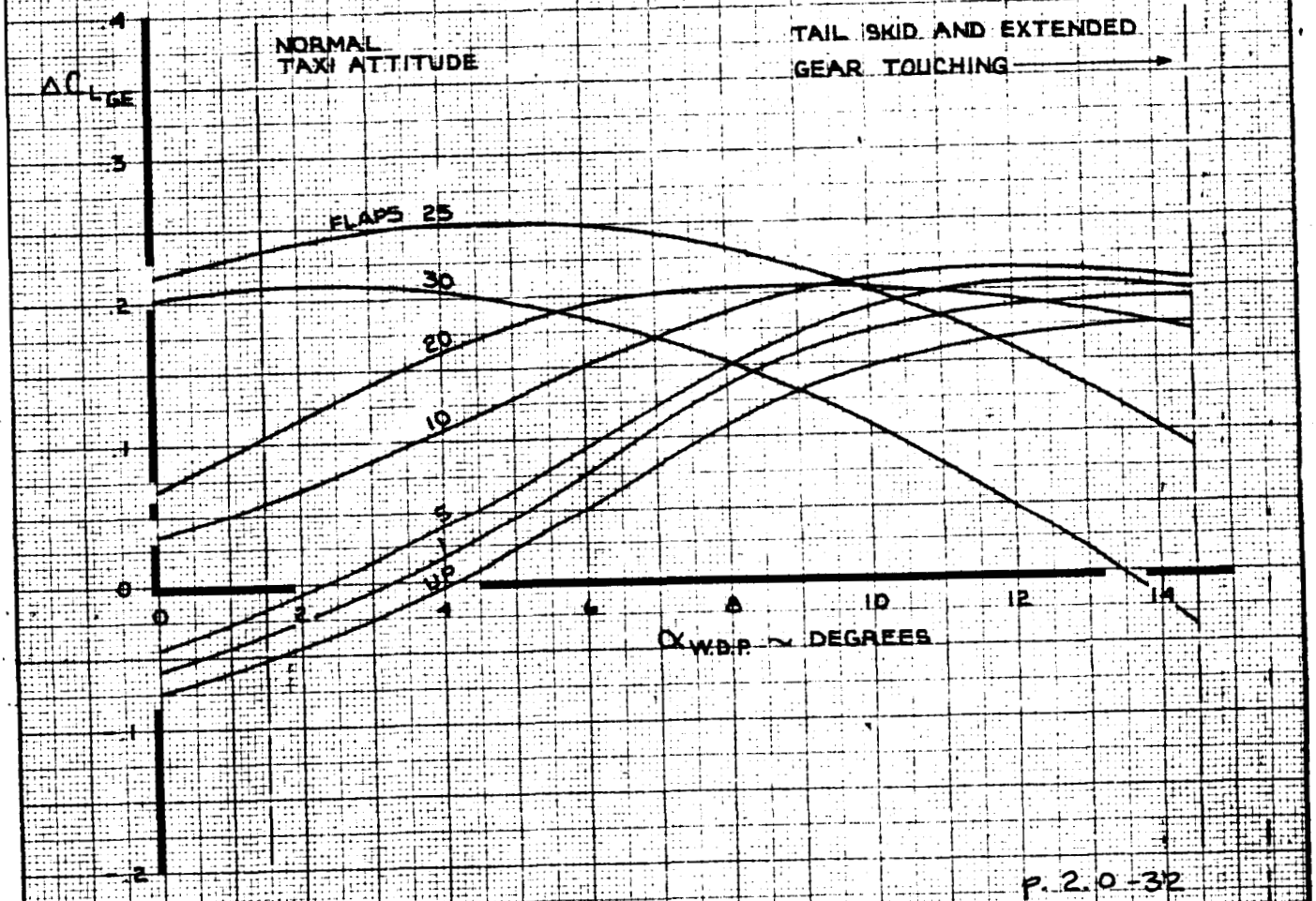

P. 2.0-32

CALC	CURNUTT	12-12-67	REVISED	DATE	LIFT COEFFICIENT GROUND EFFECT	747
CHECK	FOSTER	1-24-68	CURNUTT	3-5-70		D6-30643 Vol. II
APR			CURNUTT	9-1-70		
APR					THE BOEING COMPANY	PAGE 19.0-4
INK	KINSMAN	3-5-70				

TD 461 C-R4

K-E ALBANENE 195L TRACING PAPER REV. E

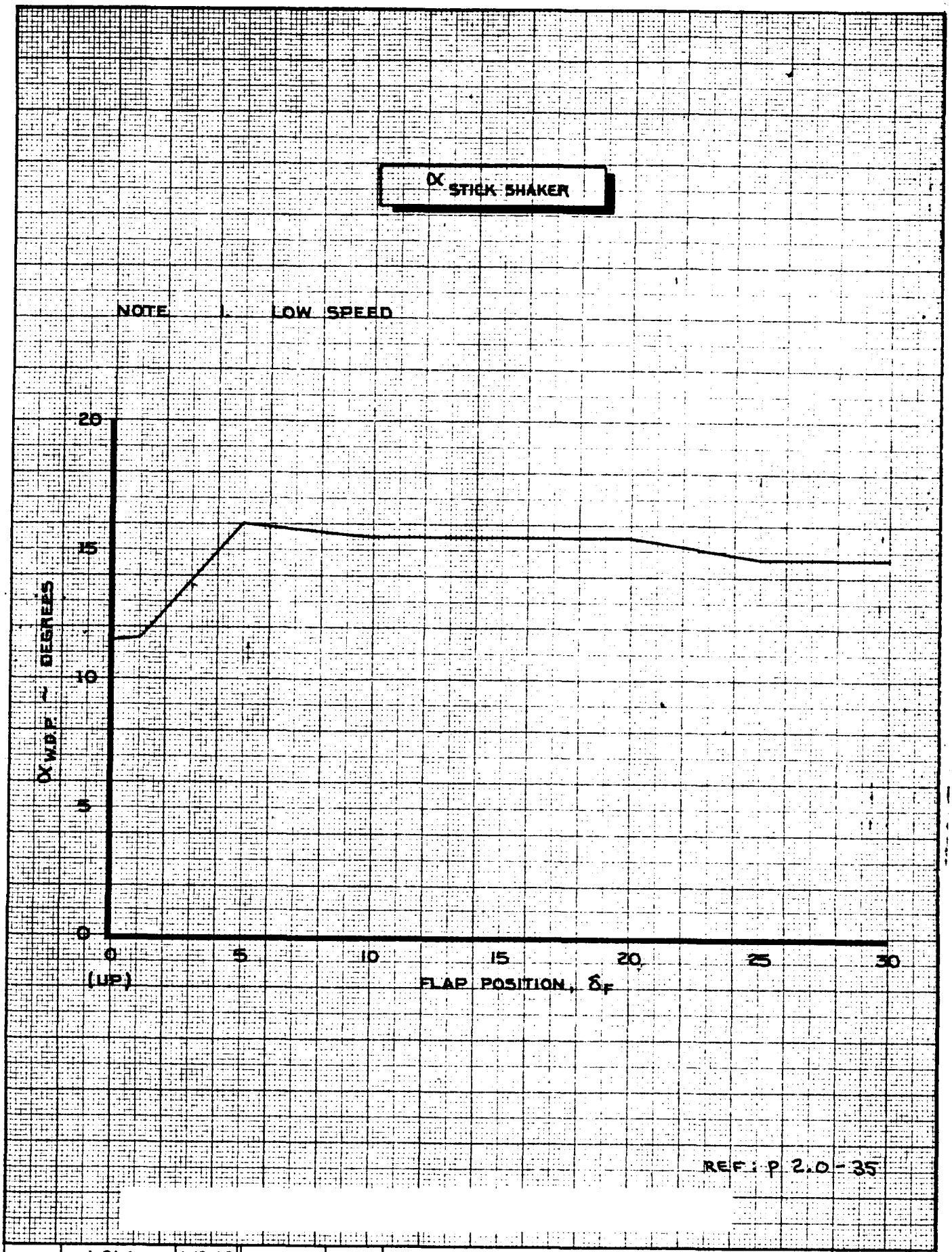

REF: P 2.0-35

CALC	LOW	1-19-68	REVISED	DATE	ANGLE OF ATTACK FOR STICK SHAKER ACTUATION	747 D6-30643 Vol. II
CHECK	FOSTER	1-24-68	LOW	6-4-69		
APR			LOW	1-28-70		
APR			BYSTROM	6-30-70		
INK	ODEGARD	6-30-70			THE BOEING COMPANY	PAGE 19.0-5

TD 441 C-R4

K-E ALBANENE 195L REV. E

α INITIAL BUFFET

NOTE 1. LOW SPEED
2. USE DATA ON P. 2.0-38 FOR FLAPS UP

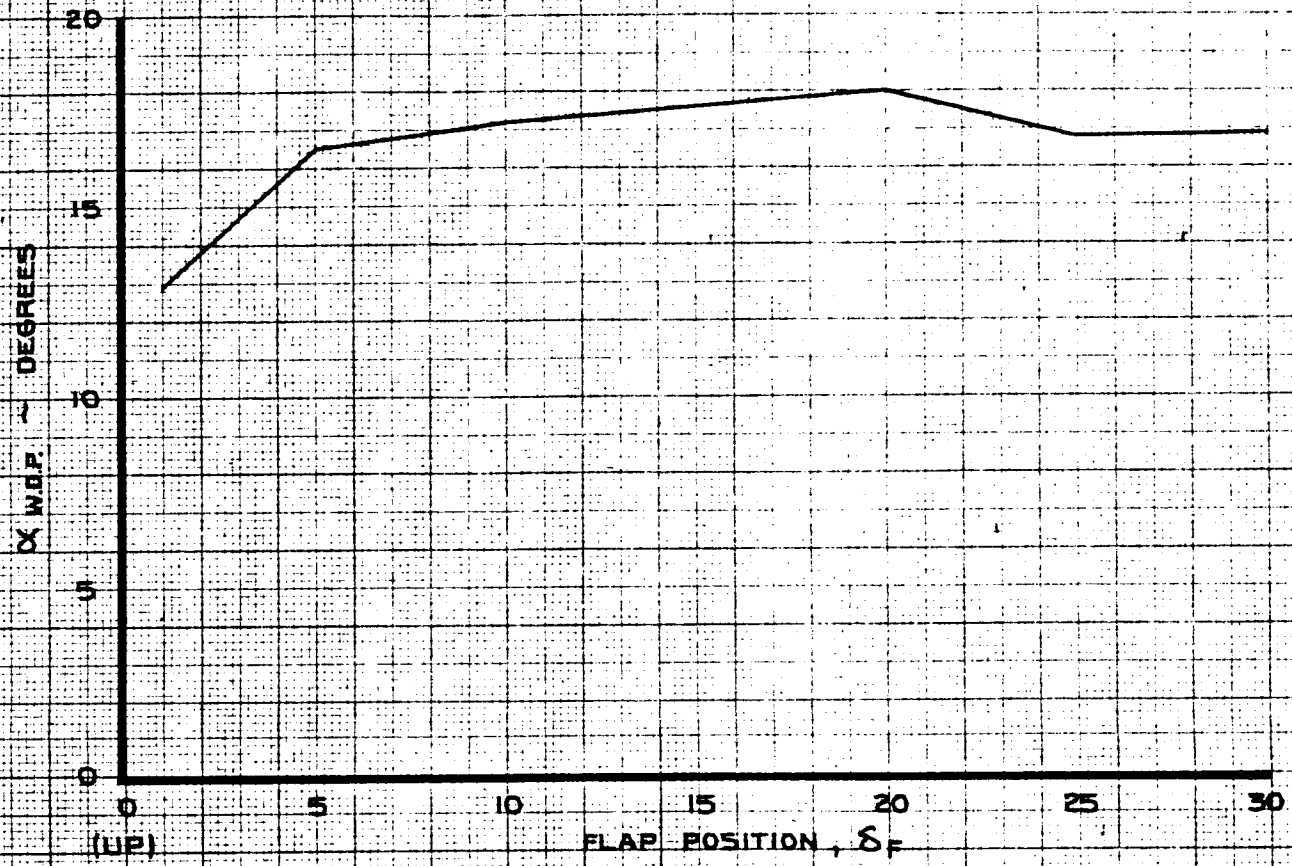

REF: P 2.0-36

CALC	LOW	1-19-68	REVISED	DATE	ANGLE OF ATTACK FOR INITIAL BUFFET
CHECK	FOSTER	1-24-68	LOW	6-4-69	
APR			LOW	1-29-70	
APR			BYSTROM	6-30-70	
INK	ODEGARD	6-30-70			

747
D6-30643 Vol. II
THE BOEING COMPANY
PAGE 19.0-6

TD 461 C-R4

K-E ALBANENE 195L REV. E

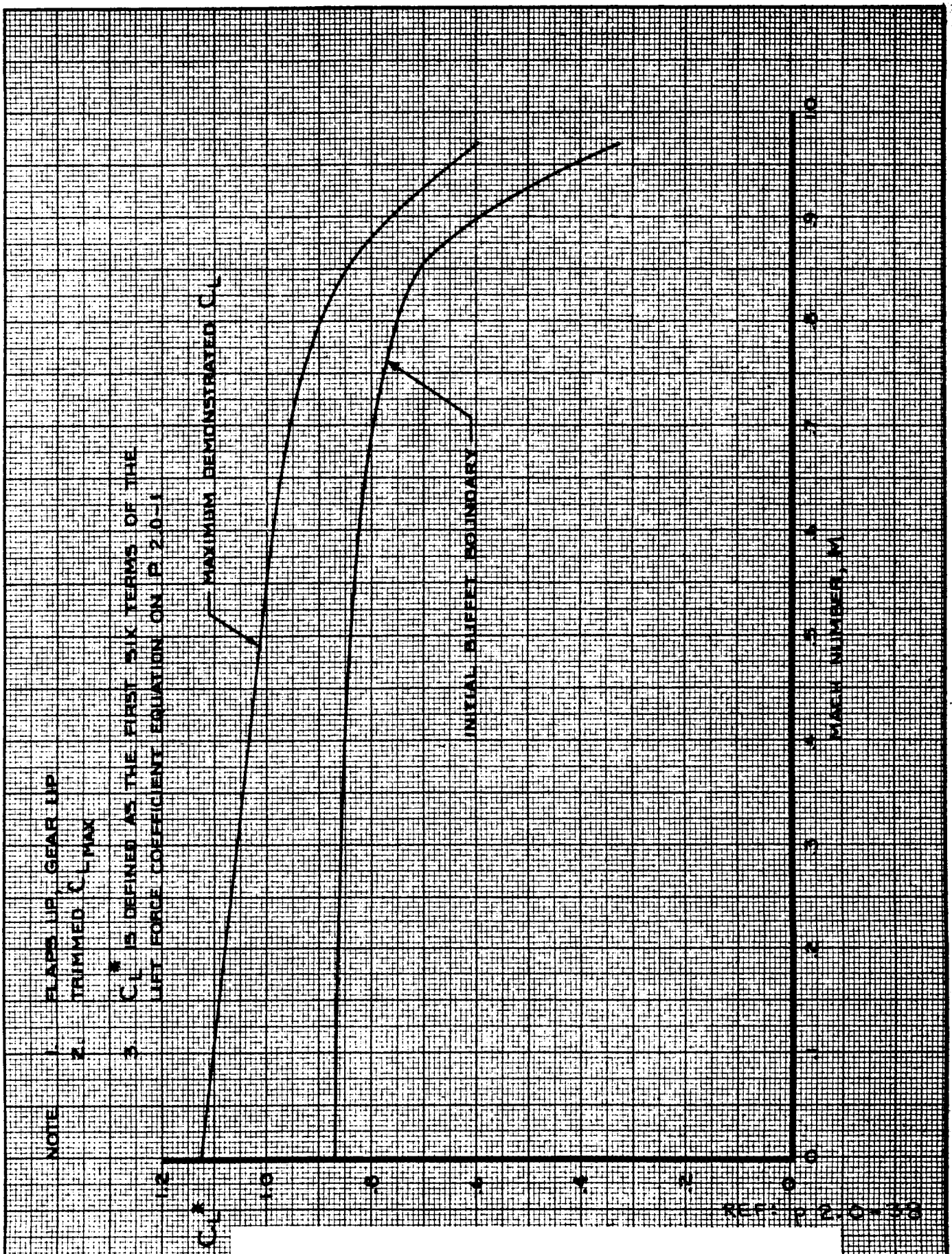

CALC	LOW	1-8-68	REVISED	DATE	LIFT COEFFICIENT BUFFET BOUNDARY AND $C_{L_{MAX}}$.
CHECK	FOSTER	1-24-68	LOW	6-4-69	
APR			LOW	1-20-70	
APR			FOSTER	6-29-70	
INK	ODEGARD	1-8-68			THE BOEING COMPANY

747
D6-30643
Vol. II
PAGE 19.0-7

AD 461 C-R4

K-E ALBANENE 100L REV. E

NOTE 1. GEAR ON GROUND

2. $K_{GE}^{A} = 1.0$

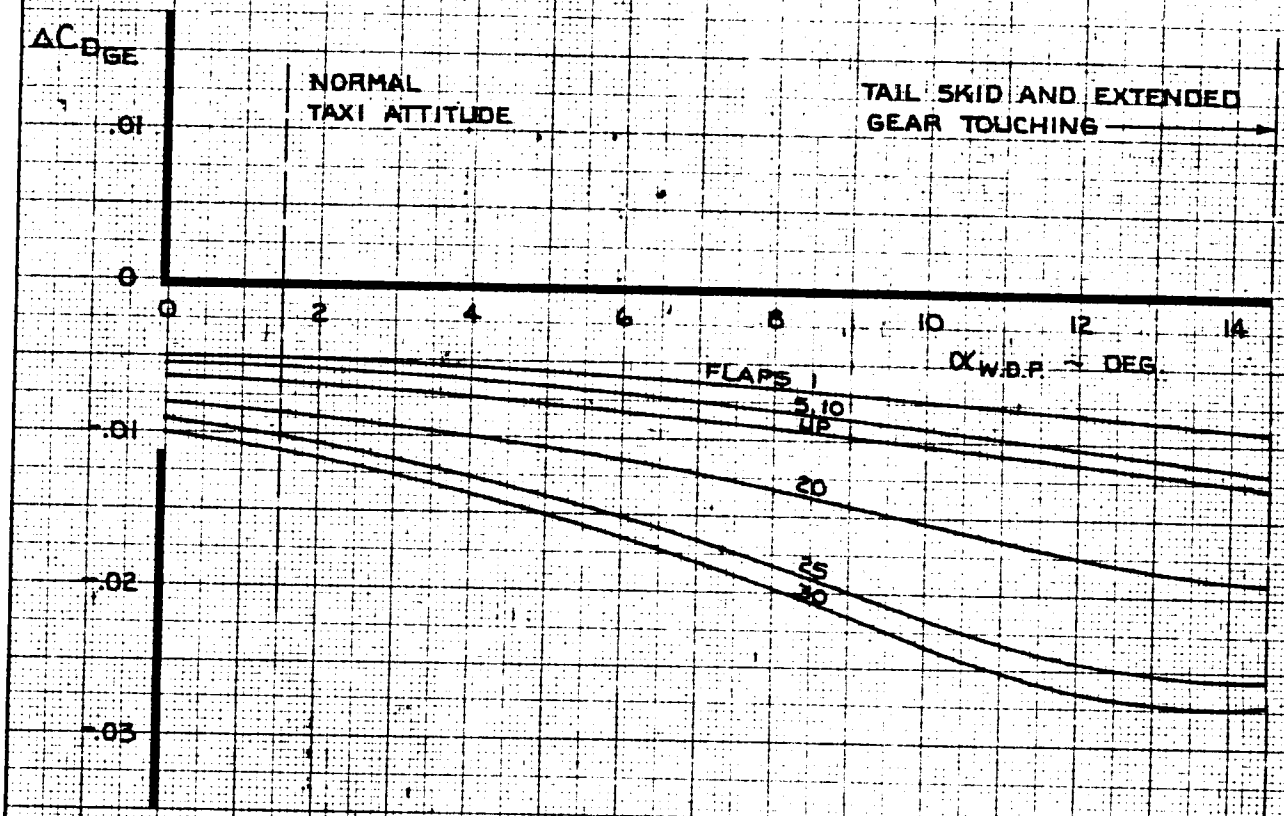

REF: P 3.0-18

CALC	CURNUTT	12-12-67	REVISED	DATE	DRAG COEFFICIENT GROUND EFFECT
CHECK	FOSTER	1-24-68	CURNUTT	3-5-70	
APR			CURNUTT	9-1-70	
APR					
INK	ODEGARD	9-1-70			THE BOEING COMPANY

747
D6-30643, Vol. II
PAGE 19.0-8

TD 461 C-R4

NOTE 1 GEAR ON GROUND

2 $K_{GE}^{\delta} = 1.0$

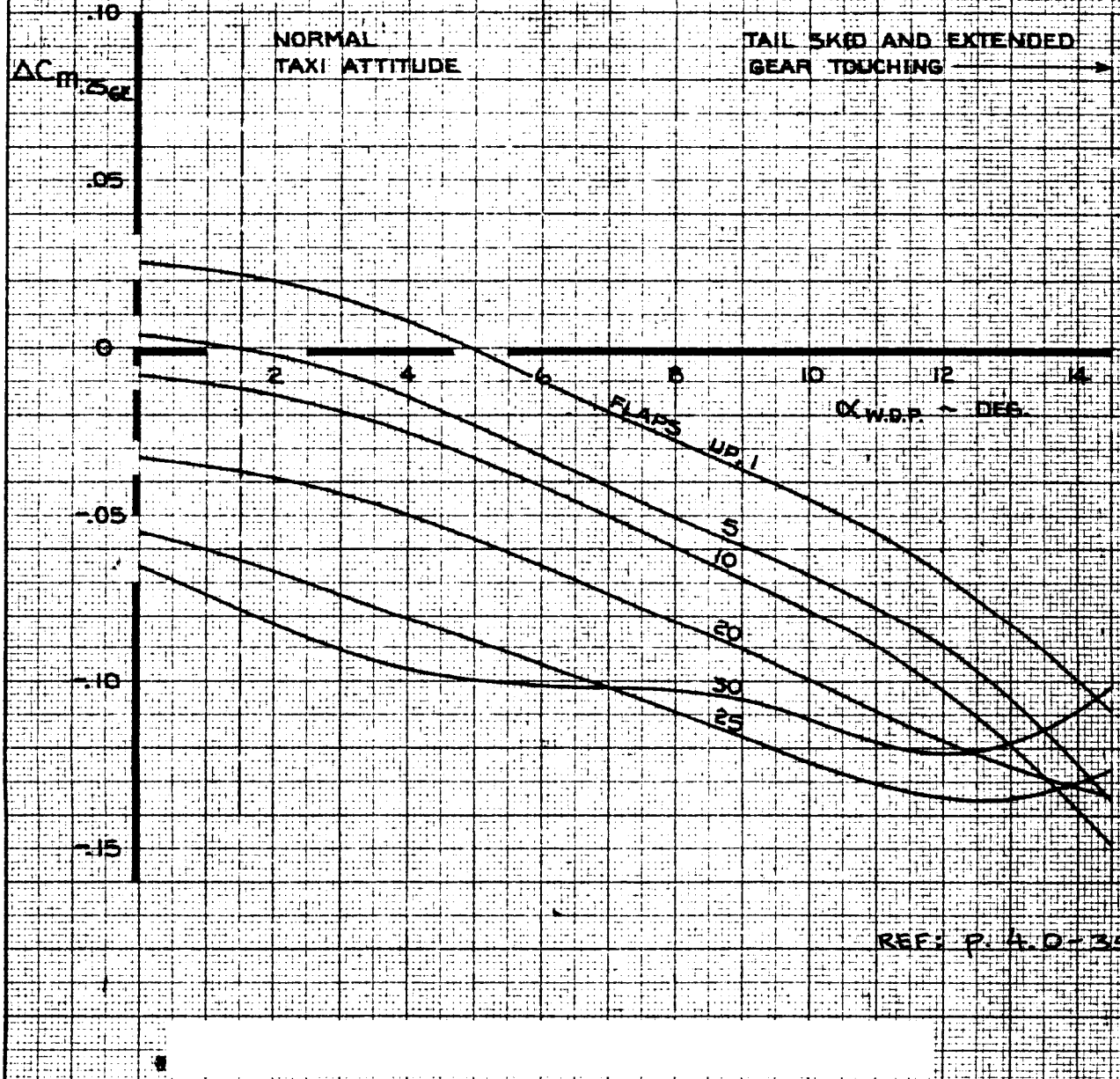

REF: P. 4.0-35

CALC	CURNUTT	12·12·67	REVISED	DATE	PITCHING MOMENT COEFFICIENT GROUND EFFECT	747
CHECK	FOSTER	1·24·68	CURNUTT	3·6·70		D6-30643 Vol. II
APR			CURNUTT	9·1·70		
APR					THE BOEING COMPANY	PAGE 19.0-9
INK	ODEGARD	9·1·70				

TD 461 C-R4

K·E ALBANENE 1951 REV. E

NOTE - FOR SPEED BRAKES AT THE GROUND STOP, USE THE IN-FLIGHT DETENT CURVES FOR PANELS 3,4,5 & 8,9,10. FOR PANELS 1&2 USE THE CURVE FOR PANELS 3,4. FOR PANELS 11&12 USE THE CURVE FOR PANELS 9,10. PANELS 6&7 REMAIN AT 20° FOR ALL WHEEL ANGLES

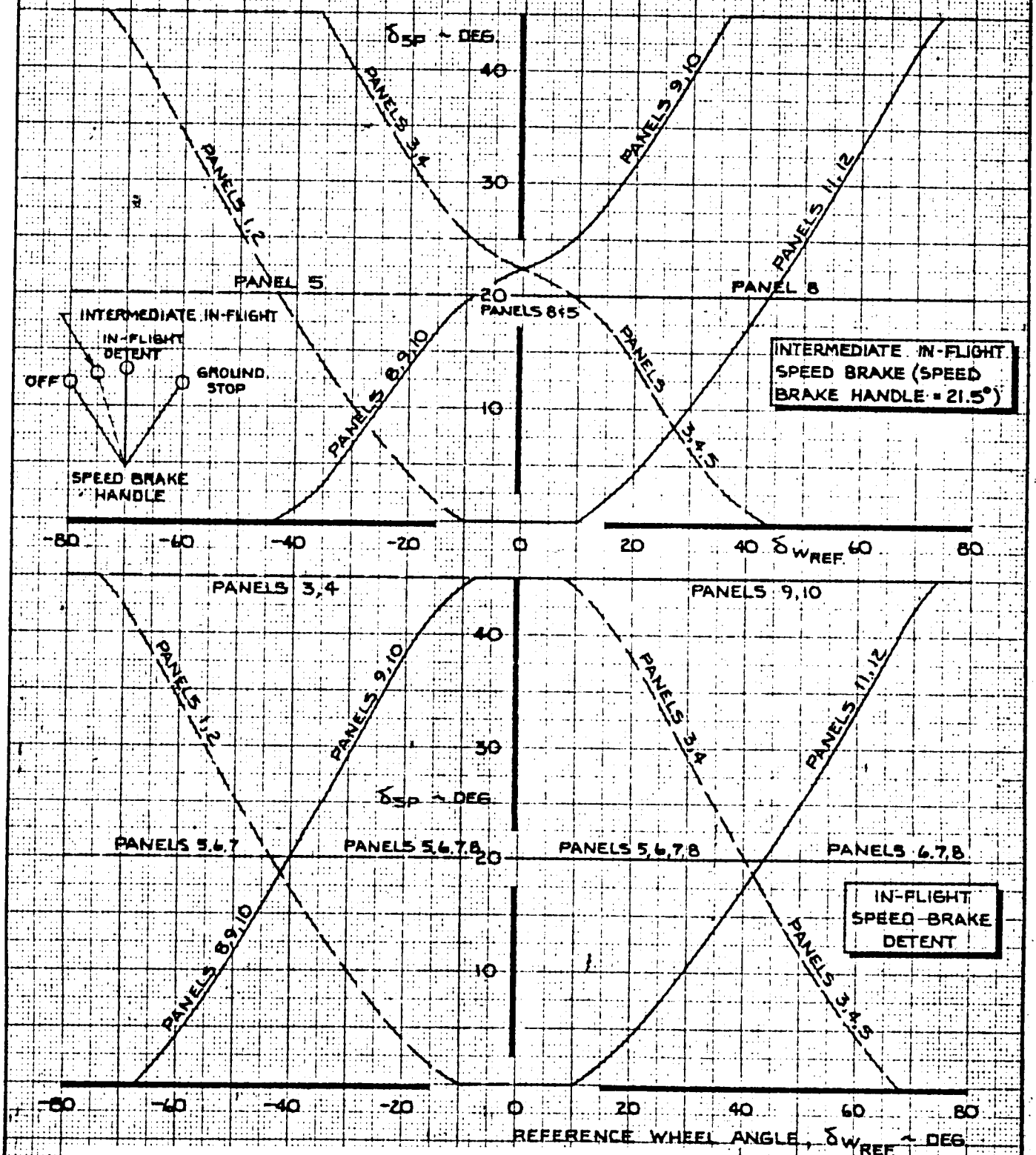

REF: P. 9.2-6

CALC	MOOIWEER	12-5-67	REVISED	DATE	LATERAL CONTROL SPOILER PROGRAM AT COMBINED LATERAL CONTROL - SPEED BRAKES
CHECK	HOLTZNER	1-15-68	KUPCIS	6-2-69	
APR			KUPCIS	8-22-69	
APR					
INK	ODEGARD	12-5-67			THE BOEING COMPANY

747
D6-30643 Vol. II
PAGE 19.0-10

NOTE 1. SPEED BRAKE HANDLE FRICTION FORCE = 20 LB. PULL, 10 LB. PUSH

2. MAXIMUM AVAILABLE IN-FLIGHT SPEED BRAKE HANDLE POSITION = 37 DEG. (IN-FLIGHT DETENT)

3. SPEED BRAKES BEYOND THE IN-FLIGHT DETENT ARE AVAILABLE ONLY ON THE GROUND

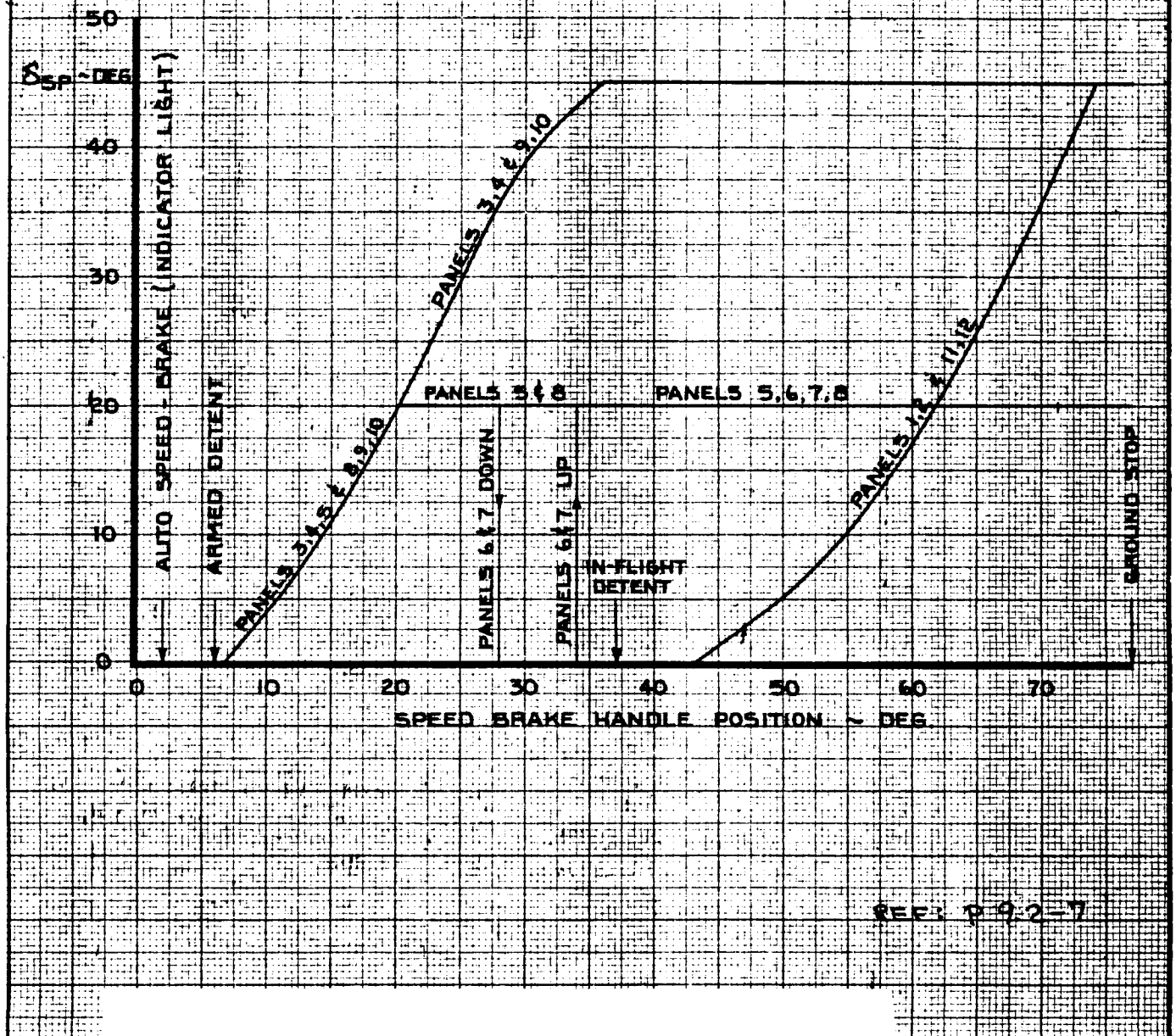

REF: P 9.2-7

CALC	MOOIWEER	12-5-67	REVISED	DATE	LATERAL CONTROL SPOILERS - SPEED BRAKE PROGRAM	747
CHECK	HOLTZNER	1-15-68	KUPCIS	6-2-69		D6-30643 Vol. II
APR			KUPCIS	8-22-69		
APR			KUPCIS	6-12-70		
	ODEGARD	6-24-70			THE BOEING COMPANY	PAGE 19.0-11

20.0 APPENDIX F - AIRPLANE RESPONSE TO CONTROL INPUTS

Time histories of airplane response to control inputs are presented in the following pages.

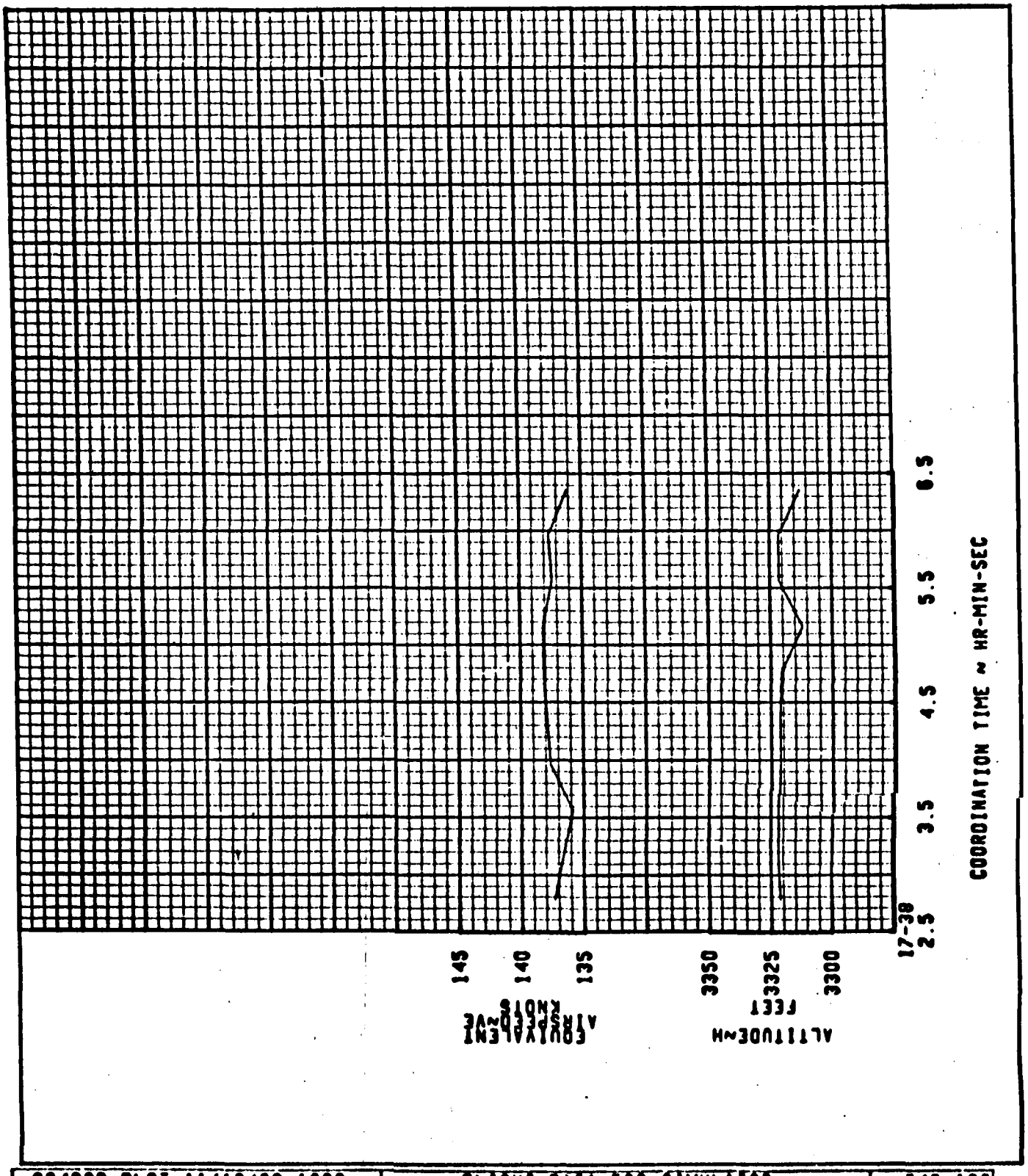

SC4020 PLOT 11/13/69 1639				
CALC			REVISED	DATE
CHECK				
APPD				
APPD				

FLIGHT DATA FOR SIMULATOR

COND NO 1.00.008.020 TEST 008-05

THE BOEING COMPANY
RENTON WASHINGTON

747-100
RA101

D6-30643
Vol. II

PAGE
20.0-8

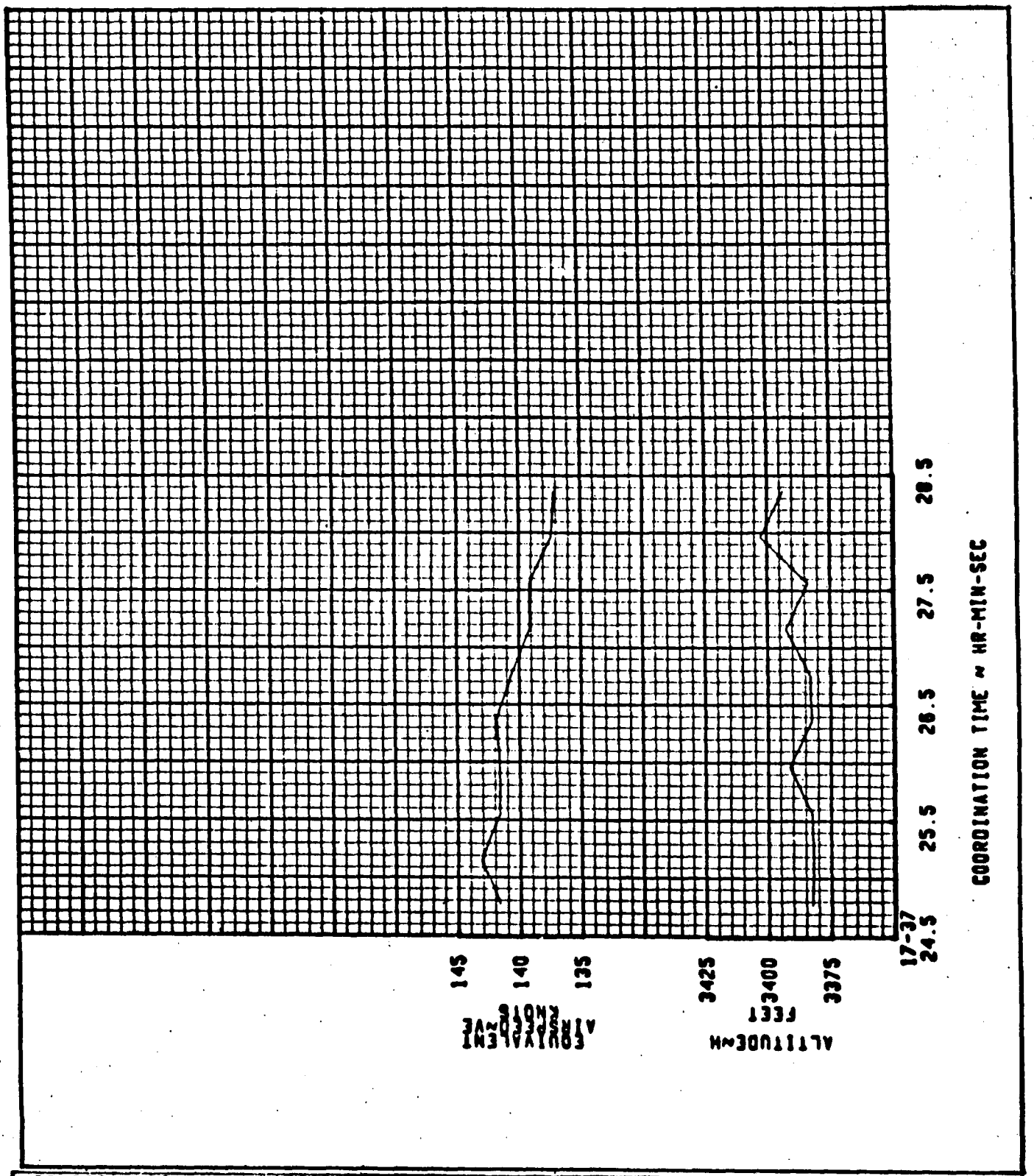

SC4020 PLOT 11/14/89 0619				
CALC			REVISED	DATE
CHECK				
APPD				
APPD				

FLIGHT DATA FOR SIMULATOR

CONO NO 1.00.008.017 TEST 008-05

THE BOEING COMPANY
RENTON WASHINGTON

747-100
RA101

D6-30643
Vol. II

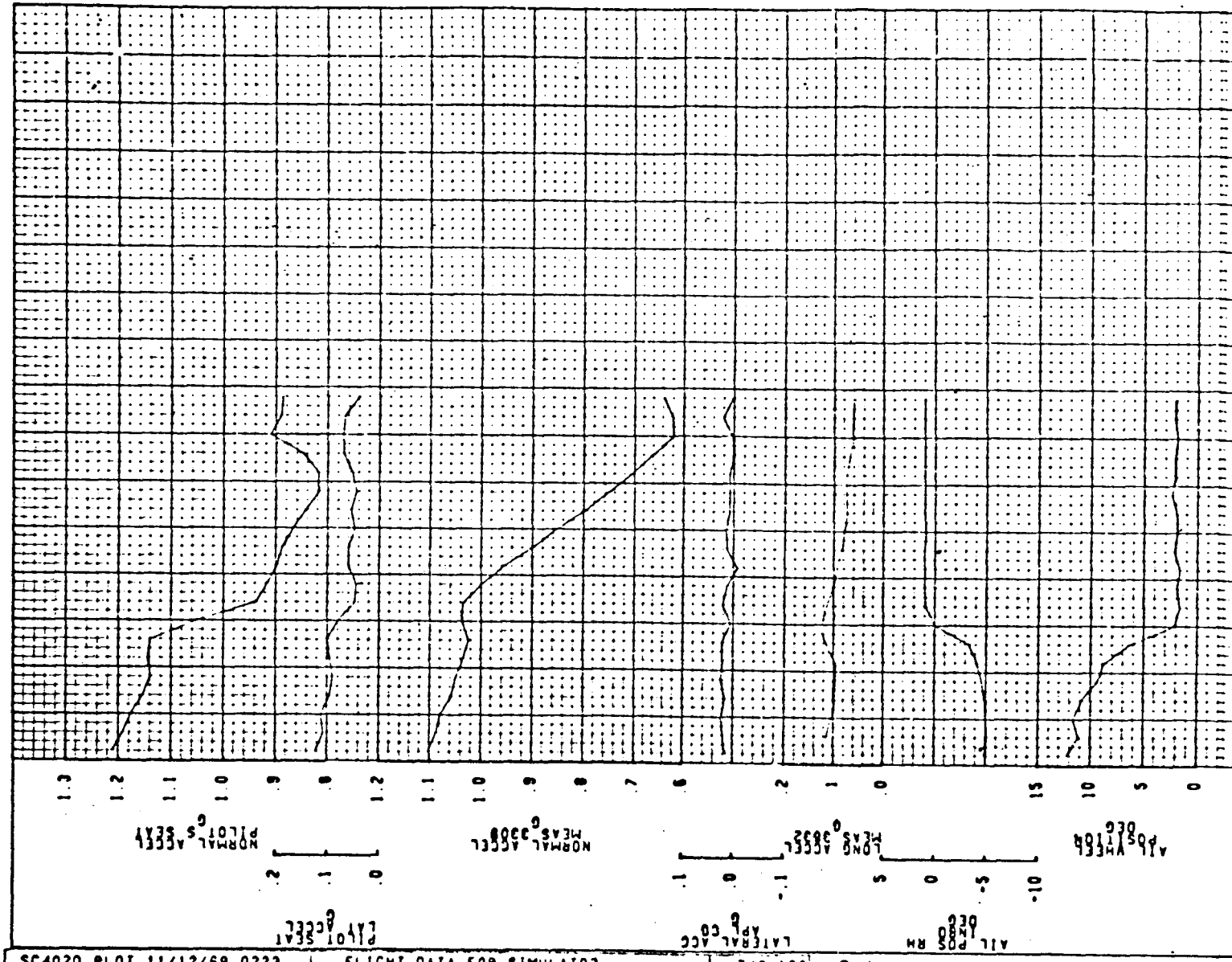

SC4020 PLOT 11/12/69 0223	FLIGHT DATA FOR SIMULATOR	747-100 RA101
CALC / CHECK / APPD / APPR — REVISED — DATE	.018 COND NO 1.00 008 ●●● 0 TEST 009-05	DS-30643 Vol. II
	THE BOEING COMPANY	PAGE 20.0-5

STEP ELEVATOR INPUT DURING
FLAPS 20° GEAR DOWN
GROSS WEIGHT = 398,100 LB.
C.G. POSITION = 27.1 % MAC

COORDINATION TIME ~ HR-MIN-SEC
28 S
29 S
30 S
31 S
32 S
17-37
PITCH RATE
ELEV POS CM
CONTROL POS
PITCH ANGLE
RPLL ANGLE
APPROACH

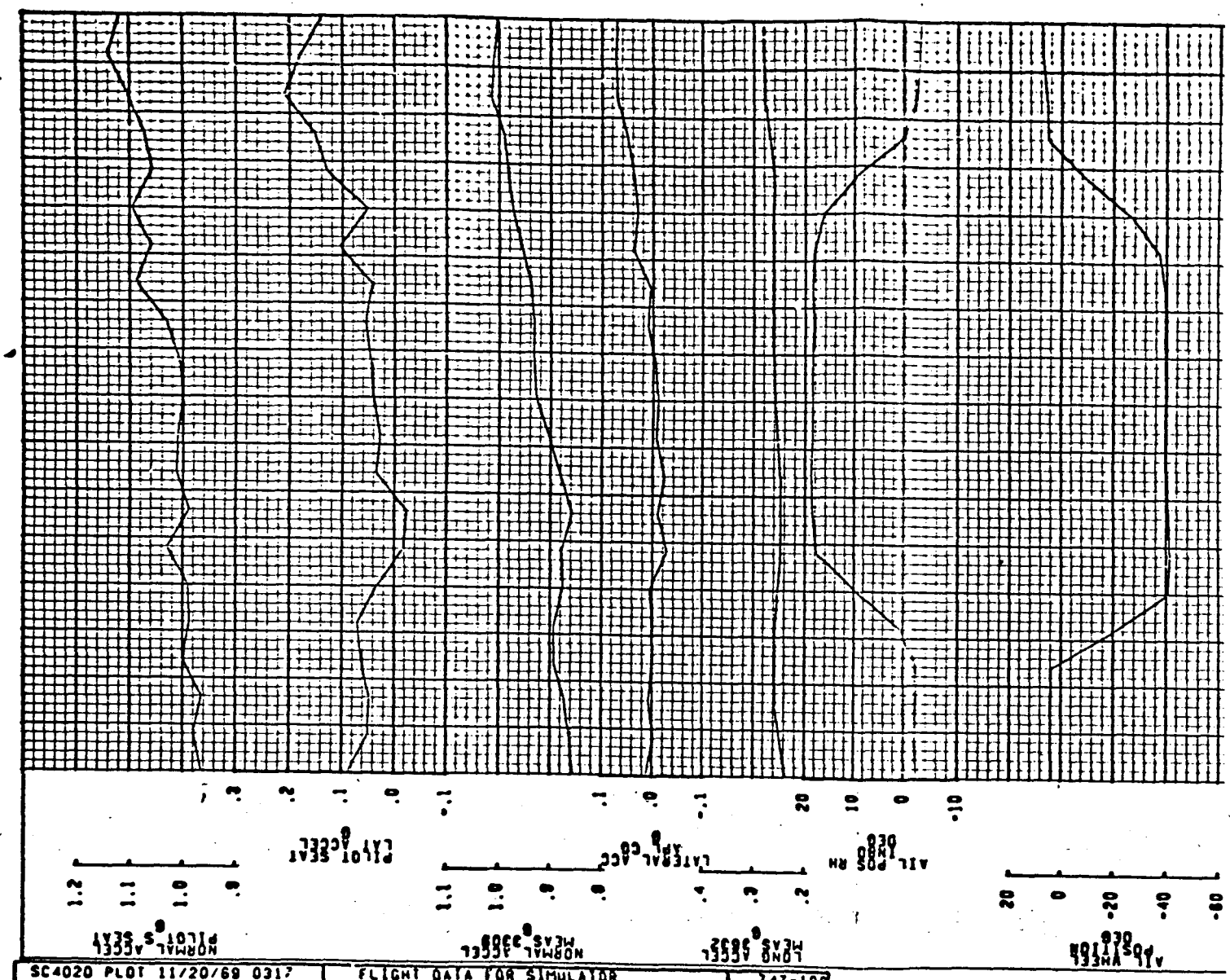

SC4020 PLOT 11/20/69 0317					FLIGHT DATA FOR SIMULATOR	747-100 RA101
CALC			REVISED	DATE		
CHECK					COND NO 1.00.008.011.0 TEST 010-01	D6-30643 Vol. II
APPD					THE BOEING COMPANY RENTON WASHINGTON	PAGE 20.0-6
APPD						

AILERON INPUTS DURING
FLAPS 10° GEAR UP
YAW DAMPER OFF
GROSS WEIGHT = 692,700 LB.
C.G. POSITION = 23.0 % MAC

CLIMB OUT

PITCH ANGLE FF GYRO DEG
ROLL ANGLE FF GYRO DEG
ROLL RATE FF GYRO DEG/S
APL ANGULAR ACCEL DEG/SS
EQUIVALENT AIRSPEED-KT
ALTITUDE-M FEET
12
10
8
6
0
-5
-10
-15
-20
5
0
-5
-10
15
10
5
0
-5
-10
-15
180
175
170
575
550
525
10-28
25.00
25.50
26.00
26.50
27.00
27.50
28.00
28.50
COORDINATION TIME ~ HR-MIN-SEC

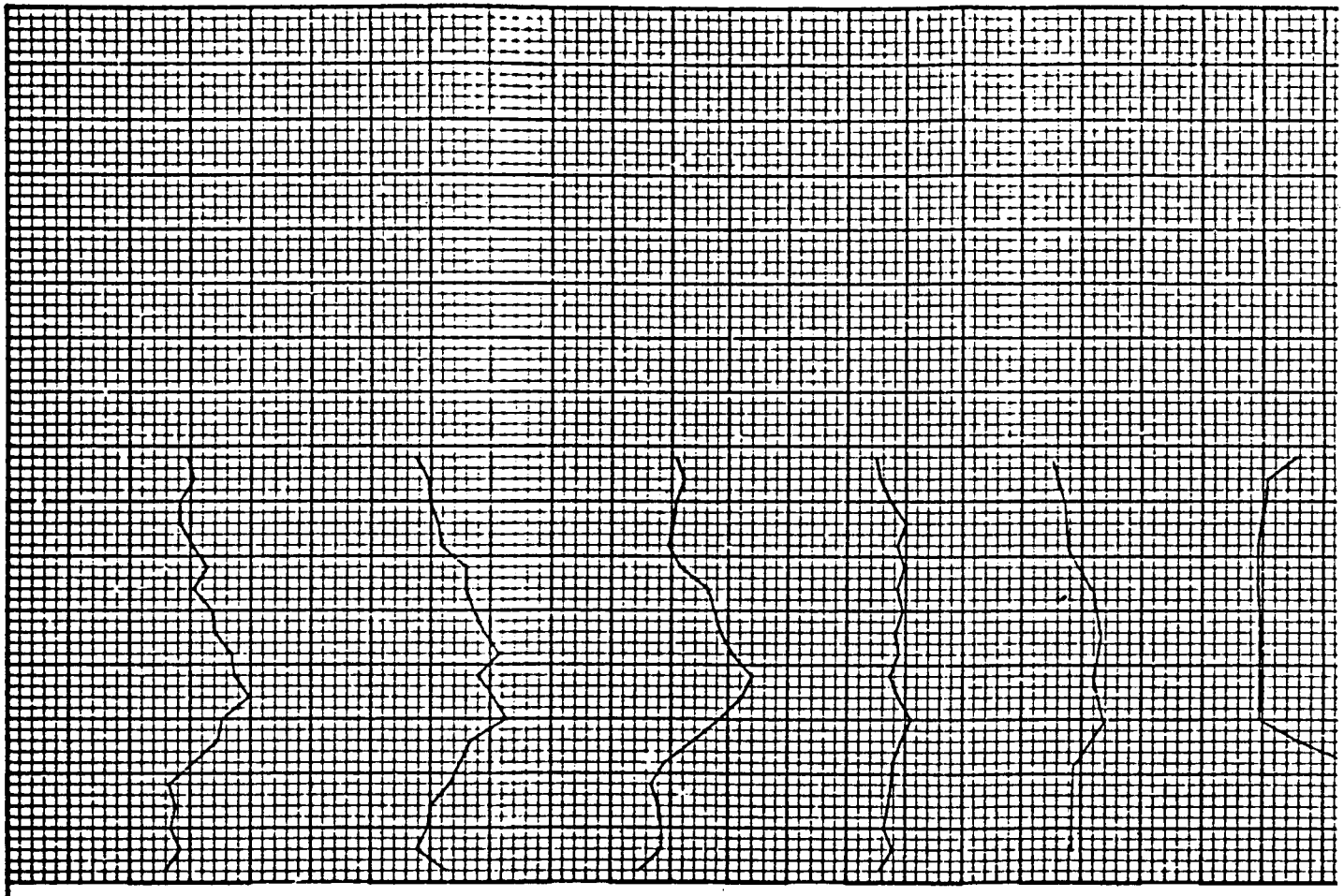

SC4020 PLOT 11/12/69 0223				
			REVISED	DATE
CALC				
CHECK				
APPD				
APPD				

FLIGHT DATA FOR SIMULATOR

.020

COND NO 1.00.000.062.0 TEST 009-05

THE BOEING COMPANY RENTON WASHINGTON

747-100 RA101

D6-30643 Vol. II

PAGE 20.0-7

STEP AILERON INPUT D'
YAW DAMPER OFF
FLAPS 20 GEAR DOWN
GROSS WEIGHT = 397,900
C.G. POSITION = 27.1 % M

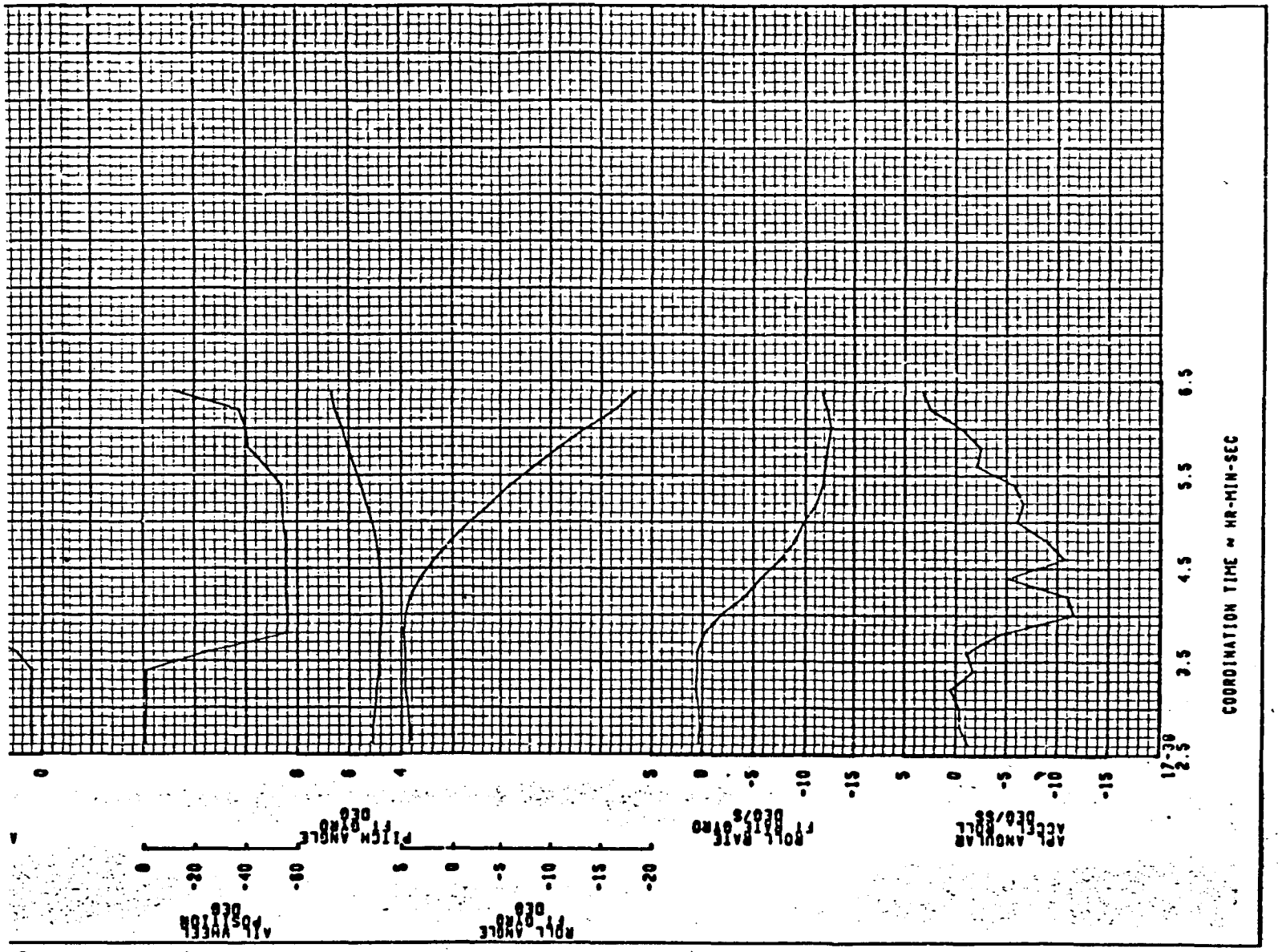

JRING APPROACH

LB.
4C

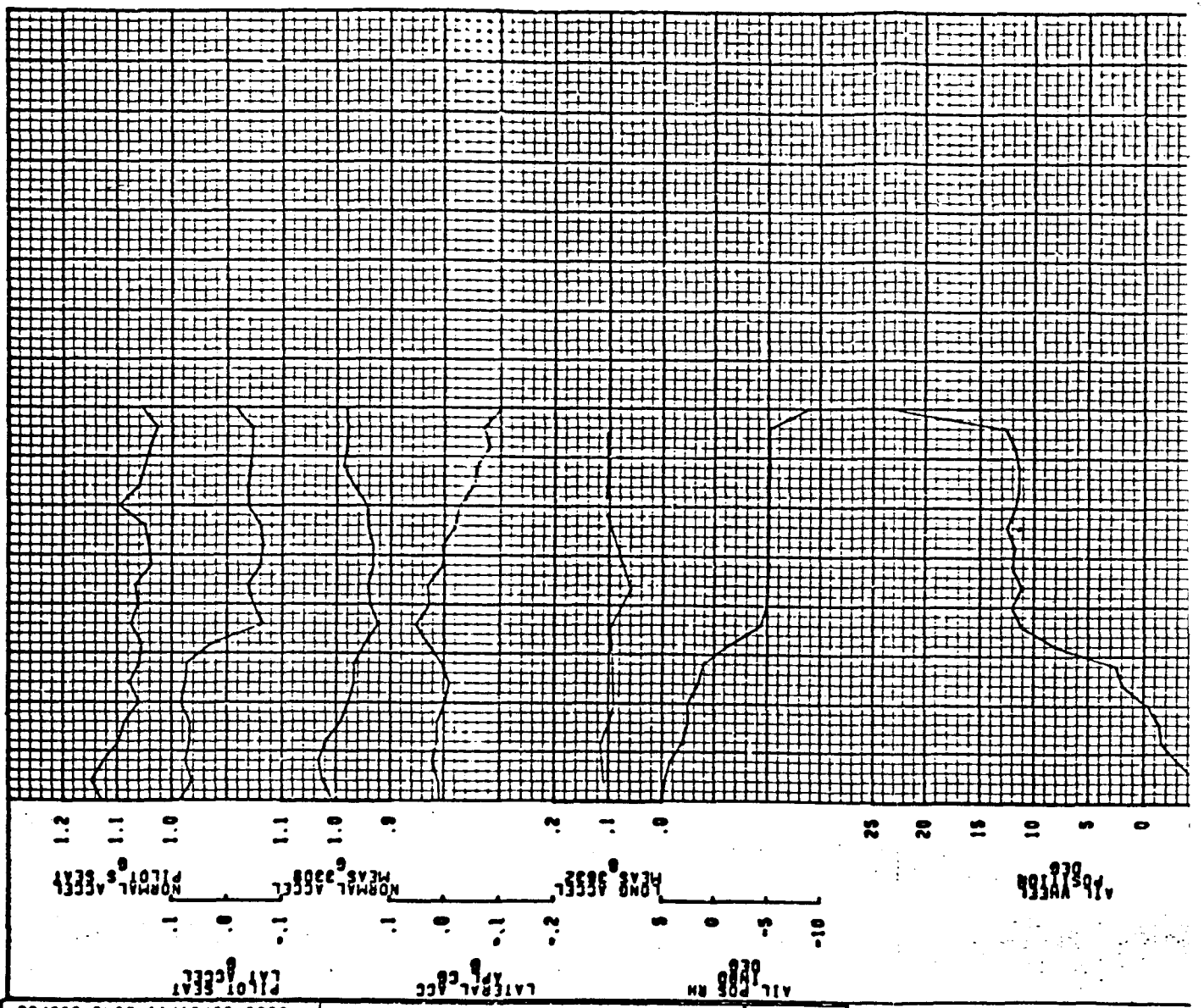

SC4020 PLOT 11/12/69 0223					
CALC			REVISED	DATE	
CHECK					
APPD					
APPD					

COND NO 1.00.008.010.0 TEST 008-05

THE BOEING COMPANY RENTON, WASHINGTON

747-100 RA101

D6-30643 Vol. II

PAGE 20.0-9

STEP RUDDER INPUT DI
FLAPS 20° GEAR DOW
GROSS WEIGHT = 397,90
C.G. POSITION = 27.1 %

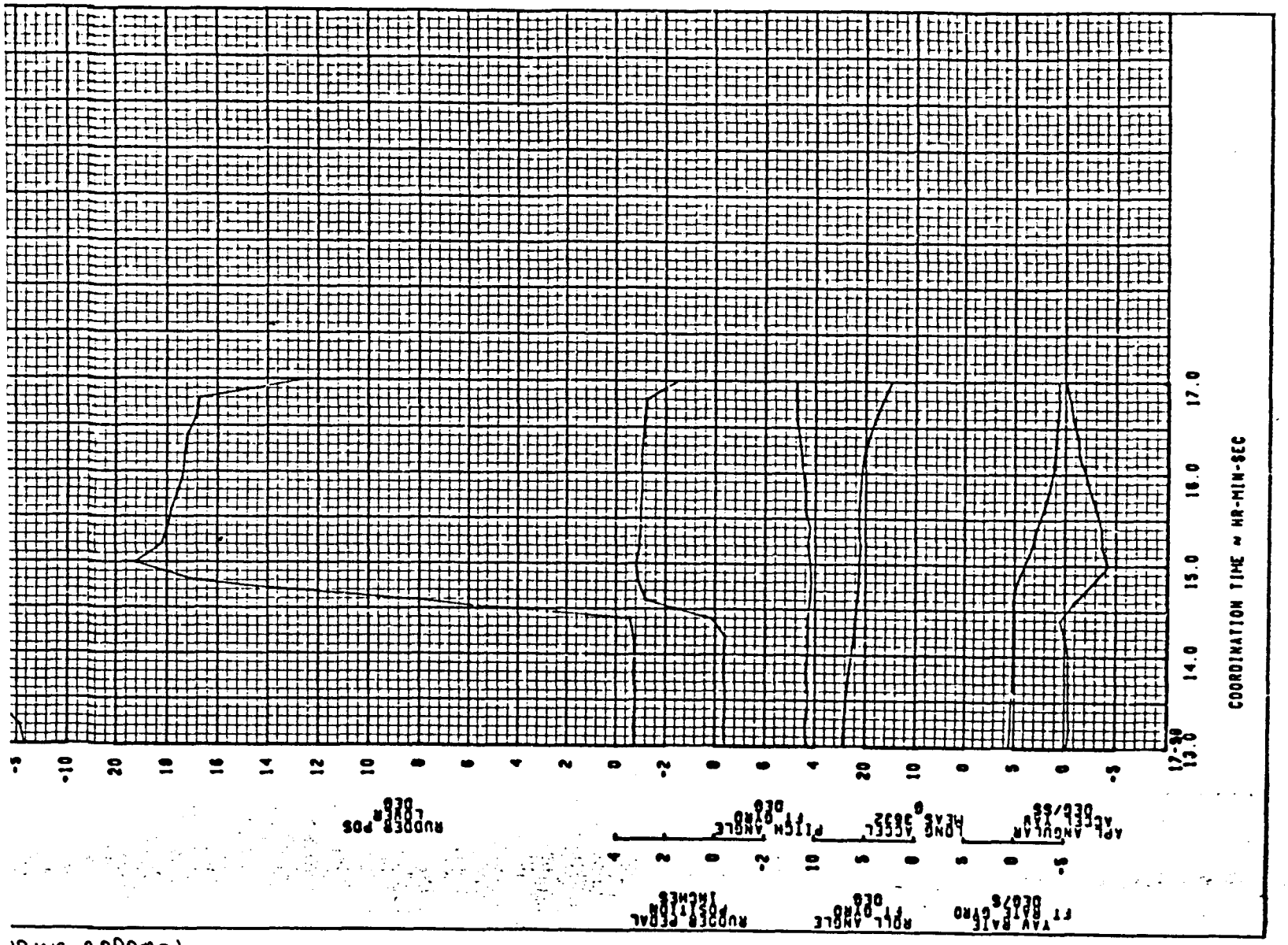

)RING APPROACH
U
) LB.
MAC

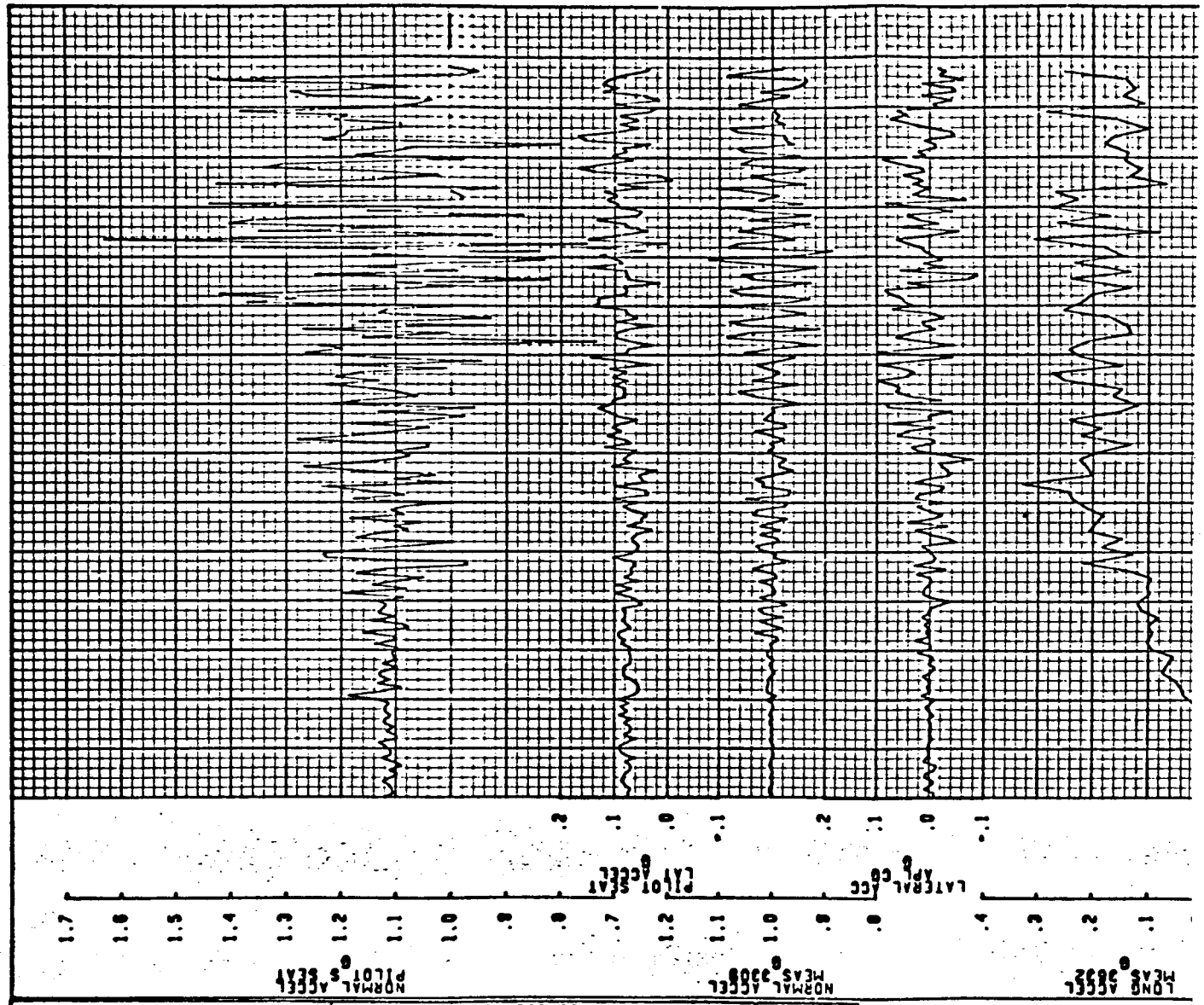

SC4020 PLOT 11/08/89 0950				FLIGHT DATA FOR SIMULATOR	747-100 RA101
CALC		REVISED	DATE		
CHECK				COND NO 1.00.000.003 0 TEST 000-01	D6-30643 Vol. II
APPD				THE BOEING COMPANY RENTON WASHINGTON	PAGE 20.0-11
APPD					

BRAKE RELEASE AND
FLAPS 10 GEAR DOWN
G.W. = 663,000 CG. 14.6
ALT. 16 FEET

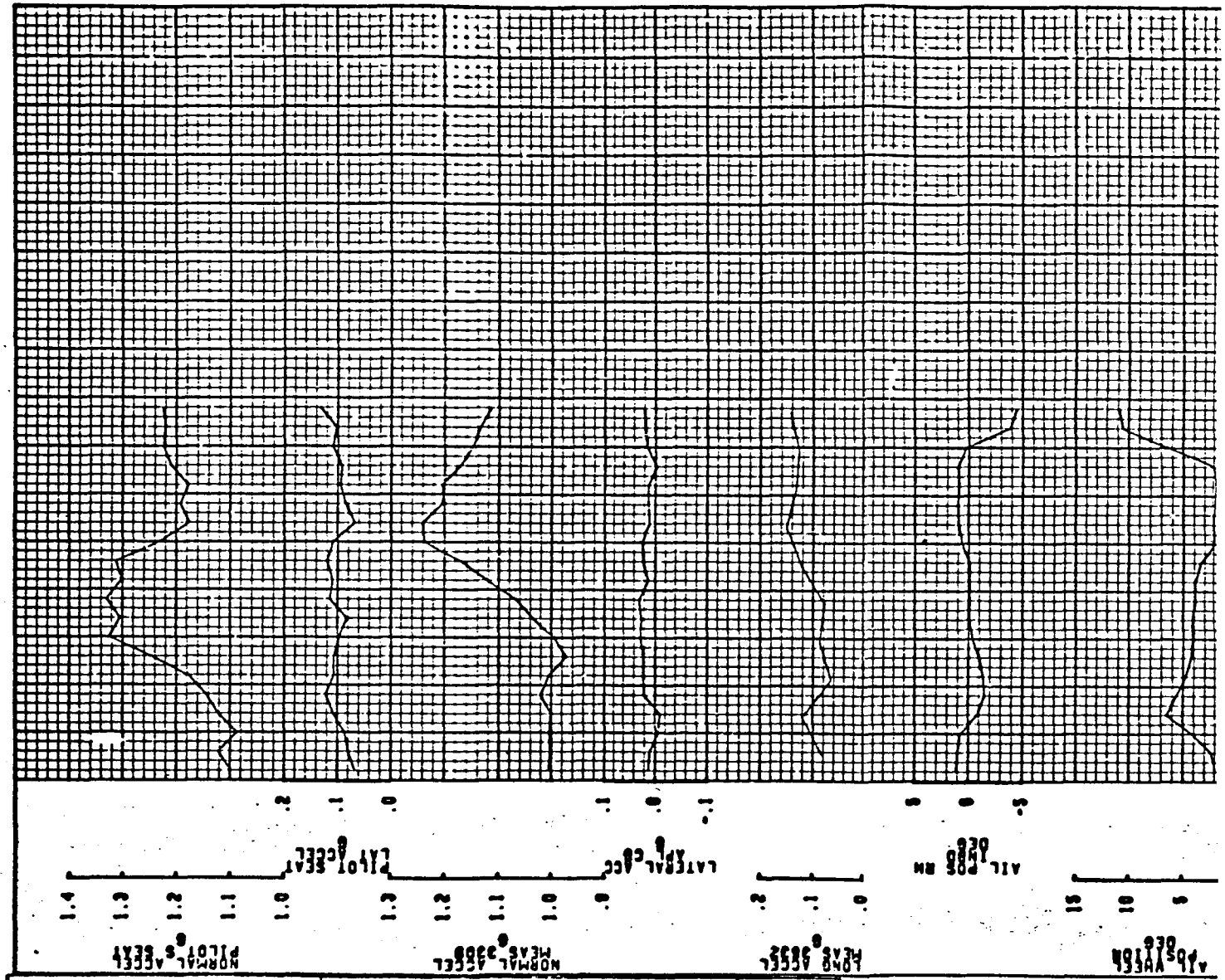

SC4020 PLOT 11/12/89 0223			FLIGHT DATA FOR SIMULATOR	747-100 RA101
CALC		REVISED	DATE	
CHECK				D6-30643 Vol. II
APPD			COND NO 1.00.008.017.0 TEST 008-05	
APPD			THE BOEING COMPANY SEATTLE WASHINGTON	PAGE 20.0-3

STEP ELEVATOR INPUT DU
FLAPS 20° GEAR DOWN
GROSS WEIGHT = 398,200 LB
C.G. POSITION = 27.1 % MAC

APPROACH
PITCH ANGLE DEG
ROLL ANGLE DEG
CONTROL COL DEG
ELEV RODS LH DEG
PITCH RATE DEG/S
AZ ANGULAR RATE DEG/SEC
12
10
8
6
4
2
0
-2
-4
-5
17-37
24.5
25.5
26.5
27.5
28.5
COORDINATION TIME ~ HR-MIN-SEC

CLIMB OUT

CONTROL COL POSITION DEG
PITCH RATE FT 2 RATE GYRO DEG/S
ROLL ANGLE FT GYRO DEG
ELEV POS LH STAB DEG
ACL ANGULAR RATE DEG/SS
EQUIVALENT AIRSPEED KNOTS
ALTITUDE-M FEET
175
170
165
300
275
250
225
200
12
10
8
6
4
2
0
-2
-4
10-20
13.0
14.0
15.0
16.0
17.0
COORDINATION TIME ~ HR-MIN-SEC

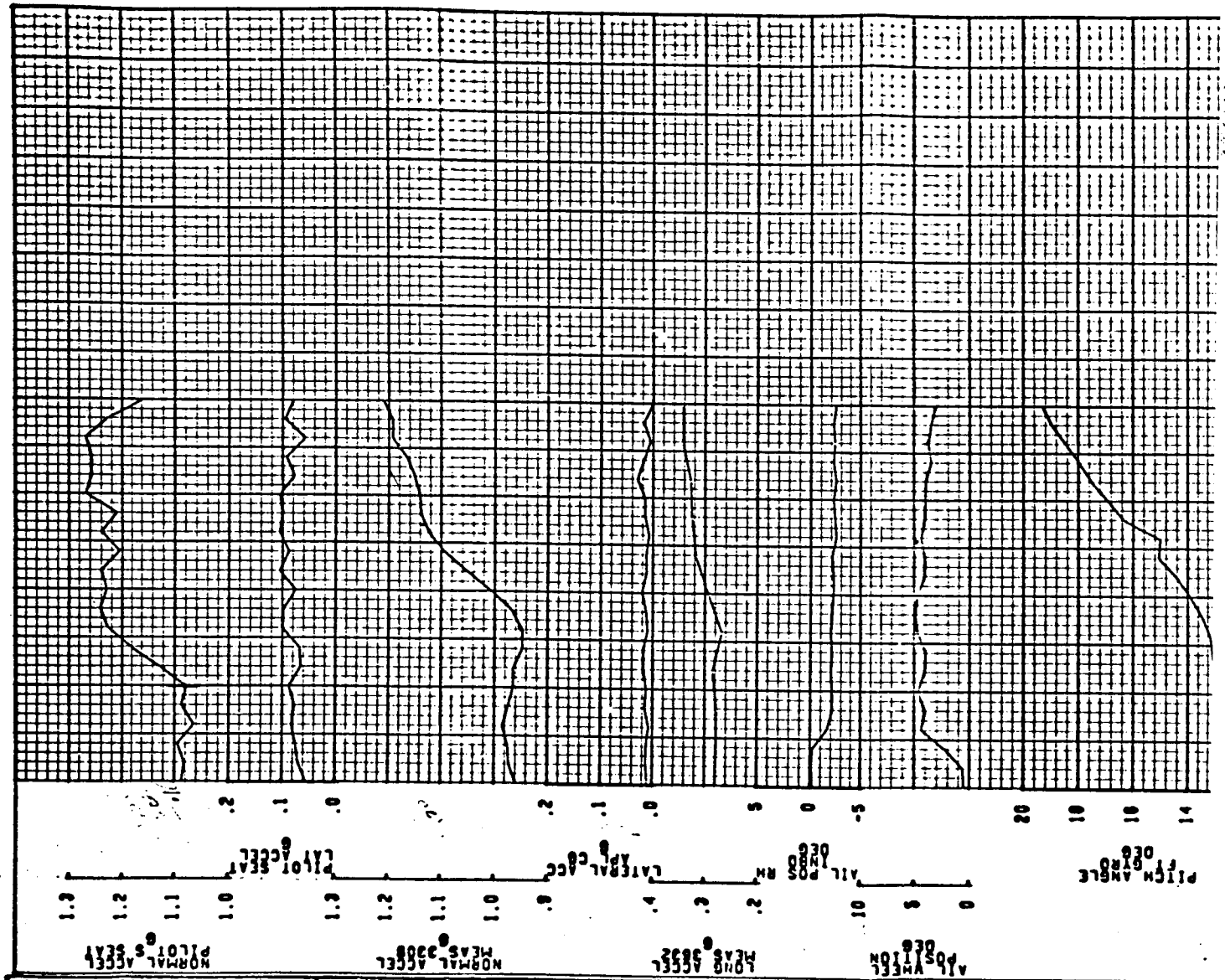

SC4020 PLOT 11/20/69 0317					FLIGHT DATA FOR SIMULATOR	747-100 RA101
CALC			REVISED	DATE		
CHECK					COND NO 1.00.000.000.0 TEST 010-01	D6-30643 Vol. II
APPD					THE BOEING COMPANY RENTON WASHINGTON	PAGE 20.0-2
APPD						

ELEVATOR INPUT DURIN
FLAPS 10° GEAR UP
GROSS WEIGHT = 693,100 l
C.G. POSITION = 23.1 % M

TABLE A - COURSE ERROR GAIN

	$\overline{DAV}$	DAV
VOR CAPTURE	2.58	2.58
VOR ON COURSE	2.58	2.58
LOC CAPTURE	0.62	0.97
LOC ON COURSE	0.62	0.97
LOC APP	—	1.60

TABLE B - LOC/VOR DISPLACEMENT GAIN

VOR CAPTURE	400.0
VOR ON COURSE	200.0
LOCALIZER	62

TABLE C - LOC/VOR INTEGRAL GAIN

VOR	0.133
LOCALIZER	.933

TABLE D - COURSE CUT LIMIT

VOR	34°
LOCALIZER	DAV 25° - $\overline{DAV}$ 35°

TABLE E - AUTOPILOT COMMAND DISPLACEMENT LIMIT

HEADING SELECT:	
TAS < 500 FT/SEC	30°
TAS > 500 FT/SEC	
OPTION A	30°
OPTION B	10°
INS, VOR, LOC:	
CAPTURE	30°
ON COURSE + LOC APPR	10°
FLARE	5°

TABLE F - AUTOPILOT COMMAND ROLL RATE LIMIT

HDG SELECT	1.5° TO 3°/SEC FUNCTION OF COMMAND
TURN KNOB	4.0°/SEC
LOC CAPTURE	7.0°/SEC
(VOR + INS) ON COURSE	1.5°/SEC
OTHER	4.0°/SEC

TABLE G - FLIGHT DIRECTOR GAIN SWITCH

AUTOPILOT A OR B IN COMMAND AND LOC MODE	.5
OTHER	1.00

TABLE H - FLIGHT DIRECTOR COMMAND DISPL LIMIT

FLARE	5°
(VOR + LOC + INS) ON COURSE	10°
OTHER	30°

TABLE I - FLIGHT DIRECTOR COMMAND, RATE LIMIT

(INS+VOR) ON COURSE	1.5°/SEC
(INS+VOR) CAPT + LOC O/C	4.0°/SEC
OTHER	9.0°/SEC

FIG a TAS GAIN PROGRAM (FOR LOC MODE, THE GAIN IS 1.59, INDEPENDENT OF TAS)

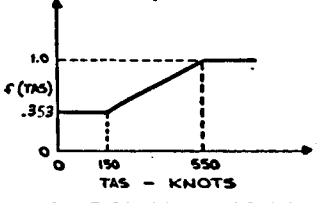

FIG b ALTITUDE GAIN PROGRAM (LOC AND RADIO ALT VALID)

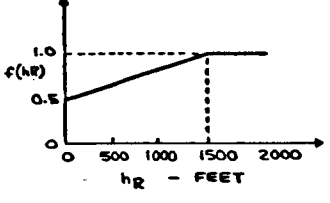

FIG c TIME BASE GAIN PROGRAM (LOC AND RADIO ALT INVALID ONLY)

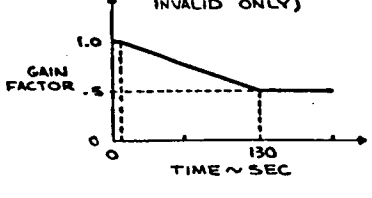

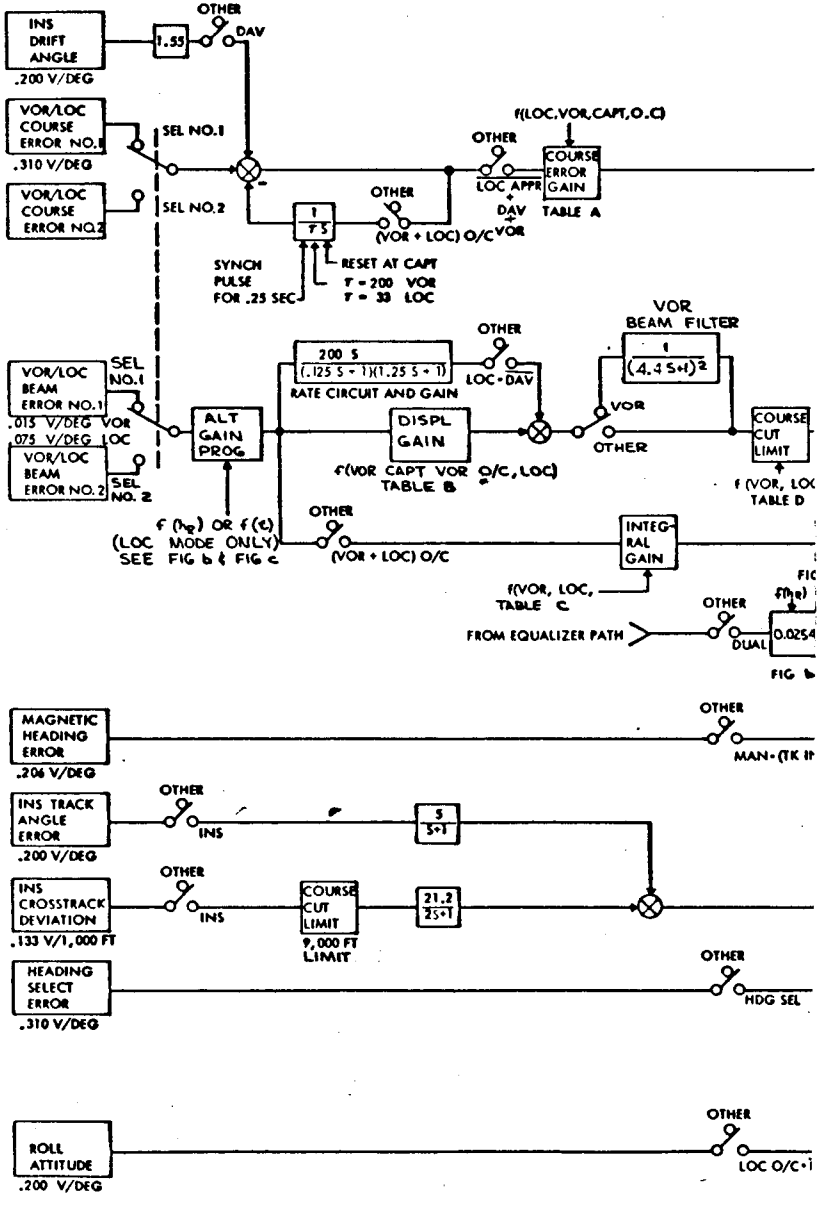

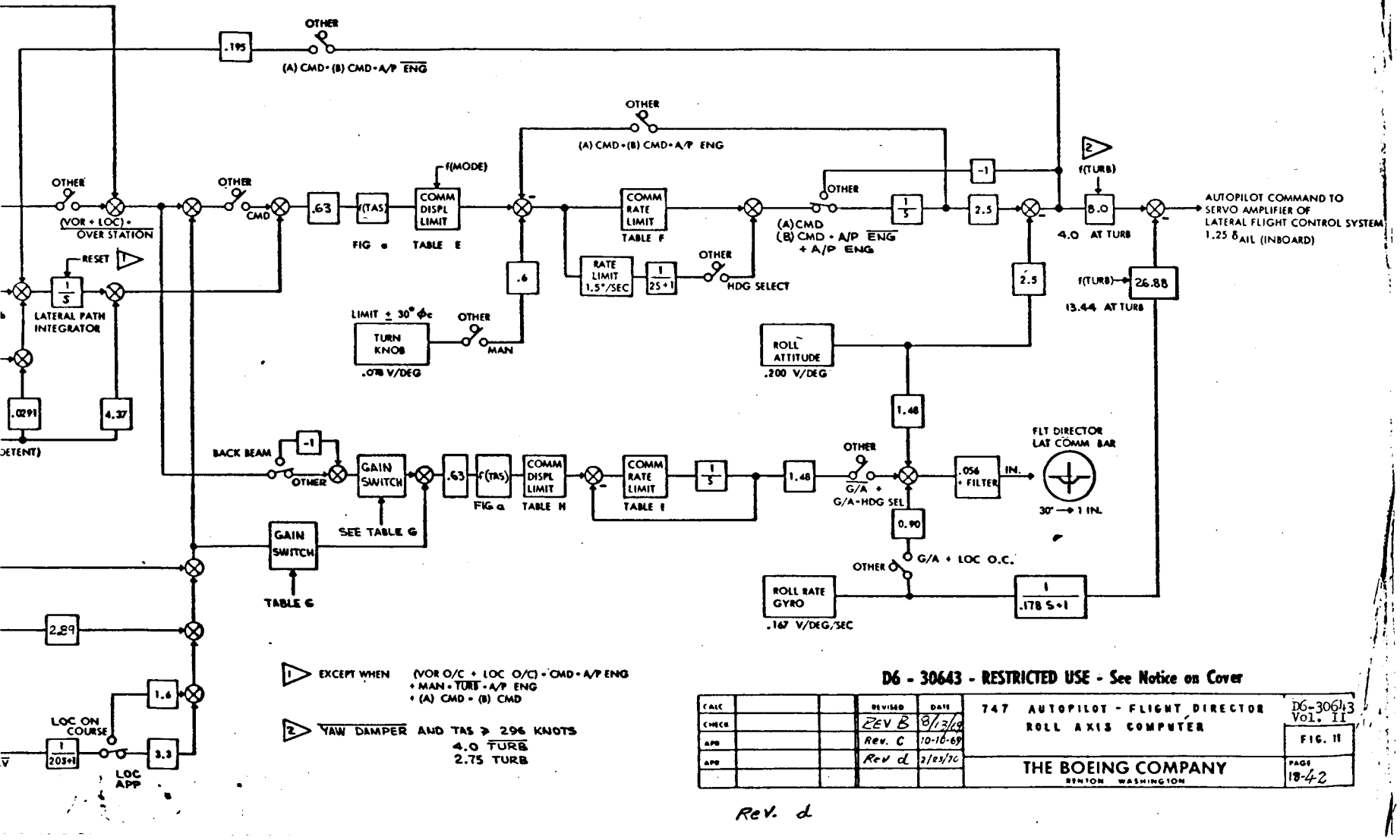

1 EXCEPT WHEN (VOR O/C • LOC O/C) • CMD • A/P ENG + MAN • TURB • A/P ENG + (A) CMD • (B) CMD

2 YAW DAMPER AND TAS ≥ 296 KNOTS
4.0 TURB
2.75 TURB

D6 - 30643 - RESTRICTED USE - See Notice on Cover

CALC			REVISED	DATE	747 AUTOPILOT - FLIGHT DIRECTOR ROLL AXIS COMPUTER	D6-30643 Vol. II	
CHECK			REV B	8/13/69		FIG. 11	
APD			Rev. C	10-16-69			
APD			Rev d	2/03/70	THE BOEING COMPANY RENTON WASHINGTON	PAGE 18-42	

Rev. d

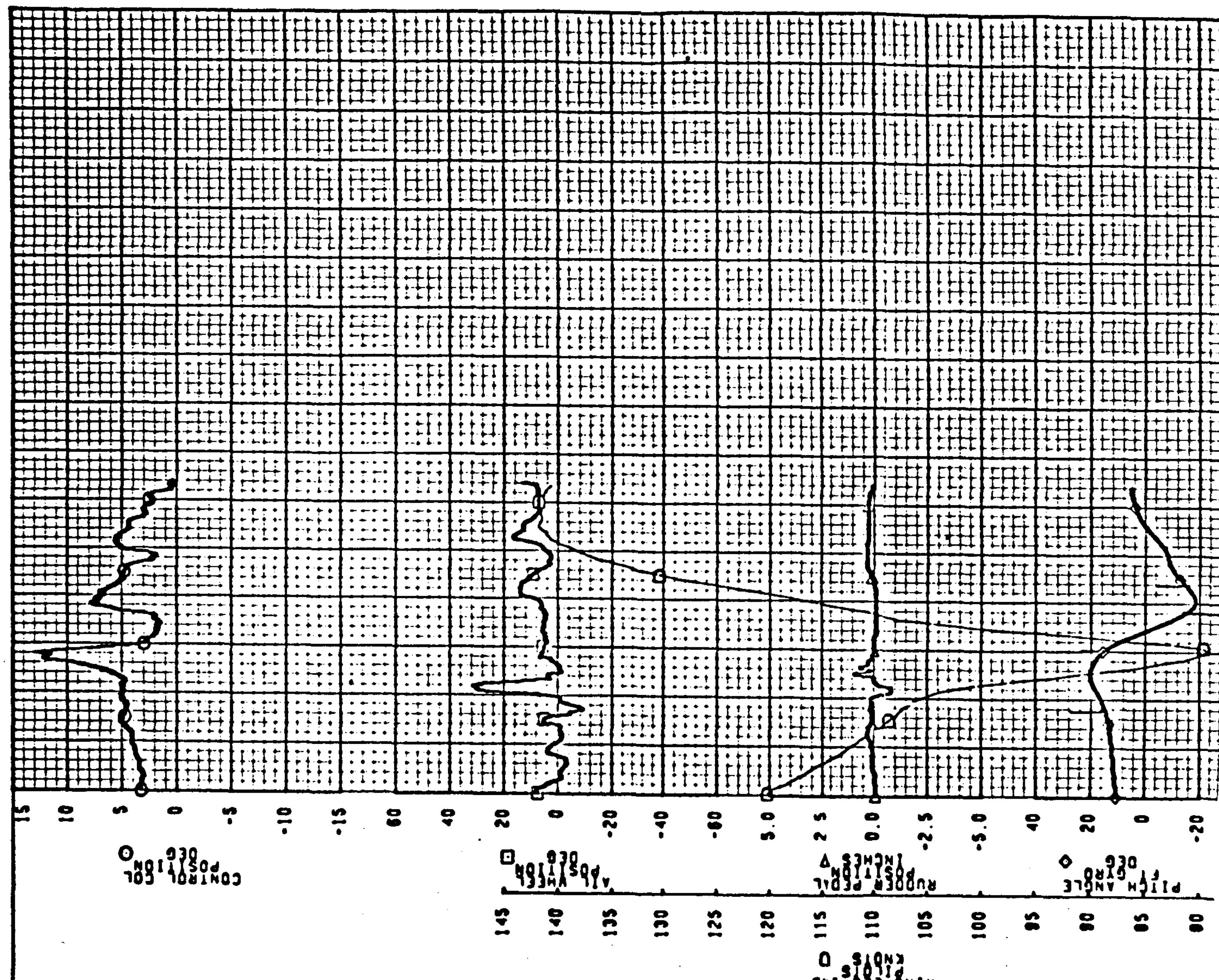

SC4020 PLOT 01/22/70 1323	747 SIMULATOR FLIGHT DECK VIBRATION ENVIRONMENT	747-100 RA101
CALC / CHECK / APPD / APPD — REVISED / DATE	COND NO 1 14 051 019 0 TEST 004-03	D6-30643 Vol. II
	THE BOEING COMPANY	PAGE 16.0-12

STALL CHARACTERISTICS
GROSS WEIGHT 525,000 LBS
CG 33.3 PERCENT MAC
FLAP SET 30 DEG—GEAR DN
ENTRY RATE 1.0 KNOTS/SEC

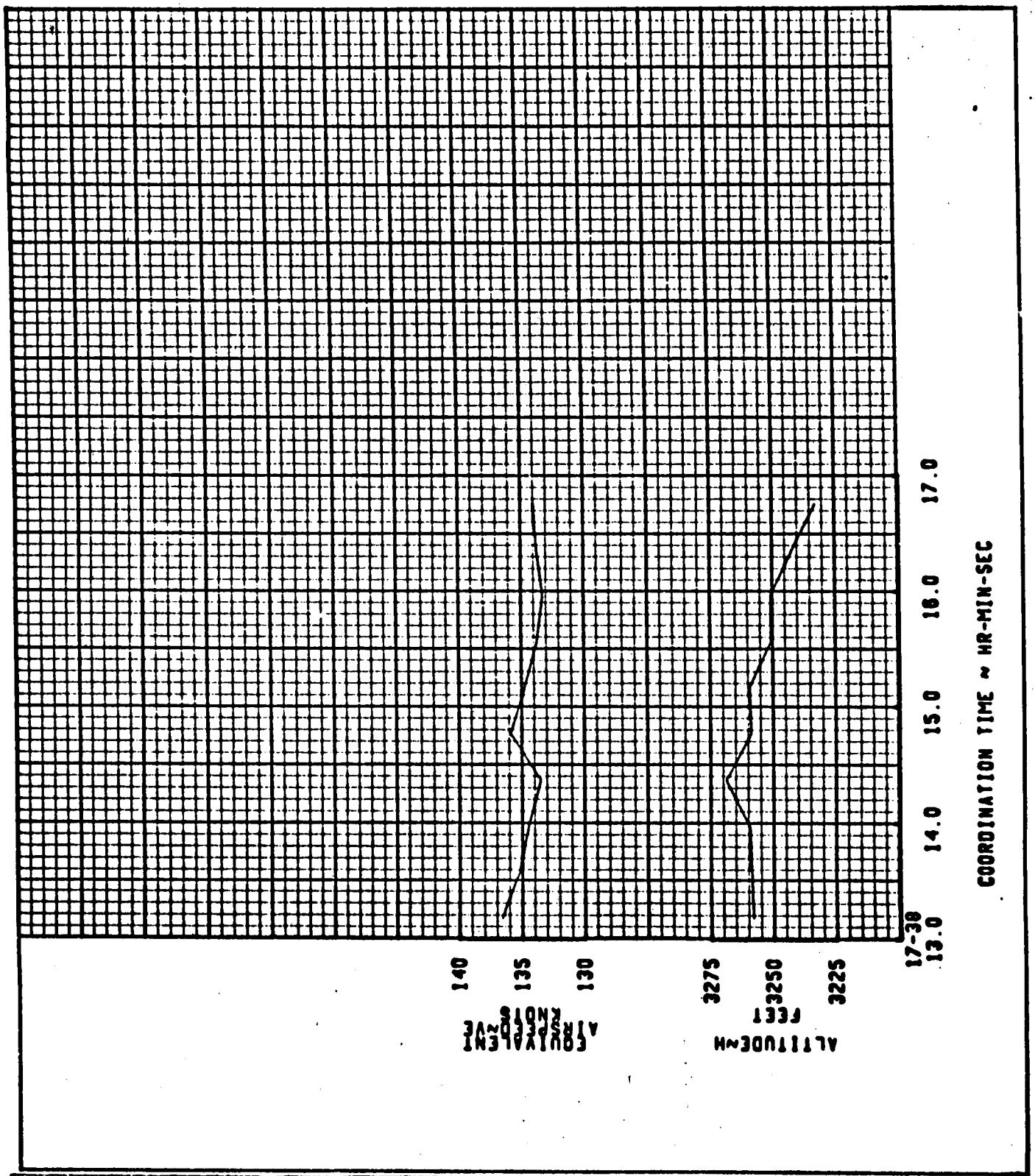

SC4020 PLOT 11/13/69 1639				
CALC			REVISED	DATE
CHECK				
APPD				
APPD				

FLIGHT DATA FOR SIMULATOR

COND NO 1.00.000.010 TEST 009-05

747-100
RA101

D6-30643
Vol. II

THE BOEING COMPANY
RENTON WASHINGTON

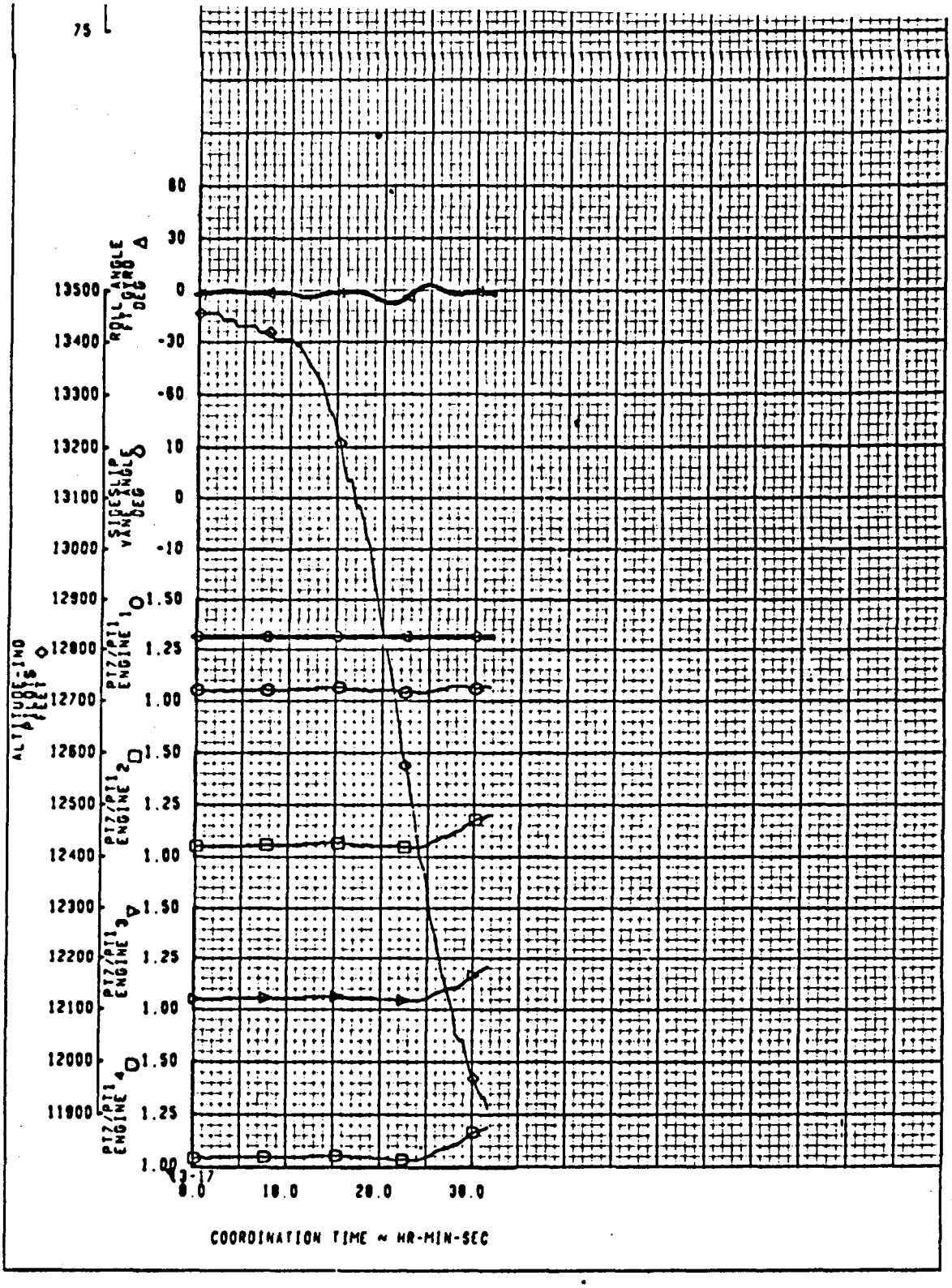
75
ALTITUDE-IND FEET ◇
13500
13400
13300
13200
13100
13000
12900
12800
12700
12600
12500
12400
12300
12200
12100
12000
11900
ROLL ANGLE DEG △
80
30
0
-30
-60
SIDESLIP VANE ANGLE DEG ▽
10
0
-10
PT2/PT1 ENGINE 1 ○
1.50
1.25
1.00
PT2/PT1 ENGINE 2 □
1.50
1.25
1.00
PT2/PT1 ENGINE 3 ▷
1.50
1.25
1.00
PT2/PT1 ENGINE 4 ○
1.50
1.25
1.00
3-17
0.0
10.0
20.0
30.0
COORDINATION TIME ~ HR-MIN-SEC

ACCELERATION
%
.1
150
125
100
75
150
125
100
75
150
125
100
75
5
0
-5
-10
120
100
80
60
40
20
0
RUDDER POS
DEG
EQUIVALENT
KNOTS
E3 PWR LEVER
DEG
E2 PWR LEVER
DEG
E1 PWR LEVER
DEG
18-21
58.0
18-22
3.0
0.0
13.0
18.0
23.0
28.0
33.0
COORDINATION TIME ~ HR-MIN-SEC

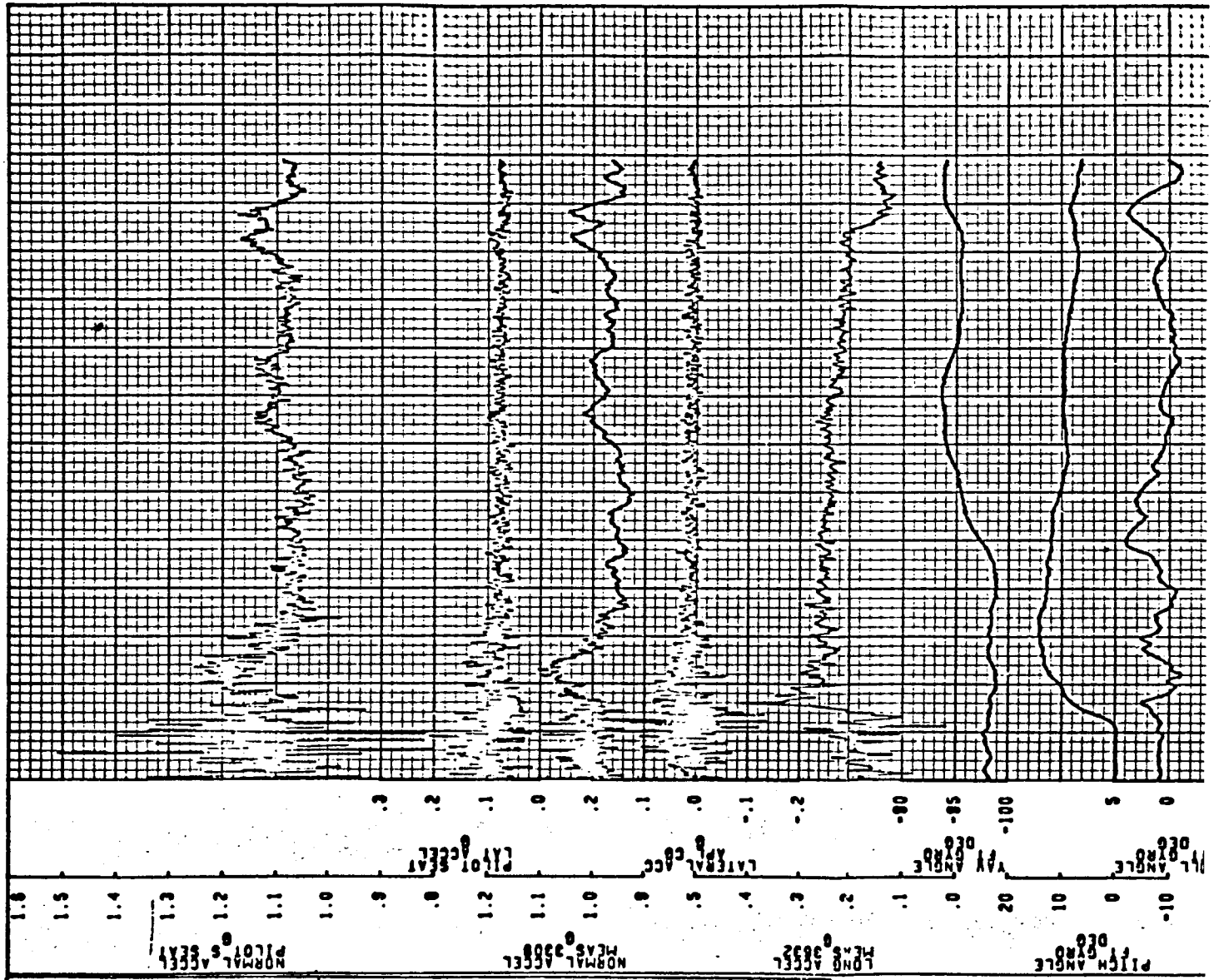

SC4020 PLOT 11/08/69 0950					FLIGHT DATA FOR SIMULATOR	747-100 RA101
CALC			REVISED	DATE		
CHECK					COND NO 1.00.000.004.0 TEST 009-01	D6-30643 Vol. II
APPD						
APPD					THE BOEING COMPANY RENTON WASHINGTON	PAGE 20.0-12

ROTATE AND INITIAL CL
FLAPS 10 GEAR DOWN
G.W. 663,000 CG 14.6

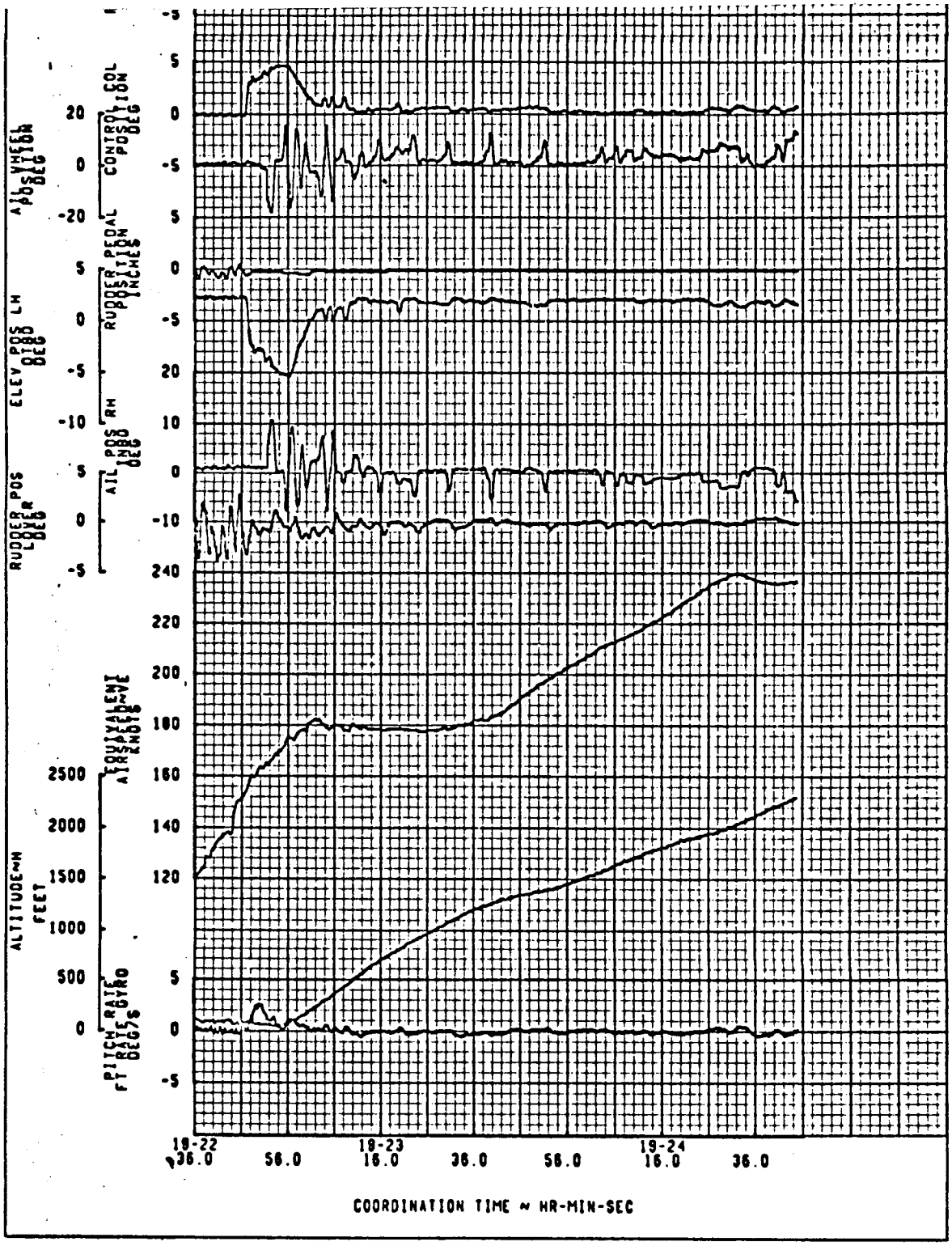
ALTITUDE-MN FEET
2500
2000
1500
1000
500
0
AIRSPEED EQUIVALENT KNOTS
240
220
200
180
160
140
120
PITCH RATE GYRO DEG/S
5
0
-5
AIL POS LWD DEG
20
10
0
-10
RUDDER PEDAL POSITION INCHES
5
0
-5
RUDDER POS LWD DEG
5
0
-5
ELEV POS LH GDS DEG
20
0
-5
-10
ABSOLUTE WHEEL POSITION DEG
20
0
-20
CONTROL COL POSITION DEG
5
0
-5
19-22 36.0
56.0
19-23 16.0
36.0
56.0
19-24 16.0
36.0
COORDINATION TIME ~ HR-MIN-SEC

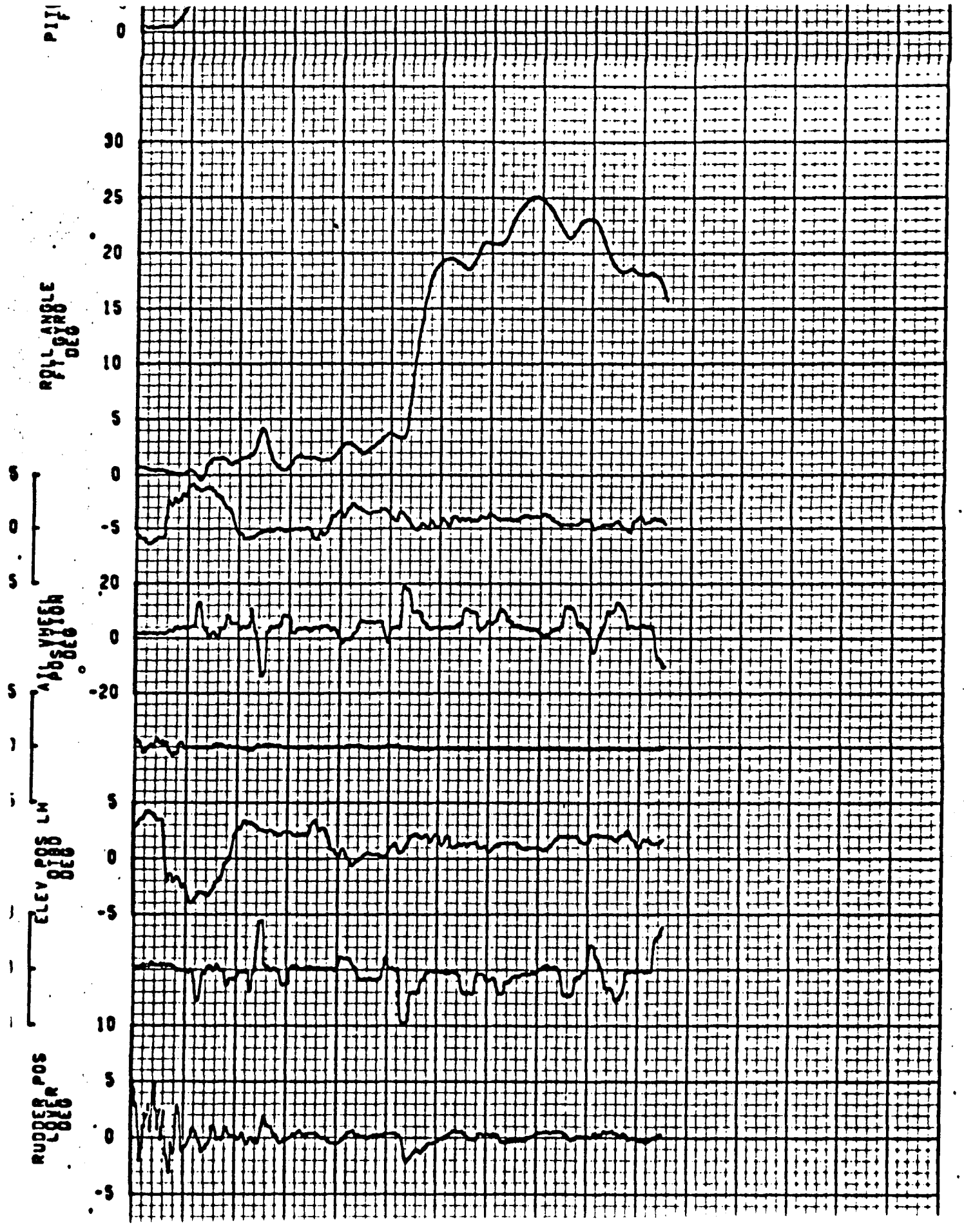
PITCH
ROLL ANGLE DEG
ABS YAW DEG
ELEV POS LH DEG
RUDDER POS DEG
0
30
25
20
15
10
5
0
-5
20
0
-20
5
0
-5
10
5
0
-5

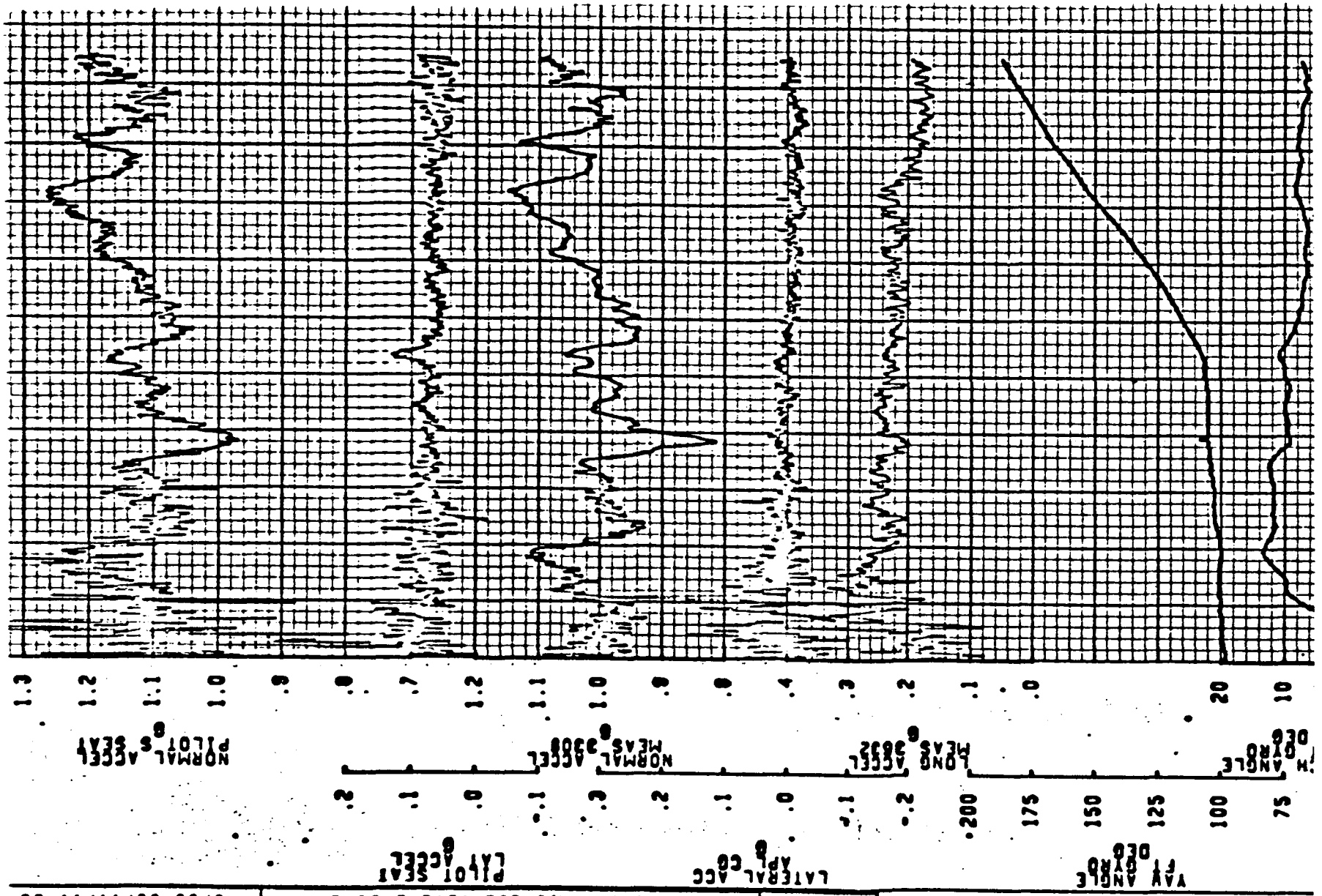

LOT 11/11/69 0246				FLIGHT DATA FOR SIMULATOR	747-100 RA101
		REVISED	DATE		
				COND NO 1.00.008.004.0 TEST 008-02	D6-30643 Vol. II
				THE BOEING COMPANY RENTON WASHINGTON	PAGE 20.0-13

TAKE OFF ROTATION A
FLAPS UP GEAR UP
GROSS WEIGHT = 564,200
C.G. POSITION = 18.2 % M

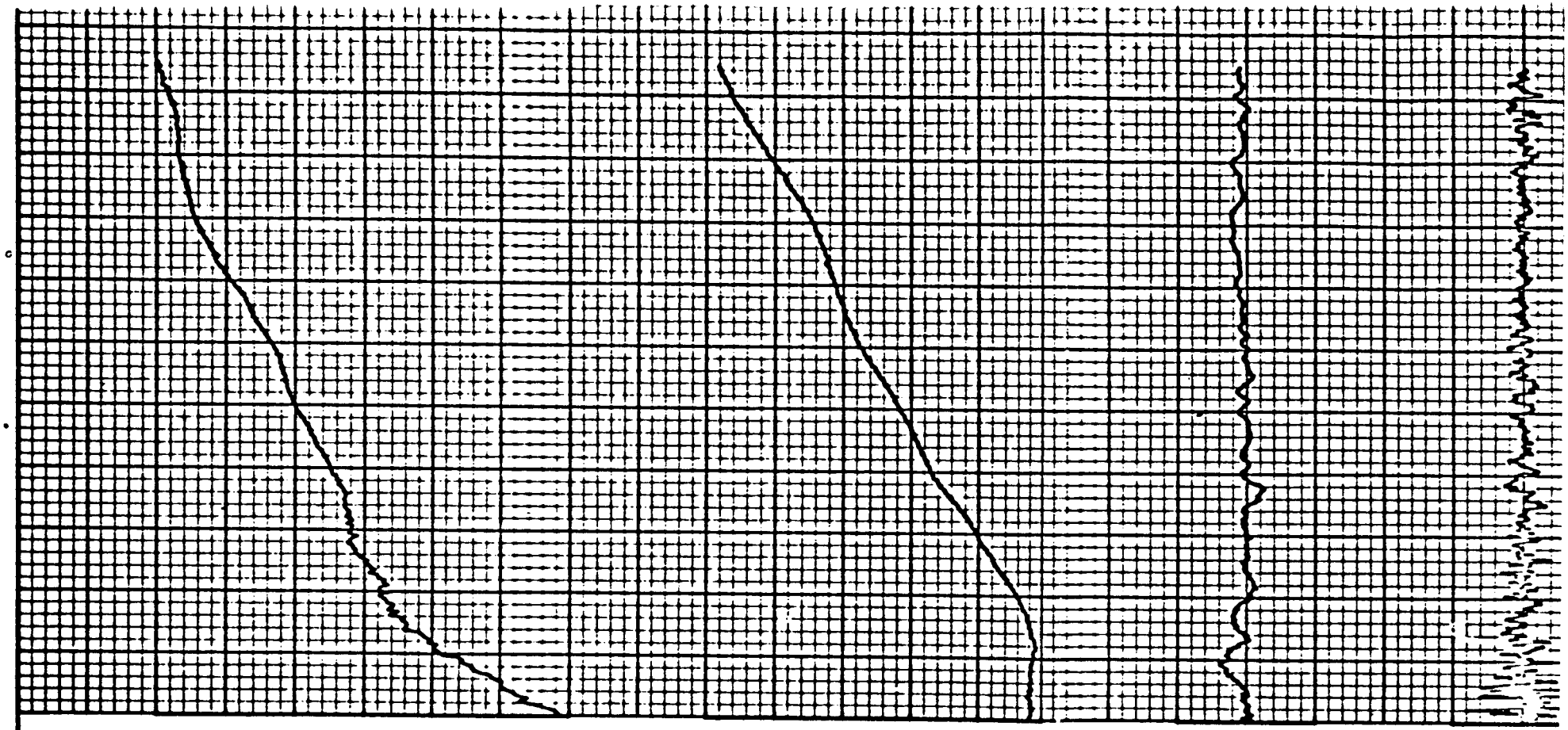

SC4020 PLOT 11/11/69 0246					FLIGHT DATA FOR SIMULATOR	747-100 RA101
CALC			REVISED	DATE		
CHECK					COND NO 1.00.008.004.0 TEST 009-02	D6-30643 Vol. II
APPD						
APPD					THE BOEING COMPANY RENTON WASHINGTON	PAGE 20.0-14

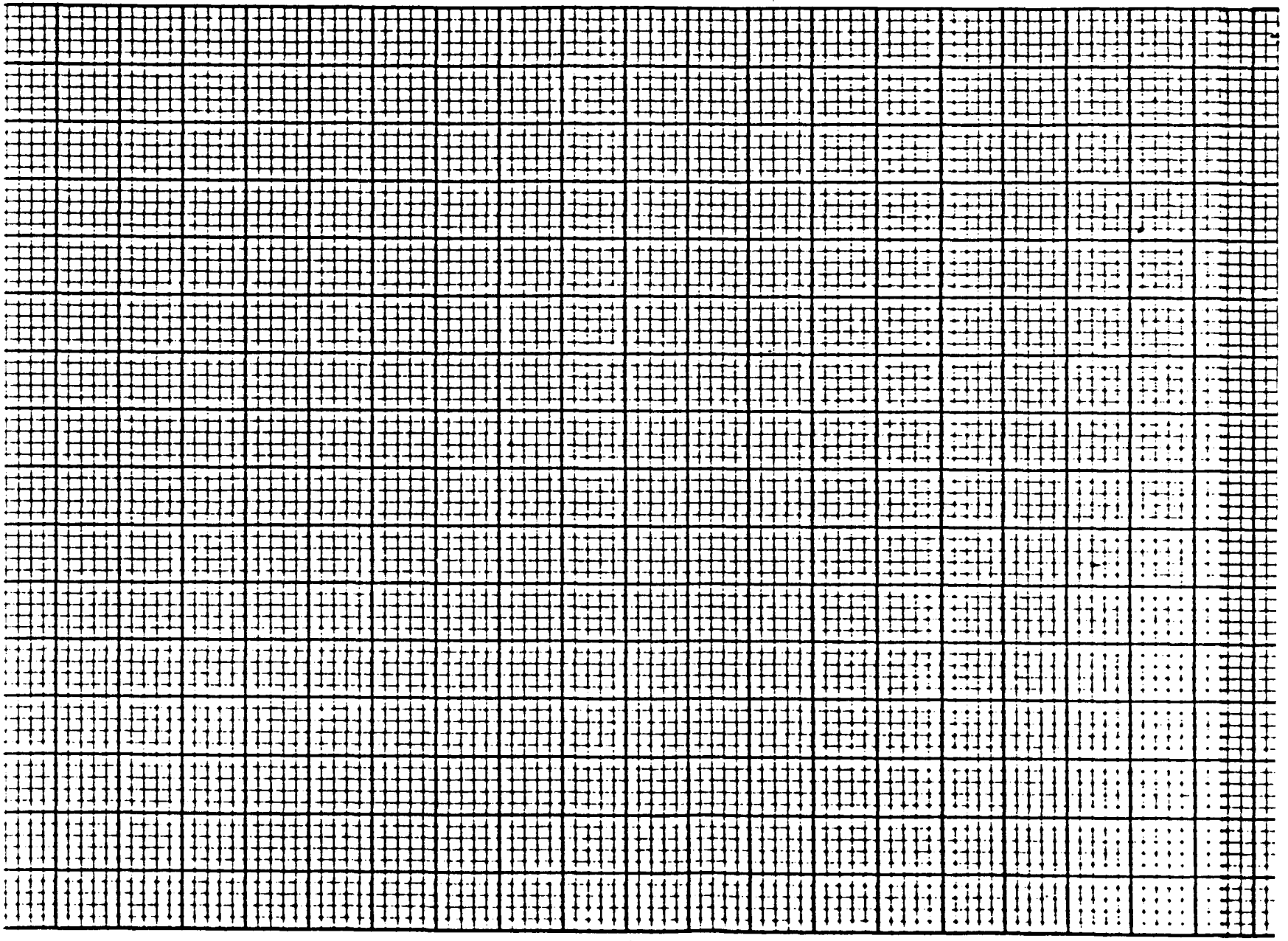

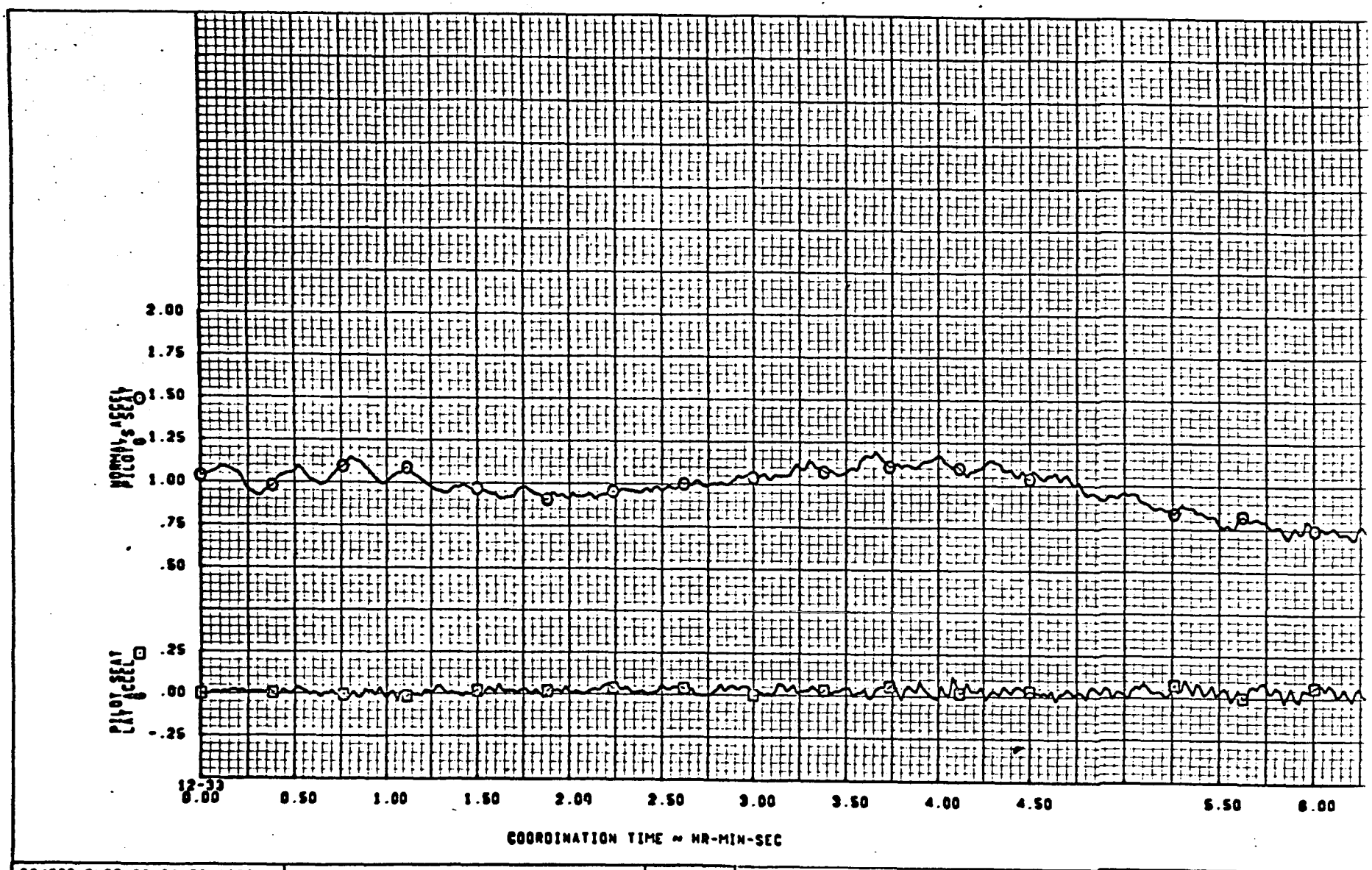

SC4020 PLOT 02/23/70 1950				
CALC			REVISED	DATE
CHECK				
APPD				
APPD				

747 SIMULATOR
FLT. DECK VIBRATION ENVIRONMENT
M_D - CLEAN AIRPLANE
COND NO 4.08.001.882.0 TEST 021-01

THE BOEING COMPANY RENTON WASHINGTON

747-100
RA001

D6-30643
Vol. II

PAGE
16.0-3

HI SPEED CHARACTERISTIC - M_D
GROSS WEIGHT 464,300 LBS
CG 26.7 PERCENT MAC
FLAP SET 0 DEG--GEAR UP

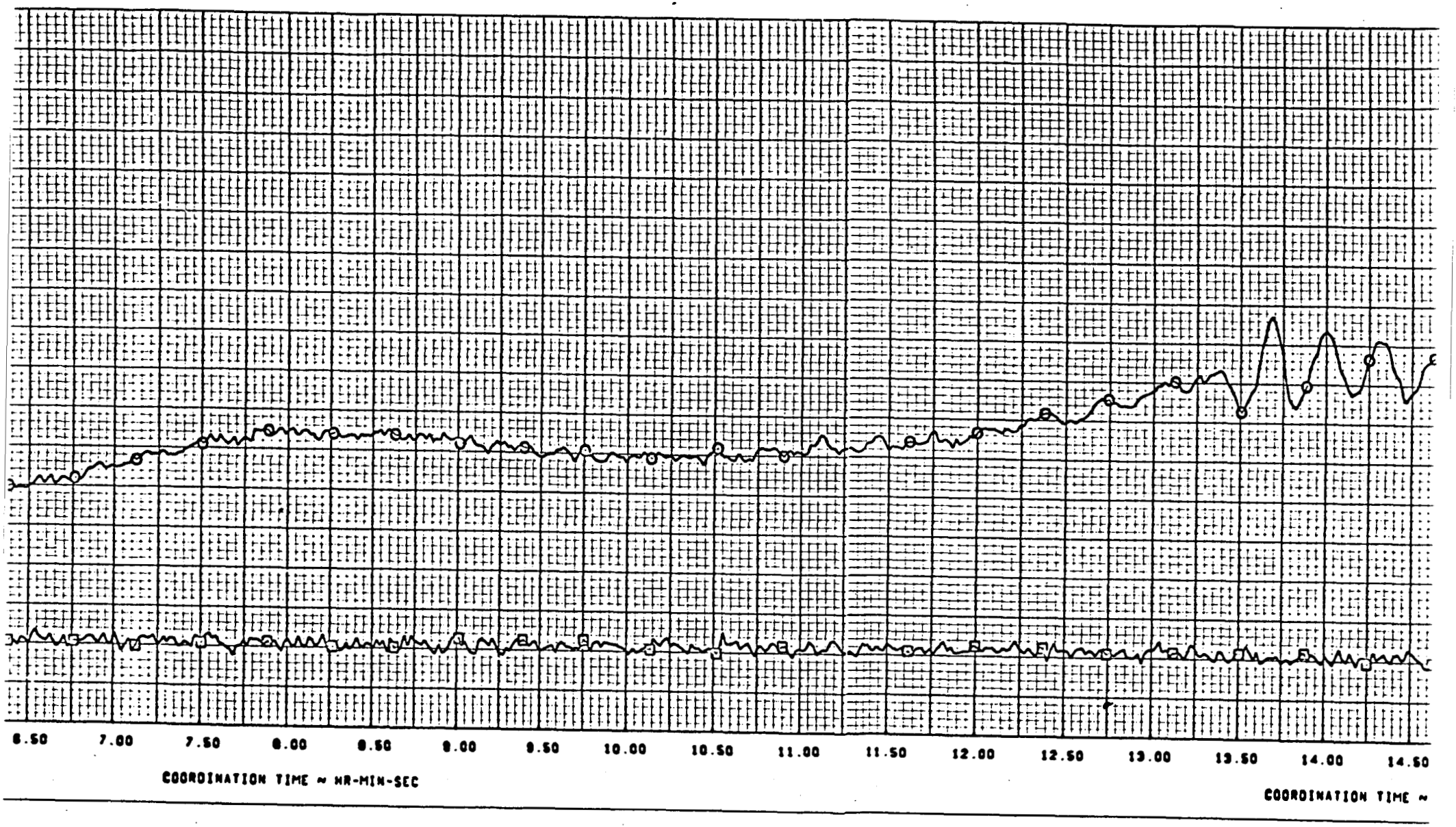
6.50
7.00
7.50
8.00
8.50
9.00
9.50
10.00
10.50
11.00
11.50
12.00
12.50
13.00
13.50
14.00
14.50
COORDINATION TIME ~ HR-MIN-SEC
COORDINATION TIME ~

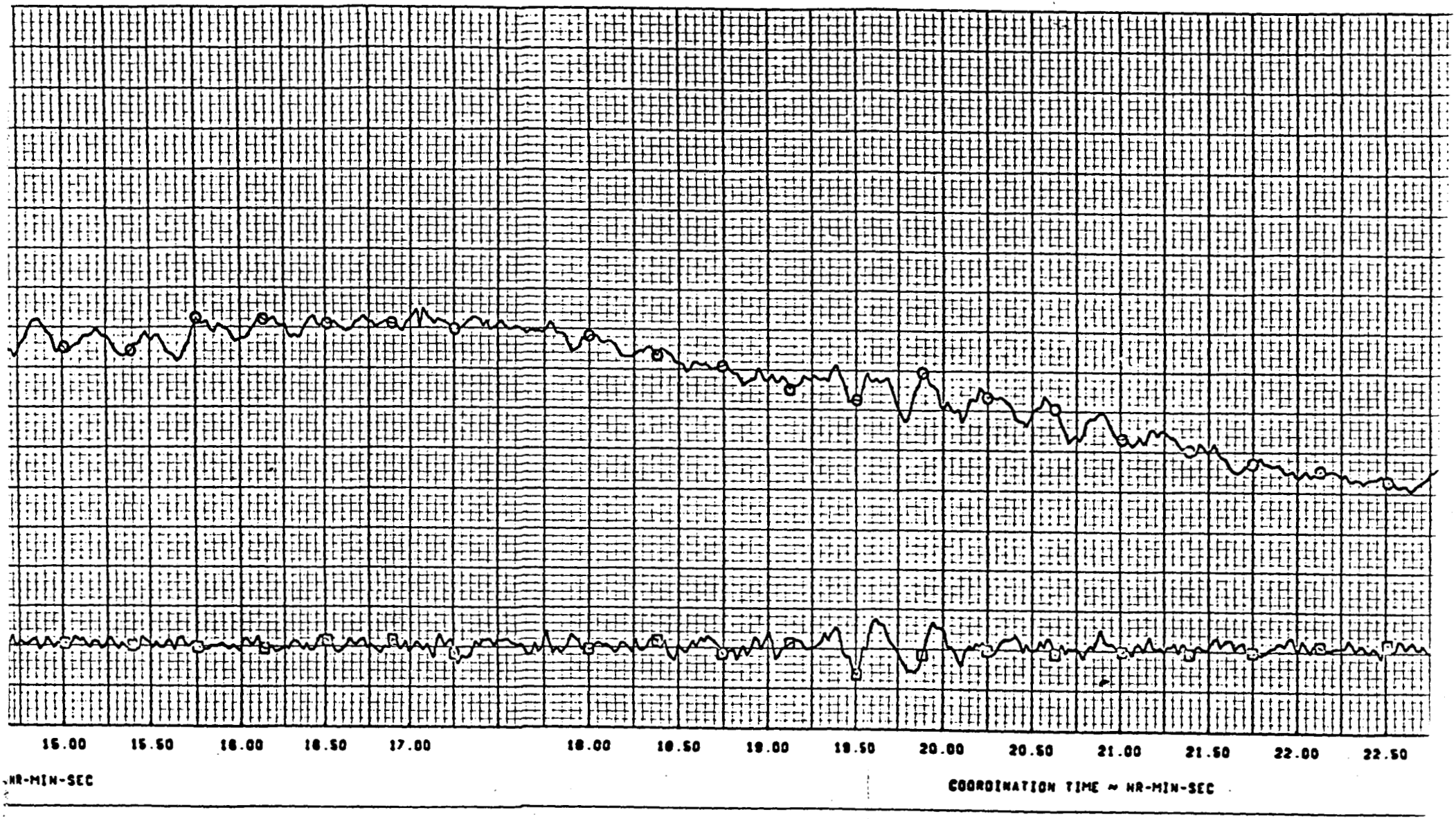
15.00
15.50
16.00
16.50
17.00
18.00
18.50
19.00
19.50
20.00
20.50
21.00
21.50
22.00
22.50
HR-MIN-SEC
COORDINATION TIME ~ HR-MIN-SEC

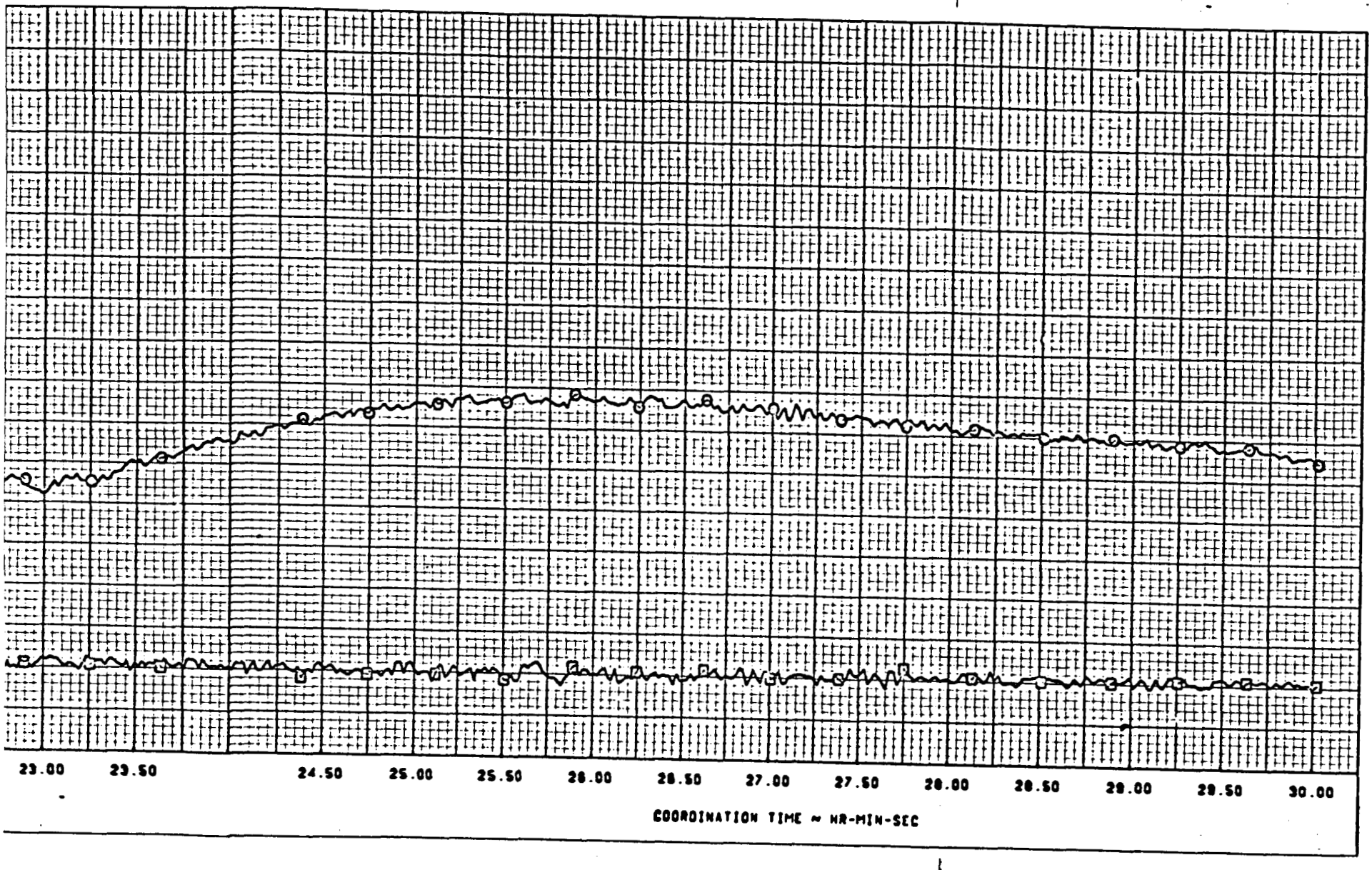
23.00
23.50
24.50
25.00
25.50
26.00
26.50
27.00
27.50
28.00
28.50
29.00
29.50
30.00
COORDINATION TIME ~ HR-MIN-SEC

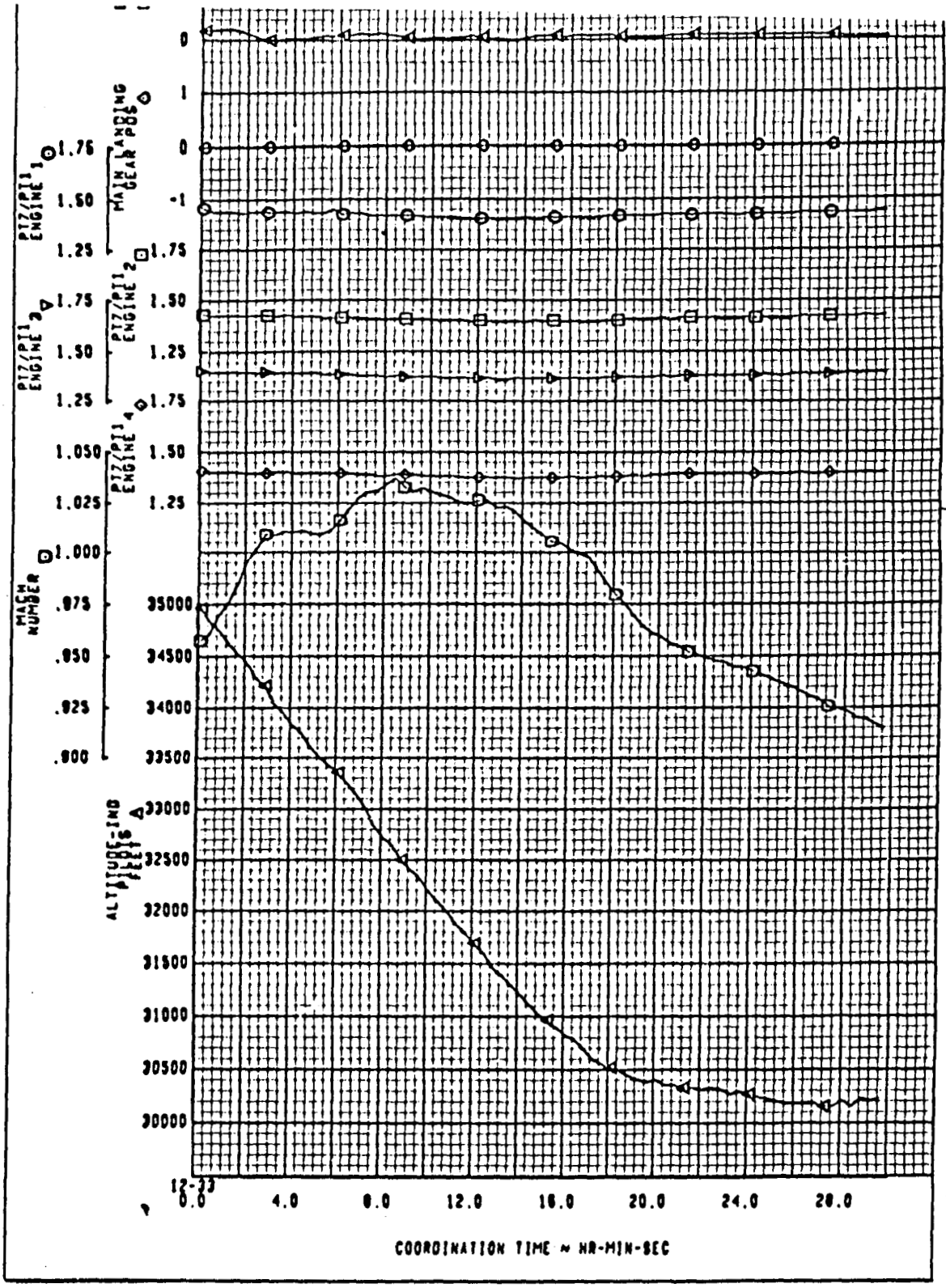
MACH NUMBER
PIZ/PI1 ENGINE 1
PIZ/PI1 ENGINE 2
PIZ/PI1 ENGINE 3
PIZ/PI1 ENGINE 4
MAIN LANDING GEAR POS
ALTITUDE-IND FEET
1.75
1.60
1.25
1.75
1.50
1.25
1.050
1.025
1.000
.975
.950
.925
.900
0
1
0
-1
1.75
1.50
1.25
1.75
1.50
1.25
35000
34500
34000
33500
33000
32500
32000
31500
31000
30500
30000
12-33
0.0
4.0
8.0
12.0
16.0
20.0
24.0
28.0
COORDINATION TIME ~ HR-MIN-SEC

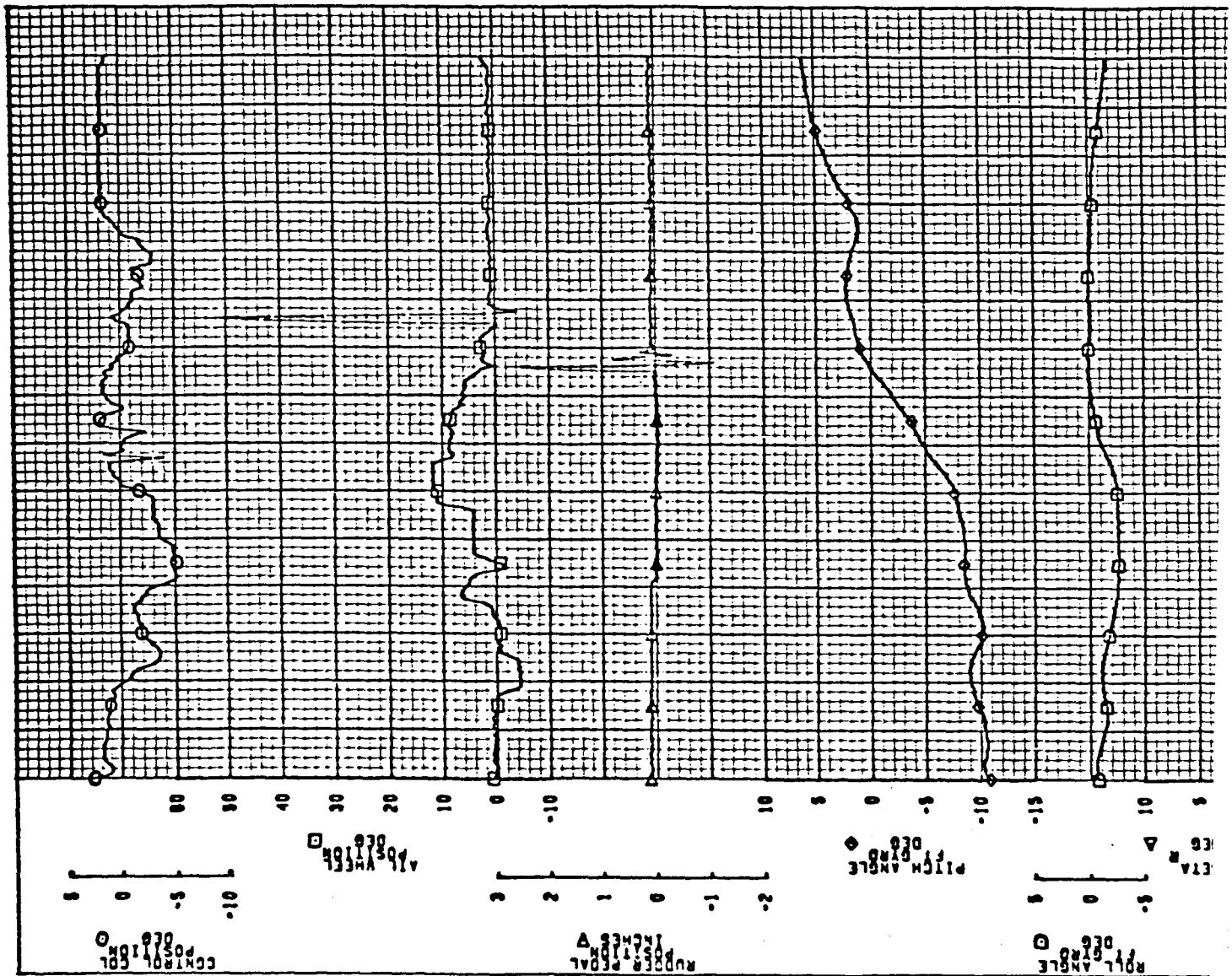

SC4020 PLOT 03/13/73 1047	747 SIMULATOR FLT. DECK VIBRATION ENVIRONMENT M_D - CLEAN AIRPLANE COND NO 4.08.001.882.0 TEST 021-01	747-100 RA001	HI SPEED CHARACTERISTIC - M_D GROSS WEIGHT 464,300 LBS CG 26.7 PERCENT MAC FLAP SET 0 DEG--GEAR UP
CALC / REVISED / DATE		D6-30643 Vol. II	
CHECK	THE BOEING COMPANY	PAGE 16.0-4	
APPD			
APPD			

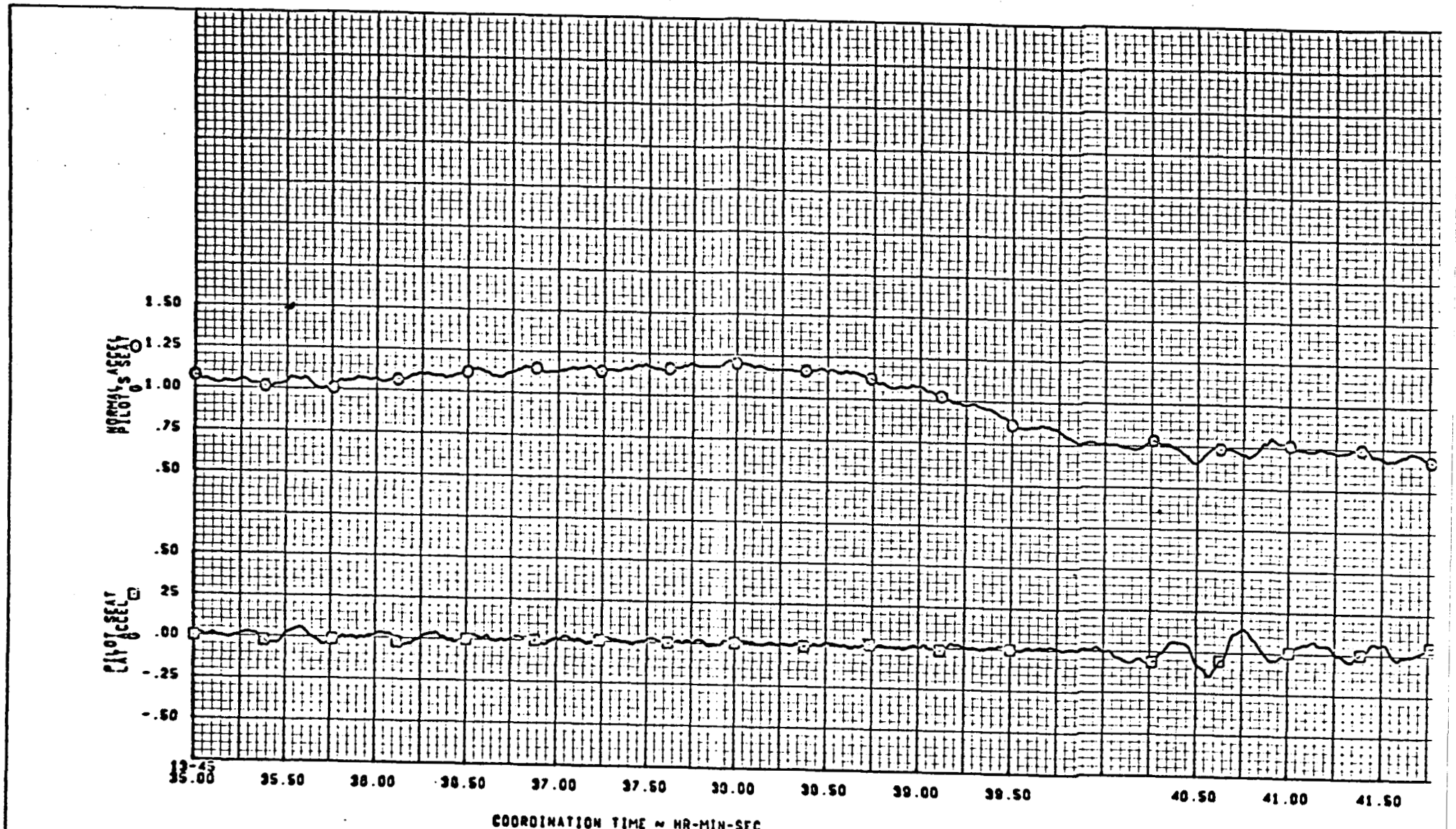

SC4020 PLOT 02/23/70 2001				
CALC			REVISED	DATE
CHECK				
APPD				
APPD				

747 SIMULATOR
FLT. DECK VIBRATION ENVIRONMENT
V_D - CLEAN AIRPLANE
COND NO 4.03.001.070.0 TEST 050-14
THE BOEING COMPANY
RENTON WASHINGTON

747-100
RA001
D6-30643
Vol. II
PAGE
16.0-5

HI SPEED CHARACTERISTIC - V_D
GROSS WEIGHT 489,500 LBS
CG 24.7 PERCENT MAC
FLAP SET 0 DEG--GEAR UP

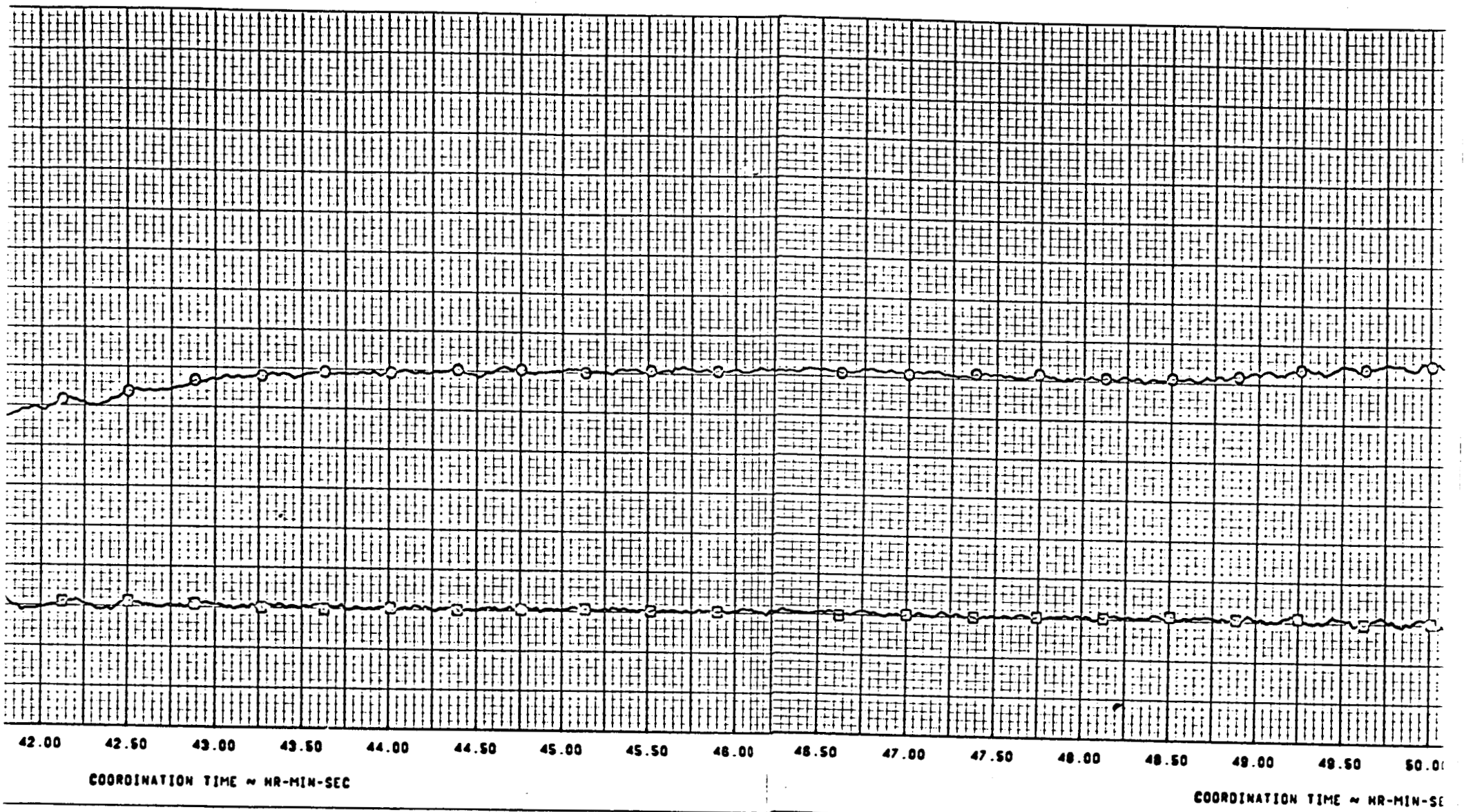
42.00
42.50
43.00
43.50
44.00
44.50
45.00
45.50
46.00
46.50
47.00
47.50
48.00
48.50
49.00
49.50
50.0
COORDINATION TIME ~ HR-MIN-SEC
COORDINATION TIME ~ HR-MIN-SE

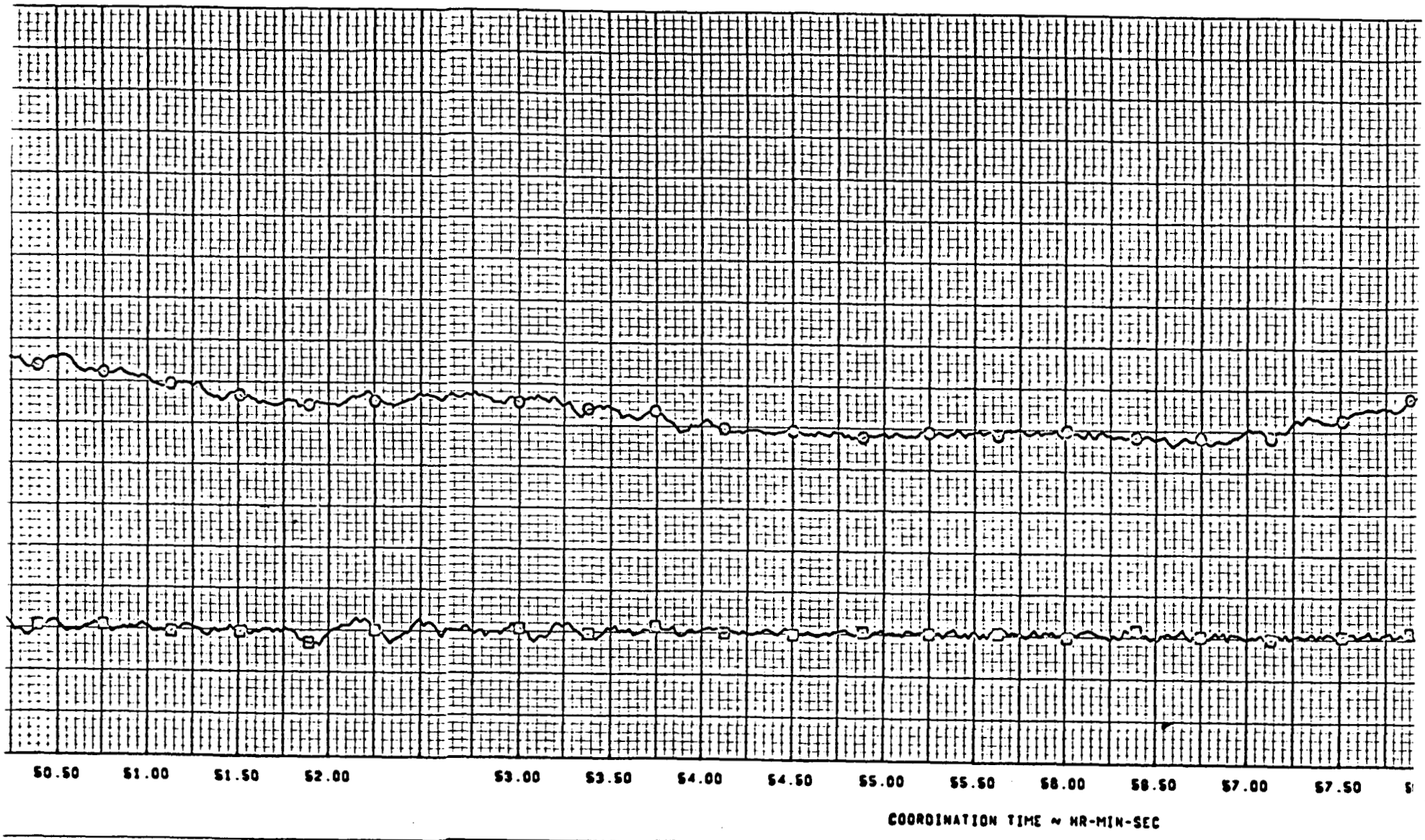
00.50
01.00
01.50
02.00
03.00
03.50
04.00
04.50
05.00
05.50
06.00
06.50
07.00
07.50
COORDINATION TIME ~ HR-MIN-SEC

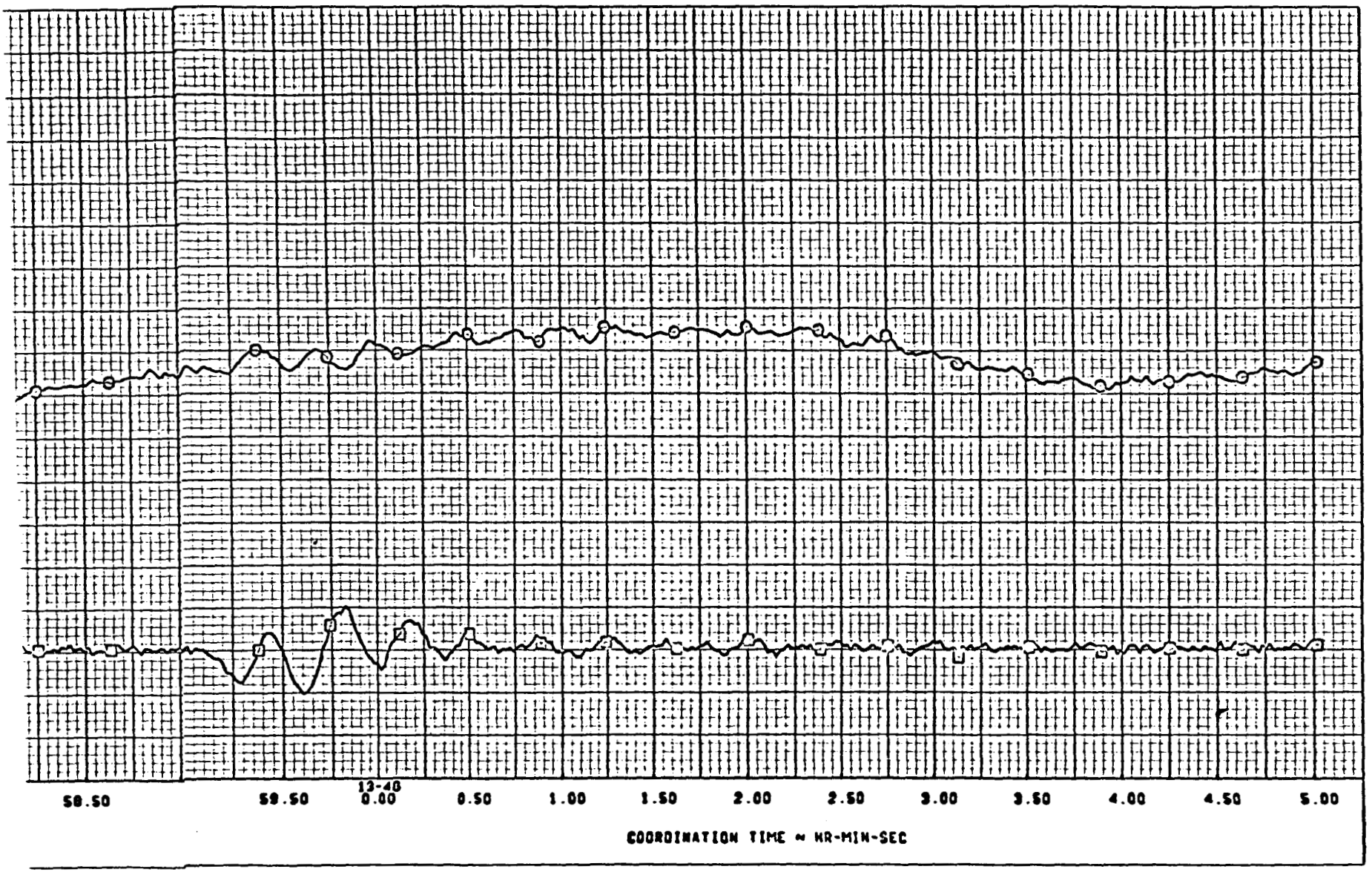
58.50
59.50
13-40
0.00
0.50
1.00
1.50
2.00
2.50
3.00
3.50
4.00
4.50
5.00
COORDINATION TIME ~ HR-MIN-SEC

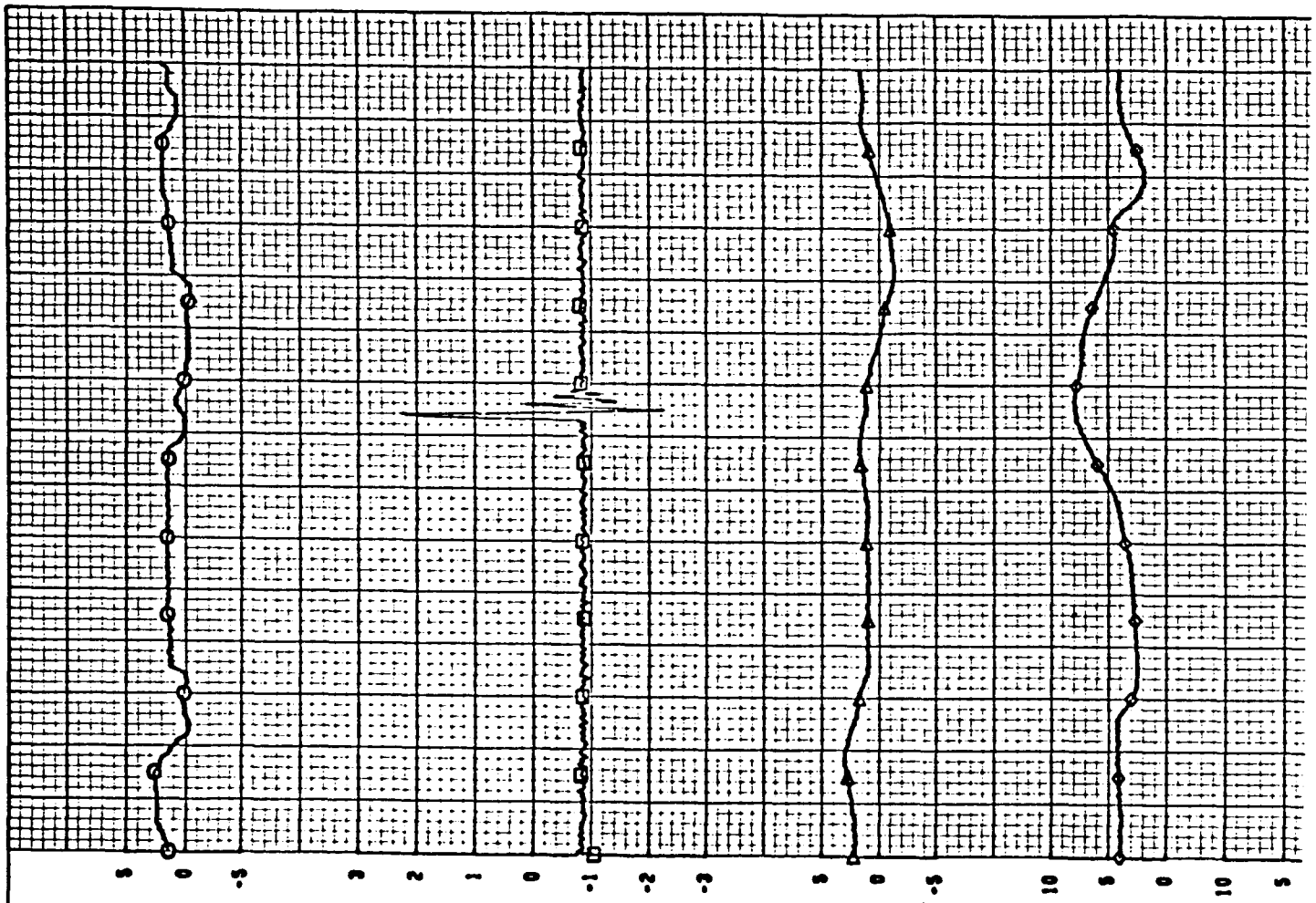

SC4020 PLOT 02/17/70 1831				
CALC			REVISED	DATE
CHECK				
APPD				
APPD				

747 SIMULATOR
FLT. DECK VIBRATION ENVIRONMENT
V_D - CLEAN AIRPLANE
CONFIG NO 4.08.001.070.0 TEST 058-14

THE BOEING COMPANY
RENTON, WASHINGTON

747-100
RA001

D6-30643
Vol. II

PAGE
16.0-6

HI SPEED CHARACTERISTIC - V_D
GROSS WEIGHT 489,500 LBS
CG 24.7 PERCENT MAC
FLAP SET 0 DEG--GEAR UP

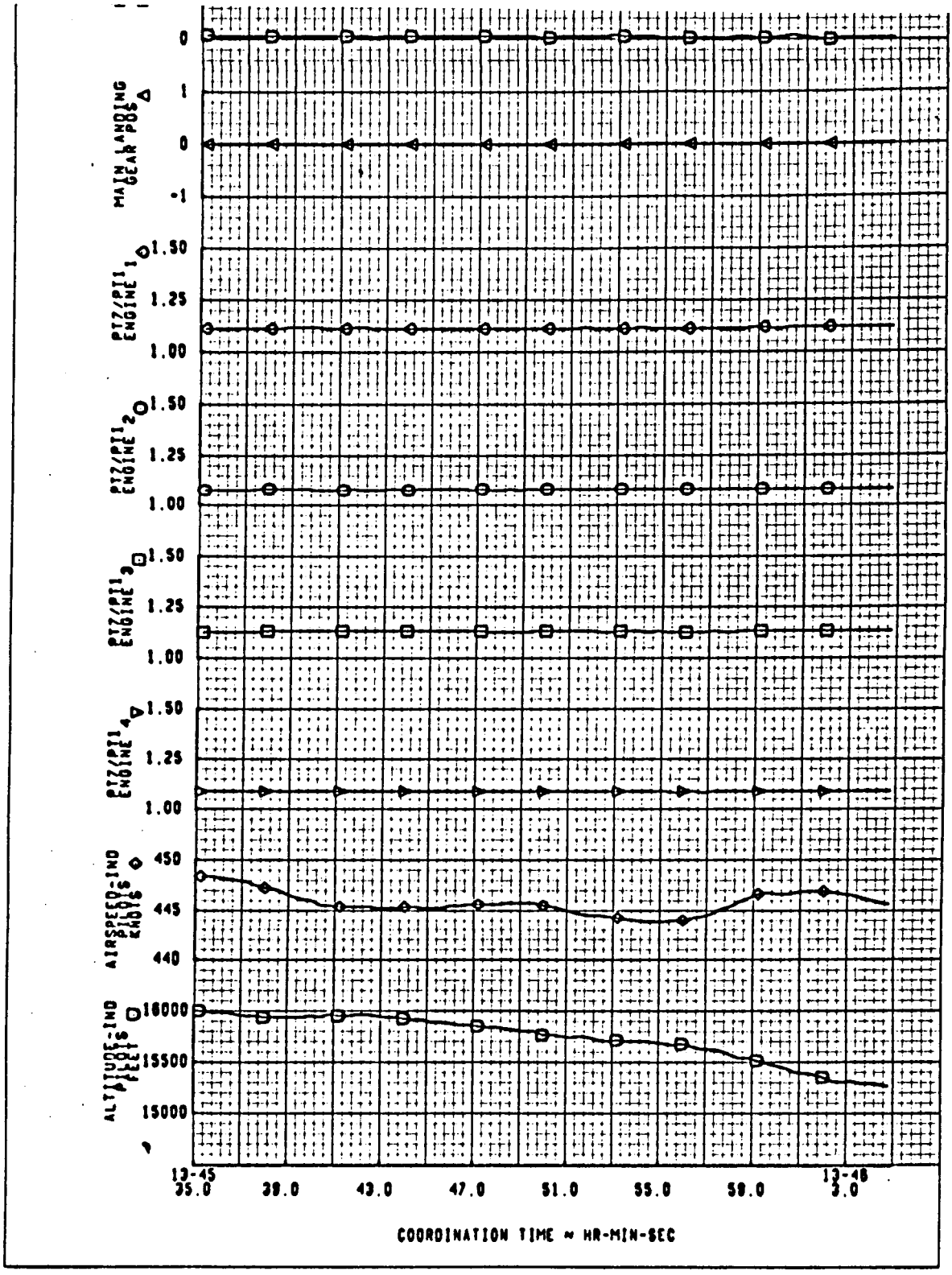
MAIN LANDING GEAR POS
0
1
0
-1
P2/P1 ENGINE 1
1.50
1.25
1.00
P2/P1 ENGINE 2
1.50
1.25
1.00
P2/P1 ENGINE 3
1.50
1.25
1.00
P2/P1 ENGINE 4
1.50
1.25
1.00
AIRSPEED-IND KNOTS
450
445
440
ALTITUDE-IND FEET
16000
15500
15000
13-45 35.0
38.0
43.0
47.0
51.0
55.0
58.0
13-46 3.0
COORDINATION TIME ~ HR-MIN-SEC

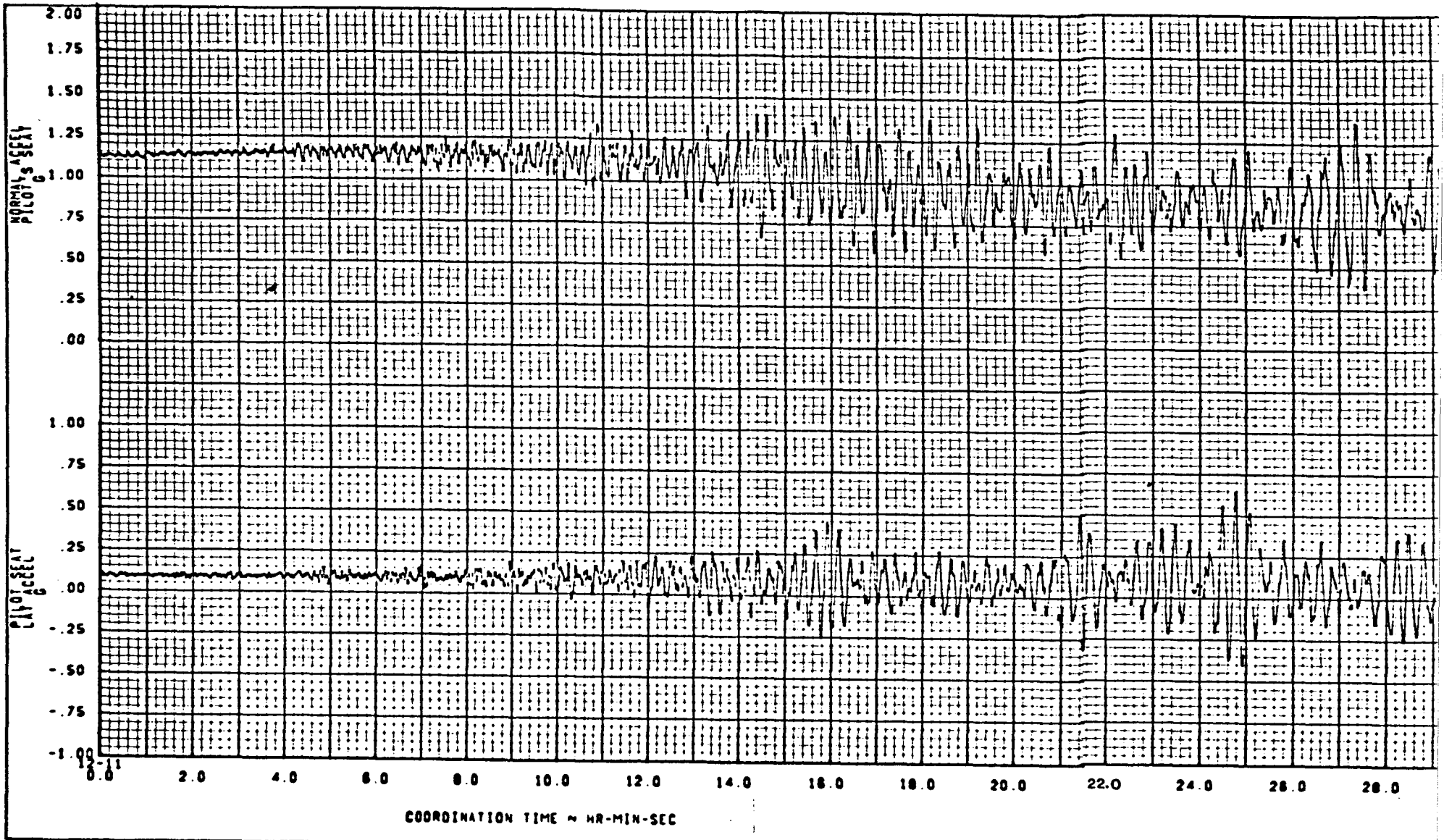

SC4020 PLOT 01/21/70 0940				
CALC			REVISED	DATE
CHECK				
APPD				
APPD				

747 SIMULATOR
FLIGHT DECK VIBRATION ENVIRONMENT

COND NO 1 14 051 002 0 TEST 004-03

THE BOEING COMPANY
RENTON, WASHINGTON

747-100
RA101

D6-30643
Vol. II

PAGE
16.0-7

STALL CHARACTERISTICS
GROSS WEIGHT 552,100 LBS
CG 32.0 PERCENT MAC
FLAP SET 0 DEG—GEAR UP
ENTRY RATE 1.0 KNOTS/SEC

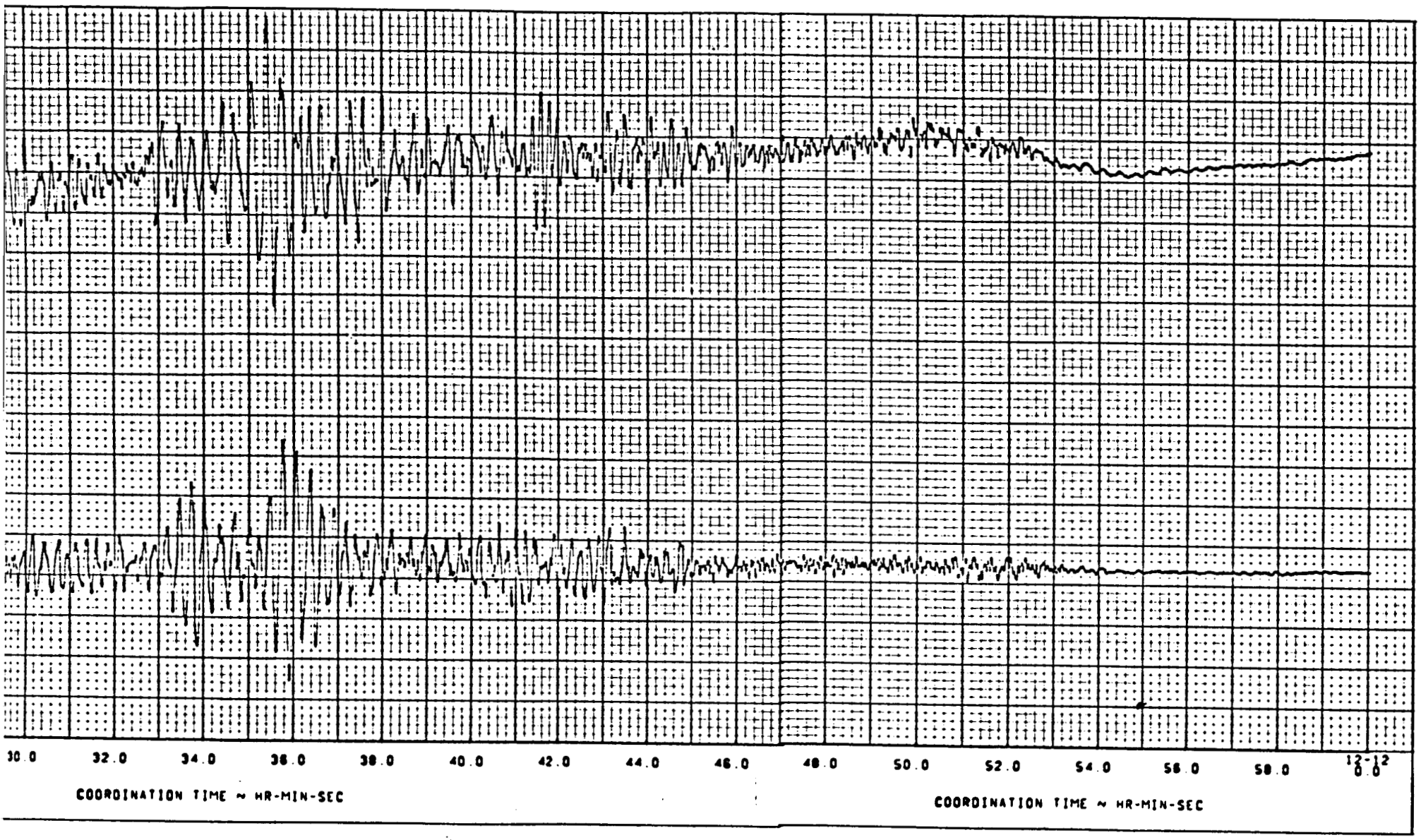
30.0
32.0
34.0
36.0
38.0
40.0
42.0
44.0
46.0
48.0
50.0
52.0
54.0
56.0
58.0
12-12
0.0
COORDINATION TIME ~ HR-MIN-SEC
COORDINATION TIME ~ HR-MIN-SEC

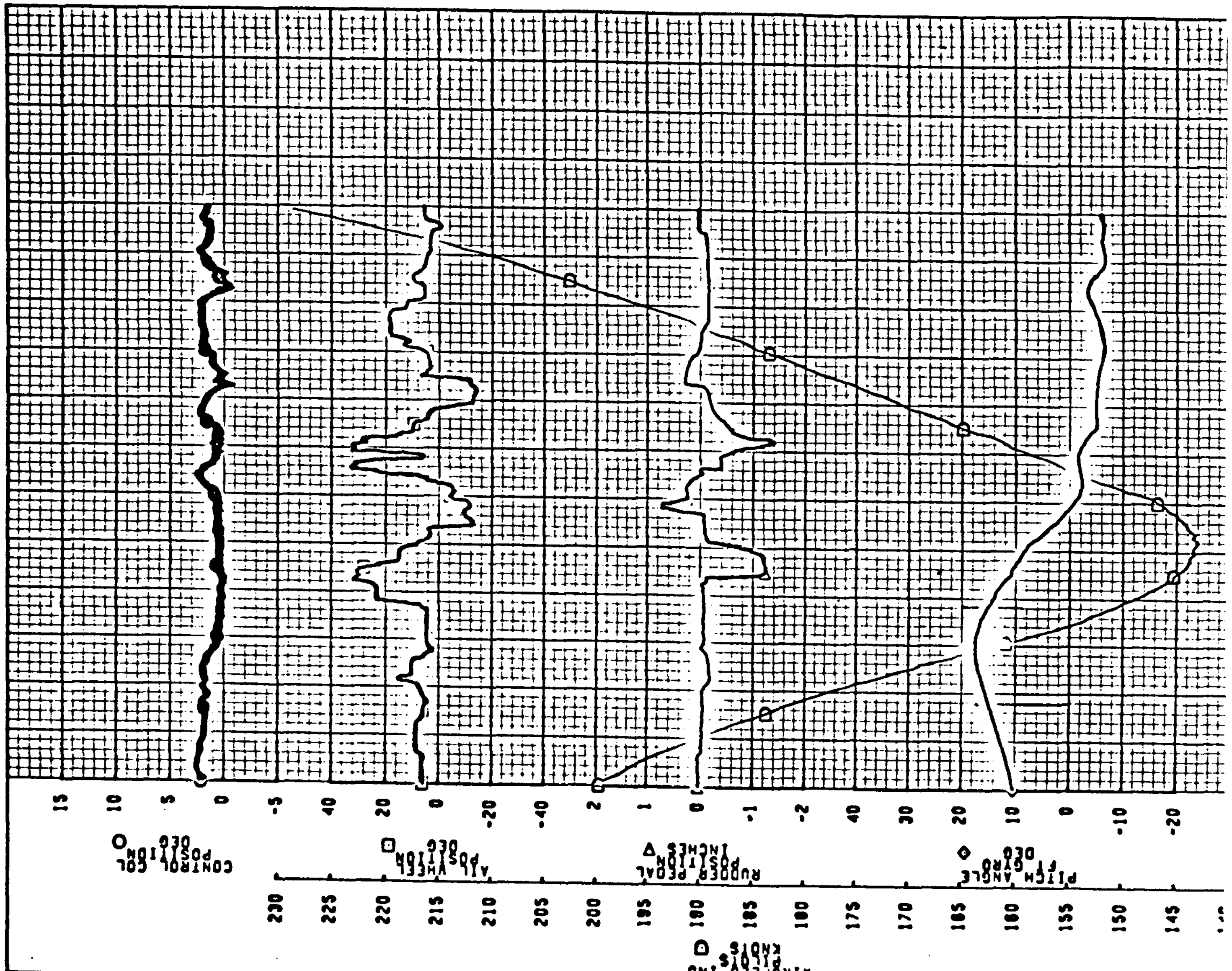

SC4020 PLOT 01/27/70 2043					747 SIMULATOR FLIGHT DECK VIBRATION ENVIRONMEN	747-100 RA101	
CALC			REVISED	DATE			
CHECK					COND NO 1.14 051 002 0 TEST 004-03	D6-30643 Vol. II	
APPD							
APPD					THE BOEING COMPANY RENTON, WASHINGTON	PAGE 16.0-8	

STALL CHARACTERISTICS
GROSS WEIGHT 552,100 LBS
CG 32.0 PERCENT MAC
FLAP SET 0 DEG—GEAR UP
ENTRY RATE 1.0 KNOTS/SEC

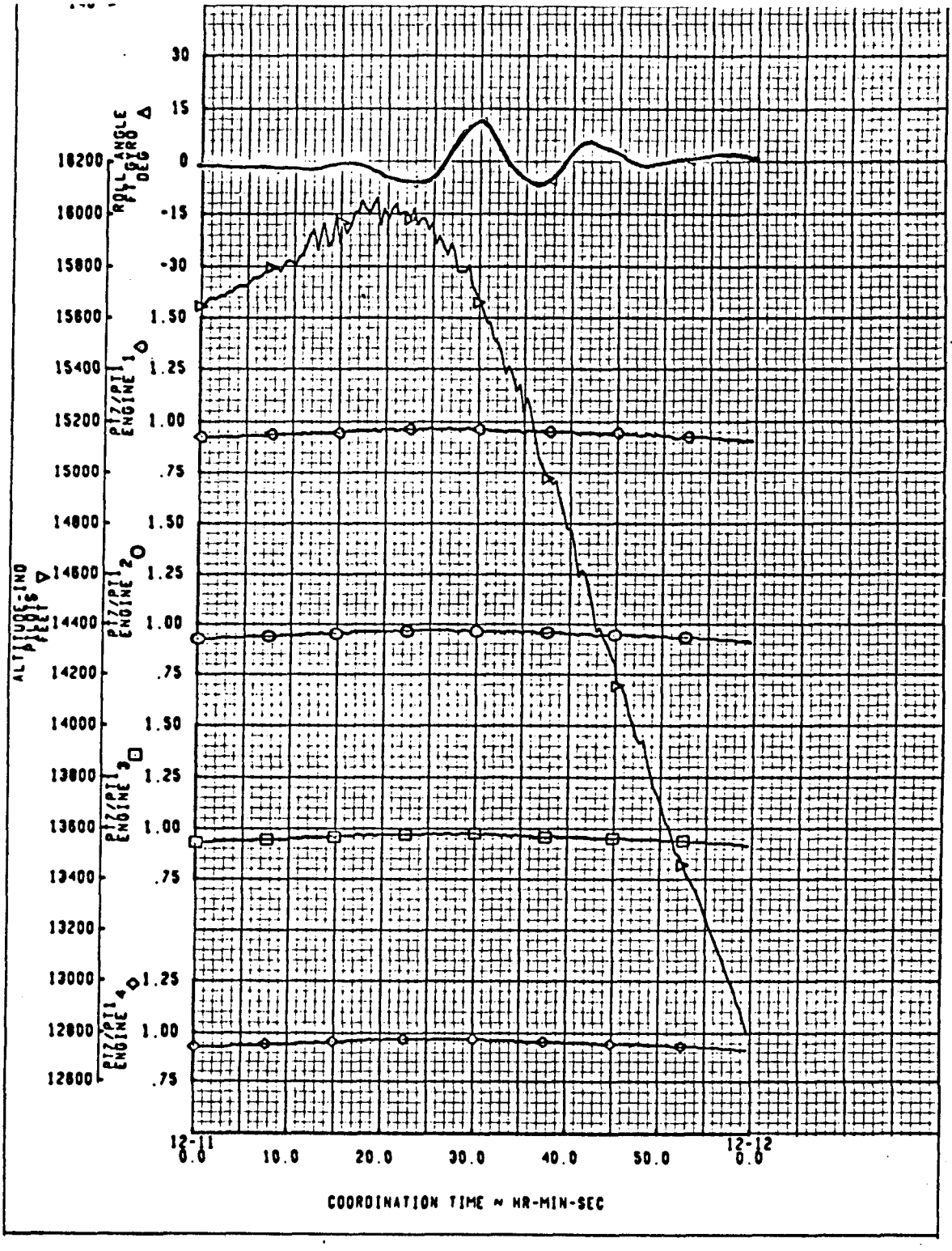
ALTITUDE-IND FEET Δ
ROLL ANGLE GYRO DEG Δ
PI2/PI1 ENGINE 1 ○
PI2/PI1 ENGINE 2 ○
PI2/PI1 ENGINE 3 □
PI2/PI1 ENGINE 4 ○
18200
16000
15800
15600
15400
15200
15000
14800
14600
14400
14200
14000
13800
13600
13400
13200
13000
12800
12600
30
15
0
-15
-30
1.50
1.25
1.00
.75
1.50
1.25
1.00
.75
1.50
1.25
1.00
.75
1.25
1.00
.75
12-11
0.0
10.0
20.0
30.0
40.0
50.0
12-12
0.0
COORDINATION TIME ~ HR-MIN-SEC

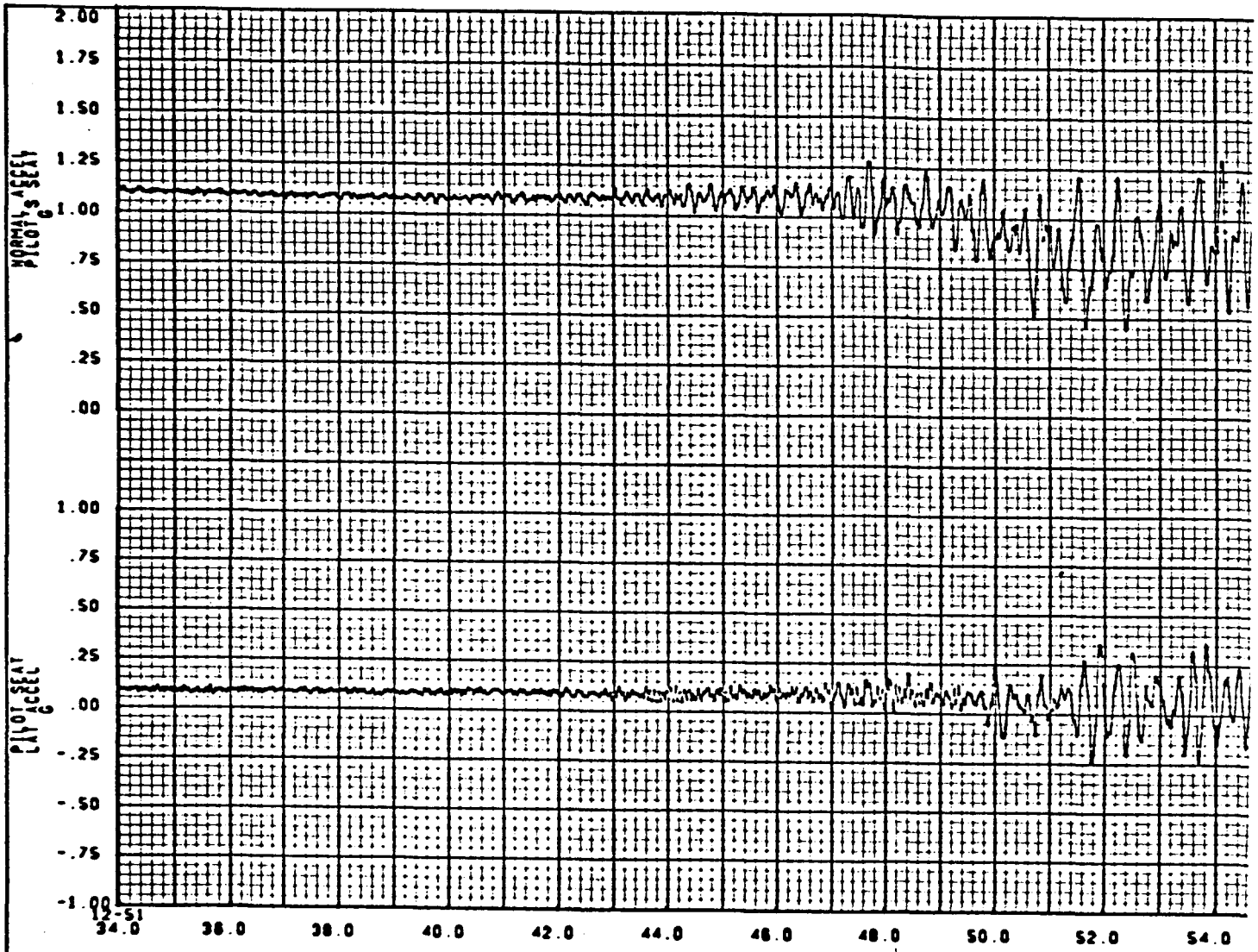

SC4020 PLOT 01/21/70 0940				
CALC			REVISED	DATE
CHECK				
APPD				
APPD				

747 SIMULATOR
FLIGHT DECK VIBRATION ENVIRONMENT

CONO NO 1 14 051 011 0 TEST 004-03

THE BOEING COMPANY

747-100
RA101
D6-30643
Vol. II
PAGE 16.0-9

STALL CHARACTERISTICS
GROSS WEIGHT 536,000 LBS
CG 32.3 PERCENT MAC
FLAP SET 10 DEG—GEAR UP
ENTRY RATE 1.0 KNOTS/SEC

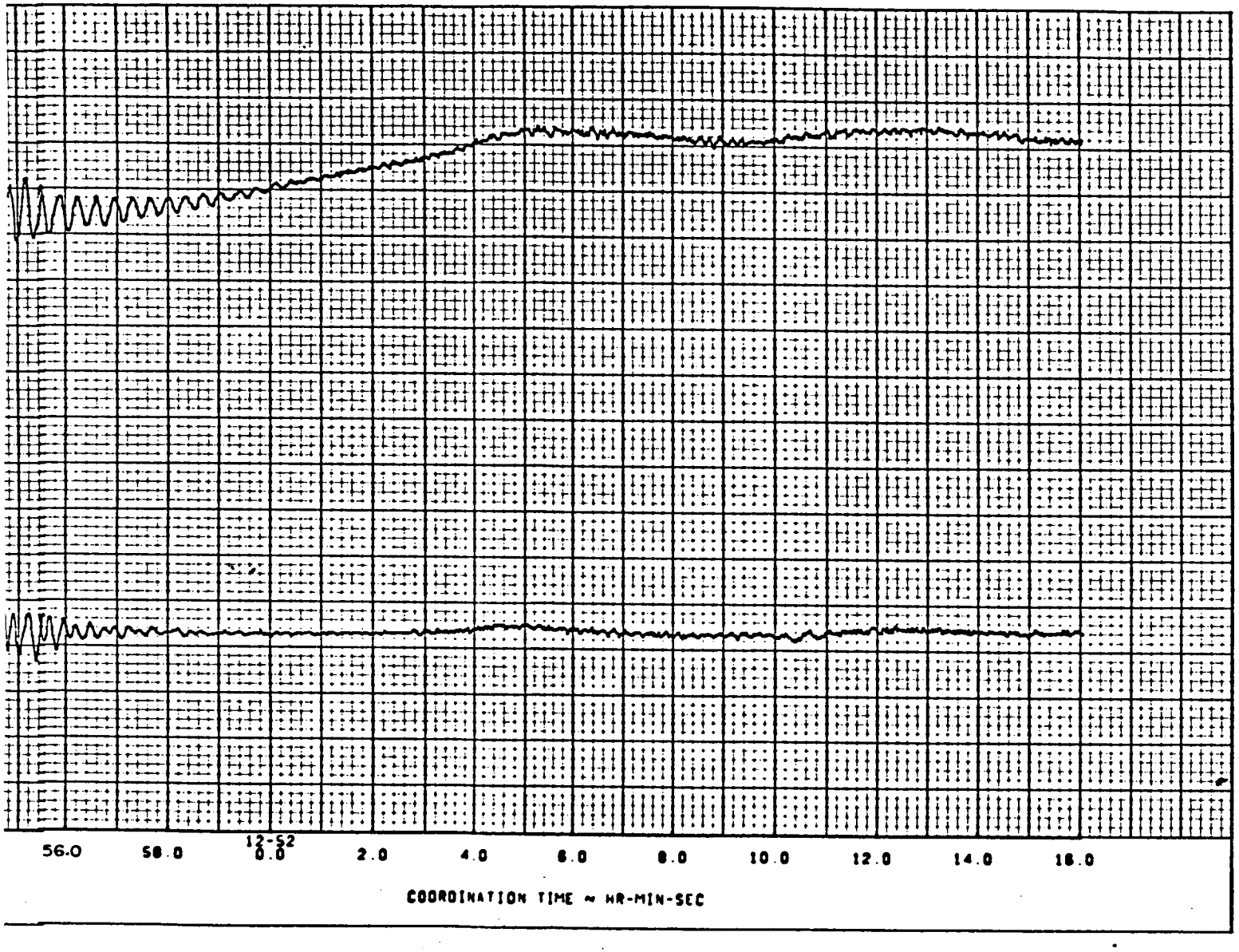
56.0
58.0
12-52
0.0
2.0
4.0
6.0
8.0
10.0
12.0
14.0
16.0
COORDINATION TIME ~ HR-MIN-SEC

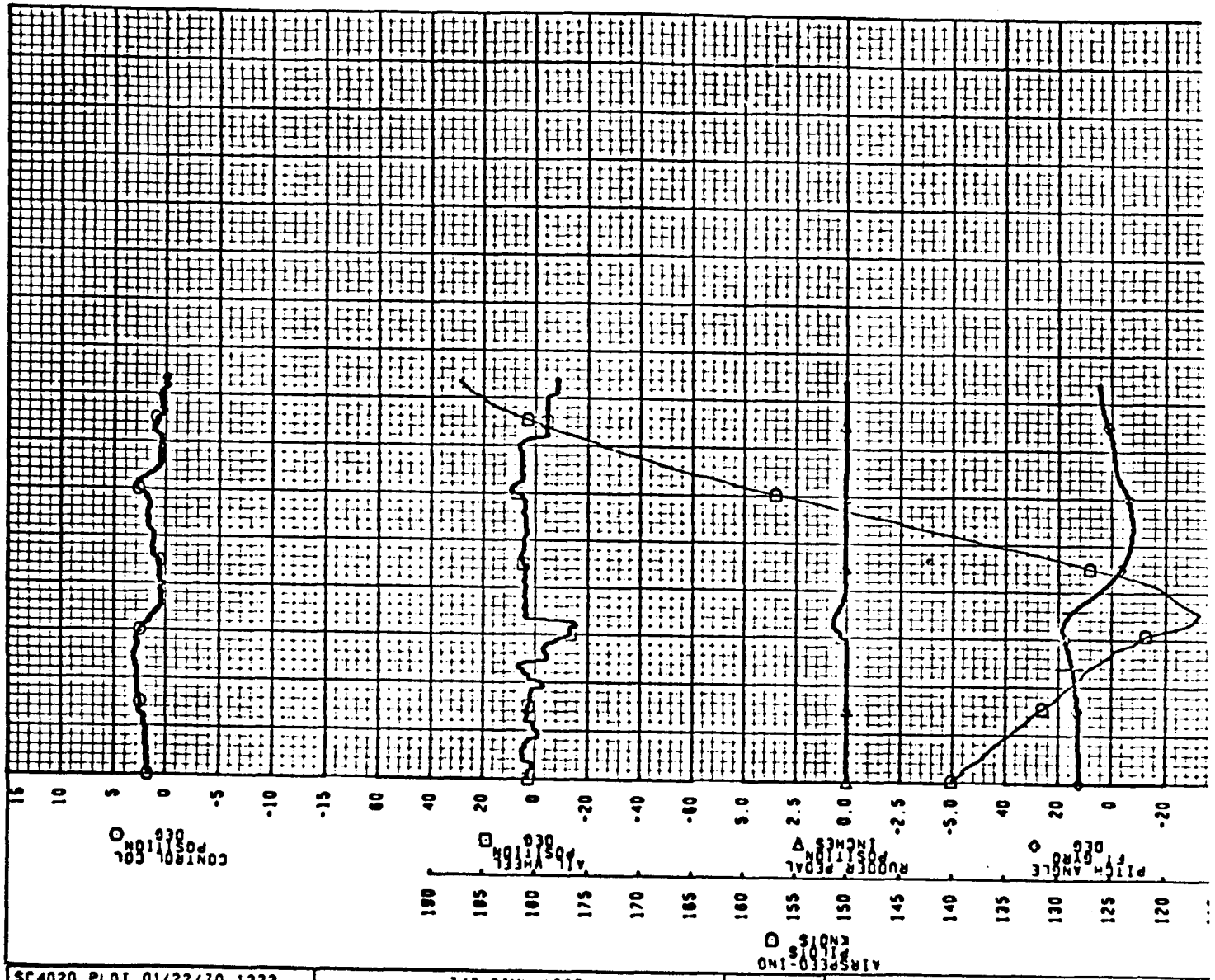
15 10 5 0 -5 -10 -15
CONTROL COL POSITION DEG
80 40 20 0 -20 -40 -80
A/S VANE POSITION DEG
5.0 2.5 0.0 -2.5 -5.0
RUDDER PEDAL POSITION INCHES
40 20 0 -20
PITCH ANGLE DEG
180 185 190 175 170 165 160 155 150 145 140 135 130 125 120
AIRSPEED-IND KNOTS
SC4020 PLOT 01/22/70 1323
CALC
CHECK
APPD
APPD
REVISED
DATE
747 SIMULATOR
FLIGHT DECK VIBRATION ENVIRONMENT
COND NO 1 14 051 011 0 TEST 004-03
THE BOEING COMPANY
747-100
RA101
D6-30643
Vol. II
PAGE
16.0-10
STALL CHARACTERISTICS
GROSS WEIGHT 536,000 LBS
CG 32.3 PERCENT MAC
FLAP SET 10 DEG—GEAR UP
ENTRY RATE 1.0 KNOTS/SEC

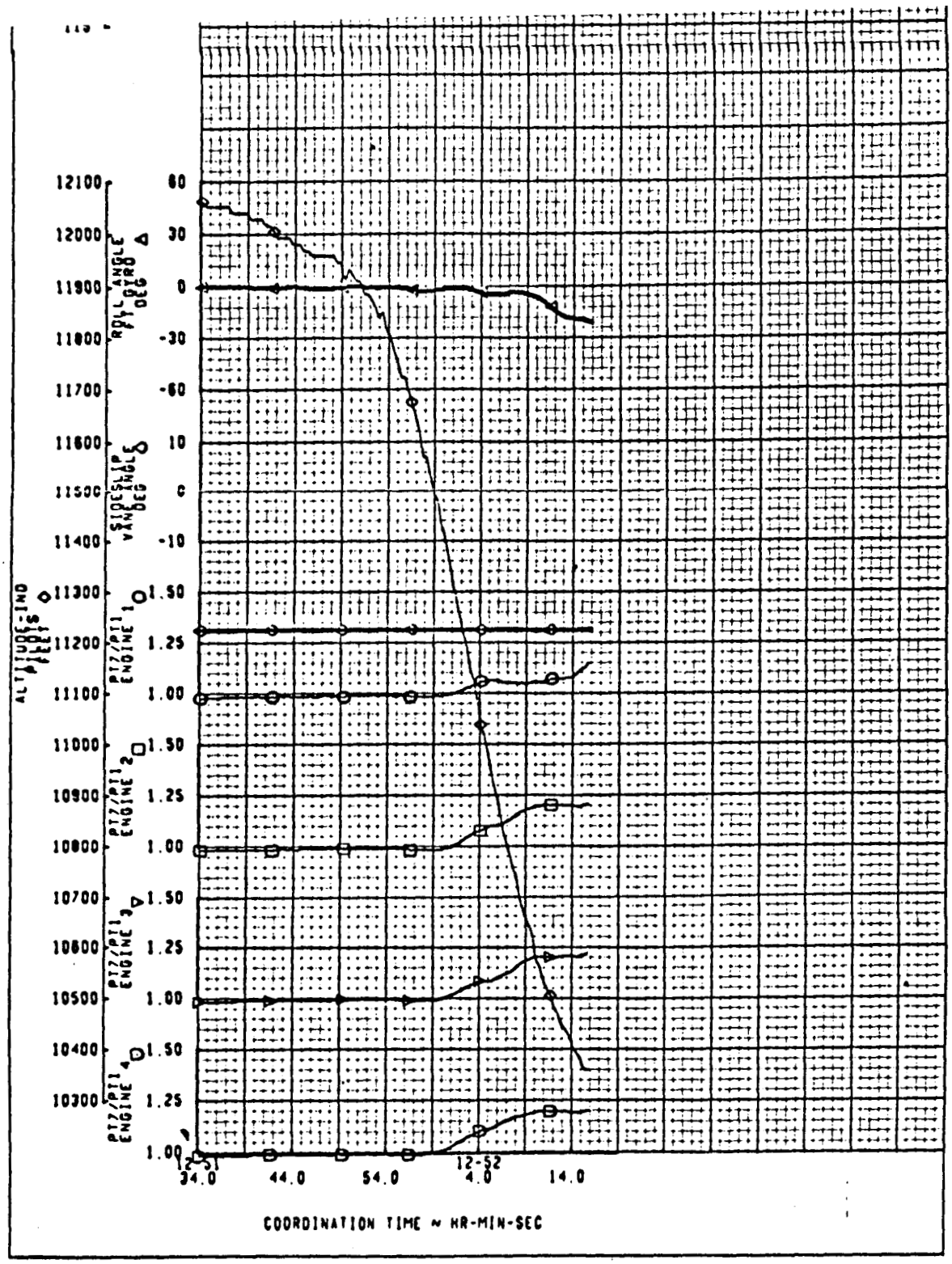
ALTITUDE IND FEET
ROLL ANGLE GYRO DEG
SIDESLIP VANE ANGLE DEG
PT7/PT1 ENGINE 1
PT7/PT1 ENGINE 2
PT7/PT1 ENGINE 3
PT7/PT1 ENGINE 4
12100
12000
11900
11800
11700
11600
11500
11400
11300
11200
11100
11000
10900
10800
10700
10600
10500
10400
10300
60
30
0
-30
-60
10
0
-10
1.50
1.25
1.00
1.50
1.25
1.00
1.50
1.25
1.00
1.50
1.25
1.00
12-51
34.0
44.0
54.0
12-52
4.0
14.0
COORDINATION TIME ~ HR-MIN-SEC

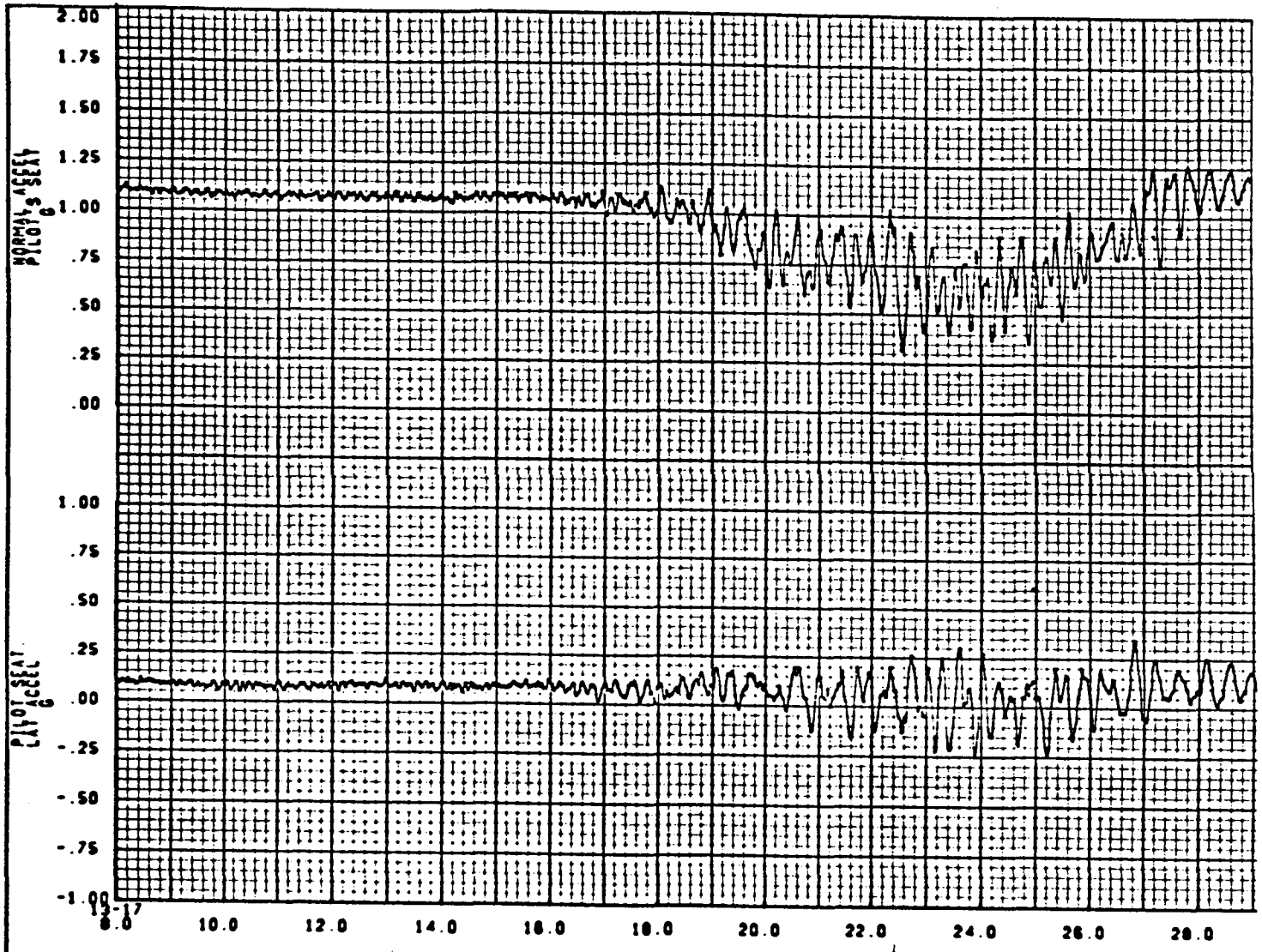

12-17

SC4020 PLOT 01/21/70 0940				
CALC			REVISED	DATE
CHECK				
APPD				
APPD				

747 SIMULATOR
FLIGHT DECK VIBRATION ENVIRONMENT

COND NO 1 14 051 019 0 TEST 004-03

THE BOEING COMPANY
RENTON, WASHINGTON

747-100
RA101

D6-30643
Vol. II

PAGE 16.0-11

STALL CHARACTERISTICS
GROSS WEIGHT 525,000 LBS
CG 33.3 PERCENT MAC
FLAP SET 30 DEG—GEAR DN
ENTRY RATE 1.0 KNOTS/SEC

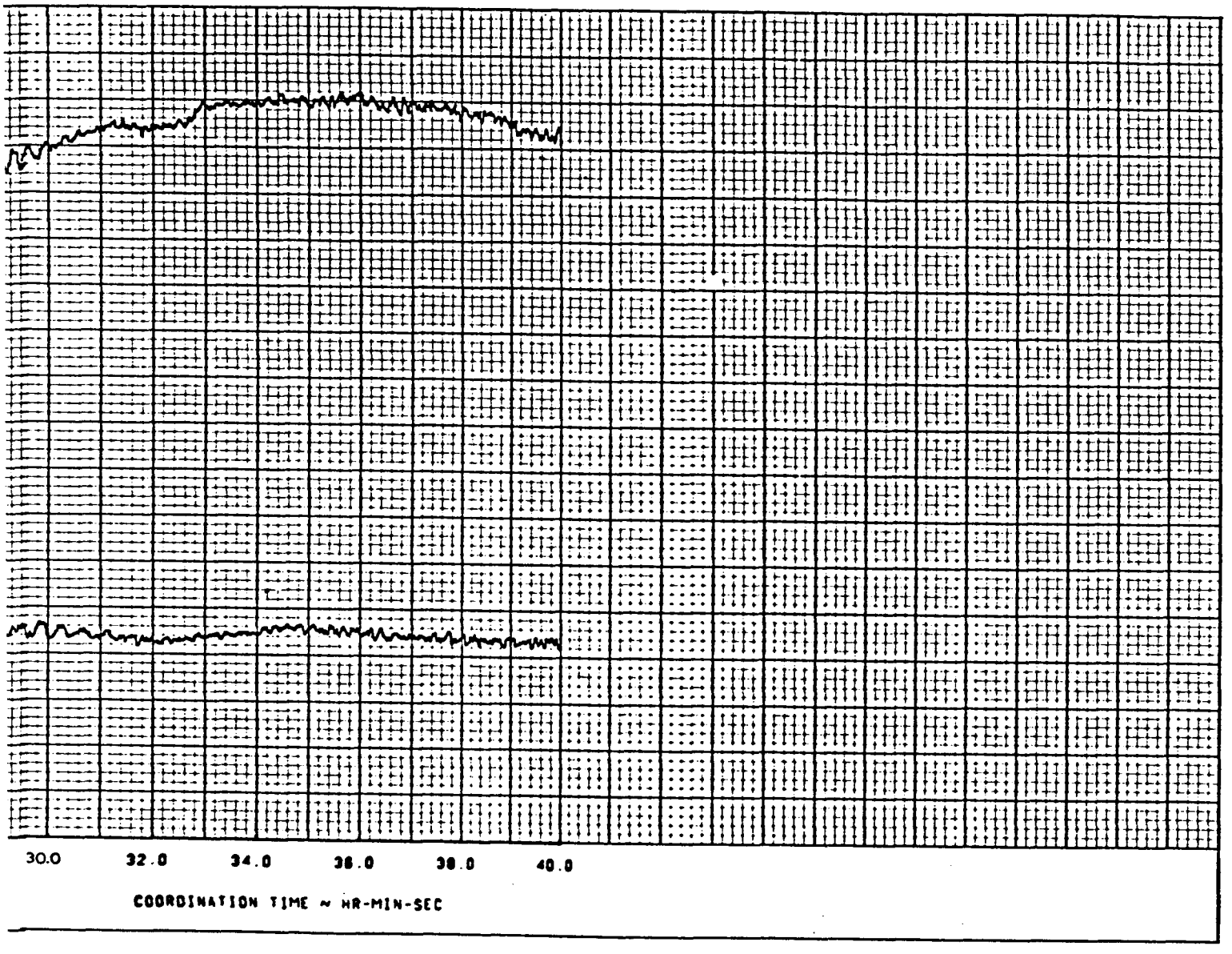
30.0
32.0
34.0
36.0
38.0
40.0
COORDINATION TIME ~ HR-MIN-SEC

APPENDIX - DERIVATION OF LANDING GEAR EQUATIONS

Gear Height

The complete equations for determining landing gear height are derived by methods of descriptive geometry as illustrated in Figure 21.

Let the coordinates of the axle of the strut be X_L, Y_L and Z_L and r be the tire radius. With zero bank angle, pitch the aircraft about the c.g. to an angle θ_B as shown in the side view of Figure 21. The height of the tire relative to the c.g. due to the pitch angle θ_B is

$$h_\theta = X_L \text{ SIN } \theta_B - Z_L \text{ COS } \theta_B - r.$$

After the pitch rotation θ_B, view the aircraft as shown in the rear view of Figure 21 and bank the aircraft to ϕ_B. In the rear view the change in vertical distance from the c.g. to tire is

$$Y_L \text{ SIN } \phi_B + (Z_L + r) \text{ COS } \phi_B - (Z_L + r).$$

Resolving this displacement of the tire relative to the c.g. from the rear view to the side view and into a change in height gives

$$h_\phi = \left[Y_L \text{ SIN } \phi_B + (Z_L + r) \text{ COS } \phi_B - (Z_L + r)\right] \text{ COS } \theta_B$$

or

$$h_\phi = \left[Y_L \text{SIN } \phi_B + (Z_L + r) \text{ (COS } \phi_B - 1)\right] \text{ COS } \theta_B.$$

In the NASA simulation $(Z_L + r)$ is replaced by an equivalent distance S_z. This simplification assumes the tire will contact the runway at a point aligned with the oleo strut as illustrated in Figure 22.

The total height of the tire above the runway is then given by

$$h_G = h + h_\theta - h_\phi.$$

If h_G is negative, the gear will be in contact with the runway and the oleo strut compression ΔS_T is obtained from

$$\Delta S_T = h_G \Big/ \text{COS } \theta_B \text{ COS } \phi_B.$$

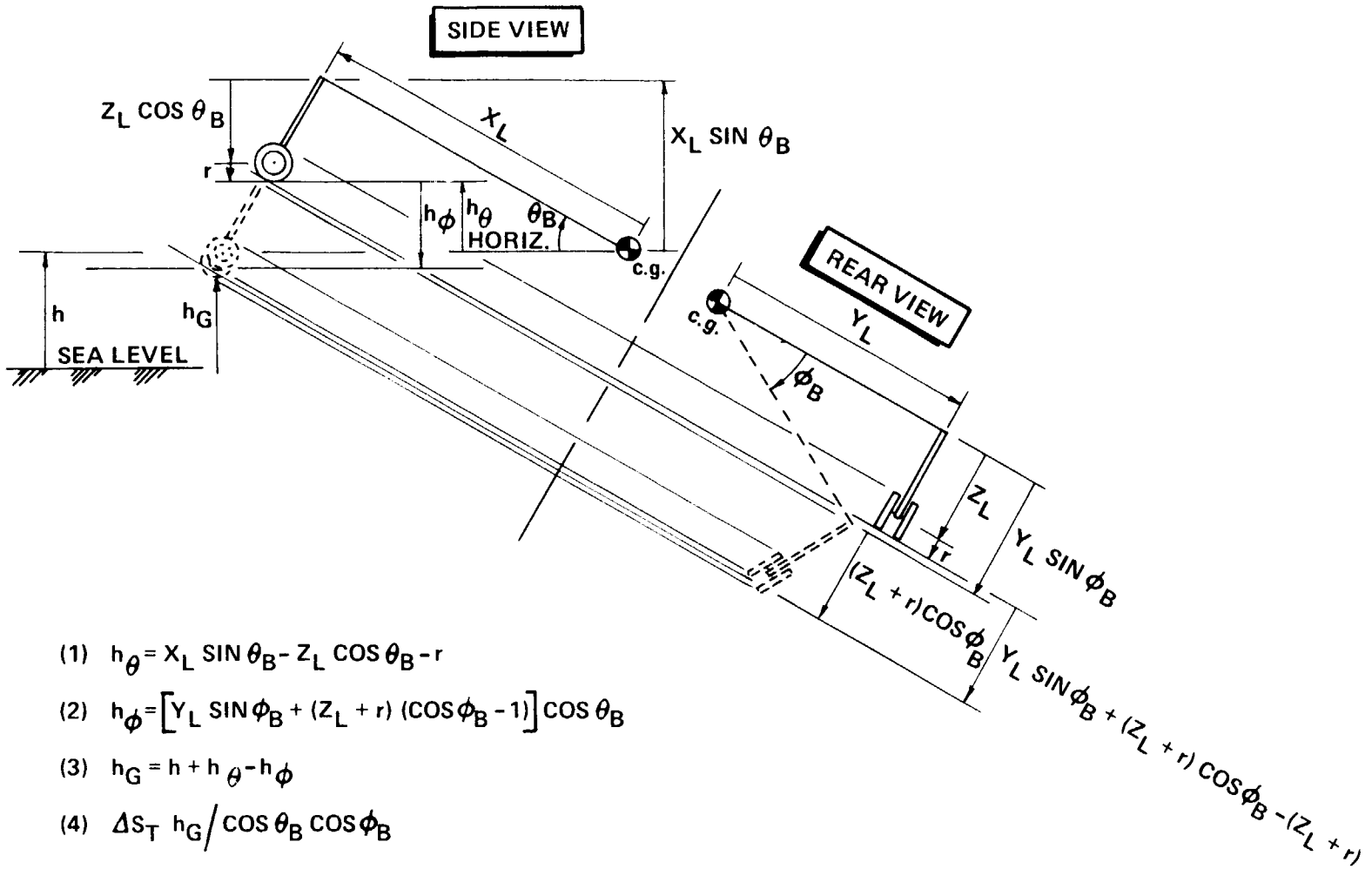

(1) $h_\theta = X_L \sin \theta_B - Z_L \cos \theta_B - r$

(2) $h_\phi = \left[Y_L \sin \phi_B + (Z_L + r)(\cos \phi_B - 1)\right] \cos \theta_B$

(3) $h_G = h + h_\theta - h_\phi$

(4) $\Delta S_T \; h_G \Big/ \cos \theta_B \cos \phi_B$

DERIVATION OF EQUATIONS FOR DETERMINING GEAR HEIGHT

FIGURE 21

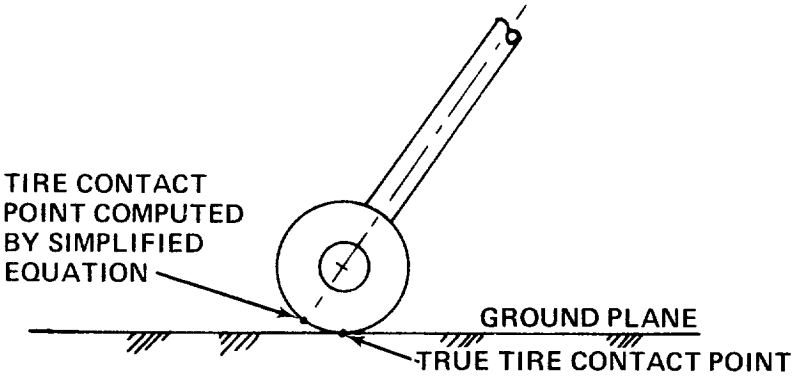

WHEEL RUNWAY CONTACT
FIGURE 22

Tire Forces

The orthogonal forces generated by a tire in contact with the runway are shown in Figure 23.

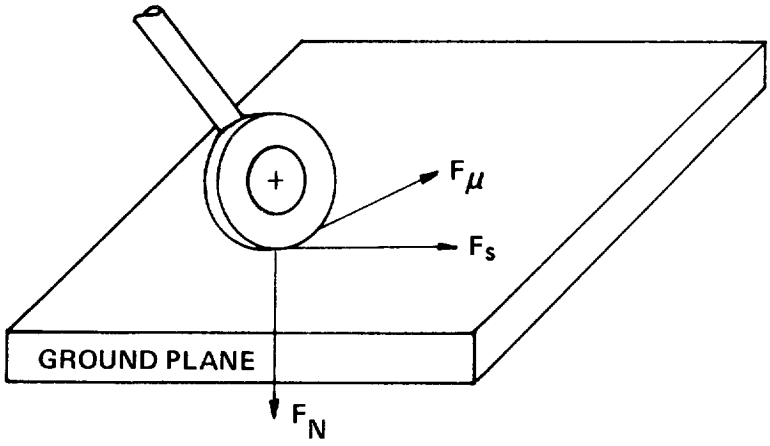

FIGURE 23

The tire drag force vector F_μ is aligned by the intersection of a plane through the tire tread and the ground plane. The normal force vector, F_N, is perpendicular to the ground plane. The side force, F_S, generated by the tire is perpendicular to the plane containing F_μ and F_N. The tire forces are resolved through the aircraft pitch attitude θ_B and bank angle ϕ_B to obtain the body axes forces exerted on the aircraft. The resultant forces in body axes are derived by descriptive geometry methods as illustrated in Figure 24 for normal force, F_N, and in Figure 25 for drag force, F_μ, and side force, F_S .

In the side view of Figure 24, prior to any axes rotation, the normal force vector F_N acts downward, perpendicular to the ground plane. If the aircraft is pitched through an angle θ_B , the normal force in body axes due to the pitch rotation is

$$F_{X_{B_\theta}} = -F_N \sin \theta_B$$

$$F_{Y_{B_\theta}} = 0$$

$$F_{Z_{B_\theta}} = F_N \cos \theta_B$$

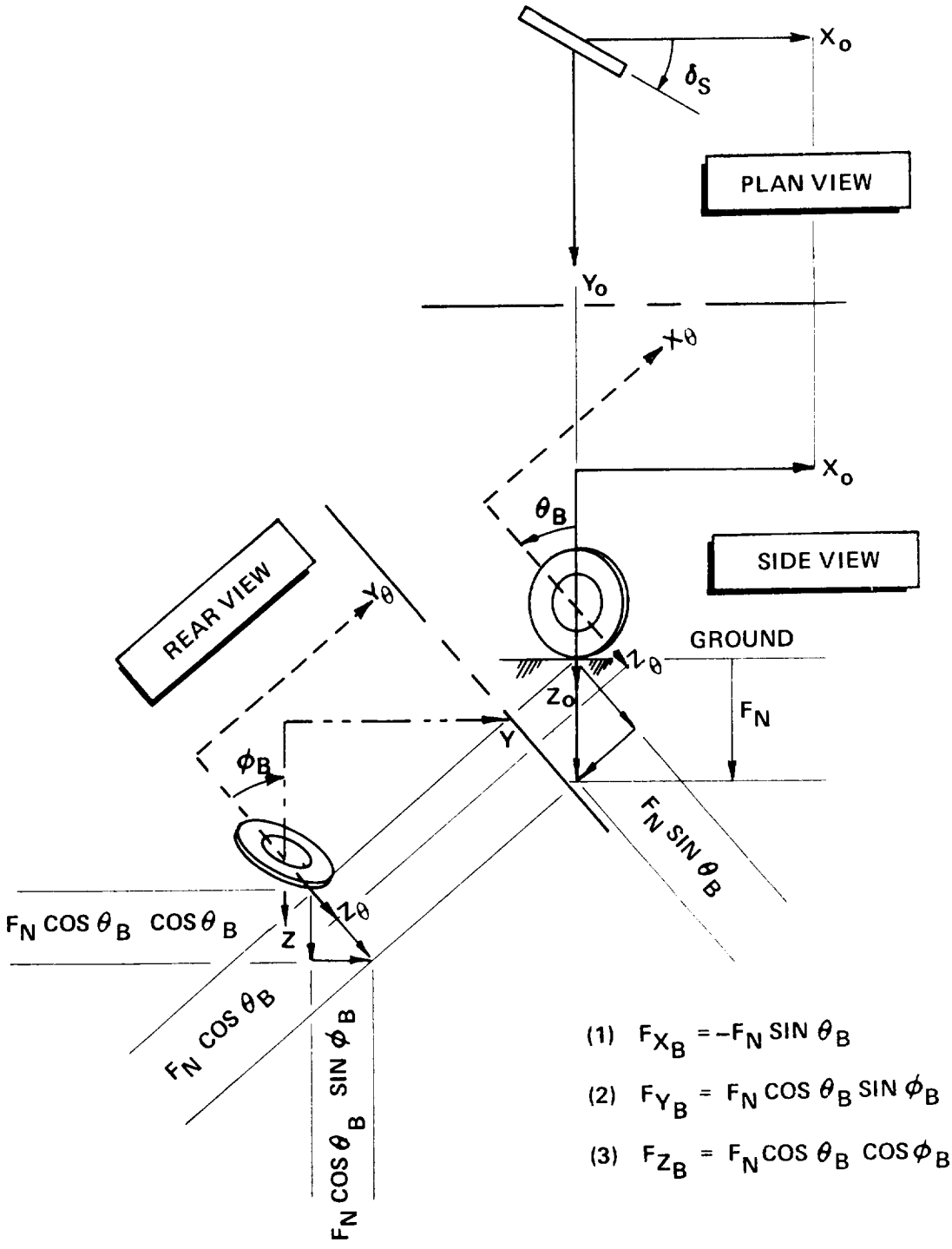

RESOLUTION OF WHEEL NORMAL FORCE INTO AIRPLANE BODY AXES

FIGURE 24

If the aircraft is viewed from the rear, as shown by the rear view of Figure 24, and is rotated through a bank angle ϕ_B, the normal force in body axes is

$$(1)\quad F_{X_B} = -F_N \sin \theta_B$$

$$(2)\quad F_{Y_B} = F_N \cos\theta_B \sin\phi_B$$

$$(3)\quad F_{Z_B} = F_N \cos\theta_B \cos\phi_B$$

Equations (1) through (3) represent the resolution of the normal force into body axes.

In the plan view of Figure 25, prior to any axes rotation, the gear drag force acts in the direction of tire rotation and the side force acts perpendicular to the side of the tire. The wheel steering angle is δ_S. The forces resolved into body axes are

$$F_{X_{B_o}} = F\mu \cos \delta_s - F_s \sin \delta_s$$

$$F_{Y_{B_o}} = F\mu \sin \delta_s + F_s \cos \delta_s$$

$$F_{Z_{B_o}} = 0$$

If the aircraft is pitched through an angle θ_B, as shown in the side view of Figure 25, the forces resolved in body axes are

$$F_{X_{B_\theta}} = (F\mu \cos \delta_s - F_s \sin \delta_s) \cos \theta_B$$

$$F_{Y_{B_\theta}} = F\mu \sin \delta_s + F_s \cos \delta_s$$

$$F_{Z_{B_\theta}} = (F\mu \cos \delta_s - F_s \sin \delta_s) \sin \theta_B$$

The bank angle axes rotation as shown in the rear view of Figure 25 gives the final value of wheel drag and side force in body axes as

$$(4)\quad F_{X_B} = (F\mu \cos \delta_s - F_s \sin \delta_s) \cos \theta_B$$

$$(5)\quad F_{Y_B} = (F\mu \sin \delta_s + F_s \cos \delta_s) \cos \phi_B + (F\mu \cos \delta_s - F_s \sin \delta_s) \sin \theta_B \sin \phi_B$$

$$(6)\quad F_{Z_B} = -(F\mu \sin \delta_s + F_s \cos \delta_s) \sin \phi_B + (F\mu \cos \delta_s - F_s \sin \delta_s) \sin \theta_B \cos \phi_B$$

Equations (4) through (6) when combined with Equations (1) through (3) represent the forces in aircraft body axes generated by a tire contacting the runway.

For the NASA simulation, small angle approximations were used to resolve the forces into body

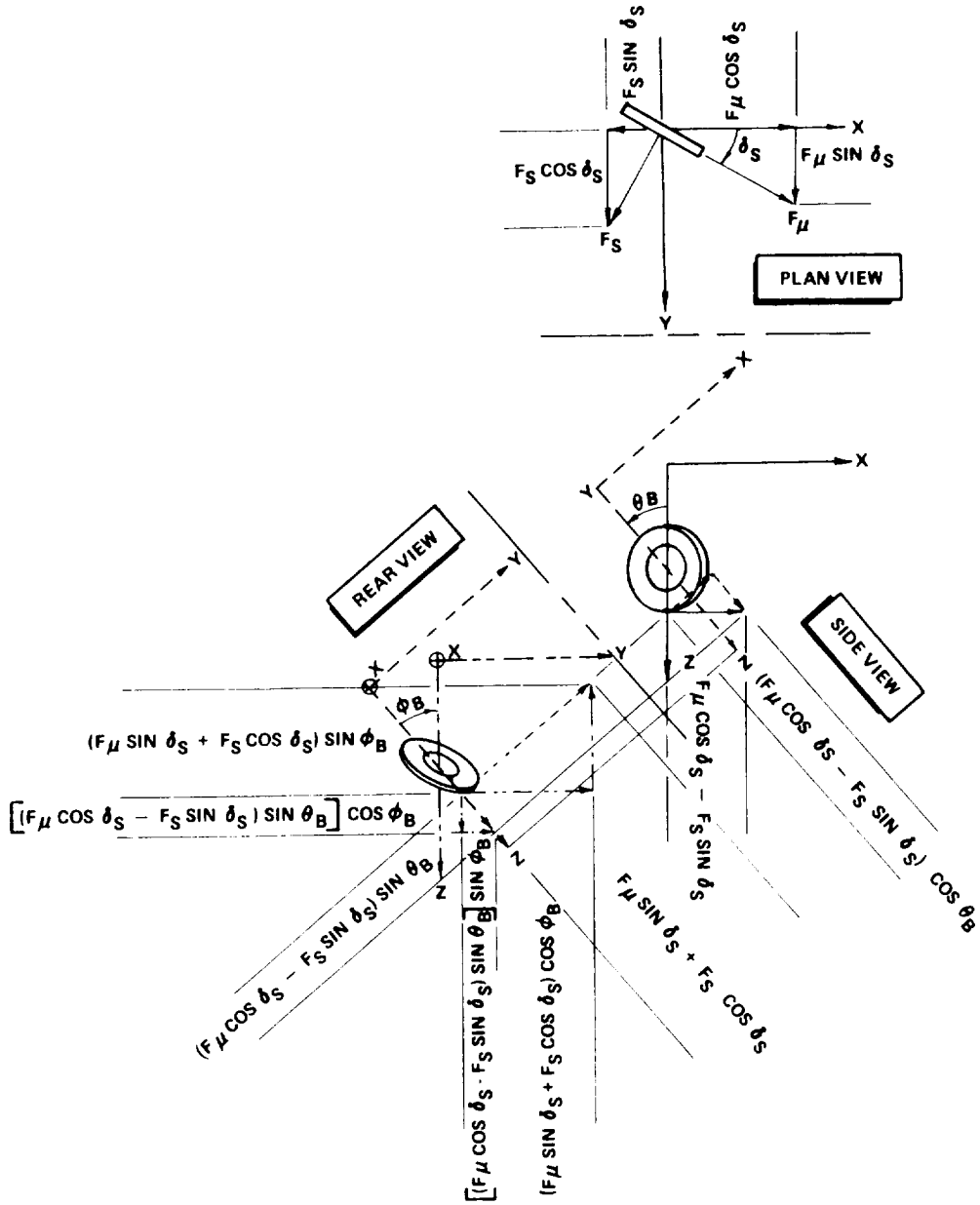

(1) $F_x = (F_\mu \cos \delta_S - F_S \sin \delta_S) \cos \theta_B$

(2) $F_y = (F_\mu \sin \delta_S + F_S \cos \delta_S) \cos \phi_B + (F_\mu \cos \delta_S - F_S \sin \delta_S) \sin \theta_B \sin \phi_B$

(3) $F_z = -(F_\mu \sin \delta_S + F_S \cos \delta_S) \sin \phi_B + (F_\mu \cos \delta_S - F_S \sin \delta_S) \sin \theta_B \cos \phi_B$

RESOLUTION OF WHEEL DRAG AND SIDE FORCE INTO AIRPLANE BODY AXES

FIGURE 25

axes. The normal force Equations (1) through (3) were simplified to

$$(7)\quad F_{X_B} = -F_N \theta_B$$

$$(8)\quad F_{Y_B} = F_N \phi_B$$

$$(9)\quad F_{Z_B} = F_N = F_{G_Z}$$

where F_{G_Z} = forces generated by compression of the oleo strut.

The drag force equations (4) through (6) were simplified to

$$(10)\quad F_{X_B} = F\mu - F_s \delta_s$$

$$(11)\quad F_{Y_B} = F\mu\ \delta_s + F_s$$

$$(12)\quad F_{Z_B} = -F_s \phi_B + F\mu \theta_B$$

Combining Equations (7) through (12) gives the final equations used for the NASA simulation

$$F_{X_B} = F\mu - F_s \delta_s - F_{G_Z} \theta_B$$

$$F_{Y_B} = F\mu\ \delta_s + F_s + F_{G_Z} \phi_B$$

$$F_{Z_B} = F\mu\ \theta_B - F_s \phi_B + F_{G_Z}$$

NASA-Langley, 1971 —— 2